

TRANSACTIONS OF THE  
American Ophthalmological Society  
VOLUME C

TRANSACTIONS OF THE  
American  
Ophthalmological Society  
ONE HUNDRED AND THIRTY-EIGHTH  
ANNUAL MEETING  
THE CLOISTER  
SEA ISLAND, GEORGIA  
2002

Published for the  
AMERICAN OPHTHALMOLOGICAL SOCIETY  
by JOHNSON PRINTING COMPANY  
Rochester, Minnesota 2002

©*American Ophthalmological Society* 2002  
*Rochester, Minnesota*  
*Printed in U.S.A.*  
*LC 43-42894*

Printed on acid-free paper effective with  
Volume XXXXVIII, 1950

## *CONTENTS*

OFFICERS AND COUNCIL	ix
PRESIDENTS OF THE SOCIETY	x-xi
RECIPIENTS OF THE HOWE MEDAL	xii-xiii
VERHOEFF LECTURERS	xiv
MEMBERS	xv-xvii
CONTRIBUTORS	xviii

## *NECROLOGY*

IN MEMORIUM	2-18
-------------	------

## *MINUTES OF THE PROCEEDINGS*

MINUTES OF THE PROCEEDINGS	19-39
----------------------------	-------

OFFICERS AND COUNCIL  
OF THE  
AMERICAN OPHTHALMOLOGICAL SOCIETY

*Elected at the Annual Meeting*  
May 20, 2002

PRESIDENT

DR MARILYN T. MILLER, CHICAGO, ILLINOIS

PRESIDENT-ELECT

DR FRONCIE A. GUTMAN, CLEVELAND, OHIO

SECRETARY-TREASURER

DR CHARLES P. WILKINSON, BALTIMORE, MARYLAND

EDITOR OF THE TRANSACTIONS

DR THOMAS J. LIESEGANG, JACKSONVILLE, FLORIDA

COUNCIL

DR DANIEL M. ALBERT, MADISON, WISCONSIN

DR JOHN G. CLARKSON, MIAMI, FLORIDA

DR DAN B. JONES, HOUSTON, TEXAS

DR SUSAN H. DAY, SAN FRANCISCO, CALIFORNIA

DR TRAVIS A. MERIDITH, CHAPEL HILL, NORTH CAROLINA

## PRESIDENTS OF THE SOCIETY

1864-1868	DR EDWARD DELAFIELD, New York
1869-1873	DR HENRY W. WILLIAMS, Boston
1874-1878	DR C. R. AGNEW, New York
1879-1884	DR HENRY D. NOYES, New York
1885-1889	DR WILLIAM F. NORRIS, Philadelphia
1890-1893	DR HASKET DERBY, Boston
1894-1898	DR GEORGE C. HARLAN, Philadelphia
1899-1902	DR O. F. WADSWORTH, Boston
1903-1905	DR CHARLES S. BULL, New York
1906	DR ARTHUR MATHEWSON, Washington, DC
1907	DR CHARLES J. KIPP, Newark
1908	DR SAMUEL D. RISLEY, Philadelphia
1909	DR S. B. ST JOHN, Hartford
1910	DR SAMUEL THEOBALD, Baltimore
1911	DR EMIL GRUENING, New York
1912	DR EDWARD JACKSON, Denver
1913	DR MYLES STANDISH, Boston
1914	DR ROBERT SATTLER, Cincinnati
1915	DR M. H. POST, St Louis
1916	DR GEORGE E. DE SCHWEINITZ, Philadelphia
1917	DR PETER A. CALLAN, New York
1918	DR WILLIAM H. WILDER, Chicago
1919	DR LUCIEN HOWE, Buffalo
1920	DR HIRAM WOODS, Baltimore
1921	DR JOHN E. WEEKS, New York
1922	DR WILLIAM M. SWEET, Philadelphia
1923	DR WILLIAM H. WILMER, Washington, DC
1924	DR ALEXANDER DUANE, New York
1925	DR CASSIUS D. WESTCOTT, Chicago
1926	DR DAVID HARROWER, Worcester
1927	DR WILLIAM ZENTMAYER, Philadelphia
1928	DR WALTER E. LAMBERT, New York
1929	DR WALTER R. PARKER, Detroit
1930	DR WILLIAM CAMPBELL POSEY, Philadelphia
1931	DR ARNOLD KNAPP, New York
1932	DR EDWARD C. ELLETT, Memphis
1933	DR THOMAS B. HOLLOWAY, Philadelphia
1934	DR W. GORDON M. BYERS, Montreal
1935	DR WALTER B. LANCASTER, Boston
1936	DR LOUIS S. GREENE, Washington, DC
1937	DR HARRY FRIEDENWALD, Baltimore
1938	DR F. H. VERHOEFF, Boston
1939	DR FREDERICK T. TOOKE, Montreal
1940	DR E. V. L. BROWN, Chicago
1941	DR F. PHINIZY CALHOUN, Atlanta
1942	DR ALLEN GREENWOOD, Boston
1943	DR HUNTER H. MCGUIRE, Winchester, Virginia
1944	DR JOHN GREEN, St Louis
1945	DR S. JUDD BEACH, Portland, Maine
1946	DR EUGENE M. BLAKE, New Haven
1947	DR JOHN W. BURKE, Washington, DC
1948	DR HENRY C. HADEN, Houston

*Presidents of the Society*

1949	DR BERNARD SAMUELS, New York
1950	DR PARKER HEATH, Boston
1951	DR JOHN H. DUNNINGTON, New York
1952	DR LAWRENCE T. POST, St Louis
1953	DR CONRAD BERENS, New York
1954	DR WILLIAM L. BENEDICT, Rochester, Minnesota
1955	DR EVERETT L. GOAR, Houston
1956	DR ALAN C. WOODS, Baltimore
1957	DR FREDERICK C. CORDES, San Francisco
1958	DR WALTER S. ATKINSON, Watertown, NY
1959	DR DERRICK VAIL, Chicago
1960	DR ALGERNON B. REESE, New York
1961	DR EDWIN B. DUNPHY, Boston
1962	DR FRANCIS HEED ADLER, Philadelphia
1963	DR PAUL A. CHANDLER, Boston
1964	DR MAYNARD C. WHEELER, New York
1965	DR FRANK B. WALSH, Baltimore
1966	DR WILFRED E. FRY, Philadelphia
1967	DR PHILLIP M. LEWIS, Memphis
1968	DR GORDON C. BRUCE, New York
1969	DR JAMES N. GREER, Reno
1970	DR C. WILBUR RUCKER, Rochester, Minnesota
1971	DR DOHRMANN K. PISCHEL, San Francisco
1972	DR TRYGVE GUNDERSEN, Boston
1973	DR ARTHUR GERARD DEVOE, New York
1974	DR WILLIAM P. MCGUIRE, Winchester, Virginia
1975	DR M. ELLIOTT RANDOLPH, Baltimore
1976	DR JOSEPH A. C. WADSWORTH, Durham
1977	DR DAVID O. HARRINGTON, San Francisco
1978	DR SAMUEL D. MCPHERSON, JR., Durham
1979	DR F. PHINIZY CALHOUN, JR., Atlanta
1980	DR JOHN WOODWORTH HENDERSON, Ann Arbor
1981	DR WILLIAM F. HUGHES, Chicago
1982	DR ROBERT W. HOLLENHORST, Rochester, Minnesota
1983	DR CLEMENT McCULLOCH, Toronto
1984	DR ROBERT N. SHAFFER, San Francisco
1985	DR DUPONT GUERRY III, Richmond
1986	DR A. EDWARD MAUMENEE, Baltimore
1987	DR FRANK W. NEWELL, Chicago
1988	DR EDWARD W. D. NORTON, Miami
1989	DR DAVID SHOCH, Chicago
1990	DR ROBERT E. KENNEDY, Rochester, New York
1991	DR FREDERICK C. BLODI, Iowa City
1992	DR THOMAS P. KEARNS, Rochester, Minnesota
1993	DR BRADLEY R. STRAATSMA, Los Angeles
1994	DR ROBERT B. WELCH, Annapolis, Maryland
1995	DR BRUCE E. SPIVEY, Chicago
1996	DR STANLEY TRUHLSEN, Omaha
1997	DR WILLIAM H. SPENCER, San Francisco
1998	DR W. RICHARD GREEN, Baltimore
1999	DR WILLIAM S. TASMAN, Wyndmoor, Pennsylvania
2000	DR W. BANKS ANDERSON, JR., Durham
2001	DR PAUL R. LICHTER, Ann Arbor
2002	DR ROBERT C. DREWS, Clayton, Missouri
2003	DR MARILYN T. MILLER, Chicago, Illinois

## RECIPIENTS OF THE HOWE MEDAL

1922	DR CARL KOLLER, New York
1923	DR ALEXANDER DUANE, New York
1924	DR ERNEST FUCHS, Vienna, Austria
1925	NO AWARD
1926	DR EDWARD JACKSON, Denver
1927	MR PRIESTLY SMITH, Birmingham, England
1928	NO AWARD
1929	DR THEODOR AXENFELD, Freiburg, Germany
1930	NO AWARD
1931	NO AWARD
1932	DR F. H. VERHOEFF, Boston
1933	NO AWARD
1934	DR GEORGE E. DE SCHWEINITZ, Philadelphia
1935	NO AWARD
1936	SIR JOHN HERBERT PARSONS, London, England
1937	DR ARNOLD KNAPP, New York
1938	NO AWARD
1939	NO AWARD
1940	NO AWARD
1941	NO AWARD
1942	DR E. V. L. BROWN, Chicago
1943	NO AWARD
1944	NO AWARD
1945	DR WALTER B. LANCASTER, Boston
1946	SIR STEWART DUCK-ELDER, London, England
1947	DR LAWRENCE T. POST, St Louis
1948	DR WILLIAM ZENTMAYER, Philadelphia
1949	DR PHILLIPS THYGESON, San Jose, California
1950	DR ALGERNON B. REESE, New York
1951	DR JONAS S. FRIEDENWALD, Baltimore
1952	DR FRANCIS H. ADLER, Philadelphia
1953	DR ALAN C. WOODS, Baltimore
1954	DR JOHN H. DUNNINGTON, New York
1955	DR ARTHUR J. BEDELL, Albany
1956	DR BERNARD SAMUELS, New York
1957	DR GEORGIANA DVORAK-THEOBALD, Oak Park, Illinois
1958	MISS IDA MANN, Nedlands, Western Australia
1959	DR LUDWIG VON SALLMANN, Bethesda, Maryland
1960	DR DERRICK T. VAIL, Chicago
1961	DR FREDERICK C. CORDES, San Francisco
1962	DR FRANK B. WALSH, Baltimore
1963	DR EDWIN B. DUNPHY, Boston
1964	DR WILLIAM L. BENEDICT, Rochester, Minnesota
1965	DR DAVID G. COGAN, Boston
1966	DR DOHRMANN K. PISCHEL, San Francisco
1967	DR PAUL A. CHANDLER, Boston
1968	DR WALTER MORTON GRANT, Boston
1969	DR A. EDWARD MAUMENEE, Baltimore
1970	DR PETER C. KRONFELD, Chicago
1971	DR C. WILBUR RUCKER, Rochester, Minnesota
1972	DR WALTER S. ATKINSON, Watertown, New York

*Recipients of the Howe Medal*

- 1973 DR GORDON M. BRUCE, Fort Lee, New Jersey  
1974 DR IRVING H. LEOPOLD, New York  
1975 DR MICHAEL J. HOGAN, San Francisco  
1976 DR EDWARD W. D. NORTON, Miami  
1977 DR KENNETH C. SWAN, Portland, Oregon  
1978 DR S. RODMAN IRVINE, Newport Beach, California  
1979 DR FRANK W. NEWELL, Chicago  
1980 DR FREDERICK C. BLODI, Iowa City  
1981 DR DAVID O. HARRINGTON, San Francisco  
1982 DR ARTHUR GERARD DEVOE, New York  
1983 DR J. DONALD M. GASS, Miami  
1984 DR HAROLD G. SCHEIE, Philadelphia  
1985 DR ROBERT N. SHAFFER, San Francisco  
1986 DR ROBERT W. HOLLENHORST, Rochester, Minnesota  
1987 DR DUPONT GUERRY III, Richmond, Virginia  
1988 DR THOMAS D. DUANE, Philadelphia  
1989 DR MARSHALL M. PARKS, Washington, DC  
1990 DR DAVID SHOCH, Chicago  
1991 DR ARNALL PATZ, Baltimore  
1992 DR BRADLEY R. STRAATSMA, Los Angeles  
1993 DR BRUCE E. SPIVEY, San Francisco  
1994 DR THOMAS P. KEARNS, Rochester, Minnesota  
1995 DR WILLIAM H. SPENCER, San Francisco  
1996 DR ROBERT MACHEMER, Durham  
1997 DR W. RICHARD GREEN, Baltimore  
1998 DR ALAN B. SCOTT, San Francisco  
1999 DR LORENZ E. ZIMMERMAN, Washington, DC  
2000 DR WILLIAM S. TASMAN, Philadelphia, Pennsylvania  
2001 DR STANLEY M. TRUHLSEN, Omaha  
2002 DR CROWELL BEARD, San Jose, California

## VERHOEFF LECTURERS

1961	DR ARTHUR J. BEDELL
1964	SIR STEWART DUKE-EDLER
1969	DR DAVID G. COGAN
1971	DR LORENZ E. ZIMMERMAN
1973	DR IRVING H. LEOPOLD
1975	DR ARTHUR GERARD DeVOE
1977	PROFESSOR JULES FRANCOIS
1979	DR SAIICHI MISHIMA
1983	DR RICHARD W. YOUNG
1989	DR FREDERICK C. BLODI
1992	DR FRANCIS I. COLLINS
1993	DR JORAM PIATIGORSKY
1997	DR GEOFFREY ARDEN
2002	DR PAUL SIEVING

## MEMBERS 2002

Aaberg Sr., Thomas M.  
Albert, Daniel M.  
Alvarado, Jorge A.  
Anderson, Douglas R.  
Anderson Jr., W. Banks  
Apple, David J.  
Asbell, Penny A.  
Augsburger, James J.  
Bartley, George B.  
Bateman, J Bronwyn  
Beauchamp, George R.  
Benson, William E.  
Berler, David K.  
Berrocal, Jose A.  
Berson, Eliot L.  
Biglan, Albert W.  
Blair, Norman P.  
Blankenship, George W.  
Bobrow, James C.  
Bourne, William M.  
Brown, Gary C.  
Bullock, John D.  
Caldwell, Delmar R.  
Cantor, Louis B.  
Caprioli, Joseph  
Char, Devron H.  
Cibis, Gerhard W.  
Clarkson, John G.  
Coleman, D. Jackson  
Crawford, J. Brooks  
Day, Susan H.  
Donshik, Peter C.  
Doughman, Donald J.  
Drews, Robert C.  
Eagle Jr., Ralph C.  
Elman, Michael J.  
Ernest, J. Terry  
Farris, R. Linsy  
Federman, Jay L.  
Feman, Stephen S.  
Ferris, Frederick L.  
Ferry, Andrew P.  
Flach, Allan J.  
Flanagan, Joseph C.  
Flynn, John T.  
Forbes, Max  
Forster, Richard K.  
Foster, C. Stephen  
France, Thomas D.  
Frank, Robert N.  
Fraunfelder, Frederick T.  
Freeman, H. MacKenzie  
Friedlaender, Mitchell H.  
Friedman, Alan H.  
Frueh, Bartley R.  
Gaasterland, Douglas E.  
Gardner, Thomas W.  
Godfrey, William A.  
Goldberg, Morton F.  
Good, William V.  
Gottsch, John D.  
Gragoudas, Evangelos S.  
Green, W. Richard  
Gross, Ronald L.  
Grossniklaus, Hans E.  
Gutman, Froncie A.  
Guyton, David L.  
Haik, Barrett G.  
Haller, Julia A.  
Harris, Gerald J.  
Heckenlively, John R.  
Helveston, Eugene M.  
Holland, Edward J.  
Horton, Jonathan C.  
Hull, David S.  
Humayun, Mark S.  
Iloff, Nicholas T.  
Iloff, W. Jackson  
Ing, Malcolm R.  
Jabs, Douglas A.  
Jaeger, Edward A.  
Jakobiec, Frederick A.  
Jampel, Henry  
Jampol, Lee M.  
Jampolsky, Arthur  
Jones, Dan B.  
Kaiser-Kupfer, Muriel I.  
Kass, Michael A.  
Katz, Barrett  
Kaufman, Paul L.  
Kelley, James S.  
Kennedy, Robert H.  
Kenyon, Kenneth R.  
Kivlin, Jane D.  
Klein, Barbara E. K.  
Klein, Ronald  
Knox, David L.  
Koch, Douglas D.  
Kolker, Allan E.  
Krachmer, Jay H.  
Kramer, Steven G.  
Kreiger, Allan E.  
Kupfer, Carl  
Laibson, Peter R.  
Lakhanpal, Vinod  
Landers III, Maurice B.  
Laties, Alan M.  
Lemp, Michael A.  
L'Esperance, Francis A.  
Lewis, Richard Alan  
Lichter, Paul R.  
Liesegang, Thomas J.  
Lindstrom, Richard L.  
Ludwig, Irene H.  
Luxenberg, Malcolm N.  
Mannis, Mark J.  
Maumenee, Irene H.  
Mazow, Malcolm L.  
McCulley, James P.  
McMeel, J. Wallace  
Meredith, Travis A.  
Merriam, John C.  
Mets, Marilyn B.  
Metz, Henry S.  
Meyer, Roger F.  
Meyers, Sanford M.  
Mieler, William F.  
Miller, Marilyn T.  
Mills, Richard P.  
Minckler, Donald S.  
Mindel, Joel S.  
Mitchell, Paul R.  
Nelson, J. Daniel  
Nirankari, Verinder S.  
Nork, T. Michael  
O'Day, Denis M.  
O'Neill John F.  
Parrish II, Richard K.  
Parver, Leonard M.  
Payne, John W.  
Podos, Steven M.  
Pollack, Irvin P.  
Pollard, Zane F.  
Pulido, Jose S.  
Raab, Edward L.  
Rao, Narsing A.  
Rich, Larry F.  
Ritch, Robert  
Robertson, Dennis M.  
Robin, Alan L.

*Members*

Rubin, Melvin L.  
Runge, Paul E.  
Ryan Jr., Stephen J.  
Sadun, Alfredo A.  
Schanzlin, David J.  
Schein, Oliver D.  
Schocket, Stanley S.  
Schwab, Ivan R.  
Scott, Alan B.  
Sergott, Robert C.  
Shields, Jerry A.  
Shields, M. Bruce  
Shields, Carol L.  
Sieving, Paul A.  
Small, Kent W.  
Smith, Ronald E.  
Smolin, Gilbert  
Sommer, Alfred  
Spaeth, George L.  
Srinivasan, B. Dobl  
Stager Sr., David R.  
Stamper, Robert L.  
Stark, Walter J.  
Steinert, Roger F.  
Stern, George A.  
Sugar, Alan  
Summers, C. Gail  
Tasman, William S.  
Taylor, Hugh R.  
Tornambe, Paul E.  
Townsend, William M.  
Tso, Mark O. M.  
Van Buskirk, E. Michael  
Van Meter, Woodford S.  
Van Newkirk, Mylan R.  
Vine, Andrew K.  
Waltman, Stephen R.  
Walton, David S.  
Waring III, George O.  
Weakley Jr., David R.  
Weinreb, Robert N.  
Welch, Robert B.  
Wilensky, Jacob T.  
Wilhelmus, Kirk R.  
Wilkinson, Charles P.  
Wilson II, Fred M.  
Wirtschafter, Jonathan D.  
Wood, Thomas O.  
Wright, Kenneth W.  
Yannuzzi, Lawrence A.  
Yanoff, Myron  
Yee, Robert D.  
Younge, Brian R.

EMERITUS MEMBERS 2002

Acers, Thomas E.  
Alper, Melvin G.  
Annesley Jr., William H.  
Armaly, Mansour F.  
Apt, Leonard  
Asbury, Taylor  
Baum, Jules L.  
Beard, Crowell  
Becker, Bernard  
Benedict, Walter H.  
Bennett, James E.  
Breinin, Goodwin M.  
Brockhurst, Robert J.  
Bronson II, Nathaniel R.  
Brubaker, Richard F.  
Burde, Ronald M.  
Burton, Thomas C.  
Campbell, Charles J.  
Campbell, Francis P.  
Carr, Ronald E.  
Carroll, Frank D.  
Chamberlain, Webb  
Cooper, William C.  
Cox Jr., Morton S.  
Curtin, Brian J.  
Darrell, Richard W.  
Davis, Matthew D.  
Day, Robert M.  
Day, Robert  
Dayton Jr., Glenn O.  
DeVoe, A. Gerard  
Dellaporta, Angelos  
Duke, James R.  
Dunlap, Edward A.  
Durham, Davis G.  
Dyer, John A.  
Elliott, James H.  
Ellis, Philip P.  
Everett, William G.  
Falls, Harold F.  
Fink, Austin I.  
Frayner, William C.  
Gass, J. Donald M.  
Glew, William B.  
Grayson, Merrill  
Guerry III, Dupont  
Hagler, William S.  
Hamilton, Ralph S.  
Harley, Robison D.

Hedges Jr., Thomas R.  
Henderson, John Warren  
Henderson, John Woodworth  
Hiatt, Roger L.  
Hilton, George F.  
Hollenhorst Sr., Robert W.  
Howard, Rufus O.  
Hyndiuk, Robert A.  
Irvine, Alexander R.  
Jarrett II, William H.  
Jones, Ira S.  
Kearns, Thomas P.  
Kennedy, Robert E.  
Knobloch, William H.  
Lawwill, Theodore  
Levene, Ralph Z.  
Little, Hunter L.  
Lloyd, Lois A.  
Locke, John C.  
Macdonald Jr., Roderick  
Manchester Jr., P. Thomas  
Marshall, Don  
McCulloch, Clement  
McDonald, James E.  
Merriam Jr., George R.  
Miranda Jr., Manuel N.  
O'Connor, G. Richard  
O'Rourke, James  
Okun, Edward  
Owens, William C.  
Parks, Marshall M.  
Patz, Arnall  
Pfeiffer, Raymond L.  
Pico Sr., Guillermo  
Regan, Ellen F.  
Richards, Richard D.  
Robb, Richard M.  
Schultz, Richard O.  
Schwartz, Ariaiah  
Sears, Marvin L.  
Shaffer, Robert N.  
Sherman, Arthur E.  
Small, Robert G.  
Snell, Albert C.  
Spalter, Harold F.  
Spaulding, Abbot G.  
Spencer, William H.  
Spivey, Bruce E.  
Straatsma, Bradley R.  
Streeten, Barbara W.  
Swan, Kenneth C.  
Taylor, Daniel M.  
Thompson, H. Stanley

*Members*

HONORARY MEMBERS

Thygeson, Phillips	
Troutman, Richard C.	
Truhlsen, Stanley M.	Zimmerman, Lorenz E.
Veronneau-Troutman, Suzanne	
von Noorden, Gunter K.	Members (includes Associates)
Waller, Robert R.	213
Watzke, Robert C.	
Weinstein, George W.	Emeritus Members
Wetzig, Paul C.	114
Wilson Sr., Fred M.	
Wilson, R. Sloan	Honorary Members
Wolff, Stewart M.	1
Wolter, J. Reimer	
Wong, Vernon G.	Total Membership
	328

## CONTRIBUTORS

DANIEL M. ALBERT MD, MS  
UNDRAA ALTANGEREL MD  
DOUGLAS R. ANDERSON MD  
W. BANKS, JR. ANDERSON MD  
RAFAEL ANDRADE MD  
ISABELLE AUDO MD  
JAMES J. AUGSBURGER MD  
AMR AZAB MD  
GEORGE B. BARTLEY MD  
JULES L. BAUM MD  
ATILLA BAYER MD  
RUBENS, JR. BELFORT MD, PhD  
ADRIANA BEREZOVSKY PhD  
ALBERT W. BIGLAN MD  
NORMAN P. BLAIR MD  
THOMAS N. BLANKENSHIP PHD  
JAMES C. BOBROW MD  
CHRISTOPHER BOWD PHD  
GEORGE J. BREWER MD  
NEDIM C. BUYUKMIHCI VMD  
LOUIS B. CANTOR MD  
VALERIO CARELLI MD, PhD  
BRIAN M. CHANG MD  
ANUWAT CHITCHARUS MD  
SOPHIA M. CHUNG MD  
ZÉLIA M. CORRÊA MD  
DAVID A. COVERT MBA  
J. BROOKS CRAWFORD MD  
SOESIWAITI R. DARJATMOKO MS  
DANIEL G. DAWSON MD  
ANNA-MARIA DENEGRI MD  
HAROLD DICKSON PHD  
DILEK DURSUN MD  
RALPH C., JR EAGLE MD  
KATHLEEN M. EGAN ScD  
HORMOZ EHYA MD  
J. TERRY ERNEST MD, PhD  
ANDREW S. FEINBERG MD  
STEPHEN S. FEMAN MD  
WILLIAM J. FEUER MS  
PAUL G. FITZGERALD PHD  
ALAN J. FLACH MD  
JOSEPH C. FLANAGAN MD  
JOHN T. FLYNN MD  
RICHARD K. FORSTER MD  
ALAN H. FRIEDMAN MD  
JARED C. FRISBIE  
BARTLEY R. FRUEH MD  
JOEL GLEISER MD  
JOHN D. GOTTSCH MD  
EVANGELOS S. GRAGOUDAS MD  
HANS E. GROSSNIKLAUS MD  
FRONCIE A. GUTMAN MD  
JULIA A. HALLER MD  
MICHAEL T. HALPERN MD, PhD  
DANIELLE HAMILTON  
DAVID R. HARDTEN MD  
SEENU M. HARIPRASAD MD  
JEFFERY D. HENDERER MD  
JEANNINE T. HOLDEN MD  
EDWARD J. HOLLAND MD  
ERIC R. HOLZ MD  
DAN B. JONES MD  
L. JAY KATZ MD  
JAMES S. KELLEY MD  
S. E. KELMAN  
MUGE KESEN MD  
VINOD LAKHANPAL MD  
R. R. LAKHANPAL MD  
MAURICE B., III LANDERS MD  
ANNE-MARIE LANE MPH  
ROBERT LAVKER PHD  
WENJUN LI MS  
PAUL R. LICHTER MD  
JEFFERY M. LIEBMANN MD  
RICHARD L. LINDSTROM MD  
MARY J. LINDSTROM PHD  
CONNIE LIU  
JANICE M. LOKKEN  
IRENE H. LUDWIG MD  
LINDA K. McLOON PHD  
JOHN C. MERRIAM MD  
JOANNA MERRIAM MD, PhD  
MARLENE M. MESSENGER  
WILLIAM F. MIELER MD  
JOHN E. MUNZENRIDER MD  
JONATHAN S. MYERS MD  
JOHN C. NICHOLS MD  
VERINDER NIRANKARI MD  
VICKIE A. NIX  
JOSE S. PULIDO MD, MS  
PETER A. QUIROS MD  
PAMELA RAYMOND PHD  
DOUGLAS RHEE MD  
ROBERT RITCH MD  
ALAN L. ROBIN MD  
TONI ROBINSON-SMITH MD  
ALFREDO A. SADUN MD, PhD  
FEDERICO SADUN MD  
SOLANGE R. SALOMAO PHD  
DONALD SANDERS MD, PhD  
STAN SCHEIN MD, PhD  
SUSAN SCHNEIDER MD  
STANLEY S. SCHOCKET MD  
IVAN R. SCHWAB MD, FACS  
NARIMAN SHARARA MD

M. BRUCE SHIELDS MD  
PAUL A. SIEVING MD, PhD  
GEORGE L. SPAETH MD  
ROBERT L. STAMPER MD  
WALTER J. STARK MD  
WILLIAM C. STEINMANN MD  
STEPHEN A. STRUGNELL PhD  
WILLIAM S. TASMAN MD, FACS  
TODD A. THEOBALD MD  
ROBERT W. THOMSEN MD  
NIKOLAOS TRICHOPOULOS MD  
RICHARD C. TROUTMAN MD  
WOODFORD S. VAN METER MD

ANDREW K. VINE MD  
GEORGE O. III WARING MD  
ROBERT N. WEINREB MD  
JONATHAN D. WIRTSCHAFTER MD  
TED H. WONJO MD  
THOMAS O. WOOD MD  
RAWIA S. YASSIN MD  
BRIAN R. YOUNGE MD  
CARLTON K. YUEN MD  
MARCO ZAIDER PhD  
LINDA M. ZANGWILL PhD  
LEI ZHENG MD  
MICHELE L. ZIMBRIC

## **NECROLOGY**

## In Memorium

DR THOMAS H. COWAN, ELECTED 1959  
DR GEORGE S. ELLIS, SR., ELECTED 1968  
DR MORTON W. GRANT, ELECTED 1956  
DR WILLIAM F. HUGHES, ELECTED 1952  
DR DAVID L. KROHN, ELECTED 1978  
DR JOHN W. MCTIGUE, ELECTED 1967  
DR ALBERT E. SLOANE, ELECTED 1950  
DR DANIEL SNYDACKER, ELECTED 1956

*Necrology*

THOMAS H. COWAN, MD

BY *George L. Spaeth, MD*



Dr Thomas Cowan died quietly at the age of 92. Dr Cowan was a long-time Philadelphian, getting his education at the most competitive public high school in the city, Central High School. He then went on to college at the University of Pennsylvania, where he received his B.A. and then continued with medical school, also at the University of Pennsylvania. Tom, as he was universally known, was affiliated with Philadelphia General Hospital, Wills Eye Hospital, and Thomas Jefferson University Medical Center. His particular interests were in the area of optics and refraction, mirroring the interests of his father, also an ophthalmologist, who wrote one of the most important texts on optics.

One of Tom's most defining characteristics was his gentleness. He always seemed to be quietly happy, with a

kind word for all. Tom loved the arts and was frequently seen at the theatre or the Philadelphia Orchestra concerts. Like his father, he was interested in antiques, he enjoyed making furniture, and was a superb craftsman. He also enjoyed playing tennis, and he continued to play tennis well into his 80s, including those times he was attending the American Ophthalmological Society meetings.

After the death of his first wife, Tom married Florence, with whom he happily spent his last 20 years. He is survived by his widow, his son Richard Cowan, his daughter Jane Hansen, and two granddaughters.

Tom will be remembered as a gentle ophthalmologist who loved his family, his community of Malvern, and the arts.



GEORGE S. ELLIS, SR., MD

BY *Barrett G. Haik, MD*



Dr George S. Ellis, Sr. died in his home in New Orleans on September 12, 2001. He was 78.

During his more than 40-year career, Dr Ellis served thousands of patients, participated in the education of more than a thousand medical students and a hundred ophthalmology residents, and he was actively involved in community, state, and national ophthalmology and medical organizations.

Born in Almonsif, Lebanon on May 30, 1923, George Ellis was raised in Port Gibson, Mississippi, and Marshall, Texas. He graduated from Marshall High School, completed his undergraduate education at the University of Texas at Austin and received his medical degree from Tulane University School of Medicine in New Orleans, interning at Charity Hospital there. He completed a residency in dermatology while in the Navy Medical Corps during World War II, practiced General Medicine in Marshall, Texas, completed a residency in ophthalmology at Charity Hospital in New Orleans, and pursued a fellowship in disorders of the eye muscles at Louisiana State University and later at the University of Iowa under the guidance of Hermann M.

Burian.

Marshall, Texas honored Dr Ellis's early service in general practice and continued service to the community with the inscription of his name on their Distinguished Citizens Wall.

Dr Ellis served as associate supervising ophthalmologist for Louisiana's Department of Public Welfare and as a clinical professor in LSU's Department of Ophthalmology and then at Tulane. He was in partnership with his brother-in-law and former chairman, George M. Haik, Sr., in private practice for more than four decades. He held appointments at the Hotel Dieu Hospital, where he was president of the medical staff one year, Mercy-Baptist Hospital, the Eye, Ear, Nose, and Throat Hospital, East Jefferson General Hospital, Children's Hospital, and DePaul Hospital.

Dr Ellis taught pediatric ophthalmology and strabismus to residents and to his peers. He was a natural teacher, excellent mentor, and, as a thoughtful listener, a constant resource for students and colleagues.

Dr Ellis's thesis for the American Ophthalmological Society, "Akinesia of the Facial Nerve: Laboratory

## *Necrology*

Investigation of the Surgical Anatomy," (Transactions of the American Ophthalmological Society 66: 746-787, 1968), contributed greatly to the understanding of seventh nerve anesthesia.

Ellis was the first Ophthalmologist elected as president of the Orleans Parish Medical Society, was active on their governing board and in other positions, and was recognized with their Outstanding Physician Award. He was president of the New Orleans Academy of Ophthalmology, which dedicated its 51st annual symposium to him, and of the Southern Eye Bank, which honored him by establishing the Dr George S. Ellis, Sr. Distinguished Service Award. He served on the board of the Southern Eye Bank, held most major offices in the Southern Medical Association, was vice president of the Eye Foundation of America, and was a member of the legislative committee of the Louisiana State Medical Society.

He was a member of the medical advisory committee for the mayor of New Orleans, volunteered his time and

expertise to numerous educational and clinical care institutions throughout Louisiana, and served as a member of the Chamber of Commerce of New Orleans, the International House, and the Rotary Club.

Preceded in death by his wife, Lorraine Haik Ellis, DrEllis is survived by two sons, Dr Robert G. Ellis, a psychiatrist, Dr George S. Ellis, Jr., an ophthalmologist, a daughter, Joan Ellis Green, seven grandchildren, a brother, Dr Michael Ellis, and a sister, Georgette Ellis.

George S. Ellis, Sr. will be remembered for his unfailing cheerfulness, humor, positive outlook, intelligence, high ethical standards, sense of duty to family, friends, patients, and colleagues, and compassionate and gentle demeanor. Dr Ellis's great love of medicine and ophthalmology and that of his partner and brother-in-law, George Haik, Sr., will live on through the lives of their more than 40 relatives who were influenced by these two men to become physicians, more than half of whom became ophthalmologists.

W. MORTON GRANT, MD

BY *M. Bruce Shields\**



Ophthalmology has lost one of its gentle giants. Dr W. Morton Grant was a world leader of the twentieth century in his chosen field of glaucoma, and yet his life was one of quietness and humility. He died on November 17, 2001, but the lessons he taught of scientific rigor and a gentle way of life will live on in those who strive to emulate his standards.

It is hard to think of Dr Grant without including his longtime friend and colleague, the late Paul A. Chandler. Together, Drs Chandler and Grant literally rewrote much of our current understanding of glaucoma. They were the perfect combination of the clinician and the scientist. While Dr Chandler was advancing new concepts in the management of the glaucomas, Dr Grant, as the David G. Cogan Professor of Ophthalmology at Harvard University Medical School and Director of the Glaucoma Consultation Service and Howe Laboratory of Ophthalmology at the Massachusetts Eye and Ear Infirmary, was revolutionizing our understanding of aqueous humor dynamics and mechanisms of the glaucomas.

When Dr Grant began his study of glaucoma in the

1940s, we did not know whether elevated intraocular pressure in the various types of glaucoma was due to decreased aqueous outflow or increased aqueous production. It was his introduction of the modern concept of tonography in 1950 and his careful application of that technology that led to the recognition that, in virtually all forms of glaucoma, the mechanism of increased pressure is obstruction of aqueous outflow. He was also a pioneer in perfusion studies of the anterior ocular segment. With his perfusion apparatus in the Howe Lab, Dr Grant and his students and associates clarified over the years much of our current knowledge regarding the physiology of aqueous outflow and the mechanisms that lead to outflow obstruction in many of the glaucomas.

It is hard to say whether Dr Grant's greatest contributions were his scientific observations or his devotion to teaching, which was also exemplary. He will be remembered for his classic Lectures on Glaucoma with Dr Chandler, which have been faithfully carried on by Dr David Epstein as *Chandler and Grant's Glaucoma*. Even in the first edition, much of the information is as relevant

## Necrology

today as when it was published in 1965, because it focuses on well-established, fundamental concepts, rather than on theories and statistics.

Not only in his writings did Dr Grant excel as a teacher, but also in the one-on-one mentoring of his fellows, residents, and students. He was never too busy to come down from his office (always using the stairs) to see a problem patient with us and to impart his invaluable knowledge in his quiet, humble way. And those of us who were fortunate enough to experience it will never forget the Wednesday morning conferences, when we would meet in Dr Grant's office with Dr Chandler and young, rising stars like Drs Richard Simmons, Thomas Hutchinson, and Robert Bellows, to talk about glaucoma. For me, that was the pinnacle of my educational experience.

Dr Grant's contributions to ophthalmology were not

limited to glaucoma. As is well known, he also had a keen interest in substances that have toxic properties injurious to the eyes. His *Toxicology of the Eye*, with which he was ably assisted by Dr Joel Schuman in later editions, will remain the classic text on this subject for many years to come.

Dr Grant is survived by his wife, Jeanette, two sons, David and Jeffrey, a daughter, Jeanne, and four grandchildren. He also leaves behind a family of devoted students who gather each year at the annual Academy meeting, as the Chandler-Grant Society, to remember the two men who set the standard that we try to follow in our careers and in our lives.

\*Reprinted, with permission, from the *Am J Ophthalmol* 2002; 133: 735.

WILLIAM F. HUGHES, MD

BY *James E. McDonald, MD*



Bill Hughes was born in Indianapolis, Indiana. His father was an ophthalmologist and Chairman of the Eye Department at the University of Indiana. He graduated from Amherst College (1934) and then Johns Hopkins Medical School (1938). He was an Ophthalmology Resident at the Wilmer Institute (1938-44) and stayed on as a young faculty member for two years. In his time at Wilmer, Dr Hughes was a very productive researcher, turning out more than 50 scientific articles on various subjects, particularly on beta radiation, corneal surgery, retinal detachment, and corneal transplantation.

After returning to Indianapolis, he entered private practice and worked at the University of Indiana for another two years. In 1947, he moved to the Chicago area, where he accepted a position as Chairman of the Eye Department at the University of Illinois and became Chief Ophthalmologist at the Illinois Eye and Ear Infirmary. The Infirmary had been founded in 1867 and was taken over by the State of Illinois in 1871 and renamed the Illinois Charitable Eye and Ear Infirmary. It served a very large indigent population with serious eye problems. There were

24 eye residents (8 per year), and about 50 volunteer attending ophthalmologists, as well as a few part-time ophthalmologists. At the infirmary, Dr Hughes organized a more efficient delivery of eye care and added faculty that raised the level of education and service. He instilled a spirit of camaraderie among the faculty, staff, and residents, and was held in high esteem by his fellow workers. He and his wife Nema were gracious hosts, entertaining residents and faculty in their home.

After directing education and patient care and encouraging research for 11 years, Dr Hughes resigned from the University of Illinois Eye and Ear Infirmary and moved his hospital and professional activities to Rush Presbyterian St. Luke Medical Center. There he had more time to personally deliver first-class eye care without as large an administrative load. He was made head of the Eye Department and Professor of Ophthalmology at Rush Medical College. Dr Hughes became Professor Emeritus in July of 1982.

Dr Hughes was associated with many of the important eye societies and boards in the country. He was a Trustee of the American Board of Ophthalmology (1967-1975), Editor

### *Necrology*

of the Yearbook of Ophthalmology (1959), Editorial Board member of the Archives of Ophthalmology (1951-62), and President of the Chicago Ophthalmological Society (1952). He held many more positions that helped keep up the standards of American ophthalmology.

He was not enamored by administration. On one occasion he told me that he used to be a good researcher at Wilmer, but now all he was doing was hiring and firing people.

Bill Hughes loved to paint (mostly with watercolors), and sometimes he would send a postcard with an original work of art (usually landscapes). He also enjoyed organ playing, tennis, and golf. He married Wanema Dickey ("Nema") in 1941, and they had three children: Frank W., Jacqueline A., and Sarah L. His wife, Nema, died in 1969, and Bill later married Jane Stockdale.

DAVID L. KROHN, MD

BY *Robert Ritch*, MD, *Ronald E. Carr*, MD



David Krohn was born September 26, 1924, in East Orange, New Jersey, and died February 20th, 2002, in New York City. He received his BA from Columbia College in 1946 and his MD from New York University College of Medicine in 1948, where he was a member of Alpha Omega Alpha. After an internship at Mount Sinai Hospital from 1948 to 1949, he was a resident in Internal Medicine at Goldwater Memorial Hospital from 1949 to 1950 and then a resident in Ophthalmology from 1950 to 1952 at Mount Sinai Hospital. He spent a year as a Captain at the USAF Hospital in Wiesbaden, West Germany, on the Ophthalmology Service. He underwent an Assistantship at the Universitäts Augenklinik in Zurich from 1954 to 1955 and became certified by the American Board of Ophthalmology that same year.

From 1957-1968 he was clinical instructor at New York University Medical Center, Department of Ophthalmology, Clinical Assistant Professor from 1968-1972, Clinical Associate Professor from 1972-1973, Associate Professor, Clinical Ophthalmology from 1974-1976, and Professor of Clinical Ophthalmology from 1976 until his death. From 1974-1999, he was director of the Glaucoma Division.

David became a member of the AOS in 1978, with his thesis entitled “Flux of Topical Pilocarpine to the Human Aqueous.” He truly cherished his membership in the Society and it was only his recent illnesses that pushed him to accept emeritus status and a less active role.

David was past President of the New York Society for Clinical Ophthalmology, the Ophthalmic Laser Surgical Society, and the New York Glaucoma Society. He was the recipient of four major research awards, two as Principal Investigator for National Eye Institute grants and two from the National Cancer Institute. He was an author on over 30 publications.

David was an avid sportsman, enjoying and excelling at tennis, skiing, and sailing. It was the game of tennis that most excited him, and while he could readily beat most of us, his unfailing graciousness and his encouragement to those of us not so adept made such an outing a pleasure.

He was a pilot with a private plane for more than 20 years and would readily fly from Westchester to Cape Cod for lunch and a swim.

He was an accomplished pianist and his interest in

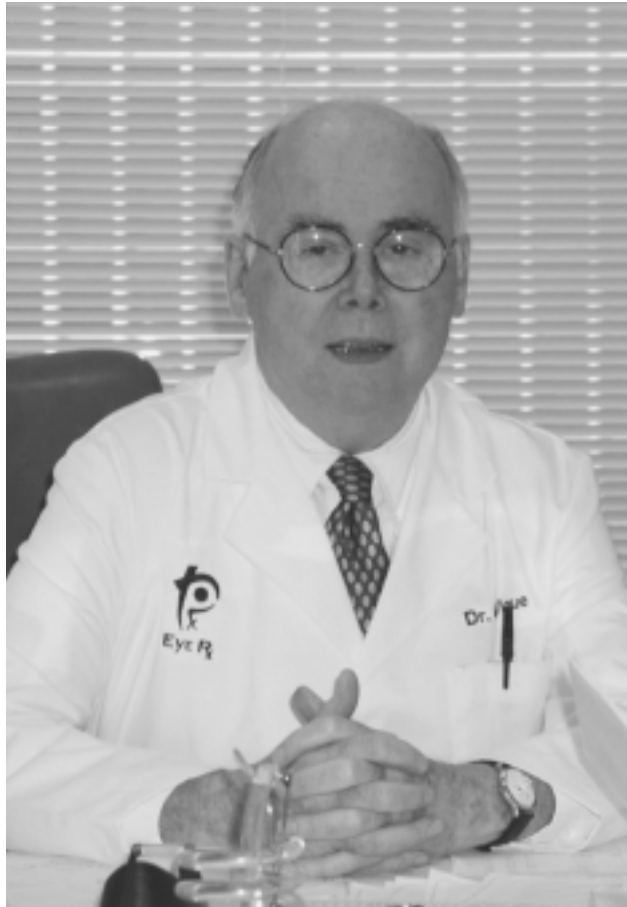
### *Necrology*

music extended to strong support of several of the excellent smaller musical societies in the New York area.

David was a courtly person, a reminder in many ways of what is often lacking today—a gentleman without being obsequious and, for the residents, a teacher who encouraged but did not cajole.

He is survived by his wife, Barbara, a ceramist, and for many years an active participant in the AOS tennis tournaments, as well as his daughters Deborah and Lisa, two grand-daughters, Livia and Martine, and his sister, Judy Lipton.

**JOHN W. MCTIGUE, MD**  
BY *William Glew, MD*



John William McTigue, the son of George and Marguerite Kenny McTigue, was born November 16, 1925 in Logan, West Virginia and died of heart disease at St. Luke's Hospital in Bethlehem, Pennsylvania at the age of seventy-six. He practiced ophthalmology in Washington, D.C from 1958 until shortly before his death on January 1, 2002.

Memorial Services and receptions were held at Trinity Episcopal Church in Bethlehem, where his son-in-law is rector, at Ascension and St. Agnes Episcopal Church in Washington, and at the Washington National Cathedral where the interment service took place on May 28th. Additional services and receptions were held at the "Kirking of the Tartans" in Montreat, North Carolina.

Dr McTigue earned his B.S. degree at the University of Virginia in 1946 and his M.D. at the University of Pennsylvania in 1950. After interning at the University of Pennsylvania Hospital and serving in the Navy, he completed his ophthalmology residency at Columbia Presbyterian Hospital in New York. He was appointed an Assistant in ophthalmology at the Institute of Ophthalmology at Columbia in 1957 and came to Washington in 1958 to begin

his practice of ophthalmology.

He immediately became active on the large teaching staff at the Washington Hospital Center and as an Instructor and Assistant Professor at the George Washington University School of Medicine. His interest in corneal diseases led to his publications on controlled freezing of corneal tissue, lyophilization of vitreous, posterior lamellar keratectomy, and many aspects of contact lenses. He co-authored with John Henry King a volume entitled "The Cornea" in 1965 based on the first World Congress on the Cornea held in Washington D.C. He served as Associate Medical Director of the International Eye Bank and was a founder at the National Lion's Eye Bank. He was named Lions Club International Humanitarian of the Year in 1987.

He was appointed Professor of Ophthalmology at George Washington in 1967 and later was Chair of the Department at Doctors Hospital. His AOS thesis "A Light and Electron Microscopic Study of the Normal Cornea and its Alteration in Various Dystrophies" was published in the 1967 *TRANSACTIONS*.

He became a member of the Cosmos Club and a

### *Necrology*

Knight of the Order of St. John of Jerusalem. He was founder of the National Eye Foundation and served as President or Chairman of many organizations including The Section of Ophthalmology of the D.C. Medical Society, The Eye Bank Association of America, The Prevention of Blindness Society, The National Cathedral Association, and the Board of Trustees of the National Cathedral School for Girls. His practice grew to include a busy surgical schedule and he served as a consultant to the White House and the State Department on many occasions.

His wife, Georgene Davis McTigue, died in 1994. Survivors include four children: Bruce D. McTigue of Pacifica, California, John W. McTigue of Houston, Texas, Amanda McTigue of Petaluma, California, Karen McTigue Kinsely of Bethlehem, Pennsylvania, and one granddaughter.

Jack was an excellent surgeon, an innovative researcher, and a lively, personable colleague at department meetings, social events, and the many AOS meetings that he attended over the past 34 years.

ALBERT E. SLOANE, MD  
BY *Eliot L. Berson, MD*



Dr Albert E. Sloane, compassionate physician and devoted teacher, died on October 24, 2001 in the Beth Israel-Deaconess Medical Center, Boston, at age 94. He was Senior Consulting Surgeon at the Massachusetts Eye and Ear Infirmary and Assistant Clinical Professor of Ophthalmology at Harvard Medical School.

Dr Sloane was born in Boston and graduated from the Massachusetts College of Optometry in 1927 and from Tufts University School of Medicine in 1933. He did his internship and residency at Boston City Hospital and Mount Auburn Hospital and was certified by the American Board of Ophthalmology in 1938. He became a member of the staff of the Massachusetts Eye and Ear Infirmary in 1936 and established the first Low Vision Clinic at that institution in 1951. He developed several eye tests including the Massachusetts Vision Test used to screen the vision of school children.

Dr Sloane taught in the Harvard Post-graduate Course in Ophthalmology, in the House Officer's Teaching Program at the Massachusetts Eye and Ear Infirmary, in the Instruction Program of the American

Academy of Ophthalmology and Otolaryngology, and in the Lancaster Course in Ophthalmology. His publications include more than fifty papers as well as a textbook entitled "Manual of Refraction." The Sloane Teaching Room is named in his honor at the Massachusetts Eye and Ear Infirmary.

Dr Sloane was a member of the American Academy of Ophthalmology and the Massachusetts Medical Society. He became a member of the American Ophthalmological Society in 1950. He was President of the New England Ophthalmological Society in 1965. He served on the advisory boards of the Massachusetts Division for the Blind and the National Society to Prevent Blindness. He was President of the American Physician Fellowship of the Israeli Ophthalmological Society and founded and supported the Low Vision Eye Clinic of Hadassah University Hospital in Jerusalem. He also supported the upgrading of the electroretinographic testing system at Hadassah that is in current use. He was a Lifetime Trustee of the Hebrew Rehabilitation Center for the Aged and, in 1999, the Albert E. Sloane Eye Clinic

### *Necrology*

was established in his honor at this Center on the Main Campus in Roslindale, Massachusetts.

His interests were quite diverse. He was an avid gardener, a skilled flutist, and an expert New York Times crossword puzzle solver. He was an accomplished needle pointer and won first prize for a petit point display of the retina at the Massachusetts Eye and Ear Infirmary in 1992.

Al was humble about his accomplishments. He will be

remembered as a man of quiet dignity with a high sensitivity for the feelings of others and a willingness to listen to others. His care of patients and his devotion to teaching were reflections of these personal attributes.

He leaves behind his wife of 70 years, Sarah "Solly" E. (Locke), two brothers, Nathan Sloane and Dr Arnold Sloane, two children, Barry and Judith, seven grandchildren, and twelve great grandchildren. He will be missed.

**DANIEL SNYDACKER, MD**

BY *James E. McDonald, MD*



Dan Snyder was born in Kenilworth, Illinois, a northern suburb of Chicago, in May of 1910. He was the son of ophthalmologist Emanuel Snyder and his wife, Ruth. He went to the University of Wisconsin as an undergraduate and to Northwestern Medical School, graduating in 1935. After an internship at Michael Reese Hospital, Dan took his eye residency at the Illinois Eye and Ear Infirmary. After a period of postgraduate work in Vienna he returned to Chicago and entered private practice with Dr Harry Gradle. He joined the Infirmary teaching staff in 1937. He later served in the Army, mostly in the Pacific Theater, from 1942 to 1946. When the war ended, he returned to his practice and resumed his professorial services at the Infirmary and Michael Reese Hospital.

Dan was on the attending staff of the Infirmary and on the faculty of the University of Illinois (now associated with the Infirmary) when I started my Ophthalmology residency in 1948. He was a dedicated, bright, and enthusiastic teacher and all of the 20 or so eye residents looked up to him for guidance in the operating room and clinics. His superb volunteer activities at the Infirmary continued for a total of

22 years, to the benefit of patients and eye residents alike. In the late fifties, Dan also donated his expertise to the University of Chicago as a Professorial Lecturer and Supervisor of Clinical Conferences. He continued this work until he retired from Ophthalmology in 1984. His contributions to the Ophthalmologic literature were impressive. He, along with Dr Frank Newell, authored the American Academy of Ophthalmology's Refraction Manual, used by all eye residents in the country.

Dan was a leader in many other areas; for example, he was an active member of the American Ophthalmological Society, a member and President of the Chicago Ophthalmological Society, Secretary of the Home Study Course of the American Academy Of Ophthalmology, and Secretary of the of the Pan American Association of Ophthalmology. He was also active in the Institute of Medicine of Chicago and the American Association for the Advancement of Science. The Illinois Society for the Prevention of Blindness and the Chicago Lighthouse for the Blind profited from his membership on their Board of Directors. Besides being a Civilian Consultant to the Fifth

### *Necrology*

Army, he was Associate Editor of both the Archives of Ophthalmology from 1960 to 1962 and the Survey of Ophthalmology 1956 until his death.

After his retirement from Ophthalmology, he became interested in botany and became an authority on the tall grass prairies of Northern Illinois. He volunteered this knowledge to the Field Museum of Natural History in

Chicago for a period of 15 years. He was alert and active until the end.

Dan was a friendly, capable, and fair-minded leader with a good sense of humor who did not tolerate ignorance or laziness in those he supervised. He was my friend. His wife Betty, his children Harry, Ruth, and Dan Jr., and ten grandchildren survive him.

## MINUTES OF THE PROCEEDINGS



# MINUTES OF THE PROCEEDINGS

*One Hundred and Thirty-Eighth Annual Meeting  
May 19-22, 2002*

The ONE HUNDRED AND THIRTY-EIGHTH ANNUAL MEETING of the American Ophthalmological Society was held at The Cloister in Sea Island, Georgia on May 19-22, 2002. President Robert C. Drews called the opening session to order at 7:30 AM on Monday morning, May 20. The program began with the Verhoeff Lecture, with a symposium following on stem cell research. The Lecture and symposium were as follows:

Verhoeff Lecture: "How Many Photoreceptors Do We Need for Vision?," Paul A. Sieving, MD, PhD (Director, National Eye Institute)

Symposium: "Stem Cells: What Are They and How Might They Be Used for Ocular Disease Treatment?"

1. "Introduction to Epithelial Stem Cells: The Eye Shows the Way," Robert Lavker, PhD (by invitation)
2. "Clinical Aspects of Ocular Surface Stem Cell Transplantation," Edward Holland, MD
3. "Retinal Stem Cells? Current Status and Future Possibilities," Pamela Raymond, PhD (by invitation)

The meeting was continued with the following scientific program:

1. "Long-Term Risk of Local Failure After Proton Therapy for Choroidal/Ciliary Body Melanoma," by Evangelos S. Gragoudas, MD, Anne Marie Lane, MPH (by invitation), John E. Munzenrider, MD (by invitation), Kathleen M. Egan, ScD (by invitation), Wenjun Li, MS (by invitation)
2. "Suturing Technique for Control of Postkeratoplasty Astigmatism and Myopia," by Dilek Dursun, MD (by invitation), Richard K. Forster, MD\*, and William J. Feuer, MS (by invitation)

\*paper was presented by R.K. Forster

3. "The Dehiscent Hughes Flap: Outcomes and Implications," by George B. Bartley, MD and Marlene M. Messenger (by invitation)

## Executive Session, May 20

President Robert C. Drews called the Annual Executive Session of the American Ophthalmological Society to order at 11:30 AM. He appointed Dr John D. Bullock to be the parliamentarian.

A motion to approve the minutes of the 2001 Executive Session, which were published in Volume XCIX of the TRANSACTIONS OF THE AMERICAN OPHTHALMOLOGICAL SOCIETY, was made, seconded, and approved.

The following reports were submitted.

## Secretary-Treasurer Report

CHARLES P. WILKINSON, MD. The AOS remains financially healthy. You will recall that our Society consists of three corporate entities: the AOS proper, the AOS Charitable, Educational, and Scientific Fund (or "CES Fund"), and the Herman Knapp Testimonial Fund (or "Knapp Fund").

All funds have suffered small reductions in assets due to the decline in market values over the past two years, and expenses have increased to some extent. But fund balances are approximately the same as they were when Banks Anderson gave his final report at this meeting four years ago.

Our fiscal year now coincides with the calendar year, and, at the end of the past fiscal year, the balance in the



The 2002 Verhoeff Lecturer, Dr Paul Sieving, the Director of the National Eye Institute.



The 2002 Verhoeff Lecturer, Dr Paul A. Sieving (left), and Dr Paul Lichter, who was his chairman when Paul was at the University of Michigan.

AOS proper was approximately \$360,000; in the CES, approximately \$1.2 million; in the Knapp Fund, approximately \$4.4 million.

Therefore, Mr. President, I recommend that dues for the coming year be continued at \$200.

### **Editor's Report**

J. BROOKS CRAWFORD, MD. The TRANSACTIONS OF THE AMERICAN OPHTHALMOLOGICAL SOCIETY, Volume XCIX, was mailed in January, 2002. The TRANSACTIONS included the Minutes of the Proceedings of the Executive Session, 3 obituaries, 21 papers, and 5 theses.

The spontaneous, secondary discussions of each paper given at the Annual Meeting were edited more extensively than in the past. The reasons for this change are as follows: (1) it allows the editor to use his/her discretion and presumed wisdom to select and edit the appropriate discussions; (2) the spoken comment (discussion) does not always translate into a well-written comment; (3) the spontaneous discussions can be improved by good editing; (4) inappropriate and often rambling comments and repetition are unnecessary (everyone congratulates the author for a great paper); and (5) many people reiterate previous discussions (with or without adding their own insights) and these comments can be eliminated. If properly executed, this change should make the papers and discussions more scholarly. The result should be a more concise and up-to-date TRANSACTIONS.

Another change this year was the placement of the TRANSACTIONS on our Website, making it available at no charge to a much wider audience. I believe this enhances our Website and will increase our visibility to the medical and scientific communities.

For the first time we have produced a CD-ROM version of the TRANSACTIONS, which we are distributing without charge to all members who are attending this meeting. This is a trial version to see if a demand exists for this format. Improvements in the format can and will be made if it is successful.

The 2001 TRANSACTIONS and this report are my final contributions as your Editor. I have very much enjoyed the work and deeply appreciate the most helpful suggestions and the tremendous cooperation that the authors of papers and theses and all the members of this Society have extended to me. You made this job a pleasure for me.

[Following his report, Dr Crawford was given a round of much deserved applause as he completed his term as Editor of the TRANSACTIONS.]

### **Report of the Program Committee**

STEPHEN S. FEMAN, MD. The Program Committee consists of Stephen S. Feman, MD, Chair, Robert C. Drews, MD, President, and Charles P. Wilkinson, MD, Secretary-Treasurer.

This year, 33 abstracts were submitted for possible inclusion in the Annual Meeting. Each abstract was reviewed independently by the committee members and assigned a grade on a scale between 1.0 and 5.0. Although many superb abstracts were submitted, time constraints limited the number of papers that could be included. The final program consists of 21 presentations. The order of appearance is related to a combination of features that incorporates grades, the order in which the abstracts were received, and their specific audio-visual requirements.

Many abstracts that could not be fit into the program contained scientific information that warranted dissemination into the membership. Some could be presented well as posters and, for this reason, were developed further. This will be the American Ophthalmological Society's first poster session and the Program Committee would like the members' suggestions about continuing this in the future.

The Program Committee would like to thank the members and guests for the participation in the scientific program of the Annual Meeting. In addition, I want to extend my personal thanks to Drs. Drews and Wilkinson for their aid in organizing the scientific meeting and their help in inviting the primary discussants. Also, I would like to thank Lisa Brown, the AOS Meeting Manager, for her great efforts on our behalf.

### **Report of the Thesis Committee**

M. BRUCE SHIELDS, MD. The members of the Committee on Theses included Bronwyn Bateman, Joel Mindel, and myself. We reviewed 10 theses submitted by anonymous authors, and none of these was a revision. We recommended that 6 be accepted, 3 be revised, and that 1 be rejected.

[Acceptance of the Report of the Committee on Theses was moved, seconded, and approved.]

### **Report of the Photographer and Archivist**

RALPH C. EAGLE, JR., MD. There were 147 photographs taken at the 2001 meeting of the American Ophthalmological Society at the Homestead in Hot Springs, Virginia. Seven photos were printed in the 2001 volume of the TRANSACTIONS of the AOS. These included photos of President Paul Lichter and his wife

Carolyn, Howe Medalist Stanley Truhlsen and his wife Dottie, and group photographs of the Council and new members. The photos were taken with a Nikon N80 camera using 35mm color print film. Two sets of color prints were prepared and prints were distributed to all new members. In addition, all photos were commercially digitized on Kodak Photo CDs. Figures for the TRANSACTIONS were prepared from the digitized images and submitted in digital format. Digital prints also were prepared for editorial review. The Society's digital photo archives now comprise 1278 images from the 1996, 1997, 1998, 1999, 2000, and 2001 meetings. These images are suitable for publication in print or digital media.

### Report of the New Members' Committee

JULIA A. HALLER, MD and JOHN D. GOTTSCH, MD. The New Members' Committee is happy to report that we have a talented and distinguished group of new members this year.

The names of the new members are:

Dr Louis B. Cantor, Indianapolis, IN

Dr William V. Good, Kentfield, CA

Dr Mark S. Humayun, Los Angeles, CA

Dr Henry D. Jampel, Baltimore, MD

Dr Robert N. Weinreb, LaJolla, CA

All of the new members attended the annual meeting at The Cloisters, Sea Island, GA.

### Report of the Emeritus Committee

STANLEY M. TRUHLSEN, MD. The American Ophthalmological Society has an Emeritus membership of 111. I am sorry to report the deaths of eight of our members:

Name	Residence	Year Inducted
Dr Thomas H. Cowan	Malvern, PA	1959
Dr George S. Ellis, Sr.	New Orleans, LA	1968
Dr David L. Krohn	New York, NY	1978
Dr William F. Hughes	Chicago, IL	1952
Dr John W. McTigue	Washington, DC	1967
Dr W. Morton Grant	Winchester, MA	1956
Dr Albert E. Sloane	Chestnut Hill, MA	1950
Dr Daniel Snyder	Lake Forest, IL	1956

[The members present rose for a moment of silence in respect to those who have passed away this past year.]

In accordance with our constitution, any Active Member who has been a member for 25 years, is 70 years of age, or has completely retired from active practice or

gainful occupation may, upon written request, become an Emeritus Member, subject to the recommendation of the Council and an affirmative vote of three quarters of the members present at the Executive Session of an Annual Meeting. New applicants for emeritus membership this year who qualify are:

Dr Leonard Apt

Dr Jules L. Baum

Dr Ronald Burde

Dr William C. Cooper

Dr Richard M. Robb

Dr Marvin Sears

Dr Bruce E. Spivey

Dr Bradley R. Straatsma

Dr Robert R. Waller

The Emeritus Members and guests have a planned annual luncheon in the Solarium on Tuesday May 21st following the scientific session.

The Emeritus membership continues to grow. We invite them by newsletter to attend the annual meeting, see old friends, participate in the scientific sessions, and enjoy the other activities of this meeting.

### Report of the Representative to the National Association for Biomedical Research Committee

EDWARD A. JAEGER, MD. The AOS has been a member of the National Association for Biomedical Research (NABR) for many years. NABR is an association that tracks the activities of animal rights activists, as well as legislation associated with the use of animals in research. Many members of the AOS have been involved in therapeutic trials and investigative studies involving the use of animals. Our organization promotes the ethical care and responsible treatment of laboratory animals. Many landmark breakthroughs in the diagnosis and treatment of diseases have been achieved through the use of laboratory animals. While alternative in vitro methods have been developed, few in the scientific community would question the continuing need for the use of animals in evaluating cancer treatments, developing an AIDS vaccine, and researching many other diseases that result in significant human mortality and morbidity.

Over the past decade, a number of animal rights and ecology protection groups have become increasingly strident and aggressive in pursuit of their goals. While most Americans (and others as well) would not question the need for the humane treatment of animals and the preservation of our environment, the extreme end of these goals, for some, conflict with our need for wooden houses to live in, energy for materials production, and medical research to continue the assault on many deadly diseases.

Four semi-clandestine organizations spearhead the "anti" movements. These groups not only are against the

use of animals in any form for anything, but also are against any research that attempts to produce better foods, insect resistant trees, et cetera. These organizations include People for the Ethical Treatment of Animals (PETA), Earth Liberation Front (ELF), Animal Liberation Front (ALF), and Physicians' Committee for Responsible Medicine (PCRM). The latter group is relatively new on the scene. Only 5% of its members are physicians. It received the bulk of its funding (\$432,000) from The Foundation to Support Animal Protection, an organization headed by Ingrid Newkirk, who is also head of PETA. The FBI has labeled some of these groups as "left wing extremists" and "terrorist" organizations. Certainly their actions are compatible with an "end justifies the means" philosophy.

This year there have been both setbacks and gains in this ongoing struggle between these competing elements. The ELF claims credit for two fires in the Northwest. One destroyed a poplar tree farm that performed research on developing hybrid trees. The other severely damaged the University of Washington Center for Urban Horticulture. Idaho's new Agriculture Biotechnical Laboratory was damaged. Five banks in New York were vandalized because of their investment association with British based Huntingdon Life Sciences, a center for research.

The ELF developed a recruiting video, "Igniting the Revolution: An Introduction to the ELF," and developed a website that discusses how to burn buildings, including "tips for arsonists." A rare humorous event occurred in July as a PETA representative streaked naked in front of Buckingham Palace, his chest painted with "Go Vegan," moments before President Bush and Queen Elizabeth II sat down for lunch.

Six states have passed legislation stiffening and expanding the penalties for terrorist facility destruction. The FBI has increased its surveillance of these activities. Congress has become increasingly cognizant of the terrorist nature of these organizations and PETA's tax exempt status is being questioned.

The inclusion of mice, rats, and birds as "animals" under the Animal Protection Act was settled with the Department of Agriculture last year, but funding for implementation was withheld. Further action has been put on hold for another year and Senator Jesse Helms (R, NC) has introduced an amendment to the Farm Bill that would permanently exclude laboratory mice, rats, and birds from the Animal Protection Act. This has been passed by the Senate but awaits House consideration at the time of this report.

NABR is a very necessary organization. It tracks the activities of anti-research groups and actively supports legislation that would protect and benefit medical research. The dues are \$500 per year. It is worthy of our support and I recommend our continued membership.

## Report of the Representative to the Pan American Association of Ophthalmology

SUZANNE VÉRONNEAU-TROUTMAN, MD. The XXIII biannual meeting of the Pan American Association of Ophthalmology took place in Buenos Aires, Argentina, from July 21-25, 2001, with Dr Gustavo Piantoni of Buenos Aires as Congress President. 3,019 ophthalmologists attended.

The economic difficulties that Argentina was facing had not yet reached their zenith by last July and Buenos Aires still had its air of a European Grand Dame, making it an outstanding venue for this meeting and further enhancing the excellent scientific and enjoyable social programs realized by the organizing committees.

There was an expanded scientific program. The number of program PAAO participants increased from the 732 at the 1999 Joint Meeting in Orlando to 1,255 in Buenos Aires in 2001. Many also contributed to the pre meeting events.

Event type	1999	2001
Symposia	21	18
Instructional Courses	124	252
Free Papers	116	281
Posters	Data unavailable	243
Videos	8	54
Scientific Photos	0	112

The traditional PAAO lectures and awards were featured events during the meeting.

- Francisco Contreras, MD gave the prestigious Gradle Lecture, "*Latin American Ophthalmology: Challenges and Options.*"
- The Pan-American Lecture, "*Advances in the Diagnosis and Treatment of Age-Related Macular Degeneration,*" another tradition of the Pan-American Association, was given by Juan Verdaguier Taradella, MD of Santiago, Chile.
- Hilel Lewis, MD, USA, gave the AJO Lecture, another perennial of the society, on "*Macular Translocation with Outpouching of the Retinal Pigment Epithelium, Choroid and Sclera Using Clips: Experimental and Clinical Studies.*"
- At every Pan-American Congress, the host national society sponsors their traditional lecture. In Buenos Aires, the Argentine Council of Ophthalmology Lecture, "*Evolution of Operated Infantile Esotropias: Late Hypercorrection,*" was given by Alberto Ciancia, MD.
- Academia Ophthalmologica Internationalis met conjointly with the XXIII Pan-American Congress and sponsored a lecture by Joaquín Barraquer, MD of Barcelona, Spain: "*Management of Allograft Rejection in Large Penetrating Keratoplasties (11-14 mm in*

diameter). *Presentation of Exceptional Cases.*"

- Enrique S. Malbrán, MD, of Buenos Aires, Argentina received the Edward A. Maumenee Medal for Distinguished Service.
- Alice R. McPherson, MD, of Houston, Texas was honored with the Benjamin F. Boyd Humanitarian Award
- Carlos Moreira Sr., MD, from Curitiba, Brazil, received the Gradle Medal for Good Teaching.

Three prizes, established primarily to encourage young ophthalmologists from the Americas to pursue academic and humanitarian interests, were awarded.

- Established in 1993, and the longest running prize in this category awarded at Pan-American Congresses, the fifth biannual \$10,000 Troutman-Véronneau Prize, funded by the Microsurgical Research Foundation, was directed this year towards Cornea and/or Corneal Refractive Surgery. It was awarded to José A. Pereira Gomes, MD, of São Paulo, Brazil, for his original paper "*Efeito do hialuronato de sódio na migração e proliferação das células do epitélio de córnea humana.*"
- Established in 1995, the three Allergan Select Free Paper Prizes were awarded to:
  - First Place: Marcel Y. Avila Castañeda, MD, of Bogotá, Colombia for his paper "*Reconstrucción de superficie ocular con injertos de membrana amniotica y epitelio limbar heterologo: una nueva técnica (modelo experimental).*"
  - Second Place: David S. Chu, MD, of Boston, Massachusetts. His paper was entitled "*HIV positive patients with intracorneal precipitates between Descemet's membrane and endothelium.*"
  - Third Place: Maria Auxiliadora Frazão Sibinelli, MD, of São Paulo, Brazil, for her paper entitled "*Manifestações oculares em pacientes com esclerose múltipla sistêmica em São Paulo (Brasil).*"
- The third Carl Kupfer Award for Prevention of Blindness, established in 1997, was given to Carlos Won Cam, MD, of Lima, Peru, for his service and dedication to prevention of blindness. He presented a paper entitled "*Veinticinco años de prevención de ceguera en el Perú.*"

Simultaneous translation from English and Spanish was provided for all symposia. The simultaneous translation of the third official language, Portuguese, was omitted on the decision of the Brazilian delegates, who were of the opinion that Spanish or English was well understood by their colleagues.

At the conclusion of the Congress, Paul R. Lichter, MD handed over the presidency gavel to Rubens Belfort Jr., MD of São Paulo, Brazil. Dr Belfort's term of office

will conclude at the end of the 2003 XXIV Pan-American Congress in San Juan, Puerto Rico. Bronwyn Bateman, MD of Denver, Colorado, will succeed Dr Belfort.

*Other Activities of the PAAO since the last report.*

During 2001, the PAAO's website, <http://pao.org>, was launched with a grant from Allergan International. The new website was used to disseminate information on the Advance Program of the XXIII Pan-American Congress in Buenos Aires. Additionally, the site is used to inform the public of the scholarships, fellowship, and other educational programs available through the Pan-American.

The PAAO continues its support of educational and cultural exchanges throughout the Western hemisphere. The Visiting Professors program, the longest running educational program of the PAAO, sent 10 visiting professors to 8 countries during 2001.

The Fellowships Committee, chaired by Alice McPherson, MD, of Houston, Texas, reported that from 1992-2001, \$638,000 has been disbursed to fund 99 candidates.

The tragedy of September 11 and the fear of travel at that time had a tremendous impact on international meetings. Attendance was down significantly at the American Academy of Ophthalmology's annual meeting in New Orleans in November 2001. This was well illustrated at the PAAO's "Best of the AAO in Spanish" that immediately followed the Orlando meeting. In 2000, over 500 people attended that meeting. In 2001, only 181 attended this popular course. This tragedy, coupled with economic hardships in other countries around the world, has greatly impacted the PAAO's membership in Latin America. The table below represents the net results from the new members gained and the attrition lost. The impact of lost membership was seen in Latin America.

<b>Membership</b>	<b>Prior year (2000)</b>	<b>Current year (2001)</b>
North America	543	589
Latin America	911	757
European		
Countries	85	86
Total	1539	1432

On March 7-9, 2002 in accordance with The Pan-American tradition to hold regional courses in less populated areas, the Guatemalan Association of Ophthalmology hosted the X Pan-American Regional Course in Antigua, Guatemala, which was attended by 277 ophthalmologists from 10 countries.

The PAAO will sponsor 11 symposia and 27 courses from October 20-23, 2002 in Orlando, Florida at the annual meeting of the American Academy of Ophthalmology.

The American Academy of Ophthalmology's publication of the two PAAO Newsletters continues: "The Pan-American" in English is sent to all members and "El Noticiero," in Spanish is distributed throughout Latin America, sponsored by Alcon.

The newest directive of the Pan-American Association of Ophthalmology is the development of the Pan-American Council of University Professors (PACUPO), which is lead by Dr Juan Verdagner of Santiago, Chile. The purpose of this program is to unite and standardize university training programs throughout Latin American through exchange programs and other means.

The XXIV biennial Pan-American Congress of Ophthalmology is scheduled for March 28 – April 1, 2003 in San Juan, Puerto Rico. Dr George Arzeno has been elected to serve as President of the Congress. The site and time of the year will favor family and social functions as well as the professional activities.

### **Report of the Representative to the American College of Surgeons Board of Governors**

BARRETT G. HAIK, MD. The Advisory Council for Ophthalmic Surgery of the American College of Surgeons is chaired by Lee R. Duffner and includes Council representatives Barrett G. Haik, James W. Karesh, Kenneth H. Musson, Aryol S. Niffenegger, A. Raymond Pilkerton, Jr., and regent William H. Coles. As of December 31, 2000, the American College of Surgeons counted 2,962 ophthalmic surgeons among its fellows, which was 6 percent of its active membership. Participation of the American Ophthalmological Society in the ACS improves interaction between ophthalmologists and other surgical specialists.

The Advisory Council met on March 3, 2001 in Fort Lauderdale, Florida to discuss the issue of out-of-field surgery. In making their recommendation to ACS, the Council attempted to address the breadth of training across the surgical subspecialties that must be included in the consideration of this topic. They concluded that the College should adopt a statement to the effect that "surgeons should not perform procedures that are beyond their education and training." The Council further stated that the College should use its website to educate the public regarding surgeries they are considering and to outline the types of training programs and certifications available in those areas.

At their June 2001 meeting in New Orleans, the Board of Regents of the American College of Surgeons approved a strategic plan for the College, with a mission including the "improvement of care of the surgical patient and the safeguarding of standards of care in an optimal and ethical practice environment." The approved vision

statement for the College describes its dedication to the role of "promoting the highest standards of surgical care through education of and advocacy for its Fellows and their patients . . . providing a cohesive voice addressing societal issues related to surgery."

To that end, at their Board meeting on October 7, 2001 in New Orleans, the Governors of the American College of Surgeons discussed a summary of the 233 annual reports submitted to them from ACS governors around the world (including representatives of 64 surgical specialties) in order to understand the concerns of the membership and to develop plans of action to address those concerns. The four areas of primary interest are broken down as follows: (1) physician reimbursement, Medicare, assistants at surgery, managed care organizations, health care reform and trauma; (2) professional liability, malpractice, and tort reform; (3) graduate medical education, funding, medical schools, medical education and research, and workforce issues; and (4) education, credentialing, new technology and hospital privileging, and peer review.

Reimbursement for services was the primary concern among Governors and fellows throughout the world. Partial and delayed payment as well as inadequate allowances for services put a strain on the system and, according to the reports, are forcing many surgeons into early retirements. The issues extend to enforcement of the Emergency Medical Treatment and Labor Act, which threatens the well-being of current systems of trauma care; the complexity of the coding system for reimbursement, which seems to provide avenues for fraud and which creates delays in payment; the burdensome nature of the utilization review processes of payors, which "delay surgical care, limit access to specialty care, and interfere with surgeons' relationships with their patients;" and the competition that has developed between hospitals for managed care contracts.

The Governors' second concern involved professional liability insurance and its legal regulation. Increases in premiums (up to 100% reported in the Philadelphia area) are ongoing, and tort reform remains slow. Insurance carriers are being forced out of business, and the costs of premiums and settlements are again causes for early retirement for some surgeons.

The third category in their list of concerns included a decline in candidates for surgical residencies, which left 68 positions in 40 programs unfilled during the 2000-2001 match program. Issues defined include long hours, non-educational tasks required of residents, the cost of training, clerkships that limit student exposure to the surgeon's patient care activities, and faculty disenchantment over the financial situations of their institutions. In the United States and Canada, shortages of nurses and allied health professionals were also cited as areas of potential crisis, as existing staff members are

required to work mandatory overtime. Within this category, Governors are concerned that the decline in research by surgeons, which may be the result of decreased funding in academic departments, may result in the review of that research by non-surgeons and so the Governors are calling for restructuring of peer review systems.

The fourth major area of concern addressed in the reports of the Governors involved education in new equipment and technologies and pertained to the availability of opportunities to learn how to use new products, the need for accredited instruction in such use, and the questions that will arise regarding competency standards and how they will meet the expectations of the surgical specialty certification boards in credentialing surgeons in these new areas.

At their adjourned meeting on October 10, 2001, the Board of Governors also discussed and approved two statements on bioterrorism prepared by the Committee on Bloodborne Infection and Environmental Risk that delineated the types of disasters that might be faced and the roles that surgeons could fill within their hospitals and communities in response to such attacks.

Included on the agenda of the ACS's Board of Regents meeting on February 8 and 9, 2002 in New Orleans, Louisiana was the approval of a plan to develop a separate 501 (c)(6) corporation, discussion of the College's current political activity, announcement of a reorganization of the Division of Education under a new associate director, reports concerning items related to patient and physician information pertaining to cancer care, and approval to establish a trauma education endowment.

Recommendations of a task force appointed to prepare a formal business plan to establish the 501 (c)(6) corporation were presented at the February meeting. To be called the American College of Surgeons Professional Association (ACSPA), the new body is intended to provide a greater presence of the College in the legislature and to allow the College's involvement in various activities precluded by its current 501 (c)(3) status as a charitable, educational, and research organization. The College's current Governors will direct the ASPCA and representatives to supervise the operation of the political program are to be appointed.

The current political activity of the ACS includes involvement in three coalitions seeking to elicit a series of changes in laws relating to medical liability. The College has also joined 12 other medical and surgical specialty societies in the Coalition for Fair Medicare Payment, in order to seek to affect legislation addressing the 5.4 percent across-the-board cut in payments for physician services under Medicare enacted in 2002 and to deal with the future effects of sustainable growth rate formulas. The decision by the Centers for Medicare and Medicaid Services to publish a final ruling on the reduced fee

schedule has been of particular concern because of its impact on vascular surgeons who perform diagnostic examinations in their offices.

With approval of a reorganization plan by the Board of Regents at their June 8 -10, 2001 meeting, all educational programs have come under the oversight of the College's Division of Education and Ajit K. Sachdeva, MD, has been appointed as associate director of the Division to help supervise the new organization of programs. Dr Daly's October report of ACS's Committee on Physician Competence and Liability to the Board of Governors called for a continued commitment to life-long learning and periodic self-assessment, and for programs emphasizing individual judgment and decision-making, with the College establishing guidelines for practice and clinical outcomes.

An update on the Journal of the American College of Surgeons, which turns 97 in July 2002, emphasized the Journal's role in offering a source of education and continuing medical education credit across all fields of surgery. As of January 16, 2002, 1,382 fellows had benefited, having earned 8,432.75 credits through the Journal, which provides up to 24 free of charge per year. The program serves to educate physicians around the world, and the American Society of Association Executives recognized the ONLINE CME-1 Program for excellence and innovation. JACS ranks 11 out of 136 surgery journals in reading popularity and the circulation was reported at 61,000 in 2001.

The Regents noted three items related to the ACS's efforts in educating the public and physicians regarding cancer care: (1) the development of a facility information profile system by the Commission on Cancer and the American Cancer Society that will enable approved programs to share information regarding their cancer programs with consumers; (2) the release of the National Cancer Data Base's benchmark reports in March that will permit physicians and cancer registrars to compare patterns of care within their own institutions with those of other similar organizations and with state, regional, and national norms; and (3) the publication in May of the sixth edition of the American Joint Committee on Cancer's Cancer Staging Manual (Springer-Verlag), which will coincide with the annual meeting of the American Society of Clinical Oncology.

The Board of Regents approved the recommendation to establish an endowment for trauma education, which is intended to enhance existing programs and to facilitate implementation of trauma education programs around the world, especially in countries with limited resources for such education.

The American College of Surgeons continues to serve the educational, clinical, and research interests of oph-

thalmologists, and continued cooperation with ACS is beneficial to the mission of the American Ophthalmological Society.

### **Report of the Representatives to the Joint Commission on Allied Health Personnel in Ophthalmology**

DONALD J. DOUGHMAN, MD. The Joint Commission on Allied Health Personnel in Ophthalmology (JCAHPO) was founded in 1969 to enhance the quality of ophthalmic patient care by providing certification of and continuing education to Ophthalmic Medical Personnel (OMP). The Commission consists of 15 sponsoring organizations, each of whom designates two commissioners as representatives. The North American Neuro-Ophthalmology Society is a provisional member organization. The American Ophthalmological Society (AOS) was one of the founding organizations. Its representatives are Drs. Robert Stamper and Donald Doughman.

During this past year, JCAHPO examined 1,734 candidates, of which 1,373 passed. Of those examined, 1,134 were at the Assistant level, 194 at the Technician level, and 25 at the Technologist level. Twenty were examined in Ophthalmic Surgical Assisting. Regarding the technician level, Skill-Evaluation tests, the hands-on evaluations of practical skills, were held three times at 39 centers, administered by 32 evaluators drawn from a pool of over 400 volunteers. As of December 31, 2001, there were 14,545 JCAHPO certified personnel including 9,599 Assistants, 4,219 Technicians, and 728 Technologists.

The 29th annual Continuing Education program (CE) was held Nov. 10-14, 2001 in New Orleans in conjunction with the annual American Academy of Ophthalmology (AAO) meeting. Over 2,900 registrants attended, with 734 individuals as first time registrants. Courses were offered in 24 subject areas by over 400 volunteer faculty.

Regional CE programs were offered in four locations throughout the United States.

Statesmanship Awards, given to a deserving Commissioner and Non-Commissioner for outstanding achievement in furthering the cause of Allied Health Personnel, were presented to Ella Rosamont-Morgan, BS, COMT and Michelle Pett Herrin, COMT, CO.

The JCAHPO Education and Research Foundation (JCAHPO-ERF) was founded 9 years ago. This past year, it awarded 48 scholarships totaling \$31,570. It has established seven endowed funds for special projects and scholarships. One of the endowments funds is in memory of Arthur H. Keeney, MD, who represented the AOS to the JCAHPO for many years. The Foundation has requested contributions from all the member organiza-

tions, including the AOS, to strengthen its appeals to the ophthalmic industry and foundations.

JCAHPO requests the continuation of active support from the American Ophthalmologic Society and further requests that Dr Donald J. Doughman and Dr Robert L. Stamper be reappointed representatives from the American Ophthalmological Society.

### **Report of the Representative to the American Orthoptic Council**

EDWARD L. RAAB, MD. The American Orthoptic Council was founded in 1935 to establish standards for orthoptic practice in the United States. Today, there are twenty members representing five sponsoring organizations, including the American Ophthalmological Society. During this past year, the Society's representatives have been Drs Thomas France, David Weakley, and Edward Raab. All serve as examiners of candidates for the Council's certificate and remain fully involved in a wide range of educational and administrative activities.

Dr France has, for several years, been highly effective as representative to the Canadian Orthoptic Council, developing and strengthening the interchange between these organizations to promote higher standards of education and practice among North American orthoptists. He continues as Editor of the American Orthoptic Journal and serves on the Bylaws, Long Range Planning, Public Relations, and Accreditation Committees.

Dr Weakley is a member of the Accreditation, Examination, Editorial, and Program Committees and again chaired the organization of the very well-attended workshop at the Annual Meeting of the American Association for Pediatric Ophthalmology and Strabismus, featuring the role of the Certified Orthoptist in the evaluation and management of all ranges of strabismus and associated conditions.

Dr Raab completed his term as Immediate Past President and a member of the Executive Committee. He chairs the Bylaws Committee, which this year undertook major revisions in the Council's nominating mechanism and committee structure, and serves on the Long Range Planning and Accreditation Committees.

During 2001, the Council approved two new programs for the education of orthoptist candidates and certified six newly graduated orthoptists. Twelve candidates will be taking the examination this fall. A manual on how to set up a program and a workshop for potential program directors are part of the Council's ongoing effort to encourage recruitment into the profession of orthoptics.

The American Orthoptic Journal has enjoyed an increase in its number of subscribing readers. While continuing its efforts to obtain listing on Medline, the Journal

has now developed its own searchable list of the contents of all volumes from 1991 to 1999.

As in previous years, action items are our requests for continuing Society representation on the American Orthoptic Council and further financial support for its programs.

### **Report of the Representative to the Council of the American Academy of Ophthalmology**

ALBERT W. BIGLAN, MD. The 2001 council fall meeting was conducted in New Orleans. Thomas A. Weingeist, PhD, MD, the Academy President-Elect, and Samuel Masket, MD, Council Chair, called the meeting to order. Regional meetings were conducted over the first three hours of the session. I presented a report on the activity of the American Ophthalmological Society at the Metro-East section of the regional meetings.

William L. Rich, III, MD presented an update on federal affairs. A 5% reduction in fees across the board is to be expected for reimbursement for Medicare services.

Randolph L. Johnston, MD presented the disappointing support of OPHTHPAC by the membership. Less than 20% of the membership contributes to this political action group. Many council members have not contributed to OPHTHPAC.

Michael W. Brennan, MD gave a report on state affairs and reviewed the political successes we have had in state and national legislatures.

H. Dunbar Hoskins, Jr., MD gave the executive Vice-President's report for the Academy.

Michael R. Redmond, MD gave a report on improving the relationship between the American Academy of Ophthalmology and subspecialty societies.

A brief review of the status of reports of the 2001 Council Advisory Recommendations (CARs) was given. Drs. Masket and Shulman recognized retiring councilors.

The American Academy of Ophthalmology (AAO) conducted its Mid Year Forum in Washington, D.C., April 2002. The focus of the forum was to address political and economic issues confronting the membership. In addition to the Council sessions, over 100 ophthalmologists visited with their Congressmen and Congresswomen on Capital Hill. During the Day of Advocacy, and throughout the Mid Year Forum, there was a plea for correcting the flaws in the payment system that are caused by linking the Medicare fee schedule to the U.S. gross domestic product. Other topics covered included re-certification, conflict of interest, and mentoring. Emerging technologies were also evaluated.

Organizations related to ophthalmology and that have more than 100 members may be approved for a seat on the AAO Council. Additionally, nominated representation

from sub-specialty societies and a population weighted representation from each state make up this august advisory body.

Addresses at the Mid Year Forum to the Council were given by H. Dunbar Hoskins, MD the Executive Vice-President of the AAO, Thomas A. Weingeist, PhD, MD, the President of the AAO, and Humphrey Taylor, MD the AAO Public Trustee.

The Council Advisory Recommendations (CARs) were reviewed and commented upon.

It is with great privilege that I submit this report to our society. This concludes my sixth year representing the American Ophthalmological Society to the Council of the American Academy of Ophthalmology.

### **Report of the Constitution and Bylaws Committee**

EDWARD L. RAAB, MD. The revisions to the Constitution and Bylaws formulated by the ad hoc committee consisting of Drs. John Clarkson, Froncie Gutman, and Edward Raab were presented for a first reading at the 2001 Annual Business Meeting and have been mailed to the membership as required, prior to final consideration at the 2002 Annual Business Meeting.

The principal effects of the proposed amendments are:

1. The category of Associate Member is eliminated. Approved individuals would enter the Society as Members.
2. Future proposed amendments would be submitted to the membership thirty days prior to an Annual Meeting and will be discussed and voted upon at the Executive Session of that Annual Meeting.
3. In voting on proposed amendments, abstentions will no longer have the effect of a "nay" vote, but will be disregarded for the purpose of calculating whether there are a sufficient number of votes favorable for passage.
4. Decisions now stated to be those of the involved committee are now officially described as those of the Council.
5. To avoid the inconvenience and expense of filing future changes to the Constitution (Articles of Incorporation) with the State of Minnesota (the state of incorporation of the Society), several sections that are at least equally appropriate as sections of the Bylaws have been moved to the latter document. Provisions of the Bylaws dealing with policy, procedures, or tradition have been removed entirely, with the present intent that they continue in force as resolutions of the Council or acts of the President.

### **Report of the Chairman of the Council**

MELVIN L. RUBIN, MD. Mr. President and members: the Council has met on two separate occasions, both of which

were preceded by a meeting of a Task Force for Membership that was chaired by Council member Dan Jones. The Fall Council meeting was held in Gainesville this past October and our second meeting yesterday here at The Cloisters. Many of our actions were aimed to improve the membership process and to allow for the participation of more of our membership, especially the newer members, in many of our activities. None of these activities that we actually implemented originated with this Council alone; you grow by stepping on the shoulders of all those that preceded you. We counted on many of the actions and suggestions of previous Councils. We have changed the Annual Meeting to include a symposium; we are welcoming your comments about the Symposium concept and I ask for any suggestions for changes in that symposium, including suggestions for topics. In order to accommodate the symposium, we had to shorten the time allotted to papers and we've added a poster session.

The AOS created a website that is functioning nicely and I hope you take advantage of viewing it. You have received notice and the passwords to have member access. There are two sections of the AOS website: the general public section and the section private to members.

We have instituted a membership committee that will help review the applications for membership. We have also modified the thesis requirements in terms of the subjects available for theses. We have broadened the subjects to make it a little bit easier for individuals to participate and to submit theses. The structure and strictness of the thesis review are still the same.

Two of the major changes in the TRANSACTIONS are the enlarged format and its the availability on the website and as a CD-ROM.

The Council has developed a medical student curriculum, chaired by the industrious leadership of a Council member Dr John Clarkson and will be offered to all medical schools.

I would like to present our Council recommendations for nominations for the coming year.

#### **Officers**

Dr Marilyn T. Miller, President  
Dr Froncie A. Gutman, President-Elect  
Dr C.P. Wilkinson, Secretary-Treasurer  
Dr Thomas J. Liesegang, Editor

#### **Committee on Publications**

Dr Thomas J. Liesegang, Chair  
Dr C.P. Wilkinson

#### **New Members' Committee**

Dr Douglas Koch, Chair

#### **Athletic Director**

Dr Woodford Van Meter

#### **Archivist/Photographer**

Dr Ralph C. Eagle, Jr.

#### **AAO Councilor**

Dr Albert W. Biglan  
Dr John O'Neill (alternate)

#### **Am. College of Surgeons Board of Governors**

Dr Barrett Haik (nominee)  
Dr Malcolm Mazow (alternate)

#### **Int. Federation of Ophthalmic Societies Representative**

Dr Bruce E. Spivey

#### **Pan American Assoc. of Ophth. Representative**

Dr Suzanne Verroneau-Troutman

[A motion was made to accept these nominations. It was seconded, no one requested a discussion, and the motion passed unanimously.]

We have one more nomination, which is to the American Academy of Ophthalmology Council. This representative must be elected every year. Dr Al Biglan has been our representative for the past few years and we are nominating him again for this coming year and, as an alternate, Dr John O'Neill.

[A motion was made to accept this nomination. It was seconded, discussed, and the motion passed unanimously]

I would now like to submit the names of those who have completely fulfilled the membership requirements for the AOS. The following is a list of our potential members. They are not members until you vote on them. They are presented to you as Dr Susan Elner, Dr Victor Elner, Dr Donald Puro, Dr David Wilson, Dr M. Roy Wilson, and Dr Steven Wilson. These six we are presenting to you for your consideration, Mr. President.

[A motion was made to accept these nominations. It was seconded, no one requested a discussion, and the motion passed unanimously.]

#### **Report of the President**

ROBERT C. DREWS, MD. As President, I make the following appointments:

#### **Council**

Dr Daniel M. Albert, Chair  
Dr John G. Clarkson

Dr Dan B. Jones  
Dr Susan H. Day  
Dr Travis H. Meredith

**Emeritus Committee**

Dr Stanley Truhlsen

**Committee on Prizes**

Dr Richard Brubaker, Chair  
Dr Bruce E. Spivey  
Dr William S. Tasman

**Committee on Theses**

Dr J. Bronwyn Bateman, Chair  
Dr Joel Mindel  
Dr James Bobrow

**Program Committee**

Dr Stephen Feman, Chair  
Dr George Bartley  
Dr C. Gail Sumner  
Dr Douglas Koch

**Membership Committee**

Dr Melvin L. Rubin, Chair  
Dr Lee Jampol  
Dr Jane Kivlin  
Dr Mark Mannis

**American Orthoptic Council Representatives**

Dr Thomas D. France  
Dr Edward L. Raab  
Dr David Weakley

**National Assoc. for Biomed. Research Representative**

Dr Edward A. Jaeger

**JCAHPO**

Dr Donald J. Doughman  
Dr Robert L. Stamper

Bylaws changes will now be discussed. The Council and the Officers have received no comments, adverse or otherwise, on these changes and revision. There are five principal effects of the changes and revision as reflected in the report of the Committee. Are the members present willing to accept these changes *in toto*?

[Dr James Bobrow offered the motion for *in toto* acceptance of the bylaws changes and it was seconded. There was no discussion and they were unanimously approved by the quorum present. ]

The Executive session will reconvene at the banquet tomorrow night to receive the reports of the New

Members committee by Dr Julia Haller, the Athletic Awards Committee by Dr Woody Van Meter, and the report of the Committee on Prizes by Dr Robert Waller. This ends the session and we adjourn for lunch, sports, and time with our spouses, and will reconvene the Executive Session at the banquet.

**Tuesday Morning, May 21**

The scientific program continued with the following papers:

4. "Endophthalmitis in Patients with Disseminated Fungal Disease" by Stephen S. Feman, MD, John C. Nichols, MD (by invitation), Sophia M. Chung, MD (by invitation), and Todd A. Theobald, MD (by invitation)
5. "Tetrathiomolybdate as an Antiangiogenesis Therapy for Subfoveal Choroidal Neovascularization Secondary to Age-Related Macular Degeneration" by Andrew K. Vine, MD and George J. Brewer, MD (by invitation)
6. "Surgical Approaches to Cystic Epithelial Ingrowth" by Julia A. Haller, MD, Walter J. Stark, MD, Amr Azab, MD (by invitation), Robert W. Thomsen, MD (by invitation), and John D. Gottsch, MD
7. "Multicenter Perspective Randomized Double-Masked Placebo Controlled Study of Rheopheresis to Treat Nonexudative AMD: Interim Analysis" by Multicenter Investigation of Rheopheresis for AMD (MIRA-1) Study Group (by invitation) and Jose S. Pulido, MD.
8. "Projected Impact of Travoprost Versus Both Timolol and Latanoprost on Visual Field Deficit Progression and Costs Among Black Glaucoma Subjects" by Michael T. Halpern, MD, PhD (by invitation), David W. Covert, MBA (by invitation), and Alan L. Robin, MD
9. "Activated Satellite Cells Are Present in Uninjured Extraocular Muscles of Mature Mice" by Linda K. McLoon, PhD (by invitation), and Jonathan D. Wirtschafter, MD\*  
\*paper was presented by J.D. Wirtschafter
10. "Toxicity and Dose-Response Studies of 1 $\alpha$ -Hydroxy Vitamin D<sub>2</sub> in LHB-Tag Transgenic Mice" by Daniel G. Dawson, MD (by invitation), Joel Gleiser, MD (by invitation), Michele L. Zimbric (by invitation), Soesiawati R. Darjatmoko, MS (by invitation), Jared C. Frisbie (by invitation), Janice M. Lokken (by invitation), Mary J. Lindstrom, PhD (by invitation), Isabell Audo, MD (by invitation), Stephen A. Strugnell, PhD (by invitation), and Daniel M. Albert, MD\*  
\*paper was presented by B.G. Haik in the absence of Dr Albert
11. "Clinical Decision-Making Based on Data from GDx: One-Year Observations" by James C. Bobrow, MD
12. "Bacterial Resistance After Short Term Exposure to

- Antibiotics” by Thomas O. Wood, MD, Harold Dickson, PhD (by invitation), Vicki A. Nix (by invitation), and Danielle Hamilton (by invitation)
13. “Long Term Analysis of LASIK for the Correction of Refractive Errors After Penetrating Keratoplasty” by David R. Hardten, MD (by invitation), Anuwat Chittcharus, MD (by invitation), and Richard L. Lindstrom, MD
  14. “Vitreous Penetration of Orally Administered Gatifloxacin in Humans” by Seenu M. Hariprasad, MD (by invitation), William F. Mieler, MD, and Eric R. Holz, MD\* (by invitation)  
\*paper was presented by E.R. Holz
  15. “Assessment of the Retinal Nerve Fiber Layer of the Normal and Glaucomatous Monkey with Scanning Laser Polarimetry” by Robert N. Weinreb, MD, Christopher Bowd, PhD (by invitation), and Linda M. Zangwill, PhD (by invitation)
  16. “A Very Large Brazilian Pedigree with 11778 Leber’s Hereditary Optic Neuropathy (LHON)” by Alfredo A. Sadun, MD, PhD, Valerio Carelli, MD, PhD (by invitation), Solange R. Salomao, PhD (by invitation), Adriana Berezovsky, PhD (by invitation), Peter Quiros, MD (by invitation), Federico Sadun, MD (by invitation), Anna-Maria DeNegri, MD (by invitation), Rafael Andrade, MD (by invitation), Stan Schein, MD, PhD (by invitation), and Rubens Belfort, MD, PhD (by invitation)

### **Tuesday Evening Banquet, May 22**

MELVIN L. RUBIN, MD. As Chairman of the Council for the 138th meeting of the AOS, it is my pleasure to welcome all of you to this special evening. One of the traditions of the Society’s Presidential Banquet is that the introductions begin with a story. Dr Fred Blodi, at this same venue, told one of my favorites fifteen years ago. Since Fred’s not here to object and since your memories of that particular meeting have probably faded, I’d like to tell you that story.

A very large (6’7”) Nebraska football player walks into a supermarket and, as he approaches the checkout clerk, he stands at his full height and says, “Sir, I would like a half a head of lettuce.” The clerk looks up at him and says, “You know, I’m trying to be nice, but we don’t have half a head of lettuce.” Now this 6’7” individual stretches up to 6’8” on his toes and says, “I said I want a half a head of lettuce.” So the clerk says, “Just a moment, sir,” and runs back to find the manager. “You’re not going to believe this, boss, but this monster man we have wants a half a head of lettuce.” The clerk turns around and sees the tall man standing directly behind him, and then he quickly says “And this nice gentleman wants the other half.”

Now, to satisfy this individual, the clerk runs off, gives him a half a head of lettuce, and then goes back to his chores. The manager later calls him in. The manager says, “You know, that was the quickest bit of thinking I’ve seen in a long time. We’re opening up a branch store in Anchorage, Alaska. Would you like to be considered for manager?” But the clerk says, “Alaska? All they have in Alaska are hookers and hockey players!” The boss now draws himself up indignantly and says, “My wife is from Alaska.” And without a blink, the clerk says, “What team did she play on?” [Laughter]

Now, I’m proud that many of the members of this audience, the AOS members, have as quick a wit as our store clerk. And especially those I wish to thank at this time are the some of the members of this honorable organization. Let’s start by asking all the Past Presidents and their spouses to rise for their accolades. [Applause]

Working with any committee or Council allows one close access to the operations of individuals and to learn about them first hand. I can’t imagine a group of individuals as wonderful as the Officers of this organization and those that I’ve worked with on the Council and I’ve been proud to be associated with them, not just during our tenure here at the AOS, but in many different venues. They have always risen to the occasion and contributed far more than they themselves have ever asked others to contribute. They are the best.

I’ll start with Dr Dan Albert, our next Council Chair. He’s a long-time friend and a most wonderful ethical scientist and clinician. Unfortunately, his wife Ellie’s illness has precluded his attendance here tonight. We miss them both, and wish her our best thoughts and prayers for a speedy recovery. The Council and the AOS have certainly benefited from his thoughtful guidance, and we look forward to his leadership this coming year.

Dr John Clarkson, currently the Dean of the University of Miami School of Medicine, is a gem, with a steady handed, pragmatic style that lets us benefit from his leadership of many other organizations.

I have known Dr Dan B. Jones since he was a resident. He brings to the Council a keen insight, organizational skills, and reliability, as well as a profound ophthalmic knowledge, which made him such a valuable addition to our early development of the OKAP exam.

Dr Susan Day is a super individual who we’ve watched grow rapidly into a true academic leader in so many organizations. Her sparkling wit, hearty laugh, and keen sense of proportion and prudence make us all proud to work with her. And if you didn’t hear her play the Mozart flute concerto with the San Francisco symphony in 1982’s Academy, or her regular performances at the Annual Academy meeting, you’ve really missed something special.

The President-Elect, Dr Marilyn Miller, is another

respected long-time friend of immense accomplishment and wise counsel, with commitment and spotless credentials for leading us next year. You'll hear more about her later, but I want to take some pride in having had a hand in training her spouse, Dr Ron Fishman, a wonderful erudite ophthalmologist with an unusually broad range of interests.

Your editor of the TRANSACTIONS, Dr Brooks Crawford, is now completing his outstanding term. He has improved the cost efficiency of the TRANSACTIONS, made many minor and major improvements, and has taken the AOS into the world of Web-based publishing. I personally thank you, Brooks, on behalf of the AOS, for a super job. [Applause]

I extend to Dr Pat Wilkinson, our Secretary-Treasurer, who wears so many well-fitting hats in ophthalmology, my sincere gratitude for always being there to provide us with guidance. He is a team player and I am very appreciative of his efforts to do what I wouldn't or couldn't do. Thank you, Pat. [Applause]

I can't even begin to thank Lisa Brown for making the AOS Council and the Annual Meeting run so smoothly. I couldn't imagine anyone who could be more thorough, compulsive, accurate, supportive, and available. I appreciate how much she and her staff, including Lisa Secretario, who is with her tonight, do on behalf of the AOS. But I want you all to know and acknowledge how much we appreciate Lisa. [Applause]

Now, before I introduce our President, I want to

acknowledge all of the spouses of the AOS; they honor us by their presence, and make this annual meeting such a congenial fun event. [Applause]

To that special spouse, my wife Lorna, I want to publicly express my appreciation for her love and her support, friendship, and tolerance, not only during my five years that I have been on the Council, but throughout the 49 years of our married life. Thank you. I love you. [Applause]

I offer a final thanks to my oldest friend in ophthalmology, Dr Bill Spencer, who is busy tonight being a new grandfather so he couldn't be here. Some 52 years ago, Bill convinced me to go to medical school and then, six years ago, as AOS president, he gave me this opportunity to serve on the Council. For those gifts, I'm very grateful, and I hope the San Francisco contingent will pass that on to him.

Now it's my great pleasure to introduce our President, Dr Robert C. Drews. Bob was born in St. Louis, and, as a stick-in-the-mud, he spent essentially his entire life there. His father, Leslie Charles Drews, was an ophthalmologist and an AOS member. He was a wonderful role model for our current AOS president. Bob was the complete Washington University alumnus. He received all his collegiate and professional training at Wash U, attending the undergraduate college, medical school, ophthalmology residency training, as well as advancing through all of the steps of clinical professorships there. He has spent 40 years in clinical practice in the St. Louis area, and has always cherished his Wash U connections. Throughout his career, Bob was not just a member of a great number of state, national, and international organizations and societies, but was extremely active. He rose to the governing boards and became an officer, or President, in just about every one. Just a few examples are the Missouri Ophthalmological Society, the Southern Medical Association (the Ophthalmology section), the American Intraocular Implant Society (now called the American Society of Cataract and Refractive Surgeons or ASCRS), where he was a founding member, and the Pan-American Association of Ophthalmology (Bob speaks Spanish fluently, and I'm sure it helped him at the Pan-American). He has been on the Board at the American Academy of Ophthalmology and a Director of the American Board of Ophthalmology, and, of course, the American Ophthalmological Society, and about a dozen more.

Bob was not just an organizational leader; he has contributed heavily to the academic scene. He has served on the editorial boards of ten different ophthalmology journals, and he still holds the editorship of the English version of the *Highlights of Ophthalmology*. Sandwiched between private practice, his family life with Lorene (his lovely wife of 52 years, who unfortunately is not able to be with us tonight to share his honors), and his four children and ten



AOS President Robert C. Drews.



AOS President Robert C. Drews presiding over the Meeting.

grandchildren at last count, his church activities, and his hobbies, he somehow made time for writing 474 papers, chapters, commentaries. Now that's being productive!

Tonight we recognize his AOS contributions: his election in 1979, his five years of service on the AOS Council as it's Chair, last year as President-Elect, and this year as President. My personal contact with Bob started when we were both residents. At that time, the ten resident associations in the Midwest met annually with their residents and faculty to share scientific papers at what was called the Midwestern Section of the Association for Research in Ophthalmology. This was before the ARVO. Even as a resident and a disciple of Dr Bernard Becker, he had that critical and evaluative style. He was outspoken, constantly asking probing questions in a way that pierced the armor of the presenting scientists and clinicians, most of whom were certainly his senior in age. Bob was a standout creative thinker, and that was evident and impressive to anyone who was in the audience. His style and intellect, as well his cogent and analytical ability and his immensely creative mind, have all been demonstrated over and over again for the 40 years that I have known him.

One final, personal, note about Bob. At dinner during one of his visits to Gainesville about 15 years ago, I was complaining about a really painful canker sore in my mouth. Bob suggested I try a dab of acetone on a Q-tip to relieve the sore. It worked amazingly well, and still does, whenever necessary. So for that bit of personal help, as well as all the scientific contributions to ophthalmology and to the AOS, I am proud indeed to present our President, Dr Robert C. Drews. [Applause]

ROBERT C. DREWS, MD. You know, it's hard to know how to respond when someone introduces you so graciously. I only wish my parents could have been here—my father would have been very proud, my mother would have believed all that. [Laughter]

This photograph (not shown here) was taken at the first AOS meeting that I was privileged to attend in 1961. I was a guest of my father's, who was a member. Unfortunately, that evening he was too ill to come down to the dinner. He died a few months later. This is my mother on your left and my wife Lorene on the right, really enjoying an AOS meeting. It was an outstanding meeting, as usual, and one of the outstanding things that occurred at that meeting was a chance to listen to Arthur Bedell deliver the first Verhoeff Lecture. Yesterday we heard another outstanding Verhoeff Lecture.

My wife Lorene is very sorry she was not able to come. She had looked forward to it very much but just could not make the trip. She sends all of her best wishes to us. Of course she realizes there has been no change in appearance of either one of us in those two photographs (not shown here). The AOS has been a marvelous organization over the years and it has been a great privilege to attend the meetings, to be a member, and finally an enormous privilege to serve as your President. What a wonderful year to serve as President—it was a terrific year and a great meeting to preside over and I thank all of the people who made that possible.

I would now like to reconvene the Executive Session of the AOS. We will make the usual exception that, for this portion of the Executive Session, the wives, spouses, and friends be invited to attend. I call on Committee reports, first from Julia Haller, to do the honors of introducing, once more, our wonderful new members. The new members are the lifeblood of the AOS, especially since so many of us are becoming Emeritus members all the time.

JULIA HALLER, MD. We have a bumper crop of new members this year, and I'd like to ask them to stand as I mention their names:

Dr Louis Cantor and his wife Linda from Indianapolis, Indiana;

Dr William Good, from San Francisco, California; we look forward to welcoming his wife Laurie in years to come;

Dr Mark Humayan and his wife Karen, formerly from Baltimore and now from Los Angeles, California;

Dr Henry Jampel and his wife Risa are not here, although they were here for the early part of the meeting; and Dr Bob Weinreb, and his guest Dr Cristiana Vasile, from LaJolla, California.

We're so pleased to welcome this wonderful group to our society. [Applause]



The AOS is proud to introduce its 2002 New Members (left to right): Dr William V. Good, San Francisco, CA; Dr Louis B. Cantor, Indianapolis, IN; Dr Robert N. Weinreb, LaJolla, CA; Dr Mark S. Humayun, Los Angeles, CA; and Dr Henry D. Jampel, Baltimore, MD.

ROBERT C. DREWS, MD. Woody Van Meter, please introduce our Athletic Award winners.

**Report of the Athletic Committee**

WOODFORD S. VAN METER, MD. Those of you who were at the meeting last year remember what disastrous weather we had and we are certainly grateful to have much better weather this year. The winners of this year's events are:

<u>Trophy</u>	<u>Event</u>	<u>Winner</u>
Beetham-Bullock Trophy	Skeet shooting	Mylan Van Newkirk
McCaslin-Fralick-Kimura Trophy	Fly fishing	Event Not Held



Dr Ed Raab and Dorothy Van Meter hold their newly acquired Wilson Trophy as mixed doubles runner-ups in tennis. Dorothy's husband, Dr Woody van Meter (right), is the AOS Athletic Awards Chairman.

Mishima-Michaels Trophy	Men's golf low gross	Verinder Nirankari
Canada-McCulloch Trophy	Men's golf low net	Michael Lemp
Truhlsen Trophy	Senior Men's low gross	William Annesley
Knapp Memorial Trophy	Men's team golf	Michael Lemp C. Pat Wilkinson
Ellsworth Trophy	Ladies' golf low gross	Carolyn Lichter
Homestead Cup	Ladies' golf low net	Dottie Truhlsen
EVL Brown Bowl	Men's tennis winners	John Gottsch Richard Lindstrom
EVL Brown Bowl	Men's tennis runners-up	Evangelos Gragoudas Woody Van Meter
Perera Bowl	Ladies' tennis winners	June Wood Alice Wilkinson
Hughes Bowl	Ladies' tennis runners-up	Nancy Brubaker Betty Van Newkirk
Wong-McDonald Trophy	Mixed Doubles winners	Jaci Lindstrom Richard Lindstrom
Wilson Trophy	Mixed Doubles runners-up	Dorothy Van Meter Edward Raab

ROBERT C. DREWS, MD. Thanks Woody, and thanks to all our participants. The athletic proceedings of the AOS are always one of the very important parts of our program.

The highlight of the evening program is always the report of the committee on prizes and, for this, I will ask Dr Robert Waller to make the presentation.

### **Report of the Committee on Prizes**

ROBERT L. WALLER, MD. Dr Drews, Dr Rubin, Officers and Councilors of the Society, distinguished members, spouses, and guests: The committee on prizes has a most pleasant assignment tonight, which is to announce the recipient of the Howe Medal winner for 2002, the highest honor bestowed by this Society, if not in all of ophthalmology.

There are only a few among us whose names are synonymous with the very beginnings of a specialty or subspecialty in ophthalmology. Tonight, we recognize such an individual, a pioneer and now the Howe Medalist for 2002. Incidentally, he has a birthday this week (we won't disclose his age, but he was born on May 23, 1912!).

He was born in Napa, California in a home that is now beautifully refurbished. He spent much of his youth there and attended local schools before going off to college. He attended U.C. Berkeley (where his father was Gold Medalist in Philosophy in the 1888 graduating class). He started his studies in economics but, apparently because he was not excited by math and statistics, he changed to pre-medicine. Our recipient also studied the violin for several years before taking up the banjo, which he carries in some of his college photos. While at Berkeley, he had a weekly half hour show on the radio playing that banjo.

Our recipient was married to Gertrude, who passed away fifteen years ago, and the two had a daughter, Nancy, and a son, Michael. He was handy around the house, as daughter

Nancy tells us, upholstering furniture and once repairing floor mats in his car with surgical needles and dental floss. He also created a solar-heating device for the roof with a series of garden hoses (but it didn't work). Incidentally, instead of Berkeley, Nancy and Michael attended Stanford, as did a physician granddaughter named Albertine, but somehow they have all been allowed to remain in the family!

Our recipient attended medical school at UC San Francisco, during which time he and his two brothers owned and operated a haberdashery near Union Square. He completed residency in Ophthalmology at Mayo Clinic, and then returned to California. He soon joined the military, as this was the time of World War II. He completed basic training in the Army at Carlisle barracks in Pennsylvania. As a side note, just before entering the military, while in private practice in San Francisco, he was asked to see a young boy for a refraction. The patient was apparently brought to the office in a reluctant state of mind, and it wasn't an easy examination. This little boy now believes that he may have influenced our Howe Medal recipient to choose a practice other than a refraction practice. The little boy grew up to be Dr Brooks Crawford.

After completing basic training, our recipient was to be posted to the South Pacific. However, at the eleventh hour he was reassigned to Dibble Hospital in Menlo Park, California, where Dr Phil Thygeson was his chief. Therein would lie a defining time in our recipient's career. He and his colleagues cared for more injuries coming from the Pacific requiring oculoplastic surgery than would have been seen in an entire career. It was a time when general plastic surgery as a specialty was in its formative stages, and it was a surgical experience which launched his life's work.

Following the war, he returned to San Jose, California, and to his first peace-time practice in partnership with Dr Phil Thygeson (perhaps our most senior AOS member, who is homebound now, but visited to this day every Thursday



Escorting the Howe Medal winner, Dr Crowell Beard (second from the left), are Dr Richard Brubaker (left), Dr Robert Waller (right) and Dr Bruce Spivey (far right).



Howe Medal winner, Dr Crowell Beard (left), receiving the Medal from AOS President Robert C. Drews.

by our recipient). He also joined the faculty of UC San Francisco; some of his house staff colleagues included Ernest Gunderson, Mike Hogan, and Harry Chong.

As we say, the rest is history. The specialty of Oculoplastic Surgery, in large measure, was literally born out of the World War II experiences of our 2002 Howe Medalist and a few of his friends: Drs Norman Cutter (with whom he devised an ingenious procedure to reconstruct full thickness defect of the upper lid), Sidney Fox, Byron Smith, Alstan Callahan, Wendell Hughes, Edmund Spaeth, and Jack Mustardé, to name a few. These pioneers then began to teach Oculoplastic Surgery at the AAO. Our recipient and a few of his friends then formed the American Society of Ophthalmic Plastic and Reconstructive Surgeons or ASOPRS, which has grown to several hundred members, prospered, and which has improved immeasurably the quality of performance in this surgical specialty.

Our recipient is the authority on ptosis, as well as the anatomy of the orbit, a master surgeon, and a master teacher. Our recipient has probably trained, mentored, encouraged, and influenced more oculoplastic surgeons than anyone in the nation, including many members of this society. As an aside, as best I can tell, he was among the first, if not the first, to publish his experience with outpatient (office) cataract surgery nearly forty years ago now.

His proven ineptitude in economics (by his own admission) drove him toward medicine, ophthalmology, military service, oculoplastic surgery, and academia, and we are so fortunate that such was the case.

Our recipient is here tonight with his wife Fran and Fran's daughter, Jeanne. Drs Bruce Spivey and Richard Brubaker from the Awards Committee will escort to the stage our distinguished 2002 Howe Medalist, Dr Crowell Beard. [Applause]

CROWELL BEARD, MD. I really don't know what to say. I'm awfully sorry. I think I'm kind of like Halle Berry at this year's Academy Awards. I've been thinking about this for some 40-odd years but I knew I would never get here. When Bob Waller called me and said that he wanted to do something nice for me, I got to thinking, "what it could be?" and I knew that it couldn't possibly be the Howe Medal, so I wrote that off. I thought that it might be an old age award that the society decided to give. And someone said I was going to have my 90th birthday in two days, I hope. The Howe Medal is something I never could have hoped for. I appreciate this honor that the Society has given me and I accept it with pride. When I think back of the last 50 years or however long the Howe Medal has been given and the big names that have been there, I don't think mine belongs on that list of ophthalmologic saints. The Howe Medal is certainly the Oscar of American Ophthalmology and I appreciate it.

I'd like to tell a brief story. About 20 or 25 years ago I

was in this audience when Dr Fred Blodi got his Howe Medal. As we were leaving the auditorium and standing in a line looking for the men's room, I said, "Gee, Fred, I thought I might get it but I'm awfully glad that, if it wasn't to be me, that it was you." Fred said, "Crowell, I think you should have gotten it. I'll give you half." About two weeks later in the mail I get this picture of the Howe Medal and it was cut in two with a note "Crowell, here's your half. Best regards, Fred." [Laughter]

It is difficult for me to tell or show you how much I appreciate this status that I never would have hoped to attain. Thank you. [Applause] ["Happy Birthday" breaks out]

DR ROBERT C. DREWS. I have one final pleasure. Dr Marilyn Miller, will you come forward please? I have the distinct honor of introducing the next President of the American Ophthalmological Society and its first woman President, Dr Marilyn Miller. [Applause]

MARILYN MILLER, MD. I'm really honored. I'm honored for the trust that this Society has put in me and given to me. I hope I meet your expectations. You're all super people, and this is a very special group. I thank you again.

ROBERT C. DREWS, MD. I'll close the Executive Session and turn the program back over to Dr Mel Rubin.

MELVIN L. RUBIN, MD. It's been a great pleasure to be Chair of the Council this year. The meeting tomorrow will start at 7:30 am; there are only five papers to be presented but I realize that some of you will have to get to the airport. I will see you all next year in Santa Barbara, California, for the 139th Annual Meeting. With that, I say good evening. The band will continue to play for around another hour or so. You're welcome to stay, mill around, and complete your dancing.



Colonel and AOS member Dr Brian Younge and his wife Gloria.

**Wednesday Morning, May 23**

The scientific meeting concluded with the following papers:

17. "The Disc Damage Likelihood Scale: Reproducibility of a New Method of Estimating the Amount of Optic Nerve Damage Caused by Glaucoma" by George L. Spaeth, MD, Jeffrey D. Henderer, MD (by invitation), Connie Liu (by invitation), Muge Kusen, MD (by invitation), Undraa Altangerel, MD (by invitation), Atilla Bayer, MD (by invitation), L. Jay Katz, MD (by invitation), Jonathan S. Myers, MD (by invitation), Douglas Rhee, MD (by invitation), and William Steinmann, MD, MSc (by invitation)
18. "Evolution of the Tapetum" by Ivan R. Schwab, MD, Carlton K. Yuen, (by invitation), Nedim C. Buyukimhci, VMD (by invitation), Thomas N. Blankenship, PhD (by invitation), and Paul G. Fitzgerald, PhD (by invitation)
19. "Angle-Closure in Younger Patients" by Brian M. Chang, MD (by invitation), Jeffrey M. Liebmann, MD (by invitation), and Robert Ritch, MD
20. "Delta-9-tetrahydrocannabinol (THC) in the Treatment of End-Stage Open-Angle Glaucoma" by Allan J. Flach, MD
21. "Diagnostic Transvitreal Fine-Needle Aspiration Biopsy of Small Melanocytic Choroidal Tumors in Nevus Versus Melanoma Category" by James J. Ausgburger, MD, Zélia M. Corrêa, MD (by invitation), Susan Schneider, MD (by invitation), Rawia S. Yassin, MD (by invitation), Toni Robinson-Smith, MD (by invitation), Hormoz Ehya, MD (by invitation), and Nikolaos Trichopoulos, MD (by invitation)

The following members were present and registered at the meeting.

Active	Aaberg Sr., Thomas M.
Emeritus	Alper, Melvin G.
Active	Anderson, Douglas R.
Active	Anderson Jr., W. Banks
Emeritus	Annesley Jr., William H.
Emeritus	Asbury, Taylor
Active	Augsburger, James J.
Active	Bartley, George B.
Emeritus	Baum, Jules L.
Emeritus	Beard, Crowell
Active	Benson, William E.
Active	Berler, David K.
Active	Berson, Eliot L.
Active	Biglan, Albert W.
Active	Blair, Norman P.

Active	Blankenship, George W.
Active	Bobrow, James C.
Active	Bourne, William M.
Emeritus	Brubaker, Richard F.
Active	Bullock, John D.
Active	Cantor, Louis B.
Active	Clarkson, John G.
Emeritus	CoxJr, Morton S.
Active	Crawford, J. Brooks
Emeritus	Day, Robert
Active	Day, Susan H.
Active	Donshik, Peter C.
Active	Doughman, Donald J.
Active	Drews, Robert C.
Active	Eagle Jr., Ralph C.
Active	Ernest, J. Terry
Active	Farris, R. Linsy
Active	Federman, Jay L.
Active	Feman, Stephen S.
Active	Ferris, Frederick L.
Active	Flach, Allan J.
Active	Flanagan, Joseph C.
Active	Flynn, John T.
Active	Forster, Richard K.
Active	Foster, C. Stephen
Active	France, Thomas D.
Active	Fraunfelder, Frederick T.
Active	Friedman, Alan H.
Active	Frueh, Bartley R.
Emeritus	Glew, William B.
Active	Godfrey, William A.
Active	Good, William V.
Active	Gottsch, John D.
Active	Gragoudas, Evangelos S.
Active	Gross, Ronald L.
Active	Grossniklaus, Hans E.
Active	Gutman, Froncie A.
Active	Haik, Barrett G.
Active	Haller, Julia A.
Active	Holland, Edward J.
Active	Hull, David S.
Active	Humayun, Mark S.
Active	Iloff, W. Jackson
Active	Jampel, Henry
Active	Jampol, Lee M.
Active	Jones, Dan B.
Active	Kelley, James S.
Active	Kennedy, Robert H.
Active	Kivlin, Jane D.
Active	Knox, David L.
Active	Laibson, Peter R.
Active	Lakhanpal, Vinod
Active	Landers III, Maurice B.

*Minutes of the Proceedings*

Active	Laties, Alan M.	Active	Srinivasan, B. Dobli
Active	Lemp, Michael A.	Active	Stamper, Robert L.
Active	Lichter, Paul R.	Active	Stark, Walter J.
Active	Liesegang, Thomas J.	Active	Sugar, Alan
Active	Lindstrom, Richard L.	Active	Summers, C. Gail
Active	Ludwig, Irene H.	Active	Tasman, William S.
Active	Luxenberg, Malcolm N.	Emeritus	Troutman, Richard C.
Active	Mazow, Malcolm L.	Emeritus	Truhlsen, Stanley M.
Active	Merriam, John C.	Active	Van Meter, Woodford S.
Active	Meyer, Roger F.	Active	Van Newkirk, Mylan R.
Active	Mieler, William F.	Emeritus	Veronneau-Troutman, Suzanne
Active	Miller, Marilyn T.	Active	Vine, Andrew K.
Active	Mindel, Joel S.	Emeritus	von Noorden, Gunter K.
Active	Mitchell, Paul R.	Active	Waller, Robert R.
Active	Nirankari, Verinder S.	Active	Waltman, Stephen R.
Active	Nork, T Michael	Active	Waring III, George O.
Active	O'Day, Denis M.	Active	Weinreb, Robert N.
Active	O'Neill, John F.	Active	Welch, Robert B.
Emeritus	Parks, Marshall M.	Active	Wilhelmus, Kirk R.
Active	Pollack, Irvin P.	Active	Wilkinson, Charles P.
Active	Pollard, Zane F.	Active	Wilson II, Fred M.
Active	Pulido, Jose S.	Active	Wirtschaftler, Jonathan D.
Active	Raab, Edward L.	Active	Wood, Thomas O.
Active	Ritch, Robert	Active	Younge, Brian R.
Active	Robin, Alan L.	Honorary	Zimmerman, Lorenz E.
Active	Rubin, Melvin L.		
Active	Runge, Paul E.	Professional Guest	Chang, Brian
Active	Sadun, Alfredo A.	Professional Guest	Grand, M. Gilbert
Active	Schein, Oliver D.	Professional Guest	Holz, Eric R.
Active	Schocket, Stanley S.	Professional Guest	Lakhanpal, Rohit R.
Active	Schwab, Ivan R.	Professional Guest	Lavker, Robert
Active	Sergott, Robert C.	Professional Guest	Raymond, Pamela A.
Active	Shields, M. Bruce	Professional Guest	Ridley, Miriam E.
Active	Sieving, Paul A.	Professional Guest	Sanders, Donald R.
Active	Spaeth, George L.	Professional Guest	Whitten, Mark
Active	Spivey, Bruce E.		

FDA STATUS DISCLAIMER

Some material on recent developments may include information on drug or device applications that are not considered community standard, that reflect indications not included in approved FDA labeling, or that are approved for use only in restricted research settings. This information is provided as education only so physicians may be aware of alternative methods of the practice of medicine, and should not be considered endorsement, promotion, or in any way encouragement to use such applications. The FDA has stated that it is the responsibility of the physician to determine the FDA status of each drug or device he or she wishes to use in clinical practice, and to use these products with appropriate patients consent and in compliance with applicable law. The Society provides the opportunity for material to be presented for educational purposes only. The material represents the approach, ideas, statement, or opinion of the presenter and/or author, not necessarily the only or best methods or procedure in every case, nor the position of the Society. The material is not intended to replace a physician's own judgement or give specific advice for case management. The Society specifically disclaims any and all liability for injury or other damages of any kind for any and all claims that may arise out of the use of any technique demonstrated or described in any material by any presenter and/or author, whether such claims are asserted by a physician or any other person.



## PAPERS



# LONG-TERM RISK OF LOCAL FAILURE AFTER PROTON THERAPY FOR CHOROIDAL/CILIARY BODY MELANOMA

---

BY Evangelos S. Gragoudas, MD, Anne Marie Lane, MPH (BY INVITATION), John Munzenrider, MD (BY INVITATION), Kathleen M. Egan, ScD (BY INVITATION), AND Wenjun Li, MS (BY INVITATION)

## ABSTRACT

*Purpose:* To quantitate long-term risk of local treatment failure after proton irradiation of choroidal/ciliary body melanomas and to evaluate risk of metastasis-related deaths after local failure.

*Methods:* We followed prospectively 1,922 patients treated at the Harvard Cyclotron between January 1975 and December 1996 for local recurrences of their tumors. Mortality surveillance was completed through June 1999. For analysis, patient follow-up continued until tumor regrowth was detected or, in patients without recurrence, until the date of the last dilated examination prior to April 1998. Actuarial methods were used to calculate rates of recurrence and metastatic deaths. Cox regression models were constructed to evaluate risk factors for these outcomes.

*Results:* Median ocular follow-up after irradiation was 5.2 years. Local recurrence was documented in 45 patients by ultrasound and/or sequential fundus photographs; in 17 more patients, the eye was enucleated due to suspected but unconfirmed tumor growth. Recurrences were documented between 2 months and 11.3 years after irradiation. The 5- and 10-year rates of regrowth, including suspected cases, were 3.2% (95% confidence interval [CI], 2.5%-4.2%), and 4.3% (95% CI, 3.3%-5.6%). Among the 45 documented recurrences, about one half (21) occurred at the margin, presumably due to treatment planning errors. The remaining cases represented extrascleral extensions (nine cases), ring melanomas (six cases), or uncontrolled tumor (nine cases). Recurrence of the tumor was independently related to risk of tumor-related death.

*Conclusion:* These data, based on relatively long-term follow-up, demonstrate that excellent local control is maintained after proton therapy and that patients with recurrences experience poorer survival.

*Trans Am Ophthalmol Soc* 2002;100:43-50

## INTRODUCTION

---

Uveal melanoma is the most common primary intraocular malignancy, with an annual incidence of six cases per million persons, or approximately 1,500 new diagnoses each year in the United States.<sup>1</sup> Over the past several decades, radiotherapy (external beam charged-particle therapy [eg, protons, helium ions] or episcleral plaque therapy) has replaced enucleation as the preferred treatment for most patients with this tumor. With radiotherapy, eye salvage is achieved, and particularly for cases in which the tumor is located away from the optic disc or macula, useful vision can be retained after treatment.<sup>2-6</sup> High rates of local control are also achieved, with 5-year control rates exceeding

95% in patients treated with charged particles.<sup>7-9</sup> Somewhat lower rates are reported for plaque therapy, ranging from 81% to 86%<sup>10-13</sup> in patients treated with cobalt 60 or iodine 125, now the most commonly used plaque. Survival rates do not appear to be compromised with conservative therapy when compared to enucleation.<sup>14-17</sup> However, some investigators have reported an increased risk of death from metastasis when the treatment has failed to control local tumor growth.<sup>7,9,18,19</sup> Previous studies evaluating local failure have been limited by small numbers and relatively short-term follow-up.

In this study, we evaluated local failure as an end point in a large series of uveal melanoma patients treated by proton irradiation, with long-term follow-up having accrued at the time of analysis. Identification of modifiable risk factors may reduce the rates of recurrence and lead to fewer complications, preservation of the eye, improved visual function and, potentially, better survival outcome.<sup>20</sup> Additionally, we evaluated local failure as a risk factor for metastatic death. Longer-term results may provide additional data that may aid in clarifying the association between local failure and metastatic risk.

From the Clinical Research Unit, Retina Service, Massachusetts Eye and Ear Infirmary, Boston (Dr Egan, Dr Gragoudas, Ms Lane); the Department of Ophthalmology, Harvard Medical School, Boston (Dr Egan, Dr Gragoudas, Ms Lane); the Department of Radiation Oncology, Massachusetts General Hospital, Boston (Dr Munzenrider); the Department of Epidemiology, Harvard School of Public Health, Boston (Dr Egan); and the Biostatistics Research Center, New England Medical Center, Boston (Mr Li). Supported by the Massachusetts Eye and Ear Infirmary Melanoma Research Fund.

## METHODS

---

We evaluated local control in a series of 1,922 patients with intraocular melanomas treated with proton therapy at the Harvard Cyclotron between 1975 and 1996 and followed prospectively through April 1998. Patients living outside the United States or Canada, patients with bilateral or iris melanomas, and patients diagnosed with metastasis at time of presentation were excluded from analysis. Additionally, patients who had received previous therapy for their tumor or adjuvant therapy after proton irradiation were excluded.

Tumor characteristics determined during the initial ophthalmologic examination included tumor size (based on indirect ophthalmoscopy, transillumination, and echography) and tumor location in relation to the optic disc, macula, equator, and ora serrata. Tumor shape and pigmentation also were estimated during the examination. Demographic and patient characteristics, including patient age, gender, and eye color, were recorded. Pretreatment workup, including liver function studies and chest x-rays, were routinely performed to rule out systemic metastasis. When liver function tests were abnormal, a liver scan was also performed.

Details concerning the treatment of intraocular melanomas at the Harvard Cyclotron Laboratory have been described previously.<sup>21-23</sup> Early in the program, doses as high as 100 Gy were administered in efforts to determine the optimal dose, while recently a lower dose of 50 Gy was administered to patients in a randomized clinical trial to establish safety and efficacy of a dose reduction.<sup>24</sup> The standard protocol requires delivery of 70 Gy in five equal fractions over 7 to 10 days. In this study most patients (94%) received the standard dose, while 5% received 50 Gy as participants in our dose reduction trial.

Ocular outcomes, including tumor regrowth, were ascertained through April 1998. The majority of patients returned to the Massachusetts Eye and Ear Infirmary (MEEI) for at least one follow-up examination after treatment. Mortality surveillance was current through June 1999. For patients not returning to MEEI, active surveillance was performed to ascertain outcomes data from referring ophthalmologists and vital status from ophthalmologists, internists, patients, or other sources (eg, the National Death Index) on an annual basis. Local recurrences were documented by ophthalmologic examination, ultrasonography, and/or sequential fundus photography for all patients evaluated at MEEI. Whenever possible, documentation of recurrences by ultrasonography and photography was also obtained from the referring ophthalmologists.

Patients were followed from completion of proton therapy to the date of diagnosis of recurrence or, in censored observations, until the date of the last dilated exam-

ination. For tumor-related mortality, patients were followed to the date of death or, for patients still alive, until the earlier of the date of last prior contact or June 30, 1999.

Using Kaplan-Meier methods,<sup>25</sup> we estimated annual incidence rates and cumulative rates at 5, 10, and 15 years after treatment, with corresponding 95% confidence intervals (CI). We calculated relative risk (RR) estimates using Cox proportional hazards regression<sup>26</sup> to determine statistically significant factors independently related to risk of tumor regrowth. Using a time-varying covariate approach, we compared risk of death from metastasis in patients with and without tumor regrowth.

## SUBJECTS

---

Approximately equal numbers of males (49%) and females (51%) were treated. There was no predilection for either eye to be affected, with 50% of cases involving the right eye. As expected, this cohort was racially homogeneous, with the proportion of Caucasian subjects approaching 100%. Median age at time of treatment was 60 years. Mean tumor dimensions were 13 mm and 5.3 mm for diameter and height, respectively. Tumors were predominantly located in the posterior fundus, and about one quarter (26%) involved the ciliary body.

## RESULTS

---

Tumor regrowth occurred in 62 patients, approximately 3% of the cohort. Of these, 45 were documented by ultrasonography and/or sequential fundus photography. A total of 17 cases were enucleated outside the Ocular Oncology Unit at MEEI. Of the confirmed cases, 27 eyes were enucleated. Median follow-up was 5.2 years. Time to recurrence ranged between 2 months and 11.3 years after proton irradiation. Of the 45 documented cases, close to half (47%) occurred at the tumor margin. The remaining cases included nine extrascleral extensions, six ring melanomas, and nine tumors exhibiting growth in all dimensions.

As shown in Table I, the highest rate of failure, 1.0%, was observed during the first year after therapy. Annual rates declined thereafter to less than 1% in subsequent years after therapy (Figure 1). Late recurrences were rare and occurred as long as 11 years after therapy. Cumulative rates of recurrence, illustrated in Table I and Figure 2, were likewise low. By 5 years after irradiation, approximately 3% of tumors had recurred. After 5 years, the cumulative rate increased little over time, with 10- and 15-year rates at 4% and 5%, respectively.

Statistically significant prognostic factors (Table II) identified in the univariate regression analysis were tumor diameter, tumor height, ciliary body involvement of the tumor, and tumor pigmentation. Factors of borderline significance included symptoms at presentation ( $P=.09$ )

TABLE I: ANNUAL AND CUMULATIVE RATES OF LOCAL FAILURE\*

YEAR AFTER THERAPY	NO. AT RISK	NO. OF FAILURES	ANNUAL RATES (%)	CUMULATIVE RATES (%)	95% CI
1	1,917	19	1.02	1.02	0.65-1.60
2	1,791	16	0.95	1.96	1.41-2.72
3	1,563	8	0.55	2.50	1.86-3.36
4	1,333	6	0.48	2.97	2.24-3.92
5	1,172	3	0.28	3.24	2.47-4.24
6	975	6	0.67	3.88	2.99-5.03
7	822	0	0.00	3.88	2.99-5.03
8	690	1	0.16	4.03	3.10-5.23
9	578	0	0.00	4.03	3.10-5.23
10	477	1	0.23	4.25	3.25-5.55
11	386	1	0.29	4.53	3.43-5.98
12	299	1	0.38	4.90	3.64-6.57
13	221	0	0.00	4.90	3.64-6.57
14	148	0	0.00	4.90	3.64-6.57
15	95	0	0.00	4.90	3.64-6.57

CI, confidence interval.

\*Includes documented and suspected cases.

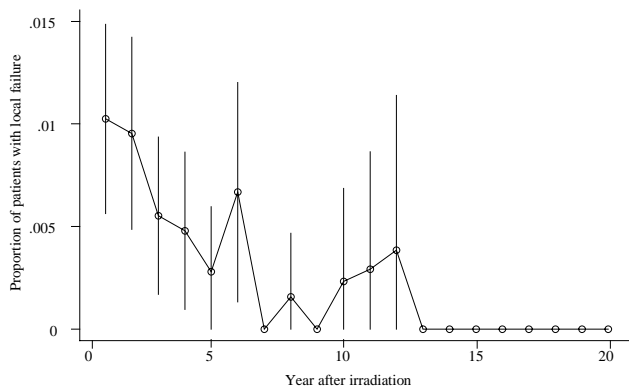


FIGURE 1

Annual rates of local failure after proton therapy, with 95% confidence intervals. Documented and suspected cases of recurrence are included.

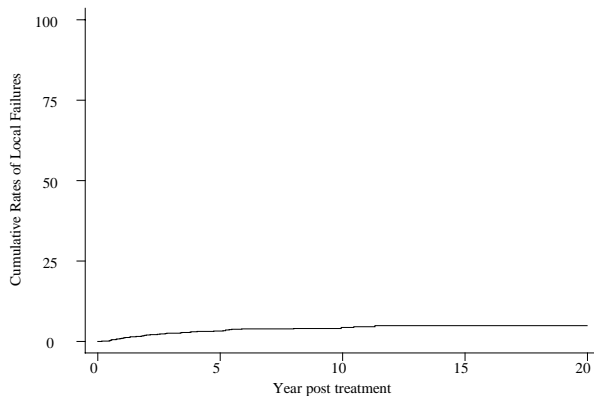


FIGURE 2

Cumulative rates of local failure after proton therapy. Documented and suspected cases of recurrence are included.

and presence or absence of extrascleral extension of the tumor ( $P=.06$ ). Eye color, age at treatment, and male or female gender were not associated with local failure.

In a multivariate analysis, we selected variables that were statistically significant ( $P \leq .05$ ) in univariate regression to enter in our model. These included tumor pigmentation, a composite tumor size variable (tumors  $>15$  mm in diameter and  $>5$  mm in height were defined as large), and ciliary body involvement, the strongest predictor of regrowth of the three variables. Tumor pigmentation was not independently associated with recurrence and was dropped from the model. Large tumors and tumors involving the ciliary body continued to be significant risk factors for recurrence in the multivariate analysis. Patients with large tumors had more than double the risk of recurrence of patients with smaller tumors (RR, 2.4; 95% CI, 1.4-4.1). Similarly, a patient's risk of treatment failure was more than doubled if the tumor involved the ciliary body rather than the choroid only (RR, 2.3; 95% CI, 1.3-4.1).

Patients experiencing tumor regrowth were at greater risk of death from metastasis. After adjustments for known risk factors for metastatic death (eg, tumor size, age, location of tumor), tumor growth was demonstrated to be highly predictive of metastatic death in a Cox regression model. The relative risk of metastasis-related death was 4.1 (95% CI, 2.6-6.6) for patients with documented growth as compared to patients who did not experience recurrence.

DISCUSSION

Results of this study confirm reports of our previous studies<sup>7,27</sup> and demonstrate that rates of regrowth decrease

TABLE II: UNIVARIATE ANALYSIS OF PROGNOSTIC FACTORS FOR LOCAL FAILURE\*

RISK FACTOR	LEVEL	RR	95% CI	P VALUE
Age	1 yr	1.01	0.99-1.03	.34
Gender	Male vs female	0.93	0.57-1.54	.79
Largest tumor diameter	1 mm	1.16	1.09-1.23	.000
Tumor height	1 mm	1.18	1.09-1.28	.000
Ciliary body involvement	No vs yes	3.35	2.03-5.51	.000
Symptoms	No vs yes	1.32	0.96-1.81	.09
Extrascleral extension	No vs yes	2.60	0.94-7.17	.065
Tumor pigmentation	None/minimal	Ref†	. . .	. . .
	Moderate	2.88	0.82-10.11	.10
	Heavy	4.74	1.44-15.64	.01
Eye color	Brown	Ref†	. . .	. . .
	Green, hazel	1.36	0.63-2.94	.44
	Blue, gray	1.31	0.63-2.71	.47

CI, confidence interval; RR, relative risk.

\*Includes documented and suspected cases.

†Referent.

with time after therapy for patients treated by protons for intraocular melanoma. Tumor recurrences may occur many years after therapy, but in this patient series none was observed after 12 years. Our findings are also consistent with reports of our group<sup>19</sup> and others,<sup>28,29</sup> identifying local recurrence after radiotherapy as a prognostic indicator for tumor-related survival.

We found that patients with ciliary body involvement and large tumors were at increased risk of local failure. One possible explanation for an increased risk of regrowth in tumors involving the ciliary body may be the increased likelihood of treatment planning errors, since visualization of the tumor margins by transillumination is more difficult when the ciliary body is involved. If this were the case, one would expect to find an overrepresentation of ciliary body tumors classified as marginal recurrences. Although over 50% of marginal recurrences involved the ciliary body, the majority of all other types of recurrences also involved the ciliary body (78%, 67%, and 44% for extrascleral extensions, ring melanomas, and uncontrolled tumors, respectively); this fact suggests that factors other than—or in addition to—inadequate radiation of the tumor are responsible for the tendency of ciliary body tumors to grow.

Studies by Folberg and colleagues<sup>30,31</sup> have demonstrated that tumor vascular networks are associated with an increased risk of metastasis and that these markers of a more aggressive tumor are found more often in ciliary body tumors.<sup>32</sup> It is possible that these vascular networks enhance the tumor's ability to regrow as well as to disseminate to other organs. Additionally, certain genetic aberrations—monosomy 3, losses of chromosome arms 6q and 1p, and additional copies of arm 8q—have been shown to be associated with metastatic uveal melanoma,<sup>33,34</sup> and alterations on chromosomes 3 and 8 in particular appear more commonly in ciliary body tumors.<sup>33,35</sup> Similar cytogenetic analyses have not been performed with samples from patients with tumor recurrences. These same mutations may be identified in association with regrowth if such analyses were to be completed.

Large tumors may be at increased risk of regrowth because they may be less radiosensitive than smaller tumors. This decrease in radiosensitivity may occur if tumor growth outpaces proliferation of tumor vasculature, thereby reducing its blood supply and the oxygenation that is necessary to optimize radiation effects.<sup>36</sup> Smaller tumors are less likely to be rendered radioresistant because they may have a more viable vasculature and thus the ability to reoxygenate. In this series, over half (56%) of the true in-field recurrences (“uncontrolled tumors” [ie, tumors with growth in height and diameter] and tumors developing extrascleral extension) occurred in larger tumors. Marginal recurrences were only somewhat less likely to involve tumors of this size (48%). In contrast, most patients with large tumors (94%)

in this series did not experience local failure. This is not unexpected, given that these patients were treated with a total dose of 70 Gy in five fractions, one of the highest doses used in external beam irradiation for any malignancy.<sup>37</sup> It may be that only a small subset of these larger tumors is radioresistant, and it is these tumors that recur.

Patients with large tumors and tumors involving the ciliary body are at increased risk not only for tumor regrowth but also for metastasis, and this increased risk is independent of local failure status.<sup>38-41</sup> Further, local recurrence is an independent prognostic factor for metastasis-related death. This suggests that local recurrence and metastasis are not interdependent outcomes. We can speculate that underlying mechanisms, which optimize viability and proliferation of these tumors, may affect malignant potential at both local and distant sites. Underlying angiogenic mechanisms may play a role by controlling growth of the primary tumor as well as growth in metastatic foci.<sup>42</sup> Primary tumors may produce angiogenic factors that inhibit angiogenesis at distant sites.<sup>43</sup> In the case of enucleation, removal of the primary tumor may halt production of angiogenesis inhibitors, allowing metastasis to occur in the presence of local control. On the other hand, patients who experience local failure after radiotherapy harbor tumors that continue to proliferate, with a higher risk of dissemination of tumor cells to distant sites. This may explain why we continue to observe rates of metastasis-related death in patients treated by enucleation that are similar to those rates achieved with radiation,<sup>14-17</sup> and suggests that metastases may develop through several mechanisms. An alternative explanation may be that tumors that recur are highly malignant and have already developed pre-clinical metastases before any therapeutic intervention, irradiation, or enucleation.

## CONCLUSIONS

These data demonstrate that excellent local control is achieved after proton irradiation of choroidal and ciliary body tumors. In this large series of patients with relatively long-term follow-up, annual and cumulative rates of regrowth were quite low, with most recurrences developing within a few years of treatment. The cumulative rate of recurrence was approximately 3% at 5 years postirradiation. This rate increased 1% between 5 and 10 years posttherapy and increased less than 1% after 10 years. Large tumors and tumors involving the ciliary body were independent predictors of regrowth, and regrowth was associated with poorer survival. It should be noted that because of the infrequency of this outcome, our findings might be due to chance, particularly with regard to multivariate analysis of risk factors. On the other hand, our results are consistent with those in previously published reports.<sup>7,19,27-29</sup>

Future refinements in treatment planning, dosing

regimen, and delivery may reduce the rate of local failure. Further exploration of underlying mechanisms of tumor cell growth is necessary to determine the pathophysiology of local failure. Elucidation of such mechanisms may lead to more effective interventions to arrest progression.

## REFERENCES

1. Scotto J, Fraumeni JF Jr, Lee JA. Melanomas of the eye and other noncutaneous sites: epidemiologic aspects. *J Natl Cancer Inst* 1976;56(3):489-491.
2. Melia BM, Abramson DH, Albert DM, et al. Collaborative ocular melanoma study (COMS) randomized trial of I-125 brachytherapy for medium choroidal melanoma. I. Visual acuity after 3 years. COMS report No. 16. *Ophthalmology* 2001;108(2):348-366.
3. Shields CL, Shields JA, Cater J, et al. Plaque radiotherapy for uveal melanoma: long-term visual outcome in 1106 consecutive patients. *Arch Ophthalmol* 2000;118(9):1219-1228.
4. Gragoudas ES. 1996 Jules Gonin Lecture of the Retina Research Foundation. Long-term results after proton irradiation of uveal melanomas. *Graefes Arch Clin Exp Ophthalmol* 1997;235(5):265-267.
5. Char DH, Kroll S, Quivey JM, et al. Long term visual outcome of radiated uveal melanomas in eyes eligible for randomisation to enucleation versus brachytherapy. *Br J Ophthalmol* 1996;80(2):117-124.
6. Augsburger JJ, Goel SD. Visual function following enucleation or episcleral plaque radiotherapy for posterior uveal melanoma. *Arch Ophthalmol* 1994;112(6):786-789.
7. Gragoudas ES, Egan KM, Seddon JM, et al. Intraocular recurrence of uveal melanoma after proton beam irradiation. *Ophthalmology* 1992;99(5):760-766.
8. Castro JR, Char DH, Petti PL, et al. 15 years experience with helium ion radiotherapy for uveal melanoma. *Int J Radiat Oncol Biol Phys* 1997;39(5):989-996.
9. Egger E, Schalenbourg A, Zografos L, et al. Maximizing local tumor control and survival after proton beam radiotherapy of uveal melanoma. *Int J Radiat Oncol Biol Phys* 2001;51(1):138-147.
10. Karlsson UL, Augsburger JJ, Shields JA, et al. Recurrence of posterior uveal melanoma after 60Co episcleral plaque therapy. *Ophthalmology* 1989;96(3):382-388.
11. Hill JC, Sealy R, Shackleton D, et al. Improved iodine-125 plaque design in the treatment of choroidal malignant melanoma. *Br J Ophthalmol* 1992;76(2):91-94.
12. Quivey JM, Augsburger J, Snelling L, et al. 125I plaque therapy for uveal melanoma. Analysis of the impact of time and dose factors on local control. *Cancer* 1996;77(11):2356-2362.
13. Char DH, Quivey JM, Castro JR, et al. Helium ions versus iodine 125 brachytherapy in the management of uveal melanoma. A prospective, randomized, dynamically balanced trial. *Ophthalmology* 1993;100(10):1547-1554.
14. Seddon JM, Gragoudas ES, Egan KM, et al. Relative survival rates after alternative therapies for uveal melanoma. *Ophthalmology* 1990;97(6):769-777.
15. Adams KS, Abramson DH, Ellsworth RM, et al. Cobalt plaque versus enucleation for uveal melanoma: comparison of survival rates. *Br J Ophthalmol* 1988;72(7):494-497.
16. Augsburger JJ, Correa ZM, Freire J, et al. Long-term survival in choroidal and ciliary body melanoma after enucleation versus plaque radiation therapy. *Ophthalmology* 1998;105(9):1670-1678.
17. Diener-West M, Earle JD, Fine SL, et al. The COMS randomized trial of iodine 125 brachytherapy for choroidal melanoma, III: Initial mortality findings. COMS report No. 18. *Arch Ophthalmol* 2001;119(7):969-982.
18. Munzenrider JE. Uveal melanomas. Conservation treatment. *Hematol Oncol Clin North Am* 2001;15(2):389-402.
19. Egan KM, Ryan LM, Gragoudas ES. Survival implications of enucleation after definitive radiotherapy for choroidal melanoma: an example of regression on time-dependent covariates. *Arch Ophthalmol* 1998;116(3):366-370.
20. Suit HD. Local control and patient survival. *Int J Radiat Oncol Biol Phys* 1992;23(3):653-660.
21. Gragoudas ES, Goitein M, Koehler A, et al. Proton irradiation of choroidal melanomas: preliminary results. *Arch Ophthalmol* 1978;96:1583-1591.
22. Gragoudas ES, Goitein M, Verhey L, et al. Proton beam irradiation of uveal melanomas: results of 5 1/2-year study. *Arch Ophthalmol* 1982;100(6):928-934.
23. Gragoudas ES, Seddon J, Goitein M, et al. Current results of proton beam irradiation of uveal melanomas. *Ophthalmology* 1985;92(2):284-291.
24. Gragoudas ES, Lane AM, Regan S, et al. A randomized controlled trial of varying radiation doses in the treatment of choroidal melanoma. *Arch Ophthalmol* 2000;118(6):773-778.
25. Kaplan E, Meier P. Nonparametric estimation from incomplete observations. *J Am Stat Assoc* 1958;53:457-481.
26. Cox D. Regression models and life-tables. *J R Stat Soc Ser* 1972;34:187-220.
27. Munzenrider JE, Verhey LJ, Gragoudas ES, et al. Conservative treatment of uveal melanoma: local recurrence after proton beam therapy. *Int J Radiat Oncol Biol Phys* 1989;17(3):493-498.
28. Vrabec TR, Augsburger JJ, Gamel JW, et al. Impact of local tumor relapse on patient survival after cobalt 60 plaque radiotherapy. *Ophthalmology* 1991;98(6):984-988.
29. Harbour JW, Char DH, Kroll S, et al. Metastatic risk for distinct patterns of postirradiation local recurrence of posterior uveal melanoma. *Ophthalmology* 1997;104(11):1785-1792.
30. Folberg R, Rummelt V, Parys-Van Ginderdeuren R, et al. The prognostic value of tumor blood vessel morphology in primary uveal melanoma. *Ophthalmology* 1993;100(9):1389-1398.
31. Folberg R, Mehaffey M, Gardner LM, et al. The microcirculation of choroidal and ciliary body melanomas. *Eye* 1997;11(Pt 2):227-238.
32. Rummelt V, Folberg R, Woolson RF, et al. Relation between the microcirculation architecture and the aggressive behavior of ciliary body melanomas. *Ophthalmology* 1995;102(5):844-851.
33. Sisley K, Rennie IG, Parsons MA, et al. Abnormalities of chromosomes 3 and 8 in posterior uveal melanoma correlate with prognosis. *Genes Chromosomes Cancer* 1997;19(1):22-28.
34. Aalto Y, Eriksson L, Seregard S, et al. Concomitant loss of chromosome 3 and whole arm losses and gains of chromosome 1, 6, or 8 in metastasizing primary uveal melanoma. *Invest Ophthalmol Vis Sci* 2001;42(2):313-317.

35. Sisley K, Cottam DW, Rennie IG, et al. Non-random abnormalities of chromosomes 3, 6, and 8 associated with posterior uveal melanoma. *Genes Chromosomes Cancer* 1992;5(3):197-200.
36. Withers HR. Biological basis of radiation therapy for cancer. *Lancet* 1992;339(8786):156-159.
37. Suit H, Urie M. Proton beams in radiation therapy. *J Natl Cancer Inst* 1992;84(3):155-164.
38. Kroll S, Char DH, Quivey J, et al. A comparison of cause-specific melanoma mortality and all-cause mortality in survival analyses after radiation treatment for uveal melanoma. *Ophthalmology* 1998;105(11):2035-2045.
39. Gragoudas ES, Seddon JM, Egan KM, et al. Prognostic factors for metastasis following proton beam irradiation of uveal melanomas. *Ophthalmology* 1986;93(5):675-680.
40. Gragoudas ES, Seddon JM, Egan KM, et al. Metastasis from uveal melanoma after proton beam irradiation. *Ophthalmology* 1988;95(7):992-999.
41. Li W, Gragoudas ES, Egan KM. Metastatic melanoma death rates by anatomic site after proton beam irradiation for uveal melanoma. *Arch Ophthalmol* 2000;118(8):1066-1070.
42. Folkman J. Angiogenesis in cancer, vascular, rheumatoid and other disease. *Nat Med* 1995;1(1):27-31.
43. O'Reilly MS, Holmgren L, Shing Y, et al. Angiostatin: a novel angiogenesis inhibitor that mediates the suppression of metastases by a Lewis lung carcinoma. *Cell* 1994;79(2):315-328.

## DISCUSSION

---

DR JAMES J. AUGSBURGER. The paper you just heard was based on more cases and slightly longer follow-up than prior reports on the same patient group by the same principal author and his coworkers. It otherwise contains no pertinent new information and provides no new insights about local relapses following proton beam irradiation.

The authors show us that the highest annual incidence of local relapses after proton beam irradiation of choroidal and ciliary body melanomas occurs during the first post-irradiation year and that annual incidence then decreases progressively thereafter. They also show us (as they have shown before) that the cumulative actuarial incidence of local relapse after proton beam irradiation is quite low, only about 5% at 15 years. They point out, as they have also done before, that this cumulative actuarial incidence of local relapse after proton beam irradiation is substantially lower than that reported after plaque radiotherapy.

The authors show us that larger tumors and those involving the ciliary body are associated with higher rates of metastasis and metastatic death than are smaller tumors and those that do not involve the ciliary body. Many authors have reported these findings over the past half-century.

The authors show us that patients who experienced local relapse had higher rates of metastasis and metastatic death than did patients who did not experience local relapse. Several groups have also reported this result pre-

viously, including Dr Gragoudas's group, since Dr Ulf Karlsson and I first described this phenomenon in 1989. The authors state (but do not present sufficient information to allow readers to verify) that local relapse is a significant prognostic factor for subsequent metastasis and metastatic death even after controlling for tumor size and tumor location in the ciliary body. This result also confirms what others and I have reported previously.

The authors state that they employed a time-varying Cox proportional hazards modeling method to control (adjust) for important prognostic covariates in this study. However, they did not indicate specifically how they set up this analysis or how they evaluated local relapse as a time-varying variable in this study. I suspect that most persons in this audience do not care about this, do not understand why this might be important, or both. Because of this, I will not expand on this point except to call it to the attention of the authors.

None of the foregoing comments should be taken as personal criticism of Dr Gragoudas, his group, or their work. I have the utmost respect for Dr Gragoudas and the work he and his group have done over the years. I am honored to comment on their work.

DR EVANGELOS GRAGOUDAS. I appreciate the opportunity to respond to Dr Augsburger's comments regarding our paper entitled "Long-term Risk of Local Failure after Proton Therapy for Choroidal/Ciliary Body Melanoma." Dr Augsburger states in his discussion that these findings have been reported previously. However, most analyses in previous studies have been limited to small patient series, with actuarial rates beyond 5 years rarely reported. In this large series of 1,922 patients, we demonstrate low rates of recurrence at 10 years (4%) and 15 years (5%) posttherapy, providing evidence that refutes the theory that in these irradiated tumors reproductive activity has not been suppressed.<sup>1</sup>

As Dr Augsburger points out, there have been other studies indicating that ciliary body involvement and large tumors increase risk of metastasis and metastatic death. However, in our paper, we focused our analysis on the influence of local recurrence on metastatic death, while controlling for the already known risk factors. We described using a multivariate Cox regression model to calculate relative risk; we estimated a fourfold increase (RR=4.1, 95% CI, 2.6-6.6) in risk of metastasis-related death for patients with documented tumor recurrence as compared to patients without a recurrence. Further, we used a more accurate statistical approach, evaluating recurrence as a time-varying covariate in a Cox regression model. We have previously demonstrated the value of this approach in measuring relative risk, and interested parties who may want to understand more about this analytic method should refer to the publication by Egan et al.<sup>2</sup>

**REFERENCES**

---

1. Manschot WA, Lee WR, van Strik R. Uveal melanoma: updated considerations on current management modalities. *Int Ophthalmol* 1996;19:203-209.
2. Egan KM, Ryan LM, Gragoudas ES. Survival implications of enucleation after definitive radiotherapy for choroidal melanoma. *Arch Ophthalmol* 1998;116:366-370.



# SUTURING TECHNIQUE FOR CONTROL OF POSTKERATOPLASTY ASTIGMATISM AND MYOPIA

---

BY *Dilek Dursun, MD* (BY INVITATION), *Richard K. Forster, MD*, AND *William J. Feuer, MS* (BY INVITATION)

## ABSTRACT

*Purpose:* We previously demonstrated that selective suture removal reduces keratoplasty astigmatism; however, a myopic shift was induced with increasing number of interrupted sutures removed. This study is an attempt to determine the effects of a modified surgical technique on postkeratoplasty myopia, astigmatism, and anisometropia.

*Methods:* Optical penetrating keratoplasties were performed on 92 eyes of 84 patients. The study group consisted of 92 consecutive penetrating keratoplasties performed using 12 interrupted 10-0 nylon sutures and a tight 12-bite continuous suture, and use of an average keratometry (K) reading of 46.00 diopters for eyes undergoing combined and intraocular lens (IOL) exchange procedures. All patients had refraction, keratometry, and videokeratometry postoperatively, starting at 6 weeks and at the completion of selective suture removal.

*Results:* Prior to suture removal, the average spherical equivalent was  $-0.160 \pm 3.59$  diopters. It was  $-1.58 \pm 3.66$  diopters at the completion of suture removal at 1 year and  $-1.44 \pm 3.72$  at the last follow-up visit, averaging 20.7 months. Final residual refractive, keratometric, and videokeratometric astigmatism was  $2.81 \pm 1.82$ ,  $4.19 \pm 2.94$ , and  $3.58 \pm 2.03$  diopters, respectively. Anisometropia, using the spherical equivalent of the operated and fellow eyes, was  $2.49 \pm 2.25$  diopters at completion of the study. A best corrected visual acuity of 20/50 or better was achieved in 50 patients (59%).

*Conclusions:* Low myopic spherical equivalent refraction and anisometropia with moderate residual astigmatism were achieved by using tighter continuous sutures, an average K reading of 46 diopters for calculation of IOL power, and selective removal of fewer sutures.

*Trans Am Ophthalmol Soc* 2002;100:51-60

## INTRODUCTION

---

Postoperative astigmatism, residual myopia, and anisometropia often determine the functional visual outcome in an otherwise successful penetrating keratoplasty. Visually successful surgery requires the reduction of astigmatism and unexpected resultant anisometropia.

The suture techniques of single or double continuous and of combined interrupted and continuous have been examined in regard to early visual rehabilitation and measurement of astigmatism, as well as final all-suture-out residual astigmatism. Reports to date differ somewhat as to which technique results in the least astigmatism and induced myopia and the earliest rehabilitation, but each usually requires either adjustment of the continuous sutures or selective removal of interrupted sutures.<sup>1-20</sup>

Laser in situ keratomileusis has become increasingly popular in the attempt to correct postoperative myopia and astigmatism.<sup>21-25</sup> However, surgical techniques and postoperative suture manipulation have not been successful in reliably reducing astigmatism and myopia. Studies to evaluate operative and postoperative techniques to

minimize visually compromising anisometropia have not been addressed to date.

We previously demonstrated that removal of selective interrupted sutures reduces keratoplasty astigmatism; however, a myopic shift was induced with increasing number of interrupted sutures removed.<sup>26</sup> The outcomes of two selective suture removal techniques were compared. In one group, removal of six alternate interrupted sutures at 6 weeks, and subsequent selective removal based on refraction, keratometry, and videokeratometry, was performed. In the other group, selective removal of interrupted sutures at the steepest meridian at 6 weeks, with repeated removal at subsequent postoperative visits, was performed. The data demonstrated that selective removal by either technique reduces keratoplasty astigmatism to 2.7 diopters or less at 1 year, with residual interrupted and continuous sutures in place. The myopic shift induced with increasing number of interrupted sutures removed resulted in an average keratometry (K) reading of 47.4 diopters in the group with more sutures removed and 46.0 diopters in the group with fewer selective sutures removed.

These results lead to the hypothesis that more interrupted sutures could be left in place, the continuous suture could be tighter, and the average predicted K

From the Department of Ophthalmology, Bascom Palmer Eye Institute, University of Miami School of Medicine, Miami, Florida.

reading could be increased for eyes undergoing intraocular lens (IOL) placement or exchange to better reduce postkeratoplasty myopia and yet control astigmatism. The present study is an attempt to determine the effects of such a modified technique on postkeratoplasty myopia, astigmatism, and anisometropia.

## **MATERIALS AND METHODS**

---

Optical penetrating keratoplasties were performed on 92 eyes of 84 patients. The study group consisted of consecutive penetrating keratoplasties performed using 12 interrupted 10-0 nylon sutures and a tight 12-bite, 10-0 nylon continuous suture, and use of an average K reading of 46.00 diopters for eyes undergoing combined and IOL exchange procedures. All patients had refraction, keratometry, and videokeratometry measurements postoperatively, starting at 6 weeks and at the completion of suture removal. Six weeks postoperatively, patients underwent selective suture removal only at the steepest meridian, if associated with greater than 3 diopters of astigmatism in that meridian. This investigation was approved by the institutional review board at the University of Miami School of Medicine.

### **SURGICAL TECHNIQUE**

All eyes underwent penetrating keratoplasty by the same surgeon (R.K.F), who prepared the donor tissue endothelial side up and used a gravity trephine with a Katena blade (7.75 to 8.25 mm). The recipient cornea was trephined to a depth of approximately 0.4 mm with a Storz guarded trephine with disposable blade (7.5 to 8 mm), and recipient corneal removal was completed with scissors. All donor corneal tissue was trephined 0.25 mm larger than the recipient trephination, except for patients with primary keratoconus, in which case same-size donor-host trephination was performed. The first four interrupted sutures were placed such that an equal-sided "square" was barely visible on the donor tissue, each suture bite was about the same tightness, and interrupted sutures were placed, at about three-quarters depth, two fifths within the donor and three fifths within the recipient. The 12-bite 10-0 nylon continuous suture was then placed somewhat more tightly than the interrupted sutures after adjustment of the intraocular pressure to approximately normal tension.

All eyes undergoing combined keratoplasty and cataract extraction, or IOL exchange procedures, had IOL power calculations using a predicted postkeratoplasty average K reading of 46.00 diopters (based on the results of our previous study<sup>11</sup>).

### **SELECTIVE SUTURE REMOVAL**

Patients underwent selective removal of sutures at the steepest meridian, if associated with greater than 3

diopters of astigmatism starting at 6 weeks postoperatively. One of two sutures in a particular meridian was removed if the topographic analysis indicated that only one of the two appeared to be tight in the steeper meridian. Interrupted sutures were then selectively removed on follow-up visits until the resultant astigmatism and overall refractive spherical equivalent best minimized anisometropia. Follow-up visits usually occurred every 4 to 6 weeks for the first 6 months postoperatively, within 1 month following selective suture removal, and then every 3 to 4 months. With patients under topical anesthesia, sutures were removed with use of a jeweler's forceps and razor blade. Antibiotic drops were applied with no patching or continuation of topical antibiotics, but with continuation of topical prednisolone acetate, or other steroid drops, at the same frequency as previously used, and of ocular hypertension-lowering agents as necessary. Refraction, keratometry, and videokeratometry measurements were performed by optometrists and/or allied health personnel.

### **DATA PARAMETERS**

All astigmatic and visual acuity data were analyzed at 6 weeks postoperatively, prior to any suture removal, after the initial sutures were removed, at 6 months postoperatively, after final selective interrupted sutures were removed, and at the final visit.

Manifest refraction was analyzed in terms of spherical equivalent, keratometric, and videokeratometric parameters; simulated keratometry (Sim K); surface regularity index (SRI); and surface asymmetry index (SAI).

For comparative purposes, the 92 eyes included in this study are referred to as *Current Study*. *Prior Study* represents those eyes in the selective suture removal group from the previous study.<sup>11</sup>

In the *Current Study*, spherical equivalent results of those eyes in which an IOL was placed at the time of penetrating keratoplasty were compared to those of eyes without IOL placement. In addition, we compared the spherical equivalent results of eyes undergoing IOL placement in the *Prior Study*, using an average K reading of 45.00 diopters, to those in the *Current Study*, in which an average K reading of 46.00 diopters was used.

### **STATISTICAL METHODS**

For each dependent variable (spherical equivalent and all astigmatism measures), the two-sample *t* test was used to compare values at each follow-up time.

## **RESULTS**

---

### **DEMOGRAPHICS, DIAGNOSES, AND PROCEDURES**

The study includes 92 eyes of 84 patients, and mean follow-up time is 20.7 months (range, 6-36 months). The

demographics included the following: 33 males (39%) and 51 females (61%); 47 right eyes (51%) and 45 left eyes (49%); and mean age, 73 years (range, 26-95 years). The preoperative diagnoses were pseudophakic corneal edema (44%), Fuchs' endothelial dystrophy with cataract (19%), aphakic corneal edema (2%), keratoconus (5%), corneal scars (9%), reoperations for failed grafts (17%), and other diagnoses, including corneal degenerations and iridocorneoendothelial syndrome (4%).

A penetrating keratoplasty only was performed in 51 eyes (56%) and a triple procedure combining a penetrating keratoplasty with extracapsular cataract extraction and IOL implantation in 22 eyes (24%). An IOL exchange was performed in 16 eyes (17%), and a secondary IOL insertion was performed in 3 eyes (3%).

**POSTOPERATIVE SPHERICAL EQUIVALENT**

The spherical equivalent prior to selective suture removal was  $-0.16 \pm 3.59$  diopters. About 1 month following selective suture removal, it was  $-0.30 \pm 3.57$  diopters; at 6 months, it was  $-1.32 \pm 3.96$  diopters; and at the completion of selective suture removal, it was  $-1.58 \pm 3.66$  diopters. At the final visit the spherical equivalent was  $-1.44 \pm 3.72$  diopters (Figure 1).

Low myopic spherical equivalent refraction could be achieved after selective suture removal, and there was somewhat more control over the postoperative residual

myopia compared to the *Prior Study* ( $P = .27$ ) at 6 months and at the last follow-up visit ( $P = .19$ ) (Table I).

**THE ROLE OF IOL POWER**

We used an average K reading of 45.00 diopters in the *Prior Study* and 46.00 diopters in the *Current Study* for calculation of IOL power to use in combined, IOL exchange, and secondary IOL cases. We compared the spherical equivalent results at the five postoperative intervals for those eyes in which an IOL was placed at the time

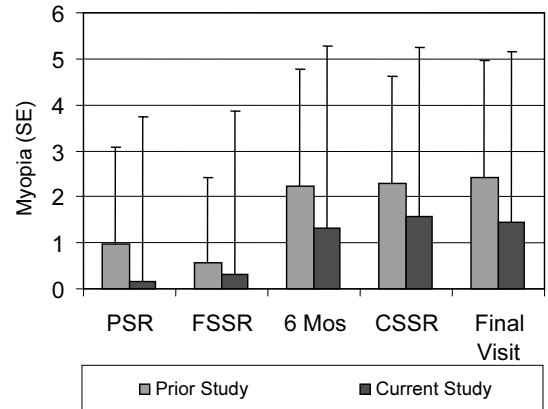


**FIGURE 1**

Postoperative myopic refractive spherical equivalent (CSSR, completion of selective suture removal; FSSR, following selective suture removal; PSR, prior to suture removal).

**TABLE I: SPHERICAL EQUIVALENT AND ASTIGMATISM AT FOLLOW-UP INTERVALS**

VARIABLE	SUTURE TYPE	PSR	FSSR	6 MO	CSSR	LAST VISIT
Spherical equivalent	Prior study	$-0.97 \pm 2.11$	$-0.58 \pm 1.83$	$-2.23 \pm 2.54$	$-2.28 \pm 2.34$	$-2.41 \pm 2.56$
	Current study	$-0.16 \pm 3.59$	$-0.30 \pm 3.57$	$-1.32 \pm 3.96$	$-1.58 \pm 3.66$	$-1.44 \pm 3.72$
	P value	.14	.60	.27	.25	.19
Refractive astigmatism	Prior study	$4.23 \pm 3.08$	$3.32 \pm 1.90$	$2.24 \pm 1.73$	$2.18 \pm 1.14$	$2.05 \pm 1.04$
	Current study	$5.13 \pm 2.60$	$3.76 \pm 2.37$	$3.07 \pm 2.02$	$2.56 \pm 1.74$	$2.81 \pm 1.82$
	P value	.13	.37	.049	.20	.008
Keratometry	Prior study	$5.48 \pm 2.75$	$3.70 \pm 2.14$	$2.59 \pm 2.34$	$2.12 \pm 1.28$	$2.02 \pm 0.93$
	Current study	$7.17 \pm 3.95$	$4.86 \pm 3.18$	$4.34 \pm 3.00$	$3.98 \pm 3.09$	$4.19 \pm 2.94$
	P value	.14	.11	.031	<.001	<.001
Simulated K	Prior study	$6.10 \pm 2.82$	$4.49 \pm 2.61$	$3.67 \pm 1.88$	$2.27 \pm 1.07$	$2.33 \pm 1.20$
	Current study	$7.13 \pm 3.93$	$5.18 \pm 3.24$	$3.64 \pm 2.56$	$3.29 \pm 2.36$	$3.58 \pm 2.03$
	P value	.18	.28	.95	.039	.001
SRI	Prior study	$1.82 \pm 0.43$	$1.58 \pm 0.48$	$1.45 \pm 0.47$	$1.32 \pm 0.46$	$1.13 \pm 0.40$
	Current study	$1.76 \pm 0.47$	$1.55 \pm 0.53$	$1.40 \pm 0.53$	$1.28 \pm 0.47$	$1.29 \pm 0.53$
	P value	.53	.77	.70	.75	.21
SAI	Prior study	$1.68 \pm 0.77$	$1.58 \pm 1.12$	$1.33 \pm 0.87$	$1.07 \pm 0.51$	$1.06 \pm 0.46$
	Current study	$1.72 \pm 0.99$	$1.50 \pm 0.98$	$1.39 \pm 1.07$	$1.29 \pm 0.95$	$1.31 \pm 0.93$
	P value	.85	.72	.84	.16	.28

CSSR, completion of selective suture removal; FSSR, following selective suture removal; PSR, prior to suture removal; SAI, surface asymmetry index; SRI, surface regularity index.

of the penetrating keratoplasty procedure and those eyes without IOL placement. Table II demonstrates the comparative results. Where significant, IOL placement in the Current Group has lower myopia; the difference, however, was not significant at the final examination.

Finally, we compared IOL placement alone in both the *Prior Study* and the *Current Study* (average K, 45.00 diopters versus 46.00 diopters). Table III shows that IOL placement has less induced myopia at all but the final visit; however, the results were statistically significant at only the presuture removal visit and were borderline at 6 months.

**POSTOPERATIVE ASTIGMATISM**

Prior to suture removal (PSR) at 6 weeks, the mean refractive astigmatism was  $5.13 \pm 2.60$  diopters, keratometric astigmatism was  $7.17 \pm 3.95$  diopters, and simulated K was  $7.13 \pm 3.93$  diopters (Figures 2, 3, and 4). Following initial

**TABLE II: SPHERICAL EQUIVALENT COMPARISON BETWEEN IOL AND NO IOL GROUPS AT FOLLOW-UP INTERVALS**

MEASUREMENT TIME	GROUP	SPHERICAL EQUIVALENT MEAN (SD)	P VALUE
PSR	IOL	1.3 (2.7)	<.001
	No IOL	-1.3 (3.8)	
FSSR	IOL	0.4 (3.2)	.14
	No IOL	-0.8 (4.0)	
6 Mo	IOL	-0.1 (2.9)	.005
	No IOL	-2.5 (4.4)	
CSSR	IOL	-0.6 (3.0)	.017
	No IOL	-2.5 (4.0)	
Final	IOL	-1.0 (3.1)	.34
	No IOL	-1.8 (4.2)	

CSSR, completion of selective suture removal; FSSR, following selective suture removal; IOL, intraocular lens; PSR, prior to suture removal.

**TABLE III: SPHERICAL EQUIVALENT COMPARISON BETWEEN PRIOR STUDY AND CURRENT STUDY FOR EYES WITH IOL PLACEMENT**

MEASUREMENT TIME	GROUP	SPHERICAL EQUIVALENT MEAN (SD)	P VALUE
PSR	Prior	-0.7 (1.7)	.003
	Current	1.3 (2.7)	
FSSR	Prior	-0.6 (1.4)	.32
	Current	0.4 (3.2)	
6 Mo	Prior	-1.7 (2.0)	.095
	Current	-0.1 (2.9)	
CSSR	Prior	-1.7 (2.3)	.22
	Current	-0.6 (3.0)	
Final	Prior	-1.5 (2.3)	.58
	Current	-1.0 (3.1)	

CSSR, completion of selective suture removal; FSSR, following selective suture removal; PSR, prior to suture removal.

suture removal (FSSR), astigmatic measurements were made about 1 month later and the mean refractive astigmatism was  $3.76 \pm 2.37$  diopters, keratometric astigmatism was  $4.86 \pm 3.18$  diopters, and simulated K was  $5.18 \pm 3.24$  diopters. Six months postoperatively, mean

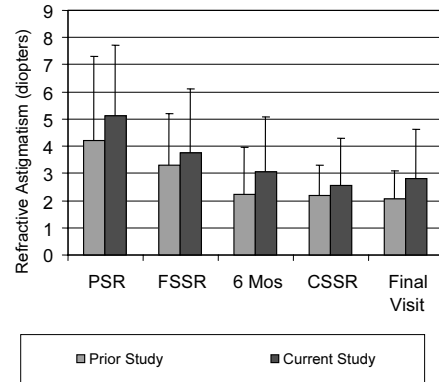


**FIGURE 2**

Postoperative refractive astigmatism equivalent (CSSR, completion of selective suture removal; FSSR, following selective suture removal; PSR, prior to suture removal).

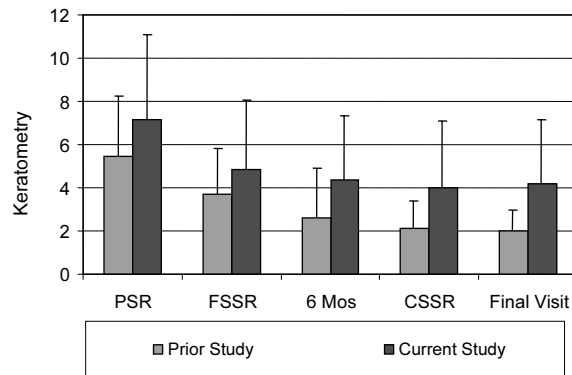


**FIGURE 3**

Postoperative keratometric astigmatism equivalent (CSSR, completion of selective suture removal; FSSR, following selective suture removal; PSR, prior to suture removal).

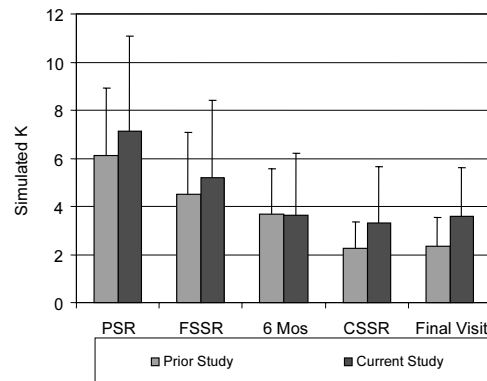


**FIGURE 4**

Postoperative videokeratoscopic astigmatism–simulated keratometry equivalent (CSSR, completion of selective suture removal; FSSR, following selective suture removal; PSR, prior to suture removal).

refractive astigmatism was  $3.07 \pm 2.02$  diopters, keratometric astigmatism was  $4.34 \pm 3.00$  diopters, and simulated K readings were  $3.64 \pm 2.56$  diopters.

After completion of selective suture removal (CSSR), refractive astigmatism was  $2.56 \pm 1.74$  diopters, keratometric astigmatism was  $3.98 \pm 3.09$  diopters, and simulated K was  $3.29 \pm 2.36$  diopters. At the final visit, refractive astigmatism was found to be  $2.81 \pm 1.82$  diopters, keratometric astigmatism was  $4.19 \pm 2.94$  diopters, and simulated K was  $3.58 \pm 2.03$  diopters (Table I).

The reduction in refractive and keratometric astigmatism was found to be statistically significant at 6 months and at the completion of suture removal compared to pre-suture removal measurements ( $P < .001$ ). The difference in the residual refractive astigmatism between the *Prior Study* group, where selective suture removal was used without a tighter continuous suture (average,  $2.05 \pm 1.04$  at final visit) and the *Current Study* group (average,  $2.81 \pm 1.82$  at final visit) was statistically significant ( $P = .008$ ) (Table I). Likewise, keratometric astigmatism and video-keratoscopy astigmatism were statistically different between the two studies.

**SURFACE REGULARITY INDEX AND SURFACE ASYMMETRY INDEX**

Prior to suture removal, the average SRI was  $1.76 \pm 0.47$ , following initial suture removal, it was  $1.55 \pm 0.53$ , at 6 months it was  $1.40 \pm 0.53$ , at completion of selective suture removal, it was  $1.28 \pm 0.47$ , and at the final examination it was  $1.29 \pm 0.53$  (Figure 5). The difference between SRI prior to suture removal and at the final visit was statistically significant ( $P < .001$ ).

Prior to suture removal, the average SAI was  $1.72 \pm 0.99$ ; following initial suture removal, it was  $1.50 \pm 0.98$ ; at 6 months,  $1.39 \pm 1.07$ ; at completion of selective suture removal,  $1.29 \pm 0.95$ ; and at the final examination, it was  $1.31 \pm 0.93$  (Figure 6). The difference from initial to final measurements was statistically significant ( $P = .05$ ) (Table I).

**ANISOMETROPIA**

Of the 92 eyes in 84 patients, 10 patients were monocular, precluding a determination of the refractive spherical equivalent in the fellow, blind eye. In addition, 5 patients had both eyes undergoing operation, and anisometropia data are reported for these patients at the final, follow-up visit. Therefore, anisometropia was analyzed in 77 patients.

The difference between the spherical equivalent of the fellow eye and the operated eye at the completion of the study was  $2.49 \pm 2.25$  diopters. This value was  $3.22 \pm 2.27$  diopters in the *Prior Study* group ( $P = .16$ ).

Of the 77 patients, 29% had 1.0 diopters or less of anisometropia, 55% had 2.0 diopters or less, 66% had 3.0 diopters or less, 86% had 4.0 diopters or less, and 87% had 5.0 diopters or less (Figure 7).

**SELECTIVE SUTURE REMOVAL**

An average of  $2.0 \pm 0.8$  sutures were initially removed at 6 weeks, and  $4.3 \pm 2.7$  sutures were removed by the final examination. In the *Prior Study* group,  $2.2 \pm 0.7$  sutures were initially removed, and an average of  $4.7 \pm 2.6$  sutures were removed by the final examination ( $P = .50$ ).

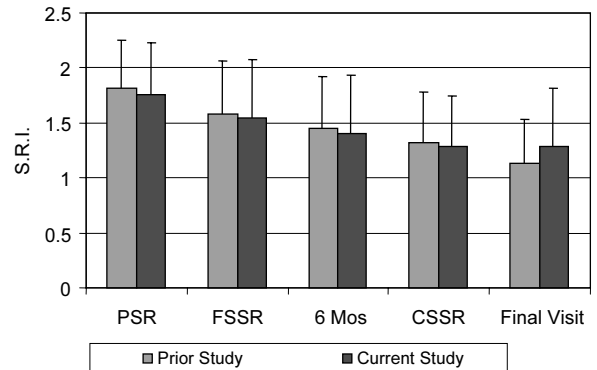


FIGURE 5

Postoperative surface regularity index (SRI) equivalent (CSSR, completion of selective suture removal; FSSR, following selective suture removal; PSR, prior to suture removal).

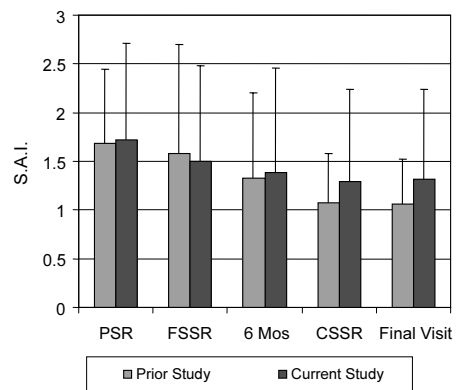


FIGURE 6

Postoperative surface asymmetry index (SAI) equivalent (CSSR, completion of selective suture removal; FSSR, following selective suture removal; PSR, prior to suture removal).

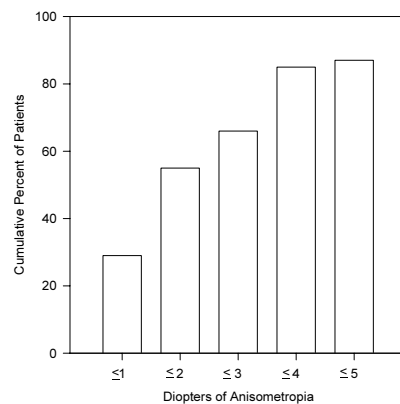


FIGURE 7

Cumulative percentage of postoperative anisometropia.

### POSTOPERATIVE VISION

Prior to any selective suture removal, 6 weeks postoperatively, 31% of eyes had a visual acuity of 20/50 or better. About 1 month following initial suture removal, 37% of eyes had a best corrected visual acuity of 20/50 or better. At 6 months, 65% achieved best corrected acuity of 20/50. At the final visit (average, 20.7 months postoperatively), acuity of 20/50 or better was achieved in 59% of eyes and 20/100 or better in 75%.

Of the 15 eyes (16%) with 20/60 to 20/100 acuity, 5 had dry age-related macular degeneration and 5 had other retinal pathologic findings, including chronic cystoid macular edema, epiretinal membrane, diabetic retinopathy, and 2 eyes that had undergone multiple retinal detachment procedures.

Visual acuity of 20/200 or less occurred in 23 eyes (25%). Nine eyes developed graft failure with corneal edema, and 2 had early edema of the graft and retinal disease. In addition, 7 eyes had age-related macular degeneration, 3 eyes had optic atrophy, and 2 eyes had both amblyopia and glaucoma.

### FINAL GRAFT STATUS

An optically clear keratoplasty was achieved in 81 eyes (88%) at the final visit. Eleven eyes (12%) had developed corneal edema.

### DISCUSSION

The goal of penetrating keratoplasty is to achieve an optically clear transplant with early visual rehabilitation and stable visual function. We strive to minimize astigmatism and anisometropia by surgical technique and, postoperatively, by suture adjustment and manipulation. We previously demonstrated that selected removal of interrupted sutures reduces keratoplasty astigmatism; however, a myopic shift was induced with increasing number of interrupted sutures removed.<sup>11</sup> Presumably, as more sutures are removed, the curvature of the cornea becomes steeper and the myopic shift increases.

In a prospective, randomized clinical trial, visual rehabilitation with decreased postkeratoplasty astigmatism and more regular corneal topography has been attained more rapidly and safely with intraoperative suture adjustment.<sup>17,18</sup> Karabatsas and associates<sup>15</sup> have concluded that postkeratoplasty astigmatism can be decreased similarly with either adjustment of a single running suture or selective removal of interrupted sutures; they also concluded that there is no advantage of single continuous adjustable suturing over interrupted and continuous suturing.

The current study was undertaken to determine whether the myopic spherical equivalent and anisometropia could be reduced while achieving an acceptable degree of

astigmatism. In an attempt to meet this goal, fewer interrupted sutures were removed, the continuous suture was made tighter than in the *Prior Study*, and the average predicted K reading was increased from 45.00 diopters in the previously reported study to 46.00 diopters in the *Current Study*, for calculations of IOL power in those eyes undergoing combined and IOL exchange or secondary placement.

Residual myopia, as measured by spherical equivalent, appears to be reduced in the *Current Study* at each of the five reported follow-up times. However, the resultant myopia was not significantly different from that obtained in the *Prior Study*. The greatest difference was demonstrated at the initial PSR time, and at the last visit, more than 1½ years following surgery.

Selective suture removal was modified in a conscious attempt to reduce anisometropia. Although we were not able to statistically demonstrate a significant reduction in myopia by eliminating those cases in which the fellow eye was myopic, nevertheless, the current study did result in a reduction in anisometropia compared to the *Prior Study* ( $2.49 \pm 2.25$  diopters versus  $3.22 \pm 2.27$  diopters). Since the *Current Study* did not have the requirement of interrupted suture removal with astigmatism over 3 diopters, somewhat fewer interrupted sutures were removed in the *Current Study*.

By comparison, although we have demonstrated a reduction in spherical equivalent myopia and anisometropia, the resultant astigmatism was significantly increased by the last visit. This increase seems to result from the tighter retained, continuous suture, rather than the number of interrupted sutures removed, since there was no difference in the selective suture removal at the final examination (*Current Study*,  $4.3 \pm 2.7$ ; *Prior Study*,  $4.7 \pm 2.6$ ).

While it might be anticipated that retention of more interrupted sutures and a tighter continuous suture would result in an increase in irregular astigmatism, there was no difference in either SRI or SAI at any time interval. Except for a trial contact lens fitting, these two indexes are probably our best indicators of residual irregular astigmatism.

There is also a suggestion that the choice of using 46.00 diopters for IOL calculations in the *Current Study*, compared to 45.00 in the *Prior Study*, may be the most significant factor contributing to a lessening of the myopic spherical equivalent. In the *Current Study*, those patients that received an IOL, either as part of a combined penetrating keratoplasty and cataract extraction or as an IOL exchange or secondary IOL placement, had a significantly less myopic result than those eyes that underwent penetrating keratoplasty without IOL placement, at the examinations prior to suture removal, at 6 months, and at the completion of suture removal, but not for the final follow-up visit (Table II). In addition, a comparison of the *Current Study* to the *Prior Study*, for eyes that received IOL placement, demonstrates a trend toward less induced

myopia in the *Current Study* prior to suture removal and at 6 months postoperatively (Table III).

## CONCLUSION

A tighter continuous suture, an increase in the average keratometry to 46.00 diopters for IOL calculation, and somewhat less aggressive selective suture removal have resulted in the following:

- A trend toward reduction in residual postoperative myopia
- A significant increase in residual astigmatism
- No significant difference in irregular astigmatism, as measured by surface regularity index (SRI) and surface asymmetry index (SAI)
- A reduction in anisometropia
- An apparent greater reduction in myopia by using 46.00 diopters for calculations of IOL power for those eyes receiving IOL placement, in contrast to eyes undergoing penetrating keratoplasty without IOL placement

## REFERENCES

1. Davidson JA, Bourne WM. Results of penetrating keratoplasty using a double running suture technique. *Arch Ophthalmol* 1981;99:1591-1595.
2. Stainer GA, Perl T, Binder PS. Controlled reduction of postkeratoplasty astigmatism. *Ophthalmology* 1982;89(6):668-676.
3. Binder PS. Selective suture removal can reduce postkeratoplasty astigmatism. *Ophthalmology* 1985;92(10):1412-1416.
4. Heidemann DG, Sugar A, Meyer RF, et al. Oversized donor grafts in penetrating keratoplasty: a randomized trial. *Arch Ophthalmol* 1985;103(12):1807-1811.
5. Musch DC, Meyer RF, Sugar A, et al. Corneal astigmatism after penetrating keratoplasty: the role of suture technique. *Ophthalmology* 1989;96(5):698-703.
6. Van Meter WS, Gussler JR, Soloman KD, et al. Postkeratoplasty astigmatism control: single continuous suture adjustment versus selective interrupted suture removal. *Ophthalmology* 1991;98(2):177-183.
7. Filatov V, Steinert RF, Talamo JH. Postkeratoplasty astigmatism with single running suture or interrupted sutures. *Am J Ophthalmol* 1993;115(6):715-721.
8. Mader TH, Yuan R, Lynn MJ, et al. Changes in keratometric astigmatism after suture removal more than one year after penetrating keratoplasty. *Ophthalmology* 1993;100(1):119-127.
9. Filatov V, Alexandrakis G, Talamo JH, et al. Comparison of suture-in and suture-out postkeratoplasty astigmatism with single running suture or combined running and interrupted sutures. *Am J Ophthalmol* 1996;122(5):696-700.
10. Van Meter W. The efficacy of a single continuous nylon suture for control of post keratoplasty astigmatism. *Trans Am Ophthalmol Soc* 1996;94:1157-1180.
11. Gross RH, Poulsen EJ, Davitt S, et al. Comparison of astigmatism after penetrating keratoplasty by experienced cornea surgeons and cornea fellows. *Am J Ophthalmol* 1997;123(5):636-643.

12. Serdarevic ON, Renard GJ, Pouliquen Y. Randomized clinical trial comparing astigmatism and visual rehabilitation after penetrating keratoplasty with and without intraoperative suture adjustment. *Ophthalmology* 1994;101(6):990-999.
13. Goren MB, Dana MR, Rapuano CJ, et al. Corneal topography after selective suture removal for astigmatism following keratoplasty. *Ophthalmic Surg Lasers* 1997;28(3):208-214.
14. Davis EA, Azar DT, Jakobs FM, et al. Refractive and keratometric results after the triple procedure: experience with early and late suture removal. *Ophthalmology* 1998;105(4):624-630.
15. Karabatsas CH, Cook SD, Figueiredo FC, et al. Combined interrupted and continuous versus single continuous adjustable suturing in penetrating keratoplasty: a prospective, randomized study of induced astigmatism during the first postoperative year. *Ophthalmology* 1998;105(11):1991-1998.
16. Hirst LW, McCoombes JA, Reedy M. Postoperative suture manipulation for control of corneal graft astigmatism. *Aust N Z J Ophthalmol* 1998;26(3):211-214.
17. Shimazaki J, Shimmura S, Tsubota K. Intraoperative versus postoperative suture adjustment after penetrating keratoplasty. *Cornea* 1998;17(6):590-594.
18. McNeill JI, Aaen VJ. Long-term results of single continuous suture adjustment to reduce penetrating keratoplasty astigmatism. *Cornea* 1999;18(1):19-24.
19. Shimazaki J, Tsubota K. Analysis of videokeratography after penetrating keratoplasty: topographic characteristics and effects of removing running sutures. *Ophthalmology* 1997;104(12):2077-2084.
20. Kagaya F, Tomidokoro A, Tanaka S, et al. Fourier series harmonic analysis of corneal topography following suture removal after penetrating keratoplasty. *Cornea* 2002;21(3):256-259.
21. Donnenfeld ED, Kornstein HS, Amin A, et al. Laser in situ keratomileusis for correction of myopia and astigmatism after penetrating keratoplasty. *Ophthalmology* 1999;106(10):1966-1975.
22. Kwitko S, Marinho DR, Rymer S, et al. Laser in situ keratomileusis after penetrating keratoplasty. *J Cataract Refract Surg* 2001;27(3):374-379.
23. Webber SK, Lawless MA, Sutton GL, et al. LASIK for post penetrating keratoplasty astigmatism and myopia. *Br J Ophthalmol* 1999;83(9):1013-1018.
24. Rashad KM. Laser in situ keratomileusis for correction of high astigmatism after penetrating keratoplasty. *J Refract Surg* 2000;16(6):701-710.
25. Forseto AS, Francesconi CM, Nose RAM, et al. Laser in situ keratomileusis to correct refractive errors after keratoplasty. *J Cataract Refract Surg* 1999;25(4):479-485.
26. Forster RK. A comparison of two selective interrupted suture removal techniques for control of post keratoplasty astigmatism. *Trans Am Ophthalmol Soc* 1997;95:193-220.

## DISCUSSION

DR WOODFORD S. VAN METER. Dr Forster and colleagues have previously published in 1997 that removal of selective interrupted sutures can decrease postkeratoplasty

astigmatism, an observation noted by multiple other corneal surgeons. The authors previously reported in 1997 that removal of multiple sutures was associated with more residual myopia than removal of fewer interrupted sutures. Today Dr Forster and Dr Dursun present a second cohort of patients in which treatment is altered to address residual myopia by (1) leaving more interrupted sutures in place (2) tying the continuous suture tighter and (3) using postoperative keratometry of 46 diopters instead of 45 diopters for the purposes of IOL calculation.

Data from the current cohort of 92 eyes in 84 patients are presented for spherical equivalent refraction, keratometry, refractive astigmatism, and three other parameters from video keratography: simulated keratometry, surface regularity index (SRI) and surface asymmetry index (SAI). Anisometropia is also examined in the current cohort, excluding monocular patients and patients with bilateral surgery. The results suggest that over 50% of patients had 2 diopters or less of anisometropia, (although the specific patient numbers and exclusion criteria were incomplete). Residual myopic spherical equivalent was reduced in the current study at each of the follow-up times, averaging 1 diopter at last visit, but the reduction was not statistically significant compared to the previous cohort. Of more interest, however, is the fact that, compared to the 1997 study, refractive astigmatism ( $P=.008$ ), keratometry ( $P=.001$ ) and simulated keratometry ( $P=.001$ ) were all higher, suggesting that the tighter continuous suture, while reducing spherical equivalent, can increase residual corneal astigmatism with sutures in place.

The manifest refraction astigmatism associated with the tighter continuous suture shows that the mitigation of astigmatism and the control of spherical equivalent refraction are not parallel processes. One might sense that corneal surgeons should use suture adjustment to control astigmatism, which has been shown to make a statistically significant difference in reduction of astigmatism, and utilize IOL adjustment to reduce postoperative spherical equivalent error.

This paper could be strengthened by better stratification of data. Ten percent of patients had surgery on both eyes. Forty-one patients had an IOL implanted with postoperative keratometry adjusted to achieve more myopia, and 51 patients had a keratoplasty only without an IOL implant, leaving two variables that contribute to final spherical equivalent. It would be helpful to note spherical equivalent in those patients with suture adjustment alone, and whether the authors think that perhaps IOL adjustment is a better means of adjusting spherical equivalent than suture tension. There was no information for 19 patients on whether the intraocular lens was in the anterior chamber or posterior chamber (or sutured), and the effect of anterior chamber depth can be significant in dealing with a final end point that varies by 1 or

2 diopters of emmetropia. Finally, one would assume that with Dr Forster's experience, some of these patients might initially have less than 3 diopters of astigmatism and not need any suture adjustment; these patients are not identified but would be a helpful control against those patients in whom suture adjustment is attempted.

The authors underscore the difficulty in objective measurement of subjective changes in surgeon-specific technique. Page 6 of the manuscript reads, "The 12-bite 10-0 nylon continuous suture was then placed somewhat more tightly than the interrupted sutures after adjustment of the intraocular pressure to approximate normal tension".

The authors should also be commended for directing attention to the problems of spherical equivalent as well as astigmatism in confronting postoperative ametropia. Corneal surgeons have long known that the morbidity of 6 diopters of unexpected myopia is nearly as debilitating as 6 diopters of unexpected astigmatism. The authors demonstrate that while IOL power may be the predominant variable in determining postoperative spherical equivalent, other features, which are surgeon controlled and surgeon-specific, come into play in determining final refractive outcome.

In conclusion, my personal thanks go to the authors for their persistent efforts to control of postkeratoplasty astigmatism using suture adjustment. Because patients usually retain corneal sutures for many years, minimizing astigmatism by selective suture removal helps early visual rehabilitation in the majority of patients undergoing penetrating keratoplasty. I encourage the authors to continue following both cohorts of patients for suture-out astigmatism evaluation. Since large, unpredictable changes in astigmatism can occur whenever multiple sutures are removed, it will be interesting to see whether these variations in suture tension and IOL power calculation affect postoperative astigmatism and spherical equivalent after all sutures are removed.

DR RICHARD C. TROUTMAN: Were the final measurements taken with all the sutures out? Why didn't you separate cases into a single pathology, which might be more revealing? Might the difference in diameter of the corneal buttons be contributing to the myopia? The final astigmatism was expressed in refractive terms but the keratometric results might be more informative. In all corneal pathologies where vision is compromised, and in particular with keratoconus, it is important to perform penetrating keratoplasty early, rather than late, before these irreversible changes that induce the myopia and astigmatism take place.

DR VERINDER S. NIRANKARI: What happens when the sutures loosen or break and need to be removed?

DR GEORGE O. WARING. I stopped using tight sutures years ago for two reasons: because it slowed the recovery time and, because it made the ocular surface more difficult to manage. Are you still tying the sutures tight? LASIK after the sutures are out can also be a reasonable adjustment technique.

DR RICHARD K. FORSTER. I'd like to thank Woody Van Meter for his comments. As for Dick Troutman's comments, the continuous sutures were retained, and the interrupted sutures were selectively removed. I do think that the use of same-size grafts, which were only used in the keratoconus cases, may have a role in reducing post-operative myopia. Further to what George Waring mentioned, I think there is a place for using same-size grafts

for reduction of anisometropia. For example, if you have a patient whom you want to achieve emmetropia or induce a little hyperopia, you may want to use a same-size graft, much like we do in keratoconus to reduce the myopia. On the other hand, if you want to induce myopia, that can be achieved with an oversized donor corneal button, slightly looser sutures, and selective suture removal. I definitely agree with the comments that the tighter sutures that we employed in this study do increase irregular astigmatism slightly and seem to induce more astigmatism in general, although they seem to reduce anisometropia and myopia. Therefore, we're trying to achieve the appropriate technique in order to ultimately achieve the best visual function after the surgical procedure.



# THE DEHISCENT HUGHES FLAP: OUTCOMES AND IMPLICATIONS

---

BY *George B. Bartley, MD* AND *Marlene M. Messenger* (BY INVITATION)

## ABSTRACT

*Purpose:* The modified Hughes procedure is used to reconstruct full-thickness lower eyelid defects. A tarsoconjunctival flap from the upper eyelid replaces the posterior lamella, whereas a skin graft, a skin flap, or a skin-muscle flap restores the anterior lamella. The conjunctival pedicle from the upper eyelid is divided after vascularization of the reconstructed lower eyelid is judged to be adequate (traditionally, at least 3 weeks postoperatively). This study reviews the outcomes of patients in whom the conjunctival flap prematurely dehisced.

*Methods:* Eight patients were identified during a 15-year interval. The posterior lamellar defects ranged in size from 13 to 30 mm horizontally and 5 to 8 mm vertically. The average age at the time of eyelid reconstruction was 72 years (range, 60-84 years). Flap dehiscence, resulting in each case from accidental trauma, occurred between 1 and 11 days postoperatively. Surgical repair of the dehiscence was unsuccessfully attempted in one case; otherwise, the eyelids were permitted to heal spontaneously with the application of erythromycin ophthalmic ointment as the sole therapy.

*Results:* Although the result was satisfactory in each case, one patient, who had dry eyes from Sjögren's syndrome, required secondary surgery to treat mild lagophthalmos and lower eyelid retraction. Follow-up ranged from 3 to 122 months (median, 6.5 months).

*Conclusions:* The ultimate functional and aesthetic outcomes after premature, traumatic dehiscence of a Hughes flap were surprisingly good, suggesting that elective division of the conjunctival pedicle in routine cases can be performed relatively soon after the primary reconstructive procedure.

*Trans Am Ophthalmol Soc* 2002;100:61-66

## INTRODUCTION

---

The Hughes procedure is a commonly used technique to reconstruct full-thickness lower eyelid defects.<sup>1-4</sup> A tarsoconjunctival flap advanced from the ipsilateral upper eyelid replaces the posterior lamella, whereas a skin graft, a skin flap, or a skin-muscle flap restores the anterior lamella. The conjunctival pedicle from the upper eyelid is divided after vascularization of the reconstructed lower eyelid is judged to be adequate (traditionally, at least 3 weeks postoperatively).<sup>5</sup> This study reviews the outcomes of patients in whom the conjunctival flap prematurely dehisced.

## METHODS

---

All patients who had undergone a modified Hughes procedure by the physician-author and whose conjunctival flap had prematurely separated were identified from a computerized database. After institutional review board approval was obtained, pertinent medical records were reviewed.

From the Department of Ophthalmology, Mayo Clinic, Rochester, Minnesota. Supported in part by a grant from Research to Prevent Blindness, New York, New York.

## RESULTS

---

Premature flap dehiscence occurred in 8 of approximately 100 patients who underwent a modified Hughes procedure during the 15-year interval January 1987 through December 2001. Clinical data are summarized in Table I. The average age at the time of eyelid reconstruction was 72 years (range, 60-84 years). The posterior lamellar defects ranged in size from 13 to 30 mm horizontally and 5 to 8 mm vertically. In all cases, Mueller muscle was dissected free from the conjunctival pedicle and was allowed to retract. The anterior lamella was reconstituted with a skin graft in three patients and a skin advancement flap in five patients. A bipedicle orbicularis flap was used to nourish the underlying tarsoconjunctival flap and the overlying skin graft or flap in two patients.

Flap dehiscence, resulting in each case from accidental trauma, occurred between 1 and 11 days postoperatively in seven of the eight patients. One patient (case 6) was unable to identify the exact day on which the flap separated. The size of the dehiscence ranged from approximately 25% of the flap in one patient to 100% in four patients. Surgical repair of the dehiscence was unsuccessfully attempted in one patient (case 4); otherwise, the eyelids were permitted

TABLE 1: CLINICAL DATA FOR EIGHT PATIENTS WITH PREMATURE FLAP DEHISCENCE FOLLOWING MODIFIED HUGHES PROCEDURE

CASE	AGE AT HUGHES (YR)	SIZE OF DEFECT (MM) HORIZONTAL × VERTICAL	SUTURE USED	ANTERIOR LAMELLA RECONSTRUCTION	DAYS UNTIL DEHISCENCE	SIZE OF DEHISCENCE	DAYS UNTIL FLAP DIVISION	SUBSEQUENT PROCEDURES	FOLLOW-UP (MO)
1	77	29 × 7	7-0 polyglactin and 6-0 plain gut	Bipedicle orbicularis oculi flap and skin graft	8	Nasal 75%	16	None	6
2	60	20 × 5	6-0 plain gut	Skin graft	3	100%	NA	None	122
3	63	15 × 7	6-0 plain gut	Skin advancement flap	11	Nasal 25%	36	Cicatricial lower eyelid retraction repair	71
4	78	15 × 8	6-0 plain gut	Skin graft	1	100%	NA	None	9
5	68	30 × 6	7-0 polyglactin and 6-0 plain gut	Skin advancement flap	2	Central 50%	31	None	3
6	69	14 × 7	6-0 polyglactin and 6-0 plain gut	Skin advancement flap	Unknown; flap had dehisced when patient returned for planned flap division	100%	NA	None	6
7	79	20 × 6	6-0 plain gut	Bipedicle orbicularis oculi flap and skin advancement flap	10	Nasal 60%	30	None	6
8	84	13 × 6	6-0 plain gut	Skin advancement flap	5	100%	NA	None	7

NA, not applicable.

to heal spontaneously with the application of erythromycin ophthalmic ointment as the sole therapy (Figures 1 and 2). Division of the residual Hughes flap was performed between 16 and 36 days in the four patients whose dehiscence did not involve the entire conjunctival pedicle.

Although the ultimate result was satisfactory in each

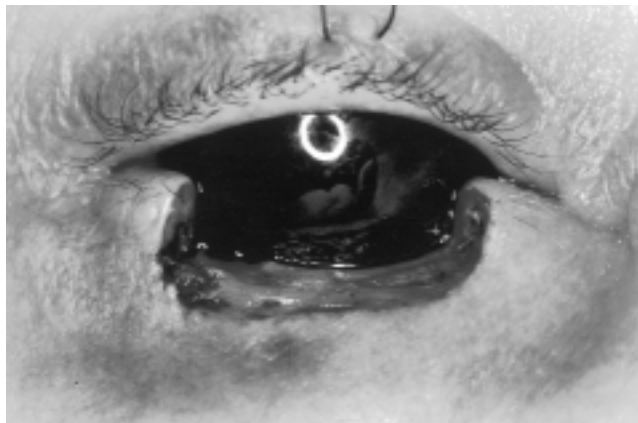


**FIGURE 1A**

Case 2. Right lower eyelid defect after tumor excision.

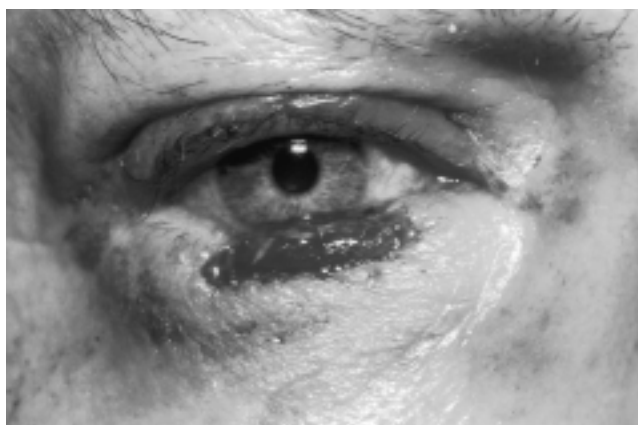


**FIGURE 1B**

Case 2. Complete dehiscence of Hughes conjunctival flap 3 days postoperatively. Eyelid left to heal spontaneously.



**FIGURE 1C**

Case 2. Appearance 5 months postoperatively.



**FIGURE 2A**

Case 4. Complete dehiscence of Hughes conjunctival flap to right lower eyelid 1 day postoperatively.



**FIGURE 2B**

Case 4. Attempted repair of Hughes flap.



**FIGURE 2C**

Case 4. Secondary dehiscence of conjunctival flap 2 days later. Eyelid left to heal spontaneously.



**FIGURE 2D**

Case 4. Appearance 9 months postoperatively.

case, one patient (case 3), who had dry eyes from Sjögren's syndrome and tight skin from chronic sun exposure, eventually required secondary surgery to treat 1 to 2 mm of eyelid retraction and mild lagophthalmos (Figure 3). Of note is that this patient had the smallest conjunctival flap dehiscence.

Follow-up ranged from 3 to 122 months (median, 6.5 months).

## DISCUSSION

The Hughes procedure is a reliable method for reconstructing full-thickness lower eyelid defects. Such defects may range in size from relatively small, segmental defects (especially nasally) to larger defects that comprise the entire lower eyelid. Although the original description involved splitting the upper eyelid margin as the tarsoconjunctival flap was elevated, the operation was modified subsequently to preserve the upper eyelid margin and decrease complications related to the donor site. Traditionally, the conjunctival pedicle was divided several weeks to months after the primary reconstruction to ensure that adequate vascularization had occurred. In contemporary practice, however, most surgeons believe that it is appropriate to divide the conjunctival pedicle after 3 to 4 weeks, especially if a bipedicle orbicularis oculi flap can be mobilized from residual eyelid tissue to provide additional nourishment to the tarsoconjunctival flap.<sup>6,7</sup>

Two recent reports by McNab and colleagues<sup>8,9</sup> have demonstrated that satisfactory results may be achieved when the conjunctival pedicle is divided 2 weeks after the initial procedure. This concept is consistent with previous reports by Hargiss,<sup>10</sup> who proposed that two tubed conjunctival flaps would provide satisfactory vascular support equivalent to an apron flap; Leone and Van Gemert,<sup>11</sup> who demonstrated that a free tarsoconjunctival graft could survive if covered by a bipedicle skin-muscle flap; and Leibsohn and associates,<sup>12</sup> who intentionally created a small optical buttonhole in the Hughes tarsoconjunctival flap without compromising the vascular supply to the reconstructed lower eyelid.

The favorable outcomes of the patients reported herein suggest that a dehiscent Hughes flap does not necessarily need to be repaired. Additionally, the results support the hypothesis that early division of the conjunctival pedicle may be performed without undue risk of functional or aesthetic complications. Limiting the eyelid-sharing interval may be useful, in particular, in patients whose opposite eye has poor vision.

## REFERENCES

1. Hughes WL. A new method for rebuilding a lower lid. Report of a case. *Arch Ophthalmol* 1937;17:1008-1017.

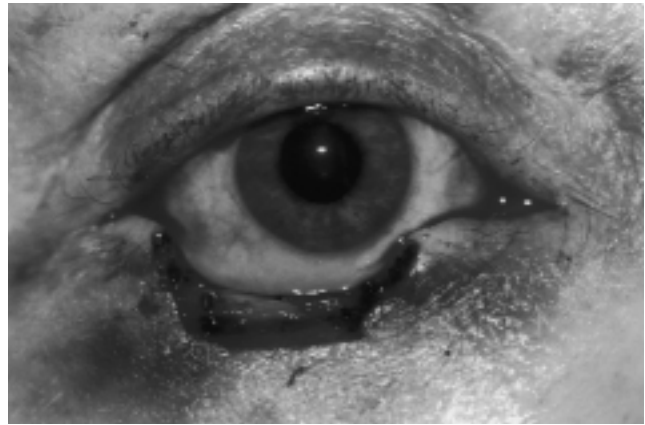


FIGURE 3A

Case 3. Right lower eyelid defect after tumor excision.

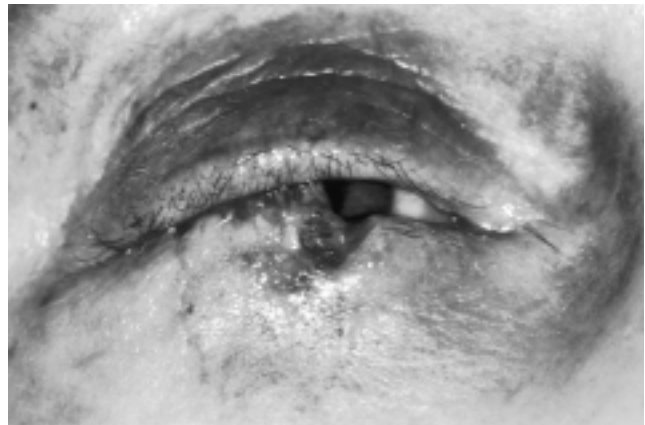


FIGURE 3B

Case 3. Dehiscence of medial 25% of Hughes conjunctival flap 11 days postoperatively. Eyelid left to heal spontaneously, and residual flap divided 36 days later.

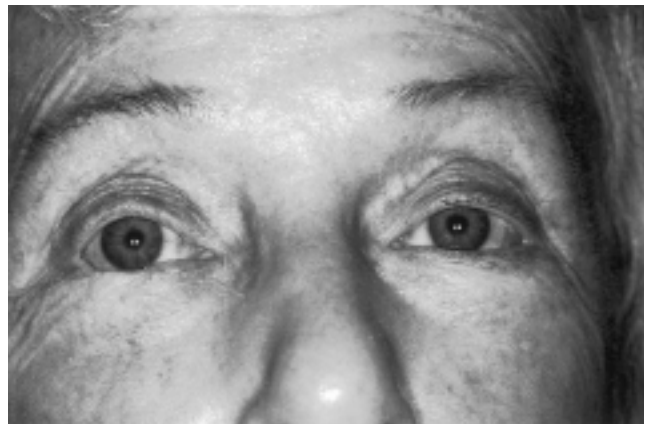


FIGURE 3C

Case 3. Appearance 20 months postoperatively, immediately prior to "split-level" grafts (hard palate mucosa graft to posterior lamella and full-thickness skin graft to anterior lamella) to decrease exposure of right eye. Patient has Sjögren's syndrome.

2. Hughes WL. Reconstruction of the lids. *Am J Ophthalmol* 1945;28:1203-1211.
3. Hughes WL. Total lower lid reconstruction: technical details. *Trans Am Ophthalmol Soc* 1976;74:321-329.
4. Bartley GB, Putterman AM. A minor modification of the Hughes' operation for lower eyelid reconstruction. *Am J Ophthalmol* 1995;119(1):96-97.
5. Rohrich RJ, Zbar RIS. The evolution of the Hughes tarsoconjunctival flap for the lower eyelid reconstruction. *Plast Reconstr Surg* 1999;104(2):518-522.
6. Doxanas MT. Orbicularis muscle mobilization in eyelid reconstruction. *Arch Ophthalmol* 1986;104(6):910-914.
7. Lowry JC, Bartley GB, Litchy WJ. Electromyographic studies of the reconstructed lower eyelid after a modified Hughes procedure. *Am J Ophthalmol* 1995;119(2):225-228.
8. McNab AA. Early division of the conjunctival pedicle in modified Hughes repair of the lower eyelid. *Ophthalmic Surg Lasers* 1996;27(6):422-424.
9. McNab AA, Martin P, Bengner R, et al. A prospective randomized study comparing division of the pedicle of modified Hughes flaps at two or four weeks. *Ophthalmic Plast Reconstr Surg* 2001;17(5):317-319.
10. Hargiss JL. Bipedicle tarsoconjunctival flap. *Ophthalmic Plast Reconstr Surg* 1989;5(2):99-103.
11. Leone CR Jr, Van Gemert JV. Lower lid reconstruction using tarsoconjunctival grafts and bipedicle skin-muscle flap. *Arch Ophthalmol* 1989;107(5):758-760.
12. Leibsohn JM, Dryden R, Ross J. Intentional buttonholing of the Hughes' flap. *Ophthalmic Plast Reconstr Surg* 1993;9(2):135-138.

## DISCUSSION

---

DR BARTLEY R. FRUEH. I recalled being taught that one should wait 2 months before taking down a Hughes flap, so I looked through textbooks on my shelf to see what they said. Merrill Reeh in 1963<sup>1</sup> said to wait for 2 months or more. Frank English in 1975<sup>2</sup> indicated 4 weeks was sufficient. In the text by Merrill Reeh, Charles Beyer, and Gerry Shannon in 1976<sup>3</sup>, they indicate that approximately 2 months is the proper interval for dividing the flap. Joe Flanagan, one of our members, in 1984<sup>4</sup> suggested that 4 to 6 weeks is the appropriate interval. And in my most recent text, Charles and Chris Stephenson in 1997<sup>5</sup> indicate the tarsoconjunctival flap may be divided after 3 to 4 weeks. We know from the recent work of McNab and colleagues<sup>6</sup> that a 2-week interval is sufficient.

In general, the indication for a Hughes flap is a relatively shallow lower lid defect that has a tarsal deficit larger than can be closed effectively with a one-stage procedure, such as a Tenzel semi-circular flap. In most patients, the loss will need to be greater than 60% of the length of the lid to meet this criterion. Half of the eight patients in this study had defects of 15 mm or less. I query whether these could have been repaired by a one-stage procedure that would have produced a lid that would be as good as, or

better than, the Hughes reconstruction functionally and cosmetically.

There are two cases in this series that are particularly instructive; cases 2 and 4, one of which had a 20-mm defect and one of which had a 15-mm defect, each with a skin graft forming the anterior lamella. Each had a 100% dehiscence of the conjunctival flap, one at day 1 and one at day 3, so very little new vessel formation from surrounding tissues could have occurred by that time. Essentially, each was then a graft on a graft, something that should not work.

In the mid 1970s, I asked Dr Hughes at a cocktail party whether he really thought there was sufficient vasculature in the conjunctiva to nourish a thick piece of tarsus at the end of it, as we suppose is happening with a Hughes flap. He assured me that the tarsal plate in a Hughes flap was nourished by its conjunctival pedicle.

Based on Bartley and Messenger's two cases, perhaps Dr Hughes was mistaken. Perhaps the nourishment for the tarsus and skin graft comes from the rich vascular supply of the remaining lid and the conjunctival flap is a secondary and nonessential contributor. Additional evidence for this is that a full-thickness lid margin graft may be taken from one lid and placed in another. Would our patients do just as well with a one-stage grafting of the tarsal plate, with the anterior lamella formed by either a flap or a skin graft, eliminating the conjunctival pedicle flap?

Thank you, Dr Bartley and Ms Messenger, for an intriguing presentation that gives us a lot of food for thought.

## REFERENCES

---

1. Reeh M. *Treatment of Lid and Epibulbar Tumors*. Springfield, Ill: Charles C Thomas; 1963:311.
2. English F. *Reconstructive and Plastic Surgery of the Eyelids*. Springfield, Ill: Charles C Thomas; 1975:10.
3. Reeh M, Beyer C, Shannon G. *Practical Ophthalmic Plastic and Reconstructive Surgery*. Philadelphia: Lea & Febiger; 1976:48.
4. Flanagan J. *Ophthalmic Plastic and Reconstructive Surgery*. Stewart WB, ed. Rochester, Minn: American Academy of Ophthalmology; 1984:251.
5. Stephenson CB, Stephenson CM. *Ophthalmic Plastic, Reconstructive, and Orbital Surgery*. Stephenson CM, ed. Boston: Butterworth-Heinemann; 1997:298.
6. McNab AA, Martin P, Bengner R, et al. A prospective randomized study comparing division of the pedicle of modified Hughes flaps at two or four weeks. *Ophthalmic Plast Reconstr Surg* 2001;17:317-319.

DR JOSEPH C. FLANAGAN. The Hughes flap could be opened much earlier than we thought in the past. There are other alternatives to this flap with the Tenzel flaps and other materials, such as a free tarsal graft from the upper eyelid with a covering flap, or materials such as Alloderm,

hard palate, or auricular cartilage have to be covered with a flap and but not a free full-thickness skin graft.

DR GEORGE B. BARTLEY. With regard to defects of 15 mm or less that could have been repaired by alternative methods, certainly there are many arrows in the quiver, if you will, that one could use. I find, though, that the Hughes flap is much easier and quicker to do than, for example, a Tenzel semicircular flap. The price one pays, of course, is the eyelid-sharing interval. A Hughes flap can sometimes be performed in 15 to 20 minutes, particularly for a nasal defect, which constituted the smaller flaps in this series. Defects close to the canaliculus are more difficult to close with a sliding flap than, for instance, a similar-sized defect laterally. With regard to the two cases that were graft-on-

graft procedures, I completely agree with Dr Frueh that by all traditionally accepted principles of surgery the tissues should have died and looked pretty bad, but in fact they turned out to be satisfactory. Bipedicle orbicularis oculi flaps as described by Doxanas were not used in those two cases, although doing so perhaps would allow us to do what Dr Frueh is suggesting. That is, the tarsoconjunctival flap could be brought down, covered with muscle that will nourish it, and then the conjunctival flap could be divided on the table. Alternatively, perhaps one could simply use a free tarsal graft for the posterior lamella and a skin graft or skin flap for the anterior lamella and avoid the eyelid-sharing portion of the procedure altogether. So, Dr Frueh is right that those two cases really are the most instructive ones in the series.

# ENDOPHTHALMITIS IN PATIENTS WITH DISSEMINATED FUNGAL DISEASE

---

BY Stephen S. Feman, MD, John C. Nichols, MD (BY INVITATION), Sophia M. Chung, MD (BY INVITATION), AND Todd A. Theobald, MD (BY INVITATION)

## ABSTRACT

**Background/Purpose:** Fungal endophthalmitis caused by dissemination from extraocular fungal infections has been reported to vary between 9% and 45%. However, recent clinical experience disagrees with that. This study is an investigation of patients in an inner city teaching hospital, the risks associated with endogenous fungal endophthalmitis, and this incidence.

**Methods:** All ophthalmology consultations between February 1995 and August 2000 that might be associated with disseminated fungal infection were examined in a prospective manner. Patients were excluded if there was no evidence of a positive fungal culture from any site at any time. Visual symptoms were recorded along with ophthalmologic and systemic examination features. Information was gathered, including the identity of cultured organisms, the sites from which the organisms were obtained, and the patients' disposition.

**Results:** During this interval, 170 consultation requests contained the words "endophthalmitis" or "retinitis" and/or indicated concern about disseminated fungal infections. Extraocular fungal infections were found in 114 patients, but only 82 of them had evidence of systemic dissemination. Some patients had more than one organism. The following are listed in decreasing frequency of occurrence: *Candida albicans*, *Torulopsis glabrata*, *Candida tropicalis*, *Candida parapsilosis*, *Candida krusei*, *Aspergillus niger*, and others. Only two patients had evidence of chorioretinitis and progressed to fungal endophthalmitis.

**Conclusions:** Endophthalmitis was rare among these patients with known fungal infections. Less than 2% had any related ophthalmic manifestations. Nevertheless, since treatment can save vision, evidence of intraocular infection should be sought as eagerly as before.

*Trans Am Ophthalmol Soc* 2002;100:67-72

## INTRODUCTION

---

Endogenous fungal endophthalmitis (EFE) is a known complication of disseminated fungal infections. The frequency of EFE among patients with systemic fungal infections has been reported to vary between 9% and 45%.<sup>1,5</sup> Those accounts that used the most exacting criteria to identify EFE had the lowest frequency. One study of this type defined EFE as the "presence of deep white infiltrative chorioretinal lesions with extension of the surrounding inflammation into the vitreous or vitreous abscess manifesting as intravitreal fluff balls" and found a frequency of 9%.<sup>1</sup> Another study, which included autopsy data, reported that 11% of patients with disseminated fungal infections had ocular involvement.<sup>2</sup>

From the Departments of Ophthalmology (Dr Feman, Dr Nichols, and Dr Chung) and Neurology (Dr Chung), and the School of Medicine (Dr Theobald), Saint Louis University Health Sciences Center, St Louis, Missouri. Supported, in part, by the Davisson Endowed Professorship in Ophthalmology (Dr Feman). The authors have no proprietary interest with respect to this manuscript.

Many different infections (eg, skin contamination, colonization of an intravenous catheter, blood-borne disease) can result in positive body fluid fungal cultures. Some may be limited to a particular site, while others may be widely disseminated. Because of the potential toxicity of antifungal therapy, it is in the patient's best interest to have proof of disease spread before starting systemic treatment. A common diagnostic method used for this in the past has been the ophthalmology consultation. Evidence of an endogenous intraocular fungal infection is a strong supporter of a decision to begin such therapy. However, the clinical practice patterns related to antifungal therapy may have changed. To better understand this, the frequency of EFE in hospitalized patients with positive fungal cultures was revisited.

## STUDY DESIGN

---

The present study is an observational case series and case report. This information was accumulated, originally, as prospective patient evaluations. To satisfy institutional

review board requirements for patient and physician anonymity, however, this data collection was reexamined in a retrospective manner.

## METHODS

In a prospective manner, at the time of the consultation, every "ophthalmology consultation service" report produced between February 1, 1995, and August 30, 2000, was entered into our research file. Appraisals were initiated whenever these records were found to contain the words "endophthalmitis" or "retinitis." Further investigation identified additional cases that included the term "fungal infection" or other phrases that could be related to a fungal infection in the consultation requests. Data analysis, however, was limited to those cases in which there was documentation of a positive fungal culture of any species from any source.

For statistical purposes, the following guidelines were used. Multiple requests for consultation made for a single patient during the same hospitalization were considered a single consultation request. When a consultation was requested for the same patient, but for a different hospital admission, the data was considered as a separate consultation.

Each patient's history was examined with a specific emphasis on the presence of ocular or visual symptoms, such as decreased vision, redness, pain, photopsias, or floaters. Medical histories were reviewed for data regarding comorbid diseases. Information collected included all signs of systemic infection and the results of the detailed ophthalmic examination. A slit-lamp biomicroscopic examination of the anterior segment of each eye was performed except when prevented by positioning concerns; in those cases, a penlight examination was conducted. All patients had dilated pupil indirect ophthalmoscopic examinations of their vitreous and retinas. The patients' laboratory test results were collected during the consultation sessions, which included information about the species and site of fungal organisms cultured. The ICD-9 diagnoses for each patient were included in the file.

A patient was considered to have a superficial site of infection if the culture was taken from the urine, the intravenous catheter, a skin swab, or sputum. A patient was considered to have a systemic infection if the culture was taken from blood, bronchial wash, deep abscess, abdominal paracentesis, or thoracentesis.

In this study, the following definitions of chorioretinitis and EFE were used. Chorioretinitis was accepted as a diagnosis only when there was a deep white infiltrative chorioretinal lesion with no evidence of direct vitreal involvement. Endogenous fungal endophthalmitis, however, was limited to those cases in which there was evidence of (1) chorioretinitis with extension of the

inflammation into the vitreous, (2) vitreous abscess manifesting as intravitreal fluff balls, or both.

## RESULTS

During this interval, a total of 170 consultation requests were initiated because of concerns about disseminated fungal infections. Each consultation request was found to include the word "retinitis" or "endophthalmitis." However, only 114 of the patients were found to have had a positive fungal culture from any site at any time during that hospitalization. Of those patients, 82 (72%) had a positive systemic fungal culture, as defined, while 32 (28%) had no evidence of widespread systemic disease.

In this study, the population with positive fungal cultures from any site (114) had the following demographic features. Median age was 55 years (range, 15-84 years). There were 64 males (56%), and 82 patients described themselves as "white" (72%). All of the patients were severely ill, and almost half (about 46%) required artificial ventilation (endotracheal intubation) at the time of initial consultation.

The subpopulation with positive fungal cultures and evidence of systemic spread was similar to the total population described previously. This subpopulation consisted of 82 patients with a median age of 55 years (range, 15-84 years). There were 44 males (54%), and 59 of the patients described themselves as "white" (72%). The members of this subpopulation were severely ill with 28 (34%) intubated at the time the consultation requests were initiated.

The 32 patients who had positive fungal cultures from superficial sites had the following organisms identified in decreasing frequency: *Candida albicans*, *Torulopsis glabrata*, *Candida tropicalis*, *Candida parapsilosis*, *Candida krusei*, *Candida lusitanae*, *Aspergillus flavus*, unidentified yeast, and *Candida guilliermondii*. Some of these patients had coexisting ocular problems associated with such disorders as diabetes mellitus, hypertension, and age-related macular degeneration. Of the 32 patients in this group, four complained of recent onset of visual symptoms, two described blurred vision, and two had "redness" in one eye. In addition, 12 had retinal findings. Six patients had new cotton-wool spots, four had local areas of "dot-blot" hemorrhages, one had a round "white-centered" hemorrhage, and one had a small, localized area of serous retinal detachment. If any systemic fungal infection had been present, these findings might have been interpreted as part of an intraocular fungal infection. However, since fungal dissemination was not present in any of these cases, these abnormalities must represent features of coexisting ocular disorders.

Most of the patients with positive fungal cultures from a systemic infection site had no visual symptoms. However,

a few complained of the following: three had “red eyes,” two described floaters and blurred vision, and one had a diffuse “ache” in one eye. Although most had no ophthalmic abnormalities detected by examination, two patients had chorioretinitis as defined previously, and both developed intravitreal “fluff balls.” In addition, three patients had hard exudates, three had local areas of dot-blot hemorrhages, two had new cotton-wool spots, one had perivascular sheathing, one had retinal pigment epithelial atrophy, and one had an area of subretinal neovascularization. One of the patients with fungal endophthalmitis complained of redness, foreign body sensation, and blurred vision in his left eye. He was found to have keratic precipitates, 3+ anterior chamber cells, posterior synechiae, cells in the vitreous, multifocal sites of chorioretinitis, and a fluff ball in the vitreous at the time of the ophthalmic examination.

Those patients with positive fungal cultures from systemic sites had the following organisms identified in decreasing frequency: *C albicans*, *T glabrata*, *C tropicalis*, *C parapsilosis*, *C krusei*, *Aspergillus niger*, *C lusitaniae*, *C norvegensis*, *Histoplasma*, *Alternaria*, *Aspergillus fumigatus*, *Cryptococcus*, *Curvularia*, unidentified fungus, *Geotrichum capitatum*, *Histoplasma capsulatum*, *Mucor*, *Mycobacterium avium*, *Mycobacterium tuberculosis*, *Penicillium*, *Pneumocystis*, *Saccharomyces cerevisiae*, and *Trichosporon beigelii*.

Some type of ophthalmic abnormality was found in approximately 17% of all patients who had a positive systemic fungal culture. However, chorioretinitis was identified in only two of these infected patients. Both patients with chorioretinitis progressed to fungal endophthalmitis. In short, fungal endophthalmitis occurred in only 2 of the 82 patients (2.4%) who had evidence of disseminated infection. The following case report describes the clinical features of one of the endogenous fungal endophthalmitis patients.

#### CASE REPORT

A 46-year-old man with a history of insulin-dependent diabetes mellitus, hypertension, and chronic hepatitis C infection was hospitalized. He had end-stage cirrhotic liver disease and was identified as a potential recipient of an organ donation. While being evaluated for a possible liver transplantation, he had several episodes of intestinal bleeding; each required hospitalization for transfusions and treatment. During one admission, he was found to have a prostate abscess infected with *Candida*. This was treated with an incision and drainage procedure and systemic therapy with fluconazole, 200 mg intravenously every 24 hours. Blood cultures were positive for *C albicans* for 3 days after the start of therapy, but the cultures were negative thereafter.

Ten days after the abscess incision and drainage, he complained of redness, foreign body sensation, and

blurred vision in his left eye. Visual acuity was 20/20 with each eye. The anterior segment and vitreous of the right eye were normal, while the left eye had 2+ cell and flare, 180° of posterior synechiae, and 2 to 3+ vitreous cell. Multifocal areas of chorioretinitis were seen scattered throughout the posterior pole of each eye. The systemic antifungal therapy was increased by the addition of amphotericin B, 45 mg intravenously every 24 hours, and flucytosine, 2,250 mg orally every 12 hours. Most of the chorioretinal lesions regressed during the next 30 days. However, when the systemic regimen was reduced, his visual acuity became worse and the lesions in the left eye were found to be enlarged (Figure 1). A pars plana vitrectomy was then performed to clear the vitreous cavity. At the end of the surgical procedure, a total of 5 µg of amphotericin B dissolved in 0.1 mL of saline was injected into the vitreous cavity. The material removed from his vitreous was cultured for bacteria and fungi. No organisms grew from these specimens, and the patient's condition rapidly improved.

Six months after the operation, the patient's visual acuity was 20/20 in each eye. The only residual findings were some pigmentary changes at the level of the retinal pigment epithelium.

#### DISCUSSION

The present study finds a much lower frequency of EFE in hospitalized patients with positive fungal cultures than previously reported.<sup>1-5</sup> When compared to the publications with the strictest definition of EFE, our data indicate a reduction in frequency.<sup>1</sup> EFE occurred in only 2 of the 82 patients (2.4%) who had evidence of disseminated disease.

It is our belief that fungal sepsis is being identified and treated earlier in its course as a consequence of greater understanding of the disease and the adverse effects of antifungal therapy. Therefore, EFE and chorioretinitis are

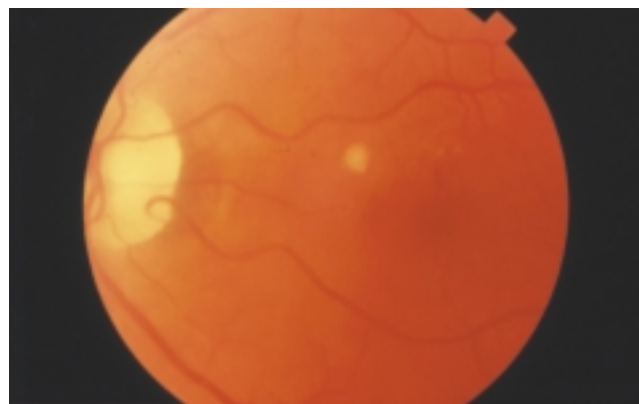


FIGURE 1

Left eye of patient with endogenous fungal endophthalmitis 25 days after systemic therapy with amphotericin B and flucytosine was begun.

being prevented because the fungemia origination sites are being treated earlier in the course of the disease process. As a corollary, however, this means that those few patients with evidence of EFE are at a great risk of harboring those infectious agents that are insensitive to their current medical therapies.

We are unaware of previous literature on EFE or chorioretinitis in patients with superficial sites of positive fungal culture. We found no EFE or chorioretinitis among the 32 patients that had only superficial fungal infections. Although we report on a small sample size, we believe that patients with a positive fungal culture from a superficial site are at very low risk for intraocular infections. If future larger studies confirm this trend, then there could be no need for ophthalmology consultations when a patient has a positive fungal culture from a superficial site.

It is important to emphasize that our findings should not be misinterpreted. The enthusiasm with which one seeks intraocular fungal infection, and the practice patterns associated with ophthalmic consultations in patients with fungal disease, should not be affected by this report. The discovery of EFE and its prompt treatment could be an organ-saving or lifesaving event. Because current therapies work so well, physicians need to maintain a constant vigil for disorders that are not sensitive to standard medical regimens. That was why a vitrectomy, along with procedures to culture and test the vitreous contents for drug sensitivity, was appropriate for the patient described in the case report.

## REFERENCES

1. Donahue SP, Greven CM, Zuravleff JJ, et al. Intraocular candidiasis in patients with candidemia. *Ophthalmology* 1994;101:1302-1309.
2. McDonnell PJ, McDonnell JM, Brown RH, et al. Ocular involvement in patients with fungal infections. *Ophthalmology* 1985;92:706-709.
3. Parke DW, Jones DB, Gentry LO. Endogenous endophthalmitis among patients with candidemia. *Ophthalmology* 1982;89:789-796.
4. Brooks RG. Prospective study of *Candida* endophthalmitis in hospitalized patients with candidemia. *Arch Intern Med* 1989;2226-2228.
5. Bross J, Talbot GH, Maislin G, et al. Risk factors for nosocomial candidemia: a case-control study in adults without leukemia. *Am J Med* 1989;87:614-620.

## DISCUSSION

DR WILLIAM TASMAN. Dr Feman and his coworkers looked at all ophthalmology consultations seen between February 1995 and August 2000 that might be associated with systemic fungal infection. Eighty-two such patients were

identified and the most common organism was *Candida albicans*. Their article then goes on to provide evidence that the frequency of ocular manifestations in systemic fungal infection is probably less than 2%, a finding that differs with reports of higher frequencies ranging anywhere from 9% to 45%.<sup>1-5</sup>

Clearly, fungal endophthalmitis under any circumstance is rare. In a review of 95 endophthalmitis cases seen by our practice during the calendar year 2001, most were postoperative and none had a fungal etiology. The last fungal endophthalmitis that I personally saw prior to last year was a case of *Candida parapsilosis* and that was in a patient who developed bilateral infection secondary to cataract extraction on both eyes.

Interestingly, however, so far in 2002 an endophthalmitis patient with hepatitis C was seen on the Retina Service of Wills Eye Hospital with disseminated *Candida albicans* infection. Consultation was also requested for another *C albicans* patient with intraocular involvement emanating from an intravenous catheter.

One of the two patients identified out of the 82 in Dr Feman's series was a 46-year-old man who had a history of insulin dependent diabetes, hypertension, chronic hepatitis C infection, and endstage cirrhotic liver disease. Predisposing factors for fungal infection include intravenous catheters, bowel surgery, corticosteroid therapy, intravenous drug use, and diabetes. In addition, a recent article in the *Archives of Ophthalmology* documented *Candida* endophthalmitis in an asplenic patient after tattooing.

A few years ago we conducted a study to see if diabetics were more prone to postoperative endophthalmitis after cataract surgery than nondiabetics. Of 162 consecutive patients treated over a 5-year period for endophthalmitis that occurred within 2 weeks of ocular surgery, 21% were diabetic. I therefore asked Dr Feman if his second affected patient had any other associated conditions that might increase the risk of fungal infection such as diabetes or an intravenous catheter. With access to more information about patient No. 2, a 48-year-old Caucasian female with acute lymphocytic leukemia, Dr Feman informed me that she was not diabetic. Although she had a vascular access device implanted as part of her cancer chemotherapy, it had been removed a few days before eye consultation was requested.

I would like to congratulate the authors on presenting evidence that the frequency of eye findings in disseminated fungal disease is probably lower than we had previously thought.

DR DAN B JONES. David Parke's prospective study in 1982 indicated a much higher incidence of fundus lesions (about 29%). A retrospective study by Howard Cupples found fundus lesions occurred in about 2%, similar to today's

presentation. In Dr Parke's study, they acted upon the report from the laboratory of a positive fungal blood culture. Most of the patients were not on treatment and only one was really immunosuppressed with corticosteroid therapy. Almost all were associated with *Candida albicans* with 10 having endophthalmitis, retinitis, or advancement to the vitreous. Why the discrepancy? Whether it's 29% or 2%, I think that the bottom line is the same—that you must respond to a positive fungus blood culture. Over that same period of time, how many other patients had *Candida* positive blood cultures in your hospital? With that, one could determine how often the primary physicians did not request ophthalmology consultations. Then we would know if there has been a change in consultation request patterns.

DR JULES L. BAUM. There might be a correlation with the interval between onset of the patient's systemic symptoms and the initiation of systemic therapy. A delay in systemic therapy might relate to the incidence of fungal endophthalmitis.

DR STEPHEN S. FEMAN. I'll answer Dr Baum's question first. We had similar concerns at our referral center, since some patients were from outside hospitals. Therefore, the interval between symptom onset and therapy initiation

may be inexact in some cases. However, in each case where it was well documented, systemic medical therapy was started in less than 24 hours.

Dr Jones raised a question about the change in incidence of this disorder. The literature and Dr Parke's paper, were well known when this study started. The difference between Dr Parke's paper and the clinical experience at my medical center was what initiated our questions. Since then, it was found that our hospital's Internal Medicine and Systemic Infectious Disease experts begin treatment earlier in the disease process, when compared to Dr Parke's paper. That is, antifungal therapy is started when blood cultures are obtained, and before their results are known. This may be why the classic ocular features rarely develop and the incidence of endogenous fungal endophthalmitis (EFE) is less.

Dr Tasman was helpful in his early communications to me. It is interesting to know that in 2001, among the 95 cases of endophthalmitis at the Wills' Eye Hospital, there was no fungal disease. However, in 2002, although the data are incomplete, one case was seen and consultation was requested on another.

In light of these comments, it is important to emphasize that this should not affect our search for intraocular fungal infection. The discovery of EFE and its prompt treatment could be an organ-saving or lifesaving event.



# TETRATHIOMOLYBDATE AS AN ANTIANGIOGENESIS THERAPY FOR SUBFOVEAL CHOROIDAL NEOVASCULARIZATION SECONDARY TO AGE-RELATED MACULAR DEGENERATION

---

BY Andrew K. Vine, MD AND George J. Brewer, MD (BY INVITATION)

## ABSTRACT

*Purpose:* Since previous studies have shown that angiogenesis requires copper, this study assessed the efficacy and safety of oral tetrathiomolybdate, an antiangiogenesis drug that binds copper, in subfoveal choroidal neovascularization (CNV) secondary to age-related macular degeneration.

*Methods:* This phase I trial involved 10 patients with age-related active subfoveal CNV. After patient consent was obtained and initial laboratory tests were performed, patients were given a loading dose of tetrathiomolybdate, followed by a maintenance dose to maintain serum ceruloplasmin (Cp) levels at 5 to 15 mg/dL. Serum Cp levels are a surrogate marker of copper status. Patient follow-up consisted of a detailed protocol that included best corrected visual acuity, measurement of extent of CNV (both classic and occult) on fluorescein angiograms, and laboratory tests to ensure that anemia did not develop. The study was approved by the institutional review board of the University of Michigan Medical Center and by the Food and Drug Administration.

*Results:* Follow-up of the 10 patients ranged from 4 to 12 months. The targeted serum Cp level was achieved in 8 of the 10 patients. Initially, patients showed stabilization of CNV, but with continued follow-up, all patients showed progression of CNV and loss of visual acuity. Initial mean visual acuity was 20/60; final mean visual acuity was 20/131. At completion of the study, 2 patients showed about a 25% increase in CNV, 1 patient a 60% increase, 1 patient a 100% increase, and 6 patients a 700% to 1,600% increase in CNV.

*Conclusion:* At the dosages used in this study, tetrathiomolybdate was ineffective in preventing the progression of CNV secondary to age-related macular degeneration.

*Trans Am Ophthalmol Soc* 2002;100:73-78

## INTRODUCTION

---

Age-related macular degeneration is the leading cause of severe, irreversible visual loss in North America. The Framingham Eye Study<sup>1</sup> showed a 28% prevalence of age-related macular degeneration in participants between the ages of 75 and 85 years. Although the nonexudative form of age-related macular degeneration is more common, the exudative form typically results in severe visual loss. The exudative form is characterized by choroidal neovascularization (CNV), which can be classified as well defined (classic) or poorly defined (occult).<sup>2</sup>

Current therapies for subfoveal CNV secondary to age-related macular degeneration are very limited. Thermal laser therapy<sup>3</sup> can be done, but the therapy destroys the central macula and results in severe visual

loss. Photodynamic therapy<sup>4</sup> with the drug Visudyne for subfoveal CNV has some efficacy but only for CNV that is predominantly classic.

CNV is a form of angiogenesis that involves a complex series of events, including degradation of extracellular matrix, endothelial cell proliferation, and migration with tube formation necessary for the formation of functional vascular vessels.<sup>5</sup> Four trials of inhibitors of angiogenesis in CNV secondary to age-related macular degeneration have been completed: isotretinoin,<sup>6</sup> intravitreal triamcinolone,<sup>7</sup> interferon alpha-2a,<sup>8</sup> and matrix metalloprotease inhibitor (Agouron Pharmaceuticals, Inc, San Diego, California, protocol AG3340). None of these trials showed a beneficial effect in controlling CNV secondary to age-related macular degeneration.

Tetrathiomolybdate (TM) is an anticopper drug developed as an orphan therapy for Wilson's disease, an autosomal recessive disorder that leads to abnormal copper accumulation, by Brewer and colleagues.<sup>9,10</sup> The drug acts by forming a tripartite complex with copper and protein.<sup>11,12</sup> Given with meals, TM complexes with copper and

From Department of Ophthalmology and Visual Sciences (Dr Vine) and the Departments of Human Genetics and Internal Medicine (Dr Brewer), University of Michigan Medical Center, Ann Arbor. Supported by a grant from The Munn Foundation.

prevents its absorption. Given between meals, TM is absorbed and complexes with serum copper and albumin, rendering the copper unavailable for cellular uptake. This complex is cleared through the kidney and liver. TM is the most potent and most rapidly acting anticopper agent known.

Copper is a major cofactor in angiogenesis.<sup>13,14</sup> Copper is a required cofactor for the function of many key mediators of angiogenesis, including basic fibroblast growth factor,<sup>15,16</sup> vascular endothelial growth factor, and angiogenin.<sup>17</sup>

Preclinical studies<sup>18,19</sup> in animal models have demonstrated that TM is an effective antiangiogenic agent in inhibiting the vascularization of mammary carcinoma and squamous cell carcinoma in mice. In a phase I study<sup>20</sup> of TM in patients with a variety of solid metastatic tumors, TM-induced copper deficiency achieved stable disease in five of six patients who were copper-deficient at the target range for at least 90 days.

The main toxic effect of TM is a reversible anemia with or without leukopenia, since the bone marrow requires copper for heme synthesis and cell production. This anemia is rapidly reversible by temporarily stopping TM. Extensive experience in treating patients with Wilson's disease and cancer has demonstrated that TM is well tolerated and is an effective anticopper agent in humans. The underlying hypothesis of an anticopper, antiangiogenesis therapy<sup>20</sup> is that the level of copper required for angiogenesis is higher than that required for essential copper-dependent cellular functions.

## METHODS

A detailed protocol was developed and was approved by the institutional review board of the University of Michigan Medical Center. The study was also approved by the Food and Drug Administration, which limited the study to 10 patients. This study was started prior to the availability of photodynamic therapy with Visudyne.<sup>4</sup> When photodynamic therapy became available, patients who met the criteria were offered it as an additive therapy.

In this phase I study, serum ceruloplasmin (Cp) was used as a surrogate marker of copper metabolism. Serum copper cannot be used because the complex of TM-copper-albumin is cleared only slowly from the blood and this conjugated copper is measured along with other copper in the serum. Cp is a copper-containing protein, and its synthesis by the liver is regulated by copper metabolism. As copper becomes less available, serum Cp levels begin to decrease, and this is the first sign of copper depletion. Cellular functions dependent on copper are not interfered with as long as there is some Cp in the blood.

The ophthalmic criteria included angiographic evidence of subfoveal CNV secondary to age-related macular degeneration. In seven patients, there had to be some

component of classic CNV but occult CNV could be present. In three patients, the CNV could be entirely occult. A best corrected visual acuity score in the study eye of  $\geq 36$  using modified EDTRS charts (Snellen equivalent of 20/200) was required. Other criteria included age greater than 50 years, clear media, adequate hematologic test results, natural liver enzyme levels, and willingness to comply with an investigational study. Exclusion criteria included the presence of any concurrent ocular disease that could possibly affect visual acuity, previous photocoagulation involving the center of the macula, foveal scarring, and the presence of any severe or unstable concurrent medical condition or active uncontrolled infections.

Study assessments consisted of best corrected visual acuity with modified ETDRS charts, complete ophthalmic examination, color photographs and fluorescein angiography of the study eye, physical examination, and the following laboratory tests: complete blood cell and platelet counts, serum urea nitrogen, creatinine, electrolytes, liver enzymes, and serum Cp. All visual acuity measurements were performed by a certified visual acuity examiner.

The extent of choroidal neovascularization was measured by a standardized grid placed over the fluorescein angiogram print at a point where the full extent of the neovascularization was evident but before extensive leakage would blur the boundaries of the neovascularization. The standardized grid consists of various circles measuring from 1 through 16 disc areas. Each disc area can be further divided into 0.25 squares and 0.01 squares. All measurements of choroidal neovascularization, both classic and occult, were measured to the nearest 0.01 square.

Induction therapy consisted of 120 mg of TM per day (given as 20 mg three times daily with meals and 60 mg at night), which typically resulted in therapeutic levels in about 4 weeks. Maintenance therapy was adjusted to maintain serum Cp levels at approximately 20% of baseline: 5 to 15 mg/dL. The normal range of serum Cp levels is 16 to 35 mg/dL. Some of our patients began the study with an elevated Cp level, which is usually due to the participation of Cp in the acute phase response to inflammation.

The primary end point was the change from baseline in best corrected visual acuity at 6 and 12 months. A secondary end point was the effect of TM on the extent and morphological changes of choroidal neovascularization as assessed by fluorescein angiography.

## RESULTS

The 10 patients consisted of 8 women and 2 men. Their mean age was 72.1 years.

The initial and final best corrected visual acuities, type and extent of CNV, baseline and mean Cp measurements after induction, and duration of follow-up are listed in

Table I. The area of choroidal neovascularization, both classic and occult, is designated in 0.01 squares as outlined in the “Methods” section.

Early in the study, patients showed initial stabilization of CNV with maintenance of good visual acuity, but with longer follow-up, all patients showed progressive loss of visual acuity and continued growth of CNV. At the termination of the study, two patients showed about a 25% increase in CNV, one patient a 60% increase, one patient a 100% increase, and six patients a 700% to 1,600% increase of CNV.

After induction, the mean Cp level was within or very close to the designated therapeutic range of 5 to 15 mg/dL in eight of the patients. In two patients (patients 2 and 8), the mean Cp level was in the mid-20s.

Four patients (1, 3, 6, and 7) who had predominantly classic CNV were also treated with photodynamic therapy with Visudyne in the prescribed manner. In comparing these patients with other nonstudy patients treated only with photodynamic therapy, no additive effect from TM could be discerned. All four patients required additional photodynamic treatments after the study was discontinued.

Complications consisted of a reversible anemia in patient 3, which necessitated that TM be withheld for 4 weeks. The study was stopped about 12 months after the initial patient entered the study. All patients were informed of the study results.

**DISCUSSION**

Angiogenesis results from a complex interplay of cellular events involving a cascade of factors that are both inhibitory and stimulatory. Surgically excised CNV or post-mortem specimens from patients with age-related macular degeneration have been shown to be immunoreactive to numerous angiogenic factors, including vascular endothelial

growth factor,<sup>21</sup> transforming growth factor-beta,<sup>1,22</sup> platelet-derived growth factor,<sup>23</sup> and basic fibroblast growth factor.<sup>22</sup> Because of the complexity of the angiogenic response, the ideal antiangiogenic therapy<sup>19</sup> would target multiple activators of angiogenesis rather than a single angiogenic factor such as vascular endothelial growth factor. Because copper is a required cofactor for numerous angiogenic mediators,<sup>15-17</sup> copper depletion therapy is an attractive approach to antiangiogenesis therapy. Two animal models<sup>15,19</sup> have dramatically shown the efficacy of TM therapy as an effective antiangiogenesis therapy in cancerous tumor control. Preliminary trials<sup>20</sup> of TM in patients with advanced metastatic disease are encouraging.

Despite this positive background, TM therapy, at the dosages used in this study, was ineffective in preventing the progression of CNV secondary to age-related macular degeneration. The reason for the lack of efficacy is not readily apparent. The majority of patients had Cp levels, reflective of total body copper levels, at the targeted level of 5 to 15 mg/dL. This degree of copper depletion was an effective antiangiogenesis therapy in animal models<sup>15,19</sup> and in patients with metastatic cancers.<sup>20</sup> More profound copper deficiency could possibly have inhibited the progression of the CNV, but greater copper depletion risks more significant potential toxicity.<sup>20</sup> Other antiangiogenesis drugs, which were effective in animal models and human tumors, have also been ineffective in age-related CNV. Systemic interferon was effective in an animal model of rubeosis<sup>24</sup> and in the treatment of human hemangioma<sup>25</sup> but was ineffective in CNV secondary to age-related macular degeneration.<sup>8</sup>

There is evidence that CNV secondary to age-related macular degeneration is particularly resilient and aggressive. Photodynamic therapy<sup>4</sup> of classic age-related CNV typically results in initial dramatic regression, but the CNV almost universally recurs, requiring multiple treatments to stabilize the disease and typically resulting in severe visual

TABLE I: CLINICAL DATA FOR TEN STUDY PATIENTS TAKING TETRATHIOMOLYBDATE

PATIENT NO.	INITIAL VISUAL ACUITY	FINAL VISUAL ACUITY	TYPE OF CNV	INITIAL EXTENT OF CNV	FINAL EXTENT OF CNV	PDT TREATMENTS	BASELINE CP (mg/dL)	MEAN CP AFTER INDUCTION (mg/dL)	FOLLOW-UP (MO)
1	20/32	20/200	Mainly classic	15	110	1	70.1	15.6	12
2	20/40	20/160	Mainly occult	14	178	0	46.7	27.6	12
3	20/32	20/200	Mainly classic	8	129	2	58.8	14.4	6
4	20/200	20/200	Occult	32	307	0	28.5	13.3	9
5	20/50	20/170	Mainly occult	35	321	0	38.4	11.7	6
6	20/80	20/200	Mainly classic	200	253	1	36.9	6.8	6
7	20/30	20/80	Mainly classic	16	233	1	35.2	18.2	6
8	20/63	20/80	Mainly occult	301	500	0	34.5	24.9	6
9	20/40	20/63	Occult	354	423	0	32.6	11.3	4
10	20/40	20/100	Mainly occult	196	370	0	32.6	11.3	4

CNV, choroidal neovascularization; Cp, ceruloplasmin; PDT, photodynamic therapy.

loss. Four of the patients in this study were treated with photodynamic therapy as an additive treatment while continuing TM therapy. In all four patients, the choroidal neovascularization recurred after initial photodynamic therapy, and multiple photodynamic treatments were required. We could not detect any benefit of TM in preventing the recurrence of the choroidal neovascularization after photodynamic therapy.

## REFERENCES

- Liebowitz HM, Krueger DE, Maunder LR, et al. The Framingham Eye Study monograph: VI. Macular degeneration. *Surv Ophthalmol* 1980;24(Suppl):428-457.
- Macular Photocoagulation Study Group. Subfoveal neovascular lesions in age-related macular degeneration. Guidelines for evaluation and treatment in the Macular Photocoagulation Study. *Arch Ophthalmol* 1991;109(9):1242-1257.
- Macular Photocoagulation Study Group. Laser photocoagulation of subfoveal neovascular lesions in age-related macular degeneration. Results of a randomized clinical trial. *Arch Ophthalmol* 1991;109(9):1220-1231.
- Treatment of Age-related Macular Degeneration with Photodynamic Therapy (TAP) Study Group. Photodynamic therapy of subfoveal choroidal neovascularization in age-related macular degeneration with verteporfin: one-year results of 2 randomized clinical trials—TAP report. *Arch Ophthalmol* 1999;117(10):1329-1345.
- Folkman J. Angiogenesis in cancer, vascular rheumatoid, and other disease. *Nat Med* 1995;1(1):27-31.
- Chu H, Garcia C, McMullen W, et al. Effect of Accutane on CNV in ARMD. *Invest Ophthalmol Vis Sci* 1996;37(Suppl):117.
- Penfield P, Gyory J, Hunyor A, et al. Exudative macular degeneration and intravitreal triamcinolone. A pilot study. *Aust N Z J Ophthalmol* 1995;23:293-298.
- Pharmacological Therapy for Macular Degeneration Study Group. Interferon alfa-2a is ineffective for patients with choroidal neovascularization secondary to age-related macular degeneration: results of a prospective randomized placebo-controlled clinical trial. *Arch Ophthalmol* 1997;115(7):865-872.
- Brewer GJ, Dick RD, Johnson V, et al. Treatment of Wilson's disease with ammonium tetrathiomolybdate. I. Initial therapy in 17 neurologically affected patients. *Arch Neurol* 1994;51(6):545-554.
- Brewer GJ, Johnson V, Dick RD, et al. Treatment of Wilson's disease with ammonium tetrathiomolybdate. II. Initial therapy in 33 neurologically affected patients and follow-up with zinc therapy. *Arch Neurol* 1996;53(10):1017-1025.
- Mills CG, El-Gallad TT, Bremner I, et al. Copper and molybdenum absorption by rats given ammonium tetrathiomolybdate. *J Inorg Biochem* 1981;14(2):163-175.
- Bremner I, Mills CF, Young BW. Copper metabolism in rats given di- or trithiomolybdates. *J Inorg Biochem* 1982;16(2):109-119.
- Raju KS, Alessandri G, Ziche M, et al. Ceruloplasmin, copper ions, and angiogenesis. *J Natl Cancer Inst* 1982;69(5):1183-1188.
- Parke A, Bhattacharjee P, Palmer RMJ, et al. Characterization and quantification of copper sulfate-induced vascularization of the rabbit cornea. *Am J Pathol* 1988;130(1):173-178.
- Engleka KA, Maciag T. Inactivation of human fibroblast growth factor-1 (FGF-1) activity by interaction with copper ions involves FGF-1 dimer formation induced by copper-catalyzed oxidation. *J Biol Chem* 1992;267(16):11307-11315.
- Patstone G, Maher P. Copper and calcium binding motifs in the extracellular domains of fibroblast growth factor receptors. *J Biol Chem* 1996;271(7):3343-3346.
- Badet J, Soncin F, Guitton JD, et al. Specific binding of angiogenin to calf pulmonary artery endothelial cells. *Proc Natl Acad Sci U S A* 1989;86(21):8427-8431.
- Merajver SD, Irani J, van Golen K, et al. Copper depletion as an anti-angiogenesis strategy in HER2-neu transgenic mice. Proceedings of the American Association for Cancer Research Special Conference on Angiogenesis and Cancer, B11, 1998.
- Cox C, Teknos TN, Barrios M, et al. The role of copper suppression as an antiangiogenic strategy in head and neck squamous cell carcinoma. *Laryngoscope* 2001;111(4 Pt 1):696-701.
- Brewer GJ, Dick RD, Grover DK, et al. Treatment of metastatic cancer with tetrathiomolybdate, an anticopper, antiangiogenic agent: phase I study. *Clin Cancer Res* 2000;6(1):1-10.
- Lopez PF, Sippy BD, Lambert HM, et al. Transdifferentiated retinal pigment epithelial cells are immunoreactive for vascular endothelial growth factor in surgically excised age-related macular degeneration-related choroidal neovascular membranes. *Invest Ophthalmol Vis Sci* 1996;37(5):855-868.
- Reddy VM, Zamora RL, Kaplan HJ. Distribution of growth factors in subfoveal neovascular membranes in age-related macular degeneration and presumed ocular histoplasmosis syndrome. *Am J Ophthalmol* 1995;120(3):291-301.
- Kliffen M, Sharma HS, Mooy CM, et al. Increased expression of angiogenic growth factors in age-related maculopathy. *Invest Ophthalmol Vis Sci* 1996;37(Suppl):203.
- Miller JW, Stinson WG, Folkman J. Regression of experimental iris neovascularization with systemic alpha-interferon. *Ophthalmology* 1993;100(1):9-14.
- Ezekowitz RA, Mulliken JB, Folkman J. Interferon alfa-2a therapy for life-threatening hemangiomas of infancy. *N Engl J Med* 1992;326(22):1456-1463.

## DISCUSSION

DR NORMAN P. BLAIR. Age-related macular degeneration is an increasingly frequent cause of severe, irreversible visual loss. Vine and Brewer are to be congratulated for attempting to improve treatment for choroidal neovascularization, which is usually responsible for this visual loss. None of the current therapeutic options has high efficacy. The authors have taken a rational approach based on the

established involvement of copper in the processes underlying angiogenesis. They have used a potent copper complexing drug, tetrathiomolybdate, which has been shown to be safe by oral administration in human disease. The study was well designed and conducted. They paid attention to admission criteria, visual acuity determination, fluorescein angiogram analysis, and ceruloplasmin measurements.

Why, then, didn't they find evidence of efficacy? First, the power of the study may have been too low with only 10 patients. However, if the efficacy actually had been substantial, one would have expected some suggestion of a benefit. Second, the reduction in copper may have been too small. A reduction in ceruloplasmin to subnormal values was achieved in only 70%, and the average reduction was only to 39%, whereas they had aimed for 20%. Furthermore, it took about four weeks to attain these levels. One wonders whether these goals could be achieved if the drug were administered differently. Third, their hypothesis may not be true. That is, the level of copper required for angiogenesis may not be higher than that required for copper-dependent cellular functions. Fourth, there may have been alternate angiogenic pathways not dependent on copper.

The authors comment that choroidal neovascularization secondary to age-related macular degeneration is particularly resilient and aggressive. While we share in the frustration that leads to this notion, we would take a more sanguine view. As common as it is, choroidal neovascularization never occurs in the majority of people, and it usually occurs only once in those eyes that do develop it. That means that the body has mechanisms to control it. When we obtain a full understanding of choroidal neovascular angiogenesis, it may be possible to devise rather simple and effective therapies. The ultimate way to prevail over this disease will be to understand its stimulus and prevent it. Much work remains before we achieve these objectives, but work such as that of Vine and Brewer represents a significant part of the process.

DR JOHN T. FLYNN. I'd like to suggest that there are a group of diseases at the other end of life, namely in premature infants, where angiogenesis also goes wild and where there are well-developed animal models in the mice, in the rat, and in the kitten. Based on the presentation from the Stem

Cell Symposium today, we should work with the University of Michigan in investigating the use of this drug in those well-defined oxygen-injured animals. We might have a very effective drug for use in premature infants with stage 4 and stage 5 ROP, for which we have no treatment that is effective at the present time.

DR ALFREDO A. SADUN. I have a concern that ethambutol also chelates copper; the mechanism of action is then that it deprives cytochrome oxidase of its proper use and blocks oxidase phosphorylation. This might well be the mechanism by which ethambutol leads to some cases of blindness. It does so by producing a relatively nonabsolute central scotoma and, in the context of this particular disease, the central scotomas, especially without any morphological findings, might well be missed and thus confound the data.

DR ALLAN J. FLACH. This is an uncontrolled study with really no basis for comparison. Looking at the data, which shows a tremendous spread in potential effect, could conceivably be part of a dose response curve of some sort. It's premature to conclude definitively that there is no effect from this therapy.

DR ANDREW K. VINE. I agree with Dr Blair's comment that the hypothesis may well be incorrect for the tissue model we are dealing with. We had looked at the possibility of suppressing copper levels lower but we were unwilling to reduce copper levels any lower because of the significant risk of increased toxicity. The drug is being used in other diseases but we have not considered retinopathy of prematurity, as suppression of angiogenesis in infants would be much more toxic. In terms of the possibility of central scotomas, we have extensive experience with the drug with patients with Wilson's disease. These patients have been documented very thoroughly with visual fields and there is no evidence that these patients developed central scotomas. I agree that our patients would not have been good candidates to pick up on the possibility of an acquired central scotoma. Our results are uncontrolled, but the results do not show any evidence or hint of possible efficacy.



# SURGICAL APPROACHES TO THE MANAGEMENT OF EPITHELIAL CYSTS

---

BY *Julia A. Haller, MD, Walter J. Stark, MD, Amr Azab, MD* (BY INVITATION), *Robert W. Thomsen, MD* (BY INVITATION), AND *John D. Gottsch, MD*

## ABSTRACT

*Purpose:* The purpose of this study was to review management strategies for treatment of epithelial cysts.

*Study Design:* Retrospective consecutive interventional case series.

*Methods:* Charts of patients treated for epithelial ingrowth over a 10-year period by a single surgeon (J.A.H.) were reviewed. Cases of epithelial cysts were identified and the following data were recorded: details of ocular history, preoperative and postoperative visual acuity, intraocular pressure (IOP), ocular examination findings, type of surgical intervention, and details of subsequent procedures performed.

*Results:* Seven eyes with epithelial cysts were identified. Patients ranged in age from 1 1/2 years to 53 years at presentation. Three patients were children. Four cysts were due to trauma, one was presumably congenital, one developed after corneal perforation in an eye with Terrien's marginal degeneration, and one developed after penetrating keratoplasty. Three patients were treated with vitrectomy, en bloc resection of the cyst and associated tissue, fluid-air exchange, and cryotherapy. Four patients were treated with conservative strategy consisting of cyst aspiration (three cases) or local excision (one "keratin pearl" cyst) and endolaser photocoagulation of the collapsed cyst wall or base. In all cases, the epithelial tissue was successfully eradicated; one case required a second excision (follow-up, 9 months to 78 months; mean, 45 months). Two eyes required subsequent surgery for elevated IOP, two for cataract extraction, and one for a second penetrating keratoplasty. Final visual acuity ranged from 20/20 to hand motions, depending on associated ocular damage. Best visual results were obtained in the more conservatively managed eyes.

*Conclusion:* Epithelial cysts can be managed conservatively in selected patients with good results. This strategy may be particularly useful in children, in whom preservation of the lens, iris, and other structures may facilitate amblyopia management.

*Trans Am Ophthalmol Soc* 2002;100:79-84

## INTRODUCTION

---

Epithelial cysts may develop as a complication of penetrating trauma or intraocular surgery, or they may be congenital.<sup>1-19</sup> Although most epithelial ingrowth is in the form of a sheetlike layer of cells growing across the ocular structures, a cystlike pattern also may occur, as an intraocular rest of implanted or congenital cells grows centripetally (Figure 1). Small, stable, and asymptomatic cysts may be observed. Larger cysts composed of proliferating epithelial tissue within the eye may require surgical therapy to prevent or treat serious problems, including pupillary obstruction, secondary glaucoma, iridocyclitis, corneal decompensation, loss of vision, and intractable pain.<sup>2-19</sup> Treatment of epithelial ingrowth has traditionally involved aggressive excision of the cellular proliferation and associated tissue as well as ablative therapy to the excision site to eradicate residual cells. One of the challenges is to identify the full

extent of ocular involvement by the epithelial cellular incursion, so as to treat it completely. In cystic ingrowths, the tissue margins are clearly defined and readily seen during surgery. Cysts may be amenable, therefore, to more conservative and less destructive surgical approaches that have the potential for commensurately less collateral damage to the delicate ocular structures, and thus better visual preservation.

Numerous conservative surgical approaches to cystic epithelial proliferations have been reported, including aspiration with and without cauterization, aspiration and diathermy, aspiration and iridectomy, injection of sclerosing agents, electrocautery, and photocoagulation.<sup>3-19</sup> Xenon arc photoablation of cysts was described by Cleasby<sup>10</sup> and Okun and Mandell.<sup>10,11</sup> Scholz and Kelley<sup>15</sup> reported long-term follow-up of two eyes in which cysts that developed after penetrating keratoplasty were successfully treated with argon laser photocoagulation. We sought to evaluate results of our surgical approach to these complicated cases, particularly with respect to a new technique of aspiration and endophotocoagulation.

From the Wilmer Ophthalmological Institute, Johns Hopkins University School of Medicine, Baltimore, Maryland.

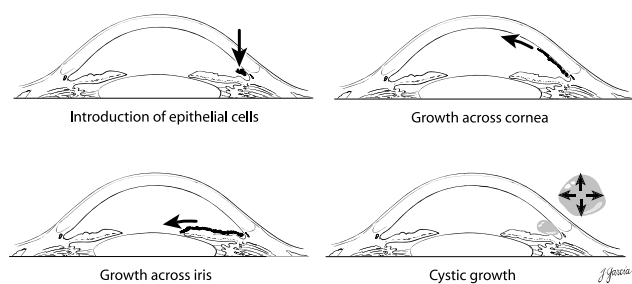


FIGURE 1

Epithelial cells implanted into anterior chamber grow in three basic patterns: initial growth anteriorly across cornea, initial growth posteriorly across iris, and centripetal expansion into a cyst.

## MATERIALS AND METHODS

We reviewed our records over the last 10 years to identify cases of epithelial ingrowth and then searched these for

eyes with cystic patterns of growth. Charts were reviewed and data collected for patient age, sex, previous ocular history and surgery, preoperative ocular examination findings (including visual acuity, intraocular pressure [IOP], and slit-lamp and fundus examination), type of surgery, postoperative complication, further postoperative surgical procedures required, and postoperative examination at last follow-up (including visual acuity, IOP, and details of slit-lamp and fundus examination).

## RESULTS

Seven eyes of seven patients were identified. Patients ranged in age from 18 months to 53 years. Three patients were children, and four were male (Table I). The epithelial cysts developed after penetrating trauma in four cases, after corneal perforation due to Terrien's marginal degeneration in one case (requiring a corneal patch graft), and following

TABLE I: PREOPERATIVE AND POSTOPERATIVE FINDINGS IN SEVEN PATIENTS WITH EPITHELIAL CYSTS

PATIENT	AGE, SEX	CYST ETIOLOGY	PREOP VA	PREOP IOP	SURGERY	FOLLOW-UP	POSTOP VA	POSTOP IOP	OTHER OPERATIONS
1	7 yr, M	Trauma	Hand motions	13	Vtx, excision of cyst and associated iris, IOL removal, cryotherapy	78 mo	Hand motions	42	Endoscopic cyclophotocoagulation
2	53 yr, M	Trauma in 1952; cyst treated with radiation but grew again in 1992	20/60	35	Lens, vtx, excision of cyst and associated iris, fluid-air exchange, cryotherapy	77 mo	Counting fingers 4ft	21	Cyclophotocoagulation
3	2 yr, F	Trauma	LP	10	Vtx, excision of cyst and associated iris, fluid-air exchange, cryotherapy	30 mo	Hand motions	23	None
4	45 yr, M	Penetrating trauma (BB)	20/25	14	Excision of "keratin pearl" cyst, endolaser to base	29 mo	20/20	15	Repeated excision and laser, phaco/IOL
5	18 mo, M	Congenital	Fix and follow		Cyst aspiration and endolaser	43 mo	20/40	15	None
6	27 yr, F	Perforation due to Terrien's marginal degeneration	20/100	10	Cyst aspiration and endolaser	51 mo	20/40	6	None
7	57 yr, F	PK	3/200	21	Cyst aspiration and endolaser	9 mo	20/40	20	Phaco/IOL, repeated PK

IOL, intraocular lens; PK, penetrating keratoplasty; vtx, vitrectomy.

penetrating keratoplasty in one case; one cyst was congenital. In all cases, the cysts were large and expanding and were causing complications such as visual axis obstruction, iritis, glaucoma, and corneal decompensation.

Surgery consisted of an aggressive ablative approach in the three eyes treated earliest; all underwent pars plana vitrectomy, en bloc excision of the cyst and associated iris tissue, fluid-air exchange to provide a thermal insulation effect, and then cryotherapy to the tissue adjacent to the excision site in an attempt to devitalize any remaining cells. The last four eyes treated were managed more conservatively, with a technique including viscodissection of the cyst wall from adjacent ocular structures, aspiration of cyst contents in three of the eyes with fluid-filled cysts, and cyst excision with a vitrectomy probe in one eye with a “keratin pearl” solid cyst, and then endolaser photocoagulation of the collapsed cyst wall or base (Figures 2 and 3). In all

cases, the epithelial tissue was successfully eradicated, although one case treated conservatively required a second excision.

Preoperative visual acuity ranged from 20/25 to hand motions; postoperative visual acuity ranged from 20/20 to counting fingers (follow-up, 9 months to 78 months; mean, 45 months), depending on associated ocular damage. Poor final visual acuity in three eyes was attributed to corneal opacity; one of these eyes also had uncontrolled glaucoma. Two eyes required subsequent procedures for glaucoma control, two eyes underwent later cataract surgery, and one eye had a second penetrating keratoplasty. Best visual results were obtained in the conservatively managed eyes (Table I, Figures 4 through 11).

## DISCUSSION

Numerous approaches to the management of epithelial cysts have been reported.<sup>1-20</sup> Small cysts that are stable in size and otherwise asymptomatic may be observed, often for years. If the cyst enlarges, however, it may require surgical treatment, since it may obstruct the visual axis and incite further complications, such as uveitis, corneal edema, or glaucoma.

Epithelial cysts have been treated with a variety of techniques, including en bloc excision, vitrectomy-instrumented cyst excision combined with cryodestruction, injection of sclerosing agents, radiation, aspiration, electrolysis, and diathermy.<sup>1-19</sup> More recently, investigators have described the use of laser photocoagulation to ablate these cysts.<sup>10,11,15</sup> Limitations of photocoagulation include recurrences requiring subsequent treatment, problems with anterior cyst wall visualization and treatment, difficulty in treating large cysts in some cases, and the risk of rupture of the cyst wall, converting the cyst into a sheetlike epithelial ingrowth.<sup>4,10,11,15</sup>

More aggressive surgical excision and devitalization of the epithelial tissues have been recommended by some investigators, with vitrectomy, sometimes lensectomy, fluid-air exchange to fill the eye with an intraocular bubble, and cryodestruction of residual cells at the excision site.<sup>4,5</sup> Other investigators have further advocated the complete excision of all epithelial layers and adjacent cornea, iris, anterior chamber angle, and ciliary body, with full-thickness corneoscleral graft.<sup>16,20</sup> These strategies involve large procedures and the possibility of considerable collateral damage to ocular structures. In children, loss of the crystalline lens and iris may complicate amblyopia therapy. As well, excision of the cyst with vitrectomy instrumentation has occasionally been reported to convert the cyst into sheetlike epithelial ingrowth, which then becomes a more difficult management issue.<sup>4,14,15</sup> We sought to evaluate our own experience with this rare clinical entity.

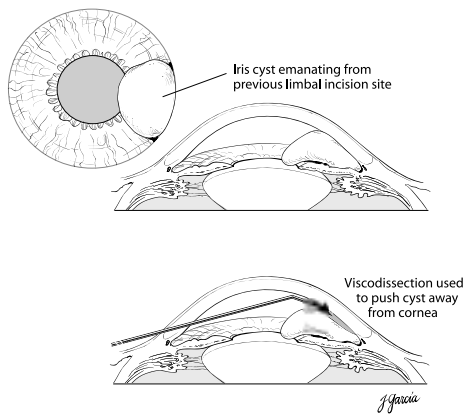


**FIGURE 2**

Conservative surgical strategy: cyst is first viscodissected from cornea and other structures.

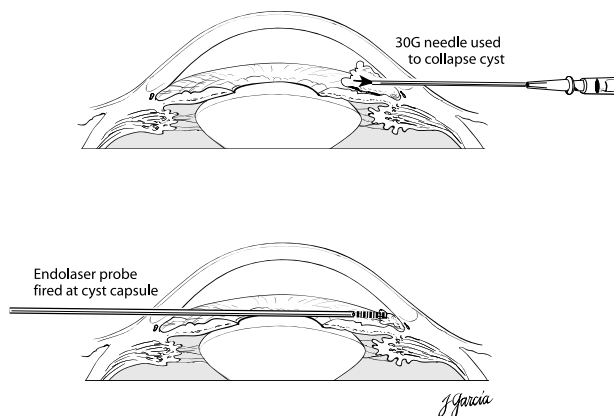


**FIGURE 3**

Conservative surgical strategy: A 30-gauge needle is inserted into apex of the cyst, and its contents are aspirated. Endolaser probe is then directed at residual cyst wall, and collapsed capsule is destroyed with photocoagulation.



**FIGURE 4A**

Patient 1. Solid "keratin pearl" epithelial cyst in 45-year-old man 2 years after he sustained a penetrating injury to the cornea from a piece of BB that embedded in his inferior angle and was subsequently removed.

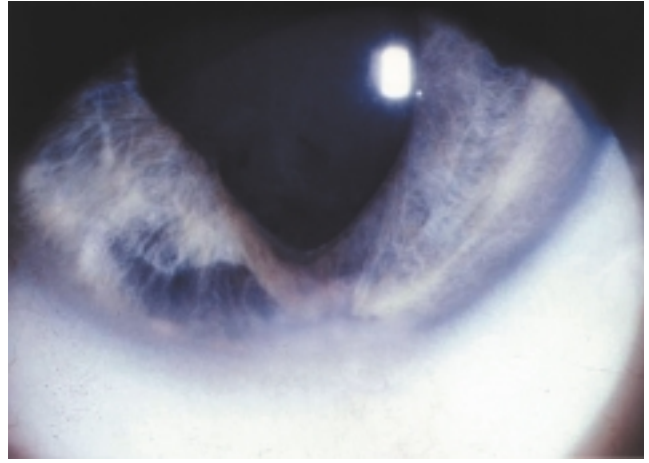


**FIGURE 4B**

Patient 1. Cyst required two local resections with endolaser to the base, leaving the patient with some inferior iris atrophy. Following cataract extraction 29 months postoperatively, visual acuity was 20/20.

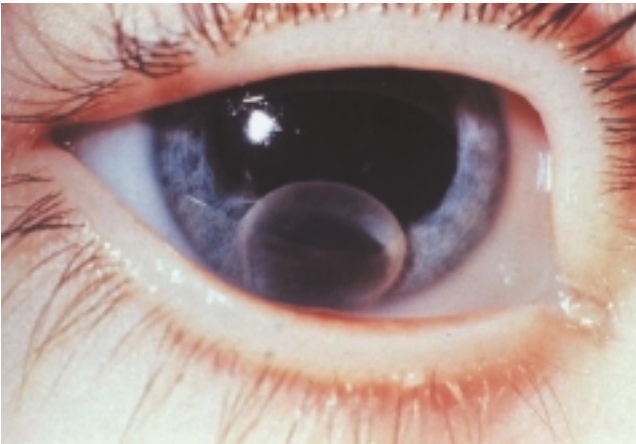


**FIGURE 5A**

Patient 2. Inferior iris cyst in 18-month-old boy. Reprinted with permission from the *American Journal of Ophthalmology*.

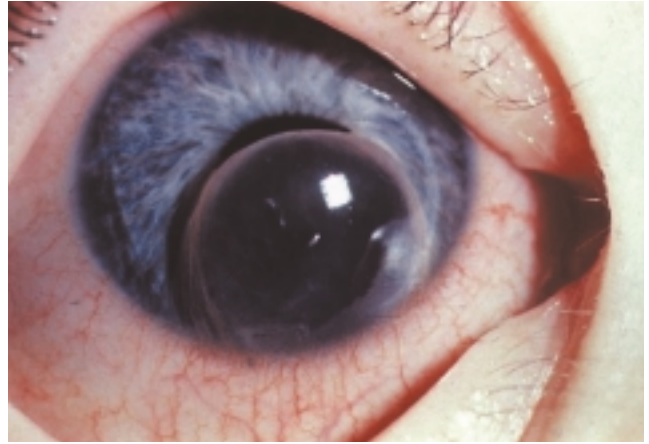


**FIGURE 5B**

Patient 2. Cyst grew over a few months to occlude the visual axis. Reprinted with permission from the *American Journal of Ophthalmology*.

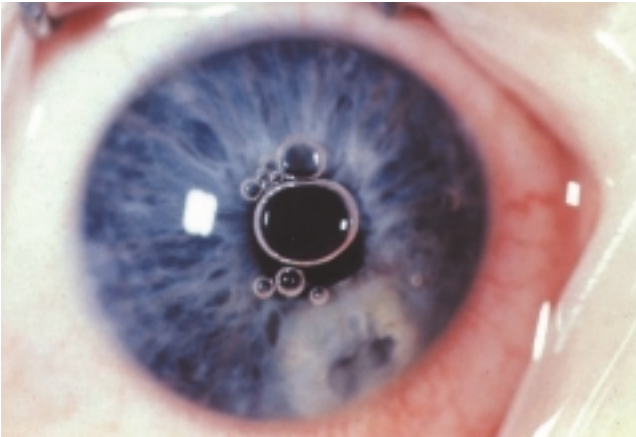


**FIGURE 5C**

Patient 2. At the close of surgery, after aspiration and endophotocoagulation, no residual cyst is seen, and iris shows thermal effect of the laser. Reprinted with permission from the *American Journal of Ophthalmology*.



**FIGURE 5D**

Patient 2. After 43 months of follow-up, no cyst recurrence is seen. Some iris atrophy was present inferiorly, the lens remained clear, and vision was 20/40 with Allen cards. Reprinted with permission from the *American Journal of Ophthalmology*.



**FIGURE 6A**

Patient 3. Epithelial cyst in 27-year-old woman that developed after corneal perforation due to Terrien's marginal degeneration. It was treated with a patch graft. Visual acuity was 20/100, with the cyst occluding the visual axis.

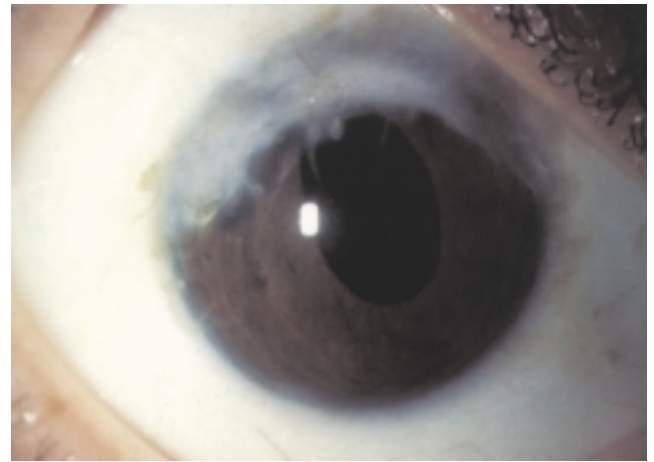


**FIGURE 6B**

Patient 3. Visual acuity had recovered to 20/40 at 14 months postoperatively, following cyst aspiration and endolaser to collapsed cyst wall.

We followed seven cases managed in two ways. The first three cases were treated with vitrectomy, cyst excision, and local cryoablation of adjacent tissue under thermal insulation by an air bubble. The last four cases were treated with aspiration or excision of just the cyst contents, followed by photocoagulation of the remaining cyst wall or base to devitalize remaining cells. Both methods were efficacious in eradicating the epithelial tissue and preserving the eyes. The more conservative approach seemed to result in better visual outcomes, but the cases were not entirely comparable, and the series is subject to the limitations of all retrospective reviews. In particular, eyes may have been preselected for a more conservative approach because of more limited and manageable disease and may have had a better prognosis to begin with. The fact that the earlier cases were more aggressively managed and all later cases more conservatively managed, however, argues against this. Three of the patients in this series were children. The eyes of children present a particular challenge to the surgeon, who seeks to salvage as much of the iris, lens, and other anterior chamber structures as possible in order to optimize vision in the face of the threat of amblyopia. The more conservative surgical approach may be particularly useful in these eyes.

## REFERENCES

1. Roy FH, Hanna C. Spontaneous congenital iris cyst. *Am J Ophthalmol* 1971;72:97-108.
2. Maumenee AE, Shannon CR. Epithelial invasion of the anterior chamber. *Am J Ophthalmol* 1956;41:929-942.
3. Maumenee AE, Paton D, Morse PH, et al. Review of 40 histologically proven cases of epithelial downgrowth following cataract extraction and suggested surgical management. *Am J Ophthalmol* 1970;60:598-603.
4. Bruner WE, Michels RG, Stark WJ, et al. Management of epithelial cysts of the anterior chamber. *Ophthalmic Surg* 1981;12:279-285.
5. Stark WJ, Michels RG, Maumenee AE, et al. Surgical management of epithelial ingrowth. *Am J Ophthalmol* 1978;85:772-780.
6. Hogan MJ, Goodner EK. Surgical treatment of epithelial cysts of the anterior chamber. *Arch Ophthalmol* 1960;64:286-291.
7. Kennedy PJ. Treatment of cysts of the iris with electrolysis. *Arch Ophthalmol* 1956;55:522-525.
8. Vail D. Treatment of cysts of the iris with diathermy coagulation. *Trans Am Ophthalmol Soc* 1953;51:371-383.
9. Wilson W. Iris cyst treated with electrolysis. *Br J Ophthalmol* 1964;48:45-49.
10. Cleasby GW. Photocoagulation of iris-ciliary-body epithelial cysts. *Trans Am Acad Ophthalmol Otolaryngol* 1971;75:638-642.
11. Okun E, Mandell A. Photocoagulation as a treatment of epithelial cysts following cataract surgery. *Trans Am Ophthalmol Soc* 1974;72:170-183.
12. Sugar HS. Further experience with posterior lamellar resection of the cornea for epithelial implantation cyst. *Am J Ophthalmol* 1967;64:291-299.
13. Ferry AP, Naghdi MR. Cryosurgical removal of epithelial cyst of iris and anterior chamber. *Arch Ophthalmol* 1967;77:86-87.
14. Harbin TS Jr, Maumenee AE. Epithelial downgrowth after surgery for epithelial cyst. *Am J Ophthalmol* 1974;78:1-4.
15. Scholz RT, Kelley JS. Argon laser photocoagulation treatment of iris cysts following penetrating keratoplasty. *Arch Ophthalmol* 1982;100:926-927.
16. Naumann GOH, Rummelt V. Block excision of cystic and diffuse epithelial ingrowth of the anterior chamber: report on 32 consecutive patients. *Arch Ophthalmol* 1992;110:223-227.
17. Shields JA, Shields CL, Lois N, et al. Iris cysts in children: classification, incidence, and management. *Br J Ophthalmol* 1999;83:334-338.

18. Tsai JC, Arrindell EL, O'Day DM. Needle aspiration and endodiathermy treatment of epithelial inclusion cyst of the iris. *Am J Ophthalmol* 2001;131:263-265.
19. Orlin SE, Rabner IM, Laibson PR, et al. Epithelial down-growth following the removal of iris inclusion cysts. *Ophthalmic Surg* 1991;22:330-335.
20. Forster RK. Corneoscleral block excision of postoperative anterior chamber cysts. *Trans Am Ophthalmol Soc* 1995;93:83-97.

## DISCUSSION

---

DR JAMES S. KELLEY. Twenty-five years ago Richard Scholz and I were confronted with two patients similar to those reported by Dr Haller and her colleagues. We had similar choices: en bloc excision, major surgery, or applying the then new technology of argon laser photocoagulation. The two patients were treated with laser and, with good luck as much as good technique, have done well. The first is a retired minister volunteering in Wales. He was treated in 1975. The second was a park service employee treated in 1976. Since that time, neither Dr Scholz nor I have seen another case of anterior chamber epithelial cyst.

Now we are a quarter century later and still faced with the same difficult clinical decisions. Is the best approach more definitive surgery or more conservative aspiration and ablation? The questions we raise are more rhetorical in nature. Can evidence-based medicine ever apply to these rare conditions? Small case series can be interesting. I am reminded that Dr James Lind in his work on scurvy had only two severely affected sailors on a diet of oranges and two "similar" crewmen on the normal ship's diet. The results were dramatic and eventually changed the history of the British navy. In general, the data from a handful of cases are insufficient.

Can new information technology help? Could there be an Internet Web site for each of these orphan conditions? By collecting worldwide statistics, we may better understand the etiology of the cysts. Are there factors in the host that increase susceptibility? The patients appear relatively young; might advanced age be a protective factor? What are the inhibiting factors? Some cysts do not enlarge aggressively, and the more common residual lens epithelium forms only the more benign pearls. Prevention is the ultimate goal. New surgical techniques such as small incisions seem to reduce epithelial down-growth incidence. A more complete database would verify this suspicion. How do we ethically apply new technology to rare

cases? Dr Scholz and I were interested in the then new application of argon laser. Dr Groh was using en bloc excision for tumors and extended that technique to epithelial cysts. There is temptation to move on to the latest technology before fully evaluating the previous methods. Will there be applications for photosensitizing dyes or growth factor inhibitors?

The patient often asks, "What if it was your mother or daughter, what would you do?" How can we answer this question when the case numbers are small and the results are conflicting? There is the fear of converting the cyst to diffuse epithelial down-growth. Rupturing the cyst with YAG laser seems particularly hazardous. The conservative approach can be followed by more extensive excision if necessary. The conservative approach appears more prudent.

I thank Dr Haller and colleagues for reporting the additional cases and adding a new management option to our arsenal. I would appeal to the national and international community to collect information on these rare conditions in some systematic fashion. Show me the data.

DR RICHARD K. FORSTER. In 1995, I presented a paper at this meeting of three similar cases requiring en bloc excision, with approximately 2-year follow-up in the three cases. And at that time, there was no evidence of recurrence; all patients had good visual function. One of the three, unfortunately, passed away shortly afterwards. Another patient presented with a recurrence of the anterior chamber cyst 39 months after initial en bloc excision; it developed contiguous with the site of en bloc excision. He still has 20/25 vision. Long-term follow-up on these cases is necessary.

DR JULIA A. HALLER. I think those are both excellent points: one being the rarity of these cysts and consequent difficulty comparing treatment options, and the second being the necessity of follow-up. One of the cases that we treated had, 53 years prior to presentation, developed epithelial ingrowth after trauma; it was treated with radiation. The patient developed a recurrent cyst 53 years later that was so large that it displaced the lens posteriorly. This one was in our initial group. Certainly, these eyes have to be followed for life, and we need better treatments. I enjoyed hearing Dr Kelly's ideas about an Internet-based system to help improve our ability to provide evidence-based data on these rare conditions, and I think that's something that the AOS might pursue.

# MULTICENTER PROSPECTIVE, RANDOMIZED, DOUBLE-MASKED, PLACEBO CONTROLLED STUDY OF RHEOPHERESIS TO TREAT NONEXUDATIVE AGE-RELATED MACULAR DEGENERATION: INTERIM ANALYSIS

---

BY *The Multicenter Investigation of Rheopheresis for AMD (MIRA-1) Study Group* (BY INVITATION)  
AND *Jose S. Pulido, MD, MS*

## ABSTRACT

**Objective:** To evaluate the safety and efficacy of Rheopheresis blood filtration to treat intermediate- to late-stage preangiogenic age-related macular degeneration (AMD) with soft drusen.

**Design:** Multicenter, prospective, randomized, double-masked, placebo-controlled clinical trial.

**Participants:** First 43 randomized patients (28 Rheopheresis and 15 placebo-control patients) with available baseline and 3-month postbaseline best corrected visual acuity (BCVA) measurements and intermediate- to late-stage preangiogenic AMD with multiple large soft drusen and elevated serum levels of targeted macromolecules.

**Intervention:** Patients were randomly assigned to receive eight Rheopheresis or eight placebo procedures over 10 weeks.

**Main Outcome Measures:** ETDRS BCVA measurements at baseline, 3, 6, 9, and 12 months postbaseline.

**Results:** In primary eyes, the mean LogMAR line difference between Rheopheresis and placebo-control eyes was 1.6 lines at 12 months postbaseline; the difference was significant throughout the first posttreatment year ( $P = .0011$ , repeated measures analysis). Thirteen percent of Rheopheresis compared with 0% of placebo-control eyes had a  $\geq 3$ -line improvement in BCVA at 12 months postbaseline. Four percent of Rheopheresis compared with 18% of placebo-control eyes had a  $\geq 3$ -line loss in BCVA.

The subgroup of patients whose primary eyes had baseline BCVA worse than 20/40 demonstrated a mean LogMAR difference between Rheopheresis and placebo-control eyes equaling 3.0 lines at 12 months postbaseline; the difference was significant throughout the first posttreatment year ( $P = .0014$ , repeated measures analysis). Sixteen percent of Rheopheresis compared with 0% of the placebo-control eyes had a  $\geq 3$ -line improvement in BCVA at 12 months postbaseline. Five percent of Rheopheresis compared with 29% of placebo-control eyes had a  $\geq 3$ -line loss in BCVA. Fifty-eight percent of Rheopheresis eyes improved to 20/40 or better, compared with 14% of placebo-control eyes. No serious treatment-related adverse events were observed.

**Conclusions:** Rheopheresis demonstrated statistically significant and clinically relevant effects on BCVA when compared with placebo controls for the 12-month study interval. Untreated patients with BCVA worse than 20/40 with intermediate- to late-stage preangiogenic AMD, soft drusen, and elevated blood factors were at risk for substantial visual loss. A sample size larger than 43 patients is important to provide a basis for widespread adoption of novel therapeutic options for AMD such as Rheopheresis. Therefore, enrollment to 150 patients is continuing.

*Trans Am Ophthalmol Soc* 2002;100:85-108

## INTRODUCTION

---

Age-related macular degeneration (AMD) is the leading cause of acquired legal blindness and visual impairment

From the Department of Ophthalmology and Visual Sciences, UIC Eye Center, University of Illinois at Chicago. Sponsored by OccuLogix Corporation, Palm Harbor, Florida.

among people older than 50 years in the United States and other Western industrialized societies.<sup>1-3</sup> According to the National Eye Institute, AMD severely impairs the vision of 1.7 million Americans older than age 60. The risk of a person older than 75 developing the disease approaches 30%, and as the population ages, the number of AMD cases with severe visual loss is expected to rise to 6.3 million by 2020 if current population growth trends

continue. New modalities of treatment are therefore needed to prevent loss of vision in the affected population.

Preangiogenic (nonexudative, or “dry”) AMD is the most common form of the disease, representing up to 90% of the affected population. The only treatment to date that has demonstrated any positive effect on visual outcomes with this stage of AMD has been the use of zinc and high-dose antioxidants. Daily oral intake of these common dietary supplements has been shown to reduce progression to the more advanced stages of the disease, including “wet” AMD, by up to 25%.<sup>4</sup>

Approximately 80% of severe vision loss caused by AMD is due to the wet form of the disease. Patients whose eyes are characterized primarily by drusen in one or both eyes typically do not manifest a significant loss of vision. However, they are at an increased risk for progression to the later stages of the disease with a concomitant loss of significant visual acuity.<sup>5</sup> Risk factors for that development include number, size, and confluence of drusen and abnormal pigment clumping.<sup>6</sup> Patients with bilateral soft drusen have a 12.4% risk of exudative AMD developing within 10 years.<sup>7</sup> Patients with exudative AMD in one eye and soft drusen in the fellow eye represent a group at high risk of becoming legally blind.<sup>6</sup>

## BACKGROUND

Over the last decade, a series of clinical trials in Germany and now the United States have evaluated the use of the Rheopheresis blood filtration technology for the treatment of AMD. The research began with several uncontrolled case series. Promising results provided the basis to initiate the first controlled randomized clinical trial to investigate the safety and efficacy of Rheopheresis in patients with AMD (the MAC-1 Trial) at the University of Cologne.<sup>8-12</sup> In each study, the Rheopheresis group consistently demonstrated statistically significant improvement in mean ETDRS (LogMAR) best corrected visual acuity (BCVA) that was sustained after the treatment period. Although many forms of AMD were evaluated at different stages of disease progression, eyes with multiple soft drusen and without evidence of neovascularization consistently demonstrated the best therapeutic results. In 1998, Swartz and colleagues (*Investigative Ophthalmology and Visual Science* 1999;40(4):5319) undertook a Food and Drug Administration (FDA) pilot study (IDE G970241) of 30 patients with preangiogenic AMD with soft drusen at the University of Utah. Its findings suggested that further study was warranted.

## THE MIRA-1 TRIAL

The current MIRA-1 (Multicenter Investigation of Rheopheresis for AMD) study design expands on these preceding trials. MIRA-1 is a 12-month randomized,

prospective, multicenter, double-masked, placebo-controlled, FDA clinical trial designed to compare Rheopheresis treatment with placebo-control treatment in 150 patients with intermediate- to late-stage (AREDS grade 3 to 4, BCVA between 20/32 and 20/125 inclusive), high-risk ( $\geq 10$  large soft drusen), preangiogenic AMD who also demonstrate the elevation of serum levels of select hemorheologic macromolecules in their blood. As such, MIRA-1 is the largest prospective, double-masked apheresis trial ever undertaken. We report on the interim results of the initial group of 43 randomized, intent-to-treat patients.

From the FDA pilot trial conducted at the University of Utah, it was determined that fibrinogen, serum IgA, and total cholesterol, as rheologically relevant high-molecular-weight proteins, were highly associated with positive treatment outcomes and might prove useful in optimizing inclusion criteria within the setting of the MIRA-1 protocol. These findings are consistent with epidemiological studies that established cholesterol, fibrinogen, alpha<sub>2</sub>-macroglobulin, vascular endothelial growth factor (VEGF), von Willebrand factor, and plasma viscosity as factors associated with AMD.<sup>13-16</sup>

## PATIENTS AND METHODS

### SITES

A total of nine clinical centers in the United States have enrolled patients in this study. Before patient enrollment began at any center, the FDA and then the local institutional review boards of the participating clinical centers reviewed the protocol, authorized the patient informed consent, and accepted the clinical design. All ophthalmic and apheresis investigators, clinical coordinators, and photographers participated in a standardized orientation. Ophthalmic examiners assessed visual acuity using the ETDRS (LogMAR) chart and a standardized refraction and visual acuity protocol. They underwent regular quality assurance audits by the study's independent clinical research organization (CRO) ProMedica International (Huntington Beach, California).

### PATIENT SELECTION AND ENTRY EVALUATIONS

The FDA has authorized up to 180 patients for enrollment with the goal of having at least 150 evaluable patients at the conclusion of the trial. All patients provided informed consent. Ophthalmologists, responsible for enrolling patients and follow-up, determined ophthalmic eligibility criteria and supervised efficacy assessments. Nephrologists, who were certified to enroll and follow the patients, performed enrollment physicals, determined medical eligibility criteria, supervised treatments, and provided safety assessments. The inclusionary

and exclusionary criteria for study eligibility are listed in Table I.

In addition, fundus photographs were obtained at baseline and at 3, 6, 9, and 12 months at follow-up visits. Fluorescein angiograms were obtained at baseline, 3 months, and 12 months. The fundus photographs and fluorescein angiograms were assessed at the UCLA Jules Stein Eye Institute Clinical Research Center Fundus Photograph Reading Unit (Los Angeles, California), where objective evaluations of the photographs and fluorescein angiograms were documented in a masked fashion. The Reading Unit was tasked with documenting all gross morphologic changes that occurred from baseline through completion with regard to (a) drusen size, character, and distribution, (b) development and progression of choroidal neovascularization, and (c) other interval fundus changes or abnormalities.

#### TREATMENT PROTOCOLS

Qualified consenting patients aged 50 to 85 were randomly assigned to one of two treatment arms—the Rheopheresis treatment group or the placebo-control group—in a 2:1 ratio, respectively. Oral supplementation consisting of zinc and high-dose vitamins and antioxidants was given to all enrolled patients. Depending on the randomization, each patient was scheduled to receive either eight Rheopheresis or eight placebo procedures, in a pulsed protocol delivered over a 10-week treatment period. In addition, any patient from either group who experienced a prospectively determined “improvement” at the 3-month postbaseline evaluation but then later showed a prospectively determined decrease at the 9-month postbaseline interval was eligible to receive two additional treatments (either Rheopheresis or placebo) 2 weeks after the 9-month postbaseline visit. Of the 43 patients included in this interim analysis, only two

TABLE I: INCLUSION AND EXCLUSION CRITERIA

#### Inclusion criteria

Patients of any race between the ages of 50 and 85 yr inclusive.

Patients must weigh  $\geq 110$  lb (50 kg).

Study eye must have a diagnosis of nonexudative “dry” AMD with  $\geq 10$  large soft, semisoft, and/or confluent drusen within 3,000 nm of the foveal center.<sup>2</sup>

Study eye must have a best corrected visual acuity using the ETDRS chart between 20/32 and 20/125 inclusive.

Geographic atrophy is allowed as long as it is less than 3 disc diameters within 3,000 nm of the foveal center.

Serous pigment epithelial detachment is allowed as long as no clearly identifiable neovascularization is present.

Patients must have elevated baseline concentrations of 2 of the following 3 rheologic factors: total serum cholesterol level  $\geq 200$  mg/dL, fibrinogen level  $\geq 300$  mg/dL, or serum immunoglobulin A (IgA) level  $\geq 200$  mg/dL, as determined at the qualifying evaluation.

Patients must have a score of no more than 75 on the VFQ-25 Visual Functioning Questionnaire.

Study eye must not have conditions that limit the view of the fundus.

Patients must have normal prothrombin (PT) and partial thromboplastin (PTT) clotting times with the exception of patients who are stable on long-term coumadin therapy.

Patients must have adequate bilateral antecubital venous access.

Patients taking lipid-lowering medication at the beginning of the treatment phase must agree to continue to take it throughout the treatment phase using their current regimen.

Patients must be available for minimum study duration of about 12 months.

Patients must be highly motivated, alert, oriented, mentally competent, and able to understand and comply with the requirements of the study.

Patients must agree to discontinue their previous vitamin regimen and to substitute their regimen with a uniform supplement regimen provided by the study, OcularRx (Science-Based Health, Corde Madera, California). This was done to ensure that every patient in the study ingested the same supplement regimen.

#### Exclusion criteria

Study eye with concomitant retinal or choroidal disorder other than AMD.

Study eye with significant central lens opacities.

Study eye with a diagnosis of exudative “wet” AMD.

Study eye with other ocular diseases.

Patients who are in poor general health.

Patients with a hematocrit  $< 35\%$ , evidence of active bleeding, or a platelet count  $< 100,000$  k/ $\mu$ L.

Patients with significant cardiac problems.

Patients with uncontrolled hypertension.

Patients with recent history of cerebral vascular disease.

Patients with severe hepatic failure or uncontrolled diabetes.

Patients with a history of HIV infection, AIDS, hepatitis, or other immunosuppressive disorders.

Patients who are allergic to fluorescein sodium and to indocyanine green.

Patients unwilling to adhere to visit or examination schedules.

Patients with a known history of alcoholism, drug abuse, or any other condition that would limit validity of consent.

AMD, age-related macular degeneration.

received booster treatments (one patient received two treatments, while the other received one treatment). All patients were shrouded from the neck down to prevent them from determining their randomization arm (see “Masking Procedure”). Rheopheresis is not typically performed by a physician. In this study, medical technicians or nurses operating with indirect apheresis physician supervision provided all 343 treatments.

Rheopheresis treatments were administered in paired 100% plasma volume processing sessions with a 2-day recovery interval between each treatment session. Each treatment session required 2 to 4 hours to complete a 100% plasma volume processing procedure, depending on the patient’s size and the adequacy of venous access. Patients were continuously monitored with ECG, automated blood pressure, oxygen saturation, and intratreatment coagulation tests. A 16-day ( $\pm 2$  days) interval of “therapeutic rest” was provided between each of the paired treatment sessions. Placebo-control treatments were administered on a similar schedule but incorporated 2-hour masked charades initiated with bilateral insertions of 21-gauge HepLok needles. Efficacy and safety parameters were evaluated midway through the 10-week treatment period (before treatment 5) and at each of the 3-, 6-, 9-, and 12-month postbaseline follow-up intervals.

#### RHEOPHERESIS BLOOD FILTRATION

Rheopheresis is a form of therapeutic plasma apheresis that utilizes a novel nanopore, hollow-fiber, membrane technology configured in a differential filtration array with two single-use, in-line, membrane filters (Figure 1). The process incorporates a protocol designed to deplete excess concentrations of soluble high-molecular-weight plasma components by mechanically sieving circulating species larger than 25 nm (as measured across their shortest linear axis) or approximately 500 kDa by weight from the blood. As such, the therapy provides physiologic depletions of a targeted bandwidth of plasma species, including immune complexes, IgM,  $\alpha_2$ -macroglobulin, fibrinogen, Von Willenbrandt Factor, low-density lipoprotein cholesterol (LDL-C), and others.<sup>17</sup>

Rheopheresis patients required bilateral insertions of 16-, 17-, or 18-gauge needles into each antecubital vein, connected to a single-use, sterile, closed-circuit, PVC tubing set. The Plasmatic blood pump (Kimal Scientific Products, Ltd, Rucorn, United Kingdom) provided blood circulation. The two-stage filtration process was provided by (a) the plasma separator (Plasmaflo 0P-05W[L]) connected in series to (b) the plasma component separator (Rheofilter AR-2000), both manufactured by Asahi Medical Co, Ltd (Tokyo, Japan).

Unlike conventional single-channel plasma exchange, this membrane differential filtration (MDF) system uses a dual-channel pumping mechanism designed to minimize

hemolysis by continuously separating native whole blood into its plasma and cellular components in a low-pressure circuit. In a separate pressurized circuit, the plasma is driven through the plasma component filter that sieves the plasma fraction, removing large ( $\geq 25$  nm), soluble, high-molecular-weight components. The sieved plasma is then recombined with the cellular fraction in a heated reservoir, and the enriched whole-blood mix is reinfused back into the patient via the sterile closed circuit.

In this euvolemic process, no more than 600 mL of blood is circulating within the continuously heparinized extracorporeal system at any one time. Of note, only autologous blood products are reintroduced into the patient’s circulation. In addition, only heparin is given. No other medications are needed, and no sedation is required. Two investigational sites performed Rheopheresis treatments in segregated, converted storage rooms as in-office procedures. One site utilized their adjacent ophthalmic surgery center in conjunction with a mobile apheresis team. Six sites partnered with affiliated or nearby dialysis or blood centers to provide treatment.

#### RANDOMIZED PROCEDURE

Treatment nurses used sequentially numbered sealed envelopes containing computer-generated random number assignments to assign the treatment arm (Rheopheresis versus placebo) at the time of the initial treatment. With respect to eyes, if both of a patient’s eyes qualified, one eye was similarly randomized into the Primary (study) Eye Cohort by the clinical coordinator.

Since multiple treatments were required, patients had to have been able to complete at least 75% of the initial plasma volume treatment in order to be considered an “intent to treat” patient. If a patient was assigned to Rheopheresis treatment but failed to complete the first treatment owing to inadequate bilateral venous access,

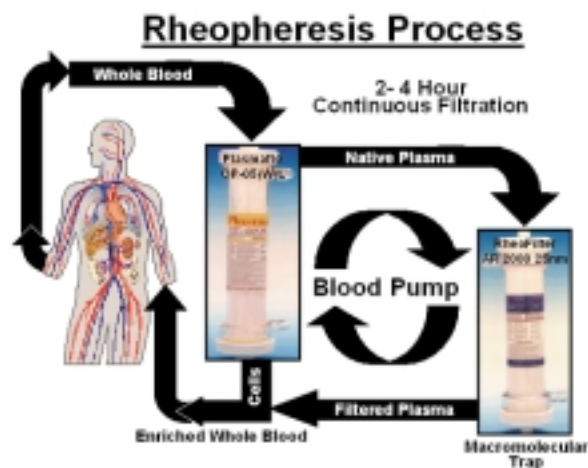


FIGURE 1  
Rheopheresis blood filtration process.

the patient was removed from the study and replaced using prespecified protocol procedures.

#### **MASKING PROCEDURE**

All patients were covered with an opaque shroud from the neck down prior to initiating each treatment in order to mask them from observing their treatment. Additionally, their arms were covered with drapes throughout the process. A partition was positioned in front of the blood pump and plasma therapy system so that the patient could not view the system. The pump was activated regardless of treatment arm assignment so that in each case the patient heard the background noise of the powered machine. Patients randomized to the placebo arm of the study received masked needlesticks with 21-gauge HepLok needles in both arms without connection to the tubing circuit. Placebo patients then underwent a 2-hour charade, complete with frequent machine alarms and checking of intravenous tube positioning.

Ophthalmologic investigators were masked, since treatments were performed at separate locations, and the treatment personnel were prohibited from discussing treatment arm assignments with the ophthalmic investigators. Physicians did not have access to study treatment envelopes, treatment forms, or the randomization log, all of which were maintained in separate areas in locked files.

#### **DATA MANAGEMENT**

Data acquisition was managed under a protocol developed with specific guidance provided prospectively by the FDA. Data were collected directly from the study sites by a third-party CRO, Promedica International (PMI, Huntington Beach, California), which had been retained from inception to provide independent, third-party, study-wide monitoring, data auditing, and database development services.

In the interim analysis, a direct, secure data transfer of the pertinent variables was made from PMI to BioStat International (BI, Tampa, Florida), which was retained specifically to perform statistical evaluation of the ophthalmic data for this interim analysis. The study's affiliate sponsor, Apheresis Technologies Inc (Palm Harbor, Florida), provided BI with a sealed copy of the randomization code for the 43 interim analysis patients only. Burkhart and Associates (BA, Salt Lake City, Utah) provided safety analysis under a similar protocol. PMI, BI, and BA do not have any relation to the study's sponsors, nor do they have any financial interests in the study's outcome.

### **STATISTICAL ANALYSIS AND METHODS**

---

#### **SAMPLE SIZE AND POWER**

The Statistical Plan for the MIRA-1 trial was based on the

results of the precedent German studies.<sup>8-10</sup> The current study called for an analysis of 150 available patients randomized into either Rheopheresis treatment or placebo-control groups on a 2:1 ratio. This sample size was expected to detect a difference with 95% to 98% power (2-sided test,  $\alpha=.05$ ) for the primary end point—comparison of mean line change in ETDRS (LogMAR) BCVA. The null hypothesis was no difference in LogMAR visual acuity from baseline in the Rheopheresis treatment group relative to the placebo-control group. With the expected power of this study, the original intent of the interim analysis was (1) to demonstrate gross trends in efficacy outcomes without anticipation of statistical significance and (2) to evaluate safety parameters and reporting procedures.

#### **BASELINE DEMOGRAPHICS**

Demographic and baseline characteristics were summarized and tested for treatment group comparability using a Fisher exact test or chi-square test for categorical values. A Wilcoxon rank sum test was used to compare continuous variables.

#### **ANALYTICAL MODEL: ANOVA WITH REPEATED MEASURES ANALYSIS**

Similar to the method used by the Age-Related Eye Disease Study (AREDS) trial, MIRA-1's end points (ie, mean changes in ETDRS [LogMAR] visual acuity from baseline through the available posttreatment interval visits) were compared using two-group ANOVA with repeated measures analysis with unstructured covariance using SAS/STAT Software (SAS Institute Inc, Cary, North Carolina). Both the group effect (rheopheresis treatment versus placebo-control efficacy) and time effect (determines if relative LogMAR acuity changes observed between Rheopheresis treatment and placebo-control are constant or change during the course of the study) were tested.

#### **PROPORTIONS ANALYSIS**

Frequency distribution of changes in ETDRS BCVA from baseline using various threshold categories ( $\geq 2$ -line improvement,  $\geq 3$ -line improvement,  $\geq 2$ -line loss,  $\geq 3$ -line loss) were presented without inferential statistics because of the inevitable loss of power when converting continuous variables into binary responses in the context of the small sample size of the interim analysis group.

#### **EFFICACY OUTCOME MEASURES**

The primary efficacy end point for the study and this interim analysis was prospectively identified as the comparison of mean change in LogMAR BCVA in the designated primary (study) eyes cohort comparing the

Rheopheresis treatment group with the placebo-control group. The interim analysis evaluated all available BCVA data on the first 43 enrolled intent-to-treat patients from baseline to the last available postbaseline follow-up visit.

Secondary efficacy outcomes included proportions of eyes with  $\geq 2$ -line (10 letters) or  $\geq 3$ -line (15 letters) loss or gain of best corrected ETDRS acuity. In addition, the proportion of cases with baseline ETDRS BCVA worse than 20/40 that achieved 20/40 or better acuity posttreatment was also determined because of the functional significance of 20/40 vision as a legal threshold criterion for maintaining a valid driver's license.

#### INTENT-TO-TREAT ANALYSIS

The primary efficacy analyses were based on a strict intent-to-treat analysis; patients were analyzed within the group to which they were randomly assigned. All 43 patients that had available baseline and 2-week posttreatment (3-month postbaseline) LogMAR BCVA measures at the time of closeout of the interim analysis database were included. One patient received only five of the planned eight Rheopheresis treatments, while another patient received seven of the planned eight Rheopheresis treatments. Two patients received one and two Rheopheresis booster treatments, respectively. The same series was later updated to include available follow-up through the 12-month postbaseline interval. The analysis presented here represents a consecutive series of cases with the following exceptions:

Three patients randomized to the Rheopheresis group were replaced, as per the protocol, at the time of their initial treatment owing to an inability to obtain adequate bilateral venous access. Two additional patients were randomized within the same time frame of the 43-case interim analysis, but their 2-week posttreatment interval data were not available to PMI at the time the interim analysis data collection period was closed. These patients' data will be included in all subsequent analyses. One patient was enrolled without documentation of baseline LogMAR BCVA, and thus no BCVA efficacy analysis was possible.

The main analysis was performed comparing the primary (study) eyes cohort of the Rheopheresis treatment group versus the placebo-control group. Since treatments were systemic, analyses were also performed for the all-qualifying-eyes and all-eyes cohorts of the 43 cases, regardless of the qualification or visual status in the contralateral eye.

All cases that had baseline ETDRS BCVA worse than 20/40 were analyzed separately as a subset.

#### SAFETY OUTCOME MEASURES

As is required of all FDA trials, safety was evaluated by

documenting evidence of any and all adverse events that occurred over the course of the study. For each adverse event occurrence, the following were recorded: (a) date of onset, (b) date of resolution, (c) severity, (d) determination as to whether the event was treatment-related or non-treatment-related, (e) determination as to whether the event was serious or not serious, (f) action or treatment required, and (g) the outcome. Anticipated treatment-related safety events included observations for episodes of dysrhythmias, hypotension, dizziness, paresthesias, flushing, nausea, vomiting, edema, lethargy, fatigue, chills, and hypoglycemia, among others.

#### HEMATOLOGY OUTCOME MEASURES

All consenting patients submitted to baseline HIV and hepatitis antigen-antibody screening. Postenrollment blood samples were collected for complete blood cell count, blood chemistry, prothrombin time (PT), partial thromboplastin time (PTT), lipid profile, fibrinogen, immunoglobulin levels, and select hemorrheologic factors ( $\alpha_2$ -macroglobulin, serum and whole-blood viscosity) at baseline, each pretreatment, each posttreatment, and at 3- and 6-month postbaseline follow-up intervals. Baseline laboratory measurements were compared between the Rheopheresis treatment and placebo-control groups using *t* tests except for several variables that were analyzed by nonparametric Mann-Whitney tests due to skewness in the data.

#### ANATOMIC OUTCOME MEASURES

With regard to the detection of gross anatomic treatment effects (ie, a decrease in drusen or development of choroidal neovascularization), given a significance level of .05 and a treatment difference of possibly 15% between the treatment and placebo-control groups, the sample size of the interim analysis population provided only an 11% power to detect a significant difference in this secondary outcome at this juncture.

## RESULTS

#### BASELINE DEMOGRAPHICS

There were 43 patients involved in the interim analysis: 28 Rheopheresis treatment and 15 placebo-control patients. Both eyes qualified for treatment based on the enrollment criteria in 11 (26%) of the enrolled patients.

The baseline characteristics of the Rheopheresis treatment and placebo-control groups with regard to age, sex, and mean baseline LogMAR acuity were not significantly different in the Rheopheresis treatment and placebo-control groups (Table II). The mean visual acuity was 20/47 for the Rheopheresis treatment group and 20/49 for the placebo-control group ( $P = .81$ ). All patients in the Rheopheresis treatment and placebo-control

TABLE II: BASELINE PATIENT CHARACTERISTICS AND DEMOGRAPHICS

VARIABLE	TREATMENT	PLACEBO	P VALUE
Age (yr)			
Mean ± SD	74.8 ± 7.8	74.7 ± 5.9	.94
Median	76.5	74.0	
Range	59-85	66-85	
Distribution:			
<60	1 (4%)	0	
60-69	7 (25%)	4 (27%)	
70-79	11 (39%)	8 (53%)	
80+	9 (32%)	3 (20%)	
Sex			
Male	16 (57%)	5 (33%)	.14
Female	12 (43%)	10 (67%)	
Mean LogMAR ± SD	0.37 ± 0.11	0.39 ± 0.17	.81
Mean visual acuity	20/47	20/49	

groups were Caucasian except one in the Rheopheresis treatment group, who was Asian.

Table III provides a listing of selected baseline laboratory values by treatment and placebo groups. With the exception of baseline serum uric acid level, which was significantly higher in the Rheopheresis treatment group than in the placebo-control group (5.24 mg/dL treatment versus 4.26 mg/dL placebo,  $P = .01$ ), there were no significant differences at baseline between the Rheopheresis treatment and placebo-control groups in any other of the 62 blood parameters tested. Nine mean baseline laboratory values were elevated in both the Rheopheresis treatment and placebo-control groups (ie, fibrinogen, international normalized ratio [INR], PT, serum intracellular adhesion molecule-1 (sICAM-1), total cholesterol, very low-density cholesterol (VLDL-C), LDL-C, serum osmolality, and whole-blood viscosity). It appears likely that these hemorrheologic abnormalities were present on account of protocol enrollment criteria that specifically preselected and sought to qualify patients with elevated levels of certain high-molecular-weight blood components (see “Inclusion Criteria,” Table I).

#### INTENT-TO-TREAT ANALYSIS

The results of the analysis of variance (ANOVA) repeated-measures analysis, as well as the mean LogMAR line difference between Rheopheresis treatment and placebo-control groups at the 12-month postbaseline interval, are shown in Table IV. In the Primary Eye cohort, the 12-month postbaseline mean LogMAR line difference between Rheopheresis treatment and placebo-control groups was 1.6 lines (group effect (GE)  $P = .0011$ ). The time effect (TE) was not significant ( $P = .2560$ ), indicating a “therapeutic plateau” (ie, there was no significant change in the therapeutic benefit of the Rheopheresis treatment group relative to the placebo-control group

over the 12-month course of the trial). These results are graphically depicted in Figure 2. Similar findings were consistently observed in both the all-qualifying-eyes cohort (GE  $P = .0053$  and TE  $P = .2570$ ), and the all-eyes cohort (GE  $P = 0.002$  and TE  $P = .4093$ ) as well.

Table V demonstrates the proportional changes in LogMAR acuity at each of the postbaseline interval visits for the primary eyes cohort. The Rheopheresis treatment group consistently had a greater proportion of cases with line improvements at each postbaseline interval, compared with the placebo-control group, regardless of which threshold criterion ( $\geq 1$  line,  $\geq 1.5$  lines,  $\geq 2$  lines,  $\geq 2.5$  lines or  $\geq 3$  lines) for BCVA, improvement was used. At 9 and 12 months postbaseline, 13% and 12% of the Rheopheresis treatment eyes had a  $\geq 3$ -line improvement in BCVA respectively, compared with 0% and 0% of the eyes in the placebo-control group (Figure 3). Similarly, the Rheopheresis treatment group consistently had a smaller proportion of cases with BCVA line losses at each postbaseline interval compared with the placebo-control group (Table V). At 12 months postbaseline, only 4.0% of the Rheopheresis treatment eyes had a  $\geq 3$ -line loss of BCVA compared with 18.2% of the eyes in the placebo-control group (Figure 4).

#### SUBGROUP ANALYSIS: EYES WITH BASELINE ETDRS BCVA WORSE THAN 20/40

In the subset of the primary eyes cohort with baseline LogMAR BCVA worse than 20/40, the mean 12-month postbaseline interval LogMAR line difference between Rheopheresis treatment and placebo-control groups was 3.0 lines (15 letters; GE  $P = .0014$  and TE  $P = .2928$ ). Figure 5 demonstrates that the mean line difference between the two groups tended to increase over time. This was largely due to the progressive loss of mean BCVA in the placebo-control eyes, while the posttreatment improvement in mean BCVA in the Rheopheresis-treated eyes remained essentially constant (1.3 lines posttreatment and 1.1 lines at the 12-month postbaseline interval). Again, the GE and TE outcomes were consistent in both the all-qualifying-eyes (GE  $P = .0122$  and TE  $P = .2747$ ) and the all-eyes (GE  $P = .0050$  and TE  $P = .3565$ ) cohorts as well.

In the subset of cases with baseline LogMAR BCVA worse than 20/40, the Rheopheresis treatment group consistently demonstrated a greater proportion of cases with ETDRS line improvements at each postbaseline interval compared with the placebo-control group (Table V). In fact, none of the placebo-control cases had a  $\geq 3$ -line improvement in vision at any postbaseline interval, compared with 18.8% and 15.8% of the Rheopheresis treatment patients achieving this level of improvement at the 9- and 12-month postbaseline intervals, respectively (Figure 6).

With respect to vision loss in the primary eyes cohort,

the Rheopheresis treatment group consistently had a smaller proportion of cases with ETDRS line losses at each postbaseline interval compared with the placebo-control group (Table V). At 12 months postbaseline, only 5.3% of Rheopheresis-treated eyes demonstrated a  $\geq 3$ -

line loss of BCVA compared to 28.6% of placebo controls (Figure 7). In the subgroup of Rheopheresis-treated primary eyes with baseline LogMAR acuity worse than 20/40, 57.9% improved to 20/40 or better at the 12-month postbaseline interval compared with only 14.3% of the

TABLE III: BASELINE LABORATORY VALUES BY TREATMENT GROUP

LABORATORY TEST	STUDY GROUP	N	MEAN	SD	MIN	MAX	P VALUE	NORMAL VALUES	
								LOW	HIGH
Albumin (g/dL)	Rheopheresis	28	4.16	0.25	3.8	4.9	.419	3.5	4.8
	Placebo	15	4.23	0.27	3.6	4.5			
Alpha <sub>2</sub> -macroglobulin (mg/dL)	Rheopheresis	25	198.6	54.5	127	357	.843	131	293
	Placebo	13	202.4	55.5	124	315			
E-selectin (ng/mL)	Rheopheresis	25	40.6	14.7	17	66.4	.179	12.0	80.4
	Placebo	13	47.9	17.1	21.2	81			
Fibrinogen (mg/dL)	Rheopheresis	25	377.6†	139.2	87	776	.716	154	494
	Placebo	14	362.4†	92.6	267	551			
Hemoglobin (g/dL)	Rheopheresis	28	14.03	1.28	11.7	16.8	.807	11.5	17.0
	Placebo	15	14.13	1.32	12.3	16.7			
Hematocrit (%)	Rheopheresis	28	41.9	3.7	35.7	48.7	.488	34	50
	Placebo	15	42.7	3.5	36.6	48			
IgA (mg/dL)	Rheopheresis	28	282.6	106.4	113	532	.560	70	400
	Placebo	15	306.4	157.9	75	698			
IgG (mg/dL)	Rheopheresis	28	1048.2	238.7	576	1567	.995	700	1600
	Placebo	15	1047.7	245.2	697	1741			
IgM (mg/dL)	Rheopheresis	28	120.7	109.6	22	584	.429	40	230
	Placebo	15	120.3	62.5	51	300			
International normalized ratio	Rheopheresis	26	1.32°	1.13	0.9	6.8	.672	2.0	3.5
	Placebo	14	1.16°	0.43	0.9	2.6			
Platelets (x10 <sup>9</sup> /μL)	Rheopheresis	28	250.7	56.0	153	360	.375	140	415
	Placebo	14	267.1	55.4	173	354			
PT (sec)	Rheopheresis	25	16.4°	15.4	11.1	89.3	.464	9.0	12.7
	Placebo	14	13.9°	5.6	10.6	32.8			
aPTT (sec)	Rheopheresis	25	29.4	6.2	24	52	.416	23	39
	Placebo	14	27.4	3.0	24	35			
sICAM-1 (ng/mL)	Rheopheresis	25	299.5†	51.9	222.2	447	.805	114.7	306.4
	Placebo	13	295.2†	47.9	235.2	384			
Total cholesterol (mg/dL)	Rheopheresis	28	220.1°	37.3	155	292	.442	100	199
	Placebo	15	229.9°	43.7	150	354			
HDL-C (mg/dL)	Rheopheresis	28	54.2	14.7	30	85	.351	30	85
	Placebo	15	59.7	23.5	34	129			
VLDL-C (mg/dL)	Rheopheresis	26	37.0†	16.0	12	74	.361	5	40
	Placebo	14	32.4†	12.9	8	58			
LDL-C (mg/dL)	Rheopheresis	26	125.6†	34.4	73	192	.478	0	129
	Placebo	14	134.4°	42.3	65	244			
Von Willebrand factor activity (%)	Rheopheresis	24	115.3	47.6	51	226	.315	50	170
	Placebo	12	134.0	60.2	54	259			
Uric acid (mg/dL)	Rheopheresis	28	5.24	1.19	2.8	7.5	.011	2.4	8.2
	Placebo	15	4.26	1.05	1.9	5.8			
Total protein (g/dL)	Rheopheresis	28	7.23	0.42	6.4	8.5	.382	6.0	8.5
	Placebo	15	7.36	0.55	6.5	8.7			
Triglyceride (mg/dL)	Rheopheresis	28	205.5	104.4	61	492	.490	10	250
	Placebo	15	182.9	96.0	44	449			
Serum osmolality (mOsm/kg)	Rheopheresis	24	301.6°	8.7	285	318	.475	280	301
	Placebo	13	299.6†	6.0	288	309			
Viscosity serum (cP, relative to saline)	Rheopheresis	23	1.65	0.13	1.4	1.9	.108	1.6	1.9
	Placebo	12	1.78	0.31	1.5	2.7			
Viscosity whole blood (cP)	Rheopheresis	25	6.56°	1.33	4.5	10.8	.757	3.6	6.0
	Placebo	11		1.67	4.2	9.8			

°Exceeds limits.

†Highest quartile.

TABLE IV: COMPARISON OF MEAN CHANGE FROM BASELINE ETDRS BCVA RHEOPHERESIS TREATMENT VERSUS PLACEBO CONTROL

COHORT	N	MEAN LOGMAR LINE DIFFERENCE (AT 12 MO)	GROUP EFFECT		TIME EFFECT	
			F	P VALUE <sup>°</sup>	F	P VALUE <sup>°</sup>
All eyes	85					
Primary eyes	43	1.6	12.22	.0011	1.41	.2560
All qualifying eyes	54	1.5	8.50	.0053	1.39	.2570
All eyes	85	1.7	9.49	.0028	0.97	.4093
All eyes with baseline BCVA worse than 20/40	56					
Primary eyes	28	3.0	12.70	.0014	1.31	.2928
All qualifying eyes	35	2.8	7.08	.0122	1.36	.2747
All eyes	56	3.2	8.55	.0050	1.10	.3565

<sup>°</sup>P values calculated by ANOVA with repeated measures analysis (with unstructured covariance).

TABLE V: PRIMARY EYES: CHANGES IN BCVA OVER TIME

EFFICACY PARAMETER	3 MONTHS		6 MONTHS		9 MONTHS		12 MONTHS	
	TREATMENT	PLACEBO	TREATMENT	PLACEBO	TREATMENT	PLACEBO	TREATMENT	PLACEBO
N=	28	15	27	13	23	13	25	11
All treatment eyes								
Visual improvement								
≥+1 line	14 (50.0%)	3 (20.0%)	13 (48.1%)	3 (23.1%)	9 (39.1%)	6 (46.2%)	12 (48.0%)	3 (27.3%)
≥+1.5 lines	10 (35.7%)	1 (6.7%)	11 (40.7%)	3 (23.1%)	6 (26.1%)	2 (15.4%)	9 (36.0%)	2 (18.2%)
≥+2 lines	8 (28.6%)	1 (6.7%)	7 (25.9%)	2 (15.4%)	4 (17.4%)	0 (0.0%)	7 (28.0%)	2 (18.2%)
≥+2.5 lines	4 (14.3%)	0 (0.0%)	3 (11.1%)	0 (0.0%)	3 (13.0%)	0 (0.0%)	5 (20.0%)	1 (9.1%)
≥+3 lines	3 (10.7%)	0 (0.0%)	2 (7.4%)	0 (0.0%)	3 (13.0%)	0 (0.0%)	3 (12.0%)	0 (0.0%)
Visual loss								
Loss of ≥3 lines BCVA	0 (0.0%)	1 (6.7%)	0 (0.0%)	1 (7.7%)	0 (0.0%)	1 (7.7%)	1 (4.0%)	2 (18.2%)
Loss of ≥2 lines BCVA	0 (0.0%)	1 (6.7%)	0 (0.0%)	1 (7.7%)	1 (4.3%)	2 (15.4%)	2 (8.0%)	2 (18.2%)
Average line change								
From baseline <sup>°</sup>	1.16	0.19	1.15	-0.43	0.90	-0.20	0.74	-0.87
Difference between treatment groups <sup>†</sup>	0.97		1.58		1.10		1.61	
N=	19	9	19	7	16	8	19	7
BCVA <20/40 pretreatment								
Visual improvement								
≥+1 line	11 (57.9%)	1 (11.1%)	9 (47.4%)	1 (14.3%)	7 (43.8%)	2 (25.0%)	11 (57.9%)	2 (28.6%)
≥+1.5 lines	9 (47.4%)	1 (11.1%)	7 (36.8%)	1 (14.3%)	4 (25.0%)	0 (0.0%)	8 (42.1%)	1 (14.3%)
≥+2 lines	8 (42.1%)	1 (11.1%)	6 (31.6%)	1 (14.3%)	4 (25.0%)	0 (0.0%)	6 (31.6%)	1 (14.3%)
≥+2.5 lines	4 (21.1%)	0 (0.0%)	3 (15.8%)	0 (0.0%)	3 (18.8%)	0 (0.0%)	4 (21.1%)	0 (0.0%)
≥+3 lines	3 (15.8%)	0 (0.0%)	2 (10.5%)	0 (0.0%)	3 (18.8%)	0 (0.0%)	3 (15.8%)	0 (0.0%)
Improvement to 20/40 or better	10 (52.6%)	1 (11.1%)	10 (52.6%)	1 (14.3%)	6 (37.5%)	1 (12.5%)	11 (57.9%)	1 (14.3%)
Visual loss								
Loss of ≥3 lines BCVA	0 (0.0%)	1 (11.1%)	0 (0.0%)	1 (14.3%)	0 (0.0%)	1 (12.5%)	1 (5.3%)	2 (28.6%)
Loss of ≥2 lines BCVA	0 (0.0%)	1 (11.1%)	0 (0.0%)	1 (14.3%)	1 (6.3%)	2 (25.0%)	1 (5.3%)	2 (28.6%)
Average line change								
From baseline <sup>°</sup>	1.35	-0.11	1.23	-1.49	1.11	-1.05	1.06	-1.91
Difference between treatment groups <sup>†</sup>	1.46		2.72		2.16		2.98	

<sup>°</sup>Positive number equals improvement; negative number equals loss.

<sup>†</sup>Positive number means treatment better than placebo.

placebo-control group (Figure 8). The proportions of cases demonstrating visual improvements or losses were similar in the all-qualifying-eyes (Table VI) and the all-eyes (Table VII) cohorts.

#### MORPHOMETRICS

Of the 43 primary eyes graded by the Fundus Photograph Reading Unit, a total of 10 primary eyes, 28.6% (8 of 28) of the Rheopheresis-treated cases, and 13.3% (2 of 15) of

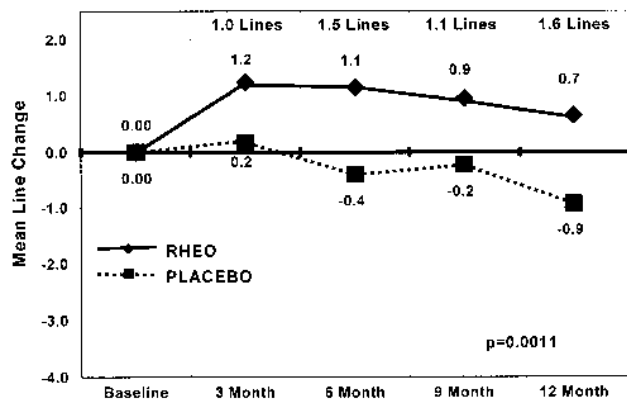


FIGURE 2

Mean ETDRS line change over time in the primary eyes randomized to receive Rheopheresis or placebo-control treatment.

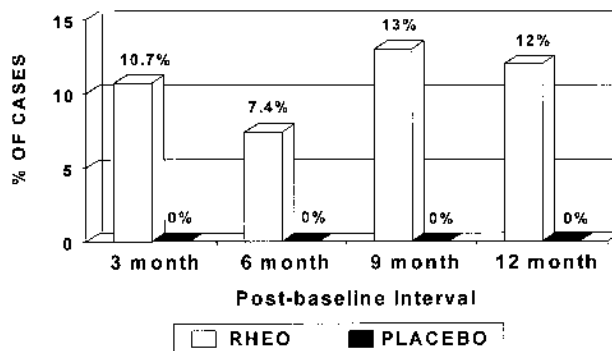


FIGURE 3

Proportion of cases with ≥3 lines of ETDRS BCVA improvement at each postbaseline interval in the primary eyes cohort of patients randomized to receive Rheopheresis or placebo-control treatment.

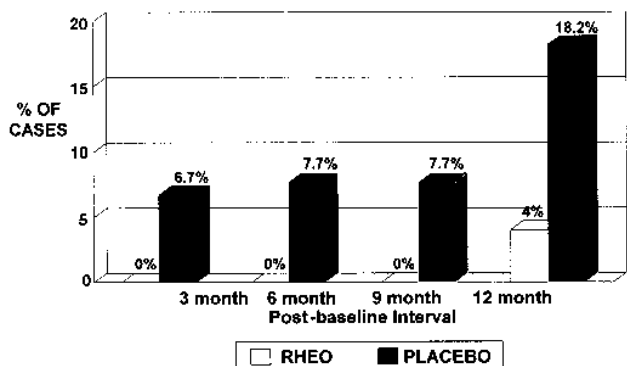


FIGURE 4

Proportion of cases with ≥3 lines of ETDRS BCVA loss at each post-baseline interval in the primary eyes cohort of patients randomized to receive Rheopheresis or placebo-control treatment.

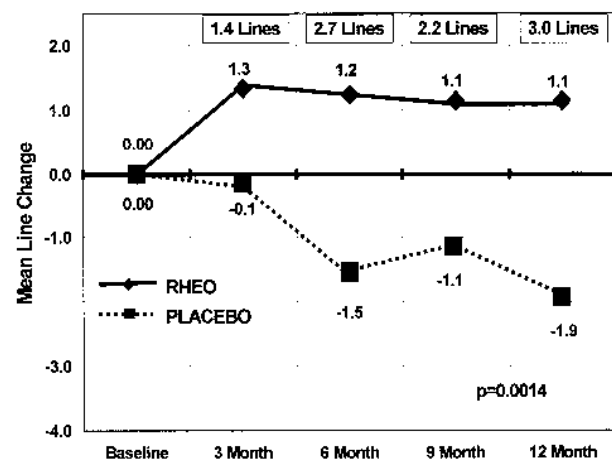


FIGURE 5

Mean ETDRS line change over time in subgroup of primary eyes with worse than 20/40 vision at baseline who were randomized to receive Rheopheresis or placebo-control treatment.

the placebo-control cases were found to have either a decrease in the number of drusen or drusen with a more atrophic (whiter) appearance over the course of the study ( $P = .28$  with Fisher's exact test). In no case was a progression to nonexudative AMD documented.

**SAFETY: REPORTING OF ADVERSE EVENTS**

*General*

In the MIRA-1 interim analysis population, a total of 40 adverse events, both treatment-related (5) and non-treatment-related (35), were recorded during 343 treatments and over the 12-month postbaseline interval for the 43 patients subject to the analysis. Table VIII provides a listing of each reported event by treatment arm, Rheopheresis (RHEO=23) versus placebo control (PBO=17). Four oph-

thalmic events were documented, two in each study group. In the Rheopheresis treatment group, one treatment-related case of bilateral lid edema occurred and resolved spontaneously within 48 hours with application of warm and cold compresses. A mild non-treatment-related case of iritis was also reported, and it resolved without sequelae. In the placebo-control group, one case of unilateral lid edema was noted and one case of capsular opacity occurred. The most common problem encountered in the trial population involved the establishment and maintenance of adequate peripheral venous access in the Rheopheresis group (38 of 223 procedures [17%]). The use of A-V shunts, percutaneous intravascular catheters (ie, PIC lines), ports, or other means, while not medically contraindicated, was prohibited in the context of this FDA study.

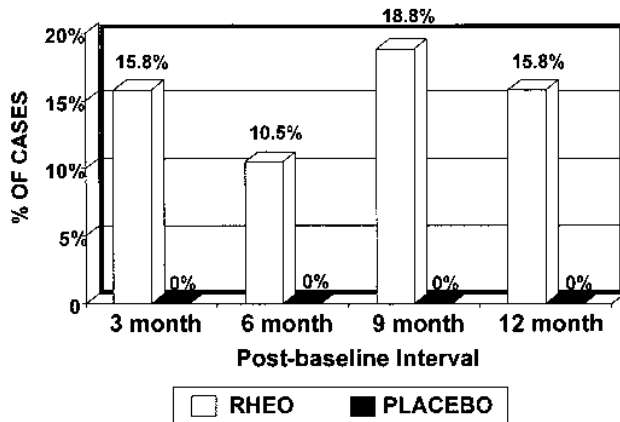


FIGURE 6

Proportion of cases with  $\geq 3$  lines of ETDRS BCVA improvement at each postbaseline interval in subgroup of primary eyes of patients with baseline BCVA of worse than 20/40 that were randomized to receive Rheopheresis or placebo-control treatment.

*Non-Treatment-Related Adverse Events*

The incidence of reported non-treatment-related adverse events was significantly lower in the Rheopheresis treatment group (8.1%, 18 of 223) than the placebo-control group (17 of 120 [14.2%]) ( $P = .03$ ). The incidence of serious non-treatment-related events for the Rheopheresis treatment group (5 of 223 [2.2%]) and the placebo-control group (2 of 120 [1.6%]) was similar ( $P = .30$ ). Two distant deaths (one by suicide and one due to leukemia) were reported in the Rheopheresis treatment group. Both deaths occurred between the 9-month and 12-month postbaseline interval. No deaths occurred in the placebo-control group.

*Treatment-Related Adverse Events*

Treatment-related adverse events were observed in 2.2%

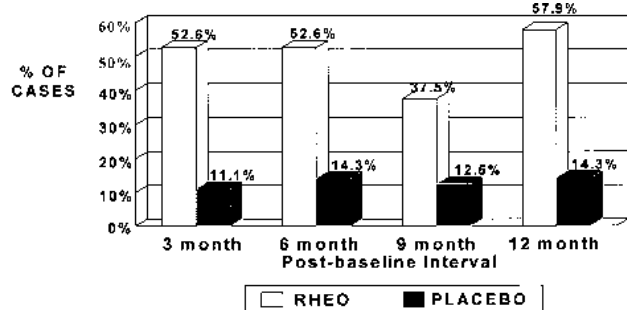


FIGURE 8

Proportion of cases with ETDRS improvements to 20/40 or better at each postbaseline interval in subgroup of primary eyes of patients with worse than 20/40 BCVA at baseline that were randomized to receive Rheopheresis or placebo-control treatment.

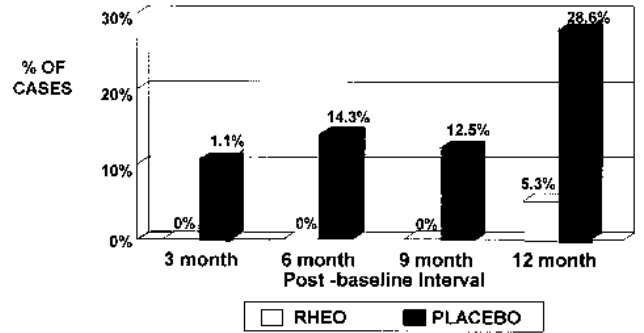


FIGURE 7

Proportion of cases with  $\geq 3$  lines of ETDRS BCVA loss at each post-baseline interval in subgroup of primary eyes of patients with baseline BCVA of worse than 20/40 that were randomized to receive Rheopheresis or placebo-control treatment.

(5 of 223) of Rheopheresis procedures and in 0% (0 of 120) of placebo-control treatments ( $P = .11$ ). None of the five Rheopheresis-related events were serious, and none were unanticipated (Figure 9). All five nonserious Rheopheresis-related events were associated with either transient or self-limited changes in intratreatment blood pressure (hypotension, 2), fluid shifts (edema, 2), or vagal response (nausea, 1). No treatment-related hospitalizations or long-term treatment-related side effects or adverse events have been reported during this study.

**DISCUSSION**

**THE MIRA-1 TRIAL**

MIRA-1 is the largest double-masked apheresis trial ever undertaken. It is the first prospective trial to evaluate the

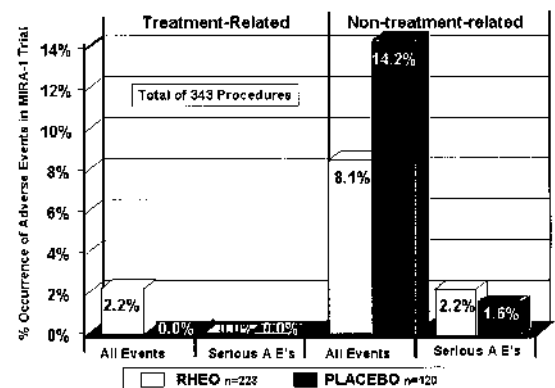


FIGURE 9

Occurrence of treatment-related and non-treatment-related adverse events in the 343 procedures performed in 43 patients randomized to receive Rheopheresis or placebo-control treatments reported as both serious and nonserious adverse events.

TABLE VI: ALL QUALIFYING EYES: CHANGES IN BCVA OVER TIME

EFFICACY PARAMETER	3 MONTHS		6 MONTHS		9 MONTHS		12 MONTHS	
	TREATMENT	PLACEBO	TREATMENT	PLACEBO	TREATMENT	PLACEBO	TREATMENT	PLACEBO
N=	36	18	35	16	30	16	32	13
All treatment eyes								
Visual improvement								
≥+1 line	18 (50.0%)	5 (27.8%)	16 (45.7%)	3 (18.8%)	13 (43.3%)	7 (43.8%)	16 (50.0%)	4 (30.8%)
≥+1.5 lines	13 (36.1%)	1 (5.6%)	14 (40.0%)	3 (18.8%)	9 (30.0%)	2 (12.5%)	12 (37.5%)	2 (15.4%)
≥+2 lines	9 (25.0%)	1 (5.6%)	10 (28.6%)	2 (12.5%)	7 (23.3%)	0 (0.0%)	10 (31.3%)	2 (15.4%)
≥+2.5 lines	4 (11.1%)	0 (0.0%)	3 (8.6%)	0 (0.0%)	4 (13.3%)	0 (0.0%)	5 (15.6%)	1 (7.7%)
≥+3 lines	3 (8.3%)	0 (0.0%)	2 (5.7%)	0 (0.0%)	4 (13.3%)	0 (0.0%)	3 (9.4%)	0 (0.0%)
Visual loss								
Loss of ≥3 lines BCVA	0 (0.0%)	1 (5.6%)	1 (2.9%)	1 (6.3%)	1 (3.3%)	2 (12.5%)	1 (3.1%)	2 (15.4%)
Loss of ≥2 lines BCVA	1 (2.8%)	1 (5.6%)	1 (2.9%)	1 (6.3%)	2 (6.7%)	3 (18.8%)	2 (6.3%)	2 (15.4%)
Average line change								
From baseline <sup>°</sup>	1.02	0.31	0.93	-0.41	0.73	-0.36	0.82	-0.69
Difference between treatment groups <sup>†</sup>		0.71		1.34		1.09		1.51
N=	24	11	24	9	20	10	23	8
BCVA <20/40 pretreatment								
Visual improvement								
≥+1 line	12 (50.0%)	2 (18.2%)	10 (41.7%)	1 (11.1%)	8 (40.0%)	2 (20.0%)	12 (52.2%)	2 (25.0%)
≥+1.5 lines	9 (37.5%)	1 (9.1%)	8 (33.3%)	1 (11.1%)	5 (25.0%)	0 (0.0%)	9 (39.1%)	1 (12.5%)
≥+2 lines	8 (33.3%)	1 (9.1%)	7 (29.2%)	1 (11.1%)	5 (25.0%)	0 (0.0%)	7 (30.4%)	1 (12.5%)
≥+2.5 lines	4 (16.7%)	0 (0.0%)	3 (12.5%)	0 (0.0%)	4 (20.0%)	0 (0.0%)	4 (17.4%)	0 (0.0%)
≥+3 lines	3 (12.5%)	0 (0.0%)	2 (8.3%)	0 (0.0%)	4 (20.0%)	0 (0.0%)	3 (13.0%)	0 (0.0%)
Improvement to 20/40 or better	11 (45.8%)	2 (18.2%)	10 (41.7%)	1 (11.1%)	7 (35.0%)	1 (10.0%)	13 (56.5%)	1 (12.5%)
Visual loss								
Loss of ≥3 lines BCVA	0 (0.0%)	1 (9.1%)	1 (4.2%)	1 (11.1%)	1 (5.0%)	2 (20.0%)	1 (4.3%)	2 (25.0%)
Loss of ≥2 lines BCVA	1 (4.2%)	1 (9.1%)	1 (4.2%)	1 (11.1%)	2 (10.0%)	3 (30.0%)	1 (4.3%)	2 (25.0%)
Average line change								
From baseline <sup>°</sup>	1.02	0.07	0.87	-1.31	0.64	-1.30	0.97	-1.78
Difference between treatment groups <sup>†</sup>		0.94		2.18		1.94		2.75

<sup>°</sup>Positive number equals improvement; negative number equals loss.

<sup>†</sup>Positive number means treatment better than placebo.

use of an extracorporeal therapy for an ophthalmic disease. Specifically, MIRA-1 is the first multicenter, prospective, randomized, double-masked, placebo-controlled study designed to investigate patients with preangiogenic AMD with soft drusen and elevated serum levels of selected hemorheologic factors. The results of the interim analysis of the first 43 intent-to-treat patients demonstrated a significant improvement in LogMAR BCVA through 12 months in the Rheopheresis-treated group relative to the placebo-control group ( $P = .001$ , repeated measures analysis).

**POSTULATED MECHANISM(S) OF ACTION**

Rheopheresis directly targets the elimination of known vascular risk factors and suspected pathophysiologically relevant factors of AMD by decreasing plasma viscosity and depleting the serum of soluble macromolecular species such as immune complexes, IgM, fibrinogen, LDL and VLDL cholesterol, von Willebrand factor,  $\alpha_2$ -

macroglobulin, and probably multimeric vitronectin, along with other acute phase reactants, chronic immunomodifiers, and cell signaling components.<sup>17</sup> These markers, however, should currently be regarded as epidemiologic risk factors. None have demonstrated any causal relationship with AMD. Indeed, our data remain insufficient to determine whether the presence or depletion of any of these compounds may prove to be predictive for determining an individual patient's potential susceptibility to obtain a therapeutic response from Rheopheresis.

Friedman and colleagues<sup>18,19</sup> have suggested a hemodynamic model of AMD pathogenesis in a series of papers. They hypothesize that impaired choroidal perfusion results from increases in vascular resistance in the choroid, possibly as a consequence of decreased compliance of the sclera and choroidal vessels with increased age combined with lipidization of Bruch's membrane and accompanying drusen biosynthesis. Such effects would

TABLE VII: ALL EYES: CHANGES IN BCVA OVER TIME

EFFICACY PARAMETER	3 MONTHS		6 MONTHS		9 MONTHS		12 MONTHS	
	TREATMENT	PLACEBO	TREATMENT	PLACEBO	TREATMENT	PLACEBO	TREATMENT	PLACEBO
N=	<b>56</b>	<b>29</b>	<b>54</b>	<b>25</b>	<b>46</b>	<b>25</b>	<b>50</b>	<b>21</b>
All treatment eyes								
Visual improvement								
≥+1 line	28 (50.0%)	7 (24.1%)	27 (50.0%)	5 (20.0%)	22 (47.8%)	10 (40.0%)	25 (50.0%)	6 (28.6%)
≥+1.5 lines	20 (35.7%)	2 (6.9%)	24 (44.4%)	4 (16.0%)	15 (32.6%)	3 (12.0%)	17 (34.0%)	3 (14.3%)
≥+2 lines	15 (26.8%)	2 (6.9%)	18 (33.3%)	3 (12.0%)	12 (26.1%)	1 (4.0%)	15 (30.0%)	3 (14.3%)
≥+2.5 lines	9 (16.1%)	1 (3.4%)	8 (14.8%)	0 (0.0%)	9 (19.6%)	1 (4.0%)	10 (20.0%)	2 (9.5%)
≥+3 lines	7 (12.5%)	1 (3.4%)	7 (13.0%)	0 (0.0%)	9 (19.6%)	1 (4.0%)	7 (14.0%)	0 (0.0%)
Visual loss								
Loss of ≥3 lines BCVA	0 (0.0%)	2 (6.9%)	1 (1.9%)	3 (12.0%)	1 (2.2%)	3 (12.0%)	1 (2.0%)	4 (19.0%)
Loss of ≥2 lines BCVA	3 (5.4%)	2 (6.9%)	2 (3.7%)	3 (12.0%)	2 (4.3%)	4 (16.0%)	3 (6.0%)	4 (19.0%)
Average line change								
From baseline <sup>o</sup>	1.12	0.21	1.16	-0.50	1.15	-0.03	1.02	-0.71
Difference between treatment groups <sup>†</sup>	0.91		1.66		1.18		1.74	
N=	38	18	38	14	32	15	36	12
BCVA <20/40 pretreatment								
Visual improvement								
≥+1 line	21 (55.3%)	3 (16.7%)	19 (50.0%)	2 (14.3%)	17 (53.1%)	3 (20.0%)	21 (58.3%)	3 (25.0%)
≥+1.5 lines	15 (39.5%)	2 (11.1%)	17 (44.7%)	2 (14.3%)	11 (34.4%)	1 (6.7%)	14 (38.9%)	2 (16.7%)
≥+2 lines	14 (36.8%)	2 (11.1%)	15 (39.5%)	2 (14.3%)	10 (31.3%)	1 (6.7%)	12 (33.3%)	2 (16.7%)
≥+2.5 lines	9 (23.7%)	1 (5.6%)	8 (21.1%)	0 (0.0%)	9 (28.1%)	1 (6.7%)	9 (25.0%)	1 (8.3%)
≥+3 lines	7 (18.4%)	1 (5.6%)	7 (18.4%)	0 (0.0%)	9 (28.1%)	1 (6.7%)	7 (19.4%)	0 (0.0%)
Improvement to 20/40	11 (28.9%)	2 (11.1%)	11 (28.9%)	1 (7.1%)	7 (21.9%)	1 (6.7%)	13 (36.1%)	1 (8.3%)
Visual loss								
Loss of ≥3 lines BCVA	0 (0.0%)	2 (11.1%)	1 (2.6%)	3 (21.4%)	1 (3.1%)	3 (20.0%)	1 (2.8%)	4 (33.3%)
Loss of ≥2 lines BCVA	3 (7.9%)	2 (11.1%)	2 (5.3%)	3 (21.4%)	2 (6.3%)	4 (26.7%)	2 (5.6%)	4 (33.3%)
Average line change								
From baseline <sup>o</sup>	1.25	0.10	1.27	-1.34	1.38	-0.71	1.32	-1.88
Difference between treatment groups <sup>†</sup>	1.15		2.62		2.08		3.21	

<sup>o</sup>Positive number equals improvement; negative number equals loss.

<sup>†</sup>Positive number means treatment better than placebo.

necessarily degrade the metabolic transport function of the pigment epithelium and other supporting posterior retinal tissues. Evidence for this hypothesis includes findings of increased scleral rigidity and increased pulsatility in the face of decreased end-diastolic blood flow velocities in the short posterior ciliary arteries in AMD patients. This hypothesis is further supported by the work of Grunwald and associates,<sup>20</sup> who, by using laser Doppler flowmetry, demonstrated a 33% decrease in choroidal blood velocity ( $P = .005$ ) and a 37% decrease in choroidal blood flow ( $P = .0005$ ) in patients with nonexudative AMD and at least 10 large soft drusen, when compared with an age-matched control group with no large drusen. Similarly, Ciulla and associates,<sup>21</sup> by using color Doppler imaging, demonstrated reduced ocular blood flow velocities in nonexudative AMD in the central retinal artery ( $P = .0007$ ), suggesting the possibility of an extrachoroidal rheopathologic process. Similar decreases in choroidal blood flow with AMD have also been documented using

fluorescein and indocyanine green angiography.<sup>22-25</sup>

These findings appear to suggest the possibility of a systemic influence in the development and progression of AMD. Recently, Mullins, Johnson, and others<sup>26-28</sup> suggested local immunobiosynthetic origins of drusen composed of compounds (complement, vitronectin, and others) also found in systemic circulation. Serum concentrations of such factors could potentially influence drusen composition as well. Putative notions of a possible connection between a molecular pathogenesis and AMD (drusen) and a systemic hemorheologic contribution become even more compelling when viewed in the context of our reported results.

Furthermore, inference of a possible systemic influence can be found in the reports of generalized risk factors that have been associated with AMD in several trials. These risk factors include smoking history,<sup>29-36</sup> systemic hypertension,<sup>37</sup> increased body mass index,<sup>38,39</sup> diets high in linoleic acid and certain lipids,<sup>40,41</sup> elevated fibrinogen lev-

TABLE VIII: MIRA-I TOTAL REPORTED ADVERSE EVENTS\*

EVENT†	RHEOPHERESIS	PLACEBO-CONTROL
Abdominal aortic aneurysm	1‡	
Abdominal pain	1‡	
Bigeminy	1‡	
Bronchospasm		1
Capsule opacity OD		1
Carpel tunnel syndrome	1	
Colon polyp		1
Common cold		1
Congestion, lung		1
Congestive heart failure		1‡
Decreased appetite	1	
Edema bilateral rms	1§	
Edema OU	1§	
Eyelid swelling		1
Fall on boat bruised groin area		1
Hand numbness	1	
Herpes zoster scalp	1	
Hip, leg, groin pain		1‡
Hyperglycemia		2
Hypertension	3	2
Hypotension	3 (2§)	
Hypovolemia	1	
Inguinal hernia		1
Leukemia, death	1‡	
Mild iritis	1	
Nausea	2 (1§)	
NSAID-induced gastritis	1	
Poison ivy		1
PVCs		1
Sinus infection	1	
Suicide, death	1‡	
Urinary tract infection		1
TOTAL ADVERSE EVENTS	23 of 223 (10.3%)	17 of 120 (14.2%)
TOTAL PATIENTS WITH ADVERSE EVENTS	16 of 28 (57%)	8 of 15 (53%)

NSAID, nonsteroidal anti-inflammatory drugs; PVC, premature ventricular contractions.

\*Excludes venous access events (difficulty in establishing or maintaining adequate access); n = 38 in 13 patients.

†If the same event was reported more than once in the same patient, it was reported above only once.

‡Serious adverse event.

§Treatment-related.

els,<sup>16,29</sup> increased serum cholesterol,<sup>13</sup> increased hemorheologic factors,<sup>16</sup> elevated von Willebrand levels,<sup>16</sup> elevated  $\alpha_2$ -macroglobulin levels,<sup>17</sup> and the presence of atherosclerosis itself.<sup>15</sup> Not all AMD studies, however, have consistently demonstrated an association with these cardiovascular and general health risk factors.<sup>42, 43</sup>

Brunner and colleagues<sup>44</sup> studied pulsatile ocular blood flow using a noninvasive quantitative assessment of the ciliary-choroidal blood flow developed by Langham and associates<sup>45</sup> immediately preceding and then subsequent to Rheopheresis treatments in 10 patients with AMD. They found a statistically significant 22% increase in ocular blood flow ( $P = .028$ ). They attributed this finding to the other changes in hemorheologic parameters that they observed in that and other similar studies,<sup>46</sup> including (1) a 14% to 17% decrease in plasma viscosity,

(2) a 12% to 18% decrease in whole-blood viscosity, and (3) a 52% to 66% decrease in erythrocyte aggregation. We agree that transient increases in blood flow may induce certain positive effects on microvascular perfusion. The durable improvements in BCVA documented in this and other studies, however, would seem to argue for a more complex mechanism than simply temporal increases in the supply of oxygen and nutrients provided by 10 to 21 weeks of therapy.

One possible answer is pointed out by Klingel and colleagues.<sup>17</sup> They state that the clinical consequences of impaired microcirculation are due to the complex interactive relationships between plasma components, blood cells, cells of the vessel wall (endothelium, vascular smooth-muscle cells, and fibroblasts), and the compartments of the surrounding tissues (cells and extracellular

TABLE IX: COMPARISON OF REPORTED SERIES OF RHEOPHERESIS MEMBRANE DIFFERENTIAL FILTRATION IN TREATMENT OF AMD

STUDY	CURRENT MIRA-1 STUDY		BRUNNER ET AL <sup>‡</sup>		BRUNNER ET AL <sup>‡</sup>	
	12 MONTHS		ALL PATIENTS 12 MONTHS		PATIENTS WITH SOFT DRUSEN 12 MONTHS	
TIME POSTBASELINE TREATMENT GROUP	TREATMENT	PLACEBO	TREATMENT	NO TREATMENT	TREATMENT	NO TREATMENT
N=	25	11	20	20	11	11
All treatment eyes						
Visual improvement						
≥+1 line	12 (48.0%)	3 (27.3%)	8 (40.0%)	1 (5.0%)	5 (45.5%)	1 (9.1%)
≥+1.5 lines	9 (36.0%)	2 (18.2%)	5 (25.0%)	1 (5.0%)	3 (27.3%)	1 (9.1%)
≥+2 lines	7 (28.0%)	2 (18.2%)	3 (15.0%)	1 (5.0%)	2 (18.2%)	1 (9.1%)
≥+2.5 lines	5 (20.0%)	1 (9.1%)	2 (10.0%)	1 (5.0%)	1 (9.1%)	1 (9.1%)
≥+3 lines	3 (12.0%)	0 (0.0%)	1 (5.0%)	1 (5.0%)	1 (9.1%)	1 (9.1%)
Visual loss						
Loss of ≥3 lines BCVA	1 (4.0%)	2 (18.2%)	2 (10.0%)	6 (30.0%)	0 (0.0%)	3 (27.3%)
Loss of ≥2 lines BCVA	2 (8.0%)	2 (18.2%)	3 (15.0%)	6 (30.0%)	0 (0.0%)	3 (27.3%)
Average line change						
From baseline <sup>°</sup>	0.74	-0.87	-0.21	-1.83	0.62	-1.33
Difference between treatment groups <sup>†</sup>		1.61		1.62		1.95
N=	19	7	19	10	11	7
BCVA <20/40 pretreatment						
Visual improvement						
≥+1 line	11 (57.9%)	2 (28.6%)	8 (42.1%)	1 (10.0%)	5 (45.5%)	1 (14.3%)
≥+1.5 lines	8 (42.1%)	1 (14.3%)	5 (26.3%)	1 (10.0%)	3 (27.3%)	1 (14.3%)
≥+2 lines	6 (31.6%)	1 (14.3%)	3 (15.8%)	1 (10.0%)	2 (18.2%)	1 (14.3%)
≥+2.5 lines	4 (21.1%)	0 (0.0%)	2 (10.5%)	1 (10.0%)	1 (9.1%)	1 (14.3%)
≥+3 lines	3 (15.8%)	0 (0.0%)	1 (5.3%)	1 (10.0%)	1 (9.1%)	1 (14.3%)
Improvement to 20/40 or better	11 (57.9%)	1 (14.3%)	7 (36.8%)	1 (10.0%)	5 (45.5%)	1 (14.3%)
Visual loss						
Loss of ≥3 lines BCVA	1 (5.3%)	2 (28.6%)	3 (10.5%)	3 (30.0%)	0 (0.0%)	2 (28.6%)
Loss of ≥2 lines BCVA	1 (5.3%)	2 (28.6%)	3 (15.8%)	3 (30.0%)	0 (0.0%)	2 (28.6%)
Average line change						
From baseline <sup>°</sup>	1.06	-1.91	-0.22	-2.12	0.62	-1.26
Difference between treatment groups <sup>†</sup>		2.98		1.90		1.88

<sup>°</sup>Positive number equals improvement - negative number equals loss.

<sup>†</sup>Positive number means Treatment better than placebo/no treatment.

<sup>‡</sup>Visual improvement and visual loss data were calculated from the raw pretreatment and posttreatment LogMAR scores reported in Table I.

matrix). In addition, physical factors such as continuous laminar flow and shear stress within the microvascular bed are variables that need to be considered. The investigators point out that when considering the potential molecular pathogenesis of AMD, it must be remembered that Rheopheresis decreases  $\alpha_2$ -macroglobulin levels by 59%, IgM by 65% to 70%, fibrinogen by 43% to 47%, LDL by 57% to 66%, and total cholesterol by 46% to 53%, while only decreasing albumin by 4% to 6% and producing no significant change in hematocrit levels.<sup>5,40</sup> While single-treatment elimination induces changes in the serum levels of these macromolecules for at least 3 to 4 days, the Rheopheresis protocol (pulsed interval apheresis) is designed to induce a prolonged hemorheologic dysequilibrium that can result in a sustained clinical benefit for months<sup>10</sup> or even years.<sup>12</sup>

As with other forms of plasma apheresis therapies, Rheopheresis may perturb both hematologic and immunologic homeostasis. Rheopheresis induces a prolonged dysequilibrium that may affect both systemic and local cytokine production in the choriocapillaris and retinal pigment epithelium (RPE).<sup>17</sup>

Another proposal has suggested the possibility that serum levels of these high-molecular-weight compounds may correlate with excessive accumulations in either Bruch's membrane or the choriocapillaris in genetically susceptible individuals over time. Deposition of these high-molecular-weight compounds at the interface of Bruch's membrane and the RPE would likely interfere with the transport-diffusion characteristics across these membranes and may induce the release of angiogenic compounds from adjacent ischemic retinal tissues (RPE

TABLE X: OTHER EUROPEAN TRIALS OF RHEOPHERESIS FOR AMD

	INDICATION	SUBJECTS	TREATMENT	EFFICACY PARAMETERS	OUTCOMES
First open-label acute study	Patients with AMD (42% CNV)	31 Eyes 17 Patients	2 Rheopheresis treatments 2 days apart	Comparison of ETDRS visual acuity 1 day prior to first treatment and 1 day after second treatment	ETDRS acuity: 15/31 (48%) of eyes gained 1 or more lines of ETDRS acuity Mean change was 4.5 lines ( $P = .005$ )
Second open-label acute study	<ul style="list-style-type: none"> <li>•Exudative AMD, not laser candidates</li> <li>•Nonexudative AMD</li> </ul>	78 Eyes 42 Patients	2 Rheopheresis treatments 2 days apart	Comparison of ETDRS visual acuity 1 day prior to first treatment and 1 day after second treatment	ETDRS acuity: 42.3% of eyes gained $\geq 1$ line and 21.8% gained $\geq 2$ lines; only 1% lost 1 line of vision and none lost $> 1$ line
Pilot randomized extended treated study	Patients with AMD: <ul style="list-style-type: none"> <li>•Wet (not candidates for laser)</li> <li>•Dry</li> </ul>	AMD: 18 eyes of 9 patients Controls: 15 eyes of 9 patients	10 Rheopheresis treatments over a period of 21 weeks	Comparison of ETDRS visual acuity 1 day prior to initial treatment and just before each of the subsequent treatments	ETDRS acuity: After initial treatment, mean improvement in ETDRS from baseline was 0.7 lines (vs 0.0 lines among controls). After final treatment, change in lines of ETDRS acuity was compared between treated and controls: median difference was 2.2 lines after final treatment

AMD, age-related macular degeneration; CNV, choroidal neovascular membrane.

and others). The Rheopheresis protocol provides a sustained decrease in the serum levels of many of these high-molecular-weight compounds. Such may induce an equilibrium shift of these materials out of Bruch's membrane and choriocapillaris tissues into the "plasma pool," thereby decreasing the rate of accumulation of these compounds. Potentially, this would improve the transport-diffusion characteristics of these macromolecules across these membranes, allowing improved oxygenation and nutrition of the overlying RPE and neurosensory retina, as well as promote removal of digested pigment wastes. This would putatively enhance neuroprotective injury repair activity as well as decrease the stimuli that promote gene-directed apoptosis (programmed cell death) and inhibit the local production of angiogenic factors leading to choroidal neovascular transformation (wet form of AMD).

Although both of these possible mechanisms of action are hypothetical, they are not without support. A recent study of 78 patients with AMD showed elevated levels of multiple rheologic factors.<sup>16</sup> This cross-sectional study compared consecutive AMD patients seen in a macula

clinic with age-matched normal controls. Plasma viscosity, von Willebrand factor, and fibrinogen were significantly elevated in the AMD patients compared with the controls ( $P < .0001$ ,  $P = .0004$ , and  $P < .0001$ , respectively). These hemorheologic elements are directly reduced or depleted by Rheopheresis treatment.

Unfortunately, our current understanding of Rheopheresis is insufficient to definitively answer questions regarding its mechanisms of action. The clinical results with Rheopheresis will be better understood with our increasing knowledge of pathogenic mechanisms of AMD. It is noteworthy, however, to recognize that this trial and completed studies and multiple case series have repeatedly demonstrated similar positive effects on vision and retinal function subsequent to intervention with Rheopheresis filtration.

#### PRECEDENT CLINICAL TRIALS

A number of German trials have reported on the efficacy of Rheopheresis in AMD.<sup>8-12</sup> Success in several uncontrolled case series led to the initiation of the first prospec-

TABLE XI: COMPARISON OF EFFICACY PARAMETERS IN UNIVERSITY OF UTAH PILOT STUDY GROUPS (2000 ANNUAL REPORT IDE# G970241)

RESULTS	ETDRS MEAN LINE CHANGE°	PEPPER SPEED SCORE CHANGE FROM BASELINE° MEAN(%) / MEDIAN(%)	VF-14 SCORE CHANGE FROM BASELINE° MEAN(%) / MEDIAN(%)	VISUAL SYMPTOM QUESTIONNAIRE (10 ITEMS) MEAN NO. OF ITEMS IMPROVED
Rheopheresis	1.8	31.5 / 34.2	7.23 / 12.5	3.3
“Sham”	1.2	0.33 / +19.8	-0.35 / 0.66	0.9
Control	0.5	6.76 / -13.6	-8.49 / -10.3	0.0
Rheopheresis vs control	$P = .017$	$P = .04$	$P = .039$	$P < .01$

°Positive value indicates improvement.

tive randomized controlled clinical trial in Germany (MAC-1). Brunner and colleagues<sup>10</sup> enrolled 40 AMD patients who were randomly assigned to receive 10 Rheopheresis treatments over a 21-week period or to the no-treatment control. The analysis of the 40 primary eyes demonstrated a mean difference in LogMAR BCVA of 1.57 lines between treatment and control groups immediately posttreatment ( $P < .01$ ). The subset of all primary eyes with soft drusen ( $n = 22$ ; 11 Rheopheresis, 11 control) demonstrated a mean difference of 2.33 lines between treatment and control groups posttreatment ( $P < .01$ ). In 92.5% of these eyes, baseline ETDRS visual acuity was worse than 20/40. Therefore, it is not unexpected that the MAC-1 results should closely parallel those reported here. The visual results of the current study and the Brunner trial, both reporting at an average of 12 months postbaseline, are given in Table IX. In addition, MAC-1 investigated electrophysiologic parameters of the retina that showed significant improvement of photopic a wave of the electroretinogram ( $P = .009$ ) and the flicker electroretinogram ( $P = .03$ ) equivalent to functional improvement of the central photoreceptor complex. In a case series of 10 patients with high-risk AMD with soft drusen, improvement in visual acuity essentially identical to the MAC-1 trial was confirmed (Fell A, et al. *Investigative Ophthalmology and Visual Science* 2000;41:S181). Results from 11 patients reported after long-term follow-up with interval “booster treatments” demonstrated that the therapeutic effect of the initial treatment series can be maintained over more than 2 years.<sup>12</sup> Eyes suffering from “dry” AMD had a mean improvement in visual acuity of 2.5 EDTRS lines of BCVA after 24 months. This study suggested that after a mean period of 12 months follow-up, provision of two to four booster treatments could be considered, depending on an individual patient’s clinical course.<sup>12</sup>

Table X summarizes the findings of three other European trials of Rheopheresis for AMD. The first and second open labeled trials demonstrated an acute effect on ETDRS acuity after only two Rheopheresis treatments 2

days apart. The randomized trial demonstrated a median difference in ETDRS line change between treatment and control group of 2.2 lines after 10 treatments were administered over a 21-week period. Improvement of the pulsatile ocular blood flow<sup>44</sup> and decrease of the arteriovenous passage time in patients with AMD after Rheopheresis treatments were demonstrated in separate trials.<sup>9,11</sup>

An FDA pilot Investigative Device Exemption (IDE) study of Rheopheresis was performed at the University of Utah (*Investigative Ophthalmology and Visual Science* 1999;40[4]:319). The inclusion criteria were similar to those of the current study, except that elevated baseline serum levels of hemorheologic factors were not considered. Thirty patients were randomized into three groups of 10 patients each: an active treatment group, a “sham” operation, and a no-treatment control group. The sham treatment consisted of circulating the patients’ blood through PVC tubing, but not through the membrane differential filters. Continuously heparinized extracorporeal circuits, however, cause many macropoteins to aggregate and adhere to the plastic tubing. As such, the sham operation induced a partial treatment effect with a documented reduction of high-molecular-weight protein concentrations of approximately 10% to 12% of that occurring for the treatment group. Active treatment consisted of 10 Rheopheresis treatments over a 16-week period instead of eight treatments over 10 weeks, as in the current study. The results immediately following the treatment period are shown in Table XI. Significant differences between Rheopheresis and control groups were observed with regard to ETDRS acuity, Pepper speed-reading scores, and two visual function questionnaires.

Given the evidence for efficacy, no significant safety concerns, and the lack of alternative therapies, the Rheopheresis system has been approved for commercial use for AMD in the European Union and Asia. Postcertification studies are ongoing within the framework of an interdisciplinary quality management program, including the incorporation of an outcomes database registry, the RheoNet System.<sup>47</sup>

### ORAL SUPPLEMENTS

Currently, several studies have demonstrated that laser photocoagulation, including that using photodynamic therapy with verteporfin, is useful in the treatment of some forms of angiogenic AMD.<sup>48,49</sup> For preangiogenic AMD, the only treatment that has been shown to have even limited efficacy is the use of zinc, high-dose vitamins C, A, and E, and beta-carotene.<sup>4</sup> The AREDS demonstrated that these oral agents decreased the development of advanced AMD and decreased severe vision loss from AMD by 25% in patients with baseline stage 3 or 4 nonexudative AMD. The patients enrolled in the MIRA-1 study would be considered to have fundus criteria that would qualify them as being in at least the grade 3 or 4 group according to the AREDS classification scheme.

It is important to note that patients in both the Rheopheresis treatment group and the placebo-control group of the current trial were provided with the same daily vitamin supplementation formula, and both groups were prohibited from using other vitamin supplements so that differential supplementation use would not be a confounding variable (See Table I, "Inclusion Criteria"). The MIRA-1 protocol provided for daily oral intake of the following: 400 mg of vitamin C (four times the recommended daily allowance [RDA]), 200 IU of vitamin E (six times the RDA), 40 mg of zinc (2.5 times the RDA), and 3,000 IU of beta carotene (1.8 times the RDA). Although these levels were considered suprathreshold at the time of the initiation of the trial, they represent only about half of those levels used in the AREDS study. Even so, the current data suggest that the observed positive effects of Rheopheresis on vision are, at minimum, additive to high-dose nutritional supplementation.

### SAFETY

Patient tolerance to extracorporeal procedures, and to needlesticks in general, varies widely among individuals, depending on resting vagal tone and other predisposing factors. Establishing and maintaining competent antecubital venous access over a 2- to 4-hour extracorporeal procedure in elderly patients remains the most frequently encountered technical challenge of Rheopheresis for AMD (17% of cannulations in this analysis experienced difficulties with vascular access).

The principle of Rheopheresis is membrane differential filtration (MDF), which is a safe and established modality of therapeutic apheresis. MDF exhibits a side-effects profile similar to that of other forms of extracorporeal therapies. These effects are typically both transient and self-limited. Historically, the safety of MDF has been reported in a number of studies. Godehardt and associates<sup>50</sup> analyzed data from 1,702 ambulatory MDF-LDL-apheresis treatments of 52 patients at nine centers (Figure

10). No severe adverse events occurred. In 98% of MDF treatments, no adverse reactions occurred. Hypotensive episodes were observed in 2%. In a trial of Rheopheresis in 10 patients with ischemic stroke, no severe adverse events were reported in 120 procedures.<sup>51</sup> In the MAC-1 trial at the University of Cologne, 20 patients, with a mean age of 72.0 years, received a total of 200 Rheopheresis treatments. Hypotension was observed in 6%, and non-significant hemolysis occurred in 2.5% of treatments.<sup>10</sup> A current RheoNet-registry analysis performed in November 2001 analyzed 1,388 Rheopheresis treatments from 273 patients with the mean age of 70.1 years. This analysis documented technical problems occurring in 1.8% and adverse reactions in 1.5% of Rheopheresis treatments. The adverse reactions included mainly hypotensive episodes, a few allergic reactions, and several observations of hemolysis. No symptomatic hemolysis occurred (R. Klingel, unpublished data). In summary, no reports document the occurrence of any serious, long-term, or unanticipated treatment-related adverse events or side effects from the use of Rheopheresis.

This dearth of reported long-term adverse effects is expected owing to the rapid reequilibration of necessary plasma components that are transiently depleted during the Rheopheresis protocol.

Theoretical concerns of induced bleeding diatheses and immunocompromise are unlikely to be realized when adhering to a conservative protocol of eight pulsed, 100% plasma volume therapies delivered over 10 weeks. Such a protocol provides for adequate intervals of "therapeutic rest," as is commonly employed with other extracorporeal procedures developed over the past 30 years for other indications, and for which a significant body of relevant clinical experience has been obtained.<sup>50,52,53</sup>

### OBSERVATIONS FOR FURTHER STUDY

Although the findings reported here have a high degree of statistical significance, our study group recognizes that a sample size larger than 43 patients is important to provide

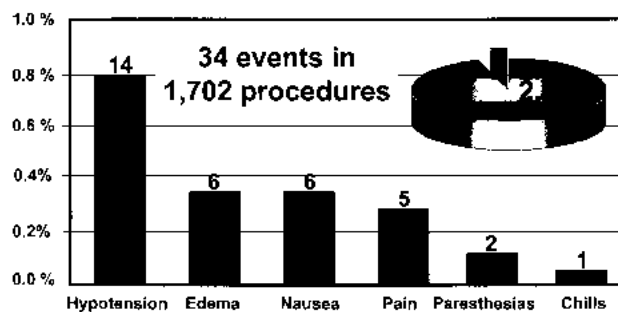


FIGURE 10

Membrane differential filtration (MDF) side effects reported in a multi-center series of 1,702 procedures. Typically, treatment effects are minor and self-limited.<sup>50</sup>

a basis for the widespread adoption of any novel technology such as Rheopheresis, whose specific mechanism of action is under investigation. Enrollment in MIRA-1 is thus continuing on to its planned 150-patient size. In addition, a sample size larger than 43 patients will be required to achieve significance in proportional differences in cases of eyes with greater than 2 or 3 lines of losses or gains in LogMAR BCVA. The final report will include all patients in the treated group as intent to treat.

Additional trials will be needed to further understand issues relating to Rheopheresis as a treatment for AMD, including (1) refining patient selection criteria, (2) determining retreatment efficacy, (3) determining mean duration of therapeutic effect and the periodicity of retreatment, (4) utility in secondary prevention of disease progression, (5) determining relevance of hemorheologic surrogate markers, and (6) the specific mechanism of action. The present study design did not provide information relative to determining the long-term efficacy beyond 1 year. Neither does it substantiate anecdotal accounts concerning the potential benefits of interval retreatment(s) on the maintenance of BCVA beyond 2 years. Also, MIRA-1 was not designed to study efficacy in cases with AREDS grades 1 and 2 AMD, and neither will it suffice as a secondary prevention trial for these earlier stages of the disease.

## CONCLUSIONS

The results of this 12-month interval interim data analysis are encouraging, and several conclusions seem reasonable:

1. Rheopheresis as a treatment for selected patients with preangiogenic AMD appears to be safe and well tolerated by most patients.
2. Relative to placebo-control, Rheopheresis provided a statistically significant and clinically relevant improvement in ETDRS BCVA and provided a therapeutic effect that is evident immediately posttreatment; the benefit for treated eyes remains essentially stable throughout the 12-month period of the MIRA-1 trial.
3. Eyes diagnosed with BCVA worse than 20/40, characterized by  $\geq 10$  large soft drusen, and without evidence of neovascular change (in selected patients with high serum concentrations of certain soluble hemorheologic macromolecules) appear to be at increased risk for substantial vision loss over the ensuing 12-month period if left untreated.
4. The results of MIRA-1 closely approximate and support the findings of precedent trials.
5. A hypothesis based on our current knowledge of pathogenic mechanisms of the development and progression of AMD may be linked with the putative mechanism of action of Rheopheresis for AMD.
6. Continuation of the MIRA-1 trial is indicated.
7. Follow-up studies are suggested.

## REFERENCES

1. National Advisory Eye Council. Report of the Retinal Disease Panel: Vision Research: A National Plan, 1994-1998. Bethesda, Md: US Dept of Health and Human Services; 1993. Publication NIH 93-3186.
2. Attebo K, Mitchell P, Smith W. Visual acuity and the causes of visual loss in Australia: the Blue Mountains Eye Study. *Ophthalmology* 1996;103:357-364.
3. Klaver DD, Wolfs RC, Vingerling JR, et al. Age-specific prevalence and causes of blindness and visual impairment in an older population: the Rotterdam study. *Arch Ophthalmol* 1998;116:653-658.
4. Age-Related Eye Disease Study Research Group. A randomized, placebo-controlled clinical trial of high-dose supplementation with vitamins C and E, beta-carotene, and zinc for age-related macular degeneration and vision loss. AREDS report No. 8. *Arch Ophthalmol* 2001;119:1417-1436.
5. Fine SL, Berger JW, Maguire MG, et al. Age-related macular degeneration. *N Engl J Med* 2000;342:483-492.
6. Sarraf D, Gin T, Yu F, et al. Long-term drusen study. *Retina* 1999;19:513-519.
7. Lanchoney DM, Maguire MG, Fine SL. A model of the incidence and consequences of choroidal neovascularization secondary to age-related macular degeneration. Comparative effects of current treatment and potential prophylaxis on visual outcomes in high-risk patients. *Arch Ophthalmol* 1998;116:1045-1052.
8. Brunner R, Widder RA, Walter P, et al. Change in hemorheological and biochemical parameters following membrane differential filtration. *Int J Artif Organs* 1995;18:794-798.
9. Brunner R, Widder RA, Fischer RA, et al. Clinical efficacy of hemorheological treatment using plasma exchange, selective adsorption and differential filtration on maculopathy, retinal vein occlusion and uveal effusion syndrome. *Transfus Sci* 1996;17:493-498.
10. Brunner R, Widder RA, Walter P, et al. Influence of membrane differential filtration on the natural course of age-related macular degeneration—a randomized trial. *Retina* 2000;20:483-491.
11. Soudavar F, Widder RA, Brunner R, et al. Changes of retinal hemodynamics after elimination of high molecular weight proteins and lipids in patients with age-related macular degeneration (Abstract). *Invest Ophthalmol Vis Sci* 1998;39:286.
12. Widder RA, Lüke C, Walter P, et al. Long-term treatment of age-related macular degeneration with extracorporeal apheresis (Abstract). *Ophthalmologie* 2000;97(Suppl 1):S172.
13. Eye Disease Case-Control Study Group. Risk factors for neovascular age-related macular degeneration. *Arch Ophthalmol* 1992;110:1701-1708.
14. Smith W, Mitchell P, Leeder SR, et al. Plasma fibrinogen levels, other cardiovascular risk factors, and age-related maculopathy. *Arch Ophthalmol* 1998;116:583, 587.

15. Vingerling JR, Dielemans I, Bots ML, et al. Age-related macular degeneration is associated with atherosclerosis. *Am J Epidemiol* 1995;142:404-409.
16. Lip PL, Blann AD, Hope-Ross M, et al. Age-related macular degeneration is associated with increased vascular endothelial growth factor, hemorheology and endothelial dysfunction. *Ophthalmology* 2001;108(4):705-710.
17. Klingel R, Fassbender C, Fassbender T, et al. Rheopheresis: rheologic, functional, and structural aspects. *Ther Apher* 2000;4(5):348-357.
18. Friedman E, Krupsky S, Lane A, et al. Ocular blood flow velocity in age-related macular degeneration. *Ophthalmology* 1995;102(4):640-646.
19. Friedman E. A hemodynamic model of the pathogenesis of age-related macular degeneration. *Am J Ophthalmol* 1997;124(5):677-682.
20. Grunwald JE, Hariprasad SM, DuPont J, et al. Foveolar choroidal blood flow in age-related macular degeneration. *Invest Ophthalmol Vis Sci* 1998;39(2):385-390.
21. Ciulla TA, Harris A, Chung HS, et al. Color Doppler imaging discloses reduced ocular blood flow velocities in nonexudative age-related macular degeneration. *Am J Ophthalmol* 1999;128(1):75-80.
22. Piguet B, Palmvang IB, Chisholm IH, et al. Evolution of age-related macular degeneration with choroidal perfusion abnormality. *Am J Ophthalmol* 1992;113:657-663.
23. Zhao J, Frambach DA, Lee PP, et al. Delayed macular choriocapillary circulation in age-related macular degeneration. *Int J Ophthalmol* 1995;19:1-12.
24. Ross R, Barofsky J, Cohen G, et al. Presumed macular choroidal watershed vascular filling, choroidal neovascularization, and systemic vascular disease in patients with age-related macular degeneration. *Am J Ophthalmol* 1998;125:71-80.
25. Ciulla TA, Harris A, Danis RP. Presumed macular choroidal watershed vascular filling, choroidal neovascularization, and systemic vascular disease in patients with age-related macular degeneration. *Am J Ophthalmol* 1998;126:153-155.
26. Mullins RF, Aptsiauri N, Hageman GS. Structure and composition of drusen associated with glomerulonephritis: implications for the role of complement activation in drusen biogenesis. *Eye* 2001;15(Pt 3):390-395.
27. Mullins RF, Russell SR, Anderson DH, et al. Drusen associated with aging and age-related macular degeneration contain proteins common to extracellular deposits associated with atherosclerosis, elastosis, amyloidosis, and dense deposit disease. *FASEB J* 2000;14(7):835-846.
28. Johnson LV, Ozaki S, Staples MK, et al. A potential role for immune complex pathogenesis in drusen formation. *Exp Eye Res* 2000;70(4):441-449.
29. Smith W, Mitchell P, Leeder SR. Smoking and age-related maculopathy: the Blue Mountains Eye Study. *Arch Ophthalmol* 1996;114:1518-1523.
30. The Eye Disease Case-Control Study Group. Risk factors for neovascular age-related macular degeneration. *Arch Ophthalmol* 1992;110:1701-1708.
31. Hyman LG, Lillienfeld AM, Ferris FL III, et al. Senile macular degeneration: case-control study. *Am J Epidemiol* 1983;118:213-227.
32. Blumenkranz MS, Russell SR, Robey MG, et al. Risk factors in age-related maculopathy complicated by choroidal neovascularization. *Ophthalmology* 1986;93:552-558.
33. Goldberg J, Flowerdew G, Smith E, et al. Factors associated with age-related macular degeneration. An analysis of data from the first National Health and Nutrition Examination Survey. *Am J Epidemiol* 1988;128:700-710.
34. Maltzman BA, Mulvihill MN, Greenbaum A. Senile macular degeneration and risk factors: case-control study. *Ann Ophthalmol* 1979;11:1197-1201.
35. Kahn HA, Leibowitz HM, Ganley JP, et al. The Framingham Eye Study. II. Association of ophthalmic pathology with single variables previously measured in the Framingham Heart Study. *Am J Epidemiol* 1977;106:33-41.
36. Seddon JM, Willett WC, Speizer FE, et al. A prospective study and age-related macular degeneration in women. *JAMA* 1996;276(14):1141-1146.
37. Sperduto RD, Hiller R. Systemic hypertension and age-related maculopathy in the Framingham Study. *Arch Ophthalmol* 1986;104:216-219.
38. Hirvela H, Luukinen H, Laara E, et al. Risk factors of age-related maculopathy in a population 70 years of age or older. *Ophthalmology* 1996;103(6):871-877.
39. Smith W, Mitchell P, Leeder SR. Plasma fibrinogen levels, other cardiovascular risk factors, and age-related maculopathy: the Blue Mountains Eye Study. *Arch Ophthalmol* 1998;116:583-587.
40. Mares-Perlman JA, Brady WE, Klein R, et al. Dietary fat and age-related maculopathy. *Arch Ophthalmol* 1995;113:743-753.
41. Seddon JM, Rosner B, Sperduto RD, et al. Dietary fat and risk for advanced age-related macular degeneration. *Arch Ophthalmol* 2001;119(8):1191-1199.
42. Klein R, Klein B, Franke T. The relationship of cardiovascular disease and its risk factors to age-related maculopathy: the Beaver Dam Eye Study. *Ophthalmology* 1993;100(3):406-414.
43. Bressler NM, Bressler SB. Preventative ophthalmology: age-related macular degeneration. *Ophthalmology* 1995;102(8):1206-1211.
44. Brunner R, Widder RA, Fischer RA. Clinical efficacy of extracorporeal hemorheological treatment in age related macular degeneration. *Jpn J Apheresis* 1997;16(1):31-34.
45. Langham ME, Farrell RA, O'Brien V, et al. Blood flow in the human eye. *Acta Ophthalmol Suppl* 1989;191:9-13.
46. Kaul D. Molecular link between cholesterol, cytokines and atherosclerosis. *Mol Cell Biochem* 2001;219(1-2): 65-71.
47. Klingel R, Fassbender C, Wahls W, et al. Implementation of rheopheresis into clinical practice—evidence based medicine and quality management. *Clin Hemorheol Microcirc* 2001;24:119-146.
48. Treatment of Age-Related Macular Degeneration With Photodynamic Therapy Study Group. Photodynamic therapy of subfoveal choroidal neovascularization in age-related macular degeneration with verteporfin: one-year results of two randomized clinical trials. TAP report 1. *Arch Ophthalmol* 1999;117:1329-1345.

49. Treatment of Age-Related Macular Degeneration With Photodynamic Therapy Study Group. Photodynamic therapy of subfoveal choroidal neovascularization in age-related macular degeneration with verteporfin. two-year results of two randomized clinical trials. TAP report 2. *Arch Ophthalmol* 2001;119:198-207.
50. Godehardt E, Messner H, Wallstab UH. Extracorporeal LDL cholesterol elimination by membrane differential filtration. In: Gotto AM, Mancini M, Richter WO, et al, eds. *Treatment of Severe Dyslipoproteinemia in the Prevention of Coronary Heart Disease*. Munich: Basel Karger; 1993;208-212.
51. Berrouschot J, Barthel H, Scheel C, et al. Extracorporeal membrane differential filtration—a new and safe method to optimize hemorheology in acute ischemic stroke. *Acta Neurol Scand* 1998;97:126-130.
52. Vucic S, Davies L. Safety of plasmapheresis in the treatment of neurological disease. *Aust N Z J Med* 1998; 28(3):301-305.
53. Furuta M, Shimizu T, Mizuno S, et al. Clinical evaluation of repeat apheresis donors in Japan. *Vox Sang* 1999; 77(1): 17-23.

## **ACKNOWLEDGMENTS**

### **Writing Committee**

Jose Pulido, MD, Reinhard Klingel, MD, PhD, and Donald R. Sanders, MD, PhD

### **The MIRA-1 Study Group is composed of the following members:**

#### Principal Ophthalmologic Investigators (in alphabetical order)

David Boyer, MD (Retina Vitreous Associates, Beverly Hills, California); David Brown, MD (Eye Centers of Florida, Fort Myers); Ronald Danis, MD (Retina and Vitreous Service, Indiana University, Indianapolis); Dana Deupree, MD (St. Luke's Cataract and Laser Institute, Tarpon Springs, Florida); Alexander Eaton, MD (Eye Centers of Florida, Fort Myers); Bert Glaser, MD (Glaser-Murphy Retina Treatment Center, Towson, Maryland); Robert Gale Martin, MD, and Greg Mincey, MD (Carolina Eye Associates, Southern Pines, North Carolina); Dan Montzka, MD (St Luke's Cataract and Laser Institute, Tarpon Springs, Florida); Robert Murphy, MD (Glaser-Murphy Retina Treatment Center, Towson, Maryland); Joseph Olk, MD (The Retina Center of St Louis County, St Louis, Missouri); Jose Pulido, MD (Department of Ophthalmology and Visual Sciences, UIC Eye Center, University of Illinois, Chicago); Mano Swartz, MD (University of Utah, Moran Eye Center, Salt Lake City)

#### Principal Investigators at Rheopheresis Therapy Units (Nephrology/Apheresis) (in alphabetical order)

Mark Aarons, MD (Pinehurst Nephrology Associates,

Pinehurst); Theresa Boyd, MD (BRT Labs, Baltimore, Maryland); Phillip DeChristopher, MD, PhD (University of Illinois, Chicago); Lawrence Dewberry, MD (Palm Harbor Nephrology Associates, Palm Harbor); Leo McCarthy, MD (Indiana University, Indianapolis); John Mellas, MD (Renex Dialysis Clinic, St Louis, Missouri); Samuel Pepkowitz, MD (Cedars-Sinai Medical Center, Los Angeles, California); Gary Rabetoy, MD (University of Utah, Salt Lake City); Joel VanSickler, MD (Southwest Florida Regional Medical Center, Fort Myers)

#### UCLA Jules Stein Fundus Photography Reading Unit

Michael Cornish, MD, Gary Holland, MD, David Saraf, MD, and Susan Ransome

#### Apheresis Research Institute, Cologne, Germany

Reinhard Klingel, MD, PhD

#### Medical BioStatistics and Data Management

Promedica International: Ginger Clasby, Pat Ticknor, Shannon Stoddard, Angel Rey, MD, Melodee Sellers, and Laura Callahan

BioStat International: Maureen Lyden, MS

Burkhart and Associates: John Burkhart, PhD

#### Study Design, Analysis and Additional Support

Center for Clinical Research: Donald R. Sanders, MD, PhD, Yolanda Gonzalez, and David Hotopp

Pepper Test Scoring: Erica Watkins and Gayle Watson, PhD

LabCorp Clinical Trials Department: Dan Herlihy, Cathleen Prokesch, Nick Niles, and Teri Olimpaito

#### Contributors and Sponsors of the MIRA-1 Trial

OccuLogix Corporation: Ray Gonzalez, MBA, Richard Davis, MD, Matt Mores, and Julie Mores

Apheresis Technologies, Inc: John Cornish, Joelle Herman, MPH, Susan Thompson, RN, Ian Tolman, RN, Sue Howard, and Angie Metelski

Asahi Medical Co Ltd, Tokyo, Japan: Messers Isobe, Enoki, Kawara, Tanaka, and Yokogi

Diamed Medizintechnik GmbH, Cologne, Germany: Hans Stock, Codula Fassbender, PhD, Bernard Erdtracht, MD

#### Clinical Coordinators, Research Associates, Treatment and Other Technical Support Staff

Stone Blacka, Sandra Gould, Jean Havercroft, Gloria Roberts, Jeff Kessinger, Linda Pratt, RN, Carrie Doub, Debra Poe, Elaine Skipworth, MTHP, Tim Steffans, Janice Brown, Shelly Peters, RN, Carla Thomas, RN, Mark Kordis, Loretta Jackson, Constance Danielson, FM, Steven Sosler, MS, Maria Touza, Marydell Augustus, James Conant, Cynthia Corres, RN, David Piironen,

Mark Janowicz, Ruth Pomykala, Harry Alcorn, MD, Deborah Harrison, RN, Melanie Christensen, RN, Kimberly Wegner, Darek Leyde, Marian West, RN, Paula Morris, Beth Snodgrass, Doug Blanchard, Roger Mitchell, PA, Cathie Kemp, Sylvia Ferrell, Carol Jones, RN, Carolyn Taylor, RN, Judy Flannigan, Jan Stivers, Bill McVerry, Karen Sayka, Shannon Hudson, LPN, Mary Flanagan, LPN, Madeline Cafano, Mark Erickson, Susan Lambert, Karen Glazener, RN, Joe Bagby, Pam Parzynski, RN, Leigh Wilson, Joanne Manrique, Bonnie Ritz, RN, Ann Wells, RN, Beth Danner, RN, Pam Vargo, Lisa Burke, Diane Gulden, Caroline Sheppard, Dale Ingram, Natalie Dixon, Michele Lucas, Tammy Boone, RN, Karen Pollack, Nancie Reichle, Wanda Batts

#### Financial Disclosure Statement and Conflicts of Interest

Drs Brown, Davis, Deupree, Dewberry, Eaton, Martin, Mincey, and Sanders beneficially own stock or stock options in OccuLogix Corporation, the principal sponsor of the Study.

The total combined beneficial ownership of the principal retina investigators is less than 1% of the fully diluted shares outstanding. Drs Brown, Davis, Martin, and Sanders are significant investors; Dr Deupree has stock options as a member of the Scientific and Medical Advisory Board; Dr Davis is OccuLogix's Chairman, President, and Chief Executive Officer.

#### **DISCUSSION**

---

DR W. BANKS ANDERSON, JR. Diseases for which there is no effective established treatment have many remedies. Whether in herbal shops or in doctor's offices, such remedies are usually profit centers. How does one decide if such treatments do more than enrich their purveyors? One method is to observe a reproducible benefit of great magnitude as, for example, when penicillin was administered for pneumococcal pneumonia. Rheopheresis treatments for age-related macular degeneration in Cologne and Florida have not met this "great magnitude" test. To the credit of Dr Pulido and the other eight in the group, they are treating patients as part of a research protocol to assess the safety and efficacy of this therapy. The criteria for a study that scientifically establishes benefit are numerous, laborious, and expensive. Some of them are as follows: prospective, randomized and safe; entry criteria that allow extrapolation; masking of both the observers and the patients as to treatment; "n" large enough to establish significance; independent monitors for safety and data collection; independent masked image graders; no outcome-dependent financial effects on the participants and; methods and outcomes are reproducible by others.

This study is prospective, randomized, and seemingly

safe. Except for one Asian, all in the study population are Caucasian. But since most AMD patients are Caucasian, the results would extrapolate to the affected population. Masking has been rigorous with study patients differing in that they have larger needle wounds. Recirculation of heparinized blood without the filters was not done as a control because it was felt that large molecule adherence to the plastic tubing, as seen in pilot studies, might contribute to a treatment effect. The results presented this morning are obtained from 43 subjects, 28 of whom are in the treatment group. The planned "n" is 150. The monitors and graders are independent. This is a multicenter trial and Dr Pulido's group does not have a major financial interest in a positive outcome; however, other groups in the study do have such an interest.

We have learned this morning that at one year, the treatment group differed from the controls by a statistically significant 1.6 lines of better vision. The 19 eyes with less than 20/40 at baseline averaged three lines of improvement. The study is ongoing.

Some questions I have for Dr Pulido are: Could heparin be responsible for the observed benefit? When do you predict completion of the 150-subject study? What is the cost of a course of treatment?

I congratulate the participating groups in electing to provide this new treatment for age-related dry macular degeneration in the context of a controlled and masked study.

DR JOHN T. FLYNN. What happened to the rheological criteria that allowed the patient to be entered into the study during the period of follow-up? Did the studies return to the baseline values or change significantly over time? The change would seem to play a role in what's happening.

DR PAUL R. LICHTER. I have a question in terms of your data and safety monitoring committee. You've shown a significance improvement in these first patients. What is the ethics of continuing to add patients to the study, since the untreated patients did considerably worse than the treated patients?

DR DONALD SANDERS (Dr Sanders was on the writing committee for this paper). I would like to address two of the issues. First, with regard to the data and safety monitoring committee: the FDA is the data and safety monitoring committee in device trials. Because of the controversy related to this technology in the ophthalmic community, it was felt that an "n" of 43 cases might not be sufficient. The study will be continued although the FDA has approved the treatment of the placebo patients after they complete the 12-month follow-up, in essence agreeing with Dr Lichter that the data is sufficiently compelling

that the placebo patients should be treated. Second, with regard to the rheological markers (total cholesterol, fibrinogen, and IgA): one of the possible ways that this technique works is to decrease plasma viscosity and therefore increase choroidal blood flow. With the procedure, the total cholesterol, IgA, and these large molecules transiently decrease, and the plasma viscosity has been demonstrated to decrease, probably for weeks. The subsequent increased choroidal blood flow possibly stops some sort of cascade causing the problem in AMD. Since we don't know what causes the etiology of AMD, however, we don't know why this is improving. The levels of those markers return to normal after the treatment is completed, although the effect appears to last a year.

DR JOSE S. PULIDO. I think Dr Lichter's question has been answered. As far as Dr Flynn's question about the rheological markers: Dr Sanders had alluded to the literature that indicates that these markers do transiently decrease a tremendous amount following rheopheresis but subsequently, with time, rise. We don't have specific data yet for the patients in this study, but it is probably the same as occurs in other patients that have been treated with rheopheresis. I appreciated Dr Banks Anderson's comments. Heparin was used in the patients that were undergoing treatment and was not used in the patients that were in the placebo group. The amount of heparin used is 5,000 units, which is the amount that you need for initial

heparinization. The subsequent amount that's needed while you're on the treatment, however, is a low amount. With a half-life of about 30 minutes for heparin, there is enough heparin to act in a therapeutic fashion for about 5 hours following treatment. I don't think the amount and time the treated patient was on heparin are substantial, but I cannot discount the fact that heparin might have some action exclusive of the study. On the other hand, one could then also argue that just having the patient's blood circulate through a machine, exclusive of a filter, might be the reason there was efficacy as well.

The results of this study may be completed by next year; the company would like to see it even faster. As far as cost is concerned: I don't know what the cost is, and, as an academic physician, I am not concerned about the cost right now. My concern is to make sure that this study is completed ethically and expeditiously. Just as in the issue of photodynamic therapy, the quality-adjusted life per year cost is a potentially significant factor. Dr Sanjay Sharma showed that for photodynamic therapy, if one eye is affected with choroidal neovascularization and the other eye is not, the cost is about \$100,000 per quality-adjusted life-years. This is very cost-ineffective compared with other medical therapies. If the study continues to show efficacy and if the FDA does approve this for the treatment, we hope that the company will keep the cost within reasonable range to make the quality-adjusted life-year cost reasonable.



# PROJECTED IMPACT OF TRAVOPROST VERSUS BOTH TIMOLOL AND LATANOPROST ON VISUAL FIELD DEFICIT PROGRESSION AND COSTS AMONG BLACK GLAUCOMA SUBJECTS

---

BY Michael T. Halpern, MD, PhD (BY INVITATION), David W. Covert, MBA (BY INVITATION),  
AND Alan L. Robin, MD

## ABSTRACT

**Purpose:** We compared differences associated with use of travoprost and latanoprost on both progression of perimetric loss over time and associated costs among black patients.

**Methods:** Patients with primary open-angle glaucoma or ocular hypertension were randomly assigned to one of four arms in a 12-month, double-masked study: travoprost (0.004% or 0.0015%), latanoprost (0.005%), or timolol (0.5%). Forty-nine patients received 0.004% travoprost, 43 received latanoprost, and 40 received timolol. We applied algorithms found in published studies that link intraocular pressure (IOP) control to visual field progression and calculated the likelihood of visual field deterioration based on IOP data. This was used to estimate differences in medical care costs.

**Results:** The average IOP was lower for patients receiving travoprost than for patients receiving latanoprost or timolol (17.3 versus 18.7 versus 20.5 mm Hg respectively,  $P < .05$ ). Travoprost-treated patients had a smaller predicted change in visual field defect score (VFDS) than latanoprost-treated patients and timolol-treated patients, and significantly fewer were expected to demonstrate visual field progression. Medical care costs would be higher for latanoprost-treated and timolol-treated patients.

**Conclusions:** Recent studies have provided algorithms linking IOP control to changes in visual fields. We found that treatment with travoprost was associated with less visual field progression and potential cost savings.

*Trans Am Ophthalmol Soc* 2002;100:109-118

## INTRODUCTION

---

Primary open-angle glaucoma (POAG) can be defined by optic nerve damage leading to progressive visual impairment. Extrapolating from both the Baltimore Eye Study and the Beaver Dam Eye Study, about 2 million to 3 million Americans have POAG, and as many as half of them may be unaware of it.<sup>1,2</sup> Prevent Blindness America just published its latest version of *Vision Problems in the US* and conservatively estimated that the number of Americans with glaucoma is 2.2 million.<sup>3</sup> Worldwide, it was estimated that the prevalence of glaucoma in the year 2000 was almost 67 million individuals.<sup>4</sup> Approximately 80,000 people in the United States are legally blind on account of glaucoma.<sup>5</sup> The total direct cost of glaucoma in the United States was estimated to be \$1.6 billion in 1991.<sup>6</sup>

From Exponent, Alexandria, Virginia (Dr Halpern); Alcon Research, Ltd, Fort Worth, Texas (Mr Covert); and the Departments of Ophthalmology at Johns Hopkins University and the University of Maryland, and the Bloomberg School of Public Health, Johns Hopkins University, Baltimore, Maryland (Dr Robin). Supported by a grant from Alcon Research, Ltd. Dr Robin is a consultant for both Pharmacia and Alcon and participates in the speaker bureau programs of both companies as well as the speaker bureau program of Merck. Mr Covert is an employee of Alcon Research, Ltd. Exponent was commissioned by Alcon for its part in this study.

Over the last decades, we have realized that elevated intraocular pressure (IOP) cannot solely be used to effectively screen for glaucoma, because it is neither sensitive nor specific, but IOP is an important risk factor for glaucoma.<sup>6,9</sup> In the treatment of glaucoma, however, IOP lowering has been found to strongly correlate with the preservation of vision. Additionally, the degree of IOP lowering achieved has a relative dose-response relationship to visual preservation.<sup>10-12</sup> Other significant risk factors for glaucoma include older age, race, and a family history of glaucoma.<sup>6,9,13</sup>

POAG is also more common in the black population. The rate of glaucoma in the United States in 1990 through 1992 was reported to be 9.9 per 1,000 individuals among the white population and 11.0 per 1,000 among the black population.<sup>14</sup> The prevalence of glaucoma in the populations of both Barbados and St Lucia is far greater, at all ages, than in whites in other studies.<sup>6</sup> Similarly, in Baltimore, Maryland, the prevalence of glaucoma is far greater among blacks than whites. The age-adjusted prevalence of open-angle glaucoma among blacks is 4.3 times that of whites.<sup>15</sup> Some investigators have suggested that open-angle glaucoma is a more severe condition among blacks, in that it appears to begin at an earlier age, resulting in the possibility that it may be more advanced at the time of diagnosis.<sup>6</sup> Further, black patients may not

respond as well to some therapies as white patients. This potential lack of efficacy may lead to greater rates of visual loss and blindness.<sup>14,16,17</sup>

Over the past decade, the number of new classes of eye pressure-lowering medications has almost doubled. These newer medications include topical carbonic anhydrase inhibitors (brinzolamide and dorzolamide), alpha agonists (apraclonidine and brimonidine), and prostaglandin analogues (latanoprost, travoprost, isopropyl unoprostone, and bimatoprost). Latanoprost (Xalatan, Pharmacia) was the first prostaglandin approved in the United States for reduction of elevated IOP in subjects with open-angle glaucoma or ocular hypertension. More recently, travoprost (Travatan, Alcon), bimatoprost (Lumigan, Allergan), and isopropyl unoprostone (Rescula, Ciba) have been approved for this indication. Travoprost is the first IOP-lowering medication used in the treatment of glaucoma that has demonstrated a comparable efficacy in white persons, yet a greater effectiveness in the black population.<sup>15</sup> This finding is potentially important, because with better screening instrumentation, more black persons may be found to have glaucoma in the coming years, and the most effective and cost-effective IOP-lowering medications may be very important.

Historically, the treatment of glaucoma has largely focused on reduction of IOP. The relationship between IOP lowering and visual field loss is likely to involve differential threshold values and patterns of IOP elevation over time. The Advanced Glaucoma Intervention Study (AGIS)<sup>12</sup> found that both the degree and the consistency of IOP lowering are directly correlated with the preservation of visual field. Some investigators have found that there is more to glaucoma damage than blindness. That is, with increasing visual field changes, prior to blindness, a subject's quality of life may directly diminish. Factors such as driving ability seem to decrease in a linear fashion with a decreasing AGIS visual field score.<sup>19</sup> We performed the current analysis to compare projections of visual field loss, and the potential financial implications of these differences in visual field loss, when either travoprost, timolol, or latanoprost is used to lower IOP in black subjects. These estimations are based on data from a previously published randomized clinical trial.<sup>20</sup>

## METHODS

Data for this analysis were obtained from a 12-month randomized, double-masked, phase III clinical trial.<sup>20</sup> In brief, this article describes subjects with open-angle glaucoma or ocular hypertension (OHT) who were randomly assigned to one of four treatment groups: travoprost 0.004%, travoprost 0.0015% (not currently available commercially), latanoprost (0.005%), or timolol (0.5%). Subjects in the timolol treatment group received one drop of timolol in each eye twice daily, at 8 AM and 8 PM. Subjects receiving

travoprost and latanoprost received one drop of active agent in each eye daily at 8 PM. These subjects also received one drop of placebo (to mask the twice-daily timolol treatment arm) in each eye daily at 8 AM. Data were collected at baseline (week 0) and at visits at weeks 2, 6, 12, 18, 24, 36, and 48. At each study visit, IOP was recorded at 8 AM, 10 AM, and 4 PM.

## STUDY POPULATIONS

We enrolled a total of 596 subjects in the travoprost (0.004%), latanoprost, and timolol arms. Of these, 132 (22%) were black. Forty-nine of the 132 were randomly assigned to receive travoprost (0.004%), 43 to receive latanoprost, and 40 to receive timolol. All 132 black subjects were included in the present analysis. Missing data were not interpolated, and IOP values for subjects discontinuing early were not "carried forward." Forty subjects in the travoprost and forty subjects in the the latanoprost groups completed all 48 weeks of the study, while 33 subjects in the timolol group completed all 48 weeks. Among those not completing 48 weeks, four subjects completed 2 study weeks (one travoprost, two latanoprost, one timolol), three subjects completed 6 study weeks, (one travoprost, two timolol), four subjects (all travoprost) completed 12 study weeks, two subjects (one travoprost, one latanoprost) completed 18 study weeks, five subjects (two travoprost, three timolol) completed 24 weeks, and one subject (timolol) completed 36 weeks. Only one subject (in the travoprost arm) discontinued early on account of an ocular adverse event.

## RELATIONSHIP OF IOP AND VISUAL FIELD DEFECT SCORES

Multiple recent reports have indicated that the likelihood of progression of visual field deficit among subjects with POAG cannot be predicted on the basis of mean IOP alone. Rather, mean IOP values above a particular threshold, the pattern of IOP over time, and incidence of IOP peaks appear to be more predictive. To evaluate the projected change in visual field over time for subjects in each treatment group, we applied the algorithms developed by the AGIS.<sup>12</sup> Changes in visual field were assessed by using the visual field deficit score (VFDS), ranging from 0 (no defect) to 20 (end-stage).

The AGIS presented two different algorithms that related IOP patterns over the study period to change in VFDS. First, in a predictive analysis, mean IOP was separated into three categories: <14 mm Hg, 14 to 18 mm Hg, and ≥18 mm Hg. (The originally published AGIS<sup>12</sup> reported 17.5 mm Hg, rather than 18 mm Hg, as the threshold compared, but we were notified of a correction by coauthor E.K. Sullivan.) The predictive AGIS analysis found that subjects with a mean IOP of <14 mm Hg during the first 18 months of follow-up, compared with those with an IOP of 14 to 18 mm Hg, had an adjusted increase in the VFDS

of 0.76 AGIS visual field units at 84 months (7 years). Subjects with an initial mean IOP of  $\geq 18$  mm Hg had an adjusted increase in the VFDS of 1.89 AGIS units over 7 years. For analysis of the travoprost, latanoprost, and timolol clinical trial data, we therefore applied a relative increase in VFDS to each subject on the basis of his or her mean IOP over the study period. For example, a subject with an average IOP of 15 mm Hg would have an adjusted increase in VFDS of 0.76. This value was added to the values for all other subjects in a treatment group and divided by the total number of subjects in a treatment group to find the average. We then determined the overall change in VFDS for each treatment group.

The second associative AGIS analysis was based on the percentage of visits during the entire study period in which a patient's IOP was  $< 18$  mm Hg. Subjects with all visits in which their IOP was  $< 18$  mm Hg served as the reference group. Those whose IOP reading was  $< 18$  mm Hg at 75% to less than 100% of visits had a relative increase in VFDS at 84 months of 1.00. Those whose IOP reading was  $< 18$  mm Hg at 50% to less than 75% of visits or at less than 50% of visits had VFDS increases of 2.05 and 1.93, respectively. We determined the proportion of visits in which subjects had IOP readings  $< 18$  mm Hg, then assigned each subject a change in VFDS value based on this proportion (ie, subjects who had an IOP reading  $< 18$  mm Hg at less than 50% of visits had a VFDS of 1.93, while those with IOP  $< 18$  mm Hg at 75% to less than 100% of visits had a VFDS of 1.0). For example, a subject with a mean IOP of  $< 18$  mm Hg at only one of the six study visits had a VFDS of 1.93. As with the first analysis, the overall change in VFDS for each treatment group was then determined.

**RELATIONSHIP OF IOP AND LIKELIHOOD OF VISUAL FIELD DEFICIT PROGRESSION**

The AGIS 7 results<sup>12</sup> provide a structure by which the likelihood of relative changes in visual field deficits can be evaluated. It is also crucial to assess the likelihood that a patient will develop further deficits in his or her visual field (ie, that the visual field deficits will progress). A number of recent studies have provided algorithms linking IOP and the likelihood of visual field deficit progression. We used algorithms from four recent publications (Mao and associates,<sup>21</sup> Odberg,<sup>22</sup> Shirakashi and colleagues,<sup>23</sup> and Stewart and coinvestigators<sup>24</sup>) to evaluate the relationship between IOP and projected progression of visual field deficit. Details of these four algorithms are presented in Table I.

For each of these four algorithms, we determined the probability of visual field deficit progression based on the overall mean IOP for all time points and for each individual subject in the study. We then determined the overall likelihood of visual field deficit progression for each treatment group, and this difference was used for the cost

analysis as described in the next section. For example, with the Mao algorithm, the travoprost group has an overall likelihood of visual field deficit progression of 37.2%, compared with 55.7% for the latanoprost group, which is a difference of 18.5% points in favor of travoprost.

**COST PROJECTIONS**

The analysis just described provided information on the likelihood of visual field deficit progression or increase in VFDS among black subjects treated with travoprost, latanoprost, or timolol. Using this information, we made various analyses to estimate the effects of VFDS on the cost of hospitalizations and cost of outpatient glaucoma care.

Differences in visual field deficit progression were used to estimate medical care cost differences based on two sources. For an estimate of the differences in hospitalization costs, we used a study by Morse and associates.<sup>25</sup> They reported that among hospitalized subjects, those with severe visual impairment had a hospital length of stay averaging 2.4 days longer than those without severe visual impairment. The difference in length of stay was applied to the difference in the rate of visual field deficit progression to determine the incremental length of stay for hospitalized subjects (ie, the difference in rate of visual field deficit progression between subjects receiving travoprost and subjects receiving other treatments was multiplied by 2.4 hospital days). The mean num-

**TABLE I: ALGORITHMS USED TO ASSESS THE RELATIONSHIP OF IOP AND LIKELIHOOD OF VISUAL FIELD DEFICIT PROGRESSION**

SOURCE	ALGORITHM
Mao et al <sup>21</sup>	Visual field deficit progression was based on categories of mean IOP. Subjects with mean IOP $\leq 16$ mm Hg had no likelihood (0%) of progression. Those with mean IOP of 17–18 mm Hg, 19–21 mm Hg, or $\geq 22$ mm Hg had likelihoods of visual field deficit progression of 29.4%, 71.4%, and 100%, respectively.
Odberg <sup>22</sup>	Visual field deficit progression was evaluated using a mean IOP threshold of 15 mm Hg. Subjects with mean IOP $\leq 15$ had a 42% likelihood of visual field deficit progression, while those with mean IOP $> 15$ had an 85% likelihood.
Shirakashi et al <sup>23</sup>	Based on a mean IOP threshold of 15 mm Hg. Over the long term, no subjects with IOP $\leq 15$ had visual field progression, while all subjects with IOP $> 15$ experienced progression.
Stewart et al <sup>24</sup>	Likelihood of visual field progression was stratified into several groups based on mean IOP. Subjects with mean IOP $\leq 16$ mm Hg had no likelihood (0%) of progression. Those with mean IOP of 17–18 mm Hg, 19–21 mm Hg, or $\geq 22$ mm Hg had likelihoods of visual field deficit progression of 15.4%, 50.0%, and 100%, respectively.

IOP, intraocular pressure.

ber of hospitalizations per year (0.183) was obtained from the 1996 National Health Interview Survey<sup>26</sup> for individuals at the median age of the patient sample (63 years). Finally, the average Medicare cost per day for hospitalization (\$1,000.36) was applied to the incremental length of stay and number of hospitalizations per year to determine the incremental hospitalization cost per year due to severe visual field deficits. As all subjects met visual field inclusion criteria (ie, none of the subjects had severe visual field loss at the time of the trial), these projections provide information on long-term cost changes (ie, these costs capture expected medical care resource utilization costs based on projected visual loss over time).

To estimate differences in outpatient costs between the various treatment groups, we used the treatment guidelines from the Preferred Practice Patterns of the American Academy of Ophthalmology.<sup>27</sup> Outpatient resource utilization rates from the guidelines and associated costs were determined for subjects with controlled IOP versus those with recent progressive damage. For controlled subjects, the mean annual rate of resource utilization was estimated as two examinations in addition to one dilated optic nerve examination and one visual field assessment. For subjects with recent progressive damage, there were approximately six examinations, two optic nerve examinations, and three visual field assessments per year. The corresponding annual costs used for controlled subjects and progressing subjects (based on 2000 Medicare reimbursement rates) were \$359 and \$818, respectively; the additional annual outpatient cost for progressing subjects is therefore assumed to be \$459. This additional cost for progressing subjects was multiplied by the difference in rate of visual field deficit progression between the three treatment groups.

#### DATA ANALYSIS

Comparisons of subject characteristics, VFDS, or likelihood of visual field deficit progression between the three treatment groups were made using *t* tests for continuous variables and chi-square tests for dichotomous variables. We also performed multivariate linear regression (for continuous variables) and logistic regression (for dichotomous variables) to evaluate the impact of treatment arm on visual field outcomes while controlling for age and sex. All calculations were performed using SAS software (release 8.01, Cary, North Carolina). *P* values at less than .05 were considered statistically significant. Finally, by using these algorithms we assumed that the efficacy of each drug demonstrated in the 1-year trial is representative of the performance of the drug on a longer-term basis.

#### RESULTS

Table II presents characteristics of study subjects. There were no statistically significant differences between the

TABLE II: CHARACTERISTICS OF SUBJECTS BY TREATMENT GROUP

CHARACTERISTICS	TRAVOPROST SUBJECTS (N=49)	LATANOPROST SUBJECTS (N=43)	TIMOLOL SUBJECTS (N=40)
Mean age, yr (SD)	62.6 (13.6)	58.6 (12.1)	62.3 (11.9)
Female	53.1%	58.1%	62.5%
Baseline mean IOP, mm Hg			
8 AM (SD)	26.8 (2.7)	27.6 (3.3)	27.2 (3.0)
1 AM (SD)	25.0 (2.7)	25.9 (3.5)	25.4 (2.8)
4 PM (SD)	24.0 (2.3)	25.2* (3.0)	24.8 (2.9)
Overall (SD)	25.3 (2.3)	26.2 (3.1)	25.8 (2.7)
Mean IOP, mm Hg			
8 AM (SD)	18.5 (2.6)	19.7* (2.4)	21.4* (3.3)
1 AM (SD)	16.6 (2.5)	18.1* (2.4)	19.9* (3.6)
4 PM (SD)	16.9 (2.8)	18.3* (3.0)	19.9* (3.7)
Overall (SD)	17.3 (2.5)	18.7* (2.4)	20.5* (3.4)

IOP, intraocular pressure.

\*Statistically significant ( $P < .05$ ) compared to travoprost.

three groups for age and sex. The difference in baseline mean IOP (before initiation of study medication) between the three groups was also not significantly different except at 4 PM between the travoprost and latanoprost groups. The mean IOP overall and throughout the day, during the 1-year study, for the travoprost group was significantly lower than that for either the latanoprost or the timolol group.

Table III presents results of changes in VFDS or likelihood of visual field deficit progression. Using either the predictive or associative AGIS analysis, the likelihood of an increase in VFDS was greater for timolol and latanoprost than for travoprost. The increase in VFDS was also greater for timolol than for latanoprost. Using both the predictive analysis (based on three categories of mean IOP) and the associative analysis (based on the percent of visits with IOP < 18 mm Hg), the differences between travoprost and the other two treatment groups were statistically significant. Similarly, the estimated proportion of subjects experiencing progression of visual field deficits was greater for timolol and latanoprost than for travoprost with each of the four algorithms used (ie, Mao and associates,<sup>21</sup> Odberg,<sup>22</sup> Shirakashi and colleagues,<sup>23</sup> and Stewart and coinvestigators<sup>24</sup>). The direct comparisons between travoprost and the other two treatment groups were statistically significant for all four algorithms.

Differences in medical care cost projections for the three groups are presented in Tables IV and V. As described in the "Methods" section, to determine inpatient cost differences, the difference in projected rate of visual field progression between the travoprost, latanoprost, and timolol groups was applied to the annual rate of hospitalization (0.183) for this age-group and increased number of days per hospitalization (2.4) for subjects with visual impairment. This produced the

Projected Impact of Travoprost Versus Both Timolol and Latanoprost on Visual Field Deficit Progression

TABLE III: PROJECTED VISUAL FIELD CHANGE RESULTS FOR BLACK SUBJECTS

SOURCE OF IOP TO VISUAL FIELD PROGRESSION LINK	VISUAL FIELD OUTCOME	TRAVOPROST	LATANOPROST	TIMOLOL	IMPACT OF TRAVOPROST VS LATANOPROST	IMPACT OF TRAVOPROST VS TIMOLOL
AGIS, 2000 predictive	Increased VFDS based on mean IOP <14, 14-18, or ≥18 mm Hg	1.18	1.48	1.66	-25.4%°	-40.7%°
AGIS, 2000 associative	Increased VFDS based on % of visits with peak IOP <18	1.40	1.81	1.89	-29.3%°	-35.0%°
Mao et al, <sup>21</sup> 1991	Visual field progression probability based on mean IOP ≤16, 17-18, 19-21, or ≥22 mm Hg	37.2%	55.7%	72.3%	-18.5%°	-35.1%°
Odberg, <sup>22</sup> 1987	Visual field progression probability based on mean IOP ≤15 vs >15 mm Hg	76.2%	84.0%	83.6%	-7.8%°	-7.4%°
Shirakashi et al, <sup>23</sup> 1993	Visual field progression probability based on mean IOP ≤15 vs >15 mm Hg	79.6%	97.7%	97.5%	-18.1%°	-17.9%
Stewart et al, <sup>24</sup> 1993	Visual field progression probability based on mean IOP ≤16, 17-18, 19-21, or ≥22 mm Hg	26.9%	41.5%	56.1%	-14.7%°	-29.2%°

AGIS, Advanced Glaucoma Intervention Study; IOP, intraocular pressure; VFDS, visual field defect score.

°Statistically significant ( $P<.05$ ) compared to travoprost.

increase in hospital days per latanoprost and timolol subject per year. For example, as shown in Table IV, patients receiving latanoprost had a 25.4% increased rate of visual field deficit progression, as compared to travoprost patients, using the first algorithm from the AGIS study. Based on this algorithm, latanoprost patients therefore had 25.4% more hospital days attributable to visual field deficits, or 25.4% times 0.183 times 2.4 (which equals 0.112) extra hospital days annually compared to travoprost patients. To determine the cost associated with this increased hospitalization, the additional hospital days (in this case, 0.112) were multiplied by the cost per day (\$1,000.36) to get the additional annual hospitalization cost (here, \$112). In Table IV, these increased costs ranged from \$34 to \$129 per latanoprost subject per year, and averaged \$83 (SD, \$34). For timolol, the increased costs ranged from \$33 to \$179 per subject per year and averaged \$121 (SD, \$55).

Tables IV and V also present similar results for outpatient medical care costs. As described in the “Methods” section, resource utilization for progressing and stable subjects was estimated by using the American Academy of Ophthalmology guidelines, and costs were assigned using Medicare 2000

reimbursement values. These costs were then applied to the differences in progression rates between travoprost, latanoprost, and timolol subjects. For example, as presented in Table V using the algorithm from Stewart and associates,<sup>24</sup> subjects receiving timolol have a 29.2% increase in the projected likelihood of visual field deficit progression. The additional outpatient cost for timolol subjects is therefore 29.2% times \$459, which equals \$133 per subject. Results are similar to those seen with increased hospital costs; the increase in annual outpatient care costs per latanoprost subject ranges from \$36 to \$134, with an average of \$87 (SD, \$35) per subject per year. For timolol subjects, the increase in annual outpatient care costs ranges from \$34 to \$186 per subject, with an average of \$126 (SD, \$57) per subject. These are conservative cost estimates, as they do not include nonphysician outpatient services and resource utilization such as systemic medications. Adding inpatient and outpatient results, the additional annual cost per latanoprost subject is projected to range from \$70 to \$263 with an average annual increase of \$170 (SD, \$69). For timolol, the range is from \$66 to \$365 with an average annual increase of \$247 (SD, \$112).

TABLE IV: COST PROJECTIONS BASED ON RATE OF VISUAL FIELD PROGRESSION: TRAVOPROST VERSUS LATANOPROST

SOURCE OF IOP TO VISUAL FIELD PROGRESSION LINK	INCREASE IN VISUAL FIELD PROGRESSION RATES, LATANOPROST VS TRAVOPROST <sup>o</sup>	INCREASE IN ANNUAL HOSPITAL DAYS PER LATANOPROST SUBJECT <sup>†</sup>	INCREASE IN ANNUAL HOSPITAL COST PER LATANOPROST SUBJECT <sup>‡</sup>	INCREASE IN ANNUAL OUTPATIENT COST PER LATANOPROST SUBJECT <sup>§</sup>	INCREASE IN ANNUAL INPATIENT PLUS OUTPATIENT COST PER LATANOPROST SUBJECT <sup>§</sup>
AGIS, predictive	25.4%	0.112	\$112	\$116	\$228
AGIS, associative	29.3%	0.129	\$129	\$134	\$263
Mao et al, <sup>21</sup> 1991	18.5%	0.081	\$81	\$85	\$166
Odlberg, <sup>22</sup> 1987	7.8%	0.034	\$34	\$36	\$70
Shirakashi et al, <sup>23</sup> 1993	18.1%	0.079	\$80	\$83	\$162
Stewart et al, <sup>24</sup> 1993	14.6%	0.064	\$64	\$67	\$131
Average	19.0%	0.083	\$83	\$87	\$170
SD of average	7.7%	0.034	\$34	\$35	\$69

AGIS, Advanced Glaucoma Intervention Study.

<sup>o</sup>For application of the AGIS measures, the increase in visual field progression is based on the percentage increase in visual field defect score.

<sup>†</sup>Assuming an average of 0.183 annual hospitalizations per patient (National Hospital Discharge Survey) and 2.4 days of additional hospitalization for patient with visual field impairment (Morse et al,<sup>25</sup> 1999).

<sup>‡</sup>Assuming an average daily cost per hospitalization of \$1,000.36 (1995 Medicare value of \$845.62 inflated to 2000 values using the medical care component of the Consumer Price Index).

<sup>§</sup>Based on outpatient resource utilization estimates from the American Academy of Ophthalmology guidelines and Medicare reimbursement rates, as described in the "Methods" section.

TABLE V: COST PROJECTIONS BASED ON RATE OF VISUAL FIELD PROGRESSION: TRAVOPROST VERSUS TIMOLOL

SOURCE OF IOP TO VISUAL FIELD PROGRESSION LINK	INCREASE IN VISUAL FIELD PROGRESSION RATES, TIMOLOL VS TRAVOPROST <sup>o</sup>	INCREASE IN ANNUAL HOSPITAL DAYS PER TIMOLOL SUBJECT <sup>†</sup>	INCREASE IN ANNUAL HOSPITAL COST PER TIMOLOL SUBJECT <sup>‡</sup>	INCREASE IN ANNUAL OUTPATIENT COST PER TIMOLOL SUBJECT <sup>§</sup>	INCREASE IN ANNUAL INPATIENT PLUS OUTPATIENT COST PER TIMOLOL SUBJECT <sup>§</sup>
AGIS, predictive	40.7%	0.179	\$179	\$186	\$365
AGIS, associative	35.0%	0.154	\$154	\$160	\$314
Mao et al, <sup>21</sup> 1991	35.1%	0.154	\$154	\$160	\$315
Odlberg, <sup>22</sup> 1987	7.4%	0.033	\$33	\$34	\$66
Shirakashi et al, <sup>23</sup> 1993	17.9%	0.079	\$79	\$82	\$160
Stewart et al, <sup>24</sup> 1993	29.2%	0.128	\$128	\$133	\$262
Average	27.5%	0.121	\$121	\$126	\$247
SD of average	12.5%	0.055	\$55	\$57	\$112

AGIS, Advanced Glaucoma Intervention Study.

<sup>o</sup>For application of the AGIS measures, the increase in visual field progression is based on the percentage increase in visual field defect score.

<sup>†</sup>Assuming an average of 0.183 annual hospitalizations per patient (National Hospital Discharge Survey) and 2.4 days of additional hospitalization for patient with visual field impairment (Morse et al,<sup>25</sup> 1999).

<sup>‡</sup>Assuming an average daily cost per hospitalization of \$1,000.36 (1995 Medicare value of \$845.62 inflated to 2000 values using the medical care component of the Consumer Price Index).

<sup>§</sup>Based on outpatient resource utilization estimates from the American Academy of Ophthalmology guidelines and Medicare reimbursement rates, as described in the "Methods" section.

## DISCUSSION

Many studies have evaluated IOP-lowering medications and often use short-term IOP lowering as a surrogate end

point for the preservation of vision. However, in glaucoma treatment, the ultimate goal of therapy is to prevent progressive vision and visual field loss. We assumed that there is a correlation between IOP decrease and long-term

vision preservation.<sup>10-12</sup> There are possibly many other factors, such as ophthalmic blood flow, that affect the long-term preservation of the optic nerve and visual function. However, there are other potential factors that cannot be quantified.

To date, the only factor that we can reliably accomplish is IOP lowering. The AGIS<sup>12</sup> evaluated the long-term impact of IOP values on a visual field progression and found a relationship between both IOP lowering and consistent IOP lowering with less visual field deterioration. Other studies<sup>21-24</sup> have also used IOP as a predictive value for progression of visual field loss. We do not currently know the exact relationship between IOP and subsequent risk of progression of visual field loss. It may not necessarily be strictly linear; rather, the likelihood of visual field loss (or increases in the VFDS) may be related to thresholds or patterns of IOP values, the degree of initial field loss, the patient's age, and the eye's unique intrinsic susceptibility to damage.

There are many costs associated with glaucoma therapy. Studies have examined the number of drops per bottle, drop size, and cost per drop. We believe a better index of cost savings is the prevention of visual deficit progression. One facet of this cost is based on the responder analysis, or the percent of subjects having a sustained satisfactory IOP lowering when given a specific therapy. A medication that is most successful initially and most likely to achieve a therapeutic goal has no tachyphylaxis and no significant systemic adverse events, and it is probably far cheaper in the long term. Also, this medication, if well tolerated, has a better chance of preserving sight and would be a very cost-effective therapy.

There are many ways to lower IOP in patients with newly diagnosed glaucoma, including drug, laser, and surgical intervention.<sup>1</sup> Each has its own advantages and disadvantages. In newly diagnosed glaucoma, surgical therapy is most likely to lower IOP the greatest. However, surgical therapy is associated with a larger risk of cataract formation and other symptoms, such as drooping eyelids.<sup>10,11</sup> Laser therapy is also a good alternative but may have a decreasing benefit with time.<sup>25</sup> All of the collaborative studies (AGIS,<sup>12</sup> the Collaborative Initial Glaucoma Treatment Study,<sup>11</sup> the Normal-Tension Glaucoma Study,<sup>10</sup> and the Glaucoma Laser Trial<sup>25</sup>) have not primarily used the prostaglandin analogues in their treatment algorithms, because the prostaglandin analogues are relatively new in glaucoma management. These prostaglandin analogues have a greater responder rate and better IOP lowering than all prior classes of medications. Until relatively recently, traditional initial pharmacotherapy for glaucoma has consisted of beta-adrenergic antagonists (beta blockers), alpha-adrenergic agonists (relatively specific alpha agonists), parasympathomimetic (cholinergic) agents, and carbonic anhydrase inhibitors. These medications have

generally been associated with potentially significant local and systemic adverse events.<sup>29-31</sup> Prostaglandin analogues represent a newer treatment for glaucoma and have minimal systemic and local side effects. Additionally, they more consistently lower IOP better and with fewer adverse events than other classes of medications. The responder rate among prostaglandin analogues is far superior to that of prior classes of medications.

In this study, we utilized IOP data from a recent large multicenter clinical trial comparing travoprost to latanoprost and timolol in order to project future changes in visual field loss. As presented in Table II, the short-term difference in IOP was apparent when comparing the three study groups; the mean IOP value for travoprost-treated subjects was significantly lower than that for latanoprost-treated and timolol-treated subjects (17.3 mm Hg versus 18.7 mm Hg versus 20.5 mm Hg, respectively). Further, regardless of which algorithm is used (the two algorithms from AGIS and the four from other studies), the projected long-term changes in VFDS and the proportion of subjects with progression of visual field loss were also significantly different among subjects using the three medications as shown in Table III. In particular, we projected that subjects receiving travoprost would have decreased rates of visual field deficit progression as compared to subjects receiving either latanoprost or timolol. By assigning costs to these projected differences, we are able to quantify both the short-term (from outpatient treatment changes) and longer-term (from changes in length of hospitalization resulting from multiple years of visual field deficit progression leading to severe visual impairment) economic changes.

There are a number of limitations to this study. First, data for this model and analysis are based on the results of a simple randomized and masked clinical trial. Subjects may behave differently depending on the trial design. Subjects may behave differently in a trial than they do in the real world. Also, the subjects in this study may or may not be comparable to those in the studies used to project changes in VFDS or visual field loss. Follow-up and compliance may be better or worse. Strict therapeutic regimens are followed, rather than less structured treatment protocols. Strict inclusion and exclusion criteria were used. These results may therefore not apply to those with other characteristics. Therefore, while randomized clinical trials allow for control of differences in a subject's characteristics (ie, they have a high degree of internal validity), they may not correspond as well to "real world" treatment patterns. This may affect the ability to generalize our results.

Also, any projection is associated with a level of uncertainty. In this analysis, projections of visual field loss (and associated costs) are subject to variability. However, the multiple projections used in this analysis all produced the same results (ie, lower rates of visual field loss progression

among subjects treated with travoprost). This consistency provides an increased foundation for the predicted results presented herein.

Finally, the results of this study are based on a fairly small sample of black subjects. Attempts to replicate the results should involve larger patient groups. Also, these models should involve subjects not in multicenter studies. Further, it is unknown whether these results are generalizable to groups beyond the study subject.

In addition to its economic impacts, progression of visual field loss is likely to result in decreased patient quality of life. It is often difficult to assign a relative cost to these items. Gutierrez and associates<sup>19</sup> evaluated the impact of the AGIS-based VFDS on patient quality of life in a number of important domains. The results clearly indicate decreasing quality of life with increasing VFDS score. For example, each 1-point increase in VFDS was associated with approximately a 3-point decrease in the driving scale score (which ranged from 100 to 0). It may thus be possible to predict changes in key visual quality-of-life domains on the basis of predicted changes in visual field.

We do not assign a cost to quality-of-life issues (eg, the value of autonomy or the value of a good driving record). We do not deal with costs associated with adverse reactions to medications (ie, the cost of a hospitalization from an asthma attack while receiving a beta blocker is quite expensive compared to the value of a bottle of eyedrops). We also do not evaluate the indirect costs associated with a patient's time or the time of a family member or friend who brings the patient in for an examination. These costs of lost productivity are very important. Thus, the cost estimates presented in this manuscript are conservative and may underestimate the true economic impact of preserving vision.

## SUMMARY

We have used data from a 12-month clinical trial to create a model and extrapolate changes in longer-term clinical outcomes (visual field) from intermediate outcomes (IOP). While these results will require replication, we initially can conclude that treatment with travoprost is projected to result in lower rates of visual field loss than is treatment with latanoprost or timolol. As a consequence, substantial cost savings and protection of patient quality of life may be associated with travoprost therapy. We urge that others also begin to consider the actual costs of therapy and further investigate the true costs of various interventions.

## REFERENCES

1. American Academy of Ophthalmology. Glaucoma Panel. *Preferred Practice Patterns: Primary Open-Angle Glaucoma*. San Francisco: American Academy of Ophthalmology; 1995.
2. Klein BEK, Klein R, Sponsel WE, et al. Prevalence of glaucoma: the Beaver Dam Eye Study. *Ophthalmology* 1992;99:1499-1504.
3. Prevent Blindness America. *Vision Problems in the US. Prevalence of Adult Vision Impairment and Age-Related Eye Disease in America*. Schaumburg, Ill: Prevent Blindness America; 2002.
4. Quigley HA. Number of people with glaucoma worldwide. *Br J Ophthalmol* 1996;80:389-393.
5. Stewart WC, Garrison PM. Beta-blocker-induced complications and the patient with glaucoma. Newer treatments to help reduce systemic adverse events. *Arch Intern Med* 1998;158:221-226.
6. Tielsch JM. The epidemiology and control of open angle glaucoma: a population-based perspective. *Ann Rev Public Health* 1996;17:121-136.
7. Anderson DR. Glaucoma: the damage caused by pressure. *Am J Ophthalmol* 1989;108:485-495.
8. Mitchell P, Smith W, Attebo K, et al. Prevalence of open-angle glaucoma in Australia: the Blue Mountain Eye Study. *Ophthalmology* 1996;103:1661-1669.
9. Dielemans I, de Jong PTVM, Stolk R, et al. Primary open-angle glaucoma, intraocular pressure, and diabetes mellitus in the general elderly population. The Rotterdam Study. *Ophthalmology* 1996;103:1271-1275.
10. Collaborative Normal-Tension Glaucoma Study Group. The effectiveness of intraocular pressure reduction in the treatment of normal-tension glaucoma. *Am J Ophthalmol* 1998;126:498-505.
11. Lichter PR, Musch DC, Gillespie BW, et al, and the CIGTS Study Group. Interim clinical outcomes in the Collaborative Initial Glaucoma Treatment Study comparing initial treatment randomized to medications or surgery. *Ophthalmology* 2001;108:1943-1953.
12. The AGIS Investigators. The Advanced Glaucoma Intervention Study (AGIS): 7. The relationship between control of intraocular pressure and visual field deterioration. *Am J Ophthalmol* 2000;130:429-440.
13. Liesegang TJ. Glaucoma: changing concepts and future directions. *Mayo Clin Proc* 1996;71:689-694.
14. Cohan RA, Van Nostrand JF. Trends in the health of older Americans: United States, 1994. National Center for Health Statistics. *Vital Health Stat* 1995;3(30):67-80.
15. Tielsch JM, Sommer A, Katz J, et al. Racial variations in the prevalence of primary open angle glaucoma: the Baltimore Eye Survey. *JAMA* 1991;266:369-374.
16. Hiller R, Kahn HA. Blindness from glaucoma. *Am J Ophthalmol* 1975;80(1):62-69.
17. Sommer A, Tielsch JM, Katz J, et al. Racial differences in the cause-specific prevalence of blindness in east Baltimore. *N Engl J Med* 1991;325(20):1412-1417.
18. Breakout data from travoprost study links effectiveness, race. *Ocular Surg News* 2001 Mar 15. Available at: <http://www.slackinc.com/eye/osn/200103b/travside.asp>.
19. Gutierrez P, Wilson MR, Johnson C, et al. Influence of glaucomatous visual field loss on health-related quality of life. *Arch Ophthalmol* 1997;115:777-784.
20. Netland PA, Landry T, Sullivan EK, et al, and the Travoprost Study Group. Travoprost compared with latanoprost and timolol in patients with open-angle glaucoma or ocular hypertension. *Am J Ophthalmol* 2001;132:472-484.

21. Mao LK, Stewart WC, Shields MB. Correlation between intraocular pressure control and progressive glaucomatous damage in primary open-angle glaucoma. *Am J Ophthalmol* 1991;111:51-55.
22. Odberg T. Visual field prognosis in advanced glaucoma. *Acta Ophthalmol* 1987;65(Suppl182):27-29.
23. Shirakashi M, Iwata K, Sawaguchi S, et al. Intraocular pressure-dependent progression of visual field loss in advanced primary open-angle glaucoma: a 15-year follow-up. *Ophthalmologica* 1993;207:1-5.
24. Stewart WC, Chorak RP, Hunt HH, et al. Factors associated with visual loss in patients with advanced glaucomatous changes in the optic nerve head. *Am J Ophthalmol* 1993;116:176-181.
25. Morse AR, Yatzkan E, Berberich B, et al. Acute care hospital utilization by patients with visual impairment. *Arch Ophthalmol* 1999;117:943-949.
26. National Center for Health Statistics. 1996 National Health Interview Survey (database on CD-ROM). Series 10(11). SETS Version 2.0. Washington, DC: US Government Printing Office; 1999.
27. American Academy of Ophthalmology. Preferred practice pattern: primary open-angle glaucoma. San Francisco (CA): American Academy of Ophthalmology, 1996.
28. Glaucoma Laser Trial Research Group. The Glaucoma Laser Trial (GLT) and Glaucoma Laser Trial Follow-Up Study: 7. Results. *Am J Ophthalmol* 1995;120:718-731.
29. Goldberg I, Goldberg H. Betaxolol eye drops. A clinical trial of safety and efficacy. *Aust N Z J Ophthalmol* 1995;23:17-24.
30. Diggory P, Cassels-Brown A, Vail A, et al. Avoiding unsuspected respiratory side-effects of topical timolol with cardioselective or sympathomimetic agents. *Lancet* 1995;345:1604-1606.
31. Diggory P, Cassels-Brown A, Fernandez C. Topical beta-blockade with intrinsic sympathomimetic activity offers no advantage for the respiratory and cardiovascular function of elderly people. *Age Ageing* 1996;25(6):424-428.

## DISCUSSION

DR M. BRUCE SHIELDS. Dr Robin and his colleagues have focused on a rather surprising finding from a previously reported multicenter trial, in which travoprost 0.004% was found to be significantly more effective in lowering intraocular pressure (IOP) among black patients than latanoprost 0.005%. What made this finding particularly surprising was the observation that travoprost 0.004% was also more effective among black patients in the clinical trial than was the same drug in the nonblack population. This is in contrast to prior studies of other topical glaucoma drugs, such as timolol, in which a higher concentration of the medication is required in eyes with darker iris pigmentation to produce the same level of pressure reduction. However, in the clinical trial cited in the present paper, travoprost 0.004% was significantly more effective than travoprost 0.0015% among black patients, which is consistent with the prior studies, and it may be that the greater affinity of travoprost for prostaglandin F receptors, as compared to latanoprost, may explain the observations in the referenced clinical trial.

In any case, it is quite appropriate that Dr Robin and his associates should pursue this question, considering the relative significance of glaucoma in the black population, in which the condition is three to four times more prevalent than in white individuals and is six times more likely to be associated with blindness. If the initial findings are correct, therefore, it would have significant implications in the treatment of black individuals with glaucoma.

Dr Robin and his colleagues have taken the IOP data within the black population of the clinical trial to estimate the long-term course of visual field progression and the economic consequences of the associated visual impairment among black patients receiving either travoprost 0.004% daily, latanoprost 0.005% daily, or timolol 0.5% twice daily. Not surprisingly, the results favor travoprost, although the magnitude of the differences is impressive.

The authors have appropriately cited limitations to their study. Specifically, two questions must be asked: How reliable is the assumed relationship between IOP data and visual field progression, and, how accurate is the IOP data upon which the assumptions are made? As the authors note, progressive visual field loss in glaucoma cannot be accurately predicted on the basis of mean IOP alone, but rather on a pattern of IOP over time. One wonders, therefore, if a 12-month study provides sufficient IOP data upon which to predict long-term visual outcome. As the authors also note, pressure is not the only factor associated with optic nerve damage and visual field loss in glaucoma, which further complicates any attempt to predict long-term visual outcome on IOP data.

Assuming for the moment, however, that the assumptions linking IOP data to visual outcome are reliable, how accurate is the IOP data on which these assumptions are based? As the authors admit, the sample size is relatively small. Furthermore, 9 of the 49 travoprost patients (18%) did not complete the study, compared to 3 of the 43 latanoprost patients (7%). It would be helpful to know the reason for the withdrawal of these patients from the study. If it were for inadequate pressure control, would this have influenced the results, since the IOP values for subjects discontinuing early were not carried forward?

As the authors correctly state, further study with a larger population of black patients and longer follow-up is first needed to confirm the IOP data in the initial clinical trial. If the findings can be confirmed, then the impact on preservation of vision, quality of life, and cost savings, as estimated by the authors, will represent a significant advance in our management of glaucoma. In any case, Dr Robin and his associates are to be complemented for focusing our attention on this important possibility and also in emphasizing the importance of considering these outcome measures in the evaluation of any glaucoma treatment.

DR ALLAN J. FLACH. The paper does involve problems of cost. The Advanced Glaucoma Intervention Study (AGIS) has recently been completed and demonstrated that intraocular pressures (IOPs) below 14 mm Hg are desirable to preserve visual function in those patients with glaucomatous visual field and disk changes. No one has disproven, however, that every individual may have his or her own susceptibility to IOP. I am alarmed by many of the individuals presenting papers in various societies that take the AGIS data and suggest that we should be striving for pressures below 15 mm Hg or 14 mm Hg in all of our patients with glaucoma. My concern that this philosophy may lead to unnecessary medical and surgical therapies.

Intraocular pressures as low as possible is a desirable goal in many, but choosing a goal pressure that is extremely low, without thinking about individual variation, may be a great financial trap.

DR ROBERT L. STAMPER. I'd like to plead that our drug and surgical studies in the future do indeed look at the primary outcome, which is, in fact, visual function and quality of life, rather than just IOP. Did you look at corneal thickness in assessing the IOP in these patients?

DR ALAN L. ROBIN. Let me address the questions in reverse order, first for Dr Stamper and then Dr Flach. I regrettably agree that many clinicians now mindlessly extrapolate from the AGIS data and create arbitrarily or artificially low IOP goals for many patients without considering the patient's age, degree of visual field and optic nerve damage, health status, or quality of life. The only way to really know of the appropriate goal for anybody is retrospectively; that is, have you preserved visual function 5 years later at the IOP level that you have chosen?

I believe that AGIS does give us some guidelines, as do the Normal Tension Glaucoma Study, Collaborative Initial Glaucoma Treatment Study (CIGTS), and the Ocular Hypertension Treatment Study (OHTS). The lessons from these studies are as follows: AGIS found that in a group of patients with advanced glaucoma, IOPs that are consistently below 18 mm Hg (averaging 12.3 mm Hg) had no net change in visual field score 6 years later. Also those

subjects whose IOPs remained below 14 mm Hg for the first 18 months after intervention had no significant change in visual function 8 years later. CIGTS found that in individuals with early glaucoma, strict IOP lowering, either medically or surgically, minimized visual field loss 5 years later, so that it occurred in less than 15% of patients. Finally the OHTS found that in subjects without glaucoma, but with elevated IOPs, a 20% decrease in IOP significantly diminished the risk of the development of glaucoma. In OHTS, corneal thickness was a significant risk factor for the development of glaucoma, as those with thinner corneas had a three times higher chance of developing the disease than those ocular hypertensives without it.

Although the results will vary from person to person and although some people are unaffected by pressure lowering, I think many ophthalmologists, regrettably, have extracted the data from AGIS and applied them to patients who don't have glaucoma or may have early glaucoma. This may be extremely inappropriate. I believe the onus and the responsibility of appropriate therapy are with the glaucoma specialists in this audience and in our society, for making sure that the right information is disseminated. We must think about the whole picture, not a "cookbook" attitude for glaucoma therapy.

Second, to answer Dr Stamper's question about pachymetry, we did not look at corneal pachymetry except for a very small number of people in this study.

Third, in response to Dr Shield's comment, there were a number of individuals, more so in the travoprost group, who were disqualified from the study. However, the disqualifications were only related to an adverse effect from Travatan in one individual. The remainder of the disqualifications were not due to either inadequate IOP lowering or drug-related adverse events. In fact, they were quite varied, including noncompliance, and car wreck.

Finally, I think that this study, in and of itself, is significant in that it finds that we should really look at therapies not only in terms of IOP lowering or visual field loss but also to analyze the cost of visual field loss preservation. The relative costs of therapy are becoming more important in choosing which therapies are most cost-efficient for our patients.

# ACTIVATED SATELLITE CELLS ARE PRESENT IN UNINJURED EXTRAOCULAR MUSCLES OF MATURE MICE

---

BY Linda K. McLoon, PhD (BY INVITATION) AND Jonathan Wirtschafter, MD

## ABSTRACT

*Purpose:* We recently demonstrated that there is a continuous process of myonuclear addition into normal, uninjured adult myofibers in rabbit extraocular muscles (EOM). This phenomenon is not seen in skeletal muscles from normal, adult limbs. These features may explain the selective involvement of the EOM in progressive external ophthalmoplegia and oculopharyngeal muscular dystrophy due to an accumulation of damaged DNA in mitochondria and nuclei within the EOM as a result of repeated cycling of the muscle satellite cells. Many testable hypotheses flow from these observations. We investigated whether continuous myonuclear addition is present in normal mouse EOM so that mouse models of genetic disorders can be used to study the pathogenic mechanisms and to test potential therapies for human muscle disorders.

*Methods:* Bromodeoxyuridine (brdU) was injected intraperitoneally into C57 adult mice every 2 hours for 12 hours. Twenty-four hours later the animals were sacrificed, and the globes with the muscles attached were prepared for immunohistochemical localization of brdU-positive nuclei within the EOM. All cross sections were immunostained for both brdU and either dystrophin or laminin.

*Results:* All the rectus muscles from the mouse EOM examined contained both satellite cells and myonuclei that were positive for brdU. This demonstrates the division of satellite cells and the fusion of their daughter cells with existing adult EOM myofibers in mice.

*Conclusions:* These data indicate that the process of continuous myonuclear addition is also active in mouse EOM. These findings will allow various mutant mouse models to be used to study the pathogenesis and treatment of various muscle disorders. The existence of continuous myonuclear addition in adult, uninjured EOM fundamentally changes the accepted notion that EOM myofibers are postmitotic.

*Trans Am Ophthalmol Soc* 2002;100:119-124

## INTRODUCTION

---

Skeletal muscles at all locations are increasingly regarded as heterogeneous at the single myofiber level. At the molecular level, it is becoming clear that even the myosin proteins are expressed in subsets that are much more heterogeneous than was originally thought.<sup>1</sup> In particular, it appears that the extraocular muscles (EOM) represent a unique allotype.<sup>2</sup> Extraocular muscles possess anatomical and physiologic features, as well as disease propensities, that distinguish them from other skeletal muscles. The EOM are distinct from limb muscle in that they have a different developmental origin as well as an unusual set of

contractile properties. The EOM express a subset of molecules that are normally down-regulated in adult skeletal muscle, such as the immature form of the acetylcholine receptor<sup>3</sup> and N-CAM,<sup>4</sup> as well as a set of molecules that are uniquely expressed in the EOM, such as the EOM-specific myosin heavy chain isoform.<sup>5</sup> These properties set them apart from other skeletal muscle groups.

Normal skeletal muscle fibers of adult mammals are not replaced or remodeled unless injured. However, skeletal muscles contain a quiescent population of progenitor cells known as satellite cells. When these cells become activated after injury, they divide and result in regeneration of the injured muscle.<sup>6</sup> We have recently shown that uninjured EOM of mature rabbits undergo a process of continuous myonuclear addition.<sup>7</sup> Using a series of bromodeoxyuridine (brdU) labeling strategies, we demonstrated brdU-positive myonuclei that became stably integrated into normal, adult rabbit EOM myofibers. The limb skeletal muscles of the same rabbits did not contain brdU-positive myonuclei. These findings suggest that the EOM of

From the Departments of Ophthalmology (Dr McLoon and Dr Wirtschafter) and Neuroscience (Dr McLoon), University of Minnesota, Minneapolis. Supported by grant EY11375 from the National Eye Institute, by the Neuro-ophthalmology Research Fund, by the Minnesota Medical Foundation (L.K.M.), by the Minnesota Lions and Lionesses, and by an unrestricted grant to the Department of Ophthalmology from Research to Prevent Blindness, Inc.

adult mammals maintain a population of activated satellite cells that divide in the normal adult muscle, and their progeny slowly fuse into existing myofibers.

The existence of continuous myonuclear addition in the EOM could be of pathogenic significance in those skeletal muscle diseases that either spare the EOM or preferentially involve them.<sup>8,9</sup> For example, the EOM are spared in Duchenne's muscular dystrophy<sup>10-12</sup> and preferentially involved in other conditions, such as progressive external ophthalmoplegia and myasthenia gravis.<sup>13</sup> The phenomenon of continuous myonuclear addition and remodeling of the EOM may have implications for understanding the etiology of strabismus, the late changes following strabismus surgery, and the responses of the EOM to denervation.

It is important to demonstrate that continuous myonuclear addition into single myofibers of adult, uninjured rabbit EOM occurs not only in rabbits but also in mammalian EOM in general. We examined whether this process of continuous myonuclear addition also occurs in the EOM of adult mice. Adult mice were injected with brdU in order to label any dividing satellite cells in the EOM. BrdU is a thymidine analogue, which is incorporated into the DNA during its synthesis in the dividing cell. Following intraperitoneal injection, brdU is rapidly absorbed into the blood and incorporated into dividing cells. Nuclei that are brdU-positive are assumed to have divided shortly after brdU injection. A series of repeated brdU injections increases the window of time for identification of dividing satellite cells. The presence of brdU-positive myonuclei within existing myofibers was demonstrated by using double-labeling techniques in order to identify and quantify the number of brdU-positive myonuclei within the dystrophin-positive sarcolemma of single EOM myofibers in cross section.

## METHODS

Adult C57 mice were obtained from Jackson Laboratories (Bar Harbor, Maine) and were housed in AALAC-approved animal quarters at the University of Minnesota. All studies were approved by the Institutional Animal Care and Use Committee at the University of Minnesota and adhered to standards for animal care as defined by the National Institutes of Health.

Mice were injected intraperitoneally with 50 mg brdU/g of body weight every 2 hours for a total of 12 hours. The animals were allowed to survive for 24 hours, after which they were euthanized with an overdose of carbon dioxide. The globes with the EOM attached were removed, embedded in tragacanth gum, and frozen in methylbutane chilled to a slurry on liquid nitrogen. Tibialis anterior muscles were also removed to serve as a control. Serial sections were prepared

at 12  $\mu$ m using a cryostat. The sections were immunostained for the presence of dystrophin and brdU using a procedure previously described.<sup>7</sup> Briefly, the sections were incubated in an antibody against dystrophin (Novocastra Labs, Vector Laboratories, Burlingame, California) at a concentration of 1:20 and reacted with the Vectastain peroxidase ABC kit. The peroxidase was developed using diaminobenzidine. For the brdU localization, the sections were incubated in 2N HCl for 1 hour at 37°C, followed by neutralization in borate buffer and a PBS rinse. The sections were incubated in the primary antibody to brdU (Boehringer Mannheim) at a concentration of 1:1,000. The sections were rinsed in PBS, incubated using reagents from the alkaline phosphatase ABC kit (Vector Laboratories), and reacted with the alkaline phosphatase purple substrate kit. The staining for dystrophin was brown, and the brdU-positive myonuclei were purple. A second set of sections was prepared and immunostained for brdU and for laminin (1:100, Sigma Chemical Co, St Louis, Missouri) in order to identify brdU-positive satellite cells. BrdU-myonuclei were identified by their position within the dystrophin-positive sarcolemma. BrdU-positive satellite cells were identified by their position with the laminin-positive basal lamina.

Cross sections through the superior and inferior rectus muscles and the tibialis anterior muscle were analyzed to determine the number of myofibers that contained a brdU-positive myonucleus or a brdU-positive satellite cell. A minimum of three cross sections was counted for each of the four sets of globes and EOM analyzed. Counts were performed with aid of the Bioquant Nova morphometry program (R & M Biometrics, Nashville, Tennessee). All data are presented as means  $\pm$  SEM. All statistical analyses were performed using the Prism and Statmate statistical software (Graphpad Software, Inc, San Diego, California). Statistical significance was defined as  $P < .05$ . The percent positive of both brdU-positive satellite cells and brdU-positive myonuclei for the global and orbital layers was compared, and there was no significant difference between the two groups using an unpaired, two-tailed  $t$  test. An F test indicated that the variances were not significantly different.

## RESULTS

Multiple brdU injections were administered in order to maximize the chance of having brdU available to all the satellite cells undergoing DNA replication during the 12-hour period that was studied. By waiting 24 hours after the final brdU injection, it was more likely that the labeled progeny of the satellite cells would have time to fuse into a myofiber. This injection schedule was based on empirical observations. By 24 hours after the last brdU injection, brdU-positive myonuclei were present and allowed definitive identification of the fate of single dividing satellite

cells. Cross sections of the EOM from the adult, uninjured mice orbits contained myofibers with brdU-positive extraocular muscle myonuclei (Figure 1A). While these brdU-labeled myonuclei were usually peripherally located, in contrast to the rabbit EOM myofibers previously studied,<sup>7</sup> myofibers were found with brdU-positive myonuclei that were centrally located within single myofiber cross sections (Figure 1B).

The percent of myofibers in cross section containing a brdU-positive myonucleus was 0.68% in the orbital layer and 0.59% in the global layer (Figure 2). Extrapolated out to a 24-hour labeling period, this would mean approximately one myofiber would have a brdU-positive nucleus out of every 80 to 90 myofibers in cross section. Interestingly, approximately 1% of the myofibers in cross

section had brdU-labeled satellite cells associated with them after the 24-hour survival period. There were essentially no brdU-positive myonuclei in the cross sections of tibialis anterior muscle.

## DISCUSSION

These studies demonstrate that myonuclei are added in a continuous manner to existing myofibers in adult mouse EOM. It has been well established that adult myonuclei are postmitotic in normal, uninjured limb musculature. We conclude that in all likelihood, the brdU-labeled myonuclei found within the uninjured EOM myofiber cross sections must have resulted from fusion of progeny from muscle satellite cells that divided during the period of brdU exposure. This is supported by evidence that activated muscle satellite cells reside within the uninjured adult EOM.<sup>7</sup> However, it is also possible that an occasional muscle progenitor cell from the blood stream may have entered the extraocular muscles. In both skeletal and cardiac muscle, a number of studies demonstrated the presence of muscle nuclei derived from blood-borne stem cells that ultimately came to reside within existing myofibers.<sup>14,15</sup>

The presence of activated and dividing satellite cells within adult, uninjured EOM is in contrast to the current view that satellite cells are quiescent in adult muscle unless injured.<sup>6</sup> Activated satellite cells can be identified using either cell cycle markers such as Ki-67<sup>16,17</sup> or myogenic lineage markers, including Pax-7<sup>18</sup> and MyoD.<sup>19</sup> Using a number of these markers, we have demonstrated that there is a population of activated satellite cells in mammalian EOM, including rabbit,<sup>7</sup> monkey, and human EOM.<sup>20</sup> It is inter-

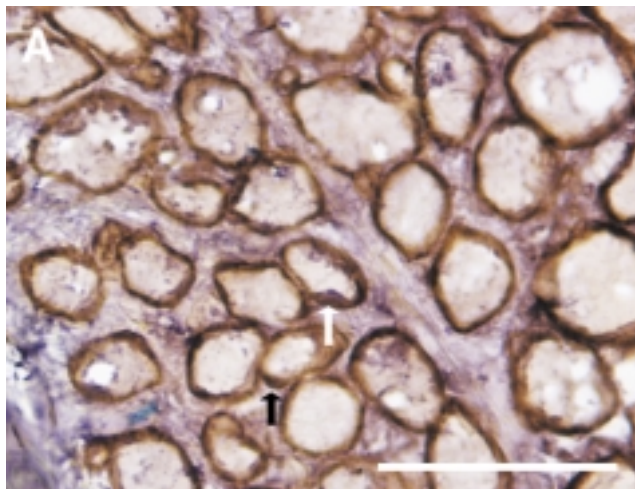


FIGURE 1A

Cross sections through inferior rectus from a mouse immunostained for both brdU (purple) and dystrophin (brown). White arrow indicates a brdU-positive myonucleus in a peripheral location within the cross section. Black arrow indicates a brdU-positive satellite cell. Bar is 50  $\mu$ m.

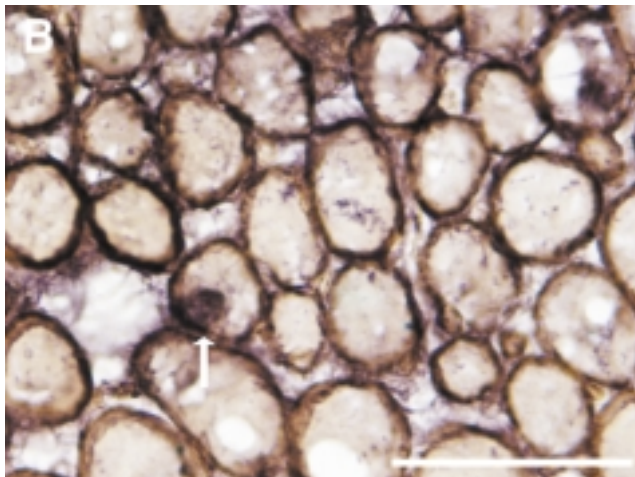


FIGURE 1B

White arrow indicates a brdU-positive myonucleus in a central location within the myofiber cross section. Bar is 50  $\mu$ m.

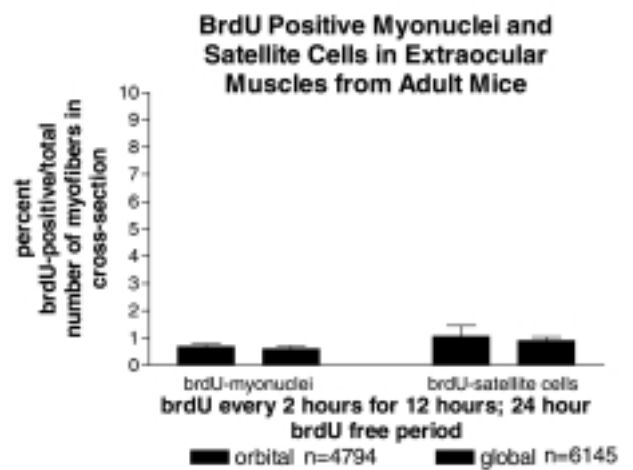


FIGURE 2

Quantification of brdU-labeling of both satellite cells and myonuclei in cross sections through adult mouse extraocular muscles. Mice received brdU injections every 2 hours for 12 hours, followed by a 24-hour brdU-free period before they were euthanized. N is the total number of myofibers counted.

esting that many of the molecules known to be involved in the control of myogenic cell division and differentiation remain up-regulated in normal adult EOM, including insulin growth factor and its receptor.<sup>21</sup> A recent study of the EOM expression profile confirmed the presence of a number of genes for muscle growth, development, and regeneration.<sup>22</sup>

We are beginning to examine possible candidates for control and maintenance of this process of myonuclear addition in mature EOM. Previous work demonstrated that the EOM are dependent for survival in vitro on innervation specifically from their cranial motor neurons; spinal motor neurons could not substitute for them.<sup>23</sup> We are currently assessing the role of innervation on this process of myonuclear addition in adult EOM. Denervation of the EOM occurs as a result of various neuropathic disorders and trauma. Temporary denervation of portions of an EOM may occur iatrogenically as a result of strabismus surgery or chemodeneration. The concept that even normal, uninjured EOM are always engaged in myofiber remodeling means that the EOM presumably respond to local changes in their environment over time. Thus the phenomenon of continuous myonuclear addition could be relevant to our understanding of the causes of strabismus, the late changes (including loss of initial success) following strabismus surgery, and the response to denervation.

There are many important implications of continuous myonuclear addition that may help explain the propensity for, or sparing of, the EOM in specific myopathic conditions.<sup>9</sup> Certain myopathies occur preferentially in extraocular muscle, such as progressive external ophthalmoplegias and oculopharyngeal muscular dystrophy. It is presumed that continuous myonuclear addition is the result of continuous myocyte addition, resulting from fusion of entire satellite cells with existing myofibers.<sup>8</sup> In progressive external ophthalmoplegia, continuous myocyte addition would mean addition of mitochondria from the replicating satellite cells, which in turn could result in increased accumulation of random mitochondrial DNA mutations. These mutated mitochondria could then become clonally amplified within individual postmitotic myofibers.<sup>24</sup> In oculopharyngeal muscular dystrophy, myonuclear addition from replicating satellite cells could result in the abnormal trinucleotide repeats seen in individual myonuclei that comprise the affected myofibers.<sup>25</sup> In oculopharyngeal muscular dystrophy, a progressive nuclear accumulation of abnormal poly(A) binding protein<sup>26</sup> results in loss of the normal function of this molecule. Myofiber loss occurs, followed by muscle regeneration. The myopathology of oculopharyngeal muscular dystrophy may be accelerated by the rate of satellite cell replication and addition into existing myofibers within the EOM. Uninjured nonocular skeletal muscle in adult mammals does not have ongoing

satellite cell division, and this may result in the protection of the body muscles from the accumulation of mutant DNA seen in the EOM.

The demonstration that the process of myonuclear addition occurs in mouse EOM opens the door for a number of studies looking at transgenic mice with muscle-specific genetic defects. This will allow us to test various hypotheses relating to possible mechanisms that control this process. Hopefully, the result will be the development of new therapeutic treatments for skeletal muscle myopathies.

## REFERENCES

1. Weiss A, Schiaffino S, Leinwand LA. Comparative sequence analysis of the complete human sarcomeric myosin heavy chain family: implications for functional diversity. *J Mol Biol* 1999;2:61-75.
2. Lucas CA, Hoh JF. Extraocular fast myosin heavy chain expression in the levator palpebrae and retractor bulbi muscles. *Invest Ophthalmol Vis Sci* 1997;38:2817-2825.
3. Horton RM, Manfredi AA, Conti-Tronconi BM. The embryonic gamma subunit of the nicotinic acetylcholine receptor is expressed in adult extraocular muscle. *Neurology* 1993;43:983-986.
4. McLoon LK, Wirtschafter JD. N-CAM is expressed in mature extraocular muscles in a pattern conserved among three species. *Invest Ophthalmol Vis Sci* 1996;37:318-327.
5. Wieczorek DF, Periasamy M, Butler-Browne GS, et al. Co-expression of multiple myosin heavy chain genes, in addition to a tissue-specific one, in extraocular muscles. *J Cell Biol* 1985;101:618-629.
6. McGeachie JK, Grounds MD. Initiation and duration of muscle precursor replication after mild and severe injury to skeletal muscle of mice. *Cell Tissue Res* 1987;248:125-130.
7. McLoon LK, Wirtschafter JD. Continuous myonuclear addition to single extraocular myofibers of uninjured adult rabbits. *Muscle Nerve* 2002;25:348-358.
8. Porter JD, Baker RS. Muscles of a different 'color': the unusual properties of the extraocular muscles may predispose or protect them in neurogenic and myogenic disease. *Neurology* 1996;46:30-37.
9. Wirtschafter JD, McLoon LK. Myopathic disease and continuous myonuclear addition to adult extraocular muscles. Submitted, 2002.
10. Karpati G, Carpenter S. Small-caliber skeletal muscle fibers do not suffer deleterious consequences of dystrophic gene expression. *Am J Med Genet* 1986;25:653-658.
11. Karpati G, Carpenter S, Prescott S. Small caliber skeletal muscle fibers do not suffer necrosis in mdx mouse dystrophy. *Muscle Nerve* 1988;11:795-803.
12. Kaminski HJ, Al-Hakim M, Leigh RJ, et al. Extraocular muscles are spared in advanced Duchenne dystrophy. *Ann Neurol* 1992;32:586-588.
13. Kaminski HJ, Maas E, Spiegel P, et al. Why are eye muscles frequently involved in myasthenia gravis? *Neurology* 1990;40:1663-1669.

14. Gussoni E, Soneoka Y, Strickland CD, et al. Dystrophin expression in the mdx mouse restored by stem cell transplantation. *Nature* 199;23:390-394.
15. Quaini F, Urbanek K, Beltrami AP, et al. Chimerism of the transplanted heart. *N Engl J Med* 2002;346:5-15.
16. Silvestrini R, Costa A, Veneroni S, et al. Comparative analysis of different approaches to investigate cell kinetics. *Cell Tissue Kinet* 1988;21:123-131.
17. Lopez F, Belloc F, Lacombe F, et al. Modalities of synthesis of Ki67 antigen during the stimulation of lymphocytes. *Cytometry* 1991;12:42-49.
18. Buckingham M. Skeletal muscle formation in vertebrates. *Current Opin Genet Dev* 2001;11:440-448.
19. Smith CK, Janney MJ, Allen RE. Temporal expression of myogenic regulatory genes during activation, proliferation and differentiation of rat skeletal muscle satellite cells. *J Cell Physiol* 1994;159:379-385.
20. McLoon LK, Wirtschafter JD. Activated satellite cells are present in uninjured extraocular muscles from normal adult humans and monkeys. *Invest Ophthalmol Vis Sci ARVO Abstr* 2002;43:1912.
21. McLoon LK, Peters E, Wirtschafter JD. Adult extraocular muscles express HSPG, Syndecan and growth factor receptor molecules that normally are down-regulated in adult skeletal muscle. *Invest Ophthalmol Vis Sci ARVO Abstr* 1999;40:S408.
22. Fisher MD, Gorospe JR, Felder E, et al. Expression profiling reveals metabolic and structural components of extraocular muscles. *Physiol Genomics* 2002;89:71-84.
23. Porter JD, Hauser KF. Survival of extraocular muscle in long-term organotypic culture: differential influence of appropriate and inappropriate motoneurons. *Dev Biol* 1993;160:39-50.
24. Hirano M, DiMauro S. ANTI, Twinkle, POLG, and TP: New genes open our eyes to ophthalmoplegia. *Neurology* 2001;57:2163-2165.
25. Brais B, Rouleau GA, Bouchard JP, et al. Oculopharyngeal muscular dystrophy. *Semin Neurol* 1999;19:59-66.
26. Uyama E, Tsukahara T, Goto K, et al. Nuclear accumulation of expanded PABP2 gene product in oculopharyngeal muscular dystrophy. *Muscle Nerve* 2000;23:1549-1554.

## **DISCUSSION**

DR IRENE H LUDWIG. The authors present microscopic evidence of the presence of cells, known to be involved in muscle fiber regeneration, in the extraocular muscles of mice. Other skeletal muscles do not show these cells. The authors also reference other work of theirs indicating similar findings in rabbits, monkeys, and humans. At the recent ARVO meeting, Dr McLoon presented evidence of markers, which indicated activation of satellite cells in normal adult human and monkey extraocular muscles.

As a clinician, I may be underqualified to evaluate the methods used in this study, but I am assured by my research colleagues at the LSU Eye Center, Drs Jacob and Gebhardt, that the methods were sound. From the

clinician's perspective, there would be less potential for bias if the observer were masked as to the origin of each tissue cross section before counting satellite cells. Although required in clinical trials, masking is not generally done in laboratory research.

The implications of the authors' findings are intriguing. They provide plausible explanations for the predilection of the extraocular muscles to be affected by conditions such as myasthenia and chronic progressive external ophthalmoplegia. They may also explain why the eye muscles are spared in Duchenne's muscular dystrophy. Perhaps they will also add to our understanding of strabismus mechanisms, leading to improved strabismus management.

For a strabismologist, it is heartening to witness the expansion of basic research in the study of extraocular muscles. At the recent ARVO meeting, numerous presentations were devoted to this subject. For too long, we have utilized diagnosis and treatment strategies based upon empirical evidence and observation. Recently, I read the correspondence surrounding a rejected strabismus paper. The reviewers had objected to findings that contradicted traditional views. One reviewer wrote, "150 years ago, the great physiologists of the 19th century...conclusively demonstrated," and used those early studies to dismiss the writer's observations.

Vision science research has led to remarkable advances in most branches of ophthalmology in recent decades. Hopefully, today's presentation, and others like it, will pave the way for meaningful discoveries in the strabismus field, which has existed in a state of "pre-science" for too long.

DR JOHN T. FLYNN. It was the great German microscopists of the late 19th and early 20th century who developed the dogma that muscles were postmitotic. They never saw a mitotic figure. What does a satellite cell look like in the resting state and when it's doing its work in making the myoblasts and putting them back to repair the muscle cell? As strabismologists, we're constantly taking pieces of extraocular muscle; should we be doing something with these specimens?

DR ALLAN J. FLACH. I wonder whether the muscles involved in presbyopia, the smooth muscles, and perhaps even cardiac muscles underlying congestive heart failure may be affected by these satellite cells?

DR JONATHAN D. WIRTSCHAFTER. Dr Ludwig, you are correct: masked counting was not used. Since there was no brdU uptake to see in one set of specimens and it was readily seen in the other, I doubt that masking would have made any difference. For me, this has been an interesting journey of discovery too, and we, in fact, did not expect to

see the satellite cells turning over.

Dr Flynn questions why both apoptosis and mitosis had not been detected previously using standard histological methods. Apoptosis of the myonucleus and mitosis of the muscle satellite cell are both processes that occur very quickly. Probably a nucleus is lost in less than an hour, so if one leaf falls from a tree, you just wouldn't see it among all the other activity going on in the forest. But if the leaves all fall at once, taking advantage of the Latin root for the word "apoptosis," you would see a lot of leaves on the ground. That's why we can see myogenic activity in skeletal muscle after a widespread injury, while we can't easily detect a very low basal turnover rate. Also, we don't see the mitosis in normal extraocular muscles because there aren't enough going on at one time. We see mitosis in tumor tissue or in skin cells, where the cells are, in fact, turning over rapidly and they have some place to grow or shed.

The extraocular muscles have to be stochastically in

balance, that is, you have the same amount of muscle mass, more or less, at the end of each day, as you had before. This concept opens a whole opportunity to rethink what we know about the extraocular muscles. They're not just meat; probably each fiber is a story of its own. I think of an extraocular muscle as a big condominium. Each myofiber is a single unit within the condominium, and the family is made up of many myonuclei that represent each of the family members. And, as each grandfather myonucleus dies, it's replaced by a baby myonucleus that's ready to be made in a little room (the muscle satellite cell) next door. That's how the myofiber keeps its number of myonuclei in balance. Still, there are many things we don't yet know. For example, is each muscle satellite cell pluripotent or is it specific to the muscle fiber type that's within its myocyte?

Dr Flach, we have not studied the smooth or cardiac muscles.

# TOXICITY AND DOSE-RESPONSE STUDIES OF 1 $\alpha$ -HYDROXYVITAMIN D<sub>2</sub> IN LH $\beta$ -TAG TRANSGENIC MICE

---

BY Daniel G. Dawson, MD (BY INVITATION), Joel Gleiser, MD (BY INVITATION), Michele L. Zimbric, BS (BY INVITATION), Soesiawaiti R. Darjatmoko, MS (BY INVITATION), Jared C. Frisbie (BY INVITATION), Janice M. Lokken (BY INVITATION), Mary J. Lindstrom, PhD (BY INVITATION), Isabelle Audo, MD (BY INVITATION), Stephen A. Strugnell, PhD (BY INVITATION), AND Daniel M. Albert, MD, MS

## ABSTRACT

**Purpose:** The study objective is to determine the effectiveness of a vitamin D analogue, 1 $\alpha$ -hydroxyvitamin D<sub>2</sub> (1 $\alpha$ -OH-D<sub>2</sub>), in inhibiting retinoblastoma in a transgenic retinoblastoma model (LH $\beta$ -Tag mouse) and to evaluate its toxicity. Previous studies of 1 $\alpha$ -OH-D<sub>2</sub> in athymic mice with human retinoblastoma xenografts suggested efficacy in tumor suppression and suitability for human treatment.

**Methods:** LH $\beta$ -Tag mice (N = 142), 8 to 10 weeks old, were randomly assigned to treatment groups receiving either control (vehicle) or 0.1, 0.3, 0.5, or 1.0  $\mu$ g/day of 1 $\alpha$ -OH-D<sub>2</sub> via oral gavage five times a week for 5 weeks. Animals were then euthanized. The eyes were enucleated, processed histologically, and serially sectioned. Three sections of each eye were microscopically examined, and mean tumor area was measured using Optimus software. Toxicity was assessed by mortality, weight loss, serum calcium levels, and kidney calcification.

**Results:** The mean tumor size in each 1 $\alpha$ -OH-D<sub>2</sub> group was smaller than in controls (*P* values <.02): control, 90,248  $\mu$ m<sup>2</sup>; 0.1  $\mu$ g, 31,545  $\mu$ m<sup>2</sup>; 0.3  $\mu$ g, 16,750  $\mu$ m<sup>2</sup>; 0.5  $\mu$ g, 30,245  $\mu$ m<sup>2</sup>; and 1.0  $\mu$ g, 16,049  $\mu$ m<sup>2</sup>. No dose-dependent response curve was evident. Mortality was higher in the groups receiving the 0.5  $\mu$ g and 1.0  $\mu$ g doses (*P* values <.01) than in the other treatment groups and the control group.

**Conclusion:** In the LH $\beta$ -Tag mouse, 1 $\alpha$ -OH-D<sub>2</sub> inhibits retinoblastoma with no increased mortality at lower doses (0.1 to 0.3  $\mu$ g). 1 $\alpha$ -OH-D<sub>2</sub> has been approved by the Food and Drug Administration as an investigative drug for cancer treatment and has shown efficacy with low levels of toxicity in adult cancer trials. 1 $\alpha$ -OH-D<sub>2</sub> meets the criteria for human clinical trials.

*Trans Am Ophthalmol Soc* 2002;100:125-130

## INTRODUCTION

---

Retinoblastoma is the most common intraocular malignancy in childhood, occurring once in 20,000 live births worldwide.<sup>1</sup> Although current methods of treatment have achieved survival rates of better than 90%,<sup>1</sup> there is a need for improved treatment alternatives to provide better visual results and decrease the risk of secondary tumors in bilateral retinoblastoma.<sup>2</sup>

A candidate compound for clinical trials in human retinoblastoma must meet the following criteria in pre-clinical studies: (1) effectively inhibit the growth of

retinoblastoma; (2) have low levels of toxicity; (3) be non-mutagenic; (4) have a defined mechanism of action; (5) be approved by the Food and Drug Administration (FDA) for investigative use in tumors; and (6) have been successfully tested in adult cancer. The vitamin D analogue 1 $\alpha$ -hydroxyvitamin D<sub>2</sub> (1 $\alpha$ -OH-D<sub>2</sub>) is a nonmutagenic compound that has previously been shown to be effective with low levels of toxicity in dose-response studies using the athymic/human retinoblastoma model.<sup>3</sup> The antineoplastic mechanism of action of related vitamin D compounds has been identified.<sup>4</sup> 1 $\alpha$ -OH-D<sub>2</sub> has been approved as an investigational drug in prostate cancer and has been successfully used in phase 1 and phase 2 studies (George Wilding, personal communication, July 30, 2001). The purpose of the present study is to determine the effectiveness of this compound in inhibiting retinoblastoma in a transgenic retinoblastoma model, the LH $\beta$ -Tag mouse,<sup>5</sup> and to evaluate its toxicity.

From the Department of Ophthalmology and Visual Sciences, University of Wisconsin Medical School, Madison (Drs Dawson, Gleiser, Audo, and Albert; Ms Zimbric, Ms Darjatmoko, Mr Frisbie, and Ms Lokken), and the Department of Biostatistics and Medical Informatics, University of Wisconsin, Madison (Dr Lindstrom); and BoneCare International, Inc, Madison, Wisconsin (Dr Strugnell). Supported by grant EYO1917 from the National Eye Institute, Bethesda, Maryland, and an unrestricted departmental grant from Research to Prevent Blindness, New York, New York.

## MATERIALS AND METHODS

### COMPOUND PREPARATION AND ADMINISTRATION

Pure crystalline  $1\alpha$ -OH- $D_2$  (graciously provided by BoneCare International, Inc, Madison, Wisconsin) was dissolved in 100% ethanol for a stock solution of 2.98 mg/mL. This solution was diluted in 0.1 mL of coconut oil to make drug concentrations of 0.1  $\mu$ g, 0.3  $\mu$ g, 0.5  $\mu$ g, and 1.0  $\mu$ g. Drug concentrations were confirmed by spectrophotometric analysis. The control group was given 0.1 mL of coconut oil. Stock solutions of drug were prepared fresh weekly and stored in amber glass bottles at  $-40^\circ\text{C}$  to protect the compound from degradation due to temperature or UV light.

### TOXICITY TRIAL

All experiments performed on animals conformed to the animal care and use policies defined by the Research Animal Resource Center at the University of Wisconsin and the ARVO statement on the Use of Animals in Ophthalmic and Vision Research.

A brief toxicity trial was done to determine the most efficacious doses of  $1\alpha$ -OH- $D_2$  for the dose-response study. Forty-two LH $\beta$ -Tag transgene-negative (as determined by polymerase chain reaction [PCR]) mice were divided into five treatment groups of seven animals each with a corresponding control group of seven animals. Drug doses were 0.3  $\mu$ g, 0.9  $\mu$ g, 1.8  $\mu$ g, 3.0  $\mu$ g, and 4.8  $\mu$ g in 0.1 mL of coconut oil. The control group received 0.1 mL of coconut oil alone.

### DOSE-RESPONSE STUDY

A total of 175 LH $\beta$ -Tag transgene-positive (as determined by PCR) 8- to 10-week-old mice were randomly assigned by sex and litter to one of five treatment groups. Doses were calculated from the preliminary toxicity study in transgene-negative mice (see "Results" section) and are as follows: vehicle (control) and 0.1  $\mu$ g, 0.3  $\mu$ g, 0.5  $\mu$ g, and 1.0  $\mu$ g of  $1\alpha$ -OH- $D_2$ . Treatment was via oral gavage with a 1-inch 22-G steel gavage needle (1.25 mm in diameter) attached to a 1-mL syringe. Treatment was given five times per week for 5 weeks. Doses were skipped for up to 3 consecutive days in mice that lost weight (25% of baseline weight) and/or became lethargic and were continued when the affected animals regained weight and health. The mice were fed a vitamin D and calcium restricted diet to remove the effect of endogenous calcium on the treatment. Individual body weights were recorded twice per week during treatment and just prior to euthanization on the last treatment day.

### TUMOR MEASUREMENT AND HISTOPATHOLOGIC STUDY

After euthanization, the eyes were enucleated and placed in

10% neutral buffered formalin for standard histopathologic sections. Four serially sectioned 5- $\mu$ m-thick sections were cut from each of the superior, middle, and inferior areas of the globe and stained with hematoxylin-eosin. The four sections from each globe area were examined under a microscope, and the section with the largest tumor was used for measurement. The outline of the tumor in each section was traced from a microscopically digitized image and the area measured with Optimas software version 6.5 (MediaCybernetics, Silver Spring, Maryland). The three tumor areas from each representative portion of the globe were averaged together to obtain the mean tumor measurement of each eye expressed in micrometers squared ( $\mu\text{m}^2$ ).

### TOXICITY ASSESSMENT

Following euthanization, both kidneys were harvested from randomly selected mice in each treatment group (control group, 15 mice; 0.1  $\mu$ g group, 14 mice; 0.3  $\mu$ g group, 16 mice; 0.5  $\mu$ g group, 17 mice; and 1.0  $\mu$ g group, 17 mice). Kidneys were fixed in 10% neutral buffered formalin, processed histologically, and serially sectioned at 5  $\mu$ m. Sections were stained by hematoxylin-eosin and von Kossa techniques. Two sections of each kidney were examined by a single masked reviewer and graded for degree of calcification according to the following scale: I, no calcium deposits; II, 1 to 7 foci of calcium deposits; III, 8 to 15 foci of calcium deposits; and IV, >15 foci of calcium deposits.

Serum samples from representative mice in each group (control group, 13 samples; 0.1  $\mu$ g group, 13 samples; 0.3  $\mu$ g group, 11 samples; 0.5  $\mu$ g group, 9 samples; and 1.0  $\mu$ g group, 11 samples) were obtained just prior to euthanization from the axillary vessels and analyzed for calcium levels by Marshfield Laboratories, Marshfield, Wisconsin.

Toxicity was assessed by percent of animals surviving the treatment schedule, changes in body weight, degree of kidney calcification, and serum calcium levels. Animals that died before the completion of the treatment were not assessed in the latter three categories.

### STATISTICAL METHODS

The effect of dose on tumor area, change in animal weight, serum calcium levels, and kidney calcification was assessed using analysis of variance. The tumor area and serum calcium levels were log transformed prior to analysis to stabilize the variance. No transformation of the kidney calcification values produced approximately normally distributed data. These data were rank transformed (the rank of a data value is its numerical ordering) to obtain an approximate nonparametric analysis. The change in animal weight (from first to last measurement) was restricted

to animals that survived until the last measurement (week 5). The effect of dose on mortality was assessed by using a generalized linear model assuming binomial variability.

The effect of layer (animal batch) on response was accounted for in all analyses by including a blocking term in the model. All significant global tests for effect of dose were followed by pairwise analyses to assess differences between specific dose groups.

## RESULTS

### PRELIMINARY TOXICITY TRIAL TO DETERMINE DOSAGES

Forty-two Lh $\beta$ -Tag transgene-negative (as determined by PCR) mice were divided into five treatment groups of 7 animals each with a corresponding control group. Toxicity was assessed by mortality. The majority of mice in the 1.8  $\mu$ g (6 of 7 animals), 3.0  $\mu$ g (6 of 7 animals), and 4.8  $\mu$ g (7 of 7 animals) groups died within 2 weeks of treatment. One animal in each of the 1.8  $\mu$ g and 3.0  $\mu$ g groups survived the 5-week treatment schedule. Two of 7 animals in the 0.9  $\mu$ g group died within 2 weeks of treatment initiation, and 3 animals in the same group died within 4 weeks of treatment. From these data, we calculated doses of 0.1  $\mu$ g, 0.3  $\mu$ g, 0.5  $\mu$ g, and 1.0  $\mu$ g of  $1\alpha$ -OH- $D_2$  for the dose-response study.

### DOSE-RESPONSE EFFICACY STUDY

Results of the dose-response data are summarized in Table I. The number of animals surviving the treatment schedule is as follows: control group, 30 of 31 mice surviving (97%); 0.1  $\mu$ g group, 32 of 35 animals surviving (91%); 0.3  $\mu$ g group, 30 of 34 animals surviving (88%); 0.5  $\mu$ g group, 26 of 37 animals surviving (70%); and 1.0  $\mu$ g group, 24 of 38 animals surviving (63%) (Figure 1). Mean tumor area of each treatment group was as follows: control, 90,248  $\mu$ m<sup>2</sup>; 0.1  $\mu$ g; 31,545  $\mu$ m<sup>2</sup>; 0.3  $\mu$ g, 16,750  $\mu$ m<sup>2</sup>; 0.5  $\mu$ g, 30,245  $\mu$ m<sup>2</sup>; and 1.0  $\mu$ g, 16,049  $\mu$ m<sup>2</sup> (Figure 2). Although no dose-dependent response curve is appreci-

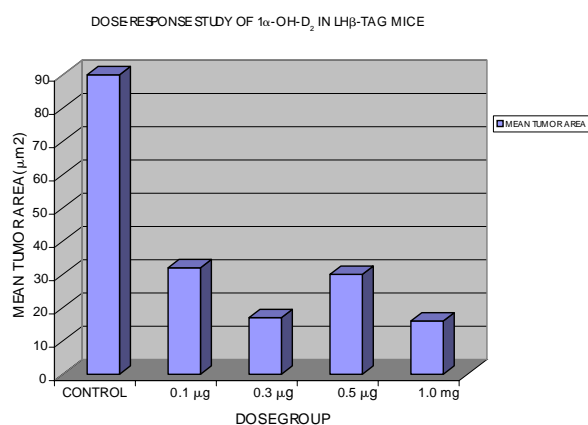


FIGURE 1

Survival curve of study animals. Survival rate was high in the 0.1  $\mu$ g and 0.3  $\mu$ g groups. However, mortality was significantly higher in the 0.5  $\mu$ g and 1.0  $\mu$ g groups when compared to control group and 0.1 and 0.3  $\mu$ g groups (all  $P$  values <.01).

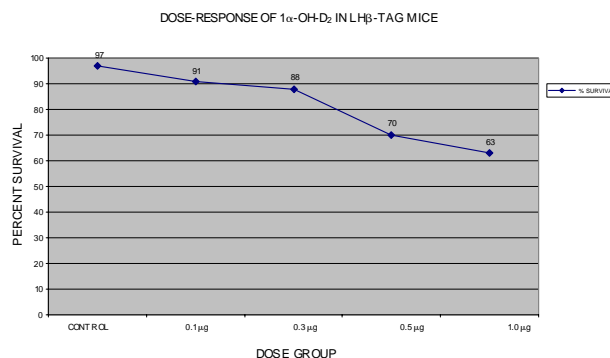


FIGURE 2

Mean tumor area of Lh $\beta$ -Tag mice treated with  $1\alpha$ -OH- $D_2$ , measured in micrometers squared ( $\mu$ m<sup>2</sup>). Reduction in tumor area is seen in all treated groups when compared to control group (all  $P$  values <.02); however, no dose-response curve is readily apparent.

TABLE I: SUMMARY OF DATA ANALYZED IN STUDY OF  $1\alpha$ -OH- $D_2$  IN Lh $\beta$ -TAG MICE

DOSE GROUP	NO. OF MICE	% SURVIVAL	TUMOR AREA*	% TUMOR INHIBITION	SERUM CALCIUM (mg/dL)†	MEAN WT CHANGE (gm)‡
Control	31	96.77	90.25 ± 32.55	NA	7.9	0.605 ± 0.34
0.1 μg	35	91.43	31.55 ± 10.83	34.9	9.9	-1.27 ± 0.33
0.3 μg	34	88.24	16.75 ± 6.11	18.6	11.3	-3.02 ± 0.35
0.5 μg	37	70.27	30.24 ± 11.72	33.5	11.4	-3.13 ± 0.36
1.0 μg	38	63.16	16.05 ± 6.57	17.8	12.2	-3.4 ± 0.39

NA, not applicable.

\*Tumor area was significant when compared to controls in all treated groups (all  $P$  values <.02).

†Serum calcium levels were higher in all treatment groups when compared to controls (all  $P$  values <.0001).

‡Body weight loss was significantly higher in the treatment groups when compared to controls (all  $P$  values <.0001).

ated, the average tumor measurement from each treatment group of  $1\alpha$ -OH- $D_2$  is statistically significant (all  $P$  values  $<.02$ ) compared to controls.

Survival rate, change in body weight, and serum calcium data are summarized in Table I. Increases in mortality, weight loss, and serum calcium levels and a higher kidney calcification grade are seen as the dose of  $1\alpha$ -OH- $D_2$  increases. Mortality in the 0.5  $\mu$ g and 1.0  $\mu$ g treatment groups was higher than in all other treatment groups and the control group (all  $P$  values  $<.01$ ). Weight loss (measured as change in weight from baseline measurement to final measurement) was statistically significant in all drug groups when compared to controls (all  $P$  values  $<.0001$ ). Kidney calcification was significantly higher in the 0.3  $\mu$ g, 0.5  $\mu$ g, and 1.0  $\mu$ g groups (all  $P$  values  $<.002$ ). Serum calcification was significantly higher in all treatment groups when compared to controls ( $P$  values  $<.0001$ ). Serum calcium was also significantly higher in the 0.3  $\mu$ g and 1.0  $\mu$ g groups when compared to the 0.1  $\mu$ g group ( $P$  values  $<.009$ ).

Some mice skipped treatment doses owing to weight loss or lethargy: control group, 0% doses skipped; 0.1  $\mu$ g group, 4.4% doses skipped; 0.3  $\mu$ g group, 6.1% doses skipped; 0.5  $\mu$ g group, 7.7% doses skipped; and 1.0  $\mu$ g group, 10.8% doses skipped. The effect of skipped dose was not statistically significant ( $P = .39$ ).

## DISCUSSION

In 1966, Frederick C. Verhoeff<sup>6</sup> proposed that retinoblastoma be treated with high doses of vitamin D. This hypothesis was based on his observations of the association of calcification of retinoblastoma with spontaneous and induced regression. To test this hypothesis, we studied the two standard forms of vitamin D, ergocalciferol (vitamin  $D_2$ ) and 1,25-dihydroxy- $D_3$  (calcitriol) (Figure 3), in the athymic/Y79 retinoblastoma xenograft mouse model.<sup>7,8</sup> Subsequently, we studied the effect of calcitriol on the growth of retinoblastomas in the LHB-Tag mouse model.<sup>9</sup> From these studies, we learned that both calcitriol and vitamin  $D_2$  inhibited the growth of human retinoblastomas and transgenic mouse retinoblastomas, but the antineoplastic effect was related to either elevated

serum calcium levels or calcification of the tumors.

We were encouraged that synthetic analogues of vitamin  $D_2$  and calcitriol with retained or increased antineoplastic effect but decreased hypercalcemic activity might prove feasible for eventual human trials. This conclusion followed our experience with the synthetic analogue of calcitriol, 1,25-dihydroxy-16-ene-23-yne-vitamin  $D_3$  (16,23- $D_3$ ). This compound was extensively studied in the athymic xenograft mouse model<sup>10</sup> and the LHB-Tag transgenic mouse models.<sup>11,12</sup> These results have recently been reviewed in detail.<sup>4</sup>

Although 16,23- $D_3$  appears to be a promising drug for use in the treatment of retinoblastoma in children, it was not approved by the FDA until March 1999 for investigational use in human cancer patients. No adult data are currently available; consequently, we have carried out preclinical studies of another analogue of vitamin  $D_2$ ,  $1\alpha$ -OH- $D_2$ . As noted,  $1\alpha$ -OH- $D_2$  has been used successfully in our laboratory in the treatment of nude mice containing human retinoblastoma xenografts, has been approved by the FDA (in 1996) as an investigational drug in prostate cancer, and has been successfully used in phase 1 and phase 2 clinical studies of prostate cancer (George Wilding, personal communication, July 30, 2001). In the athymic/Y79 mouse model, tumor weight and volume in groups receiving doses of 0.2 or 0.3  $\mu$ g/day of  $1\alpha$ -OH- $D_2$  were significantly lower than in controls and toxicity was less than with calcitriol and vitamin  $D_2$ .<sup>3</sup> In the studies now described,  $1\alpha$ -OH- $D_2$  inhibited retinoblastoma growth in the LHB-Tag transgenic mouse model, with each treatment group (0.1 to 1.0  $\mu$ g) showing a statistically significant effect as compared to the control group. The tumors in the treated animals ranged in size from 18% to 30% of the mean tumor area in the control group. There was not, however, an identifiable dose-dependent response curve. No statistically significant increase in mortality was seen between the 0.1  $\mu$ g group, the 0.3  $\mu$ g group, and the control group (Figure 1). However, statistically significant increases in mortality in the 0.5  $\mu$ g and 1.0  $\mu$ g groups were observed (both  $P$  values  $<.05$ ).

Vitamin D receptor mRNAs are detectable in Y79 retinoblastoma cells, LHB-Tag tumors, and human retinoblastoma specimens using reverse-transcriptase polymerase chain reaction (RT-PCR).<sup>4</sup> On the basis of experiments that were carried out on calcitriol and 16,23- $D_3$ ,<sup>4</sup> the mechanism of action appears to be related to increased p53-related gene expression resulting in increased apoptosis.

## CONCLUSION

$1\alpha$ -OH- $D_2$  has been effective in inhibiting retinoblastoma growth in two animal models, the LHB-Tag transgenic

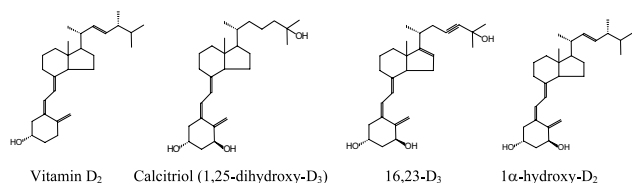


FIGURE 3

Vitamin  $D_2$  (ergocalciferol) and its analogs, calcitriol (1,25-dihydroxy- $D_3$ ), 1,25-dihydroxy-16-ene-23-yne-vitamin  $D_3$  (16,23- $D_3$ ), and  $1\alpha$ -hydroxyvitamin  $D_2$  ( $1\alpha$ -OH- $D_2$ ).

mouse, as presently described, and the athymic/Y79 model, as previously reported.<sup>3</sup> This nonmutagenic compound has low toxicity. The mechanism of antineoplastic action has been demonstrated in related compounds, and studies are under way to show whether or not the mechanism of action is similar for 1 $\alpha$ -OH-D<sub>2</sub>. The drug has been approved by the FDA for investigational use in human tumors, and phase 1 and phase 2 data show the drug to have effectiveness and low toxicity in the treatment of human prostate cancer. We are now planning to move into phase 1 and phase 2 clinical trials of this drug in children.

## REFERENCES

1. Ferris FL III, Chew EY. A new era for the treatment of retinoblastoma. *Arch Ophthalmol* 1996;114(11):1412.
2. O'Brien JM. Alternative treatment in retinoblastoma. *Ophthalmology* 1998;105(4):571-572.
3. Grostern RJ, Bryar PJ, Zimbric ML, et al. Toxicity and dose-response studies of 1 $\alpha$ -hydroxyvitamin D<sub>3</sub> in a retinoblastoma xenograft model. *Arch Ophthalmol* 2002;120(5):607-612.
4. Albert DM, Nickells RW, Gamm DM, et al. Vitamin D analogs, a new treatment for retinoblastoma: the first Ellsworth Lecture. *Ophthalmic Genet* 2002;23 (in press).
5. Windle JJ, Albert DM, O'Brien JM, et al. Retinoblastoma in transgenic mice. *Nature* 1990;343(6259):665-669.
6. Verhoeff FH. Retinoblastoma undergoing spontaneous regression. Calcifying agent suggested in treatment of retinoblastoma. *Am J Ophthalmol* 1966;62(3):573-574.
7. Albert DM, Saulenas AM, Cohen SM. Verhoeff's query: Is vitamin D effective against retinoblastoma? *Arch Ophthalmol* 1988;106(4):536-540.
8. Cohen SM, Saulenas AM, Sullivan CR, et al. Further studies of the effect of vitamin D on retinoblastoma. Inhibition with 1,25-dihydroxycholecalciferol. *Arch Ophthalmol* 1988;106(4):541-543.
9. Albert DM, Marcus DM, Gallo JP, et al. The antineoplastic effect of vitamin D in transgenic mice with retinoblastoma. *Invest Ophthalmol Vis Sci* 1992;33(8):2354-2364.
10. Sabet SJ, Darjatmoko SR, Lindstrom MJ, et al. Antineoplastic effect and toxicity of 1,24-dihydroxy-16-ene-23-yne-vitamin D<sub>3</sub> in athymic mice with Y-79 human retinoblastoma tumors. *Arch Ophthalmol* 1999;117(3):365-370.
11. Shternfeld IS, Lasudry JG, Chappell RJ, et al. Antineoplastic effect of 1,25-dihydroxy-16-ene-23-yne-vitamin D<sub>3</sub> analogue in transgenic mice with retinoblastoma. *Arch Ophthalmol* 1996;114(11):1396-1401.
12. Wilkerson CL, Darjatmoko SR, Lindstrom MJ, et al. Toxicity and dose-response studies of 1,25-(OH)<sub>2</sub>-16-ene-23-yne vitamin D<sub>3</sub> in transgenic mice. *Clin Cancer Res* 1998;4(9):2253-2256.

## DISCUSSION

DR BARRETT G. HAIK. The treatment of patients with retinoblastoma has changed dramatically over the past 10 years. Until the mid-1990s, external beam irradiation was the primary modality employed in conservative therapy. As this therapy was refined over a half century, improved delivery systems reduced the amount of damage to adjacent ocular and orbital tissue caused by radiation.

However, in 1993, Eng and colleagues presented a statistically powerful study that demonstrated an extremely high incidence of radiation-associated tumors in long-term survivors of retinoblastoma. Although the association of radiogenic neoplasms in patients with retinoblastoma had been noted for many years, Eng's study provided the largest patient series with meticulous long-term follow-up.

At approximately the same time that Dr Eng was confirming the continued risks involved with radiation therapy, Judith Kingston and John Hungerford from St. Bartholomew's Hospital in London were reporting success in treating intraocular retinoblastoma with systemic chemotherapy. Subsequently, multiple ocular oncology centers throughout North America and Europe developed individual protocols based on their own experiences with chemotherapeutic agents for tumors of neural origin. Because no single chemotherapy protocol has been proven to be totally effective and all carry significant risk of side effects, none has been universally accepted.

Today, Dr Albert and his colleagues have presented their own extremely exciting and promising findings that a nonmutagenic synthetic analog of vitamin D<sub>2</sub>, 1 $\alpha$ -hydroxyvitamin D<sub>2</sub> (1 $\alpha$ -OH-D<sub>2</sub>), effectively inhibits growth of retinoblastoma in mouse models while offering low toxicity.

The prospect of taking Dr Albert's promising findings from the laboratory to the bedside is exciting. Nevertheless, established use of 1 $\alpha$ -OH-D<sub>2</sub> will require proof of its efficacy as a single agent or as part of a multimodality regimen, and developing protocols for delivery of drugs and for monitoring side effects will take time and designing and implementing clinical trials will be complex because of the rarity of retinoblastoma. Many years of follow-up will also be required to assess the long-term impact of the incidence of second primary tumors.

Notwithstanding the time and efforts that will be required to test the use of this modality in the treatment of patients with retinoblastoma, Dr Albert's findings regarding 1 $\alpha$ -OH-D<sub>2</sub> offer new hope to children afflicted with this sight- and life-threatening disease.



# CLINICAL DECISION MAKING BASED ON DATA FROM GDx: ONE-YEAR OBSERVATIONS

---

BY James C. Bobrow, MD

## ABSTRACT

*Purpose:* To determine whether information derived from the GDx scanning laser polarimeter aids in the clinical decision-making process for patients with various types of glaucoma.

*Methods:* Over a 4-month period, 342 consecutive patients with primary open-angle glaucoma, ocular hypertension, angle-closure glaucoma, or secondary glaucomas or in whom the diagnosis of glaucoma was uncertain were evaluated with the GDx scanning laser. After 1 year, 153 patients with glaucoma underwent GDx analysis again. Chart review revealed that 42 of the 153 patients had a change in therapy as a result of the GDx evaluation combined with analysis of visual fields, optic disc cupping, and intraocular pressure (IOP). Outcomes were then compared.

*Results:* The group who had a change in therapy had a higher average GDx number ( $51.5 \pm 26.1$  vs  $37.0 \pm 23.5$  [ $P=.001$ ]) at the initial visit and higher IOP ( $18.2 \pm 4.6$  vs  $16.0 \pm 3.2$  mm Hg [ $P=.005$ ]). In spite of a change in therapy, at an average of 344 days later, IOP was unchanged ( $18.3 \pm 5.3$  vs  $15.7 \pm 3.2$  mm Hg [ $P=.001$ ]) and GDx values in the altered therapy group were higher than at baseline ( $57.3 \pm 27.9$  vs  $36.7 \pm 23.4$  [ $P=.001$ ]), although the differences within each group did not achieve statistical significance.

*Conclusion:* GDx analysis may be helpful in determining patients at risk for damage from glaucoma, even in eyes in which cup-disc ratio and field loss have not progressed. Changing medications without significantly reducing IOP may be insufficient to halt increases in GDx numbers and may indicate a need for more aggressive therapy.

*Trans Am Ophthalmol Soc* 2002;100:131-136

## INTRODUCTION

---

Attempts to find an objective discriminant function to separate patients with glaucoma from those without glaucoma have been thwarted by the redundancy of the visual system and the crudeness of the measurement techniques that have been used. Subjective testing has also suffered from individual variation in attention, comprehension, and motor function. Finally, intraocular pressure (IOP) has proved to be of uncertain value in many patients.

The final common pathway for visual loss in the glaucomas is reduction of the competency and number of nerve fibers carrying information to the processing centers in the lateral geniculate body and visual cortex. Thus, when devices purporting to measure the thickness of these layers were introduced, investigators studied the ability of these devices to discriminate between glaucomatous and nonglaucomatous eyes. The result has been a spate of studies defining the specificity and sensitivity of each system to separate the affected eyes from normal eyes.

A more practical question now awaits the ophthalmologist who seeks to use advanced methods such as nerve fiber

layer analysis: How does the information gained affect clinical decision making? In an office setting in which some patients are already receiving therapy for glaucoma, others are being followed without medication because of a disparate spectrum of abnormal findings, and still others are discovered to have abnormal findings for the first time, it would be helpful to know how the addition of measurements from a nerve fiber layer analyzer affects the decision-making process and whether these decisions preserve visual function.

Since glaucoma disturbs vision in most cases in a stealthy and slow manner, the conclusions from a 1-year study may be preliminary at best; however, before colleagues are encouraged to invest in expensive equipment, it would be helpful to prove some benefit or demonstrate an additional degree of confidence in judgment corroborated by this added information.

## METHODS

---

The author's office acquired a GDx nerve fiber layer analyzer (Laser Diagnostic Technologies, San Diego, California) in the fall of 2000. After a 2-month break-in period with instruction and training of the technical staff, reproducibility and reliability were tested on a series of normal

From the Department of Ophthalmology and Visual Sciences, Washington University School of Medicine, St Louis, Missouri.

subjects. Results indicated that values of the “number,” an age-, sex-, and race-determined derivative of the area under the receiver operating characteristic (ROC) curve, were consistent. Data collection began in December 2000. Since the study is retrospective, the decision was made in December 2001 to analyze the first 342 consecutive patients who had GDx measurements made between December 20, 2000, and April 13, 2001. Patient records were then reviewed to determine whether changes in medications, laser procedures, or surgeries were advised and what part the additional information from the GDx measurement played in the decision to alter therapy. Follow-up has continued until April 10, 2002, and includes analysis of subsequent GDx measurements when available.

Complete ophthalmologic evaluation was obtained, including refraction, slit-lamp biomicroscopy, applanation tonometry, dilated fundus examination, stereo disc photography, and Humphrey visual field evaluation using the Swedish Interactive Threshold Algorithm (SITA) and 30-2 program. Scanning laser polarimetry using the GDx was performed in all patients able to cooperate for the test and in whom the test was indicated for the diagnosis of glaucoma or to follow patients in whom the diagnosis had already been established. The data were obtained from the study population, consisting of a series of 342 consecutive patients examined between December 20, 2000, and April 13, 2001. An attempt was made to reexamine as many patients as possible about 1 year after their original enrollment. Of these individuals, 153 patients with a variety of glaucomas also underwent a second GDx analysis about 1 year following their original examination.

All data were tabulated and transferred to Epiinfo 6.04d. Statistical analysis using analysis of variance (ANOVA) methodology was performed, and results were considered statistically significant when *P* values were  $<.05$ .

## RESULTS

Table I shows the demographic characteristics of the study population. The age, sex, and racial distribution were indicative of the office population from which the study subjects were drawn. A positive family history of glaucoma was elicited in 94 (27.4%) of all patients. The types of glaucoma treated are shown in Table II. Studies were performed on patients with a spectrum of findings. In some cases, the GDx measurement was taken to establish the diagnosis, in some to differentiate ocular hypertension from glaucoma, and in others to determine whether therapy was adequate to prevent further damage. Of the 153 glaucoma patients who had a second GDx analysis, 70 eyes of 42 patients were found to require a change in therapy initiated at the time of the first visit.

Table III includes the types of glaucoma represented

TABLE I: DEMOGRAPHICS OF STUDY POPULATION

Age	69.2 ± 15.6 yr
Male-female ratio	127:215
White vs nonwhite	91.9% vs 8.1%
Family history of glaucoma	27.4%

TABLE II: TYPES OF GLAUCOMA IN STUDY POPULATION

TYPE OF GLAUCOMA	NO. OF PATIENTS	NO. OF EYES
Primary open-angle	182	360
Secondary	14	26
Low-pressure	28	55
Angle-closure	20	39
Ocular hypertension	67	133
Pigmentary	18	36
Congenital	3	5
Diagnostic testing	10	20
Total	342	674

in the 153 patients who underwent a second GDx examination. The decision to change therapy was made on the basis of IOP, visual field findings, and examination of the optic disc; but the GDx data informed the clinical decision-making process. Table IV lists the other variables measured that, taken with the GDx readings, resulted in a change in therapy.

Table V includes the data at baseline for the factors tabulated for each patient. The average IOP is consistent with a population well controlled with therapy. Visual acuities ranged from 20/15 to 20/200, since GDx measurements were found to be difficult in patients with visual acuity reduced to less than 20/400, one-eyed patients, and those unable to fixate well enough for the 300 to 400 msec necessary to obtain reliable means from three scans. In all patients for all examinations, the reliability of the GDx averaged  $87\% \pm 6\%$ . Low-reliability scans ( $<75\%$ ) were considered unreadable and were not included in the study. The overall failure rate gradually improved over the course of the first year but averaged less than 3% for the entire 17-month period.

Among the patients receiving therapy, the average

TABLE III: TYPES OF GLAUCOMA IN PATIENTS WHO UNDERWENT A SECOND GDx MEASUREMENT AT 1 YEAR

TYPE OF GLAUCOMA	NO. OF PATIENTS
Primary open-angle	101
Secondary	6
Low-tension	20
Angle-closure	12
Pigmentary	12
Congenital	2
Total	153

TABLE IV: FACTORS OTHER THAN GDX NUMBER THAT INFLUENCED A CHANGE IN THERAPY

FACTOR	NO. OF PATIENTS*
Intraocular pressure	24
Field loss	13
Increased cup-disc ratio	15

\*42 patients required a change in therapy, but total is greater than 42 because some patients had multiple factors.

number of medications used was  $1.5 \pm 0.7$ . No patient in this study required surgery for uncontrolled glaucoma during the year of observation, and only one eye was treated with laser trabeculoplasty for uncontrolled IOP.

Table V also depicts the statistically significant differences noted between the eyes in which therapy was changed and those in whom the current regimen was continued, including: (1) higher GDx number, (2) higher initial IOP, and (3) number of medications at the second examination.

## DISCUSSION

In an abstract presented at the 2002 annual meeting of the Association for Research in Vision and Ophthalmology, Choi and associates<sup>1</sup> demonstrated that longitudinal analysis over 25.9 months of retinal nerve fiber layer thickness as measured with a scanning laser polarimeter reveals that even when field loss has not progressed, the rate of thinning of the nerve fiber layer is greater in patients with open-angle glaucoma than in normal subjects.

Prior to this study, most of the published literature focused on several other issues. At first, investigators

concentrated on the reliability and reproducibility of the various machines designed to measure nerve fiber layer thickness. Zangwill and colleagues<sup>2</sup> tried to distinguish among the Heidelberg retina tomograph (HRT), the GDx nerve fiber analyzer, and the optical coherence tomograph (OCT). They found that, although the areas under the ROC curves were similar, the OCT and HRT had greater sensitivity. Colen and colleagues<sup>3</sup> reported that no significant differences appeared when both normal and glaucomatous patients were studied with the three instruments.

The next phase in studying this equipment has been to determine whether glaucoma patients may be discriminated from normal patients or those with ocular hypertension. Weinreb and coworkers<sup>4</sup> used a variety of the parameters from the GDx to study the detection of glaucoma. They found an overall difference between the normals and patients with glaucoma but also considerable overlap in parameters. Using three variables (average thickness, ellipse modulation, and average ellipse thickness), they generated a specificity of 92% and a sensitivity of 74%. They felt that the software supplied with the GDx did not perform as well as their selected parameters. Lauande-Pimentel and associates<sup>5</sup> performed a case-control study of GDx and visual field examinations together to detect glaucoma. They found the information from the GDx to be useful when added to other functional data.

Paczka and colleagues<sup>6</sup> compared various psychophysical tests to the GDx and concluded that nerve fiber layer photographs had high sensitivity values and frequency-doubling perimetry had high specificity values, but that GDx neural network parameters were almost as sensitive and required less patient cooperation. Poinosawmy and coworkers<sup>7</sup> tried to separate normal

TABLE V: DIFFERENCES BETWEEN EYES WITH AND EYES WITHOUT A CHANGE IN THERAPY\*

VARIABLE	INITIAL VISIT			SECOND VISIT		
	NO CHANGE	CHANGE	P VALUE	NO CHANGE	CHANGE	P VALUE
GDx No.	37.0 ± 23.5	51.5 ± 26.1	<b>.001</b>	36.7 ± 23.4	57.3 ± 23.9	<b>.001</b>
Reliability (%)	88.6 ± 5.2	86.3 ± 5.5	.68	87.3 ± 5.6	88.7 ± 6.0	.56
IOP	16.0 ± 3.2	18.2 ± 4.6	<b>.005</b>	15.7 ± 3.1	18.3 ± 5.3	<b>.001</b>
Cup-disc ratio	0.51 ± 0.17	0.50 ± 0.19	.36	0.50 ± 0.18	0.52 ± 0.19	.54
Visual acuity (20/)	29.1 ± 17.4	38.9 ± 35.4	.08	28.1 ± 18.5	34.4 ± 27.8	.24
No. of medications	1.5 ± 0.6	1.5 ± 0.7	.88	1.5 ± 0.8	2.2 ± 0.7	<b>.01</b>
Days to second GDx				347 ± 66	341 ± 60	.42

IOP, intraocular pressure.

\*Significant values are in bold type.

patients from those with ocular hypertension and low-pressure glaucoma by using the GDx. They found that the number value determined by the intrinsic software separated the low-tension glaucoma patients from the other groups extremely well. They concluded that a close relationship exists between the parameters measured by scanning laser polarimetry and disease severity. Sanchez-Galeana and coworkers<sup>8</sup> matched the various devices measuring nerve fiber layer thickness against judgments by two ophthalmologists and a vision scientist. They found that no instrument alone was able to provide definitive screening. Finally, Yamada and associates<sup>9</sup> used the GDx as a screening device and found that the GDx, when compared to Humphrey perimetry (Fastpac 24-2 program), separated normal patients from those with ocular hypertension and glaucoma as well and could be performed effectively on 98.5% of patients.

The practitioner who purchases a scanning laser polarimeter or other device to measure nerve fiber layer thickness has to rely on the data derived from examinations and translated by the manufacturer into a user-friendly format. This study has attempted to use just the simplest parameter—the number, extrapolated from the ROC curve and ratios of thickness of the superior and inferior nerve rim—to follow two groups of patients: (1) those in whom a change in therapy appeared to be indicated from the GDx measurement and the other clinical parameters accumulated at the time of the first examination and (2) those who seemed to be well controlled with their then-current regimen. The number was chosen as the parameter to follow in these patients because the manufacturer has communicated to prospective purchasers that with this information, the examiner should be able to distinguish those individuals with nerve fiber layer loss from those with normal nerve thicknesses.<sup>10</sup> As with all new technologies, the specific measurements that are most reliable have yet to be determined for this instrument. In addition, the problem of corneal birefringence and its effect on the repeatability and reliability of the GDx readings has been called into question.<sup>11,12</sup> It may be resolved by newer technology that, according to the manufacturer, will be available in late 2002 (personal communication, Laser Diagnostic Technologies, May 2002).

The study has definite limitations because of its retrospective nature; however, the intention to discriminate between patients who needed a change in therapy and those who did not might have affected the decision-making process. The retrospective perspective may have simulated the “in the trenches” mentality of the clinician who evaluates each patient individually.

All clinical data were collected by a single ophthalmologist and his staff experienced in obtaining IOPs and visual fields. Since the GDx number is free from subjective interpretation except by the technician creating the

ellipse from which the nerve fiber layer thickness is calculated, and since each technician was similarly trained with excellent interobserver agreement, this parameter should not be subject to significant error. The cup-disc ratio is subjective, but all patients had optic nerve stereophotography that the author reviewed for consistency.

The decision to alter therapy, armed with the data available, represents the most subjective parameter. Factors such as the patient's ability to comprehend, comply, and cooperate, as well as the establishment of an appropriate “target pressure” for control of glaucoma, are subjective at best. The fact that the groups differed in both their initial data and their subsequent follow-up information suggests that most of the poorly controlled patients were detected and that the patients who continued with their current regimen were well enough controlled, consistent with the interpretation that the GDx may be both sensitive and specific. The groups differ in that those who required a change in therapy had higher GDx numbers and higher IOP. Thus, the GDx either supported or confirmed that a change in therapy was indicated. In addition, the data demonstrate that the group in whom therapy was changed did not have an increase in IOP, an increase in cup-disc ratio, or further visual field loss in the 341-day interval between examinations. The difference in the mean GDx number ( $51.5 \pm 26.1$  initially and  $57.3 \pm 23.9$  at the second visit) for this group, although averaging 5.8 points higher, was not statistically significant.

None of the 42 patients whose medications were changed had significant enough alterations in clinical parameters during the 1-year interval to warrant additional changes in therapy, laser procedure, or surgical intervention. Longer follow-up will be necessary to accumulate measurements sufficient to perfect this hypothesis, and during that interval, the equipment will improve to enable viewing the nerve fiber layer in greater detail with improvements especially to minimize corneal birefringence. The fact that only 58% of glaucoma patients had second GDx measurements within the time limits established reduces the power of the data to distinguish between the groups; however, the demographic characteristics of the group who had second GDx analyses are not statistically different from those of the total group, including approximately the same distribution in sex, race, age, and type of glaucoma.

## CONCLUSION

The GDx can be used clinically in association with the other time-honored measurements of glaucoma—visual field loss, IOP, and cup-disc ratio—to separate controlled from uncontrolled glaucoma. The inclusion of GDx data may result in increased sensitivity to subtle changes in optic nerve fiber layer deterioration prior to changes in

the other parameters and prevention of subsequent functional loss of vision. The GDx machine reduces dependence on tests that require longer periods of concentration and attention. Finally, normative data may be less helpful than serial data in a single eye acting as its own control.

## REFERENCES

---

1. Choi K-R, Lee H-J, Moon J-I. Nerve fiber layer thickness change in open angle glaucoma. (Abstract) Presented at the 2002 annual meeting of the Association for Research in Vision and Ophthalmology, May 6-10, 2002, Fort Lauderdale, Fla.
2. Zangwill LM, Bow C, Berry CC, et al. Discriminating between normal and glaucomatous eyes using the Heidelberg Retina Tomograph, GDx Nerve Fiber Analyzer, and Optical Coherence Tomograph. *Arch Ophthalmol* 2001;119(7):985-993.
3. Colen TP, Tjon-Fo-sang MJ, Mulder PG, et al. Reproducibility of measurements with the nerve fiber analyzer (NFA/GDx). *J Glaucoma* 2000;9(5):363-370.
4. Weinreb RN, Zangwill L, Berry CC, et al. Detection of glaucoma with scanning laser polarimetry. *Arch Ophthalmol* 1998;116(12):1583-1589.
5. Lauande-Pimentel R, Carvalho RA, Oliveira HC, et al. Discrimination between normal and glaucomatous eyes with visual field and scanning laser polarimetry measurements. *Br J Ophthalmol* 2001;85(5):586-591.
6. Paczka JA, Friedman DS, Quigley HA, et al. Diagnostic capabilities of frequency-doubling technology, scanning laser polarimetry, and nerve fiber layer photographs to distinguish glaucomatous damage. *Am J Ophthalmol* 2001;131(2):188-197.
7. Poinosawmy D, Tan JC, Bunce C, et al. The ability of the GDx nerve fibre analyser neural network to diagnose glaucoma. *Graefes Arch Clin Exp Ophthalmol* 2001;239(2):122-127.
8. Sanchez-Galeana C, Bowd C, Blumenthal EZ, et al. Using optical imaging summary data to detect glaucoma. *Ophthalmology* 2001;108(10):1812-1818.
9. Yamada N, Chen PP, Mills RP, et al. Glaucoma screening using the scanning laser polarimeter. *J Glaucoma* 2000;9(3):254-261.
10. Laser Diagnostics Technologies Web site. GDx product information. Available at: [www.laserdiagnostic.com/products/reading/default.asp](http://www.laserdiagnostic.com/products/reading/default.asp). Accessed June 10, 2002.
11. Greenfield DS, Knighton RW, Huang XR. Effect of corneal polarization axis on assessment of retinal nerve fiber layer thickness by scanning laser polarimetry. *Am J Ophthalmol* 2000;129(6):715-722.
12. Greenfield DS, Knighton RW. Stability of corneal polarization axis measurements for scanning laser polarimetry. *Ophthalmology* 2001;108(6):1065-1069.

## DISCUSSION

---

DR ROBERT RITCH. Dr Bobrow has performed a retrospective chart review using the GDx nerve fiber layer analyzer on 342 consecutive patients, 153 of whom underwent a

second GDx examination approximately 1 year after the first one. The purpose was to determine if the information acquired influenced patient care by affecting the decision-making process and whether these decisions preserved visual function. Patient records were reviewed to determine whether changes in medications, laser procedures, or surgeries were advised and what part the additional information from the GDx played in the decision to alter therapy. Parameters in addition to the GDx taken into account in changing therapy included intraocular pressure, visual field loss, and an increase in cupping. The eyes in which therapy was changed had a higher mean GDx number, a higher mean initial pressure, and were receiving a greater mean number of medications. Each of these factors is associated with more severe disease, which could make it more likely that a patient would require a change in treatment.

The problem with a retrospective study is the difficulty in determining the consistency of the criteria on which decisions were based. It is not clear what relative role the GDx played in decision making nor whether any decisions were based solely on GDx data. We do not know how much weight was given to the GDx number in the decision-making. The optimal GDx criteria to establish the diagnosis of glaucoma or to determine whether therapy is adequate to prevent further damage have yet to be determined. Thus, the conclusion that the GDx can be used clinically in association with other measures to separate controlled from uncontrolled glaucoma still remains unsubstantiated.

A serious problem with the GDx is the effect of corneal birefringence on the retinal nerve fiber layer thickness assessment.<sup>1-4</sup> The wide distribution of corneal birefringence values observed in normal and glaucomatous eyes suggests that the narrow-band corneal compensator employed by the GDx is inappropriately compensating for anterior segment birefringence in most eyes and limits the discriminating power of the device. Many GDx parameters are heavily biased by the presence of corneal birefringence artifact, particularly integral and average measurements. Dr Bobrow has taken the first step in understanding the utility of this new technology in clinical practice.

A study to evaluate a device like the GDx requires a prospective design with specific well-defined end points, such as criteria for scan quality, definitions of normal or abnormal scans, repeated imaging to validate results, and defined hypotheses on which to base decisions. The recent development of a variable corneal compensator could prove to be a significant advance, allowing diagnosis of early disease and tracking of glaucoma progression.<sup>5</sup>

## REFERENCES

---

1. Greenfield DS, Knighton RW. Stability of corneal polarization axis measurements for scanning laser polarimetry. *Ophthalmology* 2001;108:1065-1069.

2. Greenfield DS, Knighton RW, Huang XR. Effect of corneal polarization axis on assessment of retinal nerve fiber layer thickness by scanning laser polarimetry. *Am J Ophthalmol* 2000;129:715-722.
3. Greenfield DS, Knighton RW, Feuer WJ, et al. Correction for corneal polarization axis improves the discriminating power of scanning laser polarimetry. *Am J Ophthalmol* 2002; in press.
4. Weinreb RN, Bowd C, Greenfield DS, et al. Measurement of the magnitude and axis of corneal polarization with scanning laser polarimetry. *Arch Ophthalmol* 2002; in press.
5. Zhou Q, Weinreb RN. Individualized compensation of anterior segment birefringence during scanning laser polarimetry. *Invest Ophthalmol Vis Sci* 2002; in press.

DR DOUGLAS R. ANDERSON. The hypothesis put to the test with this review is "Which of these various factors—intraocular pressure, increased cupping, and GDx—were used by the clinicians in reaching the decision to alter therapy"? A multivariate analysis rather than single analyses might have answered the question. Once IOP, for example, has been taken into account, what additional variables added to the decision to add therapy or not? Did the GDx number come up with a statistically significant coefficient?

DR JAMES C. BOBROW. In response to Dr Ritch's comments, this novel piece of equipment has become available commercial only recently. The scientific underpinnings

may have faults; but I felt that it would be helpful to look retrospectively at my own decision making experience, not on a multivariable or quantitative basis, but to see my "gut-level" results. No patient had a change in therapy unless another parameter plus the GDx was altered in some way, as you can see from the results I presented. The weight given to the GDx, therefore, was confirmatory. I think the value in the study, is simply that, one year later, the changes in the GDx reflected the level of control of the patient's glaucoma. Since I had previously demonstrated that the test was reliable in each individual when repeated, I felt that the changes were significant even if the compensator for corneal birefringence was not utilized (and it has been promised for late 2002 for those who already own the machines.

As far as the need for a prospective study, I agree. I will be following these patients in a prospective fashion for at least another year. In glaucoma, as we all know, trends emerge slowly. Lastly, I want to comment that, just as certain parameters such as Mean Deviation scores from Humphrey Field Analyzer (Zeiss: San Leandro, CA) have been shown to be significant after clinical use, I think that we will find that some of the individual ratios and intermediate calculations in the GDx algorithm will be much more helpful than the "number" that has been commercially derived.

# BACTERIAL RESISTANCE AFTER SHORT-TERM EXPOSURE TO ANTIBIOTICS

---

BY Thomas O. Wood, MD, Harold Dickson, PhD (BY INVITATION), Vickie A. Nix (BY INVITATION),  
AND Danielle Hamilton (BY INVITATION)

## ABSTRACT

*Purpose:* To determine if there is a difference in antibiotic sensitivity to coagulase-negative *Staphylococcus* (CNS) cultured from the host versus the donor cornea at the time of corneal transplantation. Then to apply this knowledge to preoperative preparation of patients undergoing eye surgery.

*Method:* A total of 923 donor corneas stored in Optisol and 895 host corneas with no preoperative antibiotic exposure were cultured. Forty-two CNS positive cultures grew from the donor corneas and 40 from the host corneas ( $P = .5$ ).

*Results:* There was an increase in resistance in the bacteria cultured from the donor compared with the host. The most striking changes occurred in host versus donor to: ciprofloxacin 27.5% ( $P = .0033$ ); gentamicin 27% ( $P = .0113$ ); tobramycin 31.6% ( $P = .059$ ). The combination of polymyxin, bacitracin, and neomycin (P/B/N) was significantly better than ciprofloxacin, gentamicin, and tobramycin or the combination of ciprofloxacin, gentamicin, and tobramycin (C/G/T) ( $P = .0007$ ).

*Conclusion:* The combination of C/G/T exhibited the highest change to resistant bacteria. P/B/N was the most effective commercially available preparation. These results should be considered when making the decision about which preoperative antibiotic to use, if any.

*Trans Am Ophthalmol Soc* 2002;100:137-142

## INTRODUCTION

---

Resistance to antibiotics following short-term exposure has been recognized since 1952, when Starr and Reynolds<sup>1</sup> demonstrated that bacteria in turkey intestines exhibited 100% resistance to streptomycin after 3 days of exposure to it. Gentamicin-resistant bacteria cultured from the donor is a frequent cause of endophthalmitis following corneal transplant.<sup>2,6</sup> In the ophthalmic literature, it has often been assumed that resistant bacteria are present prior to antibiotic treatment. The purpose of this study was to determine if there is a change in resistance patterns to coagulase-negative *Staphylococcus* (CNS) after constant exposure to antibiotics (gentamicin and streptomycin in Optisol) compared with bacteria from the host cornea that have had no preoperative antibiotic exposure.

## METHODS

---

We performed cultures on 923 donor corneas and 895 host corneas. There were fewer host corneas because many with endothelial dystrophy and keratoconus were used in research. In the donor corneas, the time from death to preservation averaged 3.62 hours and the time from preservation to corneal transplantation averaged 2.4 days.

Surgery was begun by preparing the eye with a 5%

solution of povidone-iodine. The donor cornea was then placed in a solution of vancomycin, 1 mg per milliliter of balanced salt solution (BSS), prior to transplantation.<sup>5</sup> The cornea from the host was also placed in the vancomycin solution. The donor cornea was safely secured in the recipient eye, and then the donor rim and host button, after about 30 minutes in the vancomycin solution, were transferred to chocolate agar transport media and taken to the laboratory. In the laboratory the corneas were ground separately and placed on blood, MacConkey, and chocolate agars, and enriched thioglycolate broth. The cultures were read daily for 7 days. Cultures were reported as follows: *rare*, when growth occurred in the first quadrant only; *few*, when growth occurred in the first and second quadrants; *several*, when growth occurred in the first three quadrants; and *many*, when there was growth on all four quadrants.

The 923 donor corneas had 42, and the host corneas 40, positive cultures for CNS or *Staphylococcus epidermidis* ( $P > .05$ , Tables I and II). Sensitivities were obtained to bacitracin, ciprofloxacin, gentamicin, neomycin, streptomycin, vancomycin, tobramycin, and polymyxin (Tables III and IV).

## RESULTS

---

The number of resistant staphylococci from the donor and host corneas was compared. Resistant strains for this study included those reported as resistant and with

From the University of Tennessee, Baptist Memorial Hospital, Memphis, Tennessee.

TABLE I: BACTERIAL RESISTANCE TO *STAPHYLOCOCCUS* IN DONOR CORNEAS

DONOR CORNEAS	BACITRACIN	CIPROFLOXACIN	GENTAMICIN	NEOMYCIN	STREPTOMYCIN	TOBRAMYCIN	VANCOMYCIN	POLYMYXIN
S. epidermidis-rare	S	R	S	S	S	R	S	R
CNS- rare	S	R	R	R	S	R	S	S
CNS- rare		S						
CNS- rare	S	R		S		S	S	S
CNS- rare	S	I	R	I	S	R	S	R
CNS- rare	S	R		R		R	S	I
S. epidermidis-rare		S					S	
CNS- rare	S	S		S		S	S	R
CNS- rare	S	S	S	S	R	S	S	S
CNS- rare	S	S	S	S	S	S	S	S
CNS- rare	S	S	S	S	S	S	S	S
CNS- rare	S	S	S	S	S	S	S	I
CNS-type I rare	S	S	S	S	S	S	S	S
CNS-type II rare	S	S	S	S	S	S	S	S
CNS-type III rare	S	S	S	S	S	S	S	I
CNS-rare	I	S	S	S	S	S	S	S
CNS-rare	S	S	S	S	S	S	S	S
CNS-rare	S	S	S	S	S	S	S	I
CNS-type I rare	S	S	R	S	S	S	S	I
CNS-type II rare	S	S	S	S	S	S	S	S
CNS-rare	S	S	S	S	S	S	S	R
CNS-rare	S	S	S	S	S	S	S	I
CNS-rare	S	S	S	S	S	S	S	S
CNS-rare	S	R	R	R	S	R	S	R
CNS-rare	S	S	S	S	S	R	S	S
CNS-CFU	S	S	S	S	S	S	S	S
CNS-rare	S	S	S	S	S	S	S	S
CNS-rare	S	S	S	S	S	S	S	I
CNS-rare	R	R	I	R	R	R	S	I
CNS-rare	S	I	R	I	S	R	S	S
CNS-rare	S	R	I	I	S	R	S	I
CNS-type I rare	S	S	S	S	S	S	S	R
CNS-type II rare	R	S	S	R	S	S	S	S
CNS-rare	S	S	S	S	S	S	S	R
CNS-rare	S	R	I	R	R	R	S	I
CNS-rare	S		S	S	S	R	S	R
CNS-Rare	S	S	R	I	S	R	S	R
CNS-rare	R	S	S	S	S	S	S	R
CNS-rare	R	R	I	S	S	S	S	I
CNS-rare	S	S	S	S	S	S	S	S
CNS-rare	S	S	S	S	S		S	
CNS-rare			S	R	S		S	
Rim resistance/total	5R/39	11R/40	10R/37	11R/40	3R/37	12R/38	0R/40	21R/38

I, intermediate; CFU, colony forming units; R, resistant; S, sensitive; CNS-, coagulase-negative *Staphylococcus*.

intermediate sensitivity. There were no significant changes in resistance patterns in donors versus host to bacitracin ( $P = .24$ ), neomycin ( $P = 0.2$ ), streptomycin ( $P = 0.5$ ), tobramycin ( $P = .059$ ), vancomycin ( $P > .05$ ), or the combination of polymyxin, bacitracin, and neomycin (P/B/N) ( $P = .5$ ). There was, however, a significant increase in resistance to ciprofloxacin ( $P = .0033$ ) and gentamicin ( $P = .0113$ ) (Table III).

Comparing resistant bacteria, without including those with intermediate sensitivities—ciprofloxacin ( $P = .01$ ), gentamicin ( $P = .07$ ), tobramycin ( $P = .025$ )—reveals that

ciprofloxacin and tobramycin have significant increases in resistance and gentamicin is almost significant (Table IV). The combination of P/B/N was the most effective commercially available topical preparation; in the bacteria cultured from the donor, only 1 of 38 was resistant to all of the antibiotics. The combination of P/B/N was significantly more effective against *Staphylococcus* than ciprofloxacin ( $P = .0029$ ), gentamicin ( $P = .003$ ), tobramycin ( $P = .003$ ) and polymyxin ( $P = .0025$ ). The total resistant strains to the combination of ciprofloxacin, and tobramycin (C/G/T) (33 of 112) revealed that P/B/N (1 of 38) was significantly

Bacterial Resistance After Short-term Exposure to Antibiotics

TABLE II: BACTERIAL RESISTANCE TO STAPHYLOCOCCUS IN HOST CORNEAS

HOST CORNEAS	BACITRACIN	CIPROFLOXACIN	GENTAMICIN	NEOMYCIN	STREPTOMYCIN	TOBRAMYCIN	VANCOMYCIN	POLYMYXIN
S. epidermidis-several	S	S		S		S	S	I
CNS- few	S	S		R		R	S	I
CNS- rare							S	
CNS- rare	S	S	S	S	S	S	S	R
CNS- rare							S	
CNS- rare	S	S		S		R	S	R
CNS- rare							S	
CNS- rare	S	S		S		S	S	R
CNS- rare	R	S		S		S	S	I
CNS- rare		S					S	
CNS- rare		S					S	
CNS- rare	R	S		R		S	S	S
CNS- rare		S					S	
CNS- few								
CNS- rare							S	
CNS- type I rare							S	
CNS-type II rare							S	
CNS- rare	R	S	S	S	S	S	S	I
CNS- rare	S	S	S	S	S	S	S	S
CNS- rare								
CNS- rare	S	S	S	S	S	S	S	S
CNS- rare	S	S	S	S	S	S	S	S
CNS- rare	S	S	S	S	S	S	S	S
CNS- rare	R	S	S	R	S	S	S	I
CNS- rare	R	S	S	S	S	S	S	S
CNS- CFU	S	S	S	S	S	S	S	S
CNS- rare								
CNS- rare							S	
CNS- rare	I	S	S	S	S	S	S	S
CNS- rare	S	S	S	S	S	S	S	I
CNS- rare e	S	S	S	S	S	S	S	S
CNS- rare	S	S	S	S	S	S	S	S
CNS-type I rare	S	S	S	S	S	S	S	I
CNS- type II rare	S	S	S	S	S	S	S	S
CNS- rare	S	S	S	S	S	S	S	S
CNS- rare	S	S	S	S	S	S	S	S
CNS- type I rare	S	S	S	S	S	S	S	S
CNS- type II rare	S	S	S	S	S	S	S	S
CNS- rare	S	S	S	R	R	I	S	R
Host resistance/total	6R/26	0R/29	0R/20	4R/26	1R/20	3R/26	0R/37	11R/26

I, intermediate; CFU, colony forming units; R, resistant; S, sensitive ; CNS-, coagulase-negative *Staphylococcus*.

more effective ( $P = .0025$ ). There was no significant difference when P/B/N was compared to bacitracin ( $P = .101$ ), neomycin ( $P = .056$ ), streptomycin ( $P = 0.29$ ), or vancomycin ( $P = .49$ ) (Table V).

**DISCUSSION**

The most common bacteria cultured in endophthalmitis following intraocular surgery were *S epidermidis* and other coagulase-negative staphylococci.<sup>6,7</sup> The bacterial flora cultured from the ocular surface is decreased following the preoperative use of topical antibiotics; there is, however, no proof that this correlates to a decreased incidence of endoph-

thalmitis.<sup>7,8</sup> Fluoroquinolone-resistant *Staphylococcus* has been demonstrated in corneal wound infections following cataract surgery in eyes treated preoperatively for 1 to 3 days with ciprofloxacin.<sup>9</sup> Our study indicates that there is a change in resistance patterns to fluoroquinolone and aminoglycosides in CNS exposed for about 2.5 days to gentamicin and streptomycin. Interestingly, the resistance changes occurred mainly in gentamicin, ciprofloxacin, and tobramycin.

- Four mechanisms may produce bacterial resistance:
- Mutation, such as gyrase gene mutation, producing quinolone resistance
  - Transduction, which is transfer by bacteriophage of

TABLE III: HOST VERSUS RIM RESISTANCE

Bacitracin			Ciprofloxacin	
Host	6/26	( $P = .24$ )	Host	0/29 ( $P = .0033$ )
Donor rim	5/39		Donor rim	11/40
Gentamicin			Neomycin	
Host	0/20	( $P = .0113$ )	Host	4/26 ( $P = .50$ )
Donor rim	10/37		Donor rim	11/40
Streptomycin			Tobramycin	
Host	1/20	( $P = .50$ )	Host	3/26 ( $P = .059$ )
Donor rim	3/37		Donor rim	12/38
Vancomycin			Polymyxin	
Host	0/36	( $P > .05$ )	Host	11/26 ( $P = .2$ )
Donor rim	0/40		Donor rim	21/38
P/B/N				
Host	1/26	( $P = .5$ )		
Donor rim	1/38			

P/B/N, polymixin, bacitracin, and neomycin.

DNA with resistance gene(s) from one bacterium to another (important in *Staphylococcus aureus* resistance)

- Transformation, when DNA that is free in the environment is taken up by the bacterium followed by homologous recombination (important in penicillin-resistant pneumococci)
- Conjugation, when DNA is transferred from one bacterium to another by direct contact. This mechanism is important in spreading DNA that produces multiple antibiotic resistance and is a frequent mechanism in the transfer of multiresistance genes from gram-negative to gram-positive organisms.<sup>10</sup>

Hoiby and colleagues<sup>11</sup> reported the development of resistance to ciprofloxacin in *S epidermidis* (CNS) cultured from axillary sweat, a relatively closed system. The resis-

TABLE IV: RESISTANCE PATTERNS WITHOUT INCLUDING INTERMEDIATE SENSITIVITIES

Bacitracin			Ciprofloxacin	
Host	5/26	( $P = .025$ )	Host	0/29 ( $P = .01$ )
Donor rim	4/39		Donor rim	9/40
Gentamicin			Neomycin	
Host	0/20	( $P = .07$ )	Host	4/26 ( $P = .50$ )
Donor rim	6/37		Donor rim	7/40
Streptomycin			Tobramycin	
Host	1/20	( $P = .50$ )	Host	2/26 ( $P = .025$ )
Donor rim	3/37		Donor rim	12/38
Polymyxin			Vancomycin	
Host	4/26	( $P = .23$ )	Host	0/36 ( $P > .05$ )
Donor rim	10/38		Donor rim	0/40

tant isolates occurred in a mean time of 2.7 days (range, 1-7 days). The CNS also exhibited the development of multiresistance to methicillin, erythromycin, sulfonamides, trimethoprim, and gentamicin. Cultures of specimens from the nose, a relatively open system, took an average of 18 days to develop resistant strains.

Occlusion causes rapid bacterial growth on the skin, providing an environment for increasing frequency of mutation and thereby increasing the chances of bacterial resistance. Corneal storage solutions are closed systems with no bacterial, antibiotic, or fluid turnover.

The conditions in corneal storage would be similar to the relatively closed environments of occluded skin, the axillae, and the intestinal tract.<sup>1,11</sup> Corneal storage solution may also be an ideal environment for transduction (phage), transformation (uptake of free DNA), and/or conjugation (DNA transfer by direct exchange) to produce resistance in CNS. This study and others, such as the 1952 report of Starr and Reynolds,<sup>1</sup> indicate that in a conducive environment, resistance as well as cross-resistance can develop following short-term antibiotic exposure.<sup>1,8,9,11-13</sup> The conjunctival cul-de-sac may provide a similar relatively closed environment. The low resistance rate in CNS cultured from the host corneas may reflect the fact that the cornea is an "open system" similar to the nose. Can this information help us decide if prophylactic antibiotics are indicated or contraindicated prior to surgery? If indicated, P/B/N appears to be the best commercially available preparation, combined with a povidone-iodine preparation.<sup>8,12-14</sup>

TABLE V: COMPARISON OF P/B/N TO SINGLE ANTIBIOTIC RESISTANCE TO *STAPHYLOCOCCUS* CULTURED FROM DONOR RIM

P/B/N	1/38		P/B/N	1/38
vs		( $P = .101$ )	vs	( $P = .0029$ )
Bacitracin	5/39		Ciprofloxacin	11/39
P/B/N	1/38		P/B/N	1/38
vs		( $P = .003$ )	vs	( $P = .0561$ )
Gentamicin	10/35		Neomycin	11/40
P/B/N	1/38		P/B/N	1/38
vs		( $P = .27$ )	vs	( $P = .003$ )
Streptomycin	3/37		Tobramycin	12/38
P/B/N	1/38		P/B/N	1/38
vs		( $P = .49$ )	vs	( $P = .0025$ )
Vancomycin	0/40		Polymyxin	21/38
C/G/T	33/112			
vs		( $P = .0007$ )		
P/B/N	1/38			

C/G/T, ciprofloxacin, gentamicin, and tobramycin; P/B/N, polymixin, bacitracin, and neomycin.

## REFERENCES

1. Starr MP, Reynolds DM. Poisonous poultry. *Sci Am* 1952 Jan;38.
2. Leveille AS, McMullan FD, Cavanaugh HD. Endophthalmitis following penetrating keratoplasty. *Ophthalmology* 1983;90(1);38-39.
3. Baer JC, Nirankari VS, Glaros DS. Streptococcal endophthalmitis from contaminated donor corneas after keratoplasty. Clinical and laboratory investigations. *Arch Ophthalmol* 1988;106(4); 517-520.
4. Poole TG, Insler BS, Insler MS. Contamination of donor cornea by gentamicin-resistant organisms. *Am J Ophthalmol* 1984;97(5);560-564.
5. Wood TO, Mohay J, McLaughlin BJ. Vancomycin in corneal transplantation. *Trans Am Ophthalmol Soc* 1993;91:391-396; discussion 396-400
6. Han DP, Wisniewski SR, Wilson LA, et al. Spectrum and susceptibilities of microbiologic isolates in the Endophthalmitis Vitrectomy Study. *Am J Ophthalmol* 1996;122(1);1-17.
7. Liesegang TJ. Perioperative antibiotic prophylaxis in cataract surgery. *Cornea* 1999;18(4);383-402.
8. Isenberg SI, Apt L, Yoshimori R, et al. Chemical preparation of the eye in ophthalmic surgery. IV. Comparison of povidone-iodine on the conjunctiva with a prophylactic antibiotic. *Arch Ophthalmol* 1985;103(9);1340-1342.
9. Cosar CB, Cohen EJ, Rapuano CJ, et al. Clear corneal wound infection after phacoemulsification. *Arch Ophthalmol* 2001;119(12);1755-1759.
10. Hardman JG, Limbird LE, Gilman AG. Antimicrobial agents buy Chambers HV. In: *Goodman and Gilman's The Pharmacological Basis of Therapeutics*. 10th ed. 2001:1143-1170.
11. Hoiby N, Jarlov JO, Kemp M, et al. Excretion of ciprofloxacin in sweat and multiresistant *Staphylococcus epidermidis*. *Lancet* 1997;349(9046):167-169.
12. Apt L, Isenberg SJ, Yoshimori R, et al. Outpatient topical use of povidone-iodine in preparing the eye for surgery. *Ophthalmology* 1989;96(3);289-292.
13. Apt L, Isenberg SJ, Yoshimori R, et al. Chemical preparation of the eye in ophthalmic surgery. III. Effect of povidone-iodine on the conjunctiva. *Arch Ophthalmol* 1984;102(5);728-729.
14. Speaker MG, Menikoff JA. Prophylaxis of endophthalmitis with topical povidone-iodine. *Ophthalmology* 1991;98(12):1769-1775.

## DISCUSSION

DR RICHARD K. FORSTER. Dr Wood and his colleagues have undertaken a study to determine if there is a change in resistance patterns of coagulase-negative staphylococci after exposure to the antibiotics gentamicin and streptomycin in Optisol corneal preservation media. They compared the sensitivity pattern of bacteria on donor rims to that of bacteria isolated from host corneas undergoing corneal transplantation. They conclude that there was a

significant increase in the resistance to ciprofloxacin and gentamicin after short-term exposure to antibiotics in the storage media.

After careful analysis of the data presented, I must conclude that Dr Wood and his coauthors may have demonstrated a difference in resistance patterns, but they have not demonstrated an increase in resistance to ciprofloxacin and gentamicin. How do I come to this conclusion? Basically, the study compares two different populations of bacteria. Those derived from the donor rims in storage media have been exposed to gentamicin and streptomycin for an average of 2.4 days. Short-term exposure to these antibiotics suppressed or killed all susceptible bacterial populations. Therefore, the resistant population of bacterial isolates was selected before being exposed to the various antibiotic sensitivity studies. By contrast, the bacteria isolated from the host corneas were not exposed to antibiotics before culturing, and thus would have higher susceptibilities to the tested antibiotics.

It is somewhat surprising that there was no demonstrable resistance to ciprofloxacin and gentamicin in 28 and 20 host cornea isolates, respectively. In South Florida, records from the ocular microbiology files of the Bascom Palmer Eye Institute in 2001 demonstrated approximately 33% resistance of *S epidermidis* to gentamicin and >50% resistance to ciprofloxacin. On the other hand, it is not surprising that 11 of 40 donor rim cultures were resistant to ciprofloxacin, since multidrug resistance probably develops from the gentamicin and streptomycin in the storage media.

Finally, in order to have two comparable populations of bacteria, cultures of the cornea and ocular surface would be required of both the donor eyes before removal and placement into the preservation media, and the host cornea and ocular surface. Standardization also assumes that no beta-dine or topical antibiotics are applied to either the donor or host eyes before obtaining cultures. In the present study the method of quantitation is unclear. In order for resistance to develop, there is need for a sufficient pool of bacteria that are growing, and therefore both groups need to be matched for temperature, time, and standard quantitation of bacterial growth. Detecting "rare" numbers of organisms in the first quadrant of the culture plate is only qualitative or at best semiquantitative.

Further to my communication with the author, I understand that this is a preliminary study, but these comments need to be considered and addressed in any prospective protocol.

DR VERINDER S. NIRANKARI. About 15 years ago, we were having significant problems with endophthalmitis from contaminated corneas coming from the eye bank. At that time the organisms were streptococcal species because we

were putting gentamicin in the solution. In our studies we found that although vancomycin was a pretty good antibiotic, there were cost issues and stability issues. Streptomycin was selected, and the incidence of clinical endophthalmitis after corneal transplantation using corneal storage media has rapidly declined

DR RICHARD L. LINDSTROM. The purpose of prophylactic antibiotics is to reduce the incidence of infection. Also, they should not be toxic to the cornea, especially the endothelium. The antibiotics selected should be uncommonly used, like streptomycin, so that if you did get an infection you'd have alternative antibiotics for treatment. We never sterilized the tissue, but you can reduce the load of bacteria that are presented. Then the body's immune system has a chance to handle the remaining organisms. I think if we took the antibiotics completely out of the media, we'd see a very high incidence of postoperative infections.

DR IVAN R. SCHWAB. *S epidermidis* is not a single organism, but rather a group of organisms, with perhaps 16 to 20 in the group, and some are more virulent than others. Did the authors look at the different variants of *S epidermidis*?

DR THOMAS O. WOOD. What led me to do this study was postoperative endophthalmitis, which occurs in about 1 in 100 cases, usually in patients who have bullous keratopathy and glaucoma. All the organisms were coagulase-negative *Staphylococcus*. Dr Forster believes that exposure to preoperative antibiotics in the optisol solution selected out resistant bacteria accounting for our results. Basically 4% CNS grew from both donor and host. Dr Dickson evaluated these numbers; the chances of selecting out the bacteria that were resistant are between 4 in 10,000 and 1 in 1,000,000. Dr Forster also mentioned a 33% resistance in bacteria to gentamicin and ciprofloxacin in South Florida, but we don't know if those cultures came from the inferior cul de sac or the cornea, or, if there were ulcers, and the corneas had been treated with antibiotics. I suspect if you have enough to get 33% resistance, a lot of those corneas, by the time they got to the Bascom Palmer, had been pretreated. Dr Schwab, we did not divide the Staphylococci into groups.

# LONG-TERM ANALYSIS OF LASIK FOR THE CORRECTION OF REFRACTIVE ERRORS AFTER PENETRATING KERATOPLASTY

---

BY David R. Hardten, MD (BY INVITATION), Anuwat Chittcharus, MD (BY INVITATION), AND Richard L. Lindstrom, MD

## ABSTRACT

*Purpose:* To determine the long-term safety and effectiveness of laser-assisted in situ keratomileusis (LASIK) in the treatment of refractive errors following penetrating keratoplasty.

*Methods:* A retrospective review was done of 57 eyes of 48 patients with anisometropia or high astigmatism who were unable to wear glasses or a contact lens after penetrating keratoplasty and who underwent LASIK for visual rehabilitation. Uncorrected visual acuity (UCVA), best spectacle-corrected visual acuity (BCVA), and corneal transplant integrity were recorded before surgery as well as up to 60 months after LASIK.

*Results:* The mean follow-up after the LASIK was  $21.4 \pm 14.2$  months (range, 3-60 months). Mean preoperative spherical equivalent (SE) was  $-4.19 \pm 3.38$  diopters (D). Mean preoperative astigmatism was  $4.67 \pm 2.18$  D. Preoperative BCVA was 20/40 or better in 42 eyes (74%). At 2 years the mean SE was  $-0.61 \pm 1.81$  D and mean astigmatism was  $1.94 \pm 1.35$  D for the 28 eyes with follow-up. UCVA was 20/40 or better in 12 eyes (43%), and BCVA was 20/40 or better in 24 eyes (86%) at 2 years. A gain in BCVA of one line or more was seen in eight eyes (29%). Two eyes (7%) had loss of two or more lines of BCVA at 2 years. Nine eyes (16%) developed epithelial ingrowth. Five eyes (9%) in this series had repeat corneal transplants.

*Conclusions:* LASIK is effective for reducing ametropia after penetrating keratoplasty. Proper patient counseling is necessary because the results of LASIK after penetrating keratoplasty are not as good as, and complications are more frequent than, in eyes with naturally occurring myopia and astigmatism. Complications are especially common in patients with mismatch of the donor and host cornea and in those with poor endothelial cell function.

*Trans Am Ophthalmol Soc* 2002;100:143-152

## INTRODUCTION

---

Visual rehabilitation after penetrating keratoplasty remains challenging. The visual success of corneal transplantation is often impaired by high degrees of regular and irregular astigmatism, which, in most cases, is accompanied by large amounts of myopia or hyperopia as well as anisometropia.<sup>1-6</sup> Usually, this is related to the inherent imprecision of corneal transplantation, with mismatch of donor and host tissue. The keratometry of the postoperative cornea is difficult to predict when performing lens power calculations in the patient undergoing combined penetrating keratoplasty and intraocular lens implantation.<sup>2,7,8</sup> High degrees of anisometropia may result in a variety of patient complaints, including diplopia and blurred vision. The use of

spectacles for visual rehabilitation is a good option for patients who have small to moderate amounts of ametropia. In more severe cases, contact lenses are often satisfactory.<sup>9,10</sup> Unfortunately, many patients, especially elderly patients, are unable to tolerate, handle, or maintain contact lenses.

Surgical intervention is considered if optical methods fail to provide adequate visual rehabilitation. Postkeratoplasty astigmatism has been treated with various forms of refractive surgery.<sup>7,11-41</sup> Unfortunately, predictability after relaxing incisions, astigmatic keratotomy, or wedge resections is not very reliable.<sup>7,13,28,29,35</sup> Relaxing incisions at the graft host interface are additionally associated with a potential risk of wound dehiscence when there is poor apposition of the posterior edges of the wound. In addition, in some patients, the graft may shift anteriorly during healing, producing irregularities in corneal topography, refraction, and keratometry. Paracentral incisional procedures have also been used in the correction of postkeratoplasty myopia and hyperopia, yet radial keratotomy performed in corneal grafts has high variability and suboptimal predictability.<sup>22</sup> Hexagonal keratotomy has been used

From Minnesota Eye Consultants, Minneapolis, Minnesota, Regions Medical Center, St Paul, Minnesota, and the Department of Ophthalmology, University of Minnesota, Minneapolis (Dr Hardten and Dr Lindstrom); and Minnesota Eye Consultants, Minneapolis, Minnesota and Bhumiphol Adulyadej Hospital, Bangkok, Thailand (Dr Chittcharus). Dr Hardten and Dr Lindstrom are consultants to and/or teach courses for VISX, Inc, Bausch & Lomb, Inc, and TLC Vision, Inc.

with limited success because of a high incidence of irregular astigmatism.<sup>42,43</sup> In the last several years, the excimer laser has acquired a significant role in the management of postkeratoplasty refractive errors. The results of photorefractive keratectomy (PRK) performed in this setting have been published in different studies, many of them reporting a significant incidence of stromal haze.<sup>11,15,21,24,27,31,36,40</sup> The haze appears to be related to the large magnitude of the ablations necessary for these cases, and it is usually coupled with regression of the obtained refractive effect and loss of best spectacle-corrected visual acuity (BCVA). In addition there are some case reports of graft rejection induced by excimer photoablation.<sup>19,23</sup>

LASIK offers several advantages over PRK in the treatment of myopia and astigmatism.<sup>44</sup> These include a more rapid visual recovery and less chance of anterior stromal haze. The major disadvantage of LASIK is the risk of complications related to the creation of the lamellar flap. Little long-term information has been reported in eyes with previous penetrating keratoplasty. This study looks at the long-term success of LASIK after penetrating keratoplasty.

## SUBJECTS AND METHODS

This study is a retrospective, noncomparative clinical trial of LASIK for visual rehabilitation of significant myopia and astigmatism after penetrating keratoplasty. All patients were intolerant of spectacle correction and contact lenses. A detailed explanation of the proposed surgical treatment was given to all patients. Informed consent was obtained from the patients. The surgery was performed by one of two surgeons in our group (R.L.L. or D.R.H.) between August 1996 and August 2000. All subjects were at least 18 years of age, and contact lens wear was discontinued at least 3 weeks prior to preoperative evaluation. Minimum time from penetrating keratoplasty to LASIK was 13 months (range, 13 months to 20 years), and all eyes had all sutures removed at least 1 month before the LASIK surgery. The study group consisted of 57 eyes of 48 patients.

Preoperative testing included a complete eye examination, consisting of uncorrected visual acuity (UCVA) and BCVA, manifest refraction, tonometry, corneal topography, and ultrasound pachymetry.

## SURGICAL PROCEDURE

The surgery was performed in a particle-free environment with patients under topical proparacaine anesthesia. The unoperated eye was taped shut to prevent drying of the cornea, eliminate cross-fixation, and aid the patient in maintaining good fixation. The corneal flap was cut using the Bausch & Lomb automated corneal shaper (ACS) or Hansatome microkeratome (Bausch & Lomb, Miami, Florida). The ACS flaps were hinged nasally (160- $\mu$ m flap

thickness, 7.5-mm average diameter), and a superior hinge was made for all eyes with the Hansatome (180- $\mu$ m flap thickness, 9.0-mm average diameter). After the flap was lifted, the photoablations were made using the VISX STAR Excimer Laser System (VISX, Inc, Santa Clara, California) with a fluence of 160 mJ/cm<sup>2</sup> using a maximum optical zone of 6.0 mm. Hydration was monitored visually during the ablation, and the cornea was moistened if it became drier than expected by the surgeon or dried if it became moister than expected.

The desired correction was emmetropia in all eyes. The correction was initially set to 100% of the manifest sphere and cylinder, but early experience showed that this nomogram resulted in residual myopia and astigmatism in many patients. Later a nomogram based on experience in normal eyes was used. Elliptical laser ablations, astigmatic keratotomy, or both, were used to correct astigmatism. For astigmatic treatment, an elliptical ablation was performed with the optical zone along the minor axis of at least 4.5 mm and no greater than 6.0 mm. For astigmatic keratotomy, a square-tipped blade was set to 50  $\mu$ m more than the thinnest central corneal depth measured under the flap after myopic ablation. An optical zone of 7 mm was used, and the length was determined by the Chiron Arc-T Lindstrom 9-mm optical zone nomogram. The flap and bed were irrigated with BSS, and the flap was floated back into position and smoothed with a dry Merocel sponge (Medtronic, Jacksonville, Florida). The eye was left open for 5 minutes to allow the endothelial cell pump to remove stromal fluid from underneath the flap and secure the flap in place. At the end of the procedure, antibiotic, steroid, and nonsteroidal anti-inflammatory drops were instilled into the eye. Patients received antibiotic and steroid drops four times daily for the first 2 postoperative weeks and then resumed their maintenance steroid regimen.

Outcome measures included UCVA accuracy and predictability of treatments (percentage within  $\pm 0.5$  D and  $\pm 1.0$  D of emmetropia), stability of refraction, loss of BCVA, and all complications at 1 day, 1 week, and 1, 3, 6, 12, and 24 months after surgery. Statistical analysis was done with Microsoft Access 97 and Microsoft Excel 97 software (Microsoft, Inc, Redmond, Washington). All means are reported with their standard deviations and ranges.

## RESULTS

Fifty-seven eyes with myopia, astigmatism, or both, were treated. Mean patient age was  $59.6 \pm 17.3$  years (range, 24-92 years). Table I shows the demographic characteristics for this population. Spherical corrections ranged from -0.75 D to -15.25 D, and cylindrical corrections ranged from 0.5 D to 10.0 D. Forty-one eyes (72%) had significant

TABLE I: PREOPERATIVE PATIENT CHARACTERISTICS OF STUDY GROUP

CHARACTERISTIC	NO.	%
Total eyes	57	
Right	28	49
Left	29	51
Mean patient age (yr)	59.6 ± 17.3	
Age range (yr)	24-92	
Gender (patients)		
Male	32	67
Female	16	33
Race (patients)		
White	46	96
Asian	1	2
Hispanic	1	2

irregular astigmatism (steep and flat meridians not 90° apart), and 16 eyes (28%) had mostly regular astigmatism. In the eyes with regular astigmatism, 13 had LASIK alone and 3 eyes had very high astigmatism and therefore had LASIK combined with astigmatic keratotomy. Twelve of the eyes with irregular astigmatism received astigmatic keratotomy combined with LASIK. The remaining 29 eyes with irregular astigmatism received LASIK alone.

In this series, many patients were elderly, and 10 eyes (17%) had significant drusen or senile macular degeneration. The most common indication for the penetrating keratoplasty in this series was keratoconus in 27 eyes (47%) and Fuchs' endothelial dystrophy in 16 eyes (28%) (Table II). Previous corneal surgeries were relaxing incisions after penetrating keratoplasty in one eye and glaucoma surgery in one eye. Two eyes had had one transplant before the transplant that received LASIK. Five eyes had glaucoma in the study group. The other anterior segment problems included 12 eyes with significant dry eye, 5 eyes with chronic significant blepharitis, 17 eyes with override of the corneal graft wound with localized ectasia, and 3 eyes with multiple corneal graft rejection episodes. Nine eyes (16%) had borderline endothelial cell count below 1,000 cells/mm<sup>2</sup> by specular microscopy. Endothelial cell counts were not performed routinely early in the study, yet

TABLE II: INDICATIONS FOR ORIGINAL PENETRATING KERATOPLASTY

DIAGNOSIS	NO. OF EYES	% OF EYES
Keratoconus	27	47
Fuchs' dystrophy	16	28
Pseudophakic corneal edema	6	11
Traumatic corneal scar	5	9
Herpes simplex keratitis	1	2
Acanthamoeba keratitis	1	2
Iridocorneal endothelial syndrome	1	2

preoperative pachymetry was over 600 µm thick in 8 of the eyes in which specular microscopy was not performed.

Six-month follow-up data are available for 53 eyes (93%), 1-year follow-up data for 52 eyes (91%), and 2-year follow-up data for 28 eyes (49%). Follow-up of 3 years or more is available for 12 eyes (21%).

**UNCORRECTED VISUAL ACUITY**

Before surgery, all eyes had UCVA worse than 20/40 (range, 20/80 to count fingers). At 1 year, follow-up is available for 52 eyes, and UCVA is 20/40 or better in 20 eyes (38%) (Figure 1). UCVA stays stable in most eyes over time (Figure 2).

**BEST SPECTACLE-CORRECTED VISUAL ACUITY**

Before surgery, 42 eyes (74%) had BCVA of 20/40 or better. At 1 year, 39 eyes (75%) had BCVA of 20/40 or better. Seven eyes (13%) had a loss of more than two lines of BCVA (Figure 3).

**REFRACTIVE ERROR**

Figure 4 shows the mean spherical equivalent manifest refractive error (SE) over time through 3 years. The SE was relatively stable by 6 months, yet 12 eyes (23%) still had more than 1 D of change in manifest refraction SE from 3 to 6 months. The mean difference in SE between 3 and 6 months was 0.4 toward the myopic direction. Figure 5 represents the accuracy of the attempted versus achieved SE correction at 1 year. Most patients had correction between -2 and +2 D (Figure 6).

**ASTIGMATIC CORRECTION**

Figure 7 shows the mean refractive cylinder over time. Most eyes were relatively stable by 3 months, yet 8% of eyes had more than 1 D of increase in astigmatism between 3 and 6 months, and 6% of eyes had more than 1 D of improvement in astigmatism between 3 and 6 months. The mean change in astigmatism between 3 and 6 months was 0.01 D.

**INTRAOCULAR PRESSURE**

None of the eyes in this study had intraocular pressure greater than 25 mm Hg or an increase in intraocular pressure of more than 10 mm Hg above preoperative baseline. Five eyes had glaucoma in this study, and pressure control was maintained with glaucoma medications.

**PACHYMETRY**

Mean central corneal thickness before LASIK was 572 ± 45 µm (range, 487-709 µm). Mean laser corneal ablation depth was 55 ± 27 µm and varied from 15 to 134 µm. Mean calculated residual stromal bed thickness was 346 ± 59 µm (range, 209-498 µm). Twelve eyes (21%) had a stromal bed

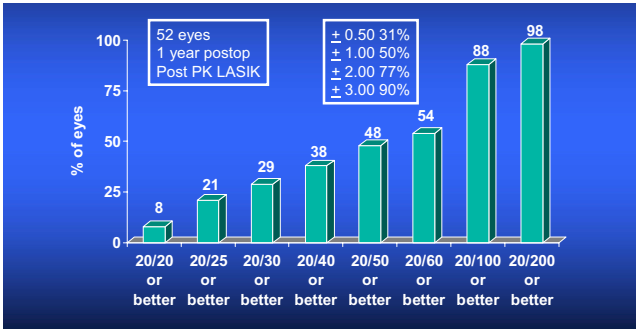


FIGURE 1

Uncorrected visual acuity of 52 eyes at 1 year.



FIGURE 2

Uncorrected visual acuity of eyes at all time points.

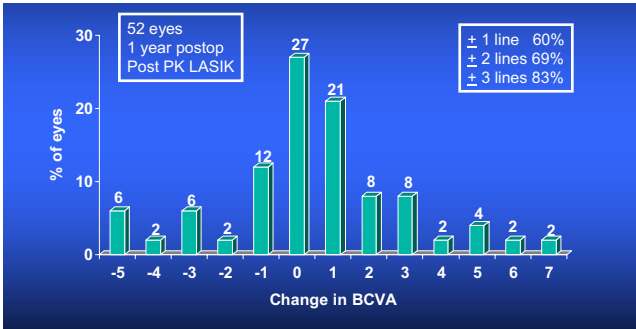


FIGURE 3

Change in best corrected visual acuity at one year. Numbers to left of zero represent patients with loss of best corrected visual acuity (BCVA). Numbers to right of zero represent patients with gains of BCVA.

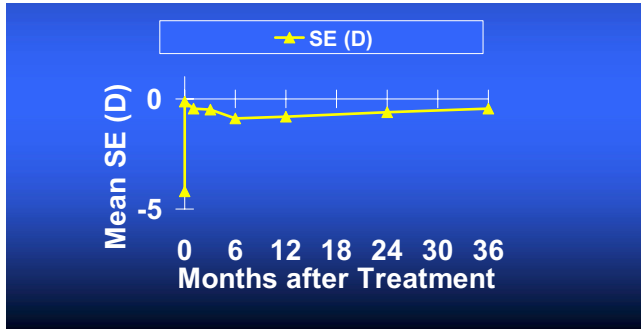


FIGURE 4

Mean spherical equivalent over time.

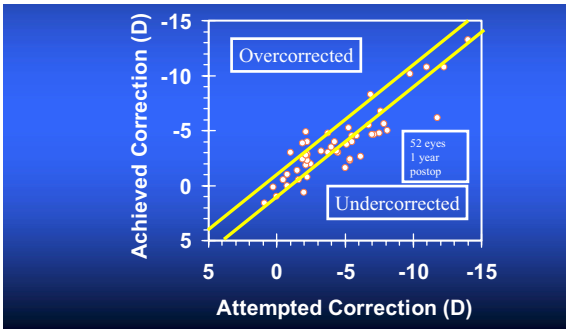


FIGURE 5

Attempted versus achieved spherical equivalent at 1 year. Points above the line represent eyes that have an overcorrection of more than 1 diopter (D). Points below the line represent eyes that have an undercorrection of more than 1 D.

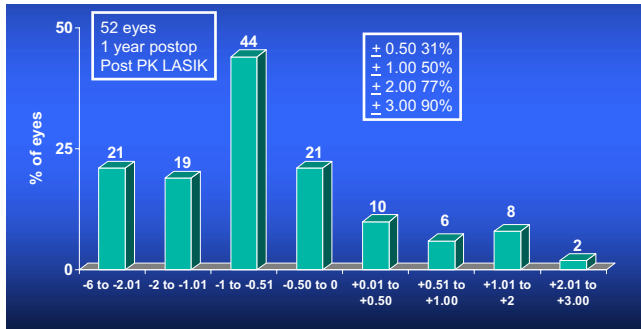


FIGURE 6

Postoperative defocus at 1 year.

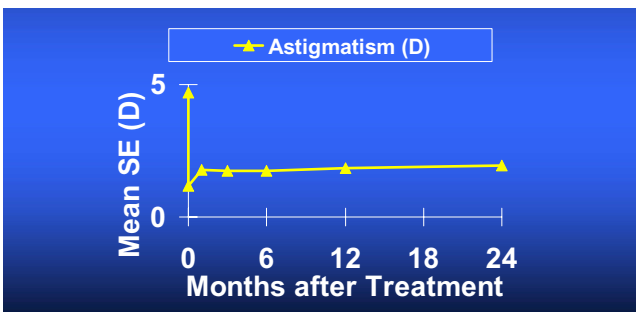


FIGURE 7

Mean residual astigmatism over time.

thickness below 300  $\mu\text{m}$ . Two eyes (4%) had a residual stromal bed thickness below 250  $\mu\text{m}$  (209 and 249  $\mu\text{m}$ ).

**CORNEAL ENDOTHELIAL CELL COUNT**

Specular microscopy was available preoperatively for 23 eyes. Mean endothelial cell count before LASIK was  $1,250 \pm 729$  cells/ $\text{mm}^2$  (range, 0-2,697 cells/ $\text{mm}^2$ ). Nine eyes had an endothelial cell count less than 1,000 cells/ $\text{mm}^2$ . Endothelial cell counts were measured postoperatively in only 10 eyes. One patient with a significant rejection episode at 2 years had a loss of over 1,000 cells/ $\text{mm}^2$ . The

other nine eyes that were measured showed no significant change in endothelial cell density.

**COMPLICATIONS AND ADVERSE REACTIONS**

A summary of complications and adverse reactions is detailed in Table III. Epithelial ingrowth occurred in nine eyes (16%), all of which had override of the donor wound over the host before the LASIK. One eye had recurrent herpes simplex keratitis at 6 months, which resolved after treatment with no loss of BCVA. Two eyes developed interface fluid pockets between 1 month and 3 months. Four other eyes had flap dislocation between 1 day and 1 week: two required sutures to stabilize the flap, one flap was removed, and one flap was repositioned successfully without sutures. Other complications occurred, including sterile interface inflammation, corneal striae, and corneal edema. In one eye a microperforation occurred during arcuate keratotomy under the flap, which required a suture of the microperforation. This suture was later lysed with the argon laser without complication. Five eyes (9%)

eventually had another penetrating keratoplasty. Two of these were for early loss of graft clarity due to low cell counts, one was due to edema from a rejection episode 2 years after the LASIK, and two were for persistent irregular astigmatism from ectasia at the interface between the graft and the host that existed prior to LASIK.

**ENHANCEMENTS**

Five eyes (9%) underwent an enhancement procedure for residual correction. Further LASIK was performed in these eyes using a lift flap technique. One of these eyes developed epithelial ingrowth, which did not require removal after the enhancement.

**DISCUSSION**

High anisometropia following penetrating keratoplasty is not uncommon and can lead to significant patient dissatisfaction. The resolution of anisometropia was the goal of LASIK in most patients in this study. Because of the differences in indication for the procedure, as well as the difference in results, we prefer to use the term *therapeutic lamellar keratectomy* (TLK) to describe the procedure in these eyes. In most of the patients, the goal of TLK was met, with improvement in the anisometropia. Many patients were older and had other associated eye problems, such as age-related macular degeneration or other anterior segment problems. Three patients had a history of multiple episodes of graft rejection prior to the TLK procedure. These associated problems limited visual acuity preoperatively in many eyes. Rehabilitation with spectacle correction or rigid gas-permeable contact lens is typically preferred over TLK; however, in elderly patients poor manual dexterity, tremor, arthritis, or decreased visual acuity in the other eye may limit the tolerance of contact lenses. Contact lenses can also be problematic in patients with chronic blepharitis and severe dry eye and may induce chronic irritation and peripheral neovascularization, also increasing the risk of corneal graft rejection.<sup>11</sup>

LASIK after penetrating keratoplasty has a higher complication rate than in patients with normal corneas, but typically management of those complications is the same.<sup>45,46</sup> In a series of LASIK in normal eyes from the same time frame from our own group, we found flap displacement on day 1 of 0.7% and epithelial ingrowth in 0.2% of eyes.<sup>46</sup> This same study showed that 97% of eyes with low myopia and 56% of eyes with high myopia have 20/40 or better visual acuity by 1 month.

In the current series, the mean preoperative astigmatism was very high at 4.7 D. Many of the eyes had significant levels of irregular astigmatism, which is not uncommon after penetrating keratoplasty.<sup>6,7,10</sup> Currently, excimer laser systems are approved in the United States to treat irregular astigmatism through a phototherapeutic

TABLE III: SUMMARY OF COMPLICATIONS AND ADVERSE REACTIONS RELATED TO SURGICAL PROCEDURE AT ANY TIME IN THE POSTOPERATIVE COURSE

COMPLICATIONS*	NO. OF EYES†	%	INTERVAL COMPLICATION NOTED
Sterile interface inflammation	3	5	1 wk to 1 mo
Epithelial ingrowth requiring removal	4	7	1 wk to 12 mo
Ingrowth not requiring removal	5	9	1 mo to 3 mo
Mild flap striae	4	7	1 day to 1 wk
Interface fluid pocket	2	4	1 mo, 3 mo
Herpes simplex keratitis recurrence	1	2	6 mo
Repeated graft for persistent irregular astigmatism	2	4	1 yr to 3 yr
Repeated graft for edema	3	5	8 mo to 3 yr
Flap dislocation	4	7	1 day, 1 wk
Microperforation	1	2	Intraoperative

\*Other complications that occurred transiently include corneal edema and punctate epitheliopathy.

†Same subject may be included in more than one complication.

approach. All eyes in our study received spherocylindrical treatments, only without any wavefront or topographic adjustments. Future modalities, such as wavefront or topographically directed treatments, may improve results in these patients, though early studies still are less satisfactory for the treatment of irregular astigmatism than regular astigmatism.<sup>47-49</sup> Proper axis alignment and centration of the laser ablation are critical in high astigmatism and difficult or impossible with standard treatments in eyes with irregular astigmatism. The success of treatment in eyes with irregular astigmatism is also difficult to measure, because the astigmatism itself is difficult to measure. We chose to use refractive astigmatism for the analysis, since wavefront testing was not available at the time the study was performed. Newer wavefront techniques may prove to be more useful in defining, measuring, or treating irregular astigmatism.<sup>50,51</sup>

There is the potential risk of damage to the corneal transplant after TLK, such as wound dehiscence, corneal graft rejection, and flap complications. The minimum time for TLK after all sutures had been removed in this study was 1 month, and the minimum time for TLK after the penetrating keratoplasty was 13 months. Mean time of TLK after penetrating keratoplasty was 70 months. This report confirms that adequate wound integrity is present to prevent disruption of the corneal wound in the treated eyes. We did perform LASIK on 17 eyes with moderate wound override due to poor healing of the corneal wound where the transplant was displaced anteriorly. These eyes were at increased risk for epithelial ingrowth. The clinical pattern in these eyes was poor early adherence of the flap in the area of the wound override, with epithelial ingrowth beginning in the area of the override. We had nine eyes (16%) overall that developed epithelial ingrowth and four eyes (7%) that required removal of the epithelial ingrowth. Eyes with wound override also have more irregular astigmatism and are less likely to achieve desired results with the TLK procedure, as evidenced by the fact that two of these patients desired another keratoplasty.

Postoperative flap dislocation or poor adherence is more likely to occur in eyes with low endothelial cell counts preoperatively. In two of our patients, fluid-filled cysts developed in the interface, both of which had very low endothelial cell function. Two cases of interface fluid have previously been reported, yet these were associated with steroid-induced ocular hypertension, not related to endothelial cell pump function from low numbers of cells.<sup>52</sup> Eyes with corneal transplants probably lose endothelial cells at a more rapid rate than normal eyes and do not always display typical guttata, so specular microscopy is helpful in identifying those eyes at risk of poor adherence.<sup>53-55</sup> LASIK probably has little detrimental effect on the endothelium.<sup>56</sup> Still, patients with low cell counts may not tolerate LASIK and may require other surgical intervention,

including repeated penetrating keratoplasty.

Preoperative topical steroid had been suggested to reduce the incidence of graft rejection, yet this was not a large problem in this series. These eyes did well with continuation of their baseline steroid dosage with a strong steroid four times daily for the first month after the TLK procedure.

Some investigators have suggested a two-step procedure, first creating the flap, then at a later time repeating refraction and the laser treatment to increase the accuracy of the procedure.<sup>17</sup> In our series, we performed the procedure in one step to allow quicker visual rehabilitation and limit the potential for complications to one surgery if possible. This is important, because the rate of epithelial ingrowth as a complication is higher in enhancement procedures (Davis, EA, Lindstrom M, Hardten DR, Lindstrom RL; Lifting versus Recutting for LASIK Enhancements, in press, *Ophthalmology*, 2002). The expectations of these patients are typically less than of patients with naturally occurring myopia or astigmatism, and despite the fact that the results were less optimal than in naturally occurring myopia, our enhancement rate was quite low (8.8%), even with an average follow-up of almost 2 years, showing the practicality of our approach.

The one arcuate keratotomy complication in our study was a microperforation, which occurred because of uneven thickness of the stromal bed in a patient with herpes simplex keratitis. Caution should be taken to avoid arcuate keratotomy incisions in areas of uneven thickness, because ultrasonic pachymetry or even scanning slit optical measurements may not adequately describe the thickness in these regions. Sutures prevented fluid leakage underneath the LASIK flap, and this eye healed uneventfully, with a good refractive result after argon laser lysis of the suture. The availability of a more diverse pattern of astigmatic treatments, such as mixed astigmatism or irregular astigmatism, should reduce the need for concomitant astigmatic keratotomy.

PRK has also been used to treat residual refractive errors after penetrating keratoplasty, yet has been associated with haze in several other studies.<sup>15,27,57</sup> Haze in eyes that have PRK after radial keratotomy has also been reported.<sup>58</sup> It may be that patients who have had ocular surgery have a higher incidence of haze. These reports are of cases that occurred before mitomycin-C was used to reduce haze after PRK or phototherapeutic keratectomy.<sup>59,60</sup> So far, use of mitomycin-C with PRK has not been reported after penetrating keratoplasty; this may be useful for cases with some override or low endothelial cell count where the risk of epithelial ingrowth or poor flap adherence is high, but further study is required.

The results of therapeutic lamellar keratectomy were not as predictable in eyes with irregular astigmatism when compared with regular astigmatism. Newer ablation profile software and newer diagnostic techniques such as topography or wavefront guidance to refine the pattern of

ablation will need to be investigated in order to improve the quality of vision in eyes with irregular astigmatism after penetrating keratoplasty. Still, therapeutic lamellar keratectomy is useful for many patients with postkeratoplasty anisometropia or astigmatism where contact lenses or glasses correction is not tolerated. Careful patient selection, especially with attention to transplant alignment and endothelial cell density, can improve results.

## REFERENCES

1. Assil KK, Zarnegar SR, Schanzlin DJ. Visual outcome after penetrating keratoplasty with double continuous or combined interrupted and continuous suture wound closure. *Am J Ophthalmol* 1992;114:63-71.
2. Binder PS. Intraocular lens powers used in the triple procedure. Effect on visual acuity and refractive error. *Ophthalmology* 1985;92:1561-1566.
3. Clinch TE, Thompson HW, Gardner BP, et al. An adjustable double running suture technique for keratoplasty. *Am J Ophthalmol* 1993;116:201-206.
4. Davis EA, Azar DT, Jakobs FM, et al. Refractive and keratometric results after the triple procedure: experience with early and late suture removal. *Ophthalmology* 1998;105:624-630.
5. Perlman EM. An analysis and interpretation of refractive errors after penetrating keratoplasty. *Ophthalmology* 1981;88:39-45.
6. Samples JR, Binder PS. Visual acuity, refractive error and astigmatism after corneal transplantation for pseudophakic bullous keratopathy. *Ophthalmology* 1985;92:1554-1560.
7. Hardten DR, Lindstrom RL. Surgical correction of refractive errors after penetrating keratoplasty. *Int Ophthalmol Clin* 1997;37(1):1-35.
8. Perl T, Charlton KH, Binder PS. Disparate diameter grafting: astigmatism, intraocular pressure and visual acuity. *Ophthalmology* 1981;88:774-781.
9. Price FW Jr, Whitson WE, Marks RG. Progression of visual acuity after penetrating keratoplasty. *Ophthalmology* 1991;98:1177-1185.
10. Speaker MG, Cohen EJ, Edelhauser HF, et al. Effect of gas-permeable contact lenses on the endothelium of corneal transplants. *Arch Ophthalmol* 1991;109:1703-1706.
11. Amm M, Duncker GI, Schroder E. Excimer laser correction of high astigmatism after keratoplasty. *J Cataract Refract Surg* 1996;22:313-317.
12. Arenas E, Maglione A. Laser in situ keratomileusis for astigmatism and myopia after penetrating keratoplasty. *J Refract Surg* 1997;13:27-32.
13. Arffa RC. Results of a graded relaxing incision technique for postkeratoplasty astigmatism. *Ophthalmic Surg* 1988;19:624-628.
14. Belquiz R, Nassaralla A, Nassaralla JJ. Laser in situ keratomileusis after penetrating keratoplasty. *J Refract Surg* 2000;16:431-437.
15. Chan WK, Hunt KE, Glasgow BJ, et al. Corneal scarring after photorefractive keratectomy in a penetrating keratoplasty. *Am J Ophthalmol* 1996;121:570-571.
16. Dada T, Vajpayee RB. Lasik for astigmatism after PKP. *J Cataract Refract Surg* 2002;28:7-8.
17. Dada T, Vajpayee RB, Gupta V, et al. Microkeratome-induced reduction of astigmatism after penetrating keratoplasty. *Am J Ophthalmol* 2001;131:507-508.
18. Donnenfeld ED, Kornstein HS, Amin A, et al. Laser in situ keratomileusis for correction of myopia and astigmatism after penetrating keratoplasty. *Ophthalmology* 1999;106:1966-1974; discussion 1974-1975.
19. Epstein RJ, Robin JB. Corneal graft rejection episode after excimer laser phototherapeutic keratectomy. *Arch Ophthalmol* 1994;112:157.
20. Forseto AS, Francesconi CM, Nose RA, et al. Laser in situ keratomileusis to correct refractive errors after keratoplasty. *J Cataract Refract Surg* 1999;25:479-485.
21. Georgaras SP, Neos G, Margetis SP, et al. Correction of myopic anisometropia with photorefractive keratectomy in 15 eyes. *Refract Corneal Surg* 1993;9(Suppl 2):S29-34.
22. Gothard TW, Agapitos PJ, Bowers RA, et al. Four-incision radial keratotomy for high myopia after penetrating keratoplasty. *Refract Corneal Surg* 1993;9:51-57.
23. Hersh PS, Jordan AJ, Mayers M. Corneal graft rejection episode after excimer laser phototherapeutic keratectomy. *Arch Ophthalmol* 1993;111:735-736.
24. John ME, Martines E, Cvintal T, et al. Photorefractive keratectomy following penetrating keratoplasty. *J Refract Corneal Surg* 1994;10(Suppl 2):S206-210.
25. Koay PY, McGhee CN, Weed KH, et al. Laser in situ keratomileusis for ametropia after penetrating keratoplasty. *J Refract Surg* 2000;16:140-147.
26. Kwitko S, Marinho DR, Rymer S, et al. Laser in situ keratomileusis after penetrating keratoplasty. *J Cataract Refract Surg* 2001;27:374-379.
27. Lazzaro DR, Haight DH, Belmont SC, et al. Excimer laser keratectomy for astigmatism occurring after penetrating keratoplasty. *Ophthalmology* 1996;103:458-464.
28. Lugo M, Donnenfeld ED, Arentson JJ. Corneal wedge resection for high astigmatism following penetrating keratoplasty. *Ophthalmic Surg* 1987;18:650-653.
29. Maguire LJ, Bourne WM. Corneal topography of transverse keratotomies for astigmatism after penetrating keratoplasty. *Am J Ophthalmol* 1989;107:323-330.
30. Nassaralla BR, Nassaralla JJ. Laser in situ keratomileusis after penetrating keratoplasty. *J Refract Surg* 2000;16:431-437.
31. Nordan LT, Binder PS, Kassir BS, et al. Photorefractive keratectomy to treat myopia and astigmatism after radial keratotomy and penetrating keratoplasty. *J Cataract Refract Surg* 1995;21:268-273.
32. Parisi A, Salchow DJ, Zirm ME, et al. Laser in situ keratomileusis after automated lamellar keratoplasty and penetrating keratoplasty. *J Cataract Refract Surg* 1997;23:1114-1118.
33. Rashad KM. Laser in situ keratomileusis for correction of high astigmatism after penetrating keratoplasty. *J Refract Surg* 2000;16:701-710.
34. Spadea L, Mosca L, Balestrazzi E. Effectiveness of LASIK to correct refractive error after penetrating keratoplasty. *Ophthalmic Surg Lasers* 2000;31:111-120.

35. Troutman RC. Corneal wedge resections and relaxing incisions for postkeratoplasty astigmatism. *Int Ophthalmol Clin* 1983;23:161-168.
36. Tuunanen TH, Ruusuvaara PJ, Uusitalo RJ, et al. Photoastigmatic keratectomy for correction of astigmatism in corneal grafts. *Cornea* 1997;16:48-53.
37. Vajpayee RB, Dada T. LASIK after penetrating keratoplasty. *Ophthalmology* 2000;107:1801-1802.
38. Webber SK, Lawless MA, Sutton GL, et al. LASIK for post penetrating keratoplasty astigmatism and myopia. *Br J Ophthalmol* 1999;83:1013-1018.
39. Wiesinger-Jendritza B, Knorz MC, Hugger P, et al. Laser in situ keratomileusis assisted by corneal topography. *J Cataract Refract Surg* 1998;24:166-174.
40. Yoshida K, Tazawa Y, Demong TT. Refractive results of post penetrating keratoplasty photorefractive keratectomy. *Ophthalmic Surg Lasers* 1999;30:354-359.
41. Zaldivar R, Davidorf J, Oscherow S. LASIK for myopia and astigmatism after penetrating keratoplasty. *J Refract Surg* 1997;13:501-502.
42. Basuk WL, Zisman M, Waring GO III, et al. Complications of hexagonal keratotomy. *Am J Ophthalmol* 1994;117:37-49.
43. Neumann AC, McCarty GR. Hexagonal keratotomy for correction of low hyperopia: preliminary results of a prospective study. *J Cataract Refract Surg* 1988;14:265-269.
44. Pallikaris IG, Papatzanaki ME, Stathi EZ, et al. Laser in-situ keratomileusis. *Lasers Surg Med* 1990;10:463-468.
45. Hardten DR, Lindstrom RL. Management of LASIK complications. *Op Tech Cataract Refract Surg* 1998;1:32-39.
46. Hardten DR, Lindstrom RL, Samuelson TW, et al. Laser in situ keratomileusis for myopia. Results in a series of 415 eyes. *Med J Allina* 1999;8:23-26.
47. Knorz MC, Jendritza B. Topographically-guided laser in situ keratomileusis to treat corneal irregularities. *Ophthalmology* 2000;107:1138-1143.
48. Tamayo G, Fernandez GE, Serrano MG. Early clinical experience using custom excimer laser ablations to treat irregular astigmatism. *J Cataract Refract Surg* 2000;26:1442-1450.
49. Hjortdal JO, Ehlers N. Treatment of post-keratoplasty astigmatism by topography supported customized laser ablation. *Acta Ophthalmol Scan* 2001;79:376-380.
50. MacRae SM, Williams DR. Wavefront guided ablation. *Am J Ophthalmol* 2001;132:915-919.
51. Panagopoulou SI, Pallikaris IG. Wavefront customized ablations with the WASCA Asclepion workstation. *J Refract Surg* 2001;17:S608-612.
52. Portellinha W, Kuchenbuk M, Nakano K, et al. Interface fluid and diffuse corneal edema after laser in situ keratomileusis. *J Refract Surg* 2001;17(Suppl):S192-S195.
53. Bell KD, Campbell RJ, Bourne WM. Pathology of late endothelial failure: study with light and electron microscopy. *Cornea* 2000;19:40-46.
54. Bourne WM, Hodge DO, Nelson LR. Corneal endothelium five years after transplantation. *Am J Ophthalmol* 1994;118:185-196.
55. Kus MM, Seitz B, Langenbucher A, et al. Endothelium and pachymetry of clear corneal grafts 15 to 33 years after penetrating keratoplasty. *Am J Ophthalmol* 1999;127:600-602.
56. Collins MJ, Carr JD, Stulting RD, et al. Effect of laser in situ keratomileusis on the corneal endothelium 3 years post-operatively. *Am J Ophthalmol* 2001;131:1-6.
57. Bilgihan K, Ozdek SC, Akata F, et al. Photorefractive keratectomy for post-penetrating keratoplasty myopia and astigmatism. *J Cataract Refract Surg* 2000;26:1590-1595.
58. Azar DT, Tuli S, Benson RA, et al. Photorefractive keratectomy for residual myopia after radial keratotomy. PRK after RK Study Group. *J Cataract Refract Surg* 1998;24:303-311.
59. Majmudar PA, Forstot SL, Dennis RF, et al. Topical mitomycin-C for subepithelial fibrosis after refractive corneal surgery. *Ophthalmology* 2000;107:89-94.
60. Schipper I, Suppelt C, Gebbers JO. Mitomycin C reduces haze formation after excimer laser (193 nm) photorefractive keratectomy in rabbits. *Eye* 1997;11:649-655.

## DISCUSSION

---

DR WALTER J. STARK. It is my pleasure to discuss the presentation by Drs Richard Lindstrom and David Hardten on the analysis of LASIK for the correction of refractive errors after penetrating keratoplasty. The authors have presented results on 57 eyes of 48 patients who underwent LASIK for a wide range of refractive errors after penetrating keratoplasty. Fifteen of the cases also had astigmatic keratotomy. The spherical errors of the eyes ranged from -0.75 diopters to -16.25 diopters and a cylindrical error ranged from 0.5 diopters to 10 diopters. Seventy-two percent of the eyes had significant irregular astigmatism, which could not be fully treated with the lasers used in the study. Forty-seven percent of patients had keratoconus, as one would expect for patients having high astigmatic and refractive errors after penetrating keratoplasty. Follow-up was 91% at a year, 41% at two years, and 21% at 3 years. Best spectacles corrected vision improved or remained the same in 74% of eyes and decreased in 28% of eyes.

The authors' results parallel the short-term results of others that have been referenced in their articles, including a paper in the journal *Ophthalmology* by Dr Eric Donnenfeld in 1999, where 59% of his 21 patients had keratoconus. After publication of Donnenfeld's article and review of Hardten's paper, I have had concern about LASIK in patients who have had keratoplasty for keratoconus. These patients have keratoconus in the recipient bed and will have instability of the recipient cornea over time. I have seen numerous keratoconus patients 20 years after keratoplasty where there is progressive thinning of the cornea at the inferior graft-host junction, with progression of the keratoconus in the inferior recipient bed. My concern is that a LASIK procedure, where the microkeratome cuts through this recipient cornea, will lead to progressive ectasia of the recipient bed and instability of the postoperative refraction. I contacted Dr Eric Donnenfeld last week to get information on long-term

follow-up on his keratoconus patients who have had LASIK after keratoplasty. He has noted some progression of ectasia in the recipient cornea, and therefore he has switched to performing PRK rather than LASIK in these keratoconus eyes. Haze has been a reported problem after PRK in corneal graft, and we have seen this in our cases. To reduce the chances of haze, he is using mitomycin-C 0.02% for 20 to 30 seconds. Also, newer lasers that give a smoother corneal bed may lead to less haze and regression in these cases.

For nonkeratoconus eyes after keratoplasty where there is good donor-recipient healing and regular astigmatism, LASIK may be the preferred option to PRK to reduce ametropia, but there are still some concerns about LASIK in eyes after keratoplasty. The keratome cut alone has been shown to cause major changes in the astigmatism. Therefore, some advocates of this procedure recommend a keratome cut of the cornea with no laser treatment, followed by refraction 1 month later, and then lifting the flap for laser treatment of the residual refractive error. In my opinion, this would increase the rate of complications, especially epithelial ingrowth under the flap, which occurred at a rate 16% in Lindstrom's series and was serious enough to require removal in 7% of eyes.

Cutting the corneal flap does put some stress on the graft-host junction. We have seen patients who have had disruption of their graft-host junction 20 years after keratoplasty from seemingly minor trauma. Therefore, disruption of the graft-host junction must be considered as a potential complication with this procedure.

Finally, a good contact lens service makes a corneal transplant service successful. Over 50% of cornea transplant recipients will have 4 diopters or more of astigmatism, and in many cases this will be irregular astigmatism. These patients will achieve their best-corrected visual acuity only with a contact lens. At this time, irregular astigmatism is difficult to treat with a laser. Therefore, we recommend repeated attempts at contact lens correction before considering LASIK or PRK in eyes after keratoplasty.

In the discussion, I would like Dr Lindstrom to comment on the percent of eyes still requiring a contact lens after LASIK for functional vision and provide some information on patient satisfaction. For contact lens-intolerant eyes we are hopeful that in the future, topographically controlled lasers and custom corneal ablations that can correct irregular astigmatism will lead to better results in complicated cases, such as those presented by Dr Lindstrom and his associates. The authors are to be commended for their work on the complicated eyes after keratoplasty.

DR VERINDER S. NIRANKARI. We presented a similar paper at the Academy two years ago looking at high

astigmatism and anisometropia in patients following PK. Our results were very similar. It would be very helpful to know which patients should not have LASIK after PK. We had three patients that developed flap adherence problems after LASIK, and all three required another PK. At what level of endothelial cell counts or pachymetry readings is the LASIK contraindicated?

DR JAMES C. BOBROW. How long after graft surgery were the LASIK procedures performed? How did you handle the problem of peripheral vascularization? Were there any special techniques for using the microkeratome? Are there any control groups or prior studies to compare these results against?

DR RICHARD C. TROUTMAN. I have no experience with LASIK. The most difficult cases of astigmatism to treat, either by relaxing incision or wedge resection, have been patients that had keratoconus for a long time. These patients had temporized with contact lenses. When you trephine the cornea in these patients, the peripheral cornea drops back on the iris. In these situations, you are going to have high astigmatism postoperatively.

DR RICHARD L. LINDSTROM. The patients were 1 year to 20 years postkeratoplasty; all were at least 1 month after all suture removal. The surgical technique with the microkeratome was routine; there were no intraoperative complications with the keratome. We are believers in a one-stage procedure, because, as we have looked at our data in routine LASIK eyes, the complication rate of an enhancement is about three times the complication rate of a primary procedure. So, in our experience, flap-lift enhancements have a higher complication rate than a primary LASIK procedure. Thus, subjecting the patient to two operations with an increased risk of complications does not make sense to us.

The cases not to do, or at least the ones that we are not going to do, Dr Nirankari, are the ones that have significant graft override, or very low cell counts. We are concerned about our keratoconus patients, Dr Stark, and we are watching those. Some of them do show inferior ectasia on their topography, and it may be progressive and that certainly would be a concern. We do have a good contact lens service, and we do fit a lot of patients with contact lenses that are referred for keratoplasty or LASIK after keratoplasty.

As an aside, I rarely disagree with my senior colleague, Dr Troutman, but there are two schools of thought on treating keratoconus. One of them is early surgery, if you will, a prophylactic keratoplasty, for keratoconus. We don't believe in that. We basically wait until patients become contact lens-intolerant before recommending

keratoplasty. We do not think that a keratoplasty stops the process of keratoconus. The same issue that was mentioned by Dr Stark, that the ectasia can continue after keratoplasty, leads us to wait until patients are contact lens-intolerant before we operate. We find one way to

make a patient contact lens-tolerant is to operate on the first eye. Bilateral contact lens-intolerant patients often become contact lens-tolerant in their second eye after they have had keratoplasty surgery in the first eye.

# VITREOUS PENETRATION OF ORALLY ADMINISTERED GATIFLOXACIN IN HUMANS

---

BY Seenu M. Hariprasad, MD (BY INVITATION), William F. Mieler, MD, AND Eric R. Holz, MD (BY INVITATION)

## ABSTRACT

**Purpose:** To investigate the penetration of gatifloxacin, a novel extended-spectrum fluoroquinolone antibiotic, into the vitreous humor after oral administration.

**Methods:** A prospective, nonrandomized clinical study of 20 consecutive patients scheduled for pars plana vitrectomy surgery between September 2001 and February 2002 at the Cullen Eye Institute, Houston, Texas. Aqueous, vitreous, and serum samples were obtained and analyzed from 20 patients after oral administration of two 400-mg gatifloxacin tablets taken 12 hours apart before surgery. Assays were performed using high-performance liquid chromatography.

**Results:** Mean gatifloxacin concentrations in serum (n=19), vitreous (n=19), and aqueous (n=10) were  $4.98 \pm 1.14$   $\mu\text{g/mL}$ ,  $1.35 \pm 0.36$   $\mu\text{g/mL}$ , and  $1.09 \pm 0.57$   $\mu\text{g/mL}$ , respectively. Mean sampling times after oral administration of the second gatifloxacin tablet for serum, vitreous, and aqueous were  $2.99 \pm 0.73$  hours,  $3.79 \pm 0.81$  hours, and  $3.71 \pm 0.87$  hours, respectively. The percentages of serum gatifloxacin concentration achieved in the vitreous and aqueous were 27.13% and 21.85%, respectively. Mean inhibitory vitreous and aqueous MIC<sub>90</sub> levels were achieved against a wide spectrum of pathogens, including *Staphylococcus epidermidis*, *Staphylococcus aureus*, *Streptococcus pneumoniae*, *Streptococcus pyogenes*, *Propionibacterium acnes*, *Haemophilus influenzae*, *Escherichia coli*, *Bacillus cereus*, *Neisseria gonorrhoeae*, *Proteus mirabilis*, and other organisms.

**Conclusions:** Gatifloxacin is a novel fourth-generation fluoroquinolone antibiotic that has MIC<sub>90</sub> levels significantly lower than those of other fluoroquinolone agents. Furthermore, it penetrates well into the vitreous cavity in the noninflamed eye. Potential uses for oral gatifloxacin may include prophylaxis against endophthalmitis in open-globe injuries, surgical prophylaxis against postoperative endophthalmitis, and adjunctive therapy for the current management of bacterial endophthalmitis.

*Trans Am Ophthalmol Soc* 2002;100:153-160

## INTRODUCTION

---

Bacterial endophthalmitis is one of the most serious complications of intraocular surgery and open-globe injuries. The microbiologic spectrum of infecting organisms in postoperative endophthalmitis was investigated in the Endophthalmitis Vitrectomy Study (EVS). The EVS represents the largest number of postoperative endophthalmitis cases from which bacteriologic data were prospectively obtained. The vast majority (94.2%) of confirmed growth isolates were gram-positive pathogens, most commonly *Staphylococcus epidermidis* and *Staphylococcus aureus*. Gram-negative pathogens, the most common being *Proteus mirabilis*, accounted for only 5.9% of confirmed growth isolates.<sup>1</sup> The spectrum of

infecting organisms in posttraumatic endophthalmitis differs from those of postoperative endophthalmitis, with *Bacillus* species playing a more prominent role.<sup>2</sup>

The EVS investigated the use of intravenous amikacin and ceftazidime in conjunction with intravitreal antibiotic injection for postoperative endophthalmitis and found no improved outcomes with the use of systemic antibiotics.<sup>3</sup> Later studies found that amikacin and ceftazidime had very poor intravitreal penetration.<sup>4,5</sup> On the basis of the EVS data, the only conclusion that can be drawn regarding the use of systemic antibiotics is that amikacin and ceftazidime specifically have no role in postoperative endophthalmitis. Since the EVS, there have been major advancements in the development of antibiotics, and the potential uses of these new-generation agents in the treatment of endophthalmitis need to be revisited. Over the past 10 years, there has been mounting evidence in the literature that agents in the fluoroquinolone class of antibiotics are able to achieve effective concentrations in the vitreous after oral administration.<sup>6-8</sup>

From the Department of Ophthalmology, Cullen Eye Institute, Baylor College of Medicine, Houston, Texas. Supported by a grant from the Bristol-Myers Squibb Company and by an unrestricted grant from Research to Prevent Blindness, Inc, New York, New York.

Gatifloxacin is a fourth-generation, 8-methoxy fluoroquinolone with a spectrum of activity encompassing gram-positive and gram-negative pathogens, including *S epidermidis*, *S aureus*, *Streptococcus pneumoniae*, *Streptococcus pyogenes*, *Haemophilus influenzae*, *Escherichia coli*, *Bacillus cereus*, *Neisseria gonorrhoeae*, and *P mirabilis*. Additionally, gatifloxacin has excellent activity against atypical pathogens, such as *Mycoplasma*, *Legionella*, and *Chlamydia* species, as well as the anaerobic organism *Propionibacterium acnes*.<sup>9,10</sup> Gatifloxacin has 96% oral bioavailability and can be administered without regard to food, reaching peak plasma concentrations 1 to 2 hours after oral dosing. Serum protein binding of gatifloxacin is only 20% and is widely distributed throughout the body into many body tissues and fluids. The new fluoroquinolones, such as gatifloxacin, grepafloxacin, moxifloxacin, and trovafloxacin, represent advances in the evolution of this antibiotic class. The more favorable pharmacokinetic properties of the previously mentioned

agents are due to alterations of the original fluoroquinolone moiety. For example, gatifloxacin and moxifloxacin possess an 8-methoxy side chain, which may be responsible for the enhanced activity against gram-positive, atypical pathogens and anaerobes while retaining potencies and broad-spectrum coverage against gram-negative organisms comparable to older-generation fluoroquinolones.<sup>10</sup>

We chose to study the intravitreal penetration of orally administered gatifloxacin in humans for two reasons. First, older-generation fluoroquinolones, such as ofloxacin, ciprofloxacin, and levofloxacin, have been shown to achieve effective levels in the vitreous after oral administration in the noninflamed eye.<sup>6,8</sup> Second, the MIC<sub>90</sub> values of gatifloxacin against the pathogens most commonly responsible for postoperative, posttraumatic, and bleb-associated endophthalmitis were generally lower than those of the other fluoroquinolone antibiotics we surveyed (Table I).<sup>9,10</sup>

TABLE I: IN VITRO SUSCEPTIBILITIES OF GATIFLOXACIN, LEVOFLOXACIN, OFLOXACIN, AND CIPROFLOXACIN SHOWING MINIMUM INHIBITORY CONCENTRATIONS AT WHICH 90% OF ISOLATES ARE INHIBITED (µg/mL)<sup>8-10</sup>

ORGANISMS	GATIFLOXACIN	LEVOFLOXACIN	OFLOXACIN	CIPROFLOXACIN
Maximum vitreous penetration	1.35 ± 0.36 µg/mL	2.39 ± 0.70 µg/mL	0.43 ± 0.47 µg/mL	0.56 ± 0.16 µg/mL
Gram-positive				
<i>Staphylococcus epidermidis</i> <sup>°†‡</sup>	0.25	0.50	0.50-0.83	0.38
<i>Staphylococcus aureus</i> (MSSA) <sup>°†</sup>	0.13	0.25	0.25-2.00	0.80
<i>Streptococcus pneumoniae</i> <sup>°†‡</sup>	0.50	2.00	2.00-4.00	3.13
<i>Streptococcus pyogenes</i>	0.50	1.00	1.00-4.00	0.78
<i>Bacillus cereus</i>	0.25	---	---	---
<i>Enterococcus faecalis</i> <sup>°</sup>	2.00	2.00	2.00-8.00	1.56
Gram-negative				
<i>Proteus mirabilis</i> †	0.25	0.25	0.12-0.39	0.27
<i>Pseudomonas aeruginosa</i>	32.0	32.0	---	0.78
<i>Haemophilus influenzae</i> ‡	0.016	0.06	0.03-0.10	0.014
<i>Escherichia coli</i>	0.008	0.03	0.12-0.39	0.08
<i>Klebsiella pneumonia</i>	0.13	0.13	0.12-0.19	0.30
<i>Neisseria gonorrhoea</i>	0.016	0.016	0.06	0.004
Anaerobic				
<i>Bacteroides fragilis</i>	1.00	2.00	4.0-12.5	---
<i>Propionibacterium acnes</i> §	0.50	0.75	1.50	---

MSSA, methicillin-sensitive *S aureus*.

<sup>°</sup>Responsible for more than 2% of postoperative endophthalmitis.<sup>1</sup>

<sup>†</sup>Associated with endophthalmitis resulting from ocular trauma.<sup>2</sup>

<sup>‡</sup>Most common causative organisms in bleb-associated endophthalmitis.<sup>14</sup>

<sup>§</sup>Most common causative organisms in chronic postoperative endophthalmitis.<sup>12</sup>

|| On file, Briston-Myers Squibb Co (SENTRY Global Antimicrobial Surveillance System 1997-2000).

¶Data not available.

**METHODS**

The study was carried out with the approval of the institutional review board of Baylor College of Medicine. Twenty adult patients (age range, 39-82 years; mean age  $\pm$ SD, 64.4  $\pm$  12.2 years) who underwent elective pars plana vitrectomy surgery between September 2001 and February 2002 at the Cullen Eye Institute were included in the study. Exclusion criteria included the following: known sensitivity to fluoroquinolones, renal disease (creatinine, >1.8 mg/dL), use of any other antibiotic in the preceding 3 weeks, pregnancy or currently breast-feeding, current use of a class IA or III antiarrhythmic agent, fresh vitreous hemorrhage as indication for vitrectomy (<1 month old), and active endophthalmitis.

Indications for operation in the 20 patients were as follows (Table II): epiretinal membrane (11 patients), macular hole (5), retinal detachment (2), nonclearing vitreous hemorrhage (1), and tractional retinal detachment secondary to proliferative diabetic retinopathy (1).

After informed consent was obtained, patients were asked to take two 400-mg gatifloxacin tablets orally 12 hours apart before surgery. Prospectively completed data forms were designed to include medical history, collection times of various samples, and concentrations of gatifloxacin in serum, aqueous, and vitreous. Patients were asked to record on each of the two gatifloxacin blister packs the exact time of oral administration. These packs

were returned on the day of surgery. Aqueous, vitreous, and serum samples were obtained before infusion of any intravenous or intraocular irrigating solution in order to obtain pure samples. Approximately 8 to 10 mL of venous blood was collected less than 1 hour prior to surgery in the preoperative holding area. In the operative suite, approximately 0.1 mL of aqueous fluid was aspirated with a 30-gauge needle attached to a syringe through a paracentesis site in those patients in whom it was felt safe to do so (ie, pseudophakic patients or phakic patients with deep anterior chambers). Within 10 minutes, 0.2 to 0.3 mL of vitreous fluid was obtained by using a vitreous cutting device attached to a syringe via a short length of tubing.

Aqueous and vitreous samples were immediately frozen at -20°C. The blood sample was centrifuged, and the serum collected from this was frozen as well. These samples were shipped with dry ice in appropriate packaging material to the Hartford Hospital Laboratory, Hartford, Connecticut. Gatifloxacin concentrations were determined in each of the samples by using a previously described high-performance liquid chromatography technique.<sup>11</sup> Serum, aqueous, and vitreous gatifloxacin concentrations were compared to already established in vitro MIC<sub>90</sub> data.<sup>9,10</sup> Student's *t* test was performed to determine if any significant differences existed between various subsets of patients, including diabetic versus nondiabetic patients and phakic status.

TABLE II: SERUM, AQUEOUS, AND VITREOUS LEVELS (µG/ML) OF GATIFLOXACIN AFTER SECOND ORAL DOSE

PATIENT NO.	AGE	HOURS FROM SECOND DOSE TO VITREOUS	INDICATION FOR SURGERY	DIABETIC	SERUM (µg/mL)	AQUEOUS (µg/mL)	VITREOUS (µg/mL)
1	70	4.67	ERM	No	5.19	*	1.27
2	77	2.20	MH	No	4.86	1.02	1.57
3	54	4.12	RD	No	4.26	0.34	1.33
4	51	3.83	MH	No	4.81	0.68	0.98
5	72	3.50	ERM	No	4.04	†	0.62
6	78	5.25	ERM	No	7.18	†	1.70
7	68	4.67	ERM	Yes	5.77	†	1.38
8	82	3.50	ERM	No	4.76	1.12	1.23
9	81	3.42	ERM	No	5.72	1.34	1.14
10	73	3.25	MH	No	6.70	2.39	2.05
11	39	5.75	ERM	No	2.93	0.932	0.95
12	55	3.25	ERM	No	5.49	1.518	1.75
13	44	3.50	NCVH	No	3.65	0.834	1.45
14	63	3.75	ERM	No	2.85	0.701	0.83
15	67	3.50	TRD	Yes	5.35	*	1.15
16‡	72	3.00	ERM	No	4.67	†	*
17	66	3.17	RD	No	4.60	†	1.46
18	67	3.67	MH	No	4.61	†	1.44
19	61	3.50	MH	No	6.15	†	1.60
20	55	3.50	ERM	No	5.65	†	1.76

ERM, epiretinal membrane; MH, macular hole; NCVH, nonclearing vitreous hemorrhage; RD, retinal detachment; TRD, tractional retinal detachment.

\*Insufficient sample volume.

†Sample not taken because of risk of compromising surgical procedure.

‡Patient data not included in study.

## RESULTS

Mean gatifloxacin concentrations in serum (n=19), vitreous (n=19), and aqueous (n=10) were  $4.98 \pm 1.14$   $\mu\text{g/mL}$ ,  $1.35 \pm 0.36$   $\mu\text{g/mL}$ , and  $1.09 \pm 0.57$   $\mu\text{g/mL}$ , respectively. Mean sampling times after oral administration of the second gatifloxacin tablet for serum, vitreous, and aqueous were  $2.99 \pm 0.73$  hours,  $3.79 \pm 0.81$  hours, and  $3.71 \pm 0.87$  hours, respectively. The percentages of serum gatifloxacin concentration achieved in the vitreous and aqueous were 27.13% and 21.85%, respectively (Table II).

Patient 16 was removed from the study because no aqueous specimen was collected and there was an insufficient vitreous sample volume to perform HPLC. Although a serum gatifloxacin concentration was determined on this patient, it was not felt that this added any value to the purpose of the study, and therefore this patient's data was removed from any data analysis.

Two of the 19 patients were diabetic. The mean gatifloxacin concentrations in the serum and vitreous for these two patients were  $5.56 \pm 0.30$   $\mu\text{g/mL}$  and  $1.26 \pm 0.16$   $\mu\text{g/mL}$ , respectively (Table II). These levels were not significantly different from those of the 17 nondiabetic patients, whose serum and vitreous concentrations were  $4.91 \pm 1.19$   $\mu\text{g/mL}$  and  $1.36 \pm 0.37$   $\mu\text{g/mL}$ , respectively ( $P=.46$  and  $P=.73$ , respectively).

Eight of the 19 patients were phakic. The mean gatifloxacin concentrations in the serum, vitreous, and aqueous for these eight patients were  $4.83 \pm 0.87$   $\mu\text{g/mL}$ ,  $1.24 \pm 0.32$   $\mu\text{g/mL}$ , and  $0.62 \pm 0.25$   $\mu\text{g/mL}$ , respectively. These levels were not significantly different from that of the one aphakic and 10 pseudophakic patients whose serum, vitreous, and aqueous concentrations were  $5.08 \pm 1.34$   $\mu\text{g/mL}$ ,  $1.43 \pm 0.38$   $\mu\text{g/mL}$ , and  $1.29 \pm 0.55$   $\mu\text{g/mL}$ , respectively ( $P=.65$ ,  $P=.28$ , and  $P=.09$ , respectively).

No serious adverse reactions were attributed to the antibiotic agent. One patient complained of mild gastrointestinal discomfort. Another patient (patient 7) vomited 30 minutes after taking the second gatifloxacin dose. The concentrations of gatifloxacin in serum and vitreous in this patient were  $5.77$   $\mu\text{g/mL}$  and  $1.38$   $\mu\text{g/mL}$ , respectively (Table II). These values were above the mean of the rest of the group.

## DISCUSSION

Endophthalmitis is one of the most serious complications of intraocular procedures or open-globe trauma. Systemic antibiotics have had an uncertain role in the prophylaxis or management of endophthalmitis as the EVS was unable to demonstrate any benefit with the use of intravenous antibiotics in postoperative infection.<sup>3</sup> Over the past 10 years, several studies have indicated that

fluoroquinolone antibiotics achieve significant concentrations in the vitreous after oral administration.<sup>6-8</sup> Unfortunately, many of the older-generation fluoroquinolones achieved intravitreal levels that barely reached the  $\text{MIC}_{90}$  against the pathogens most commonly responsible for postoperative, posttraumatic, and bleb-associated endophthalmitis. If one is to consider the use of a systemic antibiotic for the prophylaxis of, or as an adjunct in the management of, endophthalmitis, one must find a systemic antibiotic with the highest possible intravitreal penetration as well as the lowest  $\text{MIC}_{90}$  for the organisms of concern. We believe that gatifloxacin may represent a major advance in this regard.

After cataract extraction, bacterial endophthalmitis is most commonly caused by *S epidermidis* (70% of EVS isolates).<sup>1</sup> The endophthalmitis typically presents as a moderately severe infection 5 to 7 days after surgery. Less commonly, two other forms of endophthalmitis can take place after cataract extraction. The first is a chronic, indolent endophthalmitis that presents several months after surgery and is usually caused by *P acnes*.<sup>12</sup> A second, less common form of postoperative endophthalmitis is an early, fulminant type usually presenting 2 to 4 days after surgery, which is caused by streptococcal or staphylococcal species, as well as gram-negative organisms (most commonly *P mirabilis*).<sup>1</sup> In our study, vitreous levels of gatifloxacin were 5.4 times the  $\text{MIC}_{90}$  for *S epidermidis*, 10.4 times the  $\text{MIC}_{90}$  for *S aureus*, 2.7 times the  $\text{MIC}_{90}$  for *P acnes*, 2.7 times the  $\text{MIC}_{90}$  for *Streptococcus* species, and 5.4 times the  $\text{MIC}_{90}$  for *P mirabilis*. Gatifloxacin was unable to achieve intravitreal levels effective against *Enterococcus* or *Pseudomonas*. Fortunately, these two organisms are only very rarely encountered in postoperative endophthalmitis.<sup>1</sup>

The importance of finding a good bacterial endophthalmitis prophylaxis technique for cataract surgery was emphasized in a recent study by Ciulla and associates.<sup>13</sup> Performing a systematic review of the literature from 1966 to 2000 to assess commonly used techniques of bacterial endophthalmitis prophylaxis for cataract surgery, they found that only preoperative povidone-iodine preparation could receive a moderate clinical recommendation (moderately important to clinical outcome). All other measures received the lowest clinical recommendation level (possibly relevant but not definitely related to clinical outcome). Furthermore, the study revealed that no prophylactic technique in the literature could receive the highest of three possible clinical recommendations (crucial to clinical outcome).<sup>13</sup> Unfortunately, systemic antibacterial agents were not included in this study. Given our findings, one could consider the use of oral gatifloxacin before and after surgery as prophylaxis against endophthalmitis. Ciulla and associates<sup>13</sup> estimate that

there are nearly 2,000 cases of endophthalmitis after cataract surgery alone annually in the United States. If all intraocular surgeries and cases of open-globe trauma were included, this number would be far greater. Therefore, the importance of finding good prophylaxis against postoperative endophthalmitis cannot be underestimated.

Conjunctival filtering bleb-associated endophthalmitis can occur any time after trabeculectomy surgery. Infection of the bleb alone, or "blebitis," can sometimes be managed with intensive topical antibiotics. The most common causative organisms in bleb-associated endophthalmitis are *S epidermidis* and *H influenzae*.<sup>14</sup> The level of gatifloxacin achieved in the aqueous and vitreous were about 68 and 84 times the MIC<sub>90</sub> for *H influenzae*, respectively. Gatifloxacin may prove to be valuable in the management of blebitis or as an adjunct in the current management of bleb-associated endophthalmitis.

The role of systemic antibiotics in open-globe trauma deserves special attention. Posttraumatic endophthalmitis occurs in 2% to 7% of all open-globe injuries and in 7% to 13% of injuries with retained intraocular foreign bodies.<sup>15,16</sup> Injuries that occur in a rural setting result in up to a 30% incidence of endophthalmitis compared with 11% in a non-rural setting.<sup>17</sup> *Staphylococcus*, *Streptococcus*, and *Bacillus* species are the most commonly encountered organisms in posttraumatic endophthalmitis.<sup>18</sup> While the role and significance of intravenous antibiotics in the treatment of infection associated with open-globe trauma remain unresolved, Ariyasu and colleagues<sup>19</sup> studied events leading to the development of posttraumatic endophthalmitis by examining the significance of 15 factors on microbial contamination of injured eyes. Only intravenous antibiotic therapy was found to significantly reduce anterior chamber microorganisms at the time of surgical repair, supporting their prophylactic use against the development of posttraumatic endophthalmitis.

On the basis of Ariyasu's findings and the known high incidence of endophthalmitis after open-globe injuries, the prompt and routine use of systemic antibiotics for prophylaxis against infection in the setting of trauma needs to be further explored. The choice of antibiotic will be one that meets the following criteria: achieves high intravitreal concentrations well above the MIC<sub>90</sub> for the specific organisms of concern, is well tolerated, and preferably is one that achieves excellent bioavailability with oral administration. Gatifloxacin fulfills these criteria. The levels achieved in the aqueous and vitreous were several times higher than the MIC<sub>90</sub> levels for those organisms that are most commonly associated with posttraumatic endophthalmitis (Table I). In addition, previous studies suggest that intraocular penetration of systemic antibiotics may be higher in an eye that has sustained trauma, is infected, or is inflamed. This may be due to disruption of the blood-ocular barrier.<sup>20,21</sup>

The guidelines set forth by the EVS regarding the management of postoperative endophthalmitis should not be translated to posttraumatic endophthalmitis.<sup>3</sup> The incidence of endophthalmitis from open-globe trauma is many times greater than after ocular surgery. In addition, up to 42% of cases from rural areas have more than one organism cultured; often, more virulent bacteria are isolated in posttraumatic endophthalmitis than in postoperative endophthalmitis. For example, *Bacillus* infections are rare in postoperative endophthalmitis but may occur with a frequency of 20% to 46% in posttraumatic cases.<sup>17</sup> *Bacillus* produces severe, rapidly progressive endophthalmitis. Therefore, in the setting of open-globe trauma, rapid administration of an oral antibiotic known to penetrate into the posterior segment may help prevent ocular damage secondary to infection. On the basis of our data, it appears that oral administration of gatifloxacin may be a promising choice for prophylaxis against endophthalmitis in open-globe injuries before and after surgical intervention.

Two groups have recently studied the fourth-generation fluoroquinolones for possible use in ophthalmology. Mather and associates<sup>22</sup> have described the fourth-generation fluoroquinolones as "new weapons in the arsenal of ophthalmic antibiotics." They performed an in vitro study determining the differences in susceptibility patterns and potencies of second-, third-, and fourth-generation fluoroquinolones to 93 bacterial endophthalmitis isolates. They demonstrated that coagulase-negative staphylococci that were resistant to second-generation fluoroquinolones (ciprofloxacin and ofloxacin) were statistically most susceptible to the fourth-generation fluoroquinolones, specifically gatifloxacin and moxifloxacin. Additionally, *S viridans* and *S pneumoniae* were least susceptible to the older-generation fluoroquinolones. Overall, the fourth-generation fluoroquinolones retained equivalent potencies to gram-negative bacteria as compared to older-generation fluoroquinolones such as levofloxacin and ciprofloxacin while demonstrating enhanced potencies for gram-positive bacteria.

In another recent study, Garcia-Saenz and associates<sup>23</sup> investigated the penetration of orally administered moxifloxacin into the human aqueous humor as a potential prophylactic agent against bacterial endophthalmitis in cataract surgery. They found that moxifloxacin achieved a mean aqueous concentration of 2.33 ± 0.85 µg/mL; however, their reported MIC<sub>90</sub> for *S epidermidis* was 2.00. The concentration achieved is borderline for the most common causative organism in postoperative endophthalmitis. This is not the case with gatifloxacin, as intraocular concentrations after oral administration were found to be several times higher than the MIC<sub>90</sub> for *S epidermidis*. Additionally, penetration of moxifloxacin into the vitreous was not investigated; therefore, no conclusions can be made regarding its use in open-globe trauma involving the

posterior segment or its use as an adjunctive therapy for endophthalmitis management.

Overall, gatifloxacin is very well tolerated; the majority of adverse reactions are described as mild. The most common ones include nausea, vaginitis, diarrhea, headache, and dizziness. In our series, one patient complained of mild gastrointestinal discomfort and another (patient 7) vomited 30 minutes after taking the second gatifloxacin dose. The concentrations of gatifloxacin in serum and vitreous in this patient were above the mean of the rest of the group. Since gatifloxacin is eliminated primarily by renal excretion, a dosage modification is recommended for patients with a creatinine clearance of less than 40 mL/min. Gatifloxacin should be avoided in patients receiving a class IA (quinidine or procainamide) or class III (amiodarone or sotalol) antiarrhythmic agent, because gatifloxacin may have the potential to prolong the QTc interval of the electrocardiogram in some patients.

### SUMMARY

Orally administered gatifloxacin achieves therapeutic aqueous and vitreous levels in the noninflamed human eye, and the activity spectrum appears to appropriately encompass the most frequently encountered bacterial species involved in the various causes of endophthalmitis. Because of its broad spectrum of coverage, low MIC<sub>90</sub> levels for the organisms of concern, good tolerability, and excellent bioavailability with oral administration, gatifloxacin may represent a major advance in the prophylaxis or management of postoperative, posttraumatic, and bleb-associated bacterial endophthalmitis.

### ACKNOWLEDGMENTS

The authors gratefully acknowledge the following individuals for their respective contributions to this study: D'Anna Barrow, MD, Xioqui K. Sun, MD, Anita Austin, Sandy Owings, COA, Shana Noel, and the Hartford Hospital Laboratory (David P. Nicolau, PharmD, FCCP, and Christina Sutherland).

### REFERENCES

- Han DP, Wisniewski SR, Wilson LA, et al. Spectrum and susceptibilities of microbiologic isolates in the Endophthalmitis Vitrectomy Study. *Am J Ophthalmol* 1996;122:1-17.
- Affeldt JC, Flynn HW Jr, Forster RK, et al. Microbial endophthalmitis resulting from ocular trauma. *Ophthalmology* 1987;94:407-413.
- Endophthalmitis Vitrectomy Study Group. Results of the Endophthalmitis Vitrectomy Study: a randomized trial of immediate vitrectomy and of intravenous antibiotics for the treatment of postoperative bacterial endophthalmitis. *Arch Ophthalmol* 1995;113:1479-1496.
- el-Massry A, Meredith TA, Aguilar HE, et al. Aminoglycoside levels in the rabbit vitreous cavity after intravenous administration. *Am J Ophthalmol* 1996;122:684-689.
- Aguilar HE, Meredith TA, Shaarawy A, et al. Vitreous cavity penetration of ceftazidime after intravenous administration. *Retina* 1995;15:154-159.
- Keren G, Alhalel A, Barrov E, et al. The intravitreal penetration of orally administered ciprofloxacin in humans. *Invest Ophthalmol Vis Sci* 1991;32:2388-2392.
- Fiscella RG, Shapiro MJ, Solomon MJ, et al. Ofloxacin penetration into the eye after intravenous and topical administration. *Retina* 1997;17:535-539.
- Fiscella RG, Nguyen TKP, Cwik MJ, et al. Aqueous and vitreous penetration of levofloxacin after oral administration. *Ophthalmology* 1999;106:2286-2290.
- Bauernfeind A. Comparison of the antibacterial activities of the quinolones Bay 12-8039, gatifloxacin (AM 1155), trovafloxacin, cinafloxacin, levofloxacin, and ciprofloxacin. *J Antimicrob Chemother* 1997;40:639-651.
- Ednie LM, Jacobs MR, Appelbaum PC. Activities of gatifloxacin compared to those of seven other agents against anaerobic organisms. *Antimicrob Agents Chemother* 1998;42.9:2459-2462.
- Mattoes HM, Banevicius M, Li D, et al. Pharmacodynamic assessment of gatifloxacin against *Streptococcus pneumoniae*. *Antimicrob Agents Chemother* 2001;45.7:2092-2097.
- Clark WL, Kaiser PK, Flynn HW, et al. Treatment strategies and visual acuity outcomes in chronic postoperative *Propionibacterium acnes* endophthalmitis. *Ophthalmology* 1999;106:1665-1670.
- Ciulla TA, Starr MB, Masket S. Bacterial endophthalmitis prophylaxis for cataract surgery: an evidence-based update. *Ophthalmology* 2002;109:13-26.
- Kangas TA, Greenfield DS, Flynn HW Jr, et al. Delayed-onset endophthalmitis associated with conjunctival filtering blebs. *Ophthalmology* 1997;104:746-752.
- Parrish CM, O'Day DM. Traumatic endophthalmitis. *Int Ophthalmol Clin* 1987;27:112-119.
- Mieler WF, Ellis MK, Williams DF, et al. Retained intraocular foreign bodies and endophthalmitis. *Ophthalmology* 1990;97:1532-1538.
- Boldt HC, Pulido JS, Blodi CF, et al. Rural endophthalmitis. *Ophthalmology* 1989;96:1722-1726.
- Alfaro DV, Roth D, Liggett PE. Posttraumatic endophthalmitis. Causative organisms, treatment, and prevention. *Retina* 1994;14:206-211.
- Ariyasu RG, Kumar S, LaBree LD, et al. Microorganisms cultured from the anterior chamber of ruptured globes at the time of repair. *Am J Ophthalmol* 1995;119:181-188.
- Martin DF, Fisker LA, Aguilar HA, et al. Vitreous cefazolin levels after intravenous injection: effects of inflammation, repeated antibiotic doses, and surgery. *Arch Ophthalmol* 1990;108:411-414.
- Alfaro DV, Hudson SJ, Rafanan MM, et al. The effect of trauma on the ocular penetration of intravenous ciprofloxacin. *Am J Ophthalmol* 1996;122:678-683.
- Mather R, Karanchak LM, Romanowski EG, et al. Fourth generation fluoroquinolones: new weapons in the arsenal of ophthalmic antibiotics. *Am J Ophthalmol* 2002;133:463-466.

23. Garcia-Saenz MC, Arias-Puente A, Fresnadillo-Martinez MJ, et al. Human aqueous humor levels of oral ciprofloxacin, levofloxacin, and moxifloxacin. *J Cataract Refract Surg* 2001;27:1969-1974.

## DISCUSSION

---

DR MAURICE B. LANDERS III. Endophthalmitis remains a devastating complication of intraocular surgery and ocular trauma despite recent advances in diagnosis and treatment. Two thirds of these cases of endophthalmitis are postoperative. The outcome of treatment for postoperative endophthalmitis has improved dramatically during the past two decades. Some of the factors involved in these improved outcomes include: higher incidence of endophthalmitis produced by less virulent organisms; earlier diagnosis and treatment; widespread acceptance of intravitreal antibiotic therapy; employment of vitrectomy surgery; and control of the inflammation seen in endophthalmitis

The incidence of postoperative endophthalmitis over the past 2 decades, nevertheless, has declined only a little, if at all, during that time. Thus, effective prophylaxis of postoperative endophthalmitis remains an important and elusive goal for ophthalmic surgeons.

Doctors Hariprasad, Mieler, and Holz have presented a study of the vitreous penetration of orally administered fourth-generation extended-spectrum fluoroquinolone antibiotic, gatifloxacin, (TEQUIN) in humans. In a prospective, randomized clinical study of 20 consecutive patients undergoing elective pars plana vitrectomy, the serum, aqueous, and vitreous concentration of gatifloxacin was measured after the oral administration of two 400-milligram tablets taken 12 hours apart before surgery. No serious adverse reactions were found attributable to the antibiotic agent.

The levels of gatifloxacin found in the aqueous and vitreous specimens were compared to established in vitro MIC<sub>90</sub> data for a number of bacteria that may potentially cause endophthalmitis

The authors found that orally administered Gatifloxacin achieved therapeutic aqueous and vitreous levels in the non-inflamed human eye and that the antibiotic activity spectrum appears to appropriately encompass the most frequently encountered bacterial species involved in endophthalmitis. The authors found that this

novel fourth-generation fluoroquinolone antibiotic penetrates well into the vitreous cavity, exceeding MIC<sub>90</sub> levels of most bacteria of concern with the exception of the *Enterococcus faecalis* and pseudomonas bacteria. They conclude that oral gatifloxacin may prove useful for prophylaxis against post-operative endophthalmitis, traumatic endophthalmitis, and even as adjunctive therapy for the current treatment of bacterial endophthalmitis.

I have three questions for the authors of this excellent study: Is the rapidity of sterilization of the vitreous cavity in a case of endophthalmitis likely to be a function of the excess concentration of a bactericidal antibiotic over the MIC<sub>90</sub> for a particular organism?

Is anything known about the ocular toxicity of gatifloxacin given orally over a several day course of treatment? Would the administration of oral gatifloxacin in any way compromise the beneficial, antimicrobial effects of intravitreal vancomycin and ceftazidime administered in the standard doses?

DR ERIC R. HOLZ. Question 1: Is the rate of sterilization of the vitreous a function of antibiotic concentration? The answer to that, I think, is clearly yes. Drug levels have to exceed MIC<sub>90</sub> of the common pathogens in order to sterilize the anterior chamber or vitreous in endophthalmitis. Question 2, regarding the ocular toxicity of gatifloxacin: Certainly in previous studies that have been performed with oral gatifloxacin or other fourth-generation fluoroquinolones, patients receiving the drug for weeks at a time don't have any ocular toxicity that's been reported to date. Now, I must admit, we did not inject gatifloxacin into the vitreous; other fluoroquinolones injected into the vitreous have been shown to have some toxicity problems, so we have not administered this directly into the vitreous as a single injection, but we're looking, rather, at penetration after oral administration. Question 3: Could gatifloxacin compromise other antibiotic treatment? I guess the question is if you're going to put vancomycin and ceftazidime, or amikacin, into the vitreous to treat endophthalmitis, would gatifloxacin somehow compromise that treatment? I think the answer is unknown, but concurrent use should not interfere with the effectiveness of standard intravitreal antibiotics. I think gatifloxacin may be an adjunctive treatment that would not compromise the current treatment of endophthalmitis.



# ASSESSMENT OF THE RETINAL NERVE FIBER LAYER OF THE NORMAL AND GLAUCOMATOUS MONKEY WITH SCANNING LASER POLARIMETRY

---

BY Robert N. Weinreb, MD, Christopher Bowd, PhD (BY INVITATION), AND Linda M. Zangwill, PhD (BY INVITATION)

## ABSTRACT

*Purpose:* To describe and test a method for assessment of the monkey retinal nerve fiber layer (RNFL) with scanning laser polarimetry.

*Methods:* A scanning laser polarimeter was modified to accommodate a variable corneal polarization compensator. Corneal polarization magnitude (CPM) and corneal polarization axis (CPA) of the anterior segment birefringence of normal and glaucomatous cynomolgus monkey eyes were determined from a polarimetry image of the Henle fiber layer. Next, the variable compensator was adjusted to minimize the anterior segment birefringence. RNFL measurements were then obtained. All images were compared with simultaneous optic disc stereoscopic photographs.

*Results:* CPM was small in each of the eyes examined, ranging from 5.7 nm to 9.0 nm. CPA ranged from  $-62^{\circ}$  to  $79^{\circ}$ . (Nasally upward CPA values were recorded as negative; nasally downward CPA values were recorded as positive.) When eye-specific compensation was used, RNFL retardation profiles mimicked the expected appearance of the RNFL in all eyes. We also observed a substantial decrease in retardation in eyes with experimental glaucoma compared with healthy fellow eyes.

*Conclusions:* Individualized anterior segment compensation can be achieved in the monkey eye so that the measured birefringence appears to largely reflect the birefringence of the RNFL. Observed differences in retardation between healthy eyes and eyes with experimental glaucoma suggest that scanning laser polarimetry may be useful for detecting and monitoring RNFL loss in experimental primate glaucoma.

*Trans Am Ophthalmol Soc* 2002;100:161-168

## INTRODUCTION

---

Scanning laser polarimetry, an optical imaging technique based on the birefringence of the retinal nerve fiber layer (RNFL), has been used to obtain reproducible quantitative and objective measurements of the RNFL in human eyes.<sup>1-5</sup> Light refracted from the RNFL (an anisotropic structure) is polarized, resulting in two refracted rays. One of the rays travels with the same velocity along the optical axis of the tissue (fast axis of polarization), while the other ray travels with a velocity that is dependent on the propagation direction within the tissue (slow axis of polarization). The distance of separation (retardance) between the two rays increases with increasing tissue thickness. However, the RNFL is not the only birefringent structure of the eye. The cornea and, to a much lesser extent, the lens also exhibit birefringence. Further, the

Henle fiber layer of the macula is birefringent, consisting of elongated photoreceptor fibers extending radially from the fovea.

Because all birefringent structures cause a change in the polarization of an illuminating beam, the total retardance of a beam illuminating the parapapillary retina consists largely of contributions from the RNFL and cornea.<sup>6</sup> The accuracy of RNFL measurements with scanning laser polarimetry depends on the ability to extract the RNFL retardance from the measured total retardance. To compensate corneal birefringence, the commercial scanning laser polarimeter (SLP) (GDx Nerve Fiber Analyzer, Laser Diagnostic Technologies, Inc, San Diego, California) employs an integrated component that assumes all imaged eyes have a slow corneal polarization axis (CPA) of  $15^{\circ}$  nasally downward with a corneal polarization magnitude (CPM) of 60 nm.

In 1995, both eyes of 11 cynomolgus monkeys were imaged with the commercially available SLP with a fixed corneal compensator (R.N. Weinreb, unpublished data). Each of the monkeys had experimental glaucoma of the right eye and a healthy left eye. Upon inspection of the resulting images, it was apparent that the detected

From the Hamilton Glaucoma Center and Diagnostic Imaging Laboratory, University of California, San Diego. Supported in part by grant EY11008 from the National Institutes of Health and a grant from the Joseph Drown Foundation. Dr Weinreb is a consultant who has received research support from Laser Diagnostic Technologies.

retardation (change in polarization due to birefringence) did not mimic the expected appearance of the RNFL in several of the eyes. Figure 1 shows an optic disc photograph (A) and fixed-compensator SLP retardation (thickness) map (B) that were acquired from a monkey with experimental glaucoma of the right eye. Although this monkey had marked narrowing of the right neuroretinal rim (see Figure 1A), the retardation map indicated high retardance. The healthy left eye of the same monkey (Figures 1C and 1D) also had high retardance. The uniformly high retardance observed with this monkey was characteristic of the retardance in each of the other monkeys. On the basis of these observations, it was hypothesized by one of us (R.N. Weinreb) that the CPM and/or CPA in monkey eyes was significantly different from that assumed by the fixed-compensator SLP, and that only by individually compensating for corneal birefringence would it be possible to obtain retardance measurements that reflected the appearance of the monkey RNFL. However, it was not possible to measure CPM and CPA, and this hypothesis could not be tested at that time.

Recently, the commercially available SLP was modified by integrating a variable corneal polarization compensator (VCC) that allows compensation for individual eyes.<sup>7</sup> Using this modified instrument, we have measured CPM and CPA in human eyes.<sup>8</sup> Further, we have corrected SLP images using this information and determined that individually compensated images more closely resemble RNFL appearance than those acquired with a fixed-compensator SLP (unpublished data). The purpose of the current study was first to determine CPM and CPA in individual monkey eyes. Next, we sought to determine whether the VCC SLP provided retardation measurements that resembled what is expected in monkey eyes with and without experimental glaucoma.

## METHODS

### SUBJECTS

Six eyes of three adult cynomolgus (*Macaca fascicularis*) monkeys were studied. Monkey 1 (age about 7 to 10 years; young adult) had healthy eyes. The left eyes of both monkeys 2 and 3 were healthy. Monkey 2 (aged 16 years) had experimental glaucoma (right eye) of 12 years duration with considerable narrowing of the neuroretinal rim visible on simultaneous stereoscopic optic disc photographs. Monkey 3 (aged 14 years) also had experimental glaucoma (right eye) of 12 years duration, with complete absence of neuroretinal rim visible on optic disc photographs. Experimental glaucoma had been induced in the right eyes of monkeys 2 and 3 by argon laser applications to the trabecular meshwork, according to the methods of Gaasterland and Kupfer.<sup>9</sup>

### PROCEDURE

To facilitate SLP imaging, the monkeys were anesthetized with intramuscular ketamine. An intravenous catheter and endotracheal tube were placed. The animals were positioned in a restraint in the prone position with the upper jaw on a bite bar and soft pressure points at the rear of the cranium for head stabilization. Following a bolus intravenous dose of norcuronium (neuromuscular blocker), the animals were connected to a ventilator and vital signs were continuously monitored. Anesthesia was maintained with periodic intramuscular ketamine, and neuromuscular block was maintained with steady infusion of norcuronium.

### SCANNING LASER POLARIMETRY

Polarimetry images were obtained using a commercial SLP (GDx, Laser Diagnostic Technologies, Inc, San Diego, California) modified so that the original fixed corneal compensator was replaced with a VCC as described by Zhou and Weinreb.<sup>7</sup> Briefly, the VCC SLP is composed of a set of four linear retarders in the path of the measurement beam. The first two retarders are optical lenses that have equal retardance and form a variable cornea and lens compensator. The third retarder is composed of the cornea and lens, and the fourth retarder is the retinal birefringent structure (RNFL or macular Henle fibers).

The CPM and the CPA were determined by setting the compensating retarders to 0 nm and imaging the macula. The resulting retardation profile represented the additive effects of cornea, lens, and macular Henle fiber birefringence. The compensating retarders were then adjusted to minimize the effects of anterior segment birefringence, resulting in a flat low macular retardation profile. The CPM and CPA values resulting in adequate compensation were then recorded. Three macula images were obtained from both eyes of each monkey to determine mean CPM and CPA. Nasally upward CPA values (degrees) were recorded as negative; nasally downward CPA values were recorded as positive.

Next, three corneal birefringence-compensated parapapillary SLP images from each eye were obtained using the appropriate eye-specific CPM and CPA values. These three images were combined to create each composite image used for RNFL thickness analysis. In these images, each pixel is color-coded to represent the measured retardation, resulting in a retardation map.

Differences in 17 VCC SLP parameters between the right and left eyes of one healthy monkey and the glaucomatous right eyes and healthy left eyes of two other monkeys were examined to determine if SLP with eye-specific corneal birefringence compensation could detect differences between healthy eyes and those with RNFL damage. The investigated parameters were as follows:

superior maximum thickness, inferior maximum thickness, symmetry, superior nasal thickness ratio, superior temporal thickness ratio, inferior temporal thickness ratio, average thickness, ellipse modulation, maximum modulation, total polar integral, superior polar integral, inferior polar integral, ellipse average thickness, superior average thickness, temporal average thickness, inferior average thickness, and nasal average thickness. Each of these parameters has been described in detail previously.<sup>10,11</sup> Although thickness measurements are reported in micrometers ( $\mu\text{m}$ ), caution should be used when assessing these measurements. This is because the relationship between SLP retardance and RNFL thickness is not known. Therefore, thickness measurements should be considered relative, not absolute.

All experimental procedures adhered to the guidelines of the Association for Research in Vision and Ophthalmology statement for the use of animals in ophthalmic and vision research.

## RESULTS

### CPM AND CPA MEASUREMENTS IN MONKEY EYES

The measured CPM was small in the six eyes examined, ranging from 5.7 to 9.0 nm. CPA ranged from  $-62^\circ$  to  $79^\circ$ . (Nasally upward CPA values were recorded as negative; nasally downward CPA values were recorded as positive.) CPM and CPA of each eye from each subject are shown in Table I.

#### *Monkey 1: Normal Eyes*

Figure 2 shows optic disc photographs and VCC SLP retardation (thickness) maps for the right (A and B) and left eyes (C and D) of monkey 1 (both eyes healthy). The retardation maps have areas of increased retardation in the superior and inferior arcuate bundles in accordance with the expected appearance of the thicker RNFL in these regions of healthy eyes. Figure 2E shows the RNFL thickness profile for both eyes, where the x-axis represents the polar position around the optic disc and the y-axis represents RNFL thickness measured in millimeters. The measurements of parapapillary retina thickness are obtained 1.7 optic disc diameters from the optic disc margin. A large-amplitude double-hump pattern, indicative of increased thickness of the superior and inferior arcuate bundles, is apparent, and there is little difference in RNFL thickness between eyes.

#### *Monkeys 2 and 3: Experimental Glaucoma of Right Eye*

Figure 3 shows optic disc photographs and VCC SLP retardation maps for the right and left eyes of monkeys 2 and 3.

The optic disc photograph of the right eye of monkey 2 (Figure 3A) indicates considerable narrowing of the neuroretinal rim. The retardation map (Figure 3B) shows

reduced retardation, particularly superiorly, in accordance with the thin neuroretinal rim in the optic disc photograph. The optic disc photograph and retardation map from the healthy left eye are shown in Figures 3C and 3D, respectively. Figure 3E shows the RNFL thickness profile for both eyes on the same plot. The RNFL thickness of the eye with experimental glaucoma (OD) shows thinning and a reduced-amplitude double-hump pattern, particularly in the superior quadrant, compared with the healthy left eye.

The optic disc photograph of the right eye of monkey 3 (Figure 3F) indicates complete absence of neuroretinal rim. The retardation map (Figure 3G) indicates uniformly low retardance in accordance with the absence of neuroretinal rim in the optic disc photograph. The optic disc photograph and retardation map from the healthy left eye are shown in Figures 3H and 3I, respectively. Figure 3J shows the RNFL thickness profile for both eyes on the same plot. The retardation from the eye with experimental glaucoma (OD) is markedly reduced superiorly and inferiorly, and the thickness profile does not have a double-hump pattern.

### RNFL THICKNESS PARAMETERS

Table II shows RNFL thickness parameter measurements from the right and left eye of each monkey. The values are similar in each eye for monkey 1 (both eyes normal) and are quite different for monkeys 2 and 3 (glaucomatous right eye, normal left eye), with greater differences between eyes for monkey 3. For monkey 2, superior RNFL measurements (superior maximum and superior average), inferior RNFL measurements (inferior maximum and inferior average), and global RNFL measurements (average thickness and ellipse average thickness) in the eye with experimental glaucoma are 75% to 100% of those in the healthy eye. For monkey 3, superior RNFL measurements, inferior measurements, and global measurements in the eye with experimental glaucoma are 36% to 60% of those in the healthy eye.

## DISCUSSION

The most notable finding in our study is the fact that the monkey anterior segment birefringence is quite different from that described in humans, as hypothesized. Moreover, scanning laser polarimetry with variable anterior segment polarization compensation appears to objectively and quantitatively measure RNFL thickness in monkey eyes.

Currently, the commercially available SLP assumes a CPM of 60 nm and a CPA of  $15^\circ$  based on measurements from human eyes. Previous studies have shown that in healthy human eyes, CPM varies from 0 to 125 nm, with a mean of approximately 40 nm, a median of approximately

40 nm, and a mode between 40 nm and 50 nm.<sup>8,12</sup> In the current study, CPM in each of the six monkey eyes was in a narrow range, from 5.7 to 9.3 nm. Although the sample is small, these values appear quite different from values in human eyes. In contrast to the narrow range of CPM values, the range of CPA in the monkey was wide and ranged from -62° to 79°. This considerable variability is similar to

that reported in humans for CPA values.<sup>8,12,13</sup> The CPA in only one eye (monkey 1, OD, CPA = 27°) was within 15° of the value assumed by the commercially available fixed-compensator GDx (15°), indicating that SLP RNFL thickness measurements using the commercially available instrument that relies on a fixed corneal birefringence compensation are likely inaccurate in the monkey eye. In

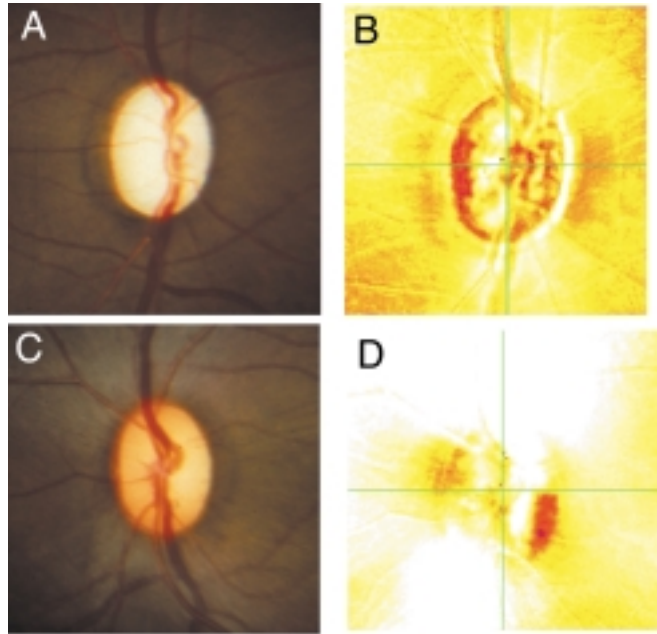


FIGURE 1

Optic disc photographs (A and C) and fixed-compensator scanning laser polarimetry retardation maps (B and D) from monkey with experimental glaucoma of right eye (A and B) and healthy left eye (C and D) (see text for description).

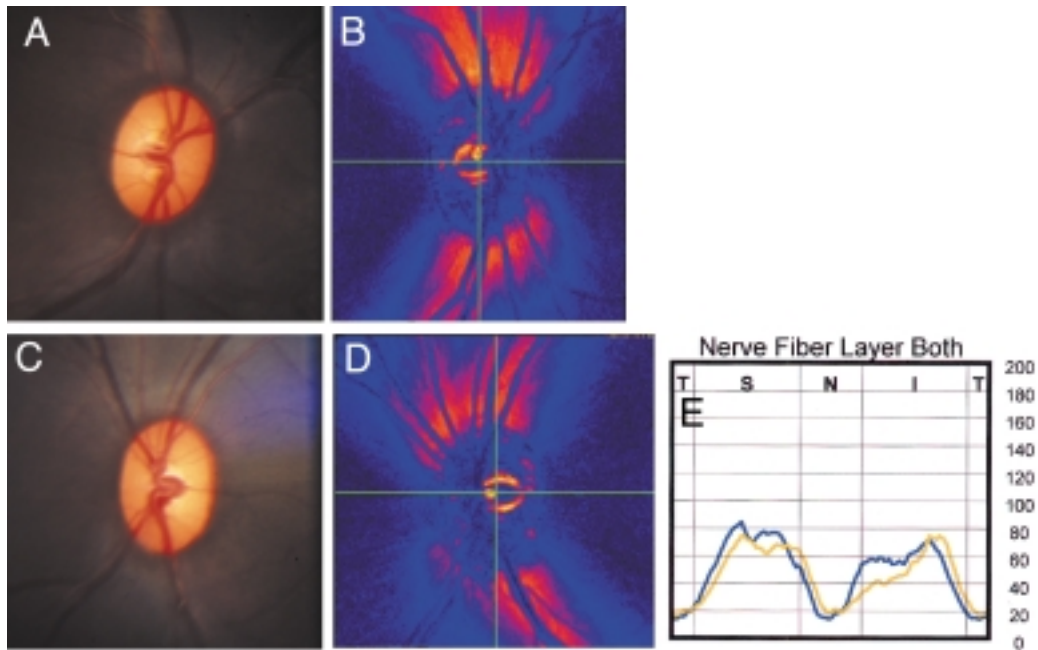


FIGURE 2

Optic disc photographs (A and C) and scanning laser polarimetry (SLP) retardation maps (B and D) using SLP with eye-specific corneal birefringence compensation from a monkey with normal eyes (monkey 1; see text for description). The x-y plot (E) shows parapapillary retinal nerve fiber layer thickness (y-axis) as a function of polar position around the optic disc (x-axis) in both eyes.

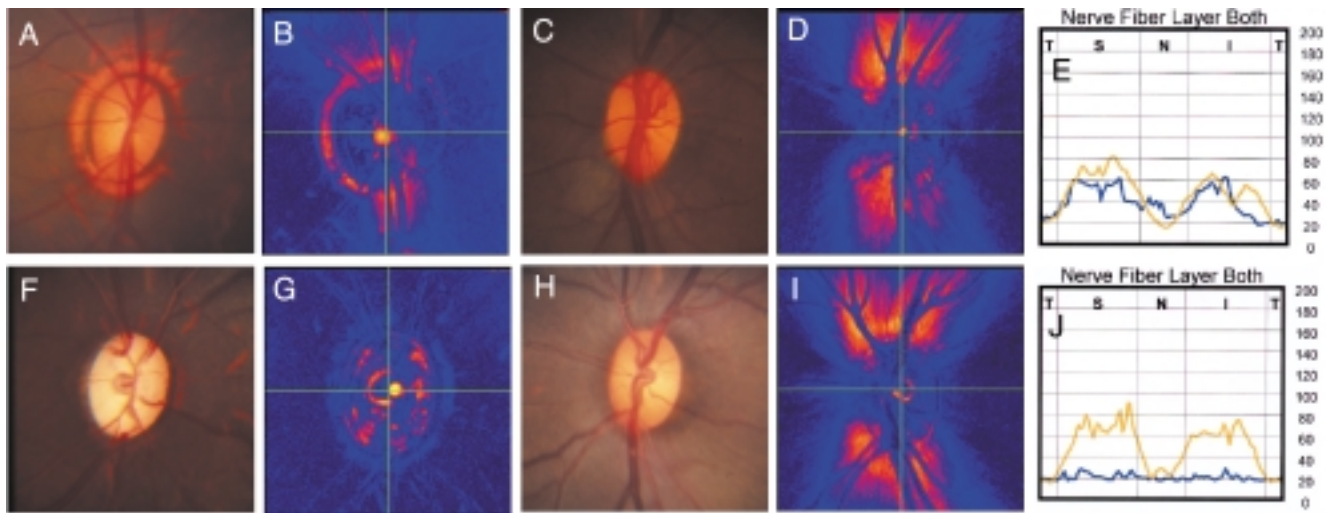


FIGURE 3

Optic disc photographs and scanning laser polarimetry (SLP) retardation maps using SLP with eye-specific corneal birefringence compensation from two monkeys with experimental glaucoma of right eye and normal left eyes (monkey 2, A through D, and monkey 3, F through I; see text for description). The x-y plots (E and J) depicts parpapillary retinal nerve fiber layer thickness (y-axis) as a function of polar position around the optic disc (x-axis) in both eyes of monkey 2 and monkey 3, respectively.

TABLE 1: CORNEAL POLARIZATION MAGNITUDE (CPM) AND CORNEAL POLARIZATION AXIS (CPA) OF EACH EYE EVALUATED

SUBJECT	EYE	STATUS	CPM (NM)	CPA
Monkey 1	OD	Healthy	8	27°
	OS	Healthy	8	53°
Monkey 2	OD	Experimental glaucoma	8	-62°
	OS	Healthy	5.7	-44.3°
Monkey 3	OD	Experimental glaucoma	7	78.7°
	OS	Healthy	8	63.7°

retrospect, the SLP images of monkey eyes obtained in 1995 were inaccurate in large part owing to incorrect compensation of corneal birefringence. Testing in additional monkeys is warranted to better validate this suggestion because it is possible that some monkeys have CPM and CPA values that closely approximate those observed in human eyes.

In the current study, there were much larger ocular asymmetries in most RNFL measurements from the monkeys with monocular glaucoma (monkeys 2 and 3) compared to the binocularly normal monkey (monkey 1). This finding indicates that differences in RNFL thickness between healthy and glaucomatous monkey eyes are detectable with SLP, as they are in humans.<sup>4,14-20</sup> Although the sample size is small, we believe that these results are compelling and are applicable to studies using the monkey experimental glaucoma model.

In the monkey model of glaucoma, the optic disc and RNFL change rapidly over several months, in contrast to the chronic and generally slowly progressing course of pri-

mary open-angle glaucoma. Results from the current study suggest that SLP with eye-specific corneal birefringence compensation can aid in the evaluation of the rapid change in RNFL thickness measurements from monkey eyes with experimental glaucoma. This may be particularly useful for evaluating the efficacy of new glaucoma therapies that purport to slow or halt the progression of disease. The present results are a first necessary step in addressing the use of SLP as a method of monitoring these effects.

Overall, the current study demonstrates that scanning laser polarimetry of the RNFL is possible in monkey eyes using variable corneal birefringence compensation, and that the resulting measurements reflect observable morphology. In addition, the large difference in SLP parameters between healthy monkey eyes and those with experimental glaucoma has implications for the future use of SLP in studies using the primate model of experimental glaucoma.

**ACKNOWLEDGMENT**

We appreciate the technical advice and support of William Hare, PhD, and Qienyuan Zhou, PhD.

**REFERENCES**

1. Kook MS, Sung K, Park RH, et al. Reproducibility of scanning laser polarimetry (GDx) of peripapillary retinal nerve fiber layer thickness in normal subjects. *Graefes Arch Clin Exp Ophthalmol* 2001;239:118-121.
2. Hoh ST, Ishikawa H, Greenfield DS, et al. Peripapillary nerve fiber layer thickness measurement reproducibility using scanning laser polarimetry. *J Glaucoma* 1998;7:12-15.

TABLE II: VCC GDx PARAMETER MEASUREMENTS FROM BOTH EYES OF EACH MONKEY\*

	MONKEY 1 (HEALTHY OU)		MONKEY 2 (GLAUCOMA OD, HEALTHY OS)		MONKEY 3 (GLAUCOMA OD, HEALTHY OS)	
	OD	OS	OD	OS	OD	OS
Superior maximum thickness	69.6	60.0	46.7	57.7	24.8	64.1
Inferior maximum thickness	56.0	59.8	38.9	52.0	22.7	57.4
Symmetry	1.24	1.00	1.20	1.11	1.09	1.12
Superior nasal ratio	4.51	3.61	1.85	3.47	1.36	3.73
Superior temporal ratio	5.16	4.06	2.72	4.00	1.34	4.56
Inferior temporal ratio	4.15	4.06	2.25	3.61	1.23	4.08
Average thickness	37.0	36.0	38.0	37.0	22.0	39.0
Ellipse modulation	5.05	3.57	2.52	4.25	0.65	5.00
Maximum modulation	4.16	3.06	1.71	3.0	0.36	3.56
Total polar integral	0.42	0.40	0.36	0.41	0.22	0.43
Superior polar integral	0.19	0.18	0.16	0.19	0.08	0.19
Inferior polar integral	0.16	0.16	0.12	0.16	0.09	0.17
Ellipse average thickness	45.9	44.1	38.8	43.9	20.6	47.1
Superior average thickness	61.3	56.1	47.3	58.5	21.8	60.0
Temporal average thickness	15.7	18.4	24.6	19.8	19.0	17.0
Inferior average thickness	60.0	48.0	37.8	45.9	20.4	53.3
Nasal average thickness	23.2	26.7	32.9	23.0	19.3	27.7

\*Thickness measures are expressed in  $\mu\text{m}$ .

3. Junghardt A, Schmid MK, Schipper I, et al. Reproducibility of the data determined by scanning laser polarimetry. *Graefes Arch Clin Exp Ophthalmol* 1996;234:628-632.
4. Weinreb RN, Shakiba S, Zangwill L. Scanning laser polarimetry to measure the nerve fiber layer of normal and glaucomatous eyes. *Am J Ophthalmol* 1995;119:627-636.
5. Waldock A, Potts MJ, Sparrow JM, et al. Clinical evaluation of scanning laser polarimetry: I. Intraoperator reproducibility and design of a blood vessel removal algorithm. *Br J Ophthalmol* 1998;82:252-259.
6. Weinreb RN. Evaluating the retinal nerve fiber layer in glaucoma with scanning laser polarimetry. *Arch Ophthalmol* 1999;117:1403-1406.
7. Zhou Q, Weinreb RN. Individualized compensation of anterior segment birefringence during scanning laser polarimetry. *Invest Ophthalmol Vis Sci* 2002;43:2221-2228.
8. Weinreb RN, Bowd C, Greenfield DS, et al. Measurement of the magnitude and axis of corneal polarization with scanning laser polarimetry. *Arch Ophthalmol* 2002;120:901-906.
9. Gaasterland D, Kupfer C. Experimental glaucoma in the rhesus monkey. *Invest Ophthalmol* 1974;13:455-457.
10. Bowd C, Zangwill L, Blumenthal E, et al. Imaging of the optic disc and retinal nerve fiber layer: the effects of age, optic disc area, refractive error, and gender. *J Optical Soc Am A* 2001;19:197-207.
11. Zangwill LM, Bowd C, Weinreb RN. Evaluating the optic disc and retinal nerve fiber layer in glaucoma II: Optical image analysis. *Sem Ophthalmol* 2000;15:206-220.
12. Knighton RW, Huang XR. Linear birefringence of the central human cornea. *Invest Ophthalmol Vis Sci* 2002;43:82-86.
13. Greenfield DS, Knighton RW, Huang XR. Effect of corneal polarization axis on assessment of retinal nerve fiber layer thickness by scanning laser polarimetry. *Am J Ophthalmol* 2000;129:715-722.
14. Bowd C, Zangwill LM, Berry CC, et al. Detecting early glaucoma by assessment of retinal nerve fiber layer thickness and visual function. *Invest Ophthalmol Vis Sci* 2001;42:1993-2003.
15. Choplin NT, Lundy DC. The sensitivity and specificity of scanning laser polarimetry in the detection of glaucoma in a clinical setting. *Ophthalmology* 2001;108:899-904.
16. Horn FK, Jonas JB, Martus P, et al. Polarimetric measurement of retinal nerve fiber layer thickness in glaucoma diagnosis. *J Glaucoma* 1999;8:353-362.
17. Sinai MJ, Essock EA, Fechtner RD, et al. Diffuse and localized nerve fiber layer loss measured with a scanning laser polarimeter: sensitivity and specificity of detecting glaucoma. *J Glaucoma* 2000;9:154-162.
18. Tribble JR, Schultz RO, Robinson JC, et al. Accuracy of scanning laser polarimetry in the diagnosis of glaucoma. *Arch Ophthalmol* 1999;117:1298-1304.
19. Weinreb RN, Zangwill L, Berry CC, et al. Detection of glaucoma with scanning laser polarimetry. *Arch Ophthalmol* 1998;116:1583-1589.
20. Zangwill LM, Bowd C, Berry CC, et al. Discriminating between normal and glaucomatous eyes using the Heidelberg Retina Tomograph, GDx Nerve Fiber Analyzer, and Optical Coherence Tomograph. *Arch Ophthalmol* 2001;119:985-993.

## DISCUSSION

DR ROBERT L. STAMPER. Over the last half century, the diagnosis and assessment of progression in glaucoma have depended on two basically subjective examinations: visual field testing, which is subjective for the patient, and optic nerve evaluation, which is subjective for the examiner.

The ultimate dream of glaucoma diagnosis and management has been an objective assessment of either visual field or optic nerve that is both sensitive to detect the earliest glaucomatous pathology and/or progression and specific enough to rule out normal variation or artifact. The scanning laser polarimeter (SLP) was touted as such an instrument and, along with two other laser scanning devices based on different principles, has become an increasingly common part of the evaluation of the glaucoma patient. The SLP is based on the true assumption that as glaucoma progresses and the ganglion cells die, that the retinal nerve fiber layer (RNFL) decreases in thickness, and that since the nerve fiber layer is made up of polarizing elements, the polarimeter can detect both relative and absolute thinning of the nerve fiber layer.

The fly in the ointment is that both the cornea and, to a smaller extent, the lens contribute to the polarizing effects of the eye, and these elements can confound the polarized signal coming from the retina. The original SLP was based on the assumption that all human corneas have approximately the same polarizing effect and that the effect was roughly in the same axis in each patient.

It became clear through clinical observations as well as unpublished data in monkeys by the author that the results did not always coincide with the observed appearance of the RNFL. The author and one of his colleagues hypothesized that corneal birefringence was variable from individual to individual and from species to species and that this variability was confounding the results. They developed an individualized, variable corneal birefringence compensator based on macular birefringence and modified the original instrument to incorporate this advance. This study reports their results in three monkeys.

Six eyes from three adult *Cynomolgus* monkeys were studied while the animals were under general anesthesia. Two eyes of two monkeys had induced glaucoma. The eye specific magnitude and axis of anterior segment (corneal and lenticular) birefringence as well as RNFL parameters were studied.

While the range of corneal polarization magnitude was small (5.7 to 0.0 nm), the corneal polarization axis ranged over 140° from -62° to 79° quite different from humans (range, 0-125; median, 40nm) in magnitude, although similar in axis. The areas of thinning of the nerve fiber layer

by SLP matched the observed areas by ophthalmoscopy.

#### **SIGNIFICANCE**

This new modification corrects the false assumption of the original polarimeter and appears to give a more accurate assessment of RNFL by eliminating a confounding variable. Thus, assessment of the RNFL thickness both in humans and in monkeys now provides more accurate diagnostic information. The modification also allows better and more objective assessment of the natural history and rate of progression of experimental glaucoma in monkeys as well as clinical glaucoma in humans.

#### **QUESTIONS**

I recognize the expenses and difficulties in expanding such a study. However, given the large range of observed polarization axis differences in monkeys even between the two eyes of the same monkey, are three animals, six eyes, enough to be comfortable that the results are representative? Furthermore, the authors have made a good start in validating this device in that the RNFL thickness measurements reflect subjective assessments. However, actual objective assessment of RNFL thickness compared to the SLP measurements would be the ultimate validation.

Corneal polarization magnitude and axis would seem to be less important for longitudinal assessment as they are probably stable over time. However, could these values change with age or other environmental stresses (not to mention LASIK, cataract, etc)? Now that a way of measuring the anterior segment polarization is available, this assumption should be assessed.

I extend my congratulations to the authors for developing and beginning the scientific assessment of a device that should move us considerably closer to the goal of objective measurement of anatomical changes in glaucoma.

DR ROBERT N. WEINREB. The small magnitude of corneal compensation that we have observed has been remarkably uniform in the monkeys that we have examined to date. Testing in larger numbers of monkeys is needed to confirm this observation. Moreover, I agree fully that it is essential to assess longitudinally this technology and to establish the stability of the compensation over time.



# A VERY LARGE BRAZILIAN PEDIGREE WITH 11778 LEBER'S HEREDITARY OPTIC NEUROPATHY

---

BY Alfredo A. Sadun, MD, PhD, Valerio Carelli, MD, PhD, (BY INVITATION), Solange R. Salomao, PhD, (BY INVITATION), Adriana Berezovsky, PhD, (BY INVITATION), Peter Quiros, MD, (BY INVITATION), Federico Sadun, MD, (BY INVITATION), Anna-Maria DeNegri, MD, (BY INVITATION), Rafael Andrade, MD, (BY INVITATION), Stan Schein, MD, PhD, (BY INVITATION), AND Rubens Belfort, MD, PhD, (BY INVITATION)

## ABSTRACT

**Purpose:** We conducted extensive epidemiological, neuro-ophthalmological, psychophysical, and blood examinations on a newly discovered, very large pedigree with molecular analysis showing mtDNA mutation for Leber's hereditary optic neuropathy (LHON).

**Methods:** Four patients representing four index cases from a remote area of Brazil were sent to Sao Paulo, where complete ophthalmological examinations strongly suggested LHON. Molecular analysis of their blood demonstrated that they were LHON, homoplasmic 11778, J-haplogroup. They had an extensive family that all lived in one rural area in Brazil. To investigate this family, we drew on a number of international experts to form a team that traveled to Brazil. This field team also included several members of the Federal University of Sao Paulo, and together we evaluated 273 of the 295 family members that were still alive. We conducted epidemiological interviews emphasizing possible environmental risk factors, comprehensive neuro-ophthalmological examinations, psychophysical tests, Humphrey visual field studies, fundus photography, and blood testing for both mitochondrial genetic analysis and nuclear gene linkage analysis.

**Results:** The person representing the first-generation case immigrated from Verona, Italy, to Colatina. Subsequent generations demonstrated penetrance rates of 71%, 60%, 34%, 15%, and 9%. The percentages of males were 60%, 50%, 64%, 100%, and 100%. Age at onset varied from 10 to 64 years, and current visual acuities varied from LP to 20/400.

**Conclusions:** Almost 95% of a nearly 300-member pedigree with LHON 11778 were comprehensively studied. Analysis of environmental risk factors and a nuclear modifying factor from this group may help address the perplexing mystery of LHON: Why do only some of the genetically affected individuals manifest the disease? This fully described database may also provide an excellent opportunity for future clinical trials of any purported neuroprotective agent.

*Trans Am Ophthalmol Soc* 2002;100:169-180

## INTRODUCTION

---

Leber's hereditary optic neuropathy (LHON) is a maternally inherited form of acute or subacute loss of central vision predominantly affecting young males.<sup>1,2</sup> This degeneration of retinal ganglion cells and their axons is due to three prevalent pathogenic mitochondrial DNA (mtDNA) point mutations.<sup>2</sup> These affect nucleotide positions 11778, 3460, and 14484, respectively, in the ND4, ND1, and ND6 subunit genes of complex I. Having this mutation is necessary but not sufficient to produce blindness. If the patient has mitochondrial homoplasmy

for one of these three mutations (all the mtDNA copies are mutant), there is a high predisposition for a catastrophic series of events in the optic nerve that ultimately leads to acute or subacute loss of central vision.<sup>2,3</sup>

These three mtDNA point mutations are pathogenic in the large majority of patients worldwide.<sup>4,5</sup> If the mutation is heteroplasmic (a mixture of normal/wild type and mtDNA mutation mitochondria), the percentage of the pedigree is reduced but the extent of visual impairment in those affected remains equally severe.<sup>7</sup>

Penetrance may be highly variable, even with the same pathogenic mutation in homoplasmic fashion within the same family.<sup>9</sup> Hence, environmental<sup>1,2</sup> and/or supplementary genetic factors, possibly in the nuclear DNA,<sup>10</sup> are probably needed to express the pathology as blindness. In particular, there is evidence that tobacco and alcohol consumption may act as risk factors that may trip the threshold in predisposed patients.<sup>9,11</sup>

From the University of Southern California-Keck School of Medicine/Doheny Eye Institute, Los Angeles (Dr A. Sadun, Dr Quiros); Dipartimento di Scienze Neurologiche, Universita di Bologna Italy (Dr Carelli); Federal University of Sao Paulo, Brazil (Dr Salomao, Dr Berezovsky, Dr Andrade, and Dr Belfort); Rome, Italy (Dr F. Sadun, Dr DeNegri); and the University of California at Los Angeles (Dr Schein).

Clinically, the patient presents with unilateral or, occasionally, bilateral visual loss of acute or subacute tempo. The vision is often in the 20/400 to count fingers range with severe dyschromatopsia.<sup>11</sup> Fundus examination may reveal telangiectatic microangiopathy in some cases that is seen very soon after, or even before (in the fellow eye), visual loss. Indeed, these vascular features may precede the onset of bilateral asynchronous visual loss and evolve in a few weeks toward optic atrophy and permanent decrease of visual acuity.<sup>12</sup> In addition, an early drop out of the papillomacular bundle, an edematous appearance of the arcuate bundle nerve fiber layer, and enlarged and tortuous peripapillar vessels can be seen on fundus examination shortly after the onset of visual loss.<sup>12</sup> Visual field examination usually reveals cecentral scotomas with relative preservation of the peripheral visual field. The visual loss usually stabilizes within a few months, leaving a picture of optic atrophy, more severely marked on the temporal side.<sup>12</sup>

Histopathological findings have been described in three cases with known mtDNA mutation.<sup>13-16</sup> These studies showed devastating losses of retinal ganglion cells and the corresponding nerve fiber layer in the eyes of the LHON patients. There was also a striking loss of fibers in the optic nerve with a variable and slight preservation of fibers in the far periphery. Electron microscopy revealed only very few retinal ganglion cells.<sup>16</sup>

Despite our extensive knowledge of the genetic and biochemical features of LHON, despite our extensive experience with its clinical presentation, and despite recent studies elucidating the morphological, morphometric, and ultrastructural features, LHON remains a great mystery. Intriguing questions include: Why does the disease selectively affect the nervous system and, more specifically, the optic nerve and, most specifically, the small fibers of the papillomacular bundle?<sup>13</sup> Even more mysteriously, Why does the disease have a selection bias to affect mostly men? Why are patients fine until early adulthood and then suddenly become profoundly blind in both eyes in an almost synchronous manner? Why do only some members of a genetically identical (in regard to mtDNA) pedigree manifest the disease?

To address this last question in particular, we recently undertook a field investigation to rural Brazil, where a previously undescribed and very large LHON pedigree was found. At minimum, we wished to examine the (nuclear) genetic and epigenetic factors that might trip the threshold of expression that leads to blindness.

## **METHODS**

We originally became aware of this extremely large pedigree when contacted (by e-mail through the

International Foundation of Optic Nerve Diseases [IFOND]) by the first index case in the summer of 2001. M.O.M. was a 51-year-old woman with no visual complaints but aware of a strong family history of LHON. Her 14-year-old son had suddenly lost vision in one eye, and she went to the Internet to research her disease with the hope that recent developments afforded some treatment for her. M.O.M. displayed a great deal of knowledge about LHON as a cause of blindness, largely as a consequence of having two brothers who had become blind bilaterally many years earlier. After several e-mail exchanges, we became convinced that she was probably right about the diagnosis, and we were astonished at her estimate of a 200-member family that carried the defective mtDNA gene.

We decided to take advantage of the generosity of funding from IFOND to have M.O.M., her son, and her two brothers properly evaluated for the diagnosis of LHON. We arranged to have them all transported to the Federal University of Sao Paulo in southern Brazil. There, they were each thoroughly examined, photographed, and evaluated by psychophysical instruments. We also drew blood samples, which were sent to three independent laboratories for molecular analysis. These samples confirmed the clinical impression that all were homoplasmic for 11778 J-haplogroup and that all three of the males had the optic neuropathy.

## **INDEX CASES**

### *Case 1*

M.O.M. was a 51-year-old woman without visual complaints. Visual acuities were 20/25 OD and 20/25 OS. FM-100 color testing did show a very mild dyschromatopsia OU without any axis. Pelli-Robson contrast sensitivity testing was borderline normal OD and normal OS. Humphrey visual field testing (24-2) was normal OU. Dilated fundus examination showed her optic discs to be flat and with evidence of slight optic atrophy OD (Figures 1A and 1B). Her left optic disc was normal. Her vessels and maculae were also normal. Clinical impression was a near-normal ophthalmological examination OD and a normal ophthalmological examination OS.

### *Case 2*

P.H.M. was the 14-year-old son of M.O.M. This young man complained of bilateral visual loss, worse OS, dating back 3 weeks. He was aware that both his maternal uncles had been bilaterally blind for decades, and he knew that many other more distant members of the family had suddenly lost their vision in young adulthood. He characterized his visual loss as occurring over a period of a few days, first in the left eye and then several days later in the right. He saw a dark cloud in the center of vision and was aware

that he had problems appreciating colors, which all ran into a dark grey.

His visual acuities by ETDRS chart were 20/250 and 20/640. FM-100 color vision testing revealed very severe dyschromatopsia OU but more severe OS. Pelli-Robson contrast sensitivity testing showed moderate losses OD and very severe losses OS. Humphrey visual field testing (24-2) demonstrated large central scotomas OS worse than OD. Dilated fundus examination showed that both optic discs were abnormal (Figures 1C and 1D). There was selective loss of the papillomacular bundle and



**FIGURE 1**

A and B, Index case 1. Right and left fundus of 51-year-old mother (LHON/carrier) without visual complaints. There is slight temporal pallor OD. C and D, Index case 2. Right and left fundus of 14-year-old son (LHON/affected) of index case 1. He had lost vision in both eyes 2 to 3 weeks earlier. Note swelling of arcuate nerve fiber layer and beginning of optic atrophy, especially OS.

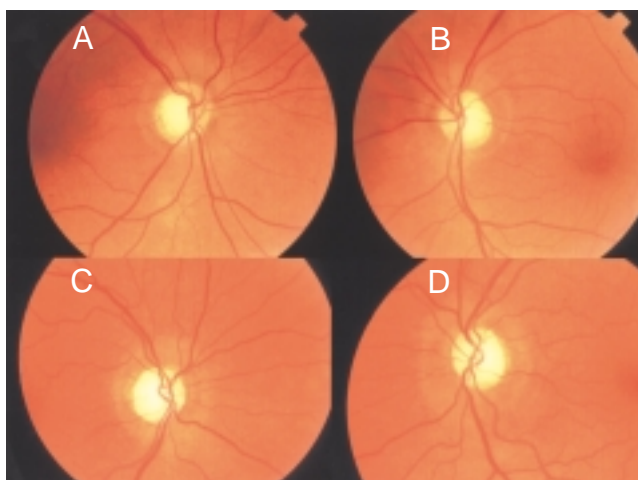


**FIGURE 2**

A and B, Index case 3. Right and left fundus of 42-year-old maternal uncle (LHON/affected) of index case 2, who had lost vision in both eyes about 7 years earlier. Note bilateral optic atrophy. C and D, Index case 4. Right and left fundus of 46-year-old maternal uncle of index case 2 (LHON/affected), who had lost vision in both eyes about 20 years before. Note severe optic atrophy OU.

swelling of the nerve fiber layer in the arcuate bundles OD. There was also hyperemia on the nasal side. The optic disc OS was similar, but the papillomacular bundle loss was more devastating and the nerve fiber layer swelling less evident. Optic atrophy was just developing in the left eye.

Blood samples were sent to our laboratories both in Los Angeles and in Bologna. They were also sent to a commercial clinical laboratory. In all cases, the findings were that of LHON, homoplasmic mtDNA mutation for G11778A. The patient was also positive for the "secondary" mutations of T4216C and G13708A. This confirmed the clinical impression of LHON, homoplasmic 11778, a J-haplogroup.

### *Case 3*

C.R.M. was the 42-year-old brother of M.O.M. He had lost his vision in February 1994, one eye a couple of weeks after the other. C.R.M. described a rapid loss of vision in each eye characterized as an inability to see straight ahead. However, he added that there may have been some slight progression of this loss over the subsequent 6 months. He described at least 26 other family members suffering visual loss presumed to be from LHON. Visual acuity by ETDRS was 10/800 OD and count fingers 1 foot OS. Color vision testing by FM-100 showed extremely severe dyschromatopsia OU. Contrast sensitivity testing showed total loss by Pelli-Robson OU. He showed complete depression on Humphrey visual field testing 24-2 OU but by confrontation demonstrated some peripheral preservation of visual field. His fundus examination OU (Figures 2A and B) revealed devastating optic atrophy with loss of the papillomacular bundle and of the superior and inferior nerve fiber layer as well. Blood test results were identical to those of his nephew P.H.M. and confirmed the clinical diagnosis of homoplasmic 11778 LHON, J-haplogroup.

### *Case 4*

P.H.M. was the other brother of M.O.M. and was 46 years old. He had lost his vision in 1983 and characterized it as cloudiness that occurred almost simultaneously in both eyes, progressed slowly over a period of a year, and then stabilized. He had been a heavy drinker of alcohol until very recently. His visual acuities by ETDRS charting were 10/800 OD and 10/800 OS. Color vision by FM-100 showed very severe dyschromatopsia OU, and contrast sensitivity by Pelli-Robson demonstrated total losses OU. Testing by tangent field showed profound and large central scotomas with some preservation of the far periphery. Fundus examination showed devastating optic atrophy and a pattern of nerve fiber layer loss almost identical to that of his younger brother (Figures 2C and 2D). Blood

test results were identical to those of his brother, mother, and nephew and confirmed the clinical diagnosis of homoplasmic 11778 LHON, J-haplogroup.

Having established the diagnosis of LHON, we began the process of assembling the extent of the pedigree and planned an international field investigation. The core of this team consisted of this manuscript's authors. In particular, it included three neuro-ophthalmologists from the United States (A.A.S., P.Q.) and Italy (F.S.), a neurologist/molecular biologist (V.C.), and an ophthalmologist/epidemiologist (A.M.D.) from Italy. An ophthalmologist/epidemiologist (R.B.) and psychophysicists/epidemiologists (S.R.S. and A.B.) from the department of ophthalmology at Federal University of Sao Paulo, Brazil, were also members, and it was this group that preceded the rest of the international team by several days to make the important arrangements. Particularly critical was their identification of a very large private clinic in Colatina, Brazil, which was suitable for our needs. This private clinic was closed for 1 week and was made available to our field investigation group, as were eight technicians from that clinic who assisted with their expertise and knowledge of Portuguese. Other volunteers, including a professional phlebotomist and photographer, were all made available for us. Furthermore, we were able to get very sophisticated equipment (eg, Humphrey visual field analyzer, high-quality fundus cameras) brought to and set up in this clinic.

The international team flew to Brazil and joined the group from Federal University of Sao Paulo in Vitoria, and then we proceeded to Colatina, a small city in a rural agricultural area further inland. The selected clinic was ideal in being spacious and having 12 excellent areas for examination spread over three floors. The international team spent a day setting up these areas and discussing the nature of LHON and, in particular, this pedigree, which had already been carefully determined and characterized over seven generations and found to contain about 300 members. We also went over our expectations for data gathering.

We designed a system of two patient streams with six stations at each. The patients would register and then proceed to Station IA, where Portuguese-speaking epidemiologists would define each individual on the pedigree and ascertain that the relations were all correct. Station IB involved going over the patient's previously completed six-page questionnaire (translated into Portuguese), which covered all sorts of environmental risk factors. At Station II, 30 mL of blood was obtained from each patient. Only a small part of this blood was used for the molecular characterizations of LHON. Most of the blood was sent to the Bologna laboratory for DNA extraction for gene linkage analysis of the nuclear DNA. Station III involved

extensive neuro-ophthalmological examinations by two of the three neuro-ophthalmologists. Translation was provided by one of three Portuguese-speaking MD-volunteers. Station IV involved careful psychophysical examinations, including standardized color vision, contrast sensitivity, and Amsler grid testing. Station V involved Humphrey visual field strategy 30-2 campimetry. Dilated fundus photography and occasional fluorescein angiographies were performed at Station VI. Four important members of the pedigree were too old and infirm and lived too far from any paved road to be brought to the Colatina clinic. We went to their homes and obtained confrontation visual fields and used a portable Kowa camera for color fundus photographs.

In total, we were able to find 295 living members of this pedigree (Figure 3) and to personally examine 273 of them. The extensive data acquisition was put into two large Excel spreadsheets containing either epigenetic or neuro-ophthalmologic factors. These were analyzed. Various parameters were compared, and we were able to obtain means or percentage involvements for each of three groups. In general, we compared (1) those who carried the mutant ND4 gene but had no serious visual impairment from optic neuropathy (labeled LHON/carriers in the tables), to (2) those with the LHON mutation and serious optic neuropathy (LHON/affected in the tables), and to (3) those who married into the family and had neither the mtDNA mutation nor any significant visual problems (controls). We were able to compute standard deviations for numerical data only (not percentage involvements), and we tested by chi-square test or Fisher exact test (if the number of cases was very small). Even so, these statistical treatments did not correct for several possible confounding factors that will be discussed later.

## RESULTS

---

### PEDIGREE

This pedigree is illustrated in Figure 3. Note that the founder was a woman born in 1861 in Verona, Italy, who immigrated to Brazil. She is depicted near the center and represents Generation I. Each subsequent generation is shown further centripetally through generation VII.

Ultimately, we found and fully examined 273 individuals of 295 living individuals identified as belonging on the pedigree. This covered seven generations. All but five of these cases clustered within 100 miles of each other between the cities of Vitoria, Colatina, and Santa Teresa. We found that the penetration of disease expression changed with these generations from over 70% in the early generations (I is the founder, so consider II), down to below 20% in the later generations V and VI (Figure 4). We also found that the percentage of cases that were male

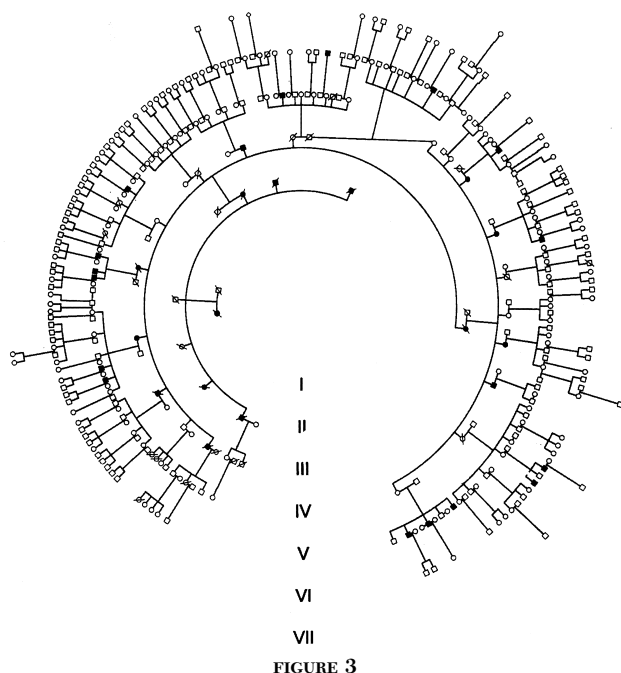


FIGURE 3

LHON pedigree.

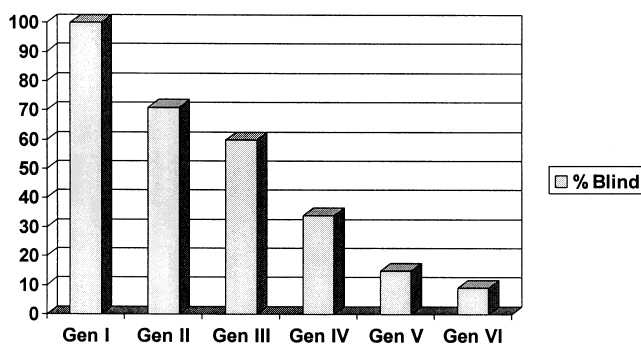


FIGURE 4

Penetrance rate in Leber's hereditary optic neuropathy. Chart showing percentage of those with the LHON mtDNA mutation who went blind in each generation. Penetrance rate diminished almost linearly.

changed with time. In the first generations after the immigrant founder, it ranged between 50% and 70%; however, in the last three generations it rose to nearly 100%.

#### GENETICS

Blood samples were analyzed in several laboratories. In all cases, the findings were that of LHON, homoplasmic mtDNA mutation for G11778A. The polymorphisms of T4216C and G13708A were also found to be homoplasmic. This confirmed the clinical impression of homoplasmic 11778 LHON, J-haplogroup. DNA was extracted from all of the blood samples.

#### EPIGENETICS

Various parameters of an extremely large spreadsheet

could be compared both for general environmental risk factors and clinical features. Our general hypothesis was that epigenetic factors might explain why only a small subset of individuals carrying the 11778 mtDNA mutation went blind. We chose to compare several parameters that might test specific associations for each of the three groups described and noted in the tables as (1) LHON/carriers, (2) LHON/affected, and (3) controls.

Table I shows that our patients varied considerably in some of their nutritional habits. Their consumption of vegetables, beef, fish, chicken, and eggs did not, however, differ significantly between our three groups. However, in regard to the consumption of fruits, group 2, composed of LHON/affected patients who had gone blind, did consume less than the other two groups ( $P < .05$  by chi-square test). In particular, group 2 averaged 1.9 fruits per day (SD, 2.4), while those in the pedigree with the same mtDNA genes who did not lose vision (group 1) averaged 3.1 (SD, 2.3) and those of the normal controls (group 3) averaged 2.9 fruits per day (SD, 2.3).

The LHON/affected group consumed more cigarettes in total (32.4 pack-years; SD, 17.2) than did group 1 (25.3 pack-years; SD, 16.4) or group 3 (14.5 pack-years; SD, 13.3). This, however, was not statistically significant.

However, as evidenced by Table II (which shows the toxic risk factors), analysis by percentage of patients smoking cigarettes did show statistical significance (by chi-square testing). We compared LHON/affected individuals (group 2) with the LHON/carriers (group 1) and found as significantly different that the blind patients were much more likely to smoke ( $P < .01$ ). Indeed, there were fewer but yet statistically significant differences ( $P < .05$ ) in that the LHON/carriers (group 1) were less likely to smoke than the general population (group 3).

Drinking alcohol was also much more common in LHON/affected patients who had gone blind. Sixty percent of these patients (group 2) drank heavily regularly or binged on weekends. This was a higher percentage than in either the LHON/carriers group (33.8% drank heavily) or controls (38.2% drank heavily). However, there was statistical significance only between the LHON/affected and LHON/carriers groups ( $P < .01$ ). In general, the LHON/affected patients consumed, on average, 5 L per week of hard alcohol (usually 86 proof Cachaça).

When we compared between the groups the tendency to both smoke and drink, the differences were even more striking. Fifty percent of the LHON/affected patients did both. In contrast, only 9.5% of LHON/carriers and 11.8% of controls both smoked and drank heavily. This was statistically significant with  $P < .01$  for comparisons of LHON/affected patients (group 2) to LHON/carriers (group 1) and  $P < .05$  between LHON/affected patients and controls (group 3).

TABLE I: NUTRITIONAL HABITS OF STUDY GROUPS

VARIABLE	LHON/CARRIERS MEAN ± SD (N=74)	LHON/AFFECTED MEAN ± SD (N=20)	CONTROLS MEAN ± SD (N=68)
Age	30.6 ± 18.4	46.8 ± 17.2	44.4 ± 13.4
Age at onset		29.2 ± 12.5	
Fruits/day*	3.1 ± 2.3	1.9 ± 2.4	2.9 ± 2.3
Vegetables/day	5.4 ± 2.4	4.6 ± 2.6	5.6 ± 2.1
Beef/day	4.4 ± 2.5	5.5 ± 2.4	5.3 ± 2.3
Fish/day	1.0 ± 1.1	1.3 ± 1.7	0.9 ± 1.2
Chicken/day	2.5 ± 1.7	2.8 ± 2.0	2.8 ± 2.0
Eggs/day	2.2 ± 2.3	2.4 ± 1.9	1.7 ± 1.6
Vitamins (use)	12.2%	5%	15.9%

\* $P < .05$  chi-squared for carriers versus affected versus controls.

TABLE II: TOXIC RISK FACTORS IN STUDY GROUPS

RISK	LHON/CARRIERS (N=75)	LHON/AFFECTED (N=20)	CONTROLS (N=69)
Toxic exposure*	9.7%	45.0%	16.2%
Cigarettes*†	13.5%	65.0%	26.1%
ETOH*	33.8%	60.0%	38.2%
Smoke and ETOH*†	9.5%	50.0%	11.8%

ETOH, ethanol; LHON, Leber's hereditary optic neuropathy.

\* $P < .01$  carriers versus affected (chi-square test).

† $P < .05$  carriers versus controls (chi-square test).

We also questioned for other possible toxic exposure (Table II). Our questionnaire and subsequent interviews revealed that there were 12 potential toxins to which these three subject populations were exposed. For many of the toxins, only a handful of those from any of the subject population were affected, and hence statistical analysis was not possible. However, when we summed all the toxins together, it was evident that LHON/affected patients were much more likely to have been exposed. The exposure rates for group 1 (LHON/carriers), group 2 (LHON/affected), and group 3 (controls) were 9.7%, 45.0%, and 16.2%, respectively. Statistical significance was found only between the LHON/carriers and the LHON/affected groups ( $P < .05$ ).

A variety of activities and diseases were also considered, as depicted in Table III. It was particularly notable that the presence of the mtDNA mutation of LHON or an associated gene was possibly protective in a variety of cardiovascular diseases. As the table shows, the prevalence of hypertension was 12.2%, 10%, and 24.6% for groups 1 (LHON/carriers), 2 (LHON/affected), and 3 (controls), respectively, and this was statistically significant ( $P < .05$ ). This was also true for diabetes mellitus, for which the rates were 2.7%, 5%, and 8.7%, respectively ( $P < .05$ ).

Elevated cholesterol levels (>230 mg) were also lower

in both groups with LHON: group 1, 8.1%; group 2, 5%; and group 3, 15.9%. Having LHON seemed protective for coronary artery disease as well, the three groups having prevalence rates of 1.4%, 5%, and 10.1%, respectively. However, these were only trends, and we could not show statistical significance. Yet, given the fact that these are all risk factors for stroke, it is not surprising that the rates of cerebral vascular disease were very low at 1.4% for LHON/carriers (group 1), 0% for the LHON/affected (group 2), and comparatively high at 8.7% for the controls (group 3). Hence there was statistical significance at  $P < .05$  with regard to both LHON groups being protective against stroke in comparison to controls.

Finally, in regard to other disease states, the prevalence of reported degenerative neurologic diseases (predominantly Alzheimer's and Parkinson's diseases) was greater at 25% in LHON/affected patients (group 2) than in either the LHON/carriers at 14.9% (group 1) or controls at 10.1% (group 3).

## DISCUSSION

These results showed several remarkable associations. However, discussion of such must begin with the recognition that there were several confounding factors that preclude us from certain conclusions and even from a confident determination of what was cause and what was effect. For example, we noted that LHON patients who were not blind exercised at almost 10 times the rate of LHON patients who were blind. Did the exercise help mitigate against blindness? Or did blind patients find it more difficult to exercise (particularly playing soccer)? The fact that the controls also exercised about as much as the LHON/affected patients at least suggests that the inability to see was not the only cause and exercise the direct effect. We suspect that the very high rate of exercise in the LHON/carriers group may have been a conscious attempt to live a healthy lifestyle among a population that knew that blindness might have been around the corner. It is quite likely that several of these effects all

TABLE III: GENERAL RISK FACTORS IN STUDY GROUPS

FACTOR	LHON/CARRIERS (%)	LHON/AFFECTED (%)	CONTROLS (%)
Exercise*	32.0	5.0	9.1
Hypertension†	12.2	10.0	24.6
Diabetes mellitus	2.7	5	8.7
High cholesterol	8.1	5	15.9
Coronary	1.4	5	10.1
CVA†	1.4	0	8.7

CVA, cerebral vascular disease; LHON, Leber's hereditary optic neuropathy.

\* $P < .05$  carriers versus both (chi-square test).

† $P < .05$  carriers versus controls and affected versus controls (chi-square test).

contributed to this dramatic association of low activity to LHON-associated blindness.

It should also be recognized that the three populations were heterogeneous in several important particulars. The LHON/carriers (group 1) were much younger (average age, 31) than their blinded counterparts (group 2, average age 47) or controls (average age, 44). This may have been due, in part, to the fact that the earlier generations, who were of course older, had a higher penetrance rate for blindness (see "Results" and Figure 4). Another difference was that the LHON/affected patients (group 2) were overwhelmingly male (85%) compared with LHON/carriers (35% male) and controls (46% male). This, too, is not surprising given that most published pedigrees showed strong male predominance. However, in interpretations of diet, smoking, or drinking, it would not be surprising that a group with a higher percentage of males eats less fruit and smokes and drinks alcohol more. Once again, this is a serious confounding factor that precludes us from concluding with certainty that these lifestyle differences determined who with the LHON gene went blind.

These and other confounding elements limit the conclusions that we can make in regard to the potency and exact effects of several epigenetic factors in determining which LHON patients with the homoplasmic 11778 mtDNA mutation would express the blindness. Nonetheless, the present study demonstrates that there are powerful associations between lifestyle, nutrition, toxic exposure, and risk factors that probably contribute to the crossing of a threshold that genetic predisposition sets. Furthermore, the present study gives us strong hints as to how these factors may exert an influence on this threshold.

This is true from examination of the pedigree itself. For example, we were struck by the remarkable decrease in penetrance demonstrated by each succeeding generation. This might have been due to a decrease of the risk factors, but the dramatic and smooth curve seen in Figure 4 strongly suggests the presence of a nuclear permissive gene, which may be diluted out in succeeding generations. If the permissive gene was autosomal recessive, then only the combination of both nuclear alleles and the LHON mtDNA mutation would result in blindness. The pedigree (Figure 3) demonstrates a few later branches of the genetic tree with a cluster of cases. Does this reflect happenstance, a different family lifestyle, or the doubling up of a permissive nuclear gene?

In regard to nutritional factors, the consumption of fruit did seem to confer benefit, as reflected by the fact that there was a statistically significant tendency for LHON/carriers to consume more fruit (slightly more than one extra per day) than their LHON relatives who had become blind. Fruits contain antioxidants, but so do the

vegetables, which both groups seemed to consume in sufficient quantity. No other eating habit appeared to differ between the groups.

The most dramatic differences between the groups were in their habits of smoking cigarettes and drinking hard liquor. As noted in Table II, there were marked and significant differences in that those with LHON who went blind were much more likely to smoke and much more likely to drink heavily. This was most dramatic when considering those that both smoked and drank heavily. Of the LHON/affected group, 50% did both, as compared to only 9.5% of their relatives harboring the identical LHON mtDNA mutation but without the visual impairment. Smoking and drinking alcohol generate reactive oxygen species (ROS).

Other toxic exposures also seemed to make a difference. Table II also shows that 45% of the LHON/affected patients were exposed to toxins at work, while their relatives with the LHON mtDNA mutation but normal vision only had a quarter of such exposure. Further analysis of these toxins (many were pesticides and others were constituents of fertilizer) will be required.

The consequences of mitochondrial dysfunction in LHON have yet to be fully worked out. The 11778, 3460, and 14484 pathogenic mutations all affect complex I activity, and when this was replicated in a cybrid cellular model, these mtDNA mutations induced a variable impairment of mitochondrial respiratory function.<sup>17</sup> These effects could be mediated by a decreased release of the quinol product or by affecting proton pumping and energy conservation.<sup>17</sup> The common feature is that all three mutations affect the site of interaction of complex I with its natural quinone (CoQ) substrate.<sup>18,19</sup> As a consequence, there probably develops a chronic increase of ROS production. In fact, a number of recent publications now implicate the important role of ROS accumulation in LHON.<sup>20-22</sup> We think that both energy depletion and oxidative stress play roles in LHON pathogenesis. Exposure to certain toxins, such as organophosphate pesticides, may exacerbate the energy depletion problem; smoking and drinking may produce more ROS, while the lack of consumption of fruits may reduce the availability of antioxidants to deal with oxidative stress.

In regard to lifestyle issues, it is interesting that the LHON/carriers group exercised 10 times more than their LHON/affected counterparts. This difference does not simply reflect the tendency of blind individuals to not participate in sports, because the controls also failed to exercise at about the rate of the LHON/affected. It is possible that the members of the LHON/carriers group were actively attempting to preclude impending blindness by the choice of a healthy lifestyle. It is also possible that we should not overlook the benefits of exercise in LHON.

One of the benefits of exercise is on the cardiovascular system. This may account for the remarkable protection afforded the LHON/carriers against hypertension, high cholesterol, and cerebral vascular accidents (see Table III). However, even the LHON/affected patients had some measure of protection from these diseases compared with the normal controls, and yet both exercised about the same. This raises the intriguing possibility that either the mtDNA mutation of LHON itself or, more likely, an associated gene may also have a protective effect against cardiovascular disease. Indeed, Carelli and associates<sup>23</sup> have suggested that haplogroup J may exert a protective rather than detrimental effect in LHON and that this protection may extend to resisting some of the ravages of aging.

The increased rate of Alzheimer's disease, and especially Parkinson's, among our LHON patients was only reported and requires autopsy confirmation. However, a family with maternally inherited adult-onset Parkinsonism and multisystem degeneration has been shown to harbor the 11778 mutation.<sup>24</sup> Going the other direction, cerebellar ataxia has been described in two LHON families with the 11778 mutation.<sup>25,26</sup>

There are several optic neuropathies that produce a clinical picture very similar to that of LHON.<sup>27</sup> At least six classes of optic neuropathies are similar in appearance and probably also in pathophysiology.<sup>12,27</sup> These are (1) LHON, (2) Cuban epidemic of optic neuropathy, (3) tobacco alcohol amblyopia, (4) nutritional deficiencies (especially folic acid and B12), (5) ethambutol, and (6) methanol, cyanide, and other toxins that specifically interfere with mitochondrial oxidative phosphorylation.<sup>26</sup> These optic neuropathies share several oddities with LHON. For example, while these diseases are metabolic and hence systemic by nature, they often have a predilection for the optic nerve and for the papillomacular bundle in particular.<sup>12,13,28</sup> Like LHON, these other mitochondrial optic neuropathies also share six prominent clinical features: (1) symmetrical visual losses, (2) loss of visual acuity and high spatial frequency contrast sensitivity, (3) early and profound dyschromatopsia, (4) centrocecal visual field defects, (5) temporal atrophy of the optic discs, and (6) preferential loss of the papillomacular nerve fiber layer.<sup>27</sup>

It is likely that for each of these mitochondrial optic neuropathies, there is, in addition to energy depletion, an accumulation of ROS. Further, through the opening of the mitochondrial permeability transition pore (mtPTP), there is a consequent release of cell death promoting factors such as cytochrome C.<sup>27</sup> These and similar mechanisms probably induce apoptosis in retinal ganglion cells.<sup>29</sup> Hence, an understanding of the role of various pro- and anti-apoptotic factors, as revealed in the study of LHON patients, may reveal principles that are generalizable to

many other optic neuropathies.

The pathophysiology of mitochondrial metabolic optic neuropathies, whether congenital or acquired, suggests certain treatment strategies. Most important, of course, is removal of the offensive element.

There may also, however, be strategies for mitigating, neutralizing, or possibly even rescuing retinal ganglion cells undergoing apoptosis due to these mechanisms. In regard to LHON, several such strategies have already been attempted. For example, Idebenone not only provides an alternate pathway around the blockage of complex I, it also scavenges ROS and concentrates within the mitochondria.<sup>30</sup>

As mentioned, we are precluded from making any definitive statement of causality between the risk factors and disease expression, owing to the many confounds in this or any statistical analysis of the many parameters measured and analyzed. However, these data and the associations presented here should help in the generation of hypotheses that can then be tested, especially in an LHON animal model. Such an animal model may predispose to blindness but will probably need additional stressors to replicate the disease. These stressors may be developed along the lines implicated in the present paper.

The present study also does not establish the specific pathophysiological consequences of mitochondrial dysfunction. Nor does it establish the relative contributions of genetic and epigenetic factors in determining penetrance, though it does suggest that both play a role. While we have accumulated a great deal of data, covering about 90 parameters in about 300 patients, the many confounding factors discussed preclude us from making definitive statements as to which factors trigger the optic neuropathy in the 11778 mtDNA mutation (that only predisposes patients to LHON-induced blindness).

However, at minimum, we hope that this study is a good start, for it focuses attention on certain newly identified intriguing associations, between epigenetic factors and the expression of blindness in LHON. From here we can propose certain hypotheses, which can be more definitively tested by more focused follow-up examinations and in animal models. We remain optimistic that these pending studies will provide insights into the relative roles of mtDNA, nuclear DNA, and epigenetic factors in determining the cytoplasmic milieu that may lead a retinal ganglion cell down the apoptotic cascade to retinal ganglion cell death.

#### ACKNOWLEDGMENTS

The authors thank Milton Moraes and Angelo Passos for the generous loan of their clinics and staff for many days, Maria Lucia Valentino for help with the genetic analysis,

Patrícia Kjaer and Josenilson Pereira for their expertise with Humphrey visual fields, Fred Ross-Cisneros for his many technical assists, and most especially Maria Odete Moschen for assembling the family pedigree and ensuring their cooperation and Fred Diehl and all the members of IFOND, whose generous support made this enterprise possible.

## REFERENCES

1. Carelli V. Leber's hereditary optic neuropathy. In: Schapira AHV, DiMauro S, eds. *Mitochondrial Disorders in Neurology 2. Blue Books of Practical Neurology*. Burlington, Mass: Butterworth-Heinemann, 2002:115-142.
2. Chalmers RM, Schapira AHV. Clinical, biochemical and molecular genetic features of Leber's hereditary optic neuropathy. *Biochim Biophys Acta* 1999;1410:147-158.
3. Howell N. Human mitochondrial diseases: answering questions and questioning answers. *Int Rev Cytol* 1999;186:49-116.
4. Wallace DC, Singh G, Lott MT, et al. Mitochondrial DNA mutation associated with Leber's hereditary optic neuropathy. *Science* 1988;242:1427-1430.
5. Huoponen K, Vilkki J, Aula P, et al. A new mtDNA mutation associated with Leber hereditary optic neuropathy. *Am J Hum Genet* 1991;48:1147-1153.
6. Howell N, Bindoff LA, McCullough DA, et al. Leber hereditary optic neuropathy: identification of the same mitochondrial ND1 mutation in six pedigrees. *Am J Hum Genet* 1991;49:939-950.
7. Mackey D, Howell N. A variant of Leber hereditary optic neuropathy characterized by recovery of vision and by an unusual mitochondrial genetic etiology. *Am J Hum Genet* 1992;51:1218-1228.
8. Johns DR, Neufeld MJ, Park RD. An ND-6 mitochondrial DNA mutation associated with Leber hereditary optic neuropathy. *Biochem Biophys Res Comm* 1992;187:1551-1557.
9. Chalmers RM, Harding AE. A case-control study of Leber's hereditary optic neuropathy. *Brain* 1996;119:1481-1486.
10. Kerrison JB, Miller NR, Hsu F, et al. A case-control study of tobacco and alcohol consumption in Leber's hereditary optic neuropathy. *Am J Ophthalmol* 2000;130:803-812.
11. Nikoskelainen EK. Clinical picture of LHON. *Clin Neurosci* 1994;2:115-120.
12. Carelli V, Ross-Cisneros FN, Sadun AA. Optic nerve degeneration and mitochondrial dysfunction: genetic and acquired optic neuropathies. *Neurochem Int* 2002;40:573-584.
13. Sadun AA, Win PH, Ross-Cisneros FN, et al. Leber's hereditary optic neuropathy differentially affects smaller axons in the optic nerve. *Trans Am Ophthalmol Soc* 2000;98:223-232.
14. Sadun AA, Kashima Y, Wurdeman AE, et al. Morphological findings in the visual system in a case of Leber's hereditary optic neuropathy. *Clin Neurosci* 1994;2:165-172.
15. Kerrison JB, Howell N, Miller NR, et al. Leber hereditary optic neuropathy. Electron microscopy and molecular genetic analysis of a case. *Ophthalmology* 1995;102:1509-1516.
16. Carelli V, Saadati HG, Madigan M, et al. Leber's hereditary optic neuropathy histopathology suggests optic nerve axoplasmic stasis as the key pathophysiologic feature. Presented at EUROMIT 4, Queens College, Cambridge, United Kingdom, September 16-19, 1999; abstract P92.
17. Brown MD, Trounce IA, Jun AS, et al. Functional analysis of lymphoblast and cybrid mitochondria containing the 3460, 11778 or 14484 Leber's hereditary optic neuropathy. *J Biol Chem* 2000;275:39831-39836.
18. Carelli V, Ghelli A, Ratta M, et al. Leber's hereditary optic neuropathy: biochemical effect of the 11778/ND4 and 3460/ND1 mutations and correlation with the mitochondrial genotype. *Neurology* 1997;48:1623-1632.
19. Carelli V, Ghelli A, Bucchi L, et al. Biochemical features of mtDNA 14484 (ND6/M64V) point mutation associated with Leber's hereditary optic neuropathy. *Ann Neurol* 1999;45:320-328.
20. Wong A, Cortopassi G. mtDNA mutations confer cellular sensitivity to oxidant stress that is partially rescued by the calcium depletion and cyclosporin A. *Biochem Biophys Res Commun* 1997;239:139-145.
21. Barrientos A, Moraes CT. Titrating the effects of mitochondrial complex I impairment in the cell physiology. *J Biol Chem* 1999;274:16188-16197.
22. Klivenyi P, Karg E, Rozsa C, et al. a-Tocopherol/lipid ratio in blood is decreased in patients with Leber's hereditary optic neuropathy and asymptomatic carriers of the 11778 mtDNA mutation. *J Neurol Neurosurg Psychiatry* 2001;70:359-362.
23. Carelli V, Vergani L, Bernazzi B, et al. Respiratory function in cybrid cell lines carrying European mtDNA haplogroups: implications for Leber's hereditary optic neuropathy. *Biochim Biophys Acta* 2002.
24. Simon DK, Pulst SM, Sutton JP, et al. Familial multisystem degeneration with parkinsonism associated with the 11778 mitochondrial DNA mutation. *Neurology* 1999;53:1787-1793.
25. Funakawa I, Kato H, Terao A, et al. Cerebellar ataxia in patients with Leber's hereditary optic neuropathy. *J Neurol* 1995;242:75-77.
26. Murakami T, Mita S, Tokunaga M, et al. Hereditary cerebellar ataxia with Leber's hereditary optic neuropathy mitochondrial DNA 11778 mutation. *J Neurol Sci* 1996;142:111-113.
27. Sadun AA. Mitochondrial optic neuropathies. A model for a unifying theory. *J Neurol Neurosurg Psychiatry* 2002;72:423-425.
28. Sadun AA. Acquired mitochondrial impairment as a cause of optic nerve disease. *Trans Am Ophthalmol Soc* 1998;96:881-923.
29. Danielson SR, Wong A, Carelli V, et al. Cells bearing mutations causing Leber's hereditary optic neuropathy are sensitized to Fas-induced apoptosis. *J Biol Chem* 2002;277(8):5810-5815.
30. Carelli V, Ghelli A, Cevoli S, et al. Idebenone therapy in Leber's hereditary optic neuropathy: Report of six cases. *Neurology* 1998;50 Suppl 4:VI-02.002:A4.

## DISCUSSION

---

DR ALAN H. FRIEDMAN. The authors are to be congratulated on the exhaustive nature of their study and the doggedness in which they pursued it.

The purpose of this study was to investigate possible contributory factors to the development of blindness in patients with LHON. Eye examinations and blood tests were administered to determine carrier status for the LHON mutation in a large Brazilian family that had homoplasmy for LHON 11778, J-haplotype. In addition, questionnaires about dietary habits, recreational activities, concurrent medical problems, and toxic exposures were studied. The data were evaluated to focus on the differences between blind versus nonblind carriers of the mutation.

Environmental factors have been suggested as possible mechanisms in LHON expression. Wilson<sup>1</sup> and Cullom and colleagues<sup>2</sup> proposed heavy tobacco smoking and secondarily undetoxified cyanide as possible factors.

The authors wrote "at minimum, they wished to examine the (nuclear) genetic and epigenetic factors that might trip the threshold of expression that leads to blindness." No further mention is made of the nuclear factors other than "Most of the blood was sent to the Bologna laboratory for DNA extraction for gene linkage analysis of the nuclear DNA." What were the authors looking for? Was anything found?

Regarding epigenetic factors, the authors provide the results of environmental and medical history questionnaires. Consumption of fruits, exposure to toxins, cigarette smoking, alcohol consumption, and exercise tendencies differed between the LHON blind and LHON nonblind. What is not clear from the results is the timing of these differences. Were these differences present prior to the development of blindness? If so, for how long were they present? If the authors are trying to examine what might alter a phenotype, then it would be important to note if and for how long the modifying factors are present prior to the onset of the phenotypic trait. Otherwise one might argue that dietary regimens, alcohol, smoking, and exercise might change as a result of the development of blindness.

The authors also looked at penetrance rates and noted that there was significantly reduced penetrance with latter generations. It might be a good idea to include the LHON nonblind carrier/obligate carrier on the pedigree to make it easier for the reader to see the actual penetrance rates of blindness. It is also important to note the average age at which each generation became blind and the average age of each generation when the study was performed. As noted, reduced penetrance in later generations may simply have to do with the fact that the subjects are younger and have not yet developed the trait.

I would like to acknowledge the assistance of Dr Melissa Wasserstein of the Department of Genetics and Dr Joel Mindel of the Department of Ophthalmology at The Mount Sinai School of Medicine in reviewing the manuscript.

## REFERENCES

---

1. Wilson J: Leber's hereditary optic atrophy: some clinical and aetiological considerations. *Brain* 1963; 86:346-362.
2. Cullom ME, Heher KL, Miller NR, Savino PJ, Johns DR: Leber's hereditary optic neuropathy masquerading as tobacco-alcohol amblyopia. *Arch Ophthalmol* 1993;111:1482-1485.

DR ALLAN J. FLACH. Do any of the visual fields reflect either a tobacco or a nutritional amblyopia? Did your histories pick up any suggestion of insecticide toxicity that might be contributing?

DR BRIAN R. YOUNGE. Do those of you who make a diagnosis of tobacco-alcohol amblyopia do testing to rule out Leber's disease on that individual, since they present in a similar fashion?

DR IVAN R. SCHWAB. If you assume that it's tobacco-alcohol related, this only accounts for approximately 50% of the affected individuals. What about the other 50%? You need to be very careful about making associations with ancillary points because the study wasn't designed to look at these ancillary points.

DR ALLAN J. FLACH. Dr Harrington taught us that there is no such thing as tobacco-alcohol amblyopia. Alcohol amblyopia is a form of nutritional amblyopia. Tobacco amblyopia exists, and these two diseases can be distinguished by visual field. One has a central scotoma, and the other has a scotoma that's not central. One has sloping margins, and the other does not have sloping margins to the visual field defect.

DR ALFREDO A. SADUN. I will begin with the questions of Dr Friedman. He was quite right in that the purpose of our study as presented today was to look only at the epigenetic factors. The gene-linkage analysis has not been completed; it's being done in conjunction between Bologna and Iowa, where Ed Stone has his hunches and we have ours. It will take another year to complete such an exhaustive study. Dr Friedman asked whether the risk factors were there at the time of the examinations or were they there at the time that the individual went blind. We have figured out a way of dividing the database to look at them separately. I think the more interesting aspect is

what the risk factors were at the time the patients went blind. I showed the numbers at the time that we did the examination. The historical numbers that reflect the risks at time of visual loss are less reliable owing to dependence on memory, but they indicate these same risk factors in even greater preponderance. We have now begun to analyze the data reflecting risks that occurred at the time that the patient went blind, notwithstanding the fact that their memories, of course, may not be accurate for an event that occurred 20 or 30 years ago. Dr Friedman also asked at what ages they went blind. The intuition is that if the penetrance rate keeps going down, perhaps the age at onset should also be going up, as we're shifting the threshold. We were amazed to discover that the opposite was the case. In the first few generations, people went blind in their 30s, and in the last few generations people have been going blind in their 20s, early 20s, and now as teenagers. For some reason, it's an all-or-none phenomenon which is becoming less frequent but occurring at a younger age when it does.

Dr Flach points out that there is a tremendous amount of overlap here between tobacco-alcohol amblyopia (or nutritional amblyopia) and the disease process discussed here. The visual fields are probably not the best way of making that distinction. They both present with central scotomas, although the central scotoma of tobacco-alcohol amblyopia tends to be relatively small, perhaps about 5° to 10°, whereas that seen in this particular disease (LHON) is enormous. We are probably looking at different ways of skinning the cat by injuring mitochondria genetically and in an acquired fashion. Dr Flach also asked if we had a chance to look at the various insecticides

that were used. It turns out that the pesticides probably are organophosphates, and the mechanism of action of organophosphates is, in fact, on the parasympathetic system, so that, in fact, they may aggravate the situation in the way that he has suggested.

Dr Younge reminds us it's very important to consider the overlap between the two diseases of LHON and nutritional deficiencies. I, too, have had patients who have called in after the blood tests were made available and in whom I had initially made a diagnosis of tobacco-alcohol amblyopia only to be surprised to later discover that they had Leber's. I do believe that some of these individuals may have suffered from the effects of smoking and drinking, although it's rather hard to say that this is the only cause when they're also carrying the mitochondrial deficiency. I'd rather think of it as tipping them over a threshold.

Dr Ivan Schwab suggested that one must be careful about ancillary associations when the study did not directly test this as a hypothesis. This is a very important point that I call the Feynman concern, since Richard Feynman was a Nobel Laureate who often found this mistake in the work of others. Even overwhelming statistics can't prove a point that wasn't hypothesized before the data were accrued. Hence I reemphasize and summarize from the conclusions of this present paper. The new associations from this study serve as a good start in looking at the relationship between genetic and epigenetic factors for the expression of blindness in LHON. These new hypotheses can then be definitively tested by more focused follow-up examinations in our LHON Brazilian population and in animal models.



# THE DISC DAMAGE LIKELIHOOD SCALE: REPRODUCIBILITY OF A NEW METHOD OF ESTIMATING THE AMOUNT OF OPTIC NERVE DAMAGE CAUSED BY GLAUCOMA

---

BY *George L. Spaeth, MD, Jeffrey Henderer, MD* (BY INVITATION), *Connie Liu, BA* (BY INVITATION), *Muge Kesen, MD* (BY INVITATION), *Undraa Altangerel, MD* (BY INVITATION), *Atilla Bayer, MD* (BY INVITATION), *L. Jay Katz, MD* (BY INVITATION), *Jonathan Myers, MD* (BY INVITATION), *Douglas Rhee, MD* (BY INVITATION), AND *William Steinmann, MD* (BY INVITATION)

## ABSTRACT

*Purpose:* The major objective of this study was to test the reproducibility of a new method of estimating the amount of optic disc damage in patients with glaucoma.

*Methods:* The Disc Damage Likelihood Scale (DDLS) is based on the appearance of the neuroretinal rim of the optic disc corrected for disc diameter. The eight stages, extending from no damage to far advanced damage, are based on the width of the neuroretinal rim or the circumferential extent of absence of neuroretinal rim. Reproducibility was measured by two masked observers staging 48 optic nerve stereoscopic photographs by two different methods, the cup/disc ratio (c/d) and the DDLS. Also, reproducibility was assessed by three observers examining 34 eyes of 24 patients.

*Results:* With regard to the photographs, the intraobserver and interobserver reproducibility was better using the DDLS than the c/d ratio (98% versus 85% for intraobserver of reproducibility, and 85% versus 74% for interobserver reproducibility). The DDLS correlated better with the Humphrey Visual Field than did any Heidelberg Retina Tomograph parameter.

*Conclusion:* In a clinical setting, the DDLS is as reproducible as, or more reproducible than, the c/d ratio system of estimating the amount of disc damage in patients with glaucoma.

*Trans Am Ophthalmol Soc* 2002;100:181-186

## INTRODUCTION

---

Glaucoma is a process in which the tissues of the eye, most importantly the optic nerve, become damaged in a characteristic fashion, at least partially related to intraocular pressure (IOP). As such, evaluation of the optic disc plays a highly important role in the diagnosis and management of patients with glaucoma. Several methods have been described to stage the amount of disc damage.<sup>1-5</sup>

The first four of these have been available for some years but have not been widely utilized. We have developed a new scale that we believe offers significant advantages over the previous four scales.<sup>5</sup> We believe that this new scale may be useful in all those areas where it is appro-

priate to know how much glaucomatous damage a patient has sustained. This new scale is called the Disc Damage Likelihood Scale (DDLS). In the present study we evaluated the DDLS in terms of reproducibility and reliability.

## METHODS

---

Patient photographs were selected by reviewing records from the Glaucoma Service Diagnostic Laboratory of the Wills Eye Hospital. Patients were placed into one of four categories according to the amount of visual field damage: no damage (15 patients), mild damage (12 patients), moderate damage (10 patients), and severe damage (11 patients). Photographs were examined using a stereo viewer by two glaucoma specialists who staged the optic nerves according to the DDLS (Table I and Figure 1) and the cup-disc (c/d) ratio method. It was assumed that all optic nerves were of average size. Graders noted both the vertical and the horizontal c/d ratios using a ruler. Each photograph was examined by each grader in three different sessions. Interobserver and intraobserver agreement was determined by the test-retest method for the DDLS and for the c/d ratio.

From William and Anna Goldberg Glaucoma Research Laboratories, Wills Eye Hospital, Jefferson Medical College, Philadelphia, Pennsylvania (Dr Spaeth, Dr Henderer, Dr Kesen, Dr Altangerel, Dr Bayer, Dr Katz, Dr Myers, and Dr Rhee); Temple University School of Medicine, Philadelphia (Ms Liu); and the Tulane Center for Clinical Effectiveness and Prevention, Tulane University Health Sciences Center, Tulane University, New Orleans, Louisiana (Dr Steinmann). Supported in part by a grant from the Glaucoma Service Foundation of the Wills Eye Hospital and an unrestricted grant from Pharmacia, Inc.

DDLS Stage	Narrowest width of rim (rim/disc ratio)			DDLS Stage	Examples		
	For Small Disc <1.50 mm	For Average Size Disc 1.50-2.00 mm	For Large Disc >2.00 mm		1.25 mm optic nerve	1.75 mm optic nerve	2.25 mm optic nerve
0a	.5 or more	.4 or more	.3 or more	0a			
0b	.4 to .49	.3 to .39	.2 to .29	0b			
1	.3 to .39	.2 to .29	.1 to .19	1			
2	.2 to .29	.1 to .19	less than .1	2			
3	.1 to .19	less than .1	0 for less than 45°	3			
4	less than .1	0 for less than 45°	0 for 46° to 90°	4			
5	0 for less than 45°	0 for 46° to 90°	0 for 91° to 180°	5			
6	0 for 46° to 90°	0 for 91° to 180°	0 for 181° to 270°	6			
7a	0 for 91° to 180°	0 for 181° to 270°	0 for more than 270°	7a			
7b	0 for more than 180°	0 for more than 270°		7b			

FIGURE 1

Disc Damage Likelihood Scale (DDLS) nomogram. DDLS is based on the radial width of the neuroretinal rim measured at its thinnest point. Unit of measurement is rim/disc ratio (ie, the radial width of the rim compared to the diameter of the disc in the same axis). When there is no rim remaining, the rim/disc ratio is 0. The circumferential extent of rim absence (0 rim/disc ratio) is measured in degrees. Caution must be taken to differentiate the actual absence of rim from sloping of the rim as, for example, can occur temporally in some patients with myopia. A sloping rim is not an absent rim. Because rim width is a function of disc size, disc size must be evaluated prior to attributing a DDLS stage. This is done with a 60D to 90D lens with appropriate corrective factors. The Volk 66D lens minimally underestimates the disc size. Corrective factors for other lenses are: Volk 60D × .88, 78D × 1.2, 90D × 1.33; Nikon 60D × 1.03, 90D × 1.63.

TABLE I: THE DISC DAMAGE LIKELIHOOD SCALE

STAGE	NARROWEST WIDTH OF RIM
0	0.3-0.5
1	0.2-0.29
2	0.1-0.19
3	0.01-0.1
4	No rim <45°
5	No rim 45°-90°
6	No rim 91°-180°
7	No rim >180°

Three observers examined 34 eyes of 24 consecutive glaucoma patients using a Haag-Strait slit lamp and a Volk 66 diopter lens,<sup>6</sup> making a single determination of the c/d ratio and the DDLS stage. The number of inter-observer agreements was tabulated using a cutoff of equal or less to 1 DDLS stage, and equal or less to 0.1 c/d ratio.

## RESULTS

Results are summarized in Tables IIA, IIB, and III.

## DISCUSSION

Diagnostic tests are valuable to the extent that they are (1) reliable, (2) "user-friendly," and (3) reproducible. *Reliable* means that the finding represents what it is supposed to represent. *User-friendly* is self-evident. *Reproducible* means on subsequent examinations the same observer or different observers will describe a particular finding the same way.

This report deals with the reproducibility of a measure to estimate the extent of any damage caused to the optic disc by glaucoma. The usual method now used to evaluate the state of the optic disc in patients with glaucoma is the c/d ratio.<sup>7</sup> This user-friendly system has resulted in better

**TABLE IIA: INTEROBSERVER AND INTRAOBSERVER AGREEMENT ( $\leq 0.1$  C/D OR  $< 1$  DDLS STAGE) FOR SELECTED DISC MEASUREMENTS**

	ARMALY VERTICAL C/D RATIO			OVERALL DDLS STAGE		
	Reading 1	Reading 2	Reading 3	Reading 1	Reading 2	Reading 3
Interobserver Grader 1 + 2	32/48	34/48	32/48	40/48	41/48	42/48
Intraobserver	Reading 1 – Reading 2	Reading 2 Reading 3	Reading 1 – Reading 3	Reading 1 – Reading 2	Reading 2 – Reading 3	Reading 1 – Reading 3
Grader 1	43/48	43/48	42/48	48/48	47/48	47/48
Grader 2	43/48	47/48	47/48	48/48	47/48	47/48

c/d, cup-disc; DDLS, Disc Damage Likelihood Scale.

**TABLE IIB: SUMMARY OF MEAN INTEROBSERVER AND INTRAOBSERVER AGREEMENT  $\leq 1$  DDLS STAGE OR  $< 0.1$  C/D RATIO/FOR REMAINING DISC CRITERIA (% AGREEMENT AND SD)**

	INTEROBSERVER		INTRAOBSERVER	
			GRADER 1	GRADER 2
Horizontal c/d ratio	69 (0.02)	89 (0.07)	92 (0)	
Vertical c/d ratio	68 (0.02)	89 (0.01)	95 (0.05)	

c/d, cup-disc; DDLS, Disc Damage Likelihood Scale.

**TABLE IIC: LEVEL OF IN VIVO INTEROBSERVER AGREEMENT ( $\leq 1$  DDLS STAGE AND  $\leq 0.1$  C/D) FOR THE THREE OBSERVERS**

	AGREEMENT OF ALL THREE OBSERVERS (%)	AGREEMENT BETWEEN 2 OF 3 OBSERVERS (%)
DDLS stage	24/34 (70.5)	34/34 (100)
Armary c/d ratio	23/34 (67.6)	33/34 (97.1)

c/d, cup-disc; DDLS, Disc Damage Likelihood Scale.

communication between observers and better care for patients. The reproducibility of the system, however, is only moderate.<sup>8-12</sup> Further, the reliability is not high.<sup>13-15</sup> That is, some patients have small c/d ratios but significant visual field loss, whereas some have large c/d ratios with little visual field loss. Finally, while the c/d ratio is of some value in patients with concentric cupping,<sup>16</sup> it may be seriously misleading when the loss of rim is limited to a single sector, as with a focal notch. In this latter situation, the c/d ratio may be recorded as small, and yet the disc and visual field may be badly damaged.

The DDLS was designed to be reliable, user-friendly, and reproducible. Reliability of the DDLS has been assessed by Bayer and colleagues,<sup>5</sup> who concluded that the DDLS correlated strongly with the amount of visual field damage.

**TABLE IID: DISTRIBUTION OF THE DDLS IN A GLAUCOMA REFERRAL PRACTICE**

DDLS SCALE	NO. OF CASES
0	271
1	500
2	447
3	330
4	176
5	105
6	136
7	186

DDLS, Disc Damage Likelihood Scale.

**TABLE IIE: POSITIVE PREDICTIVE VALUE OF DISC FINDINGS**

Disc Finding	Significance of Disc Finding As Sign of Worsening
Acquired pit of optic nerve	High
Absent rim	High
Progressive narrowing of rim greater than that seen with normal aging	High
Breaks ISNT rule	Moderately high
Disc hemorrhage	Moderate
Large c/d ratio	Low
Significance of Disc Finding As Sign of Worsening	
Narrowing of rim	High
Disc hemorrhage	Moderate

c/d, cup-disc; ISNT, inferior, superior, nasal and temporal.

Regarding user-friendliness, the DDLS is readily learned, and once the vertical diameter projected on the retina by the direct ophthalmoscope has been determined by using a strong plus lens such as the Volk 66, the only instrumentation required is the direct ophthalmoscope.

The DDLS system is now utilized as part of the routine examination in the office practice of the senior

author. Each time the disc is examined, the DDLS is recorded. This permits quantification, a characteristic considered important by Klein and associates.<sup>17</sup> The DDLS can be recorded in computer-compatible codes, so as to allow easy recovery of data. Such a code can include both the stage and the eye. For example, in our office we code all examinations with a DG (for the disc grade), followed by the eye (RT for right, and LT for left), and then the grade. Thus, DGRT 0 represents a disc grade of 0 in the right eye, and DGLT 2 represents a disc grade of 2 in the left eye.

Easy retrieval of information regarding the stage of patients with glaucoma facilitates a variety of projects related to clinical practice and research. For example, at present it is difficult to generalize results from one clinical study to another clinical study because of uncertainty regarding the similarity or dissimilarity of the populations involved. Knowing this information will allow better characterization of populations and better research. For example, Table IV lists the distribution of disc stages in the population of private patients followed by the senior author. This probably differs considerably from other practices, but whether this is indeed the case and to what extent there is a difference are at present difficult or impossible to ascertain.

Tests must also be reproducible to be valuable. The present study indicates that the DDLS is adequately reproducible. Indeed, it appears to be more so than the c/d ratio.

Diagnosis of glaucoma depends primarily on recognizing the pattern of characteristic damage (Table V). Just what is characteristic, however, is controversial. For example, hemorrhages crossing the rim of the optic disc are considered by some to be highly characteristic, and it has been shown that there is an association between the presence of hemorrhage and a worse prognosis in patients with glaucoma. However, such hemorrhages are seen in patients who do not have glaucoma and who never develop visual field loss or any other change believed to be characteristic of glaucoma. Lichter and Henderson<sup>18</sup> described a disc hemorrhage as a part of what they believed to be a stable condition different from glaucoma. Management of glaucoma depends largely on recognizing a change. Recognition of change requires reproducible quantification. The previous systems that have been suggested in this regard usually utilize the c/d ratio system and are limited to five stages, most of which describe the later stages of damage.<sup>1-4</sup> As such, detection of change becomes difficult. Additionally, these previously described systems have not been validated. Perhaps for these reasons, none of these existing systems has been widely utilized.

The DDLS was designed primarily for use in patients with glaucoma. Its value as a measure of estimating dam-

age associated with other diseases of the optic nerve has not been studied.

## CONCLUSION

---

The DDLS is a reproducible method of estimating the amount of optic nerve damage caused by glaucoma. It may provide a useful method of diagnosing and managing patients with glaucoma.

## REFERENCES

---

1. Nesterov A, Listopadova N. Classification of glaucoma. *Vestnik Oftalmolog* 1972;6:10-14.
2. Shiose Y, Kanda T. Quantitative analysis of the "optic cup" and its clinical application. Part II: Consideration of clinical cases. *Jpn J Clin Ophthalmol* 1974;38:367-374.
3. Heilmann R, Richardson KT. *Glaucoma: Concepts of a Disease*. Philadelphia: WB Saunders, 1978.
4. Jonas JB, Gusek GC, Naumann GOH. Optic disc morphometry in chronic primary open-angle glaucoma. II. Correlation of the intrapapillary morphometric data. *Graefes Arch Klin Exp Ophthalmol* 1988;226:531-538.
5. Bayer A, Harasymowycz P, Henderer JD, et al. Validity of a new disc grading scale for estimating glaucomatous damage: correlation with visual field damage. *Am J Ophthalmol* 2002 (in press).
6. Lim CS, O'Brien C, Bolton NM. A simple clinical method to measure the optic disc size in glaucoma. *J Glaucoma* 1996;5:241-245.
7. Armaly M. Genetic determination of cup/disc ratio of the optic nerve. *Arch Ophthalmol* 1967;78:35-43.
8. Tielsch J, Katz J, Quigley H, et al. Intraobserver and interobserver agreement in measurement of optic disc characteristics. *Ophthalmology* 1988;95:350-356.
9. Varma R, Steinmann W, Scott I. Expert agreement in evaluating the optic disc for glaucoma. *Ophthalmology* 1992;99:215-221.
10. Wolfs RC, Ramrattan RS, Hofman A, et al. Cup-to-disc ratio: ophthalmoscopy versus automated measurement in a general population: the Rotterdam study. *Ophthalmology* 1999;106:1597-1601.
11. Varma R, Spaeth G, Steinmann W, et al. Agreement between clinicians and an image analyzer in estimating cup-to-disc ratios. *Arch Ophthalmol* 1989;107:526-590.
12. Mikelberg F, Douglas G, Schulzer M, et al. The correlation between cup-disk ratio, neuroretinal rim area, and optic disk area measured by the video-ophthalmograph (Rodenstock analyzer) and clinical measurement. *Am J Ophthalmol* 1986;101:7-12.
13. Douglas G, Drance S, Schulzer M. A correlation of fields and discs in open angle glaucoma. *Can J Ophthalmol* 1974;9:391-398.
14. Guthauser U, Flammer J, Niesel P. The relationship between the visual field and the optic nerve head in glaucomas. *Graefes Arch Clin Exp Ophthalmol* 1987;225:129-132.

15. Miglior S, Brigatti L, Lonati C, et al. Correlation between the progression of optic disc and visual field changes in glaucoma. *Curr Eye Res* 1995;14:145-149.
16. Read RM, Spaeth GL. The practical clinical appraisal of the optic disc in glaucoma: the natural history of cup progression and some specific disc-field correlations. *Trans Am Acad Ophthalmol Otolaryngol* 1974;78:255-274.
17. Klein B, Magli Y, Richie K, et al. Quantification of optic disc cupping. *Ophthalmology* 1985;92:1654-1656.
18. Lichter PR, Henderson JW. Optic nerve infarction. *Trans Am Ophthalmol Soc* 1977;75:103-121.

## DISCUSSION

DR JAMES C. BOBROW. Each time George Spaeth reports his observations, he challenges our intellects. Whether he is assessing the anterior chamber angle or observing the optic disc, he forces us to reconsider our presumptions. As long ago as 1985 and 1989, he argued that the methods used to estimate the extent of change of the cup/disc ratio as a measurement of damage from glaucoma need revision.<sup>1,2</sup> In addition, Dr Spaeth has been in the forefront of the comparison of clinically derived measurements of optic nerve parameters with scanning laser tomography.<sup>3</sup>

Now we are being asked to reconsider the damage to the optic nerve in glaucoma from the rim in instead of from the cup out, and we are being told that the quadrants that are most vulnerable—the superior and inferior poles of the disc—are the ones on which we should focus the majority of our attention and expand the range of quantification of our observations.

Some of these data are already used in the measurements of vertical and horizontal disc size and in the emphasis on contour and depth instead of color. However, in spite of our level of confidence in our own observations, we have been confronted by several investigators with the fact that we simply don't agree about our measurements.<sup>4,6</sup> Intraobserver differences appear to be fairly consistent, but interobserver agreement is often faulty using the Armaly-derived criteria. In Dr Spaeth's presentation, interobserver agreement has been demonstrated to be improved from previous studies.

I responded to Dr Spaeth's challenge by conducting a brief reconsideration of the visual fields and three-dimensional photographs of 30 eyes of 15 patients with glaucoma in my own practice to see whether I could confirm some of his observations and whether, by applying his method of evaluation, I would gain additional insight into the relationship between the appearance of the optic disc and visual fields obtained at approximately the same time.

The results confirm Dr Spaeth's study and show that these measurements are relatively easy to learn. The DDLS scores for each three-dimensional disc photograph were plotted against a scale of field loss. Scores ranged from

1 = normal, to 10 = extensive field loss. The graph is shown in Figure 1. The  $r$  value of the curve was 0.45.

The DDLS scores were then compared to the mean deviation score from the Humphrey Visual Field Analyzer (Zeiss Instruments San Leandro, California). Figure 2 shows the plot of DDLS versus mean deviation. Here  $r = 0.68$ .

We are fortunate in ophthalmology to be able to visualize much of our patients' pathology. In conclusion, I

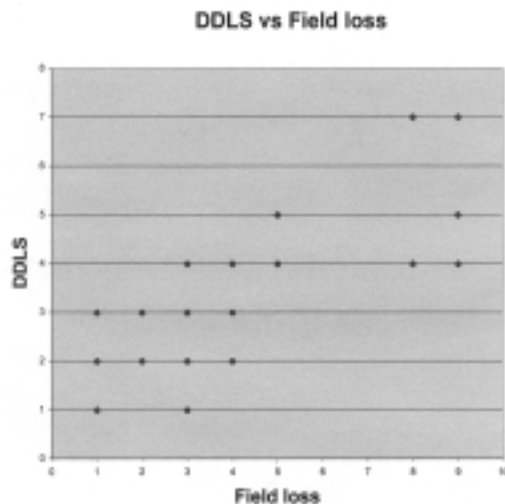


FIGURE 1

The DDLS scores for each three-dimensional disc photograph plotted against a scale of field loss. Scores ranged from 1 = normal to 10 = extensive field loss.  $r$  value of the curve was 0.45.

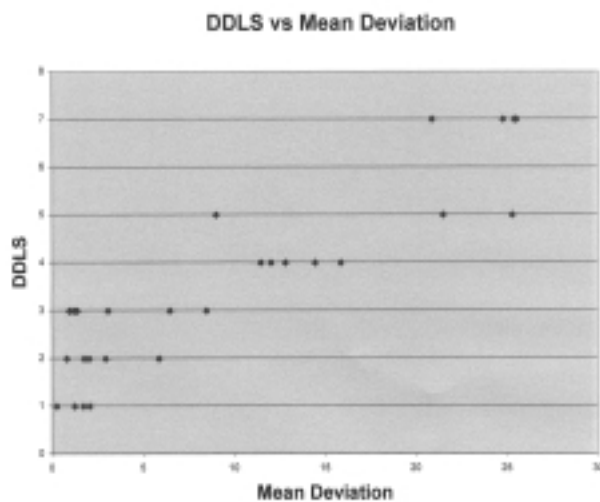


FIGURE 2

The DDLS scores compared to the mean deviation score from the Humphrey Visual Field Analyzer.  $r$  value of the curve was 0.68

want to congratulate Dr Spaeth and his coworkers for again raising our clinical awareness that careful observation of our patients will yield accurate information to assist us in caring for them.

## REFERENCES

---

1. Spaeth GL, Fellman RL, Starita RL, et al. A new management system for glaucoma based on improvement of the appearance of the optic disc or visual field. *Trans Am Ophthalmol Soc* 1985;83:268-284.
2. Katz LJ, Spaeth GL, Cantor LB, et al. Reversible optic disk cupping and visual field improvement in adults with glaucoma. *Am J Ophthalmol* 1989;107(5):485-492.
3. Eid TM, Spaeth GL, Katz LJ, et al. Quantitative estimation of retinal nerve fiber layer height in glaucoma and the relationship with optic nerve head topography and visual field. *J Glaucoma* 1997;6(4):221-230.
4. Hatch VW, Trope GE, Buys YM, et al. Agreement in assessing glaucomatous discs in a clinical teaching setting with stereoscopic disc photographs, planimetry, and laser scanning tomography. *J Glaucoma* 1999;8(2):99-104.
5. Haslett RS, Batterbury M, Cuypers M, et al. Inter-observer agreement in clinical optic disc measurement using a modified 60D lens. *Eye* 1997;11(Pt 5):692-697.
6. Feuer WJ, Parrish RK, Schiffman JC, et al. The Ocular Hypertension Treatment Study: reproducibility of cup/disk ratio measurements over time at an optic disc reading center. *Am J Ophthalmol* 2002;133(1): 19-28.

DR ROBERT RITCH. You stated that 30% of patients with hypotony get blebitis each year. There is probably more hypotony per se than bleb leaks leading to hypotony or bleb leaks leading to blebitis. You need to be careful in doing a Seidel test, since some ophthalmologists use dry

strips and actually cause bleb leaks. Use a wet strip and just touch it to the bleb.

(Editors note: Dr Spaeth's comment was in the presentation but not in the paper)

DR GEORGE SPAETH. I want to thank Dr Bobrow for his discussion. Every presenter probably wants the people who discuss their presentations to understand the substance of their talks. What better way is there to do that than to test out the presenter's hypothesis? I am delighted that Dr Bobrow actually did that. I am pleased that he found the Disc Damage Likelihood Scale to be workable and apparently useful. I thank him for taking the time to test out the new system. I hope he continues to use it and finds it useful.

I agree with Dr Ritch that one needs to be careful in performing a Seidel test. However, I believe the significance of blebs which are sufficiently thin to allow aqueous to exit through the conjunctiva is becoming increasingly clear. When aqueous can exit through those blebs, then bacteria can enter through those blebs. A telling study presented at ARVO followed patients over a period of 10 years and noted that about 3.5% of patients developed endophthalmitis each 5 years. That is a deeply disturbing finding. My prediction is that few will be using mitomycin in association with the performance of primary guarded filtration procedures within 5 years.

# EVOLUTION OF THE TAPETUM

---

BY *Ivan R. Schwab, MD, Carlton K. Yuen, BS* (BY INVITATION), *Nedim C. Buyukmihci, VMD* (BY INVITATION), *Thomas N. Blankenship, PhD* (BY INVITATION), AND *Paul G. Fitzgerald, PhD* (BY INVITATION)

## ABSTRACT

*Purpose:* To review, contrast, and compare current known tapetal mechanisms and review the implications for the evolution of the tapetum.

*Methods:* Ocular specimens of representative fish in key piscine families, including Acipenseridae, Cyprinidae, Chacidae; the reptilian family Crocodylidae; the mammalian family Felidae; and the Lepidopteran family Sphingidae were reviewed and compared histologically. All known varieties of tapeta were examined and classified and compared to the known cladogram representing the evolution of each specific family.

*Results:* Types of tapeta include tapetum cellulosum, tapetum fibrosum, retinal tapetum, invertebrate pigmented tapetum, and invertebrate thin-film tapetum. All but the invertebrate pigmented tapetum were examined histologically. Review of the evolutionary cladogram and comparison with known tapeta suggest that the tapetum evolved in the Devonian period 345 to 395 million years ago. Tapeta developed independently in at least three separate orders in invertebrates and vertebrates, and yet all have surprisingly similar mechanisms of light reflection, including thin-film interference, diffusely reflecting tapeta, Mie scattering, Rayleigh scattering, and perhaps orthogonal retroreflection.

*Conclusion:* Tapeta are found in invertebrates and vertebrates and display different physical mechanisms of reflection. Each tapetum reflects the wavelengths most relevant to the species' ecological niche. With this work, we have hypothesized that the tapetum evolved independently in both invertebrates and vertebrates as early as the Devonian period and coincided with an explosion of life forms.

*Trans Am Ophthalmol Soc* 2002;100:187-200

## INTRODUCTION

---

The tapetum lucidum (shining carpet in Latin) is a catoptric device found in the eye of many vertebrates and invertebrates, which serves to increase the amount of light absorbed by the photoreceptors. The tapetum is proximal to the photoreceptors and may be located in either the choroid or deep retina in vertebrates and proximal to the reticular cells in invertebrates. The tapetum reflects the photons that were not initially absorbed after they passed through the photoreceptors. These reflector mechanisms provide the photoreceptors a second chance at absorbing the (reflected) light, thereby enhancing an organism's visual sensitivity. This device is often a layer, and it is especially useful in lower light conditions. Animals use a wide range of materials and techniques to provide tapetal

reflectance, including guanine, riboflavin, triglycerides, pteridine, cholesterol, zinc, astaxanthin, and collagen.<sup>1</sup> Apparently, tapeta have evolved several times with these different mechanisms and represent convergent evolution of function.

## METHODS

---

Ocular specimens that are representative of fish in key piscine families, including Acipenseridae (*Acipenser medirostris*, the green sturgeon), Cyprinidae (*Cyprinus carpio*, the common carp), and Chacidae (*Ictalurus punctatus*, the channel catfish), were obtained from a local fish market. The ocular specimens were removed from the deceased fish. An ocular specimen of a member of the reptilian family Crocodylidae (*Alligator mississippiensis*, the American alligator) was obtained from Dennis Brooks, DVM, PhD, of the University of Florida in Gainesville. A fixed ocular specimen of the mammalian family Felidae (*Felis domesticus*, the domestic housecat) was obtained from Leslie Lyons, PhD, and David Maggs, BVS (hons), DACVO, of the University of California, Davis, School of Veterinary Medicine. A specimen of the Lepidopteran

From the Department of Ophthalmology, University of California, Davis, Medical Center (Dr Schwab); the University of California, Davis, School of Medicine (Dr Schwab, Mr Yuen, Dr Blankenship, Dr Fitzgerald); and the University of California, Davis, School of Veterinary Medicine (Dr Buyukmihci). Supported in part by an unrestricted grant from Research to Prevent Blindness, Inc, New York, New York, and by grant P30EY12576 from the National Institutes of Health.

family, Sphingidae (*Arctonotus lucidus*, the Pacific green sphinx moth), was obtained with the help of John Debenedictis, PhD, staff entomologist, Bohart Museum of Entomology, University of California, Davis, and the compound eyes were dissected from the specimen. Each of these ocular specimens was sectioned and stained with hematoxylin-eosin (HE), periodic acid–Schiff (PAS), or toluidine blue (TB), examined, and compared with one another histologically. The evolutionary relationship of the ocular specimens was examined and the cladistic position of each species established, evaluated, and compared.

## RESULTS

The eye of *A medirostris*, the green sturgeon, was found to contain a tapetum cellulolum. Although it resembles a tapetum fibrosum in some respects when stained (PAS), it has a cellular structure within the choroid immediately proximal to the pigment epithelium with from three to five cells aligned somewhat irregularly (Figure 1), especially when compared with the more regularly and definitely formed feline tapetum cellulolum. When stained with HE, the sturgeon eye revealed guanin granules in the superficial choroid (Figure 2). The retinal pigment epithelium (RPE) was generally clear, as is typical for animals with a choroidal RPE, but regularly spaced RPE cells contained a dense concentration of melanin with intervening clear RPE cells (Figures 1 and 2).

The tapetum lucidum of *C carpio*, the common carp, was reviewed and confirmed to be a retinal tapetum composed of guanin in an oclusible pattern. The light-adapted eye shows pigment drawn into the more inner portions of the retinal pigment epithelium and obscuring the guanin of the retinal tapetum (Figure 3).

The eye of *I punctatus*, the channel catfish, shows an oclusible retinal tapetum. A light-adapted retina shows pigment drawn up into the broad retinal pigment epithelial cells in a manner similar to the carp (Figure 4).

The eye of *Allig mississippiensis*, the American alligator, revealed fine opaque crystalline granules in the apex of the pigment epithelial cells, and represents a retinal tapetum. These granules were present in the dorsal half of the retina, although the stain (TB) has made the rodlike structures of the granules appear black (Figures 5A and 5B).

The eye of *F domesticus*, the domestic housecat, shows a regular tapetum cellulolum. This cellular structure consists of 6 to 12 flat and well-organized cells arranged in a regular distribution, resembling precision brickwork (Figure 6).

The compound eye of *Arct lucidus*, the Pacific green sphinx moth, revealed a tapetum of modified tracheoles with chitin layers alternating with layers of air. The parallel layers of chitin and air have a long axis that is perpendicular

to the long axis of the rhabdom. These chitinous layers are separated by a standard distance from rhabdom to rhabdom (Figure 7).

## DISCUSSION

### TYPES OF TAPETUM

Tapeta can be classified according to location in vertebrates and mechanism in invertebrates (Table I).

#### Vertebrate Choroidal Tapeta

Choroidal tapeta are the most common and are further classified as tapetum fibrosum and tapetum cellulolum.

Histologically, the simplest type is the tapetum fibrosum, which is found principally in mammals, including herbivorous ungulates (eg, elephants, horses, goats) (Figures 8 and 9), cetaceans (whales, dolphins), some marsupials (Tasmanian devil), and a rodent (*Cuniculus pacas*).<sup>2,3</sup> The tapetum fibrosum consists of extracellular collagen fibrils stacked in an orderly manner with the majority of the fibers running horizontally.<sup>4</sup> The number of layers of fibrils varies between species and can be up to several hundred thick.<sup>2</sup>

The most studied tapetum fibrosum among the ungulates is found in the cow. In this species, the tapetum is located posteriorly and dorsally. It is of variable thickness, increasing in thickness posteriorly. In species with a choroidal tapetum, the retinal epithelium in the area of the tapetum is unpigmented, allowing light to pass to be subsequently reflected by the tapetum. This contrasts with the pigmented retinal epithelium cells found in the same animal in nontapetal regions.<sup>4</sup>

The tapetum cellulolum is found in cartilaginous fishes (eg, sharks, dogfishes), sturgeons (Figure 1), lobe-finned fishes (coelacanth and lungfishes), seals, prosimians (eg, bush babies [Figure 10], lemurs), and most mammalian carnivores (eg, cats, dogs [Figures 6 and 11]).<sup>1,5-7</sup> This tapetum is composed of regular cells in layers of variable thickness, containing a variety of reflective material.<sup>3,8,9</sup>

In the coelacanth (*Latimeria chalumnae*), the tapetum cellulolum consists of hexagonal constant-thickness stacks of guanine crystals within the individual cells. This tapetum emits a greenish-yellow luminescence in the live specimen, with a broad maximum wavelength of reflection peaking at 476 nm, which corresponds to the peak of the wavelength of light that penetrates to depths of 7,500 feet, where the animal is found. This choroidal tapetum underlies the entire retina and appears bright silvery upon dissection. Elasmobranchs also have tapeta composed of guanine, but their tapeta differ from those of the coelacanth and others in that they are oclusible. The tapetal cells alternate with, and are separated from, one another by melanocytes that extend beyond the tapetal cells to

*Evolution of the Tapetum*

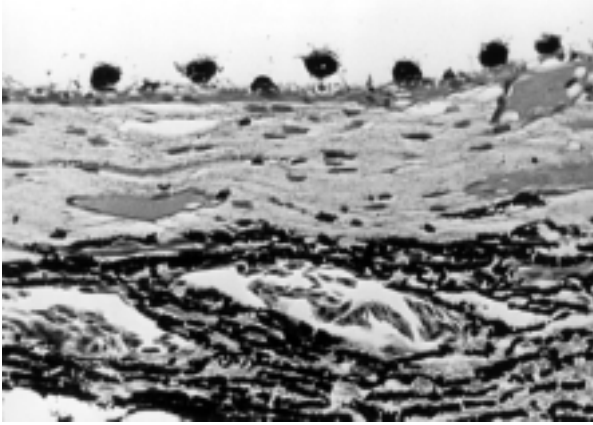


**FIGURE 1**

Sturgeon choroid stained with periodic acid-Schiff (x20). Retinal pigment epithelium (RPE) can be seen at top of photograph. Note periodicity of pigment in RPE. Intervening RPE cells contain no pigment.

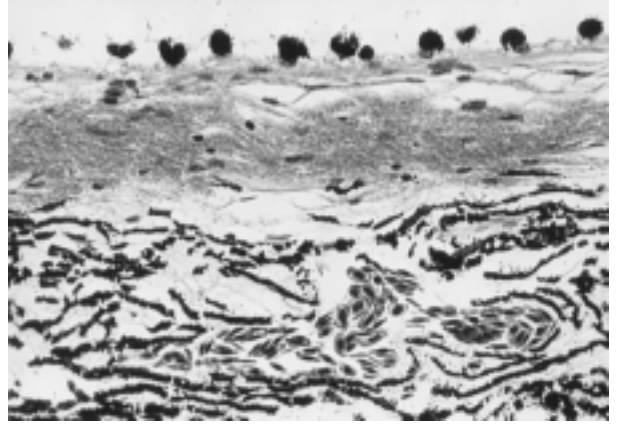


**FIGURE 2**

Sturgeon choroid stained with hematoxylin-eosin (x20). Note guanine crystals in superficial choroid immediately beneath retinal pigment epithelium (RPE). These crystals are seen as a grey coloration below pigmented deposits of RPE. Note periodicity of pigment in RPE.

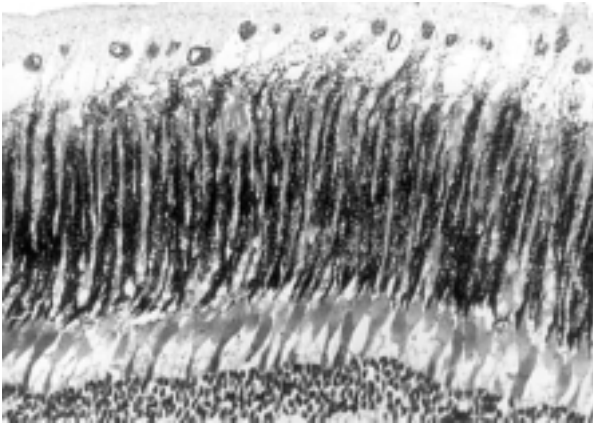


**FIGURE 3**

Carp retina stained with hematoxylin-eosin (x20). Note broadly distributed melanin throughout most of retina. This light-adapted retina exhibits an oclusable retinal tapetum. Cell bodies with nucleus of retinal pigment epithelium (RPE) can be seen at bottom of photograph. Note how little pigment is seen near base of RPE cell.

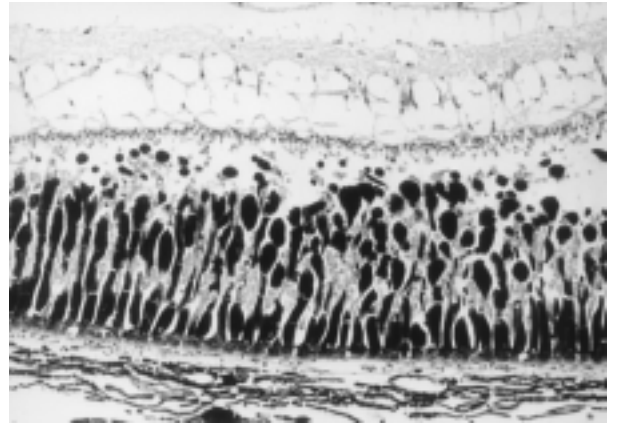


**FIGURE 4**

Light-adapted catfish retina stained with hematoxylin-eosin (x10). Note oclusable tapetum with the melanin pigment drawn nearly to outer nuclear layer, obscuring both tapetum and rod outer segments.

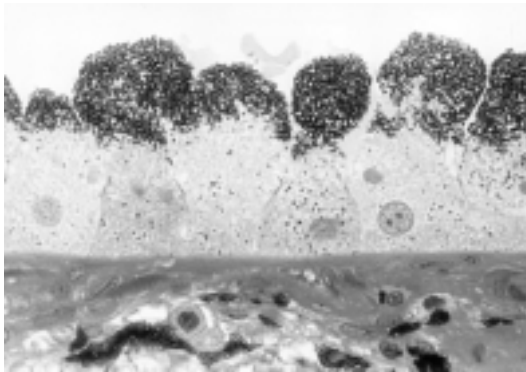


**FIGURE 5A**

Light-adapted American alligator retinal pigment epithelium (RPE) in a nontapetal region with pigment granules visible at tips of RPE stained with toluidine blue (x40). This retina is only partially oclusable and has probably lost the ability to be truly oclusable but does show some pigment migration in light adaptation. Pigment in the RPE is present in nontapetal regions of the eye.

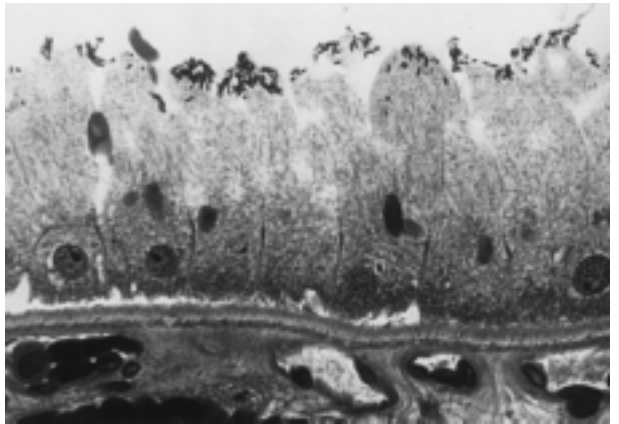


**FIGURE 5B**

Light-adapted American alligator retinal pigment epithelium (RPE) in tapetal region stained with toluidine blue (x40). Note black, flat platelike crystals in tips of RPE cells in contrast to granules of pigment seen in 5A. Many crystals were lost in preparation of specimen.

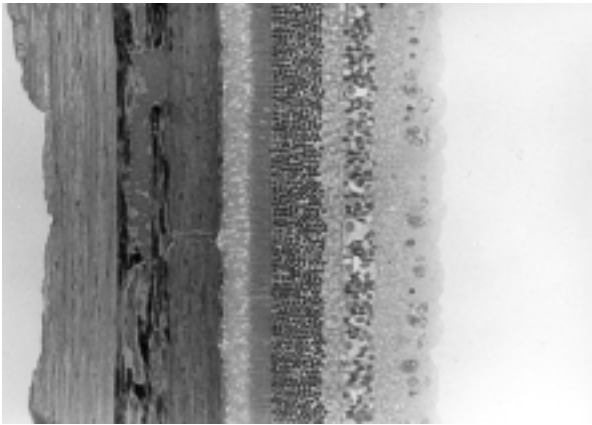


FIGURE 6

Cat choroid stained with toluidine blue (x20). Note regular tilelike cellular structure beneath retinal pigment epithelium (RPE) and photoreceptor outer segments. These cells in tapetum cellulosum are filled with many smaller platelike structures or rodlets seen with ultrastructural investigation.

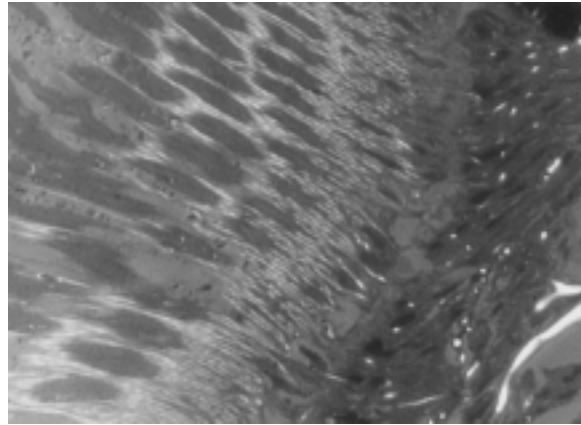


FIGURE 7

Compound eye of Pacific green sphinx moth stained with toluidine blue (x40). Larger tracheoles can be seen to right of photograph as clear spaces. As tracheoles become smaller (going toward left on photograph), they can be seen as small, clear circles. Tracheoles that become tapetum can be seen in about the middle of photograph as fine striations. Larger blue ovals toward left of photograph are undulations of rhabdoms of individual ommatidia.

intervene between the tapetal cells and incoming light. The melanocytes migrate in conditions of increased light to occlude the elasmobranch tapetum.<sup>5</sup>

The RPE and the choroidal tapetum of the sturgeon show another interesting feature. The regular deposits of pigment may serve a heretofore unrecognized purpose. The regular spacing of pigment would create a grating through which light could be channeled upon reflection, preventing extraneous photons from being scattered to adjacent photoreceptors. This would assist in the elimination of the glare of the reflection from the tapeta, which would otherwise lead to the degradation of the image owing to the scatter of the extraneous rays, and would be an alternative to an occludible tapetum as seen in the elasmobranchs.

#### *Vertebrate Retinal Tapeta*

The retinal tapetum has been found in some lampreys, certain bony fishes, crocodiles, goatsuckers, the Virginia opossum (*Didelphys virginiana*) (Figure 12), gar fishes, some old-world fruit bats, and many teleosts (Figures 3 and 4).<sup>1</sup> The retinal tapeta of fish have been further categorized as those that contain small particles in spheres or cubes, which are classified as diffuse reflectors, and those containing layered crystals, classified as specular reflectors. Specular reflectors function much like a mirror, whereas diffuse reflectors are more like the reflections from a rough surface and may use Mie scattering as their mechanism.<sup>19</sup> Diffuse tapeta can be found in many teleosts, including certain carp and cusk eels. Specular tapeta can be found in some lantern fish and other abyssal fish.<sup>9</sup>

Some species of lamprey have both diffuse and spec-

ular mechanisms. The reflecting material in teleost spheres includes nonpigmented materials (such as guanine, uric acid, and purines) and pigmented materials (including pteridine, lipid, astaxanthin, and melanoid compounds).<sup>1</sup> This represents a subclassification of the small-particle or diffuse reflectors.

In reptiles, only the crocodile and alligator have a tapetum, and it is found in the retinal pigment epithelium. This tapetum consists of several layers of crystalline platelets of guanine arranged in parallel. The tapetum appears to be somewhat occludible in certain species, such as the American alligator, and this could be explained by the diurnal and nocturnal potential of that species.<sup>10</sup> This contrasts with another crocodile, the *Caiman sclerops*, a nocturnal animal, which does not have an occludible tapetum. The tapetum of the *C sclerops* also consists of guanine crystals diffusely scattered within the RPE.<sup>11</sup>

The retinal tapetum of the opossum (*D virginiana*) is a semicircular area in the dorsal fundus. The reflecting material consists of lipoidal spheres scattered throughout the epithelial cells.<sup>12</sup> The tapeta of the crocodile and the opossum function as diffuse reflectors.

Amphibians, apparently, do not have tapeta, although a bright reflex is found in many of these species. The source of this bright reflection is unknown at present but does not conform to the currently understood mechanisms of any tapeta.

#### **INVERTEBRATE TAPETA**

##### *Pigmented Tapeta*

The invertebrate tapeta can be categorized as light-scattering pigments and those using thin-film interference.

*Evolution of the Tapetum*

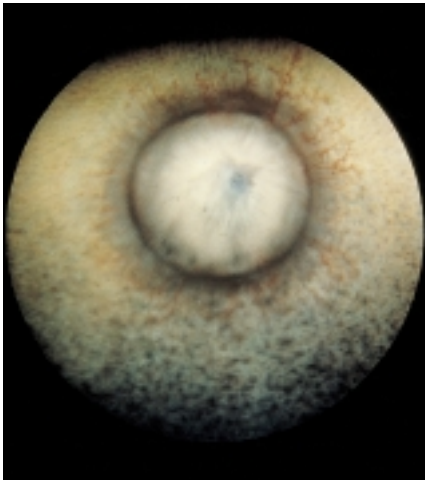


**FIGURE 8**

Fundus photograph of left eye of 6-year-old female African elephant. The elephant has a tapetum fibrosum.

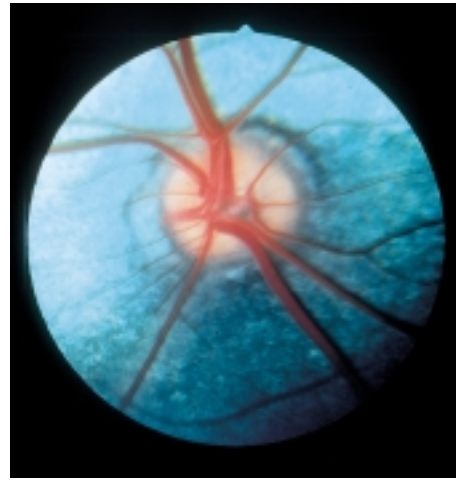


**FIGURE 9**

Fundus photograph of right eye of 6-month-old castrated male mixed-breed goat. The goat has a tapetum fibrosum.

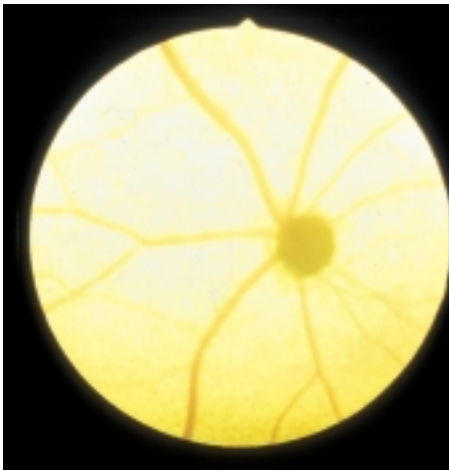


**FIGURE 10**

Fundus photograph of a galago. Bush babies have a tapetum cellulosum.



**FIGURE 11**

Fundus photograph of left eye of an adult female mixed-breed of dog. Dogs have a tapetum cellulosum.



**FIGURE 12**

Fundus photograph of right eye of adult male American opossum with retinal tapetum.

TABLE 1: TAPETA IN THE ANIMAL KINGDOM

ANIMAL KINGDOM		NO TAPETUM	CHOROICAL TAPETA		RETINAL TAPETA	LIGHT-SCATTERING TAPETA	THIN-FILM TAPETA	TAPETA REFLECTING MATERIAL	
			FIBROSUM	CELLULOSUM				UNPIGMENTED	PIGMENTED
Jawless Fishes	Lampreys	✓							
	Hag Fishes	✓							
Fishes	Sharks/Dog Fishes			+				Guanine	
	Sturgeons			+				Guanine	
	Garpikes				+				Astaxathine
	Bony Fishes		?	+	+			Several Materials	Several Materials
	Coelacanth			+			Guanine	Not Reported	Not Reported
	Lung Fishes			+					
Amphibians	Salamanders	✓							
	Frogs & Toads	✓							
Reptiles	Crocodiles and Alligators				+			Guanine	
	Most reptiles	✓							
Birds	Goatsuckers (Nighthjars)				+				Lipid
	Most Birds	✓							
	Monotremes	✓							
Mammals	Marsupials				+			Lipid (Birefringent)	
		Opossums						Collagen	
		Tasmanian Wolves		+				Collagen	
		Whales & dolphins		+				Collagen	
		Elephants & Most Hooved Animals		+				Collagen	
		Carnivores (Cats & Dogs)			+				Zinc protein
		Horses		+				Collagen	
		Lower (Bush Babies & Lemurs)			+				Riboflavin
		Aotus Monkeys	✓						
		All Other Higher Primates	✓						
Placentals		✓							
		Cuniculus Pacas		+				Collagen	
		Most Rodents	✓						
	Seals			+				Believed to be Zinc	
Mollusks	Fruit Bats				+			Phospholipid (birefringent)	
	Scallops						+	Guanine	Lipid
Arthropods	Crustaceans								
	Lobsters & Shrimp								
	Scorpions	✓							
	Arachnids						+		
	Spiders								
	Insects								
	Dragonflies						+		

In the eyes of crustaceans, light is reflected back to the rhabdoms by white or lightly colored pigments, including purines or pteridines. The reflection is less useful over shorter wavelengths but is effective over much of the spectrum and can almost double light capture.<sup>9,13</sup>

The tapeta of mesopelagic shrimps vary greatly between species, depending on the depth at which they live, and probably corresponding to individual ecological niches and the specific wavelengths required. Histologic examination of the tapetum shows that it is incomplete dorsally in some species from the upper mesopelagic zone (*Syrtellaspis debilis*, *Oplophorus spinosus*), with the amount of reflecting material increasing ventrally. Not surprisingly, peak transmission of light in oceanic species is in the blue-green region of the spectrum (450 to 500 nm). Visual pigments in crustaceans show absorbance between 470 and 490 nm, and reflecting materials appear white. The tapetum is located between the rhabdom and basement membrane.<sup>14</sup> The tapetum is complete in some deep-water species (*Syrtellaspis crsitata*, *Acanthephyra kingsleyi*, *Acanthomysis pelagica*) and is believed to be beneficial because of the lower levels of ambient light at greater depths. *Acanthephyra purpurea* has a thick tapetum peripherally but no tapetum in the central part of the eye. This is thought to interfere with the ability of predators to detect this shrimp because of decreased eye shine centrally. The tapetal adaptations of these species are believed to increase sensitivity to the dim upwelling irradiance and to bioluminescence.<sup>14</sup>

#### Thin-Film Invertebrate Tapeta

Thin-film interference is used by some invertebrates to construct a reflective tapetum. The best examples of this mechanism are found in the lycosid spiders, scallop (*Pecten maximum*), ostracod crustaceans, cockle (*Cardium edule*), and rotifers.<sup>13,15-18</sup> In the ctenid spider, a type of lycosid, the tapetum is located proximal to the rhabdomeres in the secondary eyes, while the primary anteromedial eyes do not have a tapetum. The secondary eyes are built around a "gridiron" tapetum, consisting of parallel strips of reflecting material forming a double ladder-like array.<sup>15</sup> The reflecting material in lycosid spiders has been reported as guanine.

Tapeta have also been described in only a few mollusks. In the scallop (*P. maximum*), for example, square guanine crystals have been described as a tapetum.<sup>16</sup>

Nocturnal moths and diurnal butterflies both possess a tapetum constructed of modified tracheoles, or airway cells.<sup>17</sup> The tapeta in nocturnal moths consist of air layers next to chitin, providing a large difference in refractive indices, which provides for a higher percentage of reflected light. The tapetum of these nocturnal moths appears blue-green, whereas in diurnal butterflies each rhabdom possesses its own tapetum. In many diurnal butterflies, the

tapetum consists of up to 40 overlying layers, which are regularly spaced cuticular plates, each separated from its neighbors by air spaces. Because the tapetum varies in thickness, and relies on constructive interference, dorsally it tends to reflect blue light, whereas ventrally it tends to reflect red.<sup>13,18,19</sup>

#### MECHANISMS OF THE TAPETUM

Although much is known about the structure and biochemical composition of the tapetum, there is considerably less information on the spectral reflectance characteristics and mechanisms.<sup>1,13</sup> Thin-film constructive and destructive interference probably plays a prominent role in the reflective mechanisms of the tapeta of many of these animals. Layers of crystals, or other structures with differing indices of refraction at a thickness of  $\lambda/4$  of the maximal wavelength of reflected light, support the theory that constructive interference is involved. Theoretically, 15 to 20 layers at  $\lambda/4$  should provide nearly 100% reflection of light at a wavelength of  $\lambda$ .<sup>17</sup>

Diffusely reflecting tapeta have been described in which reflection off a rough surface occurs and enhances the sensitivity of the retina, but this cannot be constructive interference. Mie scattering has been proposed as a mechanism for diffusely scattering tapeta, but this has not been studied in detail.<sup>20,21</sup> Rayleigh scattering (scattering by particles smaller than the wavelength of light with preferential scattering of the shorter wavelengths, similar to the phenomena of our atmosphere creating a blue sky), may also be involved, especially for the tapetum fibrosum.<sup>20,22</sup>

Some butterflies employ a unique form of orthogonal retroreflection that juxtaposes yellow next to blue regions, synthesizing a green color in their wings. A concave surface composed of flat and inclined regions appears yellow and blue, respectively. The juxtaposition of these colors appears green because these regions produce individual streams of photons too small to be resolved individually.<sup>23,24</sup>

Orthogonal retroreflection has never been studied as a potential mechanism for tapetal reflection, but could be involved, especially in invertebrate thin-film tapeta.<sup>1</sup> In the vertebrate world, the duplex retina of *Lestidiops*, a mesopelagic deep-sea teleost, has an anatomical configuration consistent with this form of reflection.<sup>25</sup> Other animals that may have employed orthogonal retroreflection include the bigeye fish (*Hybopsis amblops*) and cat (*F. domesticus*). The tapetum of bigeye fish is actually a mosaic of different-colored spots, where measurements of minute, singly colored areas give spectral curves with restricted bands and expected side oscillations. The spectrum of the cat tapeta is variable between animals from green to yellow, and the color varies within the eye. The cat's tapetum is composed of bundles of rodlets, when viewed microscopically, and there appear to be different colors at varying depths.<sup>1</sup>

### PIGMENTED COLORS FORMING A TAPETUM

The mechanism of individual colors produced by the tapetum has not been well studied. Constructive interference provides structural color, involving layers having the thickness of  $1/4\lambda$  (where  $\lambda$  is the wavelength of light to be reflected), and has been proposed as a common mechanism. Some tapeta, however, contain pigmented reflecting crystals. In such animals, the appearance of these tapeta correlates with the pigmented color of these reflecting crystals. For example, the galago tapetum is composed of isoalloxazine or riboflavin crystals possessing a yellow hue.<sup>26</sup> The tapetum of the garpike has also been reported as being made up of yellow pigments.<sup>27</sup> A red pigmented tapetum can be found in characin fish and garfish.<sup>28,29</sup> The pigment is found enclosed in spheres in the retinal pigment epithelium. The reflecting material of characin fish, catfish tapetal pigment, consists of oligomers of 5,6-dihydroxindole-2-carboxylic acid combined with decarbox-ylated S-adenosylmethionine.<sup>30</sup> The pigmented tapetum has conferred an advantage to deep-sea fish that exist in an environment where the predominant wavelength of light is 475 nm. Most animals at these depths have photo-receptors that predominantly absorb light at this wavelength, since that is the only wavelength that penetrates to those depths.

A mesopelagic species of fish, *Malacosteus niger*, has evolved with a mechanism that allows it to take advantage of this downwelling blue light as well as possessing red light-emitting organs (photophores) located ventrally and sub-orbitally. These red photophores emit red light that is not recognized by the photoreceptors of most deep-sea animals. The photophores are larger than most photophores, suggesting that they may assist the *M niger* in illuminating prey or signaling other individuals of the same species. It is believed that *M niger*, and not other deep-sea animals, is able to absorb the red light emitted by its own photophores because it possesses a pigmented, diffused, scarlet-red tapetum that reflects the red light emitted by the photophores. This may allow the *M niger* to effectively visualize prey undetected, as well as communicate with others of their species, without alerting their predators.<sup>28,30,31</sup>

### EVOLUTION OF THE TAPETUM

The timing of the evolution of the tapetum will probably never be determined exactly; however, we provide a model for the possible development of the tapetum according to existing evidence (Figures 13 and 14). Vertebrates are believed to have evolved from the pikaia, a primitive invertebrate and ancestor to the modern-day amphioxus. The pikaia existed in the Precambrian era, approximately 570 million years ago.<sup>32</sup> In the Silurian period (410 to 430 million years ago), fossils of the ostracoderm, the ancestor to the modern-day agnatha, had been discovered. Tapeta do not occur in amphioxus or agnatha;

therefore we make an assumption that tapeta did not exist in ostracoderms. Though fossil history does not exist, Placoderms, Chondrostei, and lobe-finned fish are all assumed to have the ostracoderm as a common ancestor, on the basis of physical characteristics.

In the Devonian period (345 to 395 million years ago), all three orders may have developed tapeta independent of each other, based on their modern progeny, namely, sharks (Placoderm), sturgeons (Chondrostei), and coelacanth (lobe-finned fish). These three orders of fish all possess a tapetum cellulosum, suggesting that this tapetum may have been the first type of tapetum to evolve in vertebrates. These species have similar enough tapeta that they may have had a common ancestor with a tapetum developing at approximately the Devonian period or, at the earliest, the very late Silurian. It is unlikely that the tapetum appeared earlier, because hagfish and most lampreys do not have tapeta and it is believed these species separated in the Silurian period. The development of the tapetum independently in fish might have occurred to allow them to explore deeper depths of the ocean, where light was not as prevalent. Conquering the depths of the ocean may have provided sources of food not previously accessible, such as detritus.

The lobe-finned fish ancestor, closely related to the coelacanth and lungfish, is believed to be the predecessor to amphibians on the basis of physical characteristics.<sup>32-34</sup> While amphibians may have possessed a tapetum at one time, none has been reported in modern species.<sup>35</sup> It would appear that, through evolution, either amphibians lost the ability to produce a tapetum or their lobe-finned fish ancestors did not possess one. Amphibians are commonly accepted as the ancestors of reptiles. The *Eryops* genus is believed to have been primitive reptiles that evolved from amphibians, dating back to the Permian period (220 to 280 million years ago). The crocodile, believed to have descended from these primitive reptiles, evolved retinal tapetum composed of guanine. This suggests that crocodiles independently evolved or re-evolved a similar retinal tapetum employing guanine, well described in jawed fishes. Guanine as a reflecting material is found widely in animals with tapeta. The crocodile also uses guanine as its reflecting material, as do many fish, the wolf spider, and many other unrelated species. The crocodile tapetum is located dorsally and temporally. It has been hypothesized that the location of the tapetum in the crocodile correlates with the need to improve the animal's ability to see in murky waters below it.<sup>20</sup>

Mammals evolved from mammal-like reptiles, which presumably did not have tapeta. This is supported by monotremes, which evolved independently from other mammals and belong to the order Docodonta. They have eyes that are much more like reptilian eyes than mam-

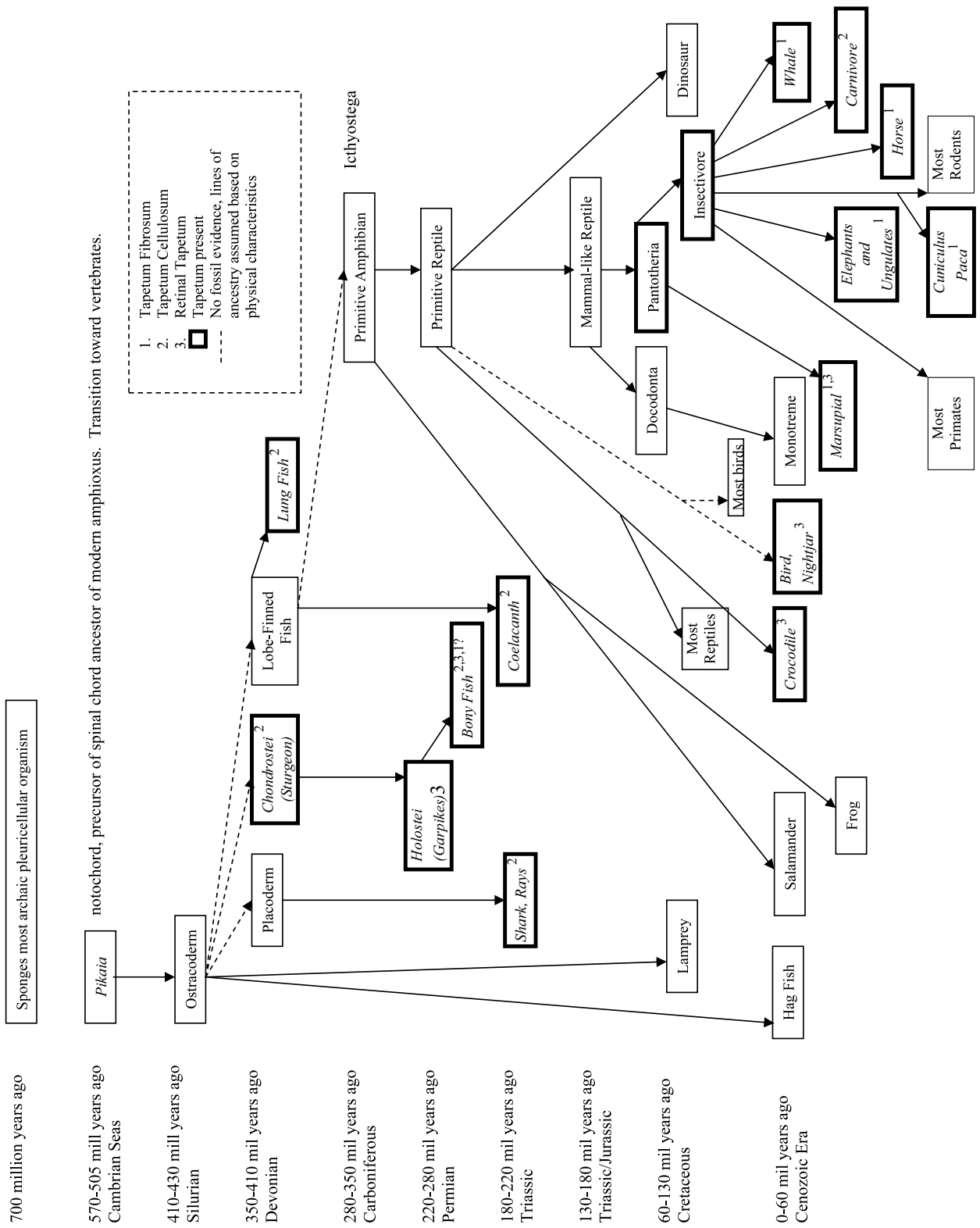


FIGURE 13  
Evolutionary diagram of vertebrate tapeta.

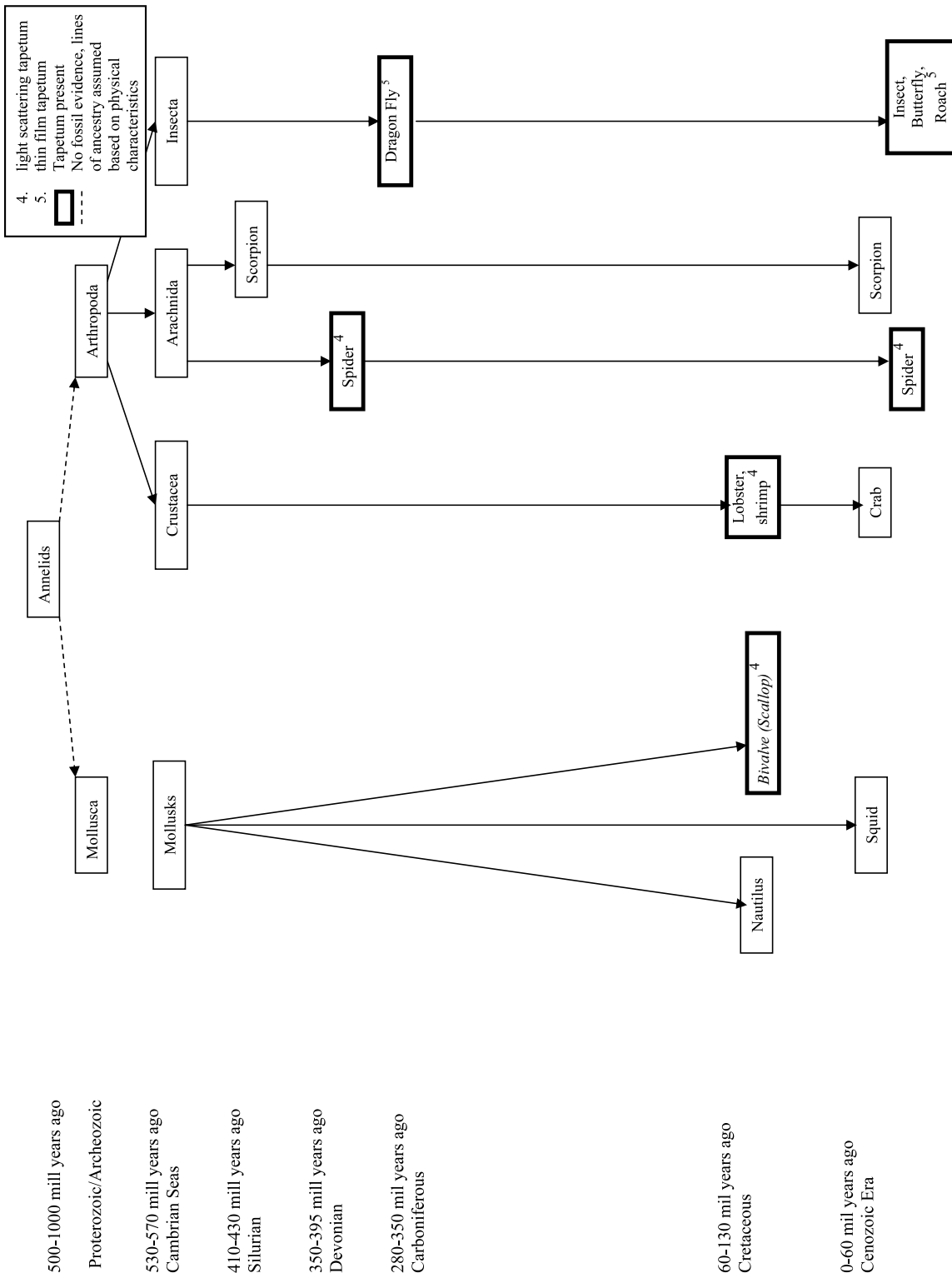


FIGURE 14  
Evolutionary diagram of invertebrate tapeta.

malian eyes, and they do not have tapeta.<sup>13</sup> With the exception of monotremes, all other mammals belong to the order Pantotheria, which gave rise to marsupials and insectivores, from which all other mammals were probably derived. There are numerous examples of marsupial tapeta, but there are some interesting differences. The Virginia opossum has a retinal tapetum with lipid reflecting material, while the Tasmanian devil has a tapetum fibrosum, suggesting independent evolution, and no common ancestor with a tapetum. Many other, but not all, mammals have tapeta, including ungulates, cetaceans, carnivores, rodents, and prosimians.<sup>1,13,18,35</sup> It seems that the tapetum was probably not present in the mammal-like reptile, but appeared later in mammals in the Cenozoic era, no more than 60 million years ago, when the tapetum seems to have evolved independently once again. Mammalian tapeta include tapetum fibrosum, cellulolum, and retinal tapeta, similar to yet different from previously evolved tapeta. Somewhat unexpectedly, tapeta are also found in strictly diurnal mammals, such as the Indian mongoose, ungulates, and dogs,<sup>1,36</sup> although dogs and ungulates may be functionally nocturnal.

The tapetum has been reported in only two phyla of invertebrates, Mollusca and Arthropoda (Figure 14). On the basis of physical characteristics, both phyla are assumed to have evolved from Annelids in the Precambrian era (1,000 million to 570 million years ago). The common ancestor to mollusks and arthropods–annelids–do not have, and probably never did have, a tapetum. Among only a few mollusks, a guanine tapeta appears to have evolved independently of the tapeta of arthropods with different mechanisms. Among the mollusks, cephalopods possess some of the most advanced eyes among the invertebrates, and even have “camera-style” eyes like most vertebrates, but they do not possess tapeta.<sup>36</sup>

Tapeta have been reported in three classes of arthropods: Arachnida, Insecta, and Crustacea. These classes appear to have evolved as separate lineages during the Precambrian era. The tapetum in invertebrates may also have evolved in the Devonian period. Spiders are credited as one of the first predators on land and can be traced back 395 million years ago, according to the fossil record.<sup>32,33</sup> This was prior to the evolution of flying insects that spiders commonly entrap in their webs.<sup>32</sup> Hence, prehistoric spiders probably hunted their prey much like lycosid spiders of today. Although the invertebrates and vertebrates both probably developed tapeta in the Devonian period, the solutions were very different for similar results. As opposed to fish, which probably developed tapeta to explore the depths of the ocean, spiders probably developed tapeta to allow them to take advantage of nocturnal conditions or to protect themselves against predators. Like sharks, the lycosid spider employs

guanine as its reflecting material organized into a thin-film reflector. In the class Insecta, dragonfly fossils have been dated to 350 million years ago, in the late Devonian to early Carboniferous period, and probably represent the earliest insect tapeta. Tapeta have been reported in dragonfly ocelli.<sup>6</sup> Because their common ancestor did not have tapeta, it appears that the dragonfly and the arachnids evolved tapeta independently of each other. Crustaceans, such as the lobster and shrimp, have pigmentary tapeta, appear to have evolved independently of insects and arthropods, and have different mechanisms.<sup>23,24</sup>

## CONCLUSIONS

---

Tapeta are found in both vertebrates and invertebrates. Not surprisingly, it appears that tapeta have a tendency to reflect wavelengths most relevant to the animal. The tapeta in vertebrates are located in either the choroid or deep retina. Choroidal tapeta are further classified as tapetum cellulolum and tapetum fibrosum, according to their appearance. The tapetum cellulolum is composed of reflecting cells stacked in depth, like tile work. The cells contain numerous refractile bodies with an orderly arrangement. The tapetum fibrosum is acellular and composed of stacks of densely packed collagen fibrils. Retinal tapeta are found in the form of small granules in spheres and cubes or regularly arranged stacked thin platelets. These tapeta reflect light by diffuse reflection and specular reflection, respectively.

A variety of reflecting material has been reported in invertebrates and vertebrates, including nonpigmented material such as uric acid, guanine, chitin, and collagen, and pigmented material such as cholesterol esters, lipids, pteridine, and astaxanthin.<sup>1</sup> Nonpigmented reflecting crystals appear to produce colors structurally, while the color produced by pigmented reflecting crystals may be a result of their pigmentation.

Mechanisms by which tapeta reflect light are incompletely understood. Constructive interference appears to be a common mechanism by which some tapeta reflect light; it does not appear, however, to be the only mechanism involved in all tapeta. In addition to thin-film interference, diffuse reflection and pigmented color granules are probably involved in tapetal reflection. Orthogonal retroreflection, a newly discovered mechanism of reflection in butterfly wings, has never been studied as a potential mechanism in butterfly tapeta and may be a more common mechanism than currently recognized.

We hypothesize that the tapetum may have arisen independently in both invertebrates and vertebrates as early as the Devonian period (390 to 345 million years ago). In vertebrates, the guanine choroidal tapetum may have arisen in sharks, sturgeon, and lobe-finned fish inde-

pendent of each other, or if there were a common ancestor, it originated in the Devonian era. This coincides with an explosion in the evolution of many different types of marine life. It appears that the choroidal tapetum was the first type of tapetum to evolve in vertebrates, with retinal tapeta appearing independently in other tetrapods.

The invertebrate tapetum appears to have evolved first in spiders, in the Devonian period, and consists of a diffusely reflecting guanine tapetum. All of these tapeta employ unpigmented guanine as their reflecting crystals, and guanine was probably the first reflecting material employed. The evolution of the tapetum appears to be highly convergent, but often with subtle differences in development. Tapeta probably arose separately in invertebrates and vertebrates and even within these broad groups, the tapetal mechanisms appear to have distinctly and separately evolved, yet with surprisingly similar mechanisms.

## REFERENCES

- Nicol JAC. Tapeta lucida of vertebrates. In: Enoch MJ, Tobey FL, eds. *Vertebrate Photoceptor Optics*. Berlin: Springer-Verlag; 1981:401-431.
- Bellairs R, Harkness ML, Harkness RD. The structure of the tapetum of the eye of the sheep. *Cell Tissue Res* 1975;157:73-91.
- Duke-Elder S. The eye in evolution. In: *System of Ophthalmology*, Vol 1. London: Henry Kimpton, 1958.
- Braekevelt CR. Fine structure of the bovine tapetum fibrosum. *Anat Hist Embryol* 1986;15:215-222.
- Braekevelt CR. Fine structure of choroidal tapetum lucidum in the Port Jackson shark (*Heterodontus phillipi*). *Anat Embryol* 1994;190:591-596.
- Collier LL, King JK, Prieur DJ. Tapetual degeneration in cats with Chediak-Higashi syndrome. *Curr Eye Res* 1985;4(7):767-773.
- Heath AR, Hindman HM. The role of cyclic AMP in the control of elasmobranch ocular tapetum lucidum pigment granule migration. *Vision Res* 1988;28(12):1277-1285.
- Walls GL. *The Vertebrate Eye and Its Adaptive Radiation*. New York: Hafner; 1963.
- Miller WE. Ocular optical filtering. In: Autrum H, ed. *Handbook of Sensory Physiology*. Vol II/6A. Berlin: Springer; 1981:69-143.
- Dieterich CE, Dieterich HJ. Electron microscopy of retinal tapetum (*Caiman crocodilus*). *Arch Klin Exp Ophthalmol* 1978;208:159-168.
- Braekevelt CR. Fine structure of the retinal epithelium of the spectacled caiman (*Caiman sclerops*). *Acta Anat* 1977;97(3):257-265.
- Braekevelt CR. Fine structure of the retinal epithelium of the opossum. *J Morphol* 1976;150:213-217.
- Douglas RH, Marshall NJ. A review of the vertebrate and invertebrate ocular filters. In: Archer, ed. *Adaptive Mechanisms in the Ecology of Vision*. Dordrecht: Kluwer Academic Publishers; 1999:95-162.
- Gaten E, Shelton PM. Regional morphological variations in the compound eyes of certain mesopelagic shrimps in relation to their habitat. *J Marine Biol Assoc* 1992;72: 61-75.
- Land MF. The quality of vision in the ctenid spider *Cupiennius salei*. *J Exp Biol* 1992;164:227-242.
- Land MF. Image formation by a concave reflector in the eye of the scallop, *Pecten maximum*. *J Physiol* 1965;179: 138-153.
- Land MF. Optics and vision in invertebrates. *Handbook of Sensory Physiology*. Vol II/6B. Berlin: Springer-Verlag; 1981:201-286.
- Nilsson DE, Howard J. Intensity and polarization of the eyeshine in butterflies. *J Comp Physiol* 1989;166:51-56.
- Miller WH, Bemard GD. Butterfly glow. *J Ultra Res* 1968; 24:286-294.
- Lockett NA. Adaptations to the deep-sea environment. In: *The Visual System in Vertebrates*. Berlin: Springer-Verlag; 1977:68-192.
- Nicol JAC. Studies on the eyes of fishes: structure and ultrastructure. In: *Vision in Fishes*. New York: Plenum Press 1975;579-608.
- Goodman LJ. Organization and physiology of the insect dorsal ocellar system. In: *Handbook of Sensory Physiology*. Berlin: Springer-Verlag; 1981:201-286.
- Vukusic P, Sambles JR, Lawrence CR. Color mixing in the wing scales of a butterfly. *Nature* 2000;404:457.
- Burgess DS. Butterfly's wings produce colors structurally. *Biol Int* 2000;7:34-36.
- Munk O. Duplex retina in the mesopelagic deep-sea teleost *Lestidiops affinis*. *Acta Zool* 1989;70:143-150.
- Braekevelt CR. Fine structure of the retinal epithelium in the bush baby. *Acta Anat* 1980;107:276-285.
- Ito S, Thurston EL, Nicol JAC. Melaniod tapeta lucida in teleost fishes. *Proc R Soc Lond B Biol Sci* 1975;194:369-385.
- Bowmaker JK, Dartnall HJ, Herring PJ. Longwave-sensitive visual pigments in some deep-sea fishes: segregation of paired rhodopsins and porphyropsins. *J Com Physiol A* 1988;163:685-698.
- Nicol JAC, Arnott HJ. Studies of gars (Lepisosteidae) with special reference to the tapetum lucidum. *Can J Zool* 1973; 51:501-508.
- Somiya H. Yellow lens eyes of a stomiatoid deep-sea fish, *Ialacosteus niger*. *Proc R Soc Lond B Biol Sci* 1982;215: 481-489.
- Angela P, Angela A. *The Extraordinary Story of Life on Earth*. New York: Prometheus Books; 1996.
- Storer TI, Usinger RL, Nybakken JW, et al. *Elements of Zoology*. 4th ed. New York: McGraw-Hill; 1977.
- Fascinating World of Animals: A Unique "Safari" Through Our Strange and Surprising Animal Kingdom*. Pleasantville, NY: Reader's Digest Association; 1971.
- Pirie A. The chemistry and structure of the tapetum lucidum in animals. In: *Aspects of Comparative Ophthalmology*. Oxford, England: Pergamon Press; 1965:57-87.
- Nellis DW, Sivak JG, McFarland WN, et al. Characteristics of the eye (*Herpestes auropunctatus*). *Can J Zool* 1989;67: 2814-2820.

36. Denton EJ, Land MF. Mechanism of reflexion in silvery layers of fish and cephalopods. *Proc R Soc London B Biol Sci* 1971;78(50):43-61.

## DISCUSSION

DR RALPH C. EAGLE, JR. Tapeta are mirrorlike structures in the choroid or outer retina that have evolved to subserve vision in low levels of light. Essentially, they reflect photons back from the eyewall, thereby increasing the probability of capture by the photoreceptors. Tapeta characteristically are found in nocturnal animals like the raccoon and fish or marine mammals like the whales that frequent the ocean depths. The authors' studies and literature review indicate that tapeta have evolved convergently in both vertebrates and invertebrates and have a tendency to reflect the wavelengths that are most relevant to the animals' environment. They hypothesize that they may have arisen as early as the Devonian period.

People probably are most familiar with the tapetal reflex or eye shine of cats. Electron microscopy of the feline tapetum cellulosum discloses myriad rodlets of osmiophilic material thought to be a zinc cysteine or taurine compound in the cytoplasm of its cells, which are stacked like brickwork. The rodlets are arranged in an exquisitely regular fashion that is reminiscent of the spacing of collagen fibrils in the corneal stroma, but the diameter of the tapetal rodlets is greater than that of corneal collagen (120 nm versus 22 to 35 nm) and they are spaced further apart (2 to 300 nm versus 42 nm).<sup>1</sup> Presumably, the size and spacing of the rodlets and fibrils are consistent with constructive interference and reflection in the feline tapetum and with destructive interference and transparency in the cornea.

Although tapeta occur in nocturnal prosimians like the bushbaby, they normally are not found in healthy higher primates, including man. Abnormal fundus reflexes that have been likened to tapeta do occur in several ocular diseases, however. Leber applied the term *tapetoretinal dystrophy* to a variety of hereditary degenerative retinal diseases including retinitis pigmentosa and fundus flavimaculatus. According to Duke-Elder, this term is derived from the tapetum nigrum or black carpet, an archaic term for the retinal pigment epithelium.<sup>2</sup> Leber thought that primary defects in the RPE were responsible for such disorders.

Shiny reflective fundus reflexes reminiscent of tapeta do occur in patients who have some of these heritable disorders, including Oguchi's disease,<sup>3,4</sup> X-linked cone dystrophy,<sup>5</sup> and the female carrier state of X-linked retinitis pigmentosa.<sup>6,7</sup> Oguchi's disease is a form of stationary night blindness caused by mutation in the gene for arrestin, a molecule involved in the recovery phase of light

transduction. Ophthalmoscopy discloses a shiny golden fundus reflex in light-adapted patients with Oguchi's disease. This golden reflex disappears after the patient has been kept in the dark for several hours, and this is called the Mizuo-Nakamura phenomenon. The eye shine in Oguchi's disease might be considered a paradoxical tapetum, for it is present in the light and disappears in darkness. I am unaware if patients with Oguchi's disease have been observed to have abnormal eye shine under non-clinical conditions.

A classic example of a human tapetal reflex occurs in children who have retinoblastoma. In 1767, Hayes initially noted that the pupil in retinoblastoma had "a bright look, something resembling a cat's eye in the dark."<sup>8</sup> The "amaurotic cat's eye reflex" is an older alternative term for leukocoria.

On a lighter note, red, glowing eyes purportedly occur in a variety of creatures that are legendary or of questionable authenticity. The latter include the Jersey Devil, the Chupacabra or goatsucker of Puerto Rico, the Mothman of Point Pleasant, West Virginia, and the Sasquatch or Bigfoot of the Pacific Northwest and its Florida relative the Myakka "skunk ape."<sup>8</sup> Because higher primates lack tapeta, the presence of a tapetal reflex in Bigfoot, would seem to cast doubt on the authenticity of this humanoid unless one postulates yet another example of convergent evolution. A photograph said to depict the Myakka skunk ape is posted on a cryptozoological Web site on the Internet.<sup>9</sup> The hairy creature in the photo does have glowing eyes.

Various sources on the Internet also indicate that creatures from the infernal regions have red glowing eyes. In fact, red eye shine, often transitory in nature, has become a ubiquitous cinematic convention for portraying devils, demons, and demonic possession in the movies. One might speculate that the latter association might stem from the eye shine of cats, which were thought to be agents of the devil in medieval Europe. Images in our collective racial memory of large feline predators lurking in the shadows around our ancestors' campfires might be a contributing factor.

The association of red eye shine with Satan and demonic possession probably is a major factor behind the general population's revulsion with the common artifact of flash photography called "red eye". Our repugnance with this unnatural appearance has led to the development of cameras equipped with repetitive flashes designed to reduce or eliminate this photographic artifact by inducing pupillary miosis before photos are taken. Computer image processing software programs such as Adobe Photoshop are also touted for their ability to correct red-eye digitally.

Red-eye reduction in amateur photography theoretically could have adverse medical consequences by delay-

ing the diagnosis of retinoblastoma. Not infrequently, parents of affected children initially detect leukocoria as a difference in character of the “red eye” in their child’s photos. Photographic pseudoleukoria may occur in healthy children, however, if the flash fortuitously happens to illuminate the optic disk in an appropriately adducted eye. I am aware of such an incident of photographic pseudoleukocoria that involved an ocular oncologist’s child, prompting expedient ophthalmoscopy.

## REFERENCES

1. Sturman JA, Wen GY, Wisniewski HM, et al. Histochemical localization of zinc in the feline tapetum. Effect of taurine depletion. *Histochemistry* 1981; 72(3):341-350.
2. Duke-Elder S, Dobree JH. The tapeto-retinal dystrophies. In Duke-Elder S, ed. *Diseases of the Retina. Vol X. System of Ophthalmology*. London: Henry Kimpton. 1967:574.
3. Bergsma DR Jr, Chen CJ. The Mizuo phenomenon in Oguchi disease. *Arch Ophthalmol* 1997;115:560-561.
4. Nakazawa M, Wada Y, Fuchs S, et al. Oguchi disease: phenotypic characteristics of patients with the frequent 1147delA mutation in the arrestin gene. *Retina* 1997;17:17-22
5. Heckenlively Jr, Weleber RG. X-linked recessive cone dystrophy with tapetal-like sheen. A newly recognized entity with Mizuo-Nakamura phenomenon. *Arch Ophthalmol* 1986;104:1322-1328.
6. Berendschot TT, DeLint PJ, van Norren D. Origin of tapetal-like reflexes in carriers of X-linked retinitis pigmentosa. *Invest Ophthalmol Vis Sci* 1996;37:2716-2723.
7. Cideciyan AV, Jacobson SG. Image analysis of the tapetal-like reflex in carriers of X-linked retinitis pigmentosa. *Invest Ophthalmol Vis Sci* 1994;35:3812-3824.
8. Hayes. *Medical Observations and Inquires*. London, 1767; 3:120.
9. Coleman L. The Myakka Skunk Ape Photos. Available at: [www.lorencoleman.com/myakka.html](http://www.lorencoleman.com/myakka.html)

DR ALFREDO A. SADUN. I am fascinated by the strategies that the tapetum use. If the tapetum were to be a quarter

wavelength in thickness, like a lens coating, then a quarter in, quarter out means that the light’s going to be half a wavelength out of phase and you have destructive interference. But that’s only for that given wavelength; for every place you have destructive interference, 25% longer or 25% shorter wavelengths will have constructive interference. So the trade-off is always choosing what you are going to construct and what you are going to destruct. So my question for Dr Schwab is, Were the shifts along the strategies of various species such that one animal like the cat is doing constructive interference at yellow and destructive interference at blue and probably destructive at the infrared? Were there shifts that reflected the animal’s behavior and needs?

DR TERRY J. ERNEST. Where do these extraordinarily difficult crystal structures in biology work, what cells make them, where do they come from? What’s evolution doing to these crystals? The last thing you want to do is put a mirror inside the eye. If you want to get better vision, you go to the standard, the eagle, and you add a fovea, but you don’t put a mirror in there, which would cause terrible reflections everywhere regardless of thickness.

DR IVAN R. SCHWAB. It is difficult to know the process that selects tapeta as we realize that evolution isn’t a force as you think of a choice; evolution is a random process—it works by mistakes and time. So, in answer to the question, I don’t know the answer, but my guess would be to maximize photons in darkness for prey capture. What are the strategies and why the different colors? That is certainly unclear, especially since certain species, such as cats, may have different colors or no color at all, depending on the species, depending on the breed; in other words, colors can be bred out. So in answer to that first question, the strategy isn’t clear because it’s even different from one cat to another. But, as I say, the strategy almost certainly is for activity in darkness.

# ANGLE CLOSURE IN YOUNGER PATIENTS

---

BY *Brian M. Chang, MD* (BY INVITATION), *Jeffrey M. Liebmann, MD* (BY INVITATION), AND *Robert Ritch, MD*

## ABSTRACT

*Purpose:* Angle-closure glaucoma is rare in children and young adults. Only scattered cases associated with specific clinical entities have been reported. We evaluated the findings in patients in our database aged 40 or younger with angle closure.

*Methods:* Our database was searched for patients with angle closure who were 40 years old or younger. Data recorded included age at initial consultation; age at the time of diagnosis; gender; results of slit-lamp examination, gonioscopy, and ultrasound biomicroscopy (from 1993 onward); clinical diagnosis; and therapy. Patients with previous incisional surgery were excluded, as were patients with anterior chamber proliferative mechanisms leading to angle closure.

*Results:* Sixty-seven patients (49 females, 18 males) met entry criteria. Mean age ( $\pm$ SD) at the time of consultation was  $34.4 \pm 9.4$  years (range, 3-68 years). Diagnoses included plateau iris syndrome (35 patients), iridociliary cysts (8 patients), retinopathy of prematurity (7 patients), uveitis (5 patients), isolated nanophthalmos (3 patients), relative pupillary block (2 patients), Weill-Marchesani syndrome (3 patients), and 1 patient each with Marfan syndrome, miotic-induced angle closure, persistent hyperplastic primary vitreous, and idiopathic lens subluxation.

*Conclusion:* The etiology of angle closure in young persons is different from that in the older population and is typically associated with structural or developmental ocular anomalies rather than relative pupillary block. Following laser iridotomy, these eyes should be monitored for recurrent angle closure and the need for additional laser or incisional surgical intervention.

*Trans Am Ophthalmol Soc* 2002;100:201-214

## INTRODUCTION

---

Angle-closure glaucoma is a disease of older persons. The incidence of primary angle closure, about 90% of which, in the United States, results from relative pupillary block, increases with age, peaking between the ages of 55 and 70 years and then declining. Angle closure is rare in children and young adults, only isolated cases and small series, primarily composed of particular entities, having been reported.<sup>1-14</sup> The purpose of this study was to evaluate the demographics and clinical information for all patients in our database with angle closure who were 40 years old or younger.

## PATIENTS AND METHODS

---

We chose age 40 as an arbitrary cutoff to define "younger" patients as being under the age of onset of presbyopia. Eligible patients were those having presented with

histories, symptoms, and findings characteristic of acute, subacute, or intermittent angle closure, chronic angle closure with peripheral anterior synechiae (PAS), or appositionally closed angles on the basis of gonioscopy or ultrasound biomicroscopic dark room provocative testing. We reviewed our database of approximately 14,000 patients for patients aged 40 years or younger at the time of initial diagnosis who fulfilled these criteria.

The following data were extracted from the medical record: date of birth, gender, clinical diagnoses, age at diagnosis of angle closure, age at time of initial consultation with us, manifest refraction (converted to spherical equivalent), axial length (when available), therapeutic intervention (medical treatment, laser iridotomy, laser iridoplasty, incisional surgery), ultrasound biomicroscopy (UBM, from 1993 onward), and the mechanism underlying the angle closure. These were classified as pupillary block, plateau iris (and pseudoplateau iris), and lens-induced angle closure. Patients with a previous history of intraocular surgery (aphakic or pseudophakic pupillary block or malignant glaucoma) were excluded, as were patients with purely anterior proliferative mechanisms,<sup>15</sup> leading to formation of PAS due to pathology at the level of the iris or iridocorneal angle.

From the Departments of Ophthalmology, the New York Eye and Ear Infirmary, New York, New York, and the New York Medical College, Valhalla, New York. Supported by the Donald Engel Research Fund of the New York Glaucoma Research Institute.

## RESULTS

Sixty-seven patients (0.48% of the patients in our database) met the entry criteria. These represented 2.34% of the 2,864 patients with angle closure in the database at the time of extraction. There were 49 females (73.1%) and 18 males (26.9%). The mean age  $\pm$  SD at the time of diagnosis of angle closure was  $31.3 \pm 8.5$  years (range, 3-40 years), while the mean age at the time of our initial consultation was  $34.4 \pm 9.4$  years (range, 3-68 years). The ages at diagnosis were 0 to 10 years (3 patients), 11 to 20 years (3 patients), 21 to 30 years (12 patients), and 31 to 40 years (49 patients). All patients older than age 40 at the time of initial consultation had been diagnosed as having angle closure prior to age 40. Some patients had been referred for UBM imaging only, resulting in incomplete historical information or incomplete refractive or biometric data, or both.

The patient diagnoses and demographics are listed in Table I. Plateau iris syndrome was the most common diagnosis, accounting for 35 (52.2%) of the patients in our series. The mean age of these patients at the time of diagnosis was  $34.9 \pm 4.6$  years (range, 23-40 years). Twenty-six (74.3%) were female. Six had presented with acute angle closure. Mean refractive error was  $+1.94 \pm 0.4$  diopters OD and  $+1.74 \pm 1.8$  diopters OS. Laser iridotomy was

performed or recommended in 69 of the 70 eyes. Twenty-seven eyes received argon laser peripheral iridoplasty (ALPI) for persistent appositional closure after iridotomy, and the remaining patients (43 eyes) were either referred back to their primary ophthalmologists or maintained under observation.

Eight patients (11.9%, 7 female, 1 male) had iridociliary cysts. The mean age at diagnosis was  $29.0 \pm 9.3$  years (range, 14-40 years). No patient presented with a history of acute angle closure. These eyes presented clinically as plateau iris, with a prominent double hump sign, and the diagnosis was made by UBM. Indentation gonioscopy in some cases in which cyst distribution was irregular provided a tentative diagnosis. Thirteen of these 16 eyes underwent laser iridotomy. Of the remaining three eyes, one had no cysts and an open angle, and two had open angles with cysts and only small areas of appositional closure. Only four eyes went on to require ALPI because of continued appositional closure after iridotomy.

Seven patients (11 eyes) were nanophthalmic (Table II). The mean refractive error of affected eyes in the seven patients was  $-1.3 \pm 6.5$  diopters (range,  $-9.00$  to  $+4.00$ ). The axial lengths ranged from 17.0 to 20.35 mm. Three patients had isolated nanophthalmos OU. The mean age at the time of diagnosis of angle closure in these patients was  $28.7 \pm 4.9$  years (range, 23-32 years). All six

TABLE I: DEMOGRAPHICS OF STUDY GROUP

DIAGNOSIS	NO. OF PATIENTS	MEAN AGE (YR) (RANGE)	GENDER
Plateau iris syndrome	35/67 (52.2%)	$34.9 \pm 4.6$ (23-40)	9/36 M (25.7%) 26/36 F (74.3%)
Iridociliary cysts	8/67 (11.9%)	$29.0 \pm 9.3$ (14-40)	1/8 M (12.5%) 7/8 F (87.5%)
Retinopathy of prematurity	7/67 (10.4%)	$24.3 \pm 13.5$ (3-37)	2/7 M (28.6%) 5/7 F (71.4%)
Uveitis	5/67 (7.5%)	$34.2 \pm 2.3$ (32-38)	3/5 M (60%) 2/5 F (40%)
Nanophthalmos	3/67 (4.5%)	$16.7 \pm 12.5$ (5-30)	1/3 M (33.3%) 2/3 F (66.7%)
Relative pupillary block	2/67 (3.0%)	$37.5 \pm 3.5$ (35-40)	2/2 F
Weill-Marchesani	3/67 (4.4%)	$26.5 \pm 3.6$ (18-30)	1/3 M 2/3 F
Marfan syndrome	1/67 (1.5%)	20	1/1 F
Miotic-induced angle closure	1/67 (1.5%)	20	1/1 M
Persistent hyperplastic primary vitreous	1/67 (1.5%)	24	1/1 F
Lens subluxation	1/67 (1.5%)	36	1/1 F

TABLE II: COEXISTING DIAGNOSES, AXIAL LENGTH, AND REFRACTION IN EYES WITH NANOPHTHALMOS

DIAGNOSIS	AXIAL LENGTH OD/OS (MM)	MEAN SPHERICAL EQUIVALENT OD/OS (D)	COMMENTS
Nanophthalmos	NA/20	+2.75/+2.75	OD excluded from analysis
Nanophthalmos	17/19	NA/NA	
Nanophthalmos	19.7/20	+3.75/+3.5	
Nanophthalmos and Weill Marchesani	19.64/19.48	-9.00/-8.75	
Nanophthalmos and Weill Marchesani	20.25/20.35	-7.75/-8.25	
Nanophthalmos and plateau iris	20.8/20.15	+4.00/+4.00	OD excluded from analysis
Nanophthalmos and ROP	21.46/19.94	NA/NA	OD excluded from analysis

NA, not available; ROP, retinopathy of prematurity.

eyes underwent laser iridotomy. One eye subsequently had ALPI. Of the four patients in other diagnostic categories who were also nanophthalmic in one or both eyes, all six of the nanophthalmic eyes underwent both laser iridotomy and ALPI.

Two patients, aged 35 and 40 years at the time of diagnosis, had relative pupillary block as determined by UBM evaluation. There was no evidence of plateau iris configuration or syndrome on gonioscopy or UBM evaluation (Figure 1). Axial lengths were not obtained.

Seven patients (10.4%) had retinopathy of prematurity (ROP). The mean age at the time of diagnosis of angle closure was  $24.3 \pm 13.5$  years (range, 3-37 years). Mean refractive error was  $-6.5 \pm 11.7$  diopters OD and  $-6.24 \pm 10.7$  diopters OS. One eye was nanophthalmic. Five eyes of five patients had presented initially with acute angle closure. Four patients were initially treated with surgical iridectomies or laser iridotomy and then required ALPI for intraocular pressure (IOP) control. Iridotomy was per-

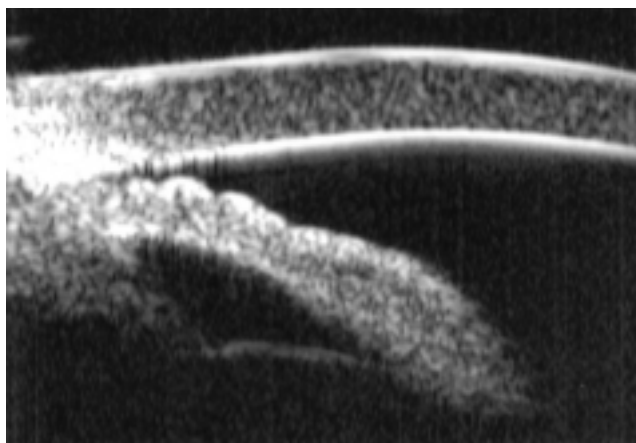


FIGURE 1

Pupillary block in 35-year-old woman. Iris contour is convex, posterior chamber is distended, and prominent ciliary sulcus is present.

formed in one patient, without additional need for ALPI. Iridotomy was recommended in one patient. Six eyes eventually underwent incisional surgery for additional pressure control.

Five patients (7.4%; 3 male, 2 female, 6 eyes) had uveitis and angle closure secondary to absolute pupillary block. Their mean age at the time of diagnosis was  $34.2 \pm 2.3$  years. All affected eyes underwent laser iridotomy, and none required ALPI.

Two patients, a brother who presented with acute angle closure and his sister, whose angle closure was detected on examination, had Weill-Marchesani syndrome and nanophthalmos with angle closure secondary to anterior lens subluxation. These patients, both successfully treated with ALPI after iridotomies, have been previously reported.<sup>16</sup> One additional patient had Weill-Marchesani syndrome and was aphakic in her only eye on presentation to us. One patient had Marfan syndrome and presented with chronic angle closure. Her refractive error was  $-17.00$  and  $-13.25$  diopters (spherical equivalent) with axial lengths of 24.71 and 23.59 mm, respectively.

One patient had persistent hyperplastic primary vitreous. One had a history of trauma at age 3 and developed acute angle closure in that eye after undergoing general anesthesia. Laser iridotomy and iridoplasty were required to control the IOP until the lens could be removed. One had miotic-induced angle closure and responded to elimination of the pilocarpine. Of the 17 patients who had a history of acute angle closure, 6 had plateau iris, 5 had ROP, 2 had uveitis, 2 had Weill-Marchesani syndrome, 1 had miotic-induced angle closure, and 1 had a subluxed lens after trauma.

## DISCUSSION

Angle closure is an anatomic disorder characterized by iris

apposition to the trabecular meshwork and is caused by abnormalities in the relative or absolute sizes or positions of anterior segment structures and/or anteriorly directed pressure in the posterior segment.<sup>17</sup> The forces posterior to the iris that lead to this situation can be conceived of as originating at four structural levels. Going from anterior to posterior, these consist of increased aqueous pressure in the posterior chamber (relative or absolute pupillary block), anatomic variations of the ciliary body (plateau iris and iridociliary cysts), the lens (phacomorphic glaucoma), and forces posterior to the lens (malignant glaucoma).

#### PUPILLARY BLOCK

Pupillary block is defined as impedence to the flow of aqueous humor from the posterior to the anterior chamber between the anterior surface of the lens and the posterior surface of the iris and is divided into relative (without posterior synechiae) and absolute (secondary to posterior synechiae) pupillary block. The ciliary sulcus is present. Indentation gonioscopy easily opens the peripheral angle because of the lack of resistance in the posterior chamber. Approximately 90% of patients with angle closure have relative pupillary block as the underlying mechanism.

Relative pupillary block typically occurs in hyperopic eyes, which have a shorter-than-average axial length, a more shallow anterior chamber, a thicker lens, a more anterior lens position, and a smaller radius of corneal curvature.<sup>18-22</sup> Angle closure caused by relative pupillary block is a disease of middle-aged and older individuals. Laser iridotomy provides the definitive treatment and results in an open angle (Figure 1).

Although many of our patients with plateau iris syndrome had an element of pupillary block, only two were deemed to have pure pupillary block based on clinical and UBM findings. Both underwent laser iridotomy with successful opening of the angle. The anterior chamber decreases in depth and volume with age.<sup>23-27</sup> Continued growth of the lens during adult life results in about 0.75 to 1.1 mm increased thickness and about 0.4 to 0.6 mm forward movement of the anterior lens surface.<sup>18-20,25</sup> The ratio of lens thickness to axial length increases with age and is greater in patients with angle closure.<sup>29</sup> Patients younger than age 40 would be least expected to exhibit these changes.

#### PLATEAU IRIS

Plateau iris is defined as an angle appearance in which the iris root angulates forward and then centrally<sup>30</sup> (Table III). The iris root is often short and inserted anteriorly on the ciliary face, so that the angle is shallow and narrow, with a sharp drop-off of the peripheral iris at the inner aspect of the angle. Classically, the iris configuration is planar and

the anterior chamber depth within the normal range. In older individuals, in whom the lens is larger and the anterior lens surface more anterior, the iris contour may be rounded, particularly when pupillary block is also present.

Plateau iris syndrome is diagnosed on the basis of continued appositional closure after laser iridotomy accompanied by a double hump sign on indentation gonioscopy and may be either complete (closure to the level of Schwalbe's line, resulting in elevated IOP) or incomplete (closure to a lower level on the trabecular meshwork so that IOP does not rise but PAS may develop over time with continued apposition).<sup>17,31-33</sup> Ultrasound biomicroscopy reveals anteriorly positioned ciliary processes and the absence of a ciliary sulcus (Figure 2).<sup>34,35</sup> The ciliary body position accounts for the double hump sign seen gonioscopically (Figure 3). This configuration persists after cataract extraction.<sup>36</sup> The definitive treatment for plateau iris is ALPI (Figure 4).<sup>37,38</sup>

Patients with plateau iris tend to be female and to be younger and less hyperopic than those with relative pupillary block, and they often have a family history of angle-closure glaucoma. Except in the youngest patients, some element of pupillary block is usually present. Iridotomy may result in an open angle (plateau iris configuration) or continue appositional closure either spontaneously or with pharmacologic dilation (plateau iris syndrome). In the former case, periodic gonioscopy is indicated, because the angle can narrow further with age due to enlargement of the lens, leading to PAS formation.

Plateau iris was the most common underlying etiology in our patients. There was a clear female preponderance (74.3%). Their mean age was notably younger than that described in the literature for angle closure secondary to relative pupillary block. Six patients (17.1%) had presented with acute angle closure. All eyes but one underwent laser iridotomy. We could not assess the total number of patients requiring ALPI, because many were seen in consultation and laser treatment had been performed elsewhere.

#### IRIDOCILIARY CYSTS

Iridociliary cysts can push the iris root anteriorly, causing a pseudoplateau configuration with or without angle closure (Figure 5). When large or extensive, they may produce angle closure<sup>39-46</sup> (Table IV). In a UBM study of 90

TABLE III: REPORTED CASES OF ANGLE CLOSURE WITH PLATEAU IRIS SYNDROME

AUTHORS	YEAR	AGE AT DIAGNOSIS	JACG/CASES REPORTED
Tornquist <sup>30</sup>	1958	44	0/1
Wand et al <sup>31</sup>	1977	37-84 yr	2/8

JACG, juvenile angle closure glaucoma.

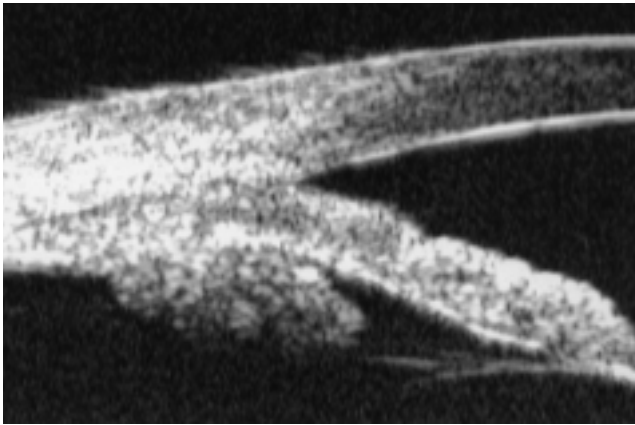


FIGURE 2

Plateau iris syndrome after laser iridotomy. Angle remains closed, anterior chamber is relatively deep, iris contour is essentially planar, posterior chamber is very small, ciliary processes are markedly centrally displaced, and no ciliary sulcus is present.



FIGURE 3

Double hump sign in eye with plateau iris. Beam follows curvature of iris over lens, reaches its deepest point at level of posterior chamber, then curves up again over ciliary processes.

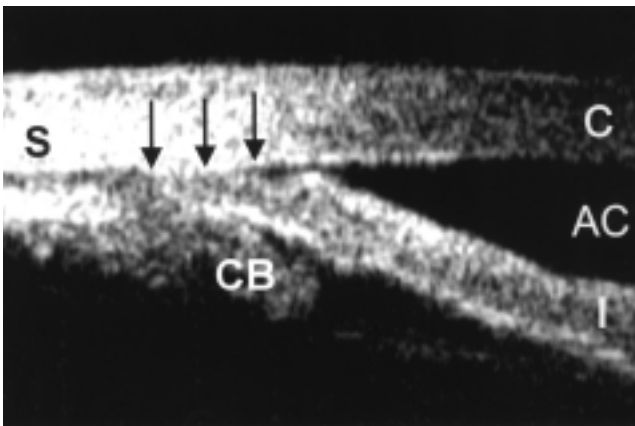


FIGURE 4A

Ultrasound biomicroscopy of eye with plateau iris syndrome before argon laser peripheral iridoplasty. Angle is closed to Schwalbe's line (arrows). S, sclera; CB, ciliary body; I, iris; AC, anterior chamber; C, cornea.

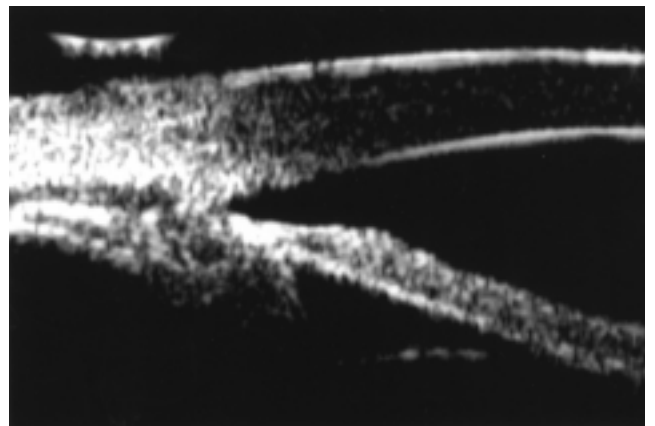


FIGURE 4B

Ultrasound biomicroscopy of eye with plateau iris syndrome after argon laser peripheral iridoplasty. Peripheral iris stroma has been compacted, creating an open angle.

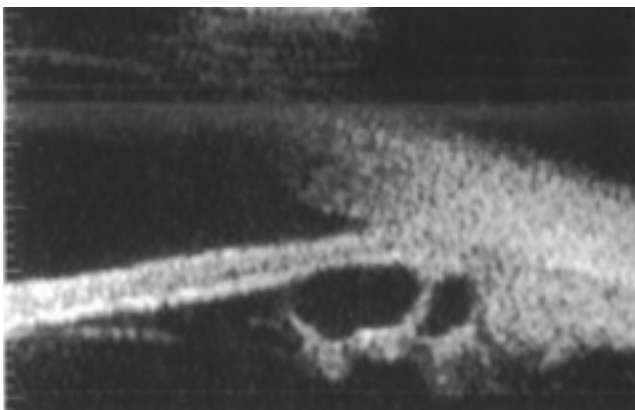


FIGURE 5

Iridociliary cysts causing angle closure with a pseudoplateau iris configuration.

eyes with primary neuroepithelial cysts, more than three cysts per eye were found in 34 eyes (37.8%).<sup>45</sup> Shields and associates<sup>11</sup> reviewed the findings in 44 children with primary iris pigment epithelial cysts, 34 of whom had iridociliary cysts. The cyst was usually detected on slit-lamp examination as bulging of the peripheral iris, and the patient was referred to rule out a tumor. In contrast, iridociliary cysts causing angle closure in our patients were multiple, extended around the circumference of the angle, produced a double hump sign on indentation gonioscopy, and were usually detected by UBM. All patients required laser iridotomy in at least one eye. Four eyes of three patients had persistent appositional closure after iridotomy and were successfully treated with ALPI.

#### LENS-INDUCED ANGLE CLOSURE

Block originating from enlargement or forward movement

TABLE IV: REPORTED CASES OF ANGLE CLOSURE AND IRIDOCILIARY BODY CYSTS

AUTHORS	YEAR	AGE AT DIAGNOSIS	JACG/CASES REPORTED	COMMENTS
Chandler and Braconier <sup>14</sup>	1958			
Vela et al <sup>39</sup>	1984	36 yr	1/11	
Shields et al <sup>15</sup>	1984	NA	0/62	No glaucoma in this series
Bron et al <sup>42</sup>	1984	28 yr	1/1	
Azuara-Blanco et al <sup>41</sup>	1996	58-70 yr	0/3	Plateau iris and cysts as combined mechanism for closure
Tanihara et al <sup>40</sup>	1997	39 yr	1/1	
Lois et al <sup>16</sup>	1998	7 mo - 70 yr	3/254	Chronic angle closure
Shields et al <sup>11</sup>	1999	<20 yr	0/251	Review of iris/ciliary body cysts in children; no separate analysis for glaucoma
Kuchenbecker et al <sup>44</sup>	2000	55 yr	0/1	
Viestenz et al <sup>43</sup>	2000	23 yr	1/1	Angle closure after mydriasis

JACG, juvenile angle closure glaucoma; NA, not available.

of the lens forces the ciliary body and iris anteriorly, closing the angle. The term *phacomorphic glaucoma* is traditionally reserved for angle closure caused by a large or intumescent lens. Indentation gonioscopy may be difficult or impossible to perform successfully. Angle closure associated with anterior lens subluxation or dislocation can occur with various syndromes that affect zonular integrity or after trauma. Indentation gonioscopy in these eyes reveals a dome-shaped central iris following the contour of the lens to its periphery and then leveling off in a flat plane to its insertion (Figure 6).

#### NANOPHTHALMOS

Nanophthalmos is a statistically derived definition and represents the short end of the spectrum of axial lengths. Isolated nanophthalmos is a bilateral, often familial form of microphthalmos unaccompanied by other congenital

malformations.<sup>47</sup> It is characterized by hyperopia, small corneal diameter, thick sclera, and narrow angles.<sup>48</sup> The axial length is between 14 and 20.5 mm, while the lens is of normal size, leading to a crowded anterior segment and a shallow anterior chamber.<sup>49</sup> The ratio of lens volume to ocular volume is four to eight times larger than that of normal eyes.<sup>50</sup> The sclera is characterized by abnormally packed, frayed, and disordered collagen fibers, loss of elastin, and an abnormal accumulation of glycosaminoglycans.<sup>51-59</sup> Uveal effusion is common, either spontaneously or after laser and surgical procedures.<sup>60-65</sup> Nanophthalmos has been described in association with retinitis pigmentosa with or without cystic macular degeneration or optic nerve head drusen<sup>66-69</sup> and Hallermann-Streiff syndrome.<sup>56</sup>

There is an inverse correlation between the degree of hyperopia and the age at onset of angle closure, which usually develops between ages 20 and 50 (Table V). The

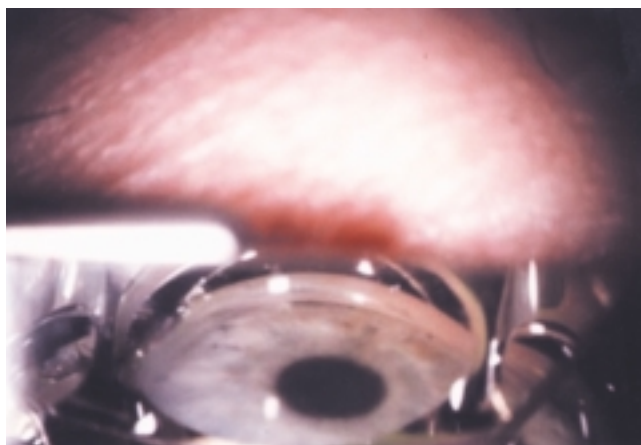


FIGURE 6A

Lens-induced angle closure. After iridotomy, angle remains closed without indentation. Black pigment at 12-o'clock position serves as reference point for Figure 6B.



FIGURE 6B

Lens-induced angle closure. With indentation, iris follows contour of lens until it reaches posterior chamber, then has a planar configuration to its insertion

TABLE V: REPORTED CASES OF ANGLE-CLOSURE GLAUCOMA AND NANOPHTHALMOS

AUTHORS	YEAR	AGE AT DIAGNOSIS	JACC/CASES REPORTED	COMMENTS
O'Grady <sup>48</sup>	1971	23 yr	1/1	
Calhoun <sup>105</sup>	1975	31 yrs	1/6	
Brockhurst <sup>60</sup>	1975	30-51 yr	1/5	
Kimbrough et al <sup>106</sup>	1979	55-58 yr	0/2	
Singh et al <sup>50</sup>	1982	19-69 yr	14/16	
Ghose et al <sup>88</sup>	1985	56 yr	0/1	Nanophthalmos with pigmentary retinopathy
Diehl et al <sup>107</sup>	1989	64-72 yr	0/2	Coexisting diagnosis of pseudoexfoliation in 1 patient
Kocak et al <sup>108</sup>	1996-1997	Mean age, 14.6 yr	8/22 eyes	
Flowers et al <sup>109</sup>	1996	65 yr	0/1	Intraoperative air bubble leading to angle closure
Caronia et al <sup>110</sup>	1998	80 yr	0/1	
Othman et al <sup>111</sup>	1998	7-77 yr	12/22	

JACC, juvenile angle closure glaucoma.

youngest reported patient with acute angle closure was a 9-year-old with 21 diopters of hyperopia.<sup>70</sup> Examination of families of affected individuals can permit detection of presymptomatic patients in early childhood.<sup>71</sup> However, acute angle closure can also develop in the elderly.<sup>72</sup>

Three of our patients had isolated nanophthalmos. All required iridotomy. Four other patients also had nanophthalmos, the two with Weill-Marchesani syndrome, one with ROP, and one eye of one patient with plateau iris (the other eye had an axial length of 20.8 mm).

#### RETINOPATHY OF PREMATUREITY

Retinopathy of prematurity occurs primarily in infants with gestational age of less than 30 weeks or 1,500 g birth weight, or both. Incomplete growth of the peripheral posterior segment vasculature leads to areas of avascular retina. Cicatricial changes may ultimately lead to retinal detachment. Retrolental fibrovascular proliferation may lead to secondary angle closure, a well-known complication of the later stages and a major cause of poor vision (Table VI).<sup>73,74</sup> Progressive lenticular myopia is often associated with shallowing of the anterior chamber.<sup>75,76</sup> Angle closure has also been reported to occur after diode laser treatment for the retinopathy<sup>77</sup> and after scleral buckling.<sup>6</sup>

Angle closure may occur in very young children with ROP due to anterior displacement of the lens-iris diaphragm.<sup>8,78-82</sup> These eyes do not respond to iridotomy or iridectomy.<sup>83</sup> In young adults with ROP, there may be a superimposed element of pupillary block, and iridotomy may be successful.<sup>84,85</sup> Chronic angle closure may develop in adults.<sup>9,79,85</sup> Iris vascular congestion may be present, mimicking neovascular glaucoma.<sup>86</sup>

In one series of 26 untreated eyes with stage IV or V ROP, 3 had angle closure for over 180°, 15 had a highly convex iris, and 16 had posterior synechiae.<sup>87</sup> Microphthalmos may occur in eyes with ROP and may

also predispose to chronic angle-closure glaucoma.<sup>88</sup> Lens extraction alone or combined with vitrectomy has been recommended.<sup>4,8,73,79,80,82,89</sup> We have found that ALPI may be beneficial in compacting the peripheral iris stroma and opening the angle in these patients.

Seven of our patients had ROP. Two patients evaluated by UBM demonstrated peripheral retinal membranes to the pars plana with peripheral vitreoretinal condensation (Figure 7). Contraction of these membranes may cause forward movement of the lens-iris diaphragm.

#### UVEITIS

Formation of posterior synechiae can lead to a secluded pupil and absolute pupillary block. Treatment includes medical management of both intraocular inflammation and elevated IOP. Iridotomy may be required to relieve a pupillary block component. In the case of significant posterior synechiae, multiple iridotomies may need to be performed to relieve segmental pupillary block.

Five of our patients (six eyes) had uveitis with angle closure secondary to total posterior synechiae. All

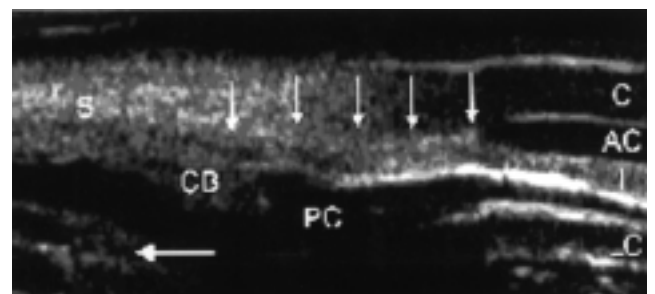


FIGURE 7

Retinopathy of prematurity. Lens (LC, lens capsule) is anteriorly displaced, anterior chamber (AC) is extremely shallow, and angle sealed with peripheral anterior synechiae onto cornea (vertical arrows). S, sclera; CB, ciliary body; PC, posterior chamber; C, cornea; horizontal arrow, proliferative membranes.

TABLE VI: REPORTED CASES OF ANGLE-CLOSURE GLAUCOMA AND RETINOPATHY OF PREMATURITY

AUTHORS	YEAR	AGE AT DIAGNOSIS	JACC/CASES REPORTED	COMMENTS
McCormick and Pratt-Johnson <sup>8</sup>	1971	<2 yr	4/5	One additional case of PHPV
Pollard <sup>90</sup>	1980	5 mo to 3.5 yr	5/5	All patients treated with PPV and PPL
Smith and Shivitz <sup>85</sup>	1984	20-28yr	3/3	
Pollard <sup>117</sup>	1984	7 mo to 3 yr	15/15	Only 3 cases described in article
Halperin and Schoch <sup>6</sup>	1988	4 yr	1/1	Angle closure after scleral buckle
Ueda and Ogino <sup>84</sup>	1988	22 yr	1/1	
Hartnett et al <sup>87</sup>	1990	4.5-35 mo	3 of 26 eyes	
Michael et al <sup>9</sup>	1991	12-45 yr	9/10	
Dhillon et al <sup>118</sup>	1992	23 wk	1/1	
Lee et al <sup>7</sup>	1998	2 yr	1/1	Post diode laser treatment
Chen and Kalina <sup>86</sup>	1998	38 yr	1/1	Late-onset NVG

JACC, juvenile angle closure glaucoma; NVG, neovascular glaucoma; PHPV, persistent hyperplastic primary vitreous; PPL, pars plana lensectomy; PPV, pars plana vitrectomy.

involved eyes had chronic angle closure with PAS, and all required iridotomies. All continued to require antiglaucoma treatment with multiple medications at last follow-up.

#### LENS SUBLUXATION

Three of our patients had Weill-Marchesani syndrome. Patients exhibit short stature, brachydactyly, brachycephaly, and microspherophakia. There is severe limitation of mobility of the fingers and wrists to both active and passive motion. The globe is usually normal in size, but two of our patients had nanophthalmos. Lenticular myopia occurs early in the second decade. Lens dislocation is common and also occurs early. In one series, 12 lenses of 10 patients were noted to be dislocated at the initial examination (average age, 20 years), and 2 dislocated subsequently.<sup>90</sup>

Glaucoma may result from either forward movement of the lens or dislocation into the anterior chamber (Table VII). Loosening of zonules permits the lens to move anteriorly, increasing its area of contact with the iris. This results in relative pupillary block, forward bowing of the peripheral iris, and gradual shallowing of the anterior chamber.<sup>91</sup> Chronic angle closure is common. Angle closure caused by microspherophakia often becomes worse with miotic therapy. If iridotomy fails to open an angle and appositional angle closure persists, ALPI may be successful.<sup>16</sup>

Marfan syndrome is an autosomal dominant disease of collagen synthesis. Patients are characterized by tall

stature, long digits, and hyperextensible joints. Ocular findings include megalocornea, keratoconus, microspherophakia, lens subluxation, and both open-angle and angle-closure glaucoma (Table VIII).

#### OTHER ETIOLOGIES

One patient had persistent hyperplastic primary vitreous, which is usually unilateral and is recognizable at birth in full-term infants with leukokoria due to a retrolental fibrovascular mass.<sup>92</sup> Angle closure can occur as a result of an intumescent cataract, forward movement of the lens-iris diaphragm associated with contracture of the retrolental membrane, or hemorrhage from persistent vessels within the fibrovascular membrane.<sup>93</sup> Angle closure in younger patients has also been reported in association with various syndromes not represented in our series (Table IX). These include Turner's syndrome,<sup>94,95</sup> Alagille syndrome,<sup>96</sup> childhood cystinosis,<sup>14</sup> oculodentodigital dysplasia,<sup>97,98</sup> congenital microcoria,<sup>99,100</sup> and familial exudative vitreoretinopathy.<sup>101</sup>

#### CONCLUSION

Persons aged 40 years or younger accounted for 2.34% of our patients with angle closure. Nevertheless, most of the patients were older than age 30 at the time of diagnosis, and angle closure in persons younger than 30, especially children, must still be considered rare. It is possible that

TABLE VII: REPORTED CASES OF ANGLE-CLOSURE GLAUCOMA AND WEILL-MARCHESANI SYNDROME

AUTHORS	YEAR	AGE AT DIAGNOSIS	JACC/CASES REPORTED
Jensen et al <sup>90</sup>	1974	12-47 yr	8/10
Wright and Chrousos <sup>102</sup>	1985	6 yr	1/1
Taylor <sup>103</sup>	1996	NA	1/1
Evereklioglu et al <sup>104</sup>	1999	19-27	2/6

JCAG, juvenile angle closure glaucoma; NA, not available.

## Angle Closure in Younger Patients

TABLE VIII: REPORTED CASES OF ANGLE-CLOSURE GLAUCOMA AND MARFAN SYNDROME

AUTHORS	YEAR	AGE AT DIAGNOSIS	JACG/CASES REPORTED
Allen et al <sup>112</sup>	1967	9-40 yr	0/6
Izquierdo et al <sup>113</sup>	1992	1-79 yr	2/13

JACG, juvenile angle closure glaucoma .

TABLE IX: REPORTED CASES OF JUVENILE ANGLE CLOSURE, VARIOUS ETIOLOGIES

AUTHORS	YEAR	JACG/CASES REPORTED	ETIOLOGY
Jones and Watson <sup>7</sup>	1967	1/1	Phospholine iodide
McCormick and Pratt-Johnson <sup>8</sup>	1971	5/5	ROP, PHPV
Mills and Robb <sup>10</sup>	1994	3/155	PHPV, congenital rubella
Mori et al <sup>119</sup>	1997	2/9	Secondary to PHPV and cataract
Yu and Chang <sup>120</sup>	1997	1/2	PHPV
Sawada et al <sup>121</sup>	2001	1/1	PHPV
Eibschitz-Tsimhoni et al	1997	1/1	Vogt-Koyanagi-Harada syndrome
Rathinam et al <sup>122</sup>	1997	2/3	Vogt-Koyanagi-Harada syndrome
Katsushima et al <sup>123</sup>	1996	1/1	Ciliary medulloepithelioma
Potamitis and Felder <sup>96</sup>	1993	1/1	Alagille syndrome
Sharir et al <sup>124</sup>	1992	1/1	Sneezing, probable elevated episcleral venous pressure
Nash and Lindquist <sup>125</sup>	1992	1/1	HIV, bilateral choroidal effusions
Kearns and Dhillon <sup>126</sup>	1990	1/1	Labor
Browning et al <sup>127</sup>	2000	1/1	Paroxetine therapy
Fivgas and Beck <sup>5</sup>	1997	1/1	Ocular albinism
Wan et al <sup>14</sup>	1986	1/1	Cystinosis
Vajpayee et al <sup>13</sup>	1991	16/16	Pseudophakic pupillary block
Appleby and Kinder <sup>1</sup>	1971	1/1	Possible nanophthalmos vs medication-induced
Faberowski et al <sup>128</sup>	2001	4/4	Congenital pupil-iris-lens membrane, ectopia lentis

JACG, juvenile angle closure glaucoma; PHPV, persistent hyperplastic primary vitreous; ROP, retinopathy of prematurity.

our patient population was skewed away from some diagnoses, such as ROP or uveitis, because of the large number of pediatric ophthalmologists in the New York area.

The mechanisms causing angle closure in younger patients differ in frequency from those in older patients. Young adults with angle closure are most likely to have plateau iris. Iridociliary cysts should be ruled out by UBM. Because angle closure in younger patients is unusual, and because gonioscopy in these patients may not be routinely performed, the clinician must maintain a high index of suspicion. We advocate performing gonioscopy on all patients undergoing initial examination. Prompt treatment with peripheral iridotomy is indicated in these patients. Furthermore, periodic gonioscopy is needed to detect further angle closure requiring iridoplasty to prevent future trabecular meshwork dysfunction, PAS formation, and chronic angle-closure glaucoma.

## REFERENCES

1. Appleby RSL, Kinder RSL. Bilateral angle closure glaucoma in a 14-year-old boy. *Arch Ophthalmol* 1971;86:449-450.
2. Boase AJ. Acute glaucoma in an adolescent. *Am J Ophthalmol* 1948;31:997-999.
3. Brosnan JD. Primary chronic angle-closure glaucoma in a young woman of 19 years: a case report. *Trans Asia-Pac Acad Ophthalmol* 1973;4:130-132.
4. Collyer R, Arstikaitis M, Pashby T. Glaucoma in children. *Trans Can Ophthalmol Soc* 1959;21:92.
5. Fivgas GD, Beck AD. Angle-closure glaucoma in a 10-year-old girl. *Am J Ophthalmol* 1997;124:251-253.
6. Halperin LS, Schoch LH. Angle closure glaucoma after scleral buckling for retinopathy of prematurity. Case report. *Arch Ophthalmol* 1988;106:453.
7. Jones DEP, Watson DM. Angle-closure glaucoma precipitated by the use of phospholine iodide for esotropia in a child. *Br J Ophthalmol* 1967;51:783-785.
8. McCormick AQ, Pratt-Johnson JA. Angle-closure glaucoma in infancy. *Can J Ophthalmol* 1971;6:38-41.

9. Michael AJ, Pesin SR, Katz LJ, et al. Management of late-onset angle-closure glaucoma associated with retinopathy of prematurity. *Ophthalmology* 1991;98:1093-1098.
10. Mills MD, Robb RM. Glaucoma following childhood cataract surgery. *J Pediatr Ophthalmol Strabismus* 1994;31:355-360.
11. Shields JA, Shields CL, Lois N, et al. Iris cysts in children: classification, incidence, and management. The 1998 Torrence A. Makley Jr Lecture. *Br J Ophthalmol* 1999;83:334-338.
12. Vajpayee RB, Talwar D. Pseudophakic malignant glaucoma in a child. *Ophthalmic Surg* 1991;22:266-267.
13. Vajpayee RB, Angra SK, Titiyal JS, et al. Pseudophakic pupillary-block glaucoma in children. *Am J Ophthalmol* 1991;111:715-718.
14. Wan WL, Minckler DS, Rao NA, et al. Pupillary-block glaucoma associated with childhood cystinosis. *Am J Ophthalmol* 1986;101:700-705.
15. Shields MD, Ritch R. Classifications and mechanisms of the glaucomas. In: Ritch R, Shields MB, eds. *The Secondary Glaucomas*. St Louis, Mo: CV Mosby, 1982.
16. Ritch R, Solomon LD. Argon laser peripheral iridoplasty for angle-closure glaucoma in siblings with Weill-Marchesani syndrome. *J Glaucoma* 1992;1:243-247.
17. Ritch R, Liebmann J, Tello C. A construct for understanding angle-closure glaucoma: the role of ultrasound biomicroscopy. *Ophthalmol Clin North Am* 1995;8:281-293.
18. Lowe RF. Primary angle-closure glaucoma: a review of ocular biometry. *Aust J Ophthalmol* 1977;5:9-17.
19. Delmarcelle Y, François J, Goes F, et al. Biometrie oculaire clinique (oculometrie). *Bull Soc Belge Ophthalmol* 1976;1:172.
20. Tomlinson A, Leighton DA. Ocular dimensions in the heredity of angle-closure glaucoma. *Br J Ophthalmol* 1973;57:475-486.
21. Lowe RF, Clark BAJ. Posterior corneal curvature: correlations in normal eyes and in eyes involved with primary angle-closure glaucoma. *Br J Ophthalmol* 1973;57:475-478.
22. Lee DA, Brubaker RF, Ilstrup DM. Anterior chamber dimensions in patients with narrow angles and angle-closure glaucoma. *Arch Ophthalmol* 1984;102:46-50.
23. Fontana SC, Brubaker RF. Volume and depth of the anterior chamber in the normal aging human eye. *Arch Ophthalmol* 1980;98:1801-1808.
24. Heim M. Photographische Bestimmung der Tiefe und des Volumens der menschlichen Vorderkammer. *Ophthalmologica* 1941;102:193-220.
25. Weekers R, Delmarcelle Y, Collignon J, et al. Mesure optique de la profondeur de la chambre antérieure. Applications cliniques. *Doc Ophthalmol* 1973;34:413-434.
26. Kondo T, Miura M, Imamichi M. Anterior chamber volume in the normal human eye. *Acta Soc Ophthalmol Jpn* 1985;89:1099-1103.
27. Grosvenor T. Reduction in axial length with age: an emmetropizing mechanism for the adult eye? *Am J Optom Physiol Optics* 1987;64:657-663.
28. Hoffer KJ. Axial dimension of the human cataractous lens. *Arch Ophthalmol* 1993;111:914-918.
29. Markowitz SN, Morin JD. Ratio of lens thickness to axial length for biometric standardization of angle-closure glaucoma. *Am J Ophthalmol* 1985;99:400.
30. Tornquist R. Angle-closure glaucoma in an eye with a plateau type of iris. *Acta Ophthalmol* 1958;36:413.
31. Wand M, Grant WM, Simmons RJ, et al. Plateau iris syndrome. *Trans Am Acad Ophthalmol Otolaryngol* 1977;83:122.
32. Lowe RF, Ritch R. Angle-closure glaucoma: clinical types. In: Ritch R, Shields MB, Krupin T, eds. *The Glaucomas*. St Louis, Mo: CV Mosby, 1989:839-853.
33. Ritch R. Plateau iris is caused by abnormally positioned ciliary processes. *J Glaucoma* 1992;1:23-26.
34. Pavlin CJ, Ritch R, Foster FS. Ultrasound biomicroscopy in plateau iris syndrome. *Am J Ophthalmol* 1992;113:390-395.
35. Ritch R, Liebmann JM. Role of ultrasound biomicroscopy in the differentiation of block glaucomas. *Curr Opin Ophthalmol* 1998;9:39-45.
36. Ritch R, Tran HV, Ishikawa H, et al. Iridociliary apposition in plateau iris syndrome persists after cataract extraction. *Am J Ophthalmol* 2002;(In Press).
37. Ritch R. Argon laser peripheral iridoplasty: an overview. *J Glaucoma* 1992;1:206-213.
38. Ritch R, Liebmann JM. Argon laser peripheral iridoplasty: a review. *Ophthalmic Surg Lasers* 1996;27:289-300.
39. Vela A, Rieser JC, Campbell DG. The heredity and treatment of angle-closure glaucoma secondary to iris and ciliary body cysts. *Ophthalmology* 1984;91:332-337.
40. Tanihara H, Akita J, Honjo M, et al. Angle closure caused by multiple, bilateral iridociliary cysts. *Acta Ophthalmol* 1997;75:216-217.
41. Azuara-Blanco A, Spaeth GL, Araujo SV, et al. Plateau iris syndrome associated with multiple ciliary body cysts. Report of 3 cases. *Arch Ophthalmol* 1996;114:666-668.
42. Bron AJ, Wilson CB, Hill AR. Laser treatment of primary ring-shaped epithelial iris cyst. *Br J Ophthalmol* 1984;68:859-865.
43. Viestenz A, Bergua A, Mardin CY, et al. Acute bilateral angle-closure glaucoma secondary to ciliary body epithelial cysts of the pars plicata: correlation with the ultrasound biomicroscope. *Klin Monatsbl Augenheilkd* 2000;217:127-129.
44. Kuchenbecker J, Motschmann M, Schmitz K, et al. Laser iridocystotomy for bilateral acute angle-closure glaucoma secondary to iris cysts. *Am J Ophthalmol* 2000;129:391-393.
45. Marigo FA, Esaki K, Finger PT, et al. Differential diagnosis of anterior segment cysts by ultrasound biomicroscopy. *Ophthalmology* 1999;106:2131-2135.
46. Thomas R, Mulligan N, Aylward GW, et al. Angle closure glaucoma due to iris and ciliary body cysts. *Aust N Z J Ophthalmol* 1989;17:317-319.
47. Ritch R, Lowe RF. Angle-closure glaucoma: clinical types. In: Ritch R, Shields MB, Krupin T, eds. *The Glaucomas*. 2nd ed. St Louis, Mo: CV Mosby, 1996:823-840.
48. O'Grady RB. Nanophthalmos. *Am J Ophthalmol* 1971;71:1251.
49. Simmons RB, Montenegro MH, Simmons RJ. Primary angle closure glaucoma. In: Tasman W, Jaeger EA, eds. *Duane's Ophthalmology*. Philadelphia: Lippincott Williams & Wilkins, 1996:1-43.
50. Singh O, Simmons RJ, Brockhurst RJ, et al. Nanophthalmos. A perspective on identification and treatment. *Ophthalmology* 1982;89:1006-1012.

51. Uyama M, Takahashi K, Kozaki J, et al. Uveal effusion syndrome. Clinical features, surgical treatment, histologic examination of the sclera and pathophysiology. *Ophthalmology* 2000;107:441-449.
52. Fukuchi T, Abe H, Sawaguchi S. Collagen fibrils in nanophthalmic sclerae. *J Jpn Ophthalmol Soc* 2000;104:706-710.
53. Yamani A, Wood I, Sugino I, et al. Abnormal collagen fibrils in nanophthalmos: a clinical and histologic study. *Am J Ophthalmol* 1999;127:106-108.
54. Forrester JV, Lee WR, Kerr PR, et al. The uveal effusion syndrome and trans-scleral flow. *Eye* 1990;4:354-365.
55. Shiono T, Shoji A, Mutoh T, et al. Abnormal sclerocytes in nanophthalmos. *Graefes Arch Clin Exp Ophthalmol* 1992;230:348-351.
56. Stewart DHI, Streeten BW, Brockhurst RJ, et al. Abnormal scleral collagen in nanophthalmos. An ultrastructural study. *Arch Ophthalmol* 1991;109:1017-1025.
57. Kawamura M, Tajima S, Azuma N, et al. Biochemical studies of glycosaminoglycans in nanophthalmic sclera. *Graefes Arch Clin Exp Ophthalmol* 1995;233:58-62.
58. Kawamura M, Tajima S, Azuma N, et al. Immunohistochemical studies of glycosaminoglycans in nanophthalmic sclera. *Graefes Arch Clin Exp Ophthalmol* 1996;234:19-24.
59. Yue BY, Duvall J, Goldberg MF, et al. Nanophthalmic sclera. Morphologic and tissue culture studies. *Ophthalmology* 1986;93:534-541.
60. Brockhurst RJ. Nanophthalmos with uveal effusion: a new clinical entity. *Arch Ophthalmol* 1975;93:1289-1299.
61. Allen KM, Meyers SM, Zegarra H. Nanophthalmic uveal effusion. *Retina* 1988;8:145-147.
62. Good WV, Stern WH. Recurrent nanophthalmic uveal effusion syndrome following laser trabeculoplasty. *Am J Ophthalmol* 1988;106:234-235.
63. Han LR, Cairns JD. Nanophthalmos with longstanding choroidal effusion and serous retinal detachment. *Aust N Z J Ophthalmol* 1997;25:181-183.
64. Ryan EA, Zwaan J, Chylack LT. Nanophthalmos with uveal effusion. Clinical and embryologic considerations. *Ophthalmology* 1982;89:1013-1017.
65. Lesnoni G, Rossi T, Nistri A, et al. Nanophthalmic uveal effusion syndrome after prophylactic laser treatment. *Eur J Ophthalmol* 1999;9:315-318.
66. MacKay CJ, Shek MS, Carr RE, et al. Retinal degeneration with nanophthalmos, cystic macular degeneration, and angle closure glaucoma: a new recessive syndrome. *Arch Ophthalmol* 1987;105:366-371.
67. Hermann P. Le syndrome microphtalmie-rétinite pigmentaire-glaucome. *Arch Ophthalmol (Paris)* 1958;18:17.
68. Ghose S, Sachdev MS, Kumar H. Bilateral nanophthalmos, pigmentary retinal dystrophy, and angle closure glaucoma—a new syndrome? *Br J Ophthalmol* 1985;69:624.
69. Buys YM, Pavlin CJ. Retinitis pigmentosa, nanophthalmos, and optic disc drusen. A case report. *Ophthalmology* 1999;106:619-622.
70. Hatcher WF. Extreme axial hyperopia. *Arch Ophthalmol* 1952;48:161-162.
71. Altintas AK, Acar MA, Yalvaç IS, et al. Autosomal recessive nanophthalmos. *Acta Ophthalmol* 1997;75:325-328.
72. Cross HE, Yoder F. Familial nanophthalmos. *Am J Ophthalmol* 1976;81:300-306.
73. Blodi F. Symposium: Retrolental fibroplasia (retinopathy of prematurity) management. *Trans Am Acad Ophthalmol Otolaryngol* 1955;59:35-38.
74. Hartnett ME, Gilbert MM, Hirose T, et al. Glaucoma as a cause of poor vision in severe retinopathy of prematurity. *Graefes Arch Clin Exp Ophthalmol* 1993;231:433-438.
75. Gordon RA, Donzis PB. Myopia associated with retinopathy of prematurity. *Ophthalmology* 1986;93:1593.
76. Ginsberg J, Bove KE. Ocular pathology of trisomy 13. *Ann Ophthalmol* 1974;6:113.
77. Lee GA, Lee LR, Gole GA. Angle-closure glaucoma after laser treatment for retinopathy of prematurity. *J Am Assoc Pediatr Ophthalmol Strabismus* 1998;2:383-384.
78. Cohen J, Alfano JE, Boshes LD, et al. Clinical evaluation of school age children with retrolental fibroplasia. *Am J Ophthalmol* 1964;57:41-57.
79. Hittner HM, Rhodes LM, McPherson AR. Anterior segment abnormalities in cicatricial retinopathy of prematurity. *Ophthalmology* 1979;86:803-816.
80. Pollard ZF. Secondary angle-closure glaucoma in cicatricial retrolental fibroplasia. *Am J Ophthalmol* 1980;89:651-653.
81. Laws DE, Haslett R, Ashby D, et al. Axial length biometry in infants with retinopathy of prematurity. *Eye* 1994;8:427-430.
82. Kushner BJ. Ciliary block glaucoma in retinopathy of prematurity. *Arch Ophthalmol* 1982;100:1078-1079.
83. Walton DS. Retrolental fibroplasia with glaucoma. In: Chandler DA, Grant WM, ed. *Glaucoma*. 2nd ed. Philadelphia: Lea & Febiger, 1979:
84. Ueda N, Ogino N. Angle-closure glaucoma with pupillary block mechanism in cicatricial retinopathy of prematurity. *Ophthalmologica* 1988;196:15-18.
85. Smith J, Shivitz I. Angle-closure glaucoma in adults with cicatricial retinopathy of prematurity. *Arch Ophthalmol* 1984;102:371-372.
86. Chen PP, Kalina RE. Chronic angle-closure mimicking rubeotic glaucoma in an adult with retinopathy of prematurity. *Arch Ophthalmol* 1998;116:1248.
87. Hartnett ME, Gilbert MM, Richardson TM, et al. Anterior segment evaluation of infants with retinopathy of prematurity. *Ophthalmology* 1990;97:122-130.
88. Kelly SP, Fielder AR. Microcornea associated with retinopathy of prematurity. *Br J Ophthalmol* 1987;71:201.
89. Kalina RE. Treatment of retrolental fibroplasia. *Surv Ophthalmol* 1980;24:229-236.
90. Jensen AD, Cross HE, Paton D. Ocular complications in the Weill-Marchesani syndrome. *Am J Ophthalmol* 1974;77:261.
91. Ritch R. Glaucoma secondary to lens intumescence and dislocation. In: Ritch R, Shields MB, eds. *The Secondary Glaucomas*. St Louis, Mo: CV Mosby, 1982:131-149.
92. Cantor LB. Glaucoma associated with congenital disorders. In: Ritch R, Shields MB, Krupin T, eds. *The Glaucomas*. 2nd ed. St Louis, Mo: CV Mosby, 1996:925-954.
93. Alward WLM, et al. PHPV with glaucoma presenting in infancy. *Arch Ophthalmol* 1991;109:1063.
94. Buckley CA, Cheng H. Intraocular melanoma, diabetes, and Turner's syndrome: presentation with proptosis. *Br J Ophthalmol* 1981;65:460.

95. Khodadoust A, Paton D. Turner's syndrome in a male: report of a case with myopia, retinal detachment, cataract, and glaucoma. *Arch Ophthalmol* 1967;77:630.
96. Potamitis T, Felder AR. Angle-closure glaucoma in Alagille syndrome. A case report. *Ophthalmic Paediatr Genet* 1993;14:101-104.
97. Kadrnka-Lovrencé M, et al. Die oculo-dento-digitale Dysplasie (das Meyer-Schwickerath syndrom). *Monatsschr Kinderheilkd* 1973;121:42.
98. Sugar HS. Oculodentodigital dysplasia syndrome with angle closure glaucoma. *Am J Ophthalmol* 1978;86:36.
99. Hyams SW, Neumann E. Congenital microcoria and combined mechanism glaucoma. *Am J Ophthalmol* 1969;68:326.
100. Veirs ER, Brown W. Congenital miosis. *Arch Ophthalmol* 1961;65:83.
101. Azuara-Blanco A, Pesin SR, Katz LJ, et al. Familial exudative vitreoretinopathy associated with nonneovascular chronic angle-closure glaucoma. *J Glaucoma* 1997;6:47-49.
102. Wright KW, Chrousos GA. Weill-Marchesani syndrome with bilateral angle closure glaucoma. *J Pediatr Ophthalmol Strabismus* 1985;22:129.
103. Taylor JN. Weill-Marchesani syndrome complicated by secondary glaucoma. Case management with surgical lens extraction. *Aust N Z J Ophthalmol* 1996;24:275-278.
104. Evereklioglu C, Hepsen IF, Mandi ER. Weill-Marchesani syndrome in three generations. *Eye* 1999;13:773-777.
105. Calhoun FP. The management of glaucoma in nanophthalmos. *Trans Am Ophthalmol Soc* 1975;73:97.
106. Kimbrough RL, Trempe CS, Brockhurst RJ, et al. Angle-closure glaucoma in nanophthalmos. *Am J Ophthalmol* 1979;88:572.
107. Diehl DLC, Feldman F, Tanzer H, et al. Nanophthalmos in sisters, one with exfoliation syndrome. *Can J Ophthalmol* 1989;24:327-330.
108. Kocak I, Altintas AG, Yalvac IS, et al. Treatment of glaucoma in young nanophthalmic patients. *Int Ophthalmol* 1996-97;20:107-111.
109. Flowers CW Jr, Reynolds D, Irvine JA, et al. Pupillary block, angle-closure glaucoma produced by an anterior chamber air bubble in a nanophthalmic eye. *Arch Ophthalmol* 1996;114:1143-1144.
110. Caronia RM, Sturm RT, Fastenberg DM, et al. Bilateral secondary angle-closure glaucoma as a complication of anticoagulation in a nanophthalmic patient. *Am J Ophthalmol* 1998;126:307-309.
111. Othman MI, Sullivan SA, Skuta GL, et al. Autosomal dominant nanophthalmos (NNO1) with high hyperopia and angle closure glaucoma maps to chromosome 11. *Am J Hum Genet* 1998;63:1411-1418.
112. Allen RA, Straatsma BR, Apt L, et al. Ocular manifestations of the Marfan syndrome. *Trans Am Acad Ophthalmol Otolaryngol* 1967;71:18.
113. Izquierdo NJ, Traboulsi EI, Enger C, et al. Glaucoma in the Marfan syndrome. *Trans Am Ophthalmol Soc* 1992;90:111-122.
114. Chandler PA, Braconier HE. Spontaneous intra-epithelial cysts of iris and ciliary body with glaucoma. *Am J Ophthalmol* 1958;45:64.
115. Shields JA, Kline MW, Augsburger JJ. Primary iris cysts: a review of the literature and report of 62 cases. *Br J Ophthalmol* 1984;68:152-166.
116. Lois N, Shields CL, Shields JA, et al. Primary cysts of the iris pigment epithelium. Clinical features and natural course in 234 patients. *Ophthalmology* 1998;105:1879-1885.
117. Pollard ZF. Lensectomy for secondary angle-closure glaucoma cicatricial retrolental fibroplasia. *Ophthalmology* 1984;91:395-398.
118. Dhillon B, Wright E, Laing I, et al. Cryotherapy for retinopathy of prematurity in a regional neonatal intensive care unit. *J Royal Coll Surg Edinb* 1992;37:83-88.
119. Mori M, Keech RV, Scott WE. Glaucoma and ocular hypertension in pediatric patients with cataracts. *J Am Acad Pediatr Ophthalmol Strabismus* 1997;1:98-101.
120. Yu YS, Chang BL. Persistent hyperplastic primary vitreous in male twins. *Korean J Ophthalmol* 1997;11:123-125.
121. Sawada H, Fukuchi T, Ohta A, et al. [Persistent hyperplastic primary vitreous—a case report of adult onset acute angle-closure glaucoma]. *Nippon Ganka Gakkai Zasshi* 2001;105:711-715.
122. Rathinam SR, Namperumalsamy P, Nozik RA, et al. Angle closure glaucoma as a presenting sign of Vogt-Koyanagi-Harada syndrome. *Br J Ophthalmol* 1997;81:608-609.
123. Katsushima H, Suzuki J, Adachi J, et al. Non-rubeotic angle-closure glaucoma associated with ciliary medullo-epithelioma. *Jpn J Ophthalmol* 1996;40:244-250.
124. Sharir M, Huntington AC, Nardin GF, et al. Sneezing as a cause of acute angle-closure glaucoma. *Ann Ophthalmol* 1992;24:214-215.
125. Nash RW, Lindquist TD. Bilateral angle-closure glaucoma associated with uveal effusion: presenting sign of HIV infection. *Surv Ophthalmol* 1992;36:255-258.
126. Kearns PP, Dhillon BJ. Angle-closure glaucoma precipitated by labour. *Acta Ophthalmol* 1990;68:225-226.
127. Browning AC, Reck AC, Chisholm IH, et al. Acute angle-closure glaucoma presenting in a young patient after administration of paroxetine. *Eye* 2000;14:406-408.
128. Faberowski N, Green J, Walton DS. Angle closure in children. *Int Ophthalmol Clin* 2001;41:35-41.

## DISCUSSION

DR LOUIS B. CANTOR. The authors present a wealth of information from their large clinical practice regarding angle-closure glaucoma in younger patients. Few articles address angle-closure glaucoma in this population and none have the variety of cases presented by the authors.

Several factors may predispose to angle-closure glaucoma. The incidence of angle-closure glaucoma varies significantly among different races and ethnic populations. While narrow angles may be found in approximately 2% of the Caucasian population, the risk of angle-closure glaucoma is small. The highest incidence of angle-closure glaucoma is in Eskimos whose risk is 30 to 40 times that of the Caucasian population. Angle-closure

glaucoma is less common among African Americans, but more common in Asians. Gender is also an important factor. Women of all races develop angle-closure glaucoma three to four times more often than men. In general, women seem to have shallower anterior chambers, small corneal diameters, and a greater lens thickness. Age, as will be discussed in more detail, is a significant risk factor for angle-closure glaucoma, and the risk of angle closure increases with age. Typically, angle-closure glaucoma occurs in eyes with hyperopia, though it may occur in eyes with any type of refractive error. In hyperopic eyes the anterior chamber depth and volume are generally smaller than in myopic eyes. Characteristics of the anterior chamber also seem to be inherited in a multifactorial fashion. Shallow anterior chambers with occludable angles may occur in first-degree relatives, with an increased risk four to six times over the general population.

Age appears to be one of the most significant predisposing factors to angle-closure glaucoma. With aging and normal lens growth, the anterior chamber decreases in depth and in volume. Because of these changes the prevalence of angle-closure glaucoma in Caucasian populations peaks between 55 to 65 years of age, and it is unusual to see angle-closure glaucoma before the age of 50. In the paper just presented, the authors looked at a unique population of patients diagnosed with angle-closure glaucoma before the age of 40. Of their extensive patient database, they discovered nearly 3,000 patients with angle-closure glaucoma representing approximately 20% of their total patient population. This would be consistent with the general population in the United States. Of these, only 67 patients met their inclusion criteria, which was only 0.48% of their total population, or only just over 2% of the angle closure glaucoma patients in their practice. The majority of these patients were female, which is typical because angle-closure glaucoma is three to four times more common in females.

The median age at diagnosis in this study was 31.5 years. Of significant interest was that 53%, or 35 patients, had plateau iris, whereas in the typical older population, approximately 90% of patients with angle-closure glaucoma will have pupillary block. This represents a very distinct difference, and only two patients in this younger population, representing a very small number of the total population, actually presented with pupillary block as the mechanism for their glaucoma.

While the authors present a very interesting overview of angle-closure glaucoma in younger individuals, many questions remain to be explored. Perhaps most important is what factors predisposed these younger patients to angle-closure glaucoma. Further information regarding the ocular status and dimensions in these younger individuals, such as corneal diameter, corneal curvature, ante-

rior chamber depth, lens thickness, axial length, lens curvature, iris insertion, ciliary body position, or other factors in these eyes, might help explain why the differences in types of glaucoma seen were identified. In addition it would be of interest to know how young patients respond to initial therapy and if they respond the same as or differently than older individuals. We do not know the long-term prognosis in these patients, though one would suspect that they would be more difficult to control with time.

Finally, was there something in the family history or racial characteristics of these patients that might have suggested that they were predisposed to angle-closure glaucoma, or might there be other ways to suspect which of these rare individuals might be at risk for developing glaucoma?

The authors are to be commended for helping to define an uncommon, though potentially serious, ocular condition that can affect younger individuals.

DR JAMES C. BOBROW. In a study published in the *American Journal of Ophthalmology* years ago about our experience with angle-closure glaucoma, we discovered that the average age of our patients was somewhere between 68 and 69. The numbers under the age of 40 were approximately 2.5% to 3% of the population. When we talk about angle closure, we talk about the diagnosis based on gonioscopy and appositional closure, but we don't talk about presenting as acute angle-closure glaucoma. Acute angle-closure glaucoma has decreased by almost 70% over the last several years and is now a rare event. We also looked at predisposing factors. Hyperopia and a keratometry reading of 42 diopters or less were significant.

DR ALLAN J. FLACH. You mentioned that your Weill-Marchesani patients respond very poorly to miotics, with all of that tension created in the sphincter. Have you had experience using the alpha-blockers, like either extemporaneously prepared thymoxamine or the commercially available dapiprozale, which would kind of ignore the sphincter and relax the dilator muscle and perhaps offer a beneficial effect in angle closure in those patients?

DR ALBERT W. BIGLAN. There were no aniridics in this series. The traditional treatment of angle closure with an iridotomy or iridectomy may not be appropriate in the patient with ROP. The mechanism there appears to be a shallowing of the anterior chamber, and lensectomy may be a way of managing this because the lens is pushing the iris forward.

DR WILLIAM TASMAN. I remember one young girl with

ROP who, while studying, noticed that her vision blurred; when she put her head back it cleared. I sent her to Dr Spaeth, who cured her with an iridectomy. More recently we've looked at 25 10-year-olds who had cryo to one eye and laser to the other. We measured with ultrasound biomicroscopy and found that the anterior chambers were shallower in the cryo eyes and the lenses were thicker. I look at them as potential candidates for perhaps angle closure in the future.

DR ROBERT RITCH. In our population, relative pupillary block accounts for about 90% of the angle closure and plateau iris or mixed plateau iris with relative pupillary block accounts for about 7%. Lens-induced angle closure, malignant glaucoma, and secondary angle-closure glaucomas account for about 3%. Plateau iris is much more common in Asia, representing nearly 30% of glaucoma diagnoses. In China, where angle closure is more common than open-angle glaucoma, there seems to be more of a lens-induced component. In Japan, on the other hand, angle closure accounts for a relatively small amount of the total glaucoma. Plateau iris is more common in women and tends to be familial. I wonder if it is a distinct entity or one end of a spectrum with pure relative pupillary block at one end and pure plateau iris in a young patient with no component of pupillary block at the other end.

I certainly agree with Dr Bobrow that acute angle-closure glaucoma has decreased markedly. I would suggest a 90% decrease in incidence. Ophthalmologists are performing gonioscopy more routinely, patients with narrow angles undergo iridotomy earlier, and cataracts are removed earlier.

Patients with Weill-Marchesani syndrome, micro-

spherophakia, and zonular weakening can respond to miotics paradoxically. If the lens is subluxed and the zonules are totally broken, miotics will open the angle, while cycloplegics allow the lens to dislocate into the anterior chamber. If intact zonules remain, cycloplegics will deepen the anterior chamber, while miotics, which contract the ciliary muscle, allow the lens to move anteriorly and worsen the angle closure. The UBM may be helpful. Thymoxamine is no longer available. We found that dapiprozale caused a lot of red eyes and patients hated it. We did not include aniridia in this series because it is not true angle closure. The iris stump slides up onto the trabecular meshwork.

Dr Tasman is correct in that patients, especially children, with ROP need to be watched for the development of angle closure. Many of the younger patients present with acute angle closure because gonioscopy in children may be difficult and the condition missed, but it is important to perform, even if an examination under anesthesia is required. A number of different mechanisms can be responsible, such as lenticular myopia shallowing the anterior chamber, proliferative fibrovascular membranes causing anterior rotation of the lens-iris diaphragm, or after cyclophotocoagulation or scleral buckling. Older patients with ROP can develop pupillary block or chronic angle closure. I don't like taking the lenses out for angle-closure if I can get away with an iridoplasty. In patients with lens-induced angle closure, where the lens is pushing forward, its effect may be transient, but it should be tried. We had a monocular 5-year-old girl with ROP who underwent combined iridotomy and iridoplasty and did well for 7 years before needing a trabeculectomy.

# DELTA-9-TETRAHYDROCANNABINOL (THC) IN THE TREATMENT OF END-STAGE OPEN-ANGLE GLAUCOMA

---

BY *Allan J. Flach, MD*

## ABSTRACT

*Purpose:* Evidence exists that the administration of cannabinoid derivatives can lower intraocular pressure. Some patients with glaucoma believe they are being deprived of a potentially beneficial treatment. Therefore, the Research Advisory Panel of California instituted the Cannabis Therapeutic Research Program to permit compassionate access to cannabinoid derivatives. Data about the potential therapeutic usefulness and toxicity of these agents were collected. This study reviews the results of this program with the specific aim of providing further direction for these investigational efforts.

*Methods:* A survey of local ophthalmologists indicated an impressive interest in participating in and contributing patients with glaucoma unresponsive to treatment to this study. Appropriate patients were treated with either orally administered delta-9-tetrahydrocannabinol capsules or inhaled marijuana in addition to their existing therapeutic regimen.

*Results:* Although 20 ophthalmologists were approved as investigators, only nine patients were enrolled in the study. An initial decrease in intraocular pressure was observed in all patients, and the investigator's therapeutic goal was met in four of the nine patients. However, the decreases in intraocular pressure were not sustained, and all patients elected to discontinue treatment within 1 to 9 months for various reasons.

*Conclusions:* This uncontrolled, unmasked, nonrandomized study does not permit definitive conclusions about the efficacy or toxicity of cannabinoids in the treatment of glaucoma. There is an impression that this treatment can lower intraocular pressure, but the development of tolerance and significant systemic toxicity appears to limit the usefulness of this potential treatment. Both patients and ophthalmologists greatly appreciated the opportunity to participate in this study.

*Trans Am Ophthalmol Soc* 2002;100:215-224

## INTRODUCTION

The hemp plant, or *Cannabis sativa*, provides leaves and flowering parts that, when dried, result in a complex pharmacologic mixture called marijuana. Hashish is the sticky resin that is secreted by the plant in hot, dry weather. These mixtures contain 420 natural products, including 28 natural cannabinoids.<sup>1</sup> The cannabinoids share several pharmacologic actions, including intraocular pressure (IOP)-lowering effects, central nervous system effects, and cardiovascular system effects.<sup>2-6</sup>

The Research Advisory Panel of California was created in 1969 by the California Legislature to encourage research into the nature and effects of abused drugs, to

review and approve research involving controlled substances, and to function as a human subject's protection committee in research involving controlled substances. Subsequently, the legislature became concerned that the status of marijuana as a stringently regulated drug might be inhibiting research into its possible therapeutic effects. Therefore, in 1979, the Cannabis Therapeutic Research Program was established to provide compassionate access for patients to marijuana or delta-9-tetrahydrocannabinol (THC) as a potential treatment for nausea and vomiting associated with cancer chemotherapy.

Evidence exists that the administration of cannabinoid derivatives can lower IOP in normal and glaucomatous eyes.<sup>2,7</sup> As a consequence, some patients with glaucoma believe that they are being deprived of a potentially vision-saving treatment and are using marijuana illegally and, in many cases, without medical supervision. Therefore, in 1984, the California legislature, by way of the Research Advisory Panel and its ongoing Cannabis Therapeutic Research Program, added to its mandate and permitted compassionate access for appropriate glaucoma

From the Department of Veteran Affairs, San Francisco, California, and the Department of Ophthalmology, University of California, San Francisco. Supported by the Research Advisory Panel of California; a Merit Review grant from the Department of Veterans Affairs, San Francisco; a grant from That Man May See, Inc; and a departmental core grant from the National Institutes of Health to the University of California, San Francisco, Department of Ophthalmology.

patients to these cannabinoid derivatives. This study allowed the collection of preliminary data about the potential therapeutic usefulness and toxicity of THC and marijuana in the treatment of end-stage open-angle glaucoma. This program was effectively ended in October 1986 when THC was marketed as dronabinol (Marinol), making the availability of free THC unnecessary. This presentation reviews the data collected during this 2-year study with the specific aim of providing direction for further investigational efforts within this area of clinical and laboratory research.

## **METHODS**

---

A 1984 survey of ophthalmologists practicing within California indicated an impressive interest in contributing patients with glaucoma unresponsive to available treatment to a study permitting access to cannabinoid derivatives. Subsequently, a protocol was designed with the goal of permitting appropriate patients to receive treatment with either orally administered THC capsules or inhaled marijuana in addition to their existing therapeutic regimen.<sup>8</sup>

### **INVESTIGATORS**

California ophthalmologists certified by the American Board of Ophthalmology could apply to become an investigator. Following application, the potential investigator was required to complete a Food and Drug Administration investigator's form and agree to follow the Cannabis Protocol for Glaucoma. Participating investigators were required to assume full responsibility for determining that their patients conformed to the admission requirements. Continued participation was conditioned upon the investigator's compliance with the protocol, including adequate record keeping on treatment outcome and timely submission of data forms to the Panel.

### **EXPERIMENTAL SUBJECTS**

A Patient Qualification Review Board appointed by the Research Advisory Panel reviewed all of the paperwork, including the patient's medical history and examinations, and referred the potential subject's material to the author for possible enrollment. The author approved a patient as an experimental subject following a lengthy discussion with the investigator and the patient to determine whether the patient met the qualifications to enter the study. Thereafter, the patient was eligible to enroll in the study and receive THC or marijuana cigarettes from an approved pharmacy within the area.

### **DESIGN OF STUDY**

This study was designed as an uncontrolled, unmasked, nonrandomized, prospective evaluation of the effects of

orally administered THC or smoked marijuana on IOP in subjects with uncontrolled IOP while receiving maximally tolerated conventional glaucoma treatment. If subjects began treatment with orally administered THC and the capsules appeared ineffective, the subject could switch to marijuana cigarettes. During the study, ancillary glaucoma medications could not be added or deleted while adjusting THC or marijuana doses without notifying the investigator.

### **EXCLUSION CRITERIA**

A complete medical history and ocular examination were submitted for each patient to determine the patient's suitability for inclusion within this study. Patients were not accepted as subjects for the study if they met one or more of the following exclusion criteria: (1) glaucoma other than primary open-angle glaucoma; (2) occludable angles; (3) not on maximally tolerated medical therapy, including an attempt to use the parasympathomimetics, sympathomimetics, carbonic anhydrase inhibitors, and topically applied beta blockers; (4) uninformed about the proven potential therapeutic advantages of conventional glaucoma surgeries, including laser trabeculoplasty; (5) younger than 18 years of age; (6) a history of any psychiatric disorder, unless approved by a psychiatrist; (7) women of child-bearing age unless using a reliable method of birth control; (8) pregnant or nursing women; (9) significant cardiovascular problems, including unstable angina pectoris, cardiac arrhythmias, or hypotensive episodes; (10) a history of dysphoric reactions to marijuana; (11) suffering from senility; (12) unwilling to abstain from driving automobiles or operating machinery; (13) impaired pulmonary or hepatic function; (14) unwilling or unable to give informed consent for this study.

### **BASELINE HISTORY AND EXAMINATION**

All subjects provided a baseline history and underwent examination to identify the presence of exclusion criteria. This included a history of glaucomatous progression and treatment, current medical management, a complete ocular examination, and the investigator's estimation of a maximum safe IOP level for protection of their optic nerves, which was then considered the goal of therapy. At the conclusion of the examination, if the patient was considered an appropriate subject for the study, the risks, benefits, and alternatives were explained to the subject, and informed consent to participate in the study was subsequently obtained.

### **INFORMED CONSENT**

All subjects read, discussed, and signed the form entitled Consent to Be a Research Subject in the California Cannabis Therapeutic Program. They were informed that the use of THC or marijuana for the treatment of

glaucoma is experimental and that there is no evidence showing that this treatment benefits open-angle glaucoma. Furthermore, they were informed about the potential risks of taking cannabinoid therapy, including changes in vision, hearing, mood, and muscle control; wheezing; decreased blood pressure; feeling faint, intoxicated, confused, nervous, or scared; and rapid heart beat, red eyes, dry mouth, daydreams, hallucinations, forgetfulness, decreased energy, sleepiness, and a distortion of perception. Subjects were warned that some of the effects may be pleasant or distressing in an unpredictable fashion and that they may persist for up to 24 hours. In addition, they were warned that marijuana cigarettes may be harmful to the lungs and have the potential to cause lung cancer, which can be lethal. They were told that they could not operate a car or any machinery while using these treatments because they would endanger themselves and others. Finally, alternative treatments, including different dose forms and higher concentrations of available medications and conventional surgery, were reviewed and clearly identified as proven and efficacious treatments well recognized to benefit glaucoma, unlike the experimental use of cannabis derivatives. In addition to signing the consent form, the subjects read and signed the Experimental Subject's Bill of Rights.

#### **MEASUREMENT OF IOP**

The subject's IOP was determined at baseline immediately prior to the start of cannabis therapy by applanation tonometry with three consecutive measurements. Thereafter, the subject's IOP was evaluated weekly, at the same time of day, until satisfactory control of IOP was achieved for 2 consecutive weeks. Satisfactory control of IOP meant a level of IOP that the investigator believed, as determined from prior experience with the subject, was safe for the health of the subject's optic nerve. When satisfactory IOP control was obtained for 2 consecutive weeks, the frequency of evaluation could be reduced to once a month. Treatment evaluation forms were returned to the Panel on a weekly basis and reviewed by the author.

#### **TREATMENT EVALUATIONS**

On subsequent visits, complete ocular examinations were performed with special attention to the subject's IOP and blood pressure, each measured at the same time of day at each visit. At the conclusion of the office visit, the investigator provided a clinical impression of the effectiveness of treatment since the last evaluation as follows: Improved, Same, Worsened, Uncertain. Cannabis side effects were recorded on both a treatment evaluation form by the investigator and a patient questionnaire by the subject.

#### **PATIENT QUESTIONNAIRE**

Subjects were required to complete a side effect and

psychosocial function questionnaire for each week until their condition stabilized with a given dose of THC or marijuana. This form was submitted to the Panel and reviewed monthly along with the investigator's treatment evaluation form. Additional comments regarding treatment and coexistent side effects were encouraged from each subject at each evaluation period in an attempt to monitor side effects and possible excessive drug accumulation.

#### **TREATMENT MEDICATIONS AND DOSING SCHEDULES**

Oral THC and marijuana cigarettes were provided without charge by the National Cancer Institute and the National Institute on Drug Abuse and dispensed by approved pharmacies. The oral THC dosage forms consisted of soft gelatin capsules containing 2.5 mg or 5 mg of THC dissolved in sesame oil. Initial dosage for each patient was 2.5 mg or 5 mg given every 4 hours (four times daily) while awake. The dose was increased or decreased by 2.5-mg increments as needed to obtain a greater effect or less toxicity, with a maximum permitted dose of 20 mg four times daily. Marijuana cigarettes marked in quarters were supplied and contained 6 mg of THC. Subjects were requested to inhale one fourth of a cigarette every 3 hours (five times daily) while awake. They were instructed to inhale deeply, hold the inhalation for 5 seconds, and then exhale; after 10 seconds the cycle is repeated until the appropriate dose is smoked in approximately 5 minutes. A flameproof holder was used to permit delivery of all the cigarette dosage. This dose was increased or decreased as needed to provide a greater effect on IOP or less toxicity. Subjects could not use "street" marijuana during the study.

#### **TERMINATION FROM STUDY**

Subjects could withdraw from the study at any time for any reason. At the time of termination, the reason for discontinuing treatment (eg, toxic effects, lack of efficacy, too tedious, geographic change, ocular surgery, other, uncertain) was noted on the final evaluation form. No subject was permitted to use these medications for more than 12 months.

#### **RESULTS**

---

During this 2-year period, 20 ophthalmologists were approved as investigators and nine patients were enrolled into the study to receive oral THC for 1 to 9 months. No subjects consented to receive smoked marijuana. The characteristics of these subjects with end-stage open-angle glaucoma are summarized in Table I. At the time of entry into the study, subjects had uncontrolled IOP despite using maximally tolerated medical treatment. Furthermore, the majority of subjects had a history of one or more glaucoma surgeries.

TABLE I: CHARACTERISTICS OF SUBJECTS

PATIENT NO. (SEX/AGE)	EYE	SNELLEN VISION (C/D)	VISUAL FIELD	SURGERY	MEDICATIONS
1. MT (M/77)	OD	HM (0.9)	Paracentral island	Laser	Methazolamide, 50 mg bid Epinephrine 2% bid Timolol 0.5% bid
	OS	20/60 (0.9)	Severe constriction	Laser	
2. WR (M/58)	OD	20/30 (0.9)	Severe constriction	Laser trabeculectomy	Acetazolamide, 250 mg qid Timolol 0.5% bid Propine bid Phospholine iodide 0.06% qd Pilocarpine 2% qid
	OS	HM (0.9)	5° field	Laser trabeculectomy, cyclocryotherapy	
3. NC (M/71)	OD	HM (0.9)	5° field	Laser trabeculectomy	Acetazolamide, 250 mg qid Timolol 0.5% bid Pilocarpine 2% qid Propine bid Phospholine iodide 0.06% qd
	OS	20/80 (0.9)	10° field	Laser trabeculectomy	
4. VD (F/60)	OD	LP (0.9)	Unable	Trabeculectomy Trabeculectomy, iridodencleisis	Acetazolamide, 250 md qid Timolol 0.5% bid Epinephrine 2% bid Pilocarpine 2% qid
	OS	HM (0.9)	Unable		
5. DF (M/50)	OD	20/60 (0.9)	10° field	Laser	Acetazolamide, 250 mg qid Timolol 0.5% bid Carbachol 0.75% bid
	OS	HM (0.9)	Unable	Laser	
6. BF (M/70)	OD	LP (0.9)	5° field	Laser	Methazolamide, 50 mg bid Carbachol 0.75% bid Timolol 0.5% bid Epinephrine 2% bid
	OS	LP (0.9)	5° field	Laser	
7. CC (F/52)	OD	HM (0.9)	Severe constriction	Trabeculectomy	Acetazolamide, 250 mg qid Epinephrine 2% bid Carbachol 0.75% bid Pilocarpine 2% qid
	OS	NLP (0.9)	Unable	Trabeculectomy	
8. MK (M/60)	OD	HM (0.9)	5° field	Trabeculectomy	Acetazolamide, 250 mg qid Epinephrine 2% bid Timolol 0.5% bid Pilocarpine 2% qid
	OS	HM (0.9)	5° field	Trabeculectomy	
9. RG (M/38)	OD	Enucleated	Enucleated	Trabeculectomy, enucleation	Acetazolamide, 250 mg qid Timolol 0.5% bid Propine bid Phospholine 0.06% qd Pilocarpine 2% qid
	OS	HM (0.9)	5° field	Trabeculectomy	

C/D, cup-disc ratio.

An initial decrease in IOP was observed in all subjects. The therapeutic goal of the investigator was achieved in four of nine subjects, and six of nine were considered “improved” during at least one visit during their treatment (Table II). Subject D.F. was improved at every visit for a 9-month period. Subject C.C. was described as “improved” during more than 50% of the follow-up visits during his 5-month treatment. Both of these subjects were improved at the time of termination from the study, when each subject underwent cataract surgery. All of the

other subjects appeared to have lost the beneficial effects of treatment on their IOP at the time of termination.

All subjects experienced toxic effects from oral THC during their treatment. Intolerable side effects forced four subjects to be terminated early from the study. These side effects and the corresponding dose of THC are summarized in Table III. No subject reported enjoying effects of THC related to the central nervous system. Subjects who did not tolerate THC were offered access to marijuana, but all of them declined.

TABLE II: INTRAOCULAR PRESSURES

PATIENT (DURATION TREATMENT)	INITIAL IOP* (GOAL IOP)	TREATMENT RANGE	CONSIDERED IMPROVED	MET GOAL
1. MT (14 wk)	19 (<12)	15-18	1 visit	No
2. WR (3 wk)	24 (<20)	20-24	Many visits	No
3. NC† (20 wk)	18-22 (<16)	14-17	2 visits	Yes†
4. VD (20 wk)	30-46 (<20)	28-40	Many visits	No
5. DF (36 wk)	19-25 (<16)	14-23	Every visit	No
6. BF (8 wk)	19-22 (<20)	15-20	3 visits	Yes
7. CC‡ (21 wk)	22-25 (<20)	16-20	More than 50% visits	Yes‡
8. MK (20 wk)	17-21 (<10)	15-16	Many visits	No
9. RG§ (28 wk)	20-24 (<15)	11-15	Many visits	Yes§

\*If IOP varied >2 mm Hg during three measurements, range given.

†Discontinued acetazolamide and propine during study.

‡Discontinued acetazolamide and carbachol during study.

§Possible increased compliance.

## DISCUSSION

The identification of brain, ocular, and peripheral cannabinoid receptors in several different mammals, the cloning of cannabinoid receptors, and the discovery of anandamide, an endogenous cannabimimetic eicosanoid, has greatly augmented the study of cannabinoid pharmacology in recent years.<sup>9-13</sup> Some of these pharmacologic investigations have attempted to develop new drugs useful for the treatment of the glaucomas.<sup>14-17</sup> However, thus far none of these efforts have included the use of cannabinoids in glaucoma patients with advanced disease. Therefore, it seemed timely to present this study, which represents the largest series of end-stage glaucoma patients treated with a cannabinoid derivative thus far completed. The data collected during this study are presented with the aim of providing direction and encouragement for further investigational efforts within this area of clinical and laboratory research.

Because this is a small, uncontrolled, unmasked, non-randomized, prospective study of short duration, it does not permit definitive conclusions about the efficacy of cannabinoids in the treatment of glaucoma. However, there is an impression from the data collected during this 2-year investigation that treatment with oral THC lowered IOP in some of this group of end-stage open-angle glaucoma patients. Following the initiation of THC treatment, all of the subjects demonstrated at least a transient improvement in the reduction of IOP (Table II). An

improvement was noted during more than 50% of the office visits in two of the nine enrolled subjects. In fact, one of the subjects was considered improved on all of the follow-up visits over a 36-week treatment period despite the fact that he never met the goal of treatment which the investigator considered ideal. The therapeutic goal of the investigator was achieved in four of nine subjects. Subjects N.C and C.C. each demonstrated an improved IOP control while using 5 mg of THC four times daily despite discontinuing coexistent carbonic anhydrase inhibitors and parasympathomimetics or sympathomimetics. Unfortunately, many of the subjects appeared to develop a tolerance to THC because their IOPs increased during the latter period of their treatment. Of course, as with any uncontrolled study, the observed improvements in IOP control may have been related to enhanced compliance associated with a subject's participation in the study or the added attention or encouragement given to the subject during the treatment period. This appeared to be the case with at least one subject (R.G.), in the opinion of the investigator, as indicated in Table II.

All subjects experienced side effects during their treatment with THC during this study (Table III). The most commonly described toxic effects were dry mouth, sleepiness, dizziness, depression, and confusion; these effects were the same as those reported by other investigators.<sup>18,19</sup> Although many of the side effects were considered mild and were of little concern to subjects, other effects were very significant. For example, the reason for

TABLE III: SIDE EFFECTS WITH THC TREATMENT

PATIENT (DURATION TREATMENT)		DOSAGE AND SIDE EFFECTS			REASON FOR TERMINATION
1. MT (14 wk)	5 mg qid: mod dizzy → mild sleepy mod light-headed mild confusion	5 mg qid: mild dizzy → mild sleepy	7.5 mg qid: mild dry mouth mod dizzy → mild sleepy	7.5 mg qid: mild dizzy	Lack efficacy
2. WR (3 wk)	2.5 mg qid: severe dizzy severe anxiety severe depression mod confused severe distortion of perception				Side effects
3. NC° (20 wk)	5 mg qid: mod dry mouth mod sleepy → mild dizzy mod sedation	5 mg qid: mild dry mouth mild sleepy weight increase			Side effects (weight increase)
4. VD (20 wk)	5 mg qid: mild dry mouth mild depression/elation → mod sleepy mild distortion of perception	15 mg qid: mod dry mouth mod dizzy mod confusion mod sleepy mod distortion of perception			Side effects
5. DF† (36 wk)	5 mg qid: mild dry mouth → mild dizzy	7.5 mg qid: mild dry mouth mod dizzy	15 mg qid: mild dry mouth mod dizzy	17.5 mg qid: mod dry mouth mild dizzy	Cataract surgery
6. BF (8 wk)	5 mg qid: mild anxiety mild sleepy mild light-headed mild elation	7.5 mg qid: severe dizzy mod anxiety mild dry mouth mild sedation mild depression mild confusion			Side effects
7. CC° (21 wk)	2.5 mg qid: mild anxiety mild elation mild dizzy mild light-headed mild dry mouth mild confusion (last 3 gone in several weeks)	5 mg qid: mod dry mouth mod dizzy mod light-headed (all gone in several weeks)			Cataract surgery
8. MK° (20 wk)	2.5 qid: mild dry mouth mild dizzy → mild depression mild sedation	2.5 qid: mild dry mouth mild dizzy			Change ophthalmologist
9. RG° (28 wk)	2.5 mg qid: mild dry mouth mild depression → mild sleepy	2.5 qid: mild dry mouth mild sleepy			Too tedious

°Possible tolerance to side effects.

†By 30th week, no side effect on 17.5 mg qid.

termination from the study for four of the nine subjects was intolerable side effects, such as distortion of perception, confusion, anxiety, depression, and severe dizziness. Changes in blood pressure have been reported with THC treatment.<sup>20,21</sup> Therefore, blood pressures were measured and the symptoms of systemic hypotension were carefully searched for at each visit. The dizziness and light-headedness reported by subjects in this study were never associated with systemic hypotension.

In most cases, the therapeutic benefit did not outweigh the toxicity associated with treatment as perceived by the subject. For example, one subject (N.C.) was unhappy because he gained weight while enrolled in the study. It was unclear whether his enhanced appetite was related to discontinuing acetazolamide or the concurrent use of THC. In any case, he was upset enough about this apparent effect that he withdrew from the study despite an improvement in IOP control and his ophthalmologist's opinion that he had met the goal of treatment. His termination from the study was considered to be due to intolerable side effects of THC.

Although the literature is unclear about the development of tolerance to the effects of cannabinoid administration, there was some evidence for tolerance in this study. There appeared to be a tendency for the beneficial effects on IOP to outlast the side effects in some patients, as demonstrated in Table III and as has been previously reported.<sup>22</sup> Unfortunately, there also appeared to be a tendency for tolerance to the beneficial IOP effects to develop in most of the subjects, as summarized in Table II.

A major limitation for applying the results of this study to present-day glaucoma therapy is that this study was completed in 1986, before many of the glaucoma medications currently in use were available. More specifically, prostaglandin derivatives, topically applied carbonic anhydrase inhibitors, and relatively  $\alpha_2$ -specific sympathomimetics were not commercially available during the 1980s. It is possible that if THC were added to the current therapeutic regimen of maximally tolerated therapy during the treatment of end-stage glaucoma, it would provide a less optimistic impression of its therapeutic usefulness.

Throughout the study, there was no observed tendency for either the physicians or the patients to abuse their access to cannabinoid derivatives. In fact, none of the subjects appeared to enjoy the psychotropic effects of THC. This is consistent with the observation made in previous studies that the environment, expectations, and reason for use of individuals during cannabinoid administration influence the overall personal experience and psychologic reaction to the effects of the cannabinoids following their administration.

Finally, it was clear that both the patients and

ophthalmologists greatly appreciated the opportunity to participate in this study. The program not only provided patients with legal and compassionate access to cannabinoid treatment as a last-resort treatment during the management of end-stage glaucoma unresponsive to conventional treatments, but it provided an opportunity for careful monitoring and extensive education of all of the patients interested in this potential treatment. Therefore, this opportunity greatly increased the safety for all of the patients who participated as subjects and even the patients who did not qualify for treatment because they were misinformed about the lack of proven value for the treatment or were ignorant of the potential dangers of taking cannabinoids in an attempt to lower IOP.

## CONCLUSIONS

---

This uncontrolled, unmasked, nonrandomized, prospective study does not permit definitive conclusions about the efficacy or toxicity of cannabinoids in the treatment of glaucoma. There is an impression from this study that treatment with oral THC lowered IOP in this group of patients with end-stage open-angle glaucoma, but the development of tolerance and the coexistence of significant systemic toxicity limited the potential usefulness of this treatment. It was particularly impressive to the investigators that throughout the study there was no observed tendency for either the physicians or the patients to abuse their access to cannabinoid derivatives. Furthermore, both the patients and ophthalmologists greatly appreciated the opportunity to participate in a study that gave them legal access to cannabinoids as a last-resort treatment for end-stage glaucoma unresponsive to conventional treatments.

## REFERENCES

---

1. Turner CE, Elsohly MA, Boeren EG. Constituents of *Cannabis sativa*: a review of the natural constituents. *J Nat Prod* 1980;43:169-234.
2. Hepler RS, Frank IM. Marijuana smoking and intraocular pressure. *J Am Med Assoc* 1971;217:1392.
3. Hepler RS, Frank IM, Ungerleider JT. Pupillary constriction after marijuana smoking. *Am J Ophthalmol* 1972;74:1185-1190.
4. Drew WG, Miller LL. Cannabis: neural mechanisms and behavior—a theoretical review. *Pharmacology* 1974;11:12-32.
5. Benowitz NL, Rosenberg J, Rogers W, et al. Cardiovascular effects of intravenous delta-9-tetrahydrocannabinol: autonomic nervous mechanisms. *Clin Pharmacol Ther* 1979;25:440-446.
6. Hollister LE. Structure-activity relationships in man of cannabis constituents and homologs and metabolites of delta-9-tetrahydrocannabinol. *Pharmacology* 1974;11:3-11.

7. Lockhart AB, West ME, Lowe HIC. The potential use of *Cannabis sativa* in ophthalmology. *West Indies Med J* 1977;26:66-70.
8. Flach AJ, Holsten DW, Icaza L, et al. Cannabis protocol for glaucoma: oral THC and smoked marijuana for treating open angle glaucoma patients. For Research Advisory Panel of California, 1984.
9. Devane WA, Dysarz FA, Johnson MR. Determination and characterization of a cannabinoid receptor in the rat brain. *Mol Pharmacol* 1988;34:605-613.
10. Munro S, Thomas KL, Abu Shaar M. Molecular characterization of a peripheral receptor for cannabinoids. *Nature* 1993;365:61-65.
11. Straiker AJ, Maguire G, Mackie K, et al. Localization of cannabinoid Cb1 receptors in the human anterior eye and retina. *Invest Ophthalmol Vis Sci* 1999;40:2442-2448.
12. Matsuda LA, Lolait SJ, Brownstein MJ, et al. Structure of a cannabinoid receptor and functional expression of the cloned DNA. *Nature* 1990;346:561-564.
13. Devane WA, Hanus L, Brever A, et al. Isolation and structure of a brain constituent that binds to the cannabinoid receptor. *Science* 1992;258:1946-1949.
14. Laine K, Jarvinen K, Pate DW, et al. Effect of the enzyme inhibitor, phenylmethylsulfonyl fluoride, on the IOP profiles of topical anandamides. *Invest Ophthalmol Vis Sci* 2002;43:393-397.
15. Buchwald A, Browne CE, Wu WM, et al. Soft cannabinoid analogues as potential anti-glaucoma agents. *Pharmazie* 2000;55:196-201.
16. Pate DW, Jarvinen K, Urtti A, et al. Ophthalmic arachidonylethanolamide decreases intraocular pressure in normotensive rabbits. *Curr Eye Res* 1995;14:779-797.
17. Beilin M, Neumann R, Belkin M, et al. Pharmacology of the intraocular pressure lowering effect of systemic dexanabinol (HU-211), a non-psychotropic cannabinoid. *J Ocular Pharm Ther* 2000;16:217-230.
18. Hollister LE, Gillespie HK. Delta-8- and delta-9-tetrahydrocannabinol. *Clin Pharmacol Ther* 1972;14:353-357.
19. Valk LEM. Hemp in connection with ophthalmology. *Ophthalmologica* 1973;167:413-421.
20. Merritt JC, Crawford WJ, Alexander PC, et al. Effect of marijuana on intraocular and blood pressure in glaucoma. *Ophthalmology* 1980;87:222-228.
21. Crawford WJ, Merritt JC. Effect of tetrahydrocannabinol on arterial and intraocular hypertension. *Int J Clin Pharm Biopharm* 1979;17:191-196.
22. Purnell WD, Gregg JM. Delta-9-tetrahydrocannabinol, euphoria and intraocular pressure in man. *Ann Ophthalmol* 1975;7:921-922.

## DISCUSSION

DR DOUGLAS R. ANDERSON. Thanks to Dr Flach for this lucid and straightforward report. To summarize the main conclusions, the author expressed surprise that fewer subjects enrolled than had been expected, despite well-known and continued public interest in use of

cannabinoids for medical purposes, including glaucoma. Perhaps a good part of the public fascination is in possible use this drug in ordinary cases of glaucoma as an alternative to already available therapy. The types of cases recruited for this study were severe cases not adequately controlled with any other treatment options, and in these cases THC was inadequately effective or impractical because of side effects.

It is, however, known that THC will lower the IOP, and that there are receptors in both the trabecular meshwork and the ciliary body. A few decades ago, I had a young patient who knew I could not prescribe marijuana for him. Having recently opened a business, he had some projects to get under control before he could proceed with the surgery I had recommended, and he asked me to monitor his IOP frequently while waiting. The readings were variable, and he revealed that on some days, at various intervals before the measurements, he had smoked marijuana. He had kept a diary of times and pressures, and also noted the quality of the particular marijuana he had smoked on each occasion, judged from the mental effects he enjoyed. From this he worked out a nice dose-response curve and the duration of the effect on IOP. I no longer remember the details, except that the effect was not long-lived and did not persist beyond the time he felt "high." The net result was that he could not focus on his work and simultaneously keep his IOP at the desired pressure level. Therefore he did undergo surgery, which worked well for him for the next several years during which he remained under my care.

At least for some patients, then, the side effects and short duration of action may simply outweigh the advantages compared to standard therapeutic options available. When patients ask about marijuana, that is exactly how I explain the situation—that THC may work to lower the IOP, but perhaps not more effectively than other available drugs, which have been better tested scientifically, have longer duration of action, and also have fewer side effects.

Do cannabinoids have a place at all? Dr Paul Palmberg has one patient under his care with glaucoma from childhood who has had all known medications, some not tolerated, and others not fully effective. The patient has had several operations, the most recent with the complication of a postoperative suprachoroidal hemorrhage, so further surgery has been avoided. The IOP can be brought from 50 mm Hg to 25 mm Hg with either timolol or marijuana, but in combination to 15 mm Hg. The patient has used marijuana in this manner for a couple of decades now. Newer alpha-adrenergic agents and prostaglandin analogues have not been satisfactory substitutes. Because of the short duration of action, this treatment requires 10 NIDA-provided marijuana cigarettes per day and is thus not so convenient, but for this patient

it is the best alternative.

Based on the experience of this patient and of others reported to him, Dr Palmberg believes marijuana can be very effective when the IOP is quite high, but seems minimally effective in patients with modestly elevated or normal IOP. He also commented that with continual use, the lowering of blood pressure and the mental effects disappear, but the favorable effects on IOP persist, so some of the problems noted in acute or short-term studies may have underestimated the potential for this class of drugs.

Dr Palmberg participated in a NIDA-workshop co-sponsored by NIH (Feb 1997) at which various potential medicinal uses of marijuana were discussed. Dr Paul Kaufman reviewed the then available studies with respect to glaucoma for the workshop, and most information dealt with acute or short-term experiments. The report of this workshop may provide those interested with a compendium of background information suggesting a potential not yet proved or developed.

Presumably, physicians can legally prescribe dronabinol (Marinol) for glaucoma as an off-label use, although prior clearance from appropriate authorities might be wise. Within the past week a well-known entertainer was arrested at an airport checkpoint for possession of marijuana, which, it was claimed, was being used to treat glaucoma. There may thus be some unanalyzed experience with cannabinoids, although even if collected, scattered anecdotal information will not substitute for further properly designed studies of long-term clinical use such as the one conducted by Dr Flach. Continued interest in the class of compounds may be warranted if longer-acting forms can be developed, and if the undesirable effects are documented to disappear after several days so that patients can work effectively and drive safely. Of particular pharmacologic interest is that cannabinoids lower IOP through mechanisms independent of those of drugs currently on the market. The implication is that cannabinoids may work when other classes of drugs don't, and that it could be additive to other drugs.

DR GEORGE L. SPAETH. I obtained tetrahydrocannabinol in 1970 and manipulated it into a form that could be used as eye drops. Masking was attempted, using one eye as control, but the eyes on the tetrahydrocannabinol turned beet red. There was no effect on IOP when we compared the treated and untreated eyes. How does this drug work to lower pressure? Is it possible to develop some type of topical product that might limit the problem of the systemic side effects?

DR LOUIS B. CANTOR. Is there any understanding of the pharmacology, and do receptors for the cannabinoids exist? Since this drug appears to lower IOP, do we know

anything about the mechanism? Is the mechanism similar to that of our other fatty acid lipid compounds that improve pressure-sensitive or pressure-insensitive out-flow pathways?

DR ALLAN J. FLACH. Dr Anderson mentioned the fascination that has existed concerning this group of drugs. This interest has been present for over 3,000 years, as recorded by one of the first clinical pharmacologists, Emperor Shen-Nung in 2737 BC. During the late 1800s, the Indian Hemp Commission Report described cannabis as the most important drug in the Indian Materia Medica. During the 20th century, tincture of cannabis was included in the 1937 United States Pharmacopoeia and, in later years, in the United States National Formulary. The preparation was considered useful as an anti-inflammatory and analgesic agent for the relief of migraine headaches and prevention of seizures. In addition, it was used to treat psychiatric illness, including depression.<sup>1</sup> In subsequent years, it was replaced with therapies that were considered less toxic and more specific in their activity.

As Dr Anderson mentioned, we might have seen greater effects on IOP following cannabinoid treatment if we included patients with a condition other than end-stage glaucoma. I believe this is probably true. However, if one properly informs glaucoma patients about the proven benefits of conventional glaucoma therapy and contrasts this with the unproven potential benefits following marijuana derivatives, one cannot avoid endorsing the commercial agents much more enthusiastically. This is particularly true since all of the available cannabinoid derivatives have significant psychotropic effects. While these effects follow dose-response relationships that include drowsiness or feeling comfortably high, which can progress to depersonalization or even a panic reaction, external stimuli can abruptly shift the apparent dose-response curve so that the patient, while experiencing a happy high, can rapidly progress into a panic reaction without additional cannabinoid treatment. This is called endogenous potentiation.<sup>2</sup>

I agree with Dr Anderson that there is good evidence that the cannabinoids are capable of lowering IOP. This was initially described by Dr Robert Hepler during the 1970s.<sup>3</sup> I have included information about US government's grown marijuana that was available for patients in this study within the text of this paper. None of the enrolled subjects wanted to use inhaled marijuana because they did not like the idea of smoking with the associated pulmonary irritation and potential risk of lung cancer.

It is interesting to me that Dr Spaeth observed excessive toxicity and a lack of therapeutic effect in his attempts to use a topical form of marijuana in glaucoma

patients. I suspect Dr Spaeth's efforts were based in part on the initial reports by Dr John Merritt, who described topically applied marijuana in experimental animals. However, Dr Merritt was unable to duplicate these potentially beneficial effects on the IOP of humans.<sup>4</sup> Therefore, Dr Spaeth's observations are not too surprising. For the past 25 years, I have had the privilege of providing a 4-day ocular pharmacology and toxicology course at Stanford University during the summer months as part of a Basic Science Course for ophthalmologists. Each year, I have included a section on the cannabinoids and their potential use within ophthalmology. One of the graduates of this course who practices in Jamaica sent me a package insert for a commercially available *Cannabis sativa* solution marketed under the name of Canasol. This topically applied liquid is described as capable of lowering IOP as effectively as timolol without the side effects. However, there are no published studies that verify this ability.

I am certain that we are all as interested as Dr Cantor in the pharmacodynamics of cannabinoids. Dr Keith Green deserves a lot of credit for the time he has devoted to this study. His research describes many different potential mechanisms by which the cannabinoids can

lower IOP.<sup>5</sup> However, I think that we need Dr Richard Brubaker, or someone with his experience studying human aqueous inflow and outflow, to conscientiously work out these effects. In conclusion, as I mentioned within the introduction to this paper, cannabinoid receptors have been identified within the human eye, but it remains to be elucidated how these receptors might be beneficially manipulated by exogenously applied or endogenously liberated cannabinoids or other lipid compounds and the mechanism underlying these activities.

1. Pars HG. The other side of marijuana research. *J Anesthesiol* 1973;38:519-520.
2. Valk LEM. Hemp in connection with ophthalmology. *Ophthalmologica* 1973;167:413-421.
3. Hepler RS, Petrus RH. Experiences with administration of marihuana to glaucoma patients. In Cohen S, Stillman RC, eds. *The Therapeutic Potential of Marihuana*, New York: Plenum 1976:63.
4. Merritt JC, Perry KDD, Russell DN, et al. Topical delta 9-tetrahydrocannabinol and aqueous dynamics in glaucoma. *J Clin Pharmacol* 1981;21:467S-471S.
5. Green K. Marijuana and the eye: a review. *J Toxicol. Cutan Ocul Toxicol* 1982;1:3-32.

## DIAGNOSTIC TRANSVITREAL FINE-NEEDLE ASPIRATION BIOPSY OF SMALL MELANOCYTIC CHOROIDAL TUMORS IN NEVUS VERSUS MELANOMA CATEGORY

---

BY James J. Augsburger, MD, Zélia M. Corrêa, MD (BY INVITATION), Susan Schneider, MD (BY INVITATION), Rawia S. Yassin, MD (BY INVITATION), Toni Robinson-Smith, MD (BY INVITATION), Hormoz Ehya, MD (BY INVITATION), AND Nikolaos Trichopoulos, MD (BY INVITATION)

### ABSTRACT

*Purpose:* To report an experience with fine-needle aspiration biopsy of selected small melanocytic choroidal tumors during the interval from April 13, 1983, through January 19, 2001.

*Methods:* Retrospective descriptive case series report of 34 patients with a small melanocytic choroidal tumor (maximal diameter,  $\leq 10$  mm; thickness,  $\geq 1.5$  mm but  $\leq 3$  mm) evaluated diagnostically by transvitreal fine-needle aspiration biopsy prior to treatment. None of the tumors had invasive features at the time of biopsy.

*Results:* Patients ranged in age from 26 to 73 years (mean, 50.9 years). The evaluated choroidal tumors had a mean maximal basal diameter of 8.0 mm and a mean maximal thickness of 2.4 mm. Eighteen of the 34 tumors (52.9%) had been documented to enlarge prior to biopsy. Biopsy was performed in all cases using a 25-gauge hollow lumen needle and a transvitreal approach via a pars plana puncture site. The biopsy yielded a sufficient aspirate for cytodiagnosis in 22 of 34 cases (64.7%). In these cases, the tumor was classified as malignant melanoma in 16 (47.1% of total), intermediate lesion in 4 (11.8%), and benign nevus in 2 (5.9%). The 12 tumors that yielded an insufficient aspirate and the four lesions that yielded intermediate cells continued to be classified as "nevus versus melanoma" and were monitored periodically for growth or other changes. Four of the 12 tumors that yielded an insufficient aspirate for cytodiagnosis and all four lesions that yielded intermediate cells were eventually reclassified as small choroidal melanomas and treated. The remaining eight tumors that yielded an insufficient aspirate and the two tumors that yielded benign nevus cells were classified as benign nevi at the most recent follow-up evaluation.

*Conclusions:* Fine-needle aspiration biopsy showed that a substantial proportion of small melanocytic choroidal tumors likely to be classified clinically as small choroidal melanomas in many centers were in fact benign nevi or intermediate lesions.

*Trans Am Ophthalmol Soc* 2002;100:225-234

### INTRODUCTION

---

Several years ago, I (J.J.A.) spoke to the American Ophthalmological Society about whether observation is really appropriate management for suspected small choroidal melanomas.<sup>1</sup> In that presentation, I indicated that there were significant potential benefits as well as significant potential risks of observing versus promptly treat-

ing such tumors. I concluded that "observation as management for patients with such tumors . . . appears to be an acceptable management approach for the time being in the absence of convincing evidence to the contrary." I went on to indicate that the prospects for resolving the question of the preferred management of a small suspected choroidal melanoma appeared bleak.

Today I would like to present evidence I have accumulated regarding the role of transvitreal fine-needle aspiration biopsy for differential diagnosis of small suspected choroidal melanomas in the nevus versus melanoma category. On the basis of my experience, I believe that diagnostic transvitreal fine-needle aspiration biopsy has an important role in distinguishing between small suspected choroidal melanomas that need to be treated promptly and those that can and probably should be managed by observation, at least initially.

For the purposes of this study, a small melanocytic

From the Department of Ophthalmology (Dr Augsburger, Dr Schneider, and Dr Trichopoulos) and the Department of Pathology and Laboratory Medicine (Dr Schneider, Dr Yassin, and Dr Robinson-Smith), University of Cincinnati College of Medicine, Cincinnati, Ohio; Santa Casa, Porto Alegre, Rio do Sol, Brasil (Dr Corrêa); and the Department of Pathology, Fox Chase Cancer Center, Philadelphia, Pennsylvania (Dr Ehya). Supported in part by an unrestricted departmental challenge grant from Research to Prevent Blindness, Inc, New York, New York, to the Department of Ophthalmology, University of Cincinnati College of Medicine.

choroidal tumor was defined as a choroidal tumor classified as probably melanocytic on the basis of its ophthalmoscopic appearance and measuring  $\leq 10$  mm in maximal basal diameter and  $\leq 3$  mm in maximal thickness, as determined by ophthalmoscopic fundus mapping and B/A-scan ultrasonography. A small melanocytic choroidal tumor was subclassified as a "nevus versus melanoma" if it did not exhibit clearly invasive clinical features such as focal nodular eruption through Bruch's membrane, retinal invasion, scleral invasion (by B-scan ultrasonography), and transcleral tumor extension (by B-scan ultrasonography). Any small melanocytic choroidal tumor that exhibited one or more of these invasive features was categorized as an unequivocal small melanoma and not a nevus versus melanoma. Similarly, a suspected melanocytic choroidal tumor that was larger than 10 mm in diameter, larger than 3 mm in thickness, or both, but exhibited no clearly invasive clinical features was subcategorized as an atypical probable melanoma and not a nevus versus melanoma. Unequivocal small choroidal melanomas and atypical probable choroidal melanomas were not evaluated in this study.

The purposes of this study were (1) to summarize the cytopathologic findings in a series of patients who underwent transvitreal fine-needle aspiration biopsy of a small melanocytic choroidal tumor in the nevus versus melanoma category and (2) to evaluate the accuracy of cytopathologic diagnosis in these cases using final diagnosis through available follow-up as our standard.

## METHODS

### PATIENTS

With the aid of my coauthors, I have developed and currently maintain a computerized database of all fine-needle aspiration biopsies performed by me personally since my initial case in 1981. As of January 31, 2001, this database contained 385 patients. Some of the early cases in this database have been reported.<sup>2-7</sup> Using a computerized records search, my coauthors and I identified 34 patients on whom a diagnostic fine-needle aspiration biopsy was performed to evaluate a small melanocytic choroidal tumor in the nevus versus melanoma category. To be categorized as a nevus versus melanoma, the tumor had to appear at least partially melanotic, measure  $\leq 10$  mm in maximal basal diameter, measure  $\geq 1.5$  mm but  $\leq 3.0$  mm in thickness, and exhibit no invasive ophthalmoscopic features (retinal invasion, optic disc invasion, eruption of the tumor through Bruch's membrane) or ultrasonographic features (scleral invasion, transcleral tumor extension). Presence or absence of overlying or surrounding serous subretinal fluid, surface clumps of orange pigment (lipofuscin), and documented lesion enlargement were

recorded in each case but were not used as classification factors in this study. The first of these biopsies was performed April 13, 1983, and the last was performed January 19, 2001. Table I contains data on demographic and ophthalmic variables in the 34 patients.

### CLINICAL DIAGNOSTIC METHODS

All patients in the database underwent comprehensive baseline prebiopsy ophthalmic evaluation by me personally. Components of the evaluation included assessment of best corrected visual acuity in each eye, evaluation of the external appearance of each eye in diffuse light, evaluation of the anterior segment features of each eye by slit-lamp biomicroscopy, measurement of the intraocular pressure in each eye by applanation tonometry, evaluation of the fundus features of each eye by non-contact lens fundus biomicroscopy and indirect ophthalmoscopy, preparation of a detailed fundus drawing of the affected eye, and performance of B/A-scan ultrasonography of the affected eye. The appearance of each lesion was documented by color fundus photography. Fluorescein angiography or indocyanine green angiography was performed in some cases but was not obtained routinely in all cases.

### INFORMED CONSENT

All patients in this series were advised completely about my clinical findings and differential diagnosis, the implications of the tumor for sight in the affected eye and survival, and the recognized potential benefits versus potential risks of available treatment options ranging from observation as management<sup>1</sup> to enucleation of the affected eye. Patients who underwent fine-needle aspiration biopsy during the first few years of the study were required to sign an investigational informed consent document that had been reviewed and approved by the institutional review board (IRB) of Wills Eye Hospital, Baltimore, Maryland. The same IRB reviewed the results obtained over the first 3 years and approved the procedure as a standard diagnostic method by the senior author in 1985. Since that time, patients have only had to review and sign a standard informed consent document for diagnostic or therapeutic procedure.

### BIOPSY TECHNIQUE

The biopsy in every case was performed in the operating room as an outpatient surgical procedure with the patient under local anesthesia (retrobulbar injection of carbocaine or xylocaine). In every patient, the biopsy was performed by means of an eye-wall puncture in the pars plana region using a 25-gauge sharp hollow-lumen biopsy needle. The meridional location of the eye-wall puncture site was selected on the basis of the intraocular tumor location. The site was prepared by making a partial-thick-

TABLE I: BASELINE PREBIOPSY FEATURES OF 34 PATIENTS AND THEIR TUMORS

CASE NO.	AGE (YR)	SEX	AFFECTED EYE	BEST CORRECTED DISTANCE VISUAL ACUITY IN AFFECTED EYE (SNELLEN)	SIZE OF TUMOR			LOCATION OF POSTERIOR TUMOR MARGIN	
					MAXIMAL BASAL DIAMETER (MM)	MINIMAL BASAL DIAMETER (MM)	THICKNESS (MM)	LOCATION RELATIVE TO FOVEA	LOCATION RELATIVE TO OPTIC DISC
1	33	F	R	20/30	7.5	7.0	1.9	subfoveal	≤3 mm from disc
2	57	F	L	20/15	8.5	7.5	2.5	>3 mm from fovea	>3 mm from disc
3	37	F	R	20/20	6.0	5.5	1.9	subfoveal	to disc margin
4	64	M	L	HM	8.0	6.0	2.0	≤3 mm from fovea	>3 mm from disc
5	27	F	R	CF	5.5	5.5	3.0	subfoveal	to disc margin
6	39	F	R	CF	7.0	5.5	2.2	subfoveal	to disc margin
7	26	F	L	20/40	8.5	7.0	2.9	≤3 mm from fovea	to disc margin
8	33	F	R	20/20	8.0	6.5	2.2	>3 mm from fovea	≤3 mm from disc
9	41	F	R	20/50	9.5	7.0	1.7	>3 mm from fovea	>3 mm from disc
10	30	M	L	20/40	5.5	5.0	2.9	≤3 mm from fovea	≤3 mm from disc
11	73	M	L	20/15	10.0	10.0	2.9	≤3 mm from fovea	>3 mm from disc
12	68	F	L	20/30	9.0	5.5	2.8	>3 mm from fovea	>3 mm from disc
13	60	M	L	20/25	8.5	4.5	2.0	>3 mm from fovea	>3 mm from disc
14	62	F	R	20/20	6.5	6.5	2.9	≤3 mm from fovea	to disc margin
15	40	M	L	20/15	7.0	5.5	2.4	>3 mm from fovea	>3 mm from disc
16	67	M	R	20/20	8.5	6.5	2.4	>3 mm from fovea	>3 mm from disc
17	44	M	R	20/15	9.5	8.5	2.7	>3 mm from fovea	>3 mm from disc
18	62	F	L	20/25	9.0	9.0	2.2	≤3 mm from fovea	>3 mm from disc
19	54	F	L	20/15	7.0	5.0	2.0	≤3 mm from fovea	>3 mm from disc
20	45	F	R	20/20	7.5	6.5	2.7	≤3 mm from fovea	>3 mm from disc
21	55	F	L	CF	8.5	8.5	2.2	subfoveal	to disc margin
22	38	F	R	20/20	8.5	7.5	2.9	>3 mm from fovea	>3 mm from disc
23	64	M	R	20/20	9.0	9.0	2.4	subfoveal	≤3 mm from disc
24	73	M	L	20/40	7.0	5.0	2.4	≤3 mm from fovea	>3 mm from disc
25	54	F	R	20/20	8.0	8.0	2.2	≤3 mm from fovea	≤3 mm from disc
26	29	F	L	CF	9.0	7.5	2.7	subfoveal	≤3 mm from disc
27	42	M	R	20/20	8.5	5.5	1.7	>3 mm from fovea	>3 mm from disc
28	64	M	L	20/100	7.0	6.0	2.2	≤3 mm from fovea	≤3 mm from disc
29	60	F	R	20/40	10.0	5.0	2.2	subfoveal	≤3 mm from disc
30	53	F	R	20/15	8.5	8.0	2.7	>3 mm from fovea	>3 mm from disc
31	46	M	L	20/20	9.0	8.0	3.0	≤3 mm from fovea	>3 mm from disc
32	57	F	L	20/50	7.5	4.5	1.7	subfoveal	≤3 mm from disc
33	59	M	L	20/60	8.0	5.0	1.7	subfoveal	to disc margin
34	60	F	R	20/15	8.5	8.0	2.4	≤3 mm from fovea	to disc margin

ness scleral incision parallel to the limbus in the selected meridian at a measured 3.5 mm from the limbus. This partial-thickness scleral incision was generally 0.5 to 1.0 mm in length. In every case, the needle was bent with a hemostat just above the end of the bevel. The angle of the bend was determined by the intraocular location of the tumor. The hub of the needle was attached via a 12- to 18-inch-long segment of sterile plastic tubing to a 10-mL aspirating syringe. Before the eye wall was punctured with the biopsy needle, the globe was fixed in appropriate position using two or more traction sutures of 4-0 black silk passed behind the insertions of selected rectus muscles. After the eye wall was punctured with the tip of the needle, the position of the needle was monitored during its passage through the vitreous and retina into the substance

of the choroidal tumor using indirect ophthalmoscopy. Once the tip of the needle was in the tumor, aspiration was performed by the surgical assistant. The tip of the needle was moved slightly in and out along its path, and aspiration was repeated after each slight repositioning. In most cases, at least 10 aspirations were performed. All suction was released, and the needle was quickly withdrawn from the eye. Light digital pressure was maintained for about 60 seconds on the puncture site to provide hemostasis.

The aspirate within the needle was submitted to our cytopathologists for analysis. In most cases, a second needle was used to sample a different portion of the tumor. In some cases, a third needle was used to sample yet another site within the tumor. The determining factors regarding

a second or third needle pass were the amount of bleeding encountered and the ability to safely visualize the tumor.

#### **PATHOLOGIC PROCESSING OF ASPIRATES**

Several different processing methods have been used by the various cytopathologists involved in this series over the years. From 1981 through 1999, all aspirates were suspended in approximately 1 to 2 mL of balanced salt solution and delivered in suspension to the cytopathologist. Until 1991, the fluid specimen was divided into two unequal portions (about 67% and 33%). The larger portion was processed by membrane filtration and stained by a modified Papanicolaou method for cytomorphologic evaluation. The smaller aliquot was processed by the cytospin method and used for histochemical (Fontana-Masson) and immunocytochemical stains when indicated.<sup>8</sup> From 1991 through 1999, the fluid specimen was processed entirely by the cytospin method. From 1999 through the present, a cytopathologist has attended the surgery, prepared at least two direct smears from each aspirate (one air-dried, the other alcohol-fixed) in the operating room, and processed the remainder of the specimens by membrane filter technique or cytospin after return to the cytopathology laboratory. The air-dried direct smears were processed by the Dif-Quik method, while the alcohol-fixed smears were stained with the Papanicolaou stain. The reserve portion of the specimen used immunocytochemical stains, including HMB-45, Melan-A, and S-100.

#### **CYTOPATHOLOGIC DIAGNOSIS**

Stained slides were interpreted with use of conventional cytomorphological criteria for distinguishing benign from malignant cells. Histochemically or immunocytochemically stained slides were reviewed to refine the diagnosis in difficult cases.

#### **REVISED DIAGNOSIS AFTER BIOPSY**

Following fine-needle aspiration biopsy, the working diagnosis was revised to reflect the cytopathologic findings in the cases with a sufficient specimen for cytodiagnosis but remained nevus versus melanoma in the cases with an insufficient aspirate for cytodiagnosis.

#### **POSTBIOPSY TUMOR MANAGEMENT**

Management of the tumor following biopsy was directed by the cytopathologic findings. In cases with a revised diagnosis of choroidal melanoma, prompt treatment of the tumor was routinely recommended. In cases with a cytopathologic diagnosis of benign choroidal nevus, observation as management was recommended after the biopsy. In cases with an insufficient specimen for cytodiagnosis or intermediate melanocytic cells (ie, borderline between

nevus and melanoma), the patient was advised of the non-diagnostic result and then managed as if the biopsy had not been performed. In some of these cases, the tumor was managed by observation, and in others the tumor was treated by a locally destructive therapy (usually plaque radiotherapy).

#### **FOLLOW-UP AND FINAL DIAGNOSIS**

The final diagnosis in each case was regarded as the diagnosis assigned the tumor on the basis of all information accumulated during available follow-up. In cases managed by enucleation following the biopsy, the final diagnosis was the histopathologic diagnosis assigned to the tumor on the official pathology report. In all other cases, the final diagnosis was determined by the clinical course. Tumors treated by a locally destructive treatment were considered to be genuine malignant melanomas. Tumors managed by observation were given a final diagnosis of choroidal melanoma if the tumor eventually exhibited invasive clinical features or substantial enlargement. In contrast, tumors managed by observation were given a final diagnosis of choroidal nevus if the tumor exhibited minimal or no subsequent enlargement and no invasive features during available follow-up.

## **RESULTS**

---

#### **PATIENTS**

The 34 study patients ranged in age from 26.5 to 73.1 years (mean, 50.9 years) (Table I). Thirteen patients were male (38.2%) and 21 were female (61.8%). The right eye was affected in 18 patients (52.9%) and the left eye in 16 (47.1%). Twenty of the 34 patients (58.8%) had visual symptoms attributable to the tumor, and 14 (41.2%) were visually asymptomatic. Visual acuity in the affected eye at the prebiopsy examination was  $\geq 20/25$  in 19 (55.9%),  $< 20/25$  but  $\geq 20/40$  in 6 (17.6%),  $< 20/40$  but  $\geq 20/200$  in 4 (11.8%), and  $< 20/200$  in 5 (14.7%).

#### **TUMORS**

The anterior margin of the tumor was at or posterior to the ocular equator in 32 of the 34 cases (94.1%) (Table I). The posterior margin of the tumor extended to the optic disc margin in 8 cases (23.5%), was within 2 disc diameters of the optic disc in 9 (26.5%), and was over 2 disc diameters from the optic disc in 17 (50.0%). It extended to or beneath the fovea in 10 eyes (29.4%), was within 2 disc diameters from the fovea in 13 (38.2%), and was over 2 disc diameters from the fovea in 11 (32.4%). The maximal basal diameter of the tumor ranged from 5.5 mm to 10.0 mm (mean, 8.0 mm), and the maximal tumor thickness ranged from 1.7 mm to 3.0 mm (mean, 2.4 mm).

#### **ASSOCIATED FEATURES**

A limited shallow serous retinal detachment was present overlying and surrounding the tumor in 13 (38.2%) of the 34 eyes, but the retina was fully attached in 21 eyes (61.8%). Prominent clumps of orange pigment were present on the surface of the tumor in 9 cases (26.5%) but were absent in 25 cases (73.5%). Eighteen of the 34 tumors (52.9%) had been documented to enlarge at least slightly following initial detection but prior to transvitreal biopsy.

#### **ADEQUACY OF ASPIRATES**

Transvitreal fine-needle aspiration biopsy yielded a sufficient aspirate for cytodiagnosis (Table II) in 22 of the 34 cases (64.7%). In the other 12 cases (35.3%), the aspirate was graded as insufficient for cytodiagnosis. Rebiopsy of the tumor was performed in two cases that yielded an insufficient specimen for cytodiagnosis initially (cases 14 and 21). In case 14, rebiopsy of the slightly enlarged tumor 42 months after the initial biopsy again produced an insufficient specimen for cytodiagnosis. We continue to regard this tumor as a benign choroidal nevus. In case 21, rebiopsy of the slightly enlarged tumor 10 months after the initial nondiagnostic biopsy yielded cells consistent with malignant melanoma of spindle-cell type. This tumor was treated by an eye-preserving therapy immediately following the second biopsy.

#### **CYTODIAGNOSIS**

Among the 22 cases with a sufficient aspirate (Table II), the cytologic diagnosis was malignant cells consistent with melanoma in 16 cases (72.7%), benign cells consistent with choroidal nevus in 2 (9.1%), and intermediate cells consistent with either atypical nevus or low-grade melanoma in 4 (18.2%). The mean thickness of the tumor in the 12 cases with an insufficient specimen for cytodiagnosis was 2.27 mm, while that for the 22 cases with an adequate specimen was 2.43 mm. This difference was not statistically significant (independent groups *t* test, *P* = .33).

#### **POSTBIOPSY TUMOR DIAGNOSIS**

Our working diagnosis following fine-needle aspiration biopsy (Table II) changed from nevus versus melanoma to choroidal melanoma in 17 of the 34 cases (50%) and to benign choroidal nevus in 2 (5.9%). Our working diagnosis remained nevus versus melanoma in 15 cases (44.1%). Among these 15 cases, the reason that the biopsy did not result in a changed working diagnosis was insufficient aspirate for cytodiagnosis in 12 cases (35.3% of the total) and identification of intermediate cells (ie, borderline between nevus and melanoma by cytologic criteria) in 3 (8.8% of the total).

#### **CYTOLOGIC-HISTOLOGIC CORRELATION**

The affected eye was enucleated in only 4 of the 34 cases in this series (cases 1, 3, 5, and 7). In case 2, enucleation was performed after a period of observation following an inconclusive biopsy. During observation, the tumor enlarged and also showed new invasive features. In the other three cases, enucleation was performed primarily following the fine-needle aspiration biopsy. In all four cases, the tumor proved to be a malignant melanoma by histopathologic criteria. It was classified as a spindle-cell melanoma in cases 1, 3, and 7 and as an epithelioid melanoma in case 5. Histopathologic study identified the same melanoma cell type as did cytopathologic study of the needle aspirates in cases 1, 3, and 5. No melanoma cell type was specified by the cytopathologist who evaluated case 7, so accuracy of cell type identification in this case cannot be determined.

#### **FOLLOW-UP AND FINAL DIAGNOSIS**

Follow-up after fine-needle aspiration biopsy in the 34 cases (Table III) ranged from just over 1 month (case 5) to 13.7 years (case 1). The mean follow-up interval was 4.2 years, and the median follow-up interval was 2.6 years. Our final diagnosis at last available follow-up examination (Table III) was choroidal melanoma in 24 cases (70.6%) and choroidal nevus in 10 cases (29.4%). The final diagnosis in the 16 cases categorized as choroidal melanoma following the biopsy remained melanoma in all 16. Similarly, the final diagnosis in the two cases categorized as benign nevus following the biopsy remained choroidal nevus in both. The final diagnosis in the four cases categorized as intermediate lesion following the biopsy was choroidal melanoma in all four. Our final diagnosis in the 12 cases that yielded an insufficient aspirate for cytodiagnosis was benign nevus in eight and malignant melanoma in four.

None of the patients in this series developed metastatic disease or died during available follow-up. No patient in the series developed any evidence of implantation tumor seeding along the needle tract in the pars plana.

#### **DISCUSSION**

If the results of this study are representative, between one fourth and one third of small melanocytic choroidal tumors in the nevus versus melanoma category (as defined in the "Methods" section) are really benign nevi and not malignant melanomas. This information is important, because tumors of this type are currently regarded by many ophthalmic tumor specialists as unequivocal small choroidal melanomas and treated accordingly. Most clinically diagnosed small choroidal melanomas are currently treated by eye-preserving, locally destructive therapies

TABLE II: RESULTS OF BIOPSY AND INITIAL POSTBIOPSY MANAGEMENT OF 34 SMALL MELANOCYTIC CHOROIDAL TUMORS CLASSIFIED AS "NEVUS VERSUS MELANOMA"

CASE	ADEQUACY OF ASPIRATE	CYTOPATHOLOGIC DIAGNOSIS	MELANOMA CELL TYPE	REVISED CLINICAL DIAGNOSIS	INITIAL MANAGEMENT
1	insufficient			nevus vs melanoma	observation
2	insufficient			nevus vs melanoma	observation
3	sufficient	malignant melanoma	spindle	choroidal melanoma	enucleation
4	sufficient	intermediate	spindle	nevus vs melanoma	observation
5	sufficient	malignant melanoma	epithelioid	choroidal melanoma	enucleation
6	insufficient			nevus vs melanoma	observation
7	sufficient	malignant melanoma	unspecified	choroidal melanoma	enucleation
8	sufficient	malignant melanoma	unspecified	choroidal melanoma	plaque radiotherapy
9	insufficient			nevus vs melanoma	plaque radiotherapy + laser
10	sufficient	malignant melanoma	unspecified	choroidal melanoma	plaque radiotherapy + laser
11	sufficient	benign nevus		choroidal nevus	observation
12	sufficient	malignant melanoma	unspecified	choroidal melanoma	plaque radiotherapy + laser
13	sufficient	malignant melanoma	spindle	choroidal melanoma	plaque radiotherapy + laser
14	insufficient			nevus vs melanoma	observation (rebiopsied)
15	sufficient	malignant melanoma	spindle	choroidal melanoma	proton beam irradiation
16	sufficient	malignant melanoma	mixed	choroidal melanoma	plaque radiotherapy + laser
17	insufficient			nevus vs melanoma	observation
18	sufficient	malignant melanoma	spindle	choroidal melanoma	plaque radiotherapy + laser
19	sufficient	malignant melanoma	spindle	choroidal melanoma	plaque radiotherapy + laser
20	sufficient	benign nevus		choroidal nevus	observation
21	insufficient			nevus vs melanoma	observation
22	sufficient	malignant melanoma	spindle	choroidal melanoma	plaque radiotherapy + laser
23	sufficient	intermediate	spindle	nevus vs melanoma	observation (rebiopsied)
24	insufficient			nevus vs melanoma	observation
25	insufficient			nevus vs melanoma	observation
26	insufficient			nevus vs melanoma	observation
27	insufficient			nevus vs melanoma	observation
28	insufficient			nevus vs melanoma	observation
29	sufficient	malignant melanoma	spindle	choroidal melanoma	plaque radiotherapy
30	sufficient	malignant melanoma	epithelioid	choroidal melanoma	plaque radiotherapy
31	sufficient	intermediate	spindle	choroidal melanoma	plaque radiotherapy
32	sufficient	malignant melanoma	spindle	choroidal melanoma	plaque radiotherapy + laser
33	sufficient	intermediate	spindle	nevus vs melanoma	plaque radiotherapy
34	sufficient	malignant melanoma	mixed	choroidal melanoma	plaque radiotherapy

such as long-duration large spot size infrared laser therapy (transpupillary thermotherapy),<sup>9-14</sup> plaque radiotherapy, or proton beam irradiation. Inclusion of benign nevi in a series of clinically diagnosed small choroidal melanomas will falsely overestimate the reported success of that treatment and underestimate the frequency of failure in true small choroidal melanomas.

The accuracy of clinical diagnosis of medium-sized and larger choroidal melanomas that exhibit classic clinical features is extremely high.<sup>15</sup> However, the accuracy of clinical diagnosis of presumed small choroidal melanomas has never been established by any clinicopathologic correlation study. Melanocytic choroidal nevi larger than the usually accepted upper limit of size of classic benign choroidal nevi (5 mm in diameter, 1 mm in thickness) but smaller than the conventional boundary dimensions for medium-sized choroidal melanomas (10 mm in diameter, 3 mm in thickness) are documented pathologically from time to time,<sup>16-18</sup> and such tumors can simulate small

malignant melanomas quite closely.<sup>19</sup> Our study suggests that such large benign choroidal nevi are substantially more common than is generally appreciated. Because most small melanocytic choroidal tumors in the nevus versus melanoma category are currently managed by eye-preserving methods, determining which lesions in this category are benign nevi or borderline lesions and which are malignant melanomas requires a method other than histopathologic study of the enucleated eye. In our opinion, fine-needle aspiration biopsy is a useful technique for obtaining this information.

The most important limitation of fine-needle aspiration biopsy of small melanocytic choroidal tumors revealed by this study is its frequent inability to obtain sufficient cells for cytodiagnosis (35.3% in this series). Early in our experience, an insufficient aspirate for cytodiagnosis caused us great concern. However, we now believe that an insufficient specimen is a meaningful nondiagnostic result. Tumors that yield a limited specimen tend to be

**TABLE III: FINAL DIAGNOSIS AND FOLLOW-UP INFORMATION ON 34 PATIENTS WITH "CHOROIDAL NEVUS VERSUS MELANOMA"  
EVALUATED BY DIAGNOSTIC FINE-NEEDLE ASPIRATION BIOPSY**

CASE	FINAL DIAGNOSIS	LIFE STATUS AT MOST RECENT ENCOUNTER	DURATION OF FOLLOW-UP (YR)
1	choroidal melanoma	alive	13.7
2	choroidal nevus	alive	2.9
3	choroidal melanoma	alive	12.6
4	choroidal melanoma	alive	10.8
5	choroidal melanoma	alive	0.1
6	choroidal nevus	alive	7.9
7	choroidal melanoma	alive	7.8
8	choroidal melanoma	alive	8.8
9	choroidal melanoma	alive	6.8
10	choroidal melanoma	alive	8.0
11	choroidal nevus	alive	5.1
12	choroidal melanoma	alive	5.6
13	choroidal melanoma	alive	7.9
14	choroidal nevus	alive	5.2
15	choroidal melanoma	alive	4.1
16	choroidal melanoma	alive	4.8
17	choroidal melanoma	alive	3.4
18	choroidal melanoma	alive	0.9
19	choroidal melanoma	alive	0.9
20	choroidal nevus	alive	0.4
21	choroidal melanoma	alive	2.0
22	choroidal melanoma	alive	1.2
23	choroidal melanoma	alive	3.1
24	choroidal nevus	alive	2.4
25	choroidal nevus	alive	2.3
26	choroidal nevus	alive	2.4
27	choroidal nevus	alive	2.2
28	choroidal nevus	alive	2.0
29	choroidal melanoma	alive	1.9
30	choroidal melanoma	alive	1.6
31	choroidal melanoma	alive	1.8
32	choroidal melanoma	alive	1.4
33	choroidal melanoma	alive	1.2
34	choroidal melanoma	alive	1.0

composed of strongly cohesive cells. Cohesiveness of tumor cells is a relative indicator of benignity. On the basis of our experience to date, small melanocytic choroidal tumors in the nevus versus melanoma category that yield an insufficient specimen for cytodiagnosis should probably be managed, at least initially, by observation rather than by prompt treatment.

I do not expect the results of this study to convince skeptics of the utility, diagnostic accuracy, or safety of diagnostic transvitreal fine-needle aspiration biopsy of small melanocytic choroidal tumors in the nevus versus melanoma category or to alter current management of such lesions at most centers. However, I do expect these results to stimulate discussion of and reflection about the nature of small melanocytic choroidal tumors and the possible role of fine-needle aspiration biopsy in their future evaluation.

## REFERENCES

1. Augsburger JJ. Is observation really appropriate for small choroidal melanomas? *Trans Am Ophthalmol Soc* 1993;91:147-175.
2. Augsburger JJ, Shields JA. Fine needle aspiration biopsy of solid intraocular tumors. *Trans Pa Acad Ophthalmol Otolaryngol* 1983;36:169-172.
3. Augsburger JJ, Shields JA. Fine needle aspiration biopsy of solid intraocular tumors: indications, instrumentation and techniques. *Ophthalmic Surg* 1984;15:34-40.
4. Augsburger JJ. Fine-needle aspiration biopsy in the diagnosis of suspected intraocular cancer. In: Jakobiec FA, Sigelman J, eds. *Advanced Techniques in Ocular Surgery*. Philadelphia: Saunders, 1984:491-521.
5. Augsburger JJ, Shields JA, Folberg R, et al. Fine needle aspiration biopsy in the diagnosis of intraocular cancer. Cytologic-histologic correlations. *Ophthalmology* 1985;92:39-49.
6. Folberg R, Augsburger JJ, Gamel JW, et al. Fine-needle aspirates of uveal melanomas and prognosis. *Am J Ophthalmol* 1985;100: 654-657.

7. Augsburger JJ. Fine needle aspiration biopsy of suspected metastatic cancers to the posterior uvea. *Trans Am Ophthalmol Soc* 1988;86:499-560.
8. Clarici JD, Lang WR. Ocular cytology: indications, techniques and preparations. *Tech Sample* 1985;CY-3:1-4.
9. Oosterhuis JA, Journee-de Korver HG, Kakebeeke-Kemme HM, et al. Transpupillary thermotherapy in choroidal melanomas. *Arch Ophthalmol* 1995;113:315-321.
10. Oosterhuis JA, Jorunee-de Korver HG, Keunen JE. Transpupillary thermotherapy: results in 50 patients with choroidal melanoma. *Arch Ophthalmol* 1998;16:157-162.
11. Shields CL, Shields JA, De Potter P, et al. Transpupillary thermotherapy in the management of choroidal melanoma. *Ophthalmology* 1996;103:1642-1650.
12. Shields CL, Shields JA, Cater J, et al. Transpupillary thermotherapy for choroidal melanoma: tumor control and visual results in 100 consecutive cases. *Ophthalmology* 1998;105:581-590.
13. Godfrey DG, Waldron RG, Capone A. Transpupillary thermotherapy for small choroidal melanoma. *Am J Ophthalmol* 1999;128:88-93.
14. Robertson DM, Buettner H, Bennett SR. Transpupillary thermotherapy as primary treatment for small choroidal melanomas. *Arch Ophthalmol* 1999;117:1512-1519.
15. The Collaborative Ocular Melanoma Study Group. Accuracy of diagnosis of choroidal melanoma in the Collaborative Ocular Melanoma Study. COMS report No. 1. *Arch Ophthalmol* 1990;108:1268-1273.
16. Hale PN, Allen RA, Straatsma BR. Benign melanomas (nevi) of the choroid and ciliary body. *Arch Ophthalmol* 1965;74:532-538.
17. McLean IW, Zimmerman LE, Evans RM. Reappraisal of Callender's spindle A type of malignant melanoma of choroid and ciliary body. *Am J Ophthalmol* 1978;86:557-564.
18. MacIlwaine WA, Anderson B, Klintworth GK. Enlargement of a histologically documented choroidal nevus. *Am J Ophthalmol* 1979;87:480-486.
19. Gass JDM. Problems in the differential diagnosis of choroidal nevi and malignant melanomas. *Am J Ophthalmol* 1977;83:299-322.

## DISCUSSION

DR HANS E. GROSSNIKLAUS. Uveal melanoma is the most common cause of death from an eye disease in the United States. During the past several decades, numerous treatments for primary uveal melanoma have been devised. The theory of cancer is that the earlier a cancer is detected and treated, the more likely it is cured. Uveal melanoma is unusual because it is generally diagnosed and treated with clinical evaluation and without examination of a biopsy. In recent years, small uveal melanomas have been treated by transpupillary thermotherapy. A problem with this treatment is that we don't know how many of these small melanomas are really nevi, if the morbidity and mortality associated with treatment outweigh the morbidity and

mortality of observing these lesions, and if the morbidity of doing an FNAB outweighs the risks of clinical diagnosis and management without doing a fine-needle aspiration biopsy. We do know that uveal melanomas treated by transpupillary thermotherapy that fail to respond or recur tend to be located near the optic nerve and may exhibit extraocular spread along emissary canals.

In this study, Dr Augsburger and coworkers attempt to answer some of these questions. Thirty-four patients with small melanocytic choroidal tumors were evaluated over an 8-year interval. The tumors had a mean maximal basal diameter of 8.0 mm and a mean maximal thickness of 2.4 mm. All patients underwent a transvitreal fine-needle aspiration biopsy of the tumor. Results showed 22 of 34 with sufficient specimen (group I) and 12 of 34 with insufficient specimen (group II). Sixteen from group I were diagnosed as having melanoma and treated. Two from group I were diagnosed as having nevus and not treated. Four tumors from group I were diagnosed as indeterminate and eventually treated as small choroidal melanomas. Of the group II patients, 8 were observed and 4 were eventually treated because of tumor enlargement. What we can learn from this study is that there is approximately a 65% diagnostic yield from fine-needle aspiration biopsy of uveal melanocytic proliferation. If we assume that all patients in the study might have had transpupillary thermotherapy for the clinical presumption of melanoma, 24% of these patients likely had nevi and didn't need the transpupillary thermotherapy.

This was a retrospective descriptive series rather than a case-control study. The fine-needle aspiration biopsy technique varied, with patients having one, two, or three needle passages. The cytological processing technique varied, with filter, cytospin, and direct smear employed. The follow-up time ranged from less than 1 month to 13.7 years. These are all weaknesses. However, as long as one doesn't try to make this a statistically sound case-control study and accepts this work as an observational case series, it provides useful information. What this study does show is that in the hands of an experienced ocular oncologist, a sizable number of small uveal melanocytic proliferations suspected to be melanoma and eligible for treatment are really nevi. We do not know if treatment of any small uveal melanocytic proliferation, nevus or melanoma, prolongs survival. According to the theory of cancer, much of the improvement in survival rates associated with early detection is due to treatment of a higher proportion of benign tumors, not curing malignancies. McLean has indicated that if this theory is correct, modifications of local treatment will not result in any significant improvement in survival. Recent evidence supports this concept, as Eskelin and coworkers have shown that it is likely that uveal melanoma forms micrometastases in

susceptible patients within 5 years prior to diagnosis of the ocular tumor. All of this information, including Augsburger and coworkers' study, needs to be considered when one develops a clinical plan for a patient with a small uveal melanocytic proliferation.

I would like to thank Dr Jackson Coleman for his comments regarding this work.

DR STEPHEN S. FEMAN. It looked like you were doing a fine-needle biopsy through the vitreous without a vitrectomy. Do you have any concerns concerning tumor growth or vitreous fibrotic reaction from doing this procedure?

DR FRONCIE A. GUTMAN. How do you select the biopsy site? You can have false negatives simply by missing that portion of the lesion that contains the melanoma. Have you modified your attitude about the associated findings? I was surprised that you don't regard the finding of an associated serous detachment significant. Have you modified the standard significant risk factors that we have used in the past to distinguish melanoma from a nevus?

DR RICHARD K. FORSTER. Have the intraoperative complications changed in association with your modifications of the technique over this 20-year period?

DR VINOD LAKHANPAL. You stated that if you document growth in these melanocytic tumors or lesions, you have done a disservice to the patient. In recent literature, it has been suggested that small melanomas should be watched. So you are suggesting a change in the management of these lesions. How do you manage those 35% of patients that remain indeterminate after the aspiration?

DR J. BROOKS CRAWFORD. The technique depends not only on the technical ability to obtain the biopsy, but also on the expertise of the cytopathologist.

DR JAMES J. AUGSBURGER. Let me respond first to Dr Feman's question about the technique. I do this technique without a vitrectomy. When I started the technique in the early 1980s, Jay Federman advised me to perform a core vitrectomy. I told him that I would try it without the vitrectomy and modify the technique if necessary. I have never had major vitreoretinal problems from the technique. In over 400 biopsies, there have been two instances of localized peripheral retinal detachment after the procedure, both of which I have walled off with laser and they have not progressed.

Now for the question of local tumor recurrence in the field. Many of you are familiar with the work of Karcioğlu and coworkers, who looked at the high frequency of

tumor cell seeding along the needle track when you biopsy directly into the tumor through the sclera. I found the same results when doing practice eyes and enucleated eyes and in postenucleation biopsies, so I do not go through the sclera. When you use the transvitreal route, or what I call the indirect technique, we have not seen a single instance of implantation tumors along the needle track at the puncture site in the pars plana nor to my knowledge has there ever been one reported. I should add a caveat on that—that although melanocytic tumors can be handled like this, I would never handle a retinoblastoma with this technique.

With regard to Dr Gutman's question on selection of the biopsy site, it depends on where the lesion is located. I tend not to go over the macula. If it is in the inferotemporal midzone of the fundus posterior to the equator, I will select a pars plana position inferotemporally and come at it from that position. As you can imagine, doing this with an indirect ophthalmoscope means I'm standing on the other side of the table from the patient's eye and viewing it on a screen with a video indirect ophthalmoscope (so my assistants can watch it) and I pass the needle directly into it under ophthalmoscopic visualization. Are there sampling errors? I'm sure that there may be sampling errors in these cases. How do I try to avoid that? It's based on our prior work with postenucleation specimens where I tried to sample at least three different sites within the tumor. I will use either a single needle or multiple needles but I will not sample only one site. Will we still miss some occasionally? I don't think we miss very many of them.

The orange pigment and the subretinal fluid are undoubtedly factors associated with the likelihood that the lesion will grow; however, there has never been a study to my knowledge that has shown that in the small melanocytic choroidal tumors, growth, especially, very slight growth without other invasive features occurring, is a clear indication of malignancy in these tumors. Nevi are almost never congenital lesions. What does that imply? They occur as adult lesions; they are acquired lesions; to be acquired, they have to grow. So growth and activity, in my opinion, are relative predictors of malignancy, but they are not the same as clear invasive features within the tumor.

With regard to Dr Forster's questions, are there intraocular complications? The major complication we see is some bleeding. As you pull the needle out, you will get a little bit of bleeding in most of those cases. I very lightly press on the eye for about a minute after the needle has been withdrawn, and at that time we will look at the bleeding site. In most of the cases the bleeding will have stopped. You will get a clot right there; that clot is actually very helpful in terms of preventing development of a retinal hole that would lead to a retinal detachment, in my opinion. In some cases, we have had enough intravitreal

bleeding that we've actually obscured the view of the fundus for up to several months. We have followed these tumors with ultrasound and we have generally not had to treat them.

What do we do now with the cases given the diagnosis "quantity not sufficient"? You might look at these numbers that I have and say, "Why did you treat some of them if you received a biopsy that indicated an insufficient aspirate?" When we started these biopsies, back in the early 1980s, I would tell the patients that we would get one of three answers. If it's malignant, I'm going to recommend that you be treated. If it's benign, I'm going to simply recommend that it be observed periodically. If we don't get enough tissue to confirm a diagnosis or if it is indeterminate, we will have to proceed as we would have routinely done in the past, without that biopsy. And in some of those cases, after discussing the options, some patients elected treatment and some did not.

We find that the frequency of a "quantity not sufficient" result varies greatly by the type of tumor. For example, take the case of a medium-sized to large melanoma, where the patient says, "Doctor, you might be a very nice guy, and I'll probably go along with your treatment recommendation, but I would rather have you confirm it with a biopsy before you do the procedure, especially if it's going to be an enucleation." We have almost 100% recov-

ery of cells in those kinds of tumors. We've found over the years that those patients that we observe after a "quantity not sufficient" diagnosis have tumors that are very dormant, on the average. Some of them will grow; a few of them will show invasive features eventually. We may treat them, but they seem to have very low metastatic risk. A lot of them turn out to be benign. Now I tell patients something different: "If we get insufficient cells, that tells me that this is a very cohesive tumor. I equate cohesiveness with a favorable prognosis for that tumor." I recommend that those tumors be observed rather than treated.

Finally, regarding my comment that if you watch a patient who has a small choroidal melanoma and his or her tumor grows during observation, you've done a disservice. Consider the survival prognosis of patients who have small, medium, and large tumors. Survival of patients having larger choroidal melanomas is clearly substantially worse than that of patients with smaller choroidal melanomas. But, prognosis is not equal for all patients having a tumor of a certain size category. If you subdivide patients into smaller categories—very small, small, a little bit bigger than small, etc, the survival prognosis decreases as tumor size increases. So if you decide to observe a choroidal melanoma, and the tumor grows during follow-up, you have not done your patient any favor.

## POSTERS



## **OCULAR ADNEXAL LYMPHOID PROLIFERATIONS: CLINICAL, HISTOLOGIC, FLOW CYTOMETRIC, AND MOLECULAR ANALYSIS OF FORTY-THREE CASES**

BY *Nariman Sharara, MD* (BY INVITATION), *Jeannine T. Holden, MD* (BY INVITATION), *Ted H. Wojno, MD* (BY INVITATION), *Andrew S. Feinberg, MD* (BY INVITATION), AND *Hans E. Grossniklaus, MD*

*Purpose:* To describe the clinical features, histologic findings, flow cytometric immunophenotypes, and molecular profiles of ocular adnexal lymphoid proliferations.

*Methods:* Patients suspected of having ocular adnexal lymphoid proliferations underwent biopsy and prospective evaluation. Provisional diagnoses were made on the basis of routine histology and immunohistochemistry for B and T cells. Results of flow cytometric immunophenotyping (FCI) and molecular assessment using polymerase chain reaction for immunoglobulin heavy chain (IgH) and T-cell receptor gamma chain gene rearrangement and bcl-2/IgH translocation were then incorporated into a final diagnosis. Demographic and clinical outcome data were collected.

*Results:* Forty-three cases were studied. Final diagnoses included lymphoma in 17 cases, chronic inflammation in 18, reactive lymphoid hyperplasia in 4, and atypical lymphoid infiltrates in 4. Preliminary evaluation accurately categorized all 43 cases as either lymphoma or nonlymphoma. FCI permitted more precise subclassification of the lymphomas according to the Revised European American Lymphoma (REAL) system of nomenclature as follows: 8 cases of marginal zone B cell (MALT-type), 3 cases of mantle cell, 2 cases of follicular, 3 cases of large cell, and 1 case of lymphoplasmacytoid lymphoma. FCI showed a clonal B-cell proliferation in 94% (16/17) of the lymphomas; FCI identified a clonal B cell population in 4% (1/25) of the nonlymphomas. Molecular evidence of clonality was identified in 88% (15/17) of lymphomas, 39% (7/18) of chronic inflammations, and 50% (4/8) of reactive lymphoid hyperplasias and atypical lymphoid infiltrates.

*Conclusions:* The histologic diagnosis of ocular adnexal lymphoid lesions is highly accurate when determined by an experienced pathologist. FCI refines the histologic diagnosis and classification. Results of molecular studies should be interpreted in conjunction with clinical, histologic, and immunophenotyping findings.

## **RECURRENT CAPSULAR OPACITY AND ERYTHROPOIETIN**

BY *James S. Kelley, MD*

*Purpose:* To note an association between erythropoietin use and recurrent capsular opacity.

*Methods:* Case report of a 75-year-old patient in whom cellular debris developed and occluded a previous YAG capsulotomy.

*Results:* The patient had been taking erythrocyte-stimulating agents weekly for 5 years. Repeated use of YAG laser in patients at this age is required in less than 1 in 5,000 cases. The debris had the typical appearance of Elschnig's pearl.

*Conclusion:* The proliferation of capsular debris may be related to the use of erythropoietin.

## **COMBINED CENTRAL RETINAL ARTERY AND VEIN OCCLUSION AND SIMULTANEOUS ANTERIOR ISCHEMIC OPTIC NEUROPATHY FROM BEHCET'S DISEASE**

BY *Rohit R. Lakhanpal, MD* (BY INVITATION), *Vinod Lakhanpal, MD*, *Shalom E. Kelman, MD* (BY INVITATION), AND *Stanley S. Schocket, MD*

*Purpose:* To report a case of Behcet's disease in which combined central retinal artery (CRA) and vein (CRV) occlusion occurred simultaneously with anterior ischemic optic neuropathy (AION) in a previously unaffected eye.

*Methods and Results:* A 40-year-old Caucasian woman who had a history of visual loss in the left eye due to retinal vasculitis and optic atrophy secondary to established Behcet's disease suddenly had complete loss of vision in the right eye. The vision gradually improved within 20 minutes. On the following day, she presented with visual acuity of 20/30 in the right eye and hand motions in the left eye. There was no afferent pupillary defect. She showed signs of anterior uveitis, vitreous cells, disc swelling with superotemporal sectoral infarct, narrowed arterioles, congested veins, and retinal hemorrhages in all quadrants. Fluorescein angiography revealed choroidal nonperfusion corresponding to the sectoral disc infarct and delayed retinal arteriolar filling. Visual field testing revealed decreased overall sensitivity and complete loss inferonasally. A diagnosis of transient CRA occlusion with visual recovery, CRV occlusion, and simultaneous AION secondary to Behcet's disease was established. The patient was hospitalized and treated with intravenous Solu-Medrol for 3 days. Follow-up examination revealed improvement of visual field, decreased anterior and posterior segment inflammation, sectoral optic atrophy, and normal retinal arteriolar filling on angiography.

*Conclusions:* Retinal vasculitis is one of the most blinding manifestations of Behcet's disease. Our patient presented not only with retinal vasculitis causing combined CRA/CRV occlusion, but also with simultaneous posterior ciliary involvement leading to segmental choroidal infarction and AION.

## **THE RELATION OF PREOPERATIVE CORNEAL ASTIGMATISM TO SURGICALLY INDUCED ASTIGMATISM AFTER CATARACT SURGERY**

BY *John C. Merriam, MD*, *Lei Zheng* (BY INVITATION), *Joanna Merriam* (BY INVITATION), AND *Marco Zaider* (BY INVITATION)

*Purpose:* To evaluate the long-term effect of preoperative corneal astigmatism on surgically induced astigmatism (SIA) following five different incisions: extracapsular cataract extraction with a 12-mm incision (ECCE), 6-mm superior scleral tunnel (6Sup), 3-mm superior scleral tunnel (3Sup), 3-mm temporal scleral tunnel (3Temp), and 3-mm temporal corneal incision (3Cor).

*Methods:* This retrospective study includes 675 eyes with preoperative "with the rule" (WTR) or "against the rule" (ATR) astigmatism: 143 ECCE, 75 6Sup, 116 3Sup, 80 3Temp, and 261 3Cor. Each surgical group was divided into eyes with preoperative WTR and ATR astigmatism, and mean SIA for each subgroup was calculated at discrete intervals by using Jaffe's vector analysis, Naeser's polar coordinates, and axis-based methods.

*Results:* SIA in eyes with preoperative WTR or ATR astigmatism was indistinguishable after the superior incisions. Preoperative astigmatism had no effect on SIA after 3Temp, but SIA after 3Cor was slightly but significantly greater at some intervals in the eyes with preoperative ATR astigmatism. Fitting a linear equation to SIA after 3Cor also suggests that SIA is slightly greater in eyes with preoperative ATR astigmatism and that this effect is detectable immediately after surgery. This difference, if confirmed, is small and may not be clinically significant.

*Conclusion:* Preoperative corneal astigmatism does not appear to have a significant effect on SIA following five standard incisions for cataract. However, the ability to detect small differences in SIA may be limited by the precision and reliability with which astigmatism is measured.

## A NEURO-OPHTHALMIC ILLUSION

BY *Brian R. Younge, MD*

*Purpose:* To explain the ophthalmoscopic stability of the fundus image in head tremor versus the great instability of the fundus image in nystagmus.

*Methods:* Observations of images seen through a strong plus lens system are seen to move opposite the direction of the lens movement. By using a diagram of head and eye movement, we demonstrate the real movement of the eye, and by means of optics we explain the apparent stability of the image. The opposite observations are made in a patient with nystagmus, and optics can be used to explain this as well.

*Results:* Optics can be used to demonstrate the phenomena of stabilized imagery during head tremor and very unstable imagery during nystagmus.

*Conclusions:* The stable fundus image of a patient with a head tremor is really an illusion of optics. In contrast, the exaggerated fundus movement in a patient with nystagmus is in excess of the actual movement of the fundus



THESES



# THE USE OF ANTIMICROBIAL PEPTIDES IN OPHTHALMOLOGY: AN EXPERIMENTAL STUDY IN CORNEAL PRESERVATION AND THE MANAGEMENT OF BACTERIAL KERATITIS

---

BY Mark J. Mannis, MD, FACS

## ABSTRACT

**Purpose:** Bacterial keratitis is an ocular infection with the potential to cause significant visual impairment. Increasing patterns of antibiotic resistance have necessitated the development of new antimicrobial agents for use in bacterial keratitis and other serious ocular infections. With a view to exploring the use of novel antimicrobial peptides in the management of ocular infection, we performed a series of experiments using synthetic antimicrobial peptides designed for the eradication of common and serious ophthalmic pathogens.

**Methods:** Experiments were performed with three clinical ocular isolates—*Pseudomonas aeruginosa*, *Staphylococcus aureus*, and *Staphylococcus epidermidis*—in three experimental settings: (1) in vitro in a controlled system of 10 mM sodium phosphate buffer, (2) in vitro in modified chondroitin sulfate-based corneal preservation media (Optisol), and (3) in an in vivo animal model (rabbit) simulating bacterial keratitis. In all cases, outcomes were measured by quantitative microbiological techniques.

**Results:** The candidate peptides (CCI A, B, and C and COL-1) produced a total reduction of the test pathogens in phosphate buffered saline. In modified Optisol, the peptides were effective against *S epidermidis* at all temperatures, demonstrated augmented activity at 23°C against the gram-positive organisms, but were ineffective against *P aeruginosa*. The addition of EDTA to the medium augmented the killing of *P aeruginosa* but made no difference in the reduction of gram-positive organisms. In an in vivo rabbit model of *Pseudomonas keratitis*, COL-1 demonstrated neither clinical nor microbicidal efficacy and appeared to have a very narrow dosage range, outside of which it appeared to be toxic to the ocular surface.

**Conclusions:** Our data indicate that the antimicrobial peptides we tested were effective in vitro but not in vivo. In an age of increasing antibiotic resistance, antimicrobial peptides, developed over millions of years as innate defense mechanisms by plants and animals, may have significant potential for development as topical agents for the management of severe bacterial keratitis. However, modifications of the peptides, the drug delivery systems, or both, will be necessary for effective clinical application.

*Trans Am Ophthalmol Soc* 2002;243-271

The emergence of multiply drug-resistant bacteria . . . would represent the most important issue in antibiotic resistance since the dawn of the antibiotic era. A common virulent and transmissible bacterial agent with no known effective therapy would set infectious diseases back 60 years.

*Annals of Internal Medicine*, 1996<sup>1</sup>

Cationic peptides have been found in all forms of life from bacteria to man and are probably the most conserved theme in nature's struggle to control aggressive microorganisms.

*Drugs*, 1997<sup>2</sup>

Most species throughout the evolutionary scale use peptides as antimicrobial agents. It is likely that resistance to peptide antibacterial agents may not develop easily. Since the problem of antibiotic resistance is presently a particularly severe one, peptide antibiotics may be the drugs of choice in the future.

*Biochimica et Biophysica Acta*, 1994<sup>3</sup>

[Peptide antibiotics] might be ideal therapeutic agents, avoiding the problem of acquired resistance.

*Nature*, 1997<sup>4</sup>

This work was performed under the auspices of the Cornea Research Laboratory, Department of Ophthalmology, University of California, Davis, in collaboration with the Dairy Food and Safety Laboratory, School of Veterinary Medicine, University of California, Davis. Financial support was provided by a Wasserman Award from Research to Prevent Blindness, Inc, New York, New York. The author is a co-owner of the University of California use-patent for defense peptides for ocular applications; he has no financial interest in any of the compounds or inventions mentioned in this thesis.

## INTRODUCTION

---

Ocular infections involving the optical media of the eye or the neurosensory retina may have profound and devastating impact on visual function. Pathogenic invasion of the cornea or the internal eye always carries the risk of significant functional visual damage because of (1) the small space in which the infection occurs, (2) structural disruption of the optics of the cornea in the case of keratitis, or (3) the rapid and irreversible destruction of neuroretinal tissue in the case of endophthalmitis. While the treatment of corneal ulcers with topical antimicrobial agents has been notably successful with an expanding array of both focused and broad-spectrum antibiotics, there has, in general, been an alarming emergence of patterns of increasing resistance to commonly used antimicrobial agents.<sup>5-9</sup> Microbes cleverly develop resistance to antibiotics as a result of chromosomal mutation, inductive expression of a latent chromosomal gene, or exchange of genetic material via transformation, bacteriophage transduction, or plasmid conjugation.<sup>5,10</sup>

Use of the fluoroquinolones in the management of external infections is the most recent example of how a new class of antibiotics has been instrumental in changing management strategies for the treatment of corneal infections. Nonetheless, emerging patterns of resistance even to these new classes of antimicrobial agents<sup>11-25</sup> have stimulated the continuing quest for an agent that provides rapid and complete microbicidal activity with minimal toxic effects and susceptibility to mechanisms of microbial resistance.

The problem of emerging antimicrobial resistance and the need to find more effective antimicrobial agents stimulated us to initiate investigation of antimicrobial peptides as a tool for the management of ocular infection. Indeed, the innate gene-encoded antimicrobial peptides are increasingly being recognized as host defense effector molecules in plants and animals,<sup>26</sup> and since they differ structurally from conventional antibiotics produced by bacteria and fungi, they may offer novel templates for pharmaceutical compounds that could be used against increasingly resistant microbes.<sup>27</sup> This thesis presents the results of a series of *in vitro* and *in vivo* experiments performed in our laboratory in an effort ultimately to expand the armamentarium of effective antimicrobial agents for the management of severe microbial keratitis.

## BACKGROUND: THE ANTIMICROBIAL PEPTIDES

---

The defense system of the eye consists of both general anatomical and specific immune responses to microbial invasion. The lids and cilia represent the first protective mechanism against pathogenic invasion. The tear film is,

likewise, an important defense against microbial invasion, both for its flushing function and its composition, which includes immunoglobulins, lysozyme, lactoferrin,  $\beta$ -lysin, and other proteins with antimicrobial capabilities.<sup>28-31</sup> These defenses notwithstanding, a breach of the corneal epithelial barrier by a pathogenic organism can render the cornea defenseless against the destructive mechanisms of a virulent pathogen. In such cases, infection management requires the application of an antimicrobial agent.

Ophthalmic researchers have paid relatively little attention to the emerging field of peptide chemistry as a tool to augment the anatomical and specific immune responses of the eye to pathogenic invasion. Yet, for the past two decades, workers have been fascinated with the cellular immune defense mechanisms elaborated by organisms in response to pathogenic infection, and for at least three decades, interest in endogenous peptides with antimicrobial properties has increased.<sup>26,32,33</sup> These peptides are part of the innate immune response to pathogenic infection that has developed throughout nature. The range of antimicrobial peptide research encompasses subject matter far too broad for the scope of this thesis. However, definition and categorization of the peptides with antimicrobial activity are necessary for consideration of the current experimentation.

## TERMINOLOGY, STRUCTURE, AND CLASSIFICATION

The terminology applied to these antimicrobial substances varies in the scientific literature. Descriptive terms that have been used include “defense peptides,” reflecting their teleological or functional role in defense against microbial invasion; “lytic peptides” or “pore-forming proteins,” reflecting their probable action as membrane-permeabilizing agents; “cationic peptides,” reflecting their electrochemical structure; and “antimicrobial peptides,” a more generic term describing their functional capabilities. For the purposes of this presentation, we will use the more generic term—antimicrobial peptides.

Antimicrobial peptides are small, basic, single gene-encoded peptides that are generally synthesized as preproteins and are activated as part of the host defense systems in plants,<sup>34,35</sup> insects,<sup>36-41</sup> fish, amphibia,<sup>42-44</sup> birds, and mammals.<sup>45-47</sup> These small proteins are an evolutionarily ancient system of immune protection that are expressed during infection, inflammatory events, and even wound repair, and their presence constitutes a key innate host defense against microbial pathogenesis.<sup>48-51</sup> Their *de novo* synthesis or release from storage sites can be induced extremely rapidly, making them particularly important in the initial phases of resistance to microbial invasion, and current scientific evidence demonstrates that they function as membrane permeabilizing agents.<sup>47</sup>

Antimicrobial peptides are produced ubiquitously throughout nature. Many of these relatively short peptides (12 to 50 residues) are lethal to bacteria, fungi, and parasites<sup>52</sup> but display minimal toxic effects on mammalian cells. Although impressively diverse in structure, most antimicrobial peptides are highly cationic (positively charged) and amphipathic. This electrochemical structure facilitates their binding to negatively charged biological membranes on which they aggregate and act as lytic pore formers.<sup>45,47,53</sup> The lytic peptides, both those with  $\alpha$ -helical and those with  $\beta$ -pleated sheet structures, are amphipathic; that is, one side of the molecule is hydrophilic and one side is hydrophobic, a design that is consistent with membrane-specific interaction.<sup>54</sup>

The origin of synthesis of the antimicrobial peptides varies according to the host species. In insects, the fat body is the primary location of peptide synthesis. In the frog, the skin is the location of synthesis. Human and other mammalian defensins are expressed in granulocytes and are formed during early hematopoiesis; they may also be found in tracheal and lung macrophages and in the Paneth cells of the small intestine.

On a chemical and biochemical basis, the antimicrobial peptides can be divided into four families:

- Cysteine-rich peptides that form amphiphilic  $\beta$ -pleated structures with two or more disulfide bonds (eg, defensins, tachyplesins, protegrins (Table IA))
- Linear molecules without cysteine (Cys) in the form of  $\alpha$ -helical peptides (eg, cecropins and magainins [both amphipathic helices], bombinins) (Table IB)
- Molecules with one disulfide bond or cysteine-disulfide ring peptides (eg, bactenecins [bovine cyclic dodecapeptides], brevinins, ranalexin) (Table IC)
- Peptides with an overrepresentation of one or two amino acids (eg, Pro, Arg, Trp, Gly): apidaecins, indolicidin, drosocin, PR-39 (Table ID)<sup>45,46</sup>

A notable characteristic of all the antimicrobial peptides is that they have well-defined tridimensional structures (secondary structure). The function of each peptide is dependent to a great extent on this conformational structure, which is specified by the amino acid sequence (primary structure), the presence or absence of disulfide bonds, and the variable terminal portions of the molecules.<sup>55,56</sup>

One can also classify the pore-forming defense peptides by their species of origin (Table II).

#### MECHANISM OF ACTION

The antimicrobial peptides, produced ubiquitously throughout nature, function as “natural” antibiotics through the mechanism of pore formation—permeabilizing and disrupting the biological membranes of target cells. These peptides, often in aggregate form, insert into cell membranes, making the target cells leaky and

ultimately killing them<sup>47,57-59</sup> (Figure 1).

The clonally based immune system alone would not be sufficient to stave off bacterial infection. It is important to recall that bacteria can double in 20 minutes, while responsive lymphocyte induction may take many hours. Therefore, throughout the evolutionary scale, multiple species from insects to mammals have developed a “rapid response” system consisting of lytic peptides that can be synthesized and excreted and that act directly and rapidly on microbial pathogens.<sup>54</sup>

The mechanism of pore formation as a strategic solution has evolved over millions of years, beginning with primitive organisms and evolving through the higher vertebrates. Primitive eukaryotes, such as *Entamoeba histolytica*, are known to elaborate pore-forming agents that allow them to kill on contact, as do simple prokaryotes. Bacteria can produce pore-forming peptides as well, an example of which are the “hemolysins,” so designated because of their ability to lyse erythrocytes. These pore-forming agents may be required for the pathogenesis of organisms, and it is through the activity of the pore-forming substances that these organisms produce clinical disease. Table III includes some examples of pore-forming agents produced by bacteria that cause disease in humans.

The mechanism of pore formation differs among various peptides. Defensins, for example, are cationic proteins that form a triple-stranded,  $\beta$ -pleated sheet at one end and a hydrophobic finger at the other. The initial contact between the target lipid cell bilayer is thought to be between the cationic arginine groups on the defensin molecule and the negatively charged target membrane. This is followed by the formation of defensin multimers, creating a channel that spans the membrane, leading to membrane permeabilization and disruption.<sup>45,60,61</sup> Similarly, the  $\alpha$ -helical cecropins bind to the target membrane electrostatically, undergo a process of multimerization, and then form membrane-spanning pores permeabilizing the outer and inner membranes of target bacteria<sup>45,62,63</sup> (see Figure 1).

A good example of the way in which peptide-induced pore formation occurs is the interaction with gram-negative bacteria.<sup>64</sup> The cell envelope of a gram-negative bacterium is composed of two membrane systems, the outer of which contains negatively charged lipopolysaccharide molecules.<sup>3</sup> Cationic antimicrobials bind to this outer lipopolysaccharide membrane and disrupt its structure. When the inner membrane is encountered, the cationic peptides form channels, altering membrane permeability. This interaction with the outer membrane of gram-negative bacteria has been confirmed for magainins, defensins, cecropins, bactenecins, and tachyplesins, among others.<sup>3</sup>

Of the substances included in the previous discussion, we will focus on a select few that have been thoroughly

TABLE IA: CYSTEINE-RICH AMPHIPHILIC  $\beta$ -PLEATED PEPTIDES

PEPTIDE	STRUCTURE	SIZE	SPECIES	TISSUE SOURCE	SPECTRUM
Defensins	6 cysteines 3 C-C bridges arginine-rich	29-45 amino acids	Mammals, insects, birds, plants	Leukocyte granules, Paneth cell granules, fat bodies (insects), plant seeds	Gram+/- bacteria, fungi, enveloped viruses
Protegrins	COOH- terminal amide	16-18 amino acids	Pig	Leukocytes	Gram+/- bacteria, fungi, enveloped viruses
Tachyplesins	4 cysteines 2 C-C bridges	16-18 amino acids	Horseshoe crab	Hemocyte granules	Gram+/- bacteria, fungi, enveloped viruses

TABLE IB: AMPHIPHILIC  $\alpha$ -HELICAL PEPTIDES

PEPTIDE	STRUCTURE	SIZE	SPECIES	TISSUE SOURCE	SPECTRUM
Magainins	Lysine-rich	20-27 amino acids	Frog	Skin (granular gland and intestinal tract)	Gram+/- bacteria, fungi, parasites
Cecropins	Lysine-rich terminal amide	34-45 amino acids	Insect	Hemolymph, hemocytes, fat body	Gram+/- bacteria, fungi, parasites

TABLE IC: CYSTEINE-DISULFIDE RING PEPTIDES

PEPTIDE	STRUCTURE	SIZE	SPECIES	TISSUE SOURCE	SPECTRUM
Cyclic dodecapeptide	Arginine-rich No amphiphilic tail	12 amino acids	Bovine	Granulocytes	Gram+/- bacteria
Ranalexin	C-C bridged ring COOH-terminal	20 amino acids	Frog	Skin	Gram+/- bacteria
Brevinins	C-C bridged ring COOH-terminal	24-30 amino acids	Frog	Skin	Gram+/- bacteria

TABLE ID: LINEAR PEPTIDES WITH A PREDOMINANCE OF AMINO ACID(S)

PEPTIDE	STRUCTURE	SIZE	SPECIES	TISSUE SOURCE	SPECTRUM
Indolicidin	Tryptophan-rich	13 amino acids	Bovine	Granulocytes	Gram+/- bacteria
PR-39	Proline- and arginine-rich	39 amino acids	Pig	Small intestine leukocytes	Gram+/- bacteria

characterized and have been of some direct relevance to ophthalmic applications. These include the magainins, the defensins, and the cecropins.

#### MAGAININS

The magainins were first reported in 1987 by Zasloff, who was attempting to find the agent to explain the curious lack of infection in the healing surgical wounds in the frog *Xenopus laevis*.<sup>42,65-67</sup> These frogs developed infection very rarely, even when they had open, healing wounds and

were kept in contaminated containers. Zasloff isolated and characterized the first of these peptides located in the skin of the frog. He called them magainins 1 and 2, after the Hebrew word *magain* (shield), since they appeared to shield the frogs from infection. Since that time, the magainins have been characterized as a family of at least a dozen ionophoric, linear, cationic amphipathic peptides, 21 to 27 amino acids in length and generally lacking cysteine.<sup>68,69</sup> The magainins are produced in the granular glands and stored in secretory vesicles, and they have a

TABLE II: SELECTED ANTIMICROBIAL PEPTIDES CLASSIFIED BY SPECIES ORIGIN

SPECIES	PEPTIDE
Amphibian ( <i>Xenopus laevis</i> )	Magainin Brevinin
Other amphibians	Dermaseptin Bimbinin
Insect	Cecropin Andropin Sarcotoxin Sapecin Apidaeicin Abaecin Hymenoptaecin Bee defensin Melittin Attacins
Mammals (rabbit, rat, guinea pig, mouse, human, cow)	Defensin Beta-defensin Indolicidin Bactenecin Azurocidin
Crustaceans (Horseshoe crab)	Tachyplesin

broad spectrum of activity against a range of gram-positive and gram-negative bacteria, fungi, and protozoa. They have also been isolated in the gastric mucosa of the frog.<sup>70</sup> They appear to serve a physiological role in defense against macroscopic predators and in the control of microbial infection following wounding.<sup>26</sup>

The magainins are highly selective, channel-forming, lytic agents that form permeabilizing membrane channels with increasing peptide concentration.<sup>69,71-85</sup> A common

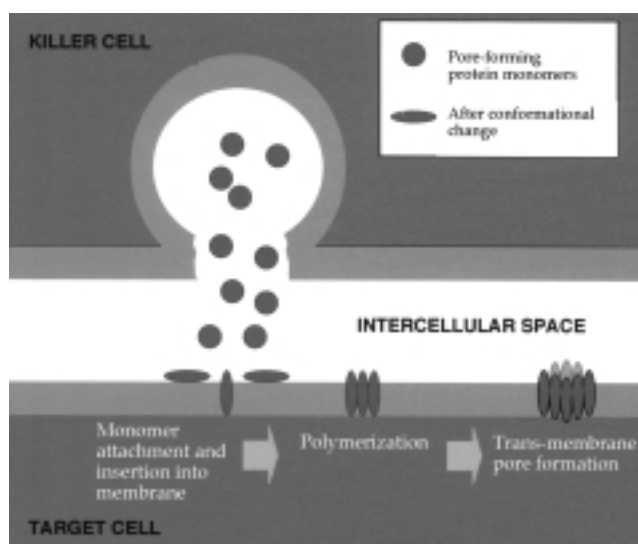


FIGURE 1

Diagrammatic representation of pore formation by antimicrobial peptides in a target cell.

TABLE III: PORE-FORMING AGENTS PRODUCED BY PATHOGENIC BACTERIA

BACTERIA	PORE-FORMING AGENT
<i>Bordetella pertussis</i>	Cytolysin
<i>Clostridium perfringens</i>	Perfringolysin
<i>Escherichia coli</i>	Alpha-hemolysin
<i>Listeria monocytogenes</i>	Listeriolysin O
<i>Pseudomonas aeruginosa</i>	Cytotoxin
<i>Staphylococcus aureus</i>	Alpha-toxin
<i>Streptococcus pneumoniae</i>	Pneumolysin
<i>Streptococcus pyogenes</i>	Streptolysin O
<i>Vibrio cholerae</i>	Hemolysin

structural feature of the magainins and similar peptides is a net positive charge due to the presence of multiple arginine and lysine residues; these amphipathic structures appear to function by binding to anionic phospholipids in the target membranes.<sup>47</sup>

The magainins exhibit a broad spectrum of antimicrobial activity, including activity against gram-positive and gram-negative bacteria, fungi, and protozoa.<sup>42,69,86-89</sup> In addition, they show selective lytic activity against a variety of transformed cells, such as human cancer cells at concentrations tenfold lower than those needed to lyse normal cells.<sup>90</sup> The magainins are the first of the antimicrobial peptides to be harnessed by the pharmaceutical industry for clinical application.

#### DEFENSINS

Stimulated neutrophils have two mechanisms for producing cellular injury. The first depends on the production of reactive oxygen intermediates, such as hydrogen peroxide, that can lyse target cells. The second mechanism is nonoxidative and is mediated by protein cytotoxins that are lodged in the cytoplasmic granules; among these are cathepsins, elastase, and defensins.<sup>91,92</sup> These mammalian defensins are small (3,000 to 4,000 daltons) cysteine- and arginine-rich antimicrobial peptides, approximately 29 to 34 amino acids in length; they contain three disulfide bonds, giving them a complex tertiary folded structure.<sup>93-97</sup> They are isolated from the azurophil granules of mammalian alveolar macrophages and neutrophils, make up about one third to one half of the total protein content of the neutrophil granules in the cells,<sup>98</sup> and constitute the major component of the oxygen-independent antimicrobial pathway of these phagocytic cells.<sup>48,98-102</sup>

Neutrophil defensins, whose structure is genetically determined, are synthesized by myeloid precursor cells in the bone marrow and are stored in the cytoplasmic azurophil granules of the mature cells.<sup>98</sup> Defensins are delivered to microbial targets after phagocytosis of an invading pathogen when the phagosomes and the azurophil granules within the neutrophil fuse.<sup>45</sup>

Originally termed lysosomal cationic peptides in rabbit and guinea pig polymorphonuclear leukocytes, crude defensin extract accounted for most of the antimicrobial activity against group D *Streptococcus*, *Proteus vulgaris*, *S aureus*, *S epidermidis*, *Candida parapsilosis*, and *Cryptococcus neoformans*. Since the original description, six defensin molecules have been isolated and purified from rabbit neutrophils<sup>101,102</sup> and also have been demonstrated in rats,<sup>103,104</sup> guinea pigs,<sup>93</sup> and humans,<sup>48,60,94</sup> where they constitute up to 7% of the total protein content of phagocytic cells (neutrophils and alveolar macrophages). The amino acid sequences of the defensins are highly conserved across species.<sup>53,93,98,105-109</sup> Table IV demonstrates the sequence of the major mammalian defensins and the remarkable homology between the peptides across mammalian species. Most of these effector protein molecules share significant structural and functional similarities, a finding that suggests their antiquity and conservation over millions of years. Defensins are, however, not limited to mammals. They have also been identified in insects.<sup>110</sup> In addition,  $\beta$ -defensins, which were discovered and isolated from bovine neutrophils, have a distinctly different structure but retain antibacterial properties similar to the defensins.<sup>111</sup>

Initially thought to be confined to cells of myeloid lineage, defensins have now been localized to other tissues. Although the largest quantity of defensins are isolated from phagocytic cells, they can also be found in bovine tracheal cells (TAP-tracheal antimicrobial peptide)<sup>112,113</sup> and in mouse intestinal cells (cryptidins).<sup>114-117</sup>

Like the magainins, the defensins appear to lyse target cells by pore formation.<sup>61,118</sup> The arginine residues associate electrostatically with the anionic portions of the target lipid membrane. These proteins then aggregate, insert into the membrane, and form a permeabilizing pore that leads to the death of the target cell.<sup>60,61</sup> The cytolytic

activity of the defensins against bacteria is extremely ion-sensitive, being greater in media of low ionic strength that lack significant concentrations of calcium or magnesium. In addition, defensin activity is dependent on pH and temperature.<sup>98</sup>

Defensins are broad-spectrum microbicides with demonstrated in vitro activity against gram-positive and gram-negative bacteria, mycobacteria, *Treponema pallidum*, and certain fungi<sup>48,119-124</sup> and enveloped viruses (herpes simplex, vesicular stomatitis virus, and influenza virus).<sup>48,102,120,121,125-129</sup>

Aside from their antimicrobial activity, specific defensins appear to have different functions. These functions include cytotoxicity,<sup>91,118,130-132</sup> chemotactic activity for monocyte recruitment,<sup>133,134</sup> inhibition of corticosteroid production,<sup>135,136</sup> release of histamine from mast cells,<sup>109</sup> augmentation of macrophage phagocytic capacity,<sup>137</sup> inhibition of protein kinase,<sup>138</sup> acceleration of wound healing,<sup>139</sup> and mitogenic effects on epithelial cells and fibroblasts.<sup>140</sup>

#### CECROPINS

Cecropins are natural antimicrobial peptides produced in a variety of insects in response to microbial infection.<sup>141</sup> First isolated from the hemolymph of *Hyalophora cecropia*, the giant silk moth, cecropins were identified as the chief component of the moth's humoral defense system against microbial infection by Boman, Merrifield and colleagues.<sup>141-146</sup> Within hours of injury or infection, a biologically active peptide is induced and is found in the insect hemolymph.<sup>147</sup>

Initially, two distinct cecropin molecules were identified (cecropins A and B).<sup>142</sup> Later, an additional five antimicrobial proteins were identified (cecropins C, D, E, F, and factor G).<sup>148</sup> The cecropins are a family of linear cationic peptides that are between 35 and 37 amino acids

TABLE IV: THE MAMMALIAN DEFENSINS

SPECIES	DEFENSIN	SEQUENCE
Human	HNP-1	ACYCRIPACIAGERRYGTCTIYQGRWLWAFCC
	HNP-2	CYCRIPACIAGERRYGTCTIYQGRWLWAFCC
	HNP-3	DCYCRIPACIAGERRYGTCTIYQGRWLWAFCC
Rabbit	NP-1	VVCACRRALCLPRERRAGFCRIRGRIHPLCCRR
	NP-2	VVCACRRALCLPLERRAGFCRIRGRIHPLCCRR
	NP-3a	GICACRRRFPCNSERFSGYCRVNGARYVRCCSRR
	NP-3b	GRCVCRKQLLSYRERRIGDCKIRGVRFPPCCPR
	NP-4	VSCTCRRFSCGFGERASGSCTVNGVRHTLCCRR
	NP-5	VFCTCRGFLCGSERASGSCTINGVRHTLCCRR
Guinea pig	GPNP	RRCICTTRTCRFYRRLGTCTIFQNRVYTFCC
Rat	RatNP-1	VTCYCRTRTCGFRERLSCACGYRGRYRLCCRR
	RatNP-2	VTCYCRSTRTCGFRERLGGACGYRGRYRLCCRR
	RatNP-3	CSCRTSSCRFCERLSGACRLNGRIYRLCC
	RatNP-4	ACYCRIGACVSGERLTGACGLNGRIYRLCCRR

Amino acid key: A=alanine; C=cysteine; D=aspartic acid; E=glutamic acid; F=phenylalanine; G=glycine; H=histidine; I=isoleucine; K=lysine; L=leucine; N=asparagine; P=proline; R=arginine; S=serine; T=threonine; V=valine; W=tryptophan; Y=tyrosine.

in length.<sup>141</sup> They are synthesized as preproteins of approximately 62 to 64 residues; these are then cleaved into the smaller active molecule.<sup>149</sup> The three principal cecropins are highly homologous and are identified as cecropins A, B, and D.<sup>148</sup> Related cecropin analogues have now been identified in a variety of insect species.<sup>32,141</sup>

The cecropins function by disrupting the cell membrane of target cells.<sup>141,150,151</sup> They are organized such that the first 11 amino acids form a highly amphipathic  $\alpha$ -helix with hydrophobic and positively charged surfaces.<sup>53,145</sup> At the N terminal of the  $\alpha$ -helix, the hydrophilic residues are located on one side of the molecule with the hydrophobic residues on the opposite side, creating the amphipathic structure.<sup>152,153</sup> These molecules have been shown to display pore-forming characteristics and have striking selectivity for prokaryotic rather than eukaryotic cells.<sup>154</sup>

Cecropins and cecropin analogues have a broad spectrum of activity, including gram-positive (eg, *Bacillus* species) and gram-negative (eg, *Pseudomonas aeruginosa*, *Salmonella typhimurium*, and *Acinetobacter calcoaceticus*) bacteria as well as fungi and parasites.<sup>52,142,143,155-160</sup> In addition to their microbicidal activity, the cecropins and synthetic analogues demonstrate markedly increased cytolytic activity against transformed cells (eg, tumor cells) as opposed to normal cells.<sup>161,162</sup>

## **ANTIMICROBIAL PEPTIDES AND OPHTHALMOLOGY**

The application of peptide antimicrobial agents in ophthalmology has been limited, although the theoretical promise of these agents in the management of corneal infection is great, given the accessibility of drug to the site of infection, rapid action, zwitterionic character for transport in biphasic corneal tissues, and potential for well-tolerated, high concentrations at the cornea. In addition, theoretically, the presence of active antimicrobial proteins such as lysozyme and lactoferrin on the ocular surface suggests that this surface has a rather low level of proteolytic enzyme activity. Moreover, the corneal epithelium is negatively charged, a circumstance that should enhance the activity of the positively charged peptide molecules. However, the majority of research on the antimicrobial peptides has remained in the sphere of structure and function, with only a relatively limited effort focused on clinical application.

For more than a decade, our laboratory has investigated the effectiveness of a variety of peptides on ocular pathogens as well as their use in the prevention of contamination in ophthalmic systems. In the following paragraphs, we will review the work that has been done with antimicrobial peptides both in our laboratory and in other centers.

### **DEFENSINS**

In 1988, the Cornea Research Laboratory in collaboration

with the Dairy Food and Safety Laboratory at the University of California, Davis, initiated the defense peptide project to explore ophthalmic applications for the defensins. The defensins constitute candidates with great potential as potent, broad-spectrum, natural antimicrobial agents. Their size, structure, and biochemical configuration suggest that they would be prime candidates for synthetic reproduction and use as biocidal agents.

Cullor, Mannis, and colleagues<sup>127,163</sup> demonstrated the effectiveness of two rabbit defensins, NP-1 and NP-5, against isolates from clinical ocular microbial infections in humans and horses. They showed for the first time the effective microbicidal activity of NP-1 (10  $\mu\text{g}/\text{mL}$ ) against all ocular pathogenic isolates tested (*Candida albicans*,  $\alpha$ -hemolytic *Streptococcus*, *Streptococcus pneumoniae*, *P aeruginosa*, and *Morganella morganii*), effecting a 2- to 3-log<sub>10</sub> (99% to 99.9%) reduction within a 60-minute incubation. NP-5, however, differed markedly, having little bactericidal activity but significant bacteriostatic activity against the isolates tested.

Mannis and colleagues<sup>164</sup> investigated the efficacy of NP-1 for antimicrobial activity against *S aureus*, *P aeruginosa*, and *S pneumoniae* in modified corneal storage media (Optisol without antibiotics) at 4°C, 23°C, and 37°C and demonstrated that at 100  $\mu\text{g}/\text{mL}$ , NP-1 successfully reduced *S pneumoniae* and *S aureus* at all temperatures, while a higher level (200  $\mu\text{g}/\text{mL}$ ) was required for killing *P aeruginosa*, suggesting that the defensin might be a potential additive for the prevention of contamination of corneal storage media.

Murphy and colleagues<sup>140,165</sup> demonstrated that the rabbit defensin NP-1 possesses significant growth factor activity in a serum-free in vitro cell culture system utilizing lens and corneal epithelial cells, suggesting that at the same concentrations at which NP-1 exhibits maximal antibacterial effects, it may also promote epithelial cell growth. This finding stimulated interest in the notion that this substance might perform two functions—antimicrobial debridement and the promotion of wound healing.

### **CECROPINS**

The cecropins have been investigated in a variety of contexts and combinations in ophthalmology.

Gunsheski and colleagues<sup>159</sup> first demonstrated the antimicrobial activity of cecropin analogs against isolates from clinical ocular microbial infections in humans. In this in vitro experiment, the investigators demonstrated greater than 3-log reduction of a panel of test pathogens, including *P aeruginosa*, *S aureus*, *S pneumoniae*, and *C albicans*, with exposure of the organisms to Shiva-11, a synthetic cecropin analogue, in the range of 10 to 100  $\mu\text{g}/\text{mL}$ . They demonstrated dose-dependent effectiveness of the

cecropin analogue against the test panel and found that solutions containing divalent cations appeared to diminish antimicrobial activity of the peptide. They theorized that the cation stabilized cell membranes, thereby inhibiting the activity of the peptide.

The same synthetic analogue was studied by Mannis and colleagues<sup>166</sup> as an antibacterial agent in preservative-free timolol and contact lens solutions. The investigators demonstrated that Shiva-11 effected greater than a 2.5-log reduction of test pathogens, including *P aeruginosa*, *S epidermidis*, and *S aureus*, in either buffered saline containing a contact lens or in preservative-free timolol, and they suggested its use as a novel ophthalmic preservative.

De Sousa and colleagues<sup>55,167</sup> evaluated a cecropin analogue (D<sub>5</sub>C) to compare the antimicrobial efficacy of the peptide against *P aeruginosa* with that of commercially available contact lens disinfecting solutions. The investigators inoculated various concentrations of bacteria into the contact disinfecting solutions and into buffered saline as a control. Samples were incubated, and at various time points, aliquots were removed and were plated and subcultured on nutrient agar. At 72 hours, all contact lens solutions tested produced greater than a 2-log reduction of the organism. However, the addition of D<sub>5</sub>C to the contact lens solutions yielded greater than 3 logs killing with a larger inoculum of bacteria and with a contact lens in the solution. The investigators demonstrated that D<sub>5</sub>C effectively augmented antimicrobial activity of the disinfecting solutions.

Schwab and colleagues<sup>168</sup> examined the effectiveness of two peptides (D<sub>5</sub>C and Nisin) against *P aeruginosa*, *S epidermidis*, *S pneumoniae*, and *C albicans* in modified corneal storage media (Optisol without antibiotics). The investigators were unable to demonstrate peptide activity in any of the testing situations at either 4°C or 27°C, although the addition of EDTA augmented killing of *P aeruginosa* in the test system.

In an extensive study of the cecropin analog D<sub>5</sub>C, de Sousa and colleagues<sup>169</sup> evaluated the efficacy of the peptide in both contact lens sterilization and corneal storage media against *P aeruginosa*, *Serratia marcescens*, *S aureus*, *S epidermidis*, *S pneumoniae*, and *C albicans*. She concluded the following:

- In concentrations greater than 5 µg/mL, the peptide demonstrated antimicrobial activity against all the pathogenic species tested, with greater than a 3-log reduction after 30 minutes of exposure to the peptide in vitro in phosphate buffered saline.
- Antimicrobial activity was dose- and exposure-dependent in phosphate buffered saline.
- At the concentration of 100 µg/mL, D<sub>5</sub>C demonstrated significant antimicrobial activity against the panel 24 hours after exposure and augmented the activity of commercial solutions.
- The peptide did not demonstrate antimicrobial activity

against the test panel in corneal preservation media (Optisol) independent of the temperature.<sup>55</sup>

Gunsheski and colleagues<sup>169</sup> demonstrated that the cecropin analog Shiva-11 (100 µg/mL) was effective against highly gentamicin-resistant organisms in vitro. Gruzensky and colleagues<sup>170</sup> evaluated the effectiveness of a synthetic cecropin analog (Hecate) in an in vitro culture of *Acanthamoeba* species (*A castellani* and *A polyphaga*). This study compared the cecropin analogue with the anti-amoebic activity of bovine neutrophil peptide (BNP-1), propamidine isethionate (Brolene), and neomycin, and demonstrated the cysticidal effect of the cecropin analogue between 250 and 500 µg/mL, with partial inhibition of organisms down to 50 µg/mL.

Murphy and colleagues<sup>171</sup> demonstrated that the cecropin analogue (Shiva-11) was mitogenic for corneal epithelial cells and fibroblasts in culture. This finding that cecropin, in specific dose ranges, possesses growth factor activity in a serum-free in vitro cell culture system suggested that it might be useful as both an antimicrobial and a wound-healing agent.

Nos-Barbera and colleagues<sup>186</sup> used an experimental rabbit model of *Pseudomonas keratitis* to investigate the antimicrobial characteristics of a hybrid peptide consisting of cecropin residues and melittin residues. Melittin is the main cytotoxic component of the *Apis mellifera* honeybee and is known to interact with lipid membranes. The hybrids demonstrated antimicrobial activity comparable to that of the parent compounds without the undesirable cytotoxicity of melittin to eukaryotic cells. Purified peptides of 18, 15, and 12 residues were compared with the antimicrobial effectiveness of 0.3% gentamicin and showed equal antimicrobial activity against both a clinical isolate and an ATCC strain of bacteria. This study confirmed in vivo the results of previous in vitro studies that demonstrated the broad antimicrobial spectrum of hybrid peptides.<sup>186</sup>

## EXPERIMENTAL DESIGN AND RATIONALE

In the present set of experiments, we endeavored to select an appropriate candidate peptide from a potential field of millions of peptides for testing against a panel of pathogens chosen for their frequency as causes of clinical keratitis in the United States. To achieve this selection, we turned to newly available computer technology for the design and choice of peptides. We elected to test these peptides in three settings: (1) in vitro, in a highly controlled system for performing quantitative microbiology, (2) in corneal storage media—a controlled system with direct relevance to corneal preservation and transplantation, and (3) in an in vivo animal model designed to assess both clinical outcomes of therapy and quantitative microbiological evaluation.

#### SELECTION OF A CANDIDATE PEPTIDE

In the vast majority of previous studies in which the rationale was the application of peptides for the testing of antimicrobial activity, researchers have worked with a candidate peptide primarily on the basis of its availability and its demonstrated in vitro spectrum of activity. The substances have either been extracted from cells or sequenced, synthesized and, in many cases, modified in order to make a synthetic peptide analogue that would theoretically demonstrate enhanced microbicidal activity. This methodology, employed by our laboratory as well as many others over the years, is limited by both availability and spectrum. That is, the candidate peptide chosen, one of potentially millions of candidates, may not be the optimal substance for the desired application and spectrum of activity. We concluded that random selection of peptides in this fashion would ultimately fail.

Therefore, for the purposes of the present research, we elected to determine the “best fit” candidate peptide according to a proprietary methodology for computational drug design devised by CyberChemics, Inc (Huntsville, Alabama). This approach is based on the use of powerful hardware- and software-based methods employing neural networks, artificial intelligence, and genetic algorithms for high-speed pattern recognition geared to identify the non-intuitive or hidden spatial pattern underlying the atoms that make one drug more effective than another. Representing a type of “computational genetic breeding,” the methodology promotes marked acceleration of the screening process for potential candidate peptide selection by the medicinal chemist. The proprietary hardware is based on a parallel processor chip that allows the screening to be performed at supercomputer speeds. This technology adds to traditional in vitro and in vivo screening what CyberChemics, Inc, has termed “in vitro” screening—a computational candidate peptide selection that enhances the traditional screening process by eliminating millions of less effective conformational structures and limits the number of compounds that actually require synthesis and testing. Using such technology,  $10^{18}$  (a billion billion) small molecular building blocks can be scanned to produce a selection of the 100 most probable candidates for synthesis and testing. This novel method of combinatorial chemistry affords the ability to both diversify and select the most probable active sequences by using specially designed computer algorithms. In this way, extremely rapid identification, synthesis, and testing of therapeutic agents for infectious diseases can be achieved. Utilizing these methods, CyberChemics, Inc, has collected a library of over a million antimicrobial agents, a subset of which have been synthesized and tested, demonstrating inhibitory concentrations against significantly resistant infectious organisms.

The selection method uses a suite of pattern recognition algorithms that sort through viable substitutions in antimicrobial peptides. This search strategically selects substitutions that have occurred previously in molecular evolution (eg, in marine, amphibian, reptilian, mammalian, and avian peptides). The algorithm uses this substitution strategy to enhance the synthetic peptides with respect to their pharmacokinetics, bioavailability (predominantly hydrophilicity), resistance to proteases, and reduction of molecular weight.

CyberChemics, Inc, de novo peptides have been tested against *Escherichia coli*, *P aeruginosa*, *Enterobacter cloacae*, *Klebsiella pneumoniae*, *Salmonella typhimurium*, *S aureus*, *S epidermidis*, *Aspergillus fumigatus*, and *C albicans*, among others. In addition, the technology has been applied to the development of peptide sequences that act as HIV-1 and hepatitis C virus protease inhibitors for the treatment of acquired immunodeficiency syndrome and hepatitis C.

For the present experiments, we used two CyberChemics, Inc, peptide sequences that were chosen on the basis of specification of organisms that are most commonly encountered in cases of human microbial keratitis in the United States. From a potential screening pool of 100 compounds, these compounds represented a cross section of sequence diversity with an available spectrum of biologic activity primarily against *Pseudomonas* species. The compounds were chosen with use of the algorithm according to behavior criteria, including bioavailability, potency, toxicity, and hydrophobicity. The activity of these peptides was reported by in 1998 (Noever D. Neural network for predicting ophthalmically relevant log P [octanol/water partition coefficients] for peptide antimicrobials. NCI Developmental Therapeutics Program. 1998 Western Multiconference, January 1998, San Diego, California).

Extensive evidence in the antimicrobial peptide literature demonstrates that the use of naturally occurring peptides (retrieved by extraction and purification) is both more expensive and less practical than the use of synthetically derived and optimized compounds. Both quantity and purity can be maximized by using synthetic techniques. There are currently no published data that directly compare the activity of the compounds used in this study with naturally occurring antimicrobial peptides.

The first group of these compounds was used in our in vitro microbial assay system as well as in corneal preservation media. Designated as CCI A, B, and C, the sequences of the compounds are as follows:

CCI A: LVLLKLLMKKYKLLKLLGGL  
CCI B: LLLLKLLKKNPKLKKLIGV  
CCI C: LLLLKLLKLMNLLKLLGHY

The second compound is designated as COL-1, and the amino acid sequence is as follows:

COL-1: LVLLKKLMMKKYKLLKLLGGL

(Note: The amino acid key is as follows: A = alanine; C = cysteine; D = aspartic acid; E = glutamic acid; F = phenylalanine; G = glycine; H = histidine; I = isoleucine; K = lysine; L = leucine; N = asparagine; P = proline; R = arginine; S = serine; T = threonine; V = valine; W = tryptophan; Y = tyrosine.)

#### SELECTION OF A PANEL OF PATHOGENS

Microbes used in this study were selected from a panel of human clinical ocular isolates from severe cases of bacterial keratitis managed in the Department of Ophthalmology, University of California, Davis, and maintained by the Microbiology Laboratory and by the Dairy Food and Safety Laboratory, School of Veterinary Medicine, University of California, Davis. The test panel of human clinical isolates maintained by our microbiology laboratory includes *P aeruginosa*, *M morgani*, *S pneumoniae*,  $\alpha$ -hemolytic *Streptococcus*, *S aureus*, *S epidermidis*, and *C albicans*.

The frequency of an organism as an ocular pathogen is modulated to some extent by local climate, the age of the population affected, and whether the country is a developing nation.<sup>30</sup> About 90% of cases of bacterial keratitis in the United States are caused by one of four groups of organisms: (1) *P aeruginosa*, (2) *S aureus* and *Micrococcaceae*, (3) *S pneumoniae*, and (4) *Enterobacteriaceae*.<sup>174</sup> *P aeruginosa* accounts for 8% to 23% of cases of bacterial keratitis in the United States, but this rate increases to 40% to 75% of the cases in contact lens wearers, while about 25% are due to *S aureus*, *S pneumoniae*, and other gram-positive cocci.<sup>175,176</sup>

*Pseudomonas* keratitis is one of the most serious corneal infections and represents one of the most threatening bacterial infections of the eye. Although it can be seen in specialized populations such as farmers and coal miners, the most common context is the population of contact lens wearers, where the infection results from an inoculum of microbes to the corneal surface in which the integrity of the epithelium has been breached. Because of its aggressive behavior and the frequency and context in which it occurs, *P aeruginosa* was chosen as the primary target pathogen in this study. *S aureus* was used as a test pathogen likewise because of its frequency as a clinical pathogen. *S epidermidis* is uncommonly a clinical corneal pathogen; however, its common presence at the ocular surface and its occasional conversion to an opportunist led to its selection as a comparison test organism. Because of the significant difficulties of managing the fastidious *S pneumoniae* in culture systems—a problem that makes bacterial quantification more difficult in the context of a quantitative, longitudinal study—we elected not to include

this organism in the panel.

#### DEVELOPMENT OF AN IN VIVO MODEL OF EXPERIMENTAL BACTERIAL KERATITIS

A number of animal models of microbial keratitis have been described in the past decade for reproducible evaluation of the pathogenesis of corneal infections and potential treatment regimens.<sup>177-192</sup> After experimentation with a number of different models, we developed a model that reliably produced a keratitis using conditions that simulate the clinical setting. This model combines a standardized epithelial defect, a single stromal crosshatch to ensure an interstice for the attachment of bacterial pathogens, and a standardized topical inoculum of bacteria. The procedure is described in detail in the “Materials and Methods” section under “In vivo experiments.”

#### MATERIALS AND METHODS

##### IN VITRO EXPERIMENTS

We tested the antimicrobial peptides COL-1 and CCI A,B, and C against the following organisms: *P aeruginosa*, *S aureus*, and *S epidermidis*. The organisms were human ocular (HO) isolates obtained from cases of severe human keratitis, cultured and stored by our microbiology laboratory. The assay employed is a quantitative microbial killing assay based on the principle that the precise amount of bacterial killing can be accurately determined only if one starts with a known quantity of organisms. This protocol allows one to obtain a stock solution of  $1 \times 10^6$  colony-forming units per milliliter (CFU/mL) in the incubation mixture.

##### Preparation of Bacteria in Log Phase of Growth

Twenty-four hours prior to the assay, we removed 2 to 5 well-isolated colonies of the desired organism from a blood agar plate and inoculated a bottle containing 40 mL of trypticase soy broth (TSB). This was incubated for 18 to 24 hours at 37°C. A 1-mL aliquot of the incubated TSB was then added to a bottle of sterile TSB and allowed to incubate in a shaking water bath at 37°C until the spectrophotometric optical density (OD) at 580 nm had increased tenfold, indicating that the bacteria were in log-phase growth (Figure 2).

The 40-mL suspension of bacteria was then centrifuged, washed with 10 mM sodium phosphate buffer (pH 7.4) twice, and resuspended in 10 to 15 mL of 10 mM sodium phosphate buffer (pH 7.4) (Figure 3).

The spectrophotometer (Beckman Du-50, Beckman Instruments, Fullerton, California) at 580 nm was used to verify a preparation of  $1 \times 10^7$  CFU/mL by comparison of the optical density to known standards.

##### Peptide Addition to Stock Solution

Ten microliters of this “stock” solution of bacteria was then

added to the test tubes containing 80  $\mu\text{L}$  of 10mM sodium phosphate buffer (pH 7.4) and 10  $\mu\text{L}$  of the antimicrobial peptide (COL-1 in 0.5% methylcellulose and 0.05% EDTA) at a specified concentration (Figure 4).

In the test circumstance, therefore, the bacterial concentration was  $1 \times 10^6$  CFU/mL. The diluted solution was plated onto trypticase soy agar (TSA) plates at 0, 30, and 60

minutes. Each test was matched with a control tube that did not contain the peptide but did contain the solvent in which the peptide was dissolved. Control tubes contained 10  $\mu\text{L}$  of bacterial suspension, 80  $\mu\text{L}$  of 10 mM sodium phosphate buffer (pH 7.4), and 10  $\mu\text{L}$  of peptide solvent. A test tube and a control tube were prepared for incubation at each of three temperatures: 4°C, 23°C, and 37°C (ie,

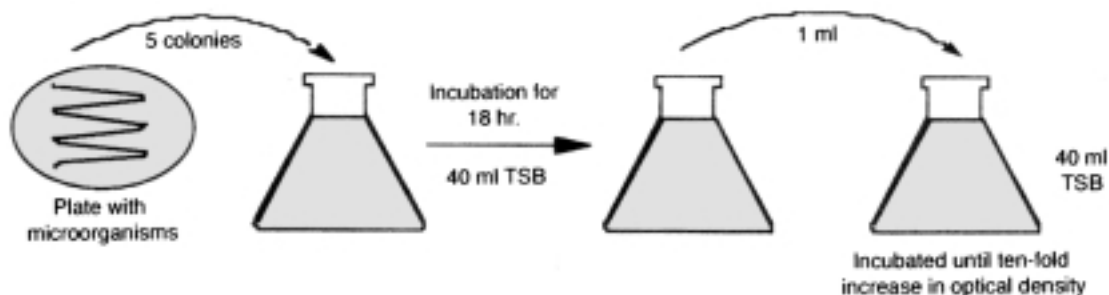


FIGURE 2  
Preparation of a solution to achieve a suspension of bacteria in log-phase growth.

Adapted from de Sousa.<sup>55</sup>

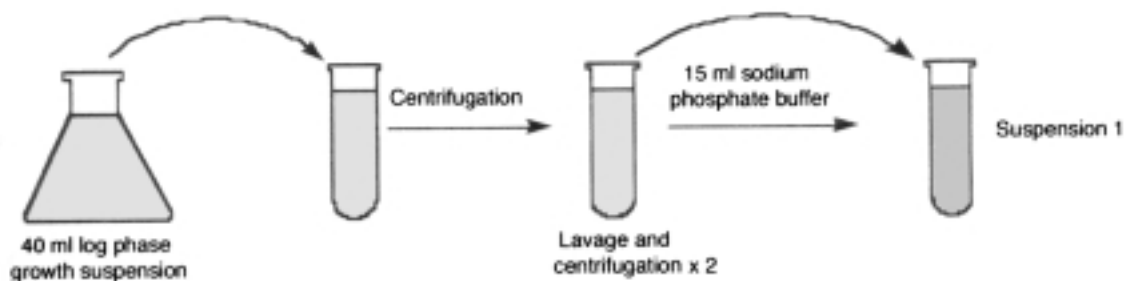


FIGURE 3  
Centrifugation and resuspension of log-phase organisms prior to spectrophotometric density verification

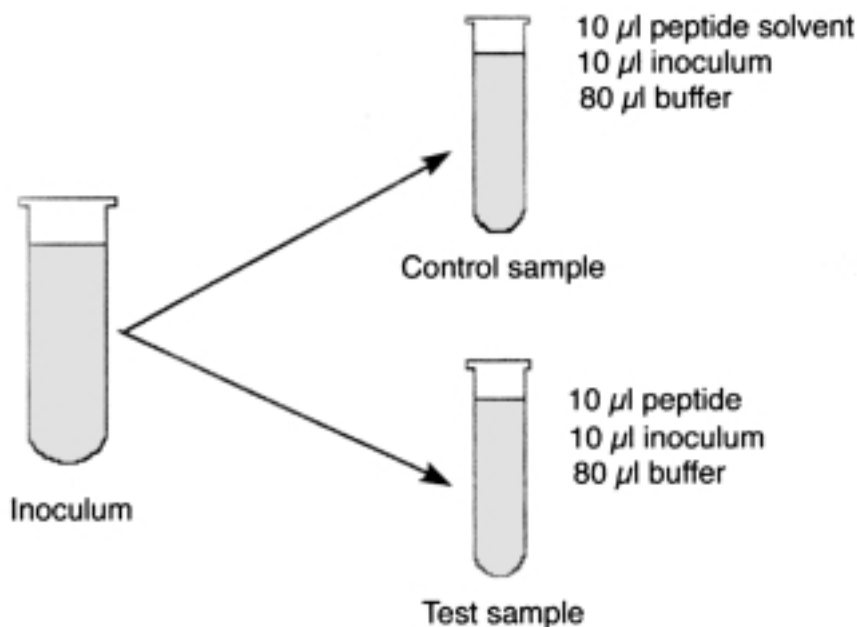


FIGURE 4  
Preparation of control and test samples.

the temperature at which corneal storage media is maintained, room temperature, and standard incubation temperature).

#### Quantitative Microbial Assay

At specified time points, 10  $\mu\text{L}$  of test solution was removed and diluted 100-fold in 10 mM sodium phosphate buffer (pH 7.4). The dilution sample was plated in duplicate with a spiral plater (model D, Spiral System Instruments, Bethesda, Maryland) (Figure 5) onto TSA plates, which were incubated at 37°C for 18 to 20 hours, a period suitable for obtaining an adequate colony growth for quantitative analysis.

The spiral plater is a device that accurately distributes a liquid sample onto the surface of a rotating agar plate for the purposes of precise bacterial enumeration and antimicrobial susceptibility testing (Figure 6). A specific aliquot of solution (test or control) is drawn into the plater and deposited on the surface of a rotating agar plate. The volume deposited is controlled by a cam-activated syringe and decreases logarithmically with distance from the center of the plate. In this fashion, we were able to achieve a precise distribution that affords extremely accurate colony counts. Counts were completed automatically by the Synoptics Protos Plus Colony Counter (Microbiology International, Frederick, Maryland) (Figure 6). This device works by producing a video image of the agar plate and projecting this image onto a computer monitor. The colonies to be counted are then highlighted and counted automatically by the software program.

The instrument takes into account the dilution of the material plated and provides an accurate count of CFU/mL. At the conclusion of these procedures, we had determined a CFU/mL value for test and control solutions at 0, 30, and 60 minutes and at 4°C, 23°C, and 37°C for each concentration of peptide. From these values and our determination of the initial concentration, we used a formula ( $\log [N \text{ CFU of control}/N \text{ CFU of test}]$ ) to calculate the log reduction for each sample. (Note: With use of the spiral plater system and Protos colony counter, there is a theoretical lower limit of detection of  $1.02 \times 10^3$  CFU/mL.) Figure 7A demonstrates the three test-panel organisms after distribution by the spiral plater and incubation

Figure 7B demonstrates the comparative results of sample plates without exposure to the antimicrobial peptide (left) and with exposure to the antimicrobial peptide, COL-1 (right).

#### CORNEAL PRESERVATION MEDIA EXPERIMENTS

We tested the antimicrobial peptides CCI A, B, and C against the following organisms: *P aeruginosa*, *S aureus*, and *S epidermidis*. The methods were identical to those described previously with the following exceptions: (1) when a solution with a concentration of  $1 \times 10^6$  CFU/mL

was achieved, the stock solution was then added to test tubes containing 80  $\mu\text{L}$  of Optisol modified by the exclusion of antibiotics (Bausch & Lomb, Irvine, California) and 10  $\mu\text{L}$  (200  $\mu\text{g}/\text{mL}$ ) of the antimicrobial peptide (CCI A, B, or C); (2) experiments were performed at 4°C and 23°C only; and (3) exposure times were extended to include time points at 90 and 120 minutes, owing to the extended time that corneas are stored in preservation media. In addition, the experiments were repeated using the test organism (10  $\mu\text{L}$ ), Optisol (70  $\mu\text{L}$ ) with 100 mM EDTA (10  $\mu\text{L}$ ), and peptide (10  $\mu\text{L}$ ).

#### IN VIVO EXPERIMENTS

This phase of the project was designed to determine the antimicrobial efficacy of COL-1 when applied topically to an experimentally induced *P aeruginosa* keratitis. (All experimental animals were managed and cared for under approved institutional review board guidelines by the Animal Resources Department at the University of California, Davis. These guidelines adhered to the principles for animal experimentation of the Association for Research in Vision and Ophthalmology.)

#### Preparation of *Pseudomonas aeruginosa*

Two to 5 colonies of *P aeruginosa* (HO-31) were selected from a pure culture plate for inoculation into 40 mL of TSB. This culture was incubated for 18 hours at 37°C, yielding approximately  $1 \times 10^9$  CFU/mL as determined by previous counts. Ten microliters of the overnight culture was diluted into 990  $\mu\text{L}$  of 10 mM sodium phosphate buffer (pH 7.4) to achieve a concentration of  $\approx 1 \times 10^7$  CFU/mL. A Hamilton microliter syringe was used to deliver two 10- $\mu\text{L}$  aliquots of this “stock” solution to the cornea, resulting in an approximate delivery to the cornea of  $2 \times 10^5$  total CFU.

#### Method of Inoculation

Each rabbit received a subcutaneous injection consisting of a mixture of xylazine hydrochloride (15 mg) and ketamine hydrochloride (125 mg). Once the rabbit was sedated, we placed 2 to 3 drops of proparacaine hydrochloride ophthalmic solution (USP 0.5%) on the right eye of the animal, and a lid speculum was introduced. Under observation with the operating microscope, a 6.5-mm trephine was used to demarcate a central area for de-epithelialization. The epithelial layer of cells was removed with a No. 15 surgical blade, exposing the stroma. A superficial crosshatch (“X”) was scored into the anterior stroma with a 22-gauge needle. Once the site for inoculation was prepared, two 10- $\mu\text{L}$  aliquots of the stock solution were dropped onto the prepared surface with the Hamilton syringe (20 to 30 seconds between doses).

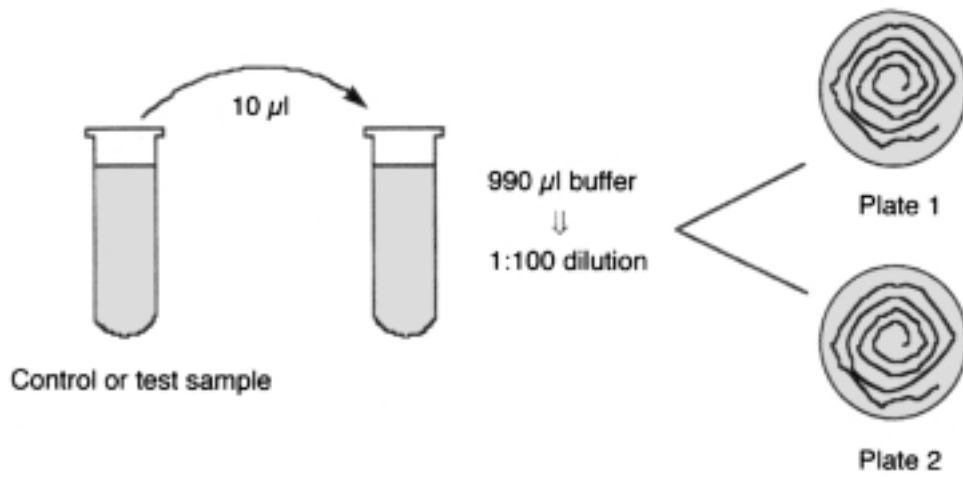


**FIGURE 5**  
Diluted samples are placed on solid agar using the spiral plater.



**FIGURE 6**  
Spiral plater system (left). Protos plate reader (right).

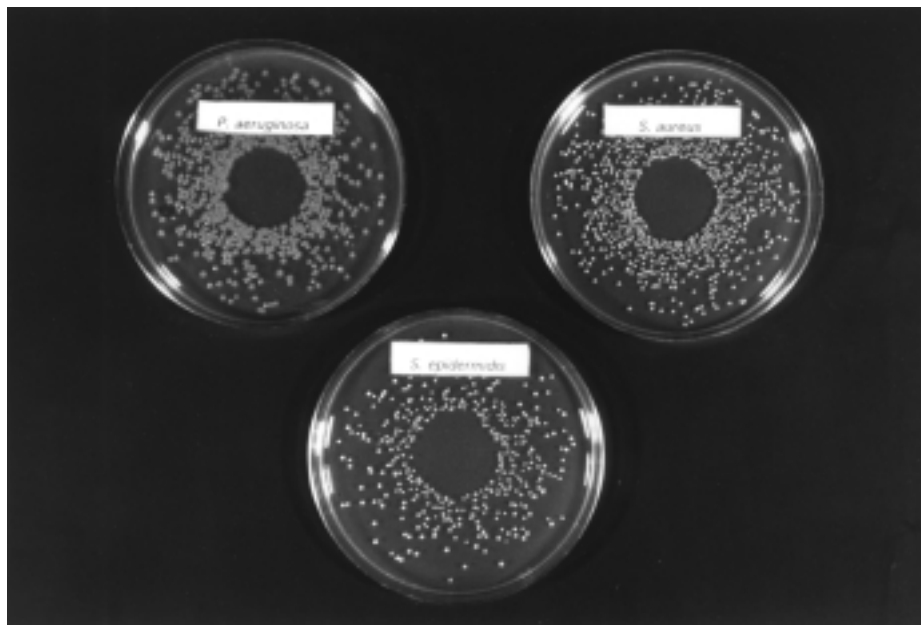
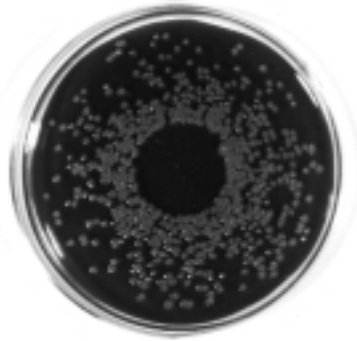


**FIGURE 7A**  
The 3 test organisms at T=0.

*P. aeruginosa*

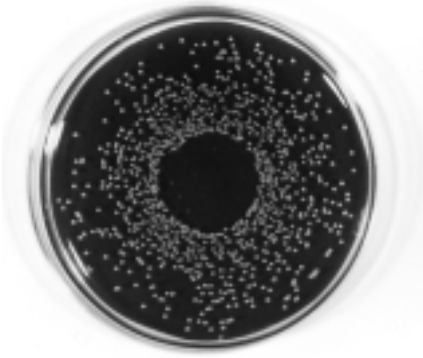


Control



Test

*S. aureus*

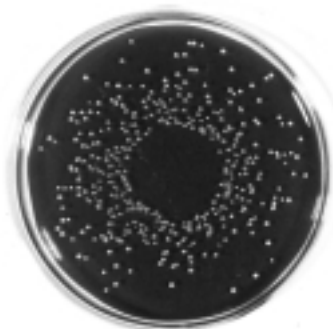


Control



Test

*S. epidermidis*



Control



Test

FIGURE 7B

Control and test plates demonstrating the activity of peptide COL-1 versus the three test organisms in this study: *P. aeruginosa* (top), *S. aureus* (middle), and *S. epidermidis* (bottom).

*Treatment Schedule*

The inoculum was allowed to incubate for 12 to 14 hours prior to initiation of treatment. The treatment schedule was as follows (except as noted):

- Day 1: One drop (containing either a specified concentration of COL-1, 10 or 50 µg/mL; tobramycin 0.3%; or 0.5% methylcellulose and .05% EDTA) every 15 minutes for the first hour, followed by 1 drop every hour for the next 9 hours. Dosage amounts of either 10 µg/mL or 50 µg/mL were chosen, since they represented the lowest effective in vitro dose and the highest dose that was not toxic to test animals in the toxicity trials.
- Days 2 through 4: One drop every hour for 10 hours. (Note: For the initial in vivo experiments, the treatment schedule differed slightly. Infection was allowed to incubate for 24 hours before treatment was initiated. The treatment schedule for days 1 through 3 was 1 drop every hour for 10 hours, and for days 4 through 6, 1 drop four times a day, 8 AM to 5 PM.)

*Observation*

During the treatments, conjunctival hyperemia, discharge, corneal opacification and suppuration, and general behavioral responses were observed and recorded.

*Euthanization*

At the conclusion of the test period, each rabbit received a mixture of 15 mg xylazine hydrochloride and 125 mg ketamine hydrochloride subcutaneously. Once anesthetized, each rabbit received an intracardiac injection of sodium pentobarbital (390 mg/mL).

*Microbiological Analysis*

A corneal-scleral button was excised from the right globe, and an 8-mm button was punched on a Teflon dish and placed into 2 mL of 10 mM sodium phosphate buffer (pH 7.4). The tissue was then homogenized using a Powergen 125 (Fisher Scientific) tissue homogenizer. The homogenate was centrifuged at 700g (1,500 rpm) for 7 minutes and the supernatant removed. Three 1:100 serial dilutions of the supernatant were made in 10 mM sodium phosphate buffer (pH 7.4), and each dilution plus an undiluted sample of the supernatant was plated on TSA plates in duplicate using the spiral plater. The plates were incubated for 18 to 20 hours at 37°C.

**EX VIVO TOXICITY STUDIES**

Because certain animals demonstrated inflammation, which the investigators thought was related directly to the peptide instillation, we performed ex vivo toxicity studies on the corneal endothelium using sheep corneas and a range of peptide concentrations.

Whole sheep globes were obtained from freshly slaughtered animals (Superior Farms, Dixon, California). Testing procedures were performed within 2 to 4 hours after harvesting of the globes. The corneas were excised using corneal-scleral scissors with care taken not to contact the corneal endothelium or to fold or compress the tissue. Corneal scleral buttons were then placed epithelial side down in a Teflon dish and exposed to COL-1 at concentrations of 25, 50, and 100 µg/mL for 15 seconds or 60 seconds. Control corneas were exposed to carrier substances alone, including phosphate buffered saline (PBS), pH 7.4; 0.5% methylcellulose and 0.05% EDTA; and 10 mM sodium phosphate buffer (pH 7.4). Immediately after exposure, corneas were gently rinsed in PBS and were stained using a vital staining technique with trypan blue and alizarin red. Vital staining was performed by exposing endothelium to 0.25% trypan blue for 90 seconds followed by a gentle rinse in PBS, after which alizarin red was applied for 45 seconds. Corneas were immediately examined under a light microscope equipped with a standardized grid for cell counting. Two grid blocks (~500 cells) placed over the central cornea were counted for each specimen, and an average count was determined. Between 3 and 6 repetitions were performed at each concentration of peptide. The results were expressed as a percentage of cells staining with trypan blue as an index of those cells with abnormal permeability.

**RESULTS**

**IN VITRO EXPERIMENTS**

*COL-1 Versus Human Ocular Isolates*

Results are expressed as log reduction in CFU/mL. Table V clarifies the relationship between log reduction and percent reduction of organisms. For example, a 3-log reduction represents eradication of 99.9% of bacterial growth.

Figures 8A, 8B, and 8C demonstrate the dose-response curves over time for *P aeruginosa* (HO-31), *S aureus* (HO-27), and *S epidermidis* (HO-29) at 37°C, 23°C, and 4°C, respectively. Each curve demonstrates reduction at times 0, 30, and 60 minutes for exposure to COL-1 at concentrations of 0.1, 1, 10, 25, and 50 µg/mL in 0.5% methylcellulose and 0.05% EDTA. Peptide in solution was added to 10 mM sodium phosphate buffer in which the microbial assay was performed. Given our

TABLE V: CORRELATION BETWEEN LOG REDUCTION AND PERCENT REDUCTION OF ORGANISMS

LOG REDUCTION	% REDUCTION
1-log	90%
2-log	99%
3-log	99.9%
4-log	99.99%

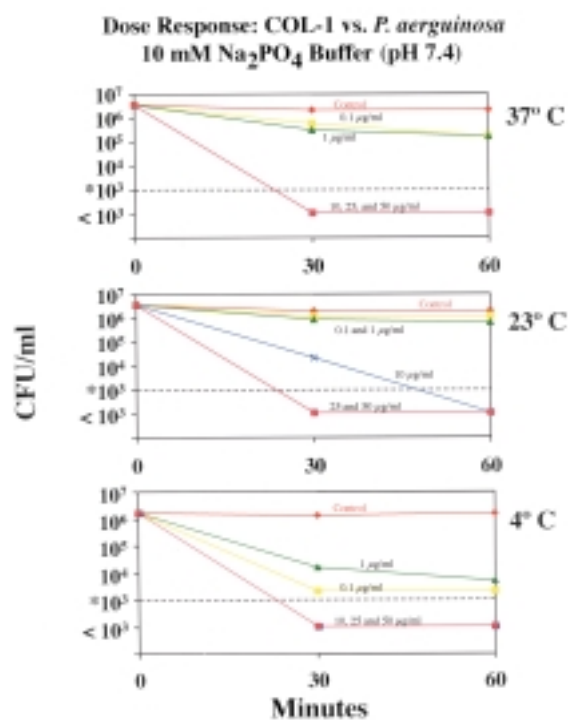


FIGURE 8A

Dose-response curve for COL-1 versus *P. aeruginosa* at 37°C, 23°C, and 4°C. Dashed line represents lower limit of detection for assay conditions. (Each curve is a representative graph of an experiment that was performed in triplicate.)

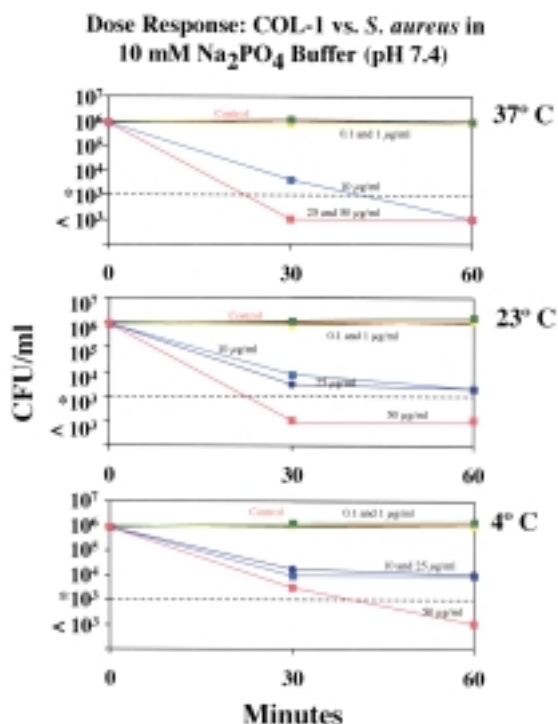


FIGURE 8B

Dose-response curve for COL-1 versus *S. aureus* at 37°C, 23°C, and 4°C. Dashed line represents lower limit of detection for assay conditions. (Each curve is a representative graph of an experiment that was performed in triplicate.)

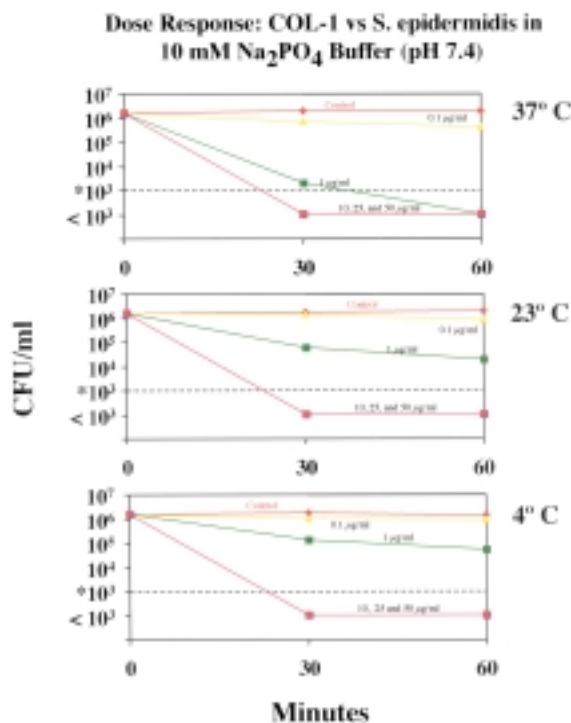


FIGURE 8C

Dose-response curve for COL-1 versus *S. epidermidis* at 37°C, 23°C, and 4°C. Dashed line represents lower limit of detection for assay conditions. (Each curve is a representative graph of an experiment that was performed in triplicate.)

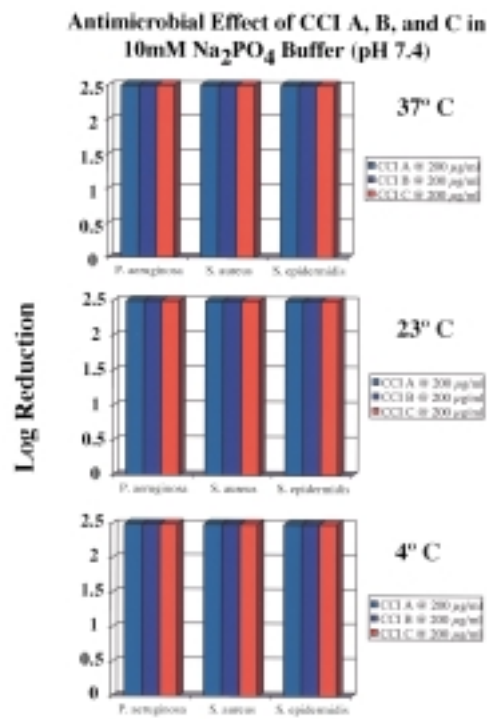


FIGURE 9

Log reduction induced by CCI A, B, and C against 3 test isolates at 37°C, 23°C, and 4°C in phosphate buffer.

lower limit of detection in this assay of  $1.02 \times 10^3$  CFU/mL, points denoted as  $<10^3$  CFU/mL represent plates with no colonies.

As indicated in Figures 8A, 8B, and 8C, for *P aeruginosa* and *S epidermidis*, there was greater than a 3-log reduction at 25 and 50  $\mu\text{g/mL}$  COL-1 at all temperatures tested. For *S aureus*, there was complete eradication with 50  $\mu\text{g/mL}$  at all temperatures. However, at 23°C, log reduction was less than 2.5 at 25  $\mu\text{g/mL}$  COL-1 but complete at 50  $\mu\text{g/mL}$ . At 4°C, complete reduction was not obtained against *S aureus*, but log reduction was 2.50 (>99% reduction). Although there is a significant decrease in organism count at lower peptide concentrations, there is, in general, a distinct fall-off of peptide activity between 10 and 25  $\mu\text{g/mL}$ , and at these lower levels, a total reduction is not obtained. The exceptions to this were *S epidermidis* at 37°C, where total eradication was obtained down to 1  $\mu\text{g/mL}$ , and *P aeruginosa* at 4°C, where total eradication was obtained down to 10  $\mu\text{g/mL}$ .

*CCI A, B, and C Versus Human Ocular Isolates (in 10 mM sodium phosphate buffer, pH 7.4)*

Figure 9 demonstrates the log reduction of CFU for *P aeruginosa* (HO-31), *S aureus* (HO-27), and *S epidermidis* (HO-29) at 37°C, 23°C, and 4°C, respectively. Results are expressed as log reduction (log killing) in CFU/mL. Each graph demonstrates killing of each organism using the three peptides CCI A, B, and C at concentrations of 200  $\mu\text{g/mL}$  in 10 mM sodium phosphate

buffer (pH 7.4). Peptide in solution was added to 10 mM sodium phosphate buffer in which the microbial assay was performed. Given our lower limit of detection in this assay, complete killing is represented as  $1.02 \times 10^3$  CFU/mL. Log reduction of 2.5 or more represents no colonies on the plates in this assay.

The peptide was effective in producing complete killing at this concentration at all three temperatures.

*CCI A, B, C in Modified Optisol*

Figure 10 demonstrates log reduction of bacterial CFU in modified Optisol (without antibiotics) at 4°C and 23°C employing CCI A, B, and C at 200  $\mu\text{g/mL}$  against three human ocular isolates.

These data demonstrate that *S epidermidis* was effectively reduced by each of the CCI compounds at 4°C, but that neither *S aureus* nor *P aeruginosa* was affected significantly by the peptide in modified Optisol. At 23°C, peptide antimicrobial activity was augmented against the gram-positive organisms but had no effect on *P aeruginosa*.

The experiment was repeated at both 4°C and 23°C in Optisol with the addition of 100 mM EDTA in order to determine if peptide activity could be augmented by this addition. Previous experiments have demonstrated that EDTA, which chelates calcium and other divalent ions, augments killing by destabilizing gram-negative bacterial cell membranes. Virtually all ophthalmic preparations are formulated with 0.05% to 0.1% EDTA as a preservative.<sup>193-195</sup>

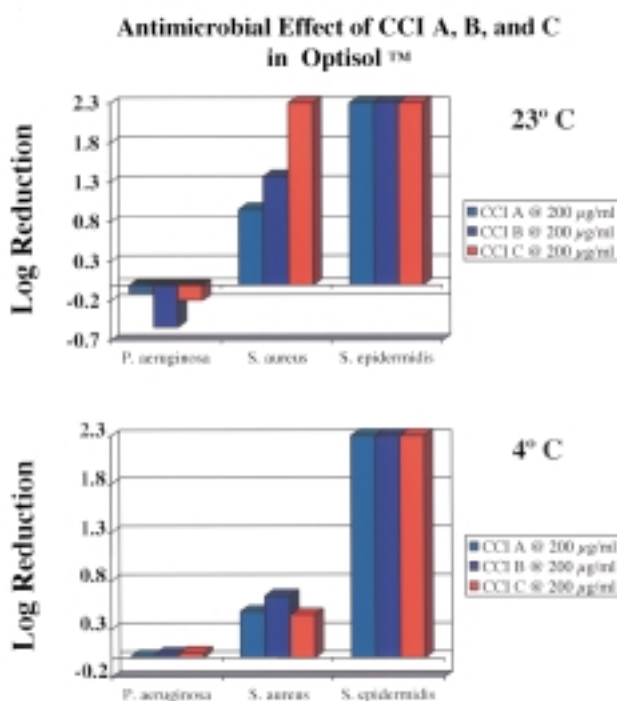


FIGURE 10

Log reduction induced by CCI A, B, and C against three test isolates at 23°C and 4°C in modified Optisol.

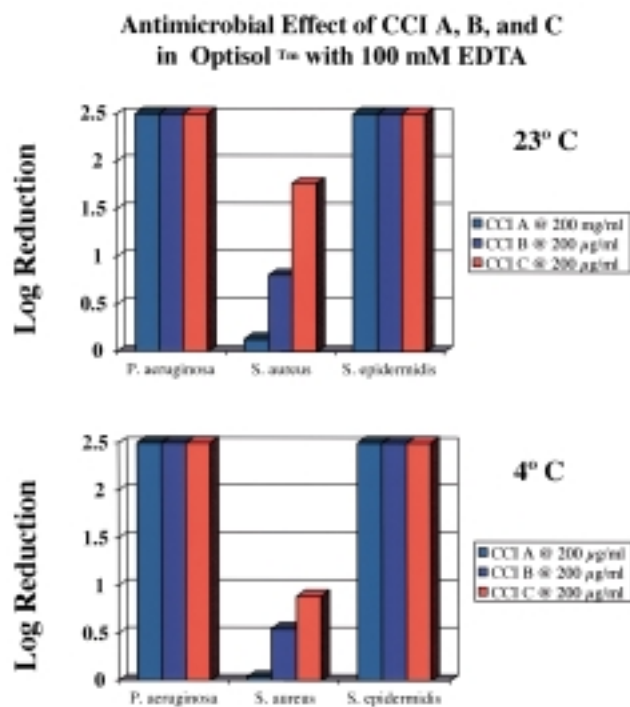


FIGURE 11

Log reduction induced by CCI A, B, and C against three test isolates at 23°C and 4°C in modified Optisol and EDTA.

### CCI A, B, C in Modified Optisol and EDTA

Figure 11 demonstrates the total log reduction of the same ocular isolates in modified Optisol and 100 mM EDTA at 4°C and 23°C. The data indicate that EDTA greatly augmented log reduction for *P. aeruginosa* but made no difference for the gram-positive organisms.

These data demonstrate that the addition of 100 mM EDTA to modified Optisol produced complete killing of *P. aeruginosa* at 4°C and 23°C but did not effectively augment killing of *S. aureus* at either temperature.

### IN VIVO EXPERIMENTS

To demonstrate the effectiveness of topical peptides in a reproducible model of bacterial keratitis, a total of 59 rabbits in a series of different experiments were employed to test COL-1 against induced *Pseudomonas* corneal infection.

Table VI demonstrates that COL-1 was not effective in either the clinical outcome or the quantitative microbial analysis when used in the in vivo model ( $P = .19-.51$ ). Since the two groups we compared were not independent and normally distributed populations, we could not use a standard *t* test for comparison; we therefore employed a non-parametric test (Wilcoxon rank sum test using the SAS/STAT program).

Because in the previous experiment there was no difference between test and control rabbits, we performed an experiment to demonstrate the growth curve of human ocular pathogens in our rabbit keratitis model. The purpose was to determine if we were missing an effect on account of natural attrition of the bacteria in the host cornea over time. We generated a longitudinal growth curve by inoculating rabbit cornea with a total of  $3.84 \times 10^5$  CFU. At 14 hours, two untreated rabbits were sacrificed to obtain a pretreatment CFU count at the end of the incubation period. Subsequently, at 24, 48, 72, and 96 hours, we euthanized two control (given only 0.5% methylcellulose and 0.05% EDTA) and 2 test rabbits (given 50 µg/mL COL-1 in 0.5% methylcellulose and 0.05% EDTA). Figure 12 demonstrates the growth curves of the

Longitudinal Growth Curve of  
*P. aeruginosa* In Vivo

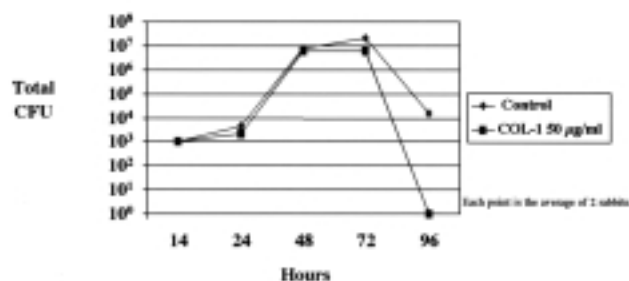


FIGURE 12

Longitudinal in vivo growth curves of *P. aeruginosa* in test and control animals over 96 hours.

*P. aeruginosa* in both test and control animals.

In either the treated or the untreated eye, bacterial counts begin to diminish naturally between 72 and 96 hours. This curve was generated so that this phenomenon of natural attrition could be separated from peptide effect, allowing us to interpret our results more accurately.

Table VII shows the results of treatment with 50 µg/mL of COL-1 in 0.5% methylcellulose and 0.05% EDTA compared with controls utilizing the methylcellulose carrier only and a control utilizing tobramycin 0.3%. All rabbits received an initial inoculum of  $4.05 \times 10^5$  CFU. The table shows that the tobramycin control was effective in eliminating both the clinical manifestations of the induced keratitis and the growth of bacteria. The activity of COL-1 showed no significant difference from the methylcellulose control in the quantitative assay ( $P = .33$ ). Clinically, the COL-1 test rabbits appeared to have more inflammation than the methylcellulose controls.

Table VIII presents the results of treatment with 50 µg/mL of COL-1 in 0.5% methylcellulose and 0.05% EDTA compared with controls utilizing the methylcellulose carrier only and a control utilizing tobramycin 0.3%. All rabbits received an initial inoculum of  $6.30 \times 10^5$  CFU.

This experiment demonstrates that the peptide was of

TABLE VI: COL-1 10 µG/ML EMPLOYED AGAINST PSEUDOMONAS KERATITIS (INOCULUM= $2.6 \times 10^5$  CFU/ML)

RABBIT	TEST/TREATMENT	CFU RECOVERED	OBSERVATIONS
1	COL-1 10 µg/mL <sup>o</sup>	150	Dense central corneal abscess
2	COL-1 10 µg/mL <sup>o</sup>	30	Diffuse conjunctiva, mildly dense central corneal infiltrate
3	COL-1 10 µg/mL <sup>†</sup>	100	Dense central infiltrate, pan corneal abscess
4	COL-1 10 µg/mL <sup>†</sup>	0	Mild central corneal infiltrate
5	0.5% Methylcellulose	100	Diffuse central abscess, dense paracentral infiltrate
6	0.5% Methylcellulose	10	Diffuse patchy infiltrate of the cornea
7	0.5% Methylcellulose plus 0.05% EDTA	150	Dense central corneal infiltrate
8	0.5% Methylcellulose plus 0.05% EDTA	170	Dense central corneal abscess

<sup>o</sup> Peptide in 0.5% methylcellulose.

<sup>†</sup> Peptide in 0.5% methylcellulose plus 0.05% EDTA.

TABLE VII: RESULTS OF TREATMENT WITH 50 µG/ML OF COL-1 IN 0.5% METHYLCELLULOSE + 0.05% EDTA COMPARED WITH CONTROLS UTILIZING THE METHYLCELLULOSE CARRIER ONLY AND CONTROLS UTILIZING TOBRAMYCIN 0.3%

RABBIT	TEST/TREATMENT	CFU RECOVERED	OBSERVATIONS
9	COL-1 50 µg/mL <sup>°</sup>	20	Small abrasion
10	COL-1 50 µg/mL <sup>°</sup>	1,070	Perforated, dense infiltrate
11	COL-1 50 µg/mL <sup>°</sup>	5,580	Perforated, dense infiltrate
12	COL-1 50 µg/mL <sup>°</sup>	874	Perforated, dense infiltrate
13	COL-1 50 µg/mL <sup>°</sup>	120	Perforated, dense infiltrate
14	COL-1 50 µg/mL <sup>°</sup>	14,100	Perforated, dense infiltrate
15	COL-1 50 µg/mL <sup>°</sup>	2,380	Perforated, dense infiltrate
16	COL-1 50 µg/mL <sup>°</sup>	3,660	Perforated, dense infiltrate
17	COL-1 50 µg/mL <sup>°</sup>	17,200	Perforated, dense infiltrate
18	Tobramycin	0	Small abrasion
19	Tobramycin	0	Small abrasion
20	Tobramycin	0	Small abrasion
21	Control†	0	Clear
22	Control†	5,020	Dense infiltrate
23	Control†	0	“X” score slightly visible
24	Control†	6,300	Perforated, dense infiltrate
25	Control†	40	Pin size abrasion
26	Control†	9,680	Dense infiltrate
27	Control†	4,920	Mild infiltrate
28	Control†	488	Perforated, dense infiltrate
29	Control†	0	2 pin size spots, mild injection

<sup>°</sup> Peptide in 0.5% methylcellulose plus 0.05% EDTA.

† Control in 0.5% methylcellulose plus 0.05% EDTA.

TABLE VIII: RESULTS OF TREATMENT WITH 50 µG/ML OF COL-1 IN 0.5% METHYLCELLULOSE AND 0.05% EDTA (BUFFERED) COMPARED WITH CONTROLS UTILIZING THE METHYLCELLULOSE CARRIER ONLY AND A CONTROL UTILIZING TOBRAMYCIN 0.3%

RABBIT	TEST/TREATMENT	CFU RECOVERED	OBSERVATIONS
30	COL-1 50 µg/mL <sup>°</sup>	0	Quiet, small abrasion
31	COL-1 50 µg/mL <sup>°</sup>	7,160	Injected, dense infiltrate
32	COL-1 50 µg/mL <sup>°</sup>	0	Injected, dense infiltrate
33	COL-1 50 µg/mL <sup>°</sup>	40	Injected, dense infiltrate
34	COL-1 50 µg/mL <sup>°</sup>	12,000	Dense infiltrate
35	Tobramycin	0	Quiet, “X” score slightly visible
36	Tobramycin	0	“X” score slightly visible
37	Control†	0	Quiet
38	Control†	23,400	Injected, dense infiltrate
39	Control†	0	Small abrasion
40	Control†	0	Small abrasion
41	Control†	0	Quiet, pin size abrasion

<sup>°</sup> Peptide in 0.5% methylcellulose plus 0.05% EDTA. (buffered)

† Control in 0.5% methylcellulose plus 0.05% EDTA. (buffered)

no advantage in the management of bacterial keratitis either clinically or microbiologically ( $P = .50$ ) and that, in fact, clinically, rabbits treated with the peptide demonstrated more inflammation than controls.

#### TOXICITY STUDY

Table IX demonstrates the results of the in vivo toxicity testing in which 1 drop of COL-1 (range, 10 to 3,000 µg/mL) was placed on the eye of a test rabbit every hour for 10 hours daily over a period of 4 days. Toxicity was

defined as diffuse conjunctival hyperemia. The trial was ended in any animal if hyperemia and edema were still present 24 hours after first initiating the medication.

Table X summarizes the results of the ex vivo endothelial toxicity studies in sheep corneas as indicated by vital staining of cells with trypan blue and alizarin red. We counted the percentage of cells demonstrating uptake of trypan blue as an indicator of cell wall damage.

These data demonstrate that COL-1 was toxic when directly applied to the corneal endothelium.

TABLE IX: RESULTS OF IN VIVO TOXICITY TESTING FOR A PREPARATION OF TOPICAL COL-1 (RANGE, 10-3,000  $\mu\text{G}/\text{ML}$ )

CONCENTRATION OF COL-1	TOXIC/NONTOXIC
10 $\mu\text{g}/\text{mL}$	Nontoxic
50 $\mu\text{g}/\text{mL}$	Nontoxic
100 $\mu\text{g}/\text{mL}$	Toxic
200 $\mu\text{g}/\text{mL}$	Toxic
380 $\mu\text{g}/\text{mL}$	Toxic
1,500 $\mu\text{g}/\text{mL}$	Toxic
3,000 $\mu\text{g}/\text{mL}$	Toxic

TABLE X: RESULTS OF EX VIVO ENDOTHELIAL TOXICITY STUDIES IN SHEEP CORNEAS

TREATMENT	TIME	AVERAGE % DAMAGE
COL-1 100 $\mu\text{g}/\text{mL}$	1 minute	37.4°
COL-1 50 $\mu\text{g}/\text{mL}$	1 minute	26
COL-1 50 $\mu\text{g}/\text{mL}$	15 seconds	21
COL-1 25 $\mu\text{g}/\text{mL}$	1 minute	16
PBS	1 minute	2.7
0.5% Methylcellulose + 0.05% EDTA	1 minute	2.5
10 mM $\text{Na}_2\text{PO}_4$ buffer (pH 7.4)	1 minute	7.9°

° Because supply of corneas was limited, only one test was done for treatments: COL-1 100  $\mu\text{g}/\text{mL}$  and 10 mM  $\text{Na}_2\text{PO}_4$  buffer (pH 7.4).

## DISCUSSION AND DATA ANALYSIS

The work outlined in this thesis is directed to the discovery and development of synthetic pore-forming antimicrobial peptides for use in the treatment of microbial keratitis and is a novel method of preventing contamination in preservation systems for corneal transplantation.

Bacterial keratitis is a cause of significant morbidity worldwide and can cause rapid and devastating visual loss.<sup>196</sup> While bacterial keratitis may be associated with poor hygienic conditions and endemic diseases such as trachoma in some parts of the world, in the United States it is linked in large part to contact lens wear. In the 29 million contact lens wearers in the United States, the incidence of bacterial keratitis is about 1 in 1,000. Typically, such keratitis is rapid in onset and may be very destructive to the host cornea and thus to visual function. An example is *Pseudomonas* keratitis, in which much of the early damage to the cornea is the result of proteases generated by the bacteria. In the case of this pathogen, which represents up to 75% of contact lens-associated bacterial keratitis, delay in effective therapy becomes an even more pressing issue. Delay in both diagnosis and initiation of effective treatment could potentially blind an eye from early suppurative proteolytic destruction of the corneal structure.

Bacterial keratitis is generally treated intensively (every 15 to 60 minutes for several days) with combinations of topical fortified antibiotics such as cefazolin and tobramycin or gentamicin.<sup>197</sup> Recently, monotherapy with a topical fluoroquinolone has become a first-line approach in selected cases, while vancomycin is generally reserved for severe vision-threatening keratitis that is not responsive to first-line agents. The antimicrobials currently in use are problematic because of their toxic effects on the ocular surface (eg, punctate keratitis, delayed re-epithelialization, hyperemia, chemosis) and, more important, the emerging and increasing patterns of resistance. Aminoglycoside resistance in cases of keratitis, endophthalmitis, and infection of corneal donor material is on the increase.<sup>198,199</sup> While the fluoroquinolones have provided a reasonable tool,<sup>200</sup> there are early, disturbing reports of resistance to these agents as well.<sup>11-25</sup> With the advent of resistance to vancomycin, there is a more pressing need to find new antimicrobial alternatives that will affect a suitable spectrum of ocular pathogens and that will not be plagued by rapidly developing resistance. To date, reports of resistance to the antimicrobial peptides have been minimal, and because of their mechanism of action, bacterial resistance to peptides is likely to develop very slowly. There are only isolated reports of resistance to peptides in the microbiological literature; some bacteria are naturally resistant (eg, *Serratia marcescens*, *Burkholderia cepacia*) by virtue of a noninteractive outer membrane or the elaboration of specific proteases.<sup>2</sup> In addition, there are isolated reports of *Salmonella* resistance.<sup>201</sup>

The problem of infection after corneal transplantation is far less common than bacterial keratitis. Of the approximately 40,000 transplants performed in the United States each year, the incidence of endophthalmitis is 0.1% (1998 Statistical Report, Eye Bank Association of America, Washington, DC). The precise incidence of postkeratoplasty keratitis is not as easily pinpointed. Nonetheless, the occurrence of keratitis or endophthalmitis after keratoplasty can represent a devastating complication and can be related to a variety of risk factors, including contamination of donor tissue, intrasurgical inoculation, and postoperative infection.<sup>202</sup> In the event of an infection following keratoplasty, early recognition of the pathogen becomes crucial for successful treatment. A variety of organisms have been implicated, including *S epidermidis*, *S aureus*, *S pneumoniae*, *Streptococcus viridans*, *P aeruginosa*, *S marcescens*, *Haemophilus influenzae*, *Bacillus* species, and *C albicans*.<sup>203-213</sup>

To diminish the risk of contamination of corneal storage media, a variety of antibiotics, antiseptics, and peptides have been investigated as additives to preservation media with emphasis on finding a nontoxic agent effective at standard storage temperatures.<sup>164,214-223</sup> Among the

antimicrobials investigated in preservation medium are penicillin, streptomycin,<sup>210,224</sup> gentamicin,<sup>210,214,225</sup> cefazolin,<sup>215</sup> povidone iodine,<sup>219</sup> and vancomycin.<sup>226</sup> Currently, gentamicin plus streptomycin is the most commonly used combination in corneal storage media, although gentamicin alone may not affect the *Streptococcus* species, *S epidermidis*, and *S aureus*, the species most commonly isolated from corneal scleral rims at the time of tissue harvest.<sup>212,227-230</sup> The special circumstance of corneal storage at 4°C and the closed system provide a challenge for adequate effective sterilization of the media without damage to the delicate corneal tissue. Although Hwang and colleagues<sup>221</sup> and Lass and colleagues<sup>223</sup> demonstrated that the antimicrobial activity of the antibiotics in preservation media can be augmented by leaving the media containing the tissue at room temperature for about 1 hour prior to preservation at 4°C, it would be ideal to employ an agent that is effective at all storage temperatures. The ideal antimicrobial agent has not been found, especially considering these storage conditions and the lengthier storage times for shipment of tissue globally for transplantation. The resistance data stress the need for an antimicrobial agent that is effective at all temperatures and that covers the common contaminants.

#### DATA ANALYSIS

##### *Interpretation of Our Data in Context*

The data selected for presentation in this series reflect a distillation of recent efforts in our laboratory to demonstrate a promising candidate peptide for application to ocular infection. We attempted to utilize a new methodology of candidate peptide selection with the greatest potential for success for use as a topical antimicrobial agent, and we employed these peptides in two in vitro situations—in a standard controlled 10 mM sodium phosphate buffer for microbiological analysis and in modified corneal preservation media. Finally, we established a working in vivo animal assay in which to test the peptide as a topical application. Our data demonstrate that although the peptides used in this study were effective against serious corneal clinical isolates in a closed in vitro system, the peptides were not effective against all bacteria tested in either corneal preservation media or at the ocular surface in an animal model.

The results demonstrate that in a highly controlled phosphate buffered saline system in which electrolytic composition and pH are rigidly controlled, the candidate peptides proved effective against the clinical isolates we tested. In a similarly controlled but very different system—that of chondroitin sulfate-based corneal storage media—the results were less impressive. And in a reliable in vivo animal model, the candidate peptides demonstrated no effect either clinically or microbiologically. The

outcome of this study will be of value for what we have learned about the selection and application of these substances in the testing for ophthalmic applications.

In summary of the experimental results, we can conclude the following:

1. The candidate peptides (CCI A, B, and C and COL-1) were successful in producing a total kill of the test clinical isolates in 10 mM sodium phosphate buffer.
2. In modified Optisol, the peptides were effective against *S epidermidis* at all temperatures, demonstrated augmented activity at 23°C against the gram-positive organisms, but were ineffective against *P aeruginosa*. The addition of EDTA to the medium augmented the killing of *P aeruginosa* but made no difference in the reduction of gram-positive organisms.
3. In an in vivo rabbit model of *Pseudomonas* keratitis, COL-1 demonstrated neither clinical nor microbicidal efficacy and appeared to have a very narrow dosage range, outside of which it appeared to be toxic to the ocular surface.

Although the peptides selected showed substantial microbicidal activity in the initial postformulation testing stage, we must try to understand why they were unsuccessful in corneal storage media and at the ocular surface, both of which represent important clinical circumstances in which infection may be a serious issue.

In the important circumstance of modified corneal storage media, there are several possibilities for inhibition of the microbicidal action. It has been well established that ionic shifts and alterations in pH affect the lytic activity of peptides.<sup>101,154,231</sup> Indeed, their capability as pore-forming agents depends on electrostatic charge distribution and their interaction with the target-cell membrane. It is possible that the chondroitin sulfate or the ionic strength of Optisol alters or masks the electrostatic distribution of the peptide. Chondroitin sulfate has 2 negative charges on its upper face, which, in contact with the peptide, could block the positive charges that are so crucial to its mechanism of action.<sup>55,232</sup> The same problem was not exhibited by defensins in previous reports with the chondroitin sulfate-based Optisol, possibly because the defensin molecule is more globular and irregular and does not expose a long positively charged face to the chondroitin sulfate polymer.<sup>218,232</sup> Other components found in Optisol, such as calcium, dextran, and Hepes buffer, could also affect peptide activity.

The fact that we were able to demonstrate some activity of the peptide in modified Optisol, especially with the addition of EDTA, suggests to us that there may be ways of altering the composition that would favor the activity of the peptide in the medium. It is also possible to

theorize that, given our differential effects on *S epidermidis* versus *S aureus*, for example, the specific organism may undergo species-specific membrane changes during incubation in Optisol, changes that might account for the differential effectiveness of the peptide.

An explanation of peptide activity, or lack thereof, on the surface of the eye is far more complex, and there may be multiple reasons for the failure of the peptide to work on the ocular surface despite its *in vitro* activity. One must take into account pharmacologic considerations such as dilutional factors, contact time, and retention time of the drug when delivered via topical application. In addition, the components of the tear film are very complex, including the lipid, aqueous, and mucin layers as well as glucose, lactate, citrate, glycoproteins, lysozyme, albumin, mucopolysaccharides, ions (Na, K, Mg, HCO<sub>3</sub>, HPO<sub>4</sub>), urea, amino acids, and sialic acid. Therefore, factors at the ocular surface, such as this complex mix of substances and the presence of proteases (both native and bacterial), could cleave or otherwise inactivate the synthetic antimicrobial peptide.

In addition, with the transition from an *in vitro* to an *in vivo* model, we must take into account a number of relevant issues, including our animal model (ie, bacterial load; incubation time prior to drug application; drug residence time, both ocular and systemic; *in vivo* immunologic factors; the isolates used) and issues of peptide and dosage delivery (pH, ionic strength, the presence of divalent ions, protease susceptibility, protein-protein interactions, membrane penetration, and pharmacokinetics).

Our *in vivo* model was developed after considerable experimentation with alternative approaches, and we designed it to yield a highly reproducible keratitis that mimicked the clinical circumstance (breach in the integrity of the epithelium plus topical challenge, rather than intrastromal injection). We intentionally chose a postinfection incubation time that we felt was comparable to the usual circumstance in human keratitis.

In our study, the rabbits uniformly progressed to corneal suppuration despite treatment with the peptide. We noted that the eyes sustained substantial damage by 96 hours, and this did not appear to be reversed in the animals tested with peptide. In the case of *P aeruginosa*, this rapid damage may be the result of potent proteases generated by the bacteria.<sup>233,234</sup> Bacteria-generated proteases may likewise be responsible for cleaving and rendering the peptide inactive. Alternatively, ocular surface proteins such as lysozyme might bind the peptide, making it inactive. In addition, *P aeruginosa* elaborates a mucoid biofilm that could conceivably serve as a barrier to the penetration of the peptide. In a previous study of the activity of defensins against *P aeruginosa*, Rich and colleagues<sup>235</sup> demonstrated that the *in vitro* antimicrobial

activity of rabbit defensin NP-3a was diminished in a linear fashion in the presence of human tears. A 3-log reduction was obtained in a test situation in which 10% tears were present. This was decreased to a 2-log reduction in the presence of 20% tears, and the peptide was rendered completely ineffective in the presence of 70% tears. These data are consistent with our findings of impaired activity at the ocular surface.

#### *Future Research Approaches to the Problem*

Each experiment, successful or unsuccessful, spawns new avenues of inquiry. Other considerations for investigating the role of peptides in the management of bacterial keratitis include alteration of the carrier media, including the use of a higher ionic strength carrier, more efficient buffering systems to maintain a pH that would favor potency of the peptide, and a more viscous carrier to increase drug residence time at the ocular surface. The hybridization of a peptide with a more traditional antibiotic such as polymixin is also a strategic option. In addition, we plan to (1) “dissect” the components of storage media and human tears to isolate inhibitory agents, (2) study peptide action over a longer period *in vitro*, and (3) further evaluate the kinetics of our animal model.

An alternative approach for the testing of *in vivo* effectiveness is a model using a “one-time” challenge in which the peptide and bacteria are mixed prior to the infection. While this does not mimic the clinical circumstance, such a model would help us distinguish between effectiveness of the peptide in the context of an infection and drug toxicity.

#### **THE FUTURE OF ANTIMICROBIAL PEPTIDES IN OPHTHALMOLOGY**

The past 50 years of the antibiotic era have witnessed an alarming increase in resistance to the natural, semisynthetic, and synthetic antibiotics.<sup>2,236</sup> The development of resistance as a phenomenon has been a reality since the widespread use of antibiotics, largely because of the short doubling times and genetic plasticity of microorganisms that allow them to test mutations that enhance their survivability.<sup>2</sup> The current “crisis” in antibiotic resistance is the result of widespread mutational changes that have brought about resistance to whole classes of antibiotics and the fact that no truly novel antibiotic agents have been developed in the past several decades.

Although we have relied on traditional antibiotic molecules like the penicillins, cephalosporins, aminoglycosides, and vancomycin for therapeutic purposes, it is interesting that most species throughout the evolutionary scale have employed peptide antimicrobials for immediate self-defense against pathogenic invasion. And yet, the employment of cationic peptide antimicrobials for the management of infectious diseases is at a very early stage

of development. Although peptide molecules clearly hold great promise for the management of infectious diseases in general and for ophthalmology specifically, indeed, very few *in vivo* studies of cationic peptide action have been published.<sup>237-239</sup> Certainly, companies involved in commercial development of these compounds have made claims of their *in vivo* applicability (eg, Applied Microbiology, Micrologix Biotech, Demeter Biotechnologies, Xoma, Magainin Pharmaceuticals, and Intrabiotics).

Theoretically, the use of the cationic peptides as antimicrobial agents has several distinct advantages:

1. They have the ability to effect killing of a broad spectrum of microorganisms, including multidrug-resistant bacteria, fungi, and even some enveloped viruses near the minimum inhibitory concentration (1 to 8  $\mu\text{g/mL}$ ), competitive with even the most potent antibiotics.
2. They kill much more rapidly than conventional antibiotics. (a 4- to 6-log reduction in survival often within 5 minutes,
3. They demonstrate a low level of resistance development *in vitro*. Since they operate on the basis of altering the permeability properties of the bacterial plasma membrane and do not interfere with cell wall or macromolecular synthesis as do traditional antibiotics, resistance to the peptide antimicrobials will not likely develop easily.
4. They have the ability in nature to protect animals against both topical and systemic infections and are able to neutralize endotoxins.<sup>237-240</sup>
5. They have demonstrated significant synergy with conventional antibiotics.<sup>238</sup>
6. Given the relatively small number of building blocks (approximately 20 amino acids on average), the peptides are quite amenable to synthesis and modification and, at the same time, offer tremendous diversity.<sup>2</sup>

However, there are some theoretical disadvantages to the use of peptides as clinical antimicrobials. Antimicrobial peptides have evolved in nature to be active within a specific and limited environment (eg, the neutrophil). Outside of this environment, the cationic peptides are programmed for deactivation so that they do not continue killing in other environments. Human defensins, outside the neutrophil, are deactivated by a variety of circumstances, such as change in ionic strength or binding to proteins. Therefore, the application of these substances in new environments (eg, the ocular surface) will require skirting those deactivating mechanisms placed so carefully by nature. In addition, peptide activity is not completely specific to prokaryotic cells, and the issues of toxicity to eukaryotic host cells need to be elaborated and resolved. Moreover, each natural peptide

has a broad but somewhat incomplete spectrum of activity, and in nature, these peptides often work together to mount an effective defense to bacterial invasion. Finding an effective application may require, therefore, the designing of a synthetic combination peptide that has a good minimal inhibitory concentration and that is nontoxic.

We face a present and emerging crisis in antibiotic therapy in which the extensive and, to some extent, indiscriminate use of antibiotics has precipitated significant resistance patterns and weakening of our armamentarium against bacterial infection.<sup>5</sup> Ophthalmic pharmaceutical companies have not rallied around the antimicrobial peptides yet, perhaps because of concern over production costs, *in vivo* stability, and unanticipated toxicity. However, the development of a new class of antimicrobials that have a broad spectrum of activity against serious ocular pathogens and a mechanism of action that would not likely generate patterns of resistance suggests that these peptides may be useful tools in the future for combating vision-threatening microbial infections of the eye. The application of the cationic peptides for the treatment of infectious disease in general and for the management of ocular infection specifically will require consideration of immunogenicity, toxicity, drug stability, formulation, and route of application. Successful achievement of this goal will require biochemical manipulation of these molecules to help overcome the problem of proteolysis that may reduce their half-life *in vivo*. Ophthalmologists and pharmacologists will need to collaborate in designing effective drugs that will achieve rapid eradication of pathogenic organisms without ocular cell toxicity. We are still at the beginning of the "peptide era." These compounds, elaborated by nature over millions of years as an effective defense system, are in their developmental infancy for application to eye disease. The future, nonetheless, holds promise.

#### **ACKNOWLEDGMENTS**

---

The author extends deepest appreciation to Kandice McGarvey for her dedicated, disciplined, and meticulous laboratory work; to Wayne Smith for his expertise and guidance in designing the antimicrobial assays and for his careful review of the manuscript; to David Noever for his thoughtful advice and for providing peptide for this study; to John Shafer for the specific peptide formulations; to Luciene Barbosa de Sousa for her expert work in the design of many of the studies performed by our laboratory; to Jim Cullor for his collegiality and support; to Tessie Smith (Bausch & Lomb, Inc) for provision of modified Optisol corneal preservation medium; and to Kelsie Luiz, Lisa Machado, and Brendan O'Donnell for their help in the laboratory. Finally, my gratitude goes to my family from whom time was taken to complete this thesis.

## REFERENCES

1. Edmond MB, Wenzel RP, Pasculle AW. Vancomycin-resistant *Staphylococcus aureus*: perspectives on measures needed for control. *Ann Intern Med* 1996;124:329-334.
2. Hancock RE. Host defence (cationic) peptides: what is their future clinical potential? *Drugs* 1999;57:469-473.
3. Saberwal G, Nagaraj R. Cell-lytic and antibacterial peptides that act by perturbing the barrier function of membranes: facets of their conformational features, structure-function correlations and membrane perturbing abilities. *Biochim Biophys Acta* 1994;1197:109-131.
4. Harder J, Bartels J, Christophers E, et al. A peptide antibiotic from human skin. *Nature* 1997;387:861.
5. Neu HC. The crisis in antibiotic resistance. *Science* 1992;257:1064-1073.
6. DeMuri GP, Hostetter MK. Resistance to antifungal agents. *Pediatr Clin North Am* 1995;42:665-685.
7. Dever LL, Handwerker S. Persistence of vancomycin-resistant *Enterococcus faecium* gastrointestinal tract colonization in antibiotic-treated mice. *Microb Drug Resist* 1996;2:415-421.
8. Glynn MK, Bopp C, Dewitt W, et al. Emergence of multidrug-resistant *Salmonella enterica* serotype typhimurium DT104 infections in the United States. *N Engl J Med* 1998;338:1333-1338.
9. Levy SB. Multidrug resistance—a sign of the times. *N Engl J Med* 1998;338:1376-1378.
10. Davies J. General mechanisms of antimicrobial resistance. *Rev Infect Dis* 1979;1:23-29.
11. Ball P. Emergent resistance to ciprofloxacin amongst *Pseudomonas aeruginosa* and *Staphylococcus aureus*: clinical significance and therapeutic approaches. *J Antimicrob Chemother* 1990;26:165-179.
12. Chin GJ, Marx Je. Resistance to antibiotics. *Science* 1994;264:359-393.
13. Fass RJ, Barnishan J, Ayers LW. Emergence of bacterial resistance to imipenem and ciprofloxacin in a university hospital. *J Antimicrob Chemother* 1995;36:343-353.
14. Garg P, Sharma S, Rao GN. Ciprofloxacin-resistant *Pseudomonas keratitis*. *Ophthalmology* 1999;106:1319-1323.
15. Goldstein MH, Kowalski RP, Gordon YJ. Emerging fluoroquinolone resistance in bacterial keratitis: a 5-year review. *Ophthalmology* 1999;106:1313-1318.
16. Humphreys H, Mulvihill E. Ciprofloxacin-resistant *Staphylococcus aureus*. (Letter) *Lancet* 1985;2:383.
17. Knauf HP, Silvany R, Southern PMJ, et al. Susceptibility of corneal and conjunctival pathogens to ciprofloxacin. *Cornea* 1996;15:66-71.
18. Maffett M, O'Day DM. Ciprofloxacin-resistant bacterial keratitis. (Letter) *Am J Ophthalmol* 1993;115:545-546.
19. Smith SM, Eng RHK, Bais P, et al. Epidemiology of ciprofloxacin resistance among patients with methicillin-resistant *Staphylococcus aureus*. *J Antimicrob Chemother* 1990;26:567-572.
20. Snyder ME, Katz HR. Ciprofloxacin-resistant bacterial keratitis. *Am J Ophthalmol* 1992;114:336-338.
21. Thomson KS, Sanders CC, Hayden ME. In vitro studies with 5 quinolones: evidence for changes in relative potency as quinolone resistance rises. *Antimicrob Agents Chemother* 1991;35:2329-2334.
22. Daum TE, Schaberg DR, Terpenning MS, et al. Increasing resistance of *Staphylococcus aureus* to ciprofloxacin. *Antimicrob Agents Chemother* 1990;34:1862-1863.
23. Drake JD, Bui D, Hwang DG. Mutagenic effects of subinhibitory levels of ciprofloxacin and their relation to antibiotic resistance. *Invest Ophthalmol Vis Sci* 1997;38:S871.
24. Cohen MA, Huband MD. Activity of clinafloxacin, trovafloxacin, quinupristin/dalfopristin, and other antimicrobial agents versus *Staphylococcus aureus* isolates with reduced susceptibility to vancomycin. *Diagn Microbiol Infect Dis* 1999;33:43-46.
25. Lai KK. Treatment of vancomycin-resistant *Enterococcus faecium* infections. *Arch Intern Med* 1996;156:2579-2584.
26. Zasloff M. Antibiotic peptides as mediators of innate immunity. *Curr Opin Immunol* 1992;4:3-7.
27. Ganz T, Lehrer RI. Antibiotic peptides from higher eukaryotes: biology and applications. *Mol Med Today* 1999;5:292-297.
28. Nassif KF. Ocular surface defense mechanisms. In: Hyndiuk RA, Tabbara KF, eds. *Infections of the Eye*. Boston: Little Brown; 1986:37-44.
29. Friedlaender MH. Immunology of ocular infections. In: Friedlaender MH, ed. *Allergy and Immunology of the Eye*. New York: Raven Press; 1993:107-138.
30. Wilhelmus KR. Bacterial keratitis. In: Pepose JS, Holland GN, Wilhelmus KR, eds. *Ocular Infection and Immunity*. St Louis: Mosby; 1996:970-1031.
31. Williams JM, Fimi ME, Cousins SW, et al. Corneal responses to infection. In: Krachmer JH, Mannis MJ, Holland EJ, eds. *Cornea*. Philadelphia: Mosby; 1997:129-162.
32. Boman HG. Antibacterial peptides: key components needed in immunity. *Cell* 1991;65:205-207.
33. Boman HG. Peptide antibiotics and their role in innate immunity. *Annu Rev Immunol* 1995;13:61-92.
34. Cammue BP, De Bolle MF, Terras MF, et al. Isolation and characterization of a novel class of plant antimicrobial peptides from *Mirabilis jalapa* L. seeds. *J Biol Chem* 1992;267(4):2228-2233.
35. Taylor RH, Acland DP, Attenborough S, et al. A novel family of small cysteine-rich antimicrobial peptides from seed of *Impatiens balsamina* is derived from a single precursor protein. *J Biol Chem* 1997;272:24480-24487.
36. Hoffmann JA, Reichhart JM, Hetru C. Innate immunity in higher insects. *Curr Opin Immunol* 1996;8:8-13.
37. Bulet P, Hetru C, Dimarcq JL, et al. Antimicrobial peptides in insects: structure and function. *Dev Comp Immunol* 1999;23:329-344.
38. Lemaitre B, Reichhart JM, Hoffmann JA. *Drosophila* host defense: differential induction of antimicrobial peptide genes after infection by various classes of microorganisms. *Proc Natl Acad Sci USA* 1997;94:14614-14619.
39. Meister M, Lemaitre B, Hoffmann JA. Antimicrobial peptide defense in *Drosophila*. *Bioessays* 1997;19:1019-1026.
40. Natori S. [Antimicrobial proteins of insect and their clinical application]. *Nippon Rinsho* 1995;53(5):1297-1304.
41. Rees JA, Moniatte M, Bulet P. Novel antibacterial peptides isolated from a European bumblebee, *Bombus pascuorum* (Hymenoptera, Apoidea). *Insect Biochem Mol Biol* 1997;27:413-422.
42. Zasloff M. Magainins, a class of antimicrobial peptides from *Xenopus* skin: isolation, characterization of 2 active forms, and partial cDNA sequence of a precursor. *Proc Natl Acad Sci USA* 1987;84(15):5449-5453.
43. Simmaco M, Mignogna G, Barra D. Antimicrobial peptides from amphibian skin: what do they tell us? *Biopolymers* 1998;47:435-450.
44. Simmaco M, Mangoni ML, Boman A, et al. Experimental infections of *Rana esculenta* with *Aeromonas hydrophila*: a molecular mechanism for the control of the normal flora. *Scand J Immunol* 1998;48(4):357-363.
45. Martin E, Ganz T, Lehrer RI. Defensins and other endogenous peptide antibiotics of vertebrates. *J Leukoc Biol* 1995;58:128-136.
46. Boman HGE. Antimicrobial peptides. *Ciba Foundation Symposium on Antimicrobial Peptides*. London: John Wiley & Sons; 1994.
47. Ojcius DM, Liu C-C, Young JD. Pore-forming proteins. *Science Med Jan/Feb* 1998:44-53.
48. Ganz T, Selsted ME, Szlerek D, et al. Defensins: natural peptide antibiotics of human neutrophils. *J Clin Invest* 1985;76:1427-1435.

## The Use Of Antimicrobial Peptides In Ophthalmology

49. Ganz T, Selsted ME, Lehrer RI. Antimicrobial activity of phagocyte granule proteins. *Semin Respir Infect* 1986;1:107-117.
50. Ganz T, Lehrer RI. Antimicrobial peptides of leukocytes. *Curr Opin Hematol* 1997;4:53-58.
51. Gallo RL, Huttner KM. Antimicrobial peptides: an emerging concept in cutaneous biology. *J Invest Dermatol* 1998;111:739-743.
52. Jaynes JM, Burton CA, Barr SB, et al. In vitro cytotoxic effect of novel lytic peptides on *Plasmodium falciparum* and *Trypanosoma cruzi*. *FASEB J* 1988;2:2878-2883.
53. Hwang PM, Vogel HJ. Structure-function relationships of antimicrobial peptides. *Biochem Cell Biol* 1998;76:235-246.
54. Boman HG. Peptide antibiotics: holy or heretic grails of innate immunity? *Scand J Immunol* 1996;43:475-482.
55. de Sousa LB. Utilização "in vitro" de um peptídeo sintético análogo à cecropina (D<sub>5</sub>C) como agente antimicrobiano perante patógenos oculares, em solução desinfetante de lente de contato e em meio de preservação. Departamento de Oftalmologia. São Paulo, Brazil: Universidade Federal de São Paulo, Escola Paulista de Medicina; 1998:207.
56. Stryer L. Protein structure and function. *Biochemistry*. 3rd ed. New York: WH Freeman; 1988:11-45.
57. Devi AS, Sitaram N, Nagaraj R. Structural features of helical aggregates of antibacterial peptides via simulated annealing and molecular modeling. *J Biomol Struct Dyn* 1998;15(4):653-661.
58. Huang HW. Peptide-lipid interactions and mechanisms of antimicrobial peptides. *Novartis Found Symp* 1999;225:188-200; discussion 200-206.
59. Oren Z, Shai Y. Mode of action of linear amphipathic  $\alpha$ -helical antimicrobial peptides. *Biopolymers* 1998;47:451-463.
60. Hill CP, Yee J, Selsted ME, et al. Crystal structure of defensin HNP-3, an amphiphilic dimer: mechanisms of membrane permeabilization. *Science* 1991;251:1481-1485.
61. Kagan BL, Selsted ME, Ganz T, et al. Antimicrobial defensin peptides form voltage-dependent ion-permeable channels in planar lipid bilayer membranes. *Proc Natl Acad Sci USA* 1990;87:210-214.
62. Sipos D, Andersson M, Ehrenberg A. The structure of the mammalian antibacterial peptide cecropin P1 in solution, determined by proton NMR. *Eur J Biochem* 1992;209:163-169.
63. Boman HG, Agerberth B, Boman A. Mechanisms of action on *Escherichia coli* of cecropin P1 and PR-39, 2 antibacterial peptides from pig intestine. *Infect Immun* 1993;61(7):2978-2984.
64. Sawyer JG, Martin NL, Hancock REW. Interaction of macrophage cationic proteins with the outer membrane of *Pseudomonas aeruginosa*. *Infect Immun* 1988;56:693-698.
65. Bevins CL, Zasloff M. Peptides from frog skin. *Ann Rev Biochem* 1990;59:395-414.
66. Soravia E, Martini G, Zasloff M. Antimicrobial properties of peptides from *Xenopus* granular gland secretions. *FEBS Lett* 1987;228:337-340.
67. Berkowitz BA, Bevins CL, Zasloff MA. Magainins: a new family of membrane-active host defense peptides. *Biochem Pharmacol* 1990;39(4):625-629.
68. Marion D, Zasloff M, Bax A. A two-dimensional NMR study of the antimicrobial peptide magainin 2. *FEBS Lett* 1988;277:21-26.
69. Duclouhier H, Molle G, Spach G. Antimicrobial peptide magainin 1 from *Xenopus* skin forms anion permeable channels in planar lipid bilayers. *Biophys J* 1989;56:1017-1021.
70. Moore KS, Bevins CL, Brasseur M, et al. Antimicrobial peptides in the stomach of *Xenopus laevis*. *J Biol Chem* 1991;266:19851-19857.
71. Westerhoff HV, Juretic D, Hendlner RW, et al. Magainins and the disruption of membrane-linked free energy transduction. *Proc Natl Acad Sci USA* 1989;86:6597-6601.
72. Westerhoff HV, Zasloff M, Rosner JL, et al. Functional synergism of the magainins PGLa and magainin-2 in *Escherichia coli*, tumor cells and liposomes. *Eur J Biochem* 1995;228:257-264.
73. Matsuzaki K, Sugishita K, Miyajima K. Interactions of an antimicrobial peptide, magainin 2, with lipopolysaccharide-containing liposomes as a model for outer membranes of gram-negative bacteria. *FEBS Lett* 1999;449:221-224.
74. Matsuzaki K, Murase O, Miyajima K. Kinetics of pore formation by an antimicrobial peptide, magainin 2, in phospholipid bilayers. *Biochemistry* 1995;34:12553-12559.
75. Matsuzaki K, Murase O, Fujii N, et al. Translocation of a channel-forming antimicrobial peptide, magainin 2, across lipid bilayers by forming a pore. *Biochemistry* 1995;34:6521-6526.
76. Matsuzaki K, Sugishita K, Fujii N, et al. Molecular basis for membrane selectivity of an antimicrobial peptide, magainin 2. *Biochemistry* 1995;34:3423-3429.
77. Matsuzaki K, Murase O, Fujii N, et al. An antimicrobial peptide, magainin 2, induced rapid flip-flop of phospholipids coupled with pore formation and peptide translocation. *Biochemistry* 1996;35:11361-11368.
78. Matsuzaki K, Yoneyama S, Fujii N, et al. Membrane permeabilization mechanisms of a cyclic antimicrobial peptide, tachyplesin I, and its linear analog. *Biochemistry* 1997;36:9799-9806.
79. Matsuzaki K, Sugishita K, Harada M, et al. Interactions of an antimicrobial peptide, magainin 2, with outer and inner membranes of gram-negative bacteria. *Biochim Biophys Acta* 1997;1327:119-130.
80. Matsuzaki K. [Molecular action mechanisms and membrane recognition of membrane-acting antimicrobial peptides]. *Yakugaku Zasshi* 1997;117:253-264.
81. Matsuzaki K, Nakamura A, Murase O, et al. Modulation of magainin 2-lipid bilayer interactions by peptide charge. *Biochemistry* 1997;36:2104-2111.
82. Matsuzaki K. Magainins as paradigm for the mode of action of pore forming polypeptides. *Biochim Biophys Acta* 1998;1376:391-400.
83. Matsuzaki K, Mitani Y, Akada KY, et al. Mechanism of synergism between antimicrobial peptides magainin 2 and PGLa. *Biochemistry* 1998;37:15144-15153.
84. Matsuzaki K, Sugishita K, Ishibe N, et al. Relationship of membrane curvature to the formation of pores by magainin 2. *Biochemistry* 1998;37:11856-11863.
85. Wieprecht T, Beyermann M, Seelig J. Binding of antibacterial magainin peptides to electrically neutral membranes: thermodynamics and structure. *Biochemistry* 1999;38:10377-10387.
86. Fuchs C, Barry AL, Brown SD. In vitro antimicrobial activity of MSI-78, a magainin analog. *Antimicrob Agents Chemother* 1998;42:1213-1216.
87. Iwahori A, Hirota Y, Sampe R, et al. Synthesis of reversed magainin 2 analogs enhanced antibacterial activity. *Biol Pharm Bull* 1997;20(3):267-270.
88. Iwahori A, Hirota Y, Sampe R, et al. On the antibacterial activity of normal and reversed magainin 2 analogs against *Helicobacter pylori*. *Biol Pharm Bull* 1997;20(7):805-808.
89. Schuster FL, Jacob LS. Effects of magainins on amoeba and cyst changes of *Acanthamoeba polyphaga*. *Antimicrob Agents Chemother* 1992;36(6):1263-1271.
90. Cruciani RA, Barke JL, Zasloff M, et al. Antibiotic magainins exert cytotoxic activity against transformed cell lines through channel formation. *Proc Natl Acad Sci USA* 1991;88:3792-3796.
91. Lichtenstein AK, Ganz T, Selsted E, et al. Synergistic cytotoxicity mediated by hydrogen peroxide combined with peptide defensins. *Cell Immunol* 1988;114(1):104-106.
92. Lehrer RI, Ganz T, Selsted ME. Oxygen-independent bactericidal systems. *Hematol/Oncol Clin North Am* 1988;2:159-169.
93. Selsted ME, Harwig SSL. Purification, primary structure, and antimicrobial activities of a guinea pig neutrophil defensin. *Infect Immun* 1987;55:2281-2286.

94. Selsted ME, Harwig SSL. Determination of the disulfide array in the human defensin HNP-2. *J Biol Chem* 1989;264:4003-4007.
95. Ganz T, Selsted ME, Lehrer RI. Defensins. *Eur J Haematol* 1990;44:1-8.
96. Lehrer RI, Ganz T, Selsted ME. Defensins: endogenous antibiotic peptides of animal cells. *Cell* 1991;64:229-230.
97. Lehrer RI, Lichtenstein AK, Ganz T. Defensins: antimicrobial and cytotoxic peptides of mammalian cells. *Ann Rev Immunol* 1993;11:105-128.
98. Lehrer RI, Ganz T, Selsted ME. Defensins: natural peptide antibiotics from neutrophils. *ASM News* 1990;56:315-318.
99. Ganz T. Extracellular release of antimicrobial defensins by human polymorphonuclear leukocytes. *Infect Immun* 1987;55:568-571.
100. Rice W, Ganz T, Kinkade JM Jr, Selsted ME, et al. Defensin-rich dense granules of human neutrophils. *Blood* 1987;70:757-765.
101. Selsted ME, Szklarek D, Lehrer RI. Purification and antibacterial activity of antimicrobial peptides of rabbit granulocytes. *Infect Immun* 1984;45:150-154.
102. Selsted ME, Brown DM, DeLange RJ, et al. Primary structures of 6 antimicrobial peptides of rabbit peritoneal neutrophils. *J Biol Chem* 1985;260:4579-4584.
103. Eisenhauer PB, Harwig SSL, Szklarek D, et al. Purification and antimicrobial properties of 3 defensins from rat neutrophils. *Infect Immun* 1989;57:2021-2027.
104. Eisenhauer P, Harwig SSL, Szklarek D, et al. Polymorphic expression of defensins in neutrophils from outbred rats. *Infect Immun* 1990;58:3899-3902.
105. Selsted ME, Brown DM, DeLange RJ, et al. Primary structures of 6 antimicrobial peptides of rabbit peritoneal neutrophils. *J Biol Chem* 1985;260:4579-4584.
106. Selsted ME, Harwig SSL, Ganz T, et al. Primary structures of 3 human neutrophil defensins. *J Clin Invest* 1985;76:1436-1439.
107. Stanfield RL, Westbrook EM, Selsted ME. Characterization of 2 crystal forms of human defensin neutrophil cationic peptide 1, a naturally occurring antimicrobial peptide of leukocytes. *J Biol Chem* 1988;263:5933-5935.
108. Pardi A, Hare DR, Selsted ME, et al. Solution structures of rabbit neutrophil defensin NP-5. *J Mol Biol* 1988;201:625-636.
109. Yamashita T, Saito K. Purification, primary structure, and biological activity of guinea pig neutrophil cationic peptides. *Infect Immun* 1989;57:2405-2409.
110. Lambert J, Keppi E, Dimarcq J-L, et al. Insect immunity: isolation from immune blood of the dipteran *Phormia terranova* of 2 insect antibacterial peptides with sequence homology to rabbit lung macrophage bactericidal peptides. *Proc Natl Acad Sci USA* 1989;86(1):262-266.
111. Selsted ME, Tang Y-Q, Morris WL, et al. Purification, primary structure, and antibacterial activities of  $\beta$ -defensins, a new family of antimicrobial peptides from bovine neutrophils. *J Biol Chem* 1993;268:6641-6648.
112. Diamond G, Zasloff M, Eck H, et al. Tracheal antimicrobial peptide, a cysteine-rich peptide from mammalian tracheal mucosa: peptide isolation and cloning of cDNA. *Proc Natl Acad Sci USA* 1991;88:3952-3956.
113. Diamond G, Russell JP, Bevins CL. Inducible expression of an antibiotic peptide gene in lipopolysaccharide-challenged tracheal epithelial cells. *Proc Natl Acad Sci USA* 1996;93:5156-5160.
114. Selsted ME, Miller SI, Henschen AH, et al. Enteric defensins: antibiotic peptide components of intestinal host defense. *J Cell Biol* 1992;118:929-936.
115. Ouellette AJ, Greco RM, James M, et al. Developmental regulation of cryptidin, a corticostatin/defensin precursor mRNA in mouse small intestinal crypt epithelium. *J Cell Biol* 1989;108:1687-1695.
116. Ouellette AJ, Lualdi JC. A novel mouse gene family coding for cationic, cysteine-rich peptides. *J Biol Chem* 1990;265:9831-9837.
117. Ouellette AJ, Selsted ME. Paneth cell defensins: endogenous peptide components of intestinal host defense. *Faseb J* 1996;10(11):1280-1289.
118. Lichtenstein AK, Ganz T, Nguyen T-M, et al. Mechanism of target cytolysis by peptide defensins: target cell metabolic activities, possibly involving endocytosis, are crucial for expression of cytotoxicity. *J Immunol* 1988;140:2686-2694.
119. Zeya HI, Spitznagel JK. Cationic proteins of polymorphonuclear leukocyte lysosomes. I. Resolution of antibacterial and enzymatic activities. *J Bacteriol* 1966;91:750-754.
120. Lehrer RI, Ladra KM, Hake RB. Nonoxidative fungicidal mechanisms of mammalian granulocytes: demonstration of components with candidacidal activity in human, rabbit, and guinea pig leukocytes. *Infect Immun* 1975;11:1226-1234.
121. Lehrer RI, Ladra KM. Fungicidal components of mammalian granulocytes active against *Cryptococcus neoformans*. *J Infect Dis* 1977;136:96-99.
122. Lehrer RI, Szklarek D, Ganz T, et al. Correlation of binding of rabbit granulocyte peptide to *Candida albicans* with candidacidal activity. *Infect Immun* 1985;49:207-211.
123. Levitz SM, Selsted ME, Ganz T, et al. In vitro killing of spores and hyphae of *Aspergillus fumigatus* and *Rhizopus oryzae* by rabbit neutrophil cationic peptides and bronchoalveolar macrophages. *J Infect Dis* 1986;154:483-489.
124. Alcoloumre MS, Ghannoum MA, Ibrahim A, et al. Fungicidal properties of defensin NP-1 and activity against *Cryptococcus neoformans* in vitro. *Antimicrob Agents Chemother* 1993;37:2628-2632.
125. Lehrer RI, Szklarek D, Ganz T, et al. Synergistic activity of rabbit granulocyte peptides against *Candida albicans*. *Infect Immun* 1986;52:902-904.
126. Daher KA, Selsted ME, Lehrer RI. Direct inactivation of viruses by human granulocyte defensins. *J Virol* 1986;60:1068-1074.
127. Cullor JS, Mannis MJ, Murphy CJ, et al. In vitro antimicrobial activity of defensins against ocular pathogens. *Arch Ophthalmol* 1990;108:861-864.
128. Cullor JS, Wood S, Smith W, et al. Bactericidal potency and mechanistic specificity of neutrophil defensins against bovine mastitis pathogens. *Vet Microbiol* 1991;29(1):49-58.
129. Lehrer RI, Ganz T. Defensins—endogenous antibiotic peptides from human leukocytes. In: Chadwick DJ, Whelan J, eds. *Secondary Metabolites: Their Function and Evolution*. Ciba Foundation Symposia. Chichester, England: Wiley; 1992:276-293.
130. Sheu MJT, Baldwin WW, Brunson KW. Cytotoxicity of rabbit macrophage peptides MCP-1 and MCP-2 for mouse tumor cells. *Antimicrob Agents Chemother* 1985;28:626-629.
131. Lichtenstein AK, Ganz T, Selsted ME, et al. In vitro tumor cell cytolysis mediated by peptide defensins of human and rabbit granulocytes. *Blood* 1986;68:1407-1410.
132. Okrent DG, Lichtenstein A, Ganz T. Direct cytotoxicity of PMN granule proteins to human lung-derived cells and endothelial cells. *Am Rev Respir Dis* 1990;141:179-185.
133. Gallin JI, Fletcher MP, Seligman BE, et al. Human neutrophil specific granule deficiency: a model to assess the role of neutrophil specific granules in the evolution of the inflammatory response. *Blood* 1982;59:1317-1329.
134. Territo MC, Ganz T, Selsted ME, et al. Monocyte-chemotactic activity of defensins from human neutrophils. *J Clin Invest* 1989;84:2017-2020.
135. Zhu Q, Hu J, Mulay S, Esch F, et al. Isolation and structure of corticostatin peptides from rabbit fetal and adult lung. *Proc Natl Acad Sci USA* 1988;85:592-596.
136. Zhu Q, Solomon S. Isolation and mode of action of rabbit corticostatic (antiadrenocorticotropin) peptides. *Endocrinology* 1992;130:1413-1423.

## The Use Of Antimicrobial Peptides In Ophthalmology

137. Fleischmann J, Selsted ME, Lehrer RI. Opsonic activity of MCP-1 and MCP-2 cationic peptides from rabbit alveolar macrophages. *Diagn Microbiol Infect Dis* 1985;3:233-242.
138. Chapp PA, Rice WG, Raynor RL, et al. Inhibition of protein kinase C by defensins, antibiotic peptides from human neutrophils. *Biochem Pharmacol* 1988;37:951-956.
139. Kudriashov BA, Kondashevskaja MV, Liapina LA, et al. Effect of defensin on the process of healing of aseptic skin wound and on the permeability of blood vessels [in Russian]. *Biull Eksp Biol Med* 1990;109:391-393.
140. Murphy CJ, Foster BA, Mannis MJ, et al. Defensins are mitogenic for epithelial cells and fibroblasts. *J Cell Physiol* 1993;155:408-413.
141. Boman HG, Hultmark D. Cell free immunity in insects. *Ann Rev Microbiol* 1987;41:102-123.
142. Hultmark D, Steiner H, Rasmuson T, et al. Insect immunity: purification and properties of 3 inducible bactericidal proteins from hemolymph of *Hyalophora cecropia*. *Eur J Biochem* 1980;106(1):7-16.
143. Boman HG, Steiner H. Humoral immunity in *Cecropia* pupae. *Curr Top Microbiol Immunol* 1981;94/95:75-91.
144. Andreu D, Merrifield RB, Steiner H, et al. N-terminal analogues of cecropin A: synthesis, antibacterial activity, and conformational properties. *Biochemistry* 1985;24:1683-1688.
145. Boman HG, Faye I, von Hofsten P, et al. On the primary structures of lysozyme, cecropins, and attacins from *Hyalophora cecropia*. *Dev Comp Immunol* 1985;9(3):551-558.
146. Hultmark D, Engstrom A, Andersson K, et al. Insect immunity: attacins, a family of antibacterial proteins from *Hyalophora cecropia*. *EMBO J* 1983;2(4):571-576.
147. Samakovlis C, Kimbrell DA, Kylsten P, et al. The immune response in *Drosophila*: pattern of cecropin expression and biological activity. *EMBO J* 1990;9(9):2969-2976.
148. Hultmark D, Engstrom A, Bemnich H, et al. Insect immunity: isolation of cecropin D and 4 minor antibacterial components from *Cecropia* pupae. *Eur J Biochem* 1982;127(1):207-217.
149. Gudmundsson GH, Lidholm DA, Åsling B, et al. The cecropin locus. Cloning and expression of a gene cluster encoding 3 antibacterial peptides in *Hyalophora cecropia*. *J Biol Chem* 1991;266(18):11510-11517.
150. Steiner H, Andreu D, Merrifield RB. Binding and action of cecropin and cecropin analogues: antibacterial peptides from insects. *Biochim Biophys Acta* 1988;939:260-266.
151. Silvestro L, Gupta K, Weiser JN, et al. The concentration-dependent membrane activity of cecropin A. *Biochemistry* 1997;36:11452-11460.
152. Steiner H. Secondary structure of the cecropins: antibacterial peptides from the moth *Hyalophora cecropia*. *FEBS Lett* 1982;137:283-287.
153. Jaynes JM. Lytic peptides portend an innovative age in the management and treatment of human disease. *Drug News Perspect* 1990;3:69-78.
154. Christensen B, Fink J, Merrifield RB, et al. Channel-forming properties of cecropins and related model compounds incorporated into planar lipid membranes. *Proc Natl Acad Sci USA* 1988;85:5072-5076.
155. Andreu D, Merrifield RB, Steiner H, et al. Solid phase synthesis of cecropin A and related peptides. *Proc Natl Acad Sci USA* 1983;80:6475-6479.
156. Boman HG, Faye I, Gudmundsson GH, et al. Cell-free immunity in *cecropia*: a model system for antibacterial proteins. *Eur J Biochem* 1991;201:23-31.
157. Arrowood MJ, Jaynes JM, Healey MC. In vitro activities of lytic peptides against the sporozoites of *Cryptosporidium parvum*. *Antimicrob Agents Chemother* 1991;35:224-227.
158. Barr SC, Rose D, Jaynes JM. Activity of lytic peptides against intracellular *Trypanosoma cruzi* amastigotes in vitro and parasitemias in mice. *J Parasitol* 1995;81:974-978.
159. Gunshefski L, Mannis MJ, Cullor J, et al. In vitro antimicrobial activity of Shiva-11 against ocular pathogens. *Cornea* 1994;13:237-242.
160. Moore AJ, Beazley WD, Bibby MC, et al. Antimicrobial activity of cecropins. *J Antimicrob Chemother* 1996;37:1077-1089.
161. Jaynes JM, Julian GR, Jeffers GW, et al. In vitro cytotoxic effect of lytic peptides on several transformed mammalian cell lines. *Peptide Res* 1989;2:157-160.
162. Moore AJ, Devine DA, Bibby MC. Preliminary experimental anticancer activity of cecropins. *Peptide Res* 1994;7:265-269.
163. Mannis MJ, Cullor J, Murphy CJ, et al. The use of defensins for the eradication of ocular pathogens. *Invest Ophthalmol Vis Sci* 1989;30:363.
164. Mannis MJ, Schwab IR, Dries D, et al. Defensins as preservative in corneal storage medium. *Invest Ophthalmol Vis Sci* 1991;32:1062.
165. Murphy CJ, Foster B, Mannis MJ, et al. The stimulation of ocular cell growth by defensins of human and rabbit origin. *Invest Ophthalmol Vis Sci* 1989;30:149.
166. Mannis M, Gunshefski L, Cullor J, et al. The use of synthetic cecropin (Shiva-11) in preservative-free timolol and contact lens solutions. *Invest Ophthalmol Vis Sci* 1993;34:859.
167. de Sousa LB, Mannis MJ, Schwab IR, et al. The use of synthetic cecropin (D<sub>5</sub>C) in disinfecting contact lens solutions. *CLAO J* 1996;22:114-117.
168. Schwab IR, de Sousa LB, Mannis MJ, et al. The use of defense peptides in corneal storage media. *Invest Ophthalmol Vis Sci* 1995;36:1017.
169. Gunshefski L, Macsai M, Granus V, et al. Are synthetic cecropins (Shiva-11) effective against gentamicin resistant organisms? *Invest Ophthalmol Vis Sci* 1993;34:850.
170. Gruzensky WD, Mannis MJ, Schwab IR, et al. The use of a cecropin analog, Hecate, against *Acanthamoeba* in vitro. *Invest Ophthalmol Vis Sci* 1994;35:1337.
171. Murphy CJ, Jaynes J, Iwahashi C, et al. The modulation of ocular cell growth by cecropins. *Invest Ophthalmol Vis Sci* 1992;33:828.
172. Andreu D, Ubach J, Boman A, et al. Shortened cecropin A-melittin hybrids. *FEBS Lett* 1992;296:190-194.
173. Andreu D, Pons M, Ubach J, et al. Antibacterial, conformational, and membrane-active properties of small size cecropin A-melittin hybrids. In: Schneider CH, Eberle AN, eds. *Peptides, 1992*. Leiden, Netherlands: ESCOM Science Publishers; 1993:763-765.
174. Jones DB. Initial therapy of suspected microbial corneal ulcers. II. Specific antibiotic therapy based on corneal smears. *Surv Ophthalmol* 1979;24:105-116.
175. Ormerod LD, Smith RE. Contact lens-associated microbial keratitis. *Arch Ophthalmol* 1986;104:79-83.
176. Ormerod LD, Hertzmark E, Gomez DS, et al. Epidemiology of microbial keratitis in Southern California: a multivariate analysis. *Ophthalmology* 1987;94:1322-1333.
177. Callegan MC, Hobden JA, Hill JM, et al. Topical antibiotic therapy for the treatment of experimental *Staphylococcus aureus* keratitis. *Invest Ophthalmol Vis Sci* 1992;33:3017-3023.
178. Kremer I, Robinson A, Braffman M, et al. The effect of topical cef-tazidime on *Pseudomonas keratitis* in rabbits. *Cornea* 1994;13:360-363.
179. Frucht-Pery J, Golan G, Hemo I, et al. Efficacy of topical gentamicin treatment after 193 nm photorefractive keratectomy in an experimental *Pseudomonas keratitis* model. *Graefes Arch Clin Exp Ophthalmol* 1995;233:532-534.
180. Lawin-Brussel CA, Refojo MF, Leong FL, et al. Scanning electron microscopy of the early host inflammatory response in experimental *Pseudomonas keratitis* and contact lens wear. *Cornea* 1995;14:3559.
181. Alio JL, Artola A, Serra A, et al. Effect of topical antioxidant therapy on experimental infectious keratitis. *Cornea* 1995;14:175-179.

182. Engel LS, Callegan MC, Hobden JA, et al. Effectiveness of specific antibiotic/steroid combinations for therapy of experimental *Pseudomonas aeruginosa* keratitis. *Curr Eye Res* 1995;14:229-234.
183. Michalova K, Moyes AL, Cameron S, et al. Povidone-iodine (betadine) in the treatment of experimental *Pseudomonas aeruginosa* keratitis. *Cornea* 1996;15:533-536.
184. Twining SS, Zhou X, Schulte DP, et al. Effect of vitamin A deficiency on the early response to experimental *Pseudomonas keratitis*. *Invest Ophthalmol Vis Sci* 1996;37(4):511-522.
185. Preston MJ, Gerciker AA, Koles NL, et al. Prophylactic and therapeutic efficacy of immunoglobulin G antibodies to *Pseudomonas aeruginosa* lipopolysaccharide against murine experimental corneal infection. *Invest Ophthalmol Vis Sci* 1997;38(7):1418-1425.
186. Nos-Barbera S, Portoles M, Morilla A, et al. Effect of hybrid peptides of cecropin A and melittin in an experimental model of bacterial keratitis. *Cornea* 1997;16:101-106.
187. Guzek JP, Cline DJ, Row PK, et al. Rabbit *Streptococcus pneumoniae* keratitis model and topical therapy. *Invest Ophthalmol Vis Sci* 1998;39:2012-2017.
188. O'Callaghan RJ. Effectiveness of ciprofloxacin-polystyrene sulfonate (PSS) ciprofloxacin and ofloxacin in a *Staphylococcus keratitis* model. *Curr Eye Res* 1998;17:808-812.
189. Er H, Turkoz Y, Ozerol IH, et al. Effect of nitric oxide synthetase inhibition in experimental *Pseudomonas keratitis* in rabbits. *Eur J Ophthalmol* 1998;8:137-141.
190. Engel LS, Hill JM, Moreau JM, et al. *Pseudomonas aeruginosa* protease IV produces corneal damage and contributes to bacterial virulence. *Invest Ophthalmol Vis Sci* 1998;39:662-665.
191. Epley KD, Katz HR, Herling I, et al. Platinum spatula versus mini-tip culturette in culturing bacterial keratitis. *Cornea* 1998;17:74-78.
192. Hume EB, Moreau JM, Conerly LL, et al. Clarithromycin for experimental *Staphylococcus aureus* keratitis. *Curr Eye Res* 1999;18:358-362.
193. Wooley RE, Jones MS, Shotts EB Jr. Uptake of antibodies in gram-negative bacteria exposed to EDTA-Tris. *Vet Microbiol* 1984;10(1):57-70.
194. Vaara M. Agents that increase the permeability of the outer membrane. *Microbiol Rev* 1992;56:395-411.
195. Zamboni FJ, Uras R, Lima ALH. Drogas utilizadas para limpeza e conservação das lentes de contato. In: Lima ALH, Melamed J, Calixto N, eds. *Terapêutica clínica ocular*. São Paulo, Brazil: Roca; 1995:191-194.
196. O'Brien TP. Bacterial keratitis. In: Krachmer JH, Mannis MJ, Holland EJ, eds. *Cornea*. Philadelphia: Mosby; 1997:1139-1189.
197. Steiner RF. Current therapy for bacterial keratitis and bacterial conjunctivitis. *Am J Ophthalmol* 1991;112:10S-14S.
198. Gelender H, Rettich C. Gentamicin-resistant *Pseudomonas aeruginosa* corneal ulcers. *Cornea* 1984;3:21-26.
199. Cameron JA, Antonios SR, Cotter JB, et al. Endophthalmitis from contaminated donor corneas following penetrating keratoplasty. *Arch Ophthalmol* 1991;105:54-59.
200. Leibowitz HM. Clinical evaluation of ciprofloxacin 0.3% ophthalmic solution in the treatment of bacterial keratitis. *Am J Ophthalmol* 1991;112:34S-47S.
201. Fields PI, Groisman EA, Heffron F. A *Salmonella* locus that controls resistance to microbicidal proteins from phagocytic cells. *Science* 1988;24:1059-1062.
202. Varley GA, Meisler DM. Complications of penetrating keratoplasty. *Refract Corneal Surg* 1991;7(1):62-66.
203. Polack FM, Locatcher-Khorazo D, Gutierrez E. Bacteriological study of donor eyes. *Arch Ophthalmol* 1967;78:219-225.
204. Mishler KE, Keates RH. Clinical safety of corneal storage media. *Ophthalmic Surg* 1977;8:23-24.
205. Olson RJ, McMain ME, Slappey TE. Donor eye contamination. *Ann Ophthalmol* 1979;Dec:1875-1878.
206. Sugar J, Liff J. Bacterial contamination of corneal donor tissue. *Ophthalmic Surg* 1980;11:250-252.
207. Pardos GJ, Gallagher MA. Microbial contamination of donor eyes. *Arch Ophthalmol* 1982;100:1611-1613.
208. Karjalainen K, Vannas A. Bacterial contamination of donor corneas. *Ophthalmic Surg* 1984;15:770-772.
209. Insler MS, Urso LF. *Candida albicans* endophthalmitis after penetrating keratoplasty. *Am J Ophthalmol* 1987;104:56-57.
210. Insler MS, Cavanagh HD, Wilson LA. Gentamicin-resistant *Pseudomonas* endophthalmitis after penetrating keratoplasty. *Br J Ophthalmol* 1985;69:189-191.
211. Baer JC, Nirankari VS, Glaros DS. *Streptococcal* endophthalmitis from contaminated corneas after keratoplasty. *Arch Ophthalmol* 1988;106:517-520.
212. Kloess PM, Stulting D, Waring GO III, et al. Bacterial and fungal endophthalmitis after penetrating keratoplasty. *Am J Ophthalmol* 1993;115:309-316.
213. Reschini RM, Kara-José N, Arieta CEL. Úlceras de córnea por *Serratia marcescens* pós ceratoplastia penetrante. *Arq Bras Oftalmol* 1991;54:265-268.
214. Hull D, Green K, McQuaig CS, et al. Modification of the antibiotic system in M-K medium. *Am J Ophthalmol* 1977;83:198-205.
215. Baum J, Barza M, Kane A. Efficacy of penicillin G cefazolin and gentamicin in M-K medium at 4°C. *Arch Ophthalmol* 1978;96:1262-1264.
216. Kowalski RP, Sundar-Raj CV, Stuart JC, et al. Antifungal synergism. A proposed dosage for corneal storage medium. *Arch Ophthalmol* 1985;103:250-256.
217. Ganz T, Liu L, Valore EV, et al. Posttranslational processing and targeting of transgenic human defensin in murine granulocyte, macrophage, fibroblast, and pituitary adenoma cell lines. *Blood* 1993;82:641-650.
218. Schwab IR, Dries D, Cullor J, et al. Corneal storage medium preservation with defensins. *Cornea* 1992;11:370-375.
219. Garcia-Ferrer FJ, Murray PR, Pepose JS. Corneal endothelial toxicity of DexSol corneal storage medium supplemented with povidone-iodine. *Arch Ophthalmol* 1992;110:1519-1520.
220. Steinemann TL, Kaufman HE, Beuerman RW, et al. Vancomycin-enriched corneal storage medium. *Am J Ophthalmol* 1992;113:555-560.
221. Hwang DG, Nakamura T, Trousdale MD, et al. Combination antibiotic supplementation of corneal storage media. *Am J Ophthalmol* 1993;115:299-308.
222. Mindrup EA, Dubbel PA, Doughman DJ. Betadine decontamination of donor globes. *Cornea* 1993;12:324-329.
223. Lass JH, Gordon JF, Sugar A, et al. Optisol containing streptomycin. *Am J Ophthalmol* 1993;116:503-504.
224. Kaufman HE, Varnell ED, Kaufman S. Chondroitin sulfate in a new corneal preservation medium. *Am J Ophthalmol* 1984;98:112-114.
225. McCarey BE, Kaufman HE. Improved corneal storage. *Invest Ophthalmol Vis Sci* 1974;13:165-173.
226. Garcia-Ferrer FJ, Pepose JS, Murray PR, et al. Antimicrobial efficacy and corneal endothelial toxicity of DexSol corneal storage medium supplemented with vancomycin. *Ophthalmology* 1991;98:863-869.
227. Poole TG, Insler MS. Contamination of donor cornea by gentamicin-resistant organisms. *Am J Ophthalmol* 1984;97:560-564.
228. Mathers WD, Lemp MA. Corneal rim cultures. *Cornea* 1987;6:231-233.
229. Farrel PL, Fan JT, Smith RE, et al. Donor cornea bacterial contamination. *Cornea* 1991;10:381-386.
230. Weckbach LS, Bloom HR, Wander AH, et al. Survival of *Streptococcus pneumoniae* in corneal storage media. *Cornea* 1992;11:200-203.

## The Use Of Antimicrobial Peptides In Ophthalmology

231. Mchaourab HS, Hyde JS, Feix J. Binding and state of aggregation of spin-labeled cecropin AD in phospholipid bilayers: effects of surface charge and fatty acyl chain length. *Biochemistry* 1994;33:6691-6694.
232. Jaynes JM. D<sub>5</sub>C activity in Optisol. 1995.
233. Kreger AS, Griffin OK. Physicochemical fractionation of extracellular cornea damaging proteases of *Pseudomonas aeruginosa*. *Infect Immunol* 1974;9:828-834.
234. Kessler E, Kennah HE, Brown SI. *Pseudomonas* protease: purification, partial characterization, and its effect on collagen, proteoglycan, and rabbit corneas. *Invest Ophthalmol Vis Sci* 1977;16:488-497.
235. Rich D, Cullor J, Mannis MJ, et al. The in vitro activity of defensins against *Pseudomonas* in the presence of human tears. *Invest Ophthalmol Vis Sci* 1990;31:449.
236. Travis J. Reviving the antibiotic miracle? *Science* 1994;1994:360-362.
237. Gough M, Hancock REW, Kelly NM. Anti endotoxic potential of cationic peptide antimicrobials. *Infect Immun* 1996;64:4922-4927.
238. Darveau RP, Cunningham MD, Seaford CL, et al. Beta-lactam antibiotics potentiate magainin 2 antimicrobial activity in vitro and in vivo. *Antimicrob Agents Chemother* 1991;35:1153-1159.
239. Ahmad I, Perkins WR, Lupan DM, et al. Liposomal entrapment of the neutrophil-derived peptide indolicidin endows it with in vivo antifungal activity. *Biochim Biophys Acta* 1995;1237:109-114.
240. Piers KL, Brown MH, Hancock REW. Improvement of outer membrane-permeabilizing and lipopolysaccharide-binding activities of an antimicrobial cationic peptide by C-terminal modification. *Antimicrob Agents Chemother* 1994;38(10):2311-2316.



# HUMAN RETINAL PIGMENT EPITHELIAL LYSIS OF EXTRACELLULAR MATRIX: FUNCTIONAL UROKINASE PLASMINOGEN ACTIVATOR RECEPTOR, COLLAGENASE, AND ELASTASE

---

BY Susan G. Elner, MD

## ABSTRACT

*Purpose:* To show (1) human retinal pigment epithelial (HRPE) expression of functional urokinase plasminogen activator receptor (uPAR; CD87), (2) HRPE secretion of collagenase and elastase, (3) uPAR-dependent HRPE migration, and (4) uPAR expression in diseased human retinal tissue.

*Methods:* Immunohistochemistry for uPAR was performed on cultured HRPE cells and in sections of human retina. Double-immunofluorescent staining of live human RPE cells with anti-CR3 antibody (CD11b) was performed to demonstrate the physical proximity of this  $\beta 2$  integrin with uPAR and determine whether associations were dependent on RPE confluence and polarity. Extracellular proteolysis by HRPE uPAR was evaluated using fluorescent bodipy-BSA and assessed for specificity by plasminogen activator inhibitor-1 (PAI-1) inhibition. The effect of interleukin-1 $\beta$  (IL-1 $\beta$ ) on uPAR expression was assessed. Collagenase and elastase secretion by unstimulated and IL-1-stimulated HRPE cells was measured by  $^3\text{H}$ -labelled collagen and elastin cleavage. HRPE-associated collagenase was also assessed by cleavage of fluorescent DQ-collagen and inhibited by phenanthroline. Using an extracellular matrix assay, the roles of uPAR and collagenase in HRPE migration were assessed.

*Results:* Immunoreactive uPAR was detected on cultured HRPE cells and increased by IL-1. On elongated, live HRPE cells, uPAR dissociated from CD11b (CR3) and translocated to anterior poles of migrating cells. Extracellular proteolysis was concentrated at sites of uPAR expression and specifically inhibited by PAI-1. Cultured HRPE cells secreted substantial, functional collagenase and elastase. IL-1 upregulated uPAR, collagenase, and elastase activities. Specific inhibition of uPAR, and to a lesser degree collagenase, reduced HRPE migration in matrix/gel assays. Immunoreactive uPAR was present along the HRPE basolateral membrane in retinal sections and in sections of diseased retinal tissue.

*Conclusions:* HRPE cells express functional uPAR, collagenase, and elastase, which may permit HRPE proteolysis and migration. uPAR polarization may concentrate proteolysis at the leading edge of migrating HRPE cells.

*Trans Am Ophthalmol Soc* 2002;100:273-299

## INTRODUCTION

---

Disruption of collagen- and elastin-rich Bruch's membrane that underlies the retinal pigment epithelium (RPE) and periretinal RPE cellular migration occur in several important retinal diseases, including age-related macular degeneration (ARMD) and proliferative vitreoretinopathy (PVR). Urokinase plasminogen activator receptor (uPAR CD87) and matrix metalloproteinases (MMPs) are important mechanisms by which leukocytes, vascular endothelial cells, reactive tissue cells, and neoplastic cells penetrate extracellular matrix (ECM) in virtually all tissues. However, uPAR, by activating plasminogen to form plasmin, yields proteolytic activity that lyses a

wide variety of ECM components when compared to the MMP.

These observations lead to the hypothesis that RPE uPAR-mediated activation of proteolysis, in contrast to secretion of enzymes cleaving elastin, interstitial collagen, and type IV collagen, mediates RPE migration through ECM and is expressed in retinal lesions.

This study demonstrates the following for the first time: (1) RPE uPAR expression in situ; (2) proinflammatory cytokine-enhanced immunoreactive and functional RPE uPAR activity; (3) RPE secretion of interstitial collagenase and elastase capable of hydrolyzing natural substrates; (4) the preeminent role of RPE uPAR in mediating RPE migration through extracellular matrix using a novel three-dimensional collagen gel assay technique; and (5) RPE uPAR expression in human lesions of subretinal choroidal neovascularization associated with Bruch's membrane disruption, proliferative vitreoretinopathy with

From the University of Michigan and University of Chicago. This work was supported by grants EY-09441 and EY-007003 from the National Institutes of Health.

RPE periretinal migration into the matrix of periretinal membranes, and uveitis with chronic active inflammation. In so doing, this study indicates that uPAR is important to RPE participation in retinal pathology.

#### BACKGROUND

Age-related macular degeneration is the most common cause of legal blindness in patients over the age of 50 from developed countries.<sup>1</sup> The early manifestations of ARMD involve Bruch's membrane thickening and formation of extracellular matrix- and lipid-containing deposits.<sup>1</sup> Focal collections of this material enlarge to form drusen, which is the hallmark finding in ARMD.<sup>2</sup> The mechanism by which this material is deposited in Bruch's membrane is not well understood, but it is commonly believed to be derived from the aged or dysfunctional RPE cells.<sup>2,3,4</sup> Accompanying the changes in Bruch's membrane are progressive degradative changes in the RPE with pigmentary and atrophic alterations in RPE that become clinically apparent. Although most patients with ARMD exhibit the atrophic form, composed of drusen and RPE alterations, severe vision loss usually results from choroidal neovascularization (CNV), which complicates ARMD. ARMD neovascularization originates from the vessels in the choriocapillaris of the choroid and grows through breaks in the altered, thickened Bruch's membrane, to extend either beneath the RPE or the sensory retina. The RPE has been noted to be a major component of CNV both in postmortem<sup>5-7</sup> and in surgical CNV specimens. RPE cells migrate from their normal position on Bruch's membrane and grow over the surface of the CNV as it penetrates through Bruch's membrane.<sup>8-12</sup>

Although a genetic component in typical ARMD is suggested by a familial tendency in some patients, a specific genetic defect has not been identified. Sorsby's fundus dystrophy is an autosomal dominant macular disorder, less common than ARMD, that strikes patients at an earlier age. It shares most of the clinical and pathophysiologic features of ARMD. In Sorsby's dystrophy, like ARMD, atrophy of the RPE, choriocapillaris, and photoreceptors may occur, with frequent development of CNV, resulting in severe visual loss. Sorsby's has been mapped to human chromosome 22, the same region to which the tissue inhibitor of matrix metalloproteinase-3 (TIMP-3) gene has been mapped.<sup>13</sup> Tissue inhibitor of matrix metalloproteinases regulate MMPs, which are a family of enzymes whose chief function is the degradation of ECM, including ECM components found in Bruch's membrane.<sup>14</sup> Point mutations in the TIMP-3 gene, which render the altered TIMP-3 defective, have been identified in affected members of Sorsby's fundus dystrophy families, implicating it in the pathogenesis of this dystrophy.<sup>15</sup> TIMP-3 is unique among TIMPs because upon

secretion, it binds to extracellular matrix components. Thickening of Bruch's membrane is a hallmark of Sorsby's dystrophy.<sup>16</sup> Studies have demonstrated increases in TIMP-3 in Bruch's membrane in Sorsby's patients, except in areas in which RPE cells have degenerated.<sup>17</sup> An accumulation of TIMP-3 in the ECM of Bruch's membrane may result in excessive ECM remodeling and lead to abnormal Bruch's membrane thickening noted in Sorsby's dystrophy and ARMD.<sup>15,18</sup> The reactive alterations in Bruch's membrane predispose to the development of breaks in this tissue through which ingrowth of new vessels from the choriocapillaris may occur.<sup>19-23</sup> However, the process of how breaks develop in Bruch's membrane remains unknown.

#### THE MATRIX METALLOPROTEINASES

The MMPs are a family of enzymes that hydrolyze protein components of the ECM and are involved in normal ECM turnover, remodeling, and connective tissue turnover.<sup>24</sup> In addition, they have been found to play important roles in many normal and pathologic processes, such as angiogenesis,<sup>25,26</sup> wound healing,<sup>24</sup> ovulation,<sup>27</sup> trophoblast invasion,<sup>28</sup> skeletal development,<sup>29,30</sup> arthritis,<sup>31,32</sup> cancer invasion and metastasis,<sup>33,34</sup> aneurysmal formation,<sup>35</sup> and atherosclerotic plaque rupture.<sup>36-38</sup>

MMPs have been categorized into more than 20 groups on the basis of their substrate specificity.<sup>39</sup> They are also known by their common group names, interstitial collagenases (MMP 1,8,13), gelatinases (MMP 2,9), stromelysins (MMP 3,10,11), and membrane-type MMPs (MT-MMP 14-17, 24,25) (Table I). MMPs are secreted as inactive proenzymes that require activation by the removal of a propeptide, to reveal a zinc-active binding site. MMP activity may be regulated at a number of stages, including (1) gene activation and transcription, (2) translation, (3) secretion of the latent proenzyme, (4) proenzyme activation, and (5) inactivation by endogenous inhibitors (ie, TIMPs).

The interstitial collagenases are primarily responsible for the degradation of structural collagens types I, II, and III.<sup>40</sup> MMP-1, or collagenase 1, is the most ubiquitously expressed and is produced at low constitutive levels by fibroblasts, macrophages, and endothelial cells and at higher constitutive levels by many tumor cells.<sup>41</sup> Expression of MMP-1 is upregulated by inflammatory cytokines and growth factors.<sup>41</sup> MMP-1 expression has been associated with low survival rates in many tumors, including esophageal and pancreatic cancer.<sup>42-44</sup>

Gelatinases A and B primarily degrade collagen type IV but can degrade collagen types I, V, and gelatin.<sup>27</sup> They are believed to play a particularly important role in angiogenesis.<sup>26</sup> Gelatinase A, MMP-2, is regulated differently than all other MMPs, both transcriptionally and extracel-

TABLE I: NOMENCLATURE OF MATRIX METALLOPROTEINASES (MMPs)

CLASS	COMMON NAME	MMP	MAJOR SUBSTRATES
Collagenases	Collagenase 1	MMP1	Types I, II, III, VII collagens
	Collagenase 2	MMP8	
	Collagenase 3	MMP13	
Gelatinases	Gelatinase A	MMP2	Types I, IV, V collagens, gelatin
	Gelatinase B	MMP9	
Stromelysins	Stromelysin 1	MMP3	Fibronectin, laminin, collagens IX, X, elastin
	Stromelysin 3	MMP11	
Membrane-type MMPs	MT1-MMP	MMP14	Activate latent gelatinase A
	MT2-MMP	MMP15	
	MT3-MMP	MMP16	

lularly.<sup>45</sup> The promoter of the gelatinase A gene lacks the TPA (12-tetradecanoylphorbol-13-acetate) responsive element and the transactivator sequences, AP-1 and PEA-3.<sup>46</sup> The promoter also lacks a transforming growth factor-beta (TGF- $\beta$ ) inhibitory element. As a result, gelatinase A is not upregulated by phorbol myristate acetate (PMA), tumor necrosis factor alpha (TNF- $\alpha$ ), interleukin-1 (IL-1), plasmin, or trypsin, nor is it inhibited by TGF- $\beta$ .<sup>30</sup> The gelatinases are inactivated either by TIMPs, which bind to their catalytic domain, or by autocatalysis, mechanisms that prevent uncontrolled proteolysis.<sup>47,48</sup>

Latent, pro-gelatinase A is constitutively secreted by vascular and synovial endothelial cells, monocytes, lymphocytes, dendritic cells, fibroblasts, and tumor cells,<sup>49, 50</sup> whereas other MMPs are not constitutively expressed. Unlike other MMPs, gelatinase A can be activated on cell surfaces via two mechanisms: (1) MT1-MMP and type I collagen, and (2) thrombin and serine protease, activated protein C.<sup>26,30</sup> When activated by the MT1-MMP pathway, TIMP-2 binds to MT1-MMP on the cell surface; pro-gelatinase A then binds to TIMP-2 and is cleaved to its active form by an adjacent MT1-MMP on the cell surface. Collagen I promotes gelatinase A activation by upregulating MT1-MMP. Activation via the activated protein C-thrombin pathway occurs more rapidly than activation via collagen I and is independent of MT1-MMP. Thrombin binds thrombomodulin on the endothelial cell surface, which leads to the conversion of protein C to activated protein C. Activated protein C, in turn, rapidly activates gelatinase A, occurring even in the absence of cells.<sup>26</sup> The thrombin-activated protein C activation pathway for gelatinase A may be particularly important in the angiogenesis of cancer and rheumatoid arthritis, since high levels of thrombin are present in these conditions.<sup>51</sup>

Gelatinase B, MMP-9, is not constitutively expressed, but is produced by a variety of cells, including epithelial

cells, fibroblasts, endothelial cells, neutrophils, monocytes, and lymphocytes in response to many stimuli, including lipopolysaccharide (LPS), viruses, cytokines, and cell-cell contact.<sup>34,50</sup> Gelatinase B is stored in both active and latent forms in the cell cytosol in secretory vesicles.<sup>52</sup> Release of gelatinase B from neutrophil granules occurs rapidly in response to interleukin-8 (IL-8). Secreted gelatinase B is bound to TIMP-1, while cytosolic gelatinase B is not bound to TIMP-1.<sup>26</sup> Because of the difference in constitutive expression between gelatinases A and B, the ratio of gelatinase B over gelatinase A has been used as a marker of inflammation in autoimmune diseases such as rheumatoid arthritis and multiple sclerosis.<sup>53,54</sup>

The gelatinases function as regulators of cytokines and chemokines. Gelatinase B promotes inflammation by converting the proform of IL-1 $\beta$  into the active cytokine.<sup>55</sup> It also cleaves IL-8, a major chemoattractant for neutrophils, into a more active form, potentiating IL-8 effects. Neutrophils attracted and stimulated by IL-8 may then release more gelatinase B, potentiating the inflammatory response.<sup>50</sup> Gelatinases also antagonize chemokine activity. Gelatinase A cleaves monocyte chemotactic protein-3 (MCP-3), a chemoattractant for monocytes, into a less active form, thereby dampening the leukocytic infiltration.<sup>56</sup>

MMP-3 or stromelysin-1 can degrade a variety of ECM proteins, including fibronectin, laminin, elastin, and collagens IX and X.<sup>57</sup> Stromelysins also indirectly contribute to the collagen degradation by their activation of other latent MMPs.<sup>40</sup> MMP-3 is expressed in atherosclerotic lesions, particularly in areas of the plaque where rupture is most common, implicating MMPs in ECM resorption that may result in plaque instability and rupture.<sup>37, 38</sup> There has also been evidence to suggest that MMP-3 may contribute to the development of aneurysms.<sup>58</sup>

MT-MMPs are membrane-bound MMPs that cleave

collagen fibrils into classic 1:3 fragments and serve to activate other latent MMPs, particularly gelatinase A. MT-MMPs are synthesized in a latent form but are activated intracellularly, by a furin-dependent mechanism. MT-MMPs have been implicated in tumor invasion, with increased levels of MT1-MMP found in normal stromal cells adjacent to tumors.<sup>41</sup>

#### MATRIX METALLOPROTEINASES IN THE RETINA

A number of MMPs have been noted in ocular tissues, most being associated with the RPE. Cultured human RPE cells have been shown to secrete basal levels of latent interstitial collagenase (MMP-1), stromelysin (MMP-3), gelatinases A (MMP-2) and B (MMP-9), and TIMP-1.<sup>59</sup> These MMPs have shown variable expression to stimulants. The phorbol ester, TPA, increases MMP-1, -2, -3, and -9, whereas TPA decreases TIMP-1.<sup>59,60</sup> The proinflammatory cytokine, IL-1, stimulates production of MMP-1 and MMP-9, but the anti-inflammatory, fibrogenic cytokine, TGF- $\beta$ , does not.<sup>61</sup> Immunohistochemical studies of sections from post-mortem human eyes have identified MMP-2 and MT1-MMP in situ in the RPE, retina, and choroid.<sup>62</sup> Studies have demonstrated TIMP-3, which has been associated with Sorsby's macular degeneration, in the RPE, implicating the RPE as a likely source of TIMP-3 found in the thickened abnormal Bruch's membrane.<sup>63</sup> MMPs of all classes have been identified in the RPE, thereby giving the RPE the capability of modulating ECM remodeling and degradation in their surrounding milieu.

#### UROKINASE PLASMINOGEN ACTIVATOR AND ITS RECEPTOR uPAR

Another well-known modulator of extracellular matrix is the serine protease, urokinase plasminogen activator (uPA), which catalyzes conversion of inactive plasminogen to its active form, plasmin.<sup>64</sup> Plasmin is a broad-spectrum protease that degrades fibrin and most substrates in the ECM, including fibronectin and laminin. uPA is secreted by a wide variety of cells in tissues, including those of the retina and choroid, as a single-chain polypeptide (pro-uPA), which is enzymatically inactive. Pro-uPA binds with high affinity to its receptor, urokinase plasminogen activator receptor (uPAR; CD87), a single-chain 55 to 60 kD glycoprotein that is anchored to cell membranes by a glucosylphosphatidylinositol (GPI) moiety.<sup>65</sup> uPAR binds the amino-terminal domain of pro-uPA, leaving the catalytic, carboxyl terminal domain open.<sup>66</sup> Pro-uPA is enzymatically cleaved in its uPAR-bound form into a two-chain active enzyme by plasmin. uPA then, in turn, converts membrane-associated plasminogen into plasmin.<sup>64</sup> uPAR has been identified on activated monocytes,<sup>66</sup> T-lymphocytes,<sup>67</sup> neutrophils,<sup>68</sup> a variety of nonhematopoietic cells (including endothelial cells, fibroblasts, hepatocytes, ker-

atinocytes),<sup>69,70,67</sup> and many tumor cells (including melanoma, breast, colon, prostate carcinoma).<sup>67,71,72</sup>

Activity of uPA and its receptor, uPAR, is correlated with ECM proteolysis, alterations in cell adhesion, cell motility, and cellular invasion through the ECM.<sup>73</sup> uPA or receptor-bound uPA can be blocked by two endogenous inhibitors known as plasminogen activator inhibitor 1 and 2 (PAI-1 and PAI-2),<sup>64</sup> which belong to the serpin protease superfamily. Several growth factors and cytokines have been implicated in uPA/uPAR regulation, including epidermal growth factor (EGF),<sup>74</sup> basic fibroblast growth factor (bFGF),<sup>75</sup> TGF- $\alpha$ ,<sup>76</sup> and TNF- $\alpha$ .<sup>77</sup>

uPAR functions to (1) bind uPA, mediate the internalization of uPA/PAI complexes, and direct uPA proteolytic activity<sup>78,79</sup>; (2) stimulate cell proliferation when bound to uPA<sup>80</sup>; (3) induce chemotactic cell migration of leukocytes and multiple other cell types through activation of uPA; (4) promote cell-cell and cell-ECM adhesion via binding to vitronectin or through interactions with  $\beta_1$  or  $\beta_2$  integrins; (5) mediate signal transduction; (6) promote differentiation in myelomonocytic cells; and (7) activate monocytes and T-lymphocytes.<sup>81,82</sup> Through these cellular functions, uPA/uPAR has been shown to play an important role in proteolysis, cell migration, angiogenesis, leukocyte chemotaxis, and tumor invasion and metastasis.

#### uPA/uPAR IN THE RETINA

Studies of uPA/uPAR in the eyes have been limited to immunohistochemical localization. These studies have shown that uPA appears to have a wide tissue distribution in the posterior segment of the eye, where it is located in the optic nerve, sclera, choroidal fibroblasts, blood vessels, vitreous, inner neural retina, and RPE.<sup>83</sup> Moreover, RPE cells in vitro have been shown to produce immunoreactive uPA<sup>84</sup> and a possible inhibitor, PAI, which is immunologically and biochemically similar to PAI-1.<sup>84,85</sup> Studies had reported indirect stimulation of uPA activity in RPE cells in response to interferon-gamma (IFN- $\gamma$ ) by suppression of PAI expression.<sup>86</sup> Limited studies have been performed on the expression of uPAR and its regulation in RPE cells. Thrombin<sup>87</sup> and TGF- $\beta$ <sup>88</sup> have been shown to induce uPAR mRNA, resulting in an increase of uPAR on the RPE cell surface. In contrast, IFN- $\gamma$ , despite increasing uPAR mRNA, was not reported to increase RPE cell-surface uPAR.<sup>88</sup> These studies, however, have not demonstrated RPE uPAR function and its modulation by proinflammatory cytokines, interactions with other RPE cell surface ligands, alterations of distribution with changes in RPE morphology, or its presence in diseased retinal tissues.

#### REGULATION OF CELL MIGRATION IN PVR

The presence of MMPs and uPAR is not only important in

the pathogenesis of ocular diseases, which involve ECM degradation, but these enzymes also may play roles in diseases that involve cell migration, such as PVR and uveitis. In PVR, RPE cells migrate from their position on Bruch's membrane, where their attachment is in part formed by  $\beta_1$  integrin binding to fibronectin, laminin, and collagen IV lining the vitreous and retinal surfaces. RPE migration and proliferation at these sites contribute to periretinal and vitreous membrane formation. PVR membranes have been shown to be composed of collagen types I, II, III, and, to a lesser degree, laminin and collagen types IV and V.<sup>99</sup> During PVR, the RPE cells have been noted to produce new ECM around themselves, which contains molecules similar to their original basement membrane firmly anchoring the RPE cells in these pathologic membranes.<sup>90</sup> MMPs may be important in the remodeling of ECM, which occurs during PVR. A number of cytokines, including IL-1, TNF- $\alpha$ , IFN- $\gamma$ , IL-6, MCP-1, and macrophage colony-stimulating factor (M-CSF), have been noted in PVR<sup>91-93</sup> and may, in part, direct migration, proliferation, and transformation of RPE cells.<sup>94</sup>

Cellular migration, however, can be affected by interactions between uPA/uPAR, integrins, and MMPs. uPA/uPAR promotes cell migration by (1) degradation of ECM proteins, allowing cells to cross basement membranes,<sup>95</sup> both directly through its activation of plasminogen to plasmin and indirectly via the activation of proMMPs by uPA,<sup>96</sup> (2) direct chemotactic effects of both uPA and uPAR on capillary endothelial cells, keratinocytes, fibroblasts, and neutrophils,<sup>97-99</sup> (3) uPAR binding to vitronectin, an adhesive glycoprotein, promoting cell migration by inhibiting adhesion to fibronectin or fibrinogen,<sup>100</sup> and (4) uPAR colocalization with adhesion molecules, integrins, and cadherins, modulating cell adhesion and migration. In particular, uPAR physically associates with the leukocyte integrin CD11b/CD18 (CR3/Mac 1), which has been demonstrated on RPE cells.<sup>101,102</sup> The association of uPAR and CD11b changes depending on cell shape. In resting cells, uPAR and CD11b colocalize, but following cell polarization (elongation) and migration, the receptors dissociate, with CD11b concentrating in the uropodia and uPAR concentrating in the lamellipodia (leading edge).<sup>103</sup> In view that CD11b regulates cell adhesion, chemotaxis, and cell migration in many cell types, uPAR may further modulate migration.

The MMPs may also modulate cell migration via a number of methods, including (1) proteolysis of ECM, (2) cleavage and inactivation of proinflammatory cytokines, which may stimulate cell chemotaxis,<sup>104</sup> (3) MMP down-regulation of uPAR-mediated proteolysis<sup>105</sup> via MMP-12 cleavage of the uPAR domain responsible for uPA binding, thereby limiting uPAR activity,<sup>106</sup> and (4) cleavage of adhesion molecules CD44 and L-selectin.<sup>107,108</sup>

Since RPE cells possess  $\beta_1$  integrins and uPA/uPAR and produce a variety of MMPs, all of which may effect migration and proteolysis, this study was undertaken to further elucidate the role of uPAR in RPE migration and proteolysis by (1) studying the modulation of uPAR by proinflammatory cytokines, (2) studying and comparing the effects of functional uPAR and interstitial collagenases on RPE migration and proteolysis, and (3) studying the expression of uPAR in diseased retinal tissues.

## **MATERIALS AND METHODS**

---

### **HUMAN RPE CELL CULTURE AND ISOLATION**

Human RPE cells were isolated from donor eyes as previously described<sup>109</sup> and cultured in Dulbecco's modified essential medium (DMEM) containing 15% fetal bovine serum. The cultured RPE cells formed monolayers showing typical polygonal morphology and pigmentation of scattered cells as well as the expression of cytokeratin.<sup>110</sup> Primary, first passaged, and second passaged RPE cell cultures were trypsinized and seeded onto either gel-coated slides for proteolysis studies, gelatin-nylon mesh matrix in 35-mm culture wells in the same media for migration studies, or glass coverslips for immunohistochemical staining. RPE cultures were maintained in the media and observed by phase contrast microscopy until they reached confluence. They were used in migration or proteolysis assays or processed for light microscopy and/or immunohistochemistry.

### **IMMUNOHISTOCHEMICAL STAINING FOR UROKINASE PLASMINOGEN ACTIVATOR RECEPTOR**

Human RPE cell culture preparations on glass coverslips, paraffin-embedded tissue sections of eyes enucleated following failed retinal detachment surgery with PVR or sections of normal retina/RPE from eyes enucleated for choroidal melanoma, or surgically excised choroidal neovascular membranes were stained for uPAR using an avidin-biotinylated enzyme complex (ABC) technique. RPE cell preparations on coverslips were gently fixed for 5 minutes in 4% paraformaldehyde. Tissue sections were deparaffinized by immersing the sections sequentially in xylene, followed by graded alcohols. Endogenous peroxidase was blocked by preincubating the fixed RPE cell preparations or tissue sections in 0.3% H<sub>2</sub>O<sub>2</sub> for 20 minutes. Nonspecific antibody binding sites were blocked using diluted normal blocking serum (Vectastain Universal Elite ABC kit, Vector Laboratories, Burlingame, California) for 20 minutes. Monoclonal antibody to uPAR (CD87; 1:25; American Diagnostica, Inc, Greenwich, Connecticut) was used as primary antibody. Platelet endothelial cell adhesion molecule-1 (PECAM-1; CD31), an antibody of similar isotype to uPAR, was used

as control primary antibody. Following a 30-minute incubation in primary antibody, sequential incubations of diluted biotinylated secondary antibody and Vectastain ABC reagent for 30 minutes each were performed (Vectastain Universal Elite ABC kit, Vector Laboratories, Burlingame, California). Reaction product was visualized by development in buffer containing 3-amino-9-ethylcarbazole (5 mg/mL) and 0.01% hydrogen peroxide to yield a red-brown, reaction product. Cell preparations were counterstained with hematoxylin and mounted in GelMount (Biomed, Foster City, California).

#### NYLON-GEL MEMBRANE PREPARATION

Nylon mesh (Nytex-3-120/52, mesh opening 120  $\mu\text{m}$ , Tetko Inc, Briarcliff Manor, New York) used for light microscopy and immunohistochemical studies was cut into 18-mm squares and rinsed in 75% ethanol for 5 minutes. Following drying under ultraviolet light for 30 minutes, the nylon mesh was placed in a 35-mm sterile Petri dish. A 4% gelatin solution was prepared by boiling gelatin in Hank's balanced salt solution (HBSS) and returning the gelatin solution to 37°C. Four drops (approximately 100  $\mu\text{L}$  each) were placed on the nylon mesh and allowed to dry on a slide warmer at 42°C until tacky. One drop of 0.5% glutaraldehyde was then placed to the gelatin-nylon matrix and allowed to dry for 15 minutes on a slide warmer. Remaining glutaraldehyde was aspirated and the cross-linked gelatin-nylon mesh matrix removed with sterile forceps and rinsed three times in HBSS, each time for 10 minutes. To obtain more substantial gelatin-nylon mesh cell culture supports, the cross-linked gelatin was laminated by repeating the process of gelatin coating with the 4% gelatin solution and cross-linking with glutaraldehyde. Following final rinsing in HBSS, the gelatin-nylon mesh supports were placed in media in an incubator overnight to leach out any remaining glutaraldehyde. They were then rinsed and placed in 35-mm Petri dishes, and 25  $\mu\text{L}$  of 10 mg/mL fibronectin solution was placed on their surfaces. The transportable, sterile cross-linked gelatin-nylon mesh matrices were allowed to dry for 20 minutes, following which RPE cells were seeded onto their surfaces in a dome-shaped drop that covered the nylon mesh. The RPE cells were allowed to attach to the mesh surfaces for 30 minutes at 37°C, following which the culture well was filled with the usual volume of regular media.

For cell migration and proteolysis studies, nylon mesh was cut into 12-mm squares and rinsed in 75% ethanol for 5 minutes. A 6% to 10% gelatin solution was prepared by boiling gelatin in HBSS containing either Bodipy-BSA (4,4-difluoro-5,7-dimethyl-4-bora-3a,4a-diaza-5-indacene-3-propionic acid-conjugated bovine serum albumin; Molecular Probes) or DQ collagen (type IV from

human placenta, fluorescein conjugate; Molecular Probes Cat No. D-12052). Bodipy-BSA and DQ collagen were used to visualize proteolytic activity in the gel-mesh matrix. Bodipy-BSA and DQ collagen become fluorescent upon exposure to uPA protease activity and to collagenase activity, respectively.

To avoid denaturation of the Bodipy-BSA or DQ collagen added to the gelatin, the solution was allowed to cool to  $\sim 42^\circ\text{C}$  before the addition of this compound. Ten microliters of cell attachment factor (Cell Systems Corporation, Kirkland, Washington) was placed on a coverslip for 15 minutes at 42°C in an incubator. After drying, a sterile nylon mesh was placed on the coverslip. Fifty microliters of 6% to 10% gelatin solution containing 10% fetal bovine serum (FBS) and Bodipy-BSA or DQ collagen (final concentration 1 mg/mL) was placed on the nylon mesh and allowed to harden in a refrigerator at 4°C for 10 minutes. The gelatin-nylon mesh matrix on the coverslip was then placed at room temperature.

#### HISTOCHEMICAL/IMMUNOHISTOCHEMICAL ANALYSIS OF NYLON MESH RPE CULTURES

RPE cultures grown on gelatin-nylon matrix were allowed to reach confluent monolayers. The cultures were monitored for confluence by observing them with phase contrast microscopy. Some cultures were then fixed with buffered 1% formaldehyde/0.5% glutaraldehyde and processed for light microscopy. For this, the cultures were sectioned with a razor blade, and portions were submitted for sequential dehydration through alcohols and embedding in plastic resin. Two-micrometer sections were then cut with a glass knife, stained with toluidine blue, and mounted on glass slides for light microscopic observation.

To detect RPE  $\text{Na}^+\text{-K}^+$  ATPase membrane protein, immunoperoxidase staining was performed on 4- $\mu\text{m}$ -section soft paraffin-embedded gelatin-nylon mesh RPE cultures.<sup>109</sup> Briefly, RPE sections were deparaffinized, rehydrated, and preincubated with blocking serum (10% goat serum) to avoid nonspecific binding. The sections were then incubated with primary rabbit-antibovine  $\text{Na}^+\text{-K}^+$ ATPase antibody (1:250 dilution, kind gift from Dr Steve Ernst, University of Michigan, Department of Anatomy and Cell Biology) for 1 hour. The sections were overlaid with 3%  $\text{H}_2\text{O}_2$  for 5 minutes to block endogenous peroxidase activity and incubated sequentially with secondary biotinylated goat anti-rabbit antibody and streptavidin conjugated to horseradish peroxidase complexes (Dakopatts Immunoenzymatic Staining kit, DAKO Corp, Carpinteria, California). Tissue-bound antibody complexes were then visualized by development in a substrate solution containing 3-amino-9-ethyl carbazole (0.5 mg/mL; Sigma Chemical Co, St Louis, Missouri) and

0.01% H<sub>2</sub>O<sub>2</sub> in 0.1 M acetate buffer, pH 5.2, to yield a granular, red-brown reaction product. The culture-preparation sections were fixed in 4% buffered formaldehyde and mounted in Gel/Mount (Biomedica Corp, Foster City, California). Negative controls included the use of normal rabbit serum (1:500) and preimmune rabbit immunoglobulin G (IgG) (1:250) in place of primary antibody.

#### **FLUORESCENT STUDIES DEMONSTRATING ASSOCIATION OF CD11b AND uPAR ON HUMAN RPE CELLS**

##### *Materials*

Fluorescein isothiocyanate (FITC) and 7-amino-4-methyl-coumarin-3 acetic acid (AMCA) were obtained from Molecular Probes (Eugene, Oregon). Ethyl diaminetetra-acetic acid (EDTA) was obtained from Fisher Scientific Co (Fair Lawn, New Jersey). Fluorescein-conjugated uPA was obtained from American Diagnostica Inc (Greenwich, Connecticut).

##### *Monoclonal Antibodies*

Mouse monoclonal antibodies (mAbs) to CD11b (CR3), uPAR (clone 3B10), and their fragments were prepared as previously described.<sup>111-117</sup> Idiotypic antibodies for uPAR and CD11b were used as controls.

##### *Preparation of FITC- and AMCA-conjugated Abs*

The AMCA- and FITC-conjugated Abs were prepared as previously described.<sup>118,119</sup> The fluorescent conjugates were separated from unreacted fluorochromes by Sephadex G-25 (Sigma Chemical Co) column chromatography. Purified conjugates were dialyzed against PBS at pH 7.4 overnight at 4°C.

##### *Fluorescence Labeling*

RPE cells were detached from culture flasks by treatment with trypsin-EDTA. After detachment, the RPE cells were resuspended in culture medium supplemented with 10% FBS for 10 minutes at room temperature to inactivate any remaining trypsin activity. RPE in suspension was labeled with nonsaturating amounts of fluorochrome-conjugated F(ab')<sub>2</sub> fragments of anti-CD11b mAb for 20 minutes at 4°C. For capping experiments, the cells were washed twice with HBSS, then labeled with second-step goat anti-mouse IgG. Cells were incubated for 30 minutes at 37°C to allow cap formation. Cells were then labeled with F(ab')<sub>2</sub> fragments of anti-uPAR mAb for 20 minutes at 4°C followed by washing with cold buffer. After staining, the cells were washed with cold HBSS by centrifugation. Samples were then transferred to a microscope stage held at 37°C. These experimental manipulations had no apparent effect on cell activation for shape change as assessed by right-angle light scatter performed as described.<sup>120</sup>

##### *Conventional Microscopy*

An axiovert 135 inverted fluorescence microscope (Carl Zeiss Inc, New York, New York) with mercury illumination interfaced to a Perceptics Biovision workstation (Knoxville, Tennessee) was employed for cell examination. The fluorescence images were collected by an intensified charge-coupled device camera, model XC-77 (Hamamatsu, Japan) and image processor. Narrow band-pass discriminating filter sets were used for FITC (excitation at 485/22 nm and emission at 530/30 nm) and AMCA (excitation of 380/15 nm and emission at 450/30 nm) (Omega Optical, Brattleboro, Vermont). Long-pass dichroic mirrors of 430 nm and 510 nm were used for AMCA and FITC, respectively. Digital images were collected using Zeiss polarizers and a charge-coupled device camera (model WV-BL200; Panasonic). The background-subtracted digitized images were averaged and then electronically stored. Fluorescence micrographs were prepared using the MultiProbe software package (Perceptics Inc, Knoxville, Tennessee) to pseudocolor and then overlay separate images of the same cell collected using different filter sets. Images were photographed using a freeze-frame video recorder (Polaroid, Boston, Massachusetts).

##### *Resonance Energy Transfer (RET) Imaging*

For RET microscopy,<sup>121</sup> the 485/22-nm narrow bandpass discriminating filter was used for excitation and the 590/30-nm filter was used for emission. The 510-nm long-pass dichroic mirror was used for RET.<sup>117,121,122</sup> Optical imaging was conducted as described in the preceding paragraph.

#### **STUDIES OF RPE CELL MIGRATION**

##### *Human RPE Cell Preparation for Transmigration Studies*

Human RPE (HPRE) cells were detached from culture flasks by treatment with trypsin-EDTA. After detachment, the RPE cells were resuspended in HBSS supplemented with 10% FBS for 10 minutes at room temperature to inactivate any remaining trypsin activity. After centrifugation at 1,000 rpm for 5 minutes, RPE cells were resuspended in HBSS at a concentration of 5×10<sup>5</sup> cells/mL. HRPE cells were stained by incubating with DiI (1,1'-dioctadecyl-3,3,3',3'-tetramethylindocarbocyanine; final concentration 20 µg/L) for 1 hour at 37°C with gentle agitation at 15-minute intervals. After labeling, the cells were washed twice by centrifugation and were seeded onto the surfaces of the gelatin-nylon mesh matrices in 50 µL of 6% gelatin solution containing 10% FBS. To visualize proteolytic activity, Bodipy-BSA (4,4-difluoro-5,7-dimethyl-4-bora-3a,4a-diaza-5-indacene-3-propionic acid-conjugated BSA; Molecular Probes) and DQ collagen (type IV from human placenta, fluorescein conjugate;

Molecular Probes Cat No. D-12052) were used. Bodipy-BSA becomes fluorescent on exposure to several proteases, especially uPA.<sup>124</sup> DQ collagen becomes fluorescent on exposure to collagenase activity. Bodipy-BSA or DQ collagen was incorporated into the gelatin-nylon mesh matrix layers at a concentration of 1 mg/mL. HRPE cells on the gelatin-nylon mesh matrices were incubated for 2 hours at 37°C in a 5% CO<sub>2</sub> incubator. The gelatin-nylon mesh matrices and coverslips were then mounted on glass slides for microscopic observation. The number of HRPE cells reaching the bottom surface of the matrix was divided by the number of cells added to the top layer to determine the fraction of cells that migrated across the matrix.

#### *Inhibition of the Collagenase Activity*

To inhibit metalloproteinase activity, 1,10-phenanthroline (Euka Chemical Corp, Ronkonkoma, New York) was used.<sup>125</sup> During some of the preparation of the gel-nylon mesh matrices, 1,10-phenanthroline was incorporated into the matrix at a final concentration of 10 mM. Control gels contained only ethanol, the solvent used for 1,10-phenanthroline.

#### *Inhibition of Urokinase-type Plasminogen Activator*

To inhibit urokinase-type plasminogen activator, PAI-1 (American Diagnostica Corporation, Joplin, Missouri) was used. During preparation of some of the gel-nylon mesh matrices, PAI-1 was incorporated into the matrix at a final concentration of 0.05 mg/mL. Control gels contained only HBSS, the solvent used for PAI-1.

#### *Fluorescence Microscopy and Image Reconstruction*

An axiovert inverted fluorescence microscope (IM-135) with HBO-100 mercury illumination (Carl Zeiss Inc, New York, New York) interfaced to a Dell 410 workstation (Round Rock, Texas) via a Scion SG-7 video card (Vay-Tek, Fairfield, Iowa) was used. The fluorescence images were collected by an intensified, cooled charged-coupled device camera (model XC-77; Hamamatsu Photonics, Bridgewater, New Jersey). Images were processed with ScionImage software and stored as TIFF files. The fluorescence of Bodipy-BSA and DQ collagen fluorescence was detected using a 485DF22-nm and 530DF30-nm filter combination and a 510 long-pass dichroic mirror (Omega Optical, Brattleboro, Vermont).

For image reconstruction, images from 50 to 70 optical sections were taken from a sample. To remove out-of-focus fluorescence, each image was deconvoluted using MicroTome software (Vay-Tek). The three-dimensional rendering was performed with VoxBlast software (Vay-Tek). Computations were performed on a Dell Precision Workstation. Images were printed using an Epson Stylus-Pro printer.

#### *Imaging Spectrophotometry*

Fluorescence emission properties of the matrices were studied using imaging spectrophotometry. Experiments were performed as described previously.<sup>126</sup> Briefly, a Zeiss IM-135 axiovert microscope was fiber-optically coupled to the input side of an Acton-150 (Acton, Massachusetts) imaging spectrophotometer. The exit side was connected to an intensifier, which was in turn attached to a Peltier-cooled I-MAX-512 camera (Princeton Instruments, Inc, Trenton, New Jersey). The collection of spectra or images was controlled by a high-speed Princeton ST-133 interface and a DG-535 delay gate generator (Stanford Research Systems, Sunnyvale, California). This equipment was interfaced to a Dell 410 workstation running Winspec/32 version 2.3.2.5 software (Princeton Instruments, Inc) to manage image acquisition, quantitate fluorescence levels, and analyze data. Cells were illuminated using an optical filter at 485DF22 nm and a 510lp dichroic mirror.

#### **PROCEDURES FOR ENZYMATIC FLUORESCENCE MICROSCOPY** *Bodipy FL-BSA and DQ FL-Collagen IV Overnight Incubation Protocol*

Slides were prepared by dissolving Bodipy-BSA FL conjugate (6%, Molecular Probes, Eugene, Oregon), bovine serum albumin (10%, Sigma, St Louis, Missouri), and D-collagen FL conjugate (12% 90, type IV from human placenta, fluorescein conjugate; Molecular Probes) in water. In some experiments human PAI-1 (5 ng/mL) (American Diagnostica, Greenwich, Connecticut) or 1,10-phenanthroline (10 mM) was added. This solution was evenly coated onto glass slides using a glass rod. The coated slides were incubated for 2 hours at 37°C in a humidified chamber. Following incubation, the slides were dipped in HBSS. The cell suspensions were then layered on top of the coated slides and allowed to adhere for 30 minutes at 37°C in a humidified box. The slides were dipped in HBSS to remove nonadherent cells, coverslips were added, and then samples were returned to the humidified box and incubated for 37°C for 8 to 16 hours. Where indicated, PAI-1 (5 ng/mL) or 1,10-phenanthroline (10 mM) was added to the cell suspension mixture immediately prior to layering the cells onto the coated slides.

*Bodipy FL-BSA Procedures for Intensified Microscopy*  
BSA (50 µg) and Bodipy FL-BSA (30 µg) DQ-collagen (60 µg) were dissolved in 20 µL of dimethyl sulfoxide (DMSO). After suspension in solvent, the entire solution volume was diluted to 0.5 mL. This stock solution could be stored for up to 1 week at 4°C. One hundred microliters of the stock solution was evenly coated onto acetone-cleaned glass coverslips and incubated for 2 hours at 37°C in a humid air atmosphere under a Petri dish (but not

allowed to dry). The coverslip was gently washed with HBSS.

#### *Intensified Microscopy*

Cells were observed using an axiovert inverted fluorescence microscope (Carl Zeiss, Inc, New York, New York) with mercury illumination interfaced to a Perceptic (Knoxville, Tennessee) Biovision image processing system. A long-pass dichroic mirror of 510 nm and a narrow bandpass discriminating filter (DF) set (Omega Optical, Brattleboro, Vermont) was used (excitation at 485 nm with a 22-nm bandpass and emission at 530 nm with a 30-nm bandpass) for FITC and Bodipy FL. The fluorescence images were collected with an intensified charge-coupled device camera (Genisys; Dage-MTI, Michigan City, Indiana). Digital photomicrographs were taken using Zeiss polarizers and a charge-coupled device camera (model 72, Dage-MTI). To distinguish extracellular from intracellular fluorescence, samples were stained with 0.5 mg/mL crystal violet as previously described.<sup>127,128</sup>

#### *Single Cell Excitation Microspectrophotometry*

Cell fluorescence was quantitated using an emission microspectrophotometer system. To minimize light losses, a Zeiss IM-135 axiovert microscope with a bottom port was employed. The bottom port was fiber-optically coupled with an efficiency near 1.0 to the input side of an Acton-150 (Acton, Massachusetts) imaging spectrophotometer. The exit side was connected to an intensifier that was attached to a Peltier-cooled I-MAX-512 camera (Princeton Instruments Inc, Trenton, New Jersey). The collection of spectra was controlled by a high-speed Princeton ST-133 interface and a Stanford Res System (Sunnyvale, California) DG-535 delay gate generator. This high-efficiency, high-sensitivity system allowed medium resolution emission spectra to be collected from individual cells in 1 second. These systems were interfaced to a Dell 410 workstation running Winspec software to manage and analyze data. Cells were illuminated using an optical filter at 485DF22 nm and a 510Ip dichroic mirror.

### **STUDIES ON THE SECRETION OF NONLYSOSOMAL HYDROLASES BY RETINAL PIGMENT EPITHELIAL CELLS**

#### *Tissue Culture and Stimulation of Monkey RPE Cells*

Monkey RPE cells were isolated and cultured by the same methods described above for human RPE cells. Cultured cells were either left unstimulated or stimulated with IL1- $\beta$  (0.02 ng/mL or 0.2 ng/mL) for 24 hours prior to collagenase and elastase studies. Monkey RPE cell cultures were preincubated with 1,10-phenanthroline (10 mM) to inhibit collagenase and elastase activity.

#### *DNA Quantitation of RPE Cell Cultures*

The DNA contents of the cultured cell monolayers

scraped from each tissue culture flask were determined according to the method of LaBarca and Paigen.<sup>129</sup> Briefly, the cells grown in tissue culture flasks were scraped into distilled water in the cold, briefly sonicated, and maintained on ice until DNA assays were performed. Twenty-five to 100- $\mu$ L aliquots of the cell lysates, raised when necessary to a total of 100  $\mu$ L by adding distilled water, were then added to 4.7 mL of a phosphate-saline buffer solution (0.05 M Na<sub>3</sub>PO<sub>4</sub>, 2.0 M NaCl) followed by addition of 0.5  $\mu$ g of Hoechst 33258, a fluorescent dye which quantitatively binds to double-stranded DNA, in 200  $\mu$ L of distilled water. The samples were then mixed vigorously and kept in the dark until fluorescence was measured using a Beckman Fluorocolorimeter with a 370-nm narrow-band interference filter for the excitation light and a Kodak 2A cutoff filter for light emission. Calf thymus DNA standards were used in each assay.

#### *Determination of Collagenase Activity in RPE-Conditioned Media and Cell Layers*

The collagenolytic activities of aliquots of RPE cell lysates were determined according to the method of Hu and associates<sup>130</sup> as modified by New England Nuclear for marketing as the "Collagenase Assay System [<sup>3</sup>H]" (Cat No. NEK-016). Briefly, [<sup>3</sup>H]-collagen fibrils were formed in chilled reaction tubes in 2.0 mM Tris HCl buffer, pH 7.6, containing 5.0 mM CaCl<sub>2</sub> for 2 hours before cell lysates were added. Forty microliters of cell lysate in distilled water was then added to the reaction tubes and incubated in the presence of 0.5 mM 4-aminophenylmercuric acetate for 24 hours at 25°C under gentle agitation to assay for both active and latent collagenase activity. Following incubation, the reaction tubes were centrifuged at 15,000g for 7 minutes at 25°C to separate the uncleaved collagen fibrils from the cleaved fragments in the supernatants. Twenty-microliter aliquots of the supernatants were removed and counted in aqueous counting solution (Awadol, New England Nuclear, Boston, Massachusetts). Samples from each culture flask were assayed in duplicate. Tissue culture flasks were run in triplicate for each culture condition. Control samples of nonconditioned media, media containing 0.5% trypsin and buffer, and media incubated with 1,10-phenanthroline (10 mM) for 30 minutes at 20°C were also assayed. The results are recorded as counts per minute/ $\mu$ g DNA.

#### *Determination of Elastase Activity in RPE-Conditioned Media and Cell Layers*

Radioactive [<sup>3</sup>H]-elastin prepared according to Banda and Werb<sup>131</sup> was supplied by Dr Harry Davis. The elastase activity was measured by determining the amount of radioactivity released after incubation of 100  $\mu$ L of each cell lysate at 37°C with 200  $\mu$ g of [<sup>3</sup>H]-elastin in 100 mM

Tris-HCl buffer, pH 7.8, containing 5 mM CaCl<sub>2</sub> and 0.2% NaNO<sub>3</sub>. The lysates and [<sup>3</sup>H]-elastin were allowed to incubate for 48 hours at 37°C. At the end of incubation, assay tubes were centrifuged for 3 minutes at 15,000g in a Beckman microfuge. The radioactivity in a 100- $\mu$ L aliquot of the supernatant was measured by liquid scintillation spectrometry. Samples from each culture flask were assayed in duplicate. In separate assays, tissue culture flasks were run in triplicate for each culture condition. Control samples of nonconditioned media, media containing 0.5% trypsin buffer, and media incubated with a broad metalloproteinase inhibitor 1,10-phenanthroline (10mM) for 30 minutes at 20°C were also assayed. The results are recorded as counts per minute/ $\mu$ g DNA/hour.

#### STATISTICAL ANALYSIS

For comparisons, unpaired Student's *t* tests were performed. Data are expressed as mean  $\pm$  standard error of the mean (SEM). Differences were considered significant at *P*<.01. All experiments were repeated on at least three independent occasions.

## RESULTS

#### IMMUNOHISTOCHEMICAL STAINING OF HUMAN RPE CELLS IN VITRO AND IN SITU

Immunohistochemical staining of cultured human RPE cells demonstrated constitutive (Figure 1A) staining, which was completely blocked by preadsorption of antibody with purified uPAR (Figure 1B). Proinflammatory cytokines, IFN- $\gamma$  (100U/mL; Figure 1C), and TNF- $\alpha$  (0.2 ng/mL)(not shown) enhanced immunoreactive uPAR expression on human RPE cells. Lipopolysaccharide also induced substantial increased uPAR immunoreactivity (Figure 1D). The proinflammatory cytokine, IL-1 $\beta$ , also induced dose-responsive increases in immunoreactive uPAR expression (Figure 2). In all cases, diffuse red-brown granular reaction product was present, with increased density of reaction product noted along cell membranes at high power (Figure 2D). Enhanced perinuclear staining was also evident in unstimulated as well as proinflammatory cytokine and LPS-stimulated cells. Human RPE cells stained with control antibody, PECAM-1, failed to show any immunoreactivity (Figure 2B).

In situ immunohistochemical staining for uPAR in formalin, paraffin-embedded sections of human eyes revealed immunoreactive uPAR to be distributed throughout the RPE cytoplasm with enhanced expression along RPE basolateral membranes (Figure 3A). Immunofluorescent staining of live, confluent cultures of human RPE cells (Figure 4A) demonstrated immunopositivity for CD11b/CD18 (Figure 4B), as previously described,<sup>101,132</sup> which was similar in distribution to that of

uPAR (Figure 4C). Noteworthy was enhanced perinuclear immunofluorescence present around the nuclei for both receptors, mimicking the staining on the fixed cell cultures (Figures 1 and 2). Simultaneous immunofluorescent staining on human RPE for uPAR and CD11b/CD18 was viewed by high-speed photomicroscopy and confirmed the close association of these receptors, inferred from the similar patterns of immunoreactive staining observed in Figure 5. Using anti-uPAR and anti-CD11b monoclonal antibodies, each labeled with a separate fluorochrome, interspersed immunoreactivity for uPAR (yellow-green) with that of CD11b (blue) was readily observed in spherical (nonpolarized) RPE cells along the circumference of the cells (Figure 5A). Resonance energy transfer between the two fluorochromes (red) yielded photochemical confirmation of the proximity of the two receptors to within 8 nm of each other (Figure 5A) (Table II; *P*<.01). In contrast, elongated (polarized), motile-appearing RPE cells exhibited segregation of the receptors with uPAR migrating to the leading edge (lamellipodia) and CD11b to the trailing edge (uropodia) (Figure 5A). This resulted in concentration of all uPAR immunoreactivity at the leading poles of the polarized RPE cells (Figure 5A).

#### RPE HYDROLYSIS OF ALBUMIN, COLLAGEN IV, COLLAGEN III, AND ELASTIN

To demonstrate functional uPAR expression in RPE cells, the RPE cells were seeded onto slides coated with gelatin containing BSA labeled with a fluorochrome (Bodipy), which only exhibits fluorescence upon albumin lysis. RPE pericellular fluorescence was evident surrounding virtually all RPE cells and was significantly reduced (*P*<.001) by inclusion of PAI-1 in the assay (Figure 6). uPAR activity was significantly increased (*P*<.001) when RPE cells were exposed to IL-1 $\beta$  (0.2 ng/mL) for 24 hours. PAI-1 significantly inhibited (*P*<.001) IL-1  $\beta$ -induced uPAR lysis of BSA (Figure 6).

To show the ability of RPE cells to cleave type IV collagen, known to be a component of Bruch's membrane, immediately underlying the RPE layer in vivo, RPE cells were seeded onto slides coated with gelatin containing collagen labeled with a fluorochrome (DQ), which only becomes fluorescent upon collagen lysis. As in the case of uPAR, pericellular proteolysis was seen around each RPE cell and was inhibited by the broad metalloproteinase inhibitor, 1,10-phenanthroline (10 mM) (*P*<.001). However, in contrast to uPAR, IL-1  $\beta$  (0.2 ng/mL) did not induce type IV collagenolysis by RPE cells over that observed surrounding unstimulated RPE cells (Figure 7). To demonstrate RPE hydrolytic activity for native interstitial collagen and elastin present within the inner lamellae of Bruch's membrane, assays employing radiolabeled

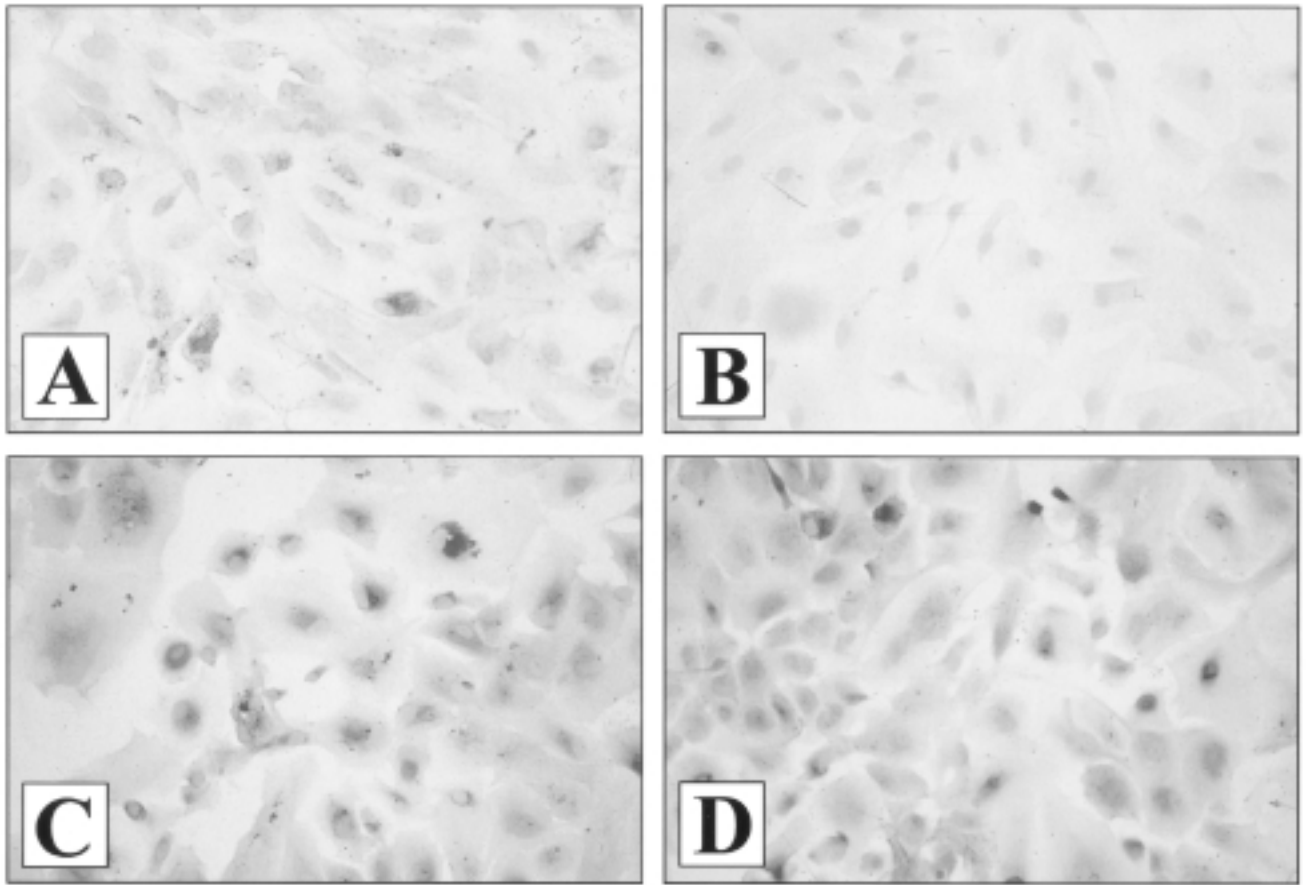


FIGURE 1

Immunohistochemical staining of nearly confluent, cultured human RPE cells for uPAR. A, Unstimulated RPE cells demonstrate predominantly perinuclear red-brown reaction product with other portions of cells lightly stained (hematoxylin counterstain, x200). B, Unstimulated RPE cells with anti-uPAR antibody preadsorbed with excess soluble uPAR show no detectable stain (hematoxylin counterstain, x200). C, RPE cells stimulated with interferon-gamma (100 U/mL) show heavy red-brown perinuclear stain as well as lighter diffuse stain (hematoxylin counterstain, x200). D, RPE cells stimulated with lipopolysaccharide (100 ng/mL) show marked increase in uPAR expression similar in distribution to that induced by interferon-gamma (hematoxylin counterstain, x200).

collagen III fibrils and radiolabeled native elastin were performed (Figures 8 and 9, respectively). Constitutive RPE hydrolysis of collagen III into classic 1/4 to 3/4 fragments was measured and significantly inhibited by 1,10-phenanthroline (Figure 8). Dose-dependent induction of collagenolytic activity resulted in significantly increased hydrolysis of collagen fibrils by RPE cells stimulated with IL-1 $\beta$  (0.2 ng/mL) ( $P < .001$ ). The proinflammatory cytokine-induced collagen III lysis was significantly inhibited by 1,10-phenanthroline ( $P < .001$ ). Elastolytic activity secreted by RPE cells demonstrated similar constitutive and IL- $\beta$ -induced profiles (Figure 9). Baseline elastin hydrolysis was significantly inhibited by 1,10-phenanthroline ( $P < .001$ ) and augmented by IL-1 $\beta$  in a dose-dependent fashion with significantly increased secreted elastolytic activity induced by IL-1 $\beta$  (0.2 ng/mL) ( $P < .001$ ). As with the collagenolytic activity, 1,10-phenanthroline significantly inhibited the cytokine-induced activity ( $P < .001$ ). Nonconditioned media and trypsin and buffer control

samples degraded less than 5% of the collagen fibrils.

#### RELATIVE CONTRIBUTIONS OF RPE EXTRACELLULAR MATRIX PROTEOLYTIC ACTIVITY TO RPE MIGRATION

To demonstrate the relative contributions of RPE-associated collagen IV, collagen III, and elastin proteolysis and of RPE uPAR-mediated proteolysis to RPE migration through extracellular matrix, three-dimensional matrices were constructed as previously described.<sup>133</sup> RPE cells were seeded onto fibronectin-coated matrices composed of collagen gel enveloping sheets of 120- $\mu$ m nylon mesh and grown to confluency (Figure 10). Confluent RPE cells on the matrices demonstrated typical polygonal arrays (Figures 10A and 10B), produced melanin (Figure 10C), and exhibited polarity with the formation of apical microvilli (Figure 10D). Immunohistochemistry for sodium-potassium-ATPase confirmed the RPE polarity by preferential immunopositivity at the cell apices (not shown).

RPE cells seeded onto Bodipy-BSA or DQ collagen-

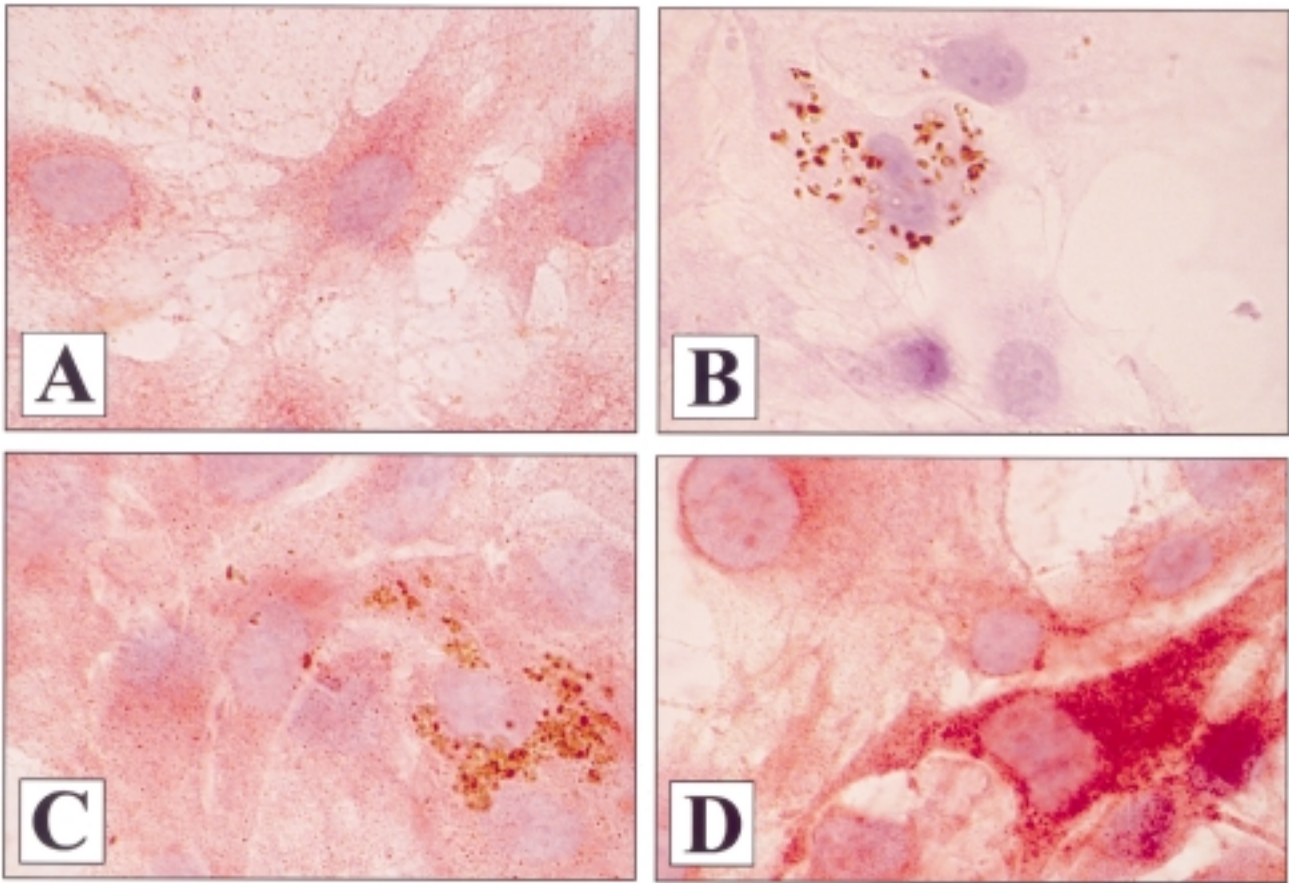


**FIGURE 2**

Immunohistochemical staining of nearly confluent, cultured human RPE cells for uPAR after exposure to interleukin-1 $\beta$ . A, Unstimulated RPE cells stained for uPAR demonstrate diffuse mild staining with increased positivity in the perinuclear region (hematoxylin counterstain, x1,000). B, Unstimulated RPE cells show no stain using idiotypic control antibody. Prominent melanin granules are visible in an RPE cell (hematoxylin counterstain, x1,000). C, RPE stimulated with 0.02 ng/mL of interleukin-1 $\beta$  exhibit more intense, diffuse deposition of red-brown reaction product when compared to unstimulated cells (hematoxylin counterstain, x1,000). D, RPE cells exposed to 0.2 ng/mL of interleukin-1 $\beta$  are heavily stained with red-brown reaction product that is enhanced in the perinuclear regions (hematoxylin counterstain, x1,000).

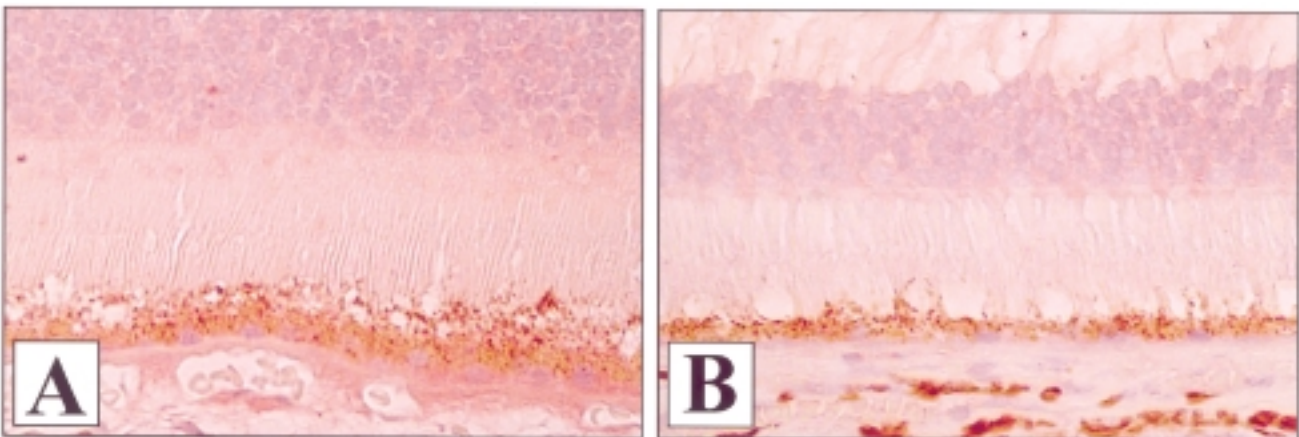


**FIGURE 3**

Immunohistochemical staining of normal human outer retina and choroid for uPAR. A, Red-brown immunohistochemical staining is present in RPE monolayer and demonstrates increased positivity along RPE basolateral membranes (hematoxylin counterstain, x1,000). B, Immunohistochemical staining performed using idiotypic control antibody fails to reveal any reaction product (hematoxylin counterstain, x1,000).

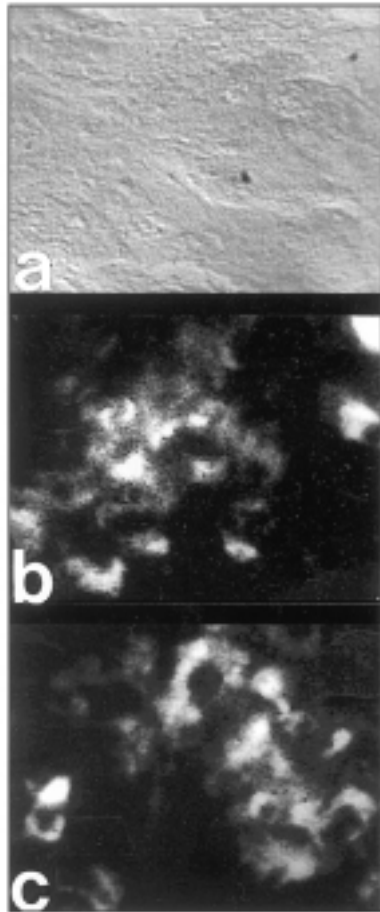


FIGURE 4

Immunofluorescent staining of live, confluent human RPE cultures for CD11b and uPAR. A, Phase contrast photomicrograph of confluent RPE cells (x400). B, Immunofluorescent staining for CD11b demonstrates diffuse membrane positivity with enhanced perinuclear immunofluorescence, mimicking results of fixed cell cultures stained for uPAR (x400). C, Immunofluorescent staining for uPAR demonstrates diffuse and enhanced pericellular distribution similar to that of CD11b (x400).

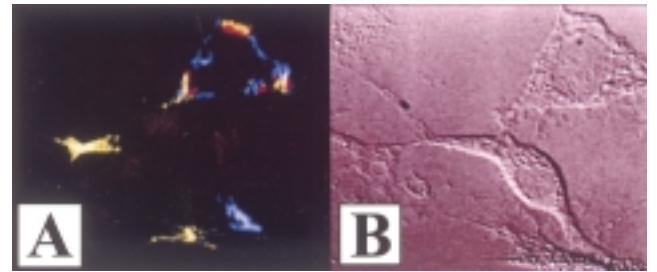


FIGURE 5

Live human RPE cells demonstrating CD11b (blue fluorescence) and uPAR (green fluorescence) due to binding of F(ab')<sub>2</sub> fragments of specific anti-CD11b and anti-uPAR monoclonal antibodies. A, Polygonal RPE cell (upper right) demonstrates circumferential, interspersed CD11b and uPAR with red fluorescence indicating resonance energy transfer (RET) between blue and green fluorochromes due to close approximation of CD11b and uPAR. Elongated RPE cells (lower left) demonstrate segregation and concentration of uPAR at leading edge of cell with concentration of CD11b at trailing edge. No RET is present in the elongated cells (x1,000). B, Phase contrast photomicrograph of same microscopic field depicted in A (x1,000).

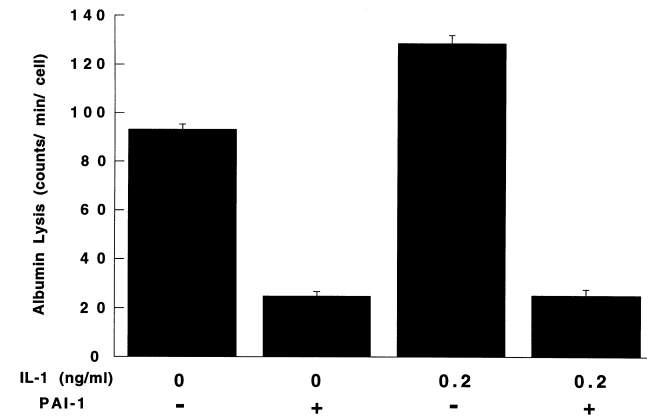


FIGURE 6

Human RPE lysis of albumin due to uPAR activity. Unstimulated and IL-1-stimulated RPE cells were assessed for pericellular proteolysis of albumin using Bodipy-BSA substrate. RPE cells exhibited constitutive activity, which was significantly enhanced by IL-1 $\beta$  (0.2 ng/mL) ( $P < .001$ ) and significantly inhibited by plasminogen activator inhibitor-1 (PAI-1) ( $P < .001$ ).

TABLE II: ASSOCIATION OF RPE uPAR AND CR3

CELL CONDITION	NO. OF CELLS	INTENSITY OF RESONANCE ENERGY TRANSFER FLUORESCENCE (COUNTS/SEC)	P
CR3-to-uPAR RPE-spherical (not polarized)	35	326 $\pm$ 36 x 10 <sup>3</sup>	<.01
CR3-to-uPAR RPE-elongated (polarized)	25	51 $\pm$ 14 x 10 <sup>3</sup>	<.01

RPE, retinal pigment epithelium.

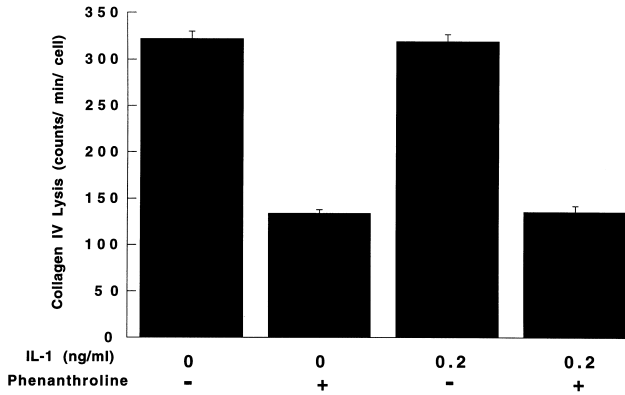


FIGURE 7

Human RPE lysis of collagen IV. Unstimulated and IL-1-stimulated RPE cells were assessed for pericellular proteolysis of collagen IV using DQ collagen substrate. RPE cells showed constitutive activity, which was significantly enhanced by IL-1 $\beta$  (0.2 ng/mL) ( $P < .001$ ) and significantly inhibited by 1,10-phenanthroline, a broad-spectrum metalloproteinase inhibitor ( $P < .001$ ).

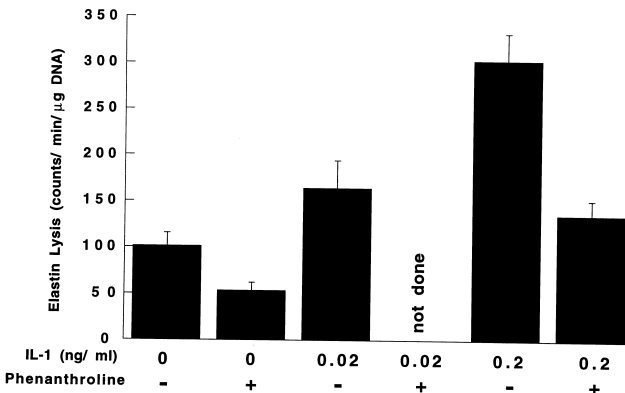


FIGURE 9

Human RPE lysis of elastin. Supernatants from unstimulated and IL-1-stimulated RPE cells, activated with trypsin, were assessed their ability to cleave radioactively-labeled native elastin. RPE cells showed constitutive activity which was significantly enhanced by IL-1 $\beta$  (0.2 ng/mL) ( $P < .001$ ) and significantly inhibited by 1,10-phenanthroline, a broad spectrum metalloproteinase inhibitor ( $P < .001$ ). IL-1 $\beta$  at lower dose (0.02 ng/mL) demonstrated increases in hydrolytic activity that were not statistically significant.

containing matrices readily migrated through the gels over 2 hours. Both fluorochromes were cleaved from the BSA or collagen as RPE migrated through the gels as depicted three-dimensionally (Figures 11A and 11B, respectively). Localized, intense RPE pericellular fluorescence was present at the site of active cleavage of the gels by the migrating RPE cells. Behind the migrated RPE cells, diffusing, cleaved fluorescent protein fragments diffused through the gels from the axes of RPE penetration, resulting in tails of weak fluorescence that expanded and dissipated with time (Figures 11A and

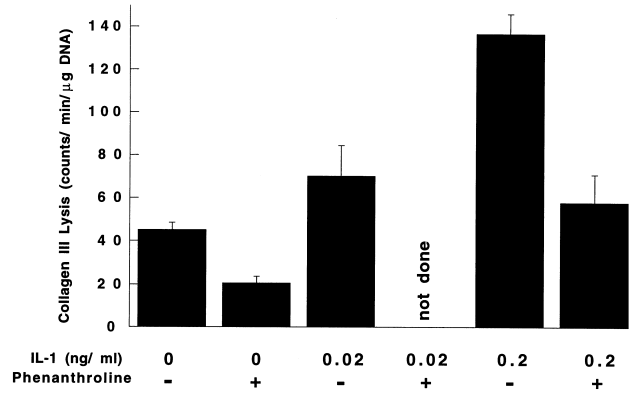


FIGURE 8

Human RPE lysis of collagen III. Supernatants from unstimulated and IL-1-stimulated RPE cells, activated with trypsin, were assessed their ability to cleave radioactively labeled collagen III fibrils. RPE cells showed constitutive activity which was significantly enhanced by IL-1 $\beta$  (0.2 ng/mL) ( $P < .001$ ) and significantly inhibited by 1,10-phenanthroline, a broad-spectrum metalloproteinase inhibitor ( $P < .001$ ). IL-1 $\beta$  at lower dose (0.02 ng/mL) demonstrated increases in hydrolytic activity that were not statistically significant.

11B). Observations made during the RPE migration assays revealed that RPE cells on the gel surface adjacent to axes of penetration migrated to reach these axes in order to penetrate the gel rather than bore their own paths (data not shown).

To assess the role of RPE uPAR opposed to the secreted RPE collagenolytic and elastolytic that were measured in this study, RPE migration assays were performed in the presence and absence of PAI-1 and in the presence and absence of 1,10-phenanthroline. PAI-1 virtually abolished RPE cell migration through the collagen matrices ( $P < .001$ ) (Figure 12A), while 1,10-phenanthroline, a known inhibitor of a wide spectrum of metalloproteinases and of the collagenases and elastases that were measured in this study, failed to demonstrate any inhibition of RPE cell migration (Figure 12B). These observations indicate a preeminent role of uPAR in RPE migration through extracellular matrix.

**IMMUNOHISTOCHEMICAL DETECTION OF uPAR IN HUMAN RETINAL LESIONS**

The presence of uPAR was confirmed in retinal lesions, characterized by disruptions in Bruch's membrane, RPE migration and proliferation, and inflammation. Examined were tissues or whole eyes with subretinal neovascular membranes (Figures 13 and 14), which emerge from the choroid through breaks in Bruch's membrane, proliferative vitreoretinopathy membranes containing migrated RPE cells (Figure 15), and eyes with end-stage uveitis (Figure 16). In whole eyes, subretinal neovascular membranes were frequently lined by RPE cells extending from Bruch's membrane over the vanguard. In surgically

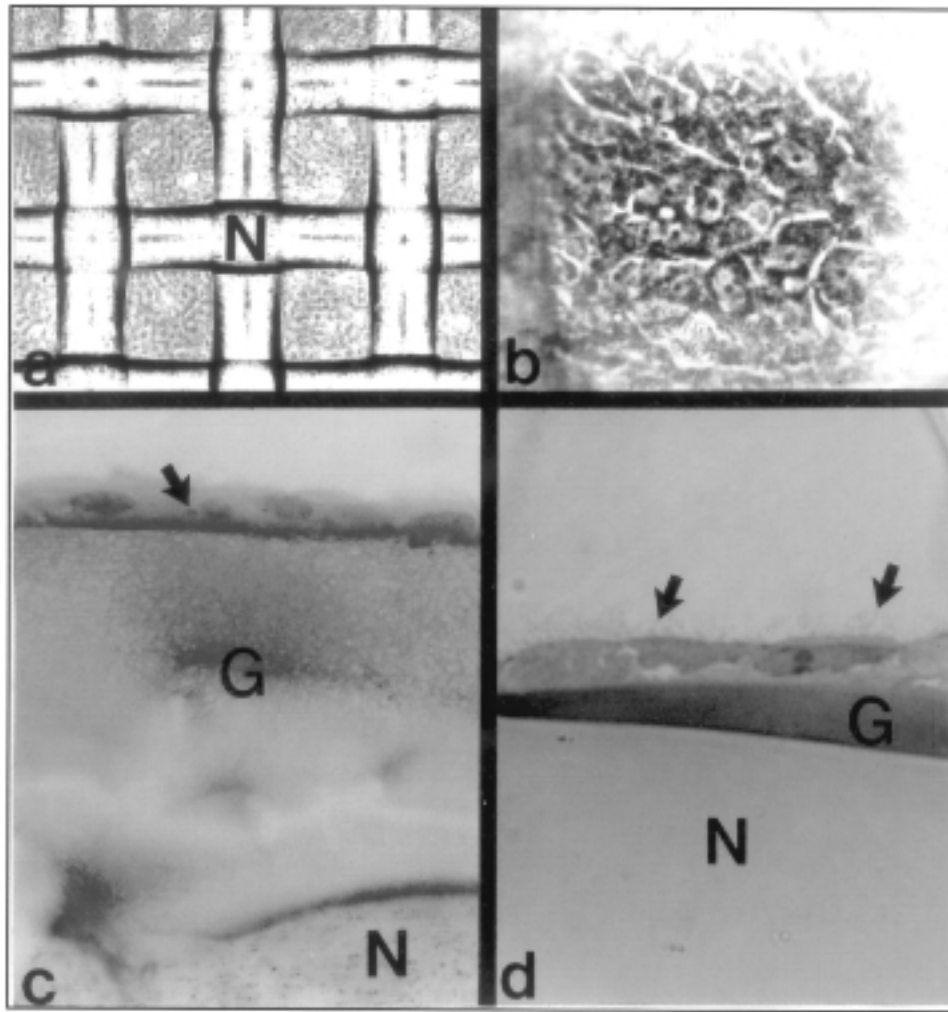


FIGURE 10

Human RPE cells cultured on novel, fibronectin-coated, gelatin/nylon (N) mesh. A, Inverted phase photomicrograph of RPE cells seen between strands of mesh exhibit typical polygonal arrays (x25). B, High-magnification photomicrograph demonstrating compact polygonal arrays of RPE cells (x200). C, Photomicrograph of formalin-fixed, paraffin-embedded section of gelatin (G)/nylon (N) mesh with confluent RPE monolayer demonstrates intracellular pigment granules (hematoxylin counterstain, x200). D, Formalin-fixed, plastic embedded gelatin(G)/nylon (N) mesh with RPE monolayer exhibiting polarization with formation of apical microvilli (arrows) (toluidine blue, x400).

excised specimens, corresponding caps of readily identifiable RPE cells lined the surfaces of the fibrovascular membranes (Figures 13 and 14). These cells exhibited intense immunoreactivity for uPAR (Figures 13A and 14A). Some endothelial cells within the fibrovascular proliferations also stained positively, as did occasional mononuclear phagocytes. Serial sections stained with control antibody failed to show significant stain.

PVR membranes were characterized by RPE cells enmeshed in connective tissue of variable densities. RPE proliferations were frequently in cords, nests, or glandular configurations (Figure 15). Mild to moderate staining was seen multifocally in many of these proliferations, with immunoreactivity also present in the pericellular stroma (Figure 15).

Immunohistochemical staining of eyes with uveitis

demonstrated immunoreactivity in the RPE monolayers and exudates overlying the choroidal inflammatory lesions. This polarized immunoreactivity was more intense than the degree observed to be constitutively present (Figure 3). Weaker but distinct immunoreactivity was exhibited by leukocytes within the choroidal lesions, as well as by some of the choroidal endothelium (Figure 16).

## DISCUSSION

Mechanisms mediating RPE motility through the ECM in retinal lesions of ARMD, PVR, and uveitis remain largely unknown. Based on immunohistochemical, gene expression, and immunochemical observations, MMP and uPAR/uPA activity has been attributed to the

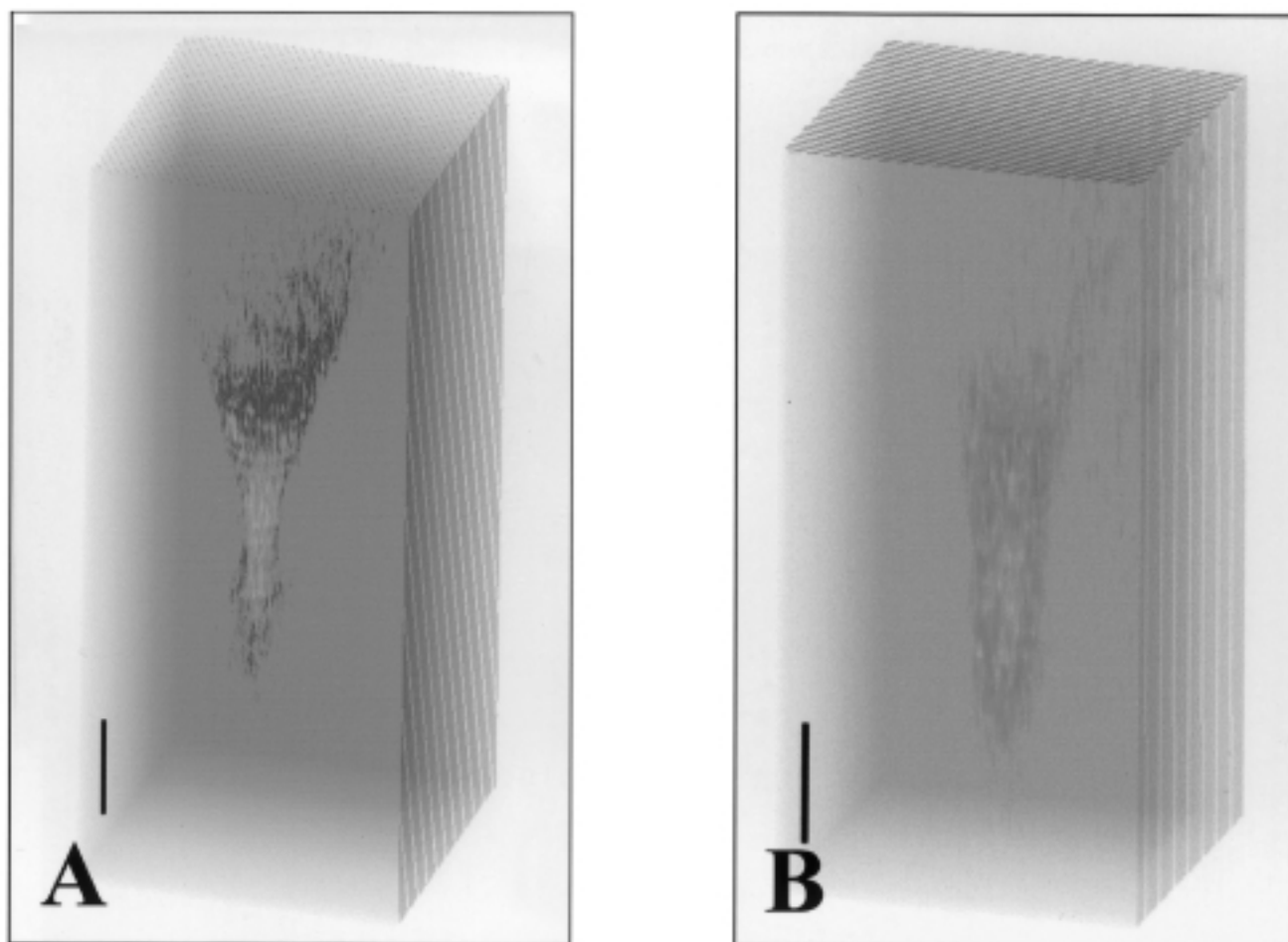


**FIGURE 11**

Three dimensional images showing RPE transmigration through gelatin/nylon mesh. A, Three-dimensional image reconstructed from multiple images acquired during migration of RPE cell through gelatin/mesh containing Bodipy BSA shows fluorescent fragments generated due to BSA cleavage by penetrating RPE cell. Concentration of fluorescence is seen where cell is cleaving albumin with a widening plume of fluorescence seen behind cell due diffusion of cleaved product from areas of prior cleavage (scale bar, 20  $\mu\text{m}$ ). B, Three-dimensional image of RPE transmigration using DQ collagen (collagen IV) substrate (scale bar, 20  $\mu\text{m}$ ).

RPE.<sup>59,60,62,63,83,84,134,135</sup> However, demonstration of uPAR immunoreactivity in RPE cells in vitro and in situ and the upregulation of RPE uPAR in response to proinflammatory cytokines that are known to be present in retinal lesions of ARMD, PVR, and uveitis have not been shown. Moreover, functional assays demonstrating actual uPAR-mediated proteolysis, its specific inhibition, its regulated expression on the RPE cell surface, and its role in RPE motility have not been investigated. With respect to MMP, this is the first study to show actual cleavage of native interstitial collagen, elastin, and collagen IV by RPE MMPs and their upregulation by a proinflammatory cytokine. Of particular interest is the demonstration of the relative contribution of uPAR/uPA and MMPs in RPE migration as assayed in a novel gelatin–nylon mesh medium using fluorescently labeled RPE cells.

RPE uPAR expression is present constitutively in

vitro (Figures 1 and 2) and in situ where it is expressed preferentially along the RPE basolateral membrane (Figure 3). RPE uPAR expression under normal conditions is not surprising, since many receptors are normally expressed, even though their functional expression may be tightly controlled under physiologic conditions. For uPAR, such control is likely to be due to the presence of PAI-1, which has been shown to be secreted by numerous cells in the posterior segment of the eye, including the RPE.<sup>84</sup> Other possible mechanisms include the activity of MMPs that are normally produced to participate in the orderly turnover of ECM, including Bruch's membrane, and are themselves regulated by TIMPs.<sup>135</sup> One MMP, stromelysin, may be of particular interest with respect to its variable effects on uPAR activity. MMP-3 can down-regulate uPA/uPAR activity, since it can (1) cleave the active portion of uPAR required for uPA activation<sup>105</sup> and

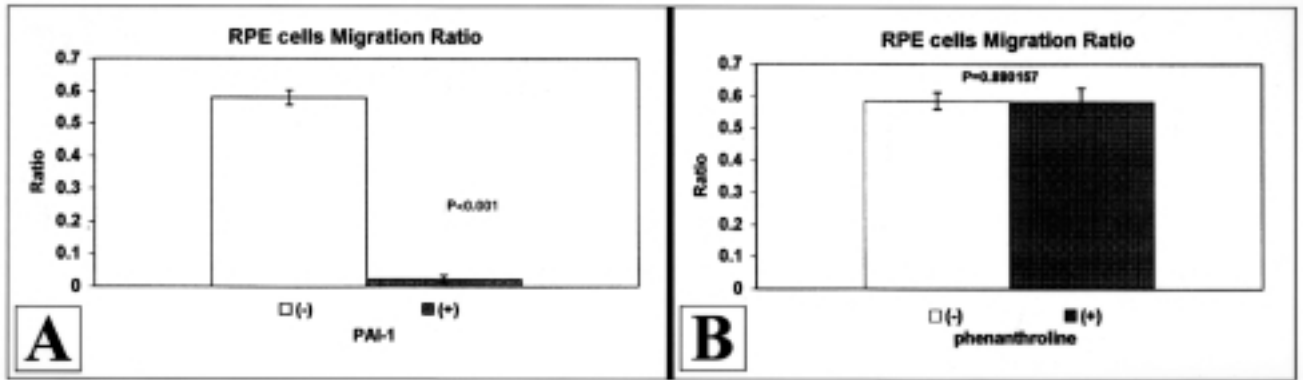


FIGURE 12

Effect of protease inhibitors on human RPE transmigration across the nylon-mesh gelatin matrices. The number of DiI, fluorescently labeled RPE cells reaching the bottom surface of the matrices after 4-hour incubations at 37°C was divided by the number of cells initially placed on top of the gelatin to determine the percentages of cells which migrated across the matrices. Experiments were performed in the presence (open bars) and absence (solid bars) of inhibitors. The uPAR/uPA inhibitor PAI-1 was found to profoundly inhibit cell migration (A), but the broad-spectrum metalloproteinase inhibitor, 1,10-phenanthroline, was found to have much less effect (B).

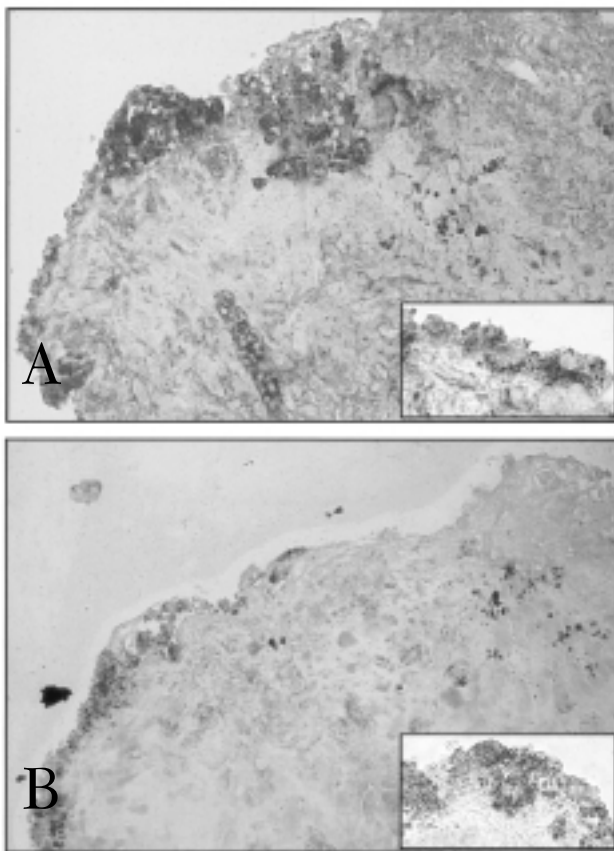


FIGURE 13

Immunohistochemical staining of surgically excised human subretinal neovascular membrane for uPAR. A, Readily identifiable RPE cells that line the surface of the membrane exhibit intense, red immunoreactivity. Some stromal cells, vascular endothelial cells, and leukocytes also show positivity. Inset shows readily visible red reaction product for uPAR (hematoxylin counterstain, x200; inset, x1,000). B, Adjacent tissue section stained using idiotypic control antibody lacks any immunoreaction (hematoxylin counterstain, x200).

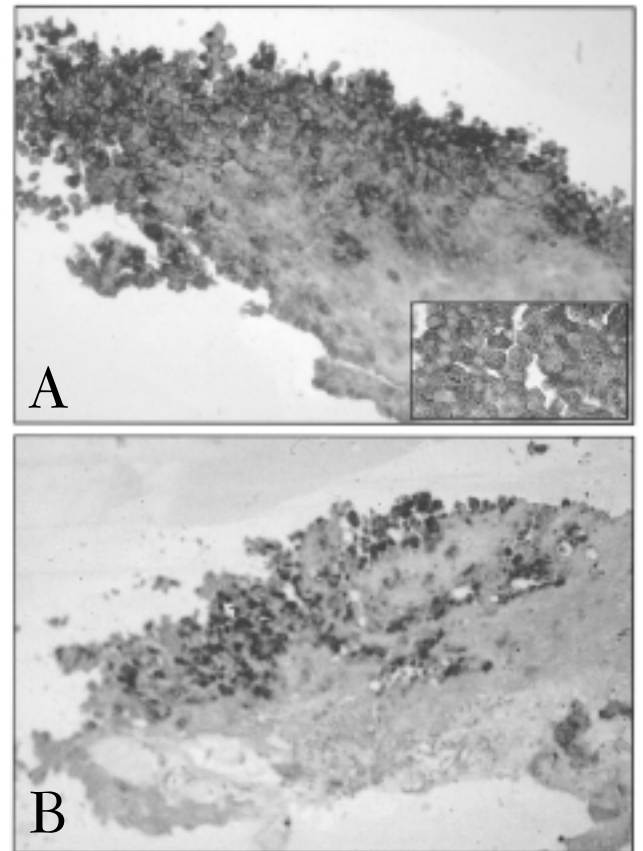


FIGURE 14

Immunodetection of uPAR in surgically excised human subretinal neovascular membrane. A, Numerous variably heavily pigmented polygonal RPE cells that occupy and line the surface of the membrane are intensely red due to uPAR immunoreactivity. Occasional stromal cells, endothelial cells, and leukocytes in the membrane also positively stained. Inset shows polygonal RPE cells decorated with deep red uPAR immunoreaction product (hematoxylin counterstain, x200; inset, x1,000). B, Adjacent tissue section stained using idiotypic control antibody is negative (hematoxylin counterstain, x200).

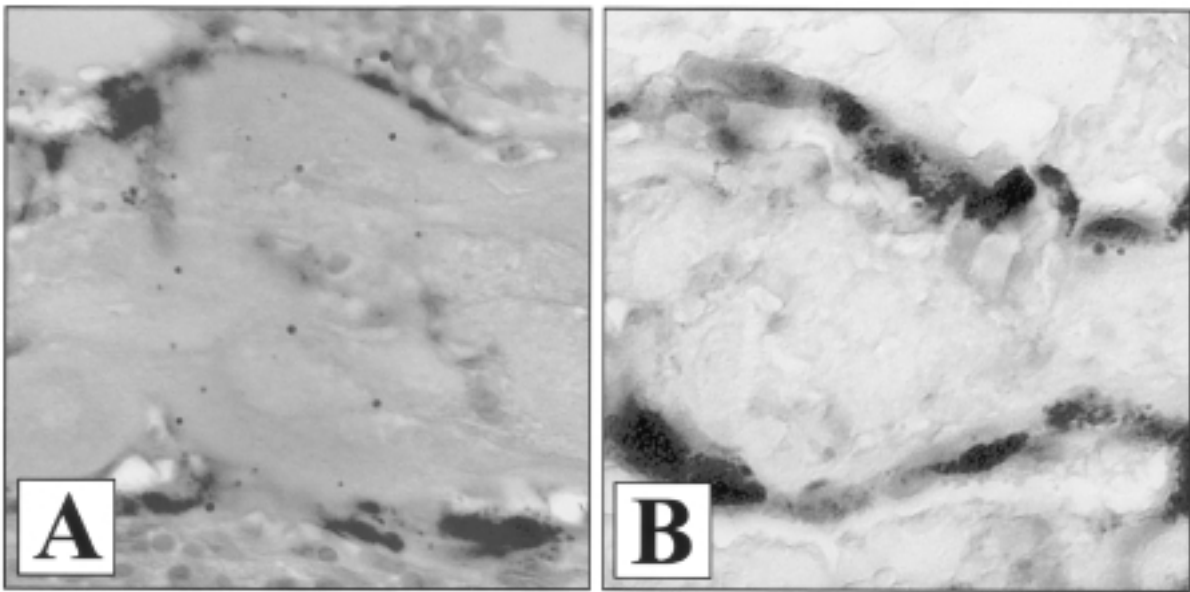


FIGURE 15

uPAR immunostaining in surgically excised human proliferative vitreoretinopathy membrane. A, Strands of infiltrating RPE cells present in moderately dense extracellular matrix of the membrane show immunoreactivity for uPAR. The stroma shows weak positivity, perhaps due to soluble uPAR in the lesion (hematoxylin counterstain,  $\times 400$ ). B, Adjacent tissue section stained with control monoclonal antibody lacks any immunohistochemical positivity (hematoxylin counterstain,  $\times 400$ ).

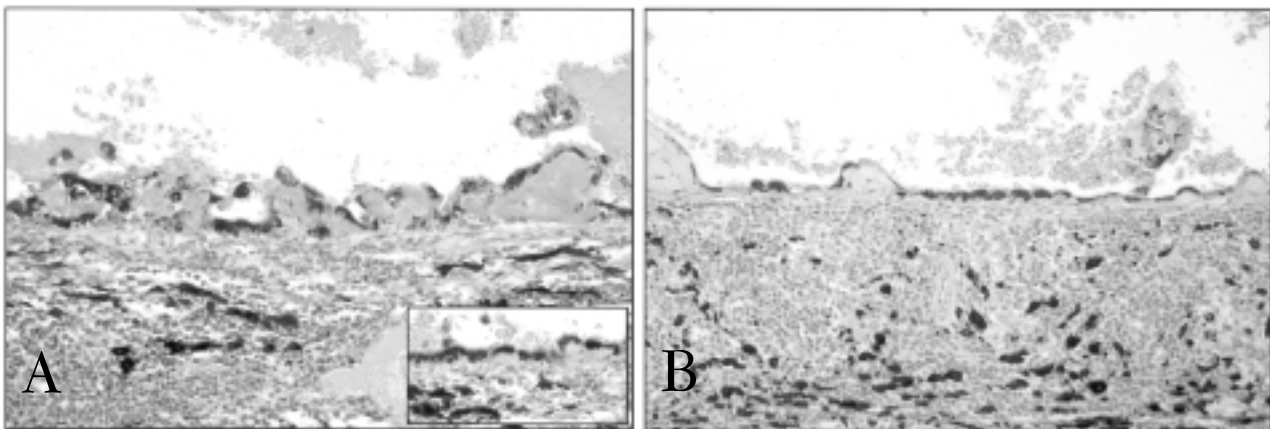


FIGURE 16

Immunohistochemical staining of posterior segment of eye with chronic uveitis for uPAR. A, RPE cells overlying Bruch's membrane demonstrate polarized immunoreactivity for uPAR along their basolateral membranes overlying chronic inflammatory infiltrate in choroid. Reaction product is also present in sub-RPE exudates between Bruch's membrane and the RPE cells. Weak positivity is also present in some leukocytes, endothelial cells, and stromal cells. Inset clearly demonstrates RPE immunoreactivity (hematoxylin counterstain,  $\times 200$ ; inset,  $\times 1,000$ ). B, Adjacent tissue section stained using idiotypic control antibody is negative (hematoxylin counterstain,  $\times 200$ ).

(2) cleave plasminogen into fragments, which cannot be activated by uPA, thereby not only reducing uPA activation but also reducing the substrate upon which uPAR/uPA acts to produce proteolytic activity.<sup>105</sup> MMP-3 may also augment uPA/uPAR activity by its proteolytic activity of PAI-1, thereby impairing the inhibitory effect of vitronectin-bound PAI-1 and enhancing uPAR activity, which may alter cell adhesion and/or migration.<sup>136</sup>

The polarized expression of uPAR along the RPE basolateral membrane (Figures 3 and 16) may be due to

its known association with other ligands and the cytoskeletal components, which has morphological and functional consequences. uPAR is known to closely associate with  $\beta 1$  integrins in a symbiotic relationship in which they mutually regulate one another.<sup>137</sup> In the RPE,  $\beta 1$  integrins are known to be involved in the development and maintenance of polarity of the monolayer and are found along the apices and at the basolateral plasma membrane, where they are involved in adhesion to fibronectin, laminin, and collagen IV.<sup>138</sup> uPAR is a GPI-linked surface receptor that

requires association with other ligands to mediate its intracellular signaling.<sup>139</sup> Associations between uPAR and  $\beta_1$  integrins regulate uPAR distribution and, hence, its inability to generate concentrated proteolytic activity that overcomes its localized physiologic control due to PAI-1 inhibition.<sup>73</sup> Conversely, uPAR stabilizes the binding of  $\beta_1$  integrins to their ECM ligands<sup>140</sup> and so assists in maintaining RPE cell polarity and adhesion to Bruch's membrane. The analogous situation to this initially recognized in leukocytes was the association of uPAR with the  $\beta_2$  integrins, namely, CD11b/CD18 and CD11c/CD18.<sup>139</sup> In leukocytes, this association helps to control receptor expression and provides for intracellular uPAR signaling. However, when leukocytes become motile or are stimulated by LPS or proinflammatory cytokines, dissociation and capping of the receptors occur. For  $\beta_2$  integrins, capping mediates localized leukocyte adhesion to activated vascular endothelium or resident tissue cells, including RPE cells, expressing adhesion molecules, most notably intercellular adhesion molecule-1 (ICAM-1). For uPAR, capping at the leading edge of the motile cell subserves highly concentrated proteolysis to facilitate directed movement through the ECM.<sup>103,141</sup>

RPE cells are noteworthy with regard to uPAR expression, since they express  $\beta_1$ ,  $\beta_2$ , and  $\beta_3$  integrins.<sup>102,142,143</sup> In so doing, the uPAR pattern of expression observed in this study suggests several consequences. First, the similar pattern of immunofluorescent staining observed for uPAR and CD11b in confluent cultures (Figure 4) and the extremely close proximity of these receptors as determined by RET of the fluorochromes labeling the receptors of rounded RPE cells (Figure 5) suggest that uPAR and CD11b/CD18 regulate the distribution and, hence, the biologic activity of one another. It is also likely that CD11b serves as the mediator for RPE uPAR, as it does in other cell types.<sup>137</sup> Dissociation of the two receptors results in homotypic aggregation and polarization of the RPE receptors, providing the polarized cells with a vanguard of proteolytic activity for ECM migration and aggregated CD11b to mediate RPE adhesion to other activated, ICAM-1-positive RPE cells as they burrow through the ECM or along surfaces coated with fibrin-rich exudates (Figure 16). The histopathologic patterns of RPE migration along subretinal neovascular membrane surfaces (Figures 13 and 14) and the strands of invading RPE cells seen in PVR membranes (Figure 15) argue for such a scenario.

The potential significance of uPAR  $\beta_1$  integrins is also suggested in the morphologic changes and RPE cell motility that were observed in each case as uPAR aggregated and migrated toward the lamellipodia of the RPE cells (Figure 5). Alterations in RPE polarity are known to be associated with changes in the distribution of  $\beta_1$  inte-

grins, and uPAR is known to stabilize  $\beta_1$  integrin binding to their extracellular matrix ligands.<sup>138</sup> These facts, taken together with our observations, imply that the uPAR polarization witnessed in real time was associated with destabilization of  $\beta_1$  integrin contact points with the ECM, thereby allowing the RPE to detach from the matrix surface, polarize, and become motile (Figure 5), as later observed in the cell migration studies (Figures 11 and 12). Release of the RPE cells from attachment to their substrata, for example, is likely to permit them to migrate over the tips of subretinal neovascular membranes as they emerge from the choroid into the subretinal space (Figures 13 and 14). RPE detachment due to release of  $\beta_1$  integrins is likely to have consequences besides loss of polarity. Among these are the binding of MMPs at sites of RPE  $\beta_1$  integrin evacuation from Bruch's membrane. The localized concentration of MMP activity and the enhanced uPAR/uPA activity on the nearby, capped RPE cell are likely to be synergistic in the ability to damage Bruch's membrane.

Another consequence of the loss of polarity is breakdown of the blood-retina barrier, which allows leakage of plasminogen and thrombin. The former is the substrate for elaboration of uPAR-generated proteolytic activity.<sup>64</sup> The latter<sup>102</sup> synergizes uPAR activity by inducing RPE uPAR gene transcription and cell surface expression. Thrombin also may activate pro-gelatinase A, which is constitutively secreted by vascular endothelial cells, monocytes, lymphocytes, and fibroblasts,<sup>49,50</sup> and is likely to be present at sites of blood-retina barrier breakdown. Activation of RPE-derived gelatinase A by the thrombin/activated protein C pathway may be particularly important in CNV, since high levels of thrombin have been shown in subretinal CNV lesions as well as in exudative sub-RPE lesions, which predispose to CNV.<sup>51</sup> Thrombin activation of RPE-derived gelatinase A would then result in proinflammatory cytokine-independent cleavage of collagen IV, since gelatinase A is not upregulated by TNF- $\gamma$  or IL-1 or by uPAR-generated plasmin.<sup>30</sup> The results of this study strongly support this possibility, since RPE collagen IV lysis was not upregulated by IL-1 (Figure 7) while IL-1 stimulation of uPAR-dependent RPE proteolysis did occur (Figure 6). These results indicate that IL-1-generated RPE uPAR activity does not activate RPE pro-gelatinase A, which, therefore, relies on IL-1-independent triggers, such as thrombin, for its activation. The proinflammatory cytokine-independent cleavage of collagen IV by thrombin at sites of blood-retina barrier breakdown might then expose collagen I in the deeper layers of Bruch's membrane. Collagen I would then accelerate gelatinase A activation,<sup>26</sup> and consequently collagen IV lysis, by upregulating cell surface-associated MT1-MMP, which cleaves pro-gelatinase A into its active form.<sup>26</sup> The

gelatinase A mechanisms of collagen IV lysis in the ECM of Bruch's membrane or PVR membranes are not likely to be modulated by therapy aimed at inhibition of proinflammatory cytokines such as IL-1 or TNF.

This is the first study to show actual cleavage of native interstitial collagen and elastin by secreted RPE MMPs. The importance of this finding is reflected in the composition of the ECM comprising Bruch's membrane and PVR membranes. Bruch's membrane is a multilayered structure composed of basement membranes of the RPE and endothelium of the choriocapillaris sandwiching central lamellae containing structural collagens and elastin, which are enmeshed in proteoglycans and glycosaminoglycans.<sup>144</sup> The basement membranes are rich in collagen IV, fibronectin, and laminin. The collagenous layers are composed principally of collagens I and III, while the central elastic layer is composed chiefly of elastin.<sup>4</sup> Exposure of the collagenous layers and central elastic layer deep in Bruch's membrane makes it subject to the effects of interstitial collagenase (collagenase 1; MMP-1) and elastase, both of which are secreted by cells, including RPE cells constitutively (Figures 8 and 9). MMP-1, secreted as a latent procollagenase 1, requires enzymatic cleavage for its activation. In vivo activation may occur by previously activated uPAR or MMP.

RPE secretion of collagenase and elastase, together with that generated by the choriocapillaris vascular endothelium, may be important to physiologic remodeling of Bruch's membrane.<sup>145,146</sup> These MMPs are almost certainly tightly regulated by TIMPs whose impairment may lead to progressive alterations. It is known that genetic alterations of TIMP-3 lead to premature severe RPE and Bruch's membrane alterations that may be due to unbridled MMP activity. Reduced RPE TIMP-3 expression also results from RPE exposure to near-ultraviolet light,<sup>147</sup> a relative risk factor for the development of ARMD. Routinely, progressive alterations in Bruch's membrane in human eyes begin in the third decade of life.<sup>148,149</sup> These include abnormal RPE basement membrane thickening due in large measure to RPE extrusion of undigested lipid, protein, and lysosomal debris into Bruch's membrane.<sup>148,150-153</sup> In eyes predisposed to ARMD, MMP-1 may also be activated by lysosomal enzymes, which are secreted directly by aging and/or dysfunctional RPE cells into Bruch's membrane in secondary lysosomes.<sup>154-158</sup> Once activated, collagenase cleaves within the triple helical domains of tropocollagen near the carboxyl terminus, resulting in one-quarter and three-quarter chain length fragments that are susceptible to further digestion by other proteolytic enzymes, including TIMPs and lysosomal enzymes.<sup>159-161</sup> Since MMP-1 hydrolyzes interstitial collagen types I, II, and III,<sup>160,161</sup> it is likely to be important in generating full-thickness defects in Bruch's membrane

that permit subretinal CNV to occur. MMP-1 might also participate in remodeling and RPE invasion into PVR membranes which have been shown to be composed principally of collagens I, II, and III. Elastase is an MMP and a neutral endopeptidase, which not only hydrolyzes elastin but also cleaves other proteins, including proteinase inhibitors, thereby potentiating the hydrolytic activities of the MMPs.<sup>162-164</sup>

In this study, the IL-1 upregulation of secreted RPE interstitial collagenase (Figure 8) and elastase (Figure 9) that hydrolyzed their native substrates indicates that this may actually occur in retinal lesions of CNV and PVR in which RPE cells, mononuclear phagocytes, vascular endothelial cells, and other cells known to generate ambient IL-1 are present. Devitalized RPE cells or RPE cells involved in reparative responses may release inappropriately high levels of MMPs. In addition to ambient proinflammatory cytokines, phagocytosis of particulate debris and growth factors may induce the RPE to secrete excessive levels of collagenase and elastase, leading to the Bruch's membrane defects which predispose to CNV.

This study also demonstrates for the first time that RPE uPAR may be upregulated by several proinflammatory cytokines known to be elaborated in retinal lesions (Figures 1, 2, and 6). TNF, as well as IL-1, is elaborated by leukocytes, vascular endothelial cells, and RPE cells. These mediators stimulate RPE cells to express cell surface receptors and secrete chemokines, most notably IL-8 and MCP-1, which recruit and activate the leukocytes perpetuating the inflammatory components of CNV, PVR, and uveitic lesions. Thrombin, known to potentiate these RPE inflammatory responses, is an important initiator of MMP-2 and uPAR/uPA proteolytic activity.<sup>26</sup> That such proinflammatory cytokine upregulation of uPAR actually occurs in vivo is confirmed by the polarized, enhanced induction of uPAR that was observed over the inflammatory choroidal uveitic infiltrates, particularly in regions where sub-RPE exudates, rich in plasma-derived proteins including thrombin, were present (Figure 16).

Low-grade inflammation is associated with the development of CNV.<sup>165-167</sup> Approximately 60% of surgically excised, active CNV membranes contain mononuclear phagocytes, regardless of the underlying disease.<sup>8-12</sup> Mononuclear phagocytes specifically have been associated with normal retinal vasculogenesis during development and in reparative and pathologic angiogenesis, in which they release factors that influence various phases of the angiogenic process.<sup>168,169</sup> These growth factors, aFGF, bFGF, TGF- $\beta$ , and vascular endothelial growth factor (VEGF), all of which have been identified in surgically excised CNV,<sup>170,171</sup> and TNF- $\alpha$  may stimulate RPE expression of VEGF<sup>172,173</sup> and chemokines IL-8 and MCP-1, the former an inducer of angiogenesis and the latter a prime

recruiter and activator of mononuclear phagocytes.<sup>174,175</sup>

uPA, uPAR, and PAI-1 are also observed during angiogenesis *in vivo* where they are found to be expressed by the proliferating vascular endothelial cells. In this study, uPAR expression was found on human RPE cells as well as on the vascular endothelium of CNV membranes (Figures 13 and 14). VEGF and bFGF increase uPA and uPAR in cultured vascular endothelial cells. Induction of uPAR is accompanied by a decreased affinity for uPA and concomitant induction of PAI-1, but the overall effect is to favor proteolysis.<sup>176</sup> TGF- $\beta$ , an inducer of RPE uPAR,<sup>88</sup> acts as a pleotropic cytokine, having both negative and positive effects on endothelial proteolytic activity by inducing both uPA and PAI-1, with an overall effect favoring PAI-1 inhibition of proteolysis.

A recent study by Davis and associates<sup>177</sup> illustrates the careful regulation of angiogenesis by coordinated activity of uPAR/uPA, interstitial collagenase (MMP-1), and gelatinase B, all of which are produced by the RPE and, as shown in this study (Figures 2, 6, and 8), all of which are increased by IL-1.<sup>59</sup> These investigators found unencumbered MMP-1 and MMP-9 activation by uPAR-induced activation of plasminogen-induced vascular endothelial cell apoptosis and capillary regression that was apparently due to overexuberant ECM digestion. Accordingly, TIMPs and PAI-1 both blocked capillary regression, while antibodies to PAI-1 accelerated it. Thus, for neovascularization, uPAR/uPA and its inhibitor, PAI-1, and MMPs and their inhibitors, TIMPs, require careful coordination so as to provide the proper degree of ECM proteolysis for new blood vessels to proliferate.

uPAR also specifically interacts with the  $\beta_3$  integrin,  $\alpha_v\beta_3$ , the major vitronectin receptor that is expressed by many cell types, including macrophages,<sup>178</sup> vascular endothelial cells,<sup>179</sup> epithelial cells,<sup>180</sup> smooth-muscle cells,<sup>181</sup> and cancer cells, including melanoma.<sup>182</sup>  $\alpha_v\beta_3$  is associated with cellular migration, ECM proteolysis, angiogenesis, and metastasis. Ligation of  $\alpha_v\beta_3$  with mAb increases gene expression of uPAR and PAI-1 mRNA and cell-surface plasmin, resulting in increased cell invasion of collagen gels that can be abolished by mAb to uPA and uPAR.<sup>183</sup> Vitronectin binding to uPAR inhibits  $\beta_1$  integrin-mediated attachment to ECM and  $\beta_2$  integrin (CD11b/CD18)-mediated phagocytosis of fibrinogen.<sup>184</sup>  $\beta_1$  integrin-mediated attachment to vitronectin also appears to be uPAR-dependent.<sup>140</sup>

In melanoma, vitronectin is a marker of malignant progression and has been implicated in apoptosis<sup>185</sup> and production of MMP-2.<sup>186</sup> Melanoma cell migration on a vitronectin matrix is inhibited by uPA, whereas PAI-1 promoted melanoma cell migration on vitronectin, supporting the concept that uPA/uPAR acts as a vitronectin receptor that plays a role in regulating cell migration and adhe-

sion.<sup>187</sup> uPA/uPAR complex can bind to vitronectin either indirectly through the vitronectin-associated PAI-1 or directly through specific uPAR domains.<sup>188</sup>

In this study, the relative contributions of uPAR and MMPs to the process of RPE migration were investigated using a novel collagen gel supported by nylon mesh to prove the hypothesis that RPE uPAR mediated activation of proteolysis mediates RPE migration through ECM. As with angiogenesis, the uPAR/uPA and MMPs are both likely to be operative. However, the relative importance of these agents to pericellular proteolysis, the key step required for the invasion of cells through basement membranes and interstitial tissues, varies among cell types<sup>124,189-196</sup> and is unknown in the RPE cells. Pericellular proteolysis due to RPE uPAR activity (Figure 6) and RPE MMP activity (Figure 7) was initially confirmed by placing the RPE cells on gels containing Bodipy-BSA (albumin) and DQ collagen (collagen IV) probes, respectively. Pericellular fluorescence due to matrix disruption and probe hydrolysis that generated fluorescent products indicated constitutive RPE expression of both activities. Disruption of matrices in the presence of the inhibitors PAI-1 and 1,10-phenanthroline substantially inhibited the release of fluorescent peptides from Bodipy-BSA and DQ collagen, respectively, demonstrating that the enzymatic activities were specific ( $P < .001$ ). IL-1 enhanced PAI-1-inhibitable, specific activity of RPE uPAR ( $P < .001$ ), but not of collagen IV MMP-hydrolytic activity, a finding consistent with the lack of induction of gelatinase by IL-1.<sup>30</sup>

To demonstrate the relative importance of uPAR and MMP in actual RPE migration, however, a novel transmigration assay system to prove the hypothesis of this thesis was developed (Figure 10).<sup>133</sup> The transmigration assay method is of considerable interest from both technologic and physiologic viewpoints. Using an open-mesh nylon grid for support, multiple gel layers were deposited on the mesh. By adding a small amount of gel to the mesh at a time, multiple layers could be built up into a thicker matrix, much like assembling plywood. The open mesh also affords the ability to use both transmitted light and epifluorescence microscopy to image events. This has considerable advantage over invasion assays that rely on cell migration through artificial pores. Another advantage of these nylon mesh-supported matrices is that most of the surface area is available for transmigration to the bottom of the matrix. In contrast, only a small fraction of a conventional filter's surface area is available in the form of small pores to permit migration to the bottom of the matrix. In most experiments using filter assays, cells must deform as they pass through the artificial matrix pores, an action event that has no clear counterpart in cell physiology. Moreover, pore assays may be measuring the abilities of cells to find an available pore rather than the kinetics of

transmigration. A clear advantage of these gel matrices is that they can also be tailored to address specific experimental hypotheses, such as the one in this study. In this study, for example, we included substrates (Bodipy-BSA and DQ collagen) within the matrix that become fluorescent upon proteolytic cleavage, thus revealing the location of functioning enzymes while imaging transmigrating red, fluorescently labeled RPE cells. When these assays were conducted for extended periods of time, the pathways followed by cells during this model transmigration process could be imaged. Our approach is particularly valuable in studying transmigration, since bright-field microscopy is unrevealing under these circumstances because the refractive index of cells matches that of the ECM. Thus, we have developed the technology suitable for addressing several critical issues surrounding the invasive ability of cells.

To demonstrate RPE migration, the novel nylon mesh-supported collagen gels were seeded with RPE cells (Figure 10) and induced to migrate with serum. Imaging of the migrating RPE cells over 4 hours revealed plumes of fluorescence generated by the RPE cells as they tunneled through the matrix (Figure 11). To confirm the relevance of uPAR and MMP activities to the transmigration of RPE cells through the novel matrices, PAI-1 and 1,10-phenanthroline were incorporated into the matrices at high concentrations before their solidification. PAI-1, but not 1,10-phenanthroline, was found to substantially inhibit ( $P < .001$ ) the ability of RPE cells to cross the matrix (Figure 12). This dramatic difference is strong evidence for a cardinal role for uPAR in RPE migration through ECM.

Studies of other cell types, including cancer cells, have shown that uPAR-positive cells are more invasive.<sup>195-199</sup> However, uPAR-negative cells can also be invasive, since the presence of uPAR-positive cells may enhance the ability of uPAR-negative cells to migrate across the ECM. Microscopy studies suggest that the ability of uPAR-negative cells to follow uPAR-positive cells across a matrix can partially account for this.<sup>133</sup> Having developed the technology to observe proteolytic trails in matrices, we examined the process of RPE invasion and found that trailing RPE cells used the paths of matrix disruption by the initial migrants, facilitating their passage. Such a process in vivo might allow a relatively few strongly expressing uPAR-positive RPE cells to pave the way for others to follow, resulting in the strands and other cellular arrangements usually seen in histopathologic sections of CNV and PVR membranes (Figures 13, 14, and 15).

In this scenario, uPAR clustering at RPE cell-substratum interfaces and at migratory fronts<sup>200-203</sup> would render the ECM susceptible to digestion by cell-associated plasmin that is activated by uPA bound to RPE uPAR. RPE uPAR, found at the lamellipodium of elongated RPE

cells in areas of blood-retina barrier breakdown, RPE cell disruption, or persistent retinal detachment, would then have focused proteolytic action in the direction of cell migration. Plasmin degradation, potentiated and controlled to some degree by the MMPs/TIMPs, would degrade ECM proteins in the path of cellular invasion.<sup>204</sup> This scenario is now a working hypothesis for current research and development of drugs to prevent cancer cell invasion and metastasis. Understanding the roles of uPAR and MMP in RPE migration may lead to the development of new pharmacologic agents targeting uPAR participation in adverse pathophysiologic mechanisms of important retinal diseases.

---

## ACKNOWLEDGMENTS

Special thanks to Victor M. Elner, MD, PhD, Howard R. Petty, PhD, Andrei L. Kindzelskii, MD, Ersalan Rahman, MD, and Mitch Gillett for their expertise and contributions in data acquisition, tissue preparation, and manuscript preparation.

---

## REFERENCES

1. Bressler NM, Bressler SB, Fine SL. Age-related macular degeneration. *Surv Ophthalmol* 1988;32:375-413.
2. Green WR, Enger C. Age related macular degeneration histopathological studies. *Ophthalmology* 1993;100:1519-1535.
3. Hogan MJ. Role of the retinal pigment epithelium in macular disease. *Trans Am Acad Ophthalmol Otolaryngol* 1972;76:64-80.
4. Feeney-Burns L, Ellersieck M. Age-related changes in the ultrastructure of Bruch's membrane. *Am J Ophthalmol* 1985;100:686-697.
5. Green WR. The retina. In: Spencer WH, ed. *Ophthalmic Pathology. An Atlas and Textbook*. Philadelphia: WB Saunders; 1996: 982-1050.
6. Green WR, Key SN III. Senile macular degeneration. A histopathologic study. *Trans Am Ophthalmol Soc* 1977;75:951-955.
7. Green WR. Clinicopathologic studies of treated choroidal neovascular membranes. A review and report of two cases. *Retina* 1991;11:328-356.
8. Lopez PF, Grossniklaus HE, Lambert HM, et al. Pathologic features of surgically excised subretinal neovascular membranes in age-related macular degeneration. *Am J Ophthalmol* 1991;112:647-656.
9. Saxe SJ, Grossniklaus HE, Lopez PF, et al. Ultrastructural features of surgically excised subretinal neovascular membranes in the ocular histoplasmosis syndrome. *Arch Ophthalmol* 1993;111:88-95.
10. Grossniklaus HE, Martinez JA, Brown VE, et al. Immunohistochemical and histochemical properties of surgically excised subretinal neovascular membranes in age-related macular degeneration. *Am J Ophthalmol* 1992;114:464-472.
11. Grossniklaus HE, Hutchinson AK, Capone A Jr, et al. Clinicopathologic features of surgically excised choroidal neovascular membranes. *Ophthalmology* 1994;101:1099-1111.
12. Grossniklaus HE, Green WR. Histopathologic and ultrastructural findings of surgically excised choroidal neovascularization. *Arch Ophthalmol* 1998;116:745-749.

13. Weber BHF, Vogt G, Wolz W, et al. Sorsby's fundus dystrophy is genetically linked to chromosome 22q13-qter. *Nature Genet* 1994;7:158-161.
14. Matrisian LM. Metalloproteinases and their inhibitors in matrix remodeling. *Trends Genet* 1990;6:121-125.
15. Weber BHF, Vogt G, Pruett RC, et al. Mutations in the tissue inhibitor of metalloproteinases-3 (TIMP3) in patients with Sorsby's fundus dystrophy. *Nature Genet* 1994;8:352-356.
16. Capon MRC, Marshall J, Krafft JI, et al. Sorsby's fundus dystrophy – A light and electron microscopic study. *Ophthalmology* 1989;96:1769-1777.
17. Fariss RN, Apte SS, Luthert PJ, et al. Accumulation of tissue inhibitor of metalloproteinases-3 in human eyes with Sorsby's fundus dystrophy or retinitis pigmentosa. *Br J Ophthalmol* 1998;82:1329-1334.
18. Kamei M, Hollyfield JG. TIMP-3 in Bruch's membrane: changes during aging and in age-related macular degeneration. *Invest Ophthalmol Vis Sci* 1999;40:2367-2375.
19. Bressler SB, Bressler NM, Alexander J, et al. Clinicopathologic correlation of occult choroidal neovascularization in age-related macular degeneration. *Arch Ophthalmol* 1992;110:827-832.
20. Gass DM. Drusen and disciform macular detachment and degeneration. *Arch Ophthalmol* 1973;90:201-217.
21. Green WR, Key SN. Pathologic features of senile macular degeneration. *Ophthalmology* 1985;92:615-627.
22. Sarkis SH. Aging and degeneration in the macular region: a clinicopathologic study. *Br J Ophthalmol* 1976;60:324-341.
23. Smiddy WE, Fine SL. Prognosis of patients with bilateral macular drusen. *Ophthalmology* 1984;91:271-284.
24. Wright JK, Cawston TE, Hazleman BL. Transforming growth factor beta stimulates the production of the tissue inhibitor of metalloproteinases (TIMP) by human synovial and skin fibroblasts. *Biochim Biophys Acta* 1991;1094:207-210.
25. Stetler S. Matrix metalloproteinases in angiogenesis: a moving target for therapeutic intervention. *J Clin Invest* 1999;103:1237-1241.
26. Nguyen M, Arkell J, Jackson CJ. Human endothelial gelatinases and angiogenesis. *Int J Biochem Cell Biol* 2001;33:960-970.
27. Butler TA, Zhu C, Mueller RA, et al. Inhibition of ovulation in the perfused rat ovary by the synthetic collagenase inhibitor SC 44463. *Biol Reprod* 1991;44:1183-1188.
28. Graham CH, Lala PK. Mechanism of control trophoblast invasion in situ. *J Cell Phys* 1991;148:228-234.
29. Ye S. Polymorphism in matrix metalloproteinase gene promoters: implication in regulation of gene expression and susceptibility of various diseases. *Matrix Biol* 2000;19:623-629.
30. Jackson C, Nguyen M, Arkell J, et al. Selective matrix metalloproteinase (MMP) inhibition in rheumatoid arthritis—targetting gelatinase A activation. *Inflamm Res* 2001;50:183-186.
31. Zucker S, Lysik RM, Zarrabi MH, et al. Elevated plasma stromelysin levels in arthritis. *J Rheumatol* 1991;21:2329-2333.
32. Naito K, Takahashi M, Kushida K, et al. Measurement of matrix metalloproteinases (MMPs) and tissue inhibitor of metalloproteinases-1 (TIMP-1) in patients with knee osteoarthritis; comparison with generalized osteoarthritis. *Rheumatology (Oxford)* 1999;38:510-515.
33. Liotta L, Steeg PS, Stetler Stevenson WG. Cancer metastasis and angiogenesis: an imbalance of positive and negative regulation. *Cell* 1991;327-336.
34. McCawley LJ, Matrisian LM. Tumor progression: defining the soil round the tumor seed. *Curr Biol* 2001;11:R25-R27.
35. McMillan WD, Pearce WH. Increased plasma levels of metalloproteinase-9 are associated with abdominal aortic aneurysms. *J Vasc Surg* 1999;29:122-127.
36. Kai H, Ikeda H, Yasukawa H, et al. Peripheral blood levels of matrix metalloproteinases-2 and -9 are elevated in patients with acute coronary syndromes. *J Am Coll Cardiol* 1998;32:368-372.
37. Henney AM, Wakeley PR, Davies MJ, et al. Localization of stromelysin gene expression in atherosclerotic plaques by in situ hybridization. *Proc Natl Acad Sci USA* 1991;88:8154-8158.
38. Galis ZS, Sukhova GK, Lark MW, et al. Increased expression of matrix metalloproteinases and matrix degrading activity in vulnerable regions of human atherosclerotic plaques. *J Clin Invest* 1994;94:2493-2503.
39. Kleiner DE, Stetler Stevenson WG. Matrix metalloproteinases and metastasis. (Abstract) *Cancer Chemo Pharmacol* 1999;43(Suppl):S42-S51.
40. Brinckerhoff CE, Rutter JL, Benbow U. Interstitial collagenases as markers of tumor progression. *Clin Cancer Res* 2000;6:4823-4830.
41. Nagase H, Woessner JF, Jr. Matrix metalloproteinases. *J Biol Chem* 1999;274:21491-21492.
42. Murray GI, Duncan ME, O'Neil P, et al. Matrix metalloproteinase-1 is associated with poor prognosis in colorectal cancer. *Nat Med* 1996;2:461-462.
43. Murray GI, Duncan ME, O'Neil P, et al. Matrix metalloproteinase-1 is associated with poor prognosis in oesophageal cancer. *J Pathol* 1998;185:256-261.
44. Ito T, Ito M, Shiozawa J, et al. Expression of the MMP-1 in human pancreatic carcinoma: relationship with prognostic factor. *Mod Pathol* 1999;12:669-675.
45. Walsh DA. Angiogenesis and arthritis. *Rheumatology* 1999;38:103-12.
46. Frisch SM, Morasaki JH. Positive and negative transcriptional elements of the human type IV collagenase gene. *Mol Biol Cell* 1990;10:6524-6532.
47. Olson MW, Gervasi DC, Mobashery S, et al. Kinetic analysis of the binding of human matrix metalloproteinase-2 and -9 to tissue inhibitor of metalloproteinase TIMP-1 and TIMP-2. *J Biol Chem* 1977;272:29975-29983.
48. Howard E, Bulleten E, Banda MJ. Regulation of the autoactivation of human 72kDa progelatinase by tissue inhibitor of metalloproteinase-2. *J Biol Chem* 1991;266:13064-13069.
49. Jackson CJ, Arkell J, Nguyen M. Rheumatoid synovial endothelial cells secrete decreased levels of tissue inhibitor of MMP (TIMP1). *Ann Rheum Dis* 1998;57:158-161.
50. Opdenakker G, Van den Steen PE, Dubois B, et al. Gelatinase B functions as regulator and effector in leukocyte biology. *J Leukoc Biol* 2002;69:851-859.
51. Fenton JW. Regulation of thrombin generation and functions. *Semin Thromb Hemost* 1988;14:234-239.
52. Nguyen M, Arkell J, Jackson CJ. Active and tissue inhibitor of matrix metalloproteinase-free gelatinase B accumulates within human microvascular endothelial vesicles. *J Biol Chem* 1998;273:5400-5404.
53. Opdenakker G, Masure S, Grillet B, et al. Cytokine-mediated regulation of human leukocyte gelatinases and role in arthritis. *Lymphokine Cytokine Res* 1991;10:317-324.
54. Gijbels K, Masure S, Carton H, et al. Gelatinase in the cerebrospinal fluid of patients with multiple sclerosis and other inflammatory neurological disorders. *J Neuroimmunol* 1992;41:29-34.
55. Schonbeck U, Mach F, Libby P. Generation of biologically active IL-1 $\beta$  by matrix metalloproteinases: a novel caspase-1-independent pathway of IL-1 $\beta$  processing. *J Immunol* 1998;161:3340-3346.

56. McQuibban GA, Gong J-H, Tam EM, et al. Inflammation dampened by gelatinase A cleavage of monocyte chemoattractant protein-3. *Science* 200;289:1202-1206.
57. Nagase H. Stromelysins 1 and 2. In: Parks WC, Mecham RP, eds. *Matrix Metalloproteinases*. San Diego: Academic Press; 1998:43-84.
58. Newman KM, Ogata Y, Malon AM, et al. Identification of matrix metalloproteinases 3 (stromelysin-1) and 9 (gelatinase B) in abdominal aortic aneurysm. *Arterioscler Thromb* 1994;14:1315-1320.
59. Alexander JP, Bradley JMB, Gabourel JD, et al. Expression of matrix metalloproteinases and inhibitor by human retinal pigment epithelium. *Invest Ophthalmol Vis Sci* 1990;31:2520-2528.
60. Schonfeld CL. Metalloproteinase stromelysin. Expression in human retinal pigment epithelium (RPE). *Ophthalmology* 1997;94:629-633.
61. Hunt RC, Fox A, Pakalnis VA, et al. Cytokines cause cultured retinal pigment epithelial cells to secrete metalloproteinases and to contract collagen gels. *Invest Ophthalmol Vis Sci* 1993;34:3179-3186.
62. Vaisanen A, Kallioinen M, Von Dickhoff K, et al. Matrix metalloproteinase-2 (MMP-2) immunoreactive protein—a new prognostic marker in uveal melanoma. *J Pathol* 1999;188:56-62.
63. Ruiz A, Brett P, Bok D. TIMP-3 is expressed in the human retinal pigment epithelium. *Biochem Biophys Res Comm* 1996;226:467-474.
64. Andreassen PA, Kjoller L, Christensen L, et al. The urokinase-type plasminogen activator system in cancer metastasis: a review. *Int J Cancer* 1997;72:1-22.
65. Ploug M, Ronne E, Behrendt N, et al. Cellular receptor for urokinase plasminogen activator. Carboxyl-terminal processing and membrane anchoring by glycosyl-phosphatidyl-inositol. *J Biol Chem* 1991;266:1926-1933.
66. Stoppelli MP, Corti A, Soffientini A, et al. Differentiation-enhanced binding of the amino-terminal fragment of human urokinase plasminogen activator to a specific receptor on U937 monocytes. *Proc Natl Acad Sci USA* 1985;82:4939-4943.
67. Dano K, Behrendt N, Brenner N, et al. The urokinase receptor. Protein structure and role in plasminogen activation and cancer invasion. *Fibrinolysis* 1994;8:189-203.
68. Plesner T, Ploug M, Ellis V, et al. The receptor for urokinase-type plasminogen activator and urokinase is translocated from two distinct intracellular compartments to the plasma membrane on stimulation of human neutrophils. *Blood* 1994;83:808-815.
69. McNeill H, Jensen PJ. A high-affinity receptor for urokinase plasminogen activator on human keratinocytes: characterization and potential modulation during migration. *Cell Regul* 1990;1:843-852.
70. Miles LA, Levin EG, Plescia J, et al. Plasminogen receptors, urokinase receptors, and their modulation on human endothelial cells. *Blood* 1988;72:628-635.
71. Hollas W, Hoosein N, Chung W, et al. Expression of urokinase and its receptor in invasive and non-invasive prostate cancer cell lines. *Thromb Haemost* 1992;68:662-666.
72. Boyd D, Florent H, Kin P, et al. Determination of the levels of urokinase and its receptor in human colon carcinoma cell lines. *Cancer Res* 1988;48:3112-3116.
73. Ghosh S, Brown R, Jones JC, et al. Urinary-type plasminogen activator (uPA) expression and uPA receptor localization are regulated by alpha 3 beta 1 integrin in oral keratinocytes. *J Biol Chem* 2000;275:23869-23876.
74. Kessler TL, Markus G. Epidermal growth factor and 12-tetradecanoyl phorbol 13-acetate induction of urokinase in A431 cells. *Semin Thromb Hemost* 1991;17:217-224.
75. Mignatti P, Mazziere R, Rifkin DB. Expression of the urokinase receptor in vascular endothelial cells is stimulated by basic fibroblast growth factor. *J Cell Biol* 1991;113:1193-1201.
76. Lund LR, Romer J, Ronne E, et al. Urokinase-receptor biosynthesis, mRNA level and gene transcription are increased by transforming growth factor beta 1 in human A549 lung carcinoma cells. *EMBO J* 1991;10:3399-3407.
77. Neidbala MJ, Stein M. Tumor necrosis factor induction of urokinase-type plasminogen activator in human endothelial cells. *Biomed Biochim Acta* 1991;50:427-436.
78. Ellis V, Scully MF, Kakkar VV. Plasminogen activation initiated by single chain urokinase-type plasminogen activator. Potentiation by U937 monocytes. *J Biol Chem* 1989;264:2185-2188.
79. Olson D, Pollanen J, Hoyer-Hansen G, et al. Internalization of the urokinase-plasminogen activator type-1 complex is mediated by the urokinase receptor. *J Biol Chem* 1992;267:9129-9133.
80. Kircheimer JC, Christ G, Binder BR. Growth stimulation of human epidermal cells by urokinase is restricted to the intact active enzyme. *Eur J Biochem* 1989;181:103-107.
81. Odekon LE, Sato Y, Rifkin DB. Urokinase-type plasminogen activator mediates basic fibroblast growth factor-induced bovine endothelial cell migration independent of its proteolytic activity. *J Cell Physiol* 1992;150:258-263.
82. Gyetko MR, Sitrin RG, Fuller JA, et al. Function receptor (CD87) in neutrophil chemotaxis. *J Leukoc Biol* 1995;58:533-538.
83. Tripathi RC, Tripathi BJ, Park JK. Localization of urokinase-type plasminogen activator in human eyes: an immunocytochemical study. *Exp Eye Res* 1990;51:545-552.
84. Siren V, Stephens RW, Salonen EM, et al. Retinal pigment epithelial cells secrete urokinase-type plasminogen activator and its inhibitor PAI-1. *Ophthalmic Res* 1992;24:203-212.
85. Campochiaro PA, Mimuro J, Sugg R, et al. Retinal pigment epithelial cells produce a latent fibrinolytic inhibitor that is antigenically and biochemically related to type 1 plasminogen activator inhibitor produced by vascular endothelial cells. *Exp Eye Res* 1989;49:195-203.
86. Siren V, Immonen I, Cantell K, et al. Interferons alpha and gamma inhibit plasminogen activator inhibitor-1 gene expression in human retinal pigment epithelial cells. *Ophthalmic Res* 1994;25:1-7.
87. Yang Z, Cohen RL, Lui GM, et al. Thrombin increases expression of urokinase receptor by activation of the thrombin receptor. *Invest Ophthalmol Vis Sci* 1995;36:2254-2261.
88. Siren V, Myohanen H, Vaheri A, et al. Transforming growth factor beta induces urokinase receptor expression in cultured retinal pigment epithelial cells. *Ophthalmic Res* 1999;31:184-191.
89. Jerdan JA, Pepose JS, Michels RG, et al. Proliferative vitreoretinopathy membranes. An immunohistochemical study. *Ophthalmology* 1989;96:801-810.
90. Marino I, Hiscott P, McKechnie N, et al. Variation in epiretinal membrane components with clinical derivation of the proliferative tissue. *Br J Ophthalmol* 1990;74:393-399.
91. Kauffmann DJH, van Meurs JC, Mertens DAE, et al. Cytokines in vitreous humor: interleukin-6 is elevated in proliferative vitreoretinopathy. *Invest Ophthalmol Vis Sci* 1994;35:900-906.
92. Elner SC, Elner VM, Jaffe GJ, et al. Cytokines in proliferative diabetic retinopathy and proliferative vitreoretinopathy. *Curr Eye Res* 1995;14:1045-1053.
93. Limb GA, Earley AO, Green W, et al. Distribution of cytokine proteins within epiretinal membranes in proliferative vitreoretinopathy. *Curr Eye Res* 1994;13:791-798.

94. Grant MB, Guay C, Marsh R. Insulin-like growth factor I stimulates proliferation, migration, and plasminogen activator release by human retinal pigment epithelial cells. *Curr Eye Res* 1990;9:323-335.
95. Reuning U, Magdolen V, Wilhelm O, et al. Multifunctional potential of the plasminogen activation system in tumor invasion and metastasis (review). *Int J Oncol* 1998;13:893-906.
96. Blasi F. uPA, uPAR, PAI-1: key intersection of proteolytic, adhesive, and chemotactic highways? *Immunol Today* 1997;18:415-417.
97. Fibbi G, Ziche M, Morbidelli L, et al. Interaction of urokinase with specific receptors stimulates mobilization of bovine adrenal capillary endothelial cells. *Exp Cell Res* 1988;179:385-395.
98. Gudewicz PW, Bilboa N. Human urokinase-type plasminogen activator stimulates chemotaxis of human neutrophils. *Biochem Biophys Res Comm* 1987;147:1176-1181.
99. Resnati M, Guttinger M, Valcamonica S, et al. Proteolytic cleavage of the urokinase receptor substitutes for the agonist-induced chemotactic effect. *EMBO J* 1996;15:1572-1582.
100. Loskutoff DJ, Curriden SA, Hu G, et al. Regulation of cell adhesion by PAI-1. *APMIS* 1999;107:54-61.
101. Elnor VM, Schaffner T, Taylor K, et al. Immunophagocytic properties of retinal pigment epithelium cells. *Science* 1982; 211:74-76.
102. Pavilack MA, Elnor SG, Feldman LE, et al. Human RPE cells express leukocyte integrins and intercellular adhesion molecules. (Abstract) *Invest Ophthalmol Vis Sci* 1990;31(Suppl):372. Abstract 1828.
103. Xue W, Kindzelskii AL, Todd III RF, et al. Physical association of complement receptor type 3 and urokinase-type plasminogen activator receptor in neutrophil membranes. *J Immunol* 1994;152:4630-4640.
104. Arribas J, Coodly L, Vollmer P, et al. Diverse cell surface protein ectodomains are shed by a system sensitive to metalloprotease inhibitors. *J Biol Chem* 1996;271:11376-11382.
105. Lijnen HR. Elements of the fibrinolytic system. *Ann NY Acad Sci* 2001;936:226-236.
106. Koolwijk P, Sidenius N, Peters E, et al. Proteolysis of the urokinase-type plasminogen activator receptor by metalloproteinase-12; implication for angiogenesis in fibrin matrices. *Blood* 2001;97:3123-3131.
107. Okamoto I, Kawano Y, Tsuiki H, et al. CD44 cleavage induced by a membrane associated metalloprotease plays a critical role in tumor cell migration. *Oncogene* 1999;18:1435-1446.
108. Preece G, Murphy G, Ager A. Metalloproteinase-mediated regulation of L-selectin levels on leucocytes. *J Biol Chem* 1996;271:11645-11640.
109. Elnor SG, Strieter RM, Elnor VM, et al. Monocyte chemotactic protein gene expression by cytokine-treated human retinal pigment epithelial cells. *Lab Invest* 1991;64:819-825.
110. Campochiaro PA, Jerdon JA, Glaser BM. The extracellular matrix of human retinal pigment epithelial cells in vivo and its synthesis in vitro. *Invest Ophthalmol Vis Sci* 1986;27:1615-1621.
111. Bohuslav J, Horejsi V, Hansmann C, et al. Urokinase plasminogen activator receptor,  $\beta_2$ -integrins, and *src*-kinases within a single receptor complex of human monocytes. *J Exp Med* 1995;181:1381-1390.
112. Min HY, Semmani R, Mizukami IF, et al. cDNA for Mo3, a monocyte activation antigen, encodes the human receptor for urokinase plasminogen activator. *J Immunol* 1992;148:3636-3642.
113. Todd RF, Nadler LM, Schlossman SF. Antigens on human monocytes identified by monoclonal antibodies. *J Immunol* 1981;126:1435-1442.
114. Todd RF, Roach JA, Arnaout MA. The modulated expression of Mo5, a human myelomonocyte plasma membrane antigen. *Blood* 1985;65:964-973.
115. Dana N, Styrts B, Griffin JD, et al. Two functional domains in the phagocyte membrane glycoprotein Mo1 identified with monoclonal antibodies. *J Immunol* 1986;137:3259-3263.
116. Petty HR, Francis JW, Todd RF, et al. Neutrophil C3bi receptors: formation of membrane clusters during cell triggering requires intracellular granules. *J Cell Physiol* 1987;133:235-242.
117. Zhou MJ, Todd RF, Petty HR. Detection of transmembrane linkages between immunoglobulin or complement receptors and the neutrophil's cortical microfilaments by resonance energy transfer microscopy. *J Mol Biol* 1991;218:263-268.
118. Zhou MJ, Todd RF III, van de Winkel JG, et al. Cocapping of the leuko adhesion molecules complement receptor type 3 and lymphocyte function-associated antigen-1 with Fc $\gamma$  receptor III on human neutrophils: possible role of lectin-like interactions. *J Immunol* 1993;150:3030-3041.
119. Wessendorf MW, Appel NM, Elde R. Simultaneous observation of fluorescent retrogradely labeled neurons and the immunofluorescently labeled fibers apposing them using fluoro-gold and antisera labeled with the blue fluorochrome 7-amino-4-methylcoumarin-3-acetic acid (AMCA). *Neurosci Lett* 1987;82:121-126.
120. Francis JW, Todd RF, Boxer LA, et al. Histamine inhibits cell-spreading and C3bi receptor clustering and diminishes hydrogen peroxide production by adherent human neutrophils. *J Cell Physiol* 1991;147:128-137.
121. Uster PS, Pagano RE. Resonance energy transfer microscopy: observations of membrane-bound fluorescent probes in model membranes and in living cells. *J Cell Biol* 1986;103:1221-1234.
122. Zhou M-J, Poo H, Todd RF, et al. Surface-bound immune complexes trigger transmembrane proximity between complement receptor type 3 and the neutrophil's cortical microfilaments. *J Immunol* 1992;148:3550-3553.
123. Maher RJ, Cao D, Boxer LA, et al. Simultaneous calcium-dependent delivery of neutrophil lactoferrin and reactive oxygen metabolites to erythrocyte targets: evidence supporting granule-dependent triggering of superoxide release. *J Cell Physiol* 1993;156:226-234.
124. Kindzelskii AL, Zhou MJ, Haugland RP, et al. Oscillatory pericellular proteolysis and oxidant deposition during neutrophil locomotion. *Biophys J* 1998;74:90-97.
125. Garbett EA, Reed MWR, Brown NJ. Proteolysis in human breast and colorectal cancer. *Br J Cancer* 1999;81:287-293.
126. Kindzelskii AL, Yang Z, Nabel GJ, et al. Ebola virus secretory glycoprotein (sGP) disrupts Fc $\gamma$ RIIb to CR3 proximity on neutrophils. *J Immunol* 2000;165:953-958.
127. Li W, Yanoff M, Li Y, et al. Artificial senescence of bovine retinal pigment epithelial cells induced by near-ultraviolet in vitro. *Mech Age Devel* 1999;110:137-155.
128. Hed J. The extinction of fluorescence by crystal violet and its use to differentiate between attached and ingested microorganisms in phagocytosis. *FEMS Microbiol Lett* 1997;1:357-361.
129. LaBarca C, Paigen K. A simple, rapid, and sensitive DNA assay procedure. *Anal Biochem* 1980;102:344-352.
130. Hu CL, Crombie G, Franzblau C. A new assay for collagenolytic activity. *Anal Biochem* 1978;88:638-643.
131. Banda MJ, Werb Z. Mouse macrophage elastase: purification and characterization as a metalloproteinase. *Biochem J* 1981;1983:589-605.
132. Elnor VM, Nielsen JC, Elnor SG, et al. Immunophenotypic modulation of cultured human retinal pigment epithelial cells by gamma interferon and phytohemagglutinin-stimulated human T-lymphocytes (Abstract). *Invest Ophthalmol Vis Sci* 1989;30(Suppl):233.

133. Horino K, Kindezeliskii AL, Elner VM, et al. Tumor cell invasion of model 3-dimensional matrices: demonstration of migratory pathways, collagen disruption, and intercellular cooperation. *FASEB J* 2001;15:932-939.
134. Esmaeli B, Elner VM, Elner SG, et al. Immunohistochemical detection of urokinase plasminogen activator receptor/Mo3 on human RPE cells (Abstract). *Invest Ophthalmol Vis Sci* 1994;35(Suppl):1759. Abstract 2334.
135. Vranka JA, Johnson E, Zhu Xianghong, et al. Discrete expression and distribution pattern of TIMP-3 in the human retina and choroid. *Curr Eye Res* 1997;15:102-110.
136. Lijnen HR, Arza B, Van Hoef B, et al. Inactivation of plasminogen activator inhibitor-1 by specific proteolysis with stromelysin-1 (MMP-3). *J Biol Chem* 2000;275:37645-37650.
137. Rizzolo LJ. Basement membrane stimulates the polarized distribution of integrins but not the Na,K-ATPase in the retinal pigment epithelium. *Cell Regul* 1991;2:939-949.
138. Simon DI, Wei Y, Zhang L, et al. Identification of urokinase receptor-integrin interaction site. Promiscuous regulator of integrin function. *J Biol Chem* 2000;275:10228-10234.
139. Ross GD. Regulation of the adhesion versus cytotoxic functions of the Mac-1/CR3/alphaM beta2-integrin glycoprotein. *Crit Rev Immun* 2000;20:197-222.
140. May AE, Neumann FJ, Schomig A, et al. VLA-4 (alpha(4)beta(1)) engagement defines a novel activation pathway for beta(2) integrin-dependent leukocyte adhesion involving the urokinase receptor. *Blood* 2000;96:506-513.
141. Estreicher A, Muhlhauser J, Carpentier JL, et al. The receptor for urokinase-type plasminogen activator polarizes expression of the protease to the leading edge of migrating monocytes and promotes degradation of enzyme inhibitor complexes. *J Cell Biol* 1990;111:783-792.
142. Chu PG, Grunwald BG. Functional inhibition of retinal pigment epithelial cell-substrate adhesion with a monoclonal antibody against the beta I subunit of integrin. *Invest Ophthalmol Vis Sci* 1991;32:1763-1769.
143. Anderson DH, Guerin CJ, Matsumoto B, et al. Identification and localization of a beta-1 receptor from the integrin family in mammalian retinal pigment epithelial cells. *Invest Ophthalmol Vis Sci* 1990;31:81-93.
144. Lin W-L. Immunogold localization of extracellular matrix molecules in Bruch's membrane of the rat. *Curr Eye Res* 1989;8:1171-1178.
145. Moscatelli D, Jaffe E, Rifkin DB. Tetradecanoyl phorbol acetate stimulates latent collagenase production by cultured human endothelial cells. *Cell* 1980;20:343-351.
146. Kalebic T, Garbisa S, Glaser B, et al. Basement membrane collagen: degradation by migrating endothelial cells. *Science* 1983;221:281-283.
147. Li W, Yanoff M, Li Y, et al. Artificial senescence of bovine retinal pigment epithelial cells induced by near-ultraviolet in vitro. *Mech Age Devel* 1999;110:137-55.
148. Spencer WH. Macular diseases: pathogenesis: light microscopy. *Trans Am Acad Ophthalmol Otolaryngol* 1965;69:662-667.
149. Hogan MJ, Alvarado JA. Studies on the human macula, IV: aging changes in Bruch's membrane. *Arch Ophthalmol* 1967;77:410-420.
150. Garron LK. The ultrastructure of the retinal pigment epithelium, with observations on the choriocapillaris and Bruch's membrane. *Trans Am Ophthalmol Soc* 1963;61:545.
151. Green WR, Key SN. Senile macular degeneration: a histopathologic study. *Trans Am Ophthalmol Soc* 1977;75:180-254.
152. Green WR. Clinicopathologic studies of senile macular degeneration. In: Nicholson DH, ed. *Ocular Pathology Update*. New York: Masson Publishing Co; 1980:118.
153. Ishibashi T, Patterson R, Ohnishi Y, et al. Formation of drusen in the human eye. *Am J Ophthalmol* 1986;101:342-343.
154. Dhaliwal BS, Steinbrecher UP. Scavenger receptors and oxidized low density lipoproteins. *Clin Chim Acta* 1999;286:191-205.
155. Eeckhout Y, Vaes G. Further studies on the activation of procollagenase, the latent precursor of bone collagenase. Effects of lysosomal cathepsin B, plasmin and kallikrein, and spontaneous activation. *Biochem J* 1977;166:21-31.
156. Dingle JT. The secretion of enzymes into the pericellular environment. *Philosoph Trans R Soc London Series B: Biol Sci* 1975;271:315-332.
157. Davies P, Allison AC. The macrophage as a secretory cell in chronic inflammation. *Agents Actions* 1976;6:60-74.
158. Unanue ER. Secretory function of mononuclear phagocytes. *Am J Pathol* 1976;83:396-417.
159. Berman M, Leary R, Gage J. Collagenase from corneal cell cultures and its modulation by phagocytosis. *Invest Ophthalmol Vis Sci* 1979;18:588-601.
160. Harper E. Collagenases. *Annu Rev Biochem* 1980;49:1063-1078.
161. Salo T, Liotta LA, Tryggvason K. Purification and characterization of a murine basement membrane collagen-degrading enzyme secreted by metastatic tumor cells. *J Biol Chem* 1983;358:3058-3063.
162. Werb Z, Gordon S. Elastase secretion by stimulated macrophages: characterization and regulation. *J Exp Med* 1975;143:361-377.
163. Banda MJ, Clark EJ, Werb Z. Limited proteolysis by macrophage elastase inactivates human a-1-proteinase inhibitor. *J Exp Med* 1980;152:1563-1570.
164. Banda MJ, Clark EJ, Werb Z. Selective proteolysis of immunoglobulins by mouse macrophage elastase. *J Exp Med* 1983;157:1184-1196.
165. Penfield PL, Provis JM, Billson FA. Age-related macular degeneration: ultrastructural studies of the relationship of leukocytes to angiogenesis. *Graefes Arch Clin Exp Ophthalmol* 1987;225:70-76.
166. Penfield PL, Killingsworth MS, Sarks SH. Senile macular degeneration: the involvement of immunocomponent cells. *Graefes Arch Clin Exp Ophthalmol* 1987;223:69-76.
167. Loeffler KU, Lee R. Basal linear deposit in the human macula. *Graefes Arch Clin Exp Ophthalmol* 1986;224:493-501.
168. Sunderkotter C, Steinbrink K, Goebeler M, et al. Macrophages and angiogenesis. *J Leuk Biol* 1994;55:410-422.
169. Polverini PJ, Cotran PS, Gimbrone MA Jr, et al. Activated macrophages induce vascular proliferation. *Nature* 1977;269:804-806.
170. Anin R, Puklin JE, Frank RN. Growth factor localization in choroidal neovascular membranes of age-related macular degeneration. *Invest Ophthalmol Vis Sci* 1994;35:3178-3188.
171. Lopez PF, Sippy BD, Lambert HM, et al. Transdifferentiated retinal pigment epithelial cells are immunoreactive for vascular endothelial growth factor in surgically excised age-related macular degeneration neovascular membranes. *Invest Ophthalmol Vis Sci* 1996;37:855-868.
172. Oh H, Takagi H, Takagi C, et al. The potential angiogenic role of macrophages in the formation of choroidal neovascular membranes. *Invest Ophthalmol Vis Sci* 1999;40:1891-1898.
173. Otani A, Takagi H, Oh H, et al. Expression of angiopoietins and Tie2 in human choroidal neovascular membranes. *Invest Ophthalmol Vis Sci* 1999;40:1912-1920.
174. Bian ZM, Elner SG, Streiter RM, et al. IL-4 potentiates IL-1 $\beta$  and TNF- $\alpha$  stimulated IL-8 and MCP-1 protein production in human retinal pigment epithelial cells. *Curr Eye Res* 1999;18:349-357.

## Human Retinal Pigment Epithelial Lysis of Extracellular Matrix

175. Elner VM, Streiter RM, Elner SG, et al. Neutrophil chemotactic factor (IL-8) gene expression by cytokine-treated retinal pigment epithelial cells. *Am J Pathol* 1990;136:745-750.
176. Pepper MS, Montesano R, Mandriota SJ, et al. Angiogenesis: a paradigm for extracellular proteolysis during cell migration and morphogenesis. *Enzyme Prot* 1996;49:138-162.
177. Davis GE, Pintar Allen KA, Salazar R, et al. Matrix metalloproteinase-1 and -9 activation by plasmin regulates a novel endothelial cell-mediated mechanism of collagen gel contraction and capillary tube regression in three-dimensional collagen matrices. *J Cell Sci* 2001;114:917-930.
178. DeNichilo MO, Burns GF. Granulocyte-macrophage and macrophage colony-stimulating factors differentially regulate alpha v integrin expression on cultured human macrophages. *PNAS* 1993;90:2517-2521.
179. Brooks PC, Stromblad S, Sanders LC, et al. Localization of matrix metalloproteinase MMP-2 to the surface of invasive cells by interaction with integrin alpha v beta 3. *Cell* 1996;85:683-685.
180. Gailit J, Welch MP, Clark RA. TGF-beta a stimulates expression of keratinocyte integrins during re-epithelialization of cutaneous wounds. *J Invest Dermatol* 1994;103:221-227.
181. Brown SL, Lundgren CH, Nordt T, et al. Stimulation of migration of human aortic smooth muscle cells by vitronectin: implications for atherosclerosis. *Cardiovasc Res* 28:1815-1820.
182. Marshall JF, Nesbitt SA, Helfrich MH, et al. Integrin expression in human melanoma cell lines: heterogeneity of vitronectin receptor composition and function. *Int J Cancer* 1991;49:9224-9231.
183. Khatib AM, Nip J, Fallavollita L, et al. Regulation of urokinase plasminogen activator/plasmin-mediated invasion of melanoma cells by the integrin vitronectin receptor. *Int J Cancer* 2001;91:300-308.
184. Kanse SM, Kost C, Wilhelm OG, et al. The urokinase receptor is a major vitronectin-binding protein on endothelial cells. *Exp Cell Res* 1996;224:344-353.
185. Montgomery AM, Reisfeld RA, Cheresch DA. Integrin alpha v beta 3 rescues melanoma cells from apoptosis in three-dimensional dermal collagen. *Proc Natl Acad Sci USA* 1994;91:8856-8860.
186. Seftor RE, Seftor EA, Gehlsen KR, et al. Role of the alpha v beta 3 integrin in human melanoma cell invasion. *Proc Natl Acad Sci USA* 1992;89:1557-1561.
187. Stahl A, Mueller BM. Melanoma cell migration on vitronectin: regulation by components of the plasminogen activation system. *Int J Cancer* 1997;71:116-122.
188. Wei Y, Waltz DA, Rao N, et al. Identification of the urokinase receptor as an adhesion receptor for vitronectin. *J Biol Chem* 1994;269:32380-32388.
189. Montgomery AMP, De Clerck YA., Langley KE, et al. Melanoma-mediated dissolution of extracellular matrix: contribution of urokinase-dependent and metalloproteinase-dependent proteolytic pathway. *Cancer Res* 1993;53:693-700.
190. Monsky WL, Lin CY, Aoyama A, et al. A potential marker protease of invasiveness, seprase, is localized on invadopodia of human malignant melanoma cells. *Cancer Res* 1994;54:5702-5710.
191. McCawley L J, Matrisian LM. Matrix metalloproteinases: multifunctional contributors to tumor progression. *Mol Med Today* 2000;4:149-156.
192. Curran S, Murray GI. Matrix metalloproteinases in tumor invasion and metastasis. *J Pathol* 1999;189:300-308.
193. Ellerbrock SM, Stack MS. Membrane associated matrix metalloproteinases in metastasis. *Bioessays* 1999;21:940-949.
194. Murphy G, Gavrilovic J. Proteolysis and cell migration: creating a path? *Curr Opin Cell Biol* 1999;11:614-621.
195. Dano K, Romer J, Nielsen BS, et al. Cancer invasion and tissue remodeling: cooperation of protease systems and cell types. *APMIS* 1999;107:120-127.
196. Reich R, Thompson EW, Iwamoto Y, et al. Effects of inhibitors of plasminogen activator, serine proteinases, and collagenases IV on the invasion of basement membranes by metastatic cells. *Cancer Res* 1988;48:3307-3312.
197. Hart IR, Fidler IJ. An in vitro quantitative assay for tumor cell invasion. *Cancer Res* 1978;38:3218-3224.
198. Poste G, Doll J, Hart IR, et al. In vitro selection of murine B 16 melanoma variants with enhanced tissue-invasive properties. *Cancer Res* 1980;40:1636-1644.
199. Towle MJ, Lee A, Maduakor EC, et al. Inhibition by 4-substituted benzo [b] thiophene-2-carboxamides: an important new class of selective synthetic urokinase inhibitor. *Cancer Res* 1993;53:2553-2559.
200. Sitrin RG, Todd RF III, Albrecht E, et al. The urokinase receptor (CD87) facilitates CD11b/CD18-mediated adhesion of human monocytes. *J Clin Invest* 1996;97:1942-1951.
201. Gytoko M, Todd III R, Wilkinson C, et al. The urokinase receptor is required for monocyte chemotaxis in vitro. *J Clin Invest* 1994;93:1380-1387.
202. Koshelnick Y, Ehart M, Stockinger H, et al. Mechanisms of signaling through urokinase receptor and the cellular response. *Thromb Haemostasis* 1999;82:305-311.
203. Sitrin R, Pan P, Harper H, et al. Urokinase receptor (CD87) aggregation triggers phosphoinositide hydrolysis and intracellular calcium mobilization in mononuclear phagocytes. *J Immunol* 1999;163:6193-6200.
204. Blasi F. Urokinase and urokinase receptor: a paracrine/autocrine system for regulating cell migration and invasiveness. *Bioessays* 1993;5:105-111.



# RETINAL PIGMENT EPITHELIAL ACID LIPASE ACTIVITY AND LIPOPROTEIN RECEPTORS: EFFECTS OF DIETARY OMEGA-3 FATTY ACIDS

---

BY Victor M. Elnor, MD, PhD

## ABSTRACT

**Purpose:** To show that fish oil–derived omega-3 polyunsaturated fatty acids, delivered to the retinal pigment epithelium (RPE) by circulating low-density lipoproteins (LDL), enhance already considerable RPE lysosomal acid lipase activity, providing for more efficient hydrolysis of intralysosomal RPE lipids, an effect that may help prevent development of age-related macular degeneration (ARMD).

**Methods:** Colorimetric biochemical and histochemical techniques were used to demonstrate RPE acid lipase in situ, in vitro, and after challenge with phagocytic stimuli. Receptor-mediated RPE uptake of fluorescently labeled native, acetoacetylated, and oxidized LDL was studied in vitro and in vivo. LDL effects on RPE lysosomal enzymes were assessed. Lysosomal enzyme activity was compared in RPE cells from monkeys fed diets rich in fish oil to those from control animals and in cultured RPE cells exposed to sera from these monkeys.

**Results:** RPE acid lipase activity was substantial and comparable to that of mononuclear phagocytes. Acid lipase activity increased significantly following phagocytic challenge with photoreceptor outer segment (POS) membranes. Receptor-mediated RPE uptake of labeled lipoproteins was determined in vitro. Distinctive uptake of labeled lipoproteins occurred in RPE cells and mononuclear phagocytes in vivo. Native LDL enhanced RPE lysosomal enzyme activity. RPE lysosomal enzymes increased significantly in RPE cells from monkeys fed fish oil–rich diets and in cultured RPE cells exposed to their sera.

**Conclusions:** RPE cells contain substantial acid lipase for efficient metabolism of lipids imbibed by POS phagocytosis and LDL uptake. Diets rich in fish oil–derived omega-3 fatty acids, by enhancing acid lipase, may reduce RPE lipofuscin accumulation, RPE oxidative damage, and the development of ARMD.

*Trans Am Ophthalmol Soc* 2002;100:301-338

## INTRODUCTION

---

The risk for development of age-related macular degeneration (ARMD) may be reduced by dietary fish oil that is rich in omega-3 polyunsaturated fatty acids.<sup>1-3</sup> This clinical observation leads to the following hypothesis: Dietary omega-3 polyunsaturated fatty acids, delivered to the retinal pigment epithelium (RPE) by circulating low-density lipoproteins (LDL), favorably enhance already considerable RPE lysosomal lipolytic activity in vivo. This mechanism would assist in the efficient degradation of intralysosomal lipid-rich material that otherwise might accumulate in RPE cells and contribute to the indigestible lipid-protein complexes of lipofuscin, which have been implicated in the development of ARMD.

To test this hypothesis, a series of studies was con-

ducted to do the following: (1) apply a simple, chromogenic biochemical assay and a novel histochemical technique for the measurement and detection of RPE lysosomal acid lipase; (2) show that purified RPE acid lipase is responsible for triglyceride and cholesteryl esterase activity and may esterify cholesterol to fatty acids, depending on substrate kinetics; (3) demonstrate that RPE acid lipase activity is comparable to the high levels known to exist in mononuclear phagocytes; (4) show that RPE acid lipase activity is enhanced by incorporation of photoreceptor outer segment (POS) membranes or LDL; (5) demonstrate avid RPE native and modified LDL uptake in vitro and in vivo; (6) show that dietary fish oil enhances RPE lysosomal acid lipase and cholesteryl esterase activities, thereby improving RPE lysosomal efficiency in live monkeys; and (7) demonstrate that the serum from fish oil–fed monkeys enhances these RPE lipolytic activities in vivo.

In so doing, this study presents a new method to study RPE lysosomal lipid metabolism, shows that the RPE monolayer incorporates circulating lipoproteins in

From the Department of Ophthalmology, University of Michigan, Ann Arbor. This work was supported in part by grants EY-09441 and EY-007003 from the National Institutes of Health and a Lew Wasserman Award from Research to Prevent Blindness, Inc.

vivo, and demonstrates that diets may be favorably altered to deliver beneficial lipids via LDL to the RPE in vivo. Caveats for dietary fish oil augmentation are likely to include the need for antioxidant supplements, avoidance of smoking and, possibly, protection from excess blue and UV light to avoid in vivo oxidation of LDL protein and lipid that may, in turn, damage RPE cells and promote RPE aging and the development of ARMD.

## BACKGROUND

The RPE consists of a monolayer of cells that is interposed between the fenestrated vasculature of the choriocapillaris and the photoreceptor cells of the neurosensory retina.<sup>4</sup> In this strategic location, the cells of this pigmented monolayer envelop the light-sensitive tips of the photoreceptor cells with their apical processes and lie on Bruch's membrane, which consists of the basement membranes of the RPE and choriocapillaris together with intervening collagen and elastic layers.<sup>4,6</sup> The continuous RPE monolayer forms the outer blood-retina barrier by virtue of the tight junctions joining adjacent RPE cells.<sup>7-10</sup> The RPE is thereby an intermediary between the systemic circulation and the avascular outer one third of the neurosensory retina, which relies on various RPE functions for its survival and homeostasis.<sup>11</sup>

Among the essential physiologic functions of the RPE are the selective diffusion and transport of ions, metabolites, and serum components to the outer retina<sup>12-17</sup>; transport, storage, and processing of vitamin A and its derivatives<sup>18-27</sup>; the absorption of scattered light by RPE melanin granules<sup>6,28,29</sup>; and the synthesis of basement membrane components, including fibronectin, laminin, collagen, and glycosaminoglycans, all of which are important to RPE adhesion to and maintenance of Bruch's membrane.<sup>30,31</sup>

A prominent and cardinal RPE function, first described by Young and Bok,<sup>32</sup> is the phagocytosis and intracellular lysosomal degradation of aged, light-sensitive membranes which are shed from the apices of the POS in a diurnal cycle.<sup>29,33-37</sup> The RPE must phagocytize approximately 10% of the POS material daily insofar as each photoreceptor renews its outer segment every 10 days.<sup>38</sup> Each RPE cell may underlie as many as 200 photoreceptors and may, therefore, ingest an equivalent of 20 entire outer segments per day.<sup>38</sup> The steps in POS phagocytosis and degradation<sup>35,36,38,39</sup> include the recognition, binding, and internalization of the shed membrane material by apical RPE processes leading to fusion of the material with lysosomes. This process is highly dependent on aerobic metabolism<sup>40</sup> and involves microtubules,<sup>41,42</sup> intermediate filaments, and actin.<sup>39,43-46</sup> The daily phagocytosis of the shed, lipid-rich POS membranes, therefore, imposes an enormous metabolic burden on the RPE. After fusion of

phagocytic debris with lysosomes, homeostasis requires efficient lysosomal enzymatic degradation of engulfed POS material as well as lysosomal elimination of autophagocytic debris derived from damaged RPE organelles.<sup>47</sup> Fusion of the phagocytic POS debris or autophagocytic and RPE-derived debris with lysosomes forms secondary lysosomes called phagosomes, in which enzymatic degradation of lipids and proteins leads to the recycling of their basic components for RPE and photoreceptor metabolism.<sup>48</sup>

RPE lysosomes contain an impressive array of nearly 40 hydrolytic enzymes that have been identified by a variety of biochemical and histochemical techniques.<sup>6,49,50</sup> In fact, RPE lysosomal fractions are sevenfold more potent than liver lysosomes in degrading POS.<sup>51</sup> Cathepsin D is the major RPE lysosomal protease and, together with cathepsin S, appears to be most important in the degradation of POS protein.<sup>52-54</sup> Opsin, a glycoprotein composing about 75% of POS mass, is completely degraded by cathepsin D and other RPE acid hydrolases.<sup>55-57</sup> To date, studies of key RPE acid hydrolases as a function of aging and in ARMD have yielded mixed results.<sup>50,58</sup> Cathepsin D,  $\beta$ -glucuronidase, and  $\beta$ -galactosidase appear to actually increase with age,<sup>59-61</sup> while acid phosphatase activity is unaffected<sup>62</sup> and glycosidases show reduced activities.<sup>63,64</sup>

The remaining 25% of POS mass consists chiefly of polyunsaturated lipids that are degraded by RPE phospholipases<sup>65,66</sup> and acid lipases,<sup>55,67-69</sup> releasing fatty acids that are recycled to photoreceptors for use in POS renewal.<sup>70,71</sup> Studies of RPE acid lipase have employed acid lipase enzyme substrates, which are notoriously insoluble,<sup>67</sup> or have used neutral triglycerides, whose hydrolyzed fatty acids require organic extraction and fractionation for their detection.<sup>68,69</sup> In a lone cytochemical study of acid lipase in humans, Feeney<sup>72</sup> showed no age-dependent reduction in detectable enzyme activity.<sup>73</sup> Other studies have examined acid lipase in the interphotoreceptor matrix<sup>74</sup> or in canine lipofuscinosis.<sup>75</sup> However, a simple, reproducible chromogenic biochemical assay and histochemical technique for acid lipase, though available,<sup>76-78</sup> has not been applied to the study of RPE lysosomal lipid metabolism and its modulation by phagocytosis or exposure to other variables.

The importance of RPE lysosomal lipid metabolism is emphasized by the fact that despite robust RPE lysosomal hydrolytic activity, particularly of the cathepsins, nondigestible material accumulates progressively in tertiary lysosomes called residual bodies.<sup>72</sup> The nondigestible material forms yellow, autofluorescent lipid-protein aggregates known as lipofuscin, which may fill up to one fifth of the RPE cytoplasm by age 80.<sup>79,80</sup> One of the putative factors leading to lipofuscin accumulation in this non-renewable, pigmented cell monolayer is the highly oxida-

tive retinal environment, which may oxidize proteins and polyunsaturated fatty acids that are abundant in POS and autophagocytic debris, rendering them refractory to lysosomal action.<sup>81-84</sup> In this scenario, the cross-linked, nondigestible residues accumulate in the RPE, which may then discharge lipid-protein complexes, as well as secondary lysosomes,<sup>85</sup> into Bruch's membrane.<sup>86,87</sup> This results in progressive lipid accumulation seen with aging<sup>88,91</sup> and the formation of basal laminar and basal linear deposits and drusen that are present in lesions of ARMD and frequently predate them.<sup>86,92-98</sup>

Another factor that may lead to the accumulation of lipofuscin may be directly related to enzymatic actions within RPE lysosomes. Acid-catalyzed, irreversible crosslinking of two retinaldehyde molecules (A2), derived slowly and incrementally from vitamin A metabolism, and an ethanolamine molecule (E), derived from POS degradation, produces the dominant fluorophore of lipofuscin granules: A2-E.<sup>99</sup> This amphiphilic, quaternary nitrogen compound concentrated in RPE tertiary lysosomes inhibits lysosomal enzyme activity, particularly if photoactivated to produce free radicals.<sup>82,83,100</sup> A2-E may also leak from lysosomes on account of its detergentlike structure or upon photoactivation, leading to RPE plasma membrane dysfunction, the formation of RPE basal deposits, and RPE detachment and apoptosis.<sup>101-103</sup> Whatever its source, lipofuscin is a photoinducible generator of reactive oxygen metabolites that cause lipid peroxidation, impairment of lysosomal enzyme activity, loss of lysosomal integrity, and eventually RPE cell death.<sup>81,104,105</sup>

In addition to the major roles of degrading engulfed, aged POS and autophagocytic debris, the RPE may incorporate other material requiring lysosomal action. Extensive studies of RPE phagocytosis have been performed in vivo and in vitro, the latter utilizing both retinal-choroidal organ cultures and cultured RPE cells. RPE phagocytosis of particulate matter, including isolated POS,<sup>45,106-111</sup> latex spheres,<sup>39,112-115</sup> liposomes,<sup>116</sup> bacteria,<sup>112,115</sup> and lectin- and sugar-coated beads,<sup>117,118</sup> have been examined. In these studies, RPE cell phagocytosis varied with the type of phagocytic stimulus, presumably on account of variable cell surface-particle binding, but receptors mediating their uptake remained unknown.

Subsequently, RPE cell surface receptors mediating the recognition and binding of specific ligands and leading to selective, rapid, and efficient incorporation of particulates into the RPE were identified. These include CD16 for immunoglobulin,<sup>119,120</sup> CD11b/CD18 and CD35 for complement,<sup>119</sup> mannose-6-phosphate receptors,<sup>121-125</sup> and CD14 for endotoxins.<sup>120,126,127</sup> Specific, high-affinity RPE uptake of lipid-laden particulates may be mediated by receptors for native (N-) LDLs and scavenger type I/II receptors for acetylated/acetoacetylated (A-) LDL, for

which RPE cells bear specific receptors.<sup>128-130</sup> Like A-LDL, oxidized (O-) LDL may be bound and internalized into lysosomes by scavenger type I/II receptors<sup>131-134</sup> and other scavenger receptors, including CD68 and CD36<sup>85,135-139</sup> that have also been identified on RPE cells.<sup>140-142</sup> CD36 is also a receptor for thrombospondin, which appears to act together with the vitronectin receptor, avb3 integrin, on macrophages to clear senescent erythrocytes and neutrophils<sup>143-146</sup> and on RPE to recognize and internalize aged POS membranes.<sup>105,147</sup> O-LDL internalized by scavenger receptors, including CD36, inhibits RPE POS membrane degradation by interfering with secondary lysosomal function.<sup>148</sup> Nevertheless, receptor-mediated uptake of native or modified LDL has not been shown on primate cells in vitro, and the RPE incorporation of these lipoproteins, which must cross Bruch's membrane, has not been demonstrated in vivo. Furthermore, the effects of these lipoproteins, whose abundance and composition may be altered by diet and other exogenous factors, on RPE lysosomal lipid hydrolytic activity has not been investigated.

The unique relationship between the photoreceptors and the RPE extends to the peculiar composition of the POS membranes and the RPE role in preserving it. The principal polyunsaturated fatty acid of POS membranes is the omega-3 fatty acid, docosahexaenoic acid (DHA), and arachidonic acid (AA).<sup>148-150</sup> Of all mammalian cells, DHA is the most abundant in POS, and dietary intake of DHA, related omega-3 fatty acids, or its precursor fatty acids, principally linoleic acid, is required for normal brain and retinal development.<sup>151</sup> Infant monkeys<sup>152,153</sup> and humans<sup>154-156</sup> deficient in dietary DHA have reduced visual acuity function. The main dietary sources of DHA and related fatty acids are fish oils, nuts, and other seeds. When ingested, hepatic processing places these fatty acids in LDLs that are delivered via the serum to tissues where receptor-mediated LDL uptake delivers the lipids containing omega-3 fatty acids to cells.<sup>157,158</sup> The RPE metabolizes the delivered lipid and transports DHA to the photoreceptors, which incorporate these fatty acids into POS. Inasmuch as the photoreceptors have an absolute requirement for DHA in substantial quantity on a daily basis to renew POS membranes, the RPE has sophisticated pathways to synthesize and conserve DHA cleaved from phagocytized POS membranes and recycle it back to the photoreceptors.<sup>159-162</sup> These pathways include transient RPE storage of cleaved DHA in triglycerides followed by efficient hydrolysis and transport of free DHA via fatty acid binding proteins.<sup>163-166</sup> Thus, the photoreceptors and the RPE have a high stake in the efficient DHA metabolism within POS-laden secondary lysosomes that is necessary for physiologic functioning and homeostasis. Alterations of this process may lead to accumulation of abnormal DHA-containing lipids driving aging and ARMD.<sup>163</sup>

Accordingly, experimental models have shown that oxidized DHA moieties including DHA hydroperoxide<sup>167</sup> and linoleic hydroperoxide are involved in oxidative-mediated retinal and RPE cell injury.<sup>168</sup> Deprivation of linoleic acid, the dietary precursor of omega-3 fatty acids in rats, reduced RPE lysosomal enzyme activity and altered the size and distribution of POS phagosomes in RPE cells and was associated with reduced electroretinographic amplitudes.<sup>169</sup> These studies imply that omega-3 fatty acids or their precursors may modulate RPE lysosomal function, DHA metabolism, and RPE cell integrity. To date, however, no investigations regarding lysosomal lipid metabolism in response to omega-3 fatty acids have been performed, perhaps in part because of difficulty in biochemically assaying lysosomal acid lipase and unavailability of a reliable histochemical stain to assess its activity in situ.

Reported epidemiologic risk factors for ARMD include cigarette smoking, atherosclerosis, high levels of serum cholesterol, low levels of serum antioxidants, and exposure to blue and UV light,<sup>130,170-177</sup> while consumption of dietary fish oils appears to have protective effects.<sup>1-3</sup> All of these factors may potentially modulate RPE lipid metabolism by altering the quantity and character of circulating lipoproteins that are delivered from the blood to the RPE monolayer and by locally oxidizing cellular and extracellular lipids and proteins, including lipoproteins that have emerged from the choriocapillaris to reach the RPE monolayer.

Cigarette smoking is the most unequivocal risk factor increasing risk for ARMD.<sup>175-177</sup> Among its protean effects, smoking causes peroxidation of circulating LDL,<sup>178,179</sup> producing elevated plasma levels of thiobarbituric acid-reactive substances (TBARS),<sup>180</sup> isoprostanes,<sup>181</sup> and other measures of lipid peroxidation.<sup>182-183</sup> Increased levels of circulating O-LDL, a known risk factor for atherosclerosis,<sup>170, 179-182</sup> have been implicated as a possible risk factor for ARMD.<sup>183</sup> Depletion of antioxidant vitamins and antioxidant enzymes<sup>172,173,184,185</sup> and increased exposure to blue or UV light<sup>174</sup> are other factors that have been purported to lead to increased oxidative stress. Oxidized LDL and other locally oxidized lipids, proteins, and extracellular matrix components are thereby altered to forms that may be recognized and engulfed by specific RPE scavenger receptors.<sup>128,129,140-142</sup> Once internalized, O-LDL has been shown to interfere with RPE POS membrane degradation, leading to oxidation of additional lipid and protein in RPE cells.<sup>148</sup>

Dietary fish oil is a newly recognized factor that may reduce the risk of developing ARMD.<sup>1-3</sup> Its main constituent, DHA, also demonstrates a trend for reduced risk.<sup>2</sup> This contrasts with high consumption of vegetable fats containing polyunsaturated fatty acids, most notably linolenic acid, which is positively associated with the

development of atherosclerosis and ARMD and mitigates the positive effects of high fish oil intake.<sup>1,186,187</sup> The mechanisms underlying this disparity are complex and involve the types of lipoprotein elaborated by the liver and their promotion of intracellular cholesterol esterification when they are incorporated into target cells.<sup>188-193</sup> These differences underlie the proatherogenic nature of linolenic acid and the antiatherogenic qualities of fish oil.<sup>186,187,194-197</sup> However, both types of unsaturated fatty acid may be readily oxidized when circulating or within tissues, resulting in oxidized forms that may be injurious to tissue, especially those containing cells expressing specific receptors for oxidized or otherwise damaged lipoproteins.<sup>182,188</sup> Therefore, better understanding of the effects of fish oil-rich diets and serum on RPE lysosomal lipid metabolism may assist in illuminating how diet and environmental oxidative factors, such as smoking and light exposure, alter the progression of RPE aging and the development of ARMD.

## MATERIALS AND METHODS

### ANIMALS, TISSUES, AND CELLS

Normal New Zealand White rabbits and monkeys (*Macaca mulatta*) were fed standard chow diets or diets supplemented with cholesterol, coconut oil, and Menhaden fish oil until sacrifice. All animals were treated and cared for according to National Institutes of Health guidelines for the humane treatment of laboratory animals. All experimental protocols were approved by committees on animal use and care in research at the University of Chicago and the University of Michigan.

### *Tissues and Cells for Comparative Acid Lipase Studies in New Zealand White Rabbits*

For histochemical studies, the albino rabbits were exsanguinated under sodium pentobarbital anesthesia. Whole eyes and tissue blocks of lung, liver, and spleen not exceeding 5 mm thick were fixed at 4°C for 24 hours in formal sucrose and rinsed in gum sucrose for 24 hours.<sup>77</sup> The fixative consisted of 4% formaldehyde prepared from paraformaldehyde by depolymerization, after which the osmolality of the fixative, buffered to pH 5.8 with 0.067 M sodium phosphate buffer, was raised by adding 7.5% wt/vol sucrose. Formal sucrose consisted of a solution of 1% (wt/vol) gum acacia and 30% (wt/vol) sucrose.<sup>198</sup>

For comparative biochemical studies in the rabbits, immediately upon death, the lungs and peritoneal cavity were lavaged with lactated Ringer's solution and cell suspensions were obtained by centrifugation for 15 minutes at 110g followed by resuspension of the cells into Eagle's minimum essential medium (MEM) supplemented with 15% fetal calf serum (FCS). Pieces of spleen were finely

minced into MEM with 15% FCS. Blood obtained at sacrifice was collected in glass tubes containing sufficient ethylenediaminetetraacetic acid (EDTA) to obtain a final concentration of 2.0 mM. White blood cells were then obtained following centrifugation and resuspension in MEM with 15% FCS. Aortic tissue samples (0.5 cm<sup>2</sup>) were excised, gently minced, and plated to establish smooth-muscle cell cultures that were maintained in MEM supplemented with 15% FCS. Rabbit eyes were removed and placed on ice and kept in darkness. Within 2 hours of death, the anterior ocular segment and vitreous were carefully removed under dim, red light. The posterior segment was immersed in Ca<sup>++</sup>- and Mg<sup>++</sup>-free Hanks' balanced salt solution (HBSS) containing 2.0 mM EDTA for 30 to 60 minutes at 4°C in darkness. The neurosensory retina was then carefully peeled from the RPE monolayer, which was subsequently collected by the method of Heller and Jones.<sup>199</sup> RPE cells were harvested by gentle brushing into phosphate-buffered saline (PBS), pelleted at 1,000g for 10 minutes, and resuspended in MEM with 15% FCS. RPE, alveolar, peritoneal, splenic, and white blood cell suspensions were overlaid onto glass beads (Microbeads class IV-C, Cataphote Corp, Toledo, Ohio) in plastic culture dishes. After 3 hours, the glass beads were rinsed thoroughly with three changes of MEM containing 15% FCS and once in PBS to remove nonadherent cells.

#### *Bovine RPE Cells for Acid Lipase Purification Studies*

Cow eyes were obtained within 1 hour of slaughter from a local abattoir and maintained on ice and in dim light. Within 2 hours, RPE cells were harvested as described for the rabbit eyes and kept on ice in MEM with 15% FCS until acid lipase extractions were performed.

#### *Monkey RPE Cells, Fibroblasts, Smooth-Muscle Cells, Alveolar Macrophages, and POS for In Vitro Studies*

At autopsy, monkey RPE cells were obtained immediately after death by exsanguination under thiamylal sodium anesthesia as described for rabbit and bovine eyes. The monkey RPE cells were established and characterized in culture as previously described. POS of monkeys was prepared by a modification of the method of Plantner and Kean.<sup>200,201</sup> Briefly, carefully peeled, fresh neurosensory retinas were gently homogenized in 5mM Tris-acetate buffer, pH 7.4, containing 0.2 mM MgCl<sub>2</sub>, 65 mM NaCl, and 36.5% sucrose (wt/wt) using a Teflon pestle and then centrifuged at 1,000g for 5 minutes. After repeating this procedure, the supernatant containing POS was centrifuged in the Tris-acetate buffer at 12,000g for 15 minutes, resuspended, and centrifuged again to obtain POS for RPE in vitro studies. POS were then resuspended in MEM, counted in a hemocytometer, and adjusted to a final concentration of 2×10<sup>6</sup>/mL for use in experimental

incubations. Alveolar macrophages were obtained by lavage with lactated Ringer's solution, and aortic smooth-muscle cells were harvested, seeded, and established as described for the rabbits. Orbital fibroblasts were obtained by mincing orbital fat into culture dishes. Fibroblasts grew from the tissue pieces and were established as cultures in MEM with 15% FCS.

#### *Tissues and Cells from Monkeys On Fish Oil or Coconut Oil Diets*

Twenty-four adult (2½- to 3-year-old) rhesus monkeys were purchased from the National Institutes of Health (Alice, Texas). The monkeys were divided into three groups of eight each and fed the diets as previously described. In brief, low-fat Purina monkey chow was used as the basic ration, to which was added 25% fat and 2% cholesterol. The 25% fat consisted of coconut oil alone, Menhaden fish oil and coconut oil (1:1), or Menhaden fish oil and coconut oil (3:1). The fish oil contained cholesterol (432 mg/dL); therefore, monkeys consumed slightly more cholesterol on the fish oil diets. Fasting serum lipid values were determined at the onset and at monthly intervals throughout the 12-month experimental period.<sup>190,192</sup> Each chow-based diet supplied sufficient essential fatty acids and other nutrients. The animals were autopsied after 12 months by exsanguination under thiamylal sodium anesthesia. For biochemical enzyme assays, the eyes from each monkey were opened in the coronal plane anterior to the equator, and the RPE cells were harvested as described for rabbit and bovine eyes. The RPE cells were harvested by gentle brushing into PBS, pelleted at 1,000g for 10 minutes, and homogenized in distilled, deionized water at 0°C in the desired volume. Portions of one of the posterior ocular segments from each monkey were fixed at 4°C for 24 hours in 4% paraformaldehyde (wt/vol) containing 7.5% sucrose (wt/vol), followed by a 24-hour wash at 4°C in 1% gum acacia (wt/vol) containing 30% sucrose (wt/vol). Frozen sections (6 µm) were cut and stained by histochemical localization of nonspecific acid esterase and acid lipase lysosomal enzyme activity.<sup>77</sup> Samples of liver, spleen, and lung were also placed in water (1/10, wt/vol) and homogenized. The homogenates of these organs were then centrifuged at 5,000g for 10 minutes, and the supernatant was collected for enzyme activity studies. Tissues for biochemical assays were used immediately or frozen at -20°C for up to 1 month until assayed.

#### **ADAPTATION OF A NOVEL CHROMOGENIC TECHNIQUE FOR ACID LIPASE ACTIVITY**

A histochemical and biochemical technique to detect and measure acid lipase activity utilizing detergent micelles containing α-naphthyl palmitate was previous reported.

This technique is adapted for use in analyzing RPE lysosomal acid lipase and nonspecific lysosomal acid esterase activity.

#### *Histochemical Assays for Acid Lipase and Acid Esterase Activity*

Histochemical staining for acid lipase activity was performed on fixed, frozen tissue sections 4 to 10  $\mu\text{m}$  thick or cultures fixed for 30 minutes in formal sucrose and rinsed for 15 minutes in gum sucrose prior to histochemical staining. Fixed sections or cultured cells rinsed in chilled 0.1 M sodium acetate buffer, pH 5.2, were transferred within 30 minutes to 40 mL of incubation medium that contained substrate micelles consisting of 1.0 mM  $\alpha$ -naphthyl palmitate (15.4 mg; Sigma Chemical Co, St Louis, Missouri), 10 mM Triton X100 (0.65% wt/vol) and 1.0 mL hexazotized pararosaniline (HPR) prepared immediately before use. HPR was obtained by vigorously mixing equal volumes of 4% sodium nitrite and 4% pararosaniline HCl (Sigma) dissolved in 2.5 N HCl for 60 seconds. After addition of the HPR solution to the buffer-containing substrate micelles, the pH was readjusted to 5.2 with 5.0 N NaOH. For acid esterase activity, the incubation medium was prepared by injecting and swirling 10 mg of  $\alpha$ -naphthyl acetate, previously dissolved in 1.0 mL acetone, into 40 mL of 0.1 M sodium acetate buffer containing 1.0 mL of freshly hexazotized pararosaniline. Incubation times, at 25°C, ranged from 15 minutes to 24 hours, depending on enzyme activity present in the tissues or cells and the purpose of the experiment. Incubations were terminated by thorough rinsing in distilled water. All sections and tissue cultures were counterstained with 1% purified methyl green in 1.0 M sodium acetate buffer, pH 4.0, and subsequently cleared with graded alcohols and xylenes prior to mounting in synthetic resin.

To inhibit acid lipase activity, fixed sections or cultures were preincubated in diethylparanitrophenylphosphate (DEPP, E600, Mintacol; Bayer Ag, Leverkusen, Germany) or parahydroxymercuribenzoate (PHMB; Sigma) in 0.1 M sodium phosphate buffer, pH 6.5, for 30 minutes at 25°C. The inhibitors were also included in the incubation media. Control sections were heat-inactivated by incubating unmounted sections in a moist chamber at 56°C for 30 minutes.

#### *Biochemical Assays for Acid Lipase and Acid Esterase Activity*

Acid lipase activity was determined with substrate micelles which were prepared using 1.0 mM  $\alpha$ -naphthyl palmitate and 10 mM Triton X100 in 0.1 M sodium acetate buffer, pH 4.2, containing 0.1% fatty acid-poor bovine serum albumin. Acid esterase activity was determined using the same buffer containing 1.0 mM  $\alpha$ -naph-

thyl acetate which was first dissolved in 0.5 to 1.5 mL of acetone and then rapidly and forcefully injected into the buffer. Aliquots (50 to 100  $\mu\text{L}$ ) of enzyme fractions, tissue homogenates, cell homogenates, or conditioned culture media or aliquots of glass beads with adherent rabbit cells were assayed in 1.0 mL of substrate at 25°C with continuous agitation for 1 to 6 hours. The reactions were stopped by placing the samples in boiling water for 2 minutes. One milliliter of 1.0 M sodium acetate buffer, pH 4.2, containing 10% Tween 20 (wt/vol) and 0.5 mg fast garnet GBC salt was added to each sample. Diazocoupling of liberated  $\alpha$ -naphthol was performed at 25°C for 16 hours. Absorbance of samples, heat-inactivated blanks, and  $\alpha$ -naphthol standards were then measured at 535 nm.

#### **QUANTITATION OF CELLS AND DNA**

For comparative acid lipase rabbit studies, cells were enumerated to normalize assayed enzyme activity. For all other studies, cell and tissue enzyme activity was normalized to DNA. DNA quantitation of cell cultures did not reveal any statistically significant differences after different cell culture treatments with phagocytic stimuli, LDL, or sera.

#### *Enumeration of Cells for Comparative Acid Lipase Studies in New Zealand White Rabbits*

Aliquots of glass beads were weighed and subsequently incubated to determine the number of glass-adherent cells per gram of glass beads to determine acid lipase activity present per cell number. Aliquots of third-passage rabbit aortic smooth-muscle cells rinsed and scraped into PBS from tissue culture flasks were also assayed for cell number to determine acid lipase activity per  $10^6$  cells/hour. Some aliquots of glass beads with adherent cells were agitated for 5 to 10 minutes in 2.0 mM EDTA according to the method of Siakotos and associates<sup>202</sup> to dislodge the glass-adherent cells, which were then smeared or dried onto glass slides. The cells in the slide preparations were either counted to assess the number of monocytes, macrophages, and RPE cells present in the various adherent cell populations or stained histochemically for up to 6 hours to determine the number of acid lipase-positive cells adherent to the glass beads. The numbers of glass-adherent monocytes, macrophages, and RPE cells per gram of glass beads were determined by enumerating cell nuclei using a modification of the method of Levine and associates.<sup>203</sup> Briefly, 0.50- to 1.0-g aliquots of glass beads with adherent cells were incubated at 37°C in 3.0-mL aliquots of 1.0 M citric acid containing 0.1% crystal violet. After 1 hour, the glass beads were agitated to dislodge cell remnants from the beads, and liberated cell nuclei were counted in a hemocytometer. For

smooth-muscle cell cultures, 100- $\mu$ L aliquots of smooth-muscle cells scraped into PBS were assayed in 1.0 mL of the citric acid–crystal violet solution.

#### *DNA Quantitation of RPE Cells and Tissue Homogenates*

The DNA contents of the cultured cell monolayers scraped from each tissue culture flask and of homogenates of freshly obtained RPE cells, liver, and spleen were determined according to the method of LaBarca and Paigen.<sup>204</sup> Briefly, the cells grown in tissue culture flasks were scraped into distilled water in the cold, briefly sonicated, and maintained on ice until DNA assays were performed. Then 25- to 100- $\mu$ L aliquots of the cell lysates, raised when necessary to a total of 100  $\mu$ L by adding distilled water, were added to 4.7 mL of a phosphate-saline buffer solution (0.05 M Na<sub>3</sub>PO<sub>4</sub>, 2.0 M NaCl), followed by addition of a 0.5- $\mu$ g Hoechst 33258, a fluorescent dye which quantitatively binds to double-stranded DNA, in 200  $\mu$ L of distilled water. The samples were then mixed vigorously and kept in the dark until fluorescence was measured using a Beckman Fluorocolorimeter with a 370-nm narrow-band interference filter for the excitation light and a Kodak 2A cutoff filter for light emission. Calf thymus DNA standards were used in each assay.

#### **ACID LIPASE PURIFICATION FROM FRESHLY ISOLATED BOVINE RPE CELLS**

To demonstrate the specificity of the chromogenic assay for acid lipase and to show that RPE acid lipase may actually esterify free fatty acids to cholesterol, acid lipase activity, corresponding to a single protein band, was purified from bovine RPE and shown to possess the ability to hydrolyze  $\alpha$ -naphthyl palmitate and esterify cholesterol to fatty acids hydrolyzed from triolein.

#### *Molecular Sieve Gel and Ion Exchange Chromatography*

Bovine RPE cell pellets were resuspended and sonicated in distilled water, 1:10 (wt/vol), and combined with 2.0 mL of 0.02 M Tris-HCl buffer, pH 7.4. The sample was then applied to and run at 4°C on a 90.0 x 2.0-cm Glenco Column of Sephadex G-150, equilibrated with degassed 0.02 M Tris-HCl buffer, pH 7.4. Column flow was 16 mL/hour and 4.0-mL fractions were collected and assayed for acid lipase activity and cholesteryl ester synthesis. Peak fractions were pooled and concentrated by ultrafiltration in 0.05 M sodium acetate buffer, pH 5.5, containing 0.025 M NaCl using an Amicon stirred cell with a UM 10 membrane (10,000 MW cutoff) under 70 psi of nitrogen. The pooled concentrate was applied to a 20.0 x 1.0-cm column of SP Sephadex C-50 equilibrated and eluted with degassed 0.05 M sodium acetate buffer, 0.025 M NaCl, pH 5.5. Two-milliliter fractions were collected and assayed for cholesteryl ester formation and for the hydroly-

ysis of  $\alpha$ -naphthyl palmitate, triglycerides, and cholesteryl esters.

#### *Polyacrylamide-SDS Gel Electrophoresis*

To test the purity of the isolated protein, electrophoresis in polyacrylamide-SDS slab gels was performed using 0.1% SDS in 0.05 M Tris-glycine buffer, pH 8.3, at an initial voltage of 200 V. The slab gels consisted of a 13% polyacrylamide running gel and a 6% stacking gel made in a 0.5 M Tris-HCl buffer at pH 8.8 and pH 6.8, respectively. Protein samples and molecular weight markers were prepared by heating a mixture containing equal volumes of 4% SDS, 20% glycerol, 10% mercaptoethanol, 0.002% bromophenol blue, and 0.05 M Tris-HCl buffer, pH 6.8, for 5 minutes at 90°C. The resulting gel profiles were stained with either Coomassie blue or silver nitrate, destained, dried, and photographed.<sup>205,206</sup>

#### *Isoelectric Focusing Zymography*

The isolated fractions were also examined by isoelectric focusing zymograms. The fractions were dialyzed against distilled water and added to a mixture of degassed 5% (wt/vol) acrylamide, 0.25% (wt/vol) bisacrylamide, 15% (wt/vol) glycerol, and either a broad-range (pH, 3.0-10.0) or narrow-range (pH, 4.0-6.5) ampholyte solution (Pharmacia, Uppsala, Sweden). Polymerization was induced by adding 50  $\mu$ L/mL of a freshly prepared 0.3% ammonium persulfate solution. Gels were poured into 10.0 x 0.5-cm glass tubes and allowed to solidify for 30 minutes. The gels were run in a Buchler disc electrophoresis cell containing 0.025 N NaOH in the cathode chamber, 0.025 N H<sub>2</sub>SO<sub>4</sub> in the anode chamber cooled to 5°C by a circulating cold water jacket. Initially, isoelectric focusing was performed at 50 V for 30 minutes, and subsequently the voltage was increased stepwise for 8 to 18 hours to a terminal voltage of 375 V and a current of 0.5 mA/gel. Some gels were stained for protein with Coomassie blue by the method of Vesterburg,<sup>206</sup> while other gels run under the same conditions were cut in 2-mm gel slices and assayed for enzyme activities.

#### **ASSAY FOR CHOLESTERYL ESTERASE AND TRIGLYCERIDE HYDROLYSIS**

Cholesteryl ester and triglyceride hydrolytic activity was determined using a radioactively labeled vesicle substrate system modified from the method of Brecher and associates.<sup>207</sup> Vesicles were prepared by drying 25 mg of egg yolk lecithin with either 2.0 mg cholesteryl oleate and 2.0  $\mu$ Ci cholesteryl-1-[<sup>14</sup>C]-oleate (66:1 phospholipid/substrate molar ratio) or 4.5 mg trioleate and 2.0  $\mu$ Ci glyceryl tri-1-[<sup>14</sup>C]-oleate. The mixtures were sonicated in 2.0 mL of glycerol, and the glycerol sonicate was added to 20 mL of 0.1 M sodium acetate buffer, pH 4.2, and resonicated.

Aliquots (200  $\mu\text{L}$ ) of media or distilled water containing sonicated cells were incubated for 4 hours in 1 mL of substrate. The reaction was terminated by adding 6.0 mL of benzene:chloroform:methanol (1.0:0.5:1.2). Free oleate was extracted by the method of Pittman and associates.<sup>208</sup> In brief, the mixture was made alkaline with 1.2 mL of 0.3 M NaOH. After phase separation, 0.5 mL of the upper phase was added to 10.0 mL of PCS scintillation cocktail (Amersham Inc, Arlington Heights, Illinois) and counted by liquid scintillation spectrometry. Counting efficiencies were determined from sample channel ratio values and quenching curves derived from quenching standards (Amersham). Appropriate blanks and controls were included in each assay.

#### ASSAY FOR ACID LIPASE CHOLESTEROL ESTERIFICATION WITH FATTY ACIDS HYDROLIZED FROM TRIOLEIN

Esterification of cholesterol to fatty acids liberated from hydrolyzed triglycerides was determined by incubating aliquots of enzyme isolates and homogenized tissue samples for 16 hours after 25°C in a substrate media containing 0.1 M sodium acetate buffer, pH 4.2, and lecithin- $^{14}\text{C}$ -cholesterol-triolein vesicles. The vesicles were prepared by drying under a nitrogen stream, 25 mg lecithin, 0.6 mg cholesterol, 9.0 mg triolein, and 2.0  $\mu\text{Ci}$  4- $^{14}\text{C}$  cholesterol (0.013 mg), sonicating the mixture in 4.0 mL of glycerol, adding 46 mL of buffer, and resonicating. The substrate vesicles were sized with a cross-linked Sephrose 6B column and were found to have an apparent  $M_r$  of  $2.5 \times 10^6$  with a calculated hydrodynamic radius of 100 angstroms, consistent with unilamellar vesicles. Incubations terminated by adding methanol and lipids were extracted by the method of Bligh and Dryer.<sup>209</sup> Extracted lipid was dried under nitrogen to a minimal volume and spotted on silica gel (IB2 Baker-Flex) thin-layer chromatography plates. The plates were developed in petroleum ether:ethyl ether:acetic acid (75:24:1). Lipid profiles were visualized with iodine vapor and cholesterol ester fractions excised and counted by liquid scintillation spectrometry.

#### ISOLATION, FLUORESCENT LABELING, AND MODIFICATION OF MONKEY LDL

Human and monkey LDL was isolated and labeled as previously described by Havel and associates.<sup>210</sup> Briefly, human or monkey LDL ( $d=1.02\text{--}1.05 \text{ g/cm}^3$ ) and lipoprotein-deficient serum (LDS) were obtained by sequential density gradient ultracentrifugation from normal plasma. For fluorescent lipoprotein uptake studies, isolated human LDL was then labeled with fluorescent, 3,3'-dioc-tadecylindocarbocyanine (DiI) according to the method of Pitas and associates.<sup>211</sup> One milligram of LDL was added to 2 mL of LDS, and the serum was sterilized with

a 0.45- $\mu\text{m}$  polycarbonate filter. Then 50  $\mu\text{L}$  of DiI (3.0 mg/mL in dimethyl sulfoxide) was added, followed by brief, gentle agitation and incubation at 37°C overnight. To reisolate the DiI-labeled LDL, the density of the incubation mixture was raised to  $1.063 \text{ g/cm}^3$  with NaCl, and the DiI-native LDL was isolated at 10°C by 24 hours of centrifugation at 29,000 rpm in a Beckman 30.2 rotor. The DiI-labeled N-LDL was then either dialyzed against 0.9% NaCl containing 0.01% EDTA, pH 7.0, or 0.1 M borate buffer, pH 8.4, in the sample to be acetoacetylated. Acetylation of LDL was performed according to the method of Basu and associates<sup>212</sup> using acetic anhydride and subsequently N,N-dimethyl-1,3-propanediamine and 1-ethyl-3-(3-dimethylaminopropyl)carbodiimide. Extensive dialyses for 24 hours at 4°C against 12 L of buffer containing 0.15 M NaCl and 0.3 mM EDTA, pH 7.4, were performed between the steps for LDL modification. For oxidation of LDL, LDL (100  $\mu\text{g/mL}$ ) was dialyzed for 16 hours at 37°C against 5  $\mu\text{M}$  copper sulfate in PBS followed by dialysis for 24 hours against PBS containing 0.5 mM EDTA to remove  $\text{Cu}^{++}$  ions according to the method of Quinn and associates.<sup>213</sup> To confirm successful acetylation and oxidation of LDL, electrophoretic mobility was assessed on 1% agarose gels.<sup>214</sup>

#### MODULATION OF LYSOSOMAL ENZYME ACTIVITY IN CULTURED MONKEY RPE CELLS BY PHAGOCYTOTIC CHALLENGE OR EXPOSURE TO LIPOPROTEINS

To begin experimental incubations, monkey RPE cells ( $5 \times 10^5$  cells/well) were rinsed twice with PBS to remove serum. They were then overlaid for 24 hours with serum-free medium or media containing 0.93  $\mu\text{m}$  latex spheres (10 mg/mL) or POS ( $5 \times 10^6$  POS/well) or LDL (50 to 100  $\mu\text{g/mL}$ ). Media were then collected and centrifuged to remove debris. The RPE cell layers were rinsed and either fixed and stained for acid lipase and acid esterase activity or scraped from the culture flasks and sonicated on ice for biochemical assays. Cell sonicates and media were maintained at -20°C for up to 1 month prior to biochemical assays.

#### RPE NATIVE AND MODIFIED LIPOPROTEIN UPTAKE

In vitro assays were performed to demonstrate receptor-mediated uptake of lipoproteins that may be specifically inhibited, while in vivo perfusions of labeled lipoproteins were used to demonstrate rapid and avid lipoprotein uptake in a primate model.

##### *Receptor-Mediated Native and Modified LDL RPE Uptake In Vitro*

Monkey RPE cells, alveolar macrophages, smooth-muscle cells, and fibroblasts were maintained in Dulbecco's modified Eagle medium (DMEM) supplemented with 15%

FCS, which was replaced with DMEM containing 10% LDS 1 to 2 days prior to incubation with DiI-labeled lipoproteins. Experimental incubations were begun by changing the medium to DMEM containing 10% LDS and 15 µg/mL of either DiI-labeled, N-, A-, or O-LDL. For competitive inhibition, tenfold excess of the corresponding unlabeled lipoprotein was used. Fucoidin, a competitive inhibitor of A-LDL and a partial inhibitor of O-LDL binding and uptake, was added to cell cultures 15 minutes prior to and during DiI-labeled, AA, and O-LDL incubations at a concentration of 150 µg/mL. Dextran sulfate (30 µg/mL), a polyanionic inhibitor of N- and A-LDL binding and uptake, was also used in some incubations. To confirm the specific uptake of the N-, A-, and O-LDL, assays on cultured macrophages, smooth-muscle cells, and fibroblasts were performed according to the method of Pitas and associates.<sup>211</sup> Experimental assays on cultured RPE cells were performed simultaneously with assays on the other cell types. Following 2-hour incubations with DiI-labeled lipoproteins at 37°C, cells were washed five times with PBS containing 2.0 mg/mL bovine serum albumin, rinsed two times with PBS, and fixed for 20 minutes in HBSS, pH 7.4, containing 4% paraformaldehyde. The cell preparations were mounted in Bacto FA fluid, pH 7.2 (Difco Inc, Detroit, Michigan) and observed using an Olympus BH microscope equipped with a BH-DMG dichroic mirror and a O-590 barrier filter. At least 200 cells were counted in each sample. Photomicrographs were taken using Ektachrome 400 film with exposures varying from 10 to 45 seconds.

#### *Native and Modified LDL RPE Uptake In Vivo*

In vivo perfusion studies were performed on monkeys under thiamylal sodium anesthesia and in rabbits under sodium pentobarbital anesthesia by catheterizing the common carotid arteries. Following carotid perfusion with 75 to 100 mL of isotonic, 0.9% saline solution at 100 mm Hg, 100 mL of DiI-labeled, N-, A-, or O-LDL (40 µg/mL) in PBS was perfused over 20 minutes in dim light. The jugular veins were then cut to permit outflow, and normal saline solution was perfused until clear fluid return was obtained. In situ fixation was obtained by subsequent perfusion with 500 mL of 4% buffered formaldehyde at a perfusion pressure of 150 mm Hg. The enucleated eyes and pieces of lung, liver, and spleen were immersed in the same fixative for 1 to 7 days. Six- and 12-µm frozen tissue sections were cut in darkness and viewed and photographed as described for cell cultures. Control tissues were obtained as described above except that in vivo perfusion was performed with 50 mL of PBS lacking lipoproteins.

#### *Statistical Analysis*

Statistical significance of differences between control and

experimental groups was determined using Student's two-tailed *t* test. Differences between groups were considered to be statistically significant for  $P < .05$ .

## RESULTS

### COMPARATIVE STUDIES ON ACID LIPASE IN RPE CELLS AND MONONUCLEAR PHAGOCYTES

A histochemical and biochemical technique to detect and measure acid lipase activity using detergent micelles containing  $\alpha$ -naphthyl palmitate was previously reported.<sup>77</sup> This technique was adapted for use in analyzing RPE lysosomal acid lipase activity and nonspecific lysosomal acid esterase activity.

Acid lipase activity was initially assessed in fixed, frozen sections of New Zealand White, albino rabbit eyes to eliminate obfuscation of staining by endogenous RPE pigment. The rabbit RPE monolayers stained selectively and intensely for acid lipase activity in full-thickness sections of the posterior ocular segment histochemical incubations of up to 6 hours (Figure 1A and 1B). The dense, red-brown reaction product was present throughout the cytoplasm of all cells in the RPE monolayer.

Histochemical staining of fixed, frozen sections of liver, spleen, and lung demonstrated selective, intense staining of mononuclear phagocytes in histochemical incubations lasting from 30 minutes to 4 hours, as previously reported in other species.<sup>76,77</sup> In liver, Kupffer cells, resident macrophages within the hepatic sinusoids, stained intensely (Figure 2A). Only faint, diffuse staining of hepatocytes was present. Histochemical staining of the spleen for acid lipase activity (Figure 2B) demonstrated heavy deposition of red-brown reaction to be limited to mononuclear phagocytes principally in interfollicular regions, but also within phagocytes distributed in the lymphoid follicles. In the lung (Figure 2C), staining for acid lipase was limited to alveolar macrophages, which exhibited deep, red-brown staining corresponding to high levels of enzyme activity in these phagocytes. Smears of peripheral monocytes and cultures of third-passage smooth-muscle cells showed no appreciable histochemical staining in overnight incubations.

To compare the acid lipase activity of freshly isolated rabbit RPE cells to that of macrophages isolated from other tissues, biochemical acid lipase assays were performed on aliquots of glass beads bearing adherent RPE cells or macrophages (Table I). The highest lipolytic activity was found in freshly isolated alveolar macrophages, followed by splenic and peritoneal mononuclear phagocytes. All macrophages demonstrated acid lipase activities well above the 36 µM/10<sup>6</sup> cells/hour threshold of  $\alpha$ -naphthyl palmitate hydrolysis required for histochemical staining in fixed, frozen tissue sections despite 80% to 90% loss of

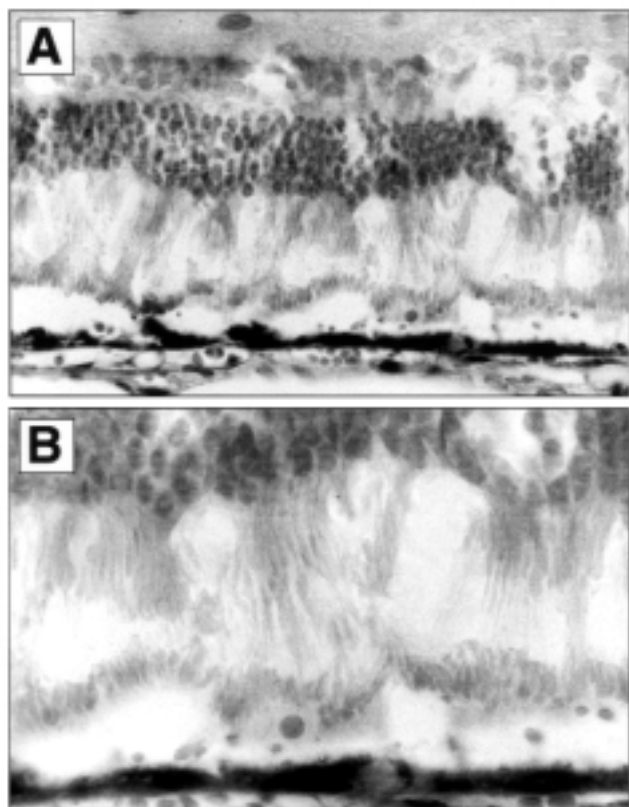


**FIGURE 1**

Histochemical staining for acid lipase activity in New Zealand White rabbit retinal pigment epithelial (RPE) cells. A, Deposition of red-brown reaction product corresponding to sites of  $\alpha$ -naphthyl palmitate hydrolysis is limited to RPE cells in fixed, frozen sections of posterior ocular segment. Variable staining of a few hyalocytes in cortical vitreous is also present (methyl green counterstain,  $\times 100$ ). B, Selective staining of RPE cells for acid lipase activity is readily visible at higher power. Lipid vacuoles are also noted in rabbit RPE monolayer (methyl green counterstain,  $\times 400$ ).

acid lipase activity associated with formal sucrose fixation.<sup>76,77</sup> Freshly isolated, glass-adherent RPE cells liberated  $81 \mu\text{M}$  of  $\alpha$ -naphthol/ $10^6$  cells/hour (Table I), which is also compatible with the positive in situ histochemical staining present in these cells (Figure 1). Subthreshold activities for histochemical staining were present in monocytes and third-passage, cultured smooth-muscle cells, the latter containing the least acid lipase activity of all cell types assayed.

Enumeration of cells adherent to glass bead aliquots was performed by counting cell nuclei extracted from cells with citric acid and stained with crystal violet. Using this technique, cell counts varied less than 10% per sample. To determine the purity of cells adherent to glass beads, adherent cells were dislodged from aliquots of glass beads using EDTA. The cells were dried onto glass slides and counted microscopically. Greater than 90% of adherent cells were macrophages, RPE cells, or monocytes in their respective preparations.

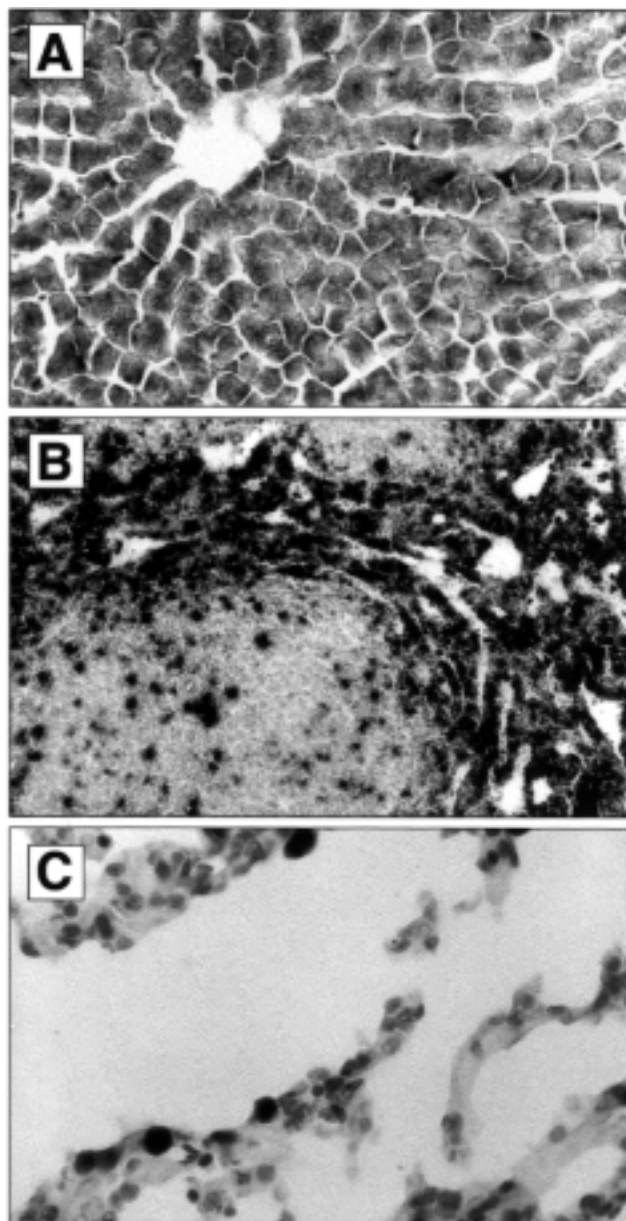


**FIGURE 2**

Histochemical staining for acid lipase activity in fixed, frozen sections of New Zealand White rabbit lung, liver, and spleen. A, Liver Kupffer cells are deeply and selectively stained with reaction product following incubation with  $\alpha$ -naphthyl palmitate substrate. Deposition of red-brown product due to enzyme activity is just visible in centroacinar hepatocytes (methyl green counterstain,  $\times 100$ ). B, Splenic acid lipase activity is detected selectively in mononuclear phagocytes of red pulp and germinal centers of spleen by red-brown reaction product (methyl green counterstain,  $\times 100$ ). C, Lung alveolar macrophages contain selective, deep red-brown reaction product following incubation with  $\alpha$ -naphthyl palmitate-Triton X100 substrate micelles (methyl green counterstain,  $\times 100$ ).

Preincubation of isolated cells or the tissue sections with the organophosphate DEPP ( $10^{-4}$  M) or the sulfhydryl blocking reagent, PHMB ( $5 \times 10^{-5}$  M), but not the carboxylic esterase inhibitor, bis-p-nitrophenylphosphate, virtually eliminated acid lipase activity in the RPE

TABLE I: ACID LIPASE ACTIVITY OF FRESHLY ISOLATED RABBIT RPE CELLS AND MONONUCLEAR PHAGOCYTES

CELL TYPE*	$\alpha$ -NAPHTHYL PALMITATE HYDROLYZED ( $\mu$ M)/10 <sup>6</sup> CELLS/HR
Alveolar macrophages (14)	4,312 $\pm$ 9,042
Splenic macrophages (24)	805 $\pm$ 2,785
Peritoneal macrophages (35)	322 $\pm$ 2,212
RPE cells (25)	81 $\pm$ 395
Blood monocytes (14)	25 $\pm$ 12
Smooth-muscle cells† (6)	10 $\pm$ 4.4

RPE, retinal pigment epithelium.

\*Number of separate glass-adherent cell samples pooled from experiments.

†Third-passage rabbit aortic smooth-muscle cells.

histochemical and biochemical assays, a feature of acid lipases in other tissue preparations.<sup>77</sup>

#### ACID LIPASE PURIFIED FROM FRESHLY ISOLATED BOVINE RPE CELLS

To demonstrate the specificity of the chromogenic assay for acid lipase and to show that RPE acid lipase may actually esterify free fatty acids to cholesterol, acid lipase activity, corresponding to a single protein band, was purified from bovine RPE cells and shown to possess the ability to hydrolyze  $\alpha$ -naphthyl palmitate and esterify cholesterol to fatty acids hydrolyzed from a triglyceride (ie, triolein). Freshly isolated RPE cells from bovine eyes were used, since adequate numbers of cells for biochemical studies could be obtained from this source.

Sonicated, isolated bovine RPE cells run on a Sephadex G-150 column exhibited similar profiles for  $\alpha$ -naphthyl palmitate hydrolysis and cholesteryl ester formation (Figure 3). The activities were associated with an apparent  $M_r$  of 66,000 d with this sizing column. Pooled peak fractions were concentrated and subsequently run on an SP-Sephadex C-50 ion exchange column under conditions that would isolate acid lipase and minimize enzyme binding to the column. This was done to obviate the need for subsequent elution with high salt or pH solutions, which decreases enzyme-specific activity. Void volume fractions showed active  $\alpha$ -naphthyl palmitate, cholesteryl ester, and triglyceride hydrolysis as well as cholesterol esterification in the same fractions (Figure 4). Polyacrylamide-SDS gel electrophoresis was performed on samples from the SP-Sephadex C-50 purification. Electrophoresis of void volume fractions following SP-Sephadex C-50 chromatography resulted in a single Coomassie blue-stained band with an apparent  $M_r$  of 65,000 d when compared to molecular weight markers. Silver staining demonstrated a similar profile with a single stainable band in gels overloaded intentionally to ascertain any other proteins that might be present (Figure 5). These findings indicated the single identity of the protein hydrolyzing  $\alpha$ -naphthyl palmitate, cholesteryl esters, and

triglycerides. Isoelectric focusing of the same void volume fractions from the Sephadex C-50 column resulted in several bands stainable by Coomassie blue at isoelectric points between pH 5.5 and 6.0. Alpha-naphthyl palmitate hydrolytic and cholesterol esterification assays at acid pH were performed on 2-mm gel slices of simultaneously run gels not stained for protein. Both enzyme activities were found in the gel slices from areas that corresponded to the Coomassie blue-stained bands (Figure 6).

#### INDUCTION OF LYSOSOMAL ENZYME ACTIVITY IN CULTURED MONKEY RPE CELLS BY PHAGOCYTTIC CHALLENGE AND LDL

To demonstrate that RPE cells may upregulate lysosomal enzyme activity in response to phagocytic stimuli, particularly to lipid-rich POS, which the RPE naturally ingests, RPE lysosomal activities were measured after phagocytic

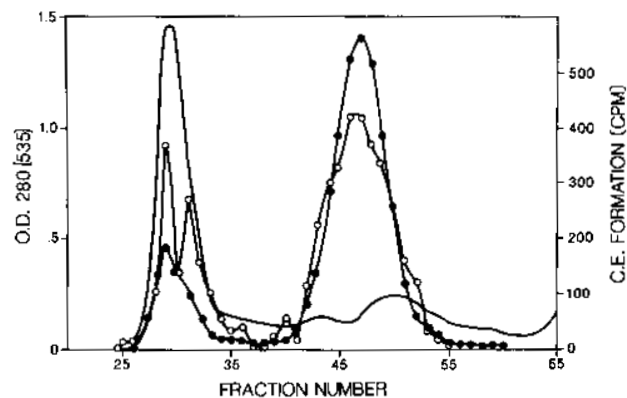


FIGURE 3

Elution profile of acid lipase activity obtained by molecular sieve gel chromatography of bovine retinal pigment epithelial (RPE) cell sonicate. Fractions collected from a Sephadex G-150 column were assayed continuously for protein (solid line) by measuring absorption at 280 nm.  $\alpha$ -Naphthyl palmitate hydrolytic (OD, 535 nm  $\bullet$ ----- $\bullet$ ) and cholesterol esterification (CPM  $\circ$ ----- $\circ$ ) activities were measured in biochemical assays at acid pH. Both enzyme activities eluted in the same fractions corresponding to an apparent  $M_r$  of 66,000. Bovine RPE cell pellets were sonicated in distilled water at a ratio of 1:10 (wt/vol) and combined with 2 mL of 0.02 M Tris-HCl, pH 7.4, and applied to and run on the column at 4°C.

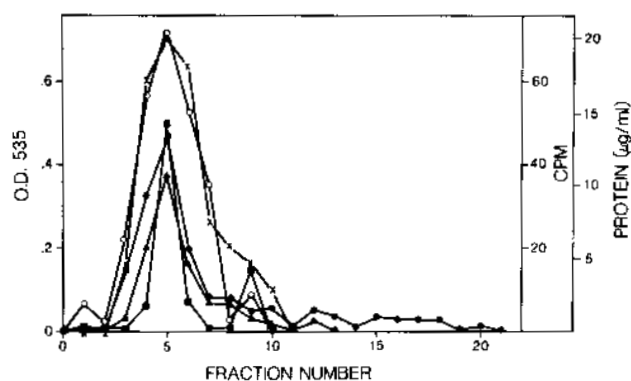


FIGURE 4

Elution profile of pooled, concentrated Sephadex G-150 fractions demonstrating peak bovine retinal pigment epithelial (RPE) acid lipase activity following application to an ion exchange column. Fractions (2 mL) eluted from SP Sephadex C-50 were assayed for protein (●-----●) and for the hydrolysis of  $\alpha$ -naphthyl palmitate (OD, 535 nm x-----x), cholesteryl esters (CPM ■-----■), and triglycerides (CPM ▲-----▲) in addition to the formation of cholesteryl esters at acid pH (CPM o-----o). All three enzyme activities are found in the same fractions. Pooled Sephadex G-150 fractions that contained peak acid lipase activity were concentrated by ultrafiltration and applied to the SP Sephadex C-50, which was equilibrated and eluted at 4°C with 0.05 M sodium acetate buffer, pH 5.5, containing 0.025 M NaCl. The low salt concentrations necessary to avoid enzyme inactivation resulted in obligate void volume elution of the enzyme activities.

challenge with POS. Latex beads were used in control preparations to assess the inductive effect of nonspecific phagocytosis on RPE lysosomal activities. Assays for acid lipase, nonspecific acid esterase, and cholesteryl esterase were performed on sonicates of control cultured monkey RPE cells and compared with cultured monkey RPE cells overlaid for 24 hours with either latex beads or POS in serum-free media (Table II). Sonicates of RPE cells that had internalized latex microspheres exhibited statistically significant increases of acid lipase activity ( $P < .05$ ) when compared with control cultured monkey RPE cells. Monkey RPE cells showed more than twofold increases in acid lipase, acid esterase, and cholesteryl esterase (all  $P < .001$ ) after phagocytic challenge with POS compared with control RPE cells (Table II).

The media of the RPE cultures were also assayed for acid lipase, acid esterase, and cholesteryl esterase activity (Table III). Media aliquots from cultures after 24 hours phagocytic challenge with latex beads revealed statistically significant increases in media for all three lysosomal enzyme activities over control media. Interestingly, RPE cell monolayers exposed to POS released substantially less lysosomal activity, reaching statistical significance only for cholesteryl esterase ( $P < .05$ ).

Histochemical studies of latex-fed and POS-fed monkey RPE cells showed readily visible staining for enzyme activity (Figure 7). The red-brown precipitates indicative

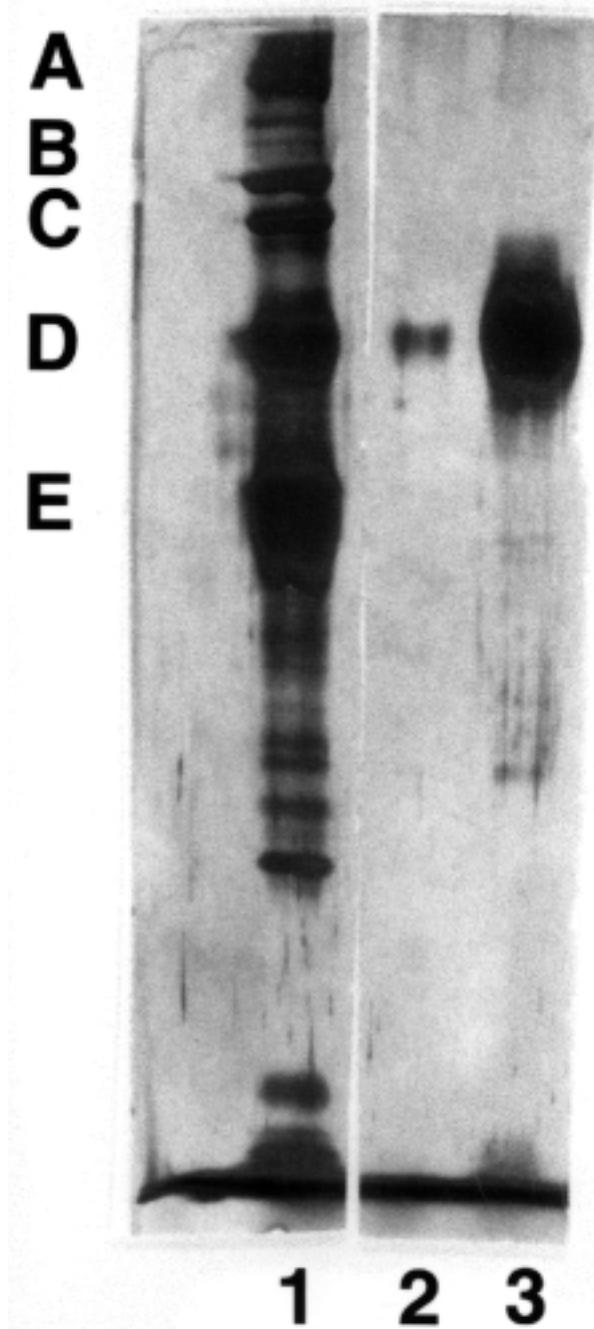


FIGURE 5

Polyacrylamide-SDS electrophoretic patterns of bovine retinal pigment epithelial (RPE) acid lipase following sequential molecular sieve gel and ion exchange chromatography. Silver-stained, polyacrylamide-SDS gel of the SP-Sephadex C-50 void volume fraction, which showed peak  $\alpha$ -naphthyl palmitate hydrolysis in biochemical assays, demonstrates a single stainable protein band (lane 2). An overloaded gel run simultaneously (lane 3) demonstrates little contamination with other proteins. Bovine RPE acid lipase (lane 2) has an apparent  $M_r$  of 65,000 when compared with molecular weight markers (lane 1): A, myosin; B,  $\beta$ -galactosidase; C, phosphorylase B; D, bovine serum albumin; E, ovalbumin.

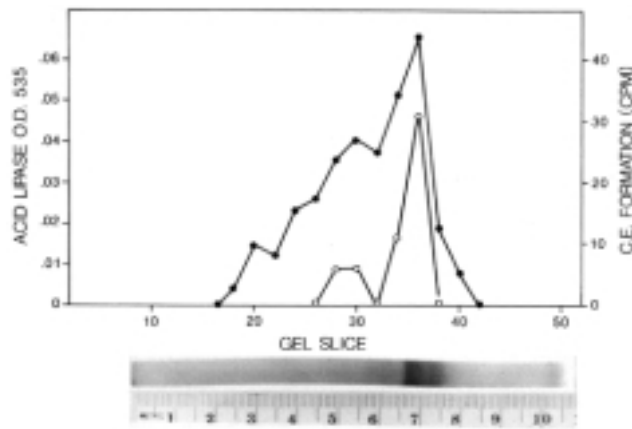


FIGURE 6

Isoelectric focusing zymogram of pooled, eluted fractions demonstrating peak bovine retinal pigment epithelial (RPE) acid lipase activity following molecular sieve gel and ion exchange chromatography.  $\alpha$ -Naphthyl palmitate hydrolytic ( $\bullet$ ----- $\bullet$ ) and cholesterol esterification (o-----o) activities were assayed in successive 2-mm gel slices at pH 4.2. Peak enzyme activities corresponded to Coomassie blue-stainable protein bands of gels run in parallel. Isoelectric focusing (pH, 4.0-6.5) of the peak SP-Sephadex C-50 void volume fractions was performed in polyacrylamide gels for 8 to 18 hours at 5°C.

of nonspecific acid esterase activity were present in control cultures, but substantially increased in intensity in cells exposed to latex particles or POS. In contrast, control RPE cell layers showed almost no reaction product when stained for acid lipase activity, but distinct reaction product corresponding to lipolytic activity after latex-bead or POS challenge.

RPE cells phagocytize substantial amounts of lipid derived from POS and enhance lysosomal lipolytic activity in response to this physiologic stimulus (Table II, Figure 7). Since circulating LDL is a rich source of lipid for which RPE cells bear specific receptors,<sup>128,129</sup> monkey RPE acid lipase, acid esterase, and cholesteryl esterase activities were assessed after 24 hours challenge with native

monkey LDL (Table IV). Exposure of cultured RPE cells to N-LDL significantly enhanced acid lipase ( $P < .01$ ) and cholesteryl esterase ( $P < .05$ ) activities. Lipoprotein-deficient serum, derived from the same samples from which the N-LDL was isolated, served as control for these assays, leading to the conclusion that LDL was responsible for enhanced RPE lysosomal activity observed. These findings paralleled those of RPE degradation assays in which <sup>99</sup>I-labeled N-LDL was actively degraded by the monkey RPE cells (results not shown).

**RECEPTOR-MEDIATED RPE UPTAKE OF N-LDL, A-LDL, O-LDL BY MONKEY RPE CELLS IN VITRO AND IN VIVO**

To demonstrate receptor-specific uptake of native and modified LDL by RPE cells, in vitro assays of fluorescently labeled lipoprotein uptake in the presence or absence of specific inhibitors was performed. In vivo 29-minute perfusions of labeled lipoproteins were then performed to demonstrate actual, rapid, and avid lipoprotein uptake in monkeys.

Specific receptor-mediated uptake of native and modified lipoproteins by monkey RPE cells was initially assessed in vitro. N-LDL labeled with the red, fluorescent dye, DiI, was avidly incorporated into approximately 90% of cultured monkey RPE cells that exhibited diffuse cytoplasmic positivity (Figure 8A). A tenfold excess of unlabeled LDL effectively inhibited RPE uptake of the labeled LDL (Figure 8B), while dextran sulfate (30  $\mu$ g/mL) completely blocked uptake of the fluorescent, native lipoprotein. Neither A nor O-LDL blocked DiI-N-LDL uptake.

Eighty percent of monkey RPE cells exposed to DiI-A-LDL displayed intense, granular cytoplasmic fluorescence (Figure 8C), presumably due to lysosomal incorporation of the modified lipoprotein.<sup>133,134</sup> Excess unlabeled A-LDL (Figure 8D) and fucoidin, (150  $\mu$ g/mL), a specific inhibitor of A-LDL binding and uptake,<sup>211,215,216</sup> were effec-

TABLE II: LYSOSOMAL ENZYME ACTIVITY INDUCED IN MONKEY RPE CELLS BY PHAGOCYTTIC CHALLENGE

LYSOSOMAL ENZYME†	LYSOSOMAL ENZYME ACTIVITY*		
	CONTROL RPE CELLS‡	LATEX-FED RPE CELLS	POS-FED RPE CELLS
Acid lipase (8)	1.00 $\pm$ 0.12 (32)	1.59 $\pm$ 0.22§	2.53 $\pm$ 0.66
Acid esterase (8)	1.00 $\pm$ 0.30 (84)	1.30 $\pm$ 0.34	2.06 $\pm$ 0.37
Cholesteryl esterase (6)	1.00 $\pm$ 0.20 (217)	1.14 $\pm$ 0.22	2.60 $\pm$ 0.37

POS, photoreceptor outer segment; RPE, retinal pigment epithelium.

\*Activities  $\pm$ SD expressed relative to mean activities of control cell groups with mean activity of each control group expressed as unity  $\pm$ SD.

†Number of separate cell samples pooled from experiments.

‡Mean activity of pooled control cell cultures expressed as  $\mu$ M substrate hydrolyzed per hour per  $\mu$ g DNA for acid lipase and acid esterase and as counts per minute per hour per  $\mu$ g DNA for cholesteryl esterase.

§ $P < .05$ , compared to control.

||  $P < .001$ , compared to control.

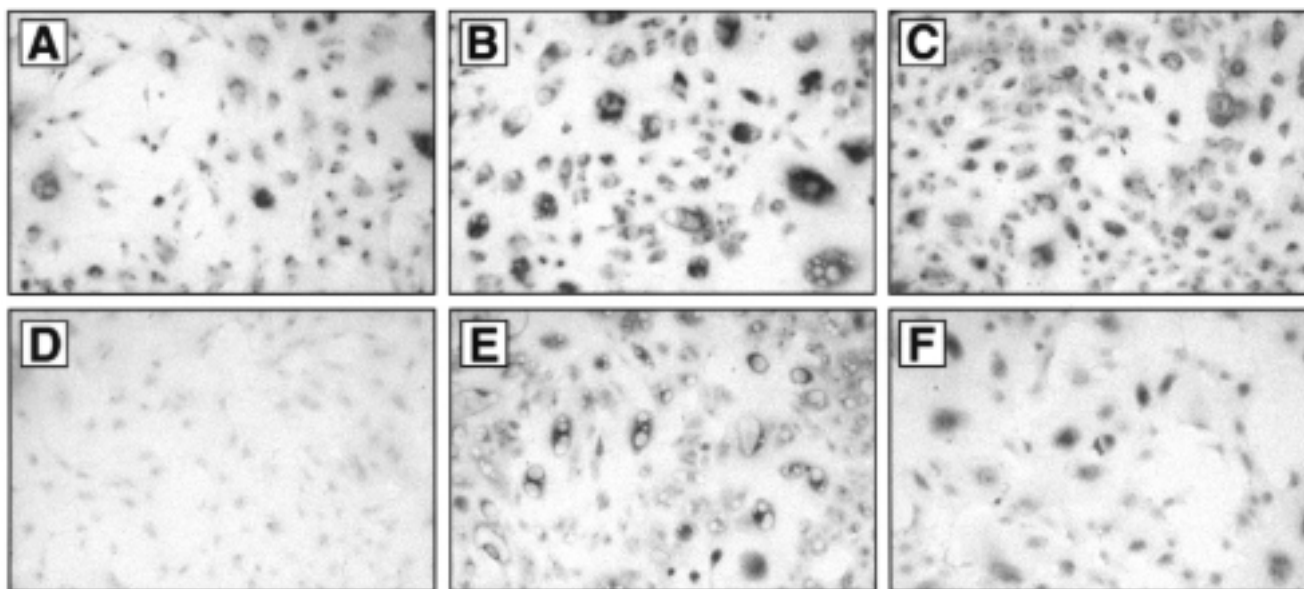


FIGURE 7

Histochemical demonstration of monkey retinal pigment epithelial (RPE) lysosomal enzyme induction following phagocytic challenge. A, Histochemical staining for nonspecific acid esterase using  $\alpha$ -naphthyl acetate demonstrates red-brown reaction product in cultured RPE cells (methyl green counterstain, x200). B, RPE cell cultures overlaid with 0.93- $\mu$ m latex microspheres (40 mg/mL) contain numerous internalized beads and increased enzyme reaction product (methyl green counterstain, x200). C, After overlay of photoreceptor outer segments (40 mg/mL), increased nonspecific esterase activity is also visualized compared with control cultures (methyl green counterstain, x200). D, Staining for acid lipase activity using  $\alpha$ -naphthyl palmitate fails to reveal distinct reaction product in control RPE cultures (methyl green counterstain x200). E, Intense, red-brown acid lipase cytoplasmic reaction product is present and surrounds latex microspheres that have been phagocytized (methyl green counterstain, x200). F, RPE cells contain distinct, enhanced visible reaction product, corresponding to acid lipase activity, after overlay of photoreceptor outer segments (methyl green counterstain, x200).

TABLE III: LYSOSOMAL ENZYME ACTIVITY RELEASED BY MONKEY RPE CELLS DURING PHAGOCYTTIC CHALLENGE

LYSOSOMAL ENZYME <sup>†</sup>	LYSOSOMAL ENZYME ACTIVITY <sup>°</sup>		
	CONTROL RPE CONDITIONED MEDIA <sup>‡</sup>	LATEX-FED RPE CONDITIONED MEDIA	POS-FED RPE CONDITIONED MEDIA
Acid lipase (6)	1.00 $\pm$ 0.29 (6.2)	2.75 $\pm$ 0.30 <sup>§</sup>	1.08 $\pm$ 0.22
Acid esterase (6)	1.00 $\pm$ 0.09 (8.4)	2.30 $\pm$ 0.47	1.18 $\pm$ 0.27
Cholesteryl esterase (6)	1.00 $\pm$ 0.10 (53)	1.58 $\pm$ 0.34 <sup>¶</sup>	1.34 $\pm$ 0.29

POS, photoreceptor outer segment; RPE, retinal pigment epithelium.

<sup>°</sup>Activities  $\pm$ SD expressed relative to mean activities of control cell groups with mean activity of each control group expressed as unity  $\pm$ SD.

<sup>†</sup>Number of separate cell samples pooled from experiments.

<sup>‡</sup>Mean activity of pooled control cell cultures expressed as  $\mu$ M substrate hydrolyzed per hour per  $\mu$ g DNA for acid lipase and acid esterase and as counts per minute per hour per  $\mu$ g DNA for cholesteryl esterase.

<sup>§</sup> $P < .001$ , compared to control.

|| $P < .05$ , compared to control.

<sup>¶</sup> $P < .01$ , compared to control.

tive inhibitors of RPE DiI-A-LDL uptake. N-LDL did not block DiI-A-LDL uptake. O-LDL reduced, but did not completely block, the RPE uptake of fluorescent A-LDL.

Seventy percent of monkey RPE cells incubated with DiI-O-LDL exhibited delicate, red granular cytoplasmic fluorescence (Figure 8E)<sup>131,132,148</sup> that was also likely due to lysosomal incorporation. DiI-O-LDL uptake was effectively inhibited by a tenfold excess of unlabeled O-LDL

(Figure 8F). Fucoidin also inhibited RPE uptake of the fluorescently labeled oxidized LDL, but it was less effective than excess unlabeled O-LDL and also less effective than when it was used to block RPE DiI-A-LDL uptake (Figure 8D). A-LDL, but not N-LDL, partially blocked DiI-O-LDL RPE uptake, presumably by blocking some, but not all, of the scavenger receptors mediating O-LDL uptake.<sup>131,132,140,142</sup>

In control incubations, about 95% of monkey fibro-

TABLE IV: EFFECTS OF LOW-DENSITY LIPOPROTEINS (LDL) ON LYSOSOMAL ENZYME ACTIVITY IN MONKEY RPE CELLS

LYSOSOMAL ENZYME <sup>†</sup>	LYSOSOMAL ENZYME ACTIVITY <sup>°</sup>	
	LIPOPROTEIN-DEFICIENT SERUM <sup>‡</sup>	NATIVE LDL
Acid lipase (6)	1.00 ± 0.14 (14)	1.28 ± 0.16§
Acid esterase (6)	1.00 ± 0.09 (20)	1.17 ± 0.23
Cholesteryl esterase (6)	1.00 ± 0.27 (170)	1.38 ± 0.31

RPE, retinal pigment epithelium.

<sup>°</sup>Activities ±SD expressed relative to mean activities of control groups with mean activity of each control group expressed as unity ±SD.

<sup>†</sup>Number of separate cell samples pooled from experiments.

<sup>‡</sup>Mean activity of pooled control cell cultures expressed as μM substrate hydrolyzed per hour per μg DNA for acid lipase and acid esterase and as counts per minute per hour per μg DNA for cholesteryl esterase.

<sup>§</sup>*P* < .01, compared to LDS.

<sup>||</sup>*P* < .05, compared to lipoprotein-deficient serum.

blasts, which are known to possess N-LDL receptors, became fluorescent when incubated with DiI-N-LDL, but less than 5% of fibroblasts incorporated A- or O-LDL. As expected, fibroblast uptake of DiI-N-LDL was inhibited by dextran sulfate or excess unlabeled LDL. Known to express both A-LDL and O-LDL receptors, 85% and 80% of monkey alveolar macrophages became brightly fluorescent upon exposure to DiI-A-LDL and DiI-O-LDL, respectively. Excess unlabeled A- and O-LDL inhibited macrophage uptake of their respective labeled, modified LDL while fucoidin was much more effective at inhibiting DiI-A-LDL uptake than DiI-O-LDL uptake. Ten percent to 40% of alveolar macrophages incubated with DiI-labeled, native LDL incorporated the lipoprotein but were less fluorescent than those exposed to either DiI-labeled, A- or O-LDL.

In vivo assessment of native and modified LDL uptake by retina, liver, spleen, and lung was performed after carotid perfusion of monkeys with DiI-labeled lipoproteins. Frozen sections of formalin-fixed monkey eyes after DiI-N-LDL perfusion revealed specific and intense diffuse red cytoplasmic fluorescence within the entire RPE monolayer (Figure 9A). Much less uptake was present in the choroid and inner neural retina. Posterior segments of eyes from monkeys perfused with A-DiI-LDL exhibited intense, red granular fluorescence along the entire RPE monolayer. The only other red fluorescence seen was delicate labeling of vascular endothelial cells within choroidal blood vessels (Figure 9C). Selective, delicate, red granular fluorescence was also present throughout the RPE monolayers of eyes from monkeys perfused with DiI-labeled O-LDL (Figure 9E) but was less intense than that observed with DiI-A-LDL. As in the case of A-LDL, no other staining was visible in the posterior ocular segment. The granular fluorescence mimicked that observed in the cultured RPE cells and presumably was due to lysosomal incorporation of the

modified lipoproteins.<sup>131-134,148</sup> In all of the monkey eyes, background, endogenous, yellow autofluorescence could be readily distinguished from the distinctive, red fluorescence of the DiI label.

To compare the patterns of DiI-labeled N-, A-, and O-LDL uptake by monkey RPE cells to those of other resident tissue phagocytes in vivo, the livers, spleens, and lungs of the same animals were harvested, fixed, frozen sectioned, and examined by fluorescence microscopy. Tissue sections of liver after DiI-N-LDL perfusion demonstrated diffuse and discrete red granular fluorescence in hepatocytes without evidence of labeled lipoprotein uptake in resident mononuclear phagocytes (Kupffer cells) or sinusoidal endothelial cells (Figure 10A). In contrast, perfusion of DiI-A-LDL resulted in selective, avid incorporation of the modified lipoprotein by Kupffer cells, which became very brightly fluorescent (Figure 10B). Lesser, but distinctive, red granular fluorescent staining of endothelial cells within the sinusoids corresponded to A-LDL uptake by these cells also. DiI-O-LDL perfusions resulted in hepatic uptake that was similar in distribution and intensity to that of DiI-A-LDL (Figure 10C) and reiterated the fluorescent pattern of uptake reported by Esbach and associates.<sup>217</sup>

Frozen sections of monkey spleens after in vivo perfusion of DiI-N-LDL demonstrated only weak paratrabeular incorporation as well as faint staining of a few stellate and fusiform cells, chiefly in interfollicular regions (Figure 10D). The splenic capsule, however, stained brightly, presumably because of the presence of fibroblasts (not shown). Fluorescence microscopy of spleens perfused with DiI-A-LDL was markedly different. The interfollicular regions contained numerous brightly fluorescent mononuclear phagocytes as well as delicate, but uniform, bright red fluorescence of vascular endothelium (Figure 10E). Mononuclear phagocytes distributed in the lymphoid follicles also displayed bright fluorescence.

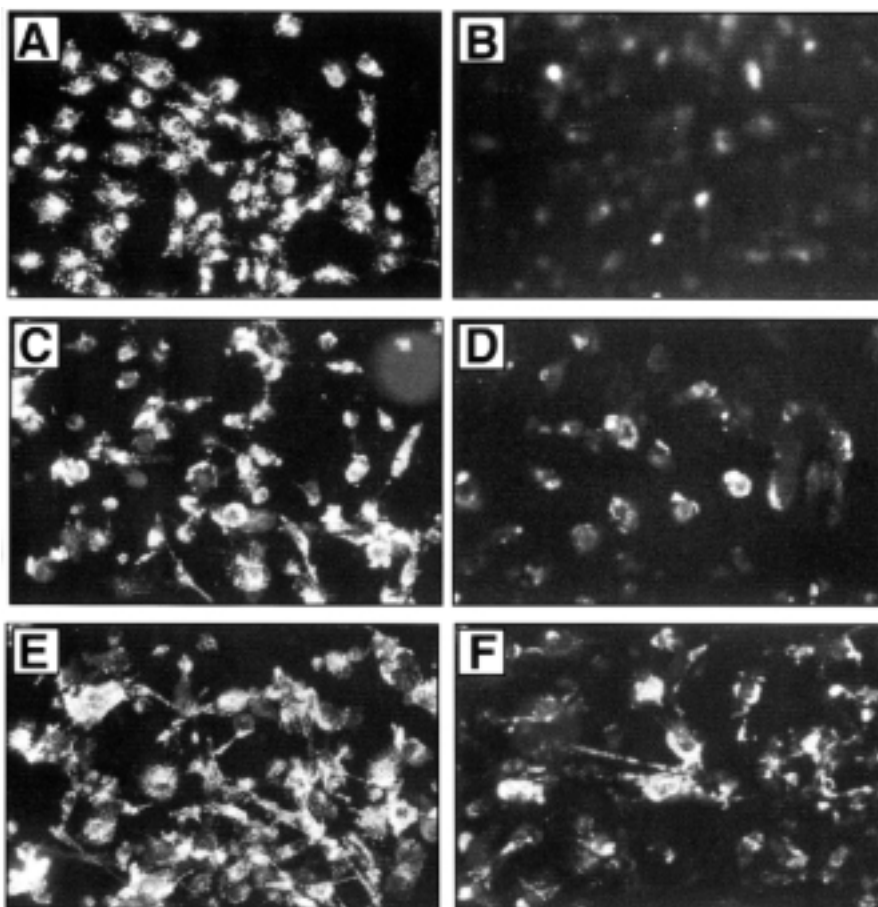


FIGURE 8

Detection of receptors for native (N)-, acetylated (A)-, and oxidized (O)-LDL on cultured monkey RPE cells. A, Photomicrograph of fluorescent, cultured RPE cells exposed to DiI-labeled N-LDL. Intense cellular fluorescence following exposure to N-LDL (15  $\mu\text{g}/\text{mL}$ ) indicates avid incorporation of the lipoprotein. Cytoplasmic fluorescence contrasts with nuclei, which are hypo-fluorescent. Uptake of the fluorescent lipoprotein is also observed in the stromal cells of the choroid (x200). B, RPE cells exposed to fluorescent N-LDL in the presence of excess unlabeled LDL (150  $\mu\text{g}/\text{mL}$ ). RPE cells are significantly less fluorescent owing to competitive inhibition of uptake by unlabeled lipoprotein. Dextran sulfate (30  $\mu\text{g}/\text{mL}$ ) completely inhibited RPE N-LDL uptake (x200). C, Monkey RPE cells after incubation with DiI-labeled A-LDL (15  $\mu\text{g}/\text{mL}$ ) display intense, red, granular fluorescence due to intracellular accumulation of modified lipoprotein. Contrasting cell nuclei are hypo-fluorescent (x200). D, Cultured RPE cells exposed to fluorescent A-LDL in the presence of excess unlabeled A-LDL (150  $\mu\text{g}/\text{mL}$ ) show substantially less fluorescence, indicating marked competitive inhibition of labeled, modified lipoprotein uptake by RPE cells. Fucoidin (100  $\mu\text{g}/\text{mL}$ ), a competitive inhibitor of A-LDL receptor binding, abolished DiI-A-LDL binding and uptake (x200). E, Moderately overexposed photomicrograph of RPE cells exposed to DiI-labeled, O-LDL. Granular fluorescence due to uptake of red, fluorescent oxidized lipoprotein within cytoplasm contrasts with hypo-fluorescent nuclei (x200). F, Competitive inhibition of DiI-labeled O-LDL uptake by excess unlabeled O-LDL (150  $\mu\text{g}/\text{mL}$ ) renders RPE cells much less fluorescent. Fucoidin also inhibited DiI-labeled O-LDL uptake, but to a lesser extent than excess unlabeled O-LDL (x200).

Perfusion with DiI-labeled, O-LDL also demonstrated fluorescence, which was limited to resident tissue macrophages and vascular endothelial cells (Figure 10F) but was less intense than that found with DiI-A-LDL.

In the lung, uptake of DiI-N-LDL was seen as intense, red fluorescence of bronchial and vascular smooth muscle as well as faint positivity in alveolar septae (Figure 10G). There was no evident uptake by alveolar macrophages or vascular endothelium. In contrast, perfusions with DiI-A-LDL and DiI-O-LDL resulted in bright fluorescence of some of the alveolar macrophages (Figure 10H,10I), but overall fluorescence was less intense than that of the liver or spleen.

New Zealand White rabbit perfusions with DiI-labeled native and modified LDL exhibited uptake patterns in retina, liver, spleen, and lung that were similar, if not identical, to those observed in the monkeys, confirming previous *in vivo* results.<sup>128</sup> *In vitro* studies on rabbit cells yielded entirely similar results to those described for monkey cells.<sup>128</sup>

#### FISH OIL MODULATION OF MONKEY RPE LYSOSOMAL ENZYMES

Since diets containing fish oil have been associated with reduced risk of ARMD and severity of atherosclerosis, presumably because of their effects on circulating lipopro-

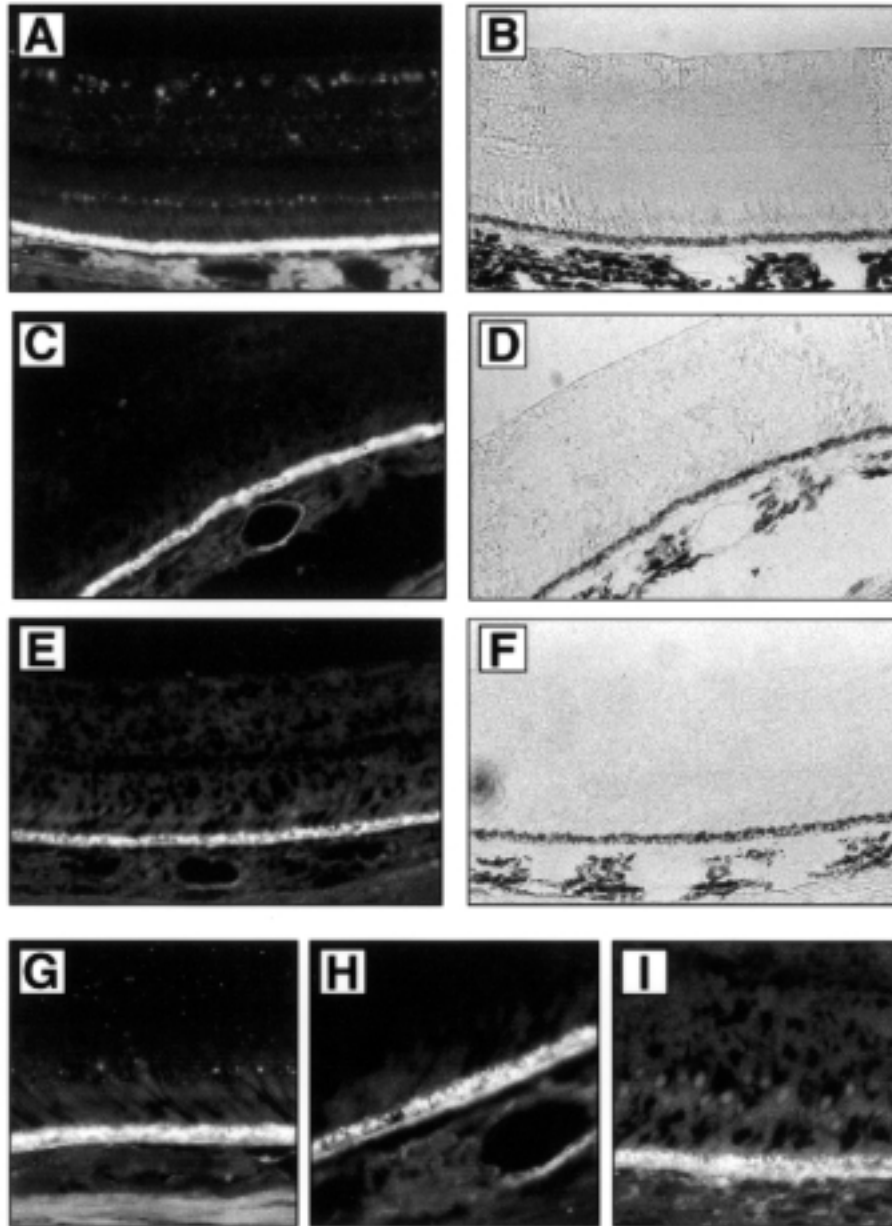


FIGURE 9

Demonstration of native (N)-, acetylated (A)-, and oxidized (O)-LDL uptake by monkey RPE in vivo. A, Histologic frozen section of formalin-fixed monkey eye after in vivo carotid arterial perfusion of DiI-labeled N-LDL (1  $\mu\text{g}/\text{mL}$ ). Intense, diffuse red fluorescence of retinal pigment epithelial (RPE) monolayer indicates avid N-LDL uptake. Less N-LDL uptake is seen within choroid and inner retinal layers (x200). B, Phase contrast photomicrograph of same field seen in A (x200). C, Frozen section of fixed monkey eye after in vivo perfusion with DiI-labeled A-LDL (1  $\mu\text{g}/\text{mL}$ ). RPE monolayer is selectively stained with intense granular fluorescence. RPE nuclei are hypofluorescent. Delicate staining of cells lining a choroidal vessel indicates endothelial incorporation of DiI-labeled A-LDL. Neural retina sclera, and other portions of choroid are unstained (x200). D, Phase contrast photomicrograph of same field seen in C (x200). E, Monkey eye following in vivo perfusion with DiI-labeled O-LDL (1  $\mu\text{g}/\text{mL}$ ). RPE monolayer exhibits selective, delicate, granular fluorescence due to uptake of the modified lipoprotein. RPE nuclei are hypofluorescent. Neural retina, sclera, and choroid are unstained (x200). F, Phase contrast photomicrograph of same field seen in E (x200). G, DiI-N-LDL uptake by RPE seen at higher power. Intense fluorescence is seen throughout cytoplasm. Uptake is also seen in sclera (x400). H, DiI-A-LDL uptake. Intense granular fluorescence, with overall less intensity than that seen due to DiI-N-LDL uptake, is present in RPE cells (x400). I, Moderately overexposed photomicrograph demonstrating DiI-O-LDL uptake as granular fluorescence within RPE cells. Uptake is also seen in vessels within choroid to a greater extent than that observed with DiI-A-LDL (x400).

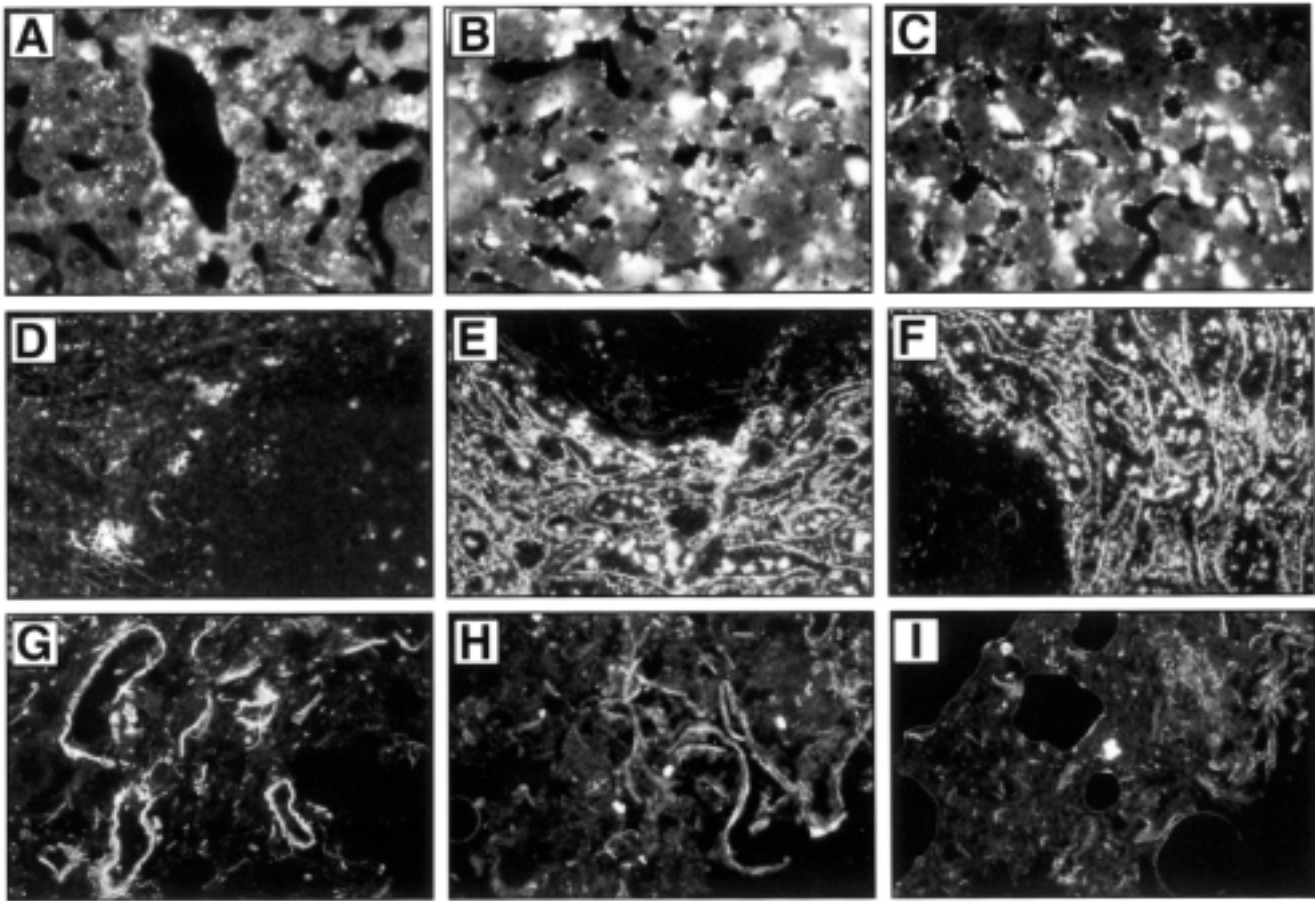


FIGURE 10

Demonstration of native (N)-, acetylated (A)-, and oxidized (O)-LDL uptake by monkey liver, spleen, and lung in vivo. A, Histologic frozen section of fixed monkey liver following in vivo perfusion of DiI-labeled N-LDL. Discrete, granular fluorescence is present in hepatocytes and surrounding central vein, indicating uptake of N-LDL. Kupffer cells and endothelium of sinusoids are not stained (x200). B, Monkey liver following in vivo perfusion of DiI-labeled A-LDL. Kupffer cells are brightly fluorescent owing to active uptake of modified lipoprotein. Sinusoidal and vascular endothelium is also distinctly fluorescent, indicating lipoprotein uptake by this cell type (x200). C, DiI-O-LDL incorporation in monkey liver after in vivo perfusion displays pattern of distribution similar to A-LDL (x200). D, Frozen section of monkey spleen following in vivo perfusion with fluorescently labeled N-LDL. Weak paratrabeular incorporation of DiI-labeled N-LDL is seen. There is faint staining of a few stellate and fusiform cells. Intense staining of splenic capsule, however, was present (not shown) (x200). E, Monkey spleen following in vivo perfusion with DiI-A-LDL. Numerous mononuclear phagocytes in interfollicular region are brightly fluorescent, as are a few mononuclear phagocytes located within lymphoid follicles. Vascular endothelium also demonstrates delicate, bright fluorescence (x200). F, DiI-O-LDL incorporation in perfused monkey spleen displays pattern of distribution similar to A-LDL (x200). G, Monkey lung after in vivo perfusion with DiI-labeled N-LDL. Intense staining of bronchial and vascular smooth muscle due to uptake of native lipoprotein is present. Weak incorporation of DiI-labeled N-LDL is seen in alveolar septae (x200). H, Fixed, frozen section of lung following DiI-A-LDL perfusion. Selective, intense fluorescence of alveolar macrophages due to uptake of labeled, modified lipoprotein is evident (x200). I, DiI-O-LDL incorporation in perfused monkey lung displays selective distribution in alveolar macrophages similar to, but less dramatic than, DiI-A-LDL (x200).

teins for which RPE cells bear receptors mediating their uptake in vivo, the effects of fish oil-rich diets on RPE lysosomal lipolytic activity were investigated. Monkeys were fed high-cholesterol diets supplemented with coconut oil (saturated fatty acids) alone or similar diets containing Menhaden fish oil (highly polyunsaturated omega-3 fatty acids) and coconut oil in 1:1 or 3:1 ratios for 12 months. Freshly isolated RPE cells from eyes removed at autopsy were assayed for lysosomal enzyme activity (Table V). Statistically significant elevations of acid lipase ( $P < .05$ ), acid esterase ( $P < .01$ ), and cholesteryl esterase

( $P < .01$ ) activity were observed when comparing the activity in RPE cells from monkeys fed the 3:1 fish oil and coconut oil diet to those from control monkeys fed coconut oil alone. RPE cells from monkeys whose diets contained equal amounts of fish oil and coconut oil (1:1 diet) also contained increased activity of all three enzymes, but these increases did not reach statistical significance.

Fixed, frozen sections of portions of a posterior ocular segment from each monkey were assayed histochemically for nonspecific acid esterase and acid lipase activity (Figure 11). Red-brown reaction product, identical to

*Retinal Pigment Epithelial Acid Lipase Activity and Lipoprotein Receptors*

**TABLE V: DIETARY FISH OIL MODULATION OF MONKEY RPE LYOSOMAL ENZYMES**

DIET	LYSOSOMAL ENZYME ACTIVITY*		
	ACID ESTERASE	ACID LIPASE	CHOLESTERYL ESTERASE
25% coconut oil/ 2% cholesterol	167 ± 61	145 ± 39	1,105 ± 150
12.5% coconut oil/12.5% fish oil/ 2% cholesterol	212 ± 65	183 ± 42	1,306 ± 327
6.25% coconut oil/ 18.75% fish oil/ 2% cholesterol	261 ± 56†	217 ± 68‡	1,778 ± 619†

RPE, retinal pigment epithelium.

\*Mean activities ±SD of RPE cell isolates from eyes of 8 monkeys in each group expressed as μM substrate hydrolyzed per hour per μg DNA for acid lipase and acid esterase and as counts per minute per hour per μg DNA for cholesteryl esterase.

†*P*<.01, compared to 25% coconut oil/2% cholesterol diet.

‡*P*<.05, compared to 25% coconut oil/2% cholesterol diet.

**TABLE VI: FISH OIL MODULATION OF HISTOCHEMICAL STAINING FOR MONKEY RPE LYOSOMAL ENZYMES**

DIET	INTENSITY OF HISTOCHEMICAL ACTIVITY*	
	ACID ESTERASE	ACID LIPASE
25% coconut oil/ 2% cholesterol	2.0 ± 1.1	1.4 ± 0.7
6.25% coconut oil/18.75% fish oil/ 2% cholesterol	3.4 ± 4†	3.2 ± 0.7‡

RPE, retinal pigment epithelium.

\*Mean grading of staining intensity ±SD of eyes from 8 monkeys in each group on a 0 to 4 scale by 2 masked observers.

†*P*<.01, compared to 25% coconut oil/2% cholesterol diet.

‡*P*<.001, compared to 25% coconut oil/2% cholesterol diet.

that observed in the albino rabbit studies (Figure 11C, 11F), could be readily discerned from endogenous RPE pigment. Staining, corresponding to enzyme activity, was greater for acid esterase (Figure 11A) and acid lipase (Figure 11D) in animals fed the 3:1 fish oil and coconut oil diet than in those fed coconut oil alone as shown in Figures 11B and 11E, respectively. The distinctive red-brown reaction product of the enzymatic histochemical assays was distinct from the red fluorescence due to DiI-labeled N-, A-, and O-LDL incorporation in RPE monolayers (Figure 11G, 11H, 11I) and in RPE cells exposed to the fluorescent lipoproteins (Figure 11D, 11K, 11L). Quantitation of the degree of histochemical staining on a scale of 0 (no stain) to 4 (intense stain) by two masked observers confirmed that the increased RPE histochemical staining was statistically significant for nonspecific acid esterase (*P*<.01) and acid lipase (*P*<.001) (Table VI).

Fish oil modulation of liver and spleen acid lipase (*P*<.001) and cholesteryl esterase activity generally cor-

roborated the RPE results (Table VII). Acid lipase and cholesteryl esterase were significantly elevated in the livers of monkeys fed a 3:1 diet of fish oil and coconut oil when compared with those fed coconut oil alone. The same was true for splenic acid lipase (*P*<.01) and cholesteryl esterase (*P*<.05). Acid lipase enzyme activity was also significantly elevated in livers of monkeys fed equal amounts of coconut and fish oils (*P*<.05). These data indicate a systemically beneficial effect in enhancing acid lipolytic efficiency.

To determine whether circulating lipoproteins from the monkeys fed diets supplemented with fish oil directly enhance RPE lysosomal enzyme activity, cultured monkey RPE cells were incubated for 24 hours with 10% sera removed at autopsy prior to RPE biochemical enzyme assays (Table VIII). Statistically significant increases in acid lipase (*P*<.01), acid esterase (*P*<.05), and cholesteryl esterase (*P*<.01) activity were present in RPE cells exposed to serum from monkeys fed a 3:1 diet of fish oil

TABLE VII: FISH OIL MODULATION OF MONKEY LIVER AND SPLEEN LYSOSOMAL ENZYMES\*

DIET/ORGAN	ACID LIPASE	CHOLESTERYL ESTERASE
<b>Liver</b>		
25% coconut oil/ 2% cholesterol	61 ± 2	1,474 ± 76
12.5% coconut oil 12.5% fish oil/ 2% cholesterol	106 ± 11†	1,380 ± 125
6.25% coconut oil/ 18.75% fish oil/ 2% cholesterol	223 ± 24‡	2,883 ± 494§
<b>Spleen</b>		
25% coconut oil/ 2% cholesterol	101 ± 10	5,053 ± 309
12.5% coconut oil 12.5% fish oil/ 2% cholesterol	120 ± 12†	4,572 ± 236
6.25% coconut oil/ 18.75% fish oil/ 2% cholesterol	194 ± 35§	5,935 ± 395†

\*Mean activities ±SD of homogenates from eyes of 8 monkeys in each group expressed as  $\mu\text{M}$  substrate hydrolyzed per hour per  $\mu\text{g}$  DNA for acid lipase and acid esterase and as counts per minute per hour per  $\mu\text{g}$  DNA for cholesteryl esterase.

† $P < .05$ , compared to 25% coconut oil/2% cholesterol diet.

‡ $P < .001$ , compared to 25% coconut oil/2% cholesterol diet.

§ $P < .01$ , compared to 25% coconut oil/2% cholesterol diet.

TABLE VIII: EFFECTS OF FISH OIL-FED MONKEY SERUM ON LYSOSOMAL ENZYME ACTIVITY IN CULTURED MONKEY RPE CELLS

LYSOSOMAL ENZYME ACTIVITY OF RPE CELLS OVERLAID WITH SERUM*				
LYSOSOMAL ENZYME†	LIPOPROTEIN- DEFICIENT SERUM‡	25% COCONUT OIL/ 2% CHOLESTEROL	12.5% COCONUT OIL/ 12.5% FISH OIL/ 2% CHOLESTEROL	6.25% COCONUT OIL/ 18.75% FISH OIL/ 2% CHOLESTEROL
Acid lipase (8)	1.00 ± 0.29 (25)	1.21 ± 0.24	1.36 ± 0.22	1.61 ± 0.26§
Acid esterase (8)	1.00 ± 0.20 (32)	1.15 ± 0.14	1.31 ± 0.22	1.43 ± 0.32
Cholesteryl esterase (8)	1.00 ± 0.13 (161)	1.22 ± 0.25	1.54 ± 0.50	1.81 ± 0.45§

\*Cells overlaid with media containing 10% vol/vol of each type of monkey serum; activities ±SD expressed relative to mean activities of control groups with the mean activity of each control group expressed as unity ±SD.

†Number of separate cell samples pooled from experiments.

‡Mean activity of pooled control cell cultures expressed as  $\mu\text{M}$  substrate hydrolyzed per hour per  $\mu\text{g}$  DNA for acid lipase and acid esterase and as counts per minute per hour per  $\mu\text{g}$  DNA for cholesteryl esterase.

§ $P < .01$ , compared to serum from 25% coconut oil/2% cholesterol-fed animal.

|| $P < .05$ , compared to serum from 25% coconut oil/2% cholesterol-fed animal.

and coconut oil when compared with the enzyme activity measured in RPE cells exposed to sera from coconut oil-fed monkeys. Elevations in RPE enzyme activity after exposure to sera from monkeys fed 1:1 fish oil and coconut oil were measurably, but not statistically significant, elevated over the levels of enzyme activity in RPE cells exposed to sera from monkeys fed coconut oil alone.

Of note, RPE cells exposed to sera from animals fed only coconut oil did not induce statistically significant increases in RPE lysosomal enzyme activity over that measured in RPE cells exposed to LDS from chow-fed monkeys (Table VIII). This finding contrasts with the significant elevations observed for native LDL from chow-fed animals (Table IV) and may indicate that even diets

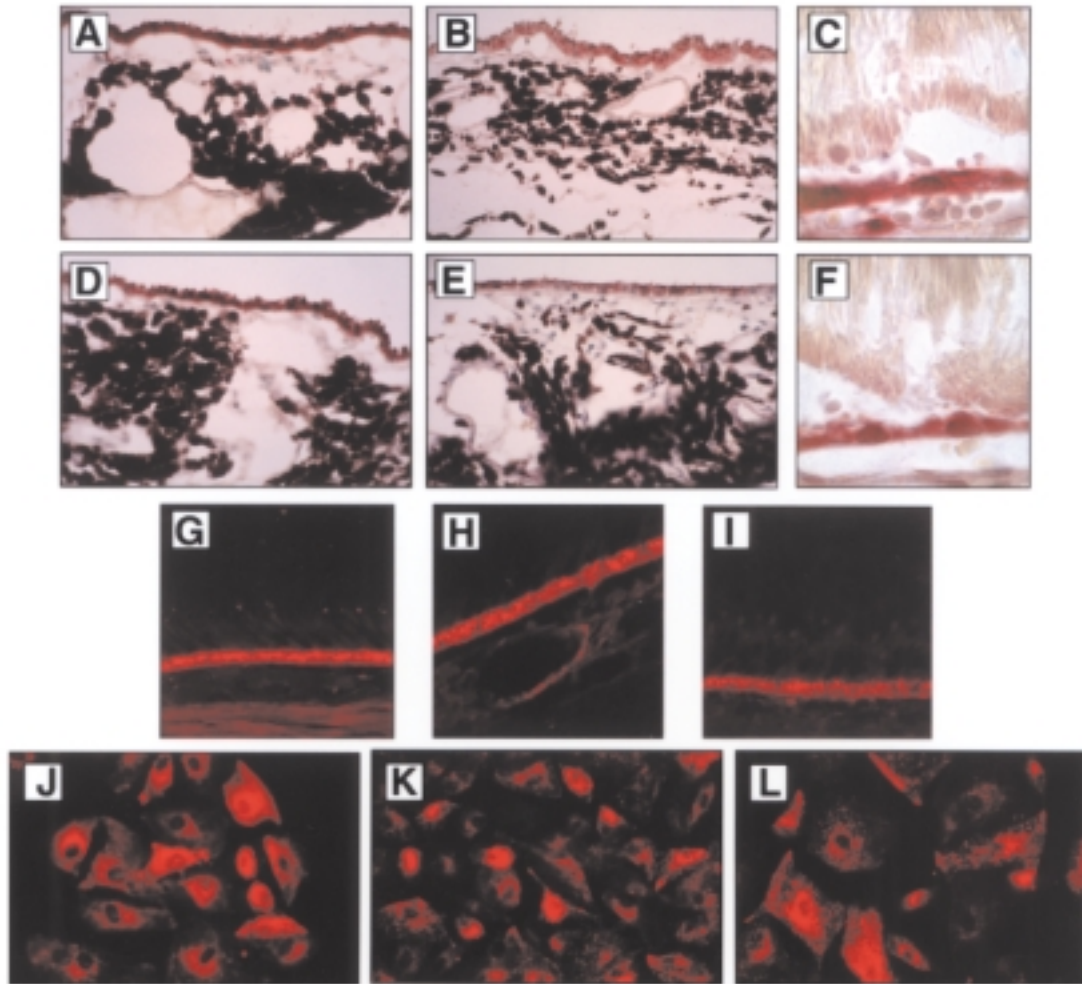


FIGURE 11

Histochemical detection of acid lipase and nonspecific acid esterase activity in fixed, frozen sections of eyes from monkeys fed coconut oil-rich and fish oil-rich diets. Retinal pigment epithelial (RPE) monolayers in monkeys fed fish oil show more intense red-brown staining for acid lipase (A) and acid esterase (B) than RPE monolayers of coconut oil-fed monkeys stained simultaneously for acid lipase (C) and acid esterase (D) activity (all methyl green counterstain, x100). Reference histochemical staining acid esterase (E) and acid lipase (F) in New Zealand White rabbit albino eye lacking autogenous brown pigment (both methyl green counterstain, x400). Comparative color of red, fluorescent DiI-labeled N-LDL (G), A-LDL (H), and O-LDL (I) uptake by RPE monolayer after in vivo perfusion of monkeys (all x400) and if DiI-labeled N-LDL (J), A-LDL (K), and O-LDL (L) uptake by RPE cells in vitro (all x400).

not supplemented with fish oil may affect RPE lysosomal function.

## DISCUSSION

### STUDIES ON ACID LIPASE IN RPE CELLS

The prominent phagocytic function of the RPE correlates with the high activities of hydrolytic lysosomal enzymes found in RPE cells.<sup>49-51</sup> Studies on RPE lipid metabolism have involved assessments of RPE lipid profiles, particularly of retinyl-fatty acid esters and phospholipids containing various saturated and unsaturated fatty acids, including high levels of DHA and arachidonic acid.<sup>21,148-150,218-221</sup> RPE lipolytic enzymes, especially acid lipase, may be of particular importance in RPE metabolism because

of the massive amount of lipid-rich, POS material that the RPE phagocytizes and degrades daily. However, a simple reproducible biochemical assay and a histochemical technique for the in situ or in vitro detection of acid lipase activity have not been applied to the study of RPE lipid metabolism.

In this study, as reported previously,<sup>76,77</sup> consistent and specific staining for acid lipase was obtained in tissues when dispersion of  $\alpha$ -naphthyl palmitate with the non-ionic detergent Triton X100 was used (Figures 1, 2, and 11). Histochemically, acid lipase activity was readily detected in cells active in the uptake and processing of neutral lipids, namely, the mononuclear phagocytes of the reticuloendothelial system, as well as in RPE cells in the eye. With use of the same artificial substrate, enzyme

activity had not been detectable in a case of human acid lipase deficiency (Wolman's disease).<sup>77</sup> One important advantage of utilizing naphthyl palmitate-Triton X 100 substrate micelles for the detection of acid lipase activity is the associated histochemical staining technique that may be employed for *in situ* or *in vitro* studies. Although albino New Zealand White rabbits initially were used in this study to avoid obscuration of the red-brown histochemical reaction product by endogenous RPE melanin (Figures 1 and 2), discrete and selective *in situ* staining for monkey RPE acid lipase activity was also obtained (Figure 11). The ability to stain for acid lipase activity may be particularly valuable in the study of human retinal lesions, since (1) eyes with retinal diseases are available only in small numbers, (2) RPE cell harvesting necessitates disruption of the specimen, and (3) RPE cells are few in number and difficult to harvest for cell culture studies, particularly when diseased.

Studies were then performed to prove that the chromogenic biochemical assay and histochemical technique were specific for acid lipase and show the lipid metabolic functions subserved by this enzyme. Acid lipase derived from isolated, sonicated bovine RPE cells hydrolyzed triglycerides and cholesteryl esters as well as the artificial substrate  $\alpha$ -naphthyl palmitate at acid pH (Figure 4). Biochemical evidence for the exclusive hydrolysis of this artificial fatty acid ester substrate by acid lipase at low pH included sequential purification of bovine RPE acid lipase activity by gel and ion exchange chromatography, followed by electrophoresis, resulting in a single silver-stained band with acid lipolytic activity. Acid lipase activity, detected by  $\alpha$ -naphthyl palmitate hydrolysis, was competitively inhibited by a natural triglyceride substrate of acid lipase, triolein, as well as by the organophosphate, DEPP, and the organomercurial, PHMB, consistent with previous observations.<sup>77</sup> Bovine RPE acid lipase activity detected by hydrolysis of triolein in triolein-lecithin substrate vesicles could not be separated from that detected by the hydrolysis of  $\alpha$ -naphthyl palmitate in  $\alpha$ -naphthyl palmitate-Triton X100 micelles at any stage in the purification process (Figures 3 through 6). The very similar, if not identical, migratory behavior of both of these hydrolytic activities purified by sequential protein purification techniques suggests that both the natural substrate, triolein, and the artificial substrate,  $\alpha$ -naphthyl palmitate, are hydrolyzed by the same enzyme. The natural substrate, triolein, was a potent competitive inhibitor of  $\alpha$ -naphthyl palmitate hydrolysis by bovine RPE cell extracts and monkey RPE cell sonicates. This effect is not due to the mere physical presence of triolein in the  $\alpha$ -naphthyl palmitate-Triton X100 micelles, since introduction of equivalent amounts of trioleylglycerylether did not produce a detectable inhibitory effect.<sup>77</sup> Bovine RPE acid lipase had

an apparent  $M_r$  of 64,000 to 66,000 d, as estimated by polyacrylamide-SDS electrophoresis (Figure 5), comparing favorably with that of rat liver acid lipase reported by Kaplan and Teng.<sup>222</sup>

Bovine RPE lysosomal acid lipase was first demonstrated by Rothman and associates<sup>67</sup> and Hayasaka and associates<sup>68,69</sup> employing substrates that were poorly soluble or required organic extraction and fractionation. Hayasaka and associates<sup>68,69</sup> purified acid lipase from crude RPE extracts. As in this study, they found acid lipase activity to be very labile, with 50% loss of activity during 12-hour dialysis at 0°C or during 48-hour storage at -20°C while purifying the enzyme using ammonium sulfate fractionation, void volume separation with Sepharose 6B gel chromatography, and diethyl-aminoethyl Sephadex ion exchange chromatography (Figure 4).

Rothman and associates<sup>67</sup> used 4-methylumbelliferyl palmitate and Hayasaka and associates<sup>68,69</sup> used [<sup>3</sup>H]-labeled triglycerides as substrates for acid lipase activity. The latter investigators found bovine RPE acid lipase to enrich in the lysosomal fractions, to have a pH optimum of 4.0 to 5.0, to be heat-sensitive, and to be inactivated by the organomercurial, p-chloromercuribenzoate. All of these findings are consistent with the enzyme activity measured with the  $\alpha$ -naphthyl palmitate-Triton X100 micelle chromogenic assay and histochemical technique. The Triton X100 activation of acid lipase found by these investigators was probably due to optimizing surfactant-substrate ratios and micellar surface properties, including charge.<sup>223</sup> The addition of this nonionic detergent thus contributed to maximally efficient substrate hydrolysis by acid lipase, a distinct advantage of the methodology used in this study.

This study also confirms the findings of Hayasaka and associates<sup>68,69</sup> and Teng and Kaplan,<sup>224</sup> who found that purification of lysosomal acid lipase by molecular sieve and/or ion exchange chromatography results in activity elution in trailing or multiple peaks and in poor enrichment of acid lipase activity due to the formation of enzyme aggregates. Pitfalls in the purification of acid lipase include not only the inactivation of even semipurified forms during storage, but also instability in the presence of inorganic salts and high affinity for hydrophobic surfaces.<sup>225</sup> In this study, bovine RPE acid lipase also was eluted from SP-Sephadex C-50 in the void volume due to the low salt concentrations necessary to avoid enzyme inactivation. Significant loss of acid lipase activity also occurred during the purification procedures in this study, presumably on account of a combination of (1) contaminating proteases, (2) denaturation, (3) aggregation, (4) exposure to salts,<sup>225</sup> and (5) extraction of the hydrophobic enzyme from cell membranes or other hydrophobic constituents necessary for maximal enzyme activity.

Copurification of triglyceride lipase, as detected by  $\alpha$ -naphthyl palmitate hydrolysis, and cholesteryl esterase activities from bovine RPE cells has been reported in other tissues. Brown and Sgoutas<sup>226</sup> purified rat liver lysosomal cholesteryl esterase with an apparent  $M_r$  of 60,000 d, and also found cholesteryl esterase and triglyceride lipase activities to cochromatograph throughout their isolation procedures. Burton and Mueller<sup>227</sup> and Warner and associates<sup>228</sup> demonstrated the hydrolysis of cholesteryl oleate, triolein, and 4-methylumbelliferyl oleate at acid pH by human placental and hepatic acid lipases during sequential purification steps, during which considerable acid lipolytic activity was lost. The authors of these studies also concluded that acid lipase was responsible for cholesteryl ester and triglyceride hydrolysis.

In addition to hydrolyzing  $\alpha$ -naphthyl palmitate, triolein, and cholesteryl oleate, the purified RPE enzyme fraction was found to form cholesteryl esters at acid pH (Figures 3 through 6). The substrate used to demonstrate cholesteryl ester formation in the present study contained no cholesteryl ester, but the kinetic conditions were in favor of cholesteryl ester synthesis by the purified enzyme. In the cholesterol esterification assay, the substrate contained only phospholipid, triglyceride, and radioactively labeled and unlabeled cholesterol in vesicle form. Since there was no free source of fatty acid to esterify to cholesterol, only hydrolysis of the lecithin or triglyceride could provide fatty acids for cholesteryl esterification. Burrier and Brecher<sup>229</sup> and Brecher and associates<sup>207</sup> used similar lecithin substrate vesicles to demonstrate cholesteryl esterase and triglyceride hydrolysis. They found that at pH 4.5, only cholesteryl esters and triglycerides were hydrolyzed, and not phospholipids. In this study, purified acid lipase from bovine RPE cells also showed triglyceride hydrolytic activity, indicating that the enzyme may hydrolyze triglycerides and subsequently esterify the liberated fatty acids to cholesterol, probably only after the free fatty acid concentration is sufficient to drive the reaction thermodynamically to form cholesteryl esters. Further support for cholesterol esterification by acid lipase is provided by a previous study of monkey splenic acid lipase, which had similar hydrolytic and esterification activities, as well as an  $M_r$  of 64,000 d when purified as described for the bovine RPE cell sonicates.<sup>77</sup>

The hydrolysis of the artificial substrate  $\alpha$ -naphthyl palmitate to free  $\alpha$ -naphthol and palmitic acid in chromogenic biochemical assays paralleled the activities for triglyceride and cholesteryl ester hydrolysis and cholesterol esterification. This simple chromogenic technique appeared to correlate well with assays for activities associated with acid lipase activity and therefore is an effective means for indirect assay of acid lipase hydrolytic and esterification activities. When applied to retinal tissue,

this methodology may demonstrate the significance of acid lipase in RPE accumulation of cholesteryl esters, lipid metabolites, and peroxidized, undigestible lipids, including lipofuscin. Cholesterol and fatty acid concentration-dependent, thermodynamically driven cholesteryl ester synthesis by acid lipase might occur in RPE cells that phagocytize lipid-rich POS membranes,<sup>29,33-37</sup> have active autophagocytic mechanisms,<sup>47</sup> and incorporate exogenous native and modified LDLs *in vivo*.

The chromogenic biochemical assay confirmed the findings of the histochemical diazocoupling technique. RPE cells were found to contain lysosomal acid lipase activity comparable to that of mononuclear phagocytes (Table I). New Zealand White rabbit RPE acid lipase activity was one fortieth of that found in alveolar macrophages, which demonstrated the highest activity of all mononuclear phagocytes assayed, but one fourth of that found in peritoneal macrophages. Although RPE cells had less activity than all of the tissue histiocytes examined, they demonstrated considerably more activity than monocytes and cultured smooth-muscle cells. The acid lipase activity found in rabbit RPE cells was consistent with the acid lipase activity necessary for positive histochemical staining in fixed, frozen tissue sections, namely, 36  $\mu$ M of hydrolyzed substrate/ $10^6$  cells/hour.<sup>76</sup> Accordingly, New Zealand White rabbit RPE cells stained selectively in sections of the posterior ocular segment (Figures 1 and 11), a finding which corresponds to the observation of selective mononuclear phagocyte staining for acid lipase activity in fixed, frozen sections of liver (Figure 2A), spleen (Figure 2B), and lung (Figure 2C). The high and histochemically stainable level of acid lipase activity in RPE cells may reflect the consequence of their prominent role in the phagocytosis and turnover of lipid-rich POS and incorporation of LDL from the systemic circulation, inasmuch as POS (Table II) and LDL (Table IV) stimulate RPE acid lipase activity.

Hayasaka and associates<sup>68,69</sup> also revealed high levels of acid lipase activity in RPE cells when compared to liver, kidney, and blood tissue homogenates, but RPE acid lipase activity was not evaluated with respect to isolated cell types. Our studies utilized a modified microcarrier culture technique, which allows comparison of freshly isolated, glass-adherent RPE cell enzyme activities to those of freshly isolated, glass-adherent mononuclear phagocytes (Table I). Assays on these cell preparations yielded direct measurements of enzyme activities in specific cell types. This technique may be adapted to cell culture studies and yield information that cannot be obtained using whole-tissue homogenates.

Deficiencies or defective augmentation of RPE lysosomal acid lipase activity in response to various metabolic, particulate, inflammatory, or immunologic stimuli may be

important to normal RPE aging and to the pathogenesis of various heritable and nonheritable retinal diseases. Of particular interest are those characterized by the accumulation of indigestible lipid residues that are incorporated into RPE cytoplasmic residual bodies as the lipopigment lipofuscin.<sup>72,82</sup> Deposition of lipofuscin has been shown to accumulate during aging<sup>79,116</sup> and reach massive proportions in various RPE degenerations<sup>5,230-243</sup> and to be extruded from RPE basal surfaces,<sup>87,154</sup> contributing to progressive lipid accumulation in Bruch's membrane,<sup>88</sup> and the formation of basal laminar and linear deposits and drusen.<sup>86,87,92-98,230,234</sup> Deficient acid lipase activity may also be important in diseases such as retinitis pigmentosa, where the inefficient elimination of POS debris<sup>37,244-249</sup> may contribute to outer retinal degeneration. A role for acid lipase deficiency in the pathogenesis of outer retinal disease is underscored by observations of tapetoretinal degeneration in patients with biochemically verified acid lipase deficiency and clinically manifest neutral lipid storage disease.<sup>250,251</sup> Alternatively, lipid esterification by acid lipase might occur under appropriate kinetic conditions as shown in this study (Figures 3, 4, and 6), thereby accumulating lipids in the RPE cytoplasm, where they may become subject to lipid peroxidation, leading to lipofuscin formation and RPE dysfunction,<sup>81,82,101-105</sup> including further loss of RPE antioxidant protection.<sup>81</sup> This scenario might then result in RPE deposition<sup>86,87</sup> of lipids, cholesterol, and cholesterol esters that are seen in Bruch's membrane with aging and in drusen.<sup>89-91</sup> The presented methodology may be helpful to assist in vitro investigations of RPE cell enzyme activity and in situ studies of the retina in health and disease that could not be previously performed.

Variations in intracellular and secreted RPE lysosomal enzyme activities in vitro may be ascribed to culture conditions and to the type and duration of inducing stimuli. Basal RPE cell activation and, hence, response to various phagocytic stimuli may be influenced by in vitro conditions, including RPE cell confluency, culture flask surface, culture media, and serum supplementation. Numerous studies have documented variable RPE avidity for and time course of uptake of various particles, including latex microspheres, under different organ culture and tissue culture conditions.<sup>39,112,114,247,252</sup> In this study, monkey RPE cells synthesized and secreted substantial basal levels of lysosomal enzymes in vitro (Tables V and VI). Significant increases over basal RPE intracellular lysosomal enzyme activities of monkey cells (Table V) were induced to a much greater degree by POS than nonspecific, control latex microsphere phagocytic challenge (Table VI). In contrast to latex, the greater POS-induced increases in RPE intracellular lysosomal enzyme activities were not accompanied by significant increases in enzyme secretion over the already substantial basal levels secreted

by the unstimulated RPE cell layers (Table VI). The specificity of RPE cellular responses to various phagocytic stimuli that was observed may be related to early-response genes such as *zif-268*, *c-fos*, and *tis-1*, which are rapidly and transiently expressed in cultured rat RPE cells during phagocytosis of bovine POS.<sup>253</sup> These inductions are thought to modulate a gene cascade of intracellular responses to POS phagocytosis, but are not activated in RPE cells during the phagocytosis of nonspecific particles such as latex beads. Moreover, increases in RPE intracellular and secreted lysosomal enzyme activities were not observed in response to the soluble, nonspecific stimulant, phorbolmyristic acid (PMA) (results not shown), further supporting the specificity of RPE cellular responses to phagocytic stimuli.

Native LDL also significantly enhanced RPE acid lipase and cholesteryl esterase activity (Table IV). Although it is likely that other serum constituents may affect RPE lysosomal function, the fact that RPE cells exposed to the lipoprotein-deficient serum from which the native LDL was derived had significantly less activity implies that the LDL per se induced RPE lysosomal lipolytic activity in this study. These increases in acid lipolytic activity suggest that receptor-mediated uptake of lipid-rich particulates may regulate RPE biochemical events after their incorporation. Such regulation may involve receptor-dependent induction of the aforementioned genetic responses<sup>253</sup> that may also assist in perpetuating the efficient uptake and subsequent degradation of the large amounts of lipid-rich material that is continually presented to these cells.

Mechanisms regulating RPE extracellular release of lysosomal enzymes have not yet been elucidated. However, acid hydrolases have been reported in the space beneath the neurosensory retina under physiologic conditions<sup>74,254</sup> and in cases of rhegmatogenous retinal detachment<sup>255</sup> and retinal dystrophies.<sup>75,256,257</sup> Moreover, the accumulation of lysosomal enzyme activities appears to be carefully controlled in a highly selective manner from excessive accumulation by specific cell surface receptors.<sup>258</sup> In this study, RPE phagocytosis of latex beads, and to a much lesser extent of POS, resulted in release of lysosomal enzyme activity into the overlying media (Table VI). This apparent stimulus-dependent release of RPE enzyme activity during phagocytosis may be due to leakage of lysosomal hydrolases when nonphysiologic or large debris are engulfed or persist in RPE cells. This observation raises the possibility that damage to patches of the RPE monolayer may occur because of leakage of RPE lysosomal enzymes when abnormal particulates are engulfed or persist in RPE cells. Such particulates may include abnormal POS in retinal dystrophies, peroxidatively damaged autophagocytic debris, oxidized or other

modified lipoproteins, and indigestible residues, including lipofuscin and A2E, which compromise RPE lysosomal function and integrity.<sup>81-83,101,148</sup> Moreover, extracellular nonlysosomal enzymes, including metalloproteinases, are known to be secreted as inactive forms that require postsecretory enzymatic cleavage for activation.<sup>259,260</sup> RPE lysosomal leakage into the extracellular space may activate these MMP by cleaving them into active forms.<sup>261-264</sup> The principal lysosomal enzymes subserving this function are cathepsins B and D,<sup>261,262</sup> the latter being the principal RPE protease that degrades engulfed POS protein.<sup>56,57</sup> Once hydrolyzed by the activated metalloproteinases, the extracellular lysosomal enzymes are then capable of further degrading fragments generated by metalloproteinase activity.<sup>265,266</sup> Thus, hydrolytic enzymes released into the pericellular environment because of inefficient lysosomal degradation of debris may also result in localized damage to connective tissues as well as neighboring RPE cells and cells of the neurosensory retina. Ultrastructural cytochemical evidence of discharge of secondary lysosomes from aged RPE cells directly into Bruch's membrane provides direct evidence that such a process indeed occurs.<sup>85</sup>

Analogous to RPE cells, intracellular mononuclear phagocyte lysosomal enzyme activity and, to a lesser extent, enzyme release may be enhanced by phagocytosis of particulates, including latex microspheres, zymosan, opsonized erythrocytes, antigen-antibody complexes, and bacteria.<sup>215,264,267-270</sup> Moreover, mononuclear phagocytes that have phagocytized indigestible bacteria or have been activated by thioglycollate synthesize and release substantially more lysosomal enzyme activities following subsequent phagocytic challenge.<sup>264,271,272</sup> These mononuclear phagocyte responses support our findings that show RPE lysosomal enzyme synthesis and secretion to be dependent on the type of phagocytic stimulus.

#### **LIPOPROTEIN UPTAKE BY MONKEY RPE CELLS IN VITRO AND IN VIVO**

DiI-labeled, A-LDL is bound and internalized by specific receptors on macrophages and may be used to distinguish bone marrow-derived mononuclear phagocytes from other cells in cell culture and in tissue sections.<sup>211,273</sup> Control incubations using cultured macrophages and smooth-muscle cells confirmed that successful modification of isolated N-LDL for our RPE studies. Accordingly, only macrophages avidly incorporated A-LDL and O-LDL while smooth-muscle cells only internalized N-LDL. Macrophage uptake of A-LDL was abolished by fucoidin, a specific A-LDL that did not block N-LDL binding and uptake and only partially reduced O-LDL uptake, presumably because of O-LDL uptake by other O-LDL receptors not blocked by fucoidin.<sup>85,132,135-137,139</sup>

RPE cells incubated with either DiI-A-LDL or O-

LDL, like macrophages, exhibited intense surface and cytoplasmic granular red fluorescence, presumably owing to lysosomal incorporation of the modified lipoproteins (Figures 8 and 11). The incomplete blockage of DiI-O-LDL uptake by fucoidin was probably due to the fact that the RPE possesses other scavenger receptors, such as CD68 and CD36, that may also mediate RPE O-LDL uptake.<sup>140-142</sup> RPE cells also avidly incorporated DiI-N-LDL, indicating that these cells do not demonstrate the selectivity of mononuclear phagocytes or smooth-muscle cells for lipoproteins but, rather, actively bind and internalize native and modified lipoproteins.<sup>128,129</sup> Following *in vivo* perfusion with the DiI-labeled, modified lipoproteins, the RPE exhibited intense fluorescence (Figures 9 and 11) comparable to that of resident mononuclear phagocytes of liver, spleen, and lung removed from the same animals (Figure 10). In these organs, perfused DiI-A-LDL and DiI-O-LDL were selectively incorporated into mononuclear phagocytes, in sharp contrast to their lack of labeling by perfused N-LDL, which was avidly incorporated into hepatocytes. In all of the tissues examined histologically, discrete uptake of labeled A-LDL and O-LDL was visualized in vascular endothelial cells as previously reported.<sup>274</sup> The lesser degree of DiI-O-LDL fluorescence present in tissues other than the liver may indicate rapid clearance by this organ in spite of the site of perfusion (ie, the carotid arteries). These *in vivo* observations, together with the selective alveolar macrophage and smooth-muscle cell lipoprotein uptake and the successful use of specific inhibitors, leads to the conclusion that RPE cells possess specific receptors for rapid, high-affinity N-, A-, and O-LDL binding and uptake *in vitro*<sup>128,129</sup> and *in vivo*.

High-affinity N-LDL receptors on RPE cells are likely to subservise physiologic functions by efficient culling of native lipoproteins from the blood to provide nourishment for the outer retina (Figures 9 and 11). It is possible that lipids derived from lipoproteins, from phagocytized, lipid-rich photoreceptor membranes, and from autophagocytosis might converge in, and possibly overwhelm, the RPE lysosomal pathway, leading to the intracellular accumulation of lipid in aging and disease. The results of this study suggest that this is unlikely, since POS membranes and N-LDL appear to induce compensatory increases in lysosomal enzyme activity (Tables II and IV).

However, RPE sequestration of modified lipoproteins, particularly oxidized LDL, may have adverse consequences. Intracellular accumulation of lipid, particularly cholesteryl esters, is specifically promoted by lysosomal hydrolysis of lipids internalized via scavenger receptor pathways.<sup>131-134,216,275</sup> Intracellular accumulation of lipid *per se* does not appear to cause cellular dysfunction and death, but light- and oxygen-induced free radicals and peroxides may cause peroxidation of accumulated lipid,

leading to indigestible lipid metabolites. The RPE contains many antioxidants for neutralizing reactive oxygen intermediates that are generated by the combined actions of high RPE oxidative metabolism and light absorption by RPE pigment.<sup>6,28,40,276,277</sup> High levels of vitamin C,<sup>278,279</sup> vitamin E,<sup>280-283</sup> peroxidase,<sup>284</sup> superoxide dismutase,<sup>285-287</sup> catalase,<sup>286,288,289</sup> glutathione,<sup>185,290</sup> and selenium<sup>291</sup> serve to protect the RPE cells and surrounding tissue by neutralizing reactive oxygen species,<sup>292,293</sup> some of which are generated in response to POS phagocytosis.<sup>294</sup> When these protective mechanisms are overwhelmed, however, extracellular modifications of N-LDL, similar to *in vitro* acetoacetylation or oxidation,<sup>133,134,216</sup> may result in forms recognized by the scavenger receptors,<sup>85,131,135,136,143</sup> some of which have been identified on RPE cells.<sup>140-142</sup> These modifications include exposure to oxidizing vascular endothelial cell metabolites,<sup>275,295,296</sup> peroxide,<sup>297</sup> and highly reactive, oxidized by-products of arachadonic acid, such as malonaldehyde and malondialdehyde, that are secreted by platelets, macrophages, and vascular endothelial cells *in vivo*.<sup>298,299</sup>

In the outer retina, RPE cells may participate in this process, since they contain high levels of POS-derived arachidonic acid<sup>218,219,300</sup> that may undergo reactive oxygen intermediate-induced lipid peroxidation to produce reactive fragments that may then oxidize or otherwise modify native LDL arriving from the choroid.<sup>301</sup> The RPE also contains significant levels of phospholipases A<sub>1</sub> and A<sub>2</sub>,<sup>51</sup> the latter of which may induce vascular endothelial cells to produce oxygen metabolites<sup>275,295,296</sup> that cause LDL oxidation and modification to forms recognized by scavenger receptors. The same local modifications of circulating LDL that are likely to occur within the choriocapillaris and at the RPE-choriocapillaris interface may also result in local denaturation and oxidation of other extracellular lipids, proteins, and glycoproteins. Such modified molecules might then become subject to uptake by RPE scavenger receptors that mediate A- or O-LDL incorporation.<sup>214,302</sup> Lysosomal dysfunction may thus be further aggravated by high-affinity uptake and lysosomal incorporation of oxidized or denatured extracellular components by means of scavenger receptors.<sup>148</sup>

Local generation of reactive oxygen intermediates may also inhibit POS membrane phagocytosis<sup>303</sup> and degradation,<sup>82,83,148</sup> perpetuating the accumulation of denatured oxidized lipids and proteins, leading to formation of lipofuscin that further embarrasses POS degradation.<sup>81-83</sup> Lipofuscin is normally found in aging RPE cells,<sup>5,47,72</sup> but massive RPE cytoplasmic accumulations and basilar excrescences of this indigestible end product are seen in ARMD and in retinas from animals and humans with dietary antioxidant deficiency.<sup>235,288</sup> Clearly, inducing robust lysosomal lipolytic activity for efficient degradation

and recycling of lipid debris may be beneficial by mitigating this pathologic sequence of events. These observations, taken together with the demonstrated ability of LDL to induce acid lipase and to penetrate the RPE monolayer *in vivo*, leads to the speculation that dietary lipids incorporated into circulating LDL may reach the RPE and modulate its role in the development of ARMD.

#### EFFECTS OF FISH OIL ON RPE ACID LIPASE ACTIVITY

This study describes RPE lipid metabolic findings in the first and only primate study on the effects of long-term dietary fish oils as a portion of dietary fat in a highly atherogenic diet.<sup>190,192,193</sup> Analysis of these animals showed that fish oil in diet may effectively reduce atherosclerotic progression during severe atherogenic stimuli, even though high-density lipoprotein cholesterol was depressed by the administration of fish oil.<sup>190,192,193</sup> Administration of fish oil depressed the concentrations of all lipoproteins, a remarkable finding, since rhesus monkeys usually show a marked rise in LDL and LDL cholesterol when fed a 2% cholesterol diet no matter what other food fat is included to a 25% level.<sup>304,305</sup> In animals fed a diet of 3:1 fish oil to coconut oil, triglycerides were less prevalent than those found in animals fed coconut oil, presumably because of the fact that there were progressive declines in triglyceride secretion by hepatocytes handling fatty acids of increasing length and unsaturation (oleate > linolenate > arachidonate > eicosapentaenoate [EPA] > DHA). The lipoproteins of animals fed the 3:1 fish oil to coconut oil diet promoted significantly less cholesterol esterification in mononuclear phagocytes than lipoproteins of monkeys fed coconut oil alone.<sup>190,192</sup> The reduction in cholesterol esterification was at least partly due to the omega-3 fatty acids contained in the fish oil, since the percentage of these fatty acids in the circulating LDL of monkeys fed the 1:1 and 3:1 fish oil to coconut oil diets correlated with reduced acyl-CoA:cholesterol acyltransferase (ACAT) cholesterol esterification in mononuclear phagocytes.<sup>192</sup> In the animals fed the 3:1 fish oil to coconut oil diet, the concentration of lipoprotein particles in the plasma, their reduced apoprotein E–apoprotein B ratios, their predominant triglyceride and reduced cholesterol ester cores, and their reduced ability to induce cholesterol esterification contributed to the reduction in atherosclerosis in these monkeys.<sup>190</sup>

RPE cells from the eyes of these monkeys fed the 3:1 fish oil to coconut oil diet also demonstrated marked differences. Enhanced lysosomal lipolytic profiles were demonstrated in histologic sections of the eyes (Table VI, Figure 11) and in biochemical assays for acid lipase, acid esterase, and cholesterol esterase activities (Table V). The effect of fish oil diets on lysosomal lipolytic activity was not limited to the RPE cells, but appeared to be a sys-

temic effect demonstrated by enhanced activities measures in liver and spleen homogenates from the same animals (Table VII). Thus, the RPE appeared to share in the beneficial systemic effects bestowed by the fish oil diet. The effect of fish oil on RPE lysosomal lipolytic profiles may be due to RPE uptake of omega-3 fatty acid containing lipoproteins, which reduce cholesterol esterification and promote acid lipase and cholesterase activities.<sup>190-192</sup>

Experiments in which cultured RPE cells were exposed to the sera of these animals confirmed that RPE lysosomal induction was likely due to favorable lipoproteins impacting the RPE monolayer *in vivo*. Because of the fact that the monkey sera were needed for several analyses,<sup>190,192,193</sup> only small amounts of sera could be used for the RPE studies. This precluded LDL isolation and incubation with RPE cells, since much more than the available sera would have been required to perform such assays. Cultured monkey RPE cells exposed to the sera from monkeys fed the 3:1 fish oil to coconut oil diet exhibited increased lysosomal hydrolytic activity (Table VIII). Of particular interest was the observation that sera from monkeys fed coconut oil alone did not significantly increase lysosomal enzyme activity in cultured RPE cells when compared with LDS from chow-fed animals (Table VIII). This finding contrasted with the significant induction of enzyme activity in RPE cells exposed to native LDL from chow-fed animals over that obtained with LDS (Table IV). These data imply that dietary alterations in LDL, even without fish oil supplementation, may affect induction of RPE lysosomal enzyme activities. Taken together, these results show that diet may modulate RPE lysosomal activity in response to alterations in circulating lipoproteins for which the RPE cells express receptors, which mediate rapid LDL uptake by the monolayer. The enhanced RPE lysosomal activities observed in RPE cells exposed to LDL from monkeys fed fish oil-containing diets, but not coconut oil-containing diets, indicates that the type of fatty acids contained in LDL is important in the modulation of RPE lysosomal activity. Such increased activity is likely to be beneficial because it results in the efficient metabolism of fats and prevents intracellular accumulation of lipids that may then be subject to oxidative processes that may embarrass RPE cellular functions.

The beneficial effects of fish oil on RPE lysosomal lipid metabolism may be only one of several mechanisms by which omega-3 polyunsaturated fatty acids may reduce the risk for ARMD. A prominent feature of ARMD lesions is the presence of leukocytes that have infiltrated diseased retinal tissue from the blood to become intimately associated with RPE cells.<sup>306-308,326</sup> Proinflammatory cytokines, including interleukin (IL)-1, tumor necrosis factor (TNF), and interferon (IFN)- $\gamma$ , derived from infiltrating leukocytes and RPE cells and

surface receptors, such as intercellular adhesion molecule (ICAM)-1, are increasingly recognized as key participants in the evolution of ARMD lesions.<sup>306,307,326</sup>

Fish oils appear to have potent immunoregulatory and anti-inflammatory effects,<sup>309</sup> including suppression of (1) arachidonic acid-derived eicosanoids<sup>309,310,327-329</sup>; (2) major histocompatibility type II (MHC II; HLA-DR) antigen expression<sup>311,312</sup>; (3) cell adhesion molecules, including ICAM-1<sup>309,330,331</sup>; (4) responses to endotoxins<sup>310,321,322,327,328,332,333</sup>, and (5) production of and response to proinflammatory cytokines.<sup>309,313,319,323</sup> Cultured cells and cells from animals fed fish oils rich in omega-3 polyunsaturated fatty acids, particularly DHA and EPA, incorporate them into their cell membranes, which become depleted of arachidonic acid.<sup>309</sup> The membranes become more fluid,<sup>329</sup> imparting reduced activity to proinflammatory surface receptors, including IFN- $\gamma$  and TNF receptors and scavenger receptors for A- and O-LDL.<sup>314-317,330</sup> DHA and EPA also inhibit the elaboration of IL-1<sup>318,328,333</sup> and TNF<sup>318,319,321,328,333</sup> from leukocytes and reduce responses to TNF, IL-1, and IFN- $\gamma$ .<sup>312,313,332</sup> The reduced inflammatory responses to these cytokines are at least partially mediated by omega-3 polyunsaturated fatty acid inhibition of intracellular signaling cascades and transcription factors controlling gene transcription.<sup>334</sup> In animal models, fish oil reduces the severity of autoimmune disease and indicators of disease activity, including TNF and IL-6.<sup>310,323-325</sup> The myriad of mechanisms by which omega-3 polyunsaturated fatty acids inhibit the production and actions of proinflammatory cytokines, reduce expression of cellular adhesion molecules that bind and stimulate leukocytes, and inhibit intracellular responses mediating inflammatory responses, all of which have been shown to be operative in RPE cells,<sup>4,306-308,326</sup> is likely to ameliorate mechanisms that lead to RPE damage and the development of ARMD.

Another important effect of dietary fish oil is omega-3 polyunsaturated fatty acid-induced reduction of nitric oxide<sup>321-323,332,335</sup> and reactive oxygen intermediates,<sup>325,336</sup> *in vitro* and *in vivo*. Reduced nitric acid and superoxide responses to TNF, IL-1, and IFN- $\gamma$  prevent the formation of peroxynitrite, a strong oxidizer causing cellular damage.<sup>310,319-322</sup> Inhibiting reactive oxygen species may be important to preventing systemic and localized LDL modification in the retina that would subject LDL<sup>317,325,330</sup> reaching the RPE monolayer to lysosomal incorporation by RPE A-LDL and O-LDL receptors.<sup>128,129</sup> Nevertheless, there is strong evidence that the LDL of animals and humans eating fish-oil-rich diets contains high levels of omega-3 polyunsaturated fatty acids that are subject to peroxidation.<sup>336-340</sup> Such oxidative processes utilize polyunsaturated fatty acids as substrates for peroxidation yielding reactive oxygen intermediates, lipoperoxides, and O-LDL, resembling the pathologic retinal process of

lipofuscin formation and toxicity in aged, damaged RPE cells.<sup>81-83,101-105,148</sup> Cells, including RPE cells, incorporating O-LDL that reaches the RPE monolayer from the blood (Figures 9 and 11) may then suffer adverse consequences, including embarrassment of RPE lysosomal, antioxidant, and POS degradative activities.<sup>81,317,325,330</sup> Ikeda and associates<sup>183</sup> provided recent clinical evidence that such processes may indeed contribute to ARMD in humans. These investigators showed that genetic polymorphisms of paroxonase, a glycoprotein that prevents O-LDL formation, represent a risk factor for ARMD. Furthermore, enhanced RPE lysosomal acid hydrolytic activity occurring in response to N-LDL (Table IV) sera from monkeys fed fish oil (Table VIII) may be antagonized by O-LDL,<sup>183</sup> negating the beneficial effects of fish oil-rich diets in reducing the risk for ARMD.<sup>122,123,127</sup> In fact, significantly reduced acid lipase, acid esterase, and cholesteryl esterase (all  $P < .05$ ) activities were observed in cultured RPE cells exposed to O-LDL when compared to LDS from the same plasma (data not shown).

The propensity for omega-3 polyunsaturated fatty acid-rich LDL to be oxidized may underlie apparently conflicting evidence from some reports.<sup>337,339,341</sup> This has led to the recommendation that dietary intake of omega-3 fatty acids should be accompanied by adequate amounts of antioxidants found in fruits and vegetables.<sup>336,338,340,341</sup> The peculiar milieu of the RPE may render adequate dietary antioxidants even more important.<sup>173,174,184,185</sup> Light,<sup>138,174</sup> vitamin C and, particularly, vitamin E deficiency result in outer retinal degeneration with RPE pathologic alterations consistent with lipid peroxidation injury.<sup>280,281</sup> Increased circulating levels of O-LDL have also been demonstrated in non-insulin-dependent diabetic patients,<sup>342-344</sup> prompting more aggressive management of hyperglycemia and hyperlipidemia, both known risk factors for vascular complications in these patients, who may require antioxidant supplementation as part of a dietary regimen high in fish oil. The most unequivocal risk factor for the development of ARMD is cigarette smoking.<sup>175-177</sup> In smokers, fish oil ingestion may actually be detrimental, insofar as they suffer significantly increased peroxidation of LDL, with O-LDL rising up to 50% above baseline levels after 4 weeks of fish oil ingestion.<sup>179</sup> Furthermore, vitamin E does not counteract oxidation of LDL in smokers as it does in smokers in whom vitamin E may idiosyncratically be pro-oxidant.<sup>179,182</sup> These observations imply that dietary fish oil, rich in omega-3 polyunsaturated fatty acids, may enhance O-LDL delivery to the RPE, aggravating RPE dysfunction that leads to ARMD.<sup>1-3</sup> Thus, dietary fish oil supplementation may potentially have negative effects on RPE metabolism in the presence of smoking, excess UV light exposure, inadequate dietary antioxidants, and diabetes with increased O-LDL levels.

The enhanced RPE lysosomal lipid hydrolytic activity due to native LDL may reflect physiologic compensation

for increased lipid incorporation and one reason that elevated lipoproteins have not been implicated as a risk factor for ARMD.<sup>345</sup> It is likely that LDL modifications, be they beneficial or pejorative, are likely to affect the RPE by efficient delivery to the RPE monolayer. In the absence of the aforementioned factors, which promote lipid oxidation, most notably smoking, dietary fish oil may be a beneficial agent that favorably modulates RPE lysosomal lipid metabolism as it reduces the risk for ARMD.<sup>1-3</sup>

## REFERENCES

1. Seddon JM, Bosner B, Sperduto RD, et al. Dietary fat and risk for advanced age-related macular degeneration. *Arch Ophthalmol* 2001;119:1191-1199.
2. Cho E, Hung S, Willett WC, et al. Prospective study of dietary fat and the risk of age-related macular degeneration. *Am J Clin Nutr* 2001;73:209-218.
3. Smith W, Mitchell P, Leeder SR. Dietary fat and fish intake and age-related maculopathy. *Arch Ophthalmol* 2000;118:401-404.
4. Marmor MF. Structure, function and disease of retinal epithelium. In: Marmor MF, Wolfensberger TJ, eds. *The Retinal Pigment Epithelium: Function and Disease*. Oxford, NY: Oxford Press; 1997:3-9.
5. Garron LK. The ultrastructure of the RPE with observations on the choriocapillaris and Bruch's membrane. *Trans Am Ophthalmol Soc* 1963;61:545-588.
6. Boulton ME, Docchio F, Dayhaw-Barker P, et al. Age-related changes in the morphology, absorption and fluorescence of melanosomes and lipofuscin granules of the retinal pigment epithelium. *Vision Res* 1990;30:1291-1303.
7. Cohen AI. A possible cytological basis for the "R" membrane in the vertebrate eye. *Nature* 1965;205:1222-1223.
8. Cunha-Vaz JG, Shakib M, Ashton N. Studies on the permeability of the blood-retinal barrier: I. On the existence, development, and site of a blood-retinal barrier. *Br J Ophthalmol* 1966;50:441-453.
9. Marmor MF. Structure and function of the retinal pigment epithelium. *Int Ophthalmol Clin* 1975;15:115-130.
10. Nguyen-Legros J. Fine structure of the pigment epithelium in the vertebrate retina. *Int Rev Cytol* 1978;7:287-329.
11. Steinberg RH. Interactions between the retinal epithelium and the neural retina. *Doc Ophthalmol* 1985;60:413-419.
12. Hughes BA, Gallemore RP, Miller SS. Transport mechanisms in the retinal pigment epithelium. In: Marmor MF, Wolfensberger TJ, eds. *The Retinal Pigment Epithelium*. Oxford, NY: Oxford Press; 1979:103-108.
13. Lake N, Marshall J, Voaden MJ. Studies on the uptake of taurine by the isolated neural retina and pigment epithelium of the frog. *Biochem Soc Trans* 1975;3:524-525.
14. Miller S, Steinberg RH. Transport of taurine, L-methionine, and 3-O methyl-D-glucose across frog retinal pigment epithelium. *Exp Eye Res* 1976;23:177-189.
15. Miller SS, Steinberg RH, Oakley B. The electrogenic sodium pump of the frog retinal pigment epithelium. *J Membr Biol* 1978;44:259-279.

16. Masterson E, Chader GJ. Characterization of glucose transport by cultured chick pigmented epithelium. *Exp Eye Res* 1981;32:279-289.
17. Trachtenberg MC, Packey DJ. Retinal carbonic anhydrase: a comparative study. *Curr Eye Res* 1984;3:599-604.
18. Rando R. Molecular mechanism in visual pigment regeneration. *Photochem Photobiol* 1992;56:1145-1156.
19. Saari J, Bredberg L, Noy N. Control of substrate flow at a branch point in the visual cycle. *Biochemistry* 1994;33:3106-3112.
20. Bok D, Heller J. Transport of retinol from the blood to the retina: an autoradiographic study of the pigment epithelial cell surface receptor for plasma retinol-binding protein. *Exp Eye Res* 1976;22:395-402.
21. Zimmerman WF. Subcellular distribution of 11-cis-retinol dehydrogenase activity in bovine pigment epithelium. *Exp Eye Res* 1976;23:59-164.
22. Berman ER, Segal N, Photiou S, et al. Inherited retinal dystrophy in RCS rats: a deficiency in vitamin A esterification in pigment epithelium. *Nature* 1981;293:217-220.
23. Liou GI, Bridges CD, Fong SL, et al. Vitamin A transport between retina and pigment epithelium—an interstitial protein carrying endogenous retinol. *Vision Res* 1982;22:1457-1467.
24. Lai YL, Tsin AT, Lam KW, et al. Distribution of retinoids in different compartments of the posterior segment of the rabbit eye. *Brain Res Bull* 1985;15:143-147.
25. Berman ER, Segal N, Rothman H, et al. Retinyl ester hydrolase of bovine retina and pigment epithelium: comparisons to the rat liver enzyme. *Curr Eye Res* 1985;4:867-876.
26. Mata JR, Mata NL, Tsin ATC. Substrate specificity of retinyl ester hydrolase activity in retinal pigment epithelium. *J Lipid Res* 1998;39:604-612.
27. Crouch RK, Chader GJ, Wiggert B, et al. Retinoids and the visual process. *Photochem Photobiol* 1996;64:613-621.
28. Sarna T. Properties and function of the ocular melanin—a photophysical view. *J Photochem Photobiol B* 1992;12:215-258.
29. Young RW. The daily rhythm of shedding and degradation of cone outer segment membranes in the chick retina. *Invest Ophthalmol Vis Sci* 1978;17:105-116.
30. Edwards RB. Glycosaminoglycan synthesis by cultured human retinal pigmented epithelium from normal post-mortem donors and a postmortem donor with retinitis pigmentosa. *Invest Ophthalmol Vis Sci* 1982;23:435-446.
31. Turksen K, Aubin JE, Sodek J, et al. Localization of laminin, type IV collagen, fibronectin, and heparan sulfate proteoglycan in chick retinal pigment epithelium basement membrane during embryonic development. *J Histochem Cytochem* 1985;33:665-671.
32. Young RW, Bok D. Participation of the retinal pigment epithelium in the rod outer segment renewal process. *J Cell Biol* 1969;42:392-403.
33. LaVail MM. Rod outer segment disc shedding in rat retina: relationship to cyclic lighting. *Science* 1976;194:1071-1074.
34. Herman KG, Steinberg RH. Phagosome movement and the diurnal pattern of phagocytosis in the tapetal retinal pigment epithelium of the opossum. *Invest Ophthalmol Vis Sci* 1982;23:277-290.
35. LaVail MM. Outer segment disc shedding and phagocytosis in the outer retina. *Trans Ophthalmol Soc U K* 1984;103:397-404.
36. Bok D. Retinal photoreceptor-pigment epithelium interaction. *Invest Ophthalmol Vis Sci* 1985;26:1659-1694.
37. Hall MO. Phagocytosis of light- and dark-adapted rod outer segments by cultured pigment epithelium. *Science* 1978;202:526-528.
38. Bok D, Young RW. Phagocytic properties of the retinal pigment epithelium. In: Zinn KM, Marmor MF, eds. *The Retinal Pigment Epithelium*. Cambridge, Mass: Harvard University Press; 1979:148-174.
39. Feeney L, Mixon N. An in vitro model of phagocytosis in bovine and human retinal pigment epithelium. *Exp Eye Res* 1976;22:533-548.
40. Masterson E, Chader GJ. Pigment epithelial cells in culture: metabolic pathways required for phagocytosis. *Invest Ophthalmol Vis Sci* 1981;20:1-7.
41. Herman KG, Steinberg RH. Phagosome movement and the diurnal pattern of phagocytosis in the tapetal retinal pigment epithelium of the opossum. *Invest Ophthalmol Vis Sci* 1982;23:277-290.
42. Beauchemin ML, Leuenberger PM. Effects of colchicines on phagosomes-lysosome interaction in retinal pigment epithelium. I. In vivo observations in albino rats. *Graefes Arch Klin Exp Ophthalmol* 1997;203:237-251.
43. Klyne MA, Ali MA. Microtubules and 10 nm filaments in the retinal pigment epithelium during the diurnal light-dark cycle. *Cell Tissue Res* 1981;214:397-405.
44. Owaribe K, Masuda H. Isolation and characterization of circumferential microfilament bundles from retinal pigment epithelial cells. *J Cell Biol* 1982;95:310-315.
45. Chaitin MH, Hall MO. The distribution of actin in cultured normal and dystrophic rat pigment epithelial cells during the phagocytosis of rod outer segments. *Invest Ophthalmol Vis Sci* 1983;24:821-831.
46. Burnside MB. Possible roles of microtubules and actin filaments in retinal pigmented epithelium. *Exp Eye Res* 1976;23:257-275.
47. Reme CE. Autophagy in visual cells and pigment epithelium. *Invest Ophthalmol Vis Sci* 1977;16:807-814.
48. Besharse JC, Defor DM. Role of the retinal pigment epithelium in photoreceptor membrane turnover. In: Marmor MF, Wolfensberger TJ, eds. *The Retinal Pigment Epithelium*. Oxford, NY: Oxford Press; 1997:152-172.
49. Eldred GE. Lipofuscin and other lysosomal storage deposits in the retinal pigment epithelium. In: Marmor MF, Wolfensberger TJ, eds. *The Retinal Pigment Epithelium*. Oxford, NY: Oxford Press; 1979:653.
50. Hayasaka S. Lysosomal enzymes in ocular tissues and diseases. *Surv Ophthalmol* 1983;27:245-258.
51. Zimmerman WF, Godchaux W, Belin M. The relative proportions of lysosomal enzyme activities in bovine retinal pigment epithelium. *Exp Eye Res* 1983;36:151-158.
52. Rakoczy PE, Mann K, Cavaney DM, et al. Detection and possible functions of cysteine protease involved in digestion of rod outer segments by retinal pigment epithelial cells. *Invest Ophthalmol Vis Sci* 1994;35:4100-4108.
53. Rakoczy P, Lai CM, Baines M, et al. Modulation of cathepsin D activity in retinal pigment epithelial cells. *Biochem J* 1977;324:935-940.

54. Deguchi J, Yamamoto A, Yoshimori T, et al. Acidification of phagosomes and degradation of rod outer segments in rat retinal pigment epithelium. *Invest Ophthalmol Vis Sci* 1994;35:568-579.
55. Hayasaka S, Hara S, Mizuno K, et al. In vitro degradation of rod outer segment lipid by acid lipase. *Jpn J Ophthalmol* 1977;21:342-347.
56. Regan CM, De Grip WJ, Daemen FJ, et al. Degradation of rhodopsin by a lysosomal fraction of retinal pigment: biochemical aspects of the visual process. *Exp Eye Res* 1980;30:183-191.
57. Kean EL, Hara S, Mizoguchi A, et al. The enzymatic cleavage of rhodopsin by the retinal pigment epithelium. II. The carbohydrate composition of the glycopeptide cleavage product. *Exp Eye Res* 1983;36:817-825.
58. Berman, ER. Retinal pigment epithelium: lysosomal enzymes and aging. *Br J Ophthalmol* 1994;78:82-83.
59. Rakoczy P, Sarks S, Daw N, et al. Distribution of cathepsin D in human eyes with or without age-related maculopathy. *Exp Eye Res* 1999;69:367-374.
60. Verdugo ME, Ray J. Age-related increase in activity of specific lysosomal enzymes in the human retinal pigment epithelium. *Exp Eye Res* 1997;65:234-240.
61. Hjelmeland LM, Cristofolo VJ, Funk W, et al. Senescence of the retinal pigment epithelium. *Mol Vis* 1999;5:33.
62. Katz ML, Robison WG Jr. Age-related changes in the retinal pigment epithelium of pigmented rats. *Exp Eye Res* 1984;38:137-151.
63. Cingle KA, Kalski RS, Bruner WE, et al. Age-related changes of glycosidases in human retinal pigment epithelium. *Curr Eye Res* 1996;15:433-438.
64. Wyszynski RE, Bruner WE, Cano DB, et al. A donor-age-dependent change in the activity of alpha-mannosidase in human cultured RPE cells. *Invest Ophthalmol Vis Sci* 1989;30:2341-2347.
65. Swartz JG, Mitchell JE. Phospholipase activity of retina and pigment epithelium. *Biochemistry* 1973;12:5273-5278.
66. Zimmerman WF, Godchaux W III, Belkin M. The relative proportions of lysosomal enzyme activities in bovine retinal pigment epithelium. *Exp Eye Res* 1983;36:151-158.
67. Rothman H, Feeney L, Berman ER. The retinal pigment epithelium, analytical subcellular fractionation with special reference to acid lipase. *Exp Eye Res* 1976;22:519-532.
68. Hayasaka S, Hara S, Takaku Y, et al. Distribution of acid lipase in the bovine retinal pigment epithelium. *Exp Eye Res* 1977;24:1-6.
69. Hayasaka S, Hara S, Mizuno K. Partial purification and properties of acid lipase in the bovine retinal pigment epithelium. *Exp Eye Res* 1977;25:317-324.
70. Gordon WC, Bazan NG. Visualization of [<sup>3</sup>H]docosahexaenoic acid trafficking through photoreceptors and retinal pigment epithelium by electron microscopic autoradiography. *Invest Ophthalmol Vis Sci* 1993;34:2402-2411.
71. Gordon WC, Rodriguez de Turco EB, Bazan NG. Retinal pigment epithelial cells play a central role in the conservation of docosahexaenoic acid by photoreceptor cells after shedding and phagocytosis. *Curr Eye Res* 1992;11:73-83.
72. Feeney L. Lipofuscin and melanin of human retinal pigment epithelium: fluorescence, enzyme cytochemical, and ultrastructural studies. *Invest Ophthalmol Vis Sci* 1978;17:583-600.
73. Feeney L. Lipofuscin and melanin of human retinal pigment epithelium: fluorescence, enzyme cytochemical, and ultrastructural studies. *Invest Ophthalmol Vis Sci* 1978;17:583-600.
74. Adler AJ. Selective presence of acid hydrolases in the interphotoreceptor matrix. *Exp Eye Res* 1989;49:1067-1077.
75. Diakotos AN, Armstrong D, Koppang N, et al. Studies on the retina and the pigment epithelium in hereditary canine ceroid lipofuscinosis. II. The subcellular distribution of lysosomal hydrolases and other enzymes. *Invest Ophthalmol Vis Sci* 1978;17:618-633.
76. Schaffner T, Elner V, Wissler RW. Histochemical localization of acid lipase with  $\alpha$ -naphthyl fatty acid esters (Abstract). *Fed Proc* 1977;36:400.
77. Schaffner T, Elner VM, Bauer M, et al. Acid lipase: a histochemical and biochemical study using Triton X100-naphthyl palmitate micelles. *J Histochem Cytochem* 1978;26:696-712.
78. Yue B, Kawa JE, Chang IL, et al. Effects of chondroitin sulfate on cultured human retinal pigment epithelial cells. *Cell Biol Int Rep* 1991;15:365-376.
79. Feeney-Burns L, Hildebrand ES, Eldridge S. Aging human RPE: morphometric analysis of macular, equatorial, and peripheral cells. *Invest Ophthalmol Vis Sci* 1984;25:195-200.
80. Dorey CK, Wu G, Ebenstein D, et al. Cell loss in the aging retina: relationship to lipofuscin accumulation and macular degeneration. *Invest Ophthalmol Vis Sci* 1989;30:1691-1699.
81. Shamsi FA, Boulton M. Inhibition of RPE lysosomal and antioxidant activity by the age pigment lipofuscin. *Invest Ophthalmol Vis Sci* 2001;42:3041-3046.
82. Holz FG, Schutt F, Kopitz J, et al. Inhibition of lysosomal degradative functions in RPE cells by a retinoid component of lipofuscin. *Invest Ophthalmol Vis Sci* 1999;40:737-743.
83. Bergmann M, Schutt F, Holz FG, et al. Does A2E, a retinoid component of lipofuscin and inhibitor of lysosomal degradative functions, directly affect the activity of lysosomal hydrolases? *Exp Eye Res* 2001;72:191-195.
84. Eldred GE. Lipofuscin fluorophore inhibits lysosomal protein degradation and may cause early stages of macular degeneration. *Gerontology* 1995;41(Suppl 2):15-28
85. Dhaliwal BS, Steinbrecher UP. Scavenger receptors and oxidized low density lipoproteins. *Clin Chim Acta* 1999;286:191-205.
86. Feeney-Burns L, Ellersieck MR. Age-related changes in the ultrastructure of Bruch's membrane. *Am J Ophthalmol* 1985;100:686-697.
87. Killingsworth MC. Age-related components of Bruch's membrane in the human eye. *Graefes Arch Clin Exp Ophthalmol* 1987;255:406-412.
88. Bird AC, Marshall J. Retinal pigment epithelial detachments in the elderly. *Trans Soc Ophthalmol U K* 1986;105:674-682.
89. Mullins RF, Russell SR, Anderson DH, et al. Drusen associated with aging and age-related macular degeneration contain proteins common to extracellular deposits associated with atherosclerosis, elastosis, amyloidosis, and dense deposit disease. *FASEB J* 2000;200;14:835-846.

90. Haimovici R, Gantz DL, Rumelt S, et al. The lipid composition of drusen, Bruch's membrane, and sclera by hot stage polarizing light microscopy. *Invest Ophthalmol Vis Sci* 2001;42:1593-1599.
91. Curcio CA, Millican CL, Bailey T, et al. Accumulation of cholesterol with age in human Bruch's membrane. *Invest Ophthalmol Vis Sci* 2001;42:265-274.
92. Sarks SH. Aging and degeneration in the macular region: a clinicopathological study. *Br J Ophthalmol* 1976;60:324-341.
93. van der Schaft TL, de Bruijn WC, Mooy CM, et al. Is basal laminar deposit unique for AMD? *Arch Ophthalmol* 1991;109:420-425.
94. van der Schaft TL, Mooy CM, Bruijn WC, et al. Histological features of the early stages of age-related macular degeneration: a statistical analysis. *Ophthalmology* 1992;99:278-286.
95. van der Schaft TL, Mooy CM, de Bruijn WC, et al. Early stages of AMD: an immunofluorescence and electron microscopic study. *Br J Ophthalmol* 1994;77:657-661.
96. Curcio CA, Millican CL. Basal linear deposit and large drusen are specific for early age-related maculopathy. *Arch Ophthalmol* 1999;117:329-339.
97. Burns RP, Feeney-Burns L. Clinicomorphologic correlations of drusen of Bruch's membrane. *Trans Am Ophthalmol Soc* 1980;78:206-225.
98. Ishibashi T, Patterson R, Ohnishi Y, et al. Formation of drusen in the human eye. *Am J Ophthalmol* 1986;101:342-343.
99. Eldred GE, Lasky MR. Retinal age pigments generated by self-assembling lysosomotropic detergents. *Nature* 1993;361:724-726.
100. Sparrow JR, Nakanishi K, Parish CA. The lipofuscin fluorophore A2E mediates blue light-induced damage to retinal pigment epithelial cells. *Invest Ophthalmol Vis Sci* 2000;41:1981-1989.
101. Schutt F, Davies S, Kopitz J, et al. Photodamage to human RPE cells by A2-E, a retinoid component of lipofuscin. *Invest Ophthalmol Vis Sci* 2000;41:2303-2308.
102. Sparrow JR, Cai B. Blue light-induced apoptosis of A2E-containing RPE: involvement of caspase-3 and protection by Bcl-2. *Invest Ophthalmol Vis Sci* 2001;42:1356-1362.
103. Berg K, Moan J. Lysosomes as photochemical targets. *Int J Cancer* 1994;59:814-822.
104. Wihlmark U, Wrigstad A, Roberg K, et al. Lipofuscin accumulation in cultured retinal pigment epithelial cells causes enhanced sensitivity to blue light irradiation. *Free Radic Biol Med* 1997;22:1229-1234.
105. Brunk UT, Wihlmark U, Wrigstad A, et al. Accumulation of lipofuscin within retinal pigment epithelial cells results in enhanced sensitivity to photoxidation. *Gerontology* 1995;41(S2):201-212.
106. Hogan MJ, Wood I, Steinberg RH. Phagocytosis by pigment epithelium of human retinal cones. *Nature* 1974;252:305-307.
107. Goldman AI, O'Brien PJ, Masterson E, et al. A quantitative system for studying phagocytosis in pigment epithelium tissue culture. *Exp Eye Res* 1979;28:455-467.
108. Masterson E, Goldman AI, Chader GJ. Phagocytosis of rod outer segments by cultured epithelial cells. *Vision Res* 1981;21:143-145.
109. Mayerson PL, Hall MO. Rat retinal pigment epithelial cells show specificity of phagocytosis in vitro. *J Cell Biol* 1986;103:299-308.
110. Edwards RB. Stimulation of rod outer segment phagocytosis by serum occurs only at the RPE apical surface. *Exp Eye Res* 1991;53:229-232.
111. Reid DM, Laird DW, Molday RS. Characterization and application of an in vitro detection system for studying the binding and phagocytosis of rod outer segments by retinal pigment epithelial cells. *Exp Eye Res* 1992;54:775-783.
112. Hollyfield JG. Phagocytic capabilities of the pigment epithelium. *Exp Eye Res* 1976;22:457-468.
113. Funahashi M, Okisaka S, Kuwabara T. Phagocytosis by the monkey pigment epithelium. *Exp Eye Res* 1976;23:217-225.
114. Essner E, Roszka Jr, Schreiber JH. Phagocytosis and surface morphology in cultured retinal pigment epithelial and rod photoreceptor cells. *Curr Eye Res* 1978;1:381-389.
115. Hayashi M, Matsumoto A, Hamashima Y, et al. Phagocytic activity of cultured retinal pigment epithelium: uptake of polystyrene spheres and *Staphylococcus aureus*. *Exp Eye Res* 1979;28:427-434.
116. Effron JT, Szamier RB, Edwards RB. Selective phagocytosis of liposomes by cultured RCS rat pigment epithelium. *Invest Ophthalmol Vis Sci* 1981;21:611-616.
117. Seyfried-Williams R, McLaughlin BJ. The use of sugar-coated beads to study phagocytosis in normal and dystrophic retina. *Vision Res* 1983;23:485-494.
118. Seyfried-Williams R, McLaughlin BJ, Cooper NG. Phagocytosis of lectin-coated beads by dystrophic and normal retinal pigment epithelium. *Gerontology* 1984;154:500-509.
119. Elner VM, Schaffner T, Taylor K, et al. Immunophagocytic properties of retinal pigment epithelium cells. *Science* 1981;211:74-76.
120. Pavlack MA, Elner SG, Feldman LE, et al. Human RPE (HRPE) cells express leukocyte integrins and intercellular adhesion molecules. (Abstract 1828) *Invest Ophthalmol Vis Sci* 1990;31(Suppl):372.
121. Elner VM, Hass A, Klusken L, et al. Immunofluorescent detection of surface receptors for glycoproteins on retinal pigment epithelium (RPE) cells. (Abstract) *Invest Ophthalmol Vis Sci* 1982; 22(Suppl):173.
122. McLaughlin BJ, Tarnowski BI, Shepherd VL. Identification of mannose 6-phosphate and mannose receptors in dystrophic and normal retinal pigment epithelium. *Prog Clin Biol Res* 1987;247-257.
123. Shepherd VL, Tarnowski BI, McLaughlin BJ. Isolation and characterization of a mannose receptor from human pigment epithelium. *Invest Ophthalmol Vis Sci* 1991;32:1779-1784.
124. Boyle DL, Tien L, Cooper NGF, et al. A mannose receptor is involved in retinal phagocytosis. *Invest Ophthalmol Vis Sci* 1991;32:1464-1470.
125. Hall MO, Abrams T. The phagocytosis of ROS by RPE cells is not inhibited by mannose-containing ligands. *Exp Eye Res* 1991;53:167-170.
126. Elner VM, Nielsen JC, Elner SG, et al. Immunophenotypic modulation of cultured human retinal pigment epithelial cells by gamma-interferon and phytohemagglutinin-stimulated human T-lymphocytes. *Invest Ophthalmol Vis Sci* 1989;30(Suppl):233.

127. Elnor SG, Elnor VM, Bian ZM, et al. RPE cell-monocyte binding induced chemokine production is mediated by CD14. (Abstract 4076) *Invest Ophthalmol Vis Sci* 2001;42(Suppl):761.
128. Elnor SG, Davis HR, Elnor VM. Acetoacetylated lipoprotein uptake by retinal pigment epithelium (RPE) cells. (Abstract) *Invest Ophthalmol Vis Sci* 1984;25(Suppl):248.
129. Hayes KC, Lindsey S, Stephan ZF, et al. Retinal pigment epithelium possesses both LDL and scavenger receptor activity. *Invest Ophthalmol Vis Sci* 1989;30:225-232.
130. Elnor VM, Elnor SG, Cornicelli JA. Human and monkey RPE cells express native and acetylated low density lipoprotein receptors in vitro and in vitro. (Abstract 1820) *Invest Ophthalmol Vis Sci* 1990;31(Suppl):370.
131. Dhaliwal BS, Steinbrecher UP. Scavenger receptors and oxidized low density lipoproteins. *Clin Chim Acta* 1999;286:191-205.
132. Loughheed M, Lum CM, Ling W, et al. High affinity saturable uptake of oxidized low density lipoprotein by macrophages from mice lacking the scavenger receptor class A type I/II. *J Biol Chem* 1997;272:12938-12944.
133. Brown MS, Basu SK, Falck JR, et al. The scavenger cell pathway for lipoprotein degradation: specificity of the binding site that mediates the uptake of negatively-charged LDL by macrophages. *J Supramol Struct* 1980;13:67-81.
134. Brown MS, Goldstein JL. Lipoprotein metabolism in the macrophage: implications for cholesterol deposition in atherosclerosis. *Ann Rev Biochem* 1983;52:223-261.
135. Endemann G, Stanton LW, Madden KS, et al. CD36 is a receptor for oxidized low density lipoprotein. *J Biol Chem* 1993;268:11811-11816.
136. Kataoka H, Kume N, Miyamoto S, et al. Expression of lectin-like oxidized low-density lipoprotein receptor-1 in human atherosclerotic lesions. *Circulation* 1999;99:3110-3117.
137. Draude G, Hrboticky N, Lorenz RL. The expression of the lectin-like oxidized low-density lipoprotein receptor (LOX-1) on human vascular smooth muscle cells and monocytes and its down-regulation by lovastatin. *Biochem Pharmacol* 1999;57:383-386.
138. Koutz CA, Weigand RD, Rapp LM, et al. Effect of dietary fat on the response of the rat retina to chronic and acute light stress. *Exp Eye Res* 1995;60:307-316.
139. van der Kooij MA, von der Mark EM, Kruijt JK, et al. Human monocyte-derived macrophages express an 120-kD Ox-LDL binding protein with strong identity to CD68. *Arterioscler Thromb Vasc Biol* 1997;17:3107-3116.
140. Elnor SG, Elnor VM, Nielsen JC, et al. CD68 antigen expression by human retinal pigment epithelial cells. *Exp Eye Res* 1992;55:21-28.
141. Ryeom SW, Sparrow JR, Silverstein RL. CD36 participates in the phagocytosis of rod outer segments by retinal pigment epithelium. *J Cell Sci* 1996;109:387-395.
142. Ryeom SW, Silverstein RL, Scotto A, et al. Binding of anionic phospholipids to retinal pigment epithelium may be mediated by the scavenger receptor CD36. *J Biol Chem* 1996;271:20536-20539.
143. Sambrano GR, Parthasarathy S, Steinberg D. Recognition of oxidatively damaged erythrocytes by a macrophage receptor with specificity for oxidized low density lipoprotein. *Proc Natl Acad Sci U S A* 1994;91:3265-3269.
144. Ren Y, Silverstein RL, Allen J, et al. CD36 gene transfer confers capacity for phagocytosis of cells undergoing apoptosis. *J Exp Med* 1995;181:1857-1862.
145. Savill J, Hogg N, Ren Y, et al. Thrombospondin cooperates with CD36 and the vitronectin receptor in macrophage recognition of neutrophils undergoing apoptosis. *J Clin Invest* 1992;90:1513-1522.
146. Savill J, Dransfield I, Hogg N, et al. Vitronectin receptor-mediated phagocytosis of cells undergoing apoptosis. *Nature* 1990;343:170-173.
147. Anderson DH, Johnson LV, Hageman GS. Vitronectin receptor expression and distribution at the photoreceptor-retinal pigment epithelial interface. *J Comp Neurol* 1995;360:1-16.
148. Hoppe G, Marmorstein AD, Pennock EA, et al. Oxidized low density lipoprotein-induced inhibition of processing of photoreceptor outer segments by RPE. *Invest Ophthalmol Vis Sci* 2001;42:2714-2720.
149. Anderson RE, Chen H, Wang N, et al. The accretion of docosahexaenoic acid in the retina. *World Rev Nutr Diet* 1994;75:124-127.
150. Bazan NG, Silvia di Fazio de Escalante M, Careaga MM, et al. High content of 22:6 (docosahexaenoate) and active [<sup>3</sup>H]glycerol metabolism of phosphatidic acid from photoreceptor membranes. *Biochim Biophys Acta* 1982;712:702-706.
151. Su HM, Huang MC, Saad NMR, et al. Fetal baboons convert 18:3n-3 to 22:6n-3 in vivo: a stable isotope tracer study. *J Lipid Res* 2001;42:581-586.
152. Neuringer M, Connor WE, Van Petten C, et al. Dietary omega-3-fatty acid deficiency and visual loss in infant rhesus monkeys. *J Clin Invest* 1984;73:272-276.
153. Neuringer M, Connor WE, Lin DS, et al. Biochemical and functional effects of prenatal and postnatal omega-3 fatty acid deficiency on retina and brain in rhesus monkeys. *Proc Natl Acad Sci U S A* 1986;83:4021-4025.
154. Yamamoto N, Saitoh M, Moriuchi A, et al. Effect of dietary alpha-linolenate/linoleate balance on brain lipid compositions and learning ability of rats. *J Lipid Res* 1987;28:144-151.
155. Uauy RD, Birch DG, Birch EE, et al. Effect of dietary omega-3 fatty-acids on retinal function of very-low-birth-weight neonates. *Pediatr Res* 1990;28:485-492.
156. Birch EE, Birch DG, Hoffman DR, et al. Dietary essential fatty acid supply and visual acuity development. *Invest Ophthalmol Vis Sci* 1992;33:3242-3253.
157. Scott BL, Bazan NG. Membrane docosahexaenoate is supplied to the developing brain and retina by the liver. *Proc Natl Acad Sci U S A* 1989;86:2903-2907.
158. Li J, Wetzel MG, O'Brien PJ. Transport of n-3 fatty acids from the intestine to the retina in rats. *J Lipid Res* 1992;33:539-548.
159. Wang N, Anderson RE. Synthesis of docosahexaenoic acid by retina and retinal pigment epithelium. *Biochemistry* 1993;32:13703-13709.
160. Gordon WC, Rodriguez de Turco EB, Bazan NG. Retinal pigment epithelial cells play a central role in the conservation of docosahexaenoic acid by photoreceptor cells after shedding and phagocytosis. *Curr Eye Res* 1992;11:73-83.
161. Anderson RE, O'Brien PJ, Wiegand RD, et al. Conservation of docosahexaenoic acid in the retina. *Adv Exp Med Biol* 1992;318:285-294.

162. Bazan NG, Gordon WC, Rodriguez de Turco EB. Docosahexaenoic acid uptake and metabolism in photoreceptors: retinal conservation by an efficient retinal pigment epithelial cell-mediated recycling process. *Adv Exp Med Biol* 1992;318:295-306.
163. Rodriguez de Turco EB, Parkins N, Ershov AV, et al. Selective retinal pigment epithelial cell lipid metabolism and remodeling conserves photoreceptor docosahexaenoic acid following phagocytosis. *J Neurosci Res* 1999;57:479-486.
164. Lee J, Jiao X, Gentleman S, et al. Soluble-binding proteins for docosahexaenoic acid are present in neural retina. *Invest Ophthalmol Vis Sci* 1995;36:2032-2039.
165. Bazan NG, Reddy TS, Redmond TM, et al. Endogenous fatty acids are covalently and noncovalently bound to interphotoreceptor retinoid-binding protein. *J Biol Chem* 1985;260:13677-13680.
166. Chen Y, Houghton LA, Brenna JT, et al. Docosahexaenoic acid modulates the interaction of the interphotoreceptor retinoid-binding protein with 11-cis-retinal. *J Biol Chem* 1996;271:20507-20515.
167. Wu GS, Rao NA. Activation of NADPH oxidase by docosahexaenoic acid hydroperoxide and its inhibition by a novel retinal pigment epithelial protein. *Invest Ophthalmol Vis Sci* 1999;40:831-839.
168. Akeo K, Hiramitsu T, Kanda T, et al. Comparative effects of linoleic acid and linoleic acid hydroperoxide on growth and morphology of bovine retinal pigment epithelial cells in vitro. *Curr Eye Res* 1996;15:467-476.
169. Ikemoto A, Fukuma A, Fujii Y, et al. Lysosomal enzyme activities are decreased in the retina and their circadian rhythms are different from those in the pineal gland of rats fed an  $\alpha$ -linolenic acid-restricted diet. *J Nutr* 2000;130:3059-3062.
170. Hyman L, Schachat AP, He Q, et al. Hypertension, cardiovascular disease, and age-related macular degeneration. *Arch Ophthalmol* 2000;117:351-358.
171. Hyman L, Lilienfeld AM, Ferris FL. Senile macular degeneration: a case-control study. *Am J Epidemiol* 1983;118:213-227.
172. Eye Disease Case-Control Study Group [EDCCS Group]. Antioxidant status and neovascular age-related macular degeneration. *Arch Ophthalmol* 1993;111:104-109.
173. Mares-Perlman J, Bride WE, Klein R, et al. Serum antioxidants and age-related macular degeneration in a population-based case-control study. *Arch Ophthalmol* 1995;113:1518-1523.
174. Taylor H, West S, Munuz B. The long term effects of visible light on the eye. *Arch Ophthalmol* 1992;110:99-104.
175. Hyman L. Epidemiology of AMD. In: Hampton G, Nelsen PT, eds. *Age-Related Macular Degeneration: Principles and Practices*. New York: Raven Press; 1992:1-35.
176. Christen WG, Glynn RJ, Manson JE, et al. A prospective study of cigarette smoking and risk of age-related macular degeneration in men. *JAMA* 1996;276:1147-1151.
177. Seddon JM, Willett WC, Speizer FE, et al. A prospective study of cigarette smoking in age-related macular degeneration in women. *JAMA* 1996;276:1141-1146.
178. Harats D, Ben-Naim M, Dabach Y, et al. Cigarette smoking renders LDL susceptible to peroxidative modification and enhanced metabolism by macrophages. *Atherosclerosis* 1989;79:245.
179. Harats D, Dabach Y, Hollander G, et al. Fish oil ingestion in smokers and nonsmokers enhances peroxidation of plasma lipoproteins. *Atherosclerosis* 1991;90:127-139.
180. Bridges AB, Scott NA, Parry GJ, et al. Age, sex, cigarette smoking and indices of free radical activity in healthy humans. *Eur J Med* 1993;2:205-208.
181. Morrow JD, Frei B, Longmire AW, et al. Increase in circulating products of lipid peroxidation ( $F^2$ -isoprostanes) in smokers. *N Engl J Med* 1995;332:1198-1203.
182. Weinberg RB, VanderWerken BS, Anderson RA, et al. Prooxidant effect of vitamin E in cigarette smokers consuming a high polyunsaturated fat diet. *Arterioscler Thromb Biol* 2002;21:1029-1033.
183. Ikeda T, Obayashi H, Hasegawa G, et al. Paraoxonase gene polymorphisms and plasma oxidized low-density lipoprotein level as possible risk factors for age-related macular degeneration. *Am J Ophthalmol* 2001;132:191-195.
184. Snodderly DM. Evidence for protection against age-related macular degeneration by carotenoids and antioxidant vitamins. *Am J Clin Nutr* 1995;62:1448S-1461S.
185. Cohen SM, Olin KL, Feuer WJ, et al. Low glutathione reductase and peroxidase activity in age-related macular degeneration. *Br J Ophthalmol* 1994;78:791-794.
186. Hu FB, Stampfer MJ, Manson JE, et al. Dietary fat intake and the risk of coronary heart disease in women. *N Engl J Med* 1997;337:1491-1499.
187. Ascherio A, Rimm EB, Giovannucci EL, et al. Dietary fat and risk of coronary heart disease in men: cohort follow-up study in the United States. *Br Med J* 1996;313:84-90.
188. Harats D, Ben-Naim M, Dabach Y, et al. Effect of vitamin C and E supplementation on susceptibility of plasma lipoproteins to peroxidation induced by acute smoking. *Atherosclerosis* 1990;85:47-54.
189. Sanders TA, Sullivan DR, Reeve J, et al. Triglyceride-lowering effect of marine polyunsaturates in patients with hypertriglyceridemia. *Arteriosclerosis* 1985;5:459-465.
190. Soltys PA, Mazzone T, Wissler RW, et al. Effects of feeding fish oil on the properties of lipoproteins isolated from rhesus monkeys consuming an atherogenic diet. *Atherosclerosis* 1989;76:103-115.
191. Davis PJ. n-3 and n-6 polyunsaturated fatty acids have different effects on acyl-CoA:cholesterol acyltransferase in J774 macrophages. *Biochem Cell Biol* 1992;70:1313-1318.
192. Davis HR, Bridenstine RT, Vesselinovitch D, et al. Fish oil inhibits development of atherosclerosis in rhesus monkeys. *Arteriosclerosis* 1987;7:441-449.
193. Wissler RW, Davis HR, Vesselinovitch D, et al. A preliminary report of acute and chronic studies of atherogenic related effects of eicosapentaenoic acid-rich rations in rhesus monkeys. In: Lands WEM, ed. *Proceedings of the AOCS Short Course on Polyunsaturated Fatty Acids and Eicosanoids*. Champaign, Ill: University of Illinois. 1987:66-69.
194. Albert CM, Hennekens CH, O'Donnell CJ, et al. Fish consumption and risk of sudden cardiac death. *JAMA* 1998;279:23-28.
195. Chan JC, McDonald BE, Gerrard JM, et al. Effect of dietary  $\alpha$ -linolenic acid and its ratio to linoleic acid on platelet and plasma fatty acids and thrombogenesis. *Lipids* 1993;28:811-817.

196. Kromhout D, Bosschieter EB, de Lezenne Coulander C. The inverse relation between fish consumption and 20-year mortality from coronary heart disease. *N Engl J Med* 1985;312:1205-1209.
197. Katan MB. Fish and heart disease. *N Engl J Med* 1995;332:1024-1025.
198. Hold SJ, Withers RF. Studies in enzyme cytochemistry: V. An appraisal of indigogenic reactions for esterase localization. *Proc R Soc (B)* 1985;148:520-532.
199. Heller J, Jones P. Purification of bovine retinal pigment epithelial cells by dissociation in calcium-free buffers and centrifugation in Ficoll density gradients followed by "recovery" in tissue culture. *Exp Eye Res* 1980;30:481-487.
200. Plantner JJ, Kean EL. Carbohydrate composition of bovine rhodopsin. *J Biol Chem* 1976;251:1548-1552.
201. Elnor SG, Strieter RM, Elnor VM, et al. Monocyte chemotactic protein gene expression by cytokine-treated human retinal pigment epithelial cells. *Lab Invest* 1991;64:819-825.
202. Siakotos AN, Aguirre G, Schuster L. Two methods for the rapid purification of the retinal pigment epithelium: adsorption and filtration. *Exp Eye Res* 1978;26:13-23.
203. Levine DW, Wong JS, Wang DIC, et al. Microcarrier cell culture: new methods for research-scale application. *Somatic Cell Genet* 1977;3:149-155.
204. Labarca C, Paigen K. A simple, rapid, and sensitive DNA assay procedure. *Anal Biochem* 1980;102:344-352.
205. Merrill CR, Goldman D, Sedman SA, et al. Ultrasensitive stain for proteins in polyacrylamide gels shows regional variation in cerebrospinal fluid proteins. *Science* 1980;211:1437-1438.
206. Vesterberg O. Isoelectric focusing of proteins in polyacrylamide gels. *Biochem Biophys Acta* 1972;257:11-19.
207. Brecher PI, Pyun HY, Chobanian AV. Effect of atherosclerosis on lysosomal cholesterol esterase activity in rabbit aorta. *J Lipid Res* 1976;18:154-163.
208. Pittman RC, Khoo JC, Steinberg D. Cholesterol esterase in rat adipose tissue: its activation by cyclic adenosine-3, 5-monophosphate-dependent protein kinase. *J Biol Chem* 1975;250:4505-4511.
209. Bligh EG, Dyer WJ. A rapid method of total lipid extraction and purification. *Can J Biochem Physiol* 1959;37:911-917.
210. Havel RJ, Eder HA, Bragdon JH. The distribution and chemical separation of ultracentrifugally separated lipoproteins in human serum. *J Clin Invest* 1955;34:1345-1353.
211. Pitas RE, Innerarity TL, Weinstein JN, et al. Acetoacetylated lipoproteins used to distinguish fibroblasts from macrophages in vitro by fluorescence microscopy. *Arteriosclerosis* 1981;1:177-185.
212. Basu SK, Goldstein JHL, Anderson RGW, Brown MS. Degradation of cationized low density lipoprotein and regulation of cholesterol metabolism in homozygous familial hypercholesterolemia fibroblasts. *Proc Natl Acad Sci U S A* 1976;73:3178-3187.
213. Quinn NT, Parthasarathy S, Fong LG, et al. Oxidatively modified low density lipoproteins: a potential role in recruitment and retention of monocytes/macrophages during atherogenesis. *Proc Natl Acad Sci U S A* 1987;84:2995-2998.
214. Steinbrecher UP, Parthasarathy S, Leake DS, et al. Modification of low density lipoprotein by endothelial cells involves lipid peroxidation and degradation of low density lipoprotein phospholipids. *Proc Natl Acad Sci U S A* 1984;81:3883-3887.
215. Colton C. Inference on Means. Colton C. Statistics in medicine. Boston, MA: Little, Brown & Co. 1974:99-150.
216. Goldstein JL, Ho YK, Basu SK, et al. Binding site on macrophages that mediates uptake and degradation of acetylated low density lipoprotein, producing massive cholesterol deposition. *Proc Natl Acad Sci U S A* 1979;76:333-337.
217. Esbach S, Pieters MN, van der Boom J, et al. Visualization of the uptake and processing of oxidized low-density lipoproteins in human and rat liver. *Hepatology* 1993;18:537-545.
218. Anderson RE, Lissandrello PM, Maude MB, et al. Lipids of bovine retinal pigment epithelium. *Exp Eye Res* 1976;23:149-157.
219. Berman ER, Schwell H, Feeney L. The retinal pigment epithelium: chemical composition and structure. *Invest Ophthalmol* 1974;13:675-687.
220. Alvarez RA, Bridges CD, Fong SL. High-pressure liquid chromatography of fatty acid esters of retinal isomers: analysis of retinyl esters stored in the eye. *Invest Ophthalmol Vis Sci* 1981;20:304-313.
221. Wiggert B, Derr JE, Israel P, et al. Cytosol binding of retinyl palmitate and palmitic acid in pigment epithelium and retina. *Exp Eye Res* 1981;32:187-196.
222. Kaplan A, Teng MH. Interaction of beef liver lipase with mixed micelles of tripalmitin and Triton X 100. *J Lipid Res* 1971;12:324-330.
223. Burrier RE, Brecher P. Effect of surface composition on triolein hydrolysis in phospholipid vesicles and microemulsions by a purified acid lipase. *Biochemistry* 1984;23:5366-5371.
224. Teng M, Kaplan A. Purification and properties of rat liver lysosomal lipase. *J Biol Chem* 1974;249:1064-1070.
225. Fowler S, Brown W. Lysosomal acid lipase. In: Borgstrom B, Brockman HL, eds. *Lipases*. New York: Elsevier-North-Holland Inc; 1984:330-354.
226. Brown WJ, Sgoutas DS. Purification of rat liver lysosomal cholesterol ester hydrolase. *Biochem Biophys Acta* 1980;617:305-317.
227. Burton BK, Mueller HW. Purification and properties of human placental acid lipase. *Biochem Biophys Acta* 1980;618:449-460.
228. Warner TG, Dambach LM, Shin JH, et al. Purification of the lysosomal acid lipase from human liver and its role in lysosomal lipid hydrolysis. *J Biol Chem* 1981;256:2952-2957.
229. Burrier RE, Brecher P. Hydrolysis of triolein in phospholipid vesicles and microemulsions by a purified rat liver acid lipase. *J Biol Chem* 1983;258:12043-12050.
230. Spencer WH. Macular diseases: pathogenesis: light microscopy. *Trans Am Acad Ophthalmol Otolaryngol* 1965;69:662-667.
231. Toussaint D, Danis P. An ocular pathologic study of Refsum's disease. *Am J Ophthalmol* 1971;72:342-347.
232. Goebel HH, Fix JD, Zeman W. The fine structure of the retina in neuronal ceroid-lipofuscinosis. *Am J Ophthalmol* 1974;77:25-39.
233. Kolb H, Gouras P. Electron microscopic observations of human retinitis pigmentosa, dominantly inherited. *Invest Ophthalmol* 1974;13:487-498.

234. Green WR, Key SN. Senile macular degeneration: a histopathologic study. *Trans Am Ophthalmol Soc* 1977;75:180-254.
235. Katz M, Stone W, Dratz E. Fluorescent pigment accumulation in the retinal pigment epithelium of antioxidant-deficient rats. *Invest Ophthalmol* 1978;17:1049-1058.
236. Szamier RB, Berson EL, Klein R, et al. Sex-linked retinitis pigmentosa: ultrastructure of photoreceptors and pigment epithelium. *Invest Ophthalmol Vis Sci* 1979;18:145-160.
237. Robison WG, Kuwabara T. Vitamin A storage and peroxisomes in retinal pigment epithelium and liver. *Invest Ophthalmol Vis Sci* 1977;16:1110-1117.
238. Eagle RC Jr, Lucier AC, Bernardino VB Jr, et al. Retinal pigment epithelial abnormalities in fundus flavimaculatus: a light and electron microscopic study. *Ophthalmology* 1980;87:1189-1200.
239. Weingeist TA, Kobrin JL, Watke RC. Histopathology of Best's macular dystrophy. *Arch Ophthalmol* 1982;100:1108-1114.
240. Miller FS, Bunt-Milam AH, Kalina RE. Clinical-ultrastructural study of thioradazine retinopathy. *Ophthalmology* 1982;89:1478-1488.
241. Frangieh GT, Green WR, Engel HM. A clinicopathologic study of Best's macular dystrophy. *Arch Ophthalmol* 1982;100:1115-1121.
242. Levin PS, Green WR, Victor DL, et al. Histopathology of the eye in Cockayne's syndrome. *Arch Ophthalmol* 1983;101:1093-1097.
243. Luckenbach MV, Green WR, Miller NR, et al. Ocular clinicopathologic correlation of Hallervorden-Spatz syndrome with acanthocytosis and pigmentary retinopathy. *Am J Ophthalmol* 1983;95:369-382.
244. Bok D, Hall MO. The role of the pigment epithelium in the etiology of inherited retinal dystrophy. *J Cell Biol* 1971;49:664-682.
245. Custer NY, Bok D. Pigment epithelium-photoreceptor interactions in normal and dystrophic rat retina. *Exp Eye Res* 1975;21:153-166.
246. Mullen RJ, LaVail MM. Inherited retinal dystrophy: primary defect in pigment epithelium determined with experimental rat chimeras. *Science* 1976;192:799-801.
247. Edwards RB, Szamier RB. Defective phagocytosis of isolated rod outer segments by RCS rat retinal epithelium in culture. *Science* 1977;197:1001-1003.
248. Goldman AI, O'Brien PJ. Phagocytosis in the retinal pigment epithelium of the RCS rat. *Science* 1978;201:1023-1025.
249. Chaitin MH, Hall MO. Defective ingestion of rod outer segments by cultured dystrophic rat pigment epithelial cells. *Invest Ophthalmol Vis Sci* 1983;24:812-820.
250. Philippart M, Den Tandt W, Borrone C, et al. Retinal-renal dysplasia and encephalopathy in a patient with triglyceride storage disease. *Acta Genet Med Gemellol (Roma)* 1974;23:201-203.
251. Philippart M, Durand P, Borrone C. Neutral lipid storage with acid lipase deficiency: a new variant of Wolman's disease with features of the Senior syndrome. *Pediatr Res* 1982;16:954-959.
252. Hayashi M, Matsumoto A, Hamashima Y, et al. Phagocytic activity of cultured retinal pigment epithelium: uptake of polystyrene spheres and *Staphylococcus aureus*. *Exp Eye Res* 1979;28:427-434.
253. Ershov AV, Lukiw WJ, Bazan NG. Selective transcription factor induction in retinal pigment epithelial cells during photoreceptor phagocytosis. *J Biol Chem* 1996;271:28458-28462.
254. Adler AJ, Klucznik DM. Interaction of bovine pigment epithelium cells, photoreceptor outer segments, and interphotoreceptor matrix: a model for retinal adhesion. *Curr Eye Res* 1981;1:579-589.
255. Feman SS, Lam KW. An enzyme histochemical analysis of human subretinal fluid. *Arch Ophthalmol* 1978;96:129-131.
256. Ansell PL, Marshall J. The distribution of extra-cellular acid phosphatase in the retinas of retinitis pigmentosa rats. *Exp Eye Res* 1974;19:273-279.
257. Seyfried-Williams R, McLaughlin BJ. Acid phosphatase localization in normal and dystrophic retinal pigment epithelium. *J Neurocytol* 1984;13:201-214.
258. Wilcox DK. Extracellular release of acid hydrolases from cultured retinal pigmented epithelium. *Invest Ophthalmol Vis Sci* 1987;28:76-82.
259. Brinckerhoff CE, Rutter JL, Benbow U. Interstitial collagenases as markers of tumor progression. *Clin Cancer Res* 2000;6:4823-4830.
260. Jackson C, Nguyen M, Arkell J, et al. Selective matrix metalloproteinase (MMP) inhibition in rheumatoid arthritis—targeting gelatinase A activation. *Inflamm Res* 2001;50:183-186.
261. Eeckhout Y, Vaes G. Further studies on the activation of procollagenase, the latent precursor of bone collagenase. Effects of lysosomal cathepsin B, plasmin and kallikrein, and spontaneous activation. *Biochem J* 1977;166:21-31.
262. Dingle JT. The secretion of enzymes into the pericellular environment. *Philos Trans R Soc Lond B Biol Sci* 1975;271:315-324.
263. Davies P, Allison AC. The macrophage as a secretory cell in chronic inflammation. *Agents Actions* 1976;6:60-74.
264. Unanue ER. Secretory function of mononuclear phagocytes. *Am J Pathol* 1976;83:396-417.
265. Maruyama K, Okazaki I, Kashiwazaki K, et al. Different appearance of hepatic collagenase and lysosomal enzymes in recovery of experimental hepatic fibrosis. *Biochem Exp Biol* 1978;14:191-201.
266. Coffey JW, Fiedler-Nagy C, Georgiadis AG, et al. Lysosomal degrading collagenolytic fragments. *J Biol Chem* 1976;251:5280-5282.
267. Cohn ZA, Wiener E. The particulate hydrolases of macrophages. II. Biologic and morphological responses to particle ingestion. *J Exp Med* 1963;118:1009-1019.
268. Axline SG, Cohn ZA. In vitro induction of lysosomal enzymes by phagocytosis. *J Exp Med* 1970;131:1239-1260.
269. Weissman G, Dukor P, Zurier RB. Effect of cyclic AMP on release of lysosomal enzymes from phagocytes. *Nature* 1971;231:131-135.
270. Cardella CJ, Davies P, Allison AC. Immune complexes induce selective release of lysosomal hydrolases from macrophages. *Nature* 1974;247:46-48.

271. Schorlemmer HU, Davies P, Allison AC. Ability of activated complement components to induce lysosomal enzyme release from macrophages. *Nature* 1976;261:48-49.
272. Bonney RJ, Wightman PD, Davies P, et al. Regulation of prostaglandin synthesis and of the selective release of lysosomal hydrolases by mouse peritoneal macrophages. *Biochem J* 1978;176:433-442.
273. Hass AJ, Davis R, Elnor VM, et al. Identification of macrophages in sections of rabbit lung using acetoacetylated lipoproteins. *J Histochem Cytochem* 1983;31:1136-1138.
274. Stein O, Stein Y. Bovine aortic endothelial cells display macrophage-like properties towards acetylated <sup>125</sup>I-labelled low density lipoprotein. *Biochem Biophys Acta* 1980;620:631-635.
275. Brown MS, Goldstein JL, Krieger M, et al. Reversible accumulation of cholesterol esters in macrophages incubated with acetylated lipoproteins. *J Cell Biol* 1979;82:597-613.
276. Crockett RS, Lawwill T. Oxygen dependence of damage by 435 nm light in cultured retinal epithelium. *Curr Eye Res* 1984;3:209-215.
277. Rozanowska M, Wessels J, Boulton M, et al. Blue light-induced singlet oxygen generation by retinal lipofuscin in non-polar media. *Free Radic Biol Med* 1998;24:1107-1112.
278. Li ZY, Tso MO, Wang HM, et al. Amelioration of photic injury in rat retina by ascorbic acid: a histopathologic study. *Invest Ophthalmol Vis Sci* 1985;26:1589-1598.
279. Tso MO. Retinal photic injury in normal and scorbutic monkeys. *Trans Am Ophthalmol Soc* 1987;85:498-556.
280. El-Hifnawi ES, Lincoln DT, Dashti H. Nutritionally induced retinal degeneration in rats. *Nutrition* 1995;11:705-707.
281. El-Hifnawi ES, Lincoln DT, Dashti H. Effects of vitamin E on the retina and retinal pigment epithelium of IRCS rats. *Nutrition* 1995;11:576-581.
282. Robison WG, Kuwabara T, Bieri JG. Vitamin E deficiency and the retina: photoreceptor and pigment epithelial changes. *Invest Ophthalmol Vis Sci* 1979;18:683-690.
283. Berger AS, Tychsen L, Rosembaum JL. Retinopathy in human vitamin E deficiency. *Am J Ophthalmol* 1991;111:774-775.
284. Armstrong D, Connole E, Feeney L, et al. Peroxidases in the neural retinal and pigment epithelium. *J Neurochem* 1978;31:761-769.
285. Feeney L, Berman ER. Oxygen toxicity: membrane damage by free radicals. *Invest Ophthalmol* 1976;15:789-792.
286. Dorey CK, Delori FC, Akeo K. Growth of cultured RPE and endothelial cells is inhibited by blue light but not green or red light. *Curr Eye Res* 1990;9:549-559.
287. Oliver PD, Newsome DA. Mitochondrial superoxide dismutase in mature and developing human retinal pigment epithelium. *Invest Ophthalmol Vis Sci* 1992;33:1909-1918.
288. Robison WG, Kuwabara T, Bieri J. Deficiencies of vitamin A and E in the rat: retinal damage and lipofuscin accumulation. *Invest Ophthalmol Vis Sci* 1980;19:103-107.
289. Robison WG, Kuwabara T. Vitamin A storage and peroxisomes in retinal pigment epithelium and liver. *Invest Ophthalmol Vis Sci* 1977;15:1110-1117.
290. Katz MI, Stone WL, Dratz EA. Fluorescent pigment accumulation in retinal pigment epithelium of antioxidant-deficient rats. *Invest Ophthalmol Vis Sci* 1978;17:1049-1058.
291. Amemiya T. Retinal changes in the selenium deficient rat. *Int J Vitam Nutr Res* 1985;55:233-237.
292. Beatty S, Koh HH, Henson D, et al. The role of oxidative stress in the pathogenesis of age-related macular degeneration. *Surv Ophthalmol* 2000;45:115-134.
293. Newsome D, Miceli M, Liles M, et al. Antioxidants in the retinal pigment epithelium. *Prog Retinal Res* 1994;13:101-123.
294. Miceli MV, Liles MR, Newsome DA. Evaluation of oxidative processes in human pigment epithelial cells associated with retinal outer segment phagocytosis. *Gerontology* 1994;214:242-249.
295. Henriksen T, Mahoney EM, Steinberg D. Enhanced macrophage degradation of biologically-modified low density lipoprotein. *Arteriosclerosis* 1983;3:149-159.
296. Nagelkerke JF, Havekes L, Van Hinsbergh VWM, et al. In vivo and in vitro catabolism of native and biologically modified LDL. *FEBS Lett* 1984;171:149-153.
297. Stahmann MA, Spencer AK. Deamination of protein lysyl ε-amino groups by peroxidase in vitro. *Biopolymers* 1977;116:1299-1306.
298. Stossel TP, Mason RJ, Smith AL. Lipid peroxidation by human blood phagocytes. *J Clin Invest* 1974;54:638-645.
299. Samuelsson B, Goldyne M, Granstrom E, et al. Prostaglandins and thromboxanes. *Ann Rev Biochem* 1978;47:997-1029.
300. Tripathi BJ, Tripathi RC. Effect of arachidonic acid on normal and dystrophic retinal pigment epithelium in tissue culture. *Invest Ophthalmol Vis Sci* 1981;20:553-557.
301. Feeney L, Berman ER. Oxygen toxicity: membrane damage by free radicals. *Invest Ophthalmol* 1976;15:789-792.
302. Parthasarathy S, Steinbrecher UP, Barnett J, et al. Essential role of phospholipase A<sub>2</sub> activity in endothelial cell-induced modification of low density lipoprotein. *Proc Natl Acad Sci U S A* 1985;82:3000-3004.
303. Becquet F, Goureau O, Soubrane G, et al. Superoxide inhibits proliferation and phagocytic internalization of photoreceptor outer segments by bovine retinal pigment epithelium in vitro. *Gerontology* 1994;212:374-382.
304. Vesselinovitsh D, Getz GS, Hughes RH, et al. Atherosclerosis in the rhesus monkey fed three food fats. *Atherosclerosis* 1974;20:303-321.
305. Vesselinovitsh D, Wissler RW, Schaffner TJ, et al. The effects of various diets on atherogenesis in rhesus monkeys. *Atherosclerosis* 1980;35:189-207.
306. Baudouin C, Peyman GA, Fredj-Reygrobellet D, et al. Immunohistological study of subretinal membranes in age-related macular degeneration. *Jpn J Ophthalmol* 1992;36:443-451.
307. Grossniklaus HE, Hutchinson AK, Capone A Jr, et al. Clinicopathologic features of surgically excised choroidal neovascular membranes. *Ophthalmology* 1994;101:1099-1111.
308. Grossniklaus HE, Green WR. Histopathologic and ultrastructural findings of surgically excised choroidal neovascularization. *Arch Ophthalmol* 1998;116:745-749.
309. Calder PC. Immunoregulatory and anti-inflammatory effects of n-3 polyunsaturated fatty acids. *Braz J Med Biol Res* 1998;31:467-490.

310. Yaqoob P, Calder P. Effects of dietary lipid manipulation upon inflammatory mediator production by murine macrophages. *Cell Immunol* 1995;153:120-128.
311. Mosquera J, Rodriguez-Iturbe B, Parra G. Brief communication. Fish oil dietary supplementation reduces Ia expression in rat and mouse peritoneal macrophages. *Clin Immunol Immunopathol* 1990;56:124-129.
312. Khair-El-Din TA, Sicher SC, Vazquez MA, et al. Docosahexaenoic acid, a major constituent of fetal serum and fish oil diets, inhibits IFN- $\gamma$ -induced Ia-expression by murine macrophages in vitro. *J Immunol* 1995;154:1296-1306.
313. Somers SD, Chapkin RS, Erickson KL. Alteration of in vitro murine peritoneal macrophage function by dietary enrichment with eicosapentaenoic and docosahexaenoic acids in menhaden fish oil. *Cell Immunol* 1989;123:201-211.
314. Shichira G, Kinoshita M, Saeki Y. Polyunsaturated fatty acid metabolism and acetylated low density lipoprotein uptake in J774A.1 cells. *Arch Biochem Biophys* 1993;303:231-237.
315. Tappia PS, Ladha S, Clark DC, et al. The influence of membrane fluidity, TNF receptor binding, camp production and GTPase activity on macrophage cytokine production in rats fed a variety of fat diets. *Mol Cell Biochem* 1997;166:135-143.
316. Feng C, Keisler DH, Fritsche KL. Dietary omega-3 polyunsaturated fatty acids reduce IFN- $\gamma$  receptor expression in mice. *J Interferon Cytokine Res* 1999;19:41-48.
317. Saito H, Saito I, Chang KJ, et al. Effect of ingestion of eicosapentaenoic acid ethyl-ester on the scavenger activity for acetylated LDL and the production of platelet-derived growth factor in rat peritoneal macrophages. *Adv Prostaglandin Thromboxane Leukotr Res* 1990;21:241-245.
318. Endres S, Ghorbani R, Kelley VE, et al. The effect of dietary supplementation with n-3 polyunsaturated fatty acids on the synthesis of interleukin-1 and tumor necrosis factor by mononuclear cells. *N Engl J Med* 1980;320:265-271.
319. Meydani SN, Endres S, Woods MM, et al. Oral (n-3) fatty acid supplementation suppresses cytokine production and lymphocyte proliferation: comparison between young and older women. *J Nutr* 1991;121:547-555.
320. Jeyarajah DR, Kielar M, Penfield J, et al. Docosahexaenoic acid, a component of fish oil, inhibits nitric oxide production in vitro. *J Surg Res* 1999;83:147-150.
321. Boutard V, Fouqueray B, Philippe C, et al. Fish oil supplementation and essential fatty acid deficiency reduce nitric oxide synthesis by rat macrophages. *Kidney Int* 1994;46:1280-1286.
322. Ohata T, Fukuda K, Takahashi M, et al. Suppression of nitric oxide production in lipopolysaccharide-stimulated macrophage cells by  $\omega$ 3 polyunsaturated fatty acids. *Jpn J Cancer Res* 1997;88:234-237.
323. Wu W-M, Chiang B-L, Chang S-C, et al. Late feeding of dietary fish oil alleviates disease severity and affects macrophage function in autoimmune NZB/W F1 mice. *J Microbiol Immunol Infect* 2000;33:79-86.
324. Robinson DR, Prickett JD, Makoul GT, et al. Dietary fish oil reduces progression of established renal disease in (NZBxNZW) F1 mice and delays renal disease in BXSb and MRL/1 strains. *Arthritis Rheum* 1986;29:539-546.
325. Fisher M, Levine PH, Weiner BH, et al. Dietary n-3 fatty acid supplementation reduces superoxide production and chemiluminescence in a monocytes-enriched preparation of leukocytes. *Am J Clin Nutr* 1990;51:804-808.
326. Yoshida Ayako, Elner SG, Bian Z-M, et al. Differential chemokine regulation by Th2 cytokines during human RPE-monocyte coculture. *Invest Ophthalmol Vis Sci* 2001;42:1631-1638.
327. Hardardottir I, Kinsella JE. Increasing the dietary (n-3) to (n-6) polyunsaturated fatty acid ratio increases tumor necrosis factor production by murine resident peritoneal macrophages without an effect on elicited peritoneal macrophages. *J Nutr* 1992;122:1942-1951.
328. Wallace FA, Miles EA, Calder PC. Activation state alters the effect of dietary fatty acids on pro-inflammatory mediator production by murine macrophages. *Cytokine* 2000;12:1374-1379.
329. Kinsella JE, Lokesh B, Stone RA. Dietary n-3 polyunsaturated fatty acids and amelioration of cardiovascular disease: possible mechanisms. *Am J Clin Nutr* 1990;52:1-28.
330. Miles EA, Wallace FA, Calder PC. Dietary fish oil reduces intercellular adhesion molecule 1 and scavenger receptor expression on murine macrophages. *Atherosclerosis* 2000;152:43-50.
331. Sanderson P, Calder PC. Dietary fish oil diminishes lymphocyte adhesion to macrophage and endothelial cell monolayers. *Immunology* 1998;94:79-87.
332. Lu CY, Penfield JG, Khair-el-Din TA, et al. Docosahexaenoic acid, a constituent of fetal and neonatal serum, inhibits nitric oxide production by murine macrophages stimulated by IFN- $\gamma$  plus LPS, or by IFN- $\gamma$  plus *Listeria monocytogenes*. *J Reprod Immunol* 1998;38:31-53.
333. Renier G, Skamene E, DeSanctis J, et al. Dietary n-3 polyunsaturated fatty acids prevent the development of atherosclerotic lesions in mice. *Arterioscler Thromb* 1993;13:1515-1524.
334. Lo CJ, Chiu KC, Fu M, et al. Fish oil modulates macrophage P44/P42 mitogen-activated protein kinase activity induced by lipopolysaccharide. *JPEN J Parenter Enteral Nutr* 2000;24:159-163.
335. Beckman JS, Beckman TW, Chen J, et al. Apparent hydroxy radical production by peroxynitrite: implications for endothelial injury from nitric oxide and superoxide. *Proc Natl Acad Sci U S A* 1990;87:1620-1624.
336. Drevon CA, Nenseter MS, Brude IR, et al. Omega-3 fatty acids—nutritional aspects. *Can J Cardiol* 1995;11(Suppl G):47-54.
337. Suzukawa M, Abbey M, Howe PR, et al. Effects of fish oil fatty acids on low density lipoprotein size, oxidizability, and uptake by macrophages. *J Lipid Res* 1995;36:473-484.
338. Suzukawa M, Abbey M, Clifton P, et al. Enhanced capacity of n-3 fatty acid-enriched macrophages to oxidize low density lipoprotein mechanisms and effects of antioxidant vitamins. *Atherosclerosis* 1996;124:157-169.
339. Nenseter MS, Rustan AC, Lund-Katz S, et al. Effect of dietary supplementation with n-3 polyunsaturated fatty acids on physical properties and metabolism of low density lipoprotein in humans. *Arterioscler Thromb* 1992;12:369-379.

340. Kim DN, Eastman A, Baker JE, et al. Fish oil, atherogenesis, and thrombogenesis. *Ann N Y Acad Sci* 1995;748:474-481.
341. Ramirez-Tortosa C, Lopez-Pedrosa JM, Suarez A, et al. Olive oil- and fish oil-enriched diets modify plasma lipids and susceptibility of LDL to oxidative modification in free-living male patients with peripheral vascular disease: the Spanish Nutrition Study. *Br J Nutr* 1999;82:31-39.
342. Harada N, Kashiwagi A, Nishio Y, et al. Fish oil, atherogenesis, and thrombogenesis. *Ann N Y Acad Sci* 1995;748:474-481.
343. Sobenin IA, Tertov V, Koshinsky T, et al. Modified low density lipoprotein from diabetic patients causes cholesterol accumulation in human intimal aortic cells. *Atherosclerosis* 1993;100:41-54.
344. Bagdade JD, Buchana WE, Kuusi T, et al. Persistent abnormalities in lipoprotein composition in non-insulin-dependent diabetes after intensive insulin therapy. *Arteriosclerosis* 1990;10:232-239.
345. Klein R, Klein B, Franke T. The relationship of cardiovascular disease and its risk factors to age-related maculopathy. The Beaver Dam Eye Study. *Ophthalmology* 1993;100:406-414.

# DIABETES-INDUCED DYSFUNCTION OF RETINAL MÜLLER CELLS

---

BY Donald G. Puro, MD, PhD

## ABSTRACT

*Purpose:* This study tested the hypothesis that the function of the glutamate transporter in retinal Müller cells is compromised early in the course of diabetes by a mechanism involving oxidation. Dysfunction of this transporter, which removes glutamate from the extracellular space, may play a critical role in the disruption of glutamate homeostasis that occurs in the diabetic retina. Because glutamate is toxic to retinal neurons and is likely to exacerbate oxidative stress, elucidation of the mechanisms by which diabetes elevates the concentration of this amino acid may help to better understand the pathogenesis of diabetic retinopathy.

*Methods:* Müller cells were freshly isolated from normal rats and those made diabetic by streptozotocin injection. The activity of the Müller cell glutamate transporter, which is electrogenic, was monitored via the perforated-patch configuration of the patch-clamp technique.

*Results:* Four weeks after the onset of hyperglycemia, dysfunction of the Müller cell glutamate transporter was detected ( $P = .005$ ). After 13 weeks of streptozotocin-induced diabetes, the activity of this transporter was decreased by 67% ( $P = .001$ ). Consistent with oxidation causing this dysfunction, exposure to a disulfide-reducing agent rapidly restored the activity of this transporter in Müller cells from diabetic retinas.

*Conclusions:* Soon after the onset of experimental diabetes, the function of the glutamate transporter in Müller cells is decreased by a mechanism that is likely to involve oxidation. The demonstration that the activity of this transporter can be rapidly restored raises the possibility that targeting this molecule for therapeutic intervention may restore glutamate homeostasis and, thereby, ameliorate sight-threatening complications of diabetic retinopathy.

*Trans Am Ophthalmol Soc* 2002;100:339-352

## INTRODUCTION

---

The focus of this thesis is on diabetes-induced changes in the function of retinal Müller cells. These glia, which are critically positioned between the vasculature and the neurons of the retina, are of particular interest because reports in the literature suggest that their role in regulating the molecular composition of the retinal microenvironment may be compromised early in the course of diabetic retinopathy.

The objective of this study was to test the hypothesis that the ability of Müller cells to remove glutamate from the extracellular space is diminished soon after the onset of experimental diabetes. Since extracellular glutamate is neurotoxic, dysfunction of the mechanisms regulating the concentration of this amino acid could contribute to nerve cell damage in the diabetic retina. In the long term,

identifying early events in diabetic retinopathy may provide therapeutic targets for preventing sight-threatening complications of this disorder.

### DIABETIC RETINOPATHY: MORE THAN A VASCULAR DISORDER

Although vascular changes are the classic hallmark of this disorder, a number of observations suggest that microangiopathy is only one aspect of a more widespread retinal dysfunction.<sup>1-3</sup> The concept that neurons as well as capillaries are affected by diabetes is not new. In the early 1960s, Wolter<sup>4</sup> and Bloodworth<sup>5</sup> documented that diabetic retinopathy is associated with degeneration of neurons, especially those located in the inner retina. In fact, diabetes-induced changes in retinal neurons and glia may precede the onset of clinically evident vascular injury.<sup>3-7</sup> For example, loss of color<sup>8-10</sup> and contrast sensitivity<sup>11-14</sup> and abnormalities in the electroretinogram<sup>15-24</sup> have been documented in patients before detection of the vascular changes that are traditionally used to diagnose diabetic retinopathy.

Early neuronal and glial alterations are also evident in rats with chemically induced diabetes. These changes include decreases in components of the electroretino-

From the Departments of Ophthalmology and Visual Sciences and Physiology, University of Michigan, Ann Arbor. This project was supported in part by grants EY07003 from the National Institutes of Health; Senior Scientist Awards from Research to Prevent Blindness, Inc; and the Mid-West Eye Bank and Transplantation Center.

gram<sup>25</sup> and increased apoptosis of retinal neurons.<sup>26,27</sup> In addition, early in the course of diabetic retinopathy, Müller cells markedly upregulate their expression of glial fibrillary acidic protein,<sup>28-31</sup> which is a nonspecific response to pathophysiological conditions.<sup>32</sup> Thus, a comprehensive understanding of diabetic retinopathy requires elucidation of the mechanisms by which diabetes affects nonvascular, as well as vascular, cells of the retina.

#### MÜLLER CELLS: CRITICAL ELEMENTS IN A HEALTHY RETINA

Müller cells are the principal glia of the retina. Although the physiology of these cells was previously thought to be rather simple, investigations during the past 2 decades have revealed that Müller cells express a diversity of ion channels and transporters, release a variety of cytokines and survival factors, and have receptors for numerous neurotransmitters and growth factors.<sup>33,34</sup> As a result, it is now evident that Müller cells play an active, dynamic role in the retina.<sup>33</sup>

A major physiological function of these cells is to regulate the ionic and molecular composition of the extracellular space (Table I). Consistent with a homeostatic role, Müller cells are well positioned to interact with the retinal microenvironment.<sup>35</sup> These glial cells are radially oriented and span the depth of the retina from the vitreal border to the interphotoreceptor matrix of the subretinal space. Their processes are in close apposition to neuronal cell bodies, neurites, and synapses as well as the blood vessels.

TABLE I: PUTATIVE FUNCTIONS OF MÜLLER CELLS

#### PHYSIOLOGICAL

##### Homeostatic

Maintain a low concentration of glutamate in the microenvironment

Redistribute extracellular potassium

Regulate pH

##### Nutritive

Store glycogen

Provide lactate for neuronal nutrition

##### Trophic:

Release photoreceptor and neuronal survival factors

##### Vascular regulation

Facilitate blood-retinal barrier development

Influence blood flow

##### Modulation of retinal function

Recycle glutamate/glutamine

Communicate with neurons

#### PATHOBIOLOGICAL

##### Protective

Decrease neurotoxic levels of glutamate at sites of blood-retinal barrier breakdown and neuronal injury

Release molecules that enhance neuronal and photoreceptor survival

Phagocytose retinal debris

Serve as an antigen-presenting cell

##### Detrimental

Migration from the retina

Proliferation

An intensively studied function of Müller cells is their uptake of synaptically released glutamate,<sup>33,34,36</sup> which is a neurotransmitter at more than 90% of the synapses in the retina.<sup>37</sup> Not only is this amino acid released by the photoreceptors, but many retinal neurons also use glutamate as a neurotransmitter. By removing extracellular glutamate, Müller cells help to terminate transmission at glutamatergic synapses.<sup>38,39</sup> After uptake via a glutamate transporter, glutamate is rapidly converted in Müller cells to glutamine, which is subsequently recycled to neurons, where it is converted back into glutamate for release at synapses.<sup>34,40</sup> Consistent with Müller cells having a vital role in regulating retinal glutamate levels, Vorwerk and colleagues<sup>41</sup> reported that treatment of rats with antisense oligonucleotides directed against the Müller cell glutamate transporter caused more than a threefold increase in the vitreal concentration of glutamate.

In addition to playing a role in terminating glutamatergic transmission, prompt removal of synaptically released glutamate is necessary, since prolonged activation of certain glutamate receptors, for example, the calcium-permeable *N*-methyl-*D*-aspartate (NMDA) receptors, can cause an excessive influx of calcium, which can kill retinal neurons.<sup>42-44</sup> Thus, mechanisms to efficiently remove synaptically released glutamate are necessary for the maintenance of a healthy retina.

#### GLUTAMATE HOMEOSTASIS: DISRUPTION IN THE DIABETIC RETINA

Despite intensive study of the mechanism by which Müller cells remove glutamate under normal conditions, much less is known about this vital function in the diabetic retina. This gap in knowledge is likely to be significant, because the role of Müller cells in maintaining a low extracellular concentration of glutamate may be particularly critical in diabetes. As in the normal retina, synaptically released glutamate must be removed. However, in addition, neurons in the diabetic retina must be protected from glutamate leaking into the retina because the blood-retinal barrier is compromised early in diabetes.<sup>45,46</sup> Since plasma contains 100 to 300  $\mu\text{M}$  of this amino acid<sup>47</sup> and as little as 5  $\mu\text{M}$  of glutamate can be lethal to retinal neurons,<sup>43,45</sup> it seems apparent that a breakdown in the blood-retinal barrier could have dire consequences for retinal function and neuronal survival. Thus, the transport of glutamate into Müller cells may be essential in order to prevent toxic levels of this amino acid from reaching neurons located near defects in the blood-retinal barrier.

Glial cells, whose processes completely ensheath the retinal vasculature,<sup>49</sup> are well positioned to remove glutamate at sites of a breakdown in the blood-retinal barrier. In diabetes, however, the ability of Müller cells to regulate the extracellular concentration of glutamate may be

compromised. Support for this possibility is that levels of this amino acid are elevated in the retinas of diabetic rats,<sup>28,50</sup> even though glutamate synthesis is unaffected.<sup>51</sup> Also, the increased concentration of glutamate in the vitreous of patients with diabetic retinopathy is likely to reflect the presence of high concentrations of this amino acid in the retina.<sup>52</sup> These various observations suggest that the regulatory mechanisms to control glutamate are dysfunctional in the diabetic retina.

**GLUTAMATE UPTAKE BY MÜLLER CELLS: A VULNERABLE STEP**

An essential step in the regulation of extracellular glutamate is the transport of this amino acid into Müller cells via a high-affinity glutamate transporter, which is named GLAST (the human analog is named EAAT1). GLAST is the only glutamate transporter detected in Müller cells, and it is not found in other types of retinal cells.<sup>53</sup> A potentially critical feature of GLAST is the presence of redox-sensing elements, which regulate this transporter via thiol-disulfide redox interconversion.<sup>54,55</sup> Consistent with the presence of redox-sensitive sites, Trotti and colleagues<sup>54</sup> demonstrated that chemical oxidation or reduction altered the activity of cloned GLAST molecules, which had been placed in artificial liposomes. These investigators found that oxidizing agents decreased GLAST function. In contrast, exposure to a chemical reductant restored the activity of this transporter.<sup>54</sup> However, although evidence is good that cloned GLAST expressed in liposomes possesses redox sensitivity, this has not been demonstrated for native GLAST molecules located in cells, such as Müller cells, which exclusively express this type of glutamate transporter.

A central premise of this thesis is that the redox sites on the GLAST molecules in Müller cells render this transporter vulnerable to diabetes-induced dysfunction (Figure 1). This idea is based, in part, on the observation that oxidative stress occurs in the retina<sup>50,56-58</sup> and other tissues<sup>59</sup> early in the course of diabetes. These observations, plus evidence that glutamate homeostasis is disrupted in the diabetic retina,<sup>28,51,52</sup> are the basis for the hypothesis that oxidation of the glutamate transporter is one mechanism by which diabetes compromises the ability of Müller cells to regulate glutamate concentration.

**EXPERIMENTAL STRATEGY**

The aim of this thesis is to test the hypothesis that early in the course of diabetic retinopathy, the function of the glutamate transporter in retinal Müller cells is compromised by a mechanism involving oxidation. To achieve this aim, this study was designed to quantify GLAST activity in Müller cells that were freshly isolated from normal rats and those made diabetic by injection of streptozotocin.

*Electrophysiological Assay of GLAST Activity*

A key feature of the glutamate transporter in Müller cells is that it is electrogenic.<sup>60-62</sup> Briefly stated, a net inward current is generated during the transport of glutamate as two sodium ions enter, but only one potassium ion exits; the influx of the negatively charged amino acid is balanced with an entering proton (Figure 2). In addition, there is an associated chloride conductance. However, this conductance is not coupled to the transport of glutamate.<sup>62</sup>

As a result of the movement of ions and glutamate during the uptake of this amino acid, the GLAST transporter generates a net influx of a positive charge as glutamate enters the cell. In standard electrophysiological terminology, a positive charge moving into a cell is classified as being an inward, negative current. Thus, GLAST activity generates an influx of positive ions that can be detected electrophysiologically as an inward (negative) current.

Because the glutamate transporter of a Müller cell is electrogenic, electrophysiological techniques can be used to detect the negative, inward current generated as glutamate is transported into the cell. The ability to use elec-

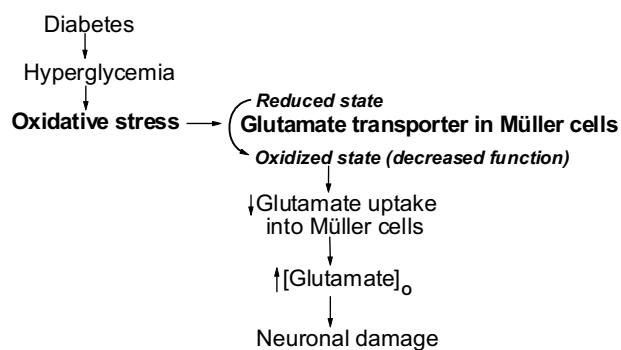


FIGURE 1

Hypothesized mechanism by which diabetes causes dysfunction of the glutamate transporter in Müller cells. [Glutamate]<sub>o</sub>, extracellular glutamate concentration.

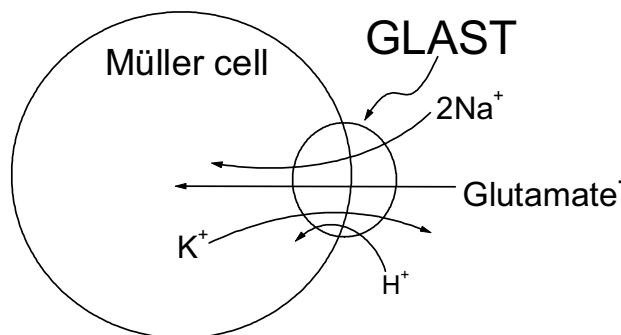


FIGURE 2

Kinetic scheme for the Müller cell glutamate transporter, GLAST. With transport of a glutamate molecule via GLAST, there is a net influx of a positive ion. Since a positive current is by definition the movement of a positive ion out of a cell, then the net influx of a positive charge, as occurs with transport of glutamate by GLAST, is an inward, negative current.

trophysiological methods to quantify in “real-time” the transporter-induced current in freshly isolated Müller cells has resulted in a detailed understanding of the physiology of this glutamate transporter.<sup>63</sup> However, despite extensive knowledge of the normal function of GLAST in Müller cells, information concerning the activity of this transporter in the diabetic retina is extremely limited.

This project appears to be the first electrophysiological assessment of the effect of diabetes on Müller cell function. In the experiments presented in this study, the currents of isolated rat Müller cells were monitored using the perforated-patch configuration of the patch-clamp technique.<sup>64,65</sup> A major advantage of the perforated-patch configuration, as compared with the standard whole-cell recording method, is that it minimally disrupts the cytoplasm of the sampled cell and, consequently, minimizes the loss of intracellular regulatory molecules, which may affect GLAST activity. Use of this recording method permitted quantification of glutamate transporter activity before, during, and after the sampled Müller cell was exposed to a perfusate supplemented with glutamate or l-trans-pyrrolidine-2, 4-dicarboxylate (PDC), which is a specific ligand for this transporter.<sup>66,67</sup>

#### *Streptozotocin Model of Diabetes*

To test the hypothesis that the function of the Müller cell glutamate transporter is decreased in the diabetic retina, Müller cells from rats with streptozotocin-induced diabetes were studied. Injection of streptozotocin creates an experimental model of type 1 diabetes.<sup>68</sup> Streptozotocin, which is essentially a glucose molecule linked to a reactive nitrosourea moiety, is internalized into cells via glucose transporters. Once inside a cell, the nitrosourea moiety is released and kills the cell by cross-linking vital structures. Because the beta cells of the pancreas are more active than other cells in taking up glucose, they are also more sensitive to streptozotocin toxicity than other cells. As a result, at an appropriate dose, streptozotocin preferentially kills beta cells and thereby causes insulin levels to plummet and blood glucose levels to rise.

The streptozotocin model of diabetes differs from the usual clinical situation in that blood glucose levels are not controlled by treatment with insulin. In contrast, patients diagnosed as having type 1 diabetes are promptly placed on insulin therapy. However, despite differing from the typical clinical course, use of this experimental model in numerous studies has provided useful insights into the effects of hyperglycemia and insulin deficiency. For this reason, a vast literature now exists on the effects of streptozotocin-induced diabetes on the rat retina. This information is useful, since new observations from this thesis project can be correlated with previously identified retinal changes that occur in this experimental model of diabetes.

#### *Isolated Müller Cells*

Because technical challenges precluded the use of an electrophysiological assay of transporter activity in Müller cells *in vivo*, or in the intact retina, the experiments performed in this study used Müller cells that were freshly isolated from the retina. Over the past 15 years, electrophysiological studies of freshly isolated Müller cells have been very fruitful. There is now a detailed understanding of the mechanisms by which GLAST molecules transport glutamate from the extracellular space into a Müller cell (Figure 2),<sup>62,63</sup> although the function of the glutamate transporter in Müller cells of diabetic retinas has not been assessed prior to this project.

A caution in the interpretation of experimental results obtained from isolated Müller cells is that any effects of diabetes on the glutamate transporter of these cells must ultimately be confirmed in the retina *in vivo*. However, despite not assaying the transporter activity in Müller cells of the intact retina, the use of the patch-clamp technique to monitor freshly isolated cells provides a powerful experimental approach. The ability to perform real-time quantification of glutamate transporter activity permits the testing of hypotheses concerning the mechanisms by which diabetes affects Müller cell function.

The results presented in this thesis revealed that the activity of the glutamate transporter in rat Müller cells decreased significantly within 4 weeks after the onset of streptozotocin-induced diabetes. With exposure of diabetic Müller cells to a chemical reductant, glutamate transporter activity was fully restored. Taken together, the experimental findings of this study support the hypothesis that early in the course of diabetic retinopathy, the function of the glutamate transporter in Müller cells is decreased by a mechanism involving oxidation.

## **METHODS**

### **MODEL OF DIABETES IN THE RAT**

This study conformed to the guidelines of the Association for Research in Vision and Ophthalmology and the University of Michigan University Committee on the Use and Care of Animals. After an overnight fast, 5- to 6-week-old Long-Evans rats (Harlan Sprague Dawley, Inc, Indianapolis, Indiana) received an intraperitoneal injection of streptozotocin (75 mg/kg) diluted in 0.8 mL of 0.03 M citrate buffer (pH 4.7). Subsequently, the animals received food and water *ad libitum*. The vivarium was maintained on a 12-hour alternating light-dark cycle. Three days after streptozotocin injection, diabetes was confirmed by assaying the glucose concentration (One Touch Basic, LifeScan, Milpitas, California) in blood obtained from the tail vein. Rats having glucose levels of greater than 250 mg/dL were classified as being diabetic.

Age-matched rats served as controls. Immediately prior to the harvesting of retinal Müller cells, the blood glucose level was  $378 \pm 6$  mg/dL in the 23 diabetic rats used in this study.

#### FRESH MÜLLER CELLS

Freshly dissociated Müller cells were prepared from rats that were euthanized with carbon dioxide. Immediately after death, the retinas were rapidly removed and incubated in 2.5 mL Earle's balanced salt solution (Invitrogen, San Diego, California), which was supplemented with 0.5 mM EDTA, 1.5 mM  $\text{CaCl}_2$ , 1 mM  $\text{MgSO}_4$ , 20 mM glucose, 26 mM sodium bicarbonate, 2 mM cysteine, 0.04% DNase, and 15 units of papain (Worthington Biochemical Corp, Freehold, New Jersey), for 40 minutes at  $30^\circ\text{C}$  while 95% oxygen–5% carbon dioxide was bubbled through to maintain pH and oxygenation. After transfer to a solution containing 140 mM NaCl, 3 mM KCl, 1.8 mM  $\text{CaCl}_2$ , 0.8 mM  $\text{MgCl}_2$ , 10 mM Na-Hepes, 15 mM mannitol, and 5 mM glucose at pH 7.4 with osmolarity adjusted to 310 mOsm  $\text{L}^{-1}$ , the retinas were gently triturated, and a suspension of cells was placed on a glass coverslip (diameter, 15 mm; Warner Instrument Corp, Hamden, Connecticut) that was positioned in a recording chamber mounted on the stage of an inverted microscope. Müller cells were identified by their characteristic morphology (Figure 3).

#### ELECTROPHYSIOLOGY

Recordings from fresh Müller cells were made at room temperature ( $22^\circ$  to  $24^\circ\text{C}$ ) within 3 hours of cell isolation. A gravity-fed system with multiple reservoirs was used to continuously perfuse ( $\sim 2$  mL/min $^{-1}$ ) the recording chamber (0.5 mL volume) with various solutions. Whole-cell currents were monitored using the perforated-patch configuration of the patch-clamp technique. Unless noted otherwise, the bathing solution (solution A) consisted of 140 mM NaCl, 3 mM KCl, 1.8 mM  $\text{CaCl}_2$ , 0.8 mM  $\text{MgCl}_2$ , 3 mM  $\text{BaCl}_2$ , 10 mM Na-Hepes, and 5 mM glucose at pH 7.4 with the osmolarity adjusted by less than 5% to 310 mOsm  $\text{L}^{-1}$ . Detection of currents generated by the glutamate transporter was facilitated by using barium to block

the large ionic currents generated by the inwardly rectifying potassium channels, which are the predominant ion channels of these glia.<sup>69-71</sup>

Using a multistage programmable puller (Sutter Instruments, San Rafael, California), patch pipettes were pulled from Corning No. 7052 glass tubing (Gardner Glass Co, Claremont, California) and heat-polished to tip diameters of 2 to 3  $\mu\text{m}$ . The pipette solution consisted of 50 mM KCl, 65 mM  $\text{K}_2\text{SO}_4$ , 6 mM  $\text{MgCl}_2$  and 10 mM K-Hepes, 240  $\mu\text{g mL}^{-1}$  amphotericin B, and 240  $\mu\text{g mL}^{-1}$  nystatin at pH 7.4 with the osmolarity adjusted to 280 mOsm  $\text{L}^{-1}$ . The resistances of the pipettes used were approximately 5 M $\Omega$  when tested in the bathing solution.

The pipettes were mounted in the holder of a Dagan 3900 patch-clamp amplifier (Dagan Corp, Minneapolis, Minnesota) and sealed to the cell bodies of Müller cells (Figure 4). Seals generally formed over a period of 1 to 30 seconds and reached resistances of greater than 1 G $\Omega$ . As amphotericin-nystatin perforated the patch, the access resistance to the cell usually decreased to less than 20 M $\Omega$  within 10 minutes for the Müller cells analyzed. Recordings were used after the ratio of cell membrane to series resistance was greater than 10. This ratio was monitored periodically; if the ratio decreased to below 10, the analysis of the cell was terminated. Series resistance was not corrected, but the error due to the voltage drop across the patch pipette was always less than 10% of the applied voltage. Cell membrane capacitance was estimated using circuits of the Dagan 3910 expander module (Dagan Corp). Adjustment for the calculated<sup>72</sup> liquid junction potential was made after data collection.

Currents were evoked by a voltage ramp protocol, which was controlled by pClamp 8 software (Axon Instruments, Inc, Foster, California). During a voltage ramp, the applied voltage changed from negative to positive membrane potentials at the rate of 66 mV  $\text{s}^{-1}$ . The recorded currents were filtered at 1 kHz with a four-pole Bessel filter, digitally sampled at 1-msec intervals using a Digidata 1200B acquisition system (Axon Instruments) and stored by a Pentium class computer that was equipped with pClamp 8 and Origin (Version 6,

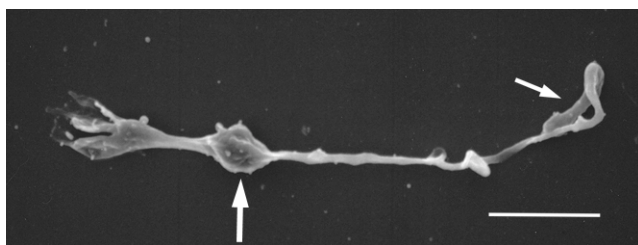


FIGURE 3

Scanning electron photomicrograph of a Müller cell freshly isolated from the rat retina. Larger arrow points to cell soma; smaller arrow points to Müller cell endfoot. Bar shows 10  $\mu\text{m}$ .

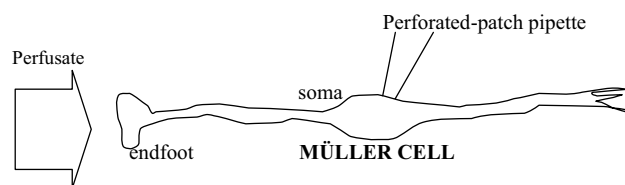


FIGURE 4

Schematic drawing of a perforated-patch recording from the soma of an isolated Müller cell.

OriginLab Corp, Northampton, Massachusetts) software for data analysis and graphics display.

The inward currents induced by glutamate or PDC were measured 1.5 to 2 minutes after the onset of exposure to the ligand. The amplitudes of the induced currents were measured at  $-120$  mV. The chord conductance for the inwardly rectifying potassium current was calculated by measuring the amplitude of the barium-sensitive current at  $-120$  mV.

#### SCANNING ELECTRON MICROSCOPY

Standard techniques, as described previously,<sup>73</sup> were used to prepare glutaraldehyde-fixed isolated Müller cells for scanning electron microscopy, which was performed by the University of Michigan Anatomy and Cell Biology Core Facility.

#### CHEMICALS

Chemicals were from Sigma (St Louis, Missouri) unless otherwise noted.

#### STATISTICS

Data are given as means  $\pm$  SEM. Probability was evaluated by the Student's *t* test.

#### RESULTS

The perforated-patch configuration of the patch-clamp technique was used to monitor the currents of isolated rat Müller cells. Because the glutamate transporter of Müller cells is electrogenic, its function can be quantitatively assessed by an electrophysiological method. An advantage of the perforated-patch configuration is that it minimizes the disruption of the recorded cell's cytoplasm and, consequently, the loss of intracellular regulatory molecules that may influence the functioning of the glutamate transporter.

Since a recording pipette detects currents generated by the activity of ion channels, as well as the electrogenic transporters such as GLAST, it was preferable in many experiments to use a ligand that is selective for the glutamate transporter. For this reason, PDC, which is more selective for GLAST than glutamate,<sup>66,67</sup> was often used in this study. The selectivity of PDC results in the activation of the glutamate transporter, without the confounding effects by also activating glutamate receptors,<sup>66,67,74</sup> which modulate the activity of ion channels in Müller cells.<sup>75,76</sup> Because PDC has not been used previously to monitor glutamate transporter function in mammalian Müller cells, however, it was necessary to establish that the PDC-induced current in rat Müller cells had characteristics consistent with GLAST activity.

#### THE PDC-INDUCED CURRENT IN MÜLLER CELLS

Figure 5 shows the effect of PDC on the inward current

monitored in a Müller cell freshly isolated from a control rat. Consistent with activation of GLAST, there was an increase in an inward (negative) current during exposure of the Müller cell to PDC. The PDC-induced current reversed rapidly when the perfusate was switched to one lacking PDC. Similar observations were made in 18 Müller cells isolated from normal retinas.

Because GLAST activity is known to be dependent on the concentration of the transported ligand,<sup>60,61,67</sup> the concentration dependence of the PDC-induced inward current in isolated rat Müller cells was determined. As shown in Figure 6, the half-maximally effective concentration of PDC was approximately  $10 \mu\text{M}$ . This concentration is very similar to the value determined by Sarantis and coworkers<sup>67</sup> for the activation by PDC of currents in salamander Müller cells. In addition, the half-maximally effective concentration for PDC is similar to that for glutamate when tested on Müller cells from the salamander,<sup>61</sup> rabbit<sup>62</sup> and rat (this thesis, Figure 12).

Similar to the electrogenic glutamate transporter observed in Müller cells from other species,<sup>61,74</sup> the PDC current induced in rat Müller cells was dependent on the voltage across the cell membrane. As illustrated in Figure 7, the PDC-induced current increased in amplitude with membrane hyperpolarization. Also, there was no sign of an induced outward current (Figure 7B), as can occur when glutamate-gated ion channels are activated.<sup>76</sup> Similar observations were made in 18 sampled Müller cells.

As reviewed (Figure 2), the transport of glutamate

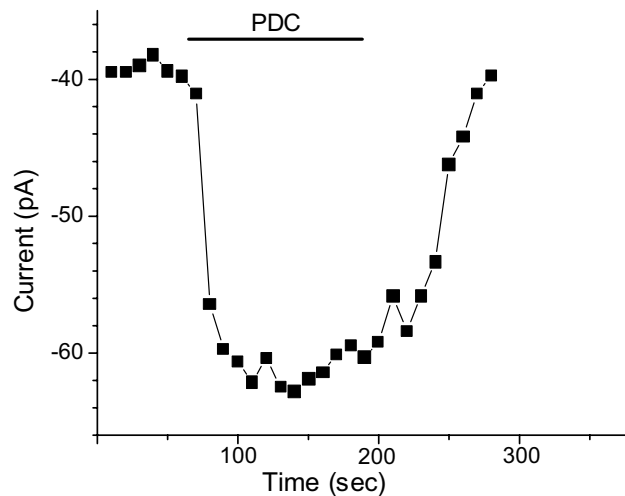


FIGURE 5

Time course for the effect of PDC on the current of a freshly isolated Müller cell monitored via a perforated-patch pipette. Amplitude of current was measured at 10-second intervals while membrane potential of Müller cell was voltage-clamped to  $-120$  mV. Bar shows time at which perfusate was supplemented with  $100 \mu\text{M}$  PDC. Induction of an inward, negative current is consistent with activation of GLAST, which causes a net movement of positive charge into a cell as this transporter moves its ligand (in this case, PDC) from extracellular space into cytoplasm.

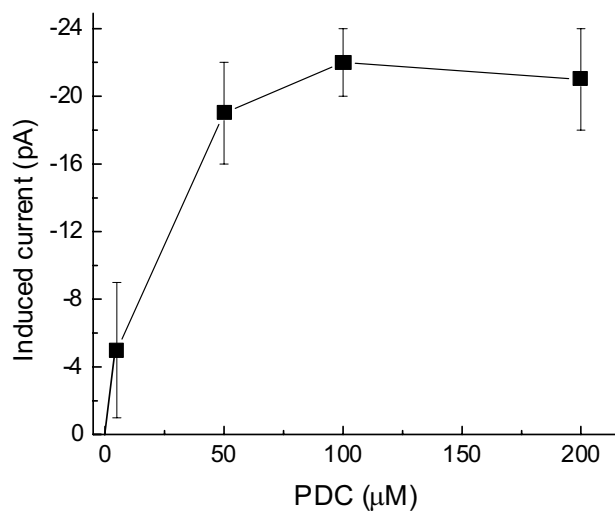


FIGURE 6

Dose response for current induced in Müller cells during exposure to PDC. Note that vertical axis indicates an increase in inward, negative current; greater transporter activity causes a more negative, inward current. A mean of  $7 \pm 4$  cells was sampled per data point. The amplitude of PDC-induced inward current in Müller cells is concentration-dependent.

into a cell via GLAST is dependent on external sodium. Consistent with a sodium dependence of the PDC-induced current, the experiment illustrated in Figure 8 demonstrated that perfusion with a sodium-free solution eliminated the PDC-induced current in a rat Müller cell. Similar observations were made in four Müller cells isolated from rat retinas. Taken together, the results of these experiments are consistent with PDC activating GLAST in Müller cells freshly isolated from the rat retina.

#### GLAST CURRENT IN MÜLLER CELLS OF DIABETIC RATS

The working hypothesis of this study was that diabetes causes dysfunction of the Müller cell glutamate transporter. To test this hypothesis, the PDC current was quantified in Müller cells isolated from control and diabetic rats (Figure 9). Four weeks after administration of streptozotocin, the amplitude of the current induced by 100  $\mu\text{M}$  PDC decreased significantly ( $P = .005$ ). At 13 weeks after streptozotocin injection, which was the maximum duration of diabetes studied in this project, the amplitude of the PDC-induced current was decreased by 67% ( $P = .001$ ) as compared with the control value.

Although there are distinct advantages to using PDC to selectively activate the GLAST, it seemed reasonable to also quantify the current induced in normal and diabetic Müller cells during exposure to 100  $\mu\text{M}$  glutamate, which is the *in vivo* ligand for this transporter. As illustrated in Figure 10, the glutamate-induced current in Müller cells from retinas of diabetic rats was significantly ( $P = .004$ ) diminished. This finding with glutamate is consistent with the observed decrease in the PDC-induced currents in

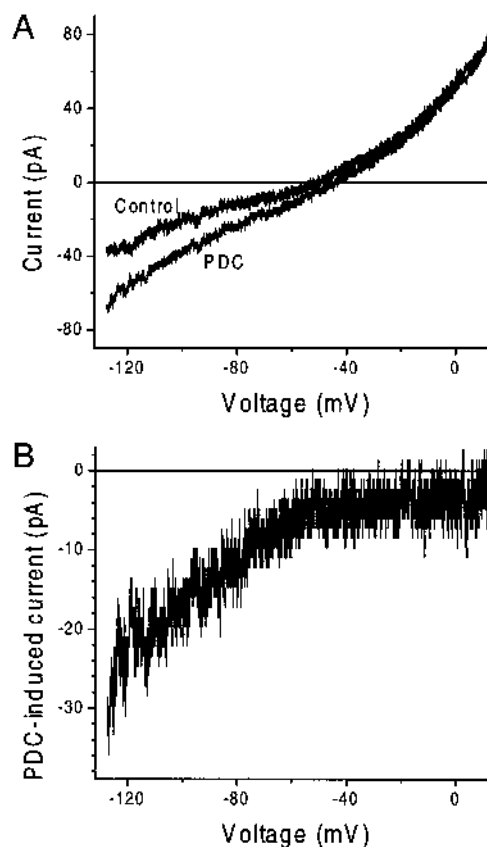


FIGURE 7

The effect PDC on the currents of a freshly isolated Müller cell. A, Effect of 100  $\mu\text{M}$  PDC on current-voltage (I-V) relationship of same Müller cell as studied in Figure 5. B, I-V plot of PDC-induced current obtained by subtracting curves in A. PDC activated a voltage-dependent inward current in Müller cells.

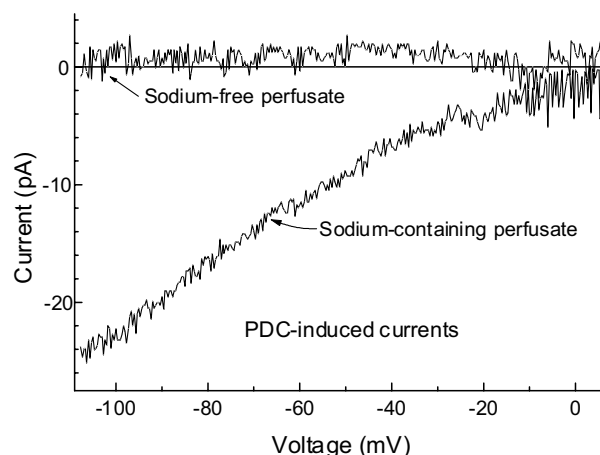


FIGURE 8

Effect of external sodium on PDC-activated current in an isolated rat Müller cell. I-V relationships of the current induced by 100  $\mu\text{M}$  PDC in a rat Müller cell perfused with either solution A, which contained 150 mM  $\text{Na}^+$ , or a modification of solution A, in which NaCl was replaced with choline chloride and *N*-methyl-*D*-glucamine-Hepes was substituted for Na-Hepes. Consistent with PDC activating GLAST, the PDC-induced current in Müller cells was dependent on external sodium.

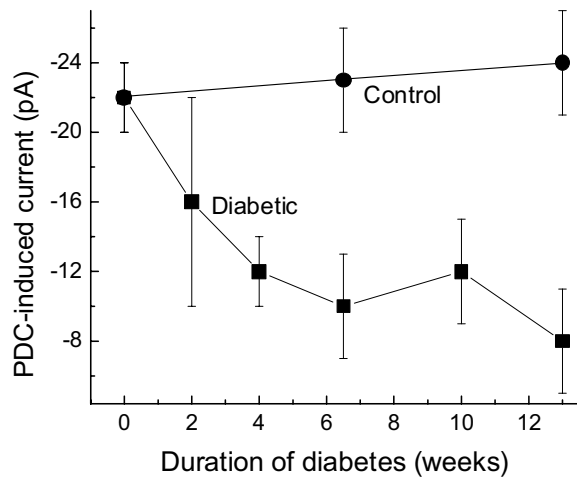


FIGURE 9

Effect of diabetes on the amplitude of the PDC-induced current in Müller cells. Inward (negative) currents induced by PDC were measured in Müller cells isolated from control (●) and diabetic (■) rats. Note that the more negative the current, the greater the PDC-induced transporter activity. Over 13-week course of streptozotocin-induced diabetes, blood glucose levels prior to sacrifice were not significantly ( $P > .1$ ) different; mean level of blood glucose was  $378 \pm 6 \text{ mg/dL}^{-1}$  in the diabetic rats. A mean of  $11 \pm 2$  Müller cells was sampled for each time point. The amplitude of the PDC-induced inward current decreases soon after the onset of experimental diabetes.

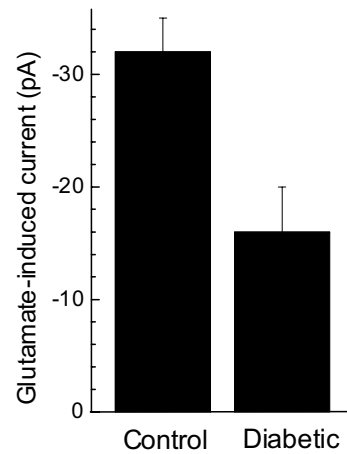


FIGURE 10

Effect of diabetes on glutamate-induced current in Müller cells. Mean induced currents in a series of 11 Müller cells from control rat retinas and 8 cells isolated from rats having diabetes for  $9 \pm 1$  weeks. Note that the greater the glutamate-induced activation of the transporter, the more negative the current. During experimental diabetes, amplitude of Müller cell current induced by glutamate decreases.

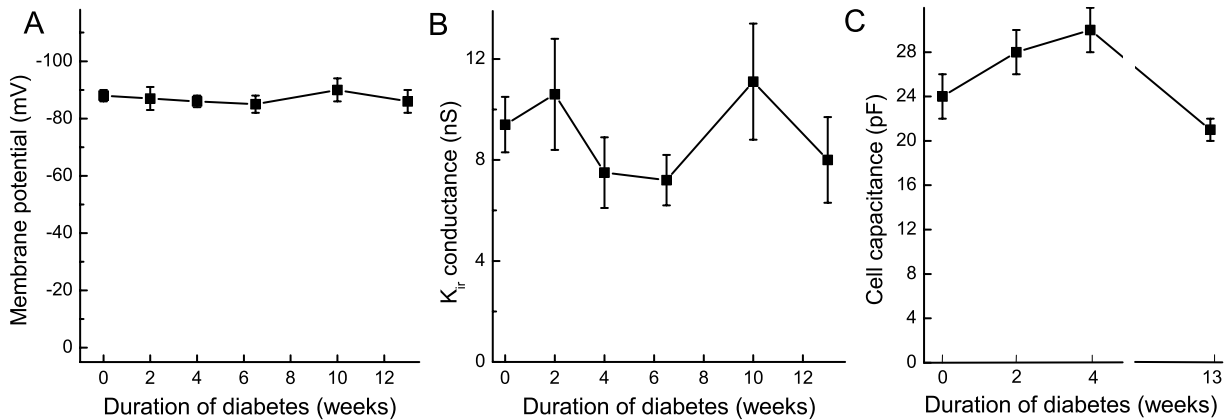


FIGURE 11

Physiological parameters of Müller cells at various times after streptozotocin injection. A, Membrane potential. B, Conductance of inwardly rectifying potassium (Kir) current. C, Cell membrane capacitance. For each panel, a mean of  $8 \pm 1$  Müller cells were sampled for each point. No significant changes occurred in these parameters of Müller cell physiology during 13 weeks of streptozotocin-induced diabetes.

Müller cells from diabetic retinas (Figure 9). Thus, it appears that early in the course of diabetes, these glia have a diminished capability to remove glutamate from the extracellular space.

One possible explanation for observation that glutamate transporter activity decreases in Müller cells from diabetic rats is that there is a generalized disturbance in physiology of these glia. However, this seems unlikely, since the membrane potentials of the sampled cells were

not significantly ( $P > .3$ ) different in the control and diabetic groups (Figure 11A). In addition, the amplitude of the inwardly rectifying potassium current, which is the predominant ionic current of Müller cells,<sup>70,71</sup> was not significantly ( $P > .16$ ) different in the Müller cells isolated from diabetic and control rats (Figure 11B).

An alternative possibility to account for the reduction in the amplitude of the current generated by the glutamate transporter is that diabetes causes Müller cells to

become smaller. With a smaller surface area, there may be fewer GLAST molecules per cell and, thereby, a smaller current generated as glutamate is transported across the membrane. However, measurements of cell membrane capacitance, which is an indicator of cell size, did not reveal a significant ( $P > .05$ ) change from control values during 13 weeks of streptozotocin-induced diabetes (Figure 11C).

The stability of the resting membrane potential, potassium conductance, and cell membrane capacitance during the initial 13 weeks of experimental diabetes suggests that the observed decrease in the activity of the glutamate transporter was not part of a generalized physiological deterioration of Müller cells. Rather, it appears likely that early in diabetic retinopathy, there is a selective vulnerability of this transporter molecule.

#### OXIDATION AND GLAST FUNCTION IN DIABETIC MÜLLER CELLS

This study also addressed the issue of the mechanism by which diabetes causes dysfunction of the glutamate transporter in Müller cells. Experiments were performed to help test the hypothesis that oxidative mechanisms play a role. This seems to be a reasonable idea because diabetes is associated with oxidative stress<sup>59</sup> and the cloned GLAST molecule possesses redox-regulatory elements.<sup>54</sup>

Because studies on cloned GLAST demonstrated that oxidation diminished transporter function without altering the half-maximally effective concentration of glutamate,<sup>54</sup> the dose-response relationship for the glutamate-induced current was assessed in Müller cells from control and diabetic rats. As shown in Figure 12, the half-maximally effective concentration of glutamate was approximately 8  $\mu\text{M}$  in both the control and experimental groups. Of further interest, this value is almost identical to the half-maximally effective concentration reported for the glutamate transporters of Müller cells from salamanders and rabbits, the only other species studied previously.<sup>60,61</sup> Thus, diabetes is associated with a significant decrease in the activity of the Müller cell glutamate transporter (Figure 9) but does not alter the half-maximally effective concentration of glutamate, at least during the initial 13 weeks of experimental diabetes. Since oxidation of GLAST is also reported to decrease the maximal activity of this transporter, the results presented here are consistent with, although not proof of, the possibility that an oxidative mechanism causes GLAST dysfunction in Müller cells of the diabetic retina.

To more directly test the hypothesis that GLAST dysfunction in diabetic Müller cells may be due to oxidation, the effect of a chemical reductant was tested. If a chemical reducing agent reversed the dysfunction of this transporter, then this would be support for the idea that the

Müller cell glutamate transporter in the diabetic retina was in an oxidized state. On the basis of this reasoning, the effect of the disulfide-reducing agent, disulfide dithiothreitol (DTT), was assessed (Figure 13).

As illustrated in Figure 13, exposure of a diabetic Müller cell to DTT promptly and markedly increased the amplitude of the inward current induced by PDC. Subsequent exposure of this Müller cell to PDC alone (without DTT) resulted in a response that was similar in amplitude to the current that was previously induced during exposure to PDC plus DTT. The persistent restoration of transporter activity is consistent with DTT having chemically modified the glutamate transporter (ie, changed this transporter molecule from being in an oxidized state to being in a reduced state).

In a series of experiments, the effect of DTT was tested on control Müller cells and those isolated from rats that were diabetic for various durations (Figure 14). Exposure to this disulfide-reducing agent completely reversed the diabetes-associated decrease in the amplitude of the PDC-induced current. This effect was not due to DTT itself inducing a current that was independent of PDC, since the basal currents of Müller cells did not change significantly ( $P > .05$ ,  $n = 5$ ) when the perfusate contained DTT without PDC.

The DTT-mediated recovery of glutamate transporter activity in diabetic Müller cells is consistent with this transporter molecule being oxidized in the diabetic retina. Taken together, the experimental results presented in this study support the hypothesis that early in the course of diabetic retinopathy, the function of the glutamate

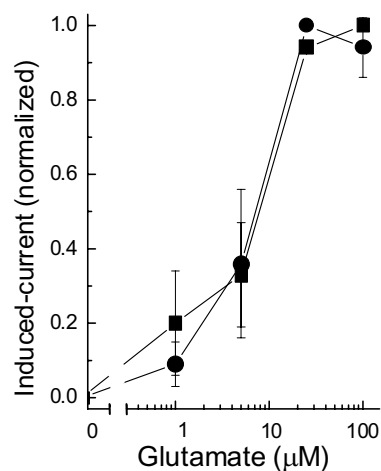
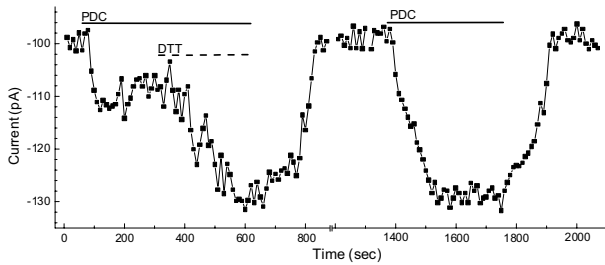


FIGURE 12

Dose-response relationship for glutamate-induced inward current in control Müller cells ( $n = 4$ ) and in Müller cells from rats that were diabetic for 9 weeks ( $n = 4$ ). Since glutamate transporter activity in diabetic Müller cells was decreased relative to controls (Figure 10), currents for each group were normalized. Concentration of glutamate that evokes a half-maximal current is similar in diabetic and control Müller cells.

■ = Diabetic, ● = Control.



**FIGURE 13**

Effect of reducing agent, DTT, on current induced by PDC in a Müller cell from a diabetic retina. Current amplitudes were measured at 10-second intervals in a Müller cell isolated from a rat made diabetic by streptozotocin injection 6 weeks earlier. Bars show times during which perfusate contained 100  $\mu$ M PDC (solid lines) and 3 mM DTT (dashed line).

mate transporter in retinal Müller cells is decreased by a mechanism involving oxidation.

## DISCUSSION

The results of this study show that the function of the glutamate transporter in rat Müller cells decreases by 67% during the initial 13 weeks of streptozotocin-induced diabetes. This conclusion is based on experiments that used an electrophysiological assay, which permitted real-time quantitative monitoring of the activity of this transporter in Müller cells freshly isolated from the rat retina. Consistent with the dysfunction of this glutamate transporter being caused by oxidation, exposure of diabetic Müller cells to a disulfide-reducing agent rapidly and fully restored the activity of this transporter. Thus, the experimental findings of this study support the hypothesis that early in the course of diabetic retinopathy, the function of the glutamate transporter in retinal Müller cells is decreased by a mechanism involving oxidation.

### DIABETIC RETINOPATHY AND THE GLUTAMATE TRANSPORTER

The finding that the activity of the Müller cell glutamate transporter is decreased in experimental diabetes provides new insight into putative mechanisms that may account for observations made in previous studies of the diabetic retina. For example, a decrease in the ability of Müller cells to transport glutamate from the extracellular space would likely cause levels of this amino acid to increase in the microenvironment. In agreement with this prediction, Lieth and colleagues<sup>28</sup> and Kowluru and colleagues<sup>50</sup> reported that the concentration of retinal glutamate is elevated early in the course of experimental diabetes. Also, the finding by Ambati and colleagues<sup>52</sup> of raised glutamate levels in the vitreous of patients with diabetic retinopathy suggests that diabetes is associated with an elevated concentration of this amino acid in the human retina.

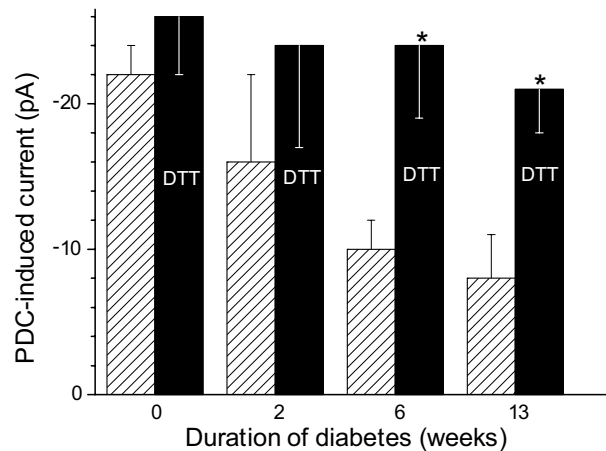


**FIGURE 14**

Effect of reducing agent, DTT, on current induced by PDC in control and diabetic Müller cells. Striped bars show current induced by 100  $\mu$ M PDC in absence of DTT. Solid bars show induced current in presence of 3mM DTT. For each value, a mean of  $9 \pm 2$  cells were sampled. Asterisk indicates a significant ( $P < .001$ ) increase in PDC-induced current during exposure to DTT. This reducing agent restores glutamate transporter activity in Müller cells isolated from diabetic rats.

Recent observations suggest that the mechanism by which glutamate levels are elevated in the diabetic retina may involve oxidative stress. For example, Kowluru and colleagues<sup>50</sup> documented that diabetic rat retinas with increased glutamate levels also had a 100% increase in thiobarbituric acid-reactive substances (TBARS), which are indicators of oxidative stress. Further support for a link between oxidative stress and elevated glutamate levels in the diabetic retina is that treatment of diabetic rats with a mixture of antioxidants blocked the increase in TBARS and in the concentration of glutamate in the retina. Taken together, the findings of Kowluru and colleagues<sup>50</sup> suggest that oxidative stress causes a rise in glutamate levels in the diabetic retina.

How are oxidative stress and glutamate homeostasis linked? The findings presented in this thesis indicate that one mechanism by which oxidative stress may increase the levels of glutamate in the diabetic retina involves an inhibition of the Müller cell glutamate transporter. Inhibition of this transporter compromises the ability of Müller cells to remove glutamate from the extracellular space. As a result, the levels of this amino acid in the retinal microenvironment would increase. Thus, on the basis of recent reports<sup>28,50,52</sup> and the experimental findings of this study, a likely scenario is that an oxidation-induced inhibition of GLAST molecules in Müller cells contributes significantly to the disruption of glutamate homeostasis in the diabetic retina.

Dysfunction of the glutamate transporter in Müller cells may augment the level of oxidative stress in the diabetic retina. Support for this idea is that glutamate

enhances the generation in the retina of oxidative stress, as indicated by an increase in TBARS.<sup>50</sup> Pharmacologic experiments indicate that the glutamate-induced increase in retinal oxidants involves the activation of *N*-methyl-*D*-aspartate receptors and the production of nitric oxide (NO).<sup>50</sup> In an environment of excess reactive oxygen species and oxidative stress, NO is readily converted into potent oxidants,<sup>77</sup> which can cause dysfunction of GLAST molecules.<sup>78</sup> These observations suggest that in the retina there is a positive feedback loop involving glutamate and oxidative stress. By failing to maintain glutamate homeostasis in the diabetic retina, Müller cells may play a key role in augmenting oxidative stress.

A positive-feedback loop involving oxidative stress and dysfunction of GLAST molecules in Müller cells may be important in the progression of diabetic retinopathy (Figure 15). This idea is based on the emerging concept<sup>39</sup> that oxidative stress initiates each of the four main molecular mechanisms implicated in the pathogenesis of diabetic complications: increased polyol synthesis, formation of advanced glycation end products, activation of protein kinase C, and enhanced flux through the hexosamine pathway. Thus, by augmenting oxidative stress in the retina, the inhibition of the Müller cell glutamate transporter may be an important step in the development of sight-threatening complications of diabetic retinopathy.

#### EXPERIMENTAL LIMITATIONS

As with any study, there are limitations in the interpretation of the experimental results. For example, although

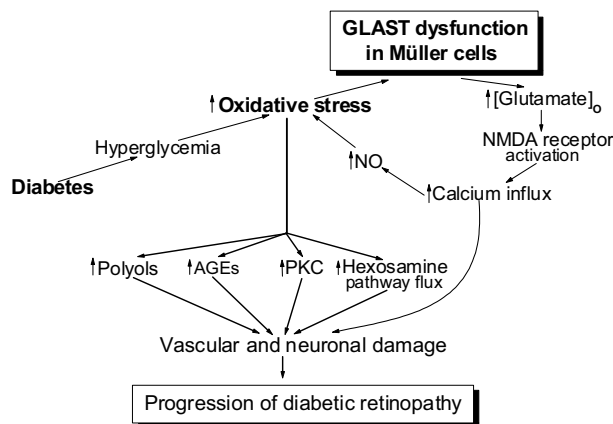


FIGURE 15

Model of putative mechanisms by which Müller cells may play a role in progression of diabetic retinopathy. Oxidative-induced dysfunction of Müller cell glutamate transporter (GLAST) and resulting elevation of glutamate levels may create a positive feedback loop that further increases oxidative stress and, thereby, progression of diabetic complications in retina. Although almost certainly overly simplistic, this model should help in formulation of future studies to assess the role of Müller cells in the pathogenesis of diabetic retinopathy. NMDA, *N*-methyl-*D*-aspartate; NO, nitric oxide; NOS, nitric oxide synthase; AGEs, advanced glycation end products; PKC, protein kinase C;  $[glutamate]_o$ , extracellular glutamate concentration.

streptozotocin-injected rats provide an intensively studied model of diabetes, they are not identical to the clinical situation. One reason for this is that uncontrolled hyperglycemia is not typical in patients. Also, of course, rats may respond differently to hyperglycemia and hypoinsulinemia than humans. Additionally, a chemically induced loss of beta cell function is very rare in humans. However, the possibility of a direct toxic effect of streptozotocin on Müller cells seems unlikely in this study, since the membrane potential, predominant ionic conductance, and cell size were not significantly changed in the sampled cells during 13 weeks of experimental diabetes. In addition, the rapid and complete recovery of glutamate transporter activity during exposure of Müller cells to a chemical reducing agent suggests a diabetes-induced oxidative effect rather than nonspecific damage caused by streptozotocin. Thus, despite some limitations, the observations made in this study of Müller cells isolated from rats with streptozotocin-induced diabetes provide a framework for future experimental work on Müller cells from human diabetic donors.

An additional experimental limitation is the use of Müller cells isolated from the retina. Because an *in vivo* application of the electrophysiologic technique used in this study seems impractical at present, it remains to be demonstrated that oxidation compromises the function of the glutamate transporter in Müller cells in the diabetic retina *in vivo*. However, although there clearly is a need for caution in extrapolating results from isolated cells to the *in vivo* situation, use of freshly isolated Müller cells provides some important experimental advantages. For example, the composition of the extracellular solution can be controlled without secondary effects of chemicals that may be released by other retinal cells. In addition, the use of isolated Müller cells in this study, which is the first electrophysiologic analysis of glia from the diabetic retina, allowed comparison with the substantial body of knowledge derived from studies of Müller cells isolated from normal retinas. Overall, it seems reasonable to predict that when electrophysiologic methods are perfected to assay Müller cells in the diabetic retina *in vivo*, the results of this thesis will help in the design of experiments to assess the functional effects of diabetes on these glia.

#### CONCLUDING COMMENTS

A review of the literature led to the formulation of the hypothesis that the ability of retinal Müller cells to remove glutamate from the extracellular space is compromised in the diabetic retina. This hypothesis was extended to also propose that, by a mechanism involving oxidation, diabetes causes dysfunction of the glutamate transporter in Müller cells. This seemed to be a reasonable hypothesis

because oxidative stress is a hallmark of diabetes and recent work indicates that the type of glutamate transporter expressed by Müller cells contains redox-sensitive elements. Experiments to test this hypothesis demonstrated that the function of the glutamate transporter in Müller cells freshly isolated from the rat retina was significantly decreased within 4 weeks after the onset of streptozotocin-induced diabetes. Furthermore, the rapid and complete recovery of transporter function during exposure of diabetic Müller cells to a chemical reducing agent supports the idea that oxidation plays a role in decreasing the function of this glutamate transporter.

Dysfunction of the Müller cell glutamate transporter is one of the earliest reported diabetes-induced changes in these glia. This change precedes the decrease in the activity of glutamine synthetase, the rate-limiting enzyme in Müller cells for the conversion of glutamate to glutamine. This enzyme's activity is not affected until after 8 weeks of experimental diabetes.<sup>51</sup> Likewise, it is not until 6 to 8 weeks of experimental diabetes that there is an up-regulation in the expression of glial fibrillary acidic protein,<sup>28-31</sup> which is an intermediate filament of uncertain function that is expressed by Müller cells in response to a multitude of retinal perturbations. Thus, the glutamate transporter of Müller cells appears to be a molecule that is particularly vulnerable early in the course of diabetes.

The demonstration in this study that the diabetes-induced dysfunction of the Müller cell glutamate transporter can be rapidly reversed, at least early in the course of diabetic retinopathy, renders GLAST as a potential target for pharmacologic intervention. In the future, enhancing the ability of Müller cells to regulate glutamate levels in the diabetic retina may prevent or diminish subsequent molecular events that lead to sight-threatening complications.

#### ACKNOWLEDGMENTS

Qing Li, MD, PhD, participated in nearly all of the experimentation. Shunji Kusaka, MD, PhD, and Kenji Sakagami, MD, PhD, participated in early phases of the study. S.K., K.S., and Q.L. were research fellows in the author's laboratory. Scanning electron microscopy was performed by the staff of the University of Michigan Anatomy and Cell Biology Core Facility.

#### REFERENCES

- Bresnick GH. Diabetic retinopathy viewed as a neurosensory disorder. *Arch Ophthalmol* 1986;104:989-990.
- Mizutani M, Gerhardinger C, Lorenzi M. Muller cell changes in human diabetic retinopathy. *Diabetes* 1998;47:445-449.
- Lieth E, Gardner TW, Barber AJ, et al. Retinal neurodegeneration: early pathology in diabetes. *Clin Exp Ophthalmol* 2000;28:3-8.
- Wolter JR. Diabetic retinopathy. *Am J Ophthalmol* 1961;51:1123-1141.
- Bloodworth JMB. Diabetic retinopathy. *Diabetes* 1962;11:1-22.
- Frank RN. On the pathogenesis of diabetic retinopathy. *Ophthalmology* 1984;91:626-634.
- Alder VA, Su EN, Yu DY, et al. Diabetic retinopathy: early functional changes. *Clin Exp Pharmacol Physiol* 1997;24:785-788.
- Terasaki H, Hirose H, Miyake Y. S-cone pathway sensitivity in diabetes measured with threshold versus intensity curves on flashed backgrounds. *Invest Ophthalmol Vis Sci* 1996;37:680-684.
- North RV, Farrell U, Banford D, et al. Visual function in young IDDM patients over 8 years of age. A 4-year longitudinal study. *Diabetes Care* 1997;20:1724-1730.
- Tregear SJ, Knowles PJ, Ripley LG, et al. Chromatic-contrast threshold impairment in diabetes. *Eye* 1997;1:537-546.
- Hyvarinen L, Laurinen P, Rovamo J. Contrast sensitivity in evaluation of visual impairment due to diabetes. *Acta Ophthalmol (Copenh)* 1983;61:94-101.
- Della Sala S, Bertoni G, Somazzi L, et al. Impaired contrast sensitivity in diabetic patients with and without retinopathy: a new technique for rapid assessment. *Br J Ophthalmol* 1985;69:136-142.
- Sokol S, Moskowitz A, Skarf B, et al. Contrast sensitivity in diabetics with and without background retinopathy. *Arch Ophthalmol* 1985;103:51-54.
- Brinchmann-Hansen O, Bangstad HJ, Hultgren S, et al. Psychophysical visual function, retinopathy, and glycemic control in insulin-dependent diabetics with normal visual acuity. *Acta Ophthalmol (Copenh)* 1993;71:230-237.
- Simonsen SE. Effect of 6 months of strict metabolic control on eye and kidney function in insulin-dependent diabetics with background retinopathy. Steno Study Group. The value of the oscillatory potential in selecting juvenile diabetics at risk of developing proliferative retinopathy. *Lancet* 1982;1:121-124.
- Brunette JR, Lafond G. Electroretinographic evaluation of diabetic retinopathy. Sensitivity amplitude time response. *Can J Ophthalmol* 1983;18:285-289.
- Bresnick GH, Palta M. Oscillatory potential amplitudes. Relation to severity of diabetic retinopathy. *Arch Ophthalmol* 1987;105:929-933.
- Coupland SG. A comparison of oscillatory potential and pattern electroretinogram measures in diabetic retinopathy. *Doc Ophthalmol* 1987;66:207-218.
- Falsini B, Porciatti V, Scalia G, et al. Steady-state pattern electroretinogram in insulin-dependent diabetics with no or minimal retinopathy. *Doc Ophthalmol* 1989;73:193-200.
- Caputo S, Di Leo MA, Falsini B, et al. Evidence for early impairment of macular function with pattern ERG in type I diabetic patients. *Diabetes Care* 1990;13:412-418.
- Juen S, Kieselbach GF. Electrophysiological changes in juvenile diabetics without retinopathy. *Arch Ophthalmol* 1990;108:372-375.

22. Prager TC, Garcia CA, Mincher CA, et al. The pattern electroretinogram in diabetes. *Am J Ophthalmol* 1990;109:279-284.
23. Holopigian K, Seiple W, Lorenzo M, et al. A comparison of photopic and scotopic electroretinographic changes in early diabetic retinopathy. *Invest Ophthalmol Vis Sci* 1992;33:2773-2780.
24. Palmowski AM, Sutter EE, Bearse MA Jr, et al. Mapping of retinal function in diabetic retinopathy using the multifocal electroretinogram. *Invest Ophthalmol Vis Sci* 1997;38:2586-2596.
25. Sakai H, Tani Y, Shirasawa E, et al. Development of electroretinographic alterations in streptozotocin-induced diabetes in rats. *Ophthalmic Res* 1995;27:57-63.
26. Barber A, Lieth E, Khin S, et al. Neural apoptosis in the retina during experimental and human diabetes: early onset effect of insulin. *J Clin Invest* 1998;102:783-791.
27. Barber AJ, Nakamura M, Wolpert EB, et al. Insulin rescues retinal neurons from apoptosis by a phosphatidylinositol 3-kinase/Akt-mediated mechanism that reduces the activation of caspase-3. *J Biol Chem* 2001;276:32814-32821.
28. Lieth E, Barber A, Xu B, et al. Glial reactivity and impaired glutamate metabolism in short-term experimental diabetic retinopathy. *Diabetes* 1998;47:815-820.
29. Barber AJ, Antonetti DA, Gardner TW. Altered expression of retinal occludin and glial fibrillary acidic protein in experimental diabetes. *Invest Ophthalmol Vis Sci* 2000;41:3561-3568.
30. Rungger-Brandle E, Dosso AA, Leuenberger PM. Glial reactivity, an early feature of diabetic retinopathy. *Invest Ophthalmol Vis Sci* 2000;41:1971-80.
31. Li Q, Zemel E, Miller B, et al. Expression of glial fibrillary acidic protein (GFAP) in the diabetic retina. *Exp Eye Res* 2002;74:615-625.
32. Eddleston M, Mucke L. Molecular profile of reactive astrocytes—implications for their role in neurologic disease. *Neuroscience* 1993;54:15-36.
33. Puro DG. Müller cells: dynamic components of the retina. In: Toyoda J, Murakami M, Kaneko A, et al, eds. *The Retinal Basis of Vision*. Amsterdam: Elsevier; 1999:233-248.
34. Sarthy V, Ripps H. *The Retinal Müller Cell*. New York: Kluwer Academic/Plenum Publishers; 2001.
35. Dreher Z, Robinson SR, Distler C. Müller cells in vascular and avascular retinopathies: a survey of seven mammals. *J Comp Neurol* 1992;323:59-80.
36. Newman E, Reichenbach A. The Müller cell: a functional element of the retina. *Trends Neurosci* 1996;19:307-312.
37. Massey SC. Cell types using glutamate as a neurotransmitter in the vertebrate retina. *Prog Retinal Res* 1990;9:399-425.
38. Derouiche A, Rauen T. Coincidence of l-glutamate/l-aspartate transporter (GLAST) and glutamine synthetase (GS) immunoreactions in retinal glia: evidence for coupling of GLAST and GS in transmitter clearance. *J Neurosci Res* 1995;42:131-143.
39. Rauen T, Taylor R, Kuhlbrodt K, et al. High-affinity glutamate transporters in the rat retina: a major role of the glial glutamate transporter GLAST-1 in transmitter clearance. *Cell Tissue Res* 1998;291:19-31.
40. Pow D, Crook DK. Direct immunocytochemical evidence for the transfer of glutamine from glial cells to neurons: use of specific antibodies directed against d-stereoisomers of glutamate glutamine. *Neuroscience* 1996;70:295-302.
41. Vorwerk CK, Naskar R, Schuettauf F, et al. Depression of retinal glutamate transporter function leads to elevated intravitreal glutamate levels and ganglion cell death. *Invest Ophthalmol Vis Sci* 2000;41:3615-3621.
42. Lucas DR, Newhouse JP. The toxic effect of sodium L-glutamate on the inner layers of the retina. *Arch Ophthalmol* 1957;58:193-201.
43. Lipton SA, Rosenberg PA. Excitatory amino acids as a final common pathway for neurologic disorders. *N Engl J Med* 1994;330:613-622.
44. Sucher NJ, Lipton SA, Dreyer EB. Molecular basis of glutamate toxicity in retinal ganglion cells. *Vis Res* 1997;37:3483-3493.
45. Cunha-Vaz JG, Faria de Abreu JR, Campos AJ, et al. Early breakdown of the blood-retinal barrier in diabetes. *Br J Ophthalmol* 1975;59:649-656.
46. Do Carmo A, Ramos P, Reis A, et al. Breakdown of the inner and outer blood retinal barrier in streptozotocin-induced diabetes. *Exp Eye Res* 1998;67:569-575.
47. Castillo J, Davalos A, Noya M. Progression of ischaemic stroke and excitotoxic amino acids. *Lancet* 1997;349:79-83.
48. Vorwerk CK, Lipton SA, Zurakowski D, et al. Chronic low-dose glutamate is toxic to retinal ganglion cells. Toxicity blocked by memantine. *Invest Ophthalmol Vis Sci* 1996;37:1618-1624.
49. Distler C, Dreher Z. Glial cells of the monkey retina. II. Müller cells. *Vis Res* 1996;36:2381-2394.
50. Kowluru RA, Engerman RL, Case GL, et al. Retinal glutamate in diabetes and effect of antioxidants. *Neurochem Int* 2001;38:385-390.
51. Lieth E, LaNoue KF, Antonetti DA, et al. Diabetes reduces glutamate oxidation and glutamine synthesis in the retina. *Exp Eye Res* 2000;70:723-730.
52. Ambati J, Chalam KV, Chawla DK, et al. Elevated gamma-aminobutyric acid, glutamate, and vascular endothelial growth factor levels in the vitreous of patients with proliferative diabetic retinopathy. *Arch Ophthalmol* 1997;115:1161-1166.
53. Rauen T. Diversity of glutamate transporter expression and function in the mammalian retina. *Amino Acids* 2000;19:53-62.
54. Trotti D, Rizzini BL, Rossi D, et al. Neuronal and glial glutamate transporters possess an SH-based redox regulatory mechanism. *Eur J Neurosci* 1997;12:1236-1243.
55. Trotti D, Danbolt NC, Volterra A. Glutamate transporters are oxidant-vulnerable: a molecular link between oxidative and excitotoxic neurodegeneration? *Trends Pharmacol Sci* 1998;19:328-334.
56. Kowluru RA, Kern TS, Engerman RL, et al. Abnormalities of retinal metabolism in diabetes or experimental galactosemia. III. Effects of antioxidants. *Diabetes* 1996;45:1233-1237.
57. Ellis EA, Grant MB, Murray FT, et al. Increased NADH oxidase activity in the retina of the BBZ/Wor diabetic rat. *Free Radic Biol Med* 1998;24:111-120.

58. Ellis EA, Guberski DL, Somogyi-Mann M, et al. Increased H<sub>2</sub>O<sub>2</sub>, vascular endothelial growth factor and receptors in the retina of the BBZ/Wor diabetic rat. *Free Radic Biol Med* 2000;28:91-101.
59. Brownlee M. Biochemistry and molecular cell biology of diabetic complications. *Nature* 2001;414:813-820.
60. Brew H, Attwell D. Electrogenic glutamate uptake is a major current carrier in the membrane of axolotl retinal glial cells. *Nature* 1987;327:707-709.
61. Saranatis M, Attwell D. Glutamate uptake in mammalian retinal glia is voltage- and potassium-dependent. *Brain Res* 1990;516:322-325.
62. Billups B, Rossi D, Attwell D. Anion conductance behavior of the glutamate uptake carrier in salamander retinal glial cells. *J Neurosci* 1996;16:6722-6731.
63. Eliasof S, Jahr CE. Retinal glial cell glutamate transporter is coupled to an anionic conductance. *Proc Natl Acad Sci U S A* 1996;93:4153-4158.
64. Horn R, Marty A. Muscarinic activation of ionic currents measured by a new whole-cell recording method. *J Gen Physiol* 1988;92:145-159.
65. Rae J, Cooper K, Gates P, et al. Low access resistance perforated patch recordings using amphotericin B. *J Neurosci Meth* 1991;37:15-26.
66. Bridges RJ, Stanley MS, Anderson MW, et al. Conformationally defined neurotransmitter analogues. Selective inhibition of glutamate uptake by one pyrrolidine-2,4-dicarboxylate diastereomer. *J Med Chem* 1991;34:717-725.
67. Sarantis M, Ballerini L, Miller B, et al. Glutamate uptake from the synaptic cleft does not shape the decay of the non-NMDA component of the synaptic current. *Neuron* 1993;11:541-549.
68. Bazan NG, Gordon WC, Marcheselli VL, et al. Experimental models and their use in studies of diabetic retinal microangiopathy. *Therapie* 1997;52:447-451.
69. Brew H, Gray PT, Mobbs P, et al. Endfeet of retinal glial cells have higher densities of ion channels that mediate K<sup>+</sup> buffering. *Nature* 1986;324:466-468.
70. Newman EA. Inward-rectifying potassium channels in retinal glial (Müller) cells. *J Neurosci* 1993;13:3333-3345.
71. Kusaka S, Puro DG. Intracellular ATP activates inwardly-rectifying K<sup>+</sup> channels in human and monkey retinal Müller (glial) cells. *J Physiol (Lond)* 1997;500:593-604.
72. Barry PH. JPCalc, a software package for calculating liquid junction potential corrections in patch-clamp, intracellular, epithelial and bilayer measurements and for correcting junction potential measurements. *J Neurosci Meth* 1993;51:107-116.
73. Agardh E, Yeh HH, Herrmann R, et al. g-Aminobutyric acid-mediated inhibition at cholinergic synapses formed by cultured retinal neurons. *Brain Res* 1985;330:323-328.
74. Kusaka S, Kapousta-Bruneau NV, Puro DG. Plasma-induced changes in the physiology of mammalian retinal glial cells: role of glutamate. *Glia* 1999;25:205-215.
75. Schwartz EA. l-glutamate conditionally modulates the K<sup>+</sup> current of Müller glial cells. *Neuron* 1993;10:1141-1149.
76. Puro DG, Yuan JP, Sucher NJ. Activation of NMDA receptor-channels in human retinal Müller glial cells inhibits inward-rectifying potassium currents. *Vis Neurosci* 1996;13:319-326.
77. Goldstein IM, Ostwald P, Roth S. Nitric oxide: a review of its role in retinal function and disease. *Vision Res* 1996;36:2979-2994.
78. Trotti D, Rossi D, Gjesdal O, et al. Peroxynitrite inhibits glutamate transporter subtypes. *J Biol Chem* 1996;271:5976-5979.

## 2-DEOXY-D-GLUCOSE UPTAKE IN THE INNER RETINA: AN IN VIVO STUDY IN THE NORMAL RAT AND FOLLOWING PHOTORECEPTOR DEGENERATION

---

BY *David J. Wilson, MD*

### ABSTRACT

*Purpose:* To evaluate, in vivo, at the cellular level, glucose metabolism in the rat inner retina, and to determine how inner retinal glucose metabolism is affected by photoreceptor degeneration.

*Methods:* Glucose metabolism was evaluated using the 2-deoxyglucose technique. This is an autoradiographic technique that permits evaluation of glucose uptake at the cellular level. The three experimental groups consisted of normal rats (n=13), dystrophic Royal College of Surgeons rats (n=3), and rats previously treated with argon green photocoagulation (n=5).

*Results:* Deoxyglucose uptake in the normal rat was not uniform across the inner retina. Uptake was greatest at the junction of the outer plexiform and inner nuclear layers, and in the inner plexiform layer. Following focal or diffuse photoreceptor loss, there was a marked decrease in the amount of deoxyglucose uptake at the junction of the outer plexiform and inner nuclear layers.

*Conclusion:* The pattern of uptake of deoxyglucose in the inner retina is consistent with abundant uptake of deoxyglucose by Müller cells and at sites of synaptic transmission. The decline in deoxyglucose uptake following diffuse or focal photoreceptor loss indicates that there is diminished inner retinal glucose uptake following photoreceptor loss. This change in inner retinal glucose metabolism following photoreceptor loss may help to explain the inner retinal vascular changes observed following photocoagulation and in retinal dystrophies.

*Trans Am Ophthalmol Soc* 2002;100:353-364

### INTRODUCTION

---

#### BACKGROUND OF RETINAL ENERGY METABOLISM AND ITS MEASUREMENT

The retina, in common with other central nervous system tissue, requires a high level of energy metabolism. Energy is used in the retina for a host of cellular functions that are common to all cells, including maintenance of ion gradients across cell membranes, protein synthesis, and nucleic acid transcription. In addition, the retina has an increased energy metabolism burden to support the energy requirements of phototransduction and neurotransmission. These latter requirements are very energy-intensive functions and account for the extremely high level of energy consumption by the retina.<sup>1,2</sup> The retina depends principally on the metabolism of glucose as a source for energy, although oxidation of aspartic acid and glutamic acid may account for a portion of retinal oxygen consumption.<sup>3-5</sup>

Retinal energy metabolism has been the subject of intensive research. However, relatively few studies have been performed to correlate retinal energy metabolism

and the cellular processes for which it is being used. This is because of the difficulty in measuring the rate of energy metabolism in small regions (eg, one cell) or in isolated units performing a specific cellular function (eg, synaptic transmission).

Most studies of retinal energy metabolism have concentrated on the role of oxygen in retinal energy metabolism rather than the role of glucose or other metabolic substrates. This is largely due to the greater ease of investigational approaches to assessing oxygen consumption and the more complex role of glucose in metabolic pathways not directly related to the production of adenosine triphosphate (ATP). However, several studies of glucose metabolism have been performed, and they are briefly summarized as follows.

#### *In Vitro Studies of Glucose Metabolism*

In vitro studies of retinal glucose metabolism have been performed in the rat,<sup>3,5</sup> the rabbit,<sup>1,2,6</sup> the guinea pig,<sup>7,8</sup> and the human.<sup>9</sup> In general, these studies have used isolated retinas maintained in perfusion chambers under very controlled conditions. The studies in the guinea pig and the human are an exception to this generality in that some of the studies involved investigations of isolated Müller

From the Casey Eye Institute, Portland, Oregon. Supported in part by an unrestricted grant from Research to Prevent Blindness, Inc.

cells<sup>8,9</sup> or Müller cell photoreceptor complexes.<sup>8</sup> These studies have been very enlightening with regard to glucose metabolism in the retina. They have raised several interesting questions that form the basis for the hypothesis to be evaluated in this thesis.

Ames and coworkers,<sup>1</sup> working in the rabbit, found that the energy for neurotransmission through the inner retina was obtained from the glycolytic metabolism of glucose. This finding was based on the abolition of the b wave of the electroretinogram and a decrease in lactate production with relatively little change in oxygen consumption when neurotransmission was blocked with specific inhibitors. These investigators found that inhibitors of neurotransmission decreased the rate of glycolysis in the dark-adapted inner retina by  $79\% \pm 9\%$ . Similarly, increased neurotransmission through the inner retina caused by a flashing light in the absence of inhibitors increased glycolysis by  $48\% \pm 4\%$ . These findings were consistent with those of Lowry and coworkers,<sup>10</sup> who found that the inner retina of the rabbit contained almost exclusively glycolytic enzymes in its inner layers. The findings by the investigators in the Ames group led them to suggest that there may be an obligatory dependence of neurotransmission on glycolytic, rather than oxidative, energy.<sup>1</sup> This would be consistent with the specific dependence of other functions in smooth muscle<sup>11</sup> and the central nervous system<sup>12-16</sup> on glycolytic energy.

Winkler<sup>5</sup> performed a comprehensive, quantitative study of glucose metabolism *in vitro* in normal and dystrophic rats. He found that 90% of glucose utilized aerobically by both normal and dystrophic rats was used in glycolysis. This finding suggested that aerobic glycolysis is the major pathway for glucose breakdown in all retina cell layers. Winkler also found that there were only small light-dark differences in retinal glycolysis and oxygen consumption. In contrast, oxidation of glucose was diminished in the light, compared with darkness, by 25% in the whole retina and by 40% in the photoreceptor cells. This suggests that light leaves unchanged or increases the amount of glucose metabolized by oxidation by the inner retina.

Poity-Yamate and coworkers,<sup>8</sup> working with Müller cells and Müller cell photoreceptor complexes isolated from guinea pig retinas, found that glucose taken up by Müller cells was metabolized to carbohydrate intermediates and that a large amount of lactate was released into the tissue bath by the isolated Müller cells. Furthermore, these investigators showed that the lactate in the tissue bath could be taken up and used as a metabolic substrate for oxidative metabolism by photoreceptors. In fact, they found that lactate was preferred over glucose by the photoreceptors. These findings led the investigators to suggest that, *in vivo*, the Müller cell transfers lactate to the photoreceptors. This is consistent with the same group's

studies using the 2-deoxyglucose technique (see below) *in vitro* to evaluate glucose metabolism in the whole retinas isolated from guinea pig<sup>7</sup> and *in vivo* in the honeybee.<sup>17</sup> In those studies, these investigators found that glucose uptake was predominantly in glial cells, leading them to suggest that some metabolite must be transferred to the photoreceptors from the glial cells to satisfy the large need of ATP in the photoreceptors.

Winkler and coworkers,<sup>9</sup> working with cultured human Müller cells, found that glycolysis accounted for 99% of the glucose consumed by these Müller cells. Oxidative metabolism of glucose by mitochondria accounted for only 1% of glucose consumed.

There have been three other *in vitro* studies of glucose metabolism using the 2-deoxyglucose technique. These were done in the frog,<sup>18</sup> goldfish,<sup>19</sup> and monkey retinas.<sup>20</sup> Interestingly, these studies showed relatively greater uptake of deoxyglucose over photoreceptors, in contrast to the findings of predominantly glial cell uptake reported by Poity-Yamate in the guinea pig.<sup>7</sup>

#### *In Vivo Studies of Glucose Metabolism*

Bill and coworkers have performed numerous studies of glucose metabolism using either the 2-deoxyglucose technique or direct measurements of glucose consumption by measuring arteriovenous differences in blood glucose concentrations. Their studies have been performed in the rabbit,<sup>21</sup> the cat,<sup>22</sup> the pig,<sup>23,24</sup> and the monkey.<sup>25-27</sup>

To briefly summarize their studies, they have concluded that in the inner retina of the pig, in the dark, 69% of the glucose is consumed in oxidative metabolism and 21% in glycolysis. In the outer retina of the pig, in the dark, 61% of the glucose is consumed in glycolytic metabolism, while 12% is consumed in oxidative metabolism. In the rabbit, both in light and dark, these investigators found that for the whole retina, 10% of glucose was consumed in oxidative metabolism and 50% in glycolysis. (The balance of the glucose utilization in all of these studies was presumed to be in other processes, such as protein synthesis).

Vitreoperfusion following cessation of retinal and choroidal blood flow after death has been used to measure total glucose consumption by the retina in cats.<sup>28</sup> This modality has the advantage of perhaps being suitable to the study of glucose metabolism in humans undergoing vitrectomy and allowing the simultaneous measurement of oxygen consumption.<sup>29</sup>

The extensive information provided by these studies raises some very interesting questions with regard to glucose metabolism in pathologic states. In diabetic retinopathy, it has long been observed that destruction of photoreceptors with photocoagulation causes a reduction in neovascularization of the inner retina. Similarly, atten-

uation of retinal vessels is a well-known occurrence in the retinal dystrophies with extensive photoreceptor atrophy. Experimentally, Wilson and coworkers<sup>30</sup> have demonstrated that destruction of photoreceptors leads to a delayed loss of inner retinal vessels in the monkey. The changes in the inner retinal vessels following loss of photoreceptors has generally been attributed to an increase in inner retinal oxygen tension. However, the studies described above raise two other possible explanations for the attenuation of the retinal vessels following destruction of photoreceptors: (1) Since Ames and coworkers<sup>1</sup> found that neurotransmission through the inner retina was responsible for a large percentage of the inner retinal energy metabolism, it is possible that following photocoagulation, there could be less of an energy requirement in the inner retina because of decreased neurotransmission through the inner retina. (2) The observation of Poitry-Yamate<sup>8</sup> that there appears to be transfer of lactate from Müller cells to photoreceptors indicates that there is a link between the metabolism of the inner retina (Müller cell) and the outer retina. In the absence of photoreceptors, one would anticipate that there would be less glucose metabolism by Müller cells. The present study was undertaken to evaluate how neurotransmission and photoreceptor atrophy affect inner retinal glucose metabolism.

#### **HYPOTHESIS**

There is diminished use of glucose in the inner retina following photocoagulation and in retinal dystrophies that result in loss of photoreceptors. This decrease in glucose utilization is due to diminished neurotransmission through the inner retina and decreased glucose consumption by Müller cells.

#### **MATERIALS AND METHODS**

---

##### **CHOICE OF TECHNIQUE**

In 1976 and 1977 Sokoloff and coworkers<sup>31,32</sup> developed a technique for the *in vivo* or *in vitro* measurement of energy metabolism called the deoxyglucose technique. This technique utilizes a radioactively labeled glucose analogue to serve as a marker of glucose metabolism. In the central nervous system and in the retina, the metabolism of glucose is utilized as the principal energy source.<sup>3,5</sup> Because of the use of glucose as an energy source, the deoxyglucose technique can be utilized to study energy metabolism in the central nervous system and retina. This technique has been of great value in the study of the central nervous system's regional differences in energy metabolism and variation in energy metabolism in different physiologic and pathologic states.<sup>12</sup> The principles of the deoxyglucose technique form the basis for positron

emission tomography (PET) scanning, which is now used as a clinical diagnostic tool for central nervous system disease. The deoxyglucose technique has been used less in the study of retinal physiology and pathology.

This technique is attractive because, unlike studies that evaluate glucose consumption using arteriovenous differences in glucose concentration, the deoxyglucose has the advantage of showing glucose uptake at the cellular level. This technique remains the only method to evaluate the relative glucose utilization of specific cells within a tissue and seems ideally suited to answer the questions of how photoreceptor degeneration and photocoagulation affect Müller cell glucose utilization. Deoxyglucose is available commercially, radioactively labeled with either <sup>14</sup>C or <sup>3</sup>H. To achieve the greatest resolution of individual cell glucose uptake, it is preferable to use deoxyglucose labeled with <sup>3</sup>H.

The deoxyglucose method may be used in a qualitative or quantitative fashion. In order to measure glucose consumption quantitatively, one must measure the entire history of the plasma deoxyglucose concentration over the course of the experiment, the steady state of the plasma glucose concentration, and the local tissue concentration of deoxyglucose. In this initial study, I have chosen to use this technique in a qualitative fashion to evaluate the local distribution of deoxyglucose. Qualitative interpretation of the autoradiograms allows one to make relative statements regarding the glucose metabolism of adjacent cells and tissues, but it does not allow one to place a numerical value on glucose utilization.

The disadvantages of the technique are that it is complex and expensive. In addition, glucose metabolism is complex, and interpretation of measurements of glucose uptake is affected by many variables. Chief among these is that tissues may metabolize glucose through either glycolysis or the tricarboxylic acid cycle. The route of metabolism of glucose affects the amount of glucose uptake by a particular tissue, as glycolysis is a much less efficient pathway for the generation of ATP than is the tricarboxylic acid cycle. Furthermore, there are other metabolic fates for glucose than the generation of ATP, and these must be kept in mind in evaluating the results of deoxyglucose studies.

##### **CHOICE OF EXPERIMENTAL ANIMAL**

As detailed in the introduction, the findings of previous studies have yielded different results for the glucose metabolism of the inner retina.<sup>1,5,6,23</sup> For example, Bill and coworkers found a much lower percentage of glucose consumed by glycolysis in the inner retina of the pig<sup>23</sup> than Winkler found in the inner retina of the rat.<sup>5</sup> These different results could be due to different experimental approaches or to species differences. I have chosen to evaluate retinal energy metabolism in the rat. To evaluate

the *in vitro* observations of Poitry-Yamate<sup>7,8</sup> and Ames<sup>1</sup> discussed above, it is preferable to work *in vivo*. Use of the 2-deoxyglucose technique to evaluate glucose metabolism at the cellular level requires working in a small animal; working in a larger animal would be prohibitively expensive because of the amount of radioactive material necessary. Furthermore, much is known about the retinal energy metabolism of the rat from previous *in vitro* studies of glucose<sup>3,5,33-36</sup> and oxygen<sup>37-39</sup> metabolism in this animal.

#### BIOCHEMICAL THEORY

The deoxyglucose method for the measurement of local glucose utilization was developed by Sokoloff.<sup>31,32</sup> 2-deoxy-D-glucose (2-DG) differs from glucose in that a hydroxyl group on the second carbon atom has been replaced by a hydrogen atom. 2-DG and glucose are transported between blood and brain tissues by the same saturable carrier. In tissues, deoxyglucose competes with glucose for hexokinase, which phosphorylates both to their respective hexose-6-phosphates. However, since 2-deoxy-D-glucose-6-phosphate (2-DG-6-P) lacks a hydroxyl group at the second carbon atom, it cannot be isomerized to fructose-6-phosphate by phosphohexoseisomerase. Consequently, 2-DG-6-P does not proceed farther down the glycolytic pathway. Since 2-DG-6-P does not appear to be a substrate for glucose-6-phosphate dehydrogenase, and since the brain and retina<sup>34</sup> have very little deoxyglucose-6-phosphatase activity, 2-DG-6-P accumulates within cells in these tissues. When radioactively labeled, 2-DG can therefore serve as a quantitative or qualitative marker of glucose utilization.

As with other methods of evaluating retinal energy metabolism, the deoxyglucose method also has its limitations. The use of this method in a quantitative fashion requires that deoxyglucose be present in trace amounts, that the arterial plasma glucose concentration remain constant, and that the glucose metabolism of the retina be maintained in a steady state. Also, it is important that 2-DG-6-P remain in the cell and not be converted to other substances. The retina contains low levels of glucose-6-phosphatase,<sup>34</sup> making it unlikely that 2-DG-6-P is converted back to 2-DG. However, another concern is that 2-DG-6-P might diffuse out of cells after fixation. Investigators have shown that 2-DG-6-P is trapped within cells prior to fixation, but that there is some ability of 2-DG-6-P to diffuse out of cells after fixation.<sup>18</sup> Therefore, to prevent diffusion of 2-DG-6-P, tissue needs to be processed to minimize exposure to aqueous solutions. Another concern is that the radioactivity initially present on deoxyglucose ends up associated with glycogen. One report has measured that as much as 30% of the radioactivity initially associated with deoxyglucose migrated with glycogen following incubation with retinal tissue.<sup>18</sup>

Finally, it is important to note that the deoxyglucose technique is a measure of glucose utilization. The uptake of 2-DG will be influenced by whether a cell or cell function is coupled with the glycolytic metabolism of glucose as opposed to the oxidative metabolism of glucose. The deoxyglucose technique would be expected to measure a much larger glucose uptake in cells or cell processes that are generating energy through the glycolytic metabolism of glucose, as this is much less efficient at generating ATP than is oxidative metabolism. Glycolytic metabolism of glucose generates only 1 molecule of ATP for every 17 or 18 molecules of ATP generated by the oxidative metabolism of glucose.<sup>16</sup> Consequently, cells relying primarily on glycolytic metabolism of glucose will be more heavily labeled on autoradiograms using the deoxyglucose technique.

#### ANIMALS

Adult male Long-Evans, Sprague-Dawley, and Royal College of Surgeons (RCS) rats were used in this study. The animals were housed in the Oregon Health Sciences University Animal Care Facility and were treated within the standards set by the Animal Care Committee at that institution. These standards conform to the guidelines established by the Association for Research in Vision and Ophthalmology. The animals received food and water *ad libitum*. They were kept at a 12-hour light, 12-hour dark-light cycle. All procedures were carried out in room light.

#### Controls

Healthy Long-Evans (n= 4), Sprague-Dawley (n= 8), and RCS nondystrophic (n=1) rats were studied with the deoxyglucose technique to determine the normal retinal distribution of deoxyglucose. In addition, the fellow eye of each of the animals treated with photocoagulation served as a control in those animals.

#### Photocoagulation

After anesthesia was obtained with a cocktail (1 mL/kg body weight) of acepromazine maleate (1 mg/mL), xylazine hydrochloride (5 mg/mL), and ketamine (50 mg/mL), five Long-Evans rats were treated with argon green photocoagulation. The photocoagulation burns were placed in a sparse pattern around the optic nerve, sparing the area centralis. The intensity of the burns was adjusted to obtain a light white burn, similar to the photocoagulation burns used to treat macular edema.

#### Dystrophic RCS Rats

Dystrophic RCS rats (n=3) were studied with the deoxyglucose technique 24, 38, and 48 days after birth.

#### DEOXYGLUCOSE TECHNIQUE

After anesthesia was obtained with a cocktail (see above)

of acepromazine, xylazine, and ketamine, each rat was injected with 25 mCi of  $^3\text{H}$ -2-deoxy-D-glucose reconstituted in 1 mL of sterile normal saline via the saphenous vein. The animal was then allowed to recover from the anesthetic. At 90 minutes after the deoxyglucose injection, the rat was anesthetized in an ether chamber and sacrificed by decapitation.

The eyes were immediately enucleated and snap frozen in Freon 22 chilled to  $-175^\circ\text{C}$  with liquid nitrogen. The eyes were then "freeze substituted" by placing them into prechilled anhydrous ether ( $-70^\circ\text{C}$ ) containing water-extracting molecular sieves. The eyes were kept at  $-70^\circ\text{C}$  for 72 hours, then at  $-4^\circ\text{C}$  for 24 hours, and then at  $12^\circ\text{C}$  for 24 hours. At room temperature the freeze-substituted eyes were fixed in 1%  $\text{OsO}_4$  in acetone. The eyes were then gradually infiltrated with epon-araldite. After polymerization, 2- $\mu\text{m}$ -thick sections were cut on a Reichert-Jung ultramicrotome. The sections were coated with NTB-2. Autoradiograms were developed at various time intervals, but exposures of 6 to 12 weeks proved to be best.

#### **BIOCHEMICAL FATE OF DEOXYGLUCOSE**

The biochemical fate of deoxyglucose was analyzed using a specific extraction for glycogen and thin-layer chromatography. One rat was treated as described above, but after enucleation the retinas from both eyes were quickly dissected free of the other tissues, frozen in liquid nitrogen, and lyophilized. The lyophilized retinas (3 mg dry weight) were homogenized in 300  $\mu\text{L}$  of 1M  $\text{HClO}_4$ ; 10  $\mu\text{L}$  was saved to determine the radioactivity of the homogenate.

To determine how much deoxyglucose was incorporated into glycogen, a specific glycogen extraction was performed on a 50- $\mu\text{L}$  aliquot of the retinal homogenate as described by Evequoz.<sup>40</sup> Briefly, the 50- $\mu\text{L}$  aliquot of retinal homogenate was combined with 50  $\mu\text{L}$  of HCL. This 100- $\mu\text{L}$  sample was applied to Whatman 3M chromatography paper, washed three times for 40 minutes in 66% ethyl alcohol, rinsed briefly in acetone, dried, and counted in a scintillation counter.

Thin-layer chromatography (TLC) was used to determine the relative concentrations of 2-DG and 2-DG-6-P. A total of 240  $\mu\text{L}$  of retinal homogenate was added to a 7.5% aqueous solution of  $\text{Ba}(\text{OH})_2$  and a 5% aqueous solution of  $\text{ZnSO}_4 \cdot 7\text{H}_2\text{O}$ ; 34  $\mu\text{L}$  of  $\text{NH}_4\text{OH}$  was added to neutralize the perchloric acid. After vortexing, the mixture was centrifuged for 20 minutes. The pellet and an aliquot of the supernatant were saved for radioactivity counting. The remaining supernatant was lyophilized and reconstituted in distilled water. 20  $\mu\text{L}$  of reconstituted supernatant and 10  $\mu\text{L}$  of cold carrier (containing 50  $\mu\text{g}$  of 2-DG and 50  $\mu\text{g}$  of 2-DG-6-P) were placed on cellulose/plastic sheets (Merck 5577) with a solvent system consisting of ethylacetate: acetic acid: pyridine:  $\text{H}_2\text{O}$  (5:1.7:2.5:2.5). The plates were sprayed with a mixture of 0.5 g carbazols, 95 mL of ethyl alcohol, and 5 mL of  $\text{H}_2\text{SO}_4$  and developed for 10 minutes at  $120^\circ\text{C}$ . Spots corresponding to 2-DG and 2-DG-6-P were scraped from the TLC plates and counted.

lose/plastic sheets (Merck 5577) with a solvent system consisting of ethylacetate: acetic acid: pyridine:  $\text{H}_2\text{O}$  (5:1.7:2.5:2.5). The plates were sprayed with a mixture of 0.5 g carbazols, 95 mL of ethyl alcohol, and 5 mL of  $\text{H}_2\text{SO}_4$  and developed for 10 minutes at  $120^\circ\text{C}$ . Spots corresponding to 2-DG and 2-DG-6-P were scraped from the TLC plates and counted.

#### **EFFECT OF AQUEOUS EXPOSURE ON DEOXYGLUCOSE LOCALIZATION**

Some investigators<sup>7,41</sup> have stressed the importance of eliminating aqueous exposure of 2-DG-containing tissues. Prior to fixation, 2-DG can freely diffuse out of cells, while 2-DG-6-P remains trapped within cells, even in aqueous environments. Following fixation, 2-DG-6-P may also diffuse out of cells. However, superior tissue morphology can be obtained on thick sections briefly exposed to water during slide preparation and application of photographic emulsion. The amount of radioactivity lost in aqueous solutions after plastic embedding has not been previously evaluated. To quantitate potential loss of radioactivity, we analyzed the loss of radioactivity in the following extreme conditions: 200 1- $\mu\text{m}$  plastic sections of rat retina were heated in 1 mL of distilled  $\text{H}_2\text{O}$  at  $40^\circ\text{C}$  for 20 minutes. The sections were then removed and the  $\text{H}_2\text{O}$  was added to 1 mL of a saturated solution of potassium hydroxide in methanol, acetone, and benzene. The amount of radioactivity present was determined in a scintillation counter. The total amount of radioactivity in 200 1- $\mu\text{m}$ -thick sections of rat retina was determined by dissolving 200 sections in 1 mL of a saturated solution of potassium hydroxide in methanol, acetone, and benzene. One milliliter of water was added, and this solution was also counted in a scintillation counter.

#### **HISTOPATHOLOGIC TECHNIQUES**

The following standard and immunohistochemical stains were prepared on sections of rat retina to allow correlation with the autoradiograms: hematoxylin-eosin, periodic acid Schiff, Feulgen (for glycogen), vimentin (Müller cells), and synaptophysin.

#### **RESULTS**

---

##### **BIOCHEMICAL FATE OF DEOXYGLUCOSE**

Only 0.31% of the retinal radioactivity was present in glycogen. The remainder of the retinal radioactivity was present as 2-DG and 2-DG-6-P. The ratio of 2-DG-6-P to 2-DG was 3:1.

##### **EFFECT OF AQUEOUS EXPOSURE ON DEOXYGLUCOSE LOCALIZATION**

Eight percent of the total radioactivity was lost into warm water after heating at  $40^\circ\text{C}$  for 20 minutes.

#### DEOXYGLUCOSE TECHNIQUE

Following freeze substitution, the retinal morphology was sufficient to allow detailed identification of the retinal layers. Certain artifacts of freezing were present but did not interfere with the interpretation of the results. Freezing results in the formation of water crystals in the tissue. Because of the rapid freezing employed in this study, the water crystals were small but still evident in some preparations. In addition, freeze substitution created a dry tissue that was prone to cracking. Again, this artifact was easily identifiable and did not interfere with interpretation of the results of the study (Figure 1). [Note: Staining of autoradiograms requires a compromise between greater visibility of the exposed grains in the photographic emulsion in an unstained section and greater visibility of the details of the retinal cells in a more darkly stained section. When necessary, unstained and variably stained sections have been provided to maximize the illustration of critical points.]

Radioactive deoxyglucose was clearly evident in various ocular tissues to a much higher level than background. This was evident in the cornea, with prominent labeling of the keratocytes and corneal endothelium, as well as in extraocular muscle. These internal controls helped to confirm that the labeling seen on autoradiograms reflected the location of deoxyglucose and deoxyglucose-6-phosphate and had not been significantly affected by diffusion of these substances in the course of processing (Figures 2 and 3).

#### DEOXYGLUCOSE UPTAKE IN CONTROL RETINAS

The pattern of deoxyglucose uptake was the same in the three different strains of rat used in this study. There was intense uptake of radioactivity in the outer plexiform, inner nuclear, and inner plexiform layers. The pattern of uptake in the outer plexiform layer was such that there were focal areas of intense uptake at the junction of the outer plexiform layer and the inner nuclear layer. This intense uptake extended into the outer portion of the inner nuclear layer. These foci of intense uptake stood out in juxtaposition to adjacent areas that had markedly less uptake of deoxyglucose. The intense areas of radioactivity in the inner nuclear layer corresponded to cells in the outer portion of the inner nuclear layer, sometimes with adjacent cells taking up almost no deoxyglucose. The intense areas of radioactivity in the outer plexiform layer appeared to correspond to the expected position of synapses between the photoreceptors and cells of the inner nuclear layer, but these synapses were not visible at the light microscopic level.

There were prominent but slightly less intense areas of radioactive labeling within the inner plexiform layer and at the junction of the inner plexiform layer and the

ganglion cell layer. In the inner plexiform layer, this labeling created two faint bands that ran parallel to the internal limiting membrane. There were also focal areas of intense radioactive labeling at the junction of the inner plexiform and ganglion cell layers. Notably, there was no labeling at the inner limiting membrane, at the junction of the Müller cells to their basement membrane (Figure 4A and B).

#### DEOXYGLUCOSE UPTAKE IN DYSTROPHIC RETINAS

At 24 days, dystrophic retinas showed markedly disarranged outer segments, but the outer nuclear layer was of normal thickness. By 38 days, there was moderate loss of the outer nuclear layer so that it was only one-half the thickness of the control RCS outer nuclear layer. There was continued disarrangement of the outer segments. By 48 days, there was marked atrophy of the outer nuclear layer so that it was only one-quarter the thickness of the control outer nuclear layer. Once again, there was marked disarrangement of the outer segments (Figure 5A and B).

The pattern of uptake in the dystrophic RCS rats was markedly different than in the control RCS animal. At the earliest time point examined (24 days), there was loss of the intense labeling at the junction of the outer plexiform and inner nuclear layers. There was relative preservation of the two less intense bands of labeling within the inner plexiform layer (Figure 6A, B, and C).

These changes were even more evident at the 48-day time point, at which there was markedly reduced deoxyglucose uptake in the region of the junction of the outer plexiform and outer nuclear layers. There was relative preservation of the two bands of deoxyglucose uptake in the inner plexiform layer. At this time point, there was striking uptake of deoxyglucose within some of the ganglion cells. There was also prominent deoxyglucose uptake within cell nuclei within the layer of disarranged outer segments (Figure 7A, B, C).

#### DEOXYGLUCOSE UPTAKE FOLLOWING PHOTOCOAGULATION

Photocoagulation burns resulted in focal areas of loss of the retinal pigment epithelium, the photoreceptor outer segments, and a variable number of the photoreceptor cell nuclei. There was some migration of pigment-containing cells into the outer plexiform and inner nuclear layers.

Deoxyglucose uptake in the area of photocoagulation was similar to that seen in photoreceptor degeneration in the RCS rat. There was loss of the intense deoxyglucose uptake at the junction of the outer plexiform layer and the inner nuclear layer. The labeling of the inner plexiform layer was relatively unaffected by the laser photocoagulation (Figure 8A, B, and C).

#### **IMMUNOHISTOCHEMICAL AND HISTOCHEMICAL STAINS**

Immunohistochemical stains for vimentin demarcated the Müller cells. Immunohistochemical stains for synaptophysin revealed prominent labeling in the inner and outer plexiform layers (Figure 9A and B).

#### **DISCUSSION**

---

This is the first in vivo study using  $^3\text{H}$ -2-DG combined with freeze substitution to localize glucose uptake at the cellular level, in the mammalian retina. As would be expected, there is a diffuse background level of glucose utilization throughout the retina. However, as described in the "Results" section, there are distinct areas of greater glucose uptake. Analysis for diffusion of 2-DG and 2-DG-6-P indicated that only 8% of 2-DG and 2-DG-6-P were lost under extreme conditions. Similarly, only 0.31% of the retinal radioactivity was present in glycogen. These findings, coupled with the internal control findings of well-defined uptake of 2-DG in the corneal endothelium and extraocular muscle, make it unlikely that the pattern of 2-DG uptake seen in the retina is artifactual.

The in vitro studies of Poitry-Yamate<sup>7,8</sup> and Ames<sup>1</sup> would suggest that there is increased glucose uptake in Müller cells and at sites of synaptic transmission. In order to compare the distribution of synapses and Müller cells to the pattern of 2-DG labeling, the retina was stained with an immunoperoxidase technique for vimentin and for synaptophysin. Vimentin is present in Müller cells and synaptophysin is a glycoprotein that is present in the presynaptic vesicles of neurons.

I would interpret the pattern of uptake of 2-DG to be consistent with a high level of uptake by Müller cells and at sites of synaptic transmission. Interestingly, the pattern of 2-DG uptake does not correspond to the entire extent of the Müller cell. Specifically, the Müller cell endfeet do not show the extent of 2-DG uptake that is present over the remainder of the cell. This could indicate that there is some intracellular compartmentalization of glucose metabolism within the Müller cell. Such compartmentalization has been reported in the central nervous system.<sup>14</sup> Alternatively, it could be that 2-DG was lost from this site on account of diffusion, but this seems unlikely because diffusion of 2-DG from other ocular tissues (corneal endothelium and extraocular muscle) was quite limited.

The pattern of 2-DG uptake in this study is similar to that reported by Poitry-Yamate and associates working in the guinea pig.<sup>7</sup> Those investigators found prominent uptake of 2-DG within Müller cells of guinea pig retinas studied in vitro. Our results differ in that in Poitry-Yamate's study there was prominent uptake of 2-DG within the Müller cell endfeet. Also, in that study there was less uptake in the outer plexiform and inner plexiform

layers than was seen in the current study.

The finding of a large amount of 2-DG uptake by Müller cells in this study is consistent with the in vitro studies of Poitry-Yamate and associates<sup>8</sup> and Winkler and colleagues<sup>9</sup> on isolated Müller cells from guinea pig and human, respectively. Those investigators have shown that there is a high rate of aerobic glycolysis in the Müller cell. Winkler concluded that the Müller cell utilized close to 99% of its glucose in glycolysis. The main products of interest from glycolysis are pyruvate (subsequently converted to lactate) and ATP. Poitry-Yamate<sup>8</sup> has shown that lactate produced by Müller cells is taken up by photoreceptors as an energy source. The ATP produced through glycolysis is used by the Müller cell for its many cellular functions, but a large portion of this ATP is undoubtedly consumed by the cells' role in maintaining ionic balances following neuronal cell depolarizations. One would expect that following loss of the photoreceptors, Müller cell glucose uptake to support photoreceptor metabolism, as well as the need for ATP for supporting ionic balance, would be reduced.

In the RCS retinas, there was loss of the pattern of deoxyglucose seen in the RCS control eye. By 24 days, even though the inner retina was intact, the distinct deoxyglucose uptake at the junction of the outer plexiform layer and the inner nuclear layer was diminished. There was some preservation of the bandlike labeling of the inner plexiform layer. By 48 days, there was even more extensive loss of 2-DG uptake at the junction of the outer plexiform and inner nuclear layers.

This change in the pattern of labeling is consistent with the observations of Poitry-Yamate and associates.<sup>7,8</sup> As already noted, these investigators have suggested that Müller cells metabolize glucose to lactate and that photoreceptors utilize the lactate as an energy source. In the RCS rat with degeneration of the photoreceptors, there is less deoxyglucose uptake by Müller cells, as there is less demand for lactate by the photoreceptors. Interestingly, the decrease in deoxyglucose uptake by the Müller cells occurs prior to the complete loss of the photoreceptors. In fact, the decrease in deoxyglucose uptake by Müller cells is readily apparent at day 24, when the cell bodies of the photoreceptors are still intact.

Similar findings are evident following photocoagulation. With local loss of the photoreceptors, there is loss of the intense deoxyglucose uptake at the junction of the outer plexiform layer and the inner nuclear layer. Once again, this is consistent with less uptake of glucose by the Müller cells as a result of the loss of photoreceptors.

In addition to deoxyglucose uptake in the Müller cells, there was clearly a fairly high level of deoxyglucose uptake in the outer plexiform layer and the inner nuclear layer that could not be accounted for by Müller cell

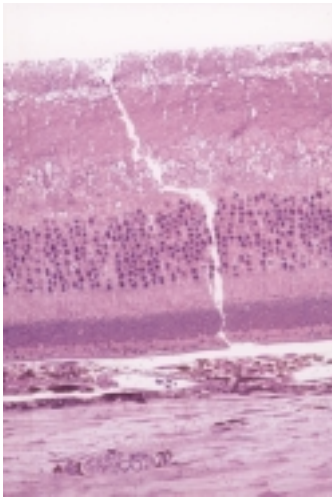


**FIGURE 1**

Histologic section of full-thickness retina, retinal pigment epithelium, choroid, and partial-thickness sclera. In center of figure is a crack resulting from drying of the tissue during freeze substitution and subsequent embedding. There are also small clear spaces due to formation of intracellular ice crystals. These are most evident in the nerve fiber and ganglion cell layers (toluidine blue, x400).

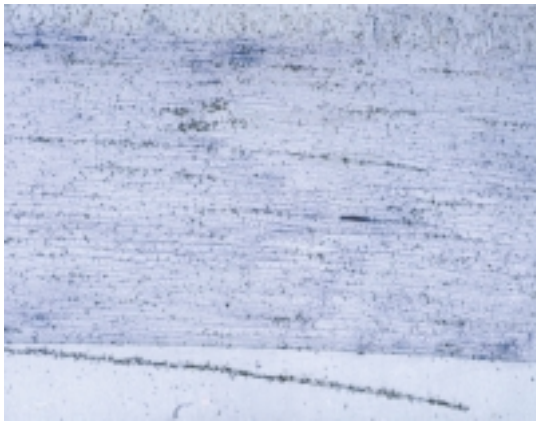


**FIGURE 3**

Autoradiogram of cornea with artifactual separation of corneal endothelium. 2-DG uptake by corneal endothelium is sharply demarcated from background, indicating limited diffusion of 2-DG or 2-DG-6-P out of cells (toluidine blue, x200).

uptake alone. My interpretation of this relatively high level of uptake is that it is due to the use of glycolytic metabolism to support synaptic transmission at these sites. As already mentioned, there is some evidence in the central nervous system<sup>12-16</sup> and in smooth muscle<sup>11</sup> that glycolytic metabolism may be used to support specific functions on demand. There are large synapses present at the junction of the outer plexiform layer and the inner nuclear layer, a site of particularly high deoxyglucose uptake, as well as numerous synapses present in the inner plexiform layer. The labeling of the rat retina with synaptophysin roughly correlates with the non-Müller cell uptake of deoxyglucose. However, the resolution of the deoxyglucose

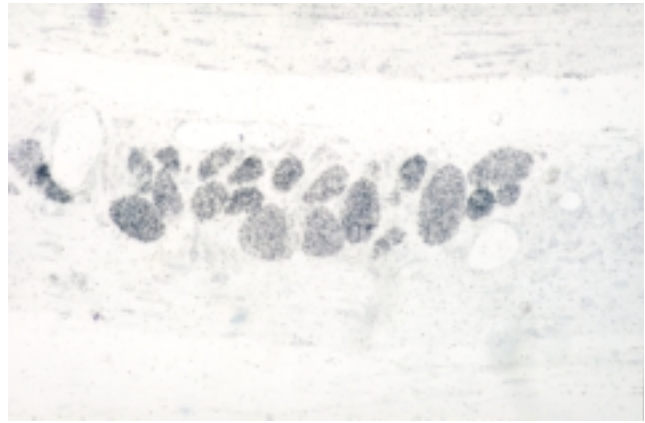


**FIGURE 2**

Autoradiogram showing 2-DG uptake by extraocular muscle relative to background. Labeling of the muscle is sharply defined relative to background. Slide is lightly stained to preserve visibility of grains of photographic emulsion (toluidine blue, x400).

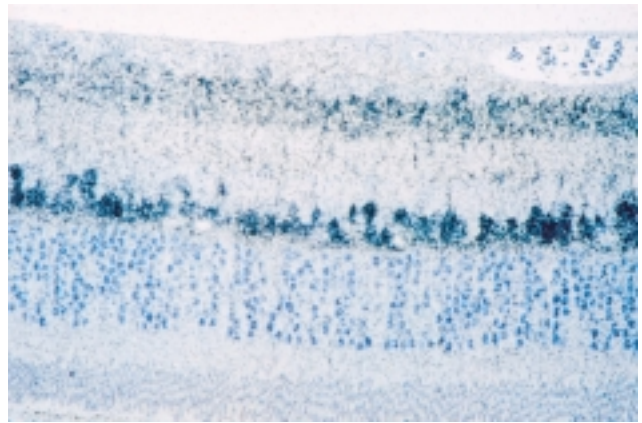


**FIGURE 4A**

Normal retina; RCS, nondystrophic. There is intense 2-DG uptake at junction of outer plexiform and inner nuclear layers, and in inner plexiform layer (toluidine blue, x400).

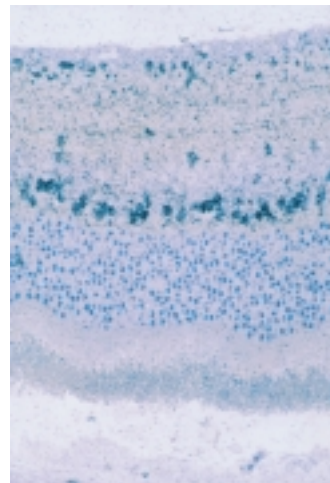


**FIGURE 4B**

Normal retina; Sprague-Dowley. Pattern of 2-DG uptake is similar to that shown in 4A, but the two faint bands of 2-DG uptake in inner plexiform layer are more prominent (toluidine blue, x400).

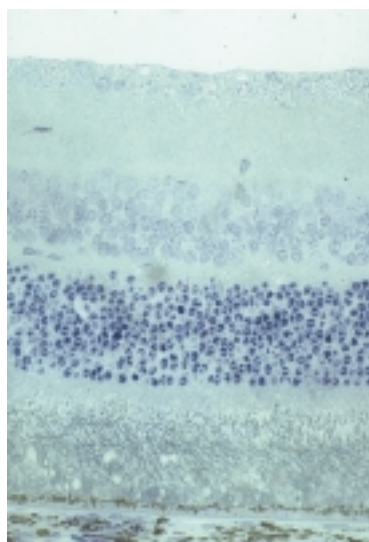


**FIGURE 5A**

24-day RCS rat retina. There is marked disarrangement of outer segments. Outer nuclear layer is of normal thickness (toluidine blue, x400).

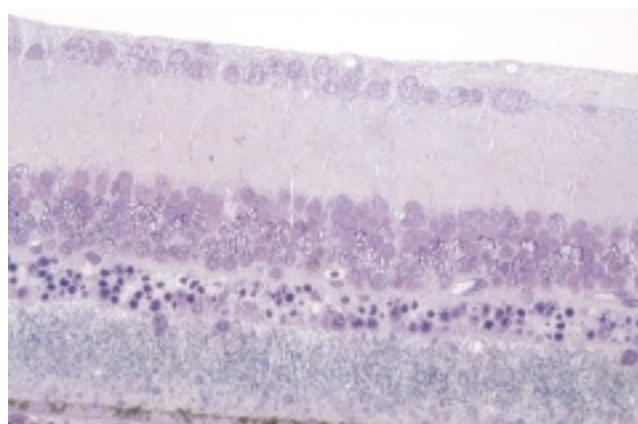


**FIGURE 5B**

48-day RCS rat retina. There is prominent atrophy of outer nuclear layer, with continued disarrangement of outer segments (toluidine blue, x400).

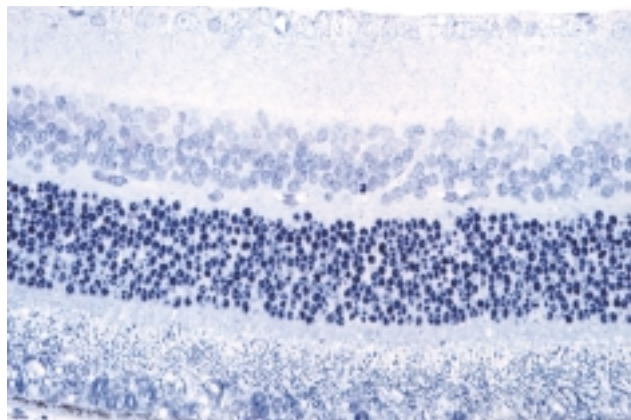


**FIGURE 6A**

24-day RCS rat retina. Histology for comparison to autoradiograms (toluidine blue, x400).

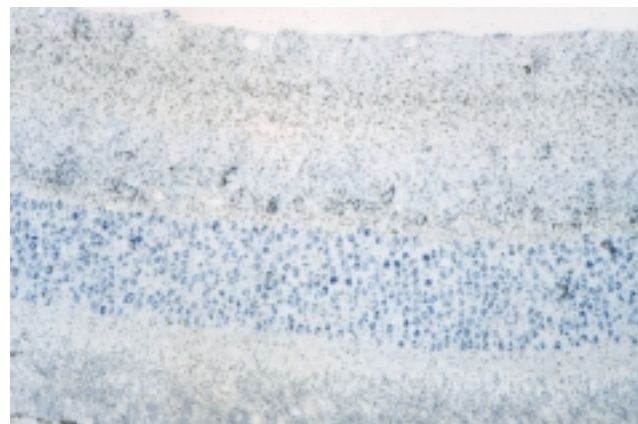


**FIGURE 6B**

24-day RCS rat retina. Lightly stained autoradiogram showing much less 2-DG uptake at junction of outer plexiform and inner nuclear layers compared to control. (See Figure 4 for comparison (toluidine blue, x400).



**FIGURE 6C**

24-day RCS rat retina. Unstained autoradiogram. Bands of 2-DG uptake are present in inner plexiform layer (x400).

localization in this study and the inadequate visualization of synapses in this light microscopic study do not permit a definite conclusion on this point. Further studies at the ultrastructural level with inhibitors of synaptic transmission might further clarify this issue.

It is more difficult to compare the results of this study to those of Bill and coworkers,<sup>25-27</sup> who studied retinal glucose uptake in the monkey using <sup>14</sup>C-2-DG. They reported that in the dark there was greater 2-DG uptake in the outer retina, as compared to the inner retina. In the light there was approximately equal uptake in the inner and the outer retina. The 2-DG uptake by individual cells was not reported in these studies.

It is of interest to try to correlate the findings in this study with studies of oxygen utilization. Glucose and

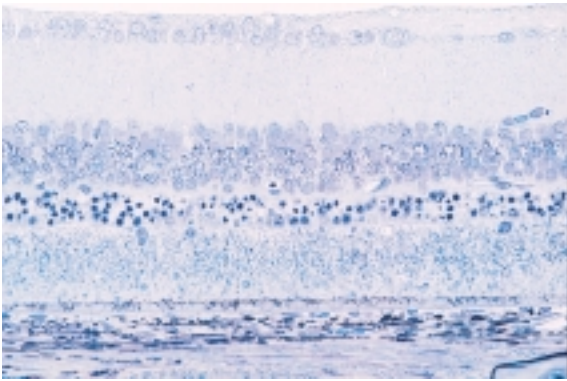


**FIGURE 7A**

48-day RCS rat. Stained section for comparison to B and C (toluidine blue, x400).

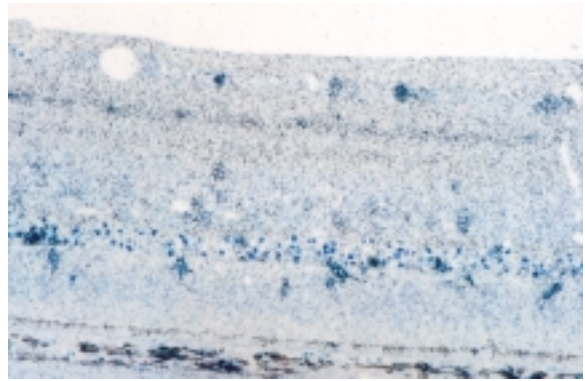


**FIGURE 7B**

48-day RCS rat. Lightly stained autoradiogram showing change of pattern of 2-DG uptake so that there is much less 2-DG uptake at junction of outer plexiform layer and inner nuclear layer (toluidine blue, x400).

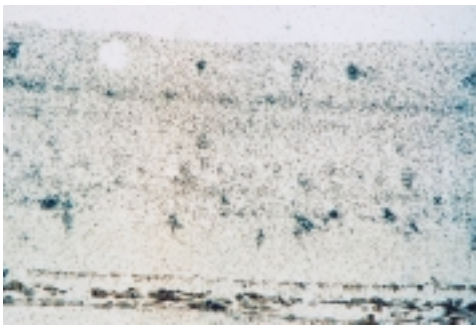


**FIGURE 7C**

48-day RCS rat. Unstained autoradiogram showing preservation of bands in inner plexiform layer and 2-DG uptake by ganglion cells and cells in photoreceptor layer (unstained, x400).

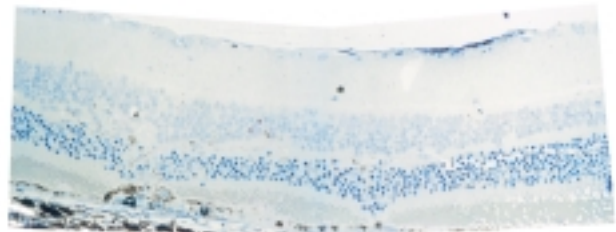


**FIGURE 8A**

Effect of photocoagulation. Photocoagulation burns are evident as focal areas of loss of photoreceptors and RPE hyperplasia (toluidine blue, x400, montage).

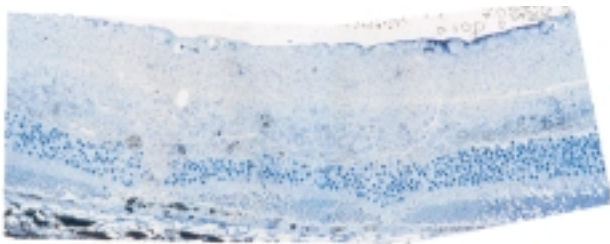


**FIGURE 8B**

Effect of photocoagulation. Lightly stained autoradiogram showing loss of 2-DG uptake at junction of inner nuclear layer and outer plexiform layer in region of photocoagulation. There is persistent 2-DG uptake at this site at periphery of montage, outside area of photocoagulation (toluidine blue, x400, montage).



**FIGURE 8C**

Unstained autoradiogram showing features similar to those shown in 8B (unstained, x400, montage).

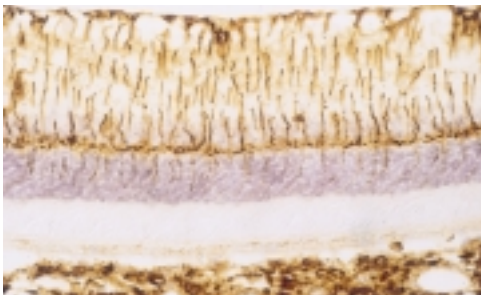


**FIGURE 9A**

Vimentin staining of Müller cells. Note linear extensions of Müller cells across inner plexiform layer and outer nuclear layer (DAB, x400).



**FIGURE 9B**

Synaptophysin: There is prominent staining of outer plexiform and inner plexiform layers (DAB, x400).

oxygen are the principal substrates of energy metabolism in the retina, so one would expect some correlative findings. Interestingly, in the perfused rabbit retina, Ames found that inhibition of neurotransmission did not affect the inner retinal oxygen consumption. Similarly, Cringle and coworkers,<sup>38,39</sup> working in vivo in the RCS rat, found that the inner retinal oxygen tension profiles were unaffected by photoreceptor degeneration. Both of these findings are consistent with the hypothesis that neurotransmission though the inner retina is supported by glycolysis, so that loss of neurotransmission would reduce glucose uptake but have no effect on oxygen consumption.

The findings in this study support the concept that there is an interaction between the glucose metabolism of the inner retina and that of the outer retina. This interaction could be important in the changes in the retinal blood vessels following photoreceptor degeneration from retinal dystrophy or from photocoagulation. In the central nervous system, capillary density has been correlated with glucose utilization in some areas of the brain. Furthermore, glial cells (astrocytes and Müller cells) have been shown to direct and guide the vascularization of the inner retina during development.<sup>42,43</sup> It is possible that changes in Müller cell metabolism following loss of the photoreceptors are responsible for the changes in the retinal vessels known to occur with photoreceptor loss.

## SUMMARY

This study shows that in vivo glucose uptake by the inner retina is not uniform. The distribution pattern of glucose uptake appears to be consistent with greatest glucose uptake by the Müller cells and at sites of synapses. Following photoreceptor degeneration, there is a marked decrease in the amount of glucose uptake at the junction of the inner plexiform and outer nuclear layers. Decreased glucose uptake in this area is consistent with decreased glucose uptake by Müller cells following photoreceptor atrophy.

## REFERENCES

1. Ames A, Li Y, Heher EC, et al. Energy metabolism of rabbit retina as related to function: high cost of  $\text{Na}^+$  transport. *J Neurosci* 1992;12:840-853.
2. Ames A. Energy requirements of CNS cells as related to their function and to their vulnerability to ischemia: a commentary based on studies on retina. *Can J Physiol Pharmacol* 1992;70:S158-S164.
3. Cohen LH, Noell WK. Glucose catabolism of rat retina before and after the development of visual function. *J Neurochem* 1960;5:253-276.
4. Noell WK. Aspects of experimental and hereditary retinal degeneration. In: Graymore C, ed. *Biochemistry of the Retina*. London: Academic Press; 1965:51-72.
5. Winkler BS. A quantitative assessment of glucose metabolism in the isolated rat retina. In: Christen Y, Doly M, Droy-Lefaix MT, eds. *Vision and adaptation. Les Seminaires Ophthalmologiques d'IPSEN*. Paris: Elsevier; 1995:79-96.
6. Ames A, Parks JM, Nesbett FB. Synthesis and degradation of retinal proteins in darkness and during photic stimulation. *J Neurochem* 1980;35:143-148.
7. Poitry-Yamate C, Tsacopoulos M. Glial (Müller) cells take up and phosphorylate [ $^3\text{H}$ ]2-deoxy-D-glucose in a mammalian retina. *Neurosci Lett* 1991;122:241-244.
8. Poitry-Yamate CL, Poitry S, Tsacopoulos M. Lactate released by Müller glial cells is metabolized by photoreceptors from mammalian retina. *J Neurosci* 1995;15:5179-5191.
9. Winkler BS, Arnold MJ, Brassell MA, et al. Energy metabolism in human retinal Müller cells. *Invest Ophthalmol Vis Sci* 2000;41:3183-3190.
10. Lowry OH, Roberts NR, Lewis C. The quantitative histochemistry of the retina. *J Biol Chem* 1956;220:879-892.
11. Paul RJ, Hardin DC, Raeymaekers L, et al. Preferential support of  $\text{Ca}^{2+}$  uptake in smooth muscle plasma membrane vesicles by an endogenous glycolytic cascade. *FASEB J* 1989;3:2298-2301.
12. Lear JL, Ackermann RF. Why the deoxyglucose method has proven so useful in cerebral activation studies: the unappreciated prevalence of stimulation-induced glycolysis. *J Cereb Blood Flow Metab* 1989;9:911-913.
13. Lipton P, Robacker K. Glycolysis and brain function: [ $\text{K}^+$ ]o stimulation of protein synthesis and  $\text{K}^+$  uptake require glycolysis. *Fed Proc* 1983;42:2875-2880.
14. Carroll EW, Wong-Riley MTT. Quantitative light and electron microscopic analysis of cytochrome oxidase-rich zones in the striate cortex of the squirrel monkey. *J Comp Neurol* 1984;222:1-17.
15. Borowsky IW, Collins RC. Metabolic anatomy of brain: a comparison of regional capillary density, glucose metabolism, and enzyme activities. *J Comp Neurol* 1989;288:401-413.
16. Erecinska M, Silver IA. ATP and brain function. *J Cereb Blood Flow Metab* 1989;9:2-19.
17. Tsacopoulos M, Evequoz-Mercier V, Perrottet P, et al. Honeybee retinal glial cells transform glucose and supply the neurons with metabolic substrate. *Proc Natl Acad Sci USA* 1988;85:8727-8731.
18. Witkovsky P, Yang C. Uptake and localization of  $^3\text{H}$ -2-deoxy-D-glucose by retinal photoreceptors. *J Comp Neurol* 1982;204:105-116.
19. Basinger SF, Gordon WC, Lam DMK. Differential labeling of retinal neurons by [ $^3\text{H}$ ]2-deoxyglucose. *Nature* 1979;280:682-683.
20. Sperling HG, Harcombe ES, Johnson C. Stimulus controlled labeling of cones in the macaque monkey with  $^3\text{H}$ -2-D-deoxyglucose. In: Hollyfield JG, Vidrio EA, eds. *The Structure of the Eye*. New York: Elsevier; 1982:56-60.
21. Wang L, Bill A. Effects of constant and flickering light on retinal metabolism in rabbits. *Acta Ophthalmol Scand* 1997;75:227-231.
22. Wang L, Kondo M, Bill A. Glucose metabolism in cat retina: effects of light and hyperoxia. *Invest Ophthalmol Vis Sci* 1997;38:48-55.

23. Wang L, Tornquist P, Bill A. Glucose metabolism of the inner retina in pigs in darkness and light. *Acta Physiol Scand* 1997;160: 71-74.
24. Wang L, Tornquist P, Bill A. Glucose metabolism in pig outer retina in light and darkness. *Acta Physiol Scand* 1977;160:75-81.
25. Bill A, Sperber GO. Aspects of oxygen and glucose consumption in the retina: effects of high intraocular pressure and light. *Graefes Arch Clin Exp Ophthalmol* 1990;228:124-127.
26. Hayreh SS, Bill A, Sperber GO. Effects of high intraocular pressure on the glucose metabolism in the retina and optic nerve in old atherosclerotic monkeys. *Graefes Arch Clin Exp Ophthalmol* 1994;232:745-752.
27. Sperber GO, Bill A. Blood flow and glucose consumption in the optic nerve, retina and brain: effects of high intraocular pressure. *Exp Eye Res* 1985;41:639-653.
28. Blair NP, Moy JJ, Tsukahara Y, et al. Ocular glucose extraction using vitreoperfusion in the cat. *Invest Ophthalmol Vis Sci* 1992;33:2791-2797.
29. Blair NP. Ocular oxygen consumption during vitreoperfusion in the cat. *Trans Am Ophthalmol Soc* 2000;98:305-329.
30. Wilson DJ, Finkelstein D, Quigley HA, et al. "Grid" macular photocoagulation: a quantitative histologic study of the effect on the primate retinal capillaries. *Arch Ophthalmol* 1988;106:100-105.
31. Sokoloff L, Reivich B, Kennedy C, et al. The [<sup>14</sup>C]deoxyglucose method for the measurement of local cerebral glucose utilization: theory, procedure, and normal values in the conscious and anesthetized albino rat. *J Neurochem* 1977;28:897-916.
32. Kennedy C, Des Rosiers MH, Sakurada O, et al. Metabolic mapping of the primary visual system of the monkey by means of the autoradiographic [<sup>14</sup>C]deoxyglucose technique. *Proc Natl Acad Sci U S A* 1976;73:4230-4234.
33. Winkler BS. Glycolytic and oxidative metabolism in relation to retinal function. *J Gen Physiol* 1981;77:667-692.
34. Blair NP, Shaw WE, Yue B. Glucose-6-phosphatase activity in the retina of the awake rat. *Invest Ophthalmol Vis Sci* 1989;30:2268-2271.
35. Graymore C. Metabolism of the developing retina. III. Respiration in the developing normal rat retina and the effect of an inherited degeneration of the retinal neuroepithelium. *Br J Ophthalmol* 1960;44:363-369.
36. Graymore C, Tansley K. Iodoacetate poisoning of the rat retina. *Br J Ophthalmol* 1959;43:486-493.
37. Medrano CJ, Fox DA. Oxygen consumption in the rat outer and inner retina: light- and pharmacologically-induced inhibition. *Exp Eye Res* 1995;61:273-284.
38. Yu D, Cringle SJ, Alder V, et al. Intraretinal oxygen distribution in the rat with graded systemic hypoxia and hypercapnia. *Invest Ophthalmol Vis Sci* 1999;40:2082-2087.
39. Yu D, Cringle SJ, Su E, et al. Intraretinal oxygen levels before and after photoreceptor loss in the RCS rat. *Invest Ophthalmol Vis Sci* 2000;41:3999-4000.
40. Evequoz V, Stadelmann A, Tsacopoulos M. The effect of light on glycogen turnover in the retina of the intact honeybee drone (*Apis mellifera*). *J Comp Physiol* 1983;150:69-75.
41. Buchner S, Buchner E. Functional neuroanatomical mapping in insects by [<sup>3</sup>H]2-deoxy-D-glucose at electron microscopical resolution. *Neurosci Lett* 1982;28:235-240.
42. Ling T, Stone J. The development of astrocytes in the cat retina: evidence of migration from the optic nerve. *Dev Brain Res* 1988;44:73-85.
43. Stone J, Itin A, Lon T, et al. Development of retinal vasculature is mediated by hypoxia-induced endothelial growth factor (VEGF) expression in neuroglia. *J Neurosci* 1997;15:4738-4747.

# PROGRESSION OF VISUAL FIELD LOSS IN UNTREATED GLAUCOMA PATIENTS AND SUSPECTS IN ST LUCIA, WEST INDIES

---

BY *M. Roy Wilson, MD, MS*

## ABSTRACT

*Purpose:* A 1986-1987 survey found an 8.8% prevalence of open-angle glaucoma in the black population of St Lucia, West Indies. This follow-up study assessed progression of visual field loss in untreated glaucoma patients and persons with suspected glaucoma 10 years later.

*Methods:* Subjects were 205 patients with or suspected of having glaucoma. The 1987 data included age, sex, visual acuity, and visual fields measured by automated threshold perimetry (Humphrey C-30-2 test). The 1997 data included intraocular pressure, visual acuity, and visual fields measured by the same test. Exclusion criteria included field unreliability, field improvement due to vision improvement, nonglaucomatous vision deterioration, glaucoma treatment since 1988, and scoring of a field as end-stage in 1987. Visual fields were scored by algorithms for the Advanced Glaucoma Intervention Study (AGIS) and Collaborative Initial Glaucoma Treatment Study (CIGTS).

*Results:* By AGIS criteria, 55% of 146 right eyes and 52% of 141 left eyes progressed. In linear regressions, progression severity was unassociated with male or female sex, intraocular pressure, or baseline visual field score, but was positively associated with age ( $P < .001$ , right;  $P = .002$ , left). By CIGTS criteria, more eyes progressed. The cumulative probability of reaching end-stage disease in 10 years in at least one eye was about 16% by AGIS criteria and was 35% by CIGTS criteria.

*Conclusions:* These data provide a unique opportunity to study progression of untreated glaucoma. A considerably larger percentage of eyes showed progression of visual field loss, and the rate of progression was greater than in studies of visual field loss in treated eyes.

*Trans Am Ophthalmol Soc* 2002;100:365-410

## INTRODUCTION

---

Despite decades of experience in the treatment of open-angle glaucoma, the natural history of this disease remains an enigma. Among the inadequately answered questions are the following:

1. Which individuals with elevated intraocular pressure will develop open-angle glaucoma?
2. How does treatment of elevated intraocular pressure affect development of open-angle glaucoma?
3. Once glaucoma develops, at what rate does it progress?
4. How does treatment affect the rate of progression?

The first of these questions, and likely also the second, undoubtedly will be answered by the Ocular Hypertension Treatment Study,<sup>1</sup> a clinical trial designed to

determine whether treatment to lower intraocular pressure prevents or delays the onset of open-angle glaucoma. Data from this study now are being analyzed. With respect to the third question, data on the rate of progression of treated open-angle glaucoma are conflicting.<sup>2,3</sup> Although widespread consensus is lacking, a few well-performed studies have reported visual field loss rates of about 2% to 3% per year.<sup>4,5</sup> Because the rate of progression of open-angle glaucoma is a topic of continuing investigation, it is likely that the progression rate estimates will soon become more precise.

Addressing the fourth question is problematic. Data are available on the progression of untreated normal-pressure glaucoma,<sup>6</sup> but no data have been reported describing the natural history of untreated open-angle glaucoma. The Early Manifest Glaucoma Trial,<sup>7</sup> a clinical trial to evaluate the effect of immediate intraocular pressure reduction in patients with early glaucoma and pressures not exceeding 30 mm Hg, potentially will provide information on the effect of treatment on progression in the very early stages. However, because it is generally agreed that open-angle glaucoma with elevated intraocular pres-

From the School of Medicine, Creighton University, Omaha, Nebraska. This study was supported in part by a grant from the Glaucoma Research Foundation and was conducted while the author was affiliated with the Jules Stein Eye Institute, University of California at Los Angeles.

sure must be treated, it would be unethical to conduct a trial to test the effect of treatment on the rate of progression of glaucoma with elevated pressures and various severity levels.

A study conducted in 1986-1987 assessed the prevalence of glaucoma and its risk factors in St Lucia, West Indies.<sup>8</sup> The high prevalence of glaucoma in this population (estimated to be 8.8%) and the availability of these baseline data (summarized below) appeared to present the opportunity for analysis of a “natural experiment” comparing the progression of open-angle glaucoma in treated and untreated eyes. At the time of the 1986-1987 survey, an infrastructure was in place to care for complicated ophthalmological disorders regardless of patients’ ability to pay, with free transportation to clinics as needed. All subjects in the 1986-1987 survey with diagnoses of glaucoma or suspected glaucoma received referrals to Victoria Hospital, in Castries, or St Jude’s Hospital, in Vieux Fort, where care was available from a faculty ophthalmologist and residents affiliated with the Massachusetts Eye and Ear Infirmary. Those with severe glaucoma received surgery; most of the others received at least one evaluation, and those requiring glaucoma medications received them at no charge. The findings of a feasibility study conducted in 1996 (described below) supported the feasibility of a follow-up study of glaucoma patients and suspects identified in the 1986-1987 survey.

Distressingly, the 1997 follow-up study showed that very few subjects were under active treatment, in part because the infrastructure for subsidized glaucoma care collapsed shortly after the Massachusetts Eye and Ear Infirmary resident rotation was discontinued, in 1988. In 1997, it was found that only a few patients had had surgery, and only a few who could afford medications had continued to receive them. Because few subjects had received treatment, the design of the follow-up study was changed to focus on the natural history and progression of untreated glaucoma.

#### ISSUES IN ANALYSIS OF GLAUCOMATOUS VISUAL FIELD LOSS PROGRESSION

Following the course of vision loss in glaucoma continues to be a major problem as more is learned about current visual field testing techniques and about the nature of the disease. No standard for identifying progression of glaucomatous visual field loss has been agreed upon. While one can be moderately certain that standard visual field tests will detect vision loss,<sup>9</sup> it still is unclear what constitutes a clinically significant, reproducible change for the worse. Visual fields may appear worse but then improve in subsequent tests. For example, the Advanced Glaucoma Intervention Study<sup>10</sup> reported that more than 30% of the fields classified as “progressed” at two follow-up examina-

tions later failed to maintain this classification. Separating true progression from changes in visual fields due to learning effects, fatigue, and the long-term fluctuation inherent in the test is extremely difficult.<sup>11,12</sup> Each visual field measurement is influenced by a variety of factors, including test-subject performance, fixation losses, pupil size, refractive correction, and changes in degree of lens opacity. These factors combine with underlying physiological changes in visual sensitivity to produce significant long-term fluctuation in visual field test results even for healthy eyes, and this long-term fluctuation is larger for eyes with visual field loss.<sup>11-15</sup> In addition, progression of visual field loss is very slow in treated glaucoma. Changes of less than 1 dB per year are difficult to detect even with a series of visual fields spanning 6 years.<sup>16</sup>

The statistical methods most commonly employed to identify visual field loss progression are the Humphrey Statpac II glaucoma change probability analysis and linear regression. Analyses by these methods have shown that variability in visual field measurements is greater for some field test locations than others and that change in variable locations must be of greater magnitude than change in stable locations to be called true progression.<sup>15,17</sup> Other commonly used analysis methods employ visual field defect scoring algorithms developed for specific clinical trials.

#### Linear Regression Over Time

Linear regression analysis requires at least 5 and preferably 7 or more visual fields to determine whether visual field loss has progressed relative to the baseline measurement.<sup>14,16,18</sup> Variables that have been evaluated for their sensitivity to progression in linear analyses include mean deviation, corrected pattern standard deviation, thresholds within glaucoma hemifield test zones, and thresholds from each of the 52 test locations. Comparing these parameters for 191 subjects over a mean follow-up period of 7.1 years, Smith and colleagues<sup>19</sup> concluded that progression rates of between 1 and 5 dB per year could be detected. While this method of detecting progression looks promising, at least 5 years of data are required in order to detect significant change in any of these field parameters via linear regression analysis.<sup>14,18</sup>

The commercially available Progressor program<sup>20</sup> uses all of an individual subject’s available visual field data in pointwise linear regression analysis for each test location from several visual fields against time of follow-up. The program produces a cumulative graphical output showing each test location as a bar graph, in which each bar represents one test. The length of the bar indicates the depth of the defect, and the color of the bar indicates the probability value of the regression slope relative to age-matched normal controls.<sup>21,22</sup> This technique is most

useful with a series of 7 visual fields.

#### *Event Analyses*

*Glaucoma Change Probability.* The glaucoma change probability analysis, included in Statpac II, looks for change by making a pointwise comparison of the standard visual field against the average of the first two reliable baseline visual fields. On the basis of the total deviation probability map, a change in sensitivity greater than the long-term fluctuation found in a reference population of stable glaucoma patients is required for deterioration to be detected at a given location.<sup>23</sup> Significant worsening of a test location is flagged with a black diamond and significant improvement with an open diamond. Because this analysis does not define cutoffs for visual field progression, the clinician must decide what number of changed points constitutes significant progression.

*Clinical Trials and Progression.* Because it often is necessary in clinical trials to determine whether progression is occurring before a series of 5 to 7 visual fields can be obtained, linear regression has not been the method of choice. Instead, the statistical methods provided by the Statpac II glaucoma change progression and global indices for identifying visual field loss progression relative to 2 baseline visual fields have been incorporated into the following large clinical trials: the Normal-Tension Glaucoma Study, the Early Manifest Glaucoma Trial, the Advanced Glaucoma Intervention Study, and the Collaborative Initial Glaucoma Treatment Study.

The Normal-Tension Glaucoma Study was designed to assess the effect of lowering intraocular pressure on the progression rate of normal-tension glaucoma. For subjects to be eligible for this study, their eyes had to show glaucomatous excavation of the optic disc and a field defect (measured by standard achromatic perimetry) consisting of a cluster of 3 nonedge points depressed by 5 dB, with 1 of the points also depressed by 10 dB. This defect had to be confirmed by two of three baseline visual field tests performed within a 4-week window. Progression was suspected if one of the following changes was observed: (1) at least 2 contiguous points within or adjacent to a baseline defect showed a reduction in sensitivity from baseline of  $\geq 10$  dB or three times the average baseline short-term fluctuation for that subject, whichever was greater, (2) the sensitivity of each suspected point was outside the range of values observed during baseline testing, or (3) a defect occurred in a previously normal part of the field. Confirmation of progression required agreement in the results of four tests.<sup>24</sup>

The Early Manifest Glaucoma Trial (EMGT) was designed to assess the effectiveness of reducing intraocular pressure in early, previously untreated open-angle glaucoma. Because visual field loss progression is used as

a study end point, a progression algorithm was developed.<sup>7</sup> The Statpac glaucoma change progression analysis was modified so that scoring is based on the pattern deviation probability map instead of the total deviation probability map. The change in pattern deviation is thought to provide a more accurate assessment of visual field loss progression because this plot is less influenced by shifts in the global hill of vision due to cataract, pupil size changes, or refractive errors.<sup>25</sup> Enrollment in EMGT required an initial screening, two preintervention visual field tests, and two baseline examinations. At both baseline examinations, the glaucoma hemifield test results had to be either (1) "outside normal limits" because of defects in the same sectors or (2) "borderline," with obvious localized change to the optic disc. Progression requires that 3 or more points be flagged by the pattern deviation version of the glaucoma change progression analysis and confirmed in 2 subsequent visual fields; the points need not be contiguous.

The Advanced Glaucoma Intervention Study (AGIS) was designed to compare two surgical management strategies for patients with advanced glaucoma inadequately controlled by medications alone. To determine eligibility and to evaluate disease progression in patients with relatively advanced glaucomatous visual fields, the AGIS investigators developed an algorithm for scoring the visual field test based on reliability and the severity of glaucomatous visual field defects. The scoring system was based on the following concepts: (1) multiple defects can occur in the upper, lower, and nasal hemifields; (2) a defect requires 2 or more adjacent defective points; (3) the severity of depression must be greater than changes due to variability; and (4) the defect must be caused by glaucoma. The score increases with increasing numbers of depressed locations and with increasing depth of the defects, ranging from 0 (no defect) to 20 (all sites deeply depressed).<sup>10</sup> (The scoring procedure is described in the "Methods" section.) Subject eligibility was determined by the results of two preintervention field tests conducted less than 60 days apart. Enrollment required an AGIS score between 1 and 16 and a reliability score of  $< 3$  for the first visual field test. The second test was used as the baseline for subsequent tests. Progression is quantified as a score increase from baseline by  $\geq 4$  points in three consecutive reliable visual field tests.<sup>26</sup>

The Collaborative Initial Glaucoma Treatment Study (CIGTS) was designed to determine whether patients with newly diagnosed open-angle glaucoma are managed better by initial treatment with medications or by immediate filtration surgery. A primary outcome measure is the visual field score, determined by a modification of the AGIS scoring method described above. The CIGTS scoring system is based on these principles: (1) the total devi-

ation probability plot adjusts the total deviation values at each point relative to the most normal region in the visual field; (2) each abnormal test location must be accompanied by at least 2 adjacent abnormal points; and (3) each abnormal point is given a score from 1 to 4 based on the probability values (5% to 0.5%) for the 3 contiguous depressed points. (The scoring procedure is described in the "Methods" section.) For CIGTS, two preintervention field tests were conducted to determine subject eligibility. Enrollment required reliability scores of  $<4$ , glaucoma hemifield test results "outside normal limits," and at least 3 contiguous points on the total deviation plot with  $P < .02$ ; if the points were in the nasal field, they could not cross the horizontal midline. The preintervention scores were averaged to create a baseline CIGTS score. If the baseline scores differed by  $>7$ , then a third field test was conducted and the three scores were used to compute a baseline CIGTS score. Progression is quantified as an increase in score from baseline reference by  $\geq 3$  points on three consecutive reliable visual field tests.<sup>27</sup>

#### *Comparison of the Analysis Methods*

Many specialists in glaucoma were involved in the development of the methods used in each of these studies. However, only a few studies have compared the various methods for identifying progression on the same series of visual fields.<sup>28-30</sup>

Comparing the AGIS, CIGTS, and EMGT methods, Katz and colleagues<sup>29</sup> evaluated the agreement among these methods and the judgment of two glaucoma specialists who graded the fields as "definite progression," "possible progression," "stable," "improved," or "too unreliable to assess." They found that the EMGT and CIGTS scoring methods and the glaucoma specialists identified similar incidences of progression, but not necessarily in the same eyes. Furthermore, the EMGT and CIGTS methods produced rates of apparent progression that were twice those obtained with the AGIS method. These results were corroborated by those of Lee and colleagues.<sup>30</sup> These studies indicate the difficulties resulting from the lack of a "gold standard" for progression of glaucoma independent of visual field test results. Until such a nonfield standard is established, only the agreement among different methods for grading progression can be determined and the sensitivity and specificity of the various techniques for determining progression will remain unknown.

### **DESCRIPTIONS AND MAJOR FINDINGS OF THE 1986-1987 ST LUCIA SURVEY**

#### *Introduction*

Although glaucoma appears to be more prevalent among blacks than whites, little information on the epidemiology

of glaucoma is available. Anecdotal reports of an unusually high prevalence of glaucoma in the relatively homogeneous black population of St Lucia, West Indies, made this an ideal site for an epidemiological study of glaucoma. A national survey of the prevalence of glaucoma in St Lucia, West Indies, was conducted in 1986-1987 by Howard University in collaboration with investigators from the Harvard Medical School.<sup>8</sup>

#### *Methods*

A cluster sampling design with systematic allocation of clusters was used to identify, from 1984 census data, a sample of 1,936 black subjects aged 30 years or older. The primary sampling units were electoral districts within St Lucia's 10 administrative areas, which were sampled with probability proportional to the size of the administrative area. A random starting point was chosen in each of the 42 districts (one per cluster), and consecutive households were listed until at least 50 subjects per cluster were recruited; all eligible individuals in a household were recruited.

All subjects underwent a screening examination, which included (1) a visual acuity test with a Snellen chart at 20 feet or a pinhole if visual acuity was 20/40 or less, (2) three measurements of intraocular pressure with a portable Perkins applanation tonometer, and (3) direct ophthalmoscopy, with clinical assessment of the horizontal and vertical cup-to-disc ratios. Height, weight, blood pressure, and pulse were measured and a risk-factor interview was completed. Screening for visual field loss by automated threshold perimetry with the Humphrey Field Analyzer full-field 120 test was attempted for every third subject and for every subject with any of the following conditions: intraocular pressure  $\geq 21$  mm Hg, cup-to-disc ratio  $\geq 0.7$ , or cup-to-disc asymmetry  $\geq 0.2$ . Some subjects could not be tested because they could not understand or comply with the testing procedure.

All subjects with elevated intraocular pressure, an abnormal cup-to-disc ratio, or 17 or more visual field defects were referred for a comprehensive glaucoma evaluation, including a slit-lamp examination, gonioscopy, and dilated direct and indirect ophthalmoscopy performed by a glaucoma subspecialist, as well as threshold visual field measurement with the Humphrey Field Analyzer (central 30-2 test). Glaucomatous visual field loss was detected by the mirror-image method.<sup>31</sup>

The primary definition of glaucoma conservatively included only visual fields with fixation loss of less than 20% and false-positive and false-negative error rates of less than 33%. All abnormal threshold visual fields were independently evaluated by two glaucoma subspecialists to confirm typical glaucomatous visual field loss. By the primary definition, cases were excluded if glaucomatous

etiology of the fields was considered questionable, regardless of the results obtained with the mirror-image method. Some referred subjects did not undergo threshold testing; these cases also were excluded by the primary definition. A more comprehensive secondary definition of glaucoma included (1) cases with unreliable visual field test results that met all other visual field criteria and (2) cases of referred subjects who did not undergo threshold visual field testing but whose examination results could not be explained by anisometropia or other ocular disease.

### *Results and Conclusions*

Publicity for the survey by the Ministry of Health and aggressive follow-up by the survey team resulted in screening of 1,679 subjects, for a participation rate of 87% (77% for men and 92% for women). Of those screened, 520 subjects were referred for a definitive examination: 306 with elevated intraocular pressure, 207 with abnormal cup-to-disc ratios, and 252 with abnormal screening visual fields. Of the 520 subjects referred, 364 (70%) underwent threshold visual field testing; visual fields were obtained for a total of 699 eyes. By the primary definition of glaucoma, 147 subjects (31% of those referred; 45 men and 102 women) were diagnosed as having glaucoma, for a prevalence of 8.8%. The remainder (217) either were diagnosed as having glaucoma by a more liberal secondary definition or were considered glaucoma suspects.

This study differed from previous glaucoma prevalence surveys in that it was based on a representative national sample and used stringent visual field criteria to diagnose glaucoma. It found much higher prevalence than had been reported in many previous surveys, leading the authors to conclude that glaucoma was a major problem in this population.

### **DESCRIPTION AND FINDINGS OF THE 1996 FEASIBILITY STUDY**

A trip to St Lucia was undertaken in December 1996 to determine the feasibility of a follow-up study of glaucoma patients and suspects identified in the 1986-1987 survey. Meetings were held with officials in the Ministry of Health and with nurses who had been trained as glaucoma diagnosticians for the initial survey. To test the feasibility of locating survey subjects and their medical records, three clusters from the 1986-1987 survey were chosen randomly, providing a sample of 37 subjects. A visit was made to each cluster to locate subjects, and medical records for the surviving subjects were sought in the Victoria Hospital medical records department.

The Ministry of Health officials and nurses expressed strong interest in and support of the proposed follow-up study. They also expressed interest in refresher training in glaucoma identification, diagnosis, and treatment.

Of the 37 subjects, 21 were interviewed, 8 had died, 3 were not home at the time of the visit, and 4 had moved to other clusters; the whereabouts of the remaining subject were unknown. Medical records were retrieved for the 28 living subjects who were located. It took 5 hours to find the 28 records. Each record provided the subject's name and address, the date of the last visit to the clinic, a summary of the ophthalmic examination, and the diagnosis and treatment plan. Thus, it was estimated that about 75% of the subjects in the 1986-1987 survey could be located to participate in the follow-up study, and that it might take about 2 weeks to retrieve their medical records. It was concluded that the follow-up study was feasible.

## **METHODS**

---

### **LOCATION AND EXAMINATION OF SUBJECTS**

The survey was approved by the responsible Institutional Review Board, and all subjects signed an informed consent form before participating in any part of the study.

Before the survey team arrived in St Lucia, the Ministry of Health generated national attention for the study through personal contacts, radio announcements, local newspapers, and other print media. Nurses and other contracted health care providers made multiple attempts to contact each of the 364 subjects identified in the 1986-1987 survey as having glaucoma or as being glaucoma suspects, and they filled out a "Record of Contacts" form (Appendix 1). Reports that subjects were deceased were verified through the national death registry. Subjects who were located were asked to report to a specific location for an eye examination and administration of a questionnaire.

The survey team consisted of an ophthalmologist and two nurses. One nurse measured visual acuity and administered the questionnaire, and the other administered the visual field tests.

The examination consisted of the following assessments: (1) measurement of visual acuity without correction, with correction (if available), and with pinhole, (2) refraction if visual acuity was less than 20/40, (3) threshold visual field measurement with the Humphrey Field Analyzer model 610 (Zeiss Humphrey Systems, Dublin, California) central 30-2 test and stimulus III, with near correction as appropriate, (4) slit-lamp biomicroscopy, (5) measurement of intraocular pressure with a portable applanation tonometer, (6) gonioscopy with a Zeiss-type lens, (7) optic nerve assessment by direct ophthalmoscopy and/or with a 90-diopter lens through dilated pupils, and (8) retina assessment by indirect ophthalmoscopy through dilated pupils. All examination findings were recorded on a standardized form (Appendix 2). If the best corrected visual acuity was less than 20/30, the ophthalmologist indi-

cated the most likely primary and secondary causes for the decreased vision.

Subjects who were not physically able to visit the examination site were examined in their homes. The modified examination consisted of measurement of visual acuity with and without correction and with pinhole, a penlight examination with loupes, intraocular pressure measurement with a portable applanation tonometer, and dilated funduscopic assessment.

All subjects completed the questionnaire (Appendix 3), which consisted of questions relating to demographic information, ocular and general medical history, eye care and general health services, medication use, and tobacco and alcohol use. To assess health-related quality of life, the National Eye Institute Visual Functioning Questionnaire 25, modified to be culturally appropriate to St Lucia, was administered. (The data unrelated to visual field loss progression, such as data on medical resource use and health-related quality of life, are not presented here but will be the subject of future analyses.)

Glaucoma progression typically is documented as changes in the optic nerve and/or progression of visual field defects. In the absence of photographic documentation, optic nerve assessment suffers from subjectivity and lack of reproducibility.<sup>32</sup> Therefore, visual field loss progression was used as a proxy for glaucoma progression.

#### SELECTION OF THE SAMPLE

Of the 364 potential subjects from 1987, 90 had died, 11 refused to participate, 21 were known to have moved from St Lucia, and 37 could not be located. Thus, data were obtained for both eyes of 205 subjects (56% of the 364 potential subjects). Among the living subjects the team was able to locate in St Lucia, the participation rate was 95%.

For each eye, 2 visual fields obtained 10 years apart were available for review. Visual fields were evaluated for reliability and excluded by the following criteria: (1) either the false-positive or the false-negative rate was 40% or greater, (2) both the false-positive and the false negative rate was 33% or greater, or (3) fixation loss was 33% or greater. Additionally, visual fields with obvious nonglaucomatous scotoma, such as near-correction lens rim artifact, were excluded.

Any eye with an improvement of vision by halving of the visual angle or deterioration of vision by doubling of the visual angle was individually considered for exclusion. An eye was excluded if it showed (1) an improvement of visual field attributable to improvement in vision or (2) a decrease in vision attributable to a cause other than glaucoma, as noted by the examining ophthalmologist. Eyes for which a Snellen acuity measurement was not available (ie, with acuity <20/400) were included in the sample but

excluded from the visual acuity analysis.

If a subject had not undergone visual field testing because of blindness, the cause was determined; if it was glaucoma, the eye was included and given the highest-severity visual field score (20) for purposes of analysis. Eyes that in 1987 had experienced end-stage glaucoma, defined as an AGIS visual field score of 17 to 20, were excluded.

A few subjects had had glaucoma surgery, and a few were receiving glaucoma medication; their eyes were excluded. Some subjects reported past use of medications. If the subjects had used medications only while they were available at no cost and had not used medications since the subsidized eye-care program ended in 1988, their eyes were included. Otherwise, the eyes of subjects who reported past use of glaucoma medications were excluded.

#### VISUAL FIELD GRADING

Visual fields were graded by methods used in two multicenter clinical trials sponsored by the National Eye Institute: the Advanced Glaucoma Intervention Study<sup>33</sup> and the Collaborative Initial Glaucoma Treatment Study.<sup>34</sup> These studies were designed to assess glaucoma at different stages of the disease.

##### *The Advanced Glaucoma Intervention Study*

An outcome measure in this trial is a score based on the 52 test locations from the Humphrey 24-2 standard full threshold visual field test (excluding the two locations nearest the blind spot). As discussed above, the AGIS algorithm for scoring visual field defects is based on reliability, the number of adjacent test locations with depressed sensitivity, and the depth of the depression (relative to normal, based on the total deviation plot of the Statpac II single-field analysis), and the region of the field affected.<sup>10</sup> The scoring procedure is described in Table I. For AGIS, progression of visual field loss is defined by worsening of the score from the baseline value by 4 points or more in three consecutive 6-month follow-up tests.<sup>26</sup>

##### *The Collaborative Initial Glaucoma Treatment Study*

The overall visual field defect score is generated from the total deviation probability plot values (rather than their corresponding decibel cut offs, used by AGIS). Any of the 52 locations on this plot (excluding the two blind spot locations) for which the probability value is  $\leq 0.05$  and which is accompanied by at least 2 adjacent abnormal points is considered defective and is scored. The score for each location is weighted by the depth of its defect and the depths of the defects of the two most defective neighboring locations (for which  $P \leq 0.05$ ).<sup>35</sup> The scoring procedure is described in Table II.

For CIGTS, progression of visual field loss is defined

TABLE I: STEPS IN SCORING VISUAL FIELD DEFECT IN AGIS

STEP AND CRITERION	SCORE
1. Score the nasal area (step or defect):	Max = 2
≥1 depressed location in nasal area and only in 1 hemifield	
or	
3 clustered depressed locations of 6 possible nasal sites	1
4 to 6 clustered locations depressed ≥12 dB	1
2. Score each hemifield (defect):	Max = 9
≥1 cluster of 2 locations with 1 depressed by ≥12 dB	1
≥1 cluster of 3 to 5 depressed locations	1
≥1 cluster of 6 to 12 depressed locations	2
≥1 cluster of 13 to 20 depressed locations	3
≥1 cluster of >20 depressed locations	4
If 50% of depressed hemifield locations are depressed by	
≥12 dB	+1
≥16 dB	+2
≥20 dB	+3
≥24 dB	+4
≥28 dB	+5
3. Sum the scores for each hemifield and for the nasal area	Max = 20

AGIS, Advanced Glaucoma Intervention Study.

TABLE II: STEPS IN SCORING VISUAL FIELD DEFECT IN CIGTS

1. Score each of the 52 test locations:		
Cluster probability	Neighboring locations	Score
≥.10		0
≤.05	0 or 1 at ≤.05	0
≤.05	2 to 8 at ≤.05	1
≤.02	2 to 8 at ≤.02	2
≤.01	2 to 8 at ≤.01	3
≤.005	2 to 8 at ≤.005	4
2. Add the scores for all 52 test locations		Max= 208
3. Divide by 10.4		Max= 20

CIGTS, Collaborative Initial Glaucoma Treatment Study.

by worsening of the score from the baseline value by ≥3 points in three consecutive separate tests.

The threshold level in decibels for each test location of the Humphrey 30-2 standard full threshold program was available for each visual field. However, many of the 1987 visual fields did not have the Statpac II indices necessary for calculation of AGIS and CIGTS scores. Conversion of the threshold decibel data into the requisite Statpac indices required the normative database from which the Statpac program was generated, and this information has not been made available by the manufacturer. The normative database developed by Drs Pamela Sample and Chris Johnson for the short-wavelength automated perimetry ancillary arm of the Ocular Hypertension Treatment Study was used instead. This normative database consists of data for one eye from each of the same 348 normal subjects between the ages of 20

and 85 tested with both standard automated perimetry (SAP) and short-wavelength automated perimetry. The normative data were collected at five centers by means of a standardized test protocol. To be included in the normative database, subjects had to have a normal eye examination, 20/30 or better visual acuity, normal color vision, no history of ocular or neurologic disease or surgery, refractive errors of less than 5 diopters spherical equivalent and 3 diopters cylinder, no diabetes mellitus, and normal optic nerve appearance, and subjects could not be taking any medications known to affect visual fields or color vision (Pamela Sample, PhD, electronic mail communication).

A Statpac-like SAP analysis package using these normative data was developed by Sample and Johnson. After age-correction for each of the 52 test locations of the Humphrey standard full-threshold 24-2 test (excluding

the two blind spot locations), the total deviation plot, the pattern deviation plot, and their associated probability cut offs and probability plots were computed. The package then computes cut off values at specific probabilities for global indices, mean deviation, and pattern standard deviation, along with an asymmetry analysis patterned after the glaucoma hemifield test analysis.<sup>36</sup> The values obtained are practically identical to values obtained from the Statpac II program (Chris Johnson, PhD, oral communication). All the visual field raw threshold values from the St Lucia study were run through the SAP analysis package to generate the information needed to perform the AGIS and CIGTS analyses for visual field loss progression.

#### ANALYTICAL METHODS

The subjects' demographic information, examination results, and questionnaire data were recorded by pencil on standardized forms and later entered into Corel Paradox database files. Snellen visual acuity measurements were converted to decimal values by division of the numerator by the denominator (eg, 20/20 = 1.0, 20/25 = 0.8, 20/30 = 0.67). Visual acuities worse than 20/400 were not given decimal values. The electronic data files were cross-checked with the raw data. Data that were considered out of range were eliminated.

The data then were transferred to a SAS 8.2 (SAS Institute, Cary, North Carolina) file for analysis. Multivariate linear regression was used to investigate the association between predictor variables and visual field loss progression based on AGIS and CIGTS scores. Logistic regression also was performed, with progression versus no progression treated as a categorical response variable. The assumptions of linear and logistic regression analysis were verified. Cross-tabulations were made between the various predictor variables and severity of visual field loss progression, and chi-square tests were used to test for associations.

#### RESULTS

##### SAMPLE SELECTION, DEMOGRAPHICS, AND EXAMINATION RESULTS

Of the 410 eyes for which data were obtained, 59 right eyes and 64 left eyes were excluded. The reasons for exclusion were as follows:

- No 1987 visual field, 4 right eyes, 6 left eyes
- No 1997 visual field because of inadequate vision due to a cause other than glaucoma, 1 right eye
- Unreliable visual field for 1987 or 1997, 20 right eyes, 21 left eyes
- Substantially improved visual field due to better vision from cataract surgery, 3 right and 3 left eyes

- Substantial worsening of vision due to a cause other than glaucoma, 11 right and 11 left eyes
- Past or present glaucoma treatment, 26 right and 26 left eyes

Some eyes satisfied more than one of the above exclusion criteria. An additional five right eyes and nine left eyes were excluded because their 1987 visual fields satisfied the AGIS criterion for end-stage glaucoma (visual field score  $\geq 17$ ). Though CIGTS score was not used as an exclusion criterion, the CIGTS scores for these eyes all were  $\geq 17$ . The final sample consisted of 146 right and 141 left eyes of 155 subjects.

The 155 subjects included 47 men and 108 women. The age distribution at baseline was as follows: 21 to 30 years, 2 patients; 31 to 40 years, 21 patients; 41 to 50 years, 57 patients; 51 to 60 years, 32 patients; 61 to 70 years, 31 patients; 71 to 80 years, 11 patients; older than 80, 1 patient.

The mean age was 52.3 years (range, 26-85 years). (Although the 1986-1987 survey was not intended to include subjects under the age of 30 years, two such subjects were found and have been included in this sample for consistency with the earlier study.) The mean intraocular pressures from the 1997 examination were 21.0 mm Hg (SD, 4.3; range, 10-39) for the right eye and 21.0 mm Hg (SD, 4.2; range, 12-43) for the left eye. Of the 155 subjects, 81 (52%) had definite visual field defects at the initial survey and had been diagnosed as having glaucoma, and 74 (48%) had either normal or inconclusive visual field test results and had been diagnosed as glaucoma suspects.

Among the eyes for which acuity measurements were available for both 1987 and 1997, vision deteriorated only minimally. The mean changes in visual acuity were -0.07 for the right eye and -0.10 for the left eye. For the subset of these eyes with visual field loss progression, the mean change in acuity was still only -0.06 for the right eye and -0.13 for the left eye. Table III summarizes the Snellen visual acuity measurements.

##### PROGRESSION OF VISUAL FIELD LOSS BY AGIS CRITERIA

AGIS visual field defect scores are summarized in Table IV. The 1987 mean scores were 3.5 for right eyes and 3.9 for left eyes, and the 1997 mean scores were 9.1 for right eyes and 9.0 for left eyes. By the AGIS criterion for definite change (score change of  $\geq 4$ ), 80 right eyes and 73 left eyes worsened, 5 right eyes and 8 left eyes improved, and 61 right eyes and 60 left eyes were unchanged. Among the eyes in which visual field loss had progressed by AGIS criteria, the 1987 mean scores were 3.3 for right eyes and 4.5 for left eyes, and the 1997 mean scores were 13.5 for right eyes and 13.1 for left eyes. The severity of progression was distributed as follows: mild progression (AGIS score

TABLE III: MEAN VISUAL ACUITY AND CHANGE IN ACUITY FROM 1987 TO 1997\*

	EYE	N	ALL EYES		EYES PROGRESSED BY AGIS CRITERIA†		
			MEAN	SD	N	MEAN	SD
1987	R	130	0.74	0.27	67	0.68	0.27
	L	124	0.76	0.26	60	0.73	0.24
1997	R	130	0.66	0.25	67	0.62	0.27
	L	124	0.66	0.26	60	0.60	0.27
Change	R	130	-0.07	-	67	-0.06	-
	L	124	-0.10	-	60	-0.13	-

\*Visual acuity is numerator divided by denominator of Snellen acuity measurement. Only eyes with Snellen acuity measurements for both 1987 and 1997 were included.

†Progression means that AGIS visual field defect score increased by  $\geq 4$ .

TABLE IV: MEAN AGIS VISUAL FIELD DEFECT SCORE AND CHANGE FROM 1987 TO 1997

	EYE	N	ALL EYES		EYES PROGRESSED BY AGIS CRITERIA*		
			MEAN	SD	N	MEAN	SD
1987	R	146	3.5	3.7	80	3.3	3.3
	L	141	3.9	4.1	73	4.5	4.4
1997	R	146	9.1	6.9	80	13.5	5.4
	L	141	9.0	6.8	73	13.1	5.5
Change	R	146	5.6	-	80	10.2	-
	L	141	5.1	-	73	8.6	-

\*Progression means that AGIS visual field defect score increased by  $\geq 4$ .

increase of 4-7), 26 right eyes (N = 80), 27 left eyes (N = 73); moderate progression (score increase of 8-11), 24 right eyes, 19 left eyes; extensive progression (score increase of 12-15), 16 right and 16 left eyes; severe progression (score increase of  $\geq 16$ ), 14 right and 11 left eyes.

In the AGIS scoring system, end-stage glaucoma is defined by a score  $\geq 18$ . Of the 80 right eyes that showed progression, 24 (30%) had progressed to end-stage glaucoma; for the 73 left eyes, the figure was 21 (29%). In 14 subjects, visual field loss had progressed to end-stage disease in both eyes. Of the eyes that had progressed to end-stage glaucoma, 14 of 24 right eyes (58%) and 13 of 21 left eyes (62%) had baseline AGIS scores of 0 to 5 (no to minimal visual field loss).

The following factors were investigated for possible association with progression of visual field loss: sex, age, intraocular pressure (1997), and baseline AGIS visual field defect score. For multiple linear regression, progression score (change in visual field score from 1987 to 1997), age, and intraocular pressure were continuous variables and sex was categorical. In this analysis, progression was not significantly associated with intraocular pressure ( $P = .91$ , right;  $P = .63$ , left) or with sex ( $P = .20$ , right;  $P = .33$ ,

left), but showed a significant positive association with age ( $P < .001$ , right;  $P = .002$ , left). The linear regression models for the right and left eyes were as follows, where  $y$  = progression severity and  $x$  = age:

Right:  $y = -6.24 + 0.21885x$ ;  
 $r^2 = 0.20$ ;  
 slope 95% CI = 0.14 to 0.29

Left:  $y = -3.9 + 0.1727x$ ;  
 $r^2 = 0.13$ ;  
 slope 95% CI = 0.09 to 0.25

Visual field loss in an eye with a high baseline score cannot progress but to a certain extent (eg, an eye with a baseline visual field score of 0 could receive a progression score of 20, whereas for an eye with a baseline score of 15, the maximum progression score would be 5). Therefore, a logistic regression was performed in which the baseline visual field score was treated as a continuous variable and the response variable was dichotomous (progression, defined as an AGIS score increase of  $\geq 4$ , versus no progression). Again, progression was significantly associated only with age ( $P = .001$ , right;  $P = .003$ , left). Progression was not significantly associated with intraocular pressure ( $P$

= .99, right;  $P = .84$ , left), sex ( $P = .14$ , right;  $P = .42$ , left), or baseline visual field score ( $P = .08$ , right;  $P = .21$ , left). The probability of progression,  $p$ , was modeled as follows, where  $x_1 =$  age and  $x_2 =$  baseline AGIS visual field score:

Right:  $\log[p/(1-p)] = -2.3204 + 0.0545x_1 - 0.0902x_2$

Left:  $\log[p/(1-p)] = -2.2454 + 0.0445x_1$

These relationships also were tested separately, with age, intraocular pressure, and baseline visual field status treated as categorical variables in chi-square tests of association with progression severity, summarized in Tables V through VII. In the analysis of baseline visual field score, the response variable was dichotomous (progression versus no progression). Again, the only significant association was between progression and age, for right eyes only ( $P = .01$ ; for left eyes,  $P = .13$ ).

**PROGRESSION OF VISUAL FIELD LOSS BY CIGTS CRITERIA**

The analyses described above also were performed with the CIGTS scores, which are summarized in Table VIII. The mean 1987 CIGTS scores were 5.6 for right eyes and 5.9 for left eyes, and the mean 1997 scores were 12.9 for right eyes and 13.6 for left eyes. By the CIGTS criterion for definite change (score change of  $\geq 3$ ), 107 right eyes and 101 left eyes worsened, 14 right eyes and 13 left eyes improved, and 25 right eyes and 27 left eyes were unchanged. Among the eyes in which visual field loss had progressed by CIGTS criteria, the 1987 mean scores were 4.6 for both right and left eyes, and the 1997 mean scores were 15.7 for right eyes and 16.2 for left eyes. The severity of progression was distributed as follows: mild progression (CIGTS score increase of 3-7), 32 right eyes ( $N = 107$ ), 28 left eyes ( $N = 101$ ); moderate progression (score increase of 8-11), 27 right eyes, 20 left eyes; extensive progression (score increase of 12-15), 17 right eyes, 24 left eyes; severe progression (score increase of  $\geq 16$ ), 31 right eyes, 29 left eyes.

The CIGTS system does not define end-stage glaucoma, but by the AGIS definition (score  $\geq 18$ ), many eyes had reached end-stage disease. Of the 107 right eyes that showed visual field loss progression, 53 (50%) had progressed to end-stage glaucoma; of the 101 left eyes, 54 (53%) had reached end-stage. In 39 subjects, visual field loss had progressed to end-stage disease in both eyes. Of the eyes that had progressed to end-stage glaucoma, 24 of 53 right eyes (45%) and 27 of 54 left eyes (50%) had baseline CIGTS scores of 0 to 5.

In the linear regression analysis, progression of visual field loss was not significantly associated with intraocular pressure ( $P = .76$ , right;  $P = .92$ , left), sex ( $P = .67$ , right;  $P = .72$ , left), or age ( $P = .14$ , right;  $P = .19$ , left). In the logistic regression analysis, the likelihood of progression

was not significantly associated with intraocular pressure ( $P = .44$ , right;  $P = .64$ , left) or sex ( $P = .65$ , right;  $P = .81$ , left), but it was significantly associated with age ( $P = .001$ , right;  $P = .008$ , left) and baseline visual field score ( $P < .001$  for both eyes); visual fields less severely affected at baseline were more likely to have progressed. The probability of progression,  $p$ , was modeled as follows, where  $x_1 =$  age and  $x_2 =$  baseline CIGTS visual field score:

Right:  $\log[p/(1-p)] = -1.1479 + 0.0588 x_1 - 0.1348 x_2$

Left:  $\log[p/(1-p)] = -0.5173 + 0.0475 x_1 - 0.1507 x_2$

The association between progression and baseline visual field status also was tested in a chi-square test, with baseline field status as a categorical variable, as shown in Table IX. In this analysis, progression was significantly associated with baseline CIGTS score ( $P < .001$  for both eyes).

**COMPARISON OF PROGRESSION BY AGIS AND CIGTS CRITERIA**

As described above, the results obtained with the AGIS and CIGTS algorithms differed. Many more eyes progressed by CIGTS than by AGIS criteria. Identification of eyes as having progressed in visual field loss by the two scoring systems differed as follows: AGIS total, 80 right eyes and 73 left eyes progressed; CIGTS total, 107 right eyes and 101 left eyes progressed; both AGIS and CIGTS, 71 right eyes and 65 left eyes progressed; AGIS only, 9 right eyes and 8 left eyes progressed; CIGTS only, 36 right eyes and 36 left eyes progressed.

The Pearson product-moment correlation coefficients for progression by the AGIS and CIGTS criteria were 0.49 for right eyes and 0.59 for left eyes ( $P < .001$  for both eyes).

**PROGRESSION BY OTHER STATPAC INDICES**

As discussed above, inadequate vision prevented some subjects from undergoing visual field testing in 1997. Because 1997 values for mean defect and corrected pattern standard deviation (CPSD) were not available for these subjects, their eyes were excluded from these analyses.

Table X summarizes the mean defect and CPSD measurements. In 1987, the mean scores for mean defect and corrected pattern standard deviation were -5.8 and 5.1, respectively, for right eyes and -6.8 and 5.9 for left eyes. In 1997, the mean scores for mean defect and CPSD were -10.3 and 7.0 for right eyes and -10.9 and 7.8 for left eyes. Among the subset of eyes that progressed by the AGIS criterion, the 1987 mean scores for mean deviation and CPSD were -6.2 and 5.4 for right eyes and -7.2 and 6.3 for left eyes. The 1997 mean scores for progressed eyes were -14.5 and 8.5 for right eyes and -16.3 and 8.7 for left eyes.

TABLE V: ASSOCIATION OF VISUAL FIELD LOSS PROGRESSION WITH INTRAOCULAR PRESSURE

INTRAOCULAR PRESSURE (MM HG)	VISUAL FIELD PROGRESSION SEVERITY*				
	<4	4-7	8-11	12-15	≥16
			Right Eyes (N); P = .55		
≤21	48	21	18	8	10
22-28	14	3	3	5	3
≥29	4	2	3	3	1
			Left Eyes (N); P = .98		
≤21	52	17	14	11	8
22-28	11	7	3	3	2
≥29	5	3	2	2	1

\*Progression severity = increase in AGIS visual field defect score.

TABLE VI: ASSOCIATION OF VISUAL FIELD LOSS PROGRESSION WITH AGE

AGE (YR)	VISUAL FIELD PROGRESSION SEVERITY*				
	<4	4-7	8-11	12-15	≥16
			Right Eyes (N); P = .01		
21-30	0	1	0	0	1
31-40	9	6	3	0	1
41-50	34	6	7	4	4
51-60	13	6	6	5	0
61-70	9	6	5	4	5
71-80	1	1	3	2	3
>80	0	0	0	1	0
			Left Eyes (N); P = .15		
21-30	0	0	0	0	0
31-40	14	4	0	2	1
41-50	29	8	9	3	4
51-60	13	7	5	2	1
61-70	9	7	3	5	4
71-80	3	1	2	3	1
>80	0	0	0	1	0

\*Progression severity = AGIS visual field defect score increased by ≥4.

TABLE VII: ASSOCIATION OF VISUAL FIELD LOSS PROGRESSION WITH BASELINE AGIS SCORE\*

BASELINE SCORE	RIGHT EYES (N)		LEFT EYES (N)	
	NO	YES	NO	YES
0 (none)	16	16	16	21
1-5 (mild)	32	47	31	31
6-11 (moderate)	13	16	15	17
12-17 (severe)	5	1	6	4
		P = .21		P = .80

\*Progression = AGIS visual field defect score increased by ≥4.

## DISCUSSION

### LIMITATIONS AND ADVANTAGES OF THIS STUDY FOR IDENTIFYING VISUAL FIELD LOSS PROGRESSION

In the present study, only 1 baseline visual field and 1 follow-up field, taken 10 years apart, were available for each eye. None of the current algorithms or protocols for

assessing progression of visual field loss allows for evaluation with only 2 visual fields; they are considered to require a series of 5 to 7 visual fields. However, the value of a sample of this size with 10 years of untreated glaucoma outweighs the disadvantage of having only 2 fields for comparison.

Normally, at least 2 baseline visual fields are required

TABLE VIII: MEAN CIGTS VISUAL FIELD DEFECT SCORE AND CHANGE FROM 1987 TO 1997

	EYE	N	ALL EYES		EYES PROGRESSED BY CIGTS CRITERIA*		
			MEAN	SD	N	MEAN	SD
1987	R	146	5.6	5.8	107	4.6	4.7
	L	141	5.9	5.3	101	4.6	4.7
1997	R	146	12.9	7.1	107	15.7	4.8
	L	141	13.6	6.8	101	16.2	4.3
Change	R	146	7.3	--	107	11.1	-
	L	141	7.7	--	101	11.6	-

\*Progression = CIGTS visual field defect score increased by  $\geq 3$ .

TABLE IX: ASSOCIATION OF VISUAL FIELD LOSS PROGRESSION WITH BASELINE CIGTS SCORE\*

BASELINE SCORE	RIGHT EYES (N)		LEFT EYES (N)	
	NO	YES	NO	YES
0 (none)	7	30	4	21
1-5 (mild)	13	38	13	45
6-11 (moderate)	5	26	7	25
12-17 (severe)	14	13	16	10
	$P < .001$		$P < .001$	

\*Progression = CIGTS visual field defect score increased by  $\geq 3$ .

TABLE X: : MEAN SCORES FOR MEAN DEFECT AND CORRECTED PATTERN STANDARD DEVIATION AND CHANGE FROM 1987 TO 1997

	EYE	N	ALL EYES		EYES PROGRESSED BY AGIS CRITERIA*		
			MEAN	SD	N	MEAN	SD
Mean Defect							
1987	R	121	-5.8	4.9	63	-6.2	4.8
	L	118	-6.8	7.5	58	-7.2	9.1
1997	R	121	-10.3	8.7	63	-14.5	8.7
	L	118	-10.9	8.5	58	-16.3	7.0
Change	R	121	-4.4	-	63	-8.3	-
	L	118	-4.3	-	58	-9.0	-
Corrected Pattern Standard Deviation							
1987	R	121	5.1	2.8	63	5.4	3.0
	L	118	5.9	5.6	58	6.3	7.4
1997	R	121	7.0	3.5	63	8.5	3.1
	L	118	7.8	8.2	58	8.7	3.0
Change	R	121	1.9	-	63	3.0	-
	L	118	1.9	-	58	2.4	-

\*Progression = AGIS visual field defect score increased by  $\geq 4$ .

for comparison with subsequent fields. Ideally, these would be obtained after training of subjects inexperienced with visual field testing. This approach reduces the effects of learning and verifies the baseline defect. It has been shown that in standard full threshold visual field tests, thresholds usually improve until the third test.<sup>4</sup> It can be assumed that most participants in the present study had never had a visual field test before the 1986-1987 survey.

In that study, they had only one screening visual field test before undergoing the visual field test that provided the baseline scores for the current study. Thus, their initial results likely were poorer than they would have been after training. On the other hand, none of the subjects had had a visual field test during the 10 years between the two studies. Therefore, it can be assumed that even on retesting, the subjects were inexperienced with visual field test-

ing. Thus, the effect of learning probably was negligible.

Another consideration is the lack of additional fields to confirm visual field loss progression. For a definitive determination of progression, many clinical trials require that 3 successive fields show a definite change from baseline. To facilitate confirmation, these trials schedule testing at 6-month intervals. In the present study, the lack of repeated evaluation for a given individual remains a limitation; however, for group statistics it might be less problematic, for several reasons. The 10-year interval in this study greatly exceeds the minimum of 5 years needed to show progression of visual field loss with serial fields.<sup>13</sup> Furthermore, the same scoring algorithms were used in both studies, as well as the same standards for inclusion and exclusion of eyes. This consistency was possible because the work of Drs Sample and Johnson enabled the use of the AGIS and CIGTS algorithms to score the baseline visual field tests.

Because eyes with improvement in vision by halving of the visual angle were excluded from this study, and because damage from chronic glaucoma is not reversible, no visual field theoretically should have improved over the 10-year period. However, in practice, intertest fluctuations not infrequently result in a better second visual field. By the AGIS criteria, the visual fields of 5 right eyes (3.4%) and 8 left eyes (5.7%) improved in this study. By the CIGTS criteria, the corresponding numbers were 14 right eyes (9.6%) and 13 left eyes (9.2%). AGIS found apparent improvement of the visual field (score decreased by  $\geq 4$  points) in 11% of eyes and deterioration (score increased by  $\geq 4$  points) in 5% of eyes retested within 6 weeks.<sup>10</sup> In a study comparing the two scoring systems, Katz and associates<sup>25</sup> found improved AGIS scores (by  $\geq 4$  points) in 11.9% of eyes and improved CIGTS scores (by  $\geq 3$  points) in 20.9% of eyes when the second visual field was obtained a year after the baseline field. In the present study, the proportion of eyes that improved (4.5%) is much lower. Although the study by Katz and associates attempted to minimize the possible effect of learning, such an effect on retesting would be greater after a year than after 10 years. Furthermore, the effect of age on visual fields is biased toward worsening rather than improvement, and the subjects in the present study were 10 years older when their second visual fields were obtained.

Although the effect of long-term fluctuation could not be measured directly, the fact that some visual fields improved implies that the visual field scores for some eyes worsened as a result of long-term fluctuation, rather than true worsening due to glaucoma. Variability alone should produce some fields showing poorer sensitivity relative to baseline and a comparable number of fields showing improved sensitivity relative to baseline. Thus, it is likely

that similar percentages of eyes worsened and improved due to long-term fluctuation. Relatively few eyes showed visual field improvement, which suggests that the effect of fluctuation on the results of this study probably was minor.

In this study, the criteria for exclusion based on the reliability measures of fixation loss ( $\geq 33\%$ ) and false-positive and false-negative error rates ( $\geq 40\%$ ) were slightly less conservative than the manufacturer's suggested reliability criteria (fixation loss  $\geq 20\%$  and false-positive or false-negative error rate  $\geq 33\%$ ).<sup>37,38</sup> Because most of the subjects were inexperienced with visual field testing, many more eyes would have been excluded had the manufacturer's criteria been used. It can be argued that the manufacturer's criteria may not be optimal, particularly for fixation loss; for example, Bickler-Bluth and colleagues<sup>39</sup> suggested that the fixation loss criterion for unreliability be increased to  $\geq 33\%$ . One strength of the present study was the large number of untreated subjects for whom visual field data were available. These data are unique; for this reason, the importance of visual field reliability was balanced against the importance of using as many of these data as possible.

A potential problem for determination of visual field loss progression with fields obtained 10 years apart is that vision typically deteriorates with time, usually because of cataracts, and decreased vision may in turn affect the visual field. This study excluded eyes with a decrease in vision by doubling of the visual angle not attributable to glaucoma. Eyes that had progressed to end-stage glaucoma for which a Snellen acuity measurement could not be obtained were not included in the visual acuity analysis. Had they been included, deterioration of vision over the 10-year period would have been more pronounced than what is shown in Table III. Nonetheless, the vast majority of the eyes upon which the visual field loss progression analysis was based had Snellen acuity measurements at both examination times, and the change in vision was minimal. Decreased vision thus does not appear to have appreciably affected the visual field loss progression data obtained in this study.

#### **VISUAL FIELD LOSS PROGRESSION IN TREATED GLAUCOMA**

A number of studies have estimated progression of visual field loss from glaucoma.<sup>2,4,5,14,16,19,40</sup> In all of these studies, most, if not all, of the patients were receiving medical treatment or had undergone surgery for glaucoma. In these studies, the design, the perimeters used, the method of assessing progression, and the length of follow-up varied greatly; therefore, these results must be compared with caution.

Studies have reported the following percentages of subjects experiencing a statistically significant visual field

decline during the following average follow-up time periods: 68% (14 years),<sup>5</sup> 73% (10 years),<sup>41</sup> 76% (7.6 years),<sup>42</sup> 38% (9 years),<sup>4</sup> 27% (7 years),<sup>19</sup> 28% (6.3 years),<sup>14</sup> and 25% (3.7 years).<sup>43</sup> The rate of visual field loss in primary open-angle glaucoma has been reported as percent loss, as well as decibel loss, per unit time. In a retrospective cohort study of 40 eyes of 40 subjects with primary open-angle glaucoma, Kwon and associates<sup>5</sup> reported annual rates of visual field loss of 1.5% for the entire cohort and 2.1% for the subset of 27 eyes that progressed. For a prospective cohort of subjects with normal-pressure glaucoma, primary open-angle glaucoma, and ocular hypertension, Rasker and associates<sup>4</sup> reported a similar annual progression rate of 1.3% for the entire cohort but a slightly higher rate of 2.9% for the subgroup whose eyes progressed. Based on their conversion factor equating 4% loss of total visual field to -1 dB, these annual progression rates would be -0.30 dB for the entire cohort and -0.73 dB for the subgroup whose eyes progressed. The corresponding annual rates in Kwon's study would be -0.35 dB for the entire group and -0.48 dB for the subgroup with progression.

In a retrospective trend analysis of 40 eyes of 40 patients with primary open-angle glaucoma, O'Brien and associates<sup>43</sup> reported a remarkably consistent annual visual field loss of -0.35 dB for the entire cohort. However, the annual rate was much higher (-1.39 dB) for the subgroup of eyes that showed visual field loss progression. Higher annual loss rates also were reported by Katz and colleagues (-0.96 dB)<sup>14</sup> and by Smith and colleagues (-1.25 dB).<sup>19</sup>

Among black subjects, AGIS found that the "average % with decrease of visual field" (score increased by  $\geq 4$ ) at 84 months (7 years) was approximately 30% (obtained from Table IV by averaging of the scores for the two surgical treatment groups).<sup>26</sup> In another AGIS study with follow-up periods ranging from 7 to 11 years, the percentage of black subjects with "sustained decrease of visual field" (score decreased at three consecutive examinations) was approximately 28%.<sup>44</sup>

The interim results of CIGTS, with follow-up completed through 4 years and partially completed through 5 years, showed relatively minimal visual field loss progression in both the medically and surgically treated groups.<sup>45</sup> The mean visual field score for the surgically treated group was 5.0 (SD = 4.3) at baseline and remained essentially unchanged. For the medically treated group, the baseline mean was 4.6 (SD = 4.2), and the score had increased to 5.0 by 5 years. Visual field loss progression (score increase by  $\geq 3$ ) was observed in 10.7% of visits of medically treated and 13.5% of visits of surgically treated subjects visits during the 5 years.

Studies have yielded conflicting results with respect to association of various factors with likelihood or rate of

progression of visual field loss. The patient's sex has not been reported to be associated with progression likelihood or rate. Some studies have found age to be positively associated with progression in subjects with glaucoma.<sup>14,45</sup> For example, CIGTS found that every 10-year increment in age increased the risk of progression by 40%. The present study corroborates the finding of greater progression with advancing age. However, other studies have reported finding no significant association between age and likelihood of progression,<sup>4,43</sup> and Kwon and associates<sup>5</sup> found no significant association between age and progression rate.

Similarly, investigations of the association between the severity of baseline visual field loss and the likelihood or rate of progression have yielded mixed results. Katz and associates<sup>14</sup> found baseline visual field loss severity to be similar in eyes that were stable and those that progressed. However, CIGTS found that eyes with higher baseline visual field scores were more likely to progress.<sup>45</sup> Wilson and associates<sup>46</sup> and Mikelberg and associates<sup>42</sup> found that the more advanced the loss of visual field at baseline, the greater the rate of further field loss. Mikelberg hypothesized that up to a certain point, axons may be lost slowly in the optic nerve, with minimal change in visual field as measured with current techniques, but that once a certain quantity of axons is lost, further loss of visual field is more linear and rapid, because very little functional nerve remains intact. However, several studies investigating this relationship found no correlation between initial visual field loss severity and subsequent rate of field loss.<sup>4,5,19,43</sup> In the present study, no statistically significant relationship between baseline severity and progression was found with the AGIS scoring system. However, with the CIGTS scoring system, better baseline visual fields were significantly associated with a greater likelihood of progression. An explanation for this finding is not obvious, and further confirmatory studies are necessary.

Intraocular pressure has long been established as a major risk factor for development of glaucoma,<sup>47</sup> as well as a prognostic factor for glaucoma progression.<sup>48</sup> It therefore logically follows that intraocular pressure would be predictive of both likelihood and rate of progression of visual field loss, and most studies that have investigated these relationships have found the likelihood and rate of progression to be positively associated with intraocular pressure.<sup>2,43,48-50</sup> However, some studies, including the present one, have not found this relationship between intraocular pressure and visual field progression.<sup>5</sup> The most likely explanation is that in the absence of diurnal intraocular pressure measurements (or at least multiple measurements), the intraocular pressure measurement obtained at a single point in time does not adequately represent the intraocular pressure throughout the duration of the study period.

#### **IMPLICATIONS FOR THE NATURAL HISTORY OF UNTREATED GLAUCOMA**

In a cross-sectional study, Quigley and associates<sup>2</sup> estimated a low probability of becoming blind from glaucoma, whereas Hattenhauer and associates,<sup>3</sup> in a community-based retrospective record review, found a 20-year cumulative probability of unilateral blindness of 54% in glaucoma patients and 27% in patients with glaucoma and/or ocular hypertension. The latter study did not distinguish between blindness from glaucoma and other causes, and it is likely that many of the eyes that became blind could have had conditions other than glaucoma. In the study by Kwon and associates,<sup>5</sup> 5 of 40 eyes became legally blind from glaucoma, which would extrapolate to a cumulative unilateral blindness rate of 19% at 22 years.

Using data from the Glasgow glaucoma trial for eyes having intraocular pressure greater than 25 mm Hg at diagnosis, Jay and Allan<sup>51</sup> estimated that it would take 38 years from the first detectable field loss to end-stage disease for optimally treated eyes and 10 years for unsatisfactorily treated eyes. In a cross-sectional record review, Jay and Murdoch<sup>49</sup> estimated that it would take 3.6 years to reach the same end point for untreated eyes with comparable intraocular pressure at diagnosis. The difference in estimated time to end-stage disease based on treatment status is striking, but it must be emphasized that the estimate for the untreated eyes was based on cross-sectional data.

The only available prospective data on untreated glaucoma are from the Normal-Tension Glaucoma Study.<sup>6</sup> The results of that study can provide only limited understanding of the natural history of untreated glaucoma, for several reasons. First, the study was limited to glaucomatous eyes with low to average intraocular pressures. Second, for obvious safety reasons, eyes were excluded once they reached a clearly defined progression end point. Nonetheless, the Normal-Tension Glaucoma Study established the beneficial effect of treatment on visual field loss progression, particularly when the impact of cataract, which was more prevalent in the treated eyes, was removed.<sup>52</sup>

Although the data vary considerably, most studies of visual field loss in treated glaucomatous eyes suggest that among eyes that progress, the average annual decline in mean defect is approximately  $-1.0 \text{ dB} \pm -0.4 \text{ dB}$ .<sup>45,14,43</sup> Although mean defect was not the primary means of assessing progression in the present study, it is interesting that among eyes that progressed, the average annual decline of mean defect was in the same range, at approximately  $-0.8$  to  $-0.9 \text{ dB}$  per year. However, it should be noted that in this study, unlike the others cited, eyes with decreased vision due to cataract (which would have had a substantial decline in mean defect) were excluded.

The best comparison of visual field loss progression in

treated versus untreated glaucomatous eyes is made by comparing the results of the present study with a study that used the same definition of progression. Although the comparison is not ideal, AGIS had subjects with varying levels of glaucoma severity, all the subjects were treated, the same visual field scoring algorithm was used, and the data allowed comparison with black subjects only.<sup>44,45</sup>

Extrapolating from the percentage of black subjects with visual field loss at 7 years in AGIS (30%)<sup>10</sup> (assuming that the percentage increases linearly), the percentage of subjects with visual field loss at 10 years would be approximately 43%. In the present study, a considerably larger percentage of eyes progressed (53%). This comparison is particularly relevant, since race is believed to be a factor in visual field progression, with blacks at greater risk of progression than whites.

CIGTS has not yet had a long follow-up period, but visual field loss progression thus far has been minimal. The visual field score from baseline to the last examination, with most subjects having 5 years of follow-up, barely changed.<sup>45</sup> The surgically treated group had a mean baseline score of 5.0 (SD = 4.3), and this group's score remained essentially unchanged; the medically treated group had a mean baseline score of 4.6 (SD = 4.2), and the score increased to about 5.0. In contrast, the mean scores in the present study changed from 5.6 in right eyes and 5.9 in left eyes in 1987 to 12.9 in right eyes and 13.6 in left eyes in 1997. Because CIGTS reported percentage of visits, rather than eyes, that showed progression, it is difficult to make a direct comparison with this study. Presumably, percentage of visits would yield a higher number than percentage of eyes, particularly if subjects who reached an end point for visual field loss were seen more frequently. Worsening of visual field was noted in 12% of visits (10.7% of medically treated and 13.5% of surgically treated subjects). Even if this is taken to represent the percentage of eyes worsening, the extrapolated percentage of eyes progressing in 10 years would be only 24%. Of the CIGTS subjects, 55.5% were white,<sup>34</sup> and nonwhites had a 50% greater risk of progression than whites.<sup>45</sup> Even so, if the extrapolation is adjusted for this race differential, the percentage of eyes that progressed at 10 years would still be markedly lower than the 72% found in the present study. It should be kept in mind, however, that CIGTS is a well-monitored clinical trial, and the experiences reported for this trial may not reflect what occurs in practice.

Using subjects enrolled in a natural history study of risk factors for glaucoma at the Johns Hopkins School of Medicine, Katz and associates<sup>29</sup> found visual field loss progression by the CIGTS criteria in 22% of the subjects over 6 years. This would extrapolate to about 37% progression over 10 years. This also was a well-monitored group of

subjects, and only 45% were black. It is possible that the progression rate would be slightly higher in a normal clinic environment and with an exclusively black population.

In the present study, 24 of 146 right eyes (16.4%) and 21 of 141 left eyes (14.9%) progressed to AGIS scores of 18 or greater, which is considered to indicate end-stage disease. Based on CIGTS scores, the corresponding numbers were 53 of 146 (36.3%) and 54 of 141 (38.3%). For purposes of comparison, if end-stage glaucoma can be considered blindness, then the cumulative probability of at least one eye becoming blind in 10 years based on AGIS score can be estimated at approximately 16%. The corresponding estimate based on CIGTS score is 35% in 10 years. These estimates can be compared with a cumulative blindness rate of 19% at 22 years reported by Kwon and associates.<sup>5</sup> Such a direct comparison is, of course, problematic. One major issue is that the definition of blindness differs. Kwon used a legal definition based on measurement of the central field with a Goldmann perimeter. By that definition, the greatest diameter of the central field must be less than 20°. Such a definition would be consistent with the AGIS and CIGTS definitions of end-stage glaucoma but would not necessarily agree with them for any given eye. Nonetheless, given that Kwon's sample consisted of confirmed primary open-angle glaucoma patients, whereas the present study included a substantial number of glaucoma suspects, the percentage of eyes reaching end-stage disease in this untreated cohort seems disproportionately high compared with the percentage among Kwon's treated patients.

Because estimation of visual field loss progression depends on how progression is defined, this study used two tested visual field scoring algorithms. The number of eyes that progressed by the CIGTS algorithm (208, or 72%) was substantially larger than the number that progressed by the AGIS algorithm (153, or 53%). Such a difference between these two scoring algorithms is consistent with the results reported by Katz and associates<sup>29</sup> in their study of glaucoma patients followed for 6 years. They reported that 11% of their subjects progressed based on AGIS score and 22% based on CIGTS score. They also reported that the CIGTS scores were systematically higher and were more likely to incorrectly identify visual field improvement than the AGIS scores. Both of these observations are confirmed by the present study.

#### LIMITATIONS ON THE INTERPRETATION AND GENERALIZATION OF THE RESULTS

The major limitation of this study is the inability to directly compare visual field loss progression in treated versus untreated eyes. Comparison of progression in this untreated cohort with progression reported in published studies of treated eyes is problematic. Inferences about the influence of treatment must be based on the magni-

tude of the differences between the progression found in this study and that found in other studies with similar methodology. However, no published study has many methodological similarities to this one. The most valid comparisons are probably with the AGIS and CIGTS results, since the same methods of defining progression were used. However, caution must be used in comparing the results of these very well performed clinical trials with those of this essentially observational study.

Another limiting factor is that this sample is generalizable to a select population. The sample was entirely black, and blacks are known to have a higher prevalence of glaucoma and experience a more aggressive clinical course. It is possible that Caribbean blacks have an even higher prevalence of glaucoma, with a more aggressive course, thus further limiting the generalizability of these findings.

Further information on the clinical course of untreated glaucoma may become available with publication of the results of the Early Manifest Glaucoma Trial, which randomized subjects with glaucoma to medical treatment versus no treatment. However, the sample in that study consists of subjects with early glaucoma only, and they will not be allowed to progress indefinitely without treatment.

Despite these limitations, the current data set is unique and not likely to be replicated. It is desirable to learn as much as possible about the natural history of glaucoma from this data set. In future analyses, statistical techniques to compensate for the small number of treated eyes will be explored to allow for direct comparison of visual field loss progression between treated and untreated eyes with glaucoma.

#### REFERENCES

1. Gordon MO, Kass MA. The Ocular Hypertension Treatment Study: design and baseline description of the participants. *Arch Ophthalmol* 1999;117:573-583.
2. Quigley HA, Tielsch JM, Katz J, et al. Rate of progression in open-angle glaucoma estimated from cross-sectional prevalence of visual field damage. *Am J Ophthalmol* 1996;122:355-363.
3. Hattenhauer MG, Johnson DH, Ing HH, et al. The probability of blindness from open-angle glaucoma. *Ophthalmology* 1998;105:2099-2104.
4. Rasker MT, van den Enden A, Bakker D, et al. Rate of visual field loss in progressive glaucoma. *Arch Ophthalmol* 2000;118:481-488.
5. Kwon YH, Kim CS, Zimmerman MB, et al. Rate of visual field loss and long-term visual outcome in primary open-angle glaucoma. *Am J Ophthalmol* 2001;132:47-56.
6. Collaborative Normal-Tension Glaucoma Study Group. Comparison of glaucomatous progression between untreated patients with normal-tension glaucoma and patients with therapeutically reduced intraocular pressures. *Am J Ophthalmol* 1998;126:487-497.

7. Leske MC, Heijl A, Hyman L, et al. Early Manifest Glaucoma Trial: design and baseline data. *Ophthalmology* 1999;106:2144-2153.
8. Mason RP, Kosoko O, Wilson MR, et al. National survey of the prevalence and risk factors of glaucoma in St Lucia, West Indies. *Ophthalmology* 1989;96:1363-1368.
9. Kass M. The Ocular Hypertension Treatment Study. *J Glaucoma* 1994;3:97-100.
10. Advanced Glaucoma Intervention Study: 2. Visual field test scoring and reliability. *Ophthalmology* 1994;101:1445-1455.
11. Flammer J, Drance SM, Zulauf M. Differential light threshold. Short- and long-term fluctuation in patients with glaucoma, normal controls, and patients with suspected glaucoma. *Arch Ophthalmol* 1984;102:704-706.
12. Wild JM, Searle AE, Dengler-Harles M, et al. Long-term follow-up of baseline learning and fatigue effects in the automated perimetry of glaucoma and ocular hypertensive patients. *Acta Ophthalmol* (Copenh) 1991;69:210-216.
13. Birch MK, Wishart PK, O'Donnell NP. Determining progressive visual field loss in serial Humphrey visual fields. *Ophthalmology* 1995;102:1227-1234.
14. Katz J, Gilbert D, Quigley HA, et al. Estimating progression of visual field loss in glaucoma. *Ophthalmology* 1997;104:1017-1025.
15. Heijl A, Lindgren A, Lindgren G. Test-retest variability in glaucomatous visual fields. *Am J Ophthalmol* 1989;108:130-135.
16. O'Brien C, Schwartz B. The visual field in chronic open angle glaucoma: the rate of change in different regions of the field. *Eye* 1990;4:557-562.
17. Heijl A, Lindgren G, Olsson J. Normal variability of static perimetric threshold values across the central visual field. *Arch Ophthalmol* 1987;105:1544-1549.
18. McNaught AI, Crabb DP, Fitzke FW, et al. Visual field progression: comparison of Humphrey Statpac2 and pointwise linear regression analysis. *Graefes Arch Clin Exp Ophthalmol* 1996;234:411-418.
19. Smith SD, Katz J, Quigley HA. Analysis of progressive change in automated visual fields in glaucoma. *Invest Ophthalmol Vis Sci* 1996;37:1419-1428.
20. Fitzke FW, Hitchings RA, Poinosawmy D, et al. Analysis of visual field progression in glaucoma. *Br J Ophthalmol* 1996;80:40-48.
21. Nouredin BN, Poinosawmy D, Fitzke FW, et al. Regression analysis of visual field progression in low tension glaucoma. *Br J Ophthalmol* 1991;75:493-495.
22. Viswanathan AC, Fitzke FW, Hitchings RA. Early detection of visual field progression in glaucoma: a comparison of PROGRESSOR and STATPAC 2. *Br J Ophthalmol* 1997;81:1037-1042.
23. Heijl A. *Extended Empirical Statistical Package for Evaluation of Single and Multiple Fields in Glaucoma: Statpac 2 in Perimetry Update*. Amsterdam: Kugler and Ghedini; 1991:303-315.
24. Schulzer M. Errors in the diagnosis of visual field progression in normal-tension glaucoma. *Ophthalmology* 1994;101:1589-1594.
25. Bengtsson B, Lindgren A, Heijl A, et al. Perimetric probability maps to separate change caused by glaucoma from that caused by cataract. *Acta Ophthalmol Scand* 1997;75:184-188.
26. The Advanced Glaucoma Intervention Study (AGIS): 4. Comparison of treatment outcomes within race. seven-year results. *Ophthalmology* 1998;105:1146-1164.
27. Lichter P. Quality of life study—determination of progression. In: Anderson DM, Drance SM, eds. [*Encounters in Glaucoma Research 3: How To Ascertain Progression and Outcome*]. Amsterdam: Kugler; 1996:149-163.
28. Katz J. Scoring systems for measuring progression of visual field loss in clinical trials of glaucoma treatment. *Ophthalmology* 1999;106:391-395.
29. Katz J, Congdon N, Friedman DS. Methodological variations in estimating apparent progressive visual field loss in clinical trials of glaucoma treatment. *Arch Ophthalmol* 1999;117:1137-1142.
30. Lee A, Sample P, Blumental EZ, et al. Infrequent confirmation of visual field progression. *Ophthalmology* (in press).
31. Sommer A, Enger C, Witt K. Screening for glaucomatous visual field loss with automated threshold perimetry. *Am J Ophthalmol* 1987;103:681-684.
32. Coleman AL, Sommer A, Enger C, et al. Interobserver and intraobserver variability in the detection of glaucomatous progression of the optic disc. *J Glaucoma* 1996;5:384-389.
33. The Advanced Glaucoma Intervention Study (AGIS): 1. Study design and methods and baseline characteristics of study patients. *Control Clin Trials* 1994;5:299-325.
34. Musch DC, Lichter PR, Guire KE, et al. The Collaborative Initial Glaucoma Treatment Study: study design, methods, and baseline characteristics of enrolled patients. *Ophthalmology* 1999;106:653-662.
35. Mills RP, Janz NK, Wren PA, et al. Correlation of visual field with quality-of-life measures at diagnosis in the Collaborative Initial Glaucoma Treatment Study (CIGTS). *J Glaucoma* 2001;10:192-198.
36. Asman P, Heijl A. Glaucoma hemifield test: automated visual field analysis. *Arch Ophthalmol* 1992;110:812-819.
37. *The Humphrey Field Analyzer Owner's Manual*. San Leandro, Calif: Allergan Humphrey; 1983.
38. *STATPAC User's Guide*. San Leandro, Calif: Allergan Humphrey; 1986.
39. Bickler-Bluth M, Trick GL, Kolker AE, et al. Assessing the utility of reliability indices for automated visual fields. *Ophthalmology* 1989;96:616-619.
40. Kidd MN, O'Connor M. Progression of field loss after trabeculectomy: a five-year follow-up. *Br J Ophthalmol* 1985;69:827-831.
41. Hart WM Jr, Becker B. The onset and evolution of glaucomatous visual field defects. *Ophthalmology* 1982;89:268-279.
42. Mikelberg FS, Schulzer M, Drance SM, et al. The rate of progression of scotomas in glaucoma. *Am J Ophthalmol* 1986;101:1-6.
43. O'Brien C, Schwartz B, Takamoto T, et al. Intraocular pressure and the rate of visual field loss in chronic open-angle glaucoma. *Am J Ophthalmol* 1991;111:491-500.
44. The Advanced Glaucoma Intervention Study (AGIS): 9. Comparison of glaucoma outcomes in black and white patients within treatment groups. *Am J Ophthalmol* 2001;132:311-320.

45. Lichter PR, Musch DC, Gillespie BW, et al. Interim clinical outcomes in the Collaborative Initial Glaucoma Treatment Study comparing initial treatment randomized to medications or surgery. *Ophthalmology* 2001;108:1943-1953.
46. Wilson R, Walker AM, Dueker DK, et al. Risk factors for rate of progression of glaucomatous visual field loss: a computer-based analysis. *Arch Ophthalmol* 1982;100:737-741.
47. Armaly MF, Krueger DE, Maunder L, et al. Biostatistical analysis of the collaborative glaucoma study. I. Summary report of the risk factors for glaucomatous visual-field defects. *Arch Ophthalmol* 1980;98:2163-2171.
48. Mao LK, Stewart WC, Shields MB. Correlation between intraocular pressure control and progressive glaucomatous damage in primary open-angle glaucoma. *Am J Ophthalmol* 1991;111:51-55.
49. Jay JL, Murdoch JR. The rate of visual field loss in untreated primary open angle glaucoma. *Br J Ophthalmol* 1993;77:176-178.
50. Shirakashi M, Iwata K, Sawaguchi S, et al. Intraocular pressure-dependent progression of visual field loss in advanced primary open-angle glaucoma: a 15-year follow-up. *Ophthalmologica* 1993;207:1-5.
51. Jay JL, Allan D. The benefit of early trabeculectomy versus conventional management in primary open angle glaucoma relative to severity of disease. *Eye* 1989;3:528-535.
52. Collaborative Normal-Tension Glaucoma Study Group. The effectiveness of intraocular pressure reduction in the treatment of normal-tension glaucoma. *Am J Ophthalmol* 1998;126:498-505.



APPENDIX 2

1 of 6

Date: \_\_\_/\_\_\_/\_\_\_

Examiner: \_\_\_\_\_

**ST. LUCIA GLAUCOMA EYE SURVEY FOLLOW-UP**

**Definitive Examination Form**

ID: \_\_\_\_\_

		<u>Right Eye</u>			<u>Left Eye</u>		
		intact	ptthis	enucleation	intact	ptthis	enucleation
1.	<u>Status of globe</u>	( 0)	( 1)	( 2)	( 0)	( 1)	( 2)
2.	<u>Pupil</u>	no		yes	no		yes
	Afferent defect	( 0)		( 1)	( 0)		( 1)
	Other	( 0)		( 1)	( 0)		( 1)
	Specify:	_____			_____		
3.	<u>Cornea</u>						
	Pigment spindle	( 0)		( 1)	( 0)		( 1)
	KP	( 0)		( 1)	( 0)		( 1)
	Edema	( 0)		( 1)	( 0)		( 1)
	Scar	( 0)		( 1)	( 0)		( 1)
	Dystrophy	( 0)		( 1)	( 0)		( 1)
	Specify:	_____			_____		
4.	<u>Iris</u>						
	Transillumination	( 0)		( 1)	( 0)		( 1)
	Posterior synechiae	( 0)		( 1)	( 0)		( 1)
	Bombe	( 0)		( 1)	( 0)		( 1)
	Rubeosis	( 0)		( 1)	( 0)		( 1)
	Laser/surgical colobama	( 0)		( 1)	( 0)		( 1)
	Other	( 0)		( 1)	( 0)		( 1)
	Specify:	_____			_____		

2 of 6

ID: \_\_\_\_\_ - \_\_\_\_\_ - \_\_\_\_\_ - \_\_\_\_\_

	<u>Right Eye</u>		<u>Left Eye</u>	
	no	yes	no	yes
5. <u>Anterior Chamber</u>				
Ray	( 0)	( 1)	( 0)	( 1)
Cell	( 0)	( 1)	( 0)	( 1)

	Open	Borderline	Closed	Open	Borderline	Closed
6. <u>Gonioscopy</u>						
Angle depth:						
Superior	( 0)	( 1)	( 2)	( 0)	( 1)	( 2)
Nasal	( 0)	( 1)	( 2)	( 0)	( 1)	( 2)
Inferior	( 0)	( 1)	( 2)	( 0)	( 1)	( 2)
Temporal	( 0)	( 1)	( 2)	( 0)	( 1)	( 2)

	no	yes	no	yes
PAS (quadrant)				
Superior	( 0)	( 1)	( 0)	( 1)
Nasal	( 0)	( 1)	( 0)	( 1)
Inferior	( 0)	( 1)	( 0)	( 1)
Temporal	( 0)	( 1)	( 0)	( 1)
Rubeosis	( 0)	( 1)	( 0)	( 1)
Recession	( 0)	( 1)	( 0)	( 1)
Other	( 0)	( 1)	( 0)	( 1)

Specify: \_\_\_\_\_

7. <u>IOP</u> (mm Hg)	Reading: 1 <sup>st</sup> _____	_____
	2 <sup>nd</sup> _____	_____
	3 <sup>rd</sup> _____	_____

3 of 6  
Rev 14

ID: \_\_\_\_\_

	<u>Right Eye</u>		<u>Left Eye</u>	
	no	yes	no	yes
8. <u>Potentially occludable angle?</u>	( 0 )	( 1 )	( 0 )	( 1 )
If yes:	dilate with		dilate with	
	1% Mydriacyl iridectomy		1% Mydriacyl iridectomy	
	( 0 )	( 1 )	( 0 )	( 1 )
If dilated with 1% Mydriacyl:	IOP 40 min	Angle 40 min	IOP 40 min	Angle 40 min
	open	closed	open	closed
	( 0 )	( 1 )	( 0 )	( 1 )

If no, dilate with regular regimen:

Dilated pupil size \_\_\_\_\_ mm                      \_\_\_\_\_ mm

	phake	pseudo	aphake	phake	pseudo	aphake
9. <u>Lens</u>	( 0 )	( 1 )	( 2 )	( 0 )	( 1 )	( 2 )
If phakic or pseudo:	no	yes		no	yes	
Exfoliation	( 0 )	( 1 )		( 0 )	( 1 )	
Dislocation	( 0 )	( 1 )		( 0 )	( 1 )	
If phakic:						
<u>Lens grading:</u>						
Nuclear	_____	_____		_____	_____	
Cortical	_____	_____		_____	_____	
PSC	_____	_____		_____	_____	

	<u>Right Eye</u>		<u>Left Eye</u>	
	Good	Poor	Good	Poor
10. <u>Vitreous</u>				
<u>Visibility:</u>	( 0 )	( 1 )	( 0 )	( 1 )
If good view:	no	yes	no	yes
Cells	( 0 )	( 1 )	( 0 )	( 1 )
Blood	( 0 )	( 1 )	( 0 )	( 1 )
Other opacity	( 0 )	( 1 )	( 0 )	( 1 )
Specify:	_____		_____	

4 of 6

ID: \_\_\_\_\_

Rev 14

11. Macula

	<u>Right Eye</u>			<u>Left Eye</u>		
Macula view:	good ( 0)	adequate ( 1)	poor ( 2)	good ( 0)	adequate ( 1)	poor ( 2)
Hole/Cyst	( 0)	( 1)		( 0)	( 1)	
Macular Edema	( 0)	( 1)		( 0)	( 1)	
Large, soft drusen/pigmentary changes	( 0)	( 1)		( 0)	( 1)	
Geographic atrophy	( 0)	( 1)		( 0)	( 1)	
Disciform scar/ Subretinal neovasc	( 0)	( 1)		( 0)	( 1)	
Other	( 0)	( 1)		( 0)	( 1)	
Specify:	_____			_____		

12. Retina

	<u>Right Eye</u>			<u>Left Eye</u>		
Retina view:	good ( 0)	adequate ( 1)	poor ( 2)	good ( 0)	adequate ( 1)	poor ( 2)
Reattachment surgery	( 0)	( 1)		( 0)	( 1)	
Pan retinal photocoag	( 0)	( 1)		( 0)	( 1)	
Focal photocoag	( 0)	( 1)		( 0)	( 1)	
Atrophy (location)	( 0)	( 1)		( 0)	( 1)	
Scar (location)	( 0)	( 1)		( 0)	( 1)	
Neovascularization	( 0)	( 1)		( 0)	( 1)	
Cotton wool spots	( 0)	( 1)		( 0)	( 1)	
IRMA	( 0)	( 1)		( 0)	( 1)	

	<u>Right Eye</u>			<u>Left Eye</u>		
	good	adequate	poor	good	adequate	poor
13. <u>NFL</u>						
NFL view:	( 0 )	( 1 )	( 2 )	( 0 )	( 1 )	( 2 )
<b>If good or adequate:</b>						
Worst diffuse atrophy grade:						
normal		( 0 )		( 0 )		
mild		( 1 )		( 1 )		
moderate		( 2 )		( 2 )		
severe		( 3 )		( 3 )		
Wedge defects:						
	no	yes		no	yes	
	( 0 )	( 1 )		( 0 )	( 1 )	

	good	adequate	poor	good	adequate	poor
14. <u>Disc &amp; Peripapilla</u>						
Visibility:	( 0 )	( 1 )	( 2 )	( 0 )	( 1 )	( 2 )
<b>If good or adequate:</b>						
Vertical C/D		_____			_____	
	no	yes		no	yes	
Notch	( 0 )	( 1 )		( 0 )	( 1 )	
Hemorrhage	( 0 )	( 1 )		( 0 )	( 1 )	
Pale disc	( 0 )	( 1 )		( 0 )	( 1 )	
Optic pit	( 0 )	( 1 )		( 0 )	( 1 )	
Drusen	( 0 )	( 1 )		( 0 )	( 1 )	
Other	( 0 )	( 1 )		( 0 )	( 1 )	
Specify:	_____			_____		

6 of 6

ID: \_ \_ - \_ \_ - \_ - \_ - \_ - \_ - \_ - \_ -

Rev. 14

15. Cause(s) of decreased acuity: only if VA < 20/30:

**RANK IN ORDER OF IMPORTANCE**

	<u>Right Eye</u>	<u>Left Eye</u>
Cataract	_ _	_ _
AMD - geographic atrophy	_ _	_ _
AMD - exudative	_ _	_ _
Glaucoma	_ _	_ _
Diabetic retinopathy	_ _	_ _
Post cataract cystoid macular edema	_ _	_ _
Other retinal pathology	_ _	_ _
Specify:	_____	_____
Corneal opacity	_ _	_ _
Non-glaucomatous Optic atrophy	_ _	_ _
Amblyopia	_ _	_ _
Uncertain	_ _	_ _
Other	_ _	_ _
Specify:	_____	_____

**ST. LUCIA EYE SURVEY  
SCREENING EXAMINATION**

**STATION #3**

**HUMPHREY VISUAL FIELD TESTING**

**SCREEN DISPLAY**

**THIS IS....**

**PATIENT ID#:**    \_\_\_ - \_\_\_ - \_\_\_ - \_\_\_

**ALONG WITH PATIENT'S NAME AND ID#, PLEASE ENTER THE FOLLOWING  
INFORMATION ONTO THE HUMPHREY FIELD ANALYZER "PATIENT  
INFORMATION SCREEN"...**

**DATE OF BIRTH** \_\_\_\_\_

**PATIENT'S DISTANCE CORRECTION**

R    \_\_\_ . \_\_\_ + \_\_\_ . \_\_\_ x \_\_\_  
L    \_\_\_ . \_\_\_ + \_\_\_ . \_\_\_ x \_\_\_

Attempt to perform 30-2 Humphrey Visual Field Test on **Right Eye**.  
Visual Field for Right Eye was .....

- Completed (1 )
- Not completed due to poor vision (2 )
- Not completed due to patient refusal (3 )
- Not completed due to patient incapability (8 )

ID \_\_\_\_\_ - \_\_\_\_\_ - \_\_\_\_\_ - \_\_\_\_\_

continued..  
Station #2

6. Perform **refractometry** and enter results here ...

6a. R \_\_\_\_\_ . \_\_\_\_\_ + \_\_\_\_\_ . \_\_\_\_\_ x \_\_\_\_\_

6b. L \_\_\_\_\_ . \_\_\_\_\_ + \_\_\_\_\_ . \_\_\_\_\_ x \_\_\_\_\_

7. **Refractometry** was performed ...

using automated refractor (1 )

manually using phoropter (2 )

8. **Visual Acuity Assessment.** First, let us check patient's **distance lane visual acuity** while they are wearing their **present correction** and record here...

8a. R \_\_\_\_ / \_\_\_\_\_ (with presenting correction)

8b. L \_\_\_\_ / \_\_\_\_\_ (with presenting correction)

9. Now, let us check patient's distance lane visual while using the **refraction correction**. Please record.

9a. R \_\_\_\_ / \_\_\_\_\_ (with refraction correction)

9b. L \_\_\_\_ / \_\_\_\_\_ (with refraction correction)

10. If patient's vision was less than 20/20 in testing both with present Rx **and** refraction please check vision again with a **multiple pinhole** in front of the **refraction correction**. Record here.

10a. R \_\_\_\_ / \_\_\_\_\_ (with multiple pinhole)

10b. L \_\_\_\_ / \_\_\_\_\_ (with multiple pinhole)

**PLEASE DIRECT PATIENT TO STATION # 3**  
**HUMPHREY VISUAL FIELDS**

APPENDIX 3

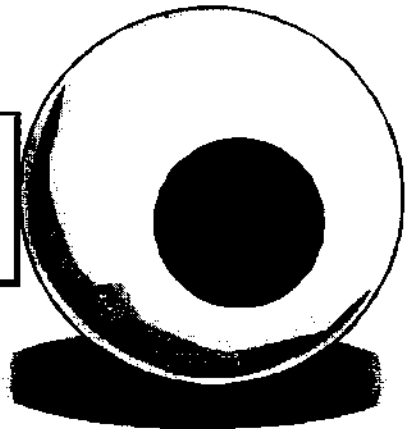
---

CASE #	....	□□	-	□□□□	-	□□	-	□□
INTERVIEWER #	.....	□□□□						
DATE	.....	□□	-	□□	-	□□		
		MM		DD		YY		
EDITOR #	.....	□□□□						
TOTAL TIME	.....	□□□						

FIELD EDIT INITIALS.....

---

**ST. LUCIA  
GLAUCOMA SURVEY**



**FOLLOW-UP STUDY  
INTERVIEW  
1997**

ID \_\_\_\_\_

DEC. 07

START TIME: [ ] [ ] : [ ] [ ]

32

ST. LUCIA GLAUCOMA SURVEY FOLLOW-UP STUDY  
INTERVIEW

**SECTION A: Demographics**

A1.	First, I would like to ask you some general background questions. How old were you on your last birthday?	AGE .....	[ ] [ ] YRS	36
A2.	What is your date of birth?	DOB .....	[ ] [ ] [ ] [ ] [ ] [ ] MM DD YY	38
A3.	Are you currently married, separated, divorced, widowed or have you never been married?	MARRIED .....	1	44
		SEPARATED .....	2	
		DIVORCED .....	3	
		WIDOWED .....	4	
		NEVER MARRIED .....	5	
		RF .....	7	
A4.	What is the highest grade in school or year of college that you completed?	GRADE:	00 01 02 03 04 05 06 07 08 09 10 11 12	45
		COLLEGE:	13 14 15 16	
		GRADUATE SCHOOL:	17	
A5.	Are you currently employed, a homemaker, retired, disabled or unemployed?  SPECIFY: _____	EMPLOYED .....	1	47
		HOMEMAKER .....	2	
		RETIRED .....	3	
		DISABLED .....	4	
		UNEMPLOYED .....	5	
		OTHER (SPECIFY) .....	6	
A6.	Not counting yourself, how many other people live in your household?	# IN HOUSEHOLD .....	[ ] [ ]	48

**SECTION C: Medical/Eye History**

DECK 03

C1.	Now I'd like to ask you some questions about your medical history and more specifically about your eye health. How satisfied are you with your vision? Are you (READ CATEGORIES)?	Very satisfied ..... 1 Satisfied ..... 2 Dissatisfied ..... 3 Very dissatisfied ..... 4	34
C2.	Do you currently wear glasses or contact lenses to see in the distance?	YES ..... 1 NO ..... 2	35
C3.	Do you currently wear glasses or bifocals specifically made for close work such as knitting or reading?	YES ..... 1 NO ..... 2	36
C4.	Using your glasses or contact lenses if you need them, can you see well enough to read ordinary newspaper print with (ASK a-c):		
a.	Your right eye?	YES ..... 1 NO ..... 2	37
b.	Your left eye?	YES ..... 1 NO ..... 2	38
c.	Both your eyes open?	YES ..... 1 NO ..... 2	39
C5.	Have you ever been told that you had a cataract in either eye?	YES ..... 1 NO ..... (GO TO C6) ..... 2	40
a.	Did your eye doctor advise you to have cataract surgery?	YES ..... 1 NO ..... (GO TO C6) ..... 2	41
b.	Did you ever have cataract surgery?	YES, ONE EYE .... (GO TO C6) ..... 1 YES, BOTH EYES .. (GO TO C6) ..... 2 NO ..... 3	42
c.	What was the reason you did not have cataract surgery? Was it because (READ CATEGORIES)?		
	It cost too much? .....	YES NO RF DK	43
	You didn't know where to go? .....	1 2 7 8	44
	You didn't have a way to get there? ....	1 2 7 8	45
	You didn't think the problem was serious enough? .....	1 2 7 8	46
	You didn't have insurance? .....	1 2 7 8	47
	You were afraid of surgery? .....	1 2 7 8	48
	Any other reason? ..... (SPECIFY) .....	1 2 7 8	49

SPECIFY:

ID \_\_\_\_\_

C6. Have you ever been told by a doctor that you have glaucoma? YES ..... 1 52  
 NO ..... (GO TO C7) ..... 2

a. How old were you when you first learned you had glaucoma? AGE .....   53

b. In the past 3 years, or since your diagnosis, how many times have you seen your eye doctor for your glaucoma? # TIMES .....   55

c. Have you ever gone more than one year without seeing your eye doctor for your glaucoma? YES ..... 1 57  
 NO ..... (GO TO e) ..... 2

d. What was the reason that you did not see your eye doctor? Was it because (READ CATEGORIES)?

	YES	NO	RF	DK	
It costs too much? .....	1	2	7	8	58
You didn't know where to go? .....	1	2	7	8	59
You didn't have a way to get there? ....	1	2	7	8	60
You didn't think the problem was serious enough? .....	1	2	7	8	61
You didn't have money? .....	1	2	7	8	62
You were afraid? .....	1	2	7	8	63
Any other reason? ..... (SPECIFY) .....	1	2	7	8	64

SPECIFY: \_\_\_\_\_   65

e. Are you taking eye drops or oral medications for your glaucoma? YES ..... 1 67  
 NO ..... (GO TO g) ..... 2

f. What medications are you taking for glaucoma?

1. \_\_\_\_\_   68

2. \_\_\_\_\_   70

3. \_\_\_\_\_   72

4. \_\_\_\_\_   74

g. Are there any medications that the doctor has prescribed for your glaucoma but that you are not taking at all or as frequently as prescribed? YES, NOT AT ALL ..... 1 76  
 YES, NOT AS FREQUENTLY ..... 2  
 NO ..... (GO TO h) ..... 3 76

END 03

DECK 04

- h. What is the main reason you are not taking your glaucoma medication as prescribed by your doctor? READ CATEGORIES.
- It costs too much ..... 1
  - Don't need it ..... 2
  - You didn't have a way to get it ..... 3
  - You don't feel good when you take it (it hurts or burns my eyes) ..... 4
  - Any other reason (SPECIFY) ..... 5

SPECIFY: \_\_\_\_\_

- i. Did your eye doctor ever tell you that you needed laser or surgery for your glaucoma?
- YES ..... 1
  - NO ..... (GO TO C7) ..... 2
- j. Did you have glaucoma surgery? PROMPT: In one eye or both eyes?
- YES, ONE EYE .... (GO TO C7) ..... 1
  - YES, BOTH EYES .. (GO TO C7) ..... 2
  - NO ..... 3

- k. What was the reason why you did not have surgery for your glaucoma? Was it because (READ CATEGORIES)?
- |  | YES | NO | RF | DK |
|--|-----|----|----|----|
|--|-----|----|----|----|

It costs too much? .....	1	2	7	8
You didn't know where to go? .....	1	2	7	8
You didn't have a way to get there? ....	1	2	7	8
You didn't think the problem was serious enough? .....	1	2	7	8
You didn't have money? .....	1	2	7	8
You were afraid of surgery? .....	1	2	7	8
Any other reason? ..... (SPECIFY) .....	1	2	7	8

SPECIFY: \_\_\_\_\_

- C7. Are you currently using any prescription eye drops or ointment to treat any other eye disease (besides glaucoma) such as ocular inflammation or an eye infection?
- YES ..... 1
  - NO ..... (GO TO C8) ..... 2

a. What eye drops or ointments are you using?

1. \_\_\_\_\_
2. \_\_\_\_\_
3. \_\_\_\_\_
4. \_\_\_\_\_
5. \_\_\_\_\_

b. What are you taking them for?

1. \_\_\_\_\_
2. \_\_\_\_\_
3. \_\_\_\_\_
4. \_\_\_\_\_
5. \_\_\_\_\_

(6)

ID \_\_\_\_\_

			DECK 04
C8.	Are you currently using any oral medication to treat any other eye disease such as ocular inflammation or an eye infection?	YES ..... 1	48
		NO ..... (GO TO C9) ..... 2	
	a. What oral medications are you taking?		
	1. _____ <input type="text"/>		49
	2. _____ <input type="text"/>		53
	3. _____ <input type="text"/>		57
	4. _____ <input type="text"/>		61
	5. _____ <input type="text"/>		65
	b. What are you taking them for?		
	1. _____ <input type="text"/>		69
	2. _____ <input type="text"/>		70
	3. _____ <input type="text"/>		71
	4. _____ <input type="text"/>		72
	5. _____ <input type="text"/>		73
C9.	Do your eyes ever feel dry?	YES ..... 1	69
		NO ..... (GO TO C10) ..... 2	
	a. HAND CARD E. Do they feel dry (READ CATEGORIES)?	All the time (4 or more days/wk) ..... 1	70
		Often (1 to 3 days/wk) ..... 2	
		Sometimes (2 to 3 days/month) ..... 3	
		Rarely (once a month or less) ... (GO TO C10) ... 4	
	b. Is this symptom worse in the morning or evening, or is it the same all day?	MORNING ..... 1	71
		EVENING ..... 2	
		SAME ..... 3	
	c. Are the symptoms (READ CATEGORIES)?	Constant year round ..... 1	72
		Seasonal ..... 2	
C10.	Do you ever feel a gritty or sandy sensation in your eyes?	YES ..... 1	73
		NO ..... (GO TO C11) ..... 2	
	a. HAND CARD E. Do they feel gritty all the time, often, sometimes, or rarely?	ALL THE TIME ..... 1	74
		OFTEN ..... 2	
		SOMETIMES ..... 3	
		RARELY ..... 4	
C11.	Do your eyes ever have a burning sensation?	YES ..... 1	75
		NO ..... (GO TO C12) ..... 2	
	a. HAND CARD E. Do they burn all the time, often, sometimes, or rarely?	ALL THE TIME ..... 1	76
		OFTEN ..... 2	
		SOMETIMES ..... 3	END 04
		RARELY ..... 4	

C12.	Are your eyes ever red?	YES .....	1	13
		NO ..... (GO TO C13) .....	2	
a.	HAND CARD E. Are they red all the time, often, sometimes, or rarely?	ALL THE TIME .....	1	14
		OFTEN .....	2	
		SOMETIMES .....	3	
		RARELY .....	4	
C13.	Do you use artificial tears or other nonprescription eye drops for dry eye?	YES .....	1	15
		NO ..... (GO TO C14) .....	2	
a.	How many times per day do you use them?	TIMES PER DAY .....	<input type="text"/>	16
b.	For how many months have you been using them?	MONTHS .....	<input type="text"/>	18
C14.	When you are in a mood to cry, can you normally produce tears?	YES .....	1	21
		NO .....	2	
C15.	Do you notice much crusting on your eye lashes?	YES .....	1	22
		NO ..... (GO TO C16) .....	2	
a.	HAND CARD E. Does this happen all the time, often, sometimes, or rarely?	ALL THE TIME .....	1	23
		OFTEN .....	2	
		SOMETIMES .....	3	
		RARELY .....	4	
C16.	Do your eyelids ever get stuck together in the morning?	YES .....	1	24
		NO ..... (GO TO C17) .....	2	
a.	HAND CARD E. Does this happen all the time, often, sometimes, or rarely?	ALL THE TIME .....	1	25
		OFTEN .....	2	
		SOMETIMES .....	3	
		RARELY .....	4	

- C17. Since the last time you were examined by Howard University Drs (DATE), have you had any surgery on your eyes? YES ..... 1 26  
 NO ..... (GO TO C18) ..... 2
- a. How many different surgeries did you have during this period? # SURGERIES .....   27

ASK b-d FOR EACH SURGERY

	FIRST SURGERY	SECOND SURGERY	THIRD SURGERY	FOURTH SURGERY
b. What eye was it on, the right or left?	29	36	43	50
RIGHT .....	1	1	1	1
LEFT .....	2	2	2	2
c. What type of surgery was it? READ CATEGORIES.	30	37	44	51
Cataract .....	01	01	01	01
Cataract (laser) .....	02	02	02	02
Glaucoma .....	03	03	03	03
Glaucoma (laser) .....	04	04	04	04
Diabetes (laser) .....	05	05	05	05
Retinal detachment .....	06	06	06	06
Other or combination (SPECIFY) ..	07	07	07	07
SPECIFY:				
DK .....	98	98	98	98
	32	39	46	53
d. When was this done?	<input type="text"/> <input type="text"/> <input type="text"/> <input type="text"/>	<input type="text"/> <input type="text"/> <input type="text"/> <input type="text"/>	<input type="text"/> <input type="text"/> <input type="text"/> <input type="text"/>	<input type="text"/> <input type="text"/> <input type="text"/> <input type="text"/>
	MM YY	MM YY	MM YY	MM YY

- C18. Now, I'm going to read you a list of eye conditions that you may have now or have had in the past. Has a doctor ever told you that you had Lazy Eye? YES ..... 1 57  
 NO ..... (GO TO C20) ..... 2
- C19. Has a doctor ever told you that you had macular degeneration? YES ..... 1 58  
 NO ..... (GO TO C20) ..... 2
- a. Were you ever treated for macular degeneration? YES ..... 1 59  
 NO ..... (GO TO C20) ..... 2
- b. What type of treatment did you receive? LASER ..... 1 60  
 SURGERY ..... 2  
 OTHER ..... (SPECIFY) ..... 3  
 DK ..... 8

SPECIFY:       61

DECK 05

- C20. Has a doctor ever told you that you had retinal detachment? YES ..... 1 63  
 NO ..... (GO TO C21) ..... 2
- a. Were you ever treated for retinal detachment? YES ..... 1 64  
 NO ..... (GO TO C21) ..... 2
- b. What type of treatment did you receive: laser, surgery, both, or some other type of treatment? LASER ..... 1 65  
 SURGERY ..... 2  
 BOTH ..... 3  
 OTHER ..... (SPECIFY) ..... 4  
 DK ..... 8

SPECIFY: \_\_\_\_\_       66

- C21. Has a doctor ever told you that you had any other eye problems? YES ..... (SPECIFY) ..... 1 68  
 NO ..... (GO TO C22) ..... 2

SPECIFY:

PROBLEM #1 \_\_\_\_\_       69

PROBLEM #2 \_\_\_\_\_       74

PROBLEM #3 \_\_\_\_\_       13

END 05

- C22. Now, I'm going to read you a list of other health conditions. At the present time, do you have any of the following conditions?

	YES	NO	RF	DK	
a. asthma? .....	1	2	7	8	18
b. chronic bronchitis or emphysema? .....	1	2	7	8	19
c. tuberculosis? .....	1	2	7	8	20
d. other chronic lung trouble? .....	1	2	7	8	21
e. repeated attacks of sinus trouble? .....	1	2	7	8	22
f. arthritis, rheumatism, or bursitis? .....	1	2	7	8	23
g. high blood pressure or hypertension? ...	1	2	7	8	24
h. hardening of the arteries? .....	1	2	7	8	25
i. a heart attack? .....	1	2	7	8	26
j. any other heart trouble? .....	1	2	7	8	27
k. a stroke? .....	1	2	7	8	28
l. stomach, bowel or intestinal trouble? ...	1	2	7	8	29
m. cancer? .....	1	2	7	8	30
n. serious kidney or bladder disease? .....	1	2	7	8	31
o. serious trouble with back or spine? .....	1	2	7	8	32
p. paralysis of any kind? .....	1	2	7	8	33

					DECK 06
C23.	Do you presently have diabetes or sugar diabetes?	YES .....	1		34
		NO .....	2	(GO TO C24)	
a.	How many years have you had diabetes?	# YEARS .....		<input type="text"/>	35
b.	How is your diabetes currently treated?	INSULIN .....	1		37
		ORAL DRUGS .....	2		
		DIET ALONE .....	3		
		NOT BEING TREATED .....	4		
c.	Did your medical doctor ever tell you to have your eyes examined every year because of your diabetes?	YES .....	1		38
		NO .....	2		
d.	When was your last complete eye examination, one that included dilating your pupils, where the doctor used bright lights to look into the back of your eyes?	WITHIN PAST 12 MONTHS .....	1		39
		1-2 YEARS AGO .....	2		
		3-5 YEARS AGO .....	3		
		OVER 5 YEARS AGO .....	4		
e.	Have you had a complete eye exam every year for the past 3 years?	YES .....	1	(GO TO g)	40
		NO .....	2		
f.	Why have you not had these annual exams? Was it because (READ CATEGORIES)?				
		YES	NO	RF	DK
	It costs too much? .....	1	2	7	8
	You didn't know where to go? .....	1	2	7	8
	You didn't have a way to get there? ....	1	2	7	8
	You didn't think the problem was serious enough? .....	1	2	7	8
	You didn't have money? .....	1	2	7	8
	You were afraid? .....	1	2	7	8
	Any other reason? .... (SPECIFY) .....	1	2	7	8
	SPECIFY: _____				<input type="text"/>
g.	Has a doctor ever told you that you had diabetic retinopathy or diabetic eye disease?	YES .....	1		50
		NO .....	2	(GO TO C24)	
h.	Has a doctor ever told you that you needed laser or surgery for your diabetic eye disease?	YES .....	1		51
		NO .....	2	(GO TO C24)	
i.	Did you have laser, surgery or both?	YES, LASER .....	1	(GO TO C24)	52
		YES, SURGERY .....	2	(GO TO C24)	
		YES, BOTH .....	3	(GO TO C24)	
		NO .....	4		

j. What was the reason you didn't have laser or surgery for your diabetic eye disease? Was it because (READ CATEGORIES)?

	YES	NO	RP	DK	
It costs too much? .....	1	2	7	8	53
You didn't know where to go? .....	1	2	7	8	54
You didn't have a way to get there? ....	1	2	7	8	55
You didn't think the problem was serious enough? .....	1	2	7	8	56
You didn't have insurance? .....	1	2	7	8	57
You were afraid of surgery? .....	1	2	7	8	58
Any other reason? ..... (SPECIFY) .....	1	2	7	8	59

SPECIFY: \_\_\_\_\_

C24. Do you presently have any other serious health problem that we have not already mentioned? SPECIFY.

YES ..... (SPECIFY) ..... 1

NO ..... (GO TO SECTION D) ..... 2

PROBLEM #1 \_\_\_\_\_

PROBLEM #2 \_\_\_\_\_

**SECTION D: Health Services**

The next few questions will be about your use of health services in general and then more specifically about your use of eye care services.

DECK 06

- |     |  |   |              |
|-----|--|---|--------------|
| D1. | In the past three years, did you stay in a hospital as a patient overnight?  | YES ..... 1<br>NO ..... (GO TO D2) ..... 2                      | 73           |
| a.  | During that period, how many different times did you stay in a hospital overnight?   | NUMBER OF TIMES ..... <input type="text"/> <input type="text"/> | 74           |
| b.  | How many were for eye problems?  | NUMBER OF TIMES ..... <input type="text"/> <input type="text"/> | 76<br>END 06 |
|     |  |   |              |
| D2. | Not counting times when you stayed overnight in a hospital, in the past three years did you ever go in and come out of a hospital on the same day for surgery? | YES ..... 1<br>NO ..... (GO TO D3) ..... 2                      | 13           |
| a.  | During that period, how many different times did you go into a hospital for one of these procedures without staying overnight?                                 | NUMBER OF TIMES ..... <input type="text"/> <input type="text"/> | 14           |
| b.  | How many were related to an eye problem?   | NUMBER OF TIMES ..... <input type="text"/> <input type="text"/> | 16           |
|     |  |   |              |
| D3. | During the last three years, did you ever have surgery done in a special surgery center outside of a hospital?   | YES ..... 1<br>NO ..... (GO TO D4) ..... 2                      | 18           |
| a.  | How many times did you have surgery at such a center?  | NUMBER OF TIMES ..... <input type="text"/> <input type="text"/> | 19           |
| b.  | How many of these surgeries were for eye problems?   | NUMBER OF TIMES ..... <input type="text"/> <input type="text"/> | 21           |
|     |  |   |              |
| D4. | During the past three years, did you stay in a nursing home, convalescent home or similar place?   | YES ..... 1<br>NO ..... (GO TO D5) ..... 2                      | 23           |
| a.  | How many times were you admitted to such a place?  | NUMBER OF TIMES ..... <input type="text"/> <input type="text"/> | 24           |
|     |  |   |              |
| D5. | During the past three years, how many times have you seen a medical doctor (not counting any doctors seen during hospital stays you already mentioned)?        | NUMBER OF TIMES ..... <input type="text"/> <input type="text"/> | 26           |

-----

DECK 07

D6. How long has it been since you last saw a doctor?      WITHIN PAST 12 MONTHS ..... 1 28  
 1-2 YEARS ..... 2  
 3-5 YEARS ..... 3  
 MORE THAN 5 YEARS ..... 4  
 DK ..... 8

D7. For what reason did you last see a doctor? CODE ONE.      ROUTINE CHECK-UP/SHOTS ..... 01 29  
 SHORT TERM ILLNESS/INJURY ..... 02  
 CARE OF A CHRONIC MEDICAL PROBLEM ..... 03  
 SURGERY OR AFTERCARE ..... 04  
 PREGNANCY/GYN EXAM ..... 05  
 DENTAL SERVICES ..... 06  
 EYE EXAM ..... 07  
 TESTS ..... 08  
 OTHER ..... (SPECIFY) ..... 09  
 DK ..... 98

SPECIFY: \_\_\_\_\_   31  
 OFFICE

D8. Where do you generally go for health care? CODE ONE.      Private MD ..... 01 31  
 Emergency Room ..... 02  
 Hospital Clinic ..... 03  
 Community Clinic ..... 04  
 Nowhere..... 05  
 Other ..... (Specify)..... 06  
 DK..... 07

SPECIFY: \_\_\_\_\_   35  
 OFFICE

D9. During the past three years, were there any times you thought you should see a doctor but did not?      YES ..... 1 37  
 NO ..... (GO TO D10) ..... 2

a. What prevented you from going for care? Was it because (READ CATEGORIES)?

	YES	NO	RF	DK	
It cost too much .....	1	2	7	8	38
You didn't know where to go? .....	1	2	7	8	39
You didn't have a way to get there? .....	1	2	7	8	40
There wasn't a health professional or medical center close enough .....	1	2	7	8	41
It was too difficult to get an appointment .....	1	2	7	8	42
Office hours were not convenient .....	1	2	7	8	43
You didn't think the problem was serious enough? .....	1	2	7	8	44
Any other reason? ..... (SPECIFY) .....	1	2	7	8	45

SPECIFY: \_\_\_\_\_   46

			DECK 07
D10.	The next few questions are about eye care you may have received from an eye doctor. People often confuse the different types of eye doctors. Just to be sure I am being clear, could you please tell me the difference between an ophthalmologist and an optometrist?	CORRECT ..... 1	48
		INCORRECT ..... (READ DEFINITION) ..... 2	
		SUBJECT DOESN'T TRY/ DOESN'T KNOW ... (READ DEFINITION) ..... 3	
	IF R IS INCORRECT OR DOESN'T KNOW, READ: DEFINITION - An ophthalmologist is an M.D. who can perform surgery and issue prescription medication. An optometrist can do visual eye exams and prescribe only eye glasses.		
D11.	In the past three years, have you seen an eye doctor, eye specialist or someone else for any type of eye care or routine eye examination?	YES ..... 1	49
		NO ..... (GO TO D12) ..... 2	
		DK ..... (GO TO D12) ..... 8	
a.	How many visits have you made for eye care in the past three years?	NUMBER OF VISITS ..... <input type="text"/> <input type="text"/>	50
b.	How many of these times were to an ophthalmologist?	# OF TIMES TO OPHTHALMOLOGIST ..... <input type="text"/> <input type="text"/>	52
c.	How many were to an optometrist?	# OF TIMES TO OPTOMETRIST ..... <input type="text"/> <input type="text"/>	54
D12.	When was the last time you went for eye care?	WITHIN PAST 12 MONTHS ..... 1	56
		1-2 YEARS ..... 2	
		3-5 YEARS ..... 3	
		MORE THAN 5 YEARS ..... 4	
		NEVER ..... (GO TO D13) ..... 5	
		DK ..... 8	
a.	What was the <u>main</u> reason for your last visit for eye care?	ROUTINE CHECK-UP ..... 01	57
		GLASSES/CONTACT LENS RELATED ..... 02	
		ACUTE/SHORT-TERM PROBLEM ..... 03	
		CHRONIC/LONG-TERM PROBLEM ..... 04	
		SURGERY OR AFTER CARE ..... 05	
		FAILED VISION TEST ..... 06	
		FAILED GLAUCOMA TEST ..... 07	
		OTHER ..... (SPECIFY) ..... 08	
		DK ..... 98	
	SPECIFY: _____	<input type="text"/> <input type="text"/>	59

ID \_\_\_\_\_

DECK 08

c. What prevented you from going for care? Was it because (READ CATEGORIES)?	YES	NO	RF	DK	
It costs too much? .....	1	2	7	8	13
You didn't know where to go? .....	1	2	7	8	14
You didn't have a way to get there? .....	1	2	7	8	15
There wasn't an eye care professional or center close enough? .....	1	2	7	8	16
It was too difficult to get an appointment? .....	1	2	7	8	17
Office hours were not convenient? .....	1	2	7	8	18
You didn't think the problem was serious enough? .....	1	2	7	8	19
Any other reason? ..... (SPECIFY) .....	1	2	7	8	20

SPECIFY: \_\_\_\_\_

D14. During the past 3 years, how many times did you purchase a new pair of glasses or contact lenses? NUMBER OF TIMES .....   23

**IF 00, GO TO SECTION E.**

a. How much have you spent on glasses and contact lenses in the past three years? DOLLAR AMOUNT ..... \$      25

**SECTION E: Medications**

Now, I'd like to ask you some questions about different medications that you may be using now or may have used in the past.

DECK OF

E1.	Have you ever taken aspirin or aspirin containing drugs, not including Tylenol, etc., on a regular basis for a month or more?	YES ..... 1 NO ..... (GO TO E2) ..... 2 DK ..... (GO TO E2) ..... 8	29
a.	On the average how many aspirin did you take per week?	# PILLS ..... <input type="text"/> <input type="text"/>	30
b.	How many months did you take (it/them) regularly?	# MONTHS ..... <input type="text"/> <input type="text"/> <input type="text"/>	32
c.	Are you taking aspirin or aspirin containing drugs now?	YES ..... 1 NO ..... (GO TO E2) ..... 2 DK ..... (GO TO E2) ..... 8	35
d.	Why were you taking (it/them)?		36
	DESCRIBE EACH: _____	<input type="text"/> <input type="text"/>	38
	_____	<input type="text"/> <input type="text"/>	38
E2.	Have you ever taken an anti-inflammatory drug on a regular basis for a month or more? These include ibuprofen, naprosyn and others. Please include both prescription and non-prescription drugs.	YES ..... 1 NO ..... (GO TO E3) ..... 2 DK ..... (GO TO E3) ..... 8	40
a.	On the average how many pills did you take per week?	# PILLS ..... <input type="text"/> <input type="text"/>	41
b.	How many months did you take (it/them) regularly?	# MONTHS ..... <input type="text"/> <input type="text"/> <input type="text"/>	43
c.	Are you taking any of these drugs now?	YES ..... 1 NO ..... (GO TO E3) ..... 2 DK ..... (GO TO E3) ..... 8	46
d.	Why were you taking (it/them)?		47
	DESCRIBE EACH: _____	<input type="text"/> <input type="text"/>	49
	_____	<input type="text"/> <input type="text"/>	49
E3.	Have you ever taken steroids, such as prednisone, on a regular basis for a month or more?	YES ..... 1 NO ..... (GO TO E4) ..... 2 DK ..... (GO TO E4) ..... 8	51
a.	On the average how many pills did you take per week?	# PILLS ..... <input type="text"/> <input type="text"/>	52
b.	How many months did you take (it/them) regularly?	# MONTHS ..... <input type="text"/> <input type="text"/> <input type="text"/>	54

		DECK OF
c.	Are you taking steroids now?	57
	YES .....	1
	NO .....	2
	DK .....	8
d.	Why were you taking (it/them)?	
	DESCRIBE EACH: _____	58
	_____	60
	_____	
E4.	Have you ever taken medicines for high blood pressure, such as lasix, reserpine, aldomet, HCTZ, inderal or others, on a regular basis for a month or more?	62
	YES .....	1
	NO ..... (GO TO E5) .....	2
	DK ..... (GO TO E5) .....	8
a.	Are you taking pills for high blood pressure now?	63
	YES .....	1
	NO .....	2
	DK .....	8
E5.	Have you ever taken medicines for heart disease, such as digoxin, isordil, nitroglycerine or others, on a regular basis for a month or more?	64
	YES .....	1
	NO ..... (GO TO E6) .....	2
	DK ..... (GO TO E6) .....	8
a.	Are you taking pills for heart disease now?	65
	YES .....	1
	NO .....	2
	DK .....	8
E6.	Have you ever taken medicines for poor circulation, such as vasodilan or others, on a regular basis for a month or more?	66
	YES .....	1
	NO ..... (GO TO SECTION F) .....	2
	DK ..... (GO TO SECTION F) .....	8
a.	Are you taking pills for poor circulation now?	67
	YES .....	1
	NO .....	2
	DK .....	8

ID \_\_\_\_\_

**SECTION G: Tobacco/Alcohol**

DECK 09

<p>G1. I'd like now to ask about smoking and drinking of alcoholic beverages. Have you ever smoked more than 100 cigarettes (5 packs) in your entire life?</p>	<p>YES ..... 1                  NO ..... (GO TO G2) ..... 2                  DK ..... (GO TO G2) ..... 8</p>	<p>28</p>
<p>a. How old were you when you first started smoking cigarettes regularly?</p>	<p>AGE ..... <input type="text"/> <input type="text"/></p>	<p>29</p>
<p>b. On the average for the entire time you smoked, how many cigarettes did you smoke per day? 20 CIG = 1 PACK</p>	<p># PER DAY ..... <input type="text"/> <input type="text"/> <input type="text"/></p>	<p>31</p>
<p>c. Did you ever stop smoking for a year or more and then start again?</p>	<p>YES ..... 1                  NO ..... (GO TO e) ..... 2                  DK ..... (GO TO e) ..... 8</p>	<p>34</p>
<p>d. For how many years did you stop?</p>	<p># YEARS ..... <input type="text"/> <input type="text"/></p>	<p>35</p>
<p>e. Do you smoke cigarettes now?</p>	<p>YES ..... (GO TO G2) ..... 1                  NO ..... 2</p>	<p>37</p>
<p>f. How old were you when you stopped?</p>	<p># YEARS ..... <input type="text"/> <input type="text"/></p>	<p>38</p>
<p>G2. The next questions are about alcoholic beverages such as beer, wine, and liquor. During the past month, on about how many different days did you drink any alcoholic beverage?</p>	<p># DAYS ..... <input type="text"/> <input type="text"/>                  NONE ..... (GO TO G3) ..... 00</p>	<p>40</p>
<p>a. On the days that you drink, how many drinks do you have on the average day?</p>	<p># DRINKS/BEERS/GLASSES OF WINE ..... <input type="text"/> <input type="text"/></p>	<p>42</p>
<p>Pint = 16 oz.                  Quart = 32 oz.                   1 oz. liquor = 8 oz beer = 6 oz. wine = 1 drink                   1 pint liquor = 16 drinks                  1 quart beer = 4 beers                  1 bottle wine = 6 glasses</p>		
<p>b. Now think back over the past month and remember the time you had the <u>most</u> to drink. About how many drinks did you have at that time?</p>	<p># DRINKS/BEERS/GLASSES OF WINE ..... <input type="text"/> <input type="text"/></p>	<p>44</p>
<p>c. During the past month, about how many days did you have 5 or more drinks?</p>	<p># DAYS ..... <input type="text"/> <input type="text"/></p>	<p>46</p>

DECK 09

d. Nowadays, what do you usually drink? READ CATEGORIES.

- Wine ..... 1
- Beer ..... 2
- Liquor ..... 3
- Combinations ..... 4
- DK ..... 8

48

e. Are you currently drinking more, less or about the same amount as you were ten years ago?

- MORE ..... (GO TO SECTION H) ..... 1
- LESS ..... (GO TO SECTION H) ..... 2
- SAME AMOUNT ..... (GO TO SECTION H) ..... 3
- DK ..... (GO TO SECTION H) ..... 8

49

G3. Was there a time in the past when you drank any alcoholic beverages or have you always been a non-drinker?

- NON-DRINKER ..... 1
- DRINKER IN PAST ..... 2
- DK ..... 8

50

# ANALYSIS OF THE KERATOCYTE APOPTOSIS, KERATOCYTE PROLIFERATION, AND MYOFIBROBLAST TRANSFORMATION RESPONSES AFTER PHOTOREFRACTIVE KERATECTOMY AND LASER IN SITU KERATOMILEUSIS

---

BY *Steven E. Wilson, MD*

## ABSTRACT

*Purpose:* To test the hypothesis that (1) there are quantitative differences in the cellular responses in the corneal stroma after photorefractive keratectomy (PRK) for low myopia compared to high myopia and (2) there are both qualitative and quantitative differences in the cellular responses in the corneal stroma after PRK for high myopia and laser in situ keratomileusis (LASIK) for high myopia.

*Methods:* PRK for low myopia (-4.5 diopters [D]), PRK for high myopia (-9.0 D), and LASIK for high myopia (-9.0 D) were performed in rabbit eyes, and corneas were obtained for examination at 4, 24, and 72 hours, 1 and 4 weeks, and 3 months after surgery. A total of 144 rabbits were included in the study. Stromal apoptosis, necrosis, mitosis, myofibroblast generation, and inflammatory cell infiltration were evaluated by immunohistochemical methods and electron microscopy.

*Results:* Keratocyte apoptosis/necrosis and the subsequent proliferation and density of myofibroblasts were qualitatively and quantitatively different in PRK for high myopia compared to either PRK for low myopia or LASIK for high myopia. Significant inflammatory cell infiltration was noted in both PRK and LASIK but appeared to be greater in PRK for high myopia.

*Conclusions:* The qualitative and quantitative differences in the cellular wound healing response after PRK for high and low myopia and LASIK for high myopia are likely determinants of the clinical differences in refractive outcome and some of the complications, such as regression and haze, seen after these procedures.

*Trans Am Ophthalmol Soc* 2002;100:411-433

## INTRODUCTION

---

It is essential to consider the evolutionary context to understand the importance of the wound-healing response in the cornea. Adequate vision was certainly essential for the survival of most animals, and this resulted in selective pressure to develop the ability to recover from a variety of corneal injuries. Abrasions to the vertebrate cornea from branches, projectiles, and other sources were probably common. Infectious agents such as herpes simplex virus, smallpox virus, or related viruses may have posed an even greater threat because of the potential for extension into the eye and even the brain. The wound-healing response to these injuries would likely have evolved to restore the protective epithelial surface, maintain the integrity of the cornea, and maintain or restore

the corneal clarity necessary for vision. Systems designed to rapidly restore the integrity of the epithelium, reestablish the structure and clarity of the stroma, and impede the spread of pathogens until the immune response eradicated the invaders would probably have provided strong selective advantages to organisms, animal or human, dependent on sight for survival.<sup>1</sup>

Within the context of modern medicine and surgery, wound healing remains critical to the maintenance of corneal health and vision. The wound-healing response is a major factor in the outcome of all corneal surgical procedures and contributes to the pathophysiology of many corneal diseases. The healing response at the donor-recipient interface plays an important role in determining the efficacy of corneal transplantation and also contributes to the development of complications, including astigmatism, graft overdrive, and others.<sup>2</sup> The stromal wound-healing response that occurs in diseases such as recurrent herpes simplex keratitis is a major determinant of the amount of corneal scarring that develops in individual eyes.<sup>3,4</sup>

The corneal wound-healing response also contributes to the efficacy and safety of refractive surgical procedures

From the Department of Ophthalmology, University of Washington School of Medicine, Seattle. This work was supported in part by US Public Health Service grants EY10056, EY01730, and EY 05665 from the National Eye Institute, National Institutes of Health, Bethesda, Maryland, and an unrestricted grant from Research to Prevent Blindness, Inc, New York, New York.

such as photorefractive keratectomy (PRK) and laser in situ keratomileusis (LASIK). It is a major factor in the development of overcorrection, undercorrection, haze, and other complications that occur when these surgeries are performed for the correction of myopia and hyperopia,<sup>5,6</sup> as well as astigmatism.<sup>7,8</sup>

Experimentally, PRK and LASIK have been used to provide standardized animal models in which to study the corneal wound-healing response. Although many of the studies performed to date have contributed important insights into wound healing in the cornea, most have been limited to some extent in terms of the number of eyes (and hence statistical analysis), choice of time points, length of follow-up, and/or aspects of the cellular responses examined. It is important, however, to understand the knowledge derived from these previous investigations in order to allow interpretation of the results of the work performed for this thesis.

#### COMPONENTS OF THE CORNEAL WOUND-HEALING CASCADE

The corneal epithelium, stroma, and nerves participate in homeostasis of the ocular surface. The lacrimal glands and tear film also contribute to maintaining ocular surface smoothness and integrity. Following most injuries, these components are involved in an orchestrated wound-healing response that efficiently restores corneal structure and function. This process is modulated by a variety of cytokines and receptors that are produced locally in the cornea and lacrimal glands. Also, immune cells that function to eliminate debris and microbes are attracted to the site of injury.

Studies performed over the past decade have revealed many of the events that make up the wound-healing cascade in the cornea. Most of these studies, however, especially those examining the stromal response, have focused on the early phase of the response—from the time of injury to a few hours after wounding. It is important to understand the contributions of each of the components of this cascade and their interactions in order to appreciate the overall corneal healing response. Figure 1 provides a framework for considering the corneal wound-healing cascade. (It should be noted that many of these events actually occur simultaneously and, therefore, the “cascade” should be viewed as such only in rough terms. Also, some of the processes that are important components in the overall wound-healing response, but are not directly related to these studies, are omitted for the sake of clarity.)

#### *Keratocyte Apoptosis*

Early studies noted that keratocytes seemed to disappear from the anterior stroma after corneal epithelial scrape injury;<sup>9-12</sup> explanations offered for this phenomenon

included osmotic changes from the loss of epithelium, exposure to the atmosphere, and artifact resulting from tissue processing. In 1996, however, it was demonstrated for the first time that the early disappearance of keratocytes after epithelial injury is mediated by a process known as apoptosis.<sup>13,14</sup> Apoptosis is a gentle, involuntal form of cell death that occurs with little release of lysosomal enzymes or other intracellular components and the resulting damage to surrounding cells or tissues that are characteristic of necrotic cell death. Subsequent studies have suggested that apoptosis is mediated by cytokines released from the injured epithelium, including interleukin-1 and tumor necrosis factor alpha.<sup>15-17</sup>

Virtually any epithelial injury induces keratocyte apoptosis. Among the causes demonstrated in animal models are mechanical scrape,<sup>13</sup> corneal surgical procedures such as PRK and LASIK,<sup>18</sup> herpes simplex keratitis,<sup>1</sup> incisions,<sup>18</sup> and the application of a plastic ring pressed firmly against the epithelial surface.<sup>14</sup> Recently, we have shown that apoptosis occurs in the keratocytes underlying Bowman's layer in the human eye after epithelial scrape injury (Figure 2) (unpublished data).

Keratocyte apoptosis near the surface of the cornea is the first observable stromal change after epithelial injury. The rapidity with which apoptosis occurs after injury can be detected by electron microscopy. If one euthanizes a mouse, enucleates the eye, performs a single scrape across the corneal epithelium, immediately places the eye into fixative, and processes the cornea for electron microscopy, one finds that the specimens already demonstrate chromatin condensation and other morphologic changes in the keratocytes consistent with apoptosis (Figure 3). Thus, the cornea is primed and ready to respond immediately to injury. Such an immediate response would be expected if one of the functions of this process is to retard dissemination of viral pathogens by removing accessible cells until the immune system can respond to the invader.<sup>1</sup>

Keratocyte apoptosis can also be demonstrated by means of the terminal deoxyribonucleotidyl transferase-mediated dUTP-digoxigenin nick end labeling (TUNEL) assay, which detects fragmented ends of the DNA strands produced in the cell during the apoptotic process. DNA fragmentation, which takes longer to develop (10 to 30 minutes) compared with the electron microscopic evidence, has been shown to be most prominent approximately 4 hours after epithelial scrape injury in mice and rabbits.<sup>13,18</sup>

Keratocytes undergo apoptosis to a depth of one third to one half of the stromal thickness, depending on the species and the type of injury. In the unwounded cornea, cellular processes called gap junctions connect keratocytes to form a syncytium.<sup>19,20</sup> Thus, cytokines released from the injured epithelium could bind to receptors on

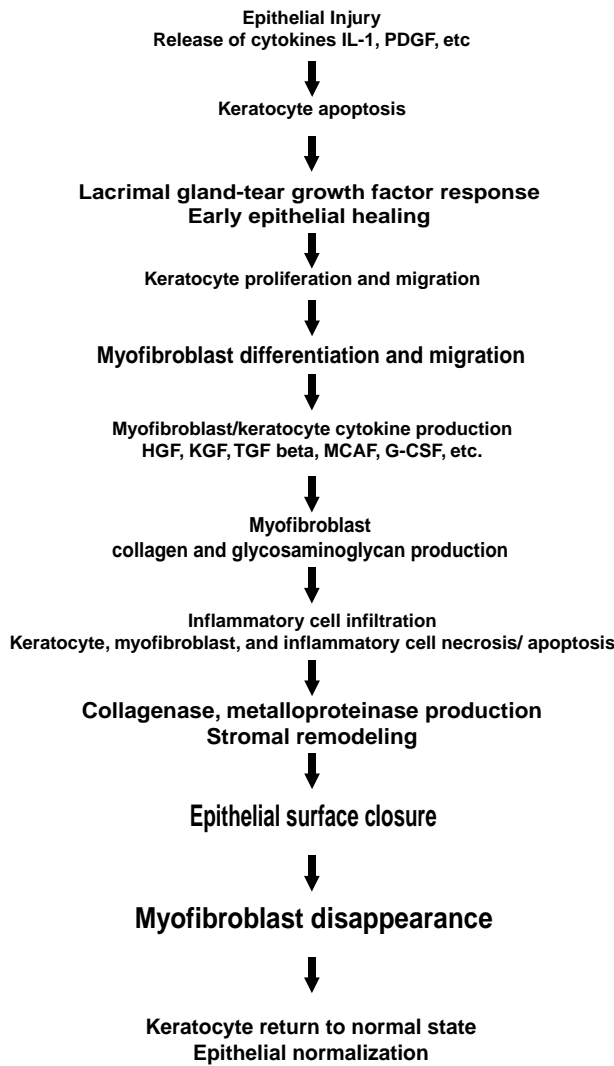


**FIGURE 1**

Schematic diagram showing some of the events that make up corneal wound-healing response that occurs after corneal epithelial injury or surgical procedures such as photorefractive keratectomy or laser in situ keratomileusis. Note that this scheme is simplified; not all events that may be important to the total wound-healing response are included. Additionally, events in the cornea do not necessarily follow the precise sequential nature of the diagram. For example, keratocyte apoptosis is the first observable phenomenon after injury, but many of the subsequent events occur in parallel.

the most superficial keratocytes and signal adjoining cells to undergo apoptosis via these intercellular communication channels. Alternatively, pro-apoptotic cytokines from the injured epithelium may penetrate into the stroma and stimulate the keratocytes directly. It has been suggested that keratocyte apoptosis continues for at least 1 week after PRK in the rabbit cornea.<sup>21</sup>

Localization of the keratocyte apoptosis response in the stroma varies with the type of corneal epithelial injury.<sup>15</sup> Injuries such as epithelial scrape and epithelial viral infection trigger keratocyte apoptosis in the superfi-

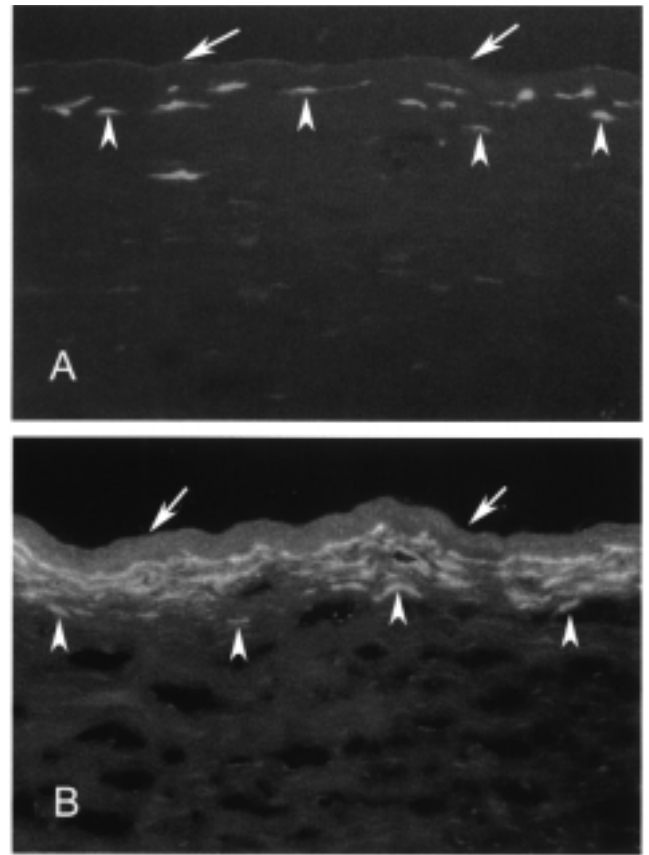


**FIGURE 2**

Keratocyte apoptosis detected at 4 hours (A) and 65 hours (B) after epithelial scrape injury in a human eye prior to enucleation for a choroidal melanoma. Terminal deoxynucleotidyl transferase-mediated dUTP nick end label (TUNEL)-positive keratocytes (arrowheads) are seen in anterior stroma beneath Bowman's layer (arrows) (magnification x200). (This experiment was approved by the institutional review board of the author's university.)

cial stroma (Figure 4A). Similarly, PRK, which is in effect an ablative epithelial scrape, results in anterior stromal keratocyte apoptosis. By contrast, a lamellar cut across the cornea produced by a microkeratome, as performed for LASIK, induces keratocyte apoptosis not only peripherally at the site of epithelial injury, as would be expected, but also along both sides of the lamellar interface created deeper in the stroma by the microkeratome cut (Figure 4B). This extension of the apoptosis-inducing effect from the site of epithelial injury is thought to be attributable to tracking of epithelial debris, including pro-apoptotic cytokines, into the interface by the microkeratome blade.<sup>15</sup> Alternatively, cytokines from the injured peripheral epithelium could diffuse along the lamellar interface and into the central stroma.<sup>15</sup>

In turn, the location of keratocyte apoptosis influences the location and effect of events that occur later in the wound-healing cascade. This may be important in determining clinical and biological differences between

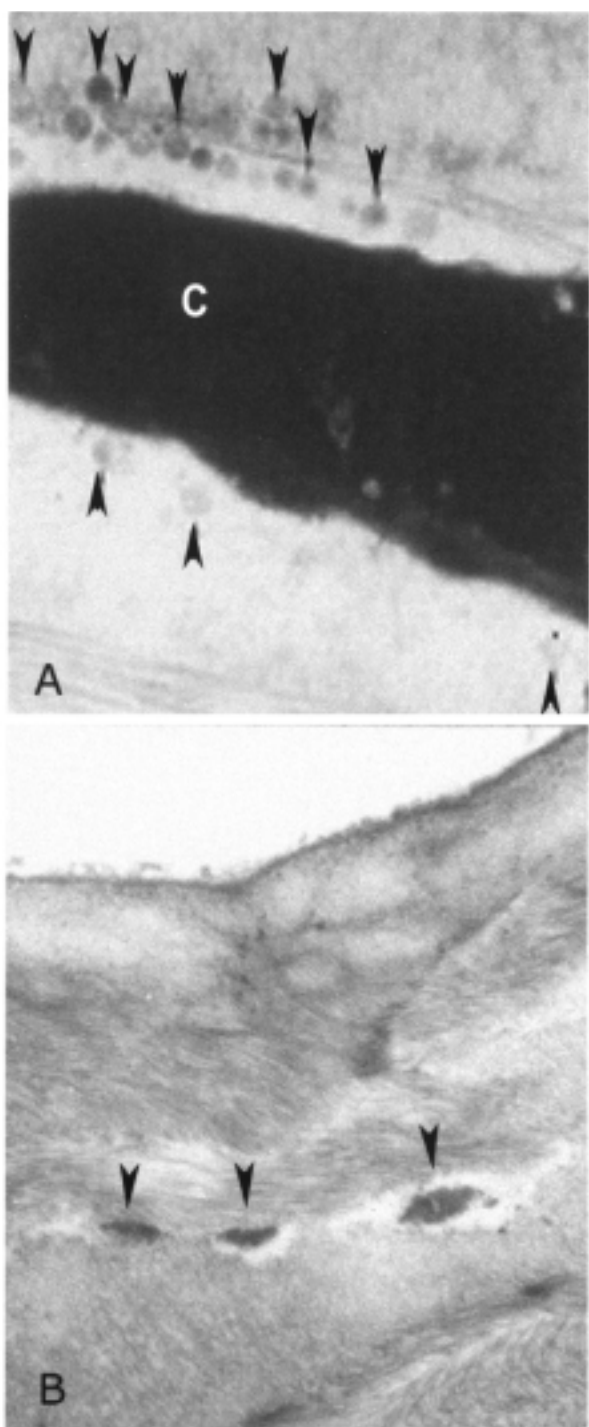


**FIGURE 3**

A, Transmission electron micrograph of keratocyte apoptosis in the mouse eye. One hour after epithelial scrape injury, superficial keratocytes show shrinkage of cytoplasm, chromatin condensation (C), and formation of apoptotic bodies (arrowheads) that contain mitochondria, lysosomes, and other cellular components. These apoptotic bodies disperse into stroma and are absorbed by other cells that remain alive (magnification x6,000). B, At 4 hours after epithelial scrape injury, only condensed chromatin (arrowheads) remains from a keratocyte that underwent apoptosis (magnification x1,000). Both figures reprinted with permission from *Experimental Eye Research*.<sup>13</sup> Copyright 1994, Academic Press, London.

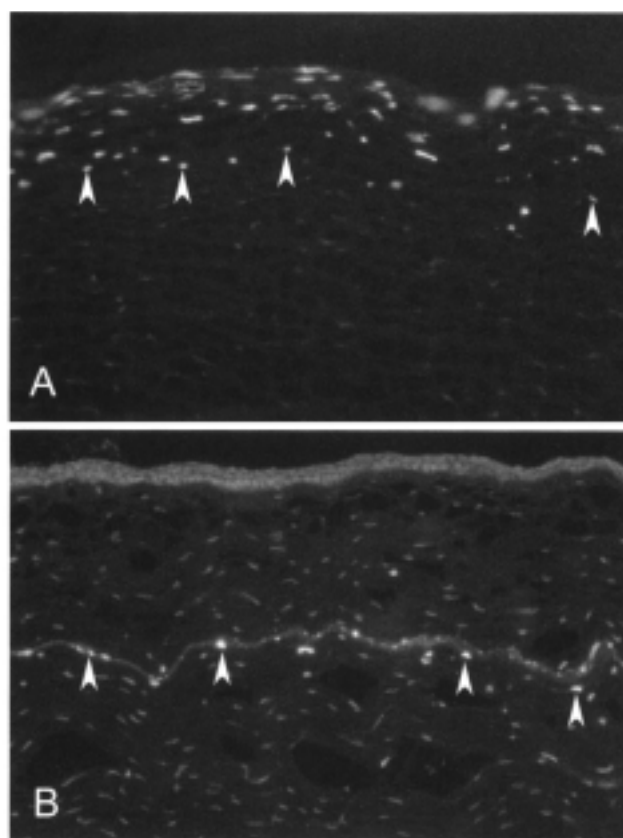


**FIGURE 4**

Localization of keratocyte apoptosis in rabbit cornea, as detected by terminal deoxynucleotidyl transferase-mediated dUTP nick end labeling (TUNEL) assay, depends on type of injury. A, Epithelial scrape injury, as occurs in photorefractive keratectomy, triggers superficial stromal keratocyte apoptosis (arrowheads). B, Lamellar microkeratome cut, such as would be made for laser in situ keratomileusis, triggers keratocyte apoptosis peripherally where blade penetrates epithelium (not shown) and along lamellar interface (arrowheads) (magnification x200).

PRK and LASIK for high myopia in terms of, for instance, epithelial hyperplasia, which characterizes later stages of corneal wound healing. Thus, superficial keratocyte apoptosis (such as that triggered by PRK) may be more likely to result in epithelial hyperplasia than deeper keratocyte apoptosis (such as that noted in LASIK) because of the localization of the epithelium-modulating growth factors produced by the proliferating keratocytes and myofibroblasts involved in repopulating the areas denuded of these cells during the early stages of wound healing.

#### *Keratocyte Proliferation and Migration: Myofibroblasts*

As noted above, the wave of keratocyte apoptosis that occurs within the first few hours of corneal epithelial injury produces an area of stroma that is devoid of keratocytes. Some of the remaining keratocytes in the posterior and peripheral cornea begin undergoing mitosis about 12 to 24 hours after injury,<sup>22</sup> as can be shown by bromodeoxyuridine incorporation or immunocytochemical stain-

ing for a mitosis-specific antigen, Ki-67.

The cytokines and other factors that regulate the proliferation and migration of the keratocytes are not well understood. Platelet-derived growth factor (PDGF) expressed by the epithelium and PDGF receptors expressed by the keratocytes may play a role, in that PDGF has a mitogenic and chemotactic effect on these cells.<sup>23-25</sup> Keratocyte proliferation after epithelial scrape injury may continue for several days.<sup>22</sup> To date, however, no studies have reported the long-term time course of keratocyte proliferation after PRK or LASIK.

Studies have suggested that keratocyte proliferation after injury results in the generation of a type of cell called the myofibroblast.<sup>26-29</sup> Most of these studies, however, have been in vitro tissue culture-based investigations. Little information is available regarding whether this transformation takes place in the keratocytes that undergo mitosis after PRK,<sup>29</sup> and nothing has been reported about the status of these cells after LASIK.

Myofibroblasts are characterized by expression of alpha smooth-muscle actin (SMA). This allows them to be detected in vitro and in situ by immunocytochemistry.<sup>26-29</sup> They are thought to have altered transparency in vivo related to corneal crystallin expression.<sup>30</sup> They are also thought to produce high levels of growth factors such as hepatocyte growth factor and keratinocyte growth factor, which have the specific functions of regulating cellular proliferation, migration, and differentiation associated with healing of the corneal epithelium.<sup>31</sup> There is also evidence that myofibroblasts express the types of collagen associated with wound healing rather than the normal collagen types produced by keratocytes.<sup>32,33</sup> They may also produce collagenases, gelatinases, and metalloproteinases associated with the remodeling of stromal collagen,<sup>34-35</sup> a process that is thought to play an important role in regression following PRK or LASIK.

The ultimate fate of the myofibroblasts that appear in the corneal stroma after PRK and LASIK is also uncertain. Two possibilities are that myofibroblasts transdifferentiate into keratocytes as the wound-healing process is completed or that myofibroblasts are terminally differentiated and are slowly eliminated by apoptosis. Greater knowledge of the role and fate of the myofibroblasts may be important in our understanding of the wound-healing events that occur after PRK and LASIK, as well as in the development of approaches to the control of these events to prevent unsatisfactory outcomes after these refractive surgical procedures.

#### *Inflammatory Cells*

Very little is known about the role of inflammatory cells in the wound-healing response after PRK and LASIK. In the only published study to date,<sup>39</sup> inflammatory cells were

identified in the stroma by hematoxylin-eosin staining beginning about 24 hours after PRK. However, this staining technique was unable to distinguish specific types of inflammatory cells in these corneas. It is important to clarify which types of inflammatory cells are involved in the corneal wound-healing response after PRK and LASIK by using more sensitive methods, such as electron microscopy.

It seems likely that the inflammatory cells attracted to the cornea after PRK and LASIK are eventually eliminated by apoptosis once the response has fulfilled its function, in that apoptosis has been shown to be the cause of immune cell death in other organs. However, there is no concrete information concerning how these cells are eliminated in the cornea after refractive surgery.

#### **RESOLUTION OF THE WOUND-HEALING RESPONSE**

In the months after injury, the wound-healing response is completed and there is a return to normal structure and function in the corneal stroma. This process is associated with elimination of some of the cells involved in wound healing, as well as remodeling of the disordered collagen produced by the myofibroblasts and/or keratocytes during the wound-healing process.<sup>40,41</sup> This remodeling process, which begins within a few weeks after injury, can continue for years, depending on the severity of the injury. Studies of later time points after laser refractive surgery are needed to understand these processes that return the cornea to its normal prewounding state.

Restoration of the epithelial cell layer after injury is also essential to the function and survival of the cornea. However, this response is often exaggerated. Eyes that have undergone identical laser refractive surgical corrections have been shown to develop widely variable amounts of epithelial hyperplasia. This phenomenon is thought to be an important mechanism in regression of the refractive effect of PRK and LASIK.<sup>42-45</sup> Additionally, remodeling of the epithelium may take place over a period of months to years, and this prolonged response may result in instability of the refractive effect of PRK and LASIK. The regulatory mechanisms that modulate the return to normal corneal epithelial morphology have not been characterized.

In the present study, we have examined several important aspects of the wound-healing response after PRK for low and high myopia and LASIK for high myopia in a large number of rabbit eyes over a substantial period of time, from the earliest observations at 4 hours to the latest at 3 months after surgery. Our goal was to test the hypotheses that (1) there are quantitative differences in the cellular responses in the corneal stroma after PRK for low and high myopia and (2) there are both qualitative and quantitative differences in the wound-healing

response after PRK for high myopia and LASIK for high myopia. We have also used the results of these experiments to draw some conclusions about possible relationships between wound healing and the complications associated with these refractive surgical procedures in the clinical setting.

## METHODS

---

### ANIMALS

All animal studies described in this thesis were approved by the Animal Control Committee at the author's university. All animals were treated in accordance with the tenets of the ARVO Statement for the Use of Animals in Ophthalmic and Vision Research.

A total of 144 12- to 15-week-old female New Zealand white rabbits weighing 2.5 kg to 3.0 kg each were included in the study. One eye of each rabbit, selected at random, was subjected to PRK or LASIK. Three corrections were performed: -4.5 D PRK (low myopia) (N=48 eyes); -9.0 D PRK (high myopia) (N=48 eyes); and -9.0 D LASIK (high myopia) (N=48 eyes). The contralateral eyes served as unoperated controls (N=144).

Anesthesia was obtained by intramuscular injection of ketamine hydrochloride (30 mg/kg) and xylazine hydrochloride (5 mg/kg). In addition, topical proparacaine hydrochloride 1% (Alcon, Fort Worth, Texas) was applied to each eye just before surgery. Euthanasia was performed with an intravenous injection of 100 mg/kg pentobarbital while the animal was under general anesthesia.

Six time points were examined: 4 hours, 24 hours, 72 hours, 1 week, 4 weeks, and 3 months. These time points were selected because they include all of the major early events that have been noted in previous studies of corneal scrape, PRK surgery, and LASIK surgery, and also provide later time points to follow the return to normalcy. Time points earlier than 4 hours were not used because previous studies found no relevant differences between earlier times and 4 hours, except that the TUNEL assay was more strongly positive at 4 hours than it was earlier.<sup>13</sup>

Eight corneas with each of the three refractive surgical procedures were examined at each of the six time points. Six of the eight corneas were preserved by cryofixation for the TUNEL assay and immunocytochemistry, and two corneas were processed for light microscopy and transmission electron microscopy (TEM).

### PRK TECHNIQUE

With the animal under general and local anesthesia, a wire lid speculum was positioned and a 7-mm-diameter area of epithelium overlying the pupil was removed by scraping with a No. 64 blade (Beaver; Becton, Dickinson & Co, Franklin Lakes, New Jersey). A laser ablation with the

corresponding sphere correction without astigmatism correction (Star S2 Excimer Laser System, VISX, Inc, Santa Clara, California) with a 6.0-mm-diameter optical zone was performed. The -4.5 D correction had a depth of 53 mm, and the -9.0 D correction had a depth of 106 mm. Two drops of ciprofloxacin hydrochloride 0.3% (Ciloxan, Alcon, Fort Worth, Texas) were instilled into the eye at the end of the procedure. A temporary tarsorrhaphy was placed with a double-armed 5.0 silk suture (Alcon) for the first 24 hours after surgery. Any eye that developed infiltration suggestive of infection or an epithelial defect persisting beyond 1 week after surgery was excluded from the study and an additional animal was included in its place.

### LASIK TECHNIQUE

With the animal under general and local anesthesia, the eye was proptosed anterior to the eyelids and temporarily retained in that position by clamping the temporal upper and lower eyelids together with a mosquito clamp. The base of the microkeratome (Hansatome, Bausch & Lomb, Rochester, New York), set to cut a flap 8.5 mm in diameter and 160  $\mu$ m in thickness, was placed on the corneal surface, and a clamp was placed on the suction tubing that runs from the microkeratome base to the power supply. This was necessary because of the difference in the curvature of the rabbit cornea, compared with that of the human, in order to allow the instrument to sense suction in the tubing. Otherwise, the safety features of the instrument would have prevented the automated microkeratome head from cutting the flap.

After the tubing was clamped, the microkeratome base was pressed firmly onto the cornea, and suction was activated with the microkeratome power supply. The microkeratome head was placed into position on the base and the forward pedal activating the motor was depressed. The base was pressed firmly against the cornea to simulate the suction obtained in the human eye while the head of the microkeratome coursed across the gear track to cut the flap. The head was returned to its original position by depressing the reverse pedal, and the base and head of the microkeratome were removed from the eye. A smooth round spatula was inserted into the stromal interface, and the flap was reflected on its hinge against the conjunctiva to expose the bed. A -9.0 D correction identical to that used in the PRK eyes was performed (Star S2 Excimer Laser System, VISX). The flap and stromal bed were irrigated with approximately 0.5 mL of 0.2  $\mu$ m filtered balanced salt solution (Alcon). The flap was returned to its original position with the spatula.

After 1 minute, two drops of ofloxacin ophthalmic solution 0.3% (Ocuflox, Allergan, Irvine, California) were instilled into the eye. Corticosteroid drops were not used to eliminate the potential confounding effect of this type

of drug on the corneal wound-healing response. The flap was protected with a contact lens (Soflens, 66 F/M base curve, Bausch & Lomb, Rochester, New York) for the first day after surgery. The eyelids were closed for 24 hours after surgery with a temporary tarsorrhaphy.

Rabbits with flaps that were displaced or that had visible striae on the first day after surgery were excluded, and replacement animals were added to complete the treatment groups.

#### **TISSUE FIXATION AND SECTIONING**

Rabbits were euthanized, and the corneoscleral rims (operated-on eyes and unoperated control eyes) were removed with 0.12 forceps and sharp Westcott scissors. For histological analyses (TUNEL assay, Ki-67 immunocytochemistry, and alpha-SMA immunocytochemistry), the corneas were embedded in liquid OCT compound (Sakura Finetek, Torrance, California) within a 24 mm x 24 mm x 5 mm mold (Fisher Scientific, Pittsburgh, Pennsylvania). The tissue specimens were centered within the mold so that the block could be bisected and transverse sections cut from the center of the cornea. The mold and tissue were rapidly frozen in 2-methyl butane within a stainless steel crucible suspended in liquid nitrogen. The frozen tissue blocks were stored at  $-85^{\circ}\text{C}$  until sectioning was performed.

Central corneal sections (7  $\mu\text{m}$  thick) were cut with a cryostat (HM 505M, Micron GmbH, Waldorf, Germany). Sections were placed on 25 mm x 75 mm x 1 mm microscope slides (Superfrost Plus, Fisher) and maintained frozen at  $-85^{\circ}\text{C}$  until staining was performed.

#### **TUNEL ASSAY AND IMMUNOCYTOCHEMISTRY ASSAYS**

To detect fragmentation of DNA associated with apoptosis,<sup>13</sup> tissue sections were fixed in acetone at  $-20^{\circ}\text{C}$  for 2 minutes, dried at room temperature for 5 minutes, and then placed in balanced salt solution. A fluorescence-based TUNEL assay was used according to the manufacturer's instructions (ApopTag, Cat No. S7165; Intergen, Purchase, New York). Positive (4-hour mechanical corneal scrape) and negative (unwounded) control slides were included in each assay. Photographs were obtained with a fluorescence microscope (Nikon E600, Melville, New York).

Immunocytochemistry for Ki-67 and alpha-SMA was performed as previously described.<sup>46</sup> The monoclonal antibody against Ki-67 (Zymed Laboratories, South San Francisco, California) was used at the stock concentration of 214.6 mg/L in 1X phosphate-buffered saline (PBS), pH 7.4, with 1% bovine serum albumin. The alpha-SMA antibody (DAKO Corporation, Carpinteria, California) was used at a concentration of 85 mg/L in PBS with 1% bovine serum albumin. In each case, the

sections were incubated with the diluted antibody for 1 to 2 hours at room temperature, followed by a 1-hour incubation with the secondary antibody (fluorescein isothiocyanate-conjugated donkey anti-mouse IgG; Jackson ImmunoResearch, West Grove, Pennsylvania). Cover slips were mounted with a protective mounting medium containing propidium iodide or 4',6-diamidino-2-phenylindole (DAPI) (Vectashield, Vector Laboratories, Burlingame, California). Negative controls (primary antibody omitted) were included with every antibody-binding experiment. Additional controls were performed with unrelated monoclonal antibodies to ensure specificity. The sections were viewed and photographed under a light microscope (Eclipse E800, Nikon) equipped with a digital SPOT camera (Micro Video Instruments, Avon, Massachusetts).

#### **LIGHT AND TRANSMISSION ELECTRON MICROSCOPY**

The corneas were fixed in a solution of 2% paraformaldehyde and 2% glutaraldehyde in a vehicle of 1.3 M sodium phosphate buffer containing 0.05%  $\text{MgCl}_2 \cdot 6 \text{H}_2\text{O}$ , pH 7.3, at  $4^{\circ}\text{C}$  for 12 to 24 hours. The specimens were then washed twice with the buffered fixative vehicle for 15 minutes at room temperature and stored at  $4^{\circ}\text{C}$  in the fixative vehicle until they were processed.

For processing, the corneas were bisected and a 1.5-mm strip was removed from the center of each cornea. This strip was again bisected, and the fragments were placed in the primary fixative vehicle prior to secondary fixation. Secondary fixation was carried out in 1%  $\text{OsO}_4$  in 1.0 M phosphate buffer, pH 7.3, for about 45 minutes at room temperature, followed by three washings in the phosphate-buffered fixative vehicle and dehydration in a graded ethanol series. The transition from 100% ethanol to epoxy was mediated by two changes of propylene oxide. An epoxy medium of Spurr's formulation<sup>47</sup> was used for infiltration and embedding. The fragments were mounted in flat molds and hardened at  $70^{\circ}\text{C}$  for 24 hours before sectioning.

Both 1- $\mu\text{m}$ -thick light microscopic sections and ultra-thin TEM sections were cut for viewing. The light microscopy sections were stained with 50% modified Richardson's stain (1% methylene blue and 1% azure II in 1% sodium borate solution diluted 1:1 with 1 M dibasic sodium phosphate solution at pH 8.5), and the TEM sections were mounted on grids coated with polyvinyl butyral (Pioloform, Sigma-Aldrich Corp, St Louis, Missouri)<sup>48</sup> and stained with saturated aqueous uranyl acetate and Reynold's<sup>49</sup> lead citrate.

Evaluation was performed by light microscopy (Nikon E600, Melville, New York) and TEM (model PW6020, CM10 transmission electron microscope, Royal Philips Electronics NV, Eindhoven, The Netherlands).

#### CELL COUNTING FOR QUANTITATION OF TUNEL ASSAYS AND IMMUNOCYTOCHEMISTRY ASSAYS

Six corneas with each surgical procedure were used for counting at each time point; in some groups one of the corneas could not be counted owing to sectioning artifact. In each cornea, all of the cells in seven nonoverlapping, full-thickness columns extending from the anterior stromal surface to the posterior stromal surface were counted by a single observer.<sup>15</sup> The diameter of each column was that of a 400× microscope field. The columns in which counts were performed were selected at random from the central cornea of each specimen. As previously reported,<sup>15</sup> this procedure was used to allow quantitative comparisons to be made between the corneas with PRK and LASIK procedures, which demonstrate healing responses at different depths.

Data were analyzed with statistical software (StatView 4.5, Abacus Concepts, Berkeley, California). Variations were expressed as standard errors of the mean (SEM). Statistical comparisons between the groups were performed using analysis of variance (ANOVA) with the Bonferroni-Dunn adjustment for repeated measures. All statistical tests were conducted at an alpha level of 0.01 because of the large number of statistical tests performed.

#### RESULTS

##### TUNEL-POSITIVE (PRESUMED APOPTOTIC) CELLS IN THE STROMA AFTER PRK AND LASIK

TUNEL-positive cells were detected in the corneal stroma at 4, 24, and 72 hours and 1 week after all three laser surgical procedures: PRK for low (-4.5 D) myopia (Figure 5), PRK for high (-9.0 D) myopia (Figure 6), and LASIK for high myopia (-9.0 D) (Figure 7). In the PRK corneas, the TUNEL-positive cells were located in the superficial stroma. In the LASIK corneas, the TUNEL-positive cells were typically scattered anterior and posterior to the lamellar interface created by the microkeratome cut. Thus, the depth of the band of TUNEL-positive cells in the stroma relative to the epithelium in the LASIK corneas was related to the thickness of the flap (Figure 7). A few of the LASIK corneas showed occasional TUNEL-positive cells in the more anterior stroma of the flap, away from the interface (Figure 7E, F, H, I). Through the 72-hour observation point, all corneas examined in all surgical groups—PRK and LASIK—showed at least some TUNEL-positive cells, but by 1 week after surgery, some corneas in each group had TUNEL-positive cells in the stroma and some did not. In the PRK groups, especially the -9.0 diopter PRK group, occasional TUNEL-positive cells were noted at 1 and 3 months after surgery in the superficial stroma. (An example of this can be seen in Figure 6I). These cells were rare, and with

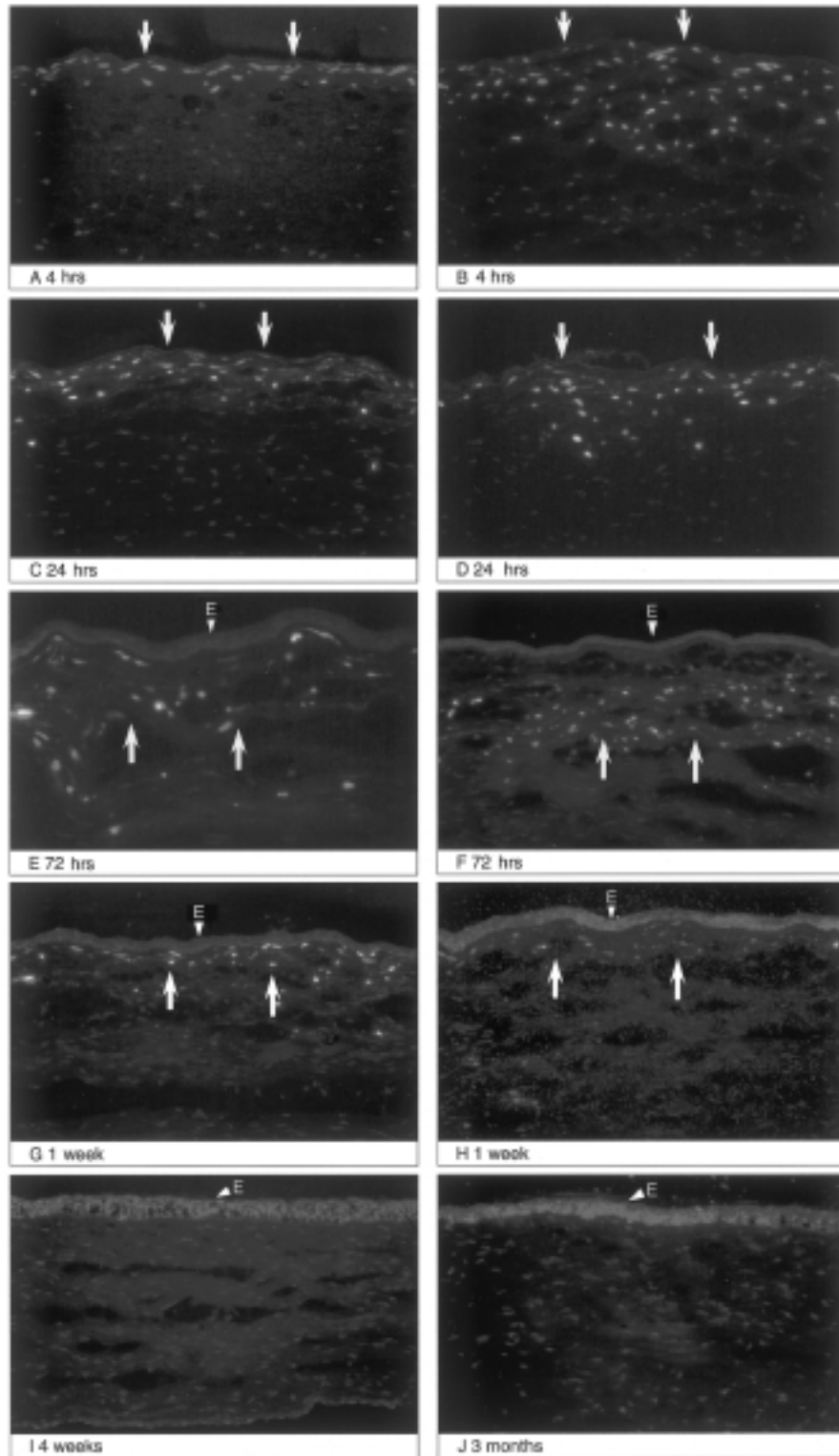
quantitation the means remained near zero.

Figure 8 shows the numbers of TUNEL-positive cells per 400× microscopic field column through the central corneal stroma at each time point from 4 hours to 3 months after PRK and LASIK. Significant numbers of TUNEL-positive stromal cells were counted in the central corneas of all three groups only at 4, 24, and 72 hours after surgery. At each of these three observation points, TUNEL-positive cells in the central cornea were most numerous in the high-myopia PRK group, fewer in the low-myopia PRK group, and fewest in the LASIK group. Although some TUNEL-positive cells were still seen at 1 week in all three groups, the numbers were small and differences between the groups were not significant. Only occasional TUNEL-positive cells were seen at 4 weeks or 3 months after surgery in each of the groups. Many of these later time point specimens in each of the three groups had no TUNEL-positive cells.

##### KI-67-POSITIVE (MITOTIC) CELLS IN THE STROMA AFTER PRK AND LASIK

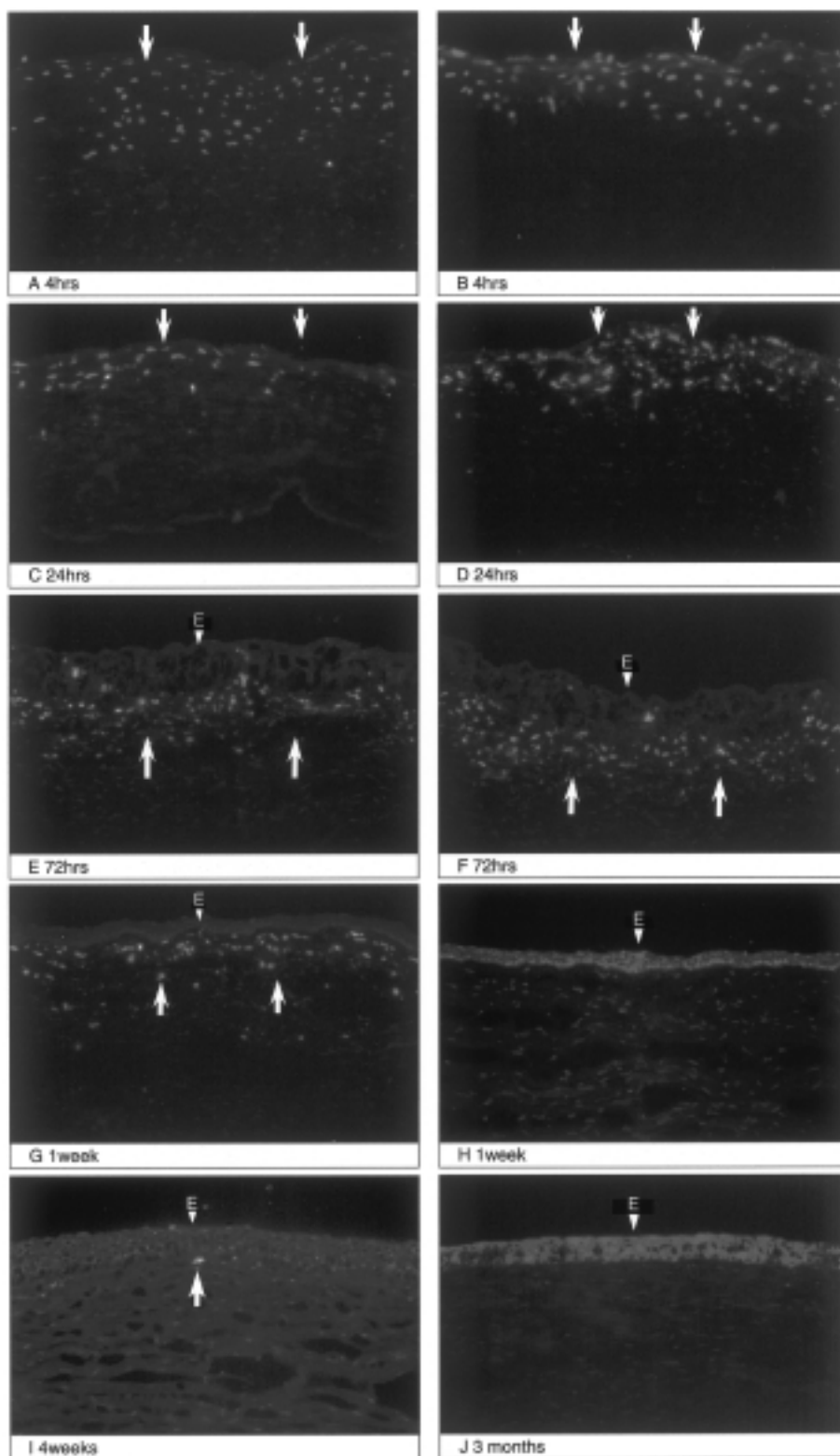
Figure 9 shows immunocytochemistry for the Ki-67 antigen associated with mitosis in the rabbit corneas that underwent PRK for low and high myopia or LASIK for high myopia. In the PRK corneas, the Ki-67-positive (mitotic) cells tended to localize in a band extending across the stroma posterior to the zone where the TUNEL-positive cells had been seen earlier. In the LASIK corneas, the Ki-67-positive (mitotic) cells were found largely in the areas anterior and posterior to the lamellar interface.

Figure 10 shows the numbers of Ki-67-positive (mitotic) cells per 400× microscopic field column through the central corneal stroma at each time point from 4 hours to 3 months after PRK and LASIK. In both the low- and high-myopia PRK corneas, significant numbers of Ki-67-positive cells were seen as early as 4 hours after surgery. In the low-myopia PRK corneas, mitosis continued to increase through 24 hours, maintained a steady rate through 72 hours, declined somewhat by 1 week, and returned to baseline (control) levels by 4 weeks after surgery. In the high-myopia PRK corneas, mitotic activity was sharply increased at 24 hours, about threefold that seen in the low-myopia PRK corneas; by 72 hours, however, the level of Ki-67-positive cells was similar to that seen in the low-myopia PRK group. By contrast, very few mitotic cells were seen in the LASIK corneas until 72 hours after surgery, when the numbers peaked at about the same levels seen in the low- and high-myopia PRK corneas at that observation point. At 4 weeks and 3 months after surgery, the numbers of mitotic cells were not significant in any of the three groups. Overall, the numbers of mitotic cells were highest in the high-myopia



**FIGURE 5**

Central cornea of rabbit eyes after PRK for low myopia (-4.5 D) assayed for apoptotic cells by terminal deoxynucleotidyl transferase-mediated dUTP nick end labeling (TUNEL). Typical results for each time point are shown: 4 hours (A, B), 24 hours (C, D), 72 hours (E, F), 1 week (G, H), 4 weeks (I), and 3 months (J) after surgery. TUNEL-positive stromal cells (arrows) are seen in all specimens from 4 hours to 72 hours. By 1 week some specimens show TUNEL-positive stromal cells (G, H) and some do not (not shown). Very few, if any, TUNEL-positive stromal cells are visible at 4 weeks or 3 months after surgery in a particular specimen (I, J). Soon after epithelial healing, epithelial cell layer (arrowhead labeled "E") is largely negative for apoptosis (E, F, G). TUNEL-positive epithelial cells begin to appear in epithelium 1 week after surgery (H) and increase in numbers thereafter (I, J), consistent with normal levels of apoptosis that occur in corneal epithelium during maturation (magnification x200) (also see Figure 6).



**FIGURE 6**

Central corneas of rabbit eyes after PRK for high myopia (-9.0 D) assayed for apoptotic cells by terminal deoxyribonucleotidyl transferase-mediated dUTP nick end labeling (TUNEL). Typical results for each time point are shown: 4 hours (A, B), 24 hours (C, D), 72 hours (E, F), 1 week (G, H), 4 weeks (I), and 3 months (J) after surgery. As with the low-myopia PRK corneas shown in Figure 5, TUNEL-positive stromal cells (arrows) are seen in all high-myopia PRK specimens from 4 hours to 72 hours (A-F). By 1 week, some specimens show TUNEL-positive stromal cells (G), and some do not (H). Rare TUNEL-positive cells (arrow in I) were visible in anterior stroma immediately beneath epithelium (arrowhead labeled "E") at 4 weeks (I) and 3 months (J) after surgery (magnification x200).

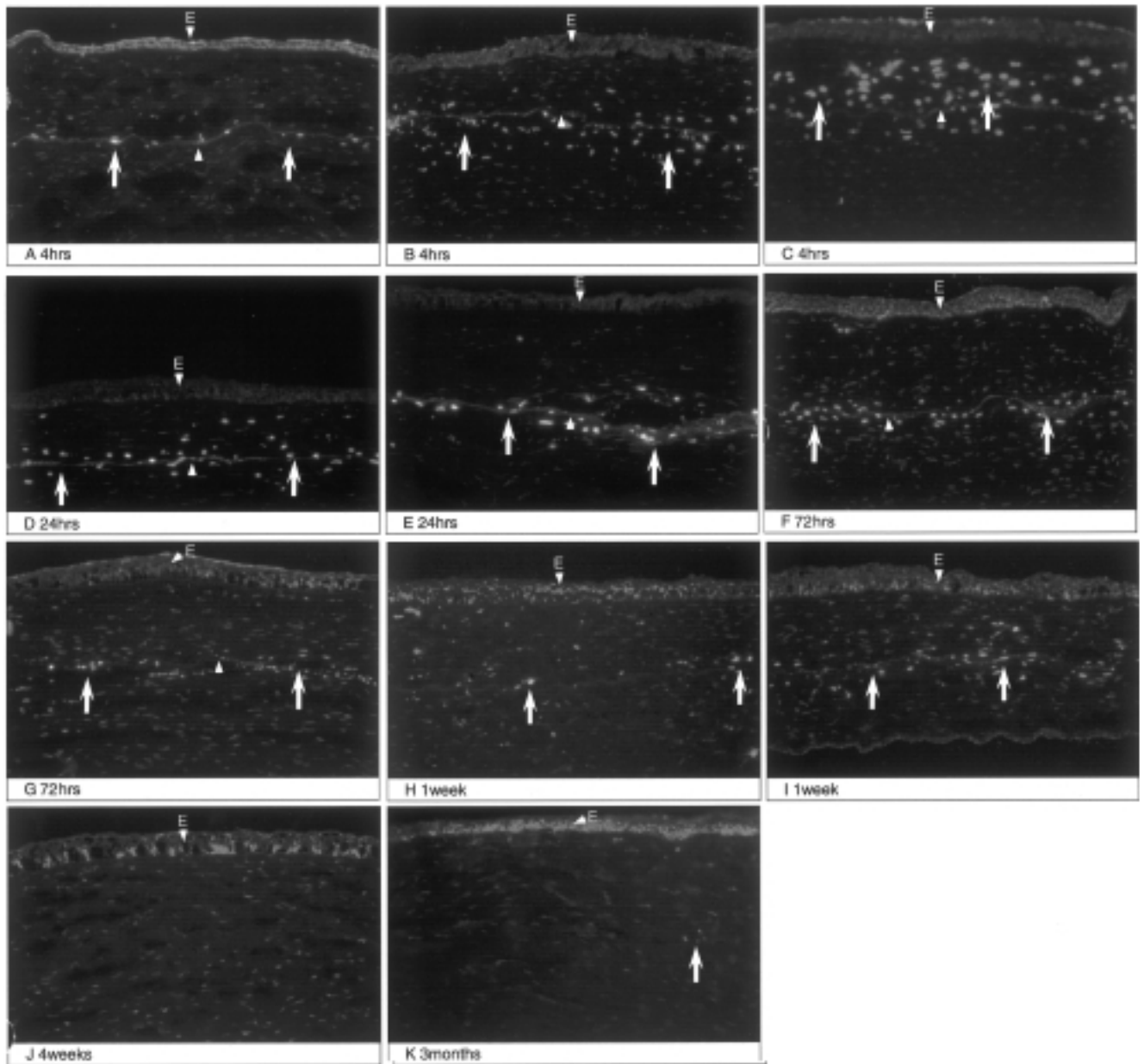


**FIGURE 7**

Central corneas from rabbit eyes after LASIK for high myopia (-9.0 D) assayed for apoptotic cells by terminal deoxynucleotidyl transferase-mediated dUTP nick end labeling (TUNEL). Typical results for each time point are shown: 4 hours (A, B, C), 24 hours (D, E), 72 hours (F, G), 1 week (H, I), 4 weeks (J), and 3 months (K) after surgery. In sections where interface between anterior flap and posterior stroma is visible (upward pointing arrowhead; A-G), apoptotic keratocytes (arrows) are seen to be distributed above and below lamellar microkeratome cut. As with both the high- and low-myopia PRK corneas in Figures 5 and 6, TUNEL-positive stromal cells are visible in all LASIK specimens from 4 hours to 72 hours (A-G). Most LASIK specimens have fewer TUNEL-positive cells in stroma (A, D, E, F, G, H) than the PRK corneas at the same time point, although a few had more (B, C, I). At 1 week after surgery, some specimens had no TUNEL-positive cells (not shown). Very few, if any, TUNEL-positive cells are seen at 4 weeks and 3 months after surgery; however, a possibly TUNEL-positive cell (arrow) is visible in at least one specimen (K) at 3 months. Note that location of apoptotic cells in cornea, in terms of stromal depth relative to epithelium (arrowhead labeled "E"), is determined directly by thickness of LASIK flap (magnification x200).

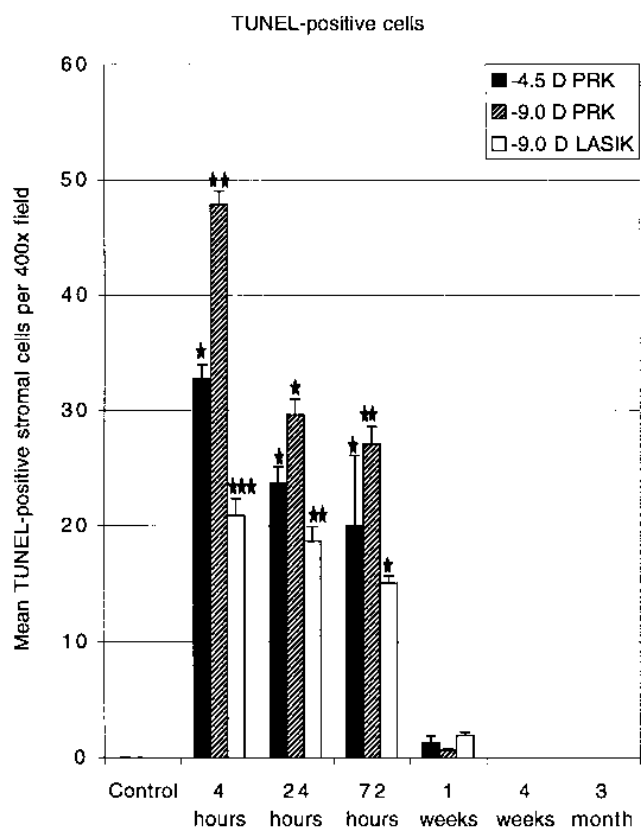


FIGURE 8

Numbers of TUNEL-positive cells in stroma after -4.5 diopters (D) PRK, -9.0 D PRK, and -9.0 D LASIK for myopia. Plotted values are numbers of cells counted in seven nonoverlapping, full-thickness columns (diameter of  $\times 400$  microscope field) extending from anterior stromal surface to posterior stromal surface. Five or six corneas were counted for each surgical procedure at each time point. Error bars represent standard error of mean. Bars marked with \*, \*\*, or \*\*\* indicate values significantly different from control ( $P < .01$ ). At a given time point, bars marked with different numbers of asterisks (\*, \*\*, and \*\*\*) indicate values significantly different from each other.

PRK corneas, lower in the low-myopia PRK corneas, and least in the LASIK cornea. Temporally, mitosis occurred earlier and persisted longer in the PRK corneas, compared with the LASIK corneas.

#### ALPHA SMOOTH-MUSCLE ACTIN-POSITIVE CELLS (MYOFIBROBLASTS) IN THE STROMA AFTER PRK AND LASIK

No alpha-SMA-positive stromal cells were seen in any of the corneas of the three groups at 4, 24, or 72 hours after surgery (not shown). Figure 11 shows immunocytochemistry for SMA associated with myofibroblasts in the central cornea of rabbit eyes that underwent PRK for high myopia. Significant numbers of alpha SMA-positive cells in the central cornea were seen only in this group. Some of the low-myopia PRK corneas had rare SMA-positive cells in the superficial stroma at 1 week, 4 weeks, and 3 months after surgery (not shown). In the high-myopia

PRK corneas, only a few SMA-positive cells were detected immediately beneath the epithelium 1 week after surgery (Figure 11, top); however, SMA staining of stromal cells was considerably increased at 4 weeks after surgery (Figure 11, middle) and persisted, albeit at a somewhat diminished level, through the end of the 3-month observation period (Figure 11, bottom). Few, if any, SMA-positive cells were detected in the central corneas of any of the LASIK eyes at any time point. A few SMA-positive cells were seen in the periphery near the edge of the flap in LASIK corneas at 1 week and 4 weeks after surgery (not shown). No such cells were seen in the 3-month LASIK corneas.

Figure 12 shows the numbers of SMA-positive cells in the stroma per 400 $\times$  microscopic field column through the central corneal stroma at each time point when staining was detected (1 week to 3 months) after PRK and LASIK. No staining was detected in the stromal cells of control corneas. A few SMA-positive cells were detected in the low-myopia PRK corneas at 1 and 4 weeks and 3 months, but the numbers of these cells did not reach statistical significance, compared with controls, at any of these observation points. By contrast, the high-myopia PRK corneas showed significant staining for myofibroblasts at 4 weeks and only slightly less staining at 3 months. In the LASIK group, the mean numbers of SMA-positive cells in the central cornea were not significantly different from control values at any time point.

#### TRANSMISSION ELECTRON MICROSCOPY

Transmission electron microscopy confirmed that the majority of dying stromal cells observed at 4 hours after PRK or LASIK showed the classic signs—cell shrinkage, chromatin condensation, and formation of apoptotic bodies (Figure 13A and B)—consistent with apoptosis, as noted in previous studies.<sup>13,14</sup> At 4 hours after surgery, all of the dying cells appeared to be keratocytes.

At 24 hours after surgery, some cells still showed morphologic changes consistent with apoptosis, but most of the dying cells had an appearance more consistent with necrosis (Figure 13C and D). By this time, large numbers of inflammatory cells had invaded the stroma, including many polymorphonuclear leukocytes and somewhat fewer monocytes/macrophages (Figure 13C, D, E, F). Many of these inflammatory cells were noted near other necrotic-appearing cells (Fig 13C and D). In some cases, the inflammatory cells appeared to be engulfing the dead cells. The inflammatory cells were most numerous in the high-myopia PRK corneas but were also seen in the low-myopia PRK corneas and the LASIK corneas. It was not possible to perform reliable quantitation of the inflammatory cells with TEM.

At 24 and 72 hours and 1 week after surgery, it was

often difficult to determine the identity of cells undergoing apoptosis or necrosis. Some appeared to be keratocytes or myofibroblasts derived from keratocytes, while others appeared to be polymorphonuclear leukocytes or monocytes/macrophages. In the PRK corneas, the necrotic and apoptotic cells were noted in the superficial stroma. In the LASIK corneas, most of the necrotic or apoptotic cells were located near the lamellar interface at a stromal depth that varied with flap thickness.

At 4 weeks and 3 months after surgery, there continued to be rare inflammatory cells. Some of the cells could be identified as probably polymorphonuclear cells or monocytes. In some cases, these cells appeared to be engulfing other cells that appeared to have died (Figure 13G). Some of the dead cells appeared to have undergone apoptosis (Figure 13G). In others, the mechanism of cell death was not clear and could have been apoptosis or necrosis. Some of the dead cells appeared to be myofibroblasts or keratocytes.

The high-myopia PRK corneas showed numerous living cells with prominent intracellular filaments and notable rough endoplasmic reticulum in the anterior stroma beneath the epithelium (Figure 13H, I, J). These cells were found in the same location where the SMA-positive cells had been detected with immunocytochemistry and were, therefore, believed to be myofibroblasts. Very few such cells were detected in the low-myopia PRK corneas, and none were noted in the LASIK corneas.

## **DISCUSSION**

---

This study represents the largest and most detailed investigation of the stromal cellular response to corneal surgery in any species. Previous studies have examined limited time intervals (4 hours or less after surgery) or have used methods such as *in vivo* confocal microscopy that are not able to detect cell death, quantitate cell proliferation, or determine cell type. Previous studies have also generally included too few animals to allow for statistical analyses. Additionally, none have looked at multiple aspects of the cellular response in the same corneal specimens over a long interval of time after surgery.

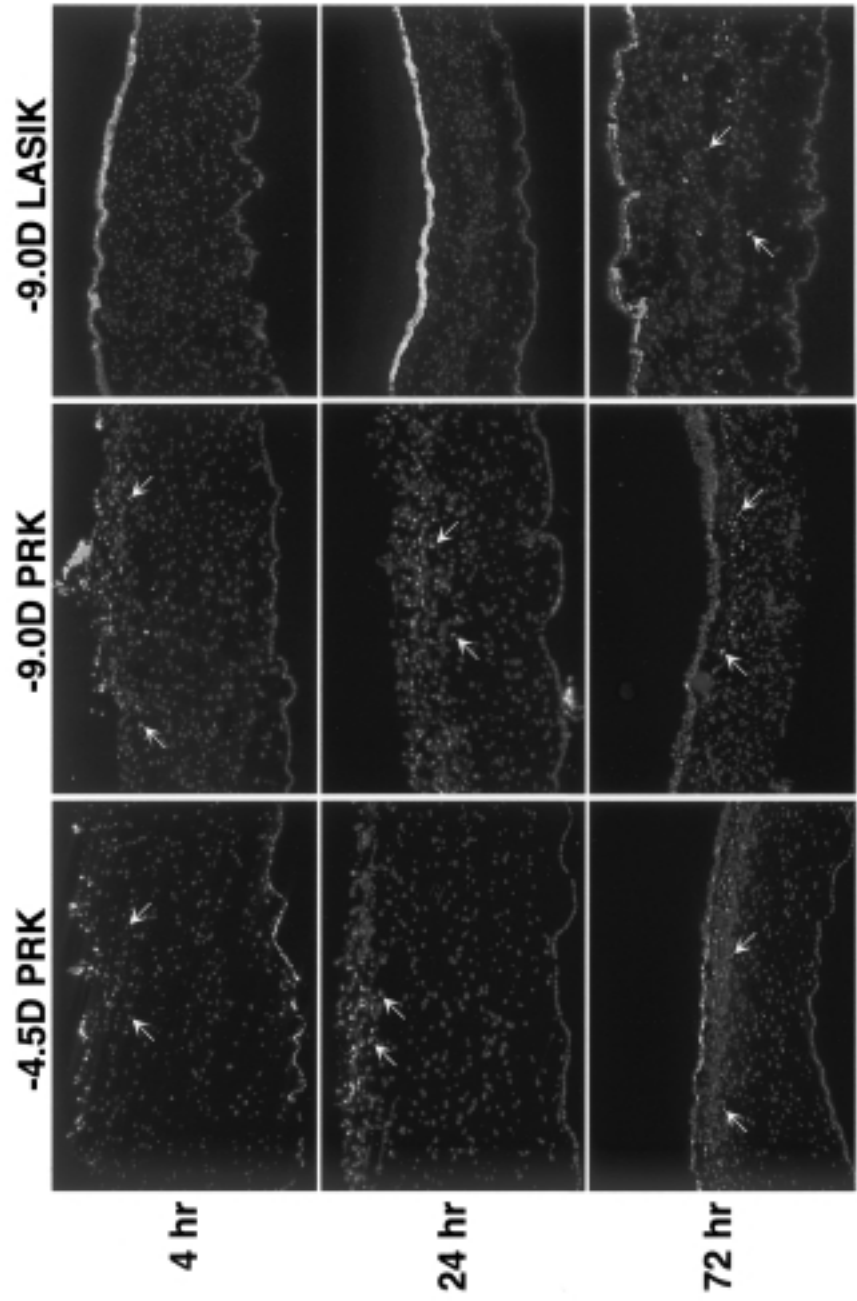
The goals of the present study were to determine whether there are quantitative differences in the cellular responses in the corneal stroma after PRK for low and high myopia and whether there are both qualitative and quantitative differences in the wound-healing response after PRK for high myopia and LASIK for high myopia. The results of this investigation provide strong evidence to support both hypotheses.

First, quantitative analysis showed statistically significant differences between low- and high-myopia PRK corneas in terms of keratocyte apoptosis (TUNEL-posi-

tive cells), keratocyte proliferation (Ki-67-positive cells), and myofibroblast cell density (SMA-positive cells). Each of these cellular responses is important in corneal wound healing, and each response was significantly greater in the high-myopia PRK corneas than in the low-myopia PRK corneas at every time point examined, from 4 hours to 1 week after surgery. These quantitative differences in the cellular responses likely underlie the clinical differences in outcome and complications such as regression and stromal haze that are seen after mechanical epithelial scrape, PRK for low myopia, and PRK for high myopia in the clinical setting.

Visually significant regression is most commonly noted after PRK for high myopia (>5 to 6 D in humans), consistent with our findings of higher levels of keratocyte apoptosis, stromal cell necrosis, keratocyte proliferation, and myofibroblast transformation. Visually significant haze is also more typically found after PRK for high myopia. The time course and localization of SMA-positive staining in the high-myopia PRK rabbit corneas is consistent with the timing and localization of dense haze that are noted in some human corneas after large PRK corrections. This correlation supports the hypothesis of Jester and coworkers<sup>28-30</sup> that myofibroblasts underlie the development of stromal haze after PRK.

Second, there were both qualitative and quantitative differences between the high-myopia PRK corneas and the high-myopia LASIK corneas in terms of the cellular responses in the stroma. Significantly greater numbers of apoptotic keratocytes, proliferating keratocytes, and myofibroblasts were seen in the -9.0 D PRK corneas, compared with the -9.0 D LASIK corneas. Furthermore, most of the TUNEL-positive cells in the LASIK corneas were located near the lamellar interface between the flap and the underlying bed, and therefore the thickness of the LASIK flap tended to determine the depth at which apoptosis and necrosis occurred. Thus, with a thin flap, the keratocyte apoptosis response was more superficially located in the stroma (Figure 7C), similar to the location of the response noted in the PRK corneas. Also in the LASIK corneas, significant keratocyte proliferation was not detected until 72 hours after surgery. By contrast, high levels of mitosis were detected at 4 hours after surgery in both the low- and high-myopia PRK corneas. Figure 10 shows that the total number of mitotic cells after surgery would likely be much greater for eyes undergoing PRK for high myopia, compared with eyes undergoing LASIK for high myopia. Mitosis is thought to give rise to the majority of wound-healing stromal cells, such as corneal fibroblasts and myofibroblasts, which in turn participate in stromal remodeling through the production and reabsorption of collagen, production of glycosaminoglycans, and other functions.



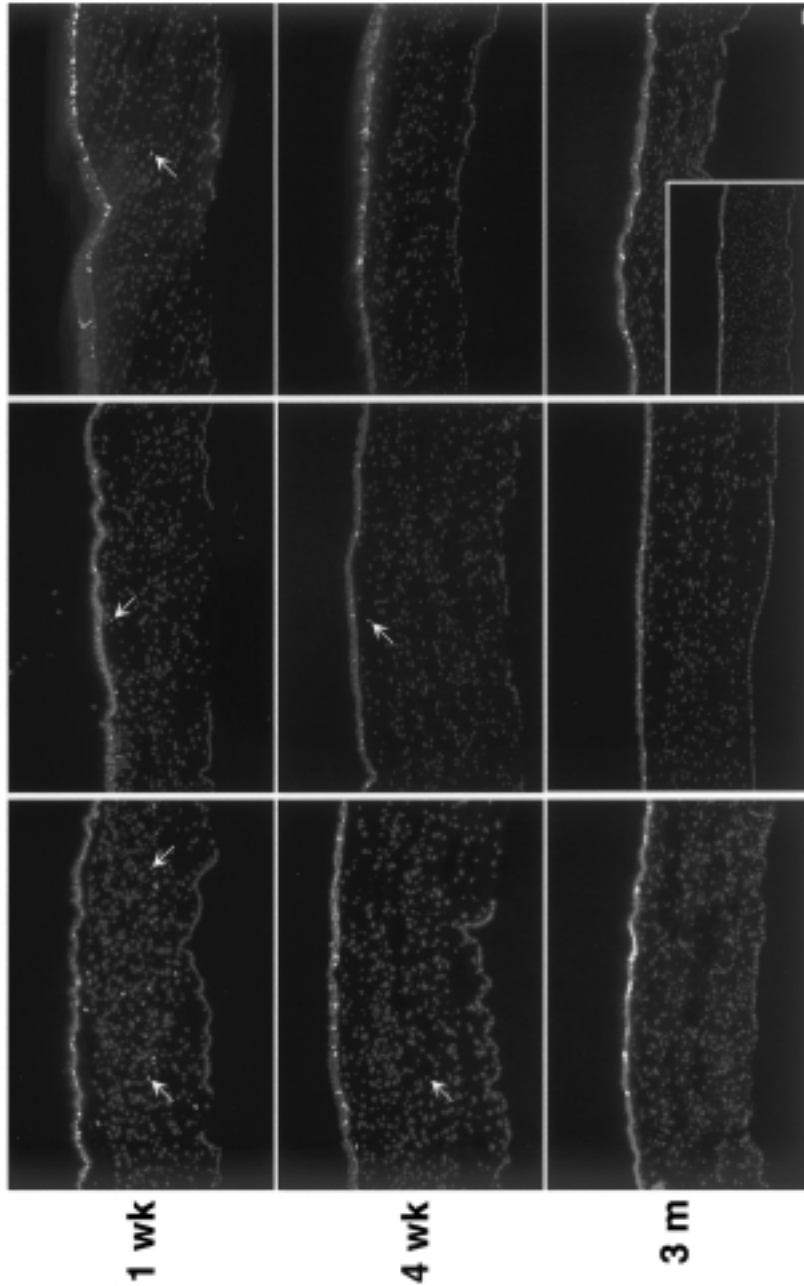


**FIGURE 9**

Immunocytochemistry to detect mitosis-associated antigen Ki-67 in corneal stroma. Cells positive for Ki-67 are stained green. Cells stained with propidium iodide counterstain appear red. In unwounded control corneas (inset), stromal cells undergoing mitosis are rare. At 4 hours after surgery, some stromal cell mitosis (arrows) is detectable in both the low- and high-myopia PRK groups, but mitotic cells are not seen in the LASIK corneas. At 24 hours, both PRK groups show increased mitosis (arrows), with larger numbers of mitotic cells visible in high-myopia PRK corneas; in these corneas, mitotic cells are located in a band beneath area where keratocyte apoptosis was noted earlier, deeper in central stroma and more superficially in peripheral stroma (not shown). Only a few mitotic stromal cells are seen at 24 hours in LASIK corneas (none in the image presented). At 72 hours and 1 week, mitotic stromal cells (arrows) are seen in both the low- and high-myopia PRK corneas. The 72-hour and 1-week LASIK corneas have mitotic cells, but they are at low levels relative to low or high PRK. After 1 week, stromal mitosis declines in all groups until, by 4 weeks, both the low- and high-myopia PRK corneas and the LASIK corneas have very few mitotic stromal cells. As would be expected, many epithelial cells stain for mitosis in the three groups at time points where epithelium is intact (magnification  $\times 200$ ).

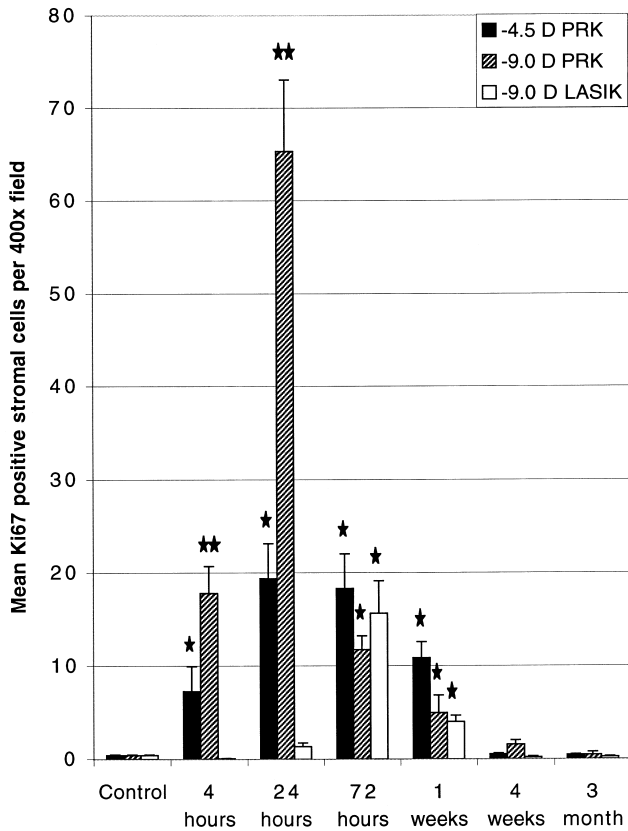


FIGURE 10

Numbers of Ki-67-positive cells in stroma after -4.5 diopter (D) PRK, -9.0 D PRK, and -9.0 D LASIK for myopia. Plotted values are numbers of cells counted in seven nonoverlapping, full-thickness columns (diameter of 400x microscope field) extending from anterior stromal surface to posterior stromal surface. Five or six corneas were counted for each surgical procedure at each time point. Error bars represent standard error of the mean. Bars marked with \* or \*\* indicate values significantly different from control ( $P < .01$ ). At a given time point, bars marked with different numbers of asterisks (\* and \*\*) indicate values significantly different from each other.

The underlying factors that delay keratocyte mitosis after LASIK, compared with PRK, are uncertain. Previous studies suggested that cytokines from the injured epithelium, such as PDGF, may have a role in triggering mitosis and migration of keratocytes after corneal injury.<sup>23-25</sup> In that there is far less epithelial injury in LASIK than in PRK, lower concentrations of these epithelial mitogens may be found in the stroma following LASIK, compared with PRK.

SMA-positive myofibroblasts were detected at significant levels in the central cornea only in the -9.0 D PRK group. Some myofibroblasts were detected in the superficial central stroma of the -4.5 D PRK corneas and near the lamellar interface in the periphery of -9.0 D LASIK corneas, but the numbers did not reach statistical significance at any time. Myofibroblast density in the -9.0 D PRK corneas determined by SMA staining peaked at 4

weeks after surgery, at which time electron microscopy showed cells with prominent rough endoplasmic reticulum and intracellular filaments consistent with myofibroblast morphology in the same locations in the anterior stroma where the SMA-positive cells had been identified by immunocytochemistry. The delayed appearance of these cells, proximity of these cells to the overlying epithelium, and their absence from corneas with the same level (-9.0 D) of LASIK correction suggests that the epithelium may have an important role in generating and maintaining myofibroblasts.

The numbers of myofibroblasts declined in the high-myopia PRK corneas between 4 weeks and 3 months after surgery. At least two possibilities could account for this phenomenon. One possibility is that some of the myofibroblasts transdifferentiate into keratocytes that do not express alpha-SMA. A second possibility is that the myofibroblasts slowly undergo apoptosis. Our detection of apoptotic cells in the anterior stroma of corneas with numerous myofibroblasts by means of both the TUNEL assay and electron microscopy supports the latter mechanism for disappearance of the myofibroblasts over time. However, our findings cannot exclude the possibility that some myofibroblasts transdifferentiate to keratocytes. It is possible that cytokines (such as transforming growth factor beta) released from the overlying epithelium act to maintain the myofibroblast phenotype,<sup>28,30,31</sup> and that the release of these factors diminishes over time as the cornea returns to a normal state. This idea is supported by the persistent localization of myofibroblasts only beneath the epithelium. Thus, we hypothesize that myofibroblasts are derived from dividing keratocytes that invade the stroma after injury, but that persistence of myofibroblasts over time requires cytokine input from the epithelium. Further support for this theory is provided by the disappearance of the transient SMA-positive cells found in the periphery near the flap-stroma interface in LASIK corneas. When present, these cells are located a considerable distance from the peripheral epithelium, and so are likely to be less affected by epithelial-derived factors.

In this study, TEM provided important new insights into the corneal wound-healing response after PRK and LASIK. At 4 hours after surgery, we saw that the majority of dying cells in the corneal stroma after PRK or LASIK were undergoing apoptosis, with chromatin condensation and formation of membrane-bound apoptotic bodies (Figure 13A and B). By contrast, at 24 hours (Fig 13C and D), 72 hours, and 1 week after PRK and LASIK, many of the dying cells had a morphology more consistent with that of necrosis, a disorganized form of cell death in which the cells appear to disintegrate, releasing their cellular contents into the surrounding tissues. Some of the cells detected at the later time points were undergoing

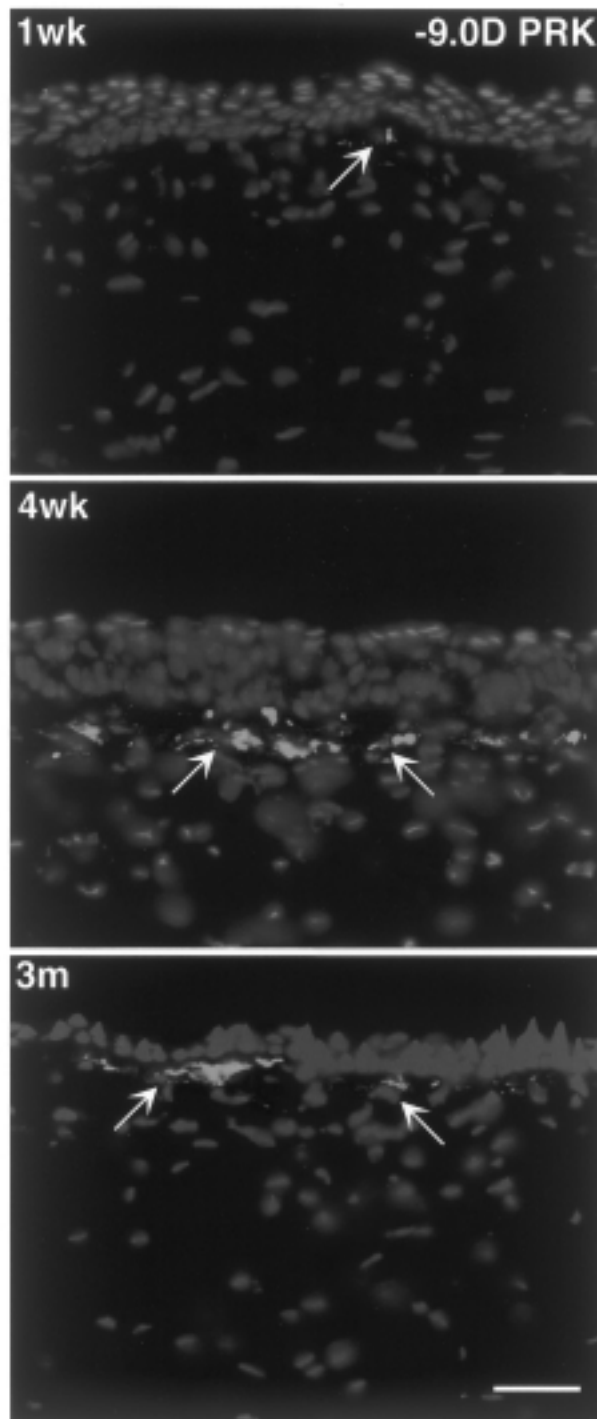


**FIGURE 11**

Immunocytochemistry to detect alpha smooth-muscle actin (SMA) myofibroblast-associated antigen in the corneal stroma. SMA-positive cells are stained green. Cells stained with propidium iodide counterstain appear red. High-myopia PRK corneas first show rare SMA-positive cells 1 week after surgery (top); greatest density of stained cells is seen at 4 weeks (middle), but numbers are still significant at 3 months after surgery (bottom). In these corneas, SMA-stained cells are located in anterior stroma immediately beneath epithelium. Few, if any, SMA-positive cells are detected in central cornea after PRK for low myopia or LASIK at any time after surgery, although LASIK corneas have some SMA-positive cells in peripheral stroma at site of perforation of epithelium by microkeratome blade at 1 week and 4 weeks after surgery (not shown) (magnification x400).

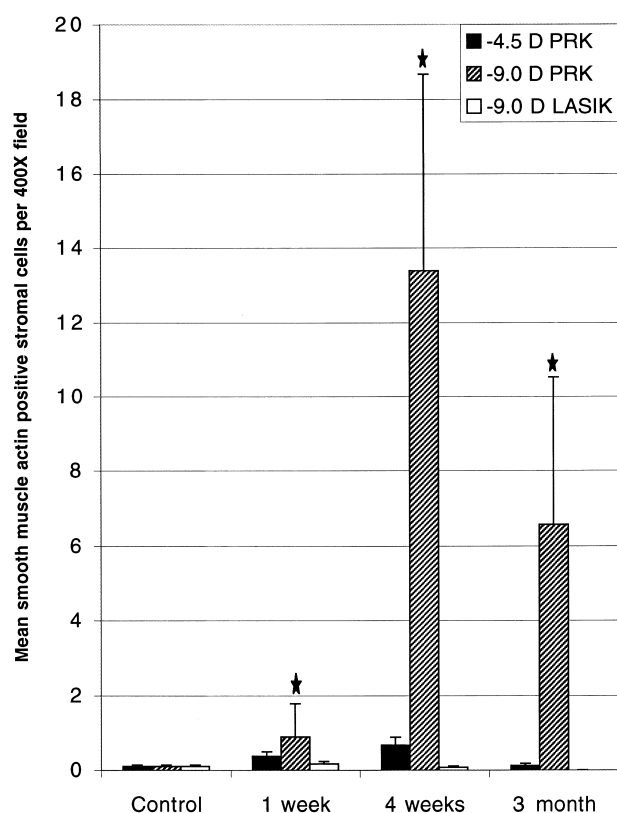


FIGURE 12

Numbers of alpha smooth muscle actin-positive cells in the central corneal stroma after -4.5 diopter (D) PRK, -9.0 D PRK, and -9.0 D LASIK for myopia. Plotted values are numbers of cells counted in seven nonoverlapping, full-thickness columns (diameter of 400x microscope field) extending from anterior stromal surface to posterior stromal surface. Five or six corneas were counted for each surgical procedure at each time point. Error bars represent standard error of mean. Bars marked with \* indicate values significantly different from control ( $P < .01$ ).

apoptosis, consistent with the findings of Gao and coworkers,<sup>21</sup> but apoptotic cells were not as common as cells undergoing necrosis. The levels of cellular necrosis were highest at 24 hours after surgery and decreased thereafter in all three groups. More necrotic cells were seen in the high-myopia PRK corneas than in the low-myopia PRK or LASIK corneas. Cells dying by either apoptosis or necrosis included keratocytes, polymorphonuclear leukocytes, and monocytes. In many cases, however, necrotic cells could not be identified by type because of the disrupted cellular morphology.

Few dying stromal cells were detected by TEM in any of the groups at 4 weeks after surgery. Of those that were seen, almost all were found in the anterior stroma of the -9.0 D PRK corneas (Figure 13G), and many were undergoing apoptosis, as determined by both electron microscopy and the TUNEL assay.

Comparison of the TUNEL assay and electron microscopy results at 24 hours, 72 hours, and 1 week

suggests that some cells that appeared to be necrotic by TEM may have also showed TUNEL-positive staining, since there were many TUNEL-positive cells, but only a relatively few cells with morphologic changes characteristic of apoptosis seen by TEM at these time points. We cannot be certain, however, since the TUNEL assay sampled many more cells than could be examined by electron microscopy. Also, the DNA fragmentation that is identified by the TUNEL assay does occur during necrosis, although usually in a more random manner that tends to make these cells invisible to the TUNEL assay. Previous studies have noted that in some situations, necrotic cells are falsely detected by the TUNEL assay.<sup>50</sup> This highlights the importance of using methods such as TEM to confirm the type of cell death detected by the TUNEL assay in a particular experimental system.<sup>50</sup>

It was difficult to identify the types of cells that underwent apoptosis or necrosis during the interval from 24 hours to 1 week after PRK or LASIK in this study. Previous studies have shown that in the early wound-healing phase (up to 4 hours after PRK or LASIK), the apoptotic cells are virtually entirely keratocytes.<sup>13,15,21</sup> However, it seems unlikely that the same keratocytes that begin apoptosis prior to 4 hours after injury are still present in the same location in the cornea a week later, since complete disappearance of the associated chromatin and the organelle-containing apoptotic bodies has been observed by 8 to 48 hours after surgery using electron microscopy.<sup>13</sup> Thus, the cells that are seen undergoing apoptosis at later time points are probably different cells; some could be keratocytes, corneal fibroblasts, or myofibroblasts<sup>26-28</sup> that migrate into the area from the peripheral and posterior cornea after injury. This migration could account for the disappearance of the SMA-positive myofibroblasts from the peripheral cornea between 1 week and 4 weeks after surgery in the LASIK group. This study found that some of these cells are polymorphonuclear leukocytes and monocytes/macrophages that are attracted to the wound-healing area.<sup>43,51</sup>

Transmission electron microscopy also showed large numbers of living inflammatory cells appearing by 24 hours after PRK and LASIK. Some of these inflammatory cells are still present, and in increased numbers compared to control corneas, at 4 weeks and 3 months after low- or high-correction PRK. To a lesser extent, some of these inflammatory cells are still present at 4 weeks and at 3 months after LASIK. These inflammatory cells included polymorphonuclear leukocytes and monocytes/macrophages. Recent studies suggest that chemokines such as monocyte chemoattractant and activating factor (MCAF) and granulocyte colony-stimulating factor (G-CSF) produced by the keratocytes during the wound-healing response attract these cells.<sup>51</sup> In the present study,

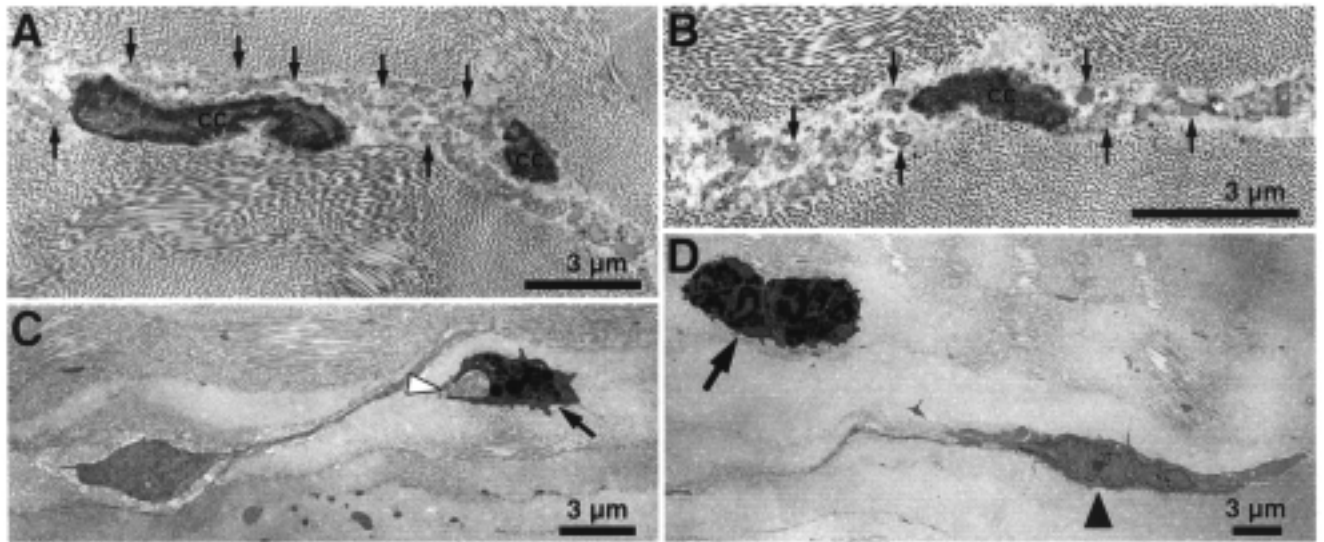


FIGURE 13A THROUGH D

Transmission electron microscopy (TEM) 4 hours after PRK or LASIK. At 4 hours after PRK for high or low PRK (A, magnification  $\times 1,500$ ) or LASIK (B, magnification  $\times 800$ ), dying cells show morphologic features consistent with apoptosis, including chromatin condensation (CC) and the formation of apoptotic bodies (arrows). At 24 hours after PRK for high myopia, TEM found cells that had cellular morphology more consistent with necrosis than apoptosis. C, Polymorphonuclear leukocyte (arrow) engulfing cellular debris (arrowhead) adjacent to a necrotic keratocyte in anterior stroma (magnification  $\times 2,950$ ). D, Polymorphonuclear leukocyte (arrow) adjacent to a necrotic-appearing keratocyte (arrowhead) in anterior stroma (magnification  $\times 3,900$ ). Findings were similar, but with fewer apoptotic or necrotic cells and inflammatory cells in the low PRK or LASIK group.

inflammatory cells were often seen in proximity to cells that appeared to be undergoing apoptosis or necrosis; in some cases the inflammatory cells were engulfing the dead cells (Figure 13C, D, G). The timing of the appearance of the inflammatory cells and detection of apoptotic and necrotic cells in the stroma suggests that the inflammatory cells themselves may trigger necrosis of some stromal cells at time points later than 4 hours. Further work is needed to elucidate these complex cellular interactions.

Within each surgical group, the magnitude of keratocyte apoptosis at the 4-hour time point appeared to correlate with the overall level of keratocyte proliferation and myfibroblast density in the stroma. Thus, the -9.0 D PRK corneas had the most TUNEL-positive cells in the stroma at 4 hours and the most Ki-67-positive, proliferating keratocytes and SMA-positive myfibroblasts at the later time points. In contrast, the LASIK corneas had the fewest TUNEL-positive cells at 4 hours after surgery and the fewest Ki-67-positive, proliferating cells and myfibroblasts at later time points. These correlations support the idea that the early keratocyte apoptosis response occurring after epithelial injury is a determinant of the overall stromal wound-healing response in the cornea.<sup>14,18,52</sup>

Considerable variation was seen among the eyes in terms of stromal cell apoptosis, keratocyte proliferation, and numbers of myfibroblasts at a given time point in a given surgical group. Figure 7 shows the variability in keratocyte apoptosis in three eyes at 4 hours after LASIK. These differences are similar to those noted clinically between the eyes of different patients, as well as between

the two eyes of a single patient, after PRK or LASIK.<sup>53-55</sup> This variability has several potential causes. One is biological variability in the healing response between individuals. Another is the unavoidable variation in surgical procedure. For example, there may be differences in the amount of cytokine-containing epithelial debris tracked into the interface by the microkeratome blade or efficiency of interface irrigation from eye to eye in LASIK.<sup>13-18,21</sup> Whatever the specific causes, it is likely that this variability in the wound-healing response ultimately leads to a significant proportion of the variability in outcome between patients undergoing refractive surgical procedures.

Localization of the wound-healing response in the cornea after PRK and LASIK is also likely to be an important determinant of clinical differences between PRK and LASIK for high myopia. Patients who undergo PRK for high myopia are more likely to experience regression and to develop corneal haze after surgery than those who undergo LASIK.<sup>53-55</sup> Regression after both PRK and LASIK is thought to result from a combination of epithelial hyperplasia and/or stromal remodeling.<sup>43-45,52,56</sup> Both of these processes are thought to be modulated via cytokine-mediated communication between the wound-healing cells of the stroma and the overlying epithelium.<sup>56</sup> It is likely that such interactions would be more pronounced in corneas that have undergone PRK, where the interacting cells are in immediate proximity to one another (Figure 5 and Figure 6), compared with LASIK corneas, in which the epithelial cells and stromal wound-healing cells are typically separated by a zone of normal stroma (Figure 7).

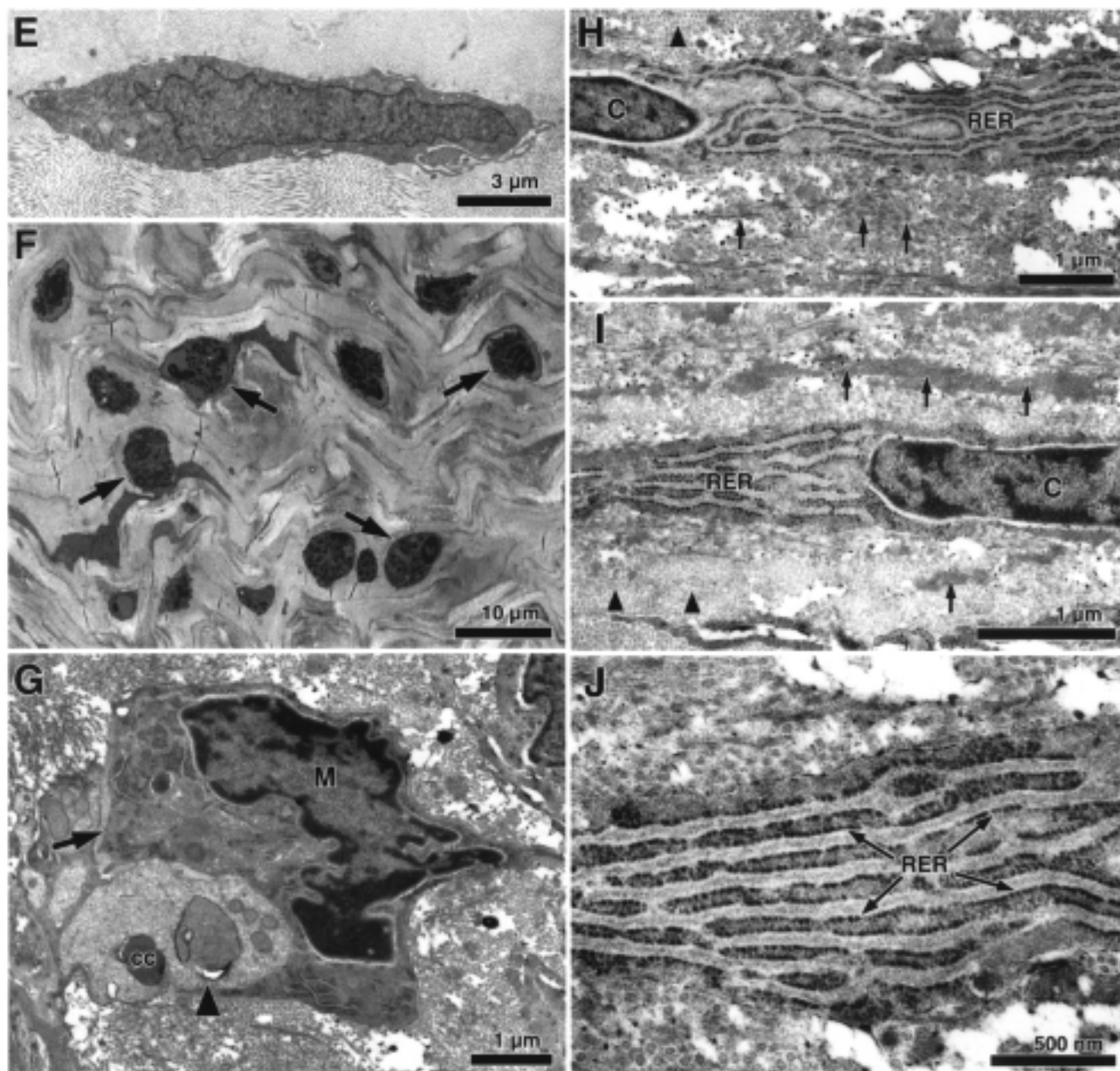


**FIGURE 13E THROUGH J**

Transmission electron microscopy. E, A monocyte in stroma at 24 hours after high PRK (magnification x1,500). F, Lower magnification of anterior stroma shows many polymorphonuclear leukocytes in anterior stroma at 24 hours after high PRK in one specimen (magnification x900). G, At 4 weeks after high PRK a monocyte/macrophage (M) is seen engulfing remnants of another cell (arrow) with condensed chromatin (CC) suggestive of apoptosis. Arrow indicates cellular membrane for monocyte/macrophage that delineates this cell from dead cell. Specific cell type of dead cell is uncertain (magnification x4,500). At 4 weeks after high PRK (H, magnification x4,200; I, magnification x5,000; J, magnification x8,000), numerous cells with large amounts of rough endoplasmic reticulum (RER), indicating a metabolically active cell with high-protein synthesis, were noted in anterior stroma. These are likely myofibroblasts. In H and I, arrowheads indicate regular collagen bundles and arrows indicate disorganized matrix material that likely includes collagen, glycosaminoglycans, and other substances. These areas of disorganized matrix material would likely be associated with corneal opacity, as would the myofibroblast cells themselves. Normal chromatin pattern of nucleus (C) is seen in H and I.

The appearance of a strong healing response with scarring at the edge of the flap in LASIK cases is also consistent with this theory. A stronger healing response with scarring is also typical of LASIK flap complications resulting when the microkeratome exits in the central cornea.<sup>57</sup> We hypothesize that this localization of the response is a major reason for the difference between PRK and LASIK in the treatment of high myopia.

The difference in myofibroblast cell density in PRK for high myopia compared with PRK for low myopia also has clinical relevance. Significant stromal haze is much more likely to occur after PRK for high myopia.<sup>58,59</sup> The author has never seen clinically significant haze in a cornea that underwent PRK for less than 5 D of myopia in more than 2,500 eyes (unpublished data, 2001). Jester and coworkers<sup>28,30</sup> suggested that loss of transparency is attributable to changes in crystallin expression in myofibroblasts that populate the stroma after PRK. Our results demonstrate a much higher density of myofibroblasts in the high-myopia PRK corneas compared with the low-myopia PRK corneas (Figure 11 and Figure 12), which is consistent with this hypothesis. The timing of the appearance of the myofibroblasts after PRK is also consistent with the clinical observation that haze may begin as early as a few weeks after PRK, but typically intensifies between 1 and 3 months after the procedure.<sup>58,59</sup> Finally, localization of myofibroblasts also suggests a role in PRK-associated haze. At the slit lamp, haze is most commonly noted immediately beneath the epithelium in humans and rabbits.<sup>58,60</sup>

## **SUMMARY**

The observations made in this study regarding the cellular responses associated with PRK and LASIK support our hypothesis that the early keratocyte apoptosis response is a good target for controlling later events in the wound-healing cascade.<sup>52</sup> Although electron microscopy revealed later cellular necrosis, apoptosis was the earliest stromal event noted after corneal injury or surgery. It remains our working hypothesis that blocking early keratocyte apoptosis could lead to diminished cellular apoptosis and necrosis, keratocyte proliferation, and myofibroblast generation later in the wound-healing process. To date, efforts to pharmacologically control early keratocyte apoptosis have not been successful<sup>50</sup>; however, studies are ongoing to identify the magic bullet that can regulate this phenomenon and its sequelae. Corneal surgeons have long sought the capacity to pharmacologically regulate the wound-healing response to clinical advantage, and early intervention in the wound-healing process still seems to be the most promising strategy. Once the early phase of keratocyte apoptosis has been initiated, the subsequent events that include late stromal cell apoptosis and necrosis, kera-

toocyte proliferation, and the generation of myofibroblasts in the stroma are highly variable and, therefore, likely to be difficult to control.

## **ACKNOWLEDGMENTS**

Rahul Mohan, PhD, Rajiv Mohan, PhD, Rosan Choi, MD, Jong-Wook Hong, MD, Jong-Soo Lee, MD, and Renato Ambrósio, MD, performed animal surgery, processed corneal tissue, and performed TUNEL assays. James Zieske, PhD, and Audrey E. K. Hutcheon, BS, performed immunocytochemistry for Ki-67 and alpha-SMA. Dan Possin performed transmission electron microscopy. Chuck Stephens provided imaging support. VISX (Santa Clara, California) provided key cards for performing the PRK and LASIK procedures in rabbits.

## **REFERENCES**

1. Wilson SE, Pedroza L, Beuerman R, et al. Herpes simplex virus type-1 infection of corneal epithelial cells induces apoptosis of the underlying keratocytes. *Exp Eye Res* 1997;64:775-779.
2. Wilson SE, Kaufman HE. Penetrating keratoplasty. *Surv Ophthalmol* 1990;34:325-356.
3. Pavan-Langston D. Herpes simplex virus ocular infections: current concepts of acute, latent and reactivated disease. *Trans Am Ophthalmol Soc* 1990;88:727-796.
4. Liesegang TJ. Ocular herpes simplex infection: pathogenesis and current therapy. *Mayo Clin Proc* 1988;63:1092-1105.
5. Shah SS, Kapadia MS, Meisler DM, et al. Photorefractive keratectomy using the Summit SVS Apex laser with or without astigmatic keratotomy. *Cornea* 1998;17:508-516.
6. Esquenazi S, Mendoza A. Two-year follow-up of laser in situ keratomileusis for hyperopia. *J Refract Surg* 1999;15:648-652.
7. Hersh PS, Abbassi R. Surgically induced astigmatism after photorefractive keratectomy and laser in situ keratomileusis. Summit PRK-LASIK Study Group. *J Cataract Refract Surg* 1999;25:389-398.
8. Kapadia MS, Krishna R, Shah S, et al. Surgically induced astigmatism after photorefractive keratectomy with the excimer laser. *Cornea* 2000;19:174-179.
9. Dohlman CH, Gasset AR, Rose J. The effect of the absence of corneal epithelium or endothelium on stromal keratocytes. *Invest Ophthalmol Vis Sci* 1968;7:520-534.
10. Nakayasu K. Stromal changes following removal of epithelium in rat cornea. *Jpn J Ophthalmol* 1988;32:113-125.
11. Crosson CE. Cellular changes following epithelial abrasion. In: Beuerman RW, Crosson CE, Kaufman HE, eds. *Healing Processes in the Cornea*. Houston, Tex: Gulf Publishing Co; 1989:3-14.
12. Campos M, Szerenyi K, Lee M, et al. Keratocyte loss after corneal deepithelialization in primates and rabbits. *Arch Ophthalmol* 1994;112:254-260.

13. Wilson SE, He Y-G, Weng J, et al. Epithelial injury induces keratocyte apoptosis: hypothesized role for the interleukin-1 system in the modulation of corneal tissue organization. *Exp Eye Res* 1996;62:325-338.
14. Wilson SE. Keratocyte apoptosis in refractive surgery: Everett Kinsey Lecture. *CLAO J* 1998;24:181-185.
15. Mohan RR, Liang Q, Kim W-J, et al. Apoptosis in the cornea: further characterization of Fas/Fas ligand system. *Exp Eye Res* 1997;65:575-589.
16. Mohan RR, Kim W-J, Mohan RR, et al. Bone morphogenic proteins 2 and 4 and their receptors in the adult human cornea. *Invest Ophthalmol Vis Sci* 1998;39:2626-2636.
17. Mohan RR, Mohan RR, Kim WJ, et al. Modulation of TNF-alpha-induced apoptosis in corneal fibroblasts by transcription factor NF-kb. *Invest Ophthalmol Vis Sci* 2000;41:1327-1336.
18. Helena MC, Baerveldt F, Kim W-J, et al. Keratocyte apoptosis after corneal surgery. *Invest Ophthalmol Vis Sci* 1998;39:276-283.
19. Watsky MA. Keratocyte gap junctional communication in normal and wounded rabbit corneas and human corneas. *Invest Ophthalmol Vis Sci* 1995;36:2568-2576.
20. Spanakis SG, Petridou S, Masur SK. Functional gap junctions in corneal fibroblasts and myofibroblasts. *Invest Ophthalmol Vis Sci* 1998;39:1320-1328.
21. Gao J, Gelber-Schwab TA, Addeo JV, et al. Apoptosis in the rabbit cornea after photorefractive keratectomy. *Cornea* 1997;16:200-208.
22. Zieske JD, Guimaraes SR, Hutcheon AEK. Kinetics of keratocyte proliferation in response to epithelial debridement. *Exp Eye Res* 2001;72:33-39.
23. Kamiyama K, Iguchi I, Wang X, et al. Effects of PDGF on the migration of rabbit corneal fibroblasts and epithelial cells. *Cornea* 1998;17:315-325.
24. Andresen JL, Ehlers N. Chemotaxis of human keratocytes is increased by platelet-derived growth factor-BB, epidermal growth factor, transforming growth factor-alpha, acidic fibroblast growth factor, insulin-like growth factor-I, and transforming growth factor-beta. *Curr Eye Res* 1998;17:79-87.
25. Kim W-J, Mohan RR, Mohan RR, et al. Effect of PDGF, IL-1 alpha, and BMP2/4 on corneal fibroblast chemotaxis: expression of the platelet-derived growth factor system in the cornea. *Invest Ophthalmol Vis Sci* 1999;40:1364-1372.
26. Masur S, Dewal HS, Dinh TT, et al. Myofibroblasts differentiate from fibroblasts when plated at low density. *Proc Natl Acad Sci U S A* 1996;93:4219-4223.
27. Jester JV, Huang J, Barry-Lane PA, et al. Transforming growth factor (beta)-mediated corneal myofibroblast differentiation requires actin and fibronectin assembly. *Invest Ophthalmol Vis Sci* 1990;40:1959-1967.
28. Jester JV, Petroll WM, Cavanagh HD. Corneal stromal wound healing in refractive surgery: the role of myofibroblasts. *Prog Retinal Eye Res* 1999;18:311-356.
29. Moller-Pedersen T, Cavanagh HD, et al. Neutralizing antibody to TGF beta modulates stromal fibrosis but not regression of photoablative effect following PRK. *Curr Eye Res* 1998;17:736-747.
30. Jester JV, Moller-Pedersen T, Huang J, et al. The cellular basis of corneal transparency: evidence for "corneal crystallins." *J Cell Sci* 1999;112:613-622.
31. Weng J, Mohan RR, Li Q, et al. IL-1 upregulates keratinocyte growth factor and hepatocyte growth factor mRNA and protein production by cultured stromal fibroblast cells: interleukin-1 beta expression in the cornea. *Cornea* 1996;16:465-471.
32. Kaji Y, Obata H, Usui T, et al. Three-dimensional organization of collagen fibrils during corneal stromal wound healing after excimer laser keratectomy. *J Cataract Refract Surg* 1998;24:1441-1446.
33. El-Shabrawi Y, Kublin CL, Cintron C. mRNA levels of alpha1(VI) collagen, alpha1(XII) collagen, and beta ig in rabbit cornea during normal development and healing. *Invest Ophthalmol Vis Sci* 1998;39:36-44.
34. Girard MT, Matsubara M, Fini ME. Transforming growth factor-beta and interleukin-1 modulate metalloproteinase expression by corneal stromal cells. *Invest Ophthalmol Vis Sci* 1991;32:2441-2454.
35. Strissel KJ, Rinehart WB, Fini ME. Regulation of paracrine cytokine balance controlling collagenase synthesis by corneal cells. *Invest Ophthalmol Vis Sci* 1997;38:546-552.
36. West-Mays JA, Strissel KJ, Sadow PM, et al. Competence for collagenase gene expression by tissue fibroblasts requires activation of an interleukin 1 alpha autocrine loop. *Proc Natl Acad Sci U S A* 1995;92:6768-6772.
37. Ye HQ, Azar DT. Expression of gelatinases A and B, and TIMPs 1 and 2 during corneal wound healing. *Invest Ophthalmol Vis Sci* 1998;39:913-921.
38. Ye HQ, Maeda M, Yu FS, et al. Differential expression of MT1-MMP (MMP-14) and collagenase III (MMP-13) genes in normal and wounded rat corneas. *Invest Ophthalmol Vis Sci* 2000;41:2894-2899.
39. O'Brien T, Li Q, Ashraf MF, et al. Inflammatory response in the early stages of wound healing after excimer laser keratectomy. *Arch Ophthalmol* 1998;116:1470-1474.
40. Lee RE, Davison PF, Cintron C. The healing of linear non-perforating wounds in rabbit corneas of different ages. *Invest Ophthalmol Vis Sci* 1982;23:660-665.
41. Cintron C, Covington HI, Kublin CL. Morphologic analyses of proteoglycans in rabbit corneal scars. *Invest Ophthalmol Vis Sci* 1990;31:1789-1798.
42. Gauthier CA, Holden BA, Epstein D, et al. Factors affecting epithelial hyperplasia after photorefractive keratectomy. *J Cataract Refract Surg* 1997;23:1042-1050.
43. Kim W-J, Helena MC, Mohan RR, et al. Changes in corneal morphology associated with chronic epithelial injury. *Invest Ophthalmol Vis Sci* 1999;40:35-42.
44. Lohmann CP, Guell JL. Regression after LASIK for the treatment of myopia: the role of the corneal epithelium. *Semin Ophthalmol* 1998;13:79-82.
45. Lohmann CP, Reischl U, Marshall J. Regression and epithelial hyperplasia after myopic photorefractive keratectomy in a human cornea. *J Cataract Refract Surg* 1999;25:712-715.
46. Zieske JD, Wasson M. Regional variation in distribution of EGF receptor in developing and adult corneal epithelium. *J Cell Sci* 1993;106:145-152.

47. Spurr AR. A low-viscosity epoxy resin embedding medium for electron microscopy. *J Ultrastruct Res* 1969;26:31-43.
48. Robards AW, Wilson AJ, eds. *Procedures in Electron Microscopy*. New York: Wiley; 1993;5:4.9.
49. Reynolds ES. The use of lead citrate at high pH as an electron-opaque stain in electron microscopy. *J Cell Biol* 1963;17:208-214.
50. Kim WJ, Mohan RR, Mohan RR, et al. Caspase inhibitor z-VAD-FMK inhibits keratocyte apoptosis, but promotes keratocyte necrosis, after corneal epithelial scrape. *Exp Eye Res* 2000;71:225-232.
51. Hong J-W, Liu JJ, Lee J-S, et al. Proinflammatory chemokine induction in keratocytes and inflammatory cell infiltration into the cornea. *Invest Ophthalmol Vis Sci* (in press).
52. Wilson SE, Kim W-J. Keratocyte apoptosis: implications on corneal wound healing, tissue organization, and disease. *Invest Ophthalmol Vis Sci* 1998;39:220-226.
53. Davidorf JM, Zaldivar R, Oscherow S. Results and complications of laser in situ keratomileusis by experienced surgeons. *J Refract Surg* 1998;14:114-122.
54. Brint SF, Ostrick DM, Fisher C, et al. Six-month results of the multicenter phase I study of excimer laser myopic keratomileusis. *J Cataract Refract Surg* 1994;20:610-615.
55. Kapadia MS, Wilson SE. One-year results of PRK in low and moderate myopia: fewer than 0.5% of eyes lose two or more lines of vision. *Cornea* 2000;19:180-184.
56. Wilson SE, Liu JJ, Mohan RR. Stromal-epithelial interactions in the cornea. *Prog Retinal Eye Res* 1999;18:293-309.
57. Wilson SE. LASIK: Management of common complications. *Cornea* 1998;17:459-467.
58. Moller-Pedersen T, Cavanagh HD, Petroll WM, et al. Corneal haze development after PRK is regulated by volume of stromal tissue removal. *Cornea* 1998;17:627-639.
59. Siganos DS, Katsanevaki VJ, Pallikaris IG. Correlation of subepithelial haze and refractive regression 1 month after photorefractive keratectomy for myopia. *J Refract Surg* 1999;15:338-342.
60. Lipshitz I, Loewenstein A, Varssano D, et al. Late onset corneal haze after photorefractive keratectomy for moderate and high myopia. *Ophthalmology* 1997;104:369-373.



# INDEX



# INDEX

- 2-Deoxy-G-Glucose Uptake in the Inner Retina : An In Vivo Study in the Normal Rat and Following Photoreceptor Degeneration, 353-364
- A Very Large Brazilian Pedigree With 11778 Leber's Hereditary Optic Neuropathy, 169-179
- Activated Satellite Cells are Present in Uninjured Extraocular Muscles of Mature Mice, 119-124
- Albert, Daniel M., 125
- Altangerel, Undraa, 181
- American Ophthalmological Society Representative to the American College of Surgeons Board of Governors  
Report of the, 26
- American Orthoptic Council,  
Report of the, 28
- Analysis of the Keratocyte Apoptosis, Keratocyte Proliferation, and Myofibroblast Transformation Responses After Photorefractive Keratectomy and Laser In Situ Keratomileusis, 411-433
- Anderson, Douglas R., 136, 222
- Anderson, W. Banks Jr., 106
- Andrade, Rafael, 169
- Angle Closure In Younger Patients, 201-214
- Appointments by the Council, 30
- Assessment of the Retinal Nerve Fiber Layer of the Normal and Glaucomatous Monkey with Scanning Laser Polarimetry, 161-168
- Athletic Committee  
Report of the, 35
- Audo, Isabelle, 125
- Augburger, James J., 48, 225, 233
- Azab, Amr, 79
- Bacterial Resistance After Short-Term Exposure to Antibiotics, 137-142
- Banquet, 32
- Bartley, George B., 61, 66
- Baum, Jules L., 71
- Bayer, Atilla, 181
- Belfort, Rubens, 169
- Berezovsky, Adriana, 169
- Biglan, Albert W., 213
- Blankenship, Thomas N., 187
- Blair, Norman P., 76
- Bobrow, James C., 131, 136, 151, 185, 213
- Bowd, Christopher, 161
- Brewer, George J., 73
- Buyukmihci, Nedim C., 187
- Cantor, Louis, B., 212, 223
- Carelli, Valerio, 169
- Chairman of the Council,  
Report of the, 29
- Chang, Brian M., 201
- Chittcharus, Anuwat, 143
- Chung, Sophia M., 67
- Clinical Decision Making Based on Data from Gdx:  
One-Year Observations, 131-136
- Committee on Prizes,  
Report of the, 36
- Constitution and Bylaws Committee  
Report of the, 29
- Contents, v
- Contributors, xviii
- Corrêa, Zélia M., 225
- Covert, David W., 109
- Crawford, J. Brooks, 233
- Darjatmoko, Soesiawaiti R., 125
- Dawson, Daniel G., 125
- Delta-9-Tetrahydrocannabinol (THC) in the Treatment of End-Stage Open-Angle Glaucoma, 215-224
- DeNegri, Anna-Maria, 169
- Diabetes-Induced Dysfunction of Retinal Müller Cells, 339-352
- Diagnostic Transvitreal Fine-Needle Aspiration Biopsy of Small Melanocytic Choroidal Tumors In Nevus Versus Melanoma Category, 225-234
- Dickson, Harold, 137
- Durson, Dilek, 51
- Eagle, Ralph C. Jr., 199
- Editors Report, 22
- Egan, Kathleen M., 43
- Elnor, Susan G., 273
- Elnor, Victor M., 301
- Emeritus Committee  
Report of the, 23
- Endophthalmitis In Patients With Disseminated Fungal Disease, 67-72
- Ernest, Terry J., 200
- Evolution of the Tapetum, 187-200
- Ehya, Hormoz, 225
- FDA Status Disclaimer, 39
- Feman, Stephen S., 67, 71, 233
- Feuer, William J., 51
- Fitzgerald, Paul G., 187
- Flach, Allan J., 77, 118, 123, 178, 213, 215, 223
- Flanagan, Joseph C., 65
- Flynn, John T., 77, 106, 123
- Forster, Richard K., 51, 59, 84, 141, 233
- Friedman, Alan H., 178
- Frisbie, Jared C., 125
- Frueh, Bartley R., 65
- Gleiser, Joel, 125
- Gottsch, John D., 79
- Gragoudas, Evangelos S., 43, 48
- Grossniklaus, Hans E., 232
- Gutman, Froncie A., 233
- Haik, Barrett G., 129
- Haller, Julia A., 79, 84
- Halpern, Michael T., 109
- Hamilton, Danielle, 137
- Hardten, David R., 143
- Hariprasad, Seenu M., 153
- Henderer, Jeffrey, 181
- Holz, Eric R., 153, 159
- Human Retinal Pigment Epithelial Lysis of Extracellular Matrix:  
Functional Urokinase Plasminogen Activator Receptor, Collagenase, and Elastase, 273-299
- In Memoriam, 2
- Joint Commission on Allied Health Personnel in Ophthalmology,  
Report of, 28
- Jones, Dan B., 70
- Katz, L. Jay, 181
- Kelley, James S., 84
- Kesen, Muge, 181
- Landers, Maurice B. III, 159
- Lakhanpal, Vinod, 233

## Index

- Lane, Anne Marie, 43  
Li, Wenjun, 43  
Lichter, Paul R., 106  
Liebmann, Jeffrey M., 201  
Lindstrom, Mary J., 125  
Lindstrom, Richard L., 142, 143, 151  
Liu, Connie, 181  
Lokken, Janice M., 125  
Long-Term Analysis Of Lasik for the Correction of Refractive Errors  
  After Penetrating Keratoplasty, 143-152  
Long-Term Risk of Local Failure after Proton Therapy for  
  Choroidal/Ciliary Body Melanoma, 43-49  
Ludwig, Irene H., 123
- Mannis, Mark J., 243  
McLoon, Linda K., 119  
Members, xv  
Messenger, Marlene M., 61  
Mieler, William F., 153  
Minutes of the Proceedings, 21  
Multicenter Prospective, Randomized, Double-Masked,  
  Placebo Controlled Study of Rheopheresis to Treat Nonexudative  
  Age-Related Macular Degeneration: Interim Analysis, 85-108  
Munzenrider, John, 43  
Myers, Jonathan, 181
- Necrology, 1  
New Members, 34  
Nichols, John C., 67  
Nirankari, Verinder S., 58, 141, 151  
Nix, Vickie A., 137
- Officers and Council of the American Ophthalmological Society, ix
- Papers, 43-234  
Photographer and Archivist  
  Report of the, 22  
Posters, 235-239  
President  
  Report of the, 30  
Presidents of the Society, x  
Proceedings of the Council of the American Academy of Ophthalmology  
  Report of the, 29  
Program Committee  
  Report of the, 22  
Progression of Visual Field Loss in Untreated Glaucoma Patients and  
  Suspects in St Lucia, West Indies, 365-410  
Projected Impact Of Travoprost Versus Both Timolol and Latanoprost  
  On Visual Field Deficit Progression and Costs Among Black  
  Glaucoma Subjects, 109-118  
Pulido, Jose S., 85, 107  
Puro, Donald G., 339
- Quiros, Peter, 169
- Recipients of the Howe Medal, xii  
Retinal Pigment Epithelial Acid Lipase Activity and Lipoprotein  
  Receptors: Effects of Dietary Omega-3 Fatty Acids, 301-338  
Rhee, Douglas, 181  
Ritch, Robert, 135, 186, 201, 214  
Robin, Alan L., 109, 118  
Robinson-Smith, Toni, 225
- Sadun, Alfredo A., 77, 169, 178, 200  
Sadun, Federico, 169  
Salomao, Solange R., 169  
Sanders, Donald, 106  
Schein, Stan, 169  
Schneider, Susan, 225  
Schwab, Ivan R., 142, 178, 187, 200  
Secretary-Treasurer Report, 21  
Shields, M. Bruce, 117  
Spaeth, George L., 181, 186, 223  
Stamper, Robert L., 118, 166  
Stark, Walter J., 79, 150  
Steinmann, William, 181  
Strugnell, Stephen A., 125  
Surgical Approaches to the Management of Epithelial Cysts, 79-84  
Suturing Technique for Control of Postkeratoplasty Astigmatism  
  and Myopia, 51-60
- Tasman, William, 70, 213  
Tetrathiomolybdate as an Antiangiogenesis Therapy for Subfoveal  
  Choroidal Neovascularization Secondary to Age-Related Macular  
  Degeneration, 73-78  
The Dehiscent Hughes Flap: Outcomes and Implications, 61-66  
The Disc Damage Likelihood Scale: Reproducibility of a New Method  
  of Estimating the Amount of Optic Nerve Damage Caused by  
  Glaucoma, 181-186  
The Multicenter Investigation of Rheopheresis for AMD (MIRA-1)  
  Study Group, 85  
The Use of Antimicrobial Peptides in Ophthalmology: An  
  Experimental Study in Corneal Preservation and the Management of  
  Bacterial Keratitis, 243-271  
Theobald, Todd A., 67  
Theses, 241  
Thesis Committee  
  Report of the, 22  
Thompson, Robert W., 79  
Toxicity and Dose-Response Studies of 1 $\alpha$ -Hydroxyvitamin D<sub>2</sub> in  
  Lh $\beta$ -Tag Transgenic Mice, 125-130  
Trichopoulos, Nikolaos, 225  
Troutman, Richard C., 58, 151
- Van Meter, Woodford S., 57  
Verhoeff Lecturers, xiv  
Vine, Andrew K., 73, 77  
Vitreous Penetration of Orally Administered Gatifloxacin  
  In Humans, 153-160
- Waring, George O., 59  
Weinreb, Robert N., 161, 167  
Wilson, David J., 353  
Wilson, M. Roy, 365  
Wilson, Steven E., 411  
Wirtschafter, Jonathan, 119, 123  
Wood, Thomas O., 137, 142
- Yassin, Rawia S., 225  
Younge, Brian R., 178  
Yuen, Carlton K., 187
- Zangwill, Linda M., 161  
Zimbrick, Michele L., 125